BIODIVERSITY, CONNECTIVITY AND ECOSYSTEM FUNCTION ACROSS THE CLARION-CLIPPERTON ZONE: A REGIONAL SYNTHESIS FOR AN AREA TARGETED FOR NODULE MINING

EDITED BY: Craig Randall Smith, Adrian Glover, Malcolm Ross Clark, Erica Goetze and Kerry Howell

PUBLISHED IN: Frontiers in Marine Science

frontiers Research Topics

frontiers

Frontiers eBook Copyright Statement

The copyright in the text of individual articles in this eBook is the property of their respective authors or their respective institutions or funders. The copyright in graphics and images within each article may be subject to copyright of other parties. In both cases this is subject to a license granted to Frontiers.

The compilation of articles constituting this eBook is the property of Frontiers.

Each article within this eBook, and the eBook itself, are published under the most recent version of the Creative Commons CC-BY licence. The version current at the date of publication of this eBook is CC-BY 4.0. If the CC-BY licence is updated, the licence granted by Frontiers is automatically updated to the new version.

When exercising any right under the CC-BY licence, Frontiers must be attributed as the original publisher of the article or eBook, as applicable.

Authors have the responsibility of ensuring that any graphics or other materials which are the property of others may be included in the CC-BY licence, but this should be checked before relying on the CC-BY licence to reproduce those materials. Any copyright notices relating to those materials must be complied with.

Copyright and source acknowledgement notices may not be removed and must be displayed in any copy, derivative work or partial copy which includes the elements in question.

All copyright, and all rights therein, are protected by national and international copyright laws. The above represents a summary only. For further information please read Frontiers' Conditions for Website Use and Copyright Statement, and the applicable CC-BY licence.

ISSN 1664-8714
ISBN 978-2-88974-126-7
DOI 10.3389/978-2-88974-126-7

About Frontiers

Frontiers is more than just an open-access publisher of scholarly articles: it is a pioneering approach to the world of academia, radically improving the way scholarly research is managed. The grand vision of Frontiers is a world where all people have an equal opportunity to seek, share and generate knowledge. Frontiers provides immediate and permanent online open access to all its publications, but this alone is not enough to realize our grand goals.

Frontiers Journal Series

The Frontiers Journal Series is a multi-tier and interdisciplinary set of open-access, online journals, promising a paradigm shift from the current review, selection and dissemination processes in academic publishing. All Frontiers journals are driven by researchers for researchers; therefore, they constitute a service to the scholarly community. At the same time, the Frontiers Journal Series operates on a revolutionary invention, the tiered publishing system, initially addressing specific communities of scholars, and gradually climbing up to broader public understanding, thus serving the interests of the lay society, too.

Dedication to Quality

Each Frontiers article is a landmark of the highest quality, thanks to genuinely collaborative interactions between authors and review editors, who include some of the world's best academicians. Research must be certified by peers before entering a stream of knowledge that may eventually reach the public - and shape society; therefore, Frontiers only applies the most rigorous and unbiased reviews.
Frontiers revolutionizes research publishing by freely delivering the most outstanding research, evaluated with no bias from both the academic and social point of view. By applying the most advanced information technologies, Frontiers is catapulting scholarly publishing into a new generation.

What are Frontiers Research Topics?

Frontiers Research Topics are very popular trademarks of the Frontiers Journals Series: they are collections of at least ten articles, all centered on a particular subject. With their unique mix of varied contributions from Original Research to Review Articles, Frontiers Research Topics unify the most influential researchers, the latest key findings and historical advances in a hot research area! Find out more on how to host your own Frontiers Research Topic or contribute to one as an author by contacting the Frontiers Editorial Office: frontiersin.org/about/contact

BIODIVERSITY, CONNECTIVITY AND ECOSYSTEM FUNCTION ACROSS THE CLARION-CLIPPERTON ZONE: A REGIONAL SYNTHESIS FOR AN AREA TARGETED FOR NODULE MINING

Topic Editors:
Craig Randall Smith, University of Hawaii at Manoa, United States
Adrian Glover, Natural History Museum (United Kingdom), United Kingdom
Malcolm Ross Clark, National Institute of Water and Atmospheric Research (NIWA), New Zealand
Erica Goetze, University of Hawaii at Manoa, United States
Kerry Howell, University of Plymouth, United Kingdom

Citation: Smith, C. R., Glover, A., Clark, M. R., Goetze, E., Howell, K., eds. (2022). Biodiversity, Connectivity and Ecosystem Function Across the Clarion-Clipperton Zone: A Regional Synthesis for an Area Targeted for Nodule Mining. Lausanne: Frontiers Media SA. doi: 10.3389/978-2-88974-126-7

Table of Contents

05 ***Editorial: Biodiversity, Connectivity and Ecosystem Function Across the Clarion-Clipperton Zone: A Regional Synthesis for an Area Targeted for Nodule Mining***
Craig R. Smith, Malcolm R. Clark, Erica Goetze, Adrian G. Glover and Kerry L. Howell

08 ***From Sea Surface to Seafloor: A Benthic Allochthonous eDNA Survey for the Abyssal Ocean***
Olivier Laroche, Oliver Kersten, Craig R. Smith and Erica Goetze

24 ***Using Habitat Classification to Assess Representativity of a Protected Area Network in a Large, Data-Poor Area Targeted for Deep-Sea Mining***
Kirsty A. McQuaid, Martin J. Attrill, Malcolm R. Clark, Amber Cobley, Adrian G. Glover, Craig R. Smith and Kerry L. Howell

45 ***Environmental Heterogeneity Throughout the Clarion-Clipperton Zone and the Potential Representativity of the APEI Network***
Travis W. Washburn, Daniel O. B. Jones, Chih-Lin Wei and Craig R. Smith

62 ***Patterns of Macrofaunal Biodiversity Across the Clarion-Clipperton Zone: An Area Targeted for Seabed Mining***
Travis W. Washburn, Lenaick Menot, Paulo Bonifácio, Ellen Pape, Magdalena Błażewicz, Guadalupe Bribiesca-Contreras, Thomas G. Dahlgren, Tomohiko Fukushima, Adrian G. Glover, Se Jong Ju, Stefanie Kaiser, Ok Hwan Yu and Craig R. Smith

84 ***Mesopelagic Scattering Layer Behaviors Across the Clarion-Clipperton Zone: Implications for Deep-Sea Mining***
Jessica N. Perelman, Eric Firing, Jesse M. A. van der Grient, Benjamin A. Jones and Jeffrey C. Drazen

98 ***Bacterial and Archaeal Communities in Polymetallic Nodules, Sediments, and Bottom Waters of the Abyssal Clarion-Clipperton Zone: Emerging Patterns and Future Monitoring Considerations***
Emma K. Wear, Matthew J. Church, Beth N. Orcutt, Christine N. Shulse, Markus V. Lindh and Craig R. Smith

114 ***Comparative Reproductive Biology of Deep-Sea Ophiuroids Inhabiting Polymetallic-Nodule Fields in the Clarion-Clipperton Fracture Zone***
Sven R. Laming, Magdalini Christodoulou, Pedro Martinez Arbizu and Ana Hilário

130 ***Eukaryotic Biodiversity and Spatial Patterns in the Clarion-Clipperton Zone and Other Abyssal Regions: Insights From Sediment DNA and RNA Metabarcoding***
Franck Lejzerowicz, Andrew John Gooday, Inés Barrenechea Angeles, Tristan Cordier, Raphaël Morard, Laure Apothéloz-Perret-Gentil, Lidia Lins, Lenaick Menot, Angelika Brandt, Lisa Ann Levin, Pedro Martinez Arbizu, Craig Randall Smith and Jan Pawlowski

153 ***The Biodiversity and Distribution of Abyssal Benthic Foraminifera and Their Possible Ecological Roles: A Synthesis Across the Clarion-Clipperton Zone***
Andrew J. Gooday, Franck Lejzerowicz, Aurélie Goineau, Maria Holzmann, Olga Kamenskaya, Hiroshi Kitazato, Swee-Cheng Lim, Jan Pawlowski, Teresa Radziejewska, Zofia Stachowska and Brygida Wawrzyniak-Wydrowska

176 ***Megafaunal Ecology of the Western Clarion Clipperton Zone***
Jennifer M. Durden, Meagan Putts, Sarah Bingo, Astrid B. Leitner, Jeffrey C. Drazen, Andrew J. Gooday, Daniel O. B. Jones, Andrew K. Sweetman, Travis W. Washburn and Craig R. Smith

198 ***Spatial Variability of Abyssal Nitrifying Microbes in the North-Eastern Clarion-Clipperton Zone***
Anita L. Hollingsworth, Daniel O. B. Jones and C. Robert Young

214 ***Biogeography and Connectivity Across Habitat Types and Geographical Scales in Pacific Abyssal Scavenging Amphipods***
Guadalupe Bribiesca-Contreras, Thomas G. Dahlgren, Tammy Horton, Jeffrey C. Drazen, Regan Drennan, Daniel O.B. Jones, Astrid B. Leitner, Kirsty A. McQuaid, Craig R. Smith, Sergio Taboada, Helena Wiklund and Adrian G. Glover

232 ***Testing the Seamount Refuge Hypothesis for Predators and Scavengers in the Western Clarion-Clipperton Zone***
Astrid B. Leitner, Jeffrey C. Drazen and Craig R. Smith

252 ***Diversity of Deep-Sea Scale-Worms (Annelida, Polynoidae) in the Clarion-Clipperton Fracture Zone***
Paulo Bonifácio, Lenka Neal and Lénaïck Menot

271 ***Regional Variation in Communities of Demersal Fishes and Scavengers Across the CCZ and Pacific Ocean***
Jeffrey C. Drazen, Astrid B. Leitner, Daniel O. B. Jones and Erik Simon-Lledó

frontiers in Marine Science

EDITORIAL
published: 03 December 2021
doi: 10.3389/fmars.2021.797516

Editorial: Biodiversity, Connectivity and Ecosystem Function Across the Clarion-Clipperton Zone: A Regional Synthesis for an Area Targeted for Nodule Mining

Craig R. Smith[1]*, *Malcolm R. Clark*[2], *Erica Goetze*[1], *Adrian G. Glover*[3] and *Kerry L. Howell*[4]

[1] Department of Oceanography, University of Hawai'i at Mānoa, Honolulu, HI, United States, [2] Deep-Sea Ecology and Fisheries Group, National Institute of Water and Atmospheric Research, Wellington, New Zealand, [3] Department of Life Sciences, The Natural History Museum, London, United Kingdom, [4] School of Biological and Marine Sciences, University of Plymouth, Plymouth, United Kingdom

Keywords: polymetallic nodule mining, deep-sea biodiversity, abyssal seafloor, APEI, connectivity, Clarion-Clipperton Zone, environmental management, marine protected areas

Editorial on the Research Topic

Biodiversity, Connectivity and Ecosystem Function Across the Clarion-Clipperton Zone: A Regional Synthesis for an Area Targeted for Nodule Mining

The Clarion Clipperton Zone (CCZ) in the equatorial Pacific Ocean is a vast region of abyssal plains and hills, polymetallic nodule fields, and seamounts. Because of the cobalt, nickel and copper content of polymetallic nodules in this region, the CCZ is targeted for deep-seabed mining. In order to safeguard seafloor biodiversity and ecosystem functions across the region in the event of mining, the International Seabed Authority (ISA) in 2012 designated nine 400×400 km no-mining areas, called Areas of Particular Environmental Interest (APEIs) (Wedding et al., 2013). The APEIs were designed based on environmental correlates of biodiversity and ecosystem function to be representative of the full range of seafloor habitats and communities potentially impacted by nodule-mining activities within the licensed mining exploration areas spanning the CCZ (Wedding et al., 2013).

Since APEI establishment in 2012, a substantial number of research expeditions have collected biodiversity and ecosystem-function data within the CCZ. These expeditions mainly focused on individual contract areas or APEIs. To date, there have been limited efforts to synthesize data at the regional level, which is critical for the further development of ISA's CCZ Environmental Management Plan (EMP). The Deep CCZ Biodiversity Synthesis Workshop was conducted in October 2019 with a new focus on the CCZ EMP, specifically to (1) compile recent deep-sea ecosystem data from across the CCZ, (2) synthesize patterns of seafloor biodiversity, ecosystem functions, and potential environmental drivers, and (3) assess the representativity of the APEIs for areas in the CCZ targeted for polymetallic nodule mining (International Seabed Authority, 2020). This Special Research Topic of *Frontiers in Marine Science* draws together scientific papers derived from the workshop, as well as others elucidating environmental variability and deep-sea biodiversity across the region.

Here, we provide a brief synthesis of the results published in this volume, highlighting aspects relevant to environmental heterogeneity, biodiversity, and environmental

OPEN ACCESS

Edited and reviewed by:
Eva Ramirez-Llodra, REV Ocean, Norway

***Correspondence:**
Craig R. Smith
craigsmi@hawaii.edu

Specialty section:
This article was submitted to Deep-Sea Environments and Ecology, a section of the journal Frontiers in Marine Science

Received: *18 October 2021*
Accepted: *09 November 2021*
Published: *03 December 2021*

Citation:
Smith CR, Clark MR, Goetze E, Glover AG and Howell KL (2021) Editorial: Biodiversity, Connectivity and Ecosystem Function Across the Clarion-Clipperton Zone: A Regional Synthesis for an Area Targeted for Nodule Mining. Front. Mar. Sci. 8:797516. doi: 10.3389/fmars.2021.797516

management in the CCZ. Six key conclusions are as follows:

1) **The CCZ has substantial environmental heterogeneity at the seafloor and in the water column.** As detailed in Washburn, et al., ecologically important environmental characteristics vary across subregions and exploration contract areas in the CCZ. In particular, seafloor depth and flux of particulate organic carbon (POC) exhibit substantial east-west and north-south gradients, varying, respectively, by factors of 1.4 and 2 across the region. The abundance of polymetallic nodules and seamounts, which provide habitat for specialized biotas (Amon et al., 2016; Laroche et al., 2020; Drazen et al.; Leitner et al., 2021; Leitner et al.), also vary >9-fold across CCZ subregions, with nodules especially abundant in the central and eastern CCZ, and seamounts abundant in the east and west, including in areas rich in nodules and exploration claims (Washburn et al.). The pelagic environment also exhibits substantial regional variability, with an intense midwater oxygen minimum zone (OMZ) along the east-west core of the CCZ overlying most nodule-rich and exploration-contract areas, causing shallower diel vertical migrations of animals in the upper water column (Perelman et al.). However, while these ecologically important variables change considerably across the CCZ, many others, especially in bottom-waters, change little; in particular, suspended particle concentrations above the abyssal seafloor across the CCZ are among the lowest in the global ocean (Washburn, et al.).
2) **Seafloor biodiversity in the CCZ is remarkable, with many 100s to 1000s of molecular/morphological "species" sampled in size classes ranging from microbes to megafauna.** Nonetheless, biodiversity remains incompletely sampled at any given site. For example, Hollingsworth et al. document >30,000 amplicon sequence variants (ASVs) among the bacteria and archaea in sediments and nodules from the eastern CCZ, a result consistent with other molecular studies showing diverse microbial communities in the region (Lindh et al., 2017; Shulse et al., 2017). For seafloor foraminifera, Gooday et al. report >1,000 morphospecies, and >6,000 molecular operational taxonomic units (MOTUs). Limited eDNA seafloor sampling in the CCZ has documented >1,200 MOTUs of metazoan meiofauna (Laroche et al., 2020; Laroche et al.; Lejzerowicz et al.). Within the macrofaunal size class, >600 molecular and morphological species have been sampled (Bribiesca-Contreras et al.; Washburn et al.), while more than 600 morphotypes of invertebrate megafauna have been resolved in seafloor images (International Seabed Authority, 2020; Durden et al.). Based on a global eDNA/eRNA survey of eukaryotic biodiversity in abyssal sediments, Lejzerowicz et al. conclude that the CCZ is a biodiversity hotspot "characterized by a high number of OTUs exclusive to the CCZ" and has "greater beta diversity" than "other abyssal regions." It should be noted that the vast majority of the many thousands of eukaryotic species detected across all size classes in the CCZ are new to science.

   Despite collections of large numbers of morphospecies, MOTUs and ASVs across the CCZ, biodiversity at any single site is still under-sampled. For example, Laroche et al. recovered only 40–74% of the estimated meiofaunal ASV richness at any site in the western CCZ. Similarly, macrofauna species accumulation curves and richness estimators indicate that that only 25–73% of the total polychaete, 16–85% of tanaid, and 20–80% of isopod morphospecies occurring at any site in the CCZ have been sampled (Washburn, Menot, et al.). Thus, across all size classes, many thousands of species remain to be sampled to achieve a full biodiversity inventory of the CCZ.
3) **Biodiversity and community structure vary substantially across the CCZ, with POC flux, manganese nodule occurrence, and seafloor topography (e.g., seamounts) implicated as key ecological drivers. This variability is a recurring theme across biotic size classes.** For example, the abundance, biodiversity and/or community structure of organisms ranging from microbes to megafauna vary with regional variations in seafloor POC flux (e.g., Bonifácio et al.; Durden et al.; Hollingsworth et al.; Washburn et al.). The occurrence/abundance of nodules also influences seafloor biodiversity, with nodules harboring distinct species and community structure from surrounding sediments for microbes (Hollingsworth et al.; Wear et al.), foraminifera (Gooday et al.), and invertebrate megafauna (Durden et al.). Seamounts also host distinct communities of microbes (Wear et al.), metazoan meiofauna (Laroche et al., 2020; Laroche et al.), invertebrate megafauna (Durden et al.) and mobile scavengers (Leitner et al., 2021; Leitner et al.).
4) **Despite many research expeditions, there are major geographic gaps in biodiversity and other ecological data across the CCZ.** Quantitative sampling of seafloor biodiversity has been heavily concentrated in the eastern CCZ in contractor areas, and in the western CCZ in APEIs. The central CCZ and most APEIs are poorly sampled, resulting in little quantitative biodiversity information for vast areas of the CCZ. These large geographic gaps are clear in quantitative studies of sediment microbes (Wear et al.; Hollingsworth et al.), foraminifera (Gooday et al.), meiofaunal eukaryotes (Lejzerowicz et al.), macrofauna (Washburn, Menot, et al.), as well as for demersal fishes and scavengers (Drazen et al.).

   Detailed studies of the ecology and evolution of benthic fauna in the CCZ, which are essential for predicting mining impacts and ecosystem recovery, are even more limited. Laming et al. present the first CCZ study of the reproductive biology of ophiuroids, which are major contributors to megafaunal abundance and biodiversity in the region, with samples available only from the eastern CCZ. Bonifácio et al. hypothesize that a highly diverse CCZ taxon, the scale-worm subfamily Macellicephalinae, may have diversified in response to variations in POC flux, again based on samples restricted to the eastern CCZ.
5) **Only a small proportion of faunal species sampled in the CCZ can be shown to have broad geographic distributions.** The vast majority of recognized foraminiferal and macrofaunal species have been found only at single sites, and often have been collected only as single individuals (Gooday et al.; Washburn et al.). A few common foraminiferal

and macrofaunal species are wide ranging across the CCZ (Gooday et al.; Washburn, Menot, et al.), but this is not true for all abundant species; for example, at least three polychaete species abundant at some stations have been collected over limited ranges of 200–700 km (Washburn et al.). Furthermore, one highly diverse family of annelid worms, the polynoids, exhibits substantial species turnover across the eastern CCZ, with evidence of diversification in more oligotrophic areas (Bonifácio et al.). Thus, even with this new biodiversity synthesis, we cannot determine whether most faunal species in the CCZ have limited geographic ranges, or are simply under sampled.

6) **Important habitat variability in the CCZ is not fully captured by the nine original APEIs.** McQuaid et al. conducted a habitat classification of the CCZ based on the key ecological drivers POC flux, nodule abundance, and bottom topography. They identified 24 habitat classes, 18 of which are represented in the original APEIs. However, six nodule-rich habitats are poorly represented in the original APEIs, but are abundant in areas targeted for mining as well as in some areas outside of license areas and APEIs. Inclusion of these nodule-rich areas in new APEIs could improve the habitat representivity of the network, and better safeguard CCZ biodiversity (McQuaid et al.).

Management implications. The Deep CCZ Biodiversity Synthesis Workshop and the papers in this special volume provide an up-to-date evaluation of biodiversity patterns across the CCZ, and highlight the habitat variability, key environmental drivers, and scales of connectivity that must be considered to assess the efficacy of the current network of APEIs. The workshop and this volume have influenced the ISA Legal and Technical Commission to recommend four new APEIs to capture nodule-rich habitats, reduce the distance between APEIs, and protect core areas of the OMZ (International Seabed Authority, 2021). If implemented, these new APEIs should substantially improve the representativity of the APEI network and further demonstrate the value of state-of-the-art scientific syntheses for enhancing environmental management in the deep sea.

AUTHOR CONTRIBUTIONS

All authors listed have made a substantial, direct, and intellectual contribution to the work and approved it for publication.

FUNDING

This work was funded by grants from the Gordon and Betty Moore Foundation (no. 5596), the Pew Charitable Trusts (no. 32871), and with support from the International Seabed Authority.

ACKNOWLEDGMENTS

We thank all the participants of the Deep CCZ Biodiversity Synthesis Workshop and the contributors to this special volume.

REFERENCES

Amon, D., Ziegler, A., Dahlgren, T., Glover, A., Goineau, A., Gooday, A., et al. (2016). First insights into the abundance and diversity of abyssal megafauna in a polymetallic-nodule region in the eastern Clarion-Clipperton Zone. *Sci. Rep.* 6:30492. doi: 10.1038/srep30492

Interational Seabed Authority (2020). *Deep CCZ Biodiversity Synthesis Workshop Report*. Available online at: https://isa.org.jm/files/files/documents/deep_ccz_biodiversity_synthesis_workshop_report_-_final.pdf (accessed June 30, 2020).

International Seabed Authority (2021). *Review of the Implementation of the Environmental Management Plan for the Clarion-Clipperton Zone*. ISBA/26/c/43. Available online at: https://isa.org.jm/files/files/documents/ISBA_26_C_43-2110787E.pdf (accessed June 1, 2021).

Laroche, O., Kersten, O., Smith, C. R., and Goetze, E. (2020). Environmental DNA surveys detect distinct metazoan communities across abyssal plains and seamounts in the western Clarion Clipperton Zone. *Mol. Ecol.* 29, 4588–4604. doi: 10.1111/mec.15484

Leitner, A. B., Durden, J. M., Smith, C. R., Klingberg, E. D., and Drazen, J. C. (2021). Synaphobranchid eel swarms on abyssal seamounts: Largest aggregation of fishes ever observed at abyssal depths. *Deep Sea Res. I Oceanogr. Res. Papers* 167:103423doi: 10.1016/j.dsr.2020.103423

Lindh, M. V., Maillot, B. M., Shulse, C. N., Gooday, A. J., Amon, D. J., Smith, C. R., et al. (2017). From the surface to the deep-sea: bacterial distributions across polymetallic nodule fields in the clarion-clipperton zone of the Pacific Ocean. *Front. Microbiol.* 8:1696. doi: 10.3389/fmicb.2017.01696

Shulse, C. N., Maillot, B., Smith, C. R., and Church, M. J. (2017). Polymetallic nodules, sediments, and deep waters in the equatorial North Pacific exhibit highly diverse and distinct bacterial, archaeal, and microeukaryotic communities. *Microbiol Open* 6:e00428. doi: 10.1002/mbo3.428

Wedding, L. M., Friedlander, A. M., Kittinger, J. N., Watling, L., Gaines, S. D., Bennett, M., et al. (2013). From principles to practice: a spatial approach to systematic conservation planning in the deep sea. *Proc. Roy. Soc. B* 280:20131684. doi: 10.1098/rspb.2013.1684

Conflict of Interest: The authors declare that the research was conducted in the absence of any commercial or financial relationships that could be construed as a potential conflict of interest.

Publisher's Note: All claims expressed in this article are solely those of the authors and do not necessarily represent those of their affiliated organizations, or those of the publisher, the editors and the reviewers. Any product that may be evaluated in this article, or claim that may be made by its manufacturer, is not guaranteed or endorsed by the publisher.

Copyright © 2021 Smith, Clark, Goetze, Glover and Howell. This is an open-access article distributed under the terms of the Creative Commons Attribution License (CC BY). The use, distribution or reproduction in other forums is permitted, provided the original author(s) and the copyright owner(s) are credited and that the original publication in this journal is cited, in accordance with accepted academic practice. No use, distribution or reproduction is permitted which does not comply with these terms.

frontiers in Marine Science

ORIGINAL RESEARCH
published: 08 September 2020
doi: 10.3389/fmars.2020.00682

From Sea Surface to Seafloor: A Benthic Allochthonous eDNA Survey for the Abyssal Ocean

Olivier Laroche[1,2], Oliver Kersten[3], Craig R. Smith[1] and Erica Goetze[1]*

[1] Department of Oceanography, School of Ocean and Earth Science and Technology, University of Hawai'i at Mānoa, Honolulu, HI, United States, [2] Institute of Marine Research, Tromsø, Norway, [3] Centre for Ecological and Evolutionary Synthesis, Department of Biosciences, University of Oslo, Oslo, Norway

Environmental DNA (eDNA) metabarcoding could facilitate rapid and comprehensive biotic surveys in the deep ocean, yet many aspects of the sources and distribution of eDNA in the deep sea are still poorly understood. In order to examine the influence of the water column on benthic eDNA surveys in regions targeted for deep-sea polymetallic nodule mining, we investigated the occurrence of pelagic eDNA across: (1) two different deep-sea habitat types, abyssal plains and seamounts, (2) benthic sample types, including nodules, sediment, and seawater within the benthic boundary layer (BBL), and (3) sediment depth horizons (0–2 and 3–5 cm). Little difference was observed between seamounts and the adjacent abyssal plains in the proportion of legacy pelagic eDNA sampled in the benthos, despite >1,000 m depth difference for these habitats. In terms of both reads and amplicon sequence variants (ASVs), pelagic eDNA was minimal within sediment and nodule samples (<2%), and is unlikely to affect benthic surveys that monitor resident organisms at the deep seafloor. However, pelagic eDNA was substantial within the BBL (up to 13% ASVs, 86% reads), derived both from the high-biomass upper ocean as well as deep pelagic residents. While most pelagic metazoan eDNA found in sediments and on nodules could be sourced from the epipelagic, protist legacy eDNA sampled on these substrates appeared to originate across a range of depths in the water column. Some evidence of eDNA degradation across a vertical sediment profile was observed for protists, with higher diversity in the 0–2 cm layer and a significantly lower proportion of legacy pelagic eDNA in deeper sediments (3–5 cm). Study-wide, our estimated metazoan sampling coverage ranged from 40 to 74%, despite relatively large sample size. Future deep-sea eDNA surveys should examine oceanographic influences on eDNA transport and residence times, consider habitat heterogeneity at a range of spatial scales in the abyss, and aim to process large amounts of material per sample (with replication) in order to increase the sampling coverage in these diverse deep ocean communities.

Keywords: environmental DNA, metabarcoding, legacy eDNA, deep sea, abyssal plains, Clarion Clipperton Zone (CCZ), deep-sea mining

OPEN ACCESS

Edited by:
Daniela Zeppilli, Institut Français de Recherche pour l'Exploitation de la Mer (IFREMER), France

Reviewed by:
Hidetaka Nomaki, Japan Agency for Marine-Earth Science and Technology (JAMSTEC), Japan
Michael Vecchione, National Oceanic and Atmospheric Administration (NOAA), United States

****Correspondence:***
Olivier Laroche
olli.laroche@gmail.com

Specialty section:
This article was submitted to Deep-Sea Environments and Ecology, a section of the journal Frontiers in Marine Science

Received: *30 May 2020*
Accepted: *27 July 2020*
Published: *08 September 2020*

Citation:
Laroche O, Kersten O, Smith CR and Goetze E (2020) From Sea Surface to Seafloor: A Benthic Allochthonous eDNA Survey for the Abyssal Ocean. Front. Mar. Sci. 7:682. doi: 10.3389/fmars.2020.00682

INTRODUCTION

Deep sea ecosystems are facing increasing pressure from anthropogenic activities, including climate change and future seabed mining (Boschen et al., 2013; Halpern et al., 2015; Sweetman et al., 2017). The deep sea, defined as the ocean and seafloor below 200 m, represents the largest habitat on our planet, covering ∼65% of Earth's surface (Thistle, 2003; Thurber et al., 2014). The deep ocean is a significant regulator of carbon sequestration and nutrient regeneration, and provides habitat and trophic support to a multitude of organisms (Le et al., 2017). Characterizing and monitoring the health of deep ocean ecosystems is important, given their role in maintaining Earth's systems.

The first large-scale deep-sea mining is likely to occur in the Clarion Clipperton Zone (CCZ), a region of particularly valuable mineral resources (nickel-, cobalt-, and copper-rich manganese nodules) in the abyssal equatorial Pacific (Wedding et al., 2013, 2015). At ∼ 6 million km^2, the CCZ spans large-scale environmental gradients in polymetallic nodule density, particulate organic carbon flux and seafloor bathymetry, and is host to diverse biological communities (Glover et al., 2002; Smith et al., 2008a; Wedding et al., 2013). Approximately 30% of the CCZ management area has been allocated to exploration nodule mining through 16 contracts granted by the International Seabed Authority (ISA). Benthic communities in the CCZ are typically characterized by high biodiversity and low biomass (Ramirez-Llodra et al., 2010; Kaiser et al., 2017; Smith et al., 2019), due to severe food limitation at abyssal depths (Smith et al., 2008a). A high proportion of species are rare, rendering adequate sampling coverage particularly difficult to achieve (Smith et al., 2008a; De Smet et al., 2017; ISA, 2019; Simon-Lledó et al., 2019). Regional species diversity is enhanced by habitat heterogeneity at a range of spatial scales, including the presence of polymetallic nodules that serve as hard substrates in a predominantly soft sediment ecosystem (Amon et al., 2016; Vanreusel et al., 2016; De Smet et al., 2017; Kaiser et al., 2017; Simon-Lledó et al., 2019; Laroche et al., 2020a), as well as deep seamounts (relief >1,000 m above the surrounding seafloor; Clark et al., 2010; Leitner et al., 2017) that may alter nutrient and particle fluxes and influence associated biological communities (Genin and Dower, 2007; Samadi et al., 2007; Lavelle and Mohn, 2010; Rowden et al., 2010). Biodiversity and species ranges remain poorly characterized across the CCZ, making predictions of the impacts of large-scale mining problematic.

Environmental DNA (eDNA) surveys could be particularly valuable for monitoring community change and environmental impacts in the deep sea, given high biodiversity, limited taxonomic descriptions of the fauna, and the challenges of sampling in remote deep-ocean habitats (Boschen et al., 2016; Sinniger et al., 2016; Kersten et al., 2019; Laroche et al., 2020a). eDNA metabarcoding is a sensitive and cost-efficient tool for biodiversity assessment (Goodwin et al., 2017; Seymour, 2019), with advantages over visual or whole-animal surveys in the ability to capture the hidden diversity of cryptic microbial eukaryotes and to indirectly detect the presence of recently living organisms through cellular debris or extra-cellular DNA (Kelly, 2016; Deiner et al., 2017). However, several methodological aspects regarding eDNA surveys in the deep ocean remain unresolved, including the extent of legacy DNA (extracellular or non-living material) that arrives in the abyss via sinking with detrital particles from overlying pelagic ecosystems (but see Pawlowski et al., 2011; Morard et al., 2017 for foraminifera). eDNA degradation rates also greatly influence organismal detection; previous studies in the upper ocean have reported eDNA half-life ranging from 10 to 50 h, and complete turnover from a few hours to several months across a range of environmental conditions (see Barnes et al., 2014; Collins et al., 2018). Both abiotic and biotic factors, including temperature, pH, oxygen concentration and microbial activity, have been found to strongly influence eDNA persistence (Strickler et al., 2015; Barnes and Turner, 2016; Seymour et al., 2018; Armbrecht et al., 2019). eDNA adsorption to sediment particles can strongly protect it against hydrolysis and DNase activity (Torti et al., 2015), with low temperatures in the deep sea favorable to DNA preservation (Corinaldesi et al., 2008). Because eDNA may be better preserved in deep sea sediments than in seawater, sample substrates from benthic boundary layer (BBL) seawater, polymetallic nodules, and sediments may integrate eDNA inputs over different timescales.

We used an eDNA metabarcoding approach to assess the influence of allochthonous pelagic eDNA on biodiversity surveys at the abyssal seafloor in the western CCZ (**Figure 1**). Specifically, our objectives were to evaluate pelagic eDNA occurrence in different: (1) deep sea habitats, including abyssal plains/hills versus seamounts, (2) benthic sample types, including polymetallic nodules, sediment, and seawater within the BBL, and (3) sediment horizons (0–2 and 3–5). We also evaluate methods for eDNA recovery from diverse sample substrates and the sampling effort required to fully capture diverse assemblages in the abyssal CCZ. We hypothesize that: (1) most pelagic eDNA recovered from the benthos will have originated in the epipelagic, as production and biomass are highest within this depth zone, (2) the proportion of eDNA shared between pelagic and abyssal samples (BBL seawater, sediment, nodules) will be highest within BBL seawater, rather than in sediments or on nodules, as a range of species may inhabit both the deeper pelagic and BBL zones (e.g., meroplankton; Kersten et al., 2017, 2019; swimming holothurians), and (3) pelagic eDNA will occur in higher proportions within the upper sediment horizon (0–2 cm) compared to deeper horizons (3–5 cm) due to detrital eDNA settlement on the surface layer and DNA degradation over time within deeper sediments.

MATERIALS AND METHODS

Sample Collection

Samples were collected in Areas of Particular Environmental Interest (APEIs) 1, 4, and 7 of the western CCZ (**Figure 1**, **Supplementary Figure S1**, **Tables 1**, **2**, and **Supplementary Table S1**), with one seamount and the adjacent abyssal plain sampled within each APEI. APEIs are seafloor areas currently closed by the International Seabed Authority to seabed mining (Wedding et al., 2013). Seamount summit depths ranged from

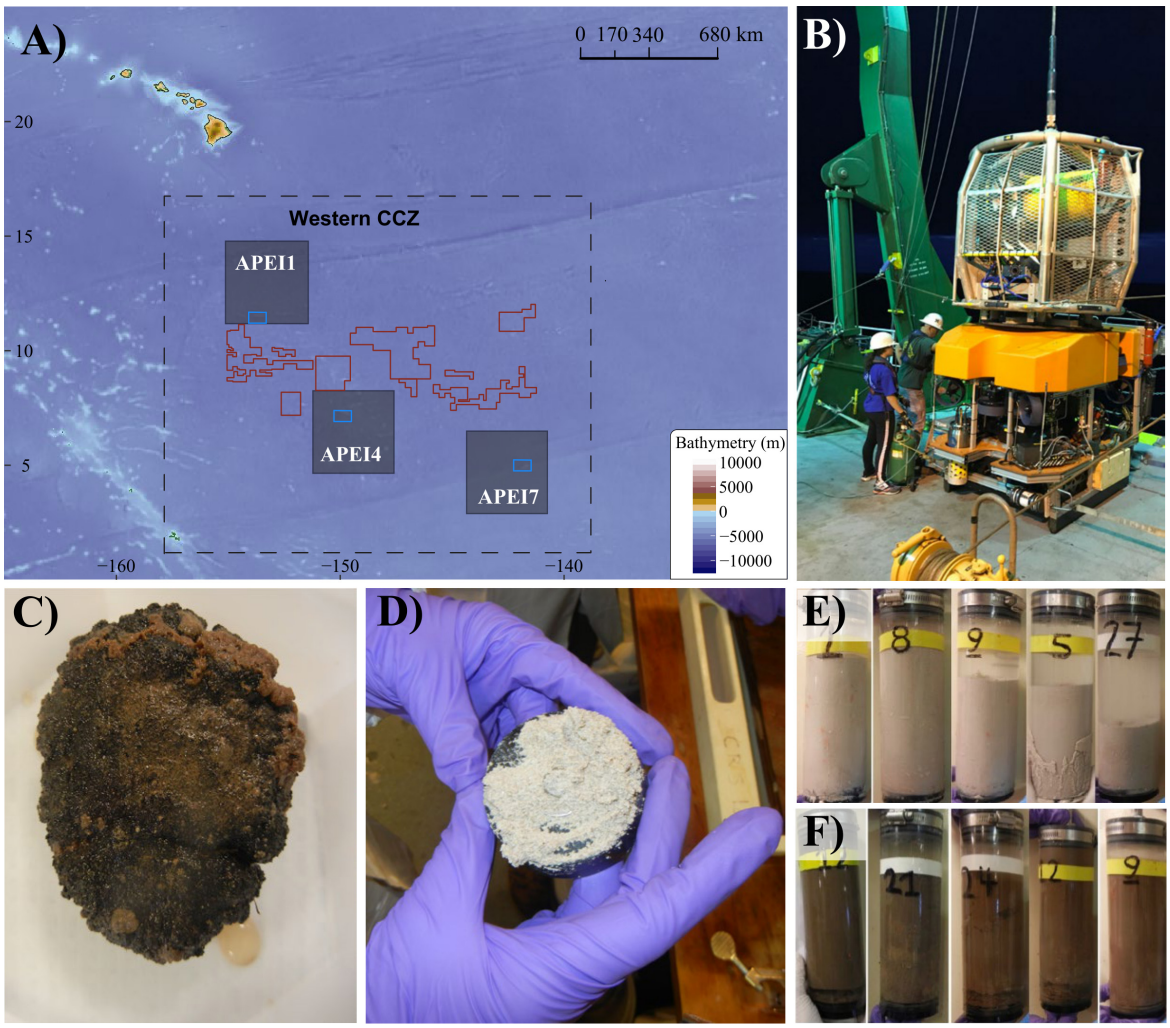

FIGURE 1 | Sampling sites, sampling tools (ROV Lu'ukai), and substrates collected. **(A)** Map of the study areas within the western Clarion Clipperton Zone (Western CCZ), with the locations of Areas of Particular Environmental Interest (APEIs 1, 4, 7) indicated (gray squares). Sampling regions within each APEI are marked by blue rectangles. Exploration mining contractor (red outline) areas within the western CCZ are also shown. See **Supplementary Figure S1** for greater detail on the sampling sites. **(B)** Remotely operated vehicle (ROV) Lu'ukai, used for collection of sediment and polymetallic nodules. **(C)** Example of a polymetallic nodule. **(D)** Example of seamount sediment texture, largely made up of foraminiferal tests. A thin slab of sediment is shown on top of a black rubber plate (push core base). **(E)** Seamount sediment cores. **(F)** Abyssal plain sediment cores.

3,100 m (APEI 7) to 3,900 m (APEI 1) and were all >1,000 m above the surrounding seafloor. Abyssal plain sites were sampled over 15 km away from the seamount ridgeline (APEI 7) or base (APEI 4/APEI 1) to reduce the effect of seamount processes on the abyssal habitats sampled. Due to ROV technical constraints, only seawater samples were collected over the seamount in APEI 1.

Sediment samples were obtained with the ROV Lu'ukai using 7-cm diameter push cores. Typical ROV dives yielded two cores in close proximity (meters) near the start of the dive and another 2 cores at mid-dive, on average 2.3 km away from the starting point. Cores were subsampled for eDNA at 0–2 and 3–5 cm sediment horizons using single-use sterile syringes (60 mL) to extract one mini-core from each sediment horizon. Samples were cryopreserved at −80°C until processing. Between ROV dives (**Table 1**), sediment-processing gear and push-core tubes were treated with 10% commercial bleach (diluted with double-distilled water [ddH_2O]), and rinsed with ddH_2O to prevent DNA contamination. Subsampling equipment (core slicer, guide) was rinsed in ddH_2O between cores from the same ROV dive. For APEI 1, two replicate subsamples were taken from each sediment horizon and core. Polymetallic nodules were collected from the same ROV dives using either push cores or the manipulator arm of the ROV, with nodules placed into a BioBox sample holder on the ROV, which was sealed during ROV recovery from the seafloor. Upon arrival on shipboard, nodules were transferred to sterile whirl-pack bags and cryopreserved (−80°C).

Seawater samples were collected using conductivity-temperature-depth (CTD) casts with a 24 Niskin bottle rosette (10 L). Four CTD casts per APEI were conducted, two

TABLE 1 | Station overview for ROV dives from which sediment and nodules were collected for eDNA.

Station #	APEI	Habitat	ROV dive #	Date	Latitude	Longitude	Water depth (m)
KM1808-25	7	Plain	4	5/25/18	5° 6.9271 N	141° 53.8015 W	4860
KM1808-33	7	Seamount	6	5/27/18	4° 53.28 N	141° 45.4299 W	3133
KM1808-36	7	Plain	7	5/28/18	5° 3.6190 N	141° 49.8836 W	4874
KM1808-43	4	Plain	8*	6/01/18	7° 2.1617 N	149° 56.3686 W	5040
KM1808-47	4	Plain	9*	6/2/18	6° 59.2646 N	149° 54.7421 W	5019
KM1808-49	4	Seamount	10	6/5/18	7° 16.2918 N	149° 46.7055 W	3562
KM1808-61	4	Plain	12*	6/6/18	6° 59.2865 N	149° 55.9757 W	5009
KM1808-66	1	Plain	13*	6/10/18	11° 16.5 N	153° 44.64 W	5240
KM1808-70	1	Plain	14*	6/11/18	11° 15.12 N	153° 36.37 W	5206

ROV dives from which nodules could be collected are indicated by a star.

TABLE 2 | List of conductivity, temperature and depth (CTD) casts from which seawater was collected for eDNA.

Station #	APEI	Habitat	Cast #	Date	Latitude	Longitude	Max. depth (m)
KM1808-12	7	Plain	1	5/22/18	5° 3.6252 N	141° 49.8395 W	4861
KM1808-13	7	Plain	2	5/22/18	5° 3.2156 N	141° 55.5066 W	4850
KM1808-27	7	Seamount	4	5/25/18	4° 53.6165 N	141° 43.7357 W	3228
KM1808-35	7	Seamount	6	5/28/18	4° 53.310 N	141° 46.1472 W	3060
KM1808-48	4	Plain	7	6/3/18	6° 58.8754 N	149° 55.6328 W	4994
KM1808-54	4	Seamount	8	6/4/18	7° 17.3894 N	149° 51.2256 W	3919
KM1808-56	4	Seamount	9	6/5/18	7° 15.8752 N	149° 46.4703 W	3560
KM1808-60	4	Plain	10	6/6/18	7° 02.2456 N	149° 56.3370 W	5034
KM1808-67	1	Plain	11	6/10/18	11° 16.4768 N	153° 44.7812 W	5232
KM1808-71	1	Plain	12	6/11/18	11° 15.1408 N	153° 36.3776 W	5196
KM1808-76	1	Seamount	13	6/12/18	11° 29.6389 N	153° 36.9525 W	4045
KM1808-77	1	Seamount	14	6/12/18	11° 29.5117 N	153° 39.0729 W	4183

Max depth (m) indicates the seafloor depth at the sampling site. Filtered seawater volume per replicate sample and per depth was 5 L at 5 meter above bottom (mab), 50 mab and in the bathypelagic (2,000–2,500 m for seamounts and 3,000 m for plains), 4 L in the deep mesopelagic (1,000 m), 2 L in the mesopelagic (500 m), and 1 L at the DCM and near surface (5 m) samples.

over the abyssal plain/hills and two over the seamount (**Table 2**). Seawater was collected at seven depths within the water column: 5 m above bottom (mab), 50 mab, bathypelagic depths (3,000 m over plains/hills, 2,500 or 2,000 m over seamounts, depending on summit depth), in the deep mesopelagic at 1,000 m, mesopelagic at 500 m, deep chlorophyll maximum (DCM; between 90 and 60 m), and at 5 m depth in near-surface waters. Eukaryotic productivity and biomass vary greatly across depth in the water column, with exponential declines in pelagic animal biomass (e.g., Vinogradov, 1970; Angel and Baker, 1982). As a result, while it is common for eDNA studies to sample the epipelagic community with small seawater volumes (e.g., 250 mL to 2 L liters, Thomsen et al., 2012; Shulse et al., 2017; Sigsgaard et al., 2017; Günther et al., 2018; Jeunen et al., 2019), larger volumes are required at greater depths to adequately sample communities to account for and offset expected declines in eDNA concentration (e.g., as in Shulse et al., 2017). Therefore, filtered seawater volumes varied across depth in this study, with 5 L per replicate sampled at 5 mab, 50 mab and bathypelagic depths, 4 L filtered in the deep mesopelagic (1,000 m), 2 L in the mesopelagic (500 m), and 1 L filtered per replicate at the DCM and in the near surface. Four to six replicates were taken from each CTD cast and depth. To assess and eliminate cross-contamination, negative controls (ddH_2O) were collected for each CTD cast (1 L for each of 2 replicates), with ddH_2O transferred to a sampling carbouy and filtration handled together with all seawater carbouys. eDNA was collected on sterile 0.2 μm Supor filters (Pall) using 47 mm inline polycarbonate filter holders and two peristaltic pumps. Two pumps with six tubing lines were run in parallel, with deep ocean samples run as a priority on the faster pump. Filters were preserved in 1 ml of RNALater (Invitrogen), flash frozen in liquid nitrogen, and held at −80°C until processing. Between CTD casts, the workspace was treated with 10% bleach for a minimum of 30 min, followed by a ddH_2O surface wipe. Sampling equipment was treated with 10% bleach for a minimum of 30 min, followed by three ddH_2O rinses and three rinses with seawater from the target sampling depth (Niskin bottle; per standard oceanographic practice for sampling from a Niskin bottle rosette). To avoid contamination during sample collection, personal protective equipment included disposable lab coats and nitrile gloves for all involved personnel. **Supplementary Table S1** reports all sediment, nodule, and seawater samples included in this study.

DNA Extraction

Sediment samples were homogenized with a sterile metallic spatula, subsampled for 10 g, and processed with the PowerMax® Soil kit (QIAGEN, CA, United States) following the

manufacturer's protocol. Purified eDNA was eluted in 1 mL of ddH_2O. Prior to eDNA extraction, polymetallic nodules were ground and homogenized inside their whirl-pack bag using a 16 g ceramic pestle. No detectable quantities of DNA could be obtained using the PowerMax® Soil kit with ∼10 g of nodule material, likely as a result of very low DNA concentrations on nodules. We therefore used the FastDNA™ Spin kit (following the manufacturer's protocols), processing ten subsamples of ca. 500 mg for each nodule. Due to low eDNA concentrations per subsample (mean concentration of 0.382 ng/μL), replicates were pooled in pairs and concentrated to ∼ 1 ng/μL with the DNA Clean & Concentrator kit (Zymo Research, CA, United States) to obtain sufficient DNA for polymerase chain reaction (PCR) amplification. Polymetallic nodules ranged between 15.4 and 144.8 g, with 3–32% of the nodule processed for DNA extractions.

For seawater samples, four extraction protocols were tested in pilot experiments: (1) a Cetyl Trimethyl Ammonium Bromide (CTAB) and ethanol precipitation protocol based on Renshaw et al. (2015), (2) the DNeasy® Blood and Tissue kit (QIAGEN, CA, United States) using a modified protocol from Djurhuus et al. (2017), (3) the E.Z.N.A® Water DNA kit (OMEGA, GA, United States), and (4) the DNeasy® Plant Mini kit (QIAGEN, CA, United States), using a modified protocol based on Paerl et al. (2008) and Shulse et al. (2017). Using biological triplicates, protocol 4 provided the highest DNA yield and best purity measurements, and was therefore used to process all seawater samples (see the **Supplementary Material** for the full protocol). Due to low DNA concentration in the 5 and 50 mab samples (mean concentration of 0.573 ng/μL), replicates (2 L × 5 L each) were pooled together and concentrated to ∼1 ng/μL with the DNA Clean & Concentrator kit (Zymo Research, CA, United States) to obtain sufficient DNA for amplification.

To assess and eliminate cross-contamination, an extraction blank was included for each sample substrate type (sediment, nodule, and seawater). All sample handling and extraction steps took place in a dedicated laboratory that had never been used for PCR amplification.

PCR Amplification and Library Preparation

The V4 region of the 18S rRNA gene [approximately 450 base pairs (bp)] was PCR amplified using the eukaryotic forward primer Uni18SF: 5′-AGG GCA AKY CTG GTG CCA GC-3′ and reverse primer Uni18SR: 5′-GRC GGT ATC TRA TCG YCT T-3′ (Zhan et al., 2013). Primers were modified to include Illumina overhang adaptors. The choice of optimal 18S rRNA hypervariable regions for biodiversity assessments remains under debate (e.g., see Hadziavdic et al., 2014; Tanabe et al., 2016). Here, preliminary tests comparing the V1–V2 region using primers from Fonseca et al. (2010) and the V4 region with primers from Zhan et al. (2013) found highest taxonomic classification and diversity at the genus level (especially for metazoans) with the latter primer set. This marker (V4 of 18S rRNA) and primer set (Zhan et al., 2013) were therefore selected for use in the full study.

Polymerase chain reaction reactions consisted of 12.5 μL of MyFi™ Mix (Bioline; hot-start, proof-reading Taq polymerase), 0.5 μL of each primer (10 μM), 0.6 μL of Bovine Serum Albumin (300 μM; BSA; Sigma), 1–3 μL of template DNA (min 2.5 ng/μL per reaction) with ddH_2O added to reach a total volume of 25 μL. The reaction cycling conditions were: 95°C for 3 min, followed by 35 cycles of 95°C for 15 s, 55°C for 30 s, 72°C for 15 s, with a final extension step at 72°C for 1 min. A negative control (no template DNA) was included with each PCR to ensure an absence of contamination.

Purification and quantification of the amplicons was performed with AMPure® XP beads (Beckman Coulter®, IN, United States) and a Qubit® Fluorometer (Life Technologies), following the manufacturer's instructions. Purified amplicons were normalized to 2 ng/μL with ddH_2O, and submitted to the Advanced Studies in Genomics Proteomics and Bioinformatics (ASGPB) of the University of Hawaii at Manoa (HI, United States) for indexing with the Nextera™ DNA library Prep Kit (Illumina, CA, United States). Samples were pooled into two libraries and sequenced on two MiSeq Illumina™ runs using V3 chemistry and paired-end sequencing (2 bp × 300 bp). Two blank samples containing ddH_2O were included during the indexing and sequencing process to assess potential contamination. Sequences are available from the NCBI Sequence Read Archive (SRA) under accession numbers SRR9199590 to SRR9199869.

Bioinformatic Analysis

Demultiplexed samples were denoised with the DADA2 pipeline (Callahan et al., 2016), as implemented in Qiime2 (Bolyen et al., 2019), using the qiime dada2 denoise-paired function and default parameters. The DADA2 pipeline is a sequence quality control process that filters low quality reads based on the maximum expected error value (default = 2), detects and removes Illumina amplicon artifacts, filters PhiX reads, and merges paired forward and reverse reads using a default minimum overlapping region of 20 bp. DADA2 is particularly efficient at eliminating spurious sequences from Illumina platforms (Callahan et al., 2016). Prior to merging, forward and reverse reads were truncated at 260 and 235 bp, respectively, to remove low quality regions and reduce the number of sequences lost during quality filtering. The DADA2 pipeline detects and removes chimeric sequences using a *de novo* approach. Here, chimera removal also was performed using the consensus approach, in which sequences found to be chimeric in a majority of samples are discarded. Taxonomic assignment was performed by training Qiime2's naive Bayes classifier (Pedregosa et al., 2012) on a SILVA 18S rRNA database (release 132 clustered at 99% similarity; Quast et al., 2013) trimmed with Qiime2's feature-classifier extract-reads function and the V4 primers. For downstream analyses, amplicon sequence variants (ASVs) were used instead of operational taxonomic unit (OTUs) in order to retain the highest possible taxonomic resolution in the data. The complete bioinformatics script is provided in **Supplementary Material**.

Data Analysis and Statistics

Sequencing depth and recovered diversity per sample were inspected using rarefaction curves with the vegan R package (Oksanen et al., 2018). Rarefaction curves indicated that all but one sample (N-26) had sufficient sequencing depth to capture total amplicon richness within the sample. This sample was excluded from all downstream analyses (**Supplementary Figure S2**). Sequences found in any of the negative controls (ddH_2O), including field, DNA extraction, and PCR blanks, were investigated and removed from the dataset. Sequences unclassified at kingdom level and those originating from non-marine taxa were also discarded (taxa assigned to birds, insects, terrestrial mammal families that likely originate from marine vessel waste). The data were then split into two groups: (1) metazoans, and (2) non-metazoans, primarily comprised of protists from the SAR supergroup (Adl et al., 2019). Amplicon sequence variant (ASV) richness for each sample type (sediment, nodule, and seawater) was estimated using the Chao2 index (per sample), an estimator of asymptotic species richness based on the frequency of rare taxa, as well as with a bootstrap method with 200 replicates as outlined in Chao and Jost (2012). When the Chao2 index is estimated per sample, as in this study, rare taxa correspond to those found in very few samples (rather than those that are rare within each sample). Calculations and visualizations were conducted using the iNEXT (version 2.0.19; Hsieh et al., 2019) and ggplot2 R packages (Wickham, 2016). The sampling coverage, or sampling completeness, estimator was based on the incidence of singletons and doubletons across samples (Chao2 index; defined in equation 4a of Chao and Jost, 2012). We used base coverage as a metric for comparison among multiple samples; this metric combines rarefaction and extrapolation, and represents the highest coverage value between minimum extrapolated values and maximum interpolated values (see Chao et al., 2014). Alpha and gamma diversity, reported as ASV richness estimated by the Chao2 index, was also compared across the water column. ASV overlap between sediment layers (0–2 and 3–5 cm) and water columns depths within the BBL (5 and 50 mab) was investigated with Venn diagrams using the Venny 2.1 program (Oliveros, 2015), in order to evaluate the importance of sampling these distinct depth horizons. Beta diversity differences between the water column depths was explored using unweighted unifrac distances (Lozupone and Knight, 2005) and a pairwise analysis of variance with the pairwiseAdonis R package (version 0.4; Martinez Arbizu, 2020).

The presence of pelagic eDNA at the seafloor, here defined as ASVs from samples of the near surface to the bathypelagic ocean (0 to 3,000 m over abyssal plains, 0 to 2,000–2,500 m over seamounts, inclusively) that were concurrently found in benthic samples, was examined from two perspectives: (1) the pelagic perspective, representing the proportion of pelagic ASVs and reads concurrently found in the benthic environment, and (2) the benthic perspective, representing the proportion of benthic ASVs and reads for each sample type (BBL seawater, sediments, and nodules) that were concurrently found within pelagic samples. The taxonomic composition and proportions of pelagic eDNA found within abyssal habitats were visualized using ggplot2. From the benthic perspective, the proportion of benthic ASVs and reads per sample was also contrasted per sample type and tested for significant differences between habitats and sediment layers with a two-sample Wilcoxon test in R (wilcox.test function), and visualized with box-plots and the ggplot2 R package. In order to ensure that results were not biased by differences in sampling completeness between habitats, an analysis of sampling coverage was conducted (**Supplementary Figure S3**).

RESULTS

High-Throughput Sequencing

A total of 10,315,003 18S reads was generated (**Supplementary Table S2**). Quality filtering, denoising, merging and chimera removal reduced read counts by 54%, leaving an average of 43,523 good quality reads per sample. Removal of sequences found in the blank samples resulted in a mean loss of 2.7% ASVs per seawater sample and 0.4% of ASVs for nodules (**Supplementary Table S3**). Removal of non-marine taxa led to a further loss of 3.3% ASVs for nodules, 1.5% for sediment and less than 1% for seawater samples (**Supplementary Table S3**). All subsequent analyses were performed on both filtered and unfiltered data to examine the effect of removing sequences found in blank samples or belonging to non-marine metazoan taxa. However, since this filtering step had no impact on the results or inferences of the study, only analyses performed on trimmed data are presented below.

Sampling Coverage and Diversity

Overall, the achieved sampling coverage was highest for seawater (74 and 84% for metazoans and non-metazoans, respectively), followed by nodules (65% for both groups) and sediment samples (40 and 64% for metazoans and non-metazoans, **Figure 2**). Gamma diversity, or ASV richness for all samples combined, was highest within sediment samples (1,271 metazoan and 6,107 protist ASVs), followed by seawater (409 and 5,953 ASVs) and nodules (407 and 2,186 ASVs, **Figure 2**). Similarly, ASV richness at base coverage was higher in sediment samples than in nodules or seawater samples for both metazoans and non-metazoans (**Figure 2**).

Sampling coverage analyzed at the level of biological replicates indicated that for sediment samples, two replicates of 10 g each led to a mean sampling coverage of 15 and 39% for metazoans and non-metazoans of the 0–2 cm layer, respectively, and 8 and 36% for the 3–5 cm layer (**Supplementary Figure S4**). Further analysis of community composition in the 0–2 and 3–5 cm layers showed modest ASV overlap between the two (10 and 19% of shared ASVs for metazoans and non-metazoans, respectively), with a large fraction of ASVs found solely in the top layer (56 and 47% for metazoans and non-metazoans, respectively) (**Supplementary Figure S5**). For nodules, five biological replicates (1 g of material each) extracted from each nodule provided a mean sampling coverage of 58% for metazoans and 43% for non-metazoans (**Supplementary Figure S3**). With three biological replicates, sampling coverage in seawater samples averaged 53% for metazoans and 69% for non-metazoans

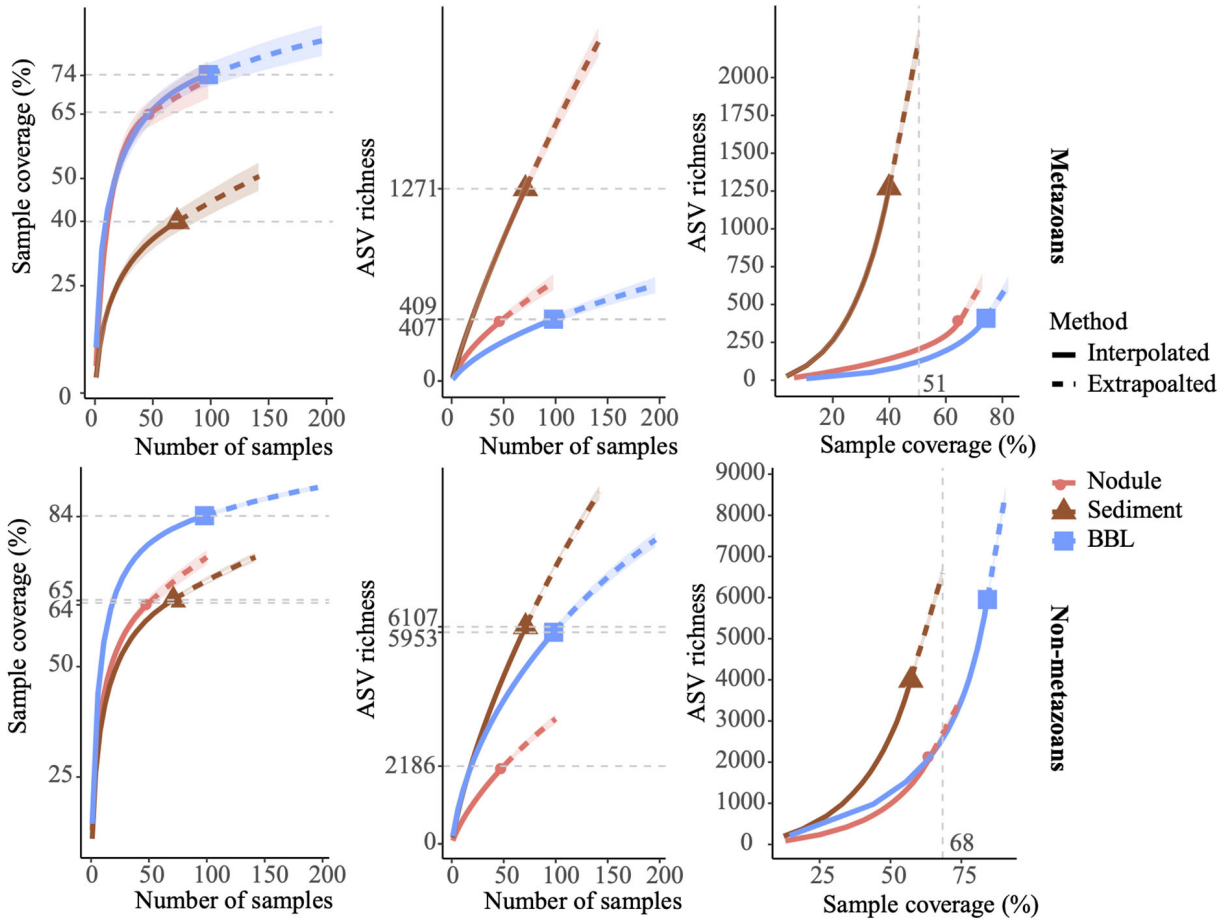

FIGURE 2 | Amplicon sequence variant (ASV) sampling coverage and richness for each sample type (nodule, sediment, and seawater). ASV richness was estimated using Chao2 (Chao and Jost, 2012). Shaded, colored areas indicate the 95% confidence intervals obtained from a bootstrap method based on 200 replicates. Horizontal dotted gray lines (left and center) indicate maximum interpolation values for each sample type. Vertical dotted gray lines (right) indicate the value at base coverage, defined as the highest coverage value between minimum extrapolated values and maximum interpolated values.

across water-column depths (**Supplementary Figure S4**). Further analysis of community overlap between the BBL water column depths showed that 5 and 50 mab samples shared 23 and 30% of metazoan and protist ASVs, respectively, with the 5 mab layer possessing the greater portion of unshared ASVs (48 and 45% for metazoans and non-metazoans) (**Supplementary Figure S5**). Overall, 66 and 73% of total benthic diversity was captured in the upper sediment horizon and the 5 mab BBL seawater sample, respectively.

Mean metazoan ASV richness per sample remained largely uniform across depths in the water column, with slightly higher values in the DCM (12 ± 4) and BBL (5 and 50 mab; 14 ± 7) (**Figure 3A**). However, sampling coverage varied greatly across water column depths (from 49 to 73%), with lowest values for the 5 mab (49%) and 50 mab (57%) samples (**Figure 3B**). Significant differences in ASV richness (absence of overlap in confidence intervals) can be observed between 5 mab and the mesopelagic, deep mesopelagic and near surface depths (**Figure 3C**). At base coverage (64%), diversity was highest within the BBL samples (∼225 and ∼100 ASVs at 5 and 50 mab, respectively), and lowest within the mesopelagic (500 m) and deep mesopelagic (1,000 m) samples (∼55 ASVs; **Figure 3C**). A comparison of the sampling effort (volume of filtered water) required at each depth to reach equivalent sampling coverage is shown in **Table 3** (at base coverage, 49%). The water column depths requiring highest sampling effort, or the largest volume of seawater filtered, are 5 and 50 mab, the bathypelagic and the DCM. Differences in beta-diversity between water column depths was found to be significant for all pairs except near surface vs. DCM, mesopelagic vs. 50 mab, and between the bathypelagic and 5 and 50 mab samples (**Supplementary Table S4**).

For non-metazoans in the water column, ASV richness per sample was highest within the DCM (304 ± 131) before gradually declining through the meso- and bathypelagic and then increasing again at 5 mab (**Figure 3A**). In contrast to metazoans, non-metazoan sampling coverage remained relatively high and uniform across depths (from 71 to 82%; **Figure 3B**), although significant differences can be observed between the near surface, BBL and the zones in between at the highest number of samples collected (14; **Figure 3B**). At base coverage, diversity

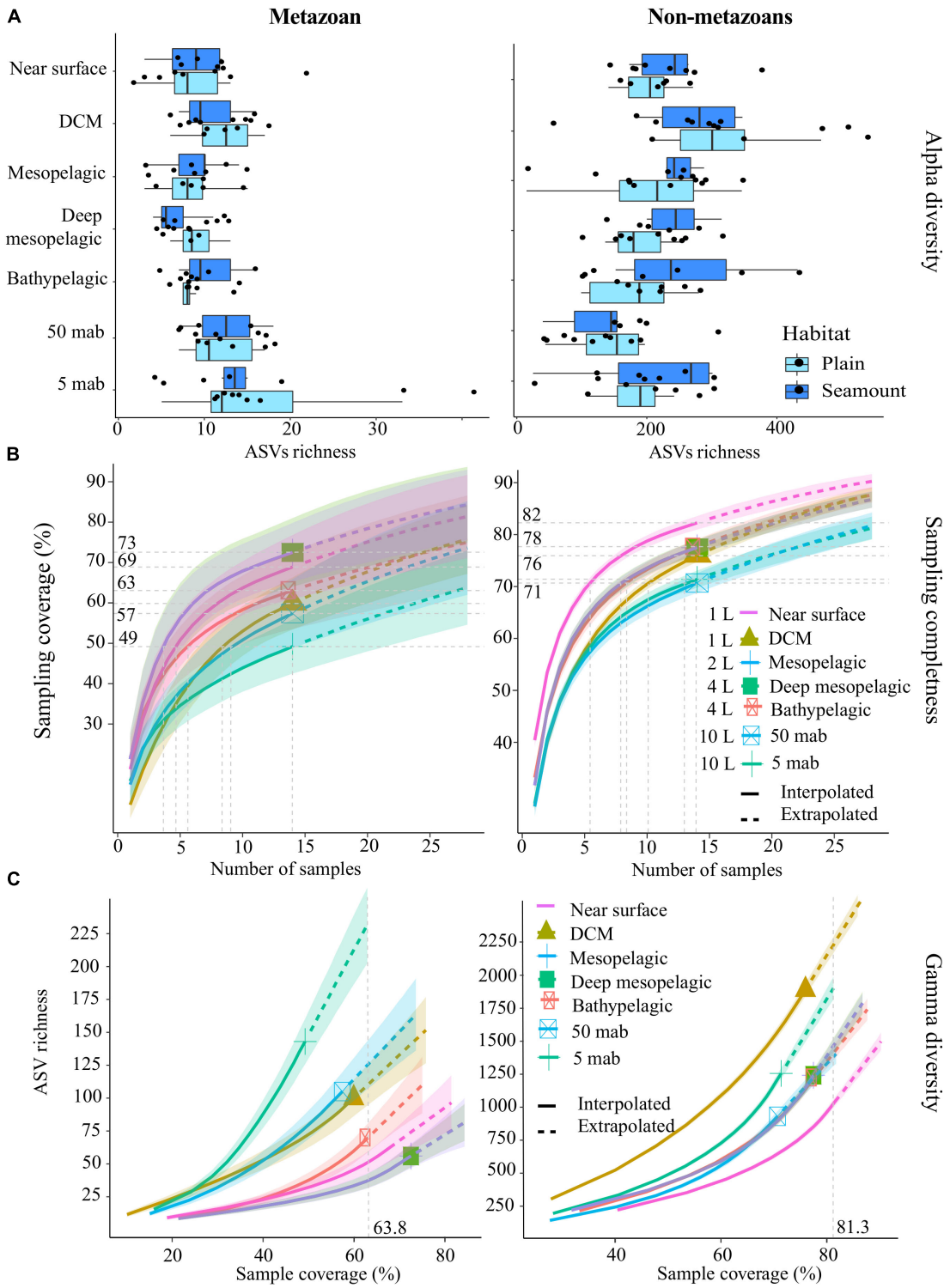

FIGURE 3 | Alpha-diversity, sampling completeness and gamma-diversity across the water column for both metazoans and non-metazoans. **(A)** Box-plot of mean amplicon sequence variant (ASV) richness observed per sample, within each habitat type (abyssal plains, seamounts). **(B)** Sampling coverage achieved across the water column, with seawater volumes filtered at each depth as listed. Horizontal gray dotted lines indicate maximum interpolated sampling coverage values for each water column depth horizon. **(C)** Estimated ASV richness as a function of sampling coverage (Chao2 estimator), across the water column. The vertical dotted gray line represents sample completeness at base coverage, defined as the highest coverage value between minimum extrapolated values and maximum interpolated values. DCM, deep chlorophyll maximum; mab, meters above bottom. For **(B,C)**, shaded colored areas indicate the 95% confidence intervals obtained by a bootstrap method based on 200 replicates.

TABLE 3 | Sampling effort required at each pelagic depth to reach the minimum sampling coverage achieved across depth (49%) for metazoans.

Pelagic zone	Number of samples	Volume per sample (L)	Total volume (L)	Sampling effort required compared to near surface
Near surface	4.66	1	4.66	–
DCM	8.43	1	8.43	1.81
Mesopelagic	2.17	2	4.33	0.93
Deep mesopelagic	1.41	4	5.67	1.22
Bathypelagic	1.84	4	7.36	1.58
50 mab	1.09	10	10.85	2.33
5 mab	2.28	10	22.77	4.89

DCM, deep chlorophyll maximum; mab, meter above bottom.

TABLE 4 | Sampling effort required at each pelagic depth to reach the minimum sampling coverage achieved across depth (71%) for non-metazoans.

Pelagic zone	Number of samples	Volume per sample (L)	Total volume (L)	Sampling effort required compared to near surface
Near surface	5.44	1	5.44	–
DCM	10.12	1	10.12	1.86
Mesopelagic	4.44	2	8.88	1.63
Deep mesopelagic	2.69	4	10.77	1.98
Bathypelagic	2.33	4	9.31	1.71
50 mab	2.29	10	22.9	4.21
5 mab	1.51	10	15.11	2.78

DCM, deep chlorophyll maximum; mab, meter above bottom.

was highest in the DCM (∼2,200 ASVs) and 5 mab (∼1,900 ASVs), and lowest at the near surface (∼1,050 ASVs; **Figure 3C**). Comparison of the sampling effort required per depth to reach equivalent sampling coverage (71%), is shown in **Table 4**, with 50 mab, 5 mab, the deep mesopelagic, and the DCM requiring the largest volumes of seawater filtered. Beta-diversity was found to be significantly different for all pairs of water column depths except 50 mab vs. 5 mab (**Supplementary Table S4**).

Pelagic eDNA in the Water Column

Metazoan eDNA within the epipelagic derived predominantly from arthropods (mean per sample of 70 ± 13% of reads), followed by chordates (15 ± 4%; essentially composed of appendicularians and thaliaceans) and cnidarians (11 ± 4%) (**Figure 4A**). Mesopelagic eDNA differed substantially from the epipelagic in that fewer arthropod reads (<17%) and a higher proportion of cnidarian reads (72%) were observed. The deep mesopelagic and bathypelagic zones contained a high proportion of cnidarian reads (>75%), which were mostly unassigned at the family level within the classes Hydrozoa (75%) and Scyphozoa (4%), but included reads assigned to families Agalmatidae (9%), Rhopalonematidae (4%), and Prayidae (2%).

Non-metazoan taxonomic composition also varied substantially across the water column, with Alveolata dominating the epipelagic (84 ± 7%) and Rhizaria dominating the meso- and bathypelagic (58 ± 10%; **Figure 4A**). Alveolate reads were primarily from Protalveolata, specifically from one of the five Syndiniales groups (31% of all pelagic reads), as well as the dinoflagellates (22%). Within the Rhizarians, most sequences belonged to Order Spumellaria (16% of all pelagic reads), Order Collodaria (9%), Class Acantharia (4%), and the RAD B class of the Retaria subphylum (3%).

Pelagic eDNA at the Seafloor

Pelagic Perspective

A relatively small fraction of the metazoan diversity observed in the upper ocean (near surface, DCM) was sampled at the abyssal seafloor, ranging from 1.2 to 24% of reads from ASVs that were simultaneously observed in both the epipelagic and abyssal sediments, nodules or seawater (**Figure 4B**). In contrast, a large fraction of the metazoan diversity in the meso- and bathypelagic ocean was found within BBL seawater samples (up to 75% of reads, 10% of ASVs; **Figure 4B**). Interestingly, the great majority of metazoan pelagic ASVs (>75%) and reads (>60%) sampled below the DCM that were also found in sediment and nodules could have been sourced from the epipelagic, as these sequences were also present in the near surface and/or DCM samples.

Many of the patterns observed for metazoans were shared for non-metazoans, including the lower proportion of epipelagic diversity sampled at abyssal depths in comparison to meso- and bathypelagic non-metazoan diversity (**Figure 4B**). In the mesopelagic and below, the proportion of pelagic protist reads found within BBL seawater samples increased gradually and substantially, from 47 to 81% and 6 to 10% for reads and ASVs, respectively. In contrast to metazoans, the proportion of non-metazoan pelagic ASVs and reads sampled below the DCM that could have been sourced in

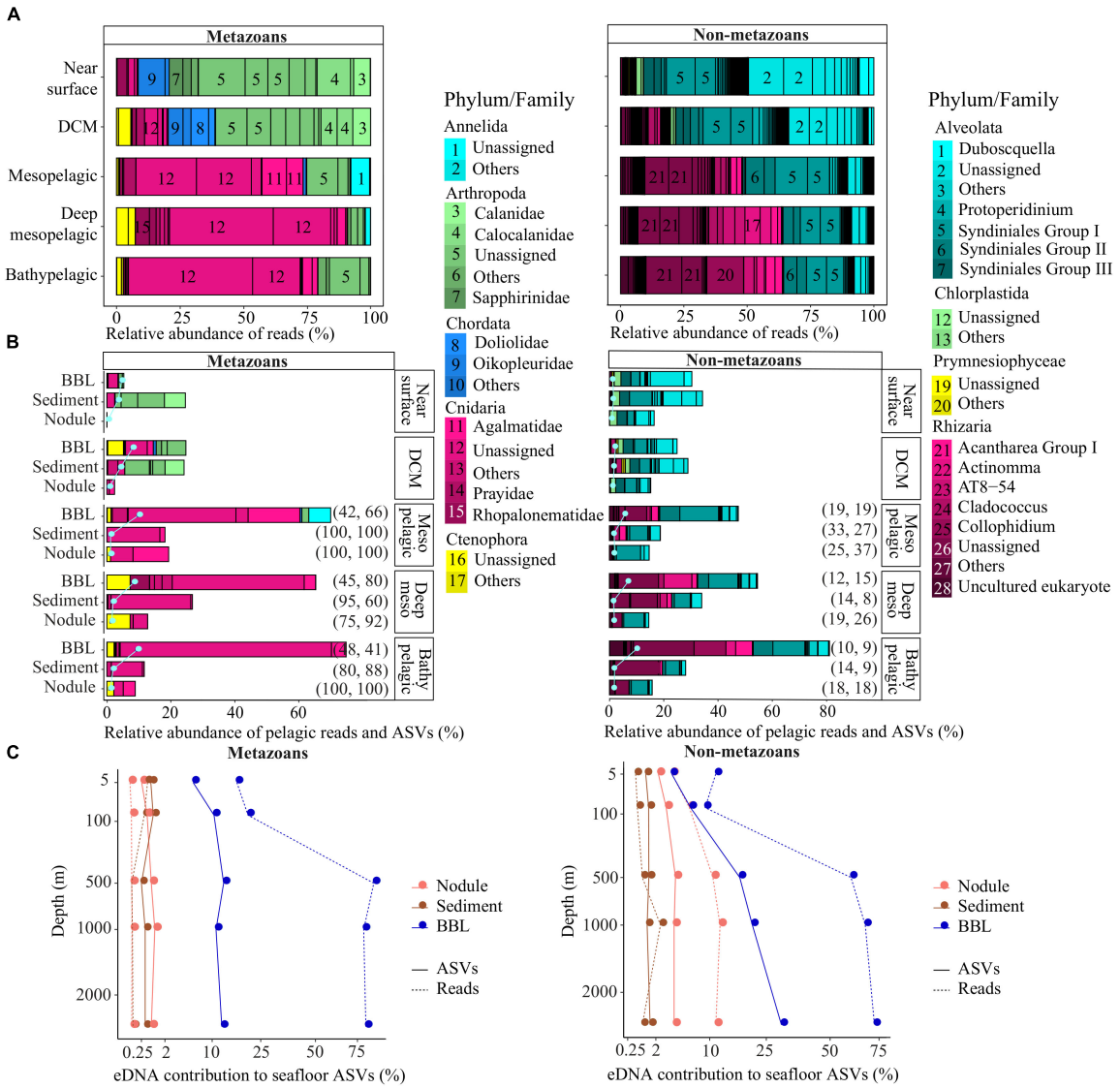

FIGURE 4 | Pelagic eDNA community composition and contribution to diversity at the seafloor. **(A)** Relative read abundance (bars) of phyla and families per pelagic depth zone within each deep ocean habitat (abyssal plains, seamounts). **(B)** Relative abundance of pelagic reads (bars) and pelagic ASVs (pale gray dots and lines) that also were sampled in abyssal sediment, nodule or BBL seawater samples, plotted relative to the diversity sampled in the water column per pelagic depth zone (pelagic perspective). The percent of pelagic ASVs and associated reads concurrently found in the epipelagic are indicated on the right side of the bars, in parentheses. Families with marginal relative abundance were combined and designated as "Others". **(C)** Proportion of sediment, nodule or BBL seawater ASVs and reads that were found within each pelagic zone sampled. Plot shows the benthic perspective, or pelagic diversity sampled at the seafloor relative to all diversity sampled at the seafloor. BBL, benthic boundary layer; DCM, deep chlorophyll maximum.

the epipelagic (also found within near surface and/or DCM samples) was much lower (<33% and <37%, respectively; **Figure 4B**). Overall, pelagic protist reads were found in the smallest proportion within nodules (15 ± 1%), followed by sediments (29 ± 6%) and seawater samples (48 ± 22%).

For both metazoans and non-metazoans, the proportion of the main pelagic eDNA phyla found within the benthos closely reflected that of the overall phyla composition of each pelagic zone (**Figures 4A,B**), with no evidence of taxonomic filtering in terms of which pelagic taxa were sampled at the abyssal seafloor.

Benthic Perspective

Because nodules, and especially sediment samples, had higher metazoan ASV richness than seawater (**Figure 2**), the proportion of diversity that was pelagic in origin represents a small fraction of the total sampled diversity at the seafloor. For example, pelagic metazoan reads and ASVs corresponded, respectively, to 0.012 and 0.64% of the diversity sampled on nodules and 0.15 and 0.53% for sediments. However, pelagic eDNA made up a much larger fraction of the BBL eDNA diversity (56% reads, 13% ASVs) (**Figure 4C**). Within the BBL, most of the pelagic diversity derives from meso- and bathypelagic depths. For metazoans, the

percentage of ASVs and associated reads per benthic sample that were also sampled in the pelagic, and inferred to be pelagic in origin, were not significantly different between seamount and abyssal-plain habitats, nor between upper and lower sediment horizons (**Figure 5**), when evaluated as combined pelagic samples of the relevant APEI and habitat (**Supplementary Table S5**).

For non-metazoans, the overall contribution of pelagic eDNA to the benthos increased gradually with depth in the water column, especially for the BBL samples (**Figure 4C**). The proportions of pelagic eDNA sampled on nodules (9 and 4% for reads and ASVs, respectively) were over an order of magnitude higher than for metazoans. In contrast to metazoans, the percentage of non-metazoan ASVs per benthic sample that were pelagic in origin was significantly higher in seamount than in abyssal plain samples (*t*-tests; $p < 0.001$) (**Figure 5** and **Supplementary Table S5**). Significantly higher proportions of pelagic reads also could be observed within the 0–2 cm versus 3–5 cm sediment layer for the abyssal plain samples (**Supplementary Table S5** and **Figure 5**).

DISCUSSION

Biodiversity assessments in the deep ocean are essential prior to large-scale anthropogenic impacts, such as polymetallic nodule mining proposed for the Clarion Clipperton Zone (Smith et al., 2008a; Wedding et al., 2013, 2015). eDNA metabarcoding methods are increasingly being applied as a biomonitoring tool for ecosystem health in marine systems (e.g., Danovaro et al., 2016; Goodwin et al., 2017; Stat et al., 2017), but have seen limited application in the deep sea (e.g., Dell'Anno et al., 2015; Guardiola et al., 2015, 2016; Sinniger et al., 2016). Here, we examine the effect of allochthonous pelagic DNA on eDNA surveys in abyssal habitats, and address several methodological issues that affect the optimal design of deep ocean eDNA biotic surveys.

Our results show that detrital pelagic eDNA represents a very small fraction of the diversity sampled in sediments and nodules at the abyssal seafloor (<2% of ASVs and their associated reads), and is unlikely to impede recovery of resident diversity in benthic eDNA surveys of the deep ocean. Pelagic eDNA sampled in the abyss appears to derive from two distinct processes: (1) True legacy eDNA that is sourced from the high biomass upper ocean (epipelagic) and sinks to the seafloor on detrital particles, including particulate organic matter (POM) and inorganic particles (e.g., foram and radiolarian tests or diatom frustules), and (2) eDNA sourced from resident populations in the bathy- and abyssopelagic ocean from organisms whose distributions range down to near the seafloor. This interpretation derives from the fact that most of the epipelagic eDNA found in the benthos was observed in sediment samples, while meso- and bathypelagic eDNA found in the benthos was overwhelmingly present within BBL seawater samples (**Figures 4B,C**). Most of the POM originating in the upper ocean is disaggregated and remineralized during its descent through the water column, such that POM flux declines exponentially with depth (Martin et al., 1987; Buesseler et al., 2007; Lutz et al., 2007; Grabowski et al., 2019), and less than 2% of primary production from the upper ocean typically reaches the abyssal seafloor (Smith

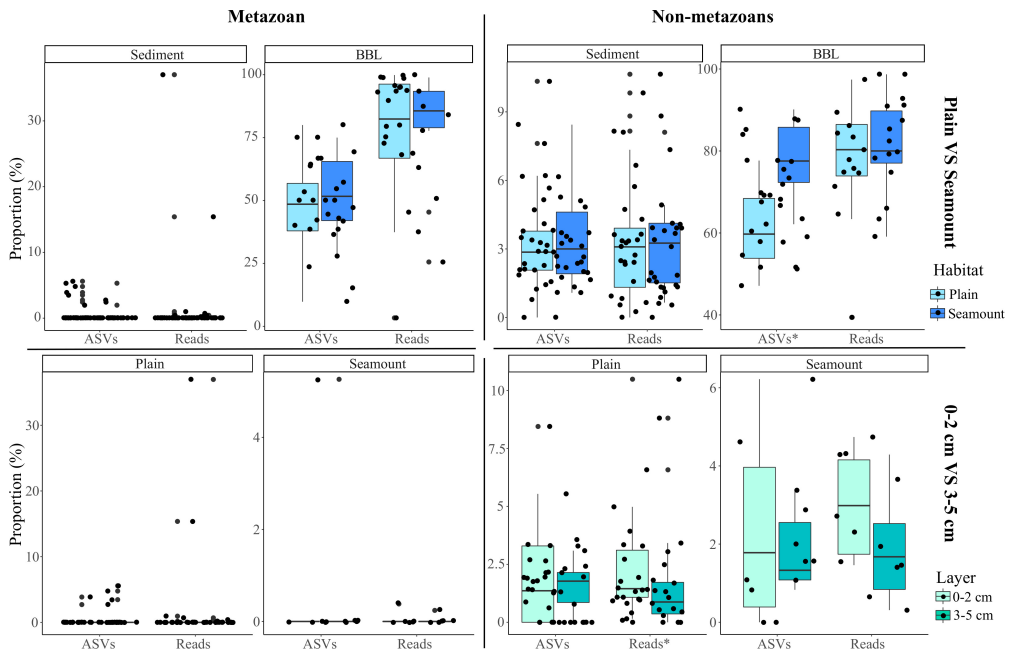

FIGURE 5 | Box-plots of the mean proportion of amplicon sequence variants (ASVs) and their respective reads that derive from pelagic ecosystems (surface to bathypelagic depths) that were sampled at the seafloor across habitats (abyssal plain, seamount) and sediment layers (0–2 and 3–5 cm) for both metazoans and non-metazoans. Plot shows the benthic perspective, or pelagic diversity sampled at the seafloor relative to all diversity sampled at the seafloor. The stars (*x*-axis labels) indicate significant differences determined by two-sample Wilcoxon tests.

et al., 2008b). This proportion is similar to that of the relative proportion of total epipelagic ASVs found in CCZ sediments (0.78 and 1.29% for metazoans and non-metazoans) and nodules (0.36 and 2.65% for metazoans and non-metazoans), suggesting that this material corresponds to true legacy eDNA and may be acting as a tracer of POC flux to the abyssal seafloor. In BBL seawater samples, the proportion of epipelagic ASVs found at the seafloor was slightly higher (8.2 and 5.8% for metazoans and non-metazoans), and BBL pelagic reads were strongly augmented by material originating in the meso- and bathypelagic (up to 86 and 72% for metazoan and non-metazoans, respectively; **Figure 4C**). Most of these deep-sourced sequences derived from hydrozoans, including siphonophore and trachymedusa families, such as Algamatidae, Rhopalonematidea, and Prayidae, as well as radiolarians (Rhizaria). High relative abundance of hydrozoans, especially siphonophores, in deep pelagic habitats is well documented (e.g., Youngbluth et al., 2008; Robison et al., 2010; Cartes et al., 2013), though there are also deep living benthic species (e.g., rhodaliids live tethered to benthic substrates; Pugh, 1983; O'Hara et al., 2016), and their presence near the seafloor of the CCZ has been reported by Dahlgren et al. (2016). Rhizaria also occur in high relative abundance in the meso- and bathypelagic (Jing et al., 2018), and have been documented to be associated with sinking POM collected at abyssal depths in the Pacific (Boeuf et al., 2019). It seems likely that a high proportion of pelagic eDNA reads concurrently found in the BBL seawater samples originate from species whose distributions extend across a broad depth range, including the bathy- and abyssopelagic, and are truncated at the seafloor. Non-metazoans and metazoans differed in the source of legacy eDNA to the seafloor, with detrital pelagic eDNA originating primarily from the epipelagic for metazoans, and across the entire water column for non-metazoans. For non-metazoans, both pelagic ASV and read proportions tended to increase with source depth in the water column (**Figure 4C**). Finally, the 18S rRNA gene is highly conserved and has relatively low taxonomic resolution (Papadopoulou et al., 2015; Creer et al., 2016; Tanabe et al., 2016), and it is possible that close pelagic and benthic relatives are not differentiated by this marker. Based on the above, we infer that most metazoan pelagic eDNA found within sediments and nodules originates from detrital material sourced primarily in the epipelagic ('true' legacy eDNA), while pelagic eDNA found within the BBL mostly derives from residents whose distributions extend upward into the bathy- and abyssopelagic ocean.

Sedimentation rates in the CCZ are relatively low, estimated to range from 0.15 to 1.15 cm kyr^{-1} (Müller and Mangini, 1980; Mewes et al., 2014; Volz et al., 2018), the mixed layer depth due to bioturbation is ∼2 cm (Smith and Rabouille, 2002), oxygen penetrates to >1 m into the sediments (Volz et al., 2018), and organic matter within the 0–5 cm layer may derive from sediment deposition over 4,000–33,000 years. Due to the low sedimentation rates and oxic conditions, most organic matter reaching the abyssal seafloor in the CCZ is remineralized within the upper few decimeters or meter of sediment (Müller and Mangini, 1980; Burdige, 2007; Volz et al., 2018). While eDNA in marine sediments can be preserved for several thousand years under certain conditions (Corinaldesi et al., 2011; Lejzerowicz et al., 2013), Dell'Anno and Danovaro (2005) found exponential declines in extracellular DNA (exDNA) in the top 5 cM of deep-sea sediments, and estimated a mean exDNA residence time of 9.5 years for the top centimeter. However, several studies suggest that most sediment eDNA degrades over time scales of hours to months due to DNase activity and hydrolysis (depurination), or is taken up by microbial organisms as a nutrient source (Nielsen et al., 2007; Corinaldesi et al., 2008; Ibáñez de Aldecoa et al., 2017). Recent deep-sea studies also suggest a marginal effect of exDNA on biodiversity assessments of contemporary eukaryotic communities (Guardiola et al., 2016; Ramírez et al., 2018; Brandt et al., 2020). In this study, using pelagic eDNA as a tracer to understand eDNA flux into and retention within the abyssal seafloor, we did not find evidence of increased pelagic eDNA degradation across a vertical profile within the sediment core for metazoans (**Supplementary Table S4**), since the majority of samples had no pelagic ASVs. However, we did find significant differences in sediment depth horizons for non-metazoans, with a higher proportion of pelagic reads in the 0–2 cm horizon in abyssal plains, and a trend toward a higher proportion of both pelagic ASVs and reads in the 0–2 cm layer across all abyssal habitats, as well as higher overall diversity within the 0–2 cm horizon (**Figure 5** and **Supplementary Figure S5**). Note that a very small fraction of sediment eDNA was found to be pelagic in origin, and the overwhelming majority of eDNA sampled in the 0–5 cm layer derives from benthic organisms (historical and/or present assemblages).

Application of eDNA biotic surveys to monitor environmental impacts on the deep seafloor requires understanding the sampling effort needed to adequately capture the resident diversity of deep benthic assemblages. Our results for abyssal sediments, polymetallic nodules and BBL seawater demonstrate highest ASV richness in sediments for both metazoans and non-metazoans at equivalent sampling coverage, with a substantial drop to the richness estimated for polymetallic nodules and BBL seawater (at base coverage, **Figure 2**). Given prior studies demonstrating the importance of sample size to recovery of eukaryotic diversity (e.g., Nascimento et al., 2018), we targeted large sample volumes in comparison to many earlier eDNA studies, extracting DNA from 10 g of sediment, 10 L of BBL seawater, and 1 g of ground polymetallic nodule for each sample. For comparison, marine protist diversity on the continental shelf is typically sampled for eDNA using ∼ 2 g of sediment (or less) in each sample (Pawlowski et al., 2014; Chariton et al., 2015; Pochon et al., 2015; Laroche et al., 2018), and metazoan surveys are often based on 1–2 L of filtered seawater (e.g., Sigsgaard et al., 2017; Grey et al., 2018; Jeunen et al., 2019) or ∼10 g per sample of the top 3–5 cm layer (deep sea examples, Guardiola et al., 2015, 2016; Sinniger et al., 2016). Despite relatively high sampling effort, including 71 sediment samples from 36 cores, 193 seawater samples from 12 CTD casts, and 50 samples from 10 polymetallic nodules, we are still under-sampling the diversity of these abyssal assemblages, with estimated sampling coverage for metazoans ranging from 40 to 74% study-wide across sample types. Our sampling coverage tended to be lower for metazoans than non-metazoans at equivalent sample size (e.g., in sediments 40% vs. 64%), as

expected since metazoans exhibit a higher degree of patchiness and because their detection relies in part on trace DNA recovery (Sinniger et al., 2016; Nascimento et al., 2018). For metazoans, diversity recovered from polymetallic nodules was approximately 6 times lower than in sediments at equivalent sampling coverage, and consequently, despite assessing only 5 g of material per nodule (∼6% of mean nodule weight) for a total of 10 nodules, sampling coverage was more complete study-wide and could be extrapolated to ∼75% of total community diversity. Nevertheless, the relatively low sampling coverage per nodule (∼50%) suggests that assessing additional material per nodule and increasing the number of sampled nodules is needed. Additional work would also yield insights into the nodule crevice-associated fauna (Thiel et al., 1993), and reveal how community composition on nodules varies as a function of nodule size (e.g., Laroche et al., 2020a). For seawater samples, metazoan ASV richness was higher at 5 mab within the BBL than any other depth sampled (at base coverage; **Figure 2**), with relatively low sampling coverage (49%, 57%, BBL samples) despite filtering 10 L per sample (2 L × 5 L). We therefore recommend increasing the number of replicates when sampling metazoan eDNA within the BBL, for example to >30 L (>3 L × 10 L replicates) to obtain sampling coverage at over 50% of the community (**Table 3**). With sampling coverage ranging from 64 to 84% for non-metazoans (all 3 substrate types), we infer that our sample sizes were adequate to capture most of the diversity of eukaryotic non-metazoans, although increased sampling effort (number of samples) across a broader range of abyssal microhabitats would improve understanding of community structure and the distribution of eDNA across these habitats. Sampling the abyssal seafloor is technically challenging and expensive relative to most marine environments, and as is commonly reported in other abyssal faunal studies (e.g., using conventional survey methods, De Smet et al., 2017; Pape et al., 2017; Washburn et al., unpublished), significant sampling effort is required to achieve high sampling completeness, in particular for the sparse but highly diverse sediment community. Additionally, the detection probability of taxa is influenced by the amount of template DNA used for PCR amplification and in studies with low amount of template material, such as ancient DNA studies, a minimum of 8 PCR replicates have been proposed to increase detection probability (Ficetola et al., 2015). While we reduced stochasticity and increased detection probability by using a minimum of 3 ng of DNA per PCR and by pooling 2 PCR replicates per sample, further research evaluating the effect of PCR replication on deep sea benthic surveys would be valuable.

Overall, our results provide some guidance on designing eDNA biotic surveys for the deep ocean, as well as insight into processes that affect the transport and distribution of eDNA across the water column and abyss. Future deep-sea eDNA surveys should aim to process large amounts of material per sample (>10 g sediment, >10 L seawater, with replication), consider habitat heterogeneity at a range of spatial scales in the abyss (Laroche et al., 2020a), and explore the temporal variability of eDNA in particular abyssal habitats and sites. Finally, research is needed to evaluate how the oceanographic setting, including current velocities and sediment-transport regime, influence eDNA delivery, retention, and persistence (e.g., degradation and winnowing) within abyssal benthic habitats.

DATA AVAILABILITY STATEMENT

The datasets generated in this study can be found on the NCBI website https://www.ncbi.nlm.nih.gov/, under project number PRJNA546001, sample accession numbers SRR9199590 to SRR9199869.

AUTHOR CONTRIBUTIONS

EG, OK, OL, and CS designed the study. EG, OK, and CS conducted field work and sampling at sea. OL generated the data and performed analyses. OL wrote the manuscript with intellectual contributions from all co-authors. EG and CS provided grant and equipment support. All authors contributed to the article and approved the submitted version.

FUNDING

Support for this project was provided by The Pew Charitable Trusts award UH30788 (to PIs EG and CS), Gordon and Betty Moore Foundation award 5596 (lead PIs CS and J. Drazen), NOAA Ocean Exploration grant NA17OAR0110209 (lead PIs J. Drazen and CS), and from the University of Hawai'i for ROV technical support at sea. The views expressed are those of the author(s) and do not necessarily reflect the views of The Pew Charitable Trusts or other funding agencies. This is contribution 11119 from SOEST, University of Hawai'i at Mānoa.

ACKNOWLEDGMENTS

We thank M. Church, E. Wear, other DeepCCZ scientists, and the captain and crew of R/V Kilo Moana for assistance at sea. We thank J. Saito from the Advanced Studies in Genomics, Proteomics, and Bioinformatics (ASGPB) core facility for laboratory support, and M. Gaither for early discussions on eDNA surveys in the deep ocean. This manuscript was released as a pre-print at bioRxiv, Laroche et al. (2020b).

SUPPLEMENTARY MATERIAL

The Supplementary Material for this article can be found online at: https://www.frontiersin.org/articles/10.3389/fmars.2020.00682/full#supplementary-material

REFERENCES

Adl, S. M., Bass, D., Lane, C. E., Lukeš, J., Schoch, C. L., Smirnov, A., et al. (2019). Revisions to the classification, nomenclature, and diversity of eukaryotes. *J. Eukaryot. Microbiol.* 66, 4–119. doi: 10.1111/jeu.12691

Amon, D. J., Ziegler, A. F., Dahlgren, T. G., Glover, A. G., Goineau, A., Gooday, A. J., et al. (2016). Insights into the abundance and diversity of abyssal megafauna in a polymetallic-nodule region in the eastern Clarion-Clipperton Zone. *Sci. Rep.* 6:30492. doi: 10.1038/srep30492

Angel, M. V., and Baker, A. D. C. (1982). Vertical distribution of the standing crop of plankton and micronekton at three stations in the northeast Atlantic. *Biol. Oceanogr.* 2, 1–30.

Armbrecht, L. H., Coolen, M. J. L., Lejzerowicz, F., George, S. C., Negandhi, K., Suzuki, Y., et al. (2019). Ancient DNA from marine sediments: precautions and considerations for seafloor coring, sample handling and data generation. *Earth Sci. Rev.* 196:102887. doi: 10.1016/j.earscirev.2019.102887

Barnes, M. A., and Turner, C. R. (2016). The ecology of environmental DNA and implications for conservation genetics. *Conserv. Genet.* 17, 1–17. doi: 10.1007/s10592-015-0775-4

Barnes, M. A., Turner, C. R., Jerde, C. L., Renshaw, M. A., Chadderton, W. L., and Lodge, D. M. (2014). Environmental conditions influence eDNA persistence in aquatic systems. *Environ. Sci. Technol.* 48, 1819–1827. doi: 10.1021/es404734p

Boeuf, D., Edwards, B. R., Eppley, J. M., Hu, S. K., Poff, K. E., Romano, A. E., et al. (2019). Biological composition and microbial dynamics of sinking particulate organic matter at abyssal depths in the oligotrophic open ocean. *Proc. Natl. Acad. Sci. U.S.A.* 116, 11824–11832. doi: 10.1073/pnas.1903080116

Bolyen, E., Rideout, J. R., Dillon, M. R., Bokulich, N. A., Abnet, C. C., Al-Ghalith, G. A., et al. (2019). Reproducible, interactive, scalable and extensible microbiome data science using QIIME 2. *Nat. Biotechnol.* 37, 852–857. doi: 10.1038/s41587-019-0209-9

Boschen, R. E., Collins, P. C., Tunnicliffe, V., Carlsson, J., Gardner, J. P. A., Lowe, J., et al. (2016). A primer for use of genetic tools in selecting and testing the suitability of set-aside sites protected from deep-sea seafloor massive sulfide mining activities. *Ocean Coast. Manage.* 122, 37–48. doi: 10.1016/j.ocecoaman.2016.01.007

Boschen, R. E., Rowden, A. A., Clark, M. R., and Gardner, J. P. A. (2013). Mining of deep-sea seafloor massive sulfides: a review of the deposits, their benthic communities, impacts from mining, regulatory frameworks and management strategies. *Ocean Coast. Manage.* 84, 54–67. doi: 10.1016/j.ocecoaman.2013.07.005

Brandt, M. I., Trouche, B., Henry, N., Liautard-Haag, C., Maignien, L., de Vargas, C., et al. (2020). An assessment of environmental metabarcoding protocols aiming at favoring contemporary biodiversity in inventories of deep-sea communities. *Front. Mar. Sci.* 7:234. doi: 10.3389/fmars.2020.00234

Buesseler, K. O., Lamborg, C. H., Boyd, P. W., Lam, P. J., Trull, T. W., Bidigare, R. R., et al. (2007). Revisiting carbon flux through the ocean's twilight zone. *Science* 316, 567–570. doi: 10.1126/science.1137959

Burdige, D. J. (2007). Preservation of organic matter in marine sediments: controls, mechanisms, and an imbalance in sediment organic carbon budgets? *Chem. Rev.* 107, 467–485. doi: 10.1021/cr050347q

Callahan, B. J., McMurdie, P. J., Rosen, M. J., Han, A. W., Johnson, A. J. A., and Holmes, S. P. (2016). DADA2: high-resolution sample inference from Illumina amplicon data. *Nat. Methods* 13, 581–583. doi: 10.1038/nmeth.3869

Cartes, J. E., Fanelli, E., López-Pérez, C., and Lebrato, M. (2013). Deep-sea macroplankton distribution (at 400 to 2300m) in the northwestern Mediterranean in relation to environmental factors. *J. Mar. Syst.* 113-114, 75–87. doi: 10.1016/j.jmarsys.2012.12.012

Chao, A., Gotelli, N. J., Hsieh, T. C., Sander, E. L., Ma, K. H., Colwell, R. K., et al. (2014). Rarefaction and extrapolation with Hill numbers: a framework for sampling and estimation in species diversity studies. *Ecol. Monogr.* 84, 45–67. doi: 10.1890/13-0133.1

Chao, A., and Jost, L. (2012). Coverage-based rarefaction and extrapolation: standardizing samples by completeness rather than size. *Ecology* 93, 2533–2547. doi: 10.1890/11-1952.1

Chariton, A. A., Stephenson, S., Morgan, M. J., Steven, A. D. L., Colloff, M. J., Court, L. N., et al. (2015). Metabarcoding of benthic eukaryote communities predicts the ecological condition of estuaries. *Environ. Pollut.* 203, 165–174. doi: 10.1016/j.envpol.2015.03.047

Clark, M. R., Rowden, A. A., Schlacher, T., Williams, A., Consalvey, M., Stocks, K. I., et al. (2010). The ecology of seamounts: structure, function, and human impacts. *Annu. Rev. Mar. Sci.* 2, 253–278. doi: 10.1146/annurev-marine-120308-081109

Collins, R. A., Wangensteen, O. S., O'Gorman, E. J., Mariani, S., Sims, D. W., and Genner, M. J. (2018). Persistence of environmental DNA in marine systems. *Commun. Biol.* 1:185. doi: 10.1038/s42003-018-0192-6

Corinaldesi, C., Barucca, M., Luna, G. M., and Dell'Anno, A. (2011). Preservation, origin and genetic imprint of extracellular DNA in permanently anoxic deep-sea sediments. *Mol. Ecol.* 20, 642–654. doi: 10.1111/j.1365-294X.2010.04958.x

Corinaldesi, C., Beolchini, F., Dell'Anno, A., and Bianche, V. B. (2008). Damage and degradation rates of extracellular DNA in marine sediments: implications for the preservation of gene sequences. *Mol. Ecol.* 17, 3939–3951. doi: 10.1111/j.1365-294X.2008.03880.x

Creer, S., Deiner, K., Frey, S., Porazinska, D., Taberlet, P., Thomas, W. K., et al. (2016). The ecologist's field guide to sequence-based identification of biodiversity. *Methods Ecol. Evol.* 56, 68–74. doi: 10.1111/2041-210X.12574

Dahlgren, T., Wiklund, H., Rabone, M., Amon, D., Ikebe, C., Watling, L., et al. (2016). Abyssal fauna of the UK-1 polymetallic nodule exploration area, Clarion-Clipperton Zone, central Pacific Ocean: Cnidaria. *Biodivers. Data J.* 4:e9277. doi: 10.3897/BDJ.4.e9277

Danovaro, R., Carugati, L., Berzano, M., Cahill, A. E., Carvalho, S., Chenuil, A., et al. (2016). Implementing and innovating marine monitoring approaches for assessing marine environmental status. *Front. Mar. Sci.* 3:213. doi: 10.3389/fmars.2016.00213

De Smet, B., Pape, E., Riehl, T., Bonifácio, P., Colson, L., and Vanreusel, A. (2017). The community structure of deep-sea macrofauna associated with polymetallic nodules in the eastern part of the Clarion-Clipperton fracture zone. *Front. Mar. Sci.* 4:103. doi: 10.3389/fmars.2017.00103

Deiner, K., Bik, H. M., Mächler, E., Seymour, M., Lacoursière-Roussel, A., Altermatt, F., et al. (2017). Environmental DNA metabarcoding: transforming how we survey animal and plant communities. *Mol. Ecol.* 5872–5895. doi: 10.1111/mec.14350

Dell'Anno, A., Carugati, L., Corinaldesi, C., Riccioni, G., and Danovaro, R. (2015). Unveiling the biodiversity of deep-sea nematodes through metabarcoding: Are we ready to bypass the classical taxonomy? *PLoS One* 10:e0144928. doi: 10.1371/journal.pone.0144928

Dell'Anno, A., and Danovaro, R. (2005). Extracellular DNA plays a key role in deep-sea ecosystem functioning. *Science* 309, 2179–2179. doi: 10.1126/science.1117475

Djurhuus, A., Port, J., Closek, C. J., Yamahara, K. M., Romero-Maraccini, O., Walz, K. R., et al. (2017). Evaluation of filtration and DNA extraction methods for environmental DNA biodiversity assessments across multiple trophic levels. *Front. Mar. Sci.* 4:314. doi: 10.3389/fmars.2017.00314

Ficetola, G. F., Pansu, J., Bonin, A., Coissac, E., Giguet-Covex, C., De Barba, M., et al. (2015). Replication levels, false presences and the estimation of the presence/absence from eDNA metabarcoding data. *Mol. Ecol. Resour.* 15, 543–556. doi: 10.1111/1755-0998.12338

Fonseca, V. G., Carvalho, G. R., Sung, W., Johnson, H. F., Power, D. M., Neill, S. P., et al. (2010). Second-generation environmental sequencing unmasks marine metazoan biodiversity. *Nat. Commun.* 1:98. doi: 10.1038/ncomms1095

Genin, A., and Dower, J. F. (2007). "Seamount plankton dynamics," in *Seamounts: Ecology, Fisheries & Conservation*, eds T. J. Pitcher, T. Morato, P. J. B. Hart, M. R. Clark, N. Haggan, and R. S. Santos (Oxford: Blackwell Publishing Ltd), 85–100. doi: 10.1002/9780470691953

Glover, A., Smith, C., Paterson, G., Wilson, G., Hawkins, L., and Sheader, M. (2002). Polychaete species diversity in the central Pacific abyss: local and regional patterns, and relationships with productivity. *Mar. Ecol. Prog. Ser.* 240, 157–170. doi: 10.3354/meps240157

Goodwin, K. D., Thompson, L. R., Duarte, B., Kahlke, T., Thompson, A. R., Marques, J. C., et al. (2017). DNA sequencing as a tool to monitor marine ecological status. *Front. Mar. Sci.* 4:107. doi: 10.3389/fmars.2017.00107

Grabowski, E., Letelier, R. M., Laws, E. A., and Karl, D. M. (2019). Coupling carbon and energy fluxes in the North Pacific Subtropical Gyre. *Nat. Commun.* 10:1895. doi: 10.1038/s41467-019-09772-z

Grey, E. K., Bernatchez, L., Cassey, P., Deiner, K., Deveney, M., Howland, K. L., et al. (2018). Effects of sampling effort on biodiversity patterns estimated from

environmental DNA metabarcoding surveys. *Sci. Rep.* 8:8843. doi: 10.1038/s41598-018-27048-2

Guardiola, M., Uriz, M. J., Taberlet, P., Coissac, E., Wangensteen, O. S., and Turon, X. (2015). Deep-sea, deep-sequencing: metabarcoding extracellular DNA from sediments of marine canyons. *PLoS One* 10:e0139633. doi: 10.1371/journal.pone.0139633

Guardiola, M., Wangensteen, O. S., Taberlet, P., Coissac, E., Uriz, M. J., and Turon, X. (2016). Spatio-temporal monitoring of deep-sea communities using metabarcoding of sediment DNA and RNA. *PeerJ* 4:e2807. doi: 10.7717/peerj.2807

Günther, B., Knebelsberger, T., Neumann, H., Laakmann, S., and Martínez Arbizu, P. (2018). Metabarcoding of marine environmental DNA based on mitochondrial and nuclear genes. *Sci. Rep.* 8:14822. doi: 10.1038/s41598-018-32917-x

Hadziavdic, K., Lekang, K., Lanzen, A., Jonassen, I., Thompson, E. M., and Troedsson, C. (2014). Characterization of the 18s rRNA gene for designing universal eukaryote specific primers. *PLoS One* 9:e87624. doi: 10.1371/journal.pone.0087624

Halpern, B. S., Frazier, M., Potapenko, J., Casey, K. S., Koenig, K., Longo, C., et al. (2015). Spatial and temporal changes in cumulative human impacts on the world's ocean. *Nat. Commun.* 6:7615. doi: 10.1038/ncomms8615

Hsieh, T. C., Ma, K. H., and Chao, A. (2019). iNEXT: an R package for rarefaction and extrapolation of species diversity (Hill numbers). *Methods Ecol. Evol.* 7, 1451–1456. doi: 10.1111/2041-210X.12613

Ibáñez de Aldecoa, A. L., Zafra, O., and González-Pastor, J. E. (2017). Mechanisms and regulation of extracellular DNA release and its biological roles in microbial communities. *Front. Microbiol.* 8:1390. doi: 10.3389/fmicb.2017.01390

ISA (2019). *Deep CCZ Biodiversity Synthesis Workshop*. Friday Harbor, WA: International Seabed Authority.

Jeunen, G. J., Knapp, M., Spencer, H. G., Lamare, M. D., Taylor, H. R., Stat, M., et al. (2019). Environmental DNA (eDNA) metabarcoding reveals strong discrimination among diverse marine habitats connected by water movement. *Mol. Ecol. Resour.* 19, 426–438. doi: 10.1111/1755-0998.12982

Jing, H., Zhang, Y., Li, Y., Zhu, W., and Liu, H. (2018). Spatial variability of Picoeukaryotic communities in the Mariana Trench. *Sci. Rep.* 8:15357. doi: 10.1038/s41598-018-33790-4

Kaiser, S., Smith, C. R., and Arbizu, P. M. (2017). Editorial: biodiversity of the Clarion Clipperton fracture zone. *Mar. Biodivers.* 47, 259–264. doi: 10.1007/s12526-017-0733-0

Kelly, R. P. (2016). Making environmental DNA count. *Mol. Ecol. Resour.* 16, 10–12. doi: 10.1111/1755-0998.12455

Kersten, O., Smith, C. R., and Vetter, E. W. (2017). Abyssal near-bottom dispersal stages of benthic invertebrates in the Clarion-Clipperton polymetallic nodule province. *Deep Sea Res. Part I Oceanogr. Res. Pap.* 127, 31–40. doi: 10.1016/j.dsr.2017.07.001

Kersten, O., Vetter, E. W., Jungbluth, M. J., Smith, C. R., and Goetze, E. (2019). Larval assemblages over the abyssal plain in the Pacific are highly diverse and spatially patchy. *PeerJ* 7:e7691. doi: 10.7717/peerj.7691

Laroche, O., Kersten, O., Smith, C. R., and Goetze, E. (2020a). Environmental DNA surveys detect distinct metazoan communities across abyssal plains and seamounts in the western Clarion Clipperton Zone. *Mol. Ecol.* doi: 10.1111/mec.15484[Epub ahead of print].

Laroche, O., Kersten, O., Smith, C. R., and Goetze, E. (2020b). From sea surface to seafloor: a benthic allochthonous eDNA survey for the abyssal ocean. *bioRxiv* [Preprint]. doi: 10.1101/2020.05.07.082602

Laroche, O., Wood, S. A., Tremblay, L. A., Ellis, J. I., Lear, G., and Pochon, X. (2018). A cross-taxa study using environmental DNA/RNA metabarcoding to measure biological impacts of offshore oil and gas drilling and production operations. *Mar. Pollut. Bull.* 127, 97–107. doi: 10.1016/j.marpolbul.2017.11.042

Lavelle, J. W., and Mohn, C. (2010). Motion, commotion, and biophysical connections at deep ocean seamounts. *Oceanography* 23, 90–103. doi: 10.5670/oceanog.2010.64

Le, J. T., Levin, L. A., and Carson, R. T. (2017). Incorporating ecosystem services into environmental management of deep-seabed mining. *Deep Sea Res. Part II Top. Stud. Oceanogr.* 137, 486–503. doi: 10.1016/j.dsr2.2016.08.007

Leitner, A. B., Neuheimer, A. B., Donlon, E., Smith, C. R., and Drazen, J. C. (2017). Environmental and bathymetric influences on abyssal bait-attending communities of the Clarion Clipperton Zone. *Deep Sea Res. Part I Oceanogr. Res. Pap.* 125, 65–80. doi: 10.1016/j.dsr.2017.04.017

Lejzerowicz, F., Esling, P., Majewski, W., Szczuciński, W., Decelle, J., Obadia, C., et al. (2013). Ancient DNA complements microfossil record in deep-sea subsurface sediments. *Biol. Lett.* 9:20130283. doi: 10.1098/rsbl.2013.0283

Lozupone, C., and Knight, R. (2005). UniFrac: a new phylogenetic method for comparing microbial communities. *Appl. Environ. Microbiol.* 71, 8228–8235. doi: 10.1128/AEM.71.12.8228-8235.2005

Lutz, M. J., Caldeira, K., Dunbar, R. B., and Behrenfeld, M. J. (2007). Seasonal rhythms of net primary production and particulate organic carbon flux to depth describe the efficiency of biological pump in the global ocean. *J. Geophys. Res.* 112:C10011. doi: 10.1029/2006JC003706

Martin, J. H., Knauer, G. A., Karl, D. M., and Broenkow, W. W. (1987). VERTEX: carbon cycling in the northeast Pacific. *Deep Sea Res. Part A Oceanogr. Res. Pap.* 34, 267–285. doi: 10.1016/0198-0149(87)90086-0

Martinez Arbizu, P. (2020). *pairwiseAdonis: Pairwise Multilevel Comparison Using Adonis. R package version* 0.4. Available online at: https://github.com/pmartinezarbizu/pairwiseAdonis (accessed February, 2019).

Mewes, K., Mogollón, J. M. M., Picard, A., Rühlemann, C., Kuhn, T., Nöthen, K., et al. (2014). Impact of depositional and biogeochemical processes on small scale variations in nodule abundance in the Clarion-Clipperton fracture zone. *Deep Sea Res. Part I Oceanogr. Res. Pap.* 91, 125–141. doi: 10.1016/j.dsr.2014.06.001

Morard, R., Lejzerowicz, F., Darling, K. F., Lecroq-Bennet, B., Winther Pedersen, M., Orlando, L., et al. (2017). Planktonic foraminifera-derived environmental DNA extracted from abyssal sediments preserves patterns of plankton macroecology. *Biogeosciences* 14, 2741–2754. doi: 10.5194/bg-14-2741-2017

Müller, P. J., and Mangini, A. (1980). Organic carbon decomposition rates in sediments of the pacific manganese nodule belt dated by 230Th and 231Pa. *Earth Planet. Sci. Lett.* 51, 94–114. doi: 10.1016/0012-821X(80)90259-9

Nascimento, F. J. A., Lallias, D., Bik, H. M., and Creer, S. (2018). Sample size effects on the assessment of eukaryotic diversity and community structure in aquatic sediments using high-throughput sequencing. *Sci. Rep.* 8:11737. doi: 10.1038/s41598-018-30179-1

Nielsen, K. M., Johnsen, P. J., Bensasson, D., and Daffonchio, D. (2007). Release and persistence of extracellular DNA in the environment. *Environ. Biosaf. Res.* 6, 37–53. doi: 10.1051/ebr:2007031

O'Hara, T. D., Hugall, A. F., MacIntosh, H., Naughton, K. M., Williams, A., and Moussalli, A. (2016). Dendrogramma is a siphonophore. *Curr. Biol.* 26, R457–R458. doi: 10.1016/j.cub.2016.04.051

Oksanen, J., Blanchet, F. G., Friendly, M., Kindt, R., Legendre, P., McGlinn, D., et al. (2018). *vegan: Community Ecology Package*. Available online at: https://cran.r-project.org/package=vegan (accessed February, 2019).

Oliveros, J. C. C. (2015). *Venny. An Interactive Tool for Comparing Lists with Venn's Diagrams*. Available online at: http://bioinfogp.cnb.csic.es/tools/venny/index.html (accessed February, 2019).

Paerl, R. W., Foster, R. A., Jenkins, B. D., Montoya, J. P., and Zehr, J. P. (2008). Phylogenetic diversity of cyanobacterial narB genes from various marine habitats. *Environ. Microbiol.* 10, 3377–3387. doi: 10.1111/j.1462-2920.2008.01741.x

Papadopoulou, A., Taberlet, P., and Zinger, L. (2015). Metagenome skimming for phylogenetic community ecology: a new era in biodiversity research. *Mol. Ecol.* 24, 3515–3517. doi: 10.1111/mec.13263

Pape, E., Bezerra, T. N., Hauquier, F., and Vanreusel, A. (2017). Limited spatial and temporal variability in meiofauna and nematode communities at distant but environmentally similar sites in an area of interest for deep-sea mining. *Front. Mar. Sci.* 4:205. doi: 10.3389/fmars.2017.00205

Pawlowski, J., Christen, R., Lecroq, B., Bachar, D., Shahbazkia, H. R., Amaral-Zettler, L., et al. (2011). Eukaryotic richness in the abyss: insights from pyrotag sequencing. *PLoS One* 6:18169. doi: 10.1371/journal.pone.0018169

Pawlowski, J., Esling, P., Lejzerowicz, F., Cedhagen, T., and Wilding, T. A. (2014). Environmental monitoring through protist NGS metabarcoding: assessing the impact of fish farming on benthic foraminifera communities. *Mol. Ecol. Resour.* 14, 1129–1140. doi: 10.1111/1755-0998.12261

Pedregosa, F., Varoquaux, G., Gramfort, A., Michel, V., Thirion, B., Grisel, O., et al. (2012). Scikit-learn: machine learning in python. *Pattern Recognit.* 45, 2041–2049. doi: 10.1016/j.patcog.2011.04.006

Pochon, X., Wood, S. A., Keeley, N. B., Lejzerowicz, F., Esling, P., Drew, J., et al. (2015). Accurate assessment of the impact of salmon farming on benthic sediment enrichment using foraminiferal metabarcoding. *Mar. Pollut. Bull.* 100, 370–382. doi: 10.1016/j.marpolbul.2015.08.022

Pugh, P. R. (1983). Benthic siphonophores: a review of the family Rhodaliidae (Siphonophora, Physonectae). *Philos. Trans. R. Soc. B Biol. Sci.* 301, 165–300. doi: 10.1098/rstb.1983.0025

Quast, C., Pruesse, E., Yilmaz, P., Gerken, J., Schweer, T., Yarza, P., et al. (2013). The SILVA ribosomal RNA gene database project: improved data processing and web-based tools. *Nucleic Acids Res.* 41, 590–596. doi: 10.1093/nar/gks1219

Ramirez-Llodra, E., Brandt, A., Danovaro, R., De Mol, B., Escobar, E., German, C. R., et al. (2010). Deep, diverse and definitely different: unique attributes of the world's largest ecosystem. *Biogeosciences* 7, 2851–2899. doi: 10.5194/bg-7-2851-2010

Ramírez, G. A., Jørgensen, S. L., Zhao, R., and D'Hondt, S. (2018). Minimal influence of extracellular DNA on molecular surveys of marine sedimentary communities. *Front. Microbiol.* 9, 1–12. doi: 10.3389/fmicb.2018.02969

Renshaw, M. A., Olds, B. P., Jerde, C. L., McVeigh, M. M., and Lodge, D. M. (2015). The room temperature preservation of filtered environmental DNA samples and assimilation into a phenol-chloroform-isoamyl alcohol DNA extraction. *Mol. Ecol. Resour.* 15, 168–176. doi: 10.1111/1755-0998.12281

Robison, B. H., Sherlock, R. E., and Reisenbichler, K. R. (2010). The bathypelagic community of Monterey Canyon. *Deep Sea Res. Part II Top. Stud. Oceanogr.* 57, 1551–1556. doi: 10.1016/j.dsr2.2010.02.021

Rowden, A. A., Dower, J. F., Schlacher, T. A., Consalvey, M., and Clark, M. R. (2010). Paradigms in seamount ecology: fact, fiction and future. *Mar. Ecol.* 31(Suppl. 1), 226–241. doi: 10.1111/j.1439-0485.2010.00400.x

Samadi, S., Schlacher, T., and de Forges, B. R. (2007). "Seamount Benthos," in *Seamounts: Ecology, Fisheries & Conservation*, ed. T. Pritcher (Oxford: Blackwell Publishing Ltd), 117–140. doi: 10.1002/9780470691953.ch7

Seymour, M. (2019). Rapid progression and future of environmental DNA research. *Commun. Biol.* 2:80. doi: 10.1038/s42003-019-0330-9

Seymour, M., Durance, I., Cosby, B. J., Ransom-Jones, E., Deiner, K., Ormerod, S. J., et al. (2018). Acidity promotes degradation of multi-species environmental DNA in lotic mesocosms. *Commun. Biol.* 1:4. doi: 10.1038/s42003-017-0005-3

Shulse, C. N., Maillot, B., Smith, C. R., and Church, M. J. (2017). Polymetallic nodules, sediments, and deep waters in the equatorial North Pacific exhibit highly diverse and distinct bacterial, archaeal, and microeukaryotic communities. *Microbiologyopen* 6:e00428. doi: 10.1002/mbo3.428

Sigsgaard, E. E., Nielsen, I. B., Carl, H., Krag, M. A., Knudsen, S. W., Xing, Y., et al. (2017). Seawater environmental DNA reflects seasonality of a coastal fish community. *Mar. Biol.* 164:128. doi: 10.1007/s00227-017-3147-4

Simon-Lledó, E., Bett, B. J., Huvenne, V. A. I., Schoening, T., Benoist, N. M. A., and Jones, D. O. B. (2019). Ecology of a polymetallic nodule occurrence gradient: implications for deep-sea mining. *Limnol. Oceanogr.* 64, 1883–1894. doi: 10.1002/lno.11157

Sinniger, F., Pawlowski, J., Harii, S., Gooday, A. J., Yamamoto, H., Chevaldonné, P., et al. (2016). Worldwide analysis of sedimentary DNA reveals major gaps in taxonomic knowledge of deep-sea Benthos. *Front. Mar. Sci.* 3:92. doi: 10.3389/fmars.2016.00092

Smith, C. R., Clark, M., Amon, D., Bonifáco, P., Bribiesca-Contreras, G., Christodoulou, M., et al. (2019). *Deep CCZ Biodiversity Synthesis Workshop Report.* Friday Harbor, WA: International Seabed Authority (ISA).

Smith, C. R., Paterson, G., Lambshead, J., Glover, A., Rogers, A., Gooday, A., et al. (2008a). *Biodiversity, Species Ranges, and Gene Flow in the Abyssal Pacific Nodule Province: Predicting and Managing the Impacts of Deep Seabed Mining. ISA Technical Study No.* 3. Friday Harbor, WA: International Seabed Authority (ISA).

Smith, C. R., De Leo, F. C., Bernadion, A. F., Sweetman, A. K., and Arbizu, P. M. (2008b). Abyssal food limitation, ecosystem structure and climate change. *Trends Ecol. Evol.* 23, 518–528. doi: 10.1016/j.tree.2008.05.002

Smith, C. R., and Rabouille, C. (2002). What controls the mixed-layer depth in deep-sea sediments? The importance of POC flux. *Limnol. Oceanogr.* 47, 418–426. doi: 10.4319/lo.2002.47.2.0418

Stat, M., Huggett, M. J., Bernasconi, R., DiBattista, J. D., Berry, T. E., Newman, S. J., et al. (2017). Ecosystem biomonitoring with eDNA: metabarcoding across the tree of life in a tropical marine environment. *Sci. Rep.* 7:12240. doi: 10.1038/s41598-017-12501-5

Strickler, K. M., Fremier, A. K., and Goldberg, C. S. (2015). Quantifying effects of UV-B, temperature, and pH on eDNA degradation in aquatic microcosms. *Biol. Conserv.* 183, 85–92. doi: 10.1016/j.biocon.2014.11.038

Sweetman, A. K., Thurber, A. R., Smith, C. R., Levin, L. A., Mora, C., Wei, C.-L., et al. (2017). Major impacts of climate change on deep-sea benthic ecosystems. *Elementa* 5:4. doi: 10.1525/elementa.203

Tanabe, A. S., Nagai, S., Hida, K., Yasuike, M., Fujiwara, A., Nakamura, Y., et al. (2016). Comparative study of the validity of three regions of the 18S-rRNA gene for massively parallel sequencing-based monitoring of the planktonic eukaryote community. *Mol. Ecol. Resour.* 16, 402–414. doi: 10.1111/1755-0998.12459

Thiel, H., Schriever, G., Bussau, C., and Borowski, C. (1993). Manganese nodule crevice fauna. *Deep Sea Res. 1 Oceanogr. Res. Pap.* 40, 419–423. doi: 10.1016/0967-0637(93)90012-R

Thistle, D. (2003). *The Deep-Sea Floor: An Overview Ecosystems of the Deep Ocean*. (Amsterdam: Elsevier).

Thomsen, P. F., Kielgast, J., Iversen, L. L., Møller, P. R., Rasmussen, M., and Willerslev, E. (2012). Detection of a diverse marine fish fauna using environmental DNA from seawater samples. *PLoS One* 7:e41732. doi: 10.1371/journal.pone.0041732

Thurber, A. R., Sweetman, A. K., Narayanaswamy, B. E., Jones, D. O. B., Ingels, J., and Hansman, R. L. (2014). Ecosystem function and services provided by the deep sea. *Biogeosciences* 11, 3941–3963. doi: 10.5194/bg-11-3941-2014

Torti, A., Lever, M. A., and Jørgensen, B. B. (2015). Origin, dynamics, and implications of extracellular DNA pools in marine sediments. *Mar. Genomics* 24, 185–196. doi: 10.1016/j.margen.2015.08.007

Vanreusel, A., Hilario, A., Ribeiro, P. A., Menot, L., and Arbizu, P. M. (2016). Threatened by mining, polymetallic nodules are required to preserve abyssal epifauna. *Sci. Rep.* 6:26808. doi: 10.1038/srep26808

Vinogradov, M. E. (1970). *Vertical Distribution of the Oceanic Zooplankton*. Jerusalem: Israel Program for Scientific Translations.

Volz, J. B., Mogollón, J. M., Geibert, W., Arbizu, P. M., Koschinsky, A., and Kasten, S. (2018). Natural spatial variability of depositional conditions, biogeochemical processes and element fluxes in sediments of the eastern Clarion-Clipperton Zone, Pacific Ocean. *Deep Sea Res. Part I Oceanogr. Res. Pap.* 140, 159–172. doi: 10.1016/j.dsr.2018.08.006

Wedding, L. M. M., Friedlander, A. M. M., Kittinger, J. N. N., Watling, L., Gaines, S. D. D., Bennett, M., et al. (2013). From principles to practice: a spatial approach to systematic conservation planning in the deep sea. *Proc. R. Soc. B* 280:20131684. doi: 10.1098/rspb.2013.1684

Wedding, L. M. M., Reiter, S. M., Smith, C. R., Gjerde, K. M., Kittinger, J. N., Friedlander, A. M., et al. (2015). Managing mining of the deep seabed. *Science* 349, 144–145. doi: 10.1126/science.aac6647

Wickham, H. (2016). *ggplot2: Elegant Graphics for Data Analysis*. New York, NY: Springer-Verlag.

Youngbluth, M., Sørnes, T., Hosia, A., and Stemmann, L. (2008). Vertical distribution and relative abundance of gelatinous zooplankton, in situ observations near the Mid-Atlantic Ridge. *Deep Sea Res. Part II Top. Stud. Oceanogr.* 55, 119–125. doi: 10.1016/j.dsr2.2007.10.002

Zhan, A., Hulák, M., Sylvester, F., Huang, X., Adebayo, A. A., Abbott, C. L., et al. (2013). High sensitivity of 454 pyrosequencing for detection of rare species in aquatic communities. *Methods Ecol. Evol.* 4, 558–565. doi: 10.1111/2041-210X.12037

Conflict of Interest: The authors declare that the research was conducted in the absence of any commercial or financial relationships that could be construed as a potential conflict of interest.

Copyright © 2020 Laroche, Kersten, Smith and Goetze. This is an open-access article distributed under the terms of the Creative Commons Attribution License (CC BY). The use, distribution or reproduction in other forums is permitted, provided the original author(s) and the copyright owner(s) are credited and that the original publication in this journal is cited, in accordance with accepted academic practice. No use, distribution or reproduction is permitted which does not comply with these terms.

frontiers in Marine Science

ORIGINAL RESEARCH
published: 09 December 2020
doi: 10.3389/fmars.2020.558860

Using Habitat Classification to Assess Representativity of a Protected Area Network in a Large, Data-Poor Area Targeted for Deep-Sea Mining

Kirsty A. McQuaid[1], Martin J. Attrill[1], Malcolm R. Clark[2], Amber Cobley[3,4], Adrian G. Glover[3], Craig R. Smith[5] and Kerry L. Howell[1]*

[1] School of Biological and Marine Sciences, University of Plymouth, Plymouth, United Kingdom, [2] National Institute of Water and Atmospheric Research, Wellington, New Zealand, [3] Department of Life Sciences, The Natural History Museum, London, United Kingdom, [4] Ocean and Earth Science, University of Southampton, Southampton, United Kingdom, [5] Department of Oceanography, University of Hawai'i at Manoa, Honolulu, HI, United States

Extractive activities in the ocean are expanding into the vast, poorly studied deep sea, with the consequence that environmental management decisions must be made for data-poor seafloor regions. Habitat classification can support marine spatial planning and inform decision-making processes in such areas. We present a regional, top–down, broad-scale, seafloor-habitat classification for the Clarion-Clipperton Fracture Zone (CCZ), an area targeted for future polymetallic nodule mining in abyssal waters in the equatorial Pacific Ocean. Our classification uses non-hierarchical, k-medoids clustering to combine environmental correlates of faunal distributions in the region. The classification uses topographic variables, particulate organic carbon flux to the seafloor, and is the first to use nodule abundance as a habitat variable. Twenty-four habitat classes are identified, with large expanses of abyssal plain and smaller classes with varying topography, food supply, and substrata. We then assess habitat representativity of the current network of protected areas (called Areas of Particular Environmental Interest) in the CCZ. Several habitat classes with high nodule abundance are common in mining exploration claims, but currently receive little to no protection in APEIs. There are several large unmanaged areas containing high nodule abundance on the periphery of the CCZ, as well as smaller unmanaged areas within the central CCZ, that could be considered for protection from mining to improve habitat representativity and safeguard regional biodiversity.

Keywords: habitat classification, marine spatial planning, deep-sea mining, polymetallic nodules, CCZ, conservation, Areas of Particular Environmental Interest (APEI), environmental management plan

OPEN ACCESS

Edited by:
Erik Cordes,
Temple University, United States

Reviewed by:
Tim O'Hara,
Museums Victoria, Australia
Dick Van Oevelen,
Royal Netherlands Institute for Sea Research (NIOZ), Netherlands

****Correspondence:***
Kirsty A. McQuaid
kirsty.mcquaid@plymouth.ac.uk

Specialty section:
This article was submitted to Deep-Sea Environments and Ecology, a section of the journal Frontiers in Marine Science

Received: *04 May 2020*
Accepted: *13 November 2020*
Published: *09 December 2020*

Citation:
McQuaid KA, Attrill MJ, Clark MR, Cobley A, Glover AG, Smith CR and Howell KL (2020) Using Habitat Classification to Assess Representativity of a Protected Area Network in a Large, Data-Poor Area Targeted for Deep-Sea Mining. Front. Mar. Sci. 7:558860. doi: 10.3389/fmars.2020.558860

INTRODUCTION

Human activities and climate change have been shown to significantly impact the deep sea (Glover and Smith, 2003; Ramirez-Llodra et al., 2011), and human influence has been recorded in even the deepest part of the ocean, the Mariana Trench (Chiba et al., 2018). With human activity continuing to expand into large, poorly known areas of the deep sea, the global community must manage

extractive activities sustainably and minimize damage to deep-sea ecosystems, particularly in Areas Beyond National Jurisdiction (ABNJ) regulated by the United Nations Convention on the Law of the Sea (UNCLOS) (Ardron et al., 2008; Altvater et al., 2019).

Ecosystem-based management is a best-practice approach to manage sustainably human activities in marine ecosystems, and is implemented through a number of different management measures, including Marine Spatial Planning (MSP). MSP is an area-based planning approach that allocates space in the marine environment to different users based on ecological, economic and social objectives, in order to balance demands for economic development with the need for environmental protection (Ehler and Douvere, 2007).

In order to achieve ecological goals in a specific area, such as to conserve biodiversity, MSP may involve the allocation of protected areas where certain human activities are limited. Marine Protected Areas (MPAs) have been shown to have numerous conservation benefits (Lubchenco et al., 2003; Mumby and Harborne, 2010; Edgar et al., 2014), and have gained political support (O'Leary et al., 2012). Whereas MPAs were historically established on an *ad hoc* and individual basis (United Nations Environment Programme World Conservation Monitoring Centre, 2008; Toropova et al., 2010), best practices now focus on establishing networks of protected areas to advance protection (Dudley, 2008; Johnson et al., 2014).

Although some nations have specific MSP requirements in their national laws or policies (e.g., the EU: Official Journal of the European Union, 2014; and South Africa: Republic of South Africa, 2017; Republic of South Africa, 2019), MSP is not mentioned explicitly in any international legislation pertaining to ABNJ (Ardron et al., 2008; Maes, 2008; De Santo, 2018). This has been highlighted as an integral component to be included in negotiations on a new, international, legally binding instrument on the conservation and sustainable use of marine biological diversity in ABNJ (United Nations Environment Programme World Conservation Monitoring Centre, 2018; Wright et al., 2018; Altvater et al., 2019). In the meantime, there are several mechanisms through which area-based management tools (ABMTs) can be implemented in ABNJ, i.e., spatial closures with "regulation of one or more or all human activities, for one or more purposes" (Molenaar, 2013). These include: closures of Vulnerable Marine Ecosystems (VMEs) to bottom-fishing, implemented through Regional Fisheries Management Organizations (RFMOs) (Food and Agriculture Organization of the United Nations, 2009; Wright et al., 2015); high seas MPAs, declared in the Southern Ocean under the Convention on the Conservation of Antarctic Marine Living Resources (CCAMLR) and in the Northeast Atlantic Ocean through the OSPAR Convention and the North-east Atlantic Fisheries Commission (NEAFC) (De Santo, 2018); and Emission Control Areas/Special Areas and Particularly Sensitive Sea Areas (PSSAs), put in place through the International Maritime Organization's (IMO) International Convention for the Prevention of Pollution from Ships (MARPOL). In addition, ecologically or biologically significant areas (EBSAs), that are important for maintaining healthy oceans (Convention on Biological Diversity, 2009), can be identified through the Convention on Biological Diversity (CBD).

Proposed deep-sea mining in the Clarion-Clipperton Fracture Zone (CCZ), eastern-central Pacific Ocean, is an important test case for MSP as it represents an example of an environmental impact that must be mitigated through spatial means, as the likely recovery times of the impacted areas are on very long, geological time-scales (Jones et al., 2017). Additionally, it is the first example of a major high-seas activity where the regulations are being put into place before the industrial activity occurs. Some MSP has been undertaken in the CCZ, with the designation of Areas of Particular Environmental Interest (APEIs) by the International Seabed Authority (ISA) to conserve regional biodiversity (International Seabed Authority, 2011). The ISA was established through UNCLOS and acts on behalf of humankind as a whole to oversee all activities for mineral prospecting, exploration and exploitation in ABNJ. The CCZ is a key area of interest for mineral exploration companies and the ISA as it contains the greatest global concentration of high-grade polymetallic nodules (International Seabed Authority, 2010), which are potato-sized mineral deposits containing commercially valuable metals such as copper, nickel, cobalt, and manganese.

The CCZ APEI network was designated through the CCZ Environmental Management Plan (EMP) and was intended to protect regional biodiversity (International Seabed Authority, 2011). The network was based on recommendations by an international collaboration of experts and was designed using the principles of: compatibility with the existing legal framework for protection; minimizing socio-economic impacts; maintaining sustainable, intact and healthy populations; accounting for regional ecological gradients; habitat representativity; creating buffer zones; and using straight-line boundaries to ease compliance (Wedding et al., 2013). Experts split the CCZ area into nine representative sub-regions based on environmental surrogates of biodiversity and community structure (nodule abundance, export production, seamount distribution, bathymetry) and macrobenthic abundance, with a 400 × 400 km APEI placed within each sub region (Wedding et al., 2013). Other MSP efforts in this area have included discussions around impact and preservation reference zones (IRZs and PRZs), which are required within exploration contract areas to facilitate monitoring of mining impacts (International Seabed Authority, 2000, Regulation 31, para. 7; International Seabed Authority, 2017c). The ISA has committed to reviewing the CCZ EMP every 5–10 years, providing an opportunity to update and improve it. Part of the first review was carried out in July 2016, and found that additional APEIs may be required in the CCZ to ensure adequate protection of regional biodiversity (International Seabed Authority, 2016).

Some of the most common and useful tools to support MSP and area-based management are habitat classifications, which partition an area into distinct groups or classes that contain environmental properties and/or a biological community that is unique to that class (United Nations Educational, Scientific and Cultural Organization, 2009; Howell, 2010). This identification and delineation of different types of marine habitats and the

communities they contain supports planning on how and where to protect habitats (Roff et al., 2003; Ehler and Douvere, 2007). For example, classifications can be used to identify habitats that are relatively rare or fragmented (United Nations Educational, Scientific and Cultural Organization, 2009; Howell, 2010). They provide a science-based framework that can be used as a tool by decision-makers (e.g., governments or international institutions) to support planning concerning what activities should (or should not) be allowed where (United Nations Educational, Scientific and Cultural Organization, 2009).

There are many different approaches for carrying out habitat classification and, due to a paucity of data, most involve the use of surrogates to represent biological diversity (e.g., Roff and Taylor, 2000; Harris and Whiteway, 2009; Howell, 2010; Clark et al., 2011; Evans et al., 2015). Surrogates used are generally chemical, physical or environmental variables that are more readily available than biological data and, critically, are identified as important factors driving the distribution and turnover of species and communities (Howell, 2010; Evans et al., 2015). Habitat maps produced through classifications using surrogates are then used to infer the distribution of a species, community, or ecosystem.

The scale of classifications varies greatly, from relatively fine-scale classifications focused on national waters (e.g., Roff and Taylor, 2000; Connor et al., 2004; Lombard et al., 2004; Leathwick et al., 2006; Lundblad et al., 2006; Snelder et al., 2006; Verfaillie et al., 2009; Last et al., 2010; Ramos et al., 2015) through regional-scale approaches (e.g., Davies et al., 2004; Grant et al., 2006; Howell, 2010; Ramos et al., 2012; Douglass et al., 2014; Evans et al., 2015), to global biogeographic classifications (e.g., Sherman, 1986; Spalding et al., 2007; Harris and Whiteway, 2009; United Nations Educational, Scientific and Cultural Organization, 2009; Clark et al., 2011; Watling et al., 2013; Sayre et al., 2017; Sutton et al., 2017).

Most classifications have been carried out in shallow and coastal waters to support management of activities at a national level (see examples above); however, a number have been applied to deep waters (>200 m) in ABNJ to classify offshore benthic (e.g., Howell, 2010; Watling et al., 2013; Douglass et al., 2014; Evans et al., 2015) and pelagic (e.g., Longhurst, 2007; United Nations Educational, Scientific and Cultural Organization, 2009; Sayre et al., 2017; Sutton et al., 2017) habitat types, as well as specific features (e.g., seamounts, Clark et al., 2011).

In the equatorial Pacific Ocean, where the CCZ is located, several global classification efforts have identified broad biogeographic provinces (see Watling et al. (2013) for a full review of deep-sea benthic classification schemes). The Global Open Oceans and Deep Seabed (GOODS) biogeographic classification used environmental and, where available, biological data to divide the global oceans into 68 provinces, with 14 of these abyssal (United Nations Educational, Scientific and Cultural Organization, 2009). The abyssal and bathyal portions of this bioregionalization were then improved by Watling et al. (2013), resulting again in 14 abyssal provinces. Harris and Whiteway (2009) also proposed a global benthic classification, based on physical and chemical variables, and identified 11 biogeographic provinces, which they called seascapes. Finally, the most recent global biogeographic classification was carried out by Sayre et al. (2017), and put forward 37 different Ecological Marine Units, identified using a classification of physical and chemical variables stratified from surface waters to the seafloor.

The CCZ EMP area falls within one or two of the biogeographic provinces identified through these above studies. While a useful starting point, these global level classifications do not offer the resolution needed to make regional management decisions. Several areas in ABNJ have received a lot of attention, for example the Northeast Atlantic Ocean (Howell, 2010; Evans et al., 2015) and the Southern Ocean (Grant et al., 2006; Douglass et al., 2014); however, there have been no detailed regional classification efforts in the equatorial Pacific to date, and a more regional approach is thus required. There have been calls for quantitative habitat mapping in the CCZ to support the spatial management of mining activities (e.g., De Smet et al., 2017; International Seabed Authority, 2017b), and the use of surrogate data is of particular benefit in this area, as it is data-poor on a regional scale.

MSP is essential to the environmental management of mining activities (Lodge et al., 2014; Wedding et al., 2015; Vanreusel et al., 2016), and habitat classifications can play a role in supporting this. Because MSP approaches are used to both design and assess effectiveness of existing MPA networks (e.g., Douglass et al., 2014; Evans et al., 2015; Foster et al., 2017), this tool is relevant to the ISA for development of environmental management frameworks for mining activities, and for future monitoring of such activities. Although some MSP has been undertaken in the CCZ as an input to the establishment of an APEI network (Wedding et al., 2013), no fully quantitative regional habitat classification has been undertaken in this area to support the EMP process.

This study is intended to support spatial planning associated with seabed mining, by bridging the gap between policy demands (e.g., the obligation of the ISA to assess the APEI network) and available scientific data. In this study, we present a broad-scale habitat map of the CCZ EMP area using a top–down habitat classification system of environmental surrogates developed through non-hierarchical cluster analysis. We then use this map to assess the habitat representativity of the current APEI network.

MATERIALS AND METHODS

Study Region

The CCZ is an area of approximately 6 million km^2, located between the Clarion and Clipperton fracture zones in the equatorial Pacific Ocean (Wedding et al., 2013). It is an abyssal plain area lying mostly between 4,000 and 6,000 m deep, with topographic features such as seamounts, abyssal hills, troughs and ridges, and the highest known global concentration of high-grade polymetallic nodules (International Seabed Authority, 2010).

There are strong environmental gradients across the CCZ, in both latitudinal and longitudinal directions. Particulate organic carbon flux to the seafloor (POC flux), depth and sediment characteristics vary across the region, resulting in differences in both nodule size and abundance as well as the composition of faunal communities (Smith et al., 1997; International Seabed Authority, 2010; Wedding et al., 2013).

The model domain for this study was defined by the boundaries in the CCZ EMP (International Seabed Authority, 2011) (shifted slightly east to encompass all contract areas comfortably): 0°–23°30′ N × 114° W-159° W (**Figure 1**). The EMP area includes APEIs, exploration contract areas, and reserved areas that are set aside for exploration by developing states or the ISA (International Seabed Authority, 2013).

Habitat Classification

We have used a two-step process to classify environmental surrogates in the CCZ. First, each environmental variable (or class of variables) was clustered (using a k-medoids, non-hierarchical clustering algorithm) to identify areas with different environmental conditions. Then, the outputs of the clustering for each environmental variable (or class of variables) were combined to give a final habitat classification.

Variable Selection

Environmental variables were selected for the classification based on evidence of key drivers of biophysical and ecological patterns and processes in the CCZ and the availability of those variables as continuous datasets across the region.

The variables used in this study were topography, POC flux to the seafloor and nodule abundance. While other variables may contribute to ecological patterns and processes in the CCZ, the selected variables are the most important variables (of those available) that have the strongest influences on biological communities in this area, as considered by an expert workshop on deep CCZ biodiversity (International Seabed Authority, 2020). It was expected that these drivers would be correlated with other parameters that were not included but may also influence species distributions. Although water-mass structure can be an important factor in determining the distribution of organisms in some marine environments (Tyler and Zibrowius, 1992; Howell et al., 2002; Miller et al., 2011), and has been used in global biogeographic classifications (e.g., Watling et al., 2013) to gain insight into species connectivity from transport and mixing processes, water-mass variables were not included because variations in water-mass structure (e.g., in temperature, salinity, dissolved oxygen concentration) are very small at the abyssal seafloor in the CCZ, and there is no evidence that water-mass structure drives differences in faunal communities across this area.

Topography

Depth and topography play an important role in determining species distributions in the deep sea, with species showing preference for certain depth ranges and topographic conditions (Rowe and Menzies, 1969; Hecker, 1990; Rice et al., 1990). In abyssal regions, and specifically the CCZ, where there are seamounts, troughs and ridges, topographic variation has been shown to influence biological communities (Durden et al., 2015; Stefanoudis et al., 2016; Leitner et al., 2017; Simon-Lledó et al., 2019a).

Although depth is a crucial factor in determining species distribution, and depth data is readily available, this parameter acts as an indirect surrogate for those variables actually driving distributions, such as temperature, pressure, oxygen, water mass structure and food supply (Evans et al., 2015), and was therefore excluded from this study. Rather, the underlying variables driving distributions were included (see below) and derivatives of bathymetry were used to represent topographic features of the region: slope, broad-scale bathymetric position index (BBPI) and fine-scale bathymetric position index (FBPI).

Slope is a first-order derivative of bathymetry, and acts as a surrogate for local hydrodynamics (Guinan et al., 2009), as benthic currents are steered by seafloor terrain and current velocities can be enhanced along steep slopes (Genin et al., 1986). Such currents affect sediment particle size distribution and drive the near-seabed horizontal flux of food particles to influence the abundance and community structure of benthic assemblages, particularly suspensions feeders (Gage and Tyler, 1996; Durden et al., 2015).

Bathymetric position index (BPI) is a second-order derivative of bathymetry, and gives the relative elevation of a point in relation to the overall landscape (Lundblad et al., 2006). Positive values indicate features rising above the surrounding terrain (e.g., peaks and crests), while negative values indicate depressions such as valleys and troughs. Areas with constant slope or flat areas are represented by near-zero values. BPI acts as a surrogate for various environmental factors that affect species distributions, such as exposure to current, current speed and sedimentation, without confounding the effects of other variables (e.g., temperature and salinity) as depth does (Evans et al., 2015).

Topographic variables were derived from the publically available General Bathymetric Chart of the Oceans (GEBCO) 2014 gridded bathymetry data[1]. All variables were generated in ArcMap 10.4 using the Benthic Terrain Modeler extension (Wright et al., 2005) (**Figure 2**). Slope is determined as the largest change in elevation between a cell and its 8 nearest neighbors. BPI was derived at both broad and fine scale (called BBPI and FBPI, respectively), to capture topographic features at different scales across the region. BBPI was derived with an inner radius of 1 and an outer radius of 100, with a scale factor of 100 km. This broad-scale layer identified large geomorphological units, such as abyssal plains, steps and troughs. FBPI was derived with an inner radius of 1 and an outer radius of 10, with a scale factor of 10 km. This finer scale layer identified smaller "megahabitats," i.e., features on the scale of kilometers to tens of kilometers, as defined in Greene et al. (1999). These features included seamounts, abyssal hills, canyons, plateaus, large banks and terraces.

Particulate organic carbon flux

Food availability plays arguably the most important role in determining the distribution of organisms at abyssal depths

[1]https://www.gebco.net/

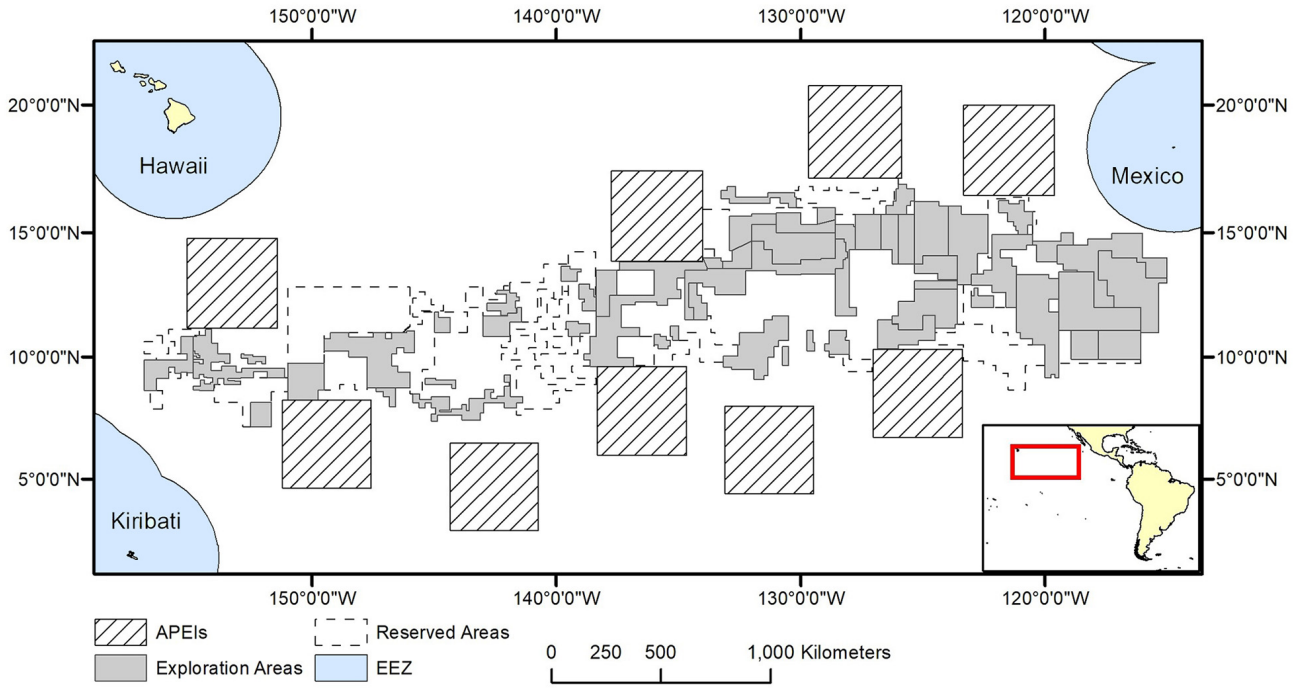

FIGURE 1 | Polymetallic nodule exploration areas in the Clarion-Clipperton Fracture Zone, showing contractor exploration areas, reserved areas and Areas of Particular Environmental Interest (APEIs).

(Cartes and Sarda, 1993; Smith et al., 1997, 2008; Levin et al., 2001; Gooday, 2002; Ruhl and Smith, 2004; Wei et al., 2011; Woolley et al., 2016). In this food-poor environment, organisms are dependent on detrital matter in the form of POC sinking from surface waters to the seafloor (POC flux), except for cases of large organic food falls and chemosynthetic habitats (Turner, 1973; Gooday et al., 1990; Van Dover, 2000; Smith and Baco, 2003). As a result, community structure, function and diversity, life history patterns, body size, and feeding type, amongst others, are all strongly dependent on POC flux to the seafloor (Smith et al., 2008).

In the CCZ there is a strong gradient in POC flux, decreasing from east to west, and from south to north (Smith et al., 1997; Pennington et al., 2006; Lutz et al., 2007). This gradient has been linked to differences in faunal communities (e.g., Smith et al., 1997, 2008; Veillette et al., 2007; Vanreusel et al., 2016; Bonifácio et al., 2020).

Estimates for POC flux to the seafloor in the CCZ were obtained from a global model produced by Lutz et al. (2007), based on water depth and seasonal variability in remote-sensed net primary productivity data between 1997 and 2004. These estimates were interpolated to a 1 km^2 resolution across the model domain using kriging (**Figure 3**).

Substrate

The use of substrate as a surrogate to represent biological diversity in deep-sea habitat classifications is well established (Howell, 2010). Although there is no global map of seabed substrate, polymetallic nodules provide most of the hard substrate in the CCZ and their abundance thus provides a proxy for hard substrate across the region.

Nodules provide habitat for encrusting and epifaunal species that depend on hard surfaces for attachment and feeding (e.g., Dugolinsky et al., 1977; Gooday et al., 2015; Amon et al., 2016), and support a range of fauna in nodule crevices (Thiel et al., 1993; Bussau et al., 1995). The increased habitat heterogeneity provided by nodules has been suggested to influence faunal standing stocks and enhance biodiversity compared to nodule-free abyssal environments (Amon et al., 2016; Vanreusel et al., 2016; Gooday et al., 2017), and a recent study provided the first quantified evidence that variations in nodule cover in the CCZ influence faunal standing stock, faunal composition, functional group composition, the distribution of individual species and some biodiversity attributes (Simon-Lledó et al., 2019b).

Modeled estimates of nodule abundance across the CCZ region were obtained from an existing geological model of nodule deposits in the CCZ, produced as part of an ISA technical study (see International Seabed Authority, 2010) (**Figure 3**). This model was developed by a group of technical experts (not the authors of the current study) and used both publicly available and proprietary data (i.e., data belonging to contractors with exploration contracts), primarily from the central CCZ. Five datasets comprising 61,583 stations provided data on nodule abundance (weight of nodules per unit of seafloor area in $kg.m^{-2}$), mainly from free-fall grab samples and some box cores. In order to protect proprietary concerns, data were grouped at one–tenth of a degree resolution, and then interpolated and extrapolated to estimate nodule abundance across the CCZ in

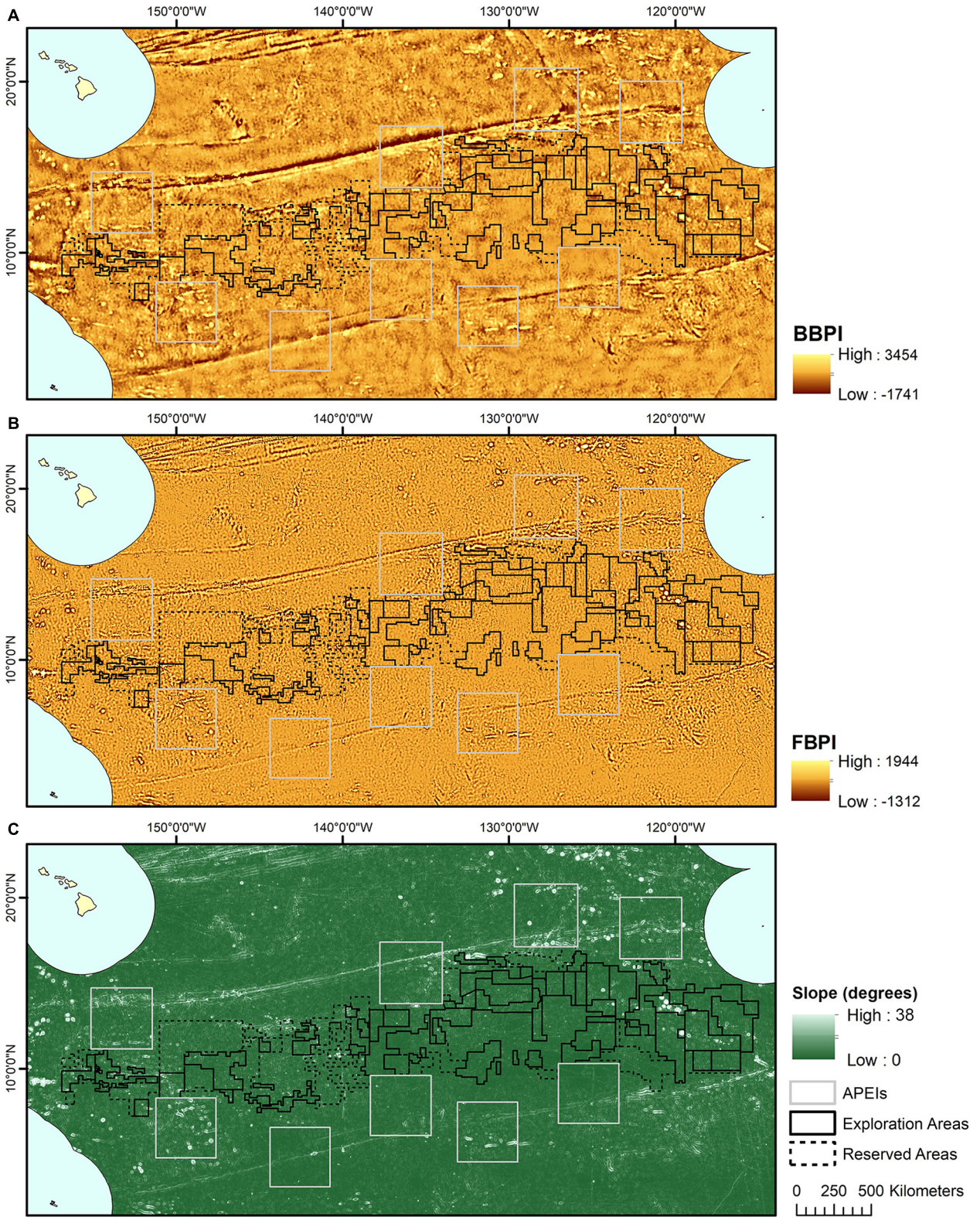

FIGURE 2 | Topographic variable layers used in initial clustering, **(A)** broad-scale bathymetric position index (BBPI), **(B)** fine-scale bathymetric position index (FBPI), and **(C)** slope, derived from GEBCO 2014 bathymetry data and interpolated to 1 km^2 resolution. Land masses are shown in cream as labeled in **Figure 1**, surrounded by EEZs in pale blue.

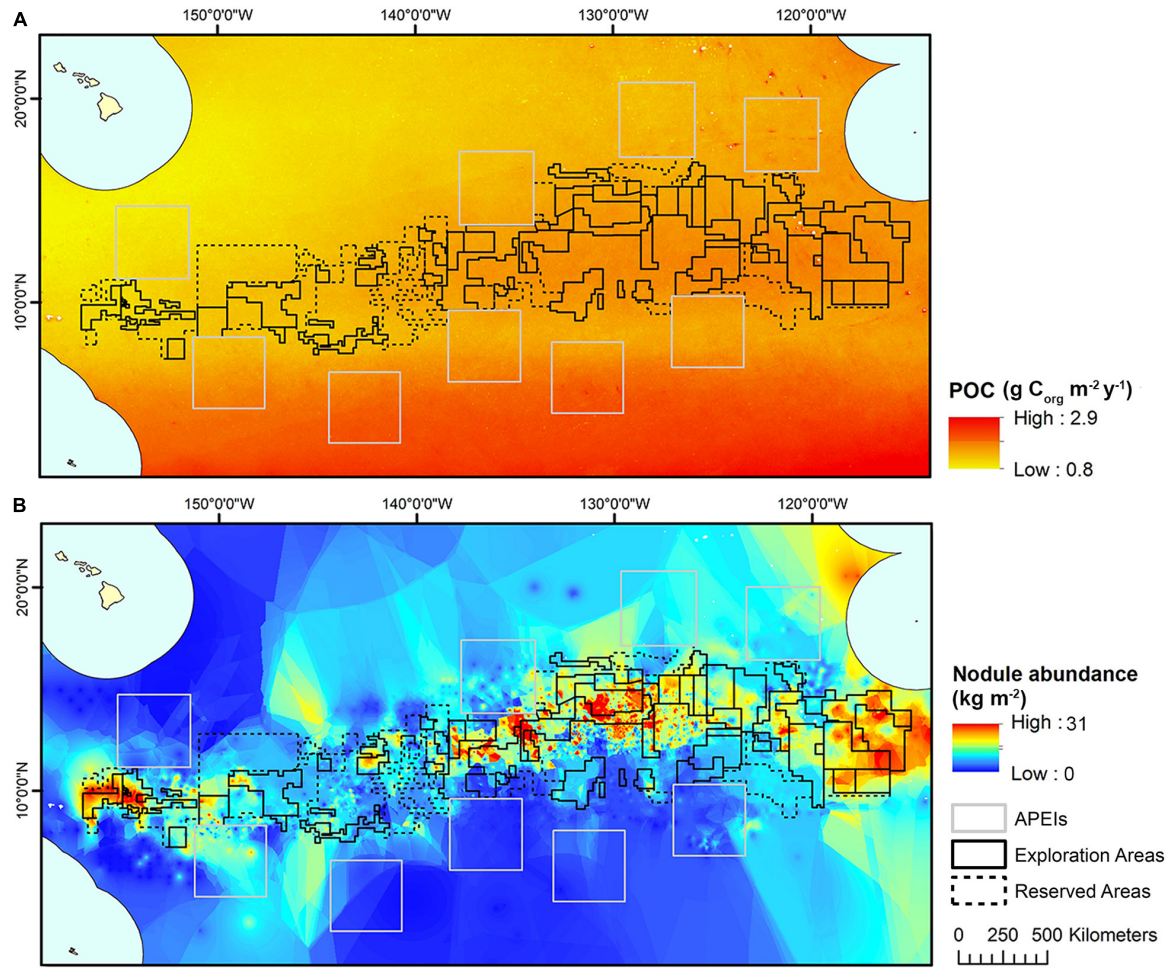

FIGURE 3 | (A) POC flux at the seafloor modeled across the CCZ by Lutz et al. (2007), interpolated to 1 km^2 resolution and used in initial clustering and **(B)** Nodule abundance modeled across the CCZ (see International Seabed Authority, 2010), interpolated to 1 km^2 resolution and used in initial clustering.

areas not covered by available data. For more information on the nodule abundance data used in this study see International Seabed Authority (2010).

Although this data layer does not reflect the high variability in nodule abundance on small spatial scales (Peukert et al., 2018), it is the best available data, and the classification makes the assumption that broad patterns in nodule abundance are more important than smaller scale heterogeneity in driving regional patterns in species distributions.

Pre-processing and Cluster Analysis

All environmental variables were interpolated to 1 km^2 and projected in WGS 1984 PDC Mercator, an equal-area projection suitable for use in the Pacific Ocean. An equal-area projection was used so that estimates of the area of each habitat class identified through the classification could be calculated. Mercator is also a popular projection for navigation as it uses straight-line segments that represent true bearings, and outputs from the classification could therefore be used to support the implementation of spatial management measures.

We used an unsupervised, non-hierarchical clustering algorithm called Clustering Large Applications (CLARA) (Kaufman and Rousseeuw, 1990). CLARA is a k-medoids technique that clusters data points around the medoids (similar in concept to centroids, but always members of the data set) and is appropriate for use with large datasets.

A separate CLARA analysis was used to carry out unsupervised clustering on each class of variable: (1) topographic variables (FBPI, BBPI and slope), (2) POC flux, and (3) nodule abundance. This step allowed the combination of multiple topographic variables to produce a single layer representing the topographic variable class, and thus providing equal weighting to all classes of variables (topography, POC flux and nodule abundance) when combined in the final classification (see below). Based on the current level of knowledge of the drivers of species distributions in the CCZ, and in abyssal plains in general, it is not yet possible to confer weighting to classes of variables. An alternative approach would be to use all five environmental variables in a single clustering step. However, we felt this was inappropriate as this would give greater weighting to the role

of topography in the resulting classification output simply due to the use of more topographic environmental variables. Our approach ensured topography, POC flux to depth, and nodule abundance contributed equally to the final output.

Pre-processing and clustering was carried out in ArcGIS 10.4 and R 3.3.1 (R Core Team, 2017), within the Rstudio environment (RStudio Team, 2015), using the "fpc" package and CLARA function (Hennig, 2015). As the focus of this study is on the deep sea in international waters, the EEZs of countries were excluded from the analysis. Prior to clustering, all variables were normalized to have equal variance and a common scale of 0–1. CLARA requires the user to define the number of clusters the dataset should be split into, and for each analysis clustering was therefore run a number of times, using a different number of clusters in each iteration, in order to identify the most parsimonious number of clusters (see below). Reproducible code for the cluster analysis is available in Supplementary Materials.

Evaluation of Clusters

In order to evaluate clustering and select appropriate numbers of clusters, two indices were used: average silhouette width (ASW) and the Calinski-Harabasz index (CH) (both built into the R CLARA function). The silhouette width of an object is a measure of how similar it is to its own cluster, compared to other clusters. ASW gives the average of all silhouette widths in a dataset, with the output being one value representing the overall silhouette width for the whole cluster analysis. This method compares the ASW of clustering iterations with different numbers of clusters, and the optimum number of clusters is the one with the highest ASW (Kaufman and Rousseeuw, 1990). The CH index assesses clustering by comparing the average between- and within-cluster sum of squares (Calinski and Harabasz, 1974). Here again the best clustering is the iteration with the largest CH value. Expert judgment based on literature and unpublished data was also used to further refine the final choice of number of clusters.

Finalization of Classification

Once the number of clusters was finalized for each variable class (topography, POC flux and nodule abundance), the three layers were combined in ArcGIS 10.4 using the "Combine" tool to produce the final habitat classification. This was a raster layer, with each cell assigned a habitat class representing a different set of environmental conditions, showing habitat heterogeneity across the region. As the modeled nodule layer displayed artifacts toward the periphery of the model domain, and certain combinations of environmental conditions were improbable (discussed below), a manual assessment of the confidence level of each habitat class was also carried out.

APEI Representativity

In order to test the habitat representativity of the current APEI network, the proportions of each habitat class from the classification located in the APEIs, exploration and/or reserved areas, and unmanaged areas of the CCZ EMP area were calculated. Under the CBD, the current target for global representation of coastal and marine areas is 10% of target regions by 2020 (Convention on Biological Diversity, 2010), with a more ambitious target of 30% advocated at the 2003 and 2014 World Parks Congress (International Union for Conservation of Nature, 2005, 2014). In addition, Foster et al. (2013) calculated that between 30 and 40% was needed to conserve 75% of bathyal deep-sea species. Proportions of each habitat class in the current APEI network were compared to these targets. In addition, the number of APEIs within which each habitat class occurs was also calculated. Habitat classes with lower confidence were included in these calculations, and where reported are accompanied by the caveat that these should be treated with caution. All analyses were carried out in ArcGIS 10.6.

RESULTS

Initial Clustering

In most cases, the clustering iteration with the highest ASW and CH values were chosen for the habitat classification, and this decision was supported by literature and expert review (**Table 1**). Topographic variables showed the best clustering with two groups. The two topographic clusters distinguished areas that were relatively flat (0 – 6 degrees slope), with small topographic features, from those that were more sloped (0 – 38 degrees), with more prominent peaks and troughs (**Table 2** and **Figure 4A**).

Seafloor POC flux clustered best into 8 and 10 groups (based on ASW and CH indices, respectively), and this highlighted what is known in the literature of trends in POC flux across the region, with a gradient of high to low POC flux from east to west and south to north (Lutz et al., 2007). However, ASW and CH indices also performed well with just 3 clusters, and in order to simplify the classification this smaller number of clusters was chosen (**Table 2** and **Figure 4B**). This clustering captured the broad pattern of seafloor POC flux across the region and supported variation in macrofauna community structure observed in the CCZ, from east to west and south to north (e.g., Glover et al., 2002; Smith et al., 2008; Bonifácio et al., 2020). It also aligned with the north-south split in biogeographic provinces in the CCZ identified by the GOODS (United Nations Educational, Scientific and Cultural Organization, 2009) and Watling et al. (2013) classifications in this region, which were both driven primarily by differences in POC flux.

Nodule abundance showed the best clustering with 4 and 8 groups (based on ASW and CH respectively). Given the current state of knowledge on the influence of nodule abundance on species distributions and the high CH value for 4 groups, 4 clusters were chosen for the final classification (**Table 2** and **Figure 4C**). These four levels allow discrimination between areas of high and low nodule density at less than 50% nodule cover and for which there is ample evidence of difference in community composition and densities (Amon et al., 2016; Vanreusel et al., 2016; Simon-Lledó et al., 2019b), but also allows for the uncertainty in what happens to reported relationships at nodules densities > 50% and for which there are no published studies. Areas of medium to high nodule abundance were concentrated in the central CCZ, with some medium to high nodule abundance areas also predicted in the north- and southeast, as well as the southwest. Predictions of high nodule abundance to the

TABLE 1 | Average silhouette width (ASW) and Calinski-Harabasz index (CH) for CLARA clustering iterations with 1–10 clusters for each class of environmental variables.

	Topography		POC flux		Nodule abundance	
Cluster iteration	**ASW**	**CH**	**ASW**	**CH**	**ASW**	**CH**
1	0	0	0	0	0	0
2	**0.55***	**4,093,629***	0.65	23,588,718	0.61	11,301,256
3	0.19	1,916,862	**0.60***	**35,745,701***	0.60	22,179,059
4	0.21	3,122,666	0.55	37,216,659	**0.66***	**34,759,846***
5	0.27	3,696,423	0.60	35,262,108	0.61	33,769,147
6	0.28	3,206,235	0.56	48,433,936	0.59	30 253 193
7	0.31	3,294,704	0.56	47,289,350	0.60	40,293,082
8	0.35	3,169,737	0.66	53,163,255	0.60	45,609,208
9	0.24	2,904,894	0.64	58,396,223	0.56	41,853,117
10	0.27	3,239,006	0.61	64,139,662	0.58	41,926,334
Justification	• Highest ASW and CH • Highly simplified interpretation of topography of the region, but captures most important aspects		• ASW and CH are relatively high • Captures broad POC flux gradient without increasing number of habitat classes • Captures variation in macrofauna community structure across region • Aligns with GOODS (United Nations Educational, Scientific and Cultural Organization, 2009) and Watling et al. (2013)		• Highest ASW and high CH score • Captures what is known of influence of nodule abundance on species distributions • Reflects modeled nodule abundance without increasing number of habitat classes	

Bold starred text indicates the iteration selected for the final habitat classification. ASW close to 1 indicates good clustering, close to 0 indicates observations lie between two clusters and close to −1 indicates observations are poorly matched to the assigned cluster. CH scores are relative, with higher values indicating better clustering.

TABLE 2 | Properties of clusters selected for the final habitat classification, produced through CLARA clustering of environmental surrogates.

Variable class	Cluster	Variable	Min	Max	Mean	Standard Deviation	Description
Topography	Cluster 1	Slope (°)	0	6	1	0.5	Flat, with some small topographic features
		BBPI	−1,700	1,230	−17	114	
		FBPI	−1,256	555	−4	44	
	Cluster 2	Slope (°)	0	38	4	2	Sloped, with more prominent peaks and troughs
		BBPI	−1,741	3,454	136	325	
		FBPI	−1,312	1,806	38	140	
POC flux (g C_{org} m^{-2} y^{-1})	Cluster 1		0.8	1.4	1.2	0.1	Low POC
	Cluster 2		1.4	1.8	1.5	0.1	Med POC
	Cluster 3		1.8	2.9	2.1	0.2	High POC
Nodule abundance (kg m^{-2})	Cluster 1		0	3	1	1	Very low nodule abundance
	Cluster 2		3	5	4	1	Low nodule abundance
	Cluster 3		5	9	7	1	Med nodule abundance
	Cluster 4		9	31	11	2	High nodule abundance

northeast reflect favorable conditions for finding undiscovered nodule deposits, while projections of medium nodule abundance in the southeast and -west may be extrapolation artifacts in the input modeled nodule data, as seafloor POC fluxes in these areas are incompatible with the occurrence of nodules (International Seabed Authority, 2010).

Final Habitat Classification

The final classification produced by combining layers of clustered environmental variables proposes 24 habitat classes (**Figure 5**). Each habitat class represents a different set of environmental conditions (**Table 3**), and is assumed to support a distinct biological community. It is worth noting that the boundaries between adjacent habitat classes will include zones of transition and will not be as abrupt as is reflected by the classification.

Habitat classes in the east are characterized by medium to high seafloor POC flux, in the north- and southeast respectively. In the west, habitat classes are mainly areas of low POC flux, with medium to high POC flux in the southwest. Habitat classes with medium to high nodule abundance are concentrated in the central CCZ, bounded by the Clarion and Clipperton fracture zones and overlapping with exploration contracts and reserved

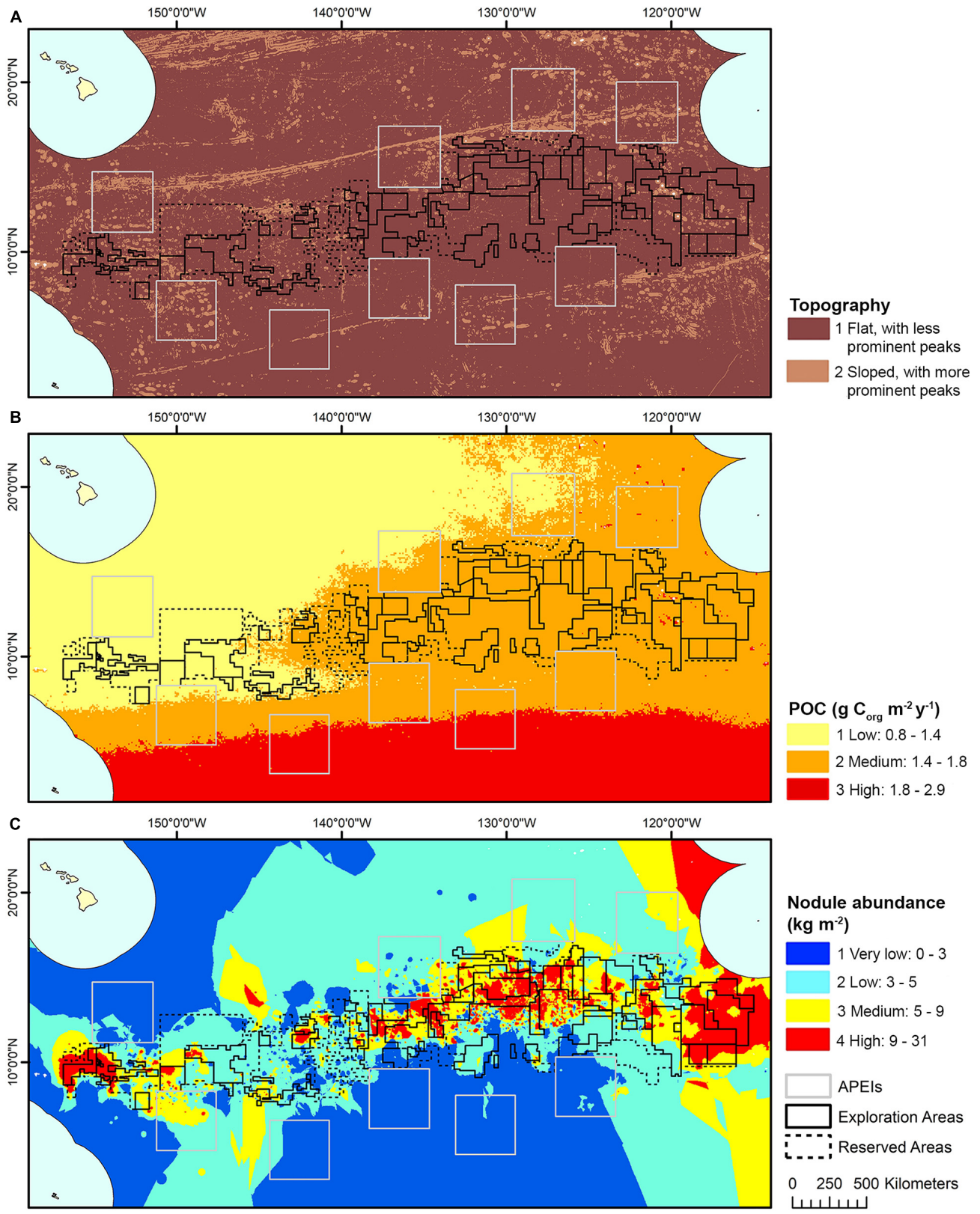

FIGURE 4 | Outputs of initial CLARA clustering on variable classes to represent **(A)** topography, **(B)** seafloor POC flux, and **(C)** nodule abundance in the CCZ region, used in the final habitat classification.

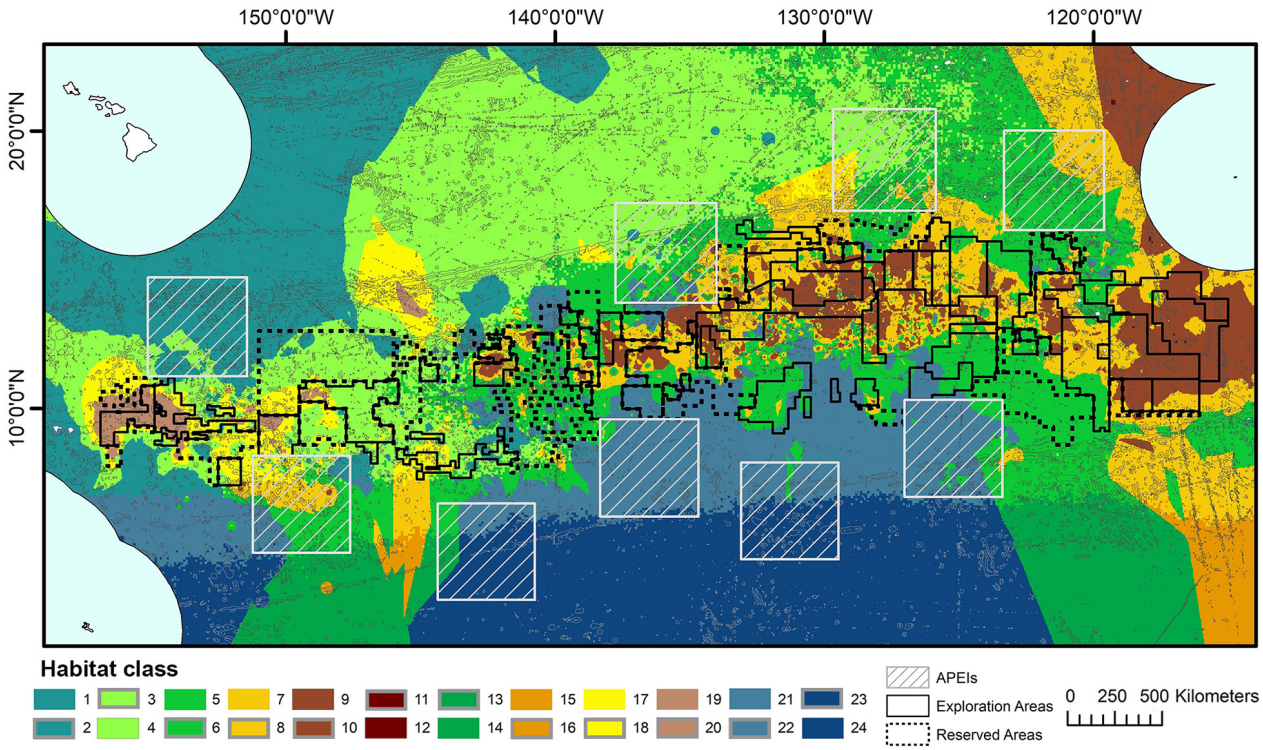

FIGURE 5 | Final 24 habitat classes produced by combining layers of clustered environmental variables. Habitat classes with high nodule abundance are shown in shades of brown, medium nodule abundance in orange/yellow, low nodule abundance in green and very low nodule abundance in blue. Within each nodule abundance group (i.e., very low, low, medium or high), habitat classes with different POC flux to the seafloor are identified by shading (i.e., darkest brown = high nodule abundance, high POC flux; lightest brown = high nodule abundance, low POC flux). Habitat classes with sloping topography are then identified by gray outlines. For example, habitat classes 1 and 2 have the same POC flux and nodule abundance conditions, but differ in topography. Habitat class 1 has very low nodule abundance, low POC flux and is flat, while habitat class 2 has very low nodule abundance, low POC flux and is more sloped.

areas. The periphery largely contains habitat classes with low and very low nodule abundance, although some medium and high nodule abundance habitat classes are also predicted in areas to the southwest, southeast and northeast of the central CCZ (but see caveats below).

Habitat classes with high nodule cover make up only 6.6% of the total area, which is otherwise dominated by low and very low nodule abundance (42 and 36% of the CCZ EMP area, respectively). The large habitat classes are also predominantly flat abyssal plain, with pockets of smaller classes distinguished by sloping topographic features like seamounts, peaks and troughs. In fact, 89% of the area is composed of habitat classes that are flat or of constant slope with small topographic features, while only 11% consist of varying slope characteristic of larger peaks and troughs.

Based on this classification, the CCZ EMP area appears to be dominated by several very large habitat classes, with many smaller pockets of different habitat classes spread across the area (**Figures 5–7**). The three most abundant habitat classes identified (numbers 4, 5, and 24, each with >1.4 million km^2, **Table 4**) are flat with some small topographic features, low to high POC flux to the seafloor, and low to very low nodule abundance. Two of these three largest habitat classes occur mainly on the periphery of the central CCZ, to the north and south, while the third occurs across parts of the central CCZ and to the northeast. In total, these habitat classes make up 44% of the EMP area. In fact, out of 24 habitat classes, the largest five form over 60% of the modeled area. These five largest habitat classes (1, 4, 5, 7, and 24) differ in terms of the level of POC input and nodule cover, but are all characterized by the same topographic conditions, i.e., flat or constant slope with some small topographic peaks and depressions.

The three smallest habitat classes in total area (classes 11, 12, and 16) all contain medium to high nodule abundance and are found predominantly to the east or in the southwest.

Confidence levels assigned to each habitat class reflect the confidence with which the class should be treated (**Table 3**). As noted above, projections of medium nodule abundance to the southeast and -west of the CCZ may be extrapolation artifacts in the input modeled nodule data (International Seabed Authority, 2010), and habitat classes in these areas (i.e., classes 15 and 16) should thus be treated with caution. In addition, certain combinations of environmental conditions are deemed to be improbable. Habitat classes with high nodule abundance and more sloped topographic features (i.e., classes 10, 11, and 20) may result from the broad-scale nodule abundance input data not reflecting small-scale heterogeneity in nodule abundance with topographic features. Nodules are not known to occur on the

TABLE 3 | Environmental characteristics (mean values) of each habitat class, indicating confidence with which the class should be treated.

Habitat class	Nodule abundance (kg m^{-2})	POC flux (g C_{org} m^{-2} y^{-1})	Slope (°)	BBPI	FBPI	Confidence	Reasoning
1	1	1.2	1	−17	−4	Higher	Not applicable
2	1	1.2	4	136	38	Higher	Not applicable
3	4	1.2	4	136	38	Higher	Not applicable
4	4	1.2	1	−17	−4	Higher	Not applicable
5	4	1.5	1	−17	−4	Higher	Not applicable
6	4	1.5	4	136	38	Higher	Not applicable
7	7	1.5	1	−17	−4	Higher	Not applicable
8	7	1.5	4	136	38	Higher	Not applicable
9	11	1.5	1	−17	−4	Higher	Not applicable
10	11	1.5	4	136	38	Lower	Steep sloping habitat with high nodule abundance unlikely.
11	11	2.1	4	136	38	Lower	Steep sloping habitat with high nodule abundance unlikely.
12	11	2.1	1	−17	−4	Higher	Not applicable
13	4	2.1	4	136	38	Higher	Not applicable
14	4	2.1	1	−17	−4	Higher	Not applicable
15	7	2.1	1	−17	−4	Lower	Artifacts in nodule data in southeast and southwest.
16	7	2.1	4	136	38	Lower	Artifacts in nodule data in southeast and southwest.
17	7	1.2	1	−17	−4	Higher	Not applicable
18	7	1.2	4	136	38	Higher	Not applicable
19	11	1.2	1	−17	−4	Higher	Not applicable
20	11	1.2	4	136	38	Lower	Steep sloping habitat with high nodule abundance unlikely.
21	1	1.5	1	−17	−4	Higher	Not applicable
22	1	1.5	4	136	38	Higher	Not applicable
23	1	2.1	4	136	38	Higher	Not applicable
24	1	2.1	1	−17	−4	Higher	Not applicable

steep flanks of seamounts, and therefore some areas with sloped topography and high nodule abundance may not actually have high nodule abundance. However, the sloped topography cluster with more prominent peaks and troughs does not identify only seamounts, but also more gently sloping topographic features that may support nodules. Slope in this cluster ranges from 0 to 38 degrees, and nodules may be found in areas of intermediate slope, up to 15 degrees (e.g., see Sharma and Kodagali, 1993; Yamazaki and Sharma, 1998; Bu et al., 2003; Kuhn et al., 2012). We therefore advise that classes with sloped topography and high nodule abundance are treated with some caution, as parts of these habitats may be improbable. The following results should be considered with the aforementioned caveats in mind.

APEI Representativity

An assessment of the habitat representativity of the CCZ APEI network shows that 21 habitat classes of a total of 24 are included in the APEIs, with 22 habitat classes occurring in exploration and/or reserved areas (**Table 4**). In the following we present results for the exploration and reserved areas combined. These are referred to as "potential mining areas," since both are ultimately intended for potential mining activities. They are up-to-date with all contracts awarded as of June 2019.

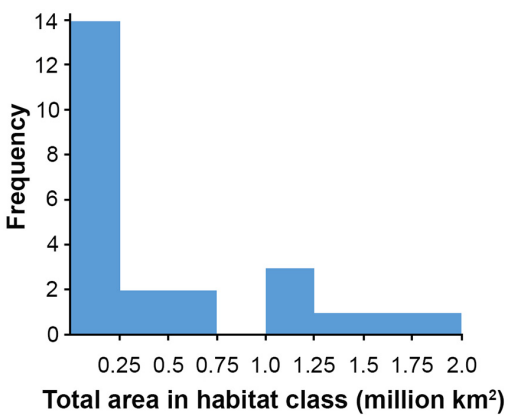

FIGURE 6 | Number of habitat classes of different total areas.

In the current APEI network, 14 habitat classes (nearly 60% of the total number of habitat classes in the area) have less than 10% of their area represented within APEIs, and 10 of these are represented by less than 5% (**Figure 8**). These 14 habitat classes have a range of environmental conditions including all

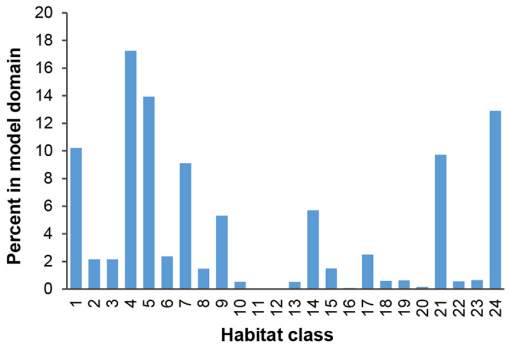

FIGURE 7 | Percentage of model domain within each habitat class.

topographic and POC flux conditions, and low to high nodule abundance levels. Seven habitat classes are represented by less than 1% (classes 9, 10, 11, 12, 13, 15, 16, 19, and 20), and of these, three receive no protection in the APEI network at all (classes 11, 12, and 15). Those habitat classes with greater than 0% but less than 1% representation in the APEIs are fairly large, ranging in total size from 9,000 to 593,000 km^2, and are generally located in large patches in the central CCZ. Those habitat classes with no protection at all have medium to high nodule abundance, high POC flux and variable topographic conditions. They include two smaller classes (numbers 11 and 12, <2,000 km^2 total area), and one larger class (number 15, >160,000 km^2). Habitat classes 11 and 12 are found in small pockets focused around topographic features with apparent high nodule abundance, and class 15 occurs in larger areas of medium nodule abundance in the southeast and southwest. Habitat classes 15 and 11 should be treated with caution, as above (**Table 3**). At the more ambitious World Park's Congress conservation target of 30% protection, which is at the lower end of what is required to conserve 75% of bathyal species (Foster et al., 2013), just two habitat classes are found to be adequately represented in the current APEI network. This means that 92% (22 classes) are not adequately protected at the 30% level.

Of the 14 habitat classes with < 10% representation in the APEIs, 10 have > 10% of their total area in potential mining areas (**Table 4** and **Figure 8**). Habitat classes 9, 10, 19, and 20 have 0% or nearly 0% representation in APEIs and a large proportion (50% to ∼ 70%) of their total extent located in exploration and/or reserved areas. These are all habitat classes with high nodule abundance located predominantly in the central CCZ (**Figure 4C**), and range in size from 17,000 km^2 to ∼ 600,000 km^2. These habitat classes also have a fairly high proportion of their area in currently unmanaged areas, which could be considered for spatial management. Two other habitat classes (11 and 12) are also unrepresented in APEIs, with a high proportion of their area in high-nodule-abundance potential mining areas; and these

TABLE 4 | Total extent of each habitat class, and percent located in potential mining areas (exploration and/or reserved areas), Areas of Particular Environmental Interest (APEI), and unmanaged areas as of June 2019.

Habitat class	Total area (km^2)	% in Potential mining areas	% in APEIs	% Unmanaged	Nodule cover
1	1,142,505	4	11	86	Very low
2	240,740	3	15	82	Very low
3	241,329	10	11	79	Low
4	1,928,272	13	8	79	Low
5	1,557,203	31	18	51	Low
6	264,740	10	28	62	Low
7	1,019,185	41	9	50	Medium
8	165,080	21	16	63	Medium
9	593,231	62	0.4	38	High
10	57,997	53	1	46	High
11	1,125	21	0	79	High
12	714	49	0	51	High
13	56,480	0.04	1	99	Low
14	636,650	0.06	3	97	Low
15	166,478	1	0	99	Medium
16	9,228	6	1	93	Medium
17	280,487	35	8	57	Medium
18	66,355	31	9	60	Medium
19	70,899	69	0.3	30	High
20	17,923	57	0.2	43	High
21	1,086,811	12	36	52	Very low
22	63,133	13	37	50	Very low
23	72,864	0	23	77	Very low
24	1,443,516	0	13	87	Very low

Habitat classes with ≤1% in APEIs are highlighted in gray.

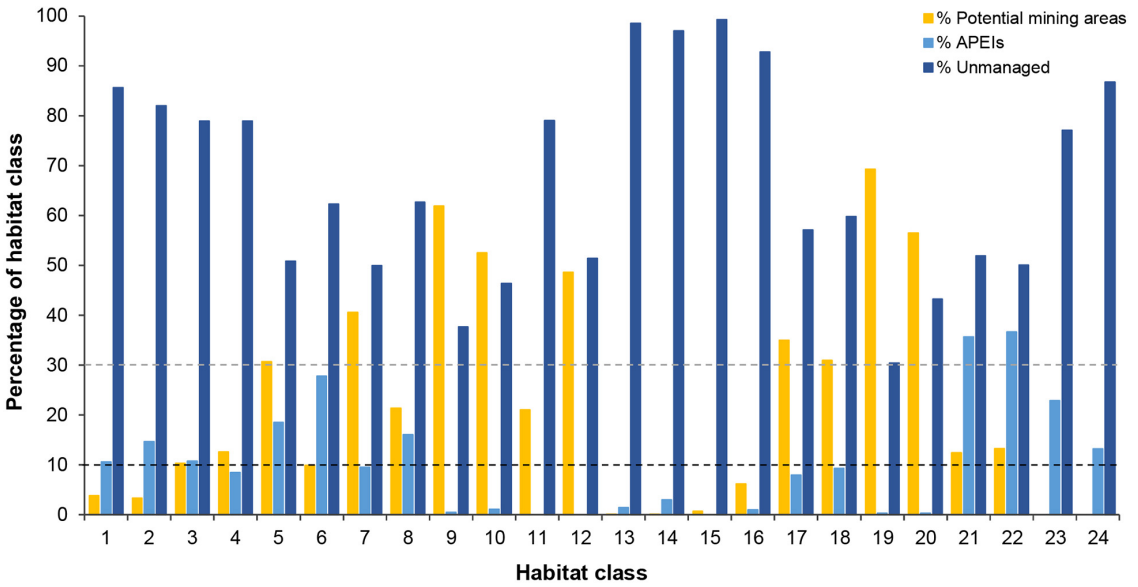

FIGURE 8 | Percentage of the total area of each habitat class occurring in APEIs, potential mining areas (exploration contracts and/or reserved areas) and unmanaged areas. Dashed lines represent conservation targets|

classes are small in total extent, focused around topographic features with high POC (**Figure 7** and **Table 4**). Of the habitat classes with <30% representation in the APEIs, 13 have >10% of their total area located within potential mining areas, while 11 have >20%, and four have >50%.

Three habitat classes (13, 15, and 16) are represented by ≤1% in APEIs and have a high proportion (>90%) of their total extent in unmanaged areas. These habitat classes are located in the southeast and southwest of the CCZ EMP area, in areas of low to medium nodule abundance, high POC flux and varying topographic conditions.

Finally, two habitat classes (classes 23 and 24) are not found in potential mining areas, but are represented in the APEI network. Both habitat classes occur to the south of the central exploration and reserved areas, and have very low nodule abundance (with other conditions varying). Four habitat classes (numbers 1, 2, 23, and 24) have > 10% (but <25%) of their total area in APEIs, and less than 5% of their area in potential mining areas. These habitat classes range in total area from 72,800 km^2 to 1,443,000 km^2 and are located in the northwest, in the south in central to western areas, and in smaller pockets in the central CCZ. These habitat classes also all have very low nodule cover.

In terms of replication of habitat classes within the APEI network, several classes (9, 10, 11, 12, 15, 16, 19, and 20) were found to occur in either no APEIs, or only one or two (**Figure 9**).

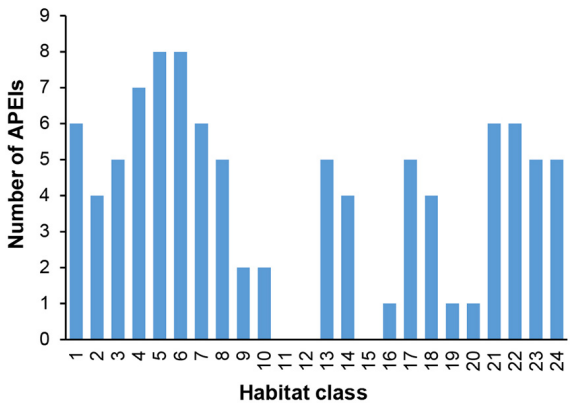

FIGURE 9 | Number of APEIs within which each habitat class is represented.

DISCUSSION

Comparison With Global Classifications

Our final habitat classification yields 24 benthic habitat classes that are assumed to support distinct faunal communities. Each of these habitat classes represents a different set of environmental conditions, based on the topographic features of the area, POC flux to the seafloor, and the abundance of nodules. According to this classification, the CCZ is dominated by several large, flat habitat classes with constant slope and relatively small topographic features, with many smaller pockets of different habitat classes interspersed across the region. Areas of high nodule abundance are predominantly located in the central CCZ, with a large patch of high nodule abundance in the northeast (**Figure 5**).

No similar, regional-scale habitat classifications have been carried out in the CCZ region, but the current classification can be compared with other global efforts that cover the region. These include the GOODS classification

United Nations Educational, Scientific and Cultural Organization (2009), Watling et al. (2013), Harris and Whiteway (2009) and Sayre et al. (2017). These are all larger scale, global classifications that describe large-scale units, in some cases based on biogeography (ecosystems with shared evolutionary processes and a suite of endemic species). The scale of the classes in these classifications is not suitable for use in regional environmental management, nevertheless, they provide a broad context for this habitat classification. Both GOODS and Watling et al. (2013) proposed two biogeographic provinces overlapping the CCZ, split in a north-south direction, with the boundaries for these driven primarily by differences in POC flux across the region. This split is captured in the current classification, which identifies habitat classes falling within areas of different POC flux, mainly in a latitudinal direction. Although a similar pattern is observed in the pelagic portions of the classification by Sayre et al. (2017), at the benthic level, the CCZ falls within a single Ecological Marine Unit. The classification produced by Harris and Whiteway (2009), on the other hand, is a somewhat finer scale, and splits the equatorial Pacific longitudinally, proposing different seascapes in the east and west, reflecting two different water masses identified in the region. Although water-mass structure may be an important factor in determining species distributions in other ocean basins (Howell et al., 2002), and has been used in previous global classifications (e.g., Watling et al., 2013), this variable was not included in the current study because there is little ecologically significant variation in water-mass characteristics across the CCZ (Watling et al., 2013), and there is no evidence that species distributions are driven by water-mass structure in this region.

It is worth noting that the underlying environmental models used to build the classification contain known, but unquantified, error. For example, the nodule abundance layer was produced using data primarily located within the central CCZ, which was then extrapolated outwards to predict nodule abundance in peripheral areas. This results in some artifacts, as previously mentioned. All layers were produced to reflect broad-scale variability only, and thus the constructed habitat classification is also only able to reflect broad-scale variability. In addition, limitations to the classification approach, including missing an important explanatory variable, not weighting input variables, issues with scale and selection of the number of clusters, and generation of clusters that represent environmental conditions that are unlikely to occur, may have impacted the model outputs. Most of these issues result from insufficient knowledge of the drivers of faunal communities in environments like the CCZ, and a general lack of both biological and environmental data. Acknowledging these potential shortcomings, this approach still has an important role to play in spatial planning, and makes use of best available data.

APEI Representativity

Representativity Assessment

Habitat representativity is a well-accepted requirement for MPA design (OSPAR Commission, 2006; Convention on Biological Diversity, 2009; O'Leary et al., 2012) and is one of the principal criteria for an MPA network to be considered ecologically coherent (Ardron, 2008; OSPAR Commission, 2010). The current CCZ APEI network does not fully meet representativity requirements, based on either the CBD conservation target of protection of 10% of the area of all habitat types (Convention on Biological Diversity, 2010), or the larger World Park's Congress target of 30% (International Union for Conservation of Nature, 2005, 2014). Recognizing the caveats previously mentioned, a large proportion of habitat classes (over half) are represented in the protected area network by less than 10% of their total extent, with the vast majority represented by less than 30% of their area. However, because the total area of current APEIs covers only 24% of the CCZ EMP area, a 30% conservation target is not realistic without additional APEIs.

Many habitat classes are represented in APEIs by <1% of their area, and some (3) are absent from the APEI network completely. Among the least protected habitat classes, many occur in large areas with high nodule abundance distributed across the central CCZ; those receiving no protection are generally found in smaller pockets on the periphery in areas of medium to high nodule abundance. Some of these are very small habitat classes, which is of concern as smaller, less common habitats may require greater protection than large, widely distributed ones (Johnson et al., 2014). Habitat classes 11 and 12, for example, occur around specific seabed features and may require additional, targeted protection at a scale that is much smaller than the size of a full APEI. Although these habitat classes are unlikely to be mined due to their topographic characteristics, they may still be vulnerable to impacts from adjacent mining such as sediment plumes. It is important to remember the caveats around habitat class 11, stated in the results (and see **Table 3**).

Several of the habitat classes with low representation (below 1%) in APEIs are found to have a large proportion of their total expanse (21 – 69%) in potential mining areas, and these are all habitat classes with high nodule abundance (numbers 9, 10, 11, 12, 19, and 20, although numbers 10, 11, and 20 should be treated with some caution, **Table 3**). The habitat heterogeneity introduced by nodules has been shown to increase megafauna abundance, with a positive relationship observed between megafauna abundance and nodule cover (Amon et al., 2016; Vanreusel et al., 2016; Simon-Lledó et al., 2019b). The link between increasing nodule cover and megafauna diversity is less clear, although no studies have yet been published from areas of high nodule abundance. Nonetheless, representation of all habitat types is required to support an ecologically coherent network of protected areas, including those with high nodule cover.

In addition, some habitat classes (13, 15, and 16) have a high proportion of their total extent in unmanaged areas, up to 99%, and <1% in APEIs. Considering habitat classes outside of exploration and reserved areas as "safe" is potentially unwise because these areas are not currently protected from mining. Exploration contracts in the CCZ are still being awarded (e.g., International Seabed Authority, 2017a), and some impacts from mining may well extend beyond the boundaries of contract areas (e.g., sediment plumes may be carried further afield by eddies, Aleynik et al., 2017). Further consideration of protection of these

habitat classes may be required, although habitats 15 and 16 should be treated with caution (**Table 3**).

Finally, those habitat classes with low replication within the APEI network are also those with low representativity. All of these habitat classes have high proportions of their total extent within potential mining areas (numbers 9, 10, 11, 12, 19, and 20) or unmanaged areas (numbers 15 and 16).

Revisiting the CCZ APEI Network

This study suggests that to reach habitat representativity conservation targets, additional protection is required in the CCZ. Protected areas are currently largely located in the periphery of the central, high-nodule-abundance habitat classes, and thus fail to adequately protect these habitats. Such a network may fall short of representing all of the unique habitats and biodiversity of the area (O'Leary et al., 2012), and we suggest that additional APEl(s) are warranted in areas of high nodule abundance to augment protection.

When the APEI network was adopted by the ISA, some of the protected areas proposed by experts within the central CCZ were shifted to the periphery to avoid any overlaps with existing exploration and/or reserved areas, resulting in the current APEI distribution (International Seabed Authority, 2011; Wedding et al., 2013). New data on dispersal distances led to calls in 2016 for two additional APEls to the northwest and southeast of the current network, but not in the central nodule area (**Figure 10**) (International Seabed Authority, 2016). Although not formally quantified in this study, this habitat classification provides support for the establishment of these additional APEIs. Proposed APEI 10 would improve representation and replication of two habitat classes currently receiving little protection, but with high proportions of their total extent within potential mining areas (see locations of classes 19 and 20 in **Figure 10**), while proposed APEI 11 would slightly increase representation and replication of habitat classes 13, 15, 16. In addition, the classification identifies areas of habitat to the east of exploration contracts, south of the Mexican EEZ, that could provide protection of another two habitat classes currently poorly represented and replicated in APEIs, and with high representation in potential mining areas (see locations of classes 9 and 10 in **Figure 10**). Although not visible in **Figure 10**, pockets of habitat classes 11 and 12 are located in unmanaged areas to the northeast of APEI 6 and could be considered for future protection, acknowledging the caveats around class 11. The addition or modification of APEls based on improved knowledge of the CCZ was a key concept in the EMP (International Seabed Authority, 2011) and is consistent with an adaptive management approach that has been advocated by many for deep-sea mining (e.g., Jaeckel, 2016).

Several habitat classes are located nearly entirely within the central CCZ, and conservation of these unique habitat classes would thus require protection measures that work around the existing mosaic of exploration and reserved areas, or utilize new space if areas are relinquished in future. These could take the form of smaller areas than a full APEI, although that would compromise the "buffer zone" that protects the core area of an APEI from possible impact from mining in an adjacent site.

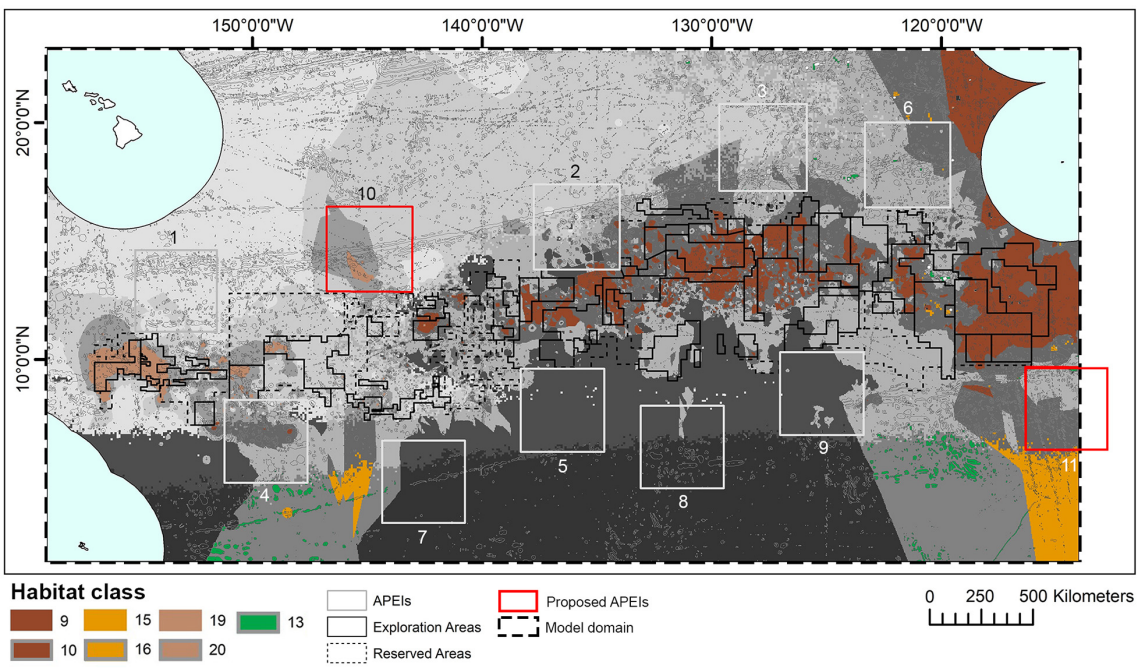

FIGURE 10 | Distribution of habitat classes 9, 10, 13, 15, 16, 19, and 20 (with 0%, or nearly 0%, representation in APEIs) in relation to two new Areas of Particular Environmental Interest (APEIs) proposed for inclusion in the current Clarion-Clipperton Fracture Zone APEI network: numbers 10, to the northwest, and 11, to the southeast. Other habitat classes shown in grayscale.

The results from the Friday Harbor Deep CCZ Biodiversity Synthesis Workshop (International Seabed Authority, 2020), that includes a preliminary account of this habitat classification work, have been incorporated into the ongoing review in 2020 of the CCZ EMP by the Legal and Technical Commission of the ISA. The classification informs the discussion of how different habitat classes (and assumed benthic communities) are distributed within the current network of APEIs, where there are clear gaps and habitat classes that are not included, where habitat classes are only protected in a single APEI (no replication), and how the location of any new APEIs can maximize the inclusion of habitat classes that are poorly represented in the existing APEI network. This includes consideration of the distance between APEIs (and the suggested inclusion of APEIs 10 and 11 from 2016), as well as options for APEIs to the east of existing potential mining areas (considering adjacent EEZs) to protect representative nodule communities and/or inside the central nodule belt and mosaic of exploration contract areas and reserved areas.

Future Applications

This study provides an example of a classification method that can be used to support spatial planning in large, data-poor areas. Specifically, it could be used to inform the development of further EMPs [termed Regional Environmental Management Plans (REMPs)] in other regions targeted by seabed mining, which are required under the draft ISA Regulations for Exploitation (International Seabed Authority, 2019a) and encouraged by UNGA Resolution 68/70 (United Nations General Assembly, 2014, para. 51). The ISA has made progress in developing further REMPs (International Seabed Authority, 2019b) and we would recommend that the use of MSP in future REMP development frameworks be formalized. A proactive approach to designating protected areas in regions of interest for mining, but currently with low levels of activity, could help to avoid a scenario like the CCZ where certain habitat classes are largely contained within potential mining areas, and therefore could be more at risk. This would support a precautionary approach and would require a large collaboration between scientists, contractors, and the ISA. Although any network of protected areas will require revision as new scientific knowledge becomes available, the development of a benthic classification coupled with an APEI network proposal developed using MSP approaches would be a positive first step for areas of interest to mining, and would ensure that any future allocation of contract areas can balance both conservation and exploitation objectives.

In addition, under ISA recommendations to contractors on biological sampling to establish environmental baselines, contractors are advised to take samples of fauna that are representative of variability of habitats, bottom topography, depth, seabed and sediment characteristics, the water column and mineral resource being targeted [International Seabed Authority, 2019c, para.15 (d)]. A similar top–down benthic classification approach as used in this study could be applied at a finer scale within contractors' exploration areas to support contractor's sampling regime.

CONCLUSION

The habitat classification method applied in this study indicates the current APEI network in the CCZ does not fully represent all of the unique habitat classes found in this area, particularly those with high nodule abundance in the central CCZ. It is recommended that consideration should be given to additional APEIs protecting areas of high nodule abundance, potentially to the east of existing contractor exploration areas, or smaller areas within the central CCZ. The habitat classification approach used here could be applied more widely to regional planning to ensure that such protected areas and networks are spatially coherent.

DATA AVAILABILITY STATEMENT

The data analyzed in this study is subject to the following licenses/restrictions: Two datasets analyzed in this study do not belong to the authors. References to the reports and papers from which the data have come are provided in the manuscript. Requests to access these datasets should be directed to https://doi.org/10.1029/2006JC003706 (for POC flux data); and https://www.isa.org.jm/documents/geological-modelpolymetallic-nodule-deposits-clarion-clipperton-fracture-zone (for nodule abundance data).

AUTHOR CONTRIBUTIONS

MA and KH obtained the funding for the study. KH and KM contributed to the conception and design. KM performed the classification, with technical input from AC and KH. All the authors contributed to the manuscript writing, read and approved the submitted version.

FUNDING

This study first appeared in the Ph.D. thesis of KM (McQuaid, 2020). The authors would like to acknowledge UK Seabed Resources Ltd., for funding this research. The funder was not involved in the study design, collection, analysis, interpretation of data, the writing of this article or the decision to submit it for publication. CS and AG were supported by the G and B Moore Foundation. This is contribution no. 11198 from SOEST, University of Hawaii.

ACKNOWLEDGMENTS

Thanks to Rebecca Ross and Nils Piechaud for technical support, and to participants of the Deep CCZ Biodiversity Synthesis Workshop for constructive feedback.

SUPPLEMENTARY MATERIAL

The Supplementary Material for this article can be found online at: https://www.frontiersin.org/articles/10.3389/fmars.2020.558860/full#supplementary-material

REFERENCES

Aleynik, D., Inall, M. E., Dale, A., and Vink, A. (2017). Impact of remotely generated eddies on plume dispersion at abyssal mining sites in the Pacific. *Sci. Rep.* 7:16959. doi: 10.1038/s41598-017-16912-2

Altvater, S., Fletcher, R., and Passarello, C. (2019). "The need for marine spatial planning in areas beyond national jurisdiction," in *Maritime Spatial Planning*, eds J. Zaucha and K. Gee (Cambridge: UN Environment World Conservation Monitoring Centre), 19.

Amon, D. J., Ziegler, A. F., Dahlgren, T. G., Glover, A. G., Goineau, A., Gooday, A. J., et al. (2016). Insights into the abundance and diversity of abyssal megafauna in a polymetallic-nodule region in the eastern Clarion-Clipperton Zone. *Sci. Rep.* 6:30492. doi: 10.1038/srep30492

Ardron, J. (2008). Three initial OSPAR tests of ecological coherence: heuristics in a data-limited situation. *ICES J. Mar. Sci.* 65, 1527–1533. doi: 10.1093/icesjms/fsn111

Ardron, J., Gjerde, K., Pullen, S., and Tilot, V. (2008). Marine spatial planning in the high seas. *Mar. Policy* 32, 832–839. doi: 10.1016/j.marpol.2008.03.018

Bonifácio, P., Martínez Arbizu, P., and Menot, L. (2020). Alpha and beta diversity patterns of polychaete assemblages across the nodule province of the eastern Clarion-Clipperton Fracture Zone (equatorial Pacific). *Biogeosciences* 17, 865–886. doi: 10.5194/bg-17-865-2020

Bu, W., Shi, X., Peng, J., and Qi, L. (2003). Geochemical characteristics of seamount ferromanganese nodules from mid-Pacific Ocean. *Chinese Sci. Bull.* 48, 98–105. doi: 10.1007/BF02900947

Bussau, C., Schriever, G., and Thiel, H. (1995). Evaluation of abyssal metazoan meiofauna from a manganese nodule area of the eastern South Pacific. *Vie Milieu* 45, 39–48.

Calinski, T., and Harabasz, J. (1974). A dendrite method for cluster analysis. *Commun. Stat.* 3, 1–27. doi: 10.1080/03610927408827101

Cartes, J. E., and Sarda, F. (1993). Zonation of deep-sea decapod fauna in the Catalan Sea (Western Mediterranean). *Mar. Ecol. Prog. Ser.* 94, 27–34. doi: 10.3354/meps094027

Chiba, S., Saito, H., Fletcher, R., Yogi, T., Kayo, M., Miyagi, S., et al. (2018). Human footprint in the abyss: 30 year records of deep-sea plastic debris. *Mar. Policy* 96, 204–212. doi: 10.1016/j.marpol.2018.03.022

Clark, M. R., Watling, L., Rowden, A. A., Guinotte, J. M., and Smith, C. R. (2011). A global seamount classification to aid the scientific design of marine protected area networks. *Ocean Coast. Manag.* 54, 19–36. doi: 10.1016/j.ocecoaman.2010.10.006

Connor, D. W., Allen, J. H., Golding, N., Howell, K. L., Lieberknecht, L. M., Northen, K. O., et al. (2004). *The Marine Habitat Classification for Britain and Ireland Version 04.05*. Peterborough: Joint Nature Conservation Committee, 49.

Convention on Biological Diversity [CBD] (2009). *Report of the Expert Workshop on Scientific and Technical Guidance on the Use of Biogeographic Classification Systems and Identification of Marine Areas Beyond National Jurisdiction in Need of Protection*. Ottawa, ON: CBD.

Convention on Biological Diversity [CBD] (2010). *Report of the Tenth Meeting of the Conference of the Parties to the Convention on Biological Diversity*. Nagoya: UNEP.

Davies, C. E., Moss, D., and Hill, M. O. (2004). *EUNIS Habitat Classification Revised 2004. Report to the European Topic Centre on Nature Protection and Biodiversity*. Copenhagen: European Environment Agency, 307.

De Santo, E. M. (2018). Implementation challenges of area-based management tools (ABMTs) for biodiversity beyond national jurisdiction (BBNJ). *Mar. Policy* 97, 34–43. doi: 10.1016/j.marpol.2018.08.034

De Smet, B., Pape, E., Riehl, T., Bonifácio, P., Colson, L., and Vanreusel, A. (2017). The community structure of deep-sea macrofauna associated with polymetallic nodules in the eastern part of the Clarion-Clipperton Fracture Zone. *Front. Mar. Sci.* 4:1–14. doi: 10.3389/fmars.2017.00103

Douglass, L. L., Turner, J., Grantham, H. S., Kaiser, S., Constable, A., Nicoll, R., et al. (2014). A hierarchical classification of benthic biodiversity and assessment of protected areas in the Southern Ocean. *PLoS One* 9:e100551. doi: 10.1371/journal.pone.0100551

Dudley, N. (2008). *Guidelines for Applying Protected Area Management Categories*. Gland: International Union for Conservation of Nature (IUCN), 86.

Dugolinsky, B. K., Margolis, S. V., and Dudley, W. C. (1977). Biogenic influence on growth of manganese nodules'. *J. Sediment. Petrol.* 47, 428–445. doi: 10.1306/212F7194-2B24-11D7-8648000102C1865D

Durden, J. M., Bett, B. J., Jones, D. O. B., Huvenne, V. A. I., and Ruhl, H. A. (2015). Abyssal hills – hidden source of increased habitat heterogeneity, benthic megafaunal biomass and diversity in the deep sea. *Prog. Oceanogr.* 137, 209–218. doi: 10.1016/j.pocean.2015.06.006

Edgar, G. J., Stuart-Smith, R. D., Willis, T. J., Kininmonth, S., Baker, S. C., Banks, S., et al. (2014). Global conservation outcomes depend on marine protected areas with five key features. *Nature* 506, 216–220. doi: 10.1038/nature13022

Ehler, C., and Douvere, F. (2007). *Visions for a Sea Change. Report of the First International Workshop on Marine Spatial Planning*. Paris: UNESCO Intergovernmental Oceanographic Commission.

Evans, J. L., Peckett, F., and Howell, K. L. (2015). Combined application of biophysical habitat mapping and systematic conservation planning to assess efficiency and representativeness of the existing High Seas MPA network in the Northeast Atlantic. *ICES J. Mar. Sci.* 72, 1–15. doi: 10.1093/icesjms/fsv012

Food and Agriculture Organization of the United Nations [FAO] (2009). *International Guidelines for the Management of Deep-sea Fisheries in the High Seas*. Rome: FAO.

Foster, N. L., Foggo, A., and Howell, K. L. (2013). Using species-area relationships to inform baseline conservation targets for the deep North East Atlantic. *PLoS One* 8:e58941. doi: 10.1371/journal.pone.0058941

Foster, N. L., Rees, S., Langmead, O., Griffiths, C., Oates, J., and Attrill, M. J. (2017). Assessing the ecological coherence of a marine protected area network in the Celtic Seas. *Ecosphere* 8:e01688. doi: 10.1002/ecs2.1688

Gage, J. D., and Tyler, P. A. (1996). *Deep-Sea Biology: A Natural History of Organisms at the Deep-Sea Floor*. Cambridge: Cambridge University Press.

Genin, A., Dayton, P. K., Lonsdale, P. F., and Spiess, F. N. (1986). Corals on seamount peaks provide evidence of current acceleration over deep-sea topography. *Nature* 322, 59–61. doi: 10.1038/322059a0

Glover, A. G., and Smith, C. R. (2003). The deep-sea floor ecosystem: current status and prospects of anthropogenic change by the year 2025. *Environ. Conserv.* 30, 219–241. doi: 10.1017/S0376892903000225

Glover, A. G., Smith, C. R., Paterson, G. L. J., Wilson, G. D. F., Hawkins, L., and Sheader, M. (2002). Polychaete species diversity in the central Pacific abyss: local and regional patterns, and relationships with productivity. *Mar. Ecol. Prog. Ser.* 240, 157–170. doi: 10.3354/meps240157

Gooday, A. J. (2002). Biological responses to seasonally varying fluxes of organic matter to the ocean floor: a review. *J. Oceanogr.* 58, 305–332. doi: 10.1023/A:1015865826379

Gooday, A. J., Goineau, A., and Voltski, I. (2015). Abyssal foraminifera attached to polymetallic nodules from the eastern Clarion Clipperton Fracture Zone: a preliminary description and comparison with North Atlantic dropstone assemblages. *Mar. Biodivers.* 45, 391–412. doi: 10.1007/s12526-014-0301-9

Gooday, A. J., Holzmann, M., Caulle, C., Goineau, A., Kamenskaya, O., Weber, A. A. T., et al. (2017). Giant protists (xenophyophores, Foraminifera) are exceptionally diverse in parts of the abyssal eastern Pacific licensed for polymetallic nodule exploration. *Biol. Conserv.* 207, 106–116. doi: 10.1016/j.biocon.2017.01.006

Gooday, A. J., Turley, C. M., Allen, J. A., Charnock, H., Edmond, J. M., McCave, I. N., et al. (1990). Responses by benthic organisms to inputs of organic material to the ocean floor: a review. *Philos. Trans. R. Soc. Lond. Ser. A Math. Phys. Sci.* 331, 119–138. doi: 10.1098/rsta.1990.0060

Grant, S., Constable, A., Raymond, B., and Doust, S. (2006). *Bioregionalisation of the Southern Ocean: Report of Expert's Workshop*. Hobart: WWF Australia and ACE CRC, 48.

Greene, H. G., Yoklavich, M. M., Starr, R. M., O'Connell, V. M., Wakefield, W. W., Sullivan, D. E., et al. (1999). A classification scheme for deep seafloor habitats. *Oceanol. Acta* 22, 663–678. doi: 10.1016/S0399-1784(00)88957-4

Guinan, J., Grehan, A., Dolan, M., and Brown, C. (2009). Quantifying relationships between video observations of cold-water coral cover and seafloor features in Rockall Trough, west of Ireland. *Mar. Ecol. Prog. Ser.* 375, 125–138. doi: 10.3354/meps07739

Harris, P. T., and Whiteway, T. (2009). High seas marine protected areas: benthic environmental conservation priorities from a GIS analysis of global ocean biophysical data. *Ocean Coast. Manag.* 52, 22–38. doi: 10.1016/j.ocecoaman.2008.09.009

Hecker, B. (1990). Variation in megafaunal assemblages on the continental margin south of New England. *Deep Sea Res. Part I Oceanogr. Res. Pap.* 37, 37–57. doi: 10.1016/0198-0149(90)90028-T

Hennig, C. (2015). *fpc: Flexible Procedures for Clustering. R package version* 2.1-10. Available online at: https://CRAN.R-project.org/package=fpc (accessed January 9, 2017).

Howell, K. L. (2010). A benthic classification system to aid in the implementation of marine protected area networks in the deep/high seas of the NE Atlantic. *Biol. Conserv.* 143, 1041–1056. doi: 10.1016/j.biocon.2010.02.001

Howell, K. L., Billet, D. S. M., and Tyler, P. A. (2002). Depth-related distribution and abundance of seastars (Echinodermata: Asteroidea) in the Porcupine Seabight and Porcupine Abyssal Plain, N.E. Atlantic. *Deep Sea Res. Part I Oceanogr. Res. Pap.* 49, 1901–1920. doi: 10.1016/S0967-0637(02)00090-0

International Seabed Authority [ISA] (2000). *Regulations on Prospecting, and Exploration for Polymetallic Nodules in theArea*. Kingston: International Seabed Authority.

International Seabed Authority [ISA] (2010). *Technical Study No. 6: A Geological Model of Polymetallic Nodule Deposits in the Clarion-Clipperton Fracture Zone*. Kingston: International Seabed Authority.

International Seabed Authority [ISA] (2011). *Environmental Management Plan for the Clarion-Clipperton Zone*. Kingston: International Seabed Authority.

International Seabed Authority [ISA] (2013). *Decision of the Council of the International Seabed Authority Relating to Amendments to the Regulations on Prospecting and Exploration for Polymetallic Nodules in the Area and Related Matters*. Kingston: International Seabed Authority.

International Seabed Authority [ISA] (2016). *Review of the Implementation of the Environmental Management Plan for the Clarion-Clipperton Fracture Zone*. Kingston: International Seabed Authority.

International Seabed Authority [ISA] (2017c). *Technical Study No. 21: Report of ISA Workshop on the Design of "Impact Reference Zones" and "Preservation Reference Zones" in Deep-Sea Mining Contract Areas*. Kingston: International Seabed Authority.

International Seabed Authority [ISA] (2017b). *Technical Study No. 17: Towards an ISA Environmental Management Strategy for the Area*. Kingston: International Seabed Authority.

International Seabed Authority [ISA] (2017a). *China Minmetals Corporation Signs Exploration Contract with the International Seabed Authority*. Kingston: International Seabed Authority.

International Seabed Authority [ISA] (2019a). *Draft Regulations for Exploitation of Mineral Resources in the Area*. Kingston: International Seabed Authority.

International Seabed Authority [ISA] (2019b). *Report of the Workshop on the Regional Environmental Management Plan for the Area of the Northern Mid-Atlantic Ridge*. Évora: International Seabed Authority.

International Seabed Authority [ISA] (2019c). *Recommendations for the Guidance of Contractors for the Assessment of the Possible Environmental Impacts Arising From Exploration for Marine Minerals in the Area*. Kingston: International Seabed Authority.

International Seabed Authority [ISA] (2020). *Deep CCZ Biodiversity Synthesis Workshop Report*. Friday Harbor: International Seabed Authority.

International Union for Conservation of Nature [IUCN] (2005). *Benefits Beyond Boundaries. Proceedings of the Vth IUCN World Parks Congress*. Durban: International Union for Conservation of Nature [IUCN].

International Union for Conservation of Nature [IUCN] (2014). *The Promise of Sydney. Sixth IUCN World Parks Congress*. Sydney: International Union for Conservation of Nature [IUCN].

Jaeckel, A. (2016). Deep seabed mining and adaptive management: the procedural challenges for the International Seabed Authority. *Mar. Policy* 70, 205–211. doi: 10.1016/j.marpol.2016.03.008

Johnson, D., Ardron, J., Billett, D., Hooper, T., Mullier, T., Chaniotis, P., et al. (2014). When is a marine protected area network ecologically coherent? A case study from the North-east Atlantic. *Aqu. Conserv.* 24, 44–58. doi: 10.1002/aqc.2510

Jones, D. O. B., Kaiser, S., Sweetman, A. K., Smith, C. R., Menot, L., Vink, A., et al. (2017). Biological responses to disturbance from simulated deep-sea polymetallic nodule mining. *PLoS One* 12:e0171750. doi: 10.1371/journal.pone.0171750

Kaufman, L., and Rousseeuw, P. (1990). *Finding Groups in Data: An Introduction to Cluster Analysis*. New York, NY: John Wiley.

Kuhn, T., Rühlemann, C., and Wiedicke-Hombach, M. (2012). "Developing a strategy for the exploration of vast seafloor areas for prospective manganese nodule fields," in *Marine Minerals: Finding the Right Balance of Sustainable Development and Environmental Protection*, eds H. Zhou and C. L. Morgan (Shanghai: The Under Water Mining Institute), K1–K9.

Last, P. R., Lyne, V. D., Williams, A., Davies, C. R., Butler, A. J., and Yearsley, G. K. (2010). A hierarchical framework for classifying seabed biodiversity with application to planning and managing Australia's marine biological resources. *Biol. Conserv.* 143, 1675–1686. doi: 10.1016/j.biocon.2010.04.008

Leathwick, J., Dey, K., and Julian, K. (2006). *Development of a Marine Environmental Classification Optimised for Demersal Fish*. Available online at: https://www.doc.govt.nz/globalassets/documents/conservation/marine-and-coastal/marine-protected-areas/mcu1.pdf (accessed on 25 September 2019)

Leitner, A. B., Neuheimer, A. B., Donlon, E., Smith, C. R., and Drazen, J. C. (2017). Environmental and bathymetric influences on abyssal bait-attending communities of the Clarion Clipperton Zone. *Deep Sea Res. Part I Oceanogr. Res. Pap.* 125, 65–80. doi: 10.1016/j.dsr.2017.04.017

Levin, L. A., Etter, R. J., Rex, M. A., Gooday, A. J., Smith, C. R., Pineda, J., et al. (2001). Environmental influences on regional deep-sea species diversity. *Annu. Rev. Ecol. Syst.* 32, 51–93. doi: 10.1146/annurev.ecolsys.32.081501.114002

Lodge, M., Johnson, D., Le Gurun, G., Wengler, M., Weaver, P., and Gunn, V. (2014). Seabed mining: international seabed authority environmental management plan for the Clarion–Clipperton Zone. A partnership approach. *Mar. Policy* 49, 66–72. doi: 10.1016/j.marpol.2014.04.006

Lombard, A. T., Strauss, T., Harris, J., Sink, K., Attwood, C., and Hutchings, L. (2004). *South African National Spatial Biodiversity Assessment 2004. Technical Report Volume 4: Marine Component*. Available online at: http://sanpcc.org.za/pssa-old/articles/includes/NSBA%20Vol%204%20Marine%20Component%20Draft%20Oct%2004.pdf (accessed on 25 September 2019).

Longhurst, A. R. (2007). "Chapter 1: Toward an ecological geography of the sea," in *Ecological Geography of the Sea*, 2nd Edn, ed. A. R. Longhurst (Burlington: Academic Press), 1–17. doi: 10.1016/b978-012455521-1/50002-4

Lubchenco, J., Palumbi, S. R., Gaines, S. D., and Andelman, S. (2003). Plugging a hole in the ocean: The emerging science of marine reserves. *Ecol. Appl.* 13, S3–S7. doi: 10.1890/1051-07612003013[0003:PAHITO]2.0.CO;2

Lundblad, E. R., Wright, D. J., Miller, J., Larkin, E. M., Rinehart, R., Naar, D. F., et al. (2006). A benthic terrain classification scheme for American Samoa. *Mar. Geodesy* 29, 89–111. doi: 10.1080/01490410600738021

Lutz, M. J., Caldeira, K., Dunbar, R. B., and Behrenfeld, M. J. (2007). Seasonal rhythms of net primary production and particulate organic carbon flux to depth describe the efficiency of biological pump in the global ocean. *J. Geophys. Res. Oceans* 112, 1–26. doi: 10.1029/2006JC003706

Maes, F. (2008). The international legal framework for marine spatial planning. *Mar. Policy* 32, 797–810. doi: 10.1016/j.marpol.2008.03.013

McQuaid, K. (2020). *Ecological Studies of an Abyssal Nodule Province to Inform the Management of Deep-Sea Mining*. PhD thesis. Plymouth: University of Plymouth.

Miller, K. J., Rowden, A. A., Williams, A., and Häussermann, V. (2011). Out of their depth? Isolated deep populations of the cosmopolitan coral Desmophyllum dianthus may be highly vulnerable to environmental change. *PLoS One* 6:e19004. doi: 10.1371/journal.pone.0019004

Molenaar, E. J. (2013). *Area-Based Management Tools*. Utrecht: Utrecht University.

Mumby, P. J., and Harborne, A. R. (2010). Marine reserves enhance the recovery of corals on Caribbean reefs. *PLoS One* 5:e8657. doi: 10.1371/journal.pone.0008657

Official Journal of the European Union [OJ] (2014). *Directive 2014/89/EU of the European Parliament and of the Council of 23 July 2014: Establishing a framework for maritime spatial planning*. Available online at: https://eur-lex.europa.eu/legal-content/EN/TXT/PDF/?uri=CELEX:32014L0089andfrom=EN (accessed on 25 September 2019).

O'Leary, B. C., Brown, R. L., Johnson, D. E., von Nordheim, H., Ardron, J., Packeiser, T., et al. (2012). The first network of marine protected areas (MPAs) in the high seas: the process, the challenges and where next. *Mar. Policy* 36, 598–605. doi: 10.1016/j.marpol.2011.11.003

OSPAR Commission (2006). *Guidance on Developing an Ecologically Coherent Network of OSPAR Marine Protected Areas. OSPAR Convention for the*

Protection of the Marine Environment of the North-East Atlantic, Reference number 2006-3. London: OSPAR Commission.

OSPAR Commission (2010). *2009/10 Status Report on the OSPAR Network of Marine Protected Areas. OSPAR Convention for the Protection of the Marine Environment of the North-East Atlantic*. London: OSPAR Commission, 62.

Pennington, J. T., Mahoney, K. L., Kuwahara, V. S., Kolber, D. D., Calienes, R., and Chavez, F. P. (2006). Primary production in the eastern tropical Pacific: a review. *Prog. Oceanogr.* 69, 285–317. doi: 10.1016/j.pocean.2006.03.012

Peukert, A., Schoening, T., Alevizos, A., Köser, K., Kwasnitschka, T., and Greinert, J. (2018). Understanding Mn-nodule distribution and evaluation of related deep-sea mining impacts using AUV-based hydroacoustic and optical data. *Biogeosciences* 15, 2525–2549. doi: 10.5194/bg-15-2525-2018

R Core Team (2017). *R: A Language and Environment for Statistical Computing*. Vienna: R foundation for statistical computing.

Ramirez-Llodra, E., Tyler, P. A., Baker, M. C., Bergstad, O. A., Clark, M. R., Escobar, E., et al. (2011). Man and the last great wilderness: human impact on the deep sea. *PLoS One* 6:e22588. doi: 10.1371/journal.pone.0022588

Ramos, E., Juanes, J. A., Galván, C., Neto, J. M., Melo, R., Pedersen, A., et al. (2012). Coastal waters classification based on physical attributes along the NE Atlantic region. An approach for rocky macroalgae potential distribution. *Estuar. Coast. Shelf Sci.* 112, 105–114. doi: 10.1016/j.ecss.2011.11.041

Ramos, E., Puente, A., and Juanes, J. A. (2015). An ecological classification of rocky shores at a regional scale: a predictive tool for management of conservation values. *Mar. Ecol.* 37, 311–328. doi: 10.1111/maec.12280

Republic of South Africa [RSA] (2017). *National Framework for Marine Spatial Planning in South Africa. Department of Environmental Affairs, Government Gazette no. 40860*. Cape Town: Department of Environmental Affairs.

Republic of South Africa [RSA] (2019). *Marine Spatial Planning Act* 16 *of 2018. Department of Environmental Affairs, Government Gazette No. 42444*. Cape Town: Department of Environmental Affairs.

Rice, A. L., Thurston, M. H., and New, A. L. (1990). Dense aggregations of a hexactinellid sponge, Pheronema carpenteri, in the Porcupine Seabight (northeast Atlantic Ocean), and possible causes. *Prog. Oceanogr.* 24, 179–196. doi: 10.1016/0079-6611(90)90029-2

Roff, J. C., and Taylor, M. E. (2000). National frameworks for marine conservation — a hierarchical geophysical approach. *Aqu. Conserv. Mar. Freshw. Ecosyst.* 10, 209–223. doi: 10.1002/1099-0755(200005/06)10:3<209::AID-AQC408<3.0.CO;2-J

Roff, J. C., Taylor, M. E., and Laughren, J. (2003). Geophysical approaches to the classification, delineation and monitoring of marine habitats and their communities. *Aqu. Conserv. Mar. Freshw. Ecosyst.* 13, 77–90. doi: 10.1002/aqc.525

Rowe, G. T., and Menzies, R. J. (1969). Zonation of large benthic invertebrates in the deep-sea off the Carolinas. *Deep Sea Res. Oceanogr. Abstracts* 16, 531–537. doi: 10.1016/0011-7471(69)90041-2

RStudio Team (2015). *RStudio: Integrated Development for R*. Boston, MA: RStudio.

Ruhl, H. A., and Smith, K. L. (2004). Shifts in deep-sea community structure linked to climate and food supply. *Science* 305, 513–515. doi: 10.1126/science.1099759

Sayre, R., Dangermond, J., Wright, D., Breyer, S., Butler, K., Van Graafeiland, K., et al. (2017). *A New Map of Global Ecological Marine Units – An Environmental Stratification Approach*. Washington, DC: American Association of Geographers.

Sharma, R., and Kodagali, V. N. (1993). Influence of seabed topography on the distribution of manganese nodules and associated features in the Central Indian Basin: a study based on photographic observations. *Mar. Geol.* 110, 153–162. doi: 10.1016/0025-3227(93)90111-8

Sherman, K. (1986). "Introduction to parts one and two: large marine ecosystems as tractable entities for measurement and management," in *Variability and Management of Large Marine Ecosystems*, eds K. Sherman and L. M. Alexander (Boulder: Westview Press), 3–7.

Simon-Lledó, E., Bett, B. J., Huvenne, V. A. I., Schoening, T., Benoist, N. M. A., Jeffreys, R. M., et al. (2019a). Megafaunal variation in the abyssal landscape of the Clarion Clipperton Zone. *Prog. Oceanogr.* 170, 119–133. doi: 10.1016/j.pocean.2018.11.003

Simon-Lledó, E., Bett, B. J., Huvenne, V. A. I., Schoening, T., Benoist, N. M. A., and Jones, D. O. B. (2019b). Ecology of a polymetallic nodule occurrence gradient: implications for deep-sea mining. *Limnol. Oceanogr.* 64, 1883–1894. doi: 10.1002/lno.11157

Smith, C. R., and Baco, A. R. (2003). Ecology of whale falls at the deep-sea floor. *Oceanogr. Mar. Biol.* 41, 311–354.

Smith, C. R., Berelson, W., Demaster, D. J., Dobbs, F. C., Hammond, D., Hoover, D. J., et al. (1997). Latitudinal variations in benthic processes in the abyssal equatorial Pacific: control by biogenic particle flux. *Deep Sea Res. Part II Top. Stud. Oceanogr.* 44, 2295–2317. doi: 10.1016/S0967-0645(97)00022-2

Smith, C. R., De Leo, F. C., Bernardino, A. F., Sweetman, A. K., and Martinez Arbizu, P. (2008). Abyssal food limitation, ecosystem structure and climate change. *Trends Ecol. Evol.* 23, 518–528. doi: 10.1016/j.tree.2008.05.002

Snelder, T., Leathwick, J., Dey, K., Rowden, A., Weatherhead, M., Fenwick, G., et al. (2006). Development of an ecologic marine classification in the New Zealand region. *Environ. Manage.* 39, 12–29. doi: 10.1007/s00267-005-0206-2

Spalding, M. D., Fox, H. E., Allen, G. R., Davidson, N., Ferdaña, Z. A., Finlayson, M., et al. (2007). Marine ecoregions of the world: a bioregionalization of coastal and shelf areas. *BioScience* 57, 573–583. doi: 10.1641/b570707

Stefanoudis, P. V., Bett, B. J., and Gooday, A. J. (2016). Abyssal hills: influence of topography on benthic foraminiferal assemblages. *Prog. Oceanogr.* 148, 44–55. doi: 10.1016/j.pocean.2016.09.005

Sutton, T. T., Clark, M. R., Dunn, D. C., Halpin, P. N., Rogers, A. D., Guinotte, J., et al. (2017). A global biogeographic classification of the mesopelagic zone. *Deep Sea Res. Part I Oceanogr. Res. Pap.* 126, 85–102. doi: 10.1016/j.dsr.2017.05.006

Thiel, H., Schriever, G., Bussau, C., and Borowski, C. (1993). Manganese nodule crevice fauna. *Deep Sea Res. Part I Oceanogr. Res. Pap.* 40, 419–423. doi: 10.1016/0967-0637(93)90012-R

Toropova, C., Meliane, I., Laffoley, D., Matthews, E., and Spalding, M. (2010). *Global Ocean Protection: Present Status and Future Possibilities*. Available online at: https://www.iucn.org/content/global-ocean-protection-present-status-and-future-possibilities-1 (accessed on 25 September 2019)

Turner, R. D. (1973). Wood-boring bivalves, opportunistic species in the deep sea. *Science* 180, 1377–1379. doi: 10.1126/science.180.4093.1377

Tyler, P. A., and Zibrowius, H. (1992). Submersible observations of the invertebrate fauna on the continental slope southwest of Ireland (NE Atlantic Ocean). *Oceanol. Acta* 15, 221–226.

United Nations Educational, Scientific and Cultural Organization [UNESCO] (2009). *Global Open Oceans and Deep Seabed (GOODS) Biogeographic Classification. UNESCO-IOC Technical Serie*. Paris: UNESCO.

United Nations Environment Programme World Conservation Monitoring Centre [UNEP-WCMC] (2008). *National and Regional Networks of Marine Protected Areas: A Review of Progress. UNEP-WCMC Biodiversity Series 30*. Cambridge: UNEP-WCMC.

United Nations Environment Programme World Conservation Monitoring Centre [UNEP-WCMC]. (2018). *A Review of Area-Based Planning Tools. What is the Potential for Cross-Sectoral Planning in Areas Beyond National Jurisdiction? Technical Document Produced as Part of the GEF ABNJ Deep Seas Project*. Cambridge: UNEP-WCMC, 71.

United Nations General Assembly [UNGA] (2014). *Oceans and the Law of the Sea. Resolution Adopted by the General Assembly on 9 December 2013*. New York, NY: United Nations General Assembly.

Van Dover, C. (2000). *The Ecology of Deep-Sea Hydrothermal Vents*. Princeton, NJ: Princeton University Press.

Vanreusel, A., Hilario, A., Ribeiro, P. A., Menot, L., and Martinez Arbizu, P. (2016). Threatened by mining, polymetallic nodules are required to preserve abyssal epifauna. *Sci. Rep.* 6:26808. doi: 10.1038/srep26808

Veillette, J., Sarrazin, J., Gooday, A. J., Galéron, J., Caprais, J.-C., Vangriesheim, A., et al. (2007). Ferromanganese nodule fauna in the Tropical North Pacific Ocean: species richness, faunal cover and spatial distribution. *Deep Sea Res. Part I Oceanogr. Res. Pap.* 54, 1912–1935. doi: 10.1016/j.dsr.2007.06.011

Verfaillie, E., Degraer, S., Schelfaut, K., Willems, W., and Van Lancker, V. (2009). A protocol for classifying ecologically relevant marine zones, a statistical approach. *Estuar. Coast. Shelf Sci.* 83, 175–185. doi: 10.1016/j.ecss.2009.03.003

Watling, L., Guinotte, J., Clark, M. R., and Smith, C. R. (2013). A proposed biogeography of the deep ocean floor. *Prog. Oceanogr.* 111, 91–112. doi: 10.1016/j.pocean.2012.11.003

Wedding, L. M., Friedlander, A. M., Kittinger, J. N., Watling, L., Gaines, S. D., Bennett, M., et al. (2013). From principles to practice: a spatial approach to

systematic conservation planning in the deep sea. *Proc. R. Soc. B Biol. Sci.* 280, 20131684. doi: 10.1098/rspb.2013.1684

Wedding, L. M., Reiter, S. M., Smith, C. R., Gjerde, K. M., Kittinger, J. N., Friedlander, A. M., et al. (2015). Managing mining of the deep seabed. *Sci. Magaz.* 349, 144–145. doi: 10.1126/science.aac6647

Wei, C.-L., Rowe, G. T., Escobar-Briones, E., Boetius, A., Soltwedel, T., Caley, M. J., et al. (2011). Global patterns and predictions of seafloor biomass using random forests. *PLoS One* 5:e15323. doi: 10.1371/journal.pone.0015323

Woolley, S. N. C., Tittensor, D. P., Dunstan, P. K., Guillera-Arroita, G., Lahoz-Monfort, J. J., Wintle, B. A., et al. (2016). Deep-sea diversity patterns are shaped by energy availability. *Nature* 533, 393–396. doi: 10.1038/nature 17937

Wright, D. J., Lundblad, E. R., Larkin, E. M., Rinehart, R. W., Murphy, J., Cary-Kothera, L., et al. (2005). *ArcGIS Benthic Terrain Modeler*. Corvallis, OR: Oregon State University.

Wright, G., Ardron, J., Gjerde, K., Currie, D., and Rochette, J. (2015). Advancing marine biodiversity protection through regional fisheries management: a review of bottom fisheries closures in areas beyond national jurisdiction. *Mar. Policy* 61, 134–148. doi: 10.1016/j.marpol.2015.06.030

Wright, G., Gjerde, K. M., Johnson, D. E., Finkelstein, A., Ferreira, M. A., Dunn, D. C., et al. (2018). *Marine Spatial Planning in Areas Beyond National Jurisdiction. Institut du Développement Durable et des Relations Internationales Issue Brief 08/18*. Paris: Institut du Développement Durable et des Relations Internationales.

Yamazaki, T., and Sharma, R. (1998). Distribution characteristics of co-rich manganese deposits on a seamount in the central Pacific Ocean. *Mar. Georesourc. Geotechnol.* 16, 283–305. doi: 10.1080/10641199809379973

Conflict of Interest: The authors declare that the research was conducted in the absence of any commercial or financial relationships that could be construed as a potential conflict of interest.

The reviewer DV declared a past co-authorship with one of the authors CS to the handling editor.

Copyright © 2020 McQuaid, Attrill, Clark, Cobley, Glover, Smith and Howell. This is an open-access article distributed under the terms of the Creative Commons Attribution License (CC BY). The use, distribution or reproduction in other forums is permitted, provided the original author(s) and the copyright owner(s) are credited and that the original publication in this journal is cited, in accordance with accepted academic practice. No use, distribution or reproduction is permitted which does not comply with these terms.

frontiers in Marine Science

ORIGINAL RESEARCH
published: 30 March 2021
doi: 10.3389/fmars.2021.661685

Environmental Heterogeneity Throughout the Clarion-Clipperton Zone and the Potential Representativity of the APEI Network

Travis W. Washburn[1], Daniel O. B. Jones[2], Chih-Lin Wei[3] and Craig R. Smith[1]*

[1] Department of Oceanography, University of Hawai'i at Mānoa, Honolulu, HI, United States, [2] National Oceanography Centre, Southampton, United Kingdom, [3] Institute of Oceanography, National Taiwan University, Taipei, Taiwan

Environmental variables such as food supply, nodule abundance, sediment characteristics, and water chemistry may influence abyssal seafloor communities and ecosystem functions at scales from meters to thousands of kilometers. Thus, knowledge of environmental variables is necessary to understand drivers of organismal distributions and community structure, and for selection of proxies for regional variations in community structure, biodiversity, and ecosystem functions. In October 2019, the *Deep CCZ Biodiversity Synthesis Workshop* was conducted to (i) compile recent seafloor ecosystem data from the Clarion-Clipperton Zone (CCZ), (ii) synthesize patterns of seafloor biodiversity, ecosystem functions, and potential environmental drivers across the CCZ, and (iii) assess the representativity of no-mining areas (Areas of Particular Environmental Interest, APEIs) for subregions and areas in the CCZ targeted for polymetallic nodule mining. Here we provide a compilation and summary of water column and seafloor environmental data throughout the CCZ used in the *Synthesis Workshop* and in many of the papers in this special volume. Bottom-water variables were relatively homogenous throughout the region while nodule abundance, sediment characteristics, seafloor topography, and particulate organic carbon flux varied across CCZ subregions and between some individual subregions and their corresponding APEIs. This suggests that additional APEIs may be needed to protect the full range of habitats and biodiversity within the CCZ.

Keywords: deep-sea mining, areas of particular environmental interest, environmental heterogeneity, Clarion-Clipperton Zone, manganese nodules, POC flux, sediment characteristics, climate change

OPEN ACCESS

Edited by:
Jacopo Aguzzi, Instituto de Ciencias del Mar (CSIC), Spain

Reviewed by:
Hiroyuki Yamamoto, Japan Agency for Marine-Earth Science and Technology (JAMSTEC), Japan
Philip Weaver, Seascape Consultants Ltd, United Kingdom

****Correspondence:***
Travis W. Washburn
Travis.Washburn@aist.go.jp

Specialty section:
This article was submitted to Deep-Sea Environments and Ecology, a section of the journal Frontiers in Marine Science

Received: *31 January 2021*
Accepted: *11 March 2021*
Published: *30 March 2021*

Citation:
Washburn TW, Jones DOB, Wei C-L and Smith CR (2021) Environmental Heterogeneity Throughout the Clarion-Clipperton Zone and the Potential Representativity of the APEI Network. Front. Mar. Sci. 8:661685. doi: 10.3389/fmars.2021.661685

INTRODUCTION

Environmental Conditions in the Deep Sea

Contrary to popular perception, the abyssal seafloor exhibits substantial variability in habitat structure and key environmental variables across a broad range of scales, with corresponding heterogeneity in benthic habitat structure and biodiversity (e.g., Lutz et al., 2007; Wei et al., 2010; Danovaro et al., 2014; Zeppilli et al., 2016; Smith et al., 2020). Commercial exploitation of deep-sea resources, including fishing, seabed mining, and deep-sea hydrocarbon drilling, have the potential to damage deep-sea ecosystems over large spatial and temporal scales

(e.g., Borowski and Thiel, 1998; Glover and Smith, 2003; Jones et al., 2017; Weaver et al., 2018; Washburn et al., 2019; Smith et al., 2020). To predict and manage the impacts of human activities in the deep sea, detailed understanding of baseline ecosystem conditions is essential. This requires assessment of the natural variability of environmental drivers and biological communities in space and time.

The International Seabed Authority (ISA) has issued 16 polymetallic nodule exploration contracts within the Clarion and Clipperton Fracture Zones (CCZ), each with an area of up to 75,000 km^2 for a total contract area of ∼1.25 million km^2 (isa.org.jm/deep-seabed-minerals-contractors). Polymetallic nodule areas of greatest economic interest occur in the Pacific Ocean, between the CCZ (Hein et al., 2013). Pacific nodules generally occur between ocean depths of 3,500–6,500 m, where low deposition rates and weak currents allow manganese and iron minerals to precipitate from bottom waters and/or from sediment pore waters, generally yielding nodule growth rates of ∼1–12 mm per million years (Hein et al., 2013). To protect regional biodiversity and ecosystem functions in the face of nodule mining, a system of nine "no-mining" areas, called Areas of Particular Environmental Interest (APEIs) have been established within the CCZ region. The APEI network was originally designed to protect the full range of deep-sea habitats in the CCZ, capturing differences in seafloor community structure and function driven by food availability (e.g., north-south and east-west gradients in seafloor particulate organic carbon flux), nodule abundance, and the occurrence of seamounts (ISA, 2008; Wedding et al., 2013).

CCZ Data Synthesis Exploring APEI Representativeness

The *Deep CCZ Biodiversity Synthesis Workshop* held at Friday Harbor Laboratories on October 1–4, 2019 (ISA, 2019) was organized by the DeepCCZ Project (led by University of Hawaii) and ISA and included experts specializing in microbes, meiofauna, macrofauna, megafauna, ecosystem-functions and habitat-mapping to address questions on biodiversity, biogeography, genetic connectivity, ecosystem functions, and habitat modeling throughout the region. Prior to this workshop, available physiographic, nodule-resource, sediment, bottom-water, flux, climate-change, and biogeographic data for the CCZ were obtained, harmonized and compiled into a data report. This report supported analyses of environmental heterogeneity across the CCZ, and helped evaluate drivers of biodiversity, community structure, and ecosystem functions at a regional scale (ISA, 2019, see other papers in this special volume). The environmental data were also used to support habitat mapping throughout the CCZ (McQuaid et al., 2020). Workshop participants' examined correlations between environmental variables and spatial patterns of benthic communities to help identify ecological drivers, and to evaluate the representativity of APEIs for nearby contractor areas. This paper is a compilation and summary of the data provided to participants in the *Deep CCZ Biodiversity Synthesis Workshop*. This compilation may help to identify environmental proxies to predict environmental and ecological patterns in poorly sampled areas of the CCZ, as well as in other deep-sea regions.

MATERIALS AND METHODS

Study Area

The CCZ is an approximately 6 million km^2 area between ∼115–155° W longitude, and ∼0–20° N latitude, containing nodule fields of interest for mining (Hein et al., 2013; Wedding et al., 2013). Locations of contract areas, reserve areas (areas reserved for mining by developing countries or the ISA itself), and APEIs were obtained from the ISA,[1] while the locations of the nine environmental subregions used in recommending APEI locations were obtained from Wedding et al. (2013) (**Figure 1**). Environmental subregions were created to capture the large north-south and east-west gradients in surface production and Particulate Organic Carbon (POC) flux to the seafloor in the CCZ (Lutz et al., 2007) which in turn drive changes in benthic communities (Wedding et al., 2013). The APEI system was originally designed such that each APEI would be located within, and representative of, a corresponding subregion (Wedding et al., 2013). However, when the APEI network was adopted by the ISA, some APEIs originally placed in subregions within the central CCZ were shifted to the periphery to avoid any overlaps with existing exploration and/or reserved areas (ISA, 2011; Wedding et al., 2013).

Environmental Data

Data sets for environmental variables compiled for and summarized in the ISA Deep CCZ workshop data report, using measured or modeled values, were collected from online resources and direct solicitations from scientists. All datasets were compiled in ArcGIS 10.7. For display purposes, the values for each variable were divided into ∼5–10 bins to illustrate heterogeneity observed throughout the CCZ. To interpolate point data throughout the CCZ, Empirical Bayesian Kriging was performed in ArcGIS using the empirical transformation and Bessel semi-variogram. All data sets in this study are based on interpolated values, with those not based on satellite data likely interpolated from a limited number of data points. Data sets were analyzed to estimate means, standard deviations, minimum and maximum values for each subregion and APEI (**Figure 1**).

Physiographic Data

Seafloor depth data were obtained from ETOPO1 for the grid calculated at 1 arc-minute intervals (Amante and Eakins, 2009; NOAA National Geophysical Data Center, 2009)[2] and extracted at 0.5-degree intervals. Means and standard deviations of depths within each subregion and APEI were calculated. Some depth points in a given region, subregion, or APEI may represent seamounts vs. abyssal seafloor; however, owing to the large number of data points and relatively few seamounts, this would

[1] www.isa.org.jm/maps

[2] https://ngdc.noaa.gov/mgg/global/global.html

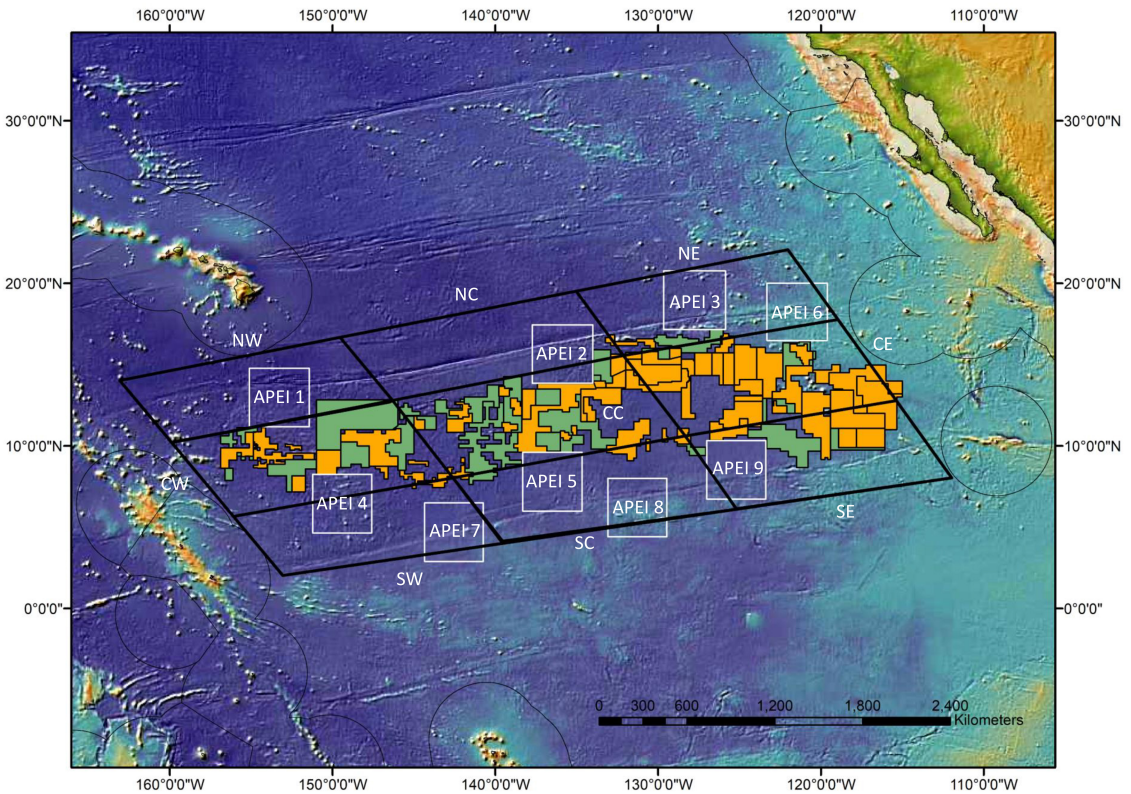

FIGURE 1 | CCZ environmental subregions (large black-outlined parallelograms—NW = northwest, NC = north-central, NE = northeast, CW = central-west, CC = central, CE = central-east, SW = southwest, SC = south-central, and SE = southeast CCZ blocks), exploration areas (orange), reserve areas (green), and APEIs (1–9, outlined in white). APEIs were located by the ISA (2011) to be representative of respective subregions as follows: NE – 1, NC – 2, NE -3, CW – 4, CC – 5, CE – 6, SW – 7, SC – 8, SE – 9. Darker blues represent deeper depths, for values see **Supplementary Figure 1**.

be unlikely to skew mean depths. Seamount and knoll data at a resolution of 30 arc-seconds were obtained from Yesson et al. (2011). Seamounts are defined as features rising >1,000 m above the surrounding seafloor, while knolls are defined as features rising between 200 and 1,000 m. Seafloor slope data at a resolution of 1 arc-minute were obtained from McQuaid et al. (2020) who derived slope from the GEneral Bathymetric Chart of the Oceans (GEBCO) bathymetry using the Benthic Terrain Modeler extension in ArcMap 10.4 to determine the largest change in elevation between a cell and its eight nearest neighbors at a scale of 1 km^2. Interpolated seafloor slope data were extracted at 1-degree intervals.

Resource Data

Most data for nodule abundance (kg/m^2), as well as percent cobalt, nickel, manganese, and copper content of nodules, were obtained from ISA Technical Study No. 6 (ISA, 2012). Nodule abundance data were available between 5.5–19°N and 119–160°W, Co-content data between 5.5–17.5°N and 114–160°W, and other nodule content data between 3–19°N and 115–160°W. Additional unpublished data for all nodule variables, compiled in 2018 were from the area delimited by 2.5–21°N and 112–160°W, excluding contractor areas (see data in **Supplementary Material**: Dr. C. Morgan, unpublished data). Finally, nodule data were unavailable from the northern 5% of the NE subregion, the western 11% of the NW subregion, and southern 1% of SW subregion as well as several contractor regions in the eastern CE and SE subregions (**Figure 1** and **Supplementary Figures 5–9**). All nodule data were in the form of point values in a 0.5-degree grid. For mapping, values of nodule variables were interpolated as described above.

Sediment Data

Sediment type, calcium-carbonate content, and biogenic-silica content were obtained from GeoMapApp,[3] and were based on sediment-type analyses of Dutkiewicz et al. (2015), the sediment calcium-carbonate compilation of Archer (2003), and the sediment biogenic-silica (opal) content compilation of Archer (1999). Raw data for sediment type were not available with specific spatial coordinates, so summaries were made based on the figures created in GeoMapApp. Raw sediment calcium carbonate and biogenic silica data were used to interpolate these variables across the entire region, and data were extracted from these interpolations at 1-degree intervals. Sediment total-organic-carbon data were obtained from Jahnke (1996) who digitized Total Organic Carbon (TOC) from Premuzic et al.

[3]http://www.geomapapp.org

(1982) at a 2-degree scale. Sediment accumulation-rate data were obtained from Jahnke (1996), who digitized accumulation rates from Cwienk (1986) at a 2-degree scale. Sediment thickness data were obtained from NOAA's National Centers of Environmental Information[4] (Straume et al., 2019). Sediment thickness data extracted at 1-degree intervals were used for calculations of summary statistics.

Water-Column Data

Bottom-water temperature, salinity, dissolved oxygen concentration, nitrate, phosphate, and silicate data were obtained from NOAA's Ocean Climate Laboratory Team in the World Ocean Atlas 2018 (WOA18).[5] The deepest value for each point below 3,000 m was used as representative of "bottom water," although data were only available to a depth of 5,500 m. Bottom-water temperature (Locarnini et al., 2019) and salinity (Zweng et al., 2019) data were averaged from 2005 to 2017 and analyzed at 15-arc-minute intervals. Bottom-water concentrations of oxygen, nitrate, phosphate, and silicate were averaged from 1960 to 2017 and calculations of summary statistics were made at 1-degree intervals (Garcia et al., 2019). Bottom-water pH was obtained from Sweetman et al. (2017) who used the program CO2SYS and inorganic CO_2, alkalinity, temperature, salinity, and pressure data from the Global Ocean Data Analysis Project and WOA 2013 average from 1998 to 2010 to estimate pH. Calculations on pH data were performed at 0.5-degree intervals. Concentrations of particulate matter in bottom water (1 value 10–15 mab) and nepheloid layer thickness were obtained from Gardner et al. (2018). The nepheloid layer thickness was defined as the distance between the seafloor and sampling depth with a particulate concentration >20 μg/L, with sampling intervals of ∼30 m. Analyses of bottom-water particulate matter concentration and nepheloid-layer thickness data were performed at 1-degree intervals. Bottom-water calcite saturation (1951–2000) was obtained from Levin et al. (2020) at a 0.5-degree scale, and calcite saturation horizon depth was estimated using maps from Yool et al. (2013).

Net Primary Production (NPP) data were obtained from Ocean Productivity website.[6] This website provides NPP based on three models: (1) Behrenfeld and Falkowski (1997), the Vertically Generalized Production Model (VGPM), (2) Behrenfeld et al. (2005), the Carbon-based Productivity Model (CBPM), and (3) Silsbe et al. (2016), the Carbon, Absorption, and Fluorescence Euphotic-resolving Model (CAFE). These models all used MODerate resolution Imaging and Spectroradiometer (MODIS) and Sea-viewing Wide Field-of-view Sensor (SeaWiFS) data as well as euphotic zone depth estimates from a model by Morel and Berthon (1989). The NPP data used here represent daily measurements averaged from 1998 to 2010 and 2010 to 2017. NPP data for the 1998–2010 time interval were used to match the interval of analyses performed previously to calculate POC flux using models from Lutz et al. (2007) by Sweetman et al. (2017), while NPP data for the 2010–2017 time interval were used to compare to NPP from the 1998–2010 dataset to examine temporal differences in patterns of surface production throughout the CCZ.

Particulate Organic-Carbon Flux

Estimated annual POC flux data to the seafloor were obtained from Lutz et al. (2007), hereafter named Lutz POC, who used 8-day SeaWiFS satellite images of chlorophyll-a concentrations (1997–2004), VGPM NPP, and ETOPO1 data to estimate seafloor flux. Comparisons were also made to estimated annual POC flux data obtained from Sweetman et al. (2017), who used monthly SeaWiFS (1998–2007) and MODIS (2008–2010) chlorophyll-a concentrations, VGPM NPP, and ETOPO1 data to estimate seafloor flux with the flux model created by Lutz et al. (2007).

Climate-Change Data

Projected changes in bottom-water temperature, oxygen, pH, POC flux, and calcite saturation (from 1951–2000 to 2081–2100), were obtained from Levin et al. (2020). All projections are based on the Representative Concentration Pathway (RCP) 8.5 climate-change scenario, and projected values (2081–2100) were subtracted from historical values (1951–2000) to get change over time. Model results were mapped at a 0.5-degree resolution using bilinear interpolation.

CCZ Biogeography

Lower-bathyal (800–3,500 m) and abyssal (3,500–6,500 m) biogeographic province boundaries were obtained from Watling et al. (2013), who used environmental variables as proxies to postulate the distribution of deep-sea biogeographic provinces. Seamount biogeographical classifications were obtained from Clark et al. (2010), who refined abyssal biogeographic province boundaries from UNESCO (2009). Pelagic marine provinces were obtained from UNESCO (2009).

Analyses

Data for all compiled environmental variables were extracted for each CCZ subregion as well as for each APEI at the spatial resolution provided in the data sources as indicated above. If the data sources were only provided as spatial rasters, then data were extracted at 1-degree intervals for our analyses. The mean, minimum, maximum, and range of values within a subregion or APEI for each variable were calculated using R version 4.0. The identification of APEIs and CCZ subregions are given in **Figure 1**.

RESULTS AND DISCUSSION

Block and APEI Descriptions

Physiographic Data

Depth

Abyssal seafloor depths at 0.5-degree resolution increase from east to west and south to north within the CCZ (**Table 1** and **Supplementary Figure 1**), yielding shallowest average abyssal depths (∼4,300–4,500 m) in the southeast and central-east near

[4]https://ngdc.noaa.gov/mgg/sedthick/

[5]https://www.nodc.noaa.gov/OC5/woa18/woa18data.html

[6]http://orca.science.oregonstate.edu/1080.by.2160.monthly.hdf.vgpm.v.chl.v.sst.php

the fracture zones, and deepest average depths (∼5,400 m) in the northwest (south of Hawaii). The central CCZ has the smallest range in abyssal seafloor depths (∼4,650–5,350 m) while the northern areas near, the Clarion Fracture Zone, have the largest range (∼3,900–5,800 m), although this range could include seamounts. The APEIs have similar depths to their designated subregions, except for APEIs 5 and 6, which are substantially shallower than their subregions (CC and CE, respectively). The greatest average depths are found in APEI 1 (∼5,400 m) (**Table 1** and **Supplementary Figure 1**). No APEI has a depth range, at 0.5-degree resolution, greater than 1,000 m.

Seamounts

Based on bathymetry at 30 arc-second resolution (Yesson et al., 2011), there were 347 seamounts (elevation >1,000 m) within the CCZ. These were distributed primarily around the fracture zones and at the eastern and western ends of the CCZ, including the peripheral exploration claim areas and APEIs, with the western CCZ having the highest abundance (**Table 1** and **Supplementary Figure 2**). APEI 9 has no seamounts, the majority of APEIs have <10, and APEI 4 had the highest number (22) (**Supplementary Table 1** and **Supplementary Figure 2**).

Average seamount summit water depth is shallowest in the east and deepest in the north, corresponding to patterns in seafloor depth (**Table 1** and **Supplementary Figure 3**). The central CCZ contained seamounts of similar summit water depths while the average depth of seamounts in the north ranged from 3,000 to 4,000 m. The average height (from base to summit) of seamounts was highest in the NW and CE (∼2,000 m). The tallest seamounts were >3,500 m tall and found in the north and east (**Supplementary Table 1** and **Supplementary Figure 4**). Most regions had a wide range of seamount heights. Average seamount area was smallest in the central CCZ and largest in the south. The seamounts with smallest areas were in the north, resulting in larger ranges of seamount size here (**Supplementary Table 1** and **Supplementary Figure 5**).

Average seamount summit water depth was lowest in APEIs 6 and 8 (∼2,600 m) and highest in APEI 1 (∼4,300 m) (**Table 1** and **Supplementary Figure 3**). APEI 6 had at least one seamount that reaches 500 m depth, which was much shallower than any seamounts found throughout the rest of the APEI system (**Supplementary Table 1**). The average height of seamounts was lowest in APEI 5 (∼1,100 m) and highest in APEI 3 (∼1,700 m) (**Table 1** and **Supplementary Figure 4**). Seamounts had smaller average areas in northern APEIs and larger areas in southern APEIs (**Supplementary Table 1** and **Supplementary Figure 5**).

Knolls

Based on bathymetry at 30 arc-second resolution (Yesson et al., 2011), knolls, with heights of 200–1,000 m above the general seafloor, were much more widely distributed than seamounts, and were common around the periphery of the CCZ. The SC region had the fewest number of knolls, while the most were found in the north and west (**Table 1** and **Supplementary Figure 6**). Subregions with the deepest and shallowest knolls mirrored average depth patterns (**Supplementary Figure 7**). Knolls were, on average, highest in the NE (∼ 600 m) and lowest in the CE (∼400 m) (**Table 1** and **Supplementary Figure 8**). Average knoll area was highest in the SW (∼700 m^2) and lowest in the NW (∼600 m^2) (**Table 1** and **Supplementary Figure 9**).

In the APEI system, there were fewer knolls in the southern APEIs and more in the west (**Table 1** and **Supplementary Figure 6**). Average knoll summit depth was lowest in APEI 6 (∼3,500 m) and highest in APEI 1 (∼5,100 m) (**Table 1** and **Supplementary Figure 7**). Average knoll height was lowest in APEI 9 (∼400 m) and highest in APEI 3 (∼600 m) (**Table 1** and **Supplementary Figure 8**). Average knoll area was lowest in APEI 7 (∼500 m^2) and highest in APEI 6 (∼700 m^2) (**Table 1** and **Supplementary Figure 9**).

Slope

High resolution multibeam bathymetry indicates that the seafloor of the CCZ is characterized by ridges and valleys varying in depth by at least 500 m (e.g., Amon et al., 2016), likely resulting from horst and graben structures formed during seafloor spreading (Johnson, 1972; Macdonald et al., 1996). However, these features are poorly resolved in the 0.5-degree bathymetric data available across the CCZ (**Supplementary Figure 1**). At the 0.5-degree scale, average seafloor slope is generally between 1 and 2 degrees for CCZ subregions and APEIs (**Table 1**). The highest and most variable slopes are found in the CC and NE (ranging ∼12–13 degrees) (**Supplementary Table 1** and **Supplementary Figure 10**). The high slopes broadly reflect the location of the fracture zones and the seamount/knoll features. Patterns of slopes in APEIs are broadly representative of their respective subregions (**Supplementary Figure 10**).

Nodule Resource Data

Nodule abundance

Mean nodule abundance in the CCZ at a resolution of 0.5 degrees is highly variable, with some areas completely devoid of nodules while others have nodule densities >18 kg/m^2 (ISA, 2012; **Supplementary Table 1** and **Supplementary Figure 11**). Nodule abundance varies over scales of <1 to 100 km apparently related to differences in sedimentation rates, organic matter content, concentration of leachable manganese, and oxygen penetration depth (Mewes et al., 2014). Mean nodule abundances were highest in the CE subregion (∼7.5 kg/m^2) and lowest in the southern subregions (∼1.5–3 kg/m^2). APEIs 1, 2, 3, 7, 8, and 9 contained lower mean abundance of nodules than their corresponding CCZ subregions (<2 kg/m^2 less) (**Table 1** and **Supplementary Figure 11**). APEIs 5 and 6, which were relocated from within their subregions by the ISA (Wedding et al., 2013), have substantially lower mean nodule abundances than their respective subregions (CC and CE; ≥3 kg/m^2 less). No APEI contained areas with nodule abundances >9 kg/m^2 (**Supplementary Table 1**). It should be emphasized that these values are from modeled data with a resolution of 0.5 degrees. Core sampling and photograph surveys indicate substantial finer-scale variations in nodule abundance than captured here (e.g., Peukert et al., 2018; Simon-Lledó et al., 2019a).

Nodule cobalt content

Mean nodule cobalt content at a resolution of 0.5 degrees was highest in the north (∼0.25%) and lowest in the south (∼0.15%).

TABLE 1 | The mean (standard deviation) of environmental variables in each CCZ subregion and APEI.

Mean	NW	APEI 1 (NW)	NC	APEI 2 (NC)	NE	APEI 3 (NE)	CW	APEI 4 (CW)	CC	APEI 5 (CC)
Physiographic Data										
Depth (etopo1) (m)	5414.49 (235.04)	5445.72 (228.4)	5216.68 (232.86)	4968.99 (186.21)	4592.95 (405.98)	4686.66 (162.85)	5112.88 (208.3)	4929.46 (145.99)	4953.94 (128.93)	4745.06 (95.62)
Seamount Abundance	64	8	24	13	46	10	57	22	7	2
Seamount Summit Depth (m)	3201.44 (1044.34)	4348.75 (340.58)	3979.79 (277.35)	3710.85 (506.64)	2692.59 (672.55)	3048.5 (512.82)	3125.86 (940.99)	3604.68 (202.27)	3249.29 (669.06)	3500 (48.08)
Seamount Summit Height (m)	2002.08 (756.86)	1338.25 (235.75)	1246.21 (146.78)	1335.92 (426.66)	1691.2 (630.52)	1657.1 (473.09)	1626.11 (569.54)	1265.45 (189.92)	1738.29 (526.19)	1092 (36.77)
Seamount Area (m^2)	869.83 (181.46)	789.04 (140.31)	734.29 (186.51)	836.13 (151.48)	833.38 (212.91)	841.03 (241.94)	881.38 (193.72)	894.58 (190.81)	733.93 (268.74)	870.59 (90.43)
Knoll Abundance	270	107	146	46	213	63	316	65	161 (	16
Knoll Summit Depth (m)	4991.7 (297.4)	5066.82 (310.29)	4676.28 (325.29)	4389.09 (221.51)	3962.6 (424.93)	4086.9 (277.77)	4665.07 (263.72)	4509.38 (256.16)	4592.44 (243.04)	4209.31 (208.62)
Knoll Summit Height (m)	522.49 (192.09)	510.09 (167.02)	549.03 (231.11)	562.48 (231.75)	582.77 (213.49)	619.57 (215.89)	506.37 (190.79)	508.06 (177.53)	494.86 (186.52)	537.19 (179.21)
Knoll Area (m^2)	598.53 (225.46)	624.13 (215.69)	687.39 (193.91)	692.03 (166.85)	662.09 (189.42)	665.6 (196.32)	654.23 (200.82)	688.87 (217.95)	647.92 (191.29)	616.95 (238.95)
Seafloor Slope (°)	1.34 (1.42)	1.78 (1.92)	1.03 (0.96)	1.28 (0.96)	1.9 (2.24)	1.5 (0.92)	1.21 (1.32)	2.82 (2.62)	1.17 (1.61)	0.79 (0.52)
Resource Data										
Nodule Abundance (kg/m2)	5.12 (2.12	3.79 (1.96)	4.81 (1.57)	4.04 (1.53)	5.56 (1.29)	5.35 (1.15)	5.25 (2.93)	5.47 (2.08)	4.79 (3.37)	1.28 (0.27)
Nodule Co (%)	0.24 (0.01)	0.24 (0.01)	0.23 (0.01)	0.24 (0.01)	0.27 (0.04)	0.26 (0.01)	0.22 (0.04)	0.20 (0.03)	0.22 (0.03)	0.17 (0.02
Nodule Ni (%)	1.13 (0.04)	1.16 (0.06)	1.06 (0.09)	1.14 (0.13)	1.12 (0.10)	1.06 (0.10)	1.20 (0.15)	1.15 (0.12)	1.33 (0.12)	1.33 (0.05)
Nodule Cu (%)	0.87 (0.04)	0.89 (0.07)	0.95 (0.11)	0.95 (0.14)	0.87 (0.12)	0.92 (0.13)	0.98 (0.19)	1.03 (0.12)	1.11 (0.11)	1.12 (0.03)
Nodule Mn (%)	24.69 (0.62)	24.79 (0.69)	24.49 (1.13)	25.73 (2.28	25.55 (1.44)	25.30 (1.29)	25.15 (2.38	23.86 (2.06)	28.35 (2.35)	29.15 (0.60)
Sediment Data										
Calcium Carbonate (%)	1.66 (3.21)	0.43 (0.15)	0.69 (0.79)	4.67 (4.74)	1.60 (1.59)	0.45 (0.14)	9.85 (12.21)	31.81 (10.16)	2.15 (3.92)	19.93 (22.43)
Biogenic Silica (%)	5.70 (1.22)	7.21 (0.43)	3.86 (0.55)	4.01 (0.31)	3.71 (0.93)	3.14 (0.61)	9.55 (2.58)	17.34 (2.76)	6.24 (1.39)	10.18 (2.16)
Sediment Thickness (m)	129 (58.56)	126.88 (41.25)	101.14 (1.36)	101.17 (0.39)	86.26 (18.19)	92.69 (3.88)	228.94 (63.14)	355.11 (53.78)	147.38 (47.06)	289.42 (54.23)
Water-Column Data										
Temperature (°C)	1.43 (0.03)	1.43 (0.02)	1.44 (0.03	1.43 (0.02)	1.48 (0.04)	1.46 (0.03)	1.43 (0.03)	1.43 (0.02)	1.44 (0.02)	1.4 (0.02)
Salinity	34.7 (0)	34.7 (0)	34.7 (0)	34.69 (0)	34.69 (0)	34.69 (0)	34.7 (0)	34.7 (0)	34.69 (0)	34.69 (0)
Dissolved Oxygen (ml/L)	4.11 (0.06)	4.12 (0.05)	3.98 (0.13)	3.92 (0.15)	3.79 (0.24)	3.86 (0.12)	4.03 (0.09)	3.94 (0.04)	3.89 (0.11)	3.92 (0.07)
Nitrate (μmol/kg)	34.09 (0.37)	34.11 (0.23)	34.19 (0.57)	34.6 (0.33)	35.37 (0.95)	34.83 (0.26)	34.31 (0.2)	34.56 (0.08)	34.68 (0.38)	34.8 (0.18)
Phosphate (μmol/kg)	2.36 (0.03)	2.35 (0.03)	2.38 (0.05)	2.37 (0.03)	2.42 (0.08)	2.38 (0.05)	2.4 (0.06)	2.41 (0.03)	2.4 (0.04)	2.42 (0.01)
Silicate (μmol/kg)	133.38 (2.5)	135.01 (0.74)	136.73 (4.74)	139.31 (5.31)	146.72 (10.13)	142.06 (2.06)	135.82 (0.21)	136.25 (1.43)	141.09 (2.38)	139.36 (2.62)
pH	7.95 (0.01)	7.96 (0)	7.95 (0)	7.95 (0)	7.94 (0.02)	7.94 (0.01)	7.96 (0)	7.96 (0.01)	7.95 (0.01)	7.92 (0)
Bottom-Water Particulate Matter (μg/L)	6.03 (1.37)	5.23 (0.39)	3.63 (0.26)	3.68 (0.11	3.81 (0.24)	3.85 (0.19)	6.04 (1.18)	5.83 (0.32	4.67 (0.46)	5.56 (0.22)

(Continued)

TABLE 1 | Continued

Mean	NW	APEI 1 (NW)	NC	APEI 2 (NC)	NE	APEI 3 (NE)	CW	APEI 4 (CW)	CC	APEI 5 (CC)
Nepheloid Thickness (m)	13.16 (8.17)	8.46 (2.15)	0 (0)	0 (0)	0 (0)	0 (0)	6.58 (8.13)	2.24 (1.32)	0 (0)	0 (0)
Calcite Saturation (%)	64.77 (1.50)	65.34 (1.84)	63.65 (1.19)	64.76 (0.86)	67.43 (2.67)	67.18 (1.20)	66.23 (1.69)	66.22 (0.81)	64.97 (0.61)	66.25 (0.89)
Net Primary Production										
VGPM 1998–2010 (g C/m^2/y)	75.99 (6.53)	80.65 (5.19)	90.41 (7.16)	100.32 (4.54)	96.53 (3.24)	90.32 (1.35)	96.33 (5.86)	110.11 (7.95)	110.67 (6.75)	114.86 (5.95)
VGPM 2010–2017 (g c/m^2/y)	66.62 (6.09)	69.01 (3.43)	84.73 (5.71	92.11 (4.93)	89.52 (3.93)	87.08 (2.42)	83.27 (6.56)	97.60 (8.07)	101.83 (6.44)	98.70 (4.51)
CBPM 1998–2010 (g C/m^2/y)	174.46 (9.95)	180.82 (8.98)	171.67 (10.46)	179.81 (10.46)	157.07 (10.65)	150.11 (6.76)	207.55 (8.46)	231.66 (14.77)	214.76 (11.02)	226.57 (11.36)
CBPM 2010–2017 (g C/m^2/y)	178.01 (8.80)	181.54 (6.32)	182.01 (12.18)	188.52 (13.20)	164.63 (12.04)	157.68 (9.60)	208.59 (11.64)	236.58 (17.74)	227.23 (12.65)	227.83 (10.76)
CAFE 2010–2017 (g C/m^2/y)	182.18 (7.40)	185.53 (6.31)	184.76 (9.11)	191.37 (9.44)	170.33 (11.37)	166.89 (9.44)	207.37 (8.59)	228.24 (9.86)	216.39 (8.02)	223.41 (8.72)
Particulate Organic Carbon Flux Data										
Lutz POC Flux 1997–2004 (g C/m^2/y)	1.02 (0.08)	1.07 (0.05)	1.24 (0.10)	1.37 (0.06)	1.40 (0.10)	1.36 (0.06)	1.25 (0.09)	1.56 (0.16)	1.47 (0.10)	1.55 (0.12)
Climate Change Data										
Temperature % change	0.02 (0)	0.02 (0)	0.02 (0)	0.01 (0)	0.01 (0)	0.01 (0)	0.02 (0)	0.02 (0)	0.01 (0)	0.01 (0)
O2 % change	−6.56 (0.99)	−7.18 (0.23)	−4.62 (1.85)	−2.23 (1)	−1.8 (0.04)	−1.53 (0.19)	−5.75 (1.4)	−3.36 (0.47)	−2.87 (1.43)	−3.01 (0.4)
pH % change	−0.21 (0.04)	−0.24 (0.01)	−0.14 (0.07)	−0.05 (0.04)	−0.04 (0.02)	−0.02 (0.01)	−0.21 (0.05)	−0.13 (0.02)	−0.09 (0.07)	−0.1 (0.02)
Calcite Saturation % change	−3.24 (0.91)	−3.87 (0.27)	−2.13 (1.28)	−0.38 (0.72)	−0.13 (0.34)	0.24 (0.19)	−3.45 (0.87)	−1.92 (0.42)	−1.11 (1.33)	−1.45 (0.34)
POC Flux % change	−25.76 (2.96)	−25.67 (1.29)	−21.08 (2.13)	−21.06 (2.17)	−18.59 (4.89)	−16.03 (2.93)	−16.98 (5.88)	−10.52 (2.07)	−17.44 (5.68)	−4 (1.92)

Mean	CE	APEI 6 (CE)	SW	APEI 7 (SW)	SC	APEI 8 (SC)	SE	APEI 9 (SE)
Physiographic Data								
Depth (etopo1) (m)	4448.23 (325.16)	4068.1 (145.3)	4879.64 (200.31)	4676.16 (244.5)	4662.54 (247.9)	4395.57 (235.5)	4282.34 (234.17)	4531.28 (92.58)
Seamount Abundance	24	9	20	3	9	6	26	0
Seamount Summit Depth (m)	2273.08 (958.06)	2600.89 (810.65)	3505.65 (366.2)	3258 (37.51)	2848.33 (447.86)	2618.67 (293.57)	2498.88 (649.65)	N/A (N/A)
Seamount Summit Height (m)	1941.79 (902.13)	1505.33 (758.04)	1315.1 (313.77)	1252.33 (49.22)	1388.56 (308.09)	1478.33 (325.82)	1590.73 (592.6)	N/A (N/A)
Seamount Area (m^2)	917.52 (159.08)	782.93 (212.53)	931.87 (109.47)	964.9 (211.21)	933.04 (118.91)	939.53 (133.79)	827.02 (184.35)	N/A (N/A)
Knoll Abundance	103	49	117	5	73	30	233	16
Knoll Summit Depth (m)	3926.29 (332.34)	3538.78 (202.84)	4493.73 (284.7)	3998.2 (469.5)	4171.1 (345.66)	3978.57 (284.97)	3676.83 (279.39)	4105.31 (155.15)
Knoll Summit Height (m)	408.75 (137.28)	563.18 (192.97)	481.78 (181.66)	579.4 (340.59)	478.58 (160.88)	451.07 (170.23)	495.94 (190.68)	437.25 (125.8)

(Continued)

TABLE 1 | Continued

Mean	CE	APEI 6 (CE)	SW	APEI 7 (SW)	SC	APEI 8 (SC)	SE	APEI 9 (SE)
Knoll Area (m^2)	646.75 (181.33)	721.49 (174.23)	695.23 (219.49)	539.81 (253.06)	633.81 (231.64)	713.96 (182.81)	628.92 (214.2)	587.11 (250.66)
Seafloor Slope (°)	0.99 (0.87)	1.63 (1.54)	0.92 (0.68)	0.7 (0.41)	0.94 (0.59)	1.29 (1.59)	1.31 (1.55)	1.02 (0.63)
Resource Data								
Nodule Abundance (kg/m2)	7.47 (3.92)	4.48 (0.56)	3.18 (2.11)	1.5 (1.17)	1.61 (0.77)	1.42 (0.28)	4.21 (1.90)	2.51 (1.09)
Nodule Co (%)	0.21 (0.03)	0.26 (0.05)	0.16 (0.04)	0.16 (0.01)	0.16 (0.03)	0.14 (0.01)	0.17 (0.02)	0.18 (0)
Nodule Ni (%)	1.31 (0.06)	1.22 (0.07)	1.32 (0.15)	1.46 (0.01)	1.26 (0.10)	1.21 (0.02)	1.22 (0.08)	1.18 (0.07)
Nodule Cu (%)	1.10 (0.16)	0.84 (0.05)	1.19 (0.15)	1.30 (0.04)	1.18 (0.09)	1.18 (0.04)	1.17 (0.11)	1.25 (0.04)
Nodule Mn (%)	29.1 (1.65)	26.60 (0.55)	26.87 (2.94)	29.87 (0.09)	29.85 (0.80)	29.98 (0.43)	30.76 (0.90)	31.43 (0.17)
Sediment Data								
Calcium Carbonate (%)	2.75 (2.59)	5.04 (1.86)	38.39 (19.80	53.78 (22.27)	32.51 (26.95)	53.39 (19.82)	26.35 (18.01)	27.1 (14.74)
Biogenic Silica (%)	8.15 (2.41)	5.87 (1.05)	20.23 (4.59)	19.43 (2.27)	13.08 (2.80)	17.2 (3.30)	12.78 (1.97)	14.52 (1.46)
Sediment Thickness (m)	80.49 (22)	51 (11.18)	361.07 (68.23)	439.44 (75.3)	332.2 (87.9)	409.31 (66.99)	125.57 (62.82)	215.42 (32.15)
Water-Column Data								
Temperature (°C)	1.45 (0.05)	1.52 (0.02)	1.41 (0.03)	1.39 (0.03)	1.42 (0.03)	1.42 (0.02)	1.47 (0.03)	1.45 (0.01)
Salinity	34.69 (0)	34.68 (0)	34.7 (0)	34.7 (0)	34.69 (0)	34.69 (0.01)	34.69 (0)	34.69 (0)
Dissolved Oxygen (ml/L)	3.65 (0.22)	3.48 (0.14)	3.94 (0.08)	3.84 (0.2)	3.83 (0.13)	3.75 (0.08)	3.58 (0.15)	3.75 (0.04)
Nitrate (μmol/kg)	35.37 (0.77)	36.41 (0.25)	34.42 (0.26)	34.32 (0.16)	34.8 (0.48)	34.99 (0.37)	35.7 (0.56)	35.6 (0.49)
Phosphate (μmol/kg)	2.36 (0.11)	2.44 (0.05)	2.4 (0.04)	2.38 (0.03)	2.43 (0.05)	2.46 (0.04)	2.45 (0.04)	2.45 (0.04)
Silicate (μmol/kg)	147.66 (5.5)	156.8 (2.4)	137.85 (2.11)	141.56 (1.09)	142.11 (3.86)	146.09 (3.27)	148.55 (2.31)	146.5 (1.62)
pH	7.94 (0.01)	7.92 (0.01)	7.95 (0.01)	7.94 (0.01)	7.93 (0.01)	7.93 (0)	7.94 (0)	7.94 (0)
Bottom-Water Particulate Matter (μg/L)	4.4 (0.21)	4.0 (0.22)	5.83 (0.69)	5.53 (0.22)	5.65 (0.38)	5.96 (0.24)	4.26 (0.36)	4.5 (0.19)
Nepheloid Thickness (m)	0 (0)	0 (0)	0.78 (1.21)	0 (0)	0 (0)	0 (0)	0 (0)	0 (0)
Calcite Saturation (%)	68.10 (2.28)	70.39 (0.53)	66.59 (1.62)	68.24 (2.29)	66.90 (1.91)	68.44 (1.80)	69.09 (1.12)	67.91 (0.51)
Net Primary Production								
VGPM 1998–2010 (g C/m^2/y)	113.14 (7.94)	99.32 (1.62)	121.86 (7.21)	127.14 (4.17)	118.30 (7.68)	124.72 (7.06)	110.50 (5.42)	111.73 (4.43)
VGPM 2010–2017 (g c/m^2/y)	103.39 (4.56)	94.79 (2.48)	107.93 (7.00)	111.34 (5.06)	102.33 (6.43)	107.32 (6.35)	97.35 (5.35)	96.60 (3.28)
CBPM 1998–2010 (g C/m^2/y)	210.34 (18.49)	168.08 (9.29)	254.41 (18.27)	261.74 (13.50)	234.21 (16.28)	248.58 (16.24)	222.91 (7.95)	220.90 (7.67)
CBPM 2010–2017 (g C/m^2/y)	221.01 (17.33)	179.75 (10.52)	259.94 (18.68)	264.32 (14.23)	235.76 (15.75)	248.03 (15.74)	226.41 (11.43)	220.94 (7.10)

(Continued)

TABLE 1 | Continued

Mean	CE	APEI 6 (CE)	SW	APEI 7 (SW)	SC	APEI 8 (SC)	SE	APEI 9 (SE)
CAFE 2010–2017 (g C/m^2/y)	213.63 (11.47)	179.75 (10.33)	241.37 (9.98)	245.25 (7.80)	229.46 (11.52)	240.56 (11.45)	220.04 (6.02)	218.05 (5.42)
Particulate Organic Carbon Flux Data								
Lutz POC Flux 1998–2010 (g C/m^2/y)	1.57 (0.08)	1.47 (0.05)	1.75 (0.17)	1.87 (0.15)	1.64 (0.20)	1.81 (0.20)	1.59 (0.09)	1.56 (0.10)
Climate Change Data								
Temperature % change	0.01 (0)	0.01 (0)	0.01 (0)	0.01 (0)	0.01 (0)	0.01 (0)	0.01 (0)	0.01 (0)
O2 % change	−1.87 (0.59)	−2.01 (0.31)	−3.08 (0.38)	−2.91 (0.34)	−2.97 (0.88)	−4.04 (1.38)	−2.73 (1.15)	−2.8 (1.33)
pH % change	−0.04 (0.02)	−0.05 (0.01)	−0.12 (0.02)	−0.11 (0.01)	−0.09 (0.03)	−0.12 (0.05)	−0.07 (0.05)	−0.06 (0.05)
Calcite Saturation % change	−0.24 (0.48)	−0.46 (0.15)	−1.66 (0.34)	−1.45 (0.23)	−1.16 (0.69)	−1.64 (0.82)	−0.88 (0.88)	−0.59 (0.94)
POC Flux % change	−19.23 (3.7)	−23.2 (3.18)	−11.85 (2.46)	−10.5 (1.39)	−2.45 (4.31)	−1.86 (4.32)	−2.99 (6.29)	2.91 (2.32)

Values for each APEI are to the right of the CCZ subregion it is meant to represent. The CCZ subregion and APEI with the highest average values for each variable are marked in dark blue while the values with the lowest average values are marked in light blue. Values marked in green represent increases due to climate change.

Cobalt values were very similar between all subregions and APEIs (within 0.02%) except for the CC, where cobalt content was 0.05% higher than in its corresponding APEI (**Table 1** and **Supplementary Figure 12**). Minimum cobalt content was lower and maximum content higher in every subregion vs. nearest APEI (differing by as much as 0.1%) except for APEI 6 (**Supplementary Table 1** and **Supplementary Figure 12**), suggesting that there is variability in nodule composition within CCZ subregions not captured in the APEI system.

Nodule nickel content

In contrast to cobalt, mean nodule nickel content at a resolution of 0.5 degrees was lowest in the north (∼1.1%) and higher in the central and west (∼1.2–1.3%) (**Table 1** and **Supplementary Figure 13**). Nickel content was generally similar between CCZ subregions and corresponding APEIs (within 0.01%), but several subregions had lower minimum and higher maximum nickel values (**Supplementary Table 1** and **Supplementary Figure 13**).

Nodule copper content

Mean nodule copper content at a resolution of 0.5 degrees increased from north to south (∼0.3–0.4%) and from west to east (∼0.1%). Copper content was also generally similar between CCZ subregions and corresponding APEIs (within 0.05%, although there is a difference of ∼0.25% between CE and APEI 6) (**Table 1** and **Supplementary Figure 14**); however, subregions in the south and west had maximum copper content ∼0.1–0.2% higher than any areas found in the APEI system (**Supplementary Table 1** and **Supplementary Figure 4**).

Nodule manganese content

Mean nodule manganese content at a resolution of 0.5 degrees increased from north to south (∼5–6% increase) and from west to east (∼4–5%), following the same trend as copper. Manganese content was generally similar (i.e., within 1%) between CCZ subregions and corresponding APEIs; however, in the central CCZ, where exploration contract areas are concentrated, maximum manganese values were several percent higher in subregions than in the nearest APEIs (**Table 1** and **Supplementary Figure 15**). Likewise, minimum manganese values were often much lower in subregions than nearby APEIs (as much as 10% between SW and APEI 7), suggesting that there is variation in nodule characteristics and, potentially, habitat structure not captured by the APEI system (**Supplementary Table 1** and **Supplementary Figure 15**).

Seafloor Sediment Data

Sediment type

According to Dutkiewicz et al. (2015), most of the northern and central CCZ is dominated by siliciclastic clay while the southern CCZ is dominated by biogenic calcareous oozes (**Supplementary Figure 16**). The NW and CW subregions have large areas of radiolarian ooze while much of the SC is comprised of fine-grained calcareous sediment. APEIs generally mirror regional sediment patterns, although much of APEI 6 is indicated to include gravel and coarser siliciclastic material; the only location in the CCZ indicated to have this sediment type (Dutkiewicz et al., 2015; **Supplementary Figure 16**). However, direct sampling

and extensive seafloor photography in APEI 6 primarily found brown-clay sediments (Menendez et al., 2019; Simon-Lledó et al., 2019a).

Sediment total organic carbon content

Total organic carbon content at a 2-degree resolution appeared to be below 0.3% in sediment throughout the CCZ, including within APEIs, with the north having lower TOC than the south (Jahnke, 1996, Plate 2).

Sediment calcium carbonate content

Mean calcium-carbonate content at a 1-degree resolution was lowest in the northern (<1–2%) and highest in the southern CCZ (as high as >75%) (**Supplementary Figure 17**). This is likely related partially to depth, because many of the northern areas tend to be deeper than the calcite compensation depth in the region (∼4,500 m) (Van Andel, 1975). Overlying productivity and sinking calcium carbonate flux most likely also play a role, since areas deeper than 4,500 m in the southern subregions still have moderate calcium carbonate content (10–20%). Sediment calcium-carbonate content varied between several CCZ subregions and corresponding APEIs by as much as 20% (**Table 1** and **Supplementary Figure 17**).

Sediment biogenic silica content

Mean sediment biogenic silica content at a 1-degree resolution appeared to increase from north (3–5%) to south, up to 25–30% in the SW subregion (**Table 1** and **Supplementary Figure 18**). Because of the extremely low number of values collected, including several APEIs with no biogenic silica values, other patterns and comparisons between subregions and APEIs are not appropriate.

Sediment thickness

Mean sediment thickness at a 1-degree resolution was highest in the SW (∼350 m) and lowest in the northeast (∼100 m), decreasing northward and eastward. Average thickness was generally similar between CCZ subregions and APEIs, although APEIs 4 and 5 differed from their respective subregions (CW and CC) (**Table 1** and **Supplementary Figure 19**).

Sediment accumulation rate

Sediment accumulation rates at a 2-degree resolution appeared to be below 0.5 g/cm^2/1,000 year in nearly all areas of the CCZ seafloor, with the north and central areas having lower sedimentation rates than the south and west (Jahnke, 1996).

Water-Column Data

Bottom-water temperature

At a resolution of 0.25 degrees, mean bottom-water temperature was nearly uniform throughout the CCZ. Nowhere did temperatures fall below 1.3 or rise above 2°C (**Table 1** and **Supplementary Figure 20**). In the west and CE, temperatures varied by ∼0.5–0.6°C, while within all other subregions and all APEIs, temperature variations did not exceed 0.3°C (**Supplementary Table 1** and **Supplementary Figure 20**).

Bottom-water salinity

At a resolution of 0.25 degrees, variations in bottom-water salinity were small throughout the CCZ subregions and APEIs, ranging from 34.68 to 34.70 (**Table 1** and **Supplementary Figure 21**).

Bottom-water dissolved-oxygen concentration

At a resolution of 1 degree, mean bottom-water oxygen concentrations were lowest in the SE (∼3.6 mL/kg) and highest in the NW (∼4.1 mL/L), decreasing eastward (by ∼0.4 μmol/L) and southward (by ∼0.2 μmol/L) (**Table 1** and **Supplementary Figure 22**). Oxygen concentrations did not fall below 3.2 mL/L throughout the CCZ while maximum oxygen concentrations did not exceed 4.3 mL/L. In the NE CCZ, oxygen concentrations varied by ∼1 mL/L while other areas had less variability. The APEIs had similar oxygen concentrations to adjacent subregions, although oxygen ranges were usually smaller (**Supplementary Table 1** and **Supplementary Figure 22**). Oxygen concentrations seemed to follow similar patterns to seafloor POC flux and organic carbon content, with increases in seafloor POC flux likely resulting in decreases in oxygen due to greater biological oxygen demand. No seafloor areas (bottom waters) in the CCZ had oxygen levels below 3 mL/L, i.e., they remained well above thresholds considered stressful for deep-sea biota (Levin, 2003).

Bottom-water nitrate

At a resolution of 1 degree, mean bottom-water nitrate concentrations were highest in the SE (∼36 μmol/kg) and lowest in the NW (∼34 μmol/kg), with slight increases moving south (increasing ∼0.5 μmol/kg) and east (∼1 μmol/kg). Average nitrate concentrations in APEIs were similar to their respective subregions (generally differing by less than 0.5 μmol/kg) (**Table 1** and **Supplementary Figure 23**). Minimum nitrate concentrations in APEIs were somewhat higher than their respective subregions, although all values were within 2 μmol/kg (**Supplementary Table 1** and **Supplementary Figure 23**).

Bottom-water phosphate

Mean bottom-water phosphate concentrations at a 1-degree resolution were relatively uniform throughout the CCZ, with all average values near 2.4 μmol/kg (**Table 1** and **Supplementary Figure 24**). The NE and CE varied by 0.5 μmol/kg, twice the variability of any other area (**Supplementary Table 1** and **Supplementary Figure 24**).

Bottom-water silicate

Mean bottom-water silicate concentrations at a 1-degree resolution were highest in the SE (∼157 μmol/kg) and lowest in the NW (∼133 μmol/kg), generally increasing from north to south and west to east. While CCZ subregions and corresponding APEIs had similar average silicate concentrations (with differences generally less than 4 μmol/kg, except between CE and APEI 6), APEIs often had higher minimum values (by ∼5–10 μmol/kg) (**Table 1** and **Supplementary Figure 25**). APEI 6 had higher concentrations than anywhere else, and minimum values (∼152 μmol/kg) here were higher than maximums found in most other areas (**Supplementary Table 1** and **Supplementary Figure 25**).

Bottom-water pH

Mean bottom-water pH at a 0.5-degree resolution was nearly constant throughout the CCZ and APEI system, with average,

minimum, and maximum pH falling between 7.9 and 7.98 (**Table 1** and **Supplementary Figure 26**).

Bottom-water particulate matter

Bottom-water particulate matter concentrations at a 1-degree resolution were extremely low in all regions of the CCZ, with means, minimums, and maximums all <10 μg/L, which is below the detectable limit for the methods (**Table 1**, **Supplementary Table 1** and **Supplementary Figure 27**). These very low values indicate little or no sediment resuspension in the region (Gardner et al., 2018).

"Strong" Nepheloid-Layer Thickness

There was no evidence of "strong" nepheloid layers in the CCZ, at a 1-degree resolution, with mean, minimum, and maximum thicknesses all <50 m, i.e., below the detectable limit for the methods used (**Table 1**, **Supplementary Table 1** and **Supplementary Figure 28**). These low values provide no evidence of "strong" nepheloid layers in the region (Gardner et al., 2018).

Calcite saturation

Bottom waters throughout the region were undersaturated with calcite, with mean calcite saturation at a 0.5-degree resolution lowest in the NC (∼64%) and highest in the CE (∼69%), increasing from north to south (by ∼2–3%) and west to east (by ∼2–3%) (**Table 1** and **Supplementary Figure 29**). Calcite saturation did not fall below 60% throughout the CCZ while it exceeded 70% in areas throughout the south and east (**Supplementary Table 1** and **Supplementary Figure 29**). Saturation levels differed by ≤2% between each subregion and its representative APEI and varied ∼10% within several subregions.

Calcite saturation horizon

Calcite saturation horizons appear to be above 3 km depth in all areas throughout the CCZ (Yool et al., 2013).

Net Primary Production Data

Vertically Generalized Production Model (VGPM) NPP

Average, minimum, and maximum NPP estimated by the VGPM model (Behrenfeld and Falkowski, 1997) were highest in the SW (∼110–120 g C/m^2/year) and lowest in the NW (∼65–75 g C/m^2/year) for both time periods examined (1998–2010 and 2010–2017). NPP increased eastward (by ∼20 g C/m^2/year) and southward (by ∼20–50 g C/m^2/year) across the CCZ for both time periods (1998–2010 and 2010–2017). NPP was relatively high along the southern CCZ, and there was also a band of higher primary production in the CC and CE subregions (**Table 1** and **Supplementary Figures 30, 31**). NPP was lower in 2010–2017 than 1998–2010 across all subregions; however, relative productivity patterns across the CCZ remained similar (**Table 1** and **Supplementary Figures 30, 31**). The minimum values of ∼55–60 g C/m^2/year in the NW were less than half of the maximum values of ∼ 125–135 in the SW. The NE had less spatial variability in NPP than other areas. NPP in APEIs also increased southward, with the highest values in APEIs 7 and 8 (∼125 and 110 g C/m^2/year, respectively) (**Table 1** and **Supplementary Figures 30, 31**). Central and western APEIs also had higher NPP than corresponding subregions, while the opposite was true for eastern APEIs.

Carbon-Based Productivity Model (CBPM) and Carbon, Absorption, and Fluorescence Euphotic-resolving model (CAFE) NPP

Average, minimum, and maximum values of NPP estimated via CBPM and CAFE were roughly twice those estimated via the VGPM model (Behrenfeld and Falkowski, 1997). Mean NPP values for CBPM and CAFE NPP were within 5% of each other in nearly all areas, and means ranged between ∼150 and 170 g C/m^2/year in the NE to ∼240–260 g C/m^2/year in the SW (**Table 1** and **Supplementary Figures 32–34**). Patterns in NPP across the CCZ were also slightly different between the CBPM/CAFE and VGPM models, with CBPM/CAFE showing the lowest values in the NE instead of NW. Comparing time periods, VGPM NPP was always higher in 1998–2010 compared to 2010–2017 while CBPM NPP was always higher in 2010–2017 compared to 1998–2010 (**Table 1** and **Supplementary Figures 30–33**). However, CBPM estimates were more variable than VGPM estimates in 2010–2017 (often 2.3–2.5× greater) compared to 1998–2010 (no more than 2–2.2× greater) illustrating that temporal variability may not be captured the same way among models (**Table 1**). Another confounding factor is that chlorophyll data used to estimate NPP was estimated using measurements from the SeaWiFs instrument up to the mid-2000s but by MODIS beyond that. Thus, while patterns in NPP across CCZ areas and APEIs are similar among the three different methods with the north and west areas having lower NPP and the south and east areas having higher NPP, the ranking of specific areas is not identical nor are differences among time periods proportional.

Particulate Organic Carbon Flux Data

Seafloor POC flux

Average Lutz POC flux mirrored NPP (measured by VGPM, which was used as an input for POC flux calculations), with lowest mean value in the NW subregion (∼1 g C/m^2/year) and highest mean value in the SW subregion (1.74 g C/m^2/year) (**Table 1** and **Supplementary Figure 35**). The lowest average Lutz POC flux for APEIs was in APEI 1 (1.07) while the highest average values were in APEIs 7 and 8 (1.8–1.9) which conformed with patterns in CCZ subregions. The NW subregion and APEI 1 were the only areas with POC flux <1 g C/m^2/year, while the NE, SW, and SC subregions had flux of ∼2 g C/m^2/year in some areas (**Supplementary Table 1**). Variations in POC fluxes were 2–3 times larger in southern areas compared to the rest of the CCZ except for the NE. When comparing POC data from 1997 to 2004 (Lutz et al., 2007) to data from 1998 to 2010 (Sweetman et al., 2017) mean values for each CCZ subregion and APEI were within 0.01 g C/m^2/year between the two time periods. Maximum and minimum Lutz POC flux values were <0.05 g C/m^2/year different in the NW, NC, CW, and CC subregions and corresponding APEIs and 0.05–0.1 different in the CE, SW, SC, and SE subregions and corresponding APEIs while maximums were 0.7 and 0.2 g higher in the Lutz et al. (2007) dataset

compared to the Sweetman et al. (2017) dataset in the NE and APEI 3 (**Supplementary Table 1**).

Climate-Change Data (Projected Changes From the Interval 1951–2000 to 2081–2100)

Bottom-water temperature

Mean bottom-water temperature at a 0.5-degree resolution is projected to change very little by 2081–2100, with all areas throughout the CCZ seeing less than 0.05% change in absolute temperature (**Table 1** and **Supplementary Figure 36**). The northwest may include areas with slightly more temperature change (0.03%) than the rest of the CCZ (≤0.02%) (**Supplementary Table 1** and **Supplementary Figure 36**).

Bottom-water oxygen concentration

Mean bottom-water oxygen at a 0.5-degree resolution is projected to change most in the northern and western CCZ, decreasing by ∼5–7% (∼0.25 mL/L), but less change will be observed in the east, decreasing by ∼ 2–3% (∼0.05 mL/L) (**Table 1** and **Supplementary Figure 37**). The NC and CW subregions include areas that may experience ∼3–4% (∼0.1 mL/L) greater decreases in oxygen concentrations compared to their respective APEIs (**Supplementary Table 1** and **Supplementary Figure 37**), although all locations within the CCZ are projected to remain well above oxygen thresholds considered stressful for deep-sea communities (Levin et al., 2009).

Bottom-water pH

Bottom-water pH at a 0.5-degree resolution is projected to change very little by 2100, with the largest decreases of ∼0.2% (0.02 pH units) observed in the NW (**Table 1** and **Supplementary Figure 38**).

Bottom-water calcite saturation

Projected bottom-water calcite saturation changes at a 0.5-degree resolution follow the same patterns as bottom-water oxygen and pH, with the largest decreases of ∼2–4% in the north and west, and the smallest decreases in the east at <1% (**Table 1** and **Supplementary Figure 39**). Several subregions include areas that may experience decreases in calcite saturation 1% greater than their corresponding APEIs (**Supplementary Table 1** and **Supplementary Figure 39**). No areas will go from saturated to unsaturated states.

Seafloor POC flux

Mean POC Flux to the seafloor at a 0.5-degree resolution is modeled to change much more by 2100 than other variables examined, although patterns of change match the other variables examined above. The largest differences in POC flux are estimated to be in the north where flux may decrease as much as 20–25% (∼0.25–0.35 g C/m^2/year), although central subregions may also see a decrease of 15–20% (∼0.25–0.35 g C/m^2/year). In contrast, seafloor POC flux in the southeast is estimated to decrease by 2–3% (<0.1 g C/m^2/year) and flux is projected to increase in APEI 9 (**Table 1** and **Supplementary Figure 40**). POC flux is projected to change by similar quantities between CCZ subregions and APEIs, except that APEIs 4 and 5 may be less impacted by future changes than their respective subregions, CW and CC. While the southern CCZ as a whole may be less impacted by climate change influences on seafloor POC flux, there are still locations in all 3 southern subregions that are projected to experience POC flux decreases of 10–20% (∼0.4–0.6 g C/m^2/year). There are also areas in the SC and SE that are projected to experience POC flux increases of ∼5% (∼0.1 g C/m^2/year) (**Supplementary Table 1** and **Supplementary Figure 40**).

CCZ Biogeography

Abyssal Provinces

The northern and CW subregions of the CCZ are almost entirely within Abyssal Province 12, while the southern, CC, and CE subregions are almost entirely within Abyssal Province 11 postulated by Watling et al. (2013) (**Supplementary Figure 41**). Likewise, APEIs 1 and 3 were entirely in Abyssal Province 12, APEIs 5, 7, 8, and 9 were entirely in Abyssal Province 11, while APEIs 2, 4, and 6 span both provinces (**Supplementary Figure 41**).

Lower-Bathyal Provinces

Seamounts in the western and central CCZ were within Bathyal Province 14 while seamounts in the eastern CCZ were within Bathyal Province 7 postulated by Watling et al. (2013) (**Supplementary Figure 42**). Likewise, western and central APEIs were in Bathyal Province 14 while western APEIs were in Bathyal Province 7 (**Supplementary Figure 42**; Watling et al., 2013).

Pelagic Provinces

The northern and central CCZ were within the North Central Pacific Gyre pelagic province with the SW in the Equatorial Pacific province and SE in the Eastern Tropical Pacific province (UNESCO, 2009). Likewise, APEIs 1, 2, 3, and 6 were in the North Central Pacific Gyre, APEIs 4, 5, and 7 were in the Equatorial Pacific, and APEIs 8 and 9 in the Eastern Tropical Pacific (**Supplementary Figure 44**).

DISCUSSION

Similarity of APEIs to Their Respective Subregions

NW Subregion vs. APEI 1

Area of Particular Environmental Interest 1 is similar in most variables considered here to its NW subregion. However, there are many shallow (<3,000 m summit depth, **Supplementary Figure 3**), tall (>2,000 m summit height, **Supplementary Figure 4**) seamounts in the northwestern corner with no shallow-tall seamounts protected in APEI 1 (**Supplementary Figure 3**). Areas of low biogenic silica content (<6%; **Supplementary Figure 18**), low bottom-water silicate (<130 μmol/kg; **Supplementary Figure 25**), very low POC flux (< ∼1 g C/m^2/year; **Supplementary Figure 35**), and greater projected changes in future bottom-water/POC flux conditions (**Supplementary Figures 36–40**) occur in the northwestern corner of the NW subregion but are not captured in APEI 1.

NC Subregion vs. APEI 2

Area of Particular Environmental Interest 2 is largely similar to its NC subregion. However, APEI 2 generally has higher POC fluxes to the seafloor than anywhere in the NC (**Supplementary Figure 35**). The absence of very low POC flux areas in the APEI could reduce its ecological representativity for this subregion (Smith et al., 2008). APEI 2 is also estimated to be less impacted by climate change than the rest of the NC (**Supplementary Figures 36–40**).

NE Subregion vs. APEI 3

Area of Particular Environmental Interest 3 is largely similar to its NE subregion. While APEI 3 appears to have less variability in many environmental variables than the NE (e.g., depth, **Supplementary Figure 1**; POC flux, **Supplementary Figure 35**), much of this range is captured by APEI 6, which is largely contained within the NE subregion (**Figure 1**).

CW Subregion vs. APEI 4

Area of Particular Environmental Interest 4, which is largely in the SW subregion (**Figure 1**), has some dissimilarities to the CW subregion it is meant to represent, including lower maximum nodule abundance, lower nodule cobalt content, and higher estimated primary production and seafloor POC flux. In addition, it does not capture the deepest abyssal areas (<5,200 m, **Supplementary Figure 1**) nor the shallow (<3,000 m, **Supplementary Figure 3**), tall (>1,500 m, **Supplementary Figure 4**) seamounts in the west. Low sediment calcium-carbonate content (<20%, **Supplementary Figure 17**), biogenic-silica content (<15%, **Supplementary Figure 18**), sediment thickness (<300 m, **Supplementary Figure 19**), NPP (**Supplementary Figures 30–34**), and POC flux (<1.35 g C/m^2/year) present throughout much of the CW region are also not represented in APEI 4. The differences in seafloor POC flux between CW and APEI 4 may be ecologically significant (Smith et al., 2008).

CC Subregion vs. APEI 5

Area of Particular Environmental Interest 5, which is almost entirely in the SC subregion (**Figure 1**), has some dissimilarities to the CC subregion it is intended to represent, including in nodule abundance/characteristics and seafloor POC flux. Relatively deep abyssal seafloor (<4,900 m, **Supplementary Figure 1**), seamounts (**Supplementary Figure 2**) and knolls (**Supplementary Figure 6**) are poorly represented in APEI 5 (although seamounts are also very rare in the CC). In addition, APEI 5 has very low nodule abundance compared to the CC subregion (an average difference of ∼3.5 kg/m^2, **Supplementary Figure 11**). Sediment calcium-carbonate content (**Supplementary Figure 17**), biogenic silica content (**Supplementary Figure 18**), sediment thickness (**Supplementary Figure 19**), and bottom-water calcite saturation (**Supplementary Figure 29**) are also lower in the CC than APEI 5. Reduced nodule abundance in APEI 5 may yield important ecological differences between APEI 5 and CC (McQuaid et al., 2020).

CE Subregion vs. APEI 6

Area of Particular Environmental Interest 6, which is almost entirely in the NE subregion (**Figure 1**), differs in nodule abundance/characteristics, sediment/bottom-water characteristics, estimated primary production, and POC flux from the CE subregion, which it is intended to represent. APEI 6 is shallower (<4,200 m, **Supplementary Figure 1**) than most of the CCZ and has lower sediment calcium-carbonate content (<∼5%, **Supplementary Figure 17**), biogenic-silica content (<∼7%, **Supplementary Figure 18**), NPP (**Supplementary Figures 30–34**), and seafloor POC flux (<1.5 g C/m^2/year; **Supplementary Figure 35**), as well as higher bottom-water nitrate concentrations (>36 μmol/kg; **Supplementary Figure 23**), bottom-water silicate concentrations (>155 μmol/kg; **Supplementary Figure 25**), and bottom-water calcite saturation (>70%; **Supplementary Figure 29**) than most of the CE. APEI 6 also includes lower nodule abundances (<5 kg/m^2; **Supplementary Figure 11**) with lower nickel, copper, and manganese contents (**Supplementary Figures 13–15**) than most of the CE subregion. While many of the sediment and bottom-water characteristic differences are likely not ecologically significant, the differences in nodule abundance/composition and seafloor POC flux may yield important ecological differences between APEI 6 and the CE subregion (Smith et al., 2008; McQuaid et al., 2020).

SW Subregion vs. APEI 7

Area of Particular Environmental Interest 7 is largely similar to it respective SW subregion. While APEI 7 protects only a few of the seamounts and knolls in SW, many of the others are located in APEI 4 (**Supplementary Figures 2**, **6**). APEI 7 does not capture the higher nodule abundances (**Supplementary Figure 11**), and lower nodule metal contents (**Supplementary Figures 12–15**), bottom-water silicate concentrations (**Supplementary Figure 25**), NPP and seafloor POC flux values (**Supplementary Figures 30–35**) found in SW, but these are captured in APEI 4, which is largely in this region (**Figure 1**).

SC Subregion vs. APEI 8

Area of Particular Environmental Interest 8 is largely similar to its SC subregion. While some variability in nodule abundance/characteristics (**Supplementary Figures 11–15**) and sediment characteristics (**Supplementary Figures 16–19**) in the SC are not fully captured by APEI 8, they are largely present in APEI 5 which is almost entirely within this region (**Figure 1**).

SE Subregion vs. APEI 9

Area of Particular Environmental Interest 9 has some dissimilarities with its SE subregion. In particular, shallower depths (<∼4,400 m, **Supplementary Figure 1**), seamounts (**Supplementary Figure 2**), most knolls (**Supplementary Figure 6**), higher nodule abundance (>4 kg/m^2, **Supplementary Figure 11**), lower bottom-water oxygen concentrations (<∼3.7 ml/L, **Supplementary Figure 22**), and higher bottom-water calcite saturation (>∼69%, **Supplementary Figure 29**) present in the eastern

SE are not captured in APEI 9. While differences in bottom-water characteristics are likely not ecologically significant, the lack of seamounts and low nodule abundances in APEI 9 may yield important ecological differences with most of the SE subregion.

While much of the environmental variability in the northern and southern CCZ appears to be captured in the APEI network, the central and SE CCZ may include areas with seafloor POC flux, nodule abundance, and seamount characteristics not found in the APEIs meant to represent them. To ensure adequate protection of biodiversity in these subregions, additional APEIs may be warranted. For detailed habitat mapping in the CCZ using the environmental data in this paper, as well as identification of potential areas for additional representative APEIs, see McQuaid et al. (2020).

Environmental Heterogeneity and Deep-Sea Mining

In the deep sea, proposed polymetallic nodule mining activities are likely to harm seafloor ecosystems, including unique habitats such as manganese nodules (Glover and Smith, 2003; Niner et al., 2018; Washburn et al., 2019; Smith et al., 2020). To protect regional biodiversity and ecosystem functions from the nodule-mining impacts in the CCZ, nine APEIs were designated as no-mining areas (Wedding et al., 2013). Thus, for the APEI network to serve its purpose in protecting biodiversity and ecosystem function throughout the CCZ, it must fully capture the full range of habitats and important environmental variables found in the region.

While there were statistically significant differences across the CCZ in every environmental variable examined, it is likely that many of these differences are not ecologically significant, and thus are likely less important for the APEI network to fully represent. Differences in seafloor slope, at a broad scale, (**Supplementary Figure 10**), sediment thickness (**Supplementary Figure 19**), bottom-water particulate concentrations, and nepheloid-layer thickness (**Supplementary Figures 27, 28**) are small or within measurement errors and likely not ecologically significant. Variations in bottom-water temperature, salinity, oxygen concentration nitrate concentration, phosphate concentration, silicate concentration, pH, particulate matter concentration, and calcite saturation (**Table 1** and **Supplementary Table 1** and **Supplementary Figures 20–29**) are relatively small and may not be ecologically significant (Levin, 2003), although little work has been done to understand how differences in many of these variables affect abyssal communities.

Several studies, including many in this volume, have found that nodule abundance (Amon et al., 2016; De Smet et al., 2017; Simon-Lledó et al., 2019b, 2020; Washburn et al., 2021) and POC flux to the seafloor (Smith et al., 2008; Bonifácio et al., 2020; Washburn et al., 2021) are major drivers of benthic community abundance, diversity, and composition. Both of these variables vary across the CCZ and between some CCZ subregions and their respective APEIs. Differences between APEIs and their subregions are most pronounced in the central CCZ (**Table 1** and **Supplementary Figures 11 and 35**), where APEIs were located away from nodule-rich areas (Wedding et al., 2013). Nodules provide habitat for apparently nodule-dependent epifauna and infauna (Amon et al., 2016; Vanreusel et al., 2016; Gooday et al., 2017; Simon-Lledó et al., 2019b) as well as metal-cycling bacteria and archaea (Shulse et al., 2016; Molari et al., 2020). Thus, differences in nodule abundance and metal composition (**Table 1** and **Supplementary Figures 11–15**) are likely to be ecological significant. Although seafloor POC flux appears to have large impacts on benthic communities (e.g., Smith et al., 2008), there are relatively few POC flux measurements from the CCZ (Lutz et al., 2007; Kim et al., 2010, 2011, 2012). Therefore, patterns of seafloor POC flux across the CCZ are estimated from models of export through the water column (e.g., Lutz et al., 2007). Substantially more direct measurements of deep POC flux are needed to better understand food availability in space and time across the CCZ.

Seamounts also serve as important habitats for benthic and pelagic communities (Clark et al., 2010; Leitner et al., 2017; Laroche et al., 2020). Seamount and knoll habitats appear to be underrepresented in the APEIs for the central CCZ (**Supplementary Figure 2**). Other variables with differences that could be ecologically significant include sediment calcium carbonate and biogenic silica content (**Table 1** and **Supplementary Figures 17, 18**), which may influence the formation of molluscan and foraminiferan shells (Wheeler, 1992; Sen Gupta, 1999). Finally, it appears that changes in bottom-water temperature, oxygen content, and pH due to climate change will likely not be ecologically significant throughout the CCZ, while it is unclear whether changes in calcite saturation will be (**Supplementary Figures 36–39**). However, estimated climate driven changes in POC flux for time intervals 1951–2000 to 2081–2100 between APEIs and their respective subregions may be as much as ∼30% (**Supplementary Figure 40**), which could significantly influence abyssal benthic communities (Smith et al., 2008; Jones et al., 2013) in the deep-sea throughout the CCZ, albeit unevenly (**Supplementary Figure 40**).

CONCLUSION

There is significant heterogeneity in all environmental variables examined across the CCZ. Much of this variability falls along north–south and east–west gradients, as postulated by Wedding et al. (2013). Most of this environmental variability is captured by the APEI system erected by the ISA's Regional Environmental Management Plan (ISA, 2011), but some APEIs differ in some important ecological characteristics (in particular nodule abundance and seafloor POC flux) from the subregions they were intended to represent, especially the central and SE CCZ. Thus, the formation of additional APEIs or other protected areas merits consideration, particularly within the nodule-rich central areas of the CCZ. Areas where additional APEIs

could be erected to help protect some of these habitats are proposed in McQuaid et al. (2020).

DATA AVAILABILITY STATEMENT

The original contributions presented in the study are included in the article/**Supplementary Material**, further inquiries can be directed to the corresponding author/s.

AUTHOR CONTRIBUTIONS

CRS and TW designed the study while TW accumulated all data sets and wrote the first draft. DJ and C-LW contributed datasets. All authors provided analytical support and revisions.

FUNDING

This work was funded by grants to CRS from the Gordon and Betty Moore Foundation (no. 5596) and the Pew Charitable Trusts (no. 32871).

ACKNOWLEDGMENTS

The authors thank the individuals and institutions who collected and/or provided data for this synthesis. In particular, we would like to thank Malcolm Clark for providing seamount and knoll data from Yesson et al. (2011), Kirsty McQuaid for providing seafloor slope data used in McQuaid et al. (2020), Charles Morgan for providing nodule abundance and metal-content data from ISA (2012) and proprietary 2018 data, Wilford Gardner and Alexey Mishonov for providing bottom-water particulate matter and nepheloid layer thickness data from Gardner et al. (2018), Robert O'Malley for assisting with NPP data provision, and Les Watling for providing CCZ ecoregion data. This is publication number 11296 from the School of Ocean and Science and Technology, University of Hawaii.

SUPPLEMENTARY MATERIAL

The Supplementary Material for this article can be found online at: https://www.frontiersin.org/articles/10.3389/fmars.2021.661685/full#supplementary-material

REFERENCES

Amante, C., and Eakins, B. W. (2009). *ETOPO1 1 Arc-Minute Global Relief Model: Procedures, Data Sources and Analysis.* NOAA Technical Memorandum NESDIS NGDC-24. Boulder, CO: National Geophysical Data Center, NOAA, doi: 10.7289/V5C8276M

Amon, D. J., Ziegler, A. F., Dahlgren, T. G., Glover, A. G., Goineau, A., Gooday, A. J., et al. (2016). Insights into the abundance and diversity of abyssal megafauna in a polymetallic-nodule region in the eastern Clarion-Clipperton Zone. *Sci. Rep.* 6:30492. doi: 10.1038/srep30492

Archer, D. E. (1999). *Opal, Quartz and Calcium Carbonate Content in Surface Sediments of the Ocean Floor*. Los Angeles, CA: PANGAEA, doi: 10.1594/PANGAEA.56017

Archer, D. E. (2003). *Interpolated Calcium Carbonate Content of the Sea Floor Sediments*. Los Angeles, CA: PANGAEA, doi: 10.1594/PANGAEA.107286

Behrenfeld, M. J., Boss, E., Siegel, D. A., and Shea, D. M. (2005). Carbon-based ocean productivity and phytoplankton physiology from space. *Glob. Biogeochem. Cycles* 19, 1–14.

Behrenfeld, M. J., and Falkowski, P. G. (1997). Photosynthetic rates derived from satellite-based chlorophyll concentrations. *Limnol. Oceanogr.* 42, 1–20. doi: 10.4319/lo.1997.42.1.0001

Bonifácio, P., Martinez-Arbizu, P., and Menot, L. (2020). Alpha and beta diversity patterns of polychaete assemblages across the nodule province of the clarion-clipperton fracture zone (Equatorial Pacific). *Biogeosciences* 17, 865–886. doi: 10.5194/bg-17-865-2020

Borowski, C., and Thiel, H. (1998). Deep-sea macrofaunal impacts of a large-scale physical disturbance experiment in the Southeast Pacific. *Deep Sea Res. II* 45, 55–81. doi: 10.1016/s0967-0645(97)00073-8

Clark, M. R., Rowden, A. A., Schlacher, T., Williams, A., Consalvey, M., Stocks, K. I., et al. (2010). The ecology of seamounts: structure, function, and human impacts. *Annu. Rev. Mar. Sci.* 2, 253–278. doi: 10.1146/annurev-marine-120308-081109

Cwienk, D. S. (1986). *Recent and Glacial Age Organic Carbon and Biogenic Silica Accumulation in Marine Sediments*. 249. Ph.D. Thesis. University of Rhode Island, Kingston, RI.

Danovaro, R., Snelgrove, P. V. R., and Tyler, P. (2014). Challenging the paradigms of deep-sea ecology. *Trends Ecol. Evol.* 29, 465–475. doi: 10.1016/j.tree.2014.06.002

De Smet, B., Paper, E., Riehl, T., Bonifácio, P., Colson, L., and Vanreusel, A. (2017). The community structure of deep-sea macrofauna associated with polymetallic nodules in the eastern part of the Clarion Clipperton Fracture Zone. *Front. Mar. Sci.* 4:103. doi: 10.3389/fmars.2017.00103

Dutkiewicz, A., Muller, R. D., O'Callaghan, S., and Jonasson, H. (2015). Census of seafloor sediments in the world's ocean. *Geology* 43, 795–798. doi: 10.1130/g36883.1

Garcia, H. E., Weathers, K. W., Paver, C. R., Smolyar, I., Boyer, T. P., Locarnini, R. A., et al. (2019). *World Ocean Atlas 2018: Dissolved Oxygen, Apparent Oxygen Utilization, and Dissolved Oxygen Saturation.* NOAA Atlas NESDIS 83, Vol. 3, ed. A. Mishonov (Silver Spring, MA: U.S. Department Of Commerce), 38.

Gardner, W. D., Richardson, M. J., Mishonov, A. V., and Biscaye, P. E. (2018). Global comparison of benthic nepheloid layers based on 52 yeas of nephelometer and transmissometer measurements. *Prog. Oceanogr.* 168, 100–111. doi: 10.1016/j.pocean.2018.09.008

Glover, A. G., and Smith, C. R. (2003). The deep-sea floor ecosystem: current status and prospects of anthropogenic change by the year 2025. *Environ. Conserv.* 30, 219–241. doi: 10.1017/S0376892903000225

Gooday, A. J., Holzmann, M., Caulle, C., Goineau, A., Kamenskaya, O., Weber, A. A.-T., et al. (2017). Giant protists (xenophyophores, Foraminifera) are exceptionally diverse in parts of the abyssal eastern Pacific licensed for polymetallic nodule exploration. *Biol. Conserv.* 107, 106–116. doi: 10.1016/j.biocon.2017.01.006

Hein, J. R., Mizell, K., Koschinsky, A., and Conrad, T. A. (2013). Deep-ocean mineral deposits as a source of critical metals for high- and green-technology applications: comparison with land-based resources. *Ore Geol. Rev.* 51, 1–14. doi: 10.1016/j.oregeorev.2012.12.001

ISA (2008). *Rationale and Recommendations for the Establishment of Preservation Reference Areas for Nodule Mining in the Clarion-Clipperton Zone: Summary Outcomes of a Workshop to Design Marine Protected Areas for Seamounts and the Abyssal Nodule Province in Pacific High Seas, Held at the University of Hawaii at Manoa, Hawaii, United States of America, from 23 to 26 October 2007.* ISBA/14/LTC/2. Kingston: International Seabed Authority, 12.

ISA (2011). *Environmental Management Plan for the Clarion-Clipperton Zone.* ISBA/17/LTC/7. Kingston: International Seabed Authority, 18.

ISA (2012). *A Geological Model of Polymetallic Nodule Deposits in the Clarion-Clipperton Fracture Zone.* ISA Technical Study No. 6. Kingston: International Seabed Authority, 106.

ISA (2019). *Deep CCZ Biodiversity Synthesis Workshop Report. Deep CCZ Biodiversity Synthesis Workshop*. Friday Harbor, WA: University of Hawaii at Manoa & International Seabed Authority.

Jahnke, R. A. (1996). The global ocean flux of particulate organic carbon: Areal distribution and magnitude. *Glob. Biogeochem. Cycles* 10, 71–88. doi: 10.1029/95gb03525

Johnson, D. A. (1972). Ocean-floor erosion in equatorial Pacific. *Geol. Soc. Am. Bull.* 83, 3121–3144. doi: 10.1130/0016-7606(1972)83[3121:oeitep]2.0.co;2

Jones, D. O. B., Kaiser, S., Sweetman, A. K., Smith, C. R., Menot, L., Vink, A., et al. (2017). Biological responses to disturbance from simulated deep-sea polymetallic nodule mining. *PLoS One* 12:e171750. doi: 10.1371/journal.pone.0171750

Jones, D. O. B., Yool, A., Wei, C.-L., Henson, S. A., Ruhl, H. A., Watson, R. A., et al. (2013). Global reductions in seafloor biomass in response to climate change. *Glob. Change Biol.* 20, 1861–1872. doi: 10.1111/gcb.12480

Kim, H. J., Hyeong, K., Yoo, C. M., Chi, S.-B., Khim, B.-K., and Kim, D. (2010). Seasonal variations of particle fluxes in the northeastern equatorial Pacific during normal and weak El Niño periods. *Geosci. J.* 14, 415–422.

Kim, H. J., Hyeong, K., Yoo, C. M., Khim, B. K., Kim, K. H., Son, J. W., et al. (2012). Impact of strong El Niño events (1997/98 and 2009/10) on sinking particle fluxes in the 10°N thermocline ridge area of the northeastern equatorial Pacific. *Deep Sea Res. I Oceanogr. Res. Pap.* 67, 111–120.

Kim, H. J., Kim, D., Yoo, C. M., Chi, S.-B., Khim, B. K., Shin, H.-R., et al. (2011). Influence of ENSO variability on sinking-particle fluxes in the northeastern equatorial Pacific. *Deep Sea Res. I* 58, 865–874. doi: 10.1016/j.dsr.2011.06.007

Laroche, O., Kersten, O., Smith, C. R., and Goetze, E. (2020). Environmental DNA surveys detect distinct metazoan communities across abyssal plains and seamounts in the western Clarion Clipperton Zone. *Mol. Ecol.* 29, 4588–4604. doi: 10.1111/mec.15484

Leitner, A. B., Neuheimer, A. B., Donlon, E., Smith, C. R., and Drazen, J. C. (2017). Environmental and bathymetric influences on abyssal bait-attending communities of the Clarion Clipperton Zone. *Deep Sea Res. I* 125, 65–80. doi: 10.1016/j.dsr.2017.04.017

Levin, L. A., Ekau, W., Gooday, A. J., Jorissen, F., Middelburg, J. J., Naqvi, S. W. A., et al. (2009). Effects of natural and human-induced hypoxia on coastal benthos. *Biogeosciences* 6, 2063–2098. doi: 10.5194/bg-6-2063-2009

Levin, L., Wei, C.-L., Dunn, D., Amon, D., Ashford, O., Cheung, W., et al. (2020). Climate change considerations are fundamental to management of deep-sea resource extraction. *Glob. Change Biol.* 26, 4664–4678. doi: 10.1111/gcb.15223

Levin, L. A. (2003). Oxygen minimum zone benthos: adaptation and community response to hypoxia. *Oceanogr. Mar. Biol.* 41, 1–45.

Locarnini, R. A., Mishonov, A. V., Baranova, O. K., Boyer, T. P., Zweng, M. M., Garcia, H. E., et al. (2019). *World Ocean Atlas 2018: Temperature. NOAA Atlas NESDIS 81*, Vol. 1, ed. A. Mishonov (Silver Spring, MD: U.S. Department Of Commerce), 52.

Lutz, M. J., Caldeira, K. R., Dunbar, R. B., and Behrenfeld, M. J. (2007). Seasonal rhythms of net primary production and particulate organic carbon flux to depth describe the efficiency of biological pump in the global ocean. *J. Geophys. Res. Oceans* 112:C10011.

Macdonald, K. C., Fox, P. J., Alexander, R. T., Pockalny, R., and Gente, P. (1996). Volcanic growth faults and the origin of Pacific abyssal hills. *Nature* 380, 125–129. doi: 10.1038/380125a0

McQuaid, K. A., Attrill, M. J., Clark, M. R., Cobley, A., Glover, A. G., Smith, C. R., et al. (2020). Using habitat classification to assess representativity of a protected area network in a large, data-poor area targeted for deep-sea mining. *Front. Mar. Sci.* 7:558860. doi: 10.3389/fmars.2020.558860

Menendez, A., James, R. H., Lichtschlag, A., Connelly, D., and Peel, K. (2019). Controls on the chemical composition of ferromanganese nodules in the Clarion-Clipperton Fracture Zone, eastern equatorial Pacific. *Mar. Geol.* 409, 1–14. doi: 10.1016/j.margeo.2018.12.004

Mewes, K., Mogollón, J. M., Picard, A., Rühlemann, C., Kuhn, T., Nöthen, K., et al. (2014). Impact of depositional and biogeochemical processes on small scale variations in nodule abundance in the Clarion-Clipperton Fracture Zone. *Deep Sea Res. I Oceanogr. Res. Pap.* 91, 125–141. doi: 10.1016/j.dsr.2014.06.001

Molari, M., Janssen, F., Vonnahme, T. R., Wenzhöfer, F., and Boetius, A. (2020). The contribution of microbial communities in polymetallic nodules to the diversity of the deep-sea microbiome of the Peru Basin (4130-4198 m depth). *Biogeosciences* 17, 3203–3222. doi: 10.5194/bg-17-3203-2020

Morel, A., and Berthon, J.-F. (1989). Surface pigments, algal biomass profiles, and potential production of the euphotic layer: relationships reinvestigated in view of remote-sensing applications. *Limnol. Oceanogr.* 34, 1545–1562. doi: 10.4319/lo.1989.34.8.1545

Niner, H. J., Ardron, J. A., Escar, E. G., Gianni, M., Jaeckel, A., Jones, D. O. B., et al. (2018). Deep-sea mining with no net loss of biodiversity – an impossible aim. *Front. Mar. Sci.* 5:53. doi: 10.3389/fmars.2018.00053

NOAA National Geophysical Data Center (2009). *ETOPO1 1 Arc-Minute Global Relief Model*. Asheville, NC: NOAA National Centers for Environmental Information.

Peukert, A., Timm, S., Alevizos, E., Köser, K., Kwasnitschka, T., and Greinert, J. (2018). Understanding Mn-nodule distribution and evaluation of related deep-sea mining impacts using AUV-based hydroacoustic and optical data. *Biogeosciences* 15, 2525–2549. doi: 10.5194/bg-15-2525-2018

Premuzic, E. T., Benkovitz, C. M., Gaffney, J. S., and Walsh, J. J. (1982). The nature and distribution of organic matter in the surface sediments of world oceans and seas. *Org. Geochem.* 4, 63–77. doi: 10.1016/0146-6380(82)90009-2

Sen Gupta, B. K. (1999). *Modern Foraminifera*. Dordrecht: Kluwer Academic Publisher, 371.

Shulse, C. N., Maillot, B., Smith, C. R., and Church, M. J. (2016). Polymetallic nodules, sediments, and deep waters in the equatorial North Pacific exhibit highly diverse and distinct bacterial, archaeal, and microeukaryotic communities. *Microbiologyopen* 6:e00428. doi: 10.1002/mbo3.428

Silsbe, G. M., Behrenfeld, M. J., Halsey, K. H., Milligan, A. J., and Westberry, T. K. (2016). The CAFE model: a net production model for global ocean phytoplankton. *Glob. Biogeochem. Cycles* 30, 1756–1777. doi: 10.1002/2016gb005521

Simon-Lledó, E., Bett, B. J., Huvenne, V. A. I., Schoening, T., Benoist, N. M. A., Jeffreys, R. M., et al. (2019a). Megafaunal variation in the abyssal landscape of the Clarion Clipperton Zone. *Prog. Oceanogr.* 170, 119–133. doi: 10.1016/j.pocean.2018.11.003

Simon-Lledó, E., Bett, B. J., Huvenne, V. A. I., Schoening, T., Benoist, N. M. A., and Jones, D. O. B. (2019b). Ecology of a polymetallic nodule occurrence gradient: implications for deep-sea mining. *Limnol. Oceanogr.* 64, 1883–1894. doi: 10.1002/lno.11157

Simon-Lledó, E., Pomee, C., Ahokava, A., Drazen, J. C., Leitner, A. B., Flynn, A., et al. (2020). Multi-scale variations in invertebrate and fish megafauna in the mid-eastern Clarion Clipperton Zone. *Prog. Oceanogr.* 187:102405. doi: 10.1016/j.pocean.2020.102405

Smith, C. R., De Leo, F. C., Bernardino, A. F., Sweetman, A. K., and Arbizu, P. M. (2008). Abyssal food limitation, ecosystem structure and climate change. *Trends Ecol. Evol.* 23, 518–528. doi: 10.1016/j.tree.2008.05.002

Smith, C. R., Tunnicliffe, V., Colaco, A., Drazen, J. C., Gollner, S., Levin, L. A., et al. (2020). Deep-sea misconceptions cause underestimation of seabed-mining impacts. *Trends Ecol. Evol.* 35, 853–857. doi: 10.1016/j.tree.2020.07.002

Straume, E. O., Gaina, C., Medvedev, S., Hochmuth, K., Gohl, K., Whittaker, J. M., et al. (2019). GlobSed: updated total sediment thickness in the world's oceans. *Geochem. Geophys. Geosyst.* 20, 1756–1772. doi: 10.1029/2018GC008115

Sweetman, A. K., Thurber, A. R., Smith, C. R., Levin, L. A., Mora, C., Wei, C. L., et al. (2017). Major impacts of climate change on deep-sea benthic ecosystems. *Elem. Sci. Anth.* 5:4. doi: 10.1525/elementa.203

UNESCO (2009). *Global Oceans and Deep Seabed – Biogeographic Classification*. IOC Technical Series, Vol. 84. Paris: UNESCO-IOC, 87.

Van Andel, T. H. (1975). Mesozoic/Cenozoic calcite compensation depth and the global distribution of calcareous sediments. *Earth Planet. Sci. Lett.* 26, 187–194. doi: 10.1016/0012-821x(75)90086-2

Vanreusel, A., Hilrio, A., Ribeiro, P. A., Menot, L., and Arbizu, P. M. (2016). Threatened by mining, polymetallic nodules are required to preserve abyssal epifauna. *Sci. Rep.* 6:26808.

Washburn, T. W., Menot, L., Bonifácio, P., Pape, E., Błazewicz, M., Bribiesca-Contreras, G., et al. (2021). Patterns of macrofaunal biodiversity across the Clarion-Clipperton Zone: an area targeted for seabed mining. *Front. Mar. Sci.* doi: 10.3389/fmars.2021.626571

Washburn, T. W., Turner, P. J., Durden, J. M., Jones, D. O. B., Weaver, P., and Van Dover, C. L. (2019). Ecological risk assessment for deep-sea mining. *Ocean Coast. Manag.* 176, 24–39. doi: 10.1016/j.ocecoaman.2019.04.014

Watling, L., Guinotte, J., Clark, M. R., and Smith, C. R. (2013). A proposed biogeography of the deep ocean floor. *Prog. Oceanogr.* 111, 91–112. doi: 10.1016/j.pocean.2012.11.003

Weaver, P. P. E., Billett, D. S. M., and Van Dover, C. L. (2018). "Environmental risks of deep-sea mining," in *Handbook on Marine Environment Protection*, eds M. Salomon and T. Markus (Cham: Spring), doi: 10.1007/978-3-319-60156-4_11

Wedding, L. M., Friedlander, A. M., Kittinger, J. N., Watling, L., Gaines, S. D., Bennett, M., et al. (2013). From principles to practice: a spatial approach to systematic conservation planning in the deep sea. *Proc. R. Soc. B* 280:20131684. doi: 10.1098/rspb.2013.1684

Wei, C.-L., Rowe, G. T., Escobar-Briones, E., Boetius, A., Soltwedel, T., Caley, M. J., et al. (2010). Global patterns and predictions of seafloor biomass using random forests. *PLoS One* 5:e15323. doi: 10.1371/journal.pone.0015323

Wheeler, A. P. (1992). *Mechanisms of Molluscan Shell Formation*. Boca Raton, FL: CRC Press.

Yesson, C., Clark, M. R., Taylor, M. L., and Rogers, A. D. (2011). The global distribution of seamounts based on 30 arc seconds bathymetry data. *Deep Sea Res. I* 58, 442–453. doi: 10.1016/j.dsr.2011.02.004

Yool, A., Popova, E. E., and Anderson, T. R. (2013). MEDUSA-2.0: an intermediate complexity biogeochemical model of the marine carbon cycle for climate change and ocean acidification studies. *Geosci. Model Dev. Discuss.* 6, 1259–1365.

Zeppilli, D., Pusceddu, A., Trincardi, F., and Danovaro, R. (2016). Seafloor heterogeneity influences the biodiversity-ecosystem functioning relationships in the deep sea. *Sci. Rep.* 6:26352.

Zweng, M. M., Reagan, J. R., Seidov, D., Boyer, T. P., Locarnini, R. A., Garcia, H. E., et al. (2019). *World Ocean Atlas 2018: Salinity*. NOAA Atlas NESDIS 82, Vol. 2, ed. A. Mishonov (Silver Spring, MA: U.S. Department Of Commerce), 50.

Conflict of Interest: The authors declare that the research was conducted in the absence of any commercial or financial relationships that could be construed as a potential conflict of interest.

Copyright © 2021 Washburn, Jones, Wei and Smith. This is an open-access article distributed under the terms of the Creative Commons Attribution License (CC BY). The use, distribution or reproduction in other forums is permitted, provided the original author(s) and the copyright owner(s) are credited and that the original publication in this journal is cited, in accordance with accepted academic practice. No use, distribution or reproduction is permitted which does not comply with these terms.

frontiers in Marine Science

ORIGINAL RESEARCH
published: 01 April 2021
doi: 10.3389/fmars.2021.626571

Patterns of Macrofaunal Biodiversity Across the Clarion-Clipperton Zone: An Area Targeted for Seabed Mining

Travis W. Washburn[1], Lenaick Menot[2], Paulo Bonifácio[2], Ellen Pape[3], Magdalena Błażewicz[4], Guadalupe Bribiesca-Contreras[5], Thomas G. Dahlgren[6,7], Tomohiko Fukushima[8], Adrian G. Glover[5], Se Jong Ju[9], Stefanie Kaiser[4], Ok Hwan Yu[9] and Craig R. Smith[1]*

[1] Department of Oceanography, University of Hawai'i at Mānoa, Honolulu, HI, United States, [2] Ifremer, Centre Bretagne, REM EEP, Laboratoire Environnement Profond, Plouzané, France, [3] Marine Biology Research Group, Ghent University, Ghent, Belgium, [4] Department of Invertebrate Zoology and Hydrobiology, University of Lodz, Łódź, Poland, [5] Department of Life Sciences, Natural History Museum, London, United Kingdom, [6] Department of Marine Sciences, University of Gothenburg, Gothenburg, Sweden, [7] Norwegian Research Centre, Bergen, Norway, [8] Japan Agency for Marine-Earth Science and Technology, Yokosuka, Japan, [9] Korea Institute of Ocean Science and Technology, Busan, South Korea

OPEN ACCESS

Edited by:
Sabine Gollner, Royal Netherlands Institute for Sea Research (NIOZ), Netherlands

Reviewed by:
Clara F. Rodrigues, University of Aveiro, Portugal
Helena Passeri Lavrado, Federal University of Rio de Janeiro, Brazil

***Correspondence:**
Travis W. Washburn
twashbur@hawaii.edu;
travis.washburn@aist.go.jp

Specialty section:
This article was submitted to Deep-Sea Environments and Ecology, a section of the journal Frontiers in Marine Science

Received: *06 November 2020*
Accepted: *26 February 2021*
Published: *01 April 2021*

Citation:
Washburn TW, Menot L, Bonifácio P, Pape E, Błażewicz M, Bribiesca-Contreras G, Dahlgren TG, Fukushima T, Glover AG, Ju SJ, Kaiser S, Yu OH and Smith CR (2021) Patterns of Macrofaunal Biodiversity Across the Clarion-Clipperton Zone: An Area Targeted for Seabed Mining. Front. Mar. Sci. 8:626571. doi: 10.3389/fmars.2021.626571

Macrofauna are an abundant and diverse component of abyssal benthic communities and are likely to be heavily impacted by polymetallic nodule mining in the Clarion-Clipperton Zone (CCZ). In 2012, the International Seabed Authority (ISA) used available benthic biodiversity data and environmental proxies to establish nine no-mining areas, called Areas of Particular Environmental Interest (APEIs) in the CCZ. The APEIs were intended as a representative system of protected areas to safeguard biodiversity and ecosystem function across the region from mining impacts. Since 2012, a number of research programs have collected additional ecological baseline data from the CCZ. We assemble and analyze macrofaunal biodiversity data sets from eight studies, focusing on three dominant taxa (Polychaeta, Tanaidacea, and Isopoda), and encompassing 477 box-core samples to address the following questions: *(1) How do macrofaunal abundance, biodiversity, and community structure vary across the CCZ, and what are the potential ecological drivers? (2) How representative are APEIs of the nearest contractor areas? (3) How broadly do macrofaunal species range across the CCZ region? and (4) What scientific gaps hinder our understanding of macrofaunal biodiversity and biogeography in the CCZ*? Our analyses led us to hypothesize that sampling efficiencies vary across macrofaunal data sets from the CCZ, making quantitative comparisons between studies challenging. Nonetheless, we found that macrofaunal abundance and diversity varied substantially across the CCZ, likely due in part to variations in particulate organic carbon (POC) flux and nodule abundance. Most macrofaunal species were collected only as singletons or doubletons, with additional species still accumulating rapidly at all sites, and with most collected species appearing to be new to science. Thus, macrofaunal diversity remains poorly sampled and described across the CCZ, especially within APEIs, where a total of nine box cores have been taken across three APEIs. Some common macrofaunal species ranged over

600–3000 km, while other locally abundant species were collected across ≤ 200 km. The vast majority of macrofaunal species are rare, have been collected only at single sites, and may have restricted ranges. Major impediments to understanding baseline conditions of macrofaunal biodiversity across the CCZ include: (1) limited taxonomic description and/or barcoding of the diverse macrofauna, (2) inadequate sampling in most of the CCZ, especially within APEIs, and (3) lack of consistent sampling protocols and efficiencies.

Keywords: macrofauna, deep-sea mining, biodiversity, polychaeta, manganese nodules, POC flux, species ranges, areas of particular environmental interest

INTRODUCTION

The Clarion-Clipperton Zone (CCZ) is an ∼ 6 million km^2 abyssal region in the equatorial Pacific Ocean targeted for polymetallic nodule mining (Wedding et al., 2013). There are currently 16 mineral exploration contract areas, each up to 75000 km^2, distributed across this region (accessed 3 January 2020[1]). While no exploitation activities have yet taken place, regulations for commercial exploitation are planned by the International Seabed Authority (ISA) to be in place by 2021 (ISA, 2018). Deep-seafloor ecosystems are expected to experience substantial impacts from nodule mining, with single mining operations potentially damaging > 1000 km^2 of seafloor annually from direct habitat disruption, turbidity, and resedimentation (Smith et al., 2008c; Washburn et al., 2019). The full range of seafloor impacts from nodule mining may include removal of sediment and nodule habitats, sediment compaction, seafloor and nodule burial, dilution of food for deposit and suspension feeders, smothering of respiratory structures, interference with photoecology, and noise pollution (Smith et al., 2008c; Washburn et al., 2019; Drazen et al., 2020). Many ecosystem impacts will be long lasting since sediment habitats will require at least many decades to recover, and natural nodule habitats will not regenerate for millions of years (Hein et al., 2013; Vanreusel et al., 2016; Jones et al., 2017; Stratmann et al., 2018a,b; Vonnahme et al., 2020).

Because impacts from nodule mining may be large-scale, intense and persistent, the ISA in 2012 established nine areas distributed across the CCZ to be protected from seabed mining, called Areas of Particular Environmental Interest (APEIs) (Wedding et al., 2013). The APEIs each cover 160000 km^2 and were designed to serve as a representative system of unmined areas to protect biodiversity and ecosystem function across the region from mining impacts (Wedding et al., 2013). Since 2012, at least thirteen sites within the CCZ region have been studied to collect new seafloor biodiversity and ecosystem data. These new data enable a scientific review and synthesis to help address the representativity of the APEI network for protecting biodiversity across the CCZ. In this paper, we review and synthesize recent biodiversity data for sediment-dwelling macrofauna, a faunal component characterized by high biodiversity in abyssal habitats (Smith et al., 2008a). The general goals of this synthesis are to: (1) consider whether the current network of APEIs appears to capture the full range of macrofaunal biodiversity and species distributions in the CCZ; (2) identify needs for additional APEIs; and (3) identify key gaps in our knowledge of macrofaunal biodiversity that impede APEI evaluation and assessment of risks from nodule mining to regional biodiversity.

For this synthesis, macrofauna are considered to be animals retained on 250 – 300 μm sieves. This size fraction contributes substantially to biodiversity and ecosystem functions at the abyssal seafloor (Smith et al., 2008a). The abyssal CCZ macrofauna are primarily sediment-dwelling and are numerically dominated by polychaete worms, and tanaid and isopod crustaceans (Borowski and Thiel, 1998; Smith and Demopoulos, 2003; De Smet et al., 2017; Wilson, 2017; Pasotti et al., 2021). Polychaetes in particular account for ∼35 – 65% of macrofaunal abundance, biomass, and species richness in nodule regions (e.g., Borowski and Thiel, 1998; Smith and Demopoulos, 2003; Chuar et al., 2020). Macrofaunal community abundance in abyssal nodule regions of the CCZ is relatively low compared to shallower continental margins, and typically totals 200 – 500 individuals m^{-2} (Glover et al., 2002; Smith and Demopoulos, 2003; De Smet et al., 2017). Despite low abundances, the CCZ appears to host high levels of macrobenthic biodiversity (Smith et al., 2008a,b).

In this paper, we address the following questions for the sediment macrofauna:

(1) *Do abundance, species/family richness and evenness, and community structure vary along and across the CCZ? What are the ecological drivers of these variations?*
(2) *Do mining exploration claim areas have similar levels of species/taxon richness and evenness, and similar community structure, to the proximal APEI(s)?*
(3) *Are macrofaunal species ranges (based on morphology and/or barcoding) generally large compared to the distances between APEIs and contractor areas? What is the degree of species overlap between different study locations across the CCZ?*
(4) *What scientific gaps hinder biodiversity and biogeographic syntheses for the macrofauna (e.g., how well is the macrofauna known taxonomically)?*

Our results indicate that macrofaunal abundance, diversity, and community structure vary across the CCZ, driven in part by differences in particulate organic carbon (POC) flux to the seafloor. However regional macrofaunal diversity is still poorly characterized, with sampling at all studied sites still rapidly

[1]https://www.isa.org.jm/deep-seabed-minerals-contractors

accumulating species, and major areas of the CCZ (including most APEIs) with little or no macrofaunal sampling.

MATERIALS AND METHODS

CCZ Macrofaunal Box-Core Data Sets

Data were assembled from the peer-reviewed scientific literature and from a variety of unpublished sources through direct solicitation from scientists and contractors, and online posting by the ISA of a general data solicitation[2]. The abyssal macrofaunal data assembled were collected by box corer with a sample area of 0.25 m^2 (Hessler and Jumars, 1974). Data sets were restricted to box cores because they can provide quantitative samples of adequate size for macrofaunal community studies, and there is some (albeit, not complete) standardization of box-core sampling and processing protocols for deep-sea macrofauna (Hessler and Jumars, 1974; Glover et al., 2016; De Smet et al., 2017). The box corer is a more quantitative, and less biased, sampler of infaunal macrobenthic community structure and diversity than devices such as epibenthic sleds that collect larger, but qualitative, samples. In addition, the box core has been shown to be a highly efficient sampler per unit area (Jóźwiak et al., 2020). For our synthesis, macrofauna consisted of animals retained on 250- or 300-μm sieves collected to a sediment depth of 10 cm. Nematodes, harpacticoid copepods, and ostracods were omitted from macrofaunal counts because these taxa are poorly retained by 250 – 300-μm sieves and thus are generally considered to be meiofaunal taxa (Hessler and Jumars, 1974; Dinet et al., 1985; De Smet et al., 2017). Counts per box core at species and higher taxonomic levels were assembled for all samples available from the CCZ and the broader equatorial Pacific, which included nine cores in total collected across three APEIs (**Figure 1** and **Table 1**).

Data sets were obtained from eight different studies that collected samples from eleven different contractor areas and three APEIs (Glover et al., 2002; De Smet et al., 2017; Wilson, 2017; Błażewicz et al., 2019b; Bonifácio et al., 2020; Chuar et al., 2020; Pasotti et al., 2021). Data sets were obtained from the National University of Singapore (*NUS*), the Abyssal Biological Baseline Project (*ABYSSLINE*), multiple projects funded by the National Oceanic and Atmospheric Administration analyzed by Wilson (2017) (*Wilson*), U.S. Joint Global Ocean Flux Study (JGOFS) (*Smith*), Joint Programming Initiative Healthy and Productive Seas and Oceans (JPIO) project (*JPIO*), the Belgian company Global Sea Mineral Resources (GSR) through Ghent University (*Ghent*), Korea Deep Ocean Study (*KODOS*), and Yuzhmorgeologiya of the Russian Federation (*Yuzhmor*) (**Figure 1** and **Table 1**). Macrofaunal data from a total of 477 box cores were analyzed for this synthesis. Sampling sites ranged

[2]www.isa.org.jm/workshop/deep-ccz-biodiversity-synthesis-workshop

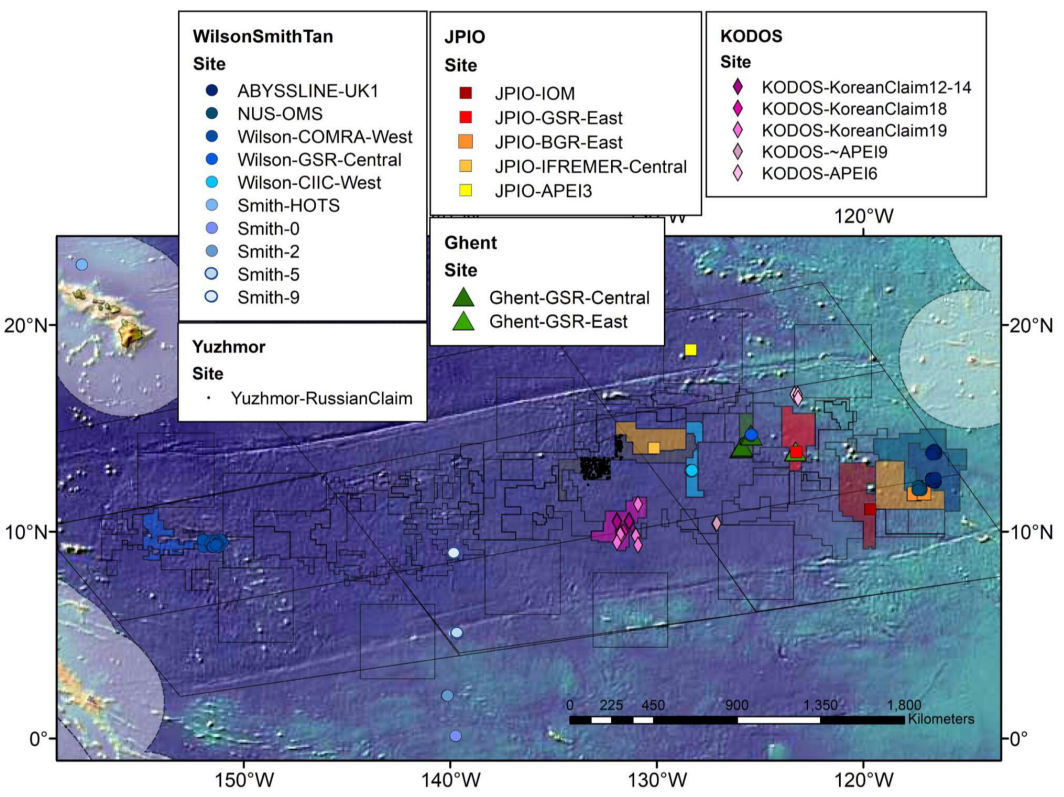

FIGURE 1 | Map of the CCZ showing study sites from which macrofaunal box-core data were assembled for use in this study. The characteristics of the data sets collected at these sites are presented in **Tables 1**, **2**.

TABLE 1 | Sources, numbers (#) of box cores, locations, and depths for macrofaunal box-core data used in this study.

Study	Site	Source of Data (Name and Email or citation)	# of Box Cores	Area of Box Core Sampled (m^2)	Latitude (N) (Decimal Deg.)	Longitude (W) (Decimal Deg.)	Sample Dates	Depth (m)
NUS	NUS-OMS	Tan Koh Siang – tmstanks@nus.edu.sg Chuar et al., 2020	12	0.2267–0.2275	12.01–12.22	117.18–117.38	2015	4041–4183
ABYSSLINE	ABYSSLINE-UK1	Craig Smith – craigsmi@hawaii.edu	24	0.25	12.37–13.96	116.46–116.72	2013–2015	4036–4218
Wilson	Wilson-COMRA-West	Wilson, 2017	54	0.2454	9.25–9.61	151.01–151.97	1977–1978	4842–5283
Wilson	Wilson-GSR-Central	Wilson, 2017	15	0.25	14.62–14.71	125.37–125.46	1983	4480 – 4567
Wilson	Wilson-CIIC-West	Wilson, 2017	16	0.25	12.91–12.98	128.28–128.37	1989	4708 – 4854
Smith	Smith-HOTS	Craig Smith – craigsmi@hawaii.edu Glover et al., 2002	4	0.15	22.91–22.92	157.83–157.84	1992	4843 – 4867
Smith	Smith-0°	Craig Smith – craigsmi@hawaii.edu Glover et al., 2002	3	0.18	0.11–0.12	139.73–139.74	1992	4300 – 4305
Smith	Smith-2°	Craig Smith – craigsmi@hawaii.edu Glover et al., 2002	4	0.18	2.06–2.07	140.13–140.15	1992	4408 – 4414
Smith	Smith-5°	Craig Smith – craigsmi@hawaii.edu Glover et al., 2002	3	0.18	5.07–5.08	139.64–139.65	1992	4320–4446
Smith	Smith-9°	Craig Smith – craigsmi@hawaii.edu Glover et al., 2002	3	0.18	8.93	139.86–139.88	1992	4981–4991
JPIO	JPIO-IOM	Lenaick Menot – lenaick.menot@ifremer.fr Martinez Arbizu and Haeckel(eds), 2015; Błażewicz et al., 2019b; Bonifácio et al., 2020	8	0.25	11.07–11.08	119.65–119.66	2015	4414–4434
JPIO	JPIO-GSR-East	Lenaick Menot – lenaick.menot@ifremer.fr Martinez Arbizu and Haeckel(eds), 2015; Błażewicz et al., 2019b; Bonifácio et al., 2020	5	0.25	13.84–13.86	123.23–123.25	2015	4503–4516
JPIO	JPIO-BGR-East	Lenaick Menot – lenaick.menot@ifremer.fr Martinez Arbizu and Haeckel(eds), 2015; Błażewicz et al., 2019b; Bonifácio et al., 2020	8	0.25	11.81–11.86	117.05–117.55	2015	4118–4370
JPIO	JPIO-IFREMER-Central	Lenaick Menot – lenaick.menot@ifremer.fr Martinez Arbizu and Haeckel(eds), 2015; Błażewicz et al., 2019b; Bonifácio et al., 2020	6	0.25	14.04–14.05	130.13–130.14	2015	4921–4964
JPIO	JPIO-APEI3	Lenaick Menot – lenaick.menot@ifremer.fr Martinez Arbizu and Haeckel(eds), 2015; Błażewicz et al., 2019b; Bonifácio et al., 2020	3	0.25	18.77–18.80	128.34–128.36	2015	4816–4847
Ghent	Ghent-GSR-Central	Ellen Pape – Ellen.Pape@ugent.be De Smet et al., 2017; Pasotti et al., 2021	19	0.25	14.02–14.71	125.51–125.93	2015–2017	4477–4629
Ghent	Ghent-GSR-East	Ellen Pape – Ellen.Pape@ugent.be De Smet et al., 2017	5	0.25	13.88–13.89	123.28–123.31	2015–2017	4535–4560
KODOS	KODOS-KoreanClaim-2018	Se-Jong Ju – sjju@kiost.ac.kr	15	0.23–0.25	9.85–10.52	131.33–131.93	2018	4995–5174
KODOS	KODOS-KoreanClaim-2012-14	Se-Jong Ju – sjju@kiost.ac.kr	36	0.23–0.25	10.48–10.52	131.29–131.94	2012–2014	4772–5206
KODOS	KODOS-KoreanClaim-2019	Se-Jong Ju – sjju@kiost.ac.kr	10	0.25	9.35–11.33	130.90–131.93	2019	4712–5220
KODOS	KODOS-APEI9	Se-Jong Ju – sjju@kiost.ac.kr	2	0.23–0.25	10.40–10.41	127.09–127.12	2018	4784–4792
KODOS	KODOS-APEI6	Se-Jong Ju – sjju@kiost.ac.kr	4	0.23–0.25	16.44–16.64	123.15–123.33	2018	4232–4290
Yuzhmor	Yuzhmor-RussianClaim	Slava Melnik – melnikvf@ymg.ru	214	0.2175–0.225	12.26–14.66	131.68–133.64	2010–2016	4713–5254

Site includes both the study and contractor area, APEI, or station name.

TABLE 2 | Results of linear mixed-effects models examining abundance, family richness, and species richness (taxa within a core) for polychaetes, tanaids, and isopods within the CCZ.

Mixed-effects Models	Polychaete Abundance	Polychaete Family Richness	Polychaete Species Richness	Tanaid Abundance	Tanaid Family Richness	Tanaid Species Richness	Isopod Abundance	Isopod Family Richness	Isopod Species Richness
Fixed Effects	4.8	3.1	1.7	46.9	52.6	32.2	18.5	10.8	7.7
Lutz POC	19.1[1]	2.3	2.6	26.1	42	17.7	9.2	8.8	5.2
Depth	0	1	0	42**	32.2	35.4**	21.7**	21.3**	4.5
Nodule Abundance	0.7	2*	0.3	0	3.8*	1.4	0	0	0.5
Dissolved Oxygen	13.8	2.6	0	3.6	27.2	9	0.1	0.1	3.8
Random Effects	74.8	73.1	72.6	20.7	9.4	32.5	43.2	63.6	29.3
Best Model	POC + Depth	POC + Depth + O2	POC + Depth + O2	POC + Depth	All Variables	POC + Depth	POC + Depth	POC + Depth + Nodules	POC + Depth + Nodules
R2	23	12.7	2.9	51.2	52.6	36.2	26.1	24.9	12.2
Random Effects of Best	56.6	63.5	71.4	16.4	9.4	28.5	35.6	49.5	24.8

[1] *0.05–0.1*

** < 0.05; ** < 0.01; *** < 0.001.*

Numbers represent R^2 values for all four fixed effects combined, each fixed effect alone, and the random effect (study/site). The best model represents the combination of fixed effects with the highest R^2 value. KODOS, except KoreanClaim19, and Yuzhmor are excluded from these analyses due to apparent differences in sampling efficiencies; Smith_HOTS, Smith_0^o, and Smith_2^o are excluded from analyses because they fall outside of the CCZ. Asterisks denote variables with significant differences in ANOVA at the p-levels indicated below table.

in depth from ∼ 4000 – 5300 m and were collected between 0 – 23° N and 116 –158° W (data sources and shorthand names for data sets are given in **Table 1**). Macrofaunal data were compiled for each research group at the site level, i.e., within a contract area or APEI (**Figure 1** and **Table 1**). Most studies differentiated only a subset of macrofaunal taxa (i.e., polychaetes, tanaids, and isopods) to the species level; however, *NUS* data were resolved only to the family level and *Yuzhmor* data to the class level (**Supplementary Table 1**). All studies used a 0.25 m^2 box corer although some removed small subsamples for other analyses (**Table 1**). Abundance data for all box-core samples were normalized to 1 m^2. All studies used 300-μm sieves except for *NUS*, which used 250-μm. Sampling years ranged from 1977 to 2019 (**Table 1**).

The Comparability of Box-Core Data Sets

There was substantial variability among "quantitative" box-core data sets in taxa counted and taxonomic resolution obtained. In addition, box-core samples were collected by different research programs (**Table 1**) using a range of box-core designs, box-core deployment protocols (e.g., lowering speed, stern vs. side A-frame, etc.), and sample-washing procedures (e.g., sieve size, washing-water temperature, on-board vs. in-laboratory sieving, etc.), all of which may influence sampling efficiency and the ability to resolve macrofauna at the species level (Glover et al., 2016). Most macrofaunal box-core data sets distinguished polychaetes, tanaids, and isopods to morphospecies. However, taxonomic and systematic resolution differed among these groups (e.g., many tanaid species were not classified into families), and only one study (*ABYSSLINE*) distinguished species for all macrofauna collected (**Supplementary Table 1**).

In addition, the thousands of sediment macrofaunal species in the CCZ are mostly undescribed (Glover et al., 2002; Smith et al., 2008a,b; Glover et al., 2018; Błażewicz et al., 2019b; Jakiel et al., 2019), research programs use different taxonomists with different morphological reference collections to resolve species, and some programs have combined morpho-taxonomy with DNA barcoding (**Supplementary Table 1**). Since reference collections have not been intercalibrated across all research programs and only a small proportion of macrofaunal species from the CCZ have been DNA barcoded or formally described, we conducted between-site species-level comparisons primarily *within* research programs to assure consistency in sampling protocols and species-level determinations. However, within one data set (*KODOS*), box cores collected on different cruises (2012–2014, 2018, and 2019) appear to have different sampling biases, with the percentage of polychaetes resolvable to species level, polychaete abundances, and species/family accumulation curves exhibiting large differences among sampling times; we thus analyzed the *KODOS* samples as three different data sets. It should be noted that the box-core data sets contributed by Wilson (*Wilson*), Smith (*ABYSSLINE* and *Smith*), and Tan (*NUS*) were collected and processed with similar protocols [first described in Hessler and Jumars (1974), and more recently in Glover et al. (2016)] by lead personnel trained in a single laboratory (that of R. R. Hessler), so these samples were considered to be a single *Wilson–Smith–Tan* data set for abundance analyses.

To allow diversity comparisons across data sets, we analyzed patterns at the family level after harmonizing the family level taxonomy using the World Register of Marine Species (WoRMS[3]).

[3] www.marinespecies.org

Analytical Methods

Analyses of the Comparability of Data Sets

Macrofaunal patterns across sites were first explored with regression analyses between macrofaunal abundances and individual environmental parameters, in particular POC flux, nodule abundance estimated from the ISA (2010) Geological Model, and ocean depth. Direct deep POC flux measurements (e.g., from sediment traps) are not available from the study sites considered here. Thus, to explore the relationship between seafloor particulate organic carbon (POC) flux and polychaete abundance, we estimated seafloor POC flux for sampling localities using the Lutz et al. (2007) POC-flux model and the data set created by Lutz et al. (2007), which was calculated for the period 1997 – 2004, an interval near the middle of the range in sampling times (1977–2019) of box cores used in this study; we call these estimates "Lutz POC flux." The Lutz et al. (2007) POC flux model is trained with sediment-trap data from the CCZ and the equatorial Pacific region generally, and yields results consistent with diagenetic modeling of seafloor POC in the CCZ (Volz et al., 2018). This model has been widely used to evaluate regional patterns of seafloor POC flux in the deep sea (e.g., Sweetman et al., 2017; Snelgrove et al., 2018). Type II regression analyses of polychaete abundance versus Lutz POC flux were performed using linear and exponential functions in *Excel*, and the function 'lmodel2' (Legendre, 2018) in R. The functionality (either linear or exponential) with the highest R^2 was selected, and ordinary least squares (OLS) regressions were used for all studies since they produced the best fit to the data. Linear mixed-effects modeling, 'lmer' (Bates et al., 2015), in R, with "POC flux" as the fixed effect and "Research Program" as the random effect was used to explore the amount of variation explained by POC flux versus study in polychaete abundance. If studies had different sampling efficiencies, we would expect that the "Research Program" effect would explain a relatively high proportion of the variance.

Analyses of Macrofaunal Abundance/Diversity, Environmental Drivers, and Community Structure

Biodiversity patterns were further explored with species and family accumulation curves, Chao 1 species richness estimators, rarefaction, and Pielou's evenness, as described in Magurran (2004) using EstimateS (Colwell, 2013), R (Venables et al., 2019), or PRIMER 7 (Clarke and Gorley, 2015). Rarefaction curves with 95% confidence limits were calculated in EstimateS for each site by pooling box-core samples within a site. Species accumulation curves and Chao 1 richness were calculated using 100 permutations and the UGE index (Ugland et al., 2003) in EstimateS for each site using box cores as replicates. Pielou's species and family evenness were calculated in PRIMER 7 for each box core and then averaged within a site. The number of species at each site with abundances of 1 or 2 individuals (singletons or doubletons) was calculated and compared to the total number of species found within each site. A similarity percentages (SIMPER) analysis was used to examine community similarity within study sites while an analysis of similarity (ANOSIM) test was used to examine community differences among sites within a study (Clarke and Gorley, 2015). Finally, the number of species found in more than one contractor area was calculated within studies for "working species," and across studies for "described species." "Working species" (i.e., "morphospecies") have been differentiated by a taxonomist but have not been assigned to a described species (i.e., they are likely new to science); working species are assigned numbers or letters that vary across taxonomists and studies. The number of species shared between sites was explored in the *JPIO* data set (Błażewicz et al., 2019b; Bonifácio et al., 2020) using UpSet plots generated in R (Conway et al., 2017). UpSet is a technique which visualizes data intersections and sizes of these intersections (Conway et al., 2017).

Linear Mixed-Effects Modeling, 'lmer,' in R, was used to explore which environmental variables best explained macrofaunal abundance and taxonomic richness across individual box cores (Bates et al., 2015). Sample depth, Lutz seafloor POC flux (Lutz et al., 2007), nodule abundance (kg/m^2) (Morgan, 2012), bottom-water oxygen concentration, bottom-water salinity, bottom-water temperature, bottom-water nitrate, phosphate, and silicate concentrations (all downloaded from World Ocean Atlas 2018[4]; Washburn et al., 2021), bottom slope (largest change in elevation between a cell and its eight neighbors), broad-scale bathymetric position index (BBPI; with an inner radius of 100 km and outer radius of 10000 km) and fine-scale bathymetric position index (FBPI, with an inner radius of 10 km and outer radius of 100 km) (McQuaid et al., 2020) were obtained for each box-core sample location. Since environmental data were not available for many individual locations and several studies, and to ensure data were consistent across studies, data for all environmental variables (except depth, which was provided for each sample) were extracted for each box-core location from interpolated rasters in ArcGis (see Washburn et al., 2021). Environmental variables were standardized, and abundance/richness data were log-transformed to facilitate linearity in the relationship between abundance/richness and environmental variables. If the relationship between an environmental variable and taxon abundance or richness did not appear linear (e.g., appearing parabolic in many cases), a second-order relationship was examined. A linear mixed-effect model was then created with abundance or taxon richness per core as the dependent variable, the standardized environmental variables set as fixed-effect explanatory variables, and site as the random-effect variable. Correlations among environmental variables were explored by calculating the variance inflation factors (VIF) in the 'car' package (Fox et al., 2020) and any variables with scores near or above 10 were removed (Montgomery and Peck, 1992). Studies were removed from the model if they appeared to have skewed residuals, and models with all possible combinations of variables were examined using 'dredge' in the 'MuMIn' package (Barton, 2020). Exploratory analyses found that the majority of variables explained less than 1% of the variation in abundances or richness, so models were refined to include only the variables explaining > 5% of the variance, i.e., depth, Lutz POC flux, nodule abundance, and bottom-water oxygen concentration. Relationships between environmental variables and abundance

[4]www.nodc.noaa.gov/OC5/woa18/

or richness in the best models, measured by AIC and R^2 values, were explored further with ANOVAs and regression plots (Zuur et al., 2009).

Community composition for polychaetes at the species level, and for other taxa at the family level, was compared among sites using non-metric multidimensional scaling on square-root transformed abundances/m^2 in PRIMER 7. SIMPER analysis was then used to explore which taxa were responsible for similarities/differences within and among studies.

RESULTS

The Comparability of Box-Core Data Sets

Because polychaetes typically constituted > 50% of macrofaunal abundance, and polychaete abundance was tabulated in all the box-core data sets, polychaete abundance was used to explore comparability (e.g., sampling efficiency) across research programs. Based on previous abyssal studies of the relationships between seafloor POC flux and macrofaunal abundance (Glover et al., 2002; Smith et al., 2008a; Wei et al., 2010), it was expected that polychaete abundance across the CCZ would exhibit a positive relationship (exponential or linear) with estimated annual seafloor POC flux (Lutz et al., 2007). Abundances per box core spanned an order of magnitude across studies (**Supplementary Figure 1**), likely in part due to variations in POC flux.

When box-core samples were pooled across all studies, polychaete abundance was exponentially related to POC flux (**Figure 2**), with 20% of the variation explained. However, the data from individual sampling programs were not evenly distributed above and below the overall regression curve, as would be expected if they were from the same statistical population, with a number of data sets falling largely above or essentially entirely below the curve. This suggests that individual data sets may have different relationships between POC flux and polychaete abundance, as might be expected if sampling protocols (and sampling efficiency) varied among research programs. Furthermore, in the linear mixed effect model including all data with research program as the random effect and POC flux as the fixed effect, the research program effect explained 51% of the variation while POC flux explained 19% ($p < 0.0001$). This is also consistent with the hypothesis that sampling efficiency varied among research programs.

We then conducted regressions of POC flux versus polychaete abundance for individual research programs, i.e., studies that were conducted by investigators trained within the same laboratory and thus expected to use similar sampling protocols. The *Wilson–Smith–Tan* and *JPIO* studies exhibited positive exponential relationships with high R^2 values (>0.7), while all other studies, except for KODOS, showed positive but weaker exponential relationships to Lutz POC flux (**Figure 2**). The KODOS data showed a negative exponential relationship to POC flux, driven largely by relatively low values in box cores collected prior to 2019 (**Figure 2**), potentially due to differences in sampling protocols, sea states, and/or seasonal/temporal trends in the KODOS area. The *Wilson–Smith–Tan* data covered the broadest ranges of longitude, latitude and POC fluxes while *JPIO* data covered the second broadest ranges of these variables (**Table 1**), providing robust support for the importance of POC flux as an ecosystem driver across the CCZ (cf. Smith et al., 2008a; Wedding et al., 2013; Bonifácio et al., 2020). Due to the differing relationships between polychaete abundance and POC flux across studies, we hypothesized that different studies had

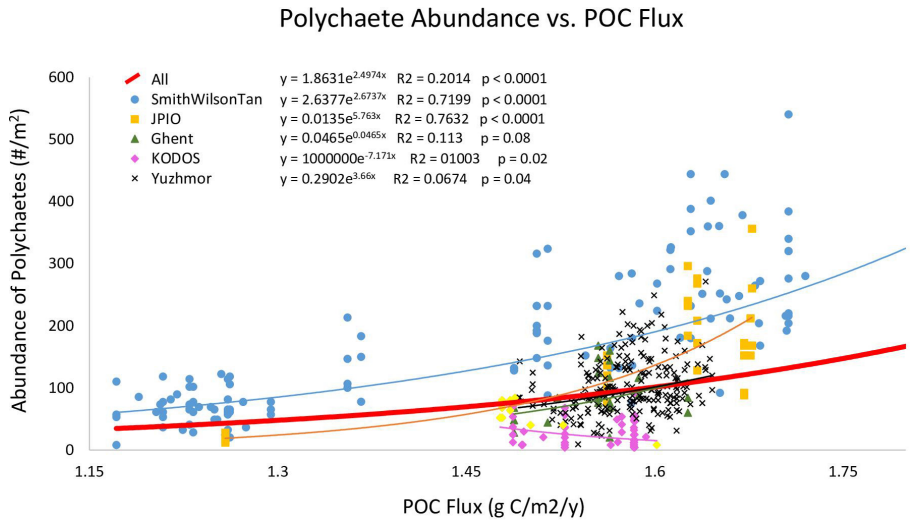

FIGURE 2 | Polychaete abundance in individual box cores versus Lutz POC flux. Curves are Type II regressions conducted in R, with regression equations, R^2 values, and p levels of regressions indicated. The bold red line is the exponential regression for all sampling programs combined. Regression lines for data sets match the colors of their symbols in the upper left. The pink regression line represents all *KODOS* data, while yellow diamonds represent *KODOS* samples collected in 2019. This figure does not show data points for Smith-0, Smith-2, or Smith-5 (which are included in the regressions/curves) as they have much larger POC fluxes and abundances than all other sites making observations of trends for other studies difficult.

different sampling efficiencies and were not directly comparable, so further analyses were performed separately on data sets from individual research programs.

Question 1: Do Abundance, Species/Family Richness and Evenness, and Community Structure, Vary Along and Across the CCZ? What Are the Ecological Drivers of These Variations?

Abundance Patterns

Regional patterns of polychaete abundance

Polychaete abundance showed strong variations along and across the CCZ, including within data sets (e.g., the *Wilson–Smith–Tan* data in blue and the *JPIO* data in yellow) (**Supplementary Figure 2**). Many of the between-site differences are clearly statistically significant, as indicated by the small size of within-site standard errors compared to between-site differences. As noted above (**Figure 2**), regression analyses indicate that these variations in polychaete abundance across the region are strongly related to Lutz POC flux (Lutz et al., 2007), supporting the use of seafloor POC flux to divide the CCZ management area into ecological subregions (Wedding et al., 2013).

Lutz POC flux explained >70% of the variability in polychaete abundances across the CCZ for two studies and 20% of variability for all studies combined. Regional nodule abundance, when assessed individually with Type II regression, exhibited little relationship with polychaete abundance for all data sets combined, but explained 38 and 48% of variation in the *Wilson–Smith–Tan* and *JPIO* data sets, respectively (**Figure 3**, Smith-0, Smith-2, and Smith-5 not shown). The relationships between depth and polychaete abundance were generally negative, explaining 25% of variability among polychaete abundances when all data sets were combined, and 41 and 35% of abundances for the *Wilson-Smith-Tan* and *JPIO* data sets, respectively (**Figure 3**).

We also explored the relationship between average polychaete abundance at all sites sampled across the region (**Figure 1**) versus Lutz POC flux to the seafloor, depth, bottom-water oxygen concentration, nodule abundance, and measures of seafloor slope using linear mixed-effects models. Measures of seafloor slope (i.e., slope, BBPI, FBPI) explained little to no variation in polychaete abundances and were thus removed. ANOVA found that only POC flux had a nearly significant p-value (p = 0.06). Fixed effects (i.e., environmental variables) in the model explained 23% of variation in polychaete abundance when *KODOS* from 2012 – 2018 and *Yuzhmor* data (i.e., data sets with very different apparent sampling efficiencies) were excluded. This was almost solely due to POC flux, since the model containing POC flux alone explained 19% of the variation. Neither depth nor nodule abundance explained substantial variation while the inclusion of oxygen concentration actually decreased the R^2 of the model (**Table 2**). It is noteworthy that random (study/site) effects explained three times as much variability in polychaete abundance (57%) as the fixed effects, highlighting that there are large differences among sampling programs and/or sites not explained by the current set of environmental variables; these differences are likely caused, at least in part, by differences in sampling efficiency among studies.

Regional patterns of tanaid and isopod abundance

Regression relationships between tanaid and isopod abundances and Lutz POC flux were similar to those for polychaete abundance. POC flux explained 57 and 47% of variability in tanaid abundances for the *Wilson–Smith–Tan* and *JPIO* data sets, respectively, and 26% of tanaid variability for all studies combined. POC flux explained 21 and 17% of variability in isopod abundances for the *Wilson–Smith–Tan* and *JPIO* data sets, respectively, and only 7% of isopod variability for all studies combined (**Supplementary Figures 3A, 4A**). Nodule abundance explained approximately 10% or less of the variation for both tanaid and isopod abundances for all data sets combined as well as for each data set independently, except *JPIO*; there, nodule abundance explained 27 and 33% of tanaid and isopod abundances, respectively. However, unlike all other studies, the relationships between nodule abundance and polychaete, tanaid, and isopod abundances in *JPIO* samples were best described by second-order polynomial functions with maximum animal abundances at intermediate nodule abundances (**Supplementary Figures 3B, 4B**).

Depth explained 31% of variability of tanaid abundances for all data sets combined and 39 and 47% of abundances for the *Wilson–Smith–Tan* and *JPIO* data sets, respectively. Depth

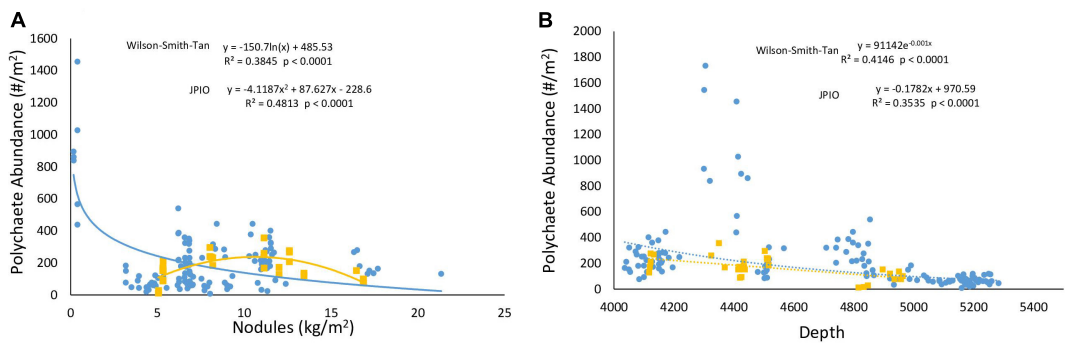

FIGURE 3 | (A) Nodule abundance and **(B)** depth versus polychaete abundance in the *Wilson–Smith–Tan* (blue) and *JPIO* (yellow) data sets. Lines shown are Type II regressions conducted in R. All regressions are highly statistically significant (p < 0.0001).

exhibited little relationship with isopod abundances for all data sets combined. Depth explained 27, 43, and 47% of variability of isopod abundances for the *Wilson–Smith–Tan*, *JPIO*, and *Ghent* data sets, respectively. However, unlike polychaetes and tanaids, regression relationships for isopod abundances were best represented by second-order polynomial functions with maximum abundances at intermediate depths for *Wilson–Smith–Tan,* but with minimum abundances at intermediate depths for *JPIO* and *Ghent*. Measures of slope explained little to no variation in tanaid or isopod abundances (**Supplementary Figures 3C, 4C**).

Overall, these regression relationships suggest that on regional scales across the CCZ, POC flux, and to lesser degrees nodule abundance and depth, are likely to be important drivers of tanaid and isopod abundances. The differences in these relationships among studies and the lack of relationships to POC flux, nodule abundance, and depth for the *Ghent*, *KODOS*, and *Yuzhmor* data sets further suggest differences in sampling efficiencies among studies. These differences may also be due in part to the narrow range of variation among explanatory variables in the above data sets due to their limited geographical extents.

Linear mixed-effects models for both tanaid and isopod abundance indicated that environmental variables were important, with fixed effects explaining over 50% of the variability in tanaid abundances and 25% for isopod abundances in the best models. ANOVA indicated that depth was significant for both tanaids (p = 0.004) and isopods (p = 0.006). The inclusion of oxygen and nodule abundance in either model decreased its ability to explain variations in abundances. For both tanaids and isopods, depth alone explained nearly all the variability attributed to fixed effects. POC flux explained roughly half of the variability in either model (tanaids ∼25%, isopods ∼10%). Removal of POC flux did not appear to affect the quality of the model when depth was left in, suggesting that half of the variability related to depth may be caused by covarying POC flux. Nodule abundance explained 0% of the variability for either tanaid or isopod abundance (**Table 2**).

Biodiversity Patterns at the Species Level

Polychaetes

All sites with species-level, box-core data for polychaetes exhibited rising species accumulation curves, in many cases with steep slopes and with none approaching a plateau (**Figure 4**). These curves indicate that polychaete species richness at all sites remains under-sampled, i.e., species are still accumulating rapidly and additional sampling at any site will collect previously unsampled species, even when large numbers of box cores have already been collected (e.g., >50 at COMRA-West; **Table 1**). The rapidly rising curves reflect the fact that many/most species at each site are rare; ≥49% of species were singletons or doubletons, i.e., represented by only one or two individuals, in the pooled samples from any site (**Figure 5**). Within internally consistent data sets (e.g., within the *Wilson* and within the *JPIO* data sets), there are substantial between-site differences in the slopes and apparent asymptotes of species accumulation curves (**Figure 4**).

Because species were still accumulating at all sites, the Chao 1 statistic (**Figure 6**) was used to estimate the total number of species expected to be collected at each site (Magurran, 2004). Chao 1 estimates range from ∼25 to ∼370 species, with all the relatively well-sampled sites estimated to have > 100 species of polychaetes. Estimated total species richness at all sites substantially exceeds the number of species collected, i.e., only 25 – 73% of estimated polychaete species richness has been recovered at any site (**Supplementary Figure 5**). It is important to note that for many sites (ABYSSLINE-UK1, Wilson-CIIC-West, all five *JPIO* sites), the Chao 1 curves are increasing

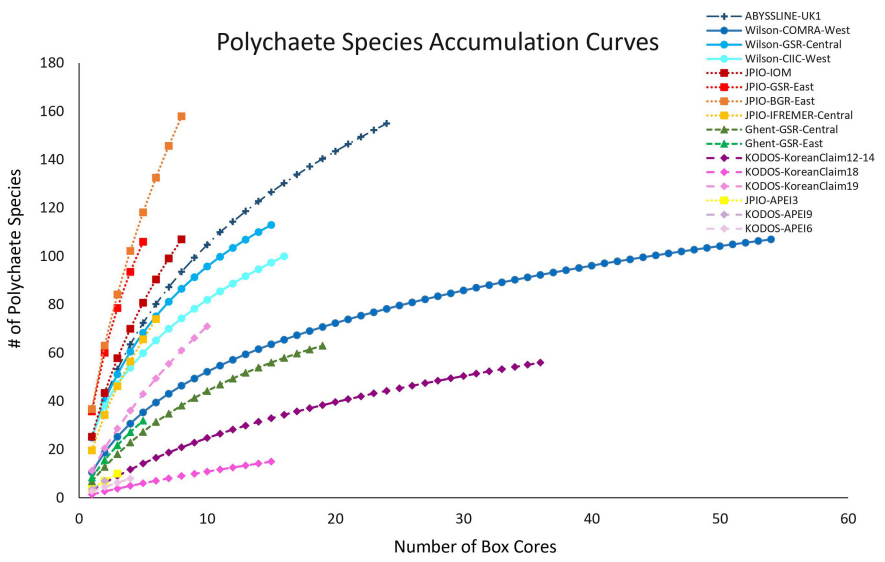

FIGURE 4 | Mean polychaete species accumulation as a function of number of box-core samples (UGE plot from EstimateS, 100 permutations) at different sites in the CCZ region. Note that KODOS-KoreanClaim data come from a single site sampled in different years. Data sets that are considered to have been sampled with similar protocols and to have used a consistent taxonomy are indicated by similar symbols.

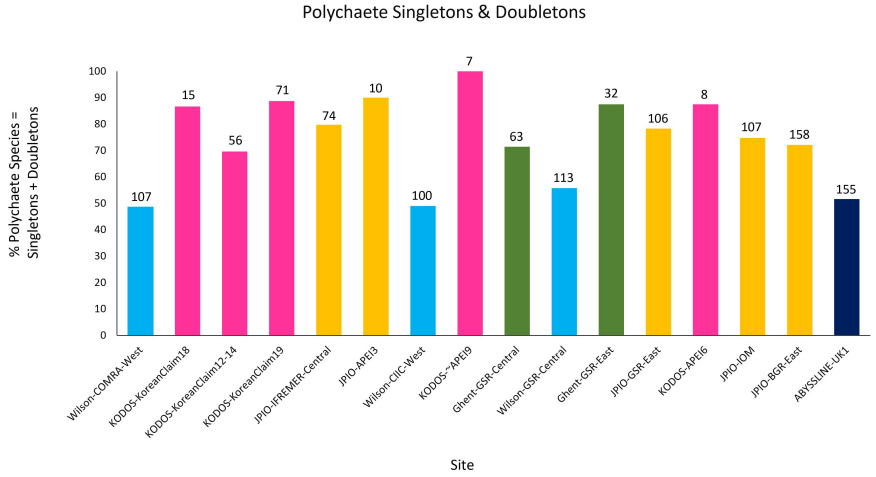

FIGURE 5 | Percentage of total polychaete species represented by singletons + doubletons in pooled collections from each site and study. The total number of polychaete species collected in each data set is indicated at the top of each bar. Note that KODOS-KoreanClaim data come from a single site sampled in different years, and potentially with different sampling efficiencies. Data sets considered to have been sampled with similar protocols and to have used a consistent taxonomy are indicated by similar colors.

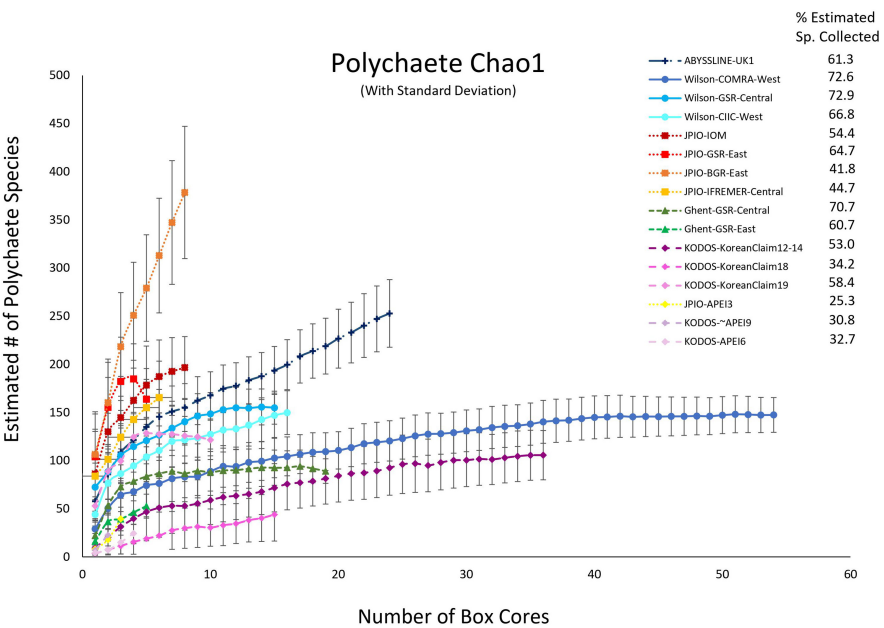

FIGURE 6 | Chao 1 (±SD) estimates of polychaete species richness as a function of number of box cores collected at 16 sites across the CCZ region. Note that KODOS-KoreanClaim data come from a single site sampled in different years. Data sets considered to have been sampled with similar protocols and to have used a consistent taxonomy are indicated by similar symbols.

rapidly with additional box cores (**Figure 6**) suggesting that at these sites, estimated species richness will increase substantially with additional sampling (i.e., the current Chao 1 number is an underestimate). Species diversity (including richness) can only be directly compared between those sites with a common polychaete taxonomy (i.e., internally consistent species differentiation), and only one internally consistent box-core data set, *JPIO*, has sampled > 3 sites (n = 5) across a substantial range (1400 km) of the CCZ (**Figure 1**; Bonifácio et al., 2020). The *JPIO* data (based on morphological and molecular differentiation of species) indicate substantial variability in species richness across sites (**Supplementary Figure 5**), which appears to be driven by differences in POC flux and nodule abundance (Bonifácio et al., 2020).

Individual-based species rarefaction curves for all sites exhibit similar initial slopes (with overlapping 95% confidence limits) suggesting similar, high levels of species evenness across sites (**Supplementary Figure 6**). However, rarefaction diversity at

higher numbers of individuals, i.e., toward the right ends of curves and at $Es_{(130)}$, exhibit significant variability across sites within data sets (**Figure 7** and **Supplementary Figure 6**). These between-site differences in rarefaction diversity were not strongly related to POC flux (**Supplementary Figure 6**), in agreement with the findings of Bonifácio et al. (2020) for the JPIO data set.

Mean Pielou Evenness J', calculated at the box-core level, was generally high (near 1.0) and showed little variation across sites, except that the Wilson-CIIC-West site value was unusually low (∼0.9) (**Supplementary Figure 7**). Overall, this result is consistent with the similarity of initial slopes of species rarefactions curves in **Figure 7**.

No environmental variables in the linear mixed-effects model for polychaete species richness per core were significant in ANOVA. The fixed effects (POC flux, Depth, O_2, and nodule abundance) explained less than 5% of species richness. On the other hand, the random variable explained over 70% of richness differences (**Table 2**), suggesting that differences in sampling efficiency and taxonomy among research programs may have contributed to differences in species richness among studies.

The similarity of polychaete communities among box cores from single studies, measured by SIMPER, ranged from 0 to 49%. ANOSIM tests found communities differed significantly among the three sites in the *Wilson* data set and the five sites in the *JPIO* data set. Generally, communities at sites further away were more different. However, evenness and the proportion of species represented as singletons are high, which means that samples with few individuals are likely to be dissimilar to other samples. For the *Wilson* data set, communities at GSR-Central and CIIC-West clustered together vs. COMRA-West, but abundances were also lower in COMRA-West vs. the other sites. Samples from COMRA-West appeared to have decreasing similarity with decreasing abundance (**Supplementary Figure 8**). A similar trend was observed in samples from the *JPIO* data set, with IOM, BGR-East, and GSR-East clustered together and different from Ifremer, which had lower abundances per sample than the other three sites (**Supplementary Figure 8**).

Tanaids and isopods

Rapid rates of species accumulation were observed across all sites for tanaid and isopod crustaceans, as for polychaetes, indicating that these crustacean assemblages remain poorly sampled (**Figure 8**). As for polychaetes, large proportions of the species at all sites (>45%) were represented by singletons + doubletons, and a substantial percentage of Chao-1 estimated species richness remained uncollected (>15%), indicating that these assemblages are incompletely sampled, even with >50 box cores (Wilson-COMRA-West). Within data sets, there was some heterogeneity between sites in accumulation curves and estimated species richness (**Figures 8**, **9**). Estimated total species richness at most sites substantially exceeds the number of species collected for both tanaids and isopods with only 16–85% of estimated tanaid species richness, and 20–80% of isopod richness, recovered at any site (**Figure 9**). Unlike polychaetes, individual-based species rarefaction curves for tanaids exhibit similar curves across most sites. Only one data set, *Wilson*, collected more than 30 isopods at two or more sites, and rarefaction curves for these three sites were similar as well (**Supplementary Figure 9**).

Unlike polychaete species richness, the fixed (environmental) effects in the best mixed effects model for tanaid species richness explained over 35% of variation. ANOVA results for this model show a significant difference for depth, and nearly all the variation explained in the model was attributed to depth. POC flux explained roughly half of the variation in tanaid richness as depth, suggesting that half of the apparent influence of depth on tanaid richness is due to POC flux. Nodule abundance explained less than 2% of variation. The fixed effects in the mixed effects model for isopod species richness

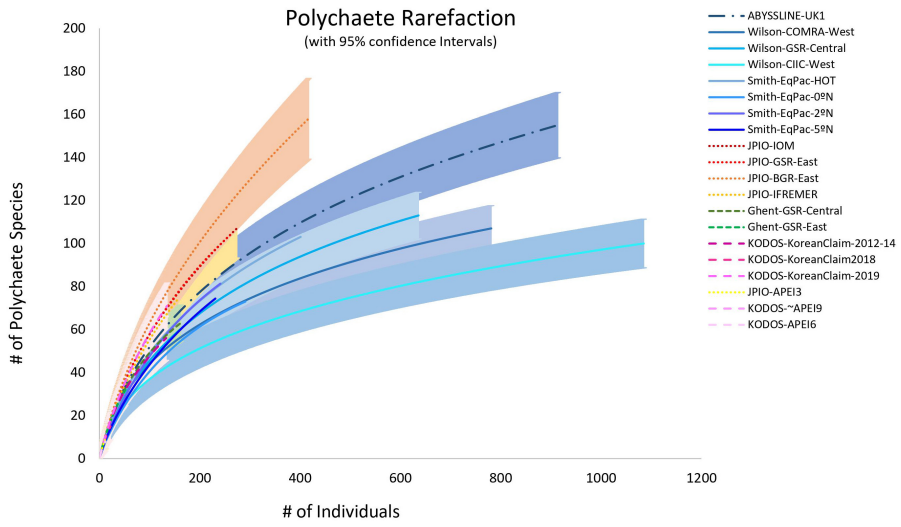

FIGURE 7 | Individual-based polychaete species rarefaction curves by site. Envelopes indicate 95% confidence limits for curves. Note that the KODOS-KoreanClaim data come from a single site sampled in different years. Data sets considered to have been sampled with similar protocols and to have used a consistent taxonomy, are indicated by similar line types.

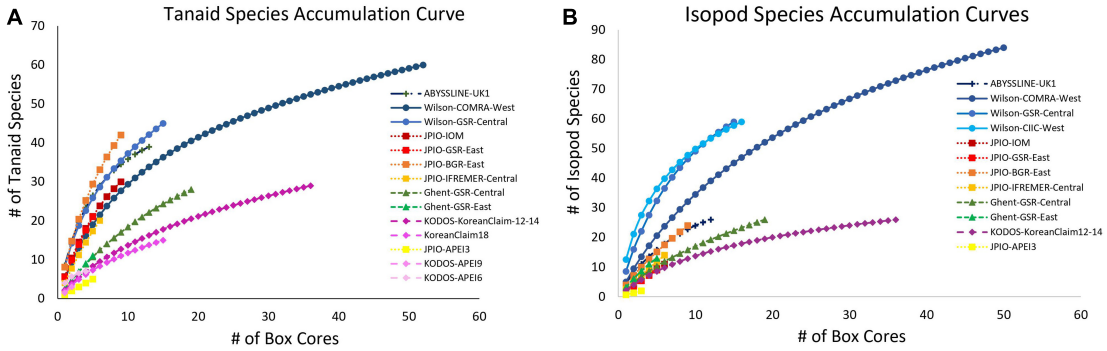

FIGURE 8 | Mean **(A)** tanaid and **(B)** isopod species accumulation as a function of number of box-core samples (UGE plot from EstimateS, 100 permutations) at different sites in the CCZ region. Note that the Korean Claim data come from a single site sampled in different years. Data sets considered to have been sampled with similar protocols and to have used a consistent taxonomy, are indicated by similar symbols.

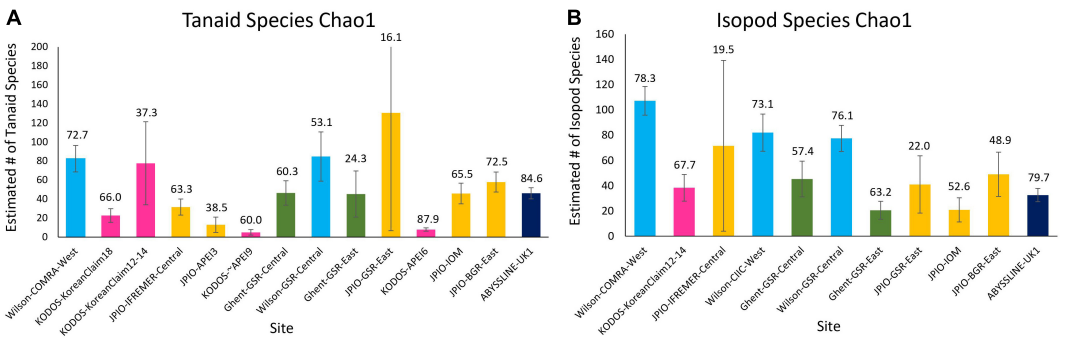

FIGURE 9 | Chao 1 (±SD) estimate of species richness for **(A)** tanaid and **(B)** isopod assemblages at the various sites sampled across the CCZ. Numbers over bars indicate the percentage of estimated species richness that has been collected at each site.

explained roughly 10% of variation while ANOVA results showed no significant differences in any environmental variables for this model (**Table 2**). The random effect explained over 30% of variation in tanaid species richness and over 40% in isopod species richness, again suggesting that differences in sample efficiency inhibit comparisons across studies.

Within study sites, community similarities at the species level among tanaid communities, based on SIMPER, ranged from 0 – 24%, and from 0 – 28% among isopod communities. ANOSIM analyses found communities differed significantly among all study sites in the *Wilson* data set for both tanaids and isopods, and in the *JPIO* data set for tanaids. nMDS plots separated sites in the *Wilson* data set for isopods but not for tanaids, while *JPIO* sites were spatially separated for tanaids and isopods (with very low abundances, **Supplementary Figures 10, 11**). As for polychaetes, much of the dissimilarity appeared to be directly related to samples with small numbers of individuals.

Biodiversity Patterns at the Family Level

To minimize differences in taxonomy among data sets, we also explored patterns of diversity and community structure at the family level. Identifications at the family level are generally standardized across taxonomists and sampling programs, and the sampling of families is usually more complete and less biased than sampling of many hundreds of rare, undescribed species. For older data sets (e.g., Wilson, 2017), we updated family classifications to the current family taxonomy using WoRMS.

Polychaetes

For most sites with >10 box-core samples, polychaete family accumulation curves were leveling off (**Figure 10**), and the number of families collected was generally > 80% of Chao-1 family richness estimates (**Supplementary Figure 12**), suggesting that most sites are well sampled for polychaete families. There was substantial across-site variability in estimated family richness, both within and across sampling programs.

A linear mixed-effects model exploring the relationship between polychaete family richness per core and four explanatory environmental variables (Lutz POC flux, depth, nodule density in kg/m^2, and bottom-water oxygen concentration) found that fixed effects in the best model explained approximately 15% of variation in family richness, but only nodule abundance was statistically significant ($p < 0.05$) and explained only 2% of the variation. The random effect explained over 60% of the variation (**Table 2**). Thus, differences in sampling efficiency or unmeasured environmental, or biotic, variables may be largely driving differences in polychaete family richness per core among the study sites.

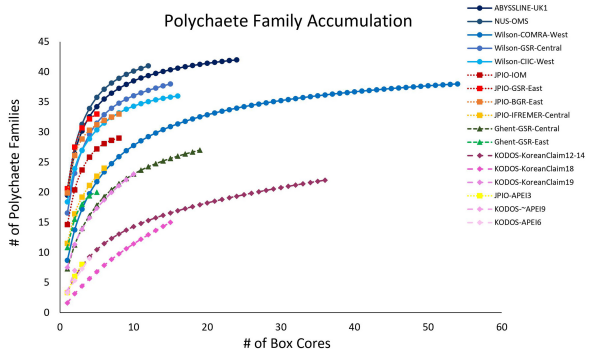

FIGURE 10 | Mean polychaete family accumulation versus number of box-core samples (UGE plot from EstimateS, 100 permutations) at different sites in the CCZ region. Note that *KODOS* data come from a single site sampled in different years. Data sets considered to have been sampled with similar protocols are indicated by similar symbols.

Community structure at the family level also differed across sites, with some carnivorous families (e.g., lumbrinerids and goniadids) being relatively common at sites with higher POC flux and rare or absent from sites with low POC flux (**Figure 11**, purple and brown wedges). While both lumbrinerids and goniadids were almost completely absent at sites with the lowest POC fluxes, lumbrinerids exhibited a positive linear relationship with POC flux while goniadids exhibited a parabolic relationship with POC flux with highest abundances at intermediate levels (**Supplementary Figure 13**). However, *p*-values for both lumbrinerids and goniadids relationships with POC flux were not significant.

Question 2: Do Claim Areas Have Similar Levels of Species/Taxon Richness and Evenness, and Similar Community Structure, to the Proximal APEI(s)?

The sediment macrofaunal data from APEIs are extremely limited, with only APEI 3 sampled within its core region (at a single site) with three box cores, and single sites on the edges of APEIs 6 and 9 sampled with four and two box cores, respectively. Polychaete community abundance, and Chao 1 species and family richness were substantially lower in the core of APEI 3 than in license areas 600 – 900 km away (IFREMER-Central and GSR-East) sampled during the *JPIO* program (**Supplementary Figures 2, 5, 12**). These differences appear to be related to lower POC flux and nodule abundance in APEI 3 (**Figure 2**) (Bonifácio et al., 2020). Polychaete abundance and Chao 1 species richness were also lower on the edges of APEI 6 and 9 than in the KODOS area 600 –1200 km away sampled during the same cruise (**Supplementary Figures 2, 5**). These differences may also be related to differences in POC flux.

Species level comparisons between APEIs and contract areas are very problematic because so few macrofaunal individuals were collected in/near APEIs (e.g., only 13 polychaete, 5 tanaid, and 2 isopod individuals in APEI 3). Six of the 10 polychaete species found in APEI 3 were not found at any other *JPIO* site. In fact, only one species (*Aphelochaeta* sp. 2062) was found in more than one core in APEI 3, making it impossible to characterize macrofaunal communities from these samples. There were only five tanaid species and two isopod species collected in APEI 3 (all singletons) with one species of each crustacean taxon found at additional *JPIO* sites.

At the polychaete family level, nMDS analyses show all three sites inside or near APEIs as outliers in community structure compared to sites sampled within license areas (**Figure 12**). However, these differences could well be caused by the very limited number of box cores (3 – 4) and polychaetes ($\leq$16) collected in or near the APEIs. It is noteworthy that KODOS 2018, which also has very few polychaetes identifiable to family level (n = 28), is an outlier compared to the sites with larger samples. For tanaid families, APEIs 3 and 9 appear as outliers, but, once again, these sites are very poorly sampled with $\leq$4 tanaids identified to family. Both sites in the *Wilson* data set also had very different tanaid communities than all other studies; however, these individuals were identified $\sim$ 40 years ago and the family level taxonomy of tanaids has been revised since that time. While we updated tanaid families using the current taxonomy in WoRMS, tanaid species in *Wilson* were only identified by number so may not have been assigned reliably to current tanaid families.

Question 3: Are Species Ranges (Based on Morphology and/or Barcoding) Generally Large Compared to the Distances Between APEIs and Contractor Areas? What Is the Degree of Species Overlap Between Different Study Locations Across the CCZ?

Distribution of Described Polychaete Species Among Box-Core Studies

For the purpose of this analysis we assume that described species can be consistently identified across taxonomists, although that is not necessarily the case. There were 54 described species of polychaetes identified in our combined macrofaunal data set. Some of these identifications included "cf.", i.e., to be compared with a given described species. Again, for the purpose of this analysis, we assume that individuals identified with a "cf." belong to the referenced species. Thirteen of the 54 identified species were found at more than one contractor site. Eleven species were shared between the Korean Claim and UK1, and seven species were shared between GSR and UK1. Two species were found in the BGR, GSR-East, GSR-Central, IFREMER, UK1, and Korean claim sites as well as APEI 6. These two species, the spionid *Aurospio cf. dibranchiata* and the goniadid *Bathyglycinde cf. profunda*, were the most commonly collected described species in the CCZ data set and have been found in other ocean basins (Maciolek, 1981; Mincks et al., 2009; Boggemann, 2016). *Aurospio cf. dibranchiata, Bathyglycinde cf. profunda, Ceratocephale cf. regularis, Levinsenia cf. uncinata, Paralacydonia cf. paradoxa, Paraonella abranchiata, Prionospio branchilucida, Progoniada cf. regularis, Pseudomystides rarica,* and *Terebellides cf. abyssalis* were found at sites separated by

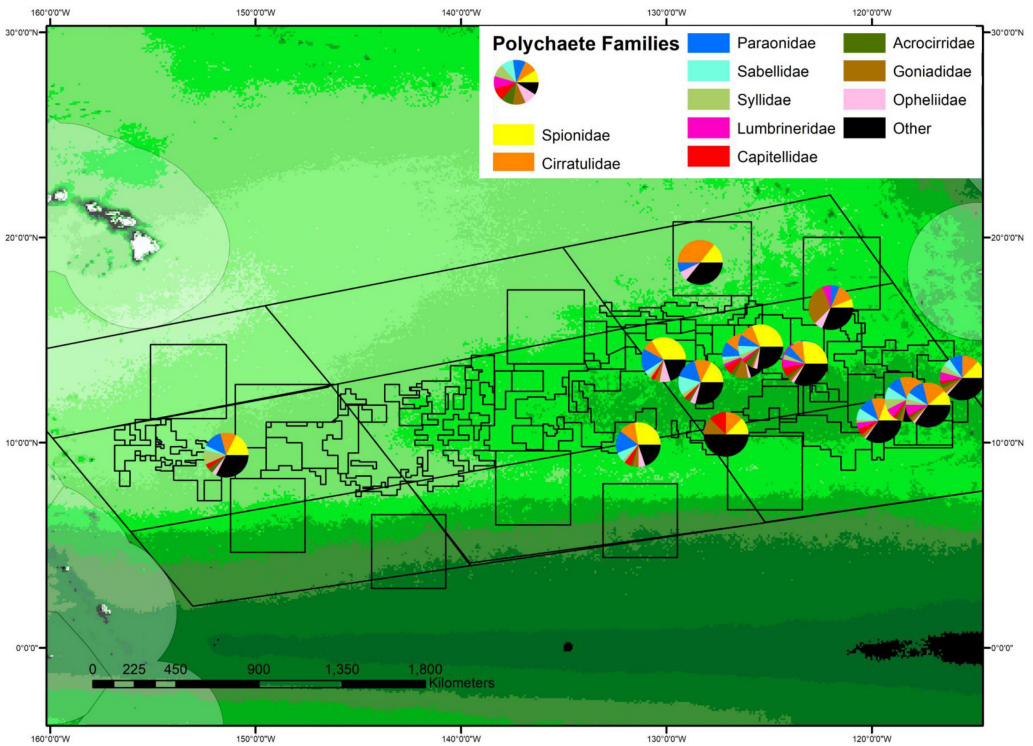

FIGURE 11 | Percent composition of polychaetes by family plotted on the regional map of POC flux. The percent abundance of the 10 most common families is shown, with the size of wedges of circles proportional to percent abundance. The center of each chart in the map indicates site location, with some offsets to allow all pie charts to be visible. See **Supplementary Figure S2** for POC flux scale.

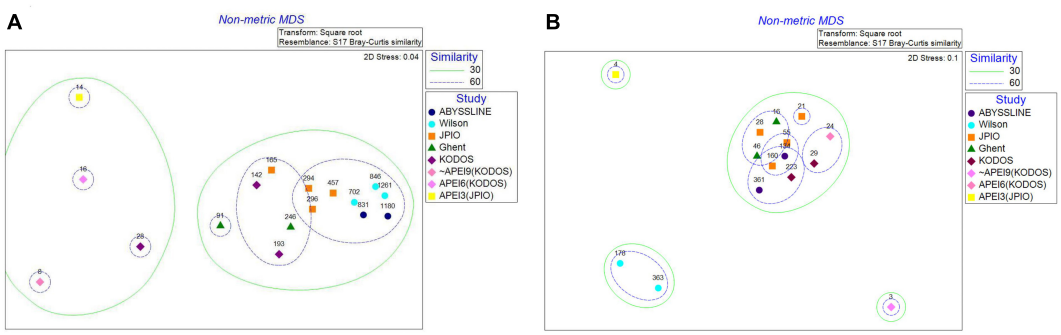

FIGURE 12 | NMDS plots of **(A)** polychaete and **(B)** tanaid family community structure for contractor areas and in or near APEIs. Dashed lines bound sites with 30 and 60% similarity. Numbers above points represent the number of individuals collected at each site.

1500 – 2000 km (**Supplementary Figure 14**). However, one polychaete species (*Lumbrinerides cf. laubieri*) represented by many individuals (68) was identified from stations within only one site separated by ∼200 km. Thus, three-quarters of the described polychaetes, including one collected many times, were sampled from only a small geographic range (≤200 km) while some commonly collected polychaete species show evidence of broad geographic ranges (**Supplementary Figure 14**). Among the fourteen described species of tanaids (Błażewicz et al., 2019a; Jakiel et al., 2019), only one (*Stenotanais arenasi*) was found at more than one study site; this was the only described tanaid species for which numerous individuals (16) were collected (**Supplementary Figure 14**) while there were no described species of isopods.

Distribution of "Working Species" Within Box-Core Studies

The *JPIO* study included the largest number of different sites and spans ∼1400 km (**Figure 1**), although all the *JPIO* sites are in the eastern CCZ. Roughly 30% of working species of polychaetes and 5 – 10% of tanaid and isopod working species in the *JPIO* data set range over 600 – 1200 km, with four polychaete

and one tanaid species occurring in APEI 3 and contract areas separated by 1250 – 1400 km (**Figure 13**). However, roughly 60% of polychaete, 80% of tanaid, and nearly 90% of isopod species were found only at single sites, with 60 – 80% of species found at only one site as singletons (**Figure 13**).

These results suggest that the ranges of some relatively common macrofaunal species are broad, while many other species, including some with high local abundance, may have small ranges compared to the size of exploration contract areas (up to 75000 km^2) and the distance from contractor areas to the nearest APEIs (often 100s of kilometers). However, because most macrofaunal species sampled are rare, it is very difficult to distinguish whether species typically are endemic to single sites (i.e., have small ranges compared the spacing of samples across the region, **Figure 1**), or are present but not yet sampled at multiple sites.

DISCUSSION

Our analyses of abundance patterns of polychaetes (which dominate the macrofauna), tanaids and isopods strongly suggest the hypothesis that different sampling programs have had differing sampling efficiencies for macrofauna, although

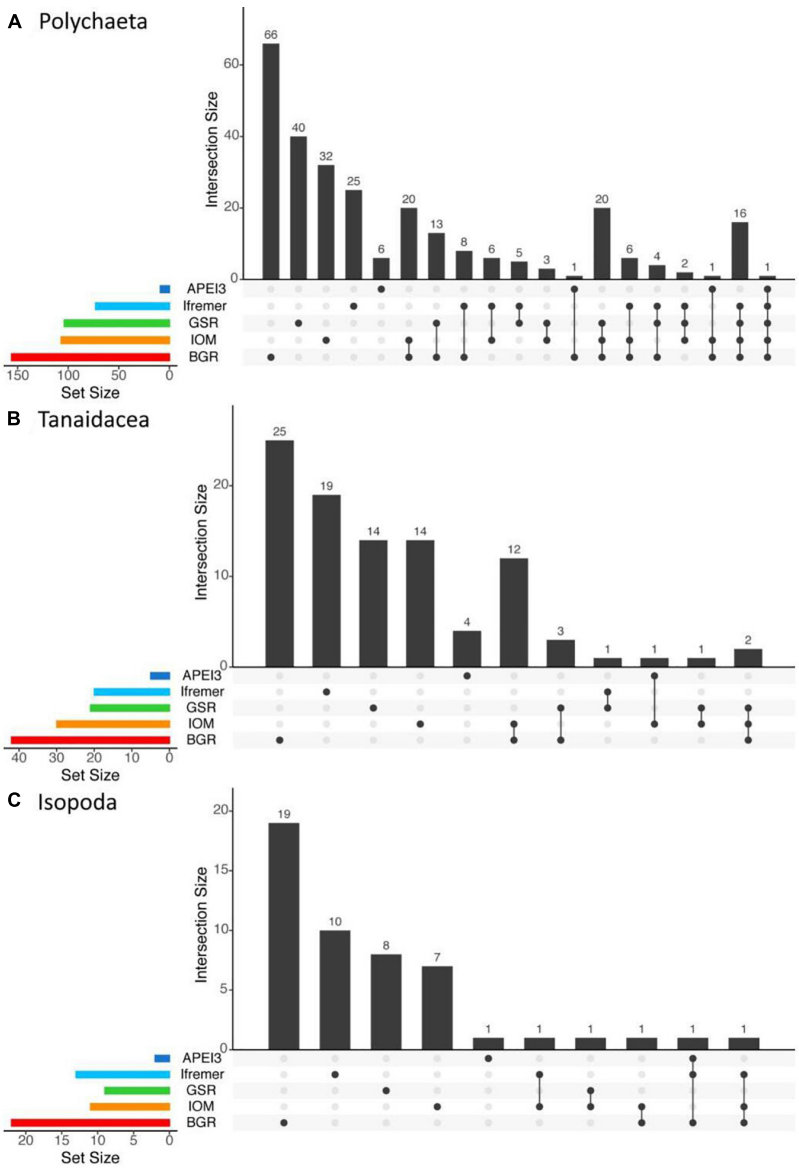

FIGURE 13 | UpSet plots showing the intersection of sediment macrofaunal species resolved by morphological and/or molecular approaches across the five JPIO sites (i.e., sites with a common species-level taxonomy) for **(A)** polychaetes, **(B)** tanaids, and **(C)** isopods. Vertical bars on the main plots represent the number of the unique species in each area (indicated by dots in the bottom part of the graph) or number of species shared across sites (dots connected by lines). Bars on the left are the total number of morphological species and MOTUs (Molecular Operational Taxonomic Units) identified in each of the five areas.

spatial and temporal variations in ecological drivers likely also have contributed to variations among studies. Differing sampling efficiencies were indicated by regression analyses of polychaete abundance versus POC flux, and as random effects in our linear mixed models for multiple taxa. Variations in sampling efficiencies may be caused by differences in box-coring equipment, lowering protocols, characteristics of ship motion, deployment locations (e.g., stern versus side A-frames), and sample-washing and preservation protocols (Glover et al., 2016). These potential differences in sampling efficiencies highlight the need for detailed, standardized sampling protocols, and training and scientific exchange programs, as well as inter-calibrated taxonomy, to allow "quantitative" box-core data to be compared across study programs and sites, facilitating a synthesis for macrofaunal baselines in diversity and community structure across the CCZ.

Question 1: Do Abundance, Species/Family Richness and Evenness, and Community Structure, Vary Along and Across the CCZ? What Are the Ecological Drivers of These Variations?

Macrofaunal Abundances

Abundances of sediment-dwelling polychaetes, tanaids, and isopods varied across the CCZ with polychaetes, and to a lesser extent tanaids and isopods, varying with estimated POC flux to the seafloor (**Figure 2** and **Supplementary Figure 2**). It should be noted that macrofaunal data were collected over a broad time range (1977 – 2019), and seafloor POC flux was estimated near the middle of this interval (1997 – 2004) (Lutz et al., 2007). While there is evidence that POC flux can vary seasonally and inter-annually at abyssal locations including in the CCZ (e.g., Dymond and Collier, 1998; Kim D. et al., 2011; Kim H. J. et al., 2011; Smith et al., 2013), regional variation in POC flux across the CCZ is large (>2X) and relatively stable on decadal time scales (Lutz et al., 2002, 2007; Washburn et al., 2021) and appears to be an important driver of macrofaunal abundances in this study. Previous studies have also found strong relationships between deep POC flux integrated over decadal time scales and macrofaunal abundance in abyssal regions (Smith et al., 2008a; Wei et al., 2010; Bonifácio et al., 2020). For example, within the CCZ, polychaete, tanaid, and isopod abundances varied with export productivity across three sites spanning 2500 km (Paterson et al., 1998; Glover et al., 2002; Wilson, 2017). Polychaete and tanaid abundances also varied with POC flux across the JPIO sites spanning 1440 km (Błażewicz et al., 2019b; Bonifácio et al., 2020). Within the GSR contract area, differences in polychaete abundance and diversity have been attributed to differences in POC flux integrated over a decadal time scale (De Smet et al., 2017).

The relationships between sediment macrofaunal abundance and nodule abundance in the CCZ, as well as other environmental variables, was less clear than for POC flux. For some studies, polychaete abundance covaried with regional nodule abundance and depth (**Figure 3**). For tanaids and isopods, only the *JPIO* data revealed a relationship between nodule abundance and faunal abundance, possibly because this study sampled more sites (5) than any other in our synthesis. A previous analysis within the GSR contract area found that polychaete and nodule abundances in box cores were significantly positively correlated across three sites, in which all sites had relatively high mean nodule abundance ($\geq$19 kg/m^2) (De Smet et al., 2017). Across JPIO sites, polychaete abundance was also significantly correlated with nodule abundance in individual box cores, but not with nodule abundance from regional models (Bonifácio et al., 2020). This could be because nodule abundance can be heterogeneous at local scales within JPIO sites, varying from 0 to over 25 kg/m^2 within hundreds of meters. This fine-scale variation in nodule abundance is not captured by the regional model used here. For example, at the JPIO-BGR site, nodule abundance in individual box cores ranged from 0 to 27 kg/m^2 while the regional model predicted an abundance of ∼12 kg/m^2 (Bonifácio et al., 2020). The *JPIO* data set also showed a different relationship between macrofaunal abundances and nodule abundance than other data sets, with abundances peaking at intermediate nodule densities estimated from regional models. If the relationship between nodule abundance and the abundance of sediment-dwelling macrofauna is indeed parabolic, then analyses of samples from sites lacking a broad range of nodule densities could fail to show this relationship.

Many other environmental variables examined changed little across the CCZ, with temperature, salinity, and oxygen concentration varying by 0.1°C, 0.02 psu, and 1.1 ml/l (from 3.2 to 4.2 ml/l), respectively. We found no strong macrofaunal relationships with these variables and we doubt that such small variations are ecologically significant. However, site specific differences, or differences in sampling efficiency across studies, may have masked relationships between macrofauna and environmental variables; when data sets were combined into mixed-effects models, the random variable "study effects" explained the most variance.

We conclude that the most robust data sets assembled here (i.e., *WilsonSmithTan* and *JPIO*) indicate that deep POC flux (as estimated over a decadal time scale with the Lutz model) is a good predictor of polychaete and macrofaunal abundance over regional scales in the CCZ. This result is consistent with expectations of macrofaunal food limitation in this region based on direct measurements of POC flux versus macrofaunal parameters at many different abyssal sites (Smith et al., 2008a), and with the reasonable match of Lutz POC fluxes (within 20%) with results from sediment diagenetic models (Volz et al., 2018). Thus, POC flux is likely a major driver of polychaete, tanaid, and isopod abundances across the CCZ, an important contributor to habitat quality, and an important variable to consider when setting up and evaluating APEIs across the CCZ (as in Wedding et al., 2013; McQuaid et al., 2020).

Macrofaunal Species and Family Richness

Measured species and family richness (number of species or families within a sample) of major taxa also varied across the CCZ. Polychaete species and family richness were not strongly related to any of the environmental variables examined, but study/site effects explained more than 70% of variation

(**Table 2**). This suggests that differences in sampling efficiency among studies, taxonomy, and/or spatio-temporal variations in environmental variables not examined in this study were largely responsible for heterogeneity in polychaete taxonomic richness. In contrast, POC flux and/or depth explained a substantial portion of variation in tanaid species and family richness. The fact that models with either depth or POC flux had similar R^2 values to those with both variables indicates that POC flux is likely the underlying driver for the depth relationships. It is well established that POC flux varies with water column depth in the deep sea (e.g., Lutz et al., 2007), and depth is often used as a proxy for food availability from vertical POC flux (e.g., Rex et al., 2005; McClain et al., 2012). Variations in isopod species richness were poorly explained by environmental and study/site variables, suggesting that other factors may influence isopod diversity (**Table 2**).

Previous studies have also found relationships between POC flux and number of species collected, with some variations across taxa. Wilson (2017) found the number of polychaete and tanaid species collected were highest at one of three sites with highest POC flux, and lowest in the low flux site, but isopod species richness showed the opposite trend. Bonifácio et al. (2020) found a positive relationship between polychaete species richness and POC flux within JPIO sites but no relationship between ES163 or bootstrap diversity and POC flux across the CCZ. Nematode richness was also found to have a positive relationship with POC flux in the CCZ (Lambshead et al., 2003; Pape et al., 2017). Veillette et al. (2007) attributed differences in species richness of nodule communities in part to differences in POC flux, and Woolley et al. (2016) found that POC flux may partially drive ophiuroid diversity on the abyssal seafloor. However, many other abyssal studies have found no clear correlation between various metrics of species diversity and productivity (e.g., Thistle et al., 1985; Wilson and Hessler, 1987; Watts et al., 1992; Paterson et al., 1998; Levin et al., 2001; Glover et al., 2002).

Polychaete and tanaid family richness (taxa per sample) were significantly related to nodule abundance, while species richness was not (**Table 2**). However, there appeared to be different relationships between richness and nodule abundance among studies. For JPIO, which sampled the largest range in nodule abundance, the relationship between nodules and taxonomic richness was parabolic for all taxa sampled, suggesting that the highest number of species and families may be found at intermediate levels of nodule cover. In the GSR data, nodule abundance showed positive correlations with H' and ET_{50} (De Smet et al., 2017).

Macrofaunal Community Structure

Between-site differences within studies appeared to be driven largely by under-sampling of sites with low abundances, due to low number of box cores and low faunal densities (**Figure 8** and **Supplementary Figures 8, 10, 11**). When abundances are low in cores, and species richness and evenness are high, each sample collects a small subset of the community and may appear to be different from all other samples. Family diversity was clearly different among sites (**Figure 10** and **Supplementary Figure 12**), but many of these differences cannot be differentiated from possible differences in sampling efficiency among studies. Because abundances were positively correlated with POC flux, oligotrophic areas require higher sampling effort to provide statistically robust community comparisons. Because we cannot compare communities among individual cores (due to low abundances) or among many studies with cores pooled by site (due to different sampling efficiencies), changes in community structure throughout the CCZ remain very poorly characterized.

Similarity in community structure *within sites* was always highest for polychaete species and generally lower but similar for tanaid and isopod species. This could be due to differences in taxon abundances since polychaetes were always the most abundant taxon (typically 2- to 4-fold more abundant than tanaids and isopods). Differences in site similarity among taxa may also be caused by differences in life-history characteristics among the taxa, because tanaids and isopods are obligate brooders and may have more limited dispersal than polychaetes with planktonic larvae. Although polychaetes as a group have a broad range of life histories, some CCZ species may have planktonic development and disperse over large distances. Thus, higher similarity in polychaete communities within sites in the CCZ may in part be due to differences in dispersal ability (Janssen et al., 2015; Wilson, 2017; Jakiel et al., 2019). It should be noted that analyses at higher taxonomic levels (e.g., Polychaeta, Tanaidacea, and Isopoda) can mask trends occurring at the species level (Wilson, 2017). For instance, scale-worm species of the family Polynoidae showed different patterns of dispersion between APEI 3 and other areas (Bonifácio et al., 2021). Polychaetes and isopods at the species level previously showed different correlations with environmental variables in the CCZ, with polychaete species richness positively correlated with POC flux, but isopod species richness negatively correlated (Wilson, 2017).

For polychaetes, carnivores appeared to be relatively less abundant at sites with lower POC flux (**Supplementary Figure 11**). A similar pattern has been documented previously in the CCZ (Smith et al., 2008b; Bonifácio et al., 2020) and in the oligotrophic gyre in the North Pacific (Hessler and Jumars, 1974). This is consistent with previous observations of fewer trophic levels in food webs from oligotrophic systems (Moore and de Ruiter, 2000; Post, 2002).

Question 2: Do Claim Areas Have Similar Levels of Species/Taxon Richness and Evenness, and Similar Community Structure, to the Proximal APEI(s)?

Very limited data from a single site in APEI 3 suggest lower macrofaunal abundance and diversity compared to contractor license areas 600 – 900 km away in areas with higher POC flux. No other direct macrofaunal comparisons can be made between APEIs and contractor areas because of lack of data. At the same site in APEI 3, Vanreusel et al. (2016) also found reduced megafaunal abundance, and Hauquier et al. (2019) found reduced nematode abundance relative to contract areas in more productive and nodule-rich portions of the CCZ. However, this reduced macrofaunal abundance did not result in lower diversity in the area (Jakiel et al., 2019). For isopods

and mobile scale-worms (Polynoidae), previous studies (Brix et al., 2020; Bonifácio et al., 2021) found similar or higher diversity levels in APEI 3 compared to other contractor areas sampled by *JPIO*, but species composition varied significantly. Reduced abundances of megafauna and nematodes in APEI 3 are consistent with an influence of POC flux and nodule cover on benthic communities, as found in this synthesis. It is worth noting that the APEI system was designed to capture the range of POC fluxes and nodule abundances present in the CCZ as proxies for the different communities likely present throughout the area (Wedding et al., 2013). APEI 3 likely represents an end-member in terms of low POC flux in the CCZ, and may be representative of the relatively oligotrophic northeastern CCZ subregion (Wedding et al., 2013; Washburn et al., 2021). Much more sampling in APEIs is required to adequately assess the representativity of the APEI system for contract areas, including sample collections in all APEIs, collections at multiple locations within APEIs, and adequate sample replication per site.

Question 3: Are Species Ranges (Based on Morphology and/or Barcoding) Generally Large Compared to the Distances Between APEIs and Contractor Areas? What Is the Degree of Species Overlap Between Different Study Locations Across the CCZ?

Some common macrofaunal species (identified with morphology and/or DNA barcoding) ranged over 600 – 900 km, and a few ranged over 1500 – 3000 km (**Supplementary Figure 14**). However, some species common at single sites were collected over ranges of $\leq$ 200 km. For described species and *JPIO* data, less than 20% of species were found at more than one site (**Figure 13** and **Supplementary Figure 14**), but the vast majority of identified macrofaunal species were represented by singletons and doubletons (**Figure 5**) hindering the examination of species ranges. Previous work examining species ranges in the CCZ have shown mixed results. In the GSR site, 26% of polychaete species and 11% of isopod species were shared among three sample sites 10 – 100's of km apart (De Smet et al., 2017). Some isopods species, capable of swimming were distributed over 5000 km, but a large proportion of species (40.5%) were singletons (Brix et al., 2020). At a very oligotrophic site northeast of the CCZ, nearly two-thirds of macrofaunal species were represented by singletons (Hessler and Jumars, 1974). More recent studies found CCZ macrofaunal communities were dominated by rare species, with 50% or more of all species represented by singletons (Błażewicz et al., 2019b; Janssen et al., 2019; Bonifácio et al., 2020; Bonifácio et al., 2021). In the CCZ and surrounding abyssal Pacific, some (but not all) locally common species appear to be widespread biogeographically over scales of 3000 km. However, there was also a long list of rare species, and some locally common species, found over restricted ranges ($<$ 200 km) due to either incomplete sampling or high species turnover (Glover et al., 2002). Previous studies have used beta diversity metrics to estimate macrofaunal species ranges in the CCZ of 25 – 180 km for polychaetes (Wilson, 2017; Bonifácio et al., 2020), 84 km for isopods (Wilson, 2017), and 1245 km for tanaids (Jakiel et al., 2019). Similarly, narrow geographical ranges were found in the NW Pacific (Jakiel et al., 2020; Kakui et al., 2020).

Two described polychaete species were found in high abundances in multiple data sets. *Aurospio cf. dibranchiata* and *Bathyglycinde cf. profunda* were both found in six contractor areas and two APEIs, suggesting they are likely part of a group of abundant, widely distributed polychaetes (Glover et al., 2002). Both species are reported to be widespread or cosmopolitan (Maciolek, 1981; Paterson et al., 2016). However, some of these widespread species may represent cryptic species or species complexes. Molecular techniques and more careful morphological taxonomy have revealed that many species considered to have wide ranges have been misidentified or were cryptic species (Sun et al., 2016; Alvarez-Campos et al., 2017; Glover et al., 2018; Hutchings and Kupriyanova, 2018; Nygren et al., 2018). DNA barcoding of 16s and 18s rRNA indicates that *A. dibranchiata* may indeed be pan-oceanic, but many individuals identified morphologically as *A. dibranchiata* also comprise several species (Guggolz et al., 2020). Abundant polychaete species may be useful to target in monitoring studies since their absence is less likely to be due to under-sampling than other taxa. However, until their ecology is better understood, it is not clear whether they are sensitive or insensitive to mining disturbance. Widely distributed species may also be more likely to be ecological generalists and particularly good dispersers, and thus both less sensitive to mining stress and more rapid recolonizers than the many rare species constituting the bulk of abyssal communities. It is also important to note that, in better known ecosystems than the CCZ, rarity is often correlated with small species ranges (Pimm et al., 2014). Thus, we cannot assume that the numerous rare species in the CCZ are widely distributed, and simply under-sampled.

Question 4: What Scientific Gaps Hinder Biodiversity and Biogeographic Syntheses for the Macrofauna Across the CCZ?

Under-sampling

Although quantitative box-core samples for macrofauna have been collected at widespread sites in the North Pacific, there are huge, unsampled gaps within the CCZ, particularly in the central and western portions (**Figure 1**). Thus, for over $>$50% of the management area, sediment macrofaunal biodiversity patterns remain poorly studied or unevaluated. There has been no quantitative macrofaunal sampling in the core of eight APEIs and extremely limited sampling in the ninth (APEI 3), making direct evaluation of the representativeness of the APEI network for sediment macrofauna currently impossible. Macrofaunal species accumulation curves are rising rapidly at all sampled sites, even where large numbers of box cores ($>$50) have been collected, indicating that species diversity at every site studied remains under-sampled. This results in very limited understanding of macrofaunal diversity at any site, and of species distributions across the CCZ.

Sample collection/processing differences

Based on differing relationships between POC flux and macrofaunal abundance in box cores, sampling efficiencies likely varied across data sets and sampling programs in the CCZ (**Figure 2**). In addition, the random variable in the mixed effects models (which incorporated study) for polychaete and isopod abundance and taxonomic richness explained much more variation among communities than all environmental variables combined (**Table 2**). These potential variations in sampling efficiencies, plus differences between sampling programs in the identification of working species, makes quantitative comparisons of macrofaunal biodiversity across research programs, as well as the delineations of species ranges and community types, problematic.

While the linear mixed-effects models for tanaid abundance and diversity had similar R^2 values to polychaetes and isopods, much more of the variability in tanaids was explained by the environmental fixed effects suggesting that tanaid communities may be less susceptible to biases from box-core sampling and processing. Tanaids (Tanaidomorpha) are often tube-dwelling (Hassack and Holdich, 1987) and thus may be resistant to bow-wave effects from the box corer, and their robust exoskeleton and compact body habitus supported with short legs may make them less susceptible to damage during sieving.

Future Directions

Much more extensive macrofaunal sampling in the western and central CCZ, as well as in all APEIs, is required to elucidate patterns of biodiversity, community structure, and species ranges throughout the CCZ. Direct measurements of environmental variables at multiple sampling locations (e.g., POC flux from sediment traps, nodule cover within box cores, slope calculations from high resolution multibeam sonar) will help explore local-scale heterogeneity and identify ecosystem drivers at local and regional spatial scales. Time-series measurements of seafloor macrofaunal parameters, and key ecosystem drivers including POC flux, are also required to provide baselines of temporal variability across the CCZ.

The adoption of standard sampling methods (e.g., box-core design, lowering speed, use of side A-frames, sieving procedures, etc.), and ensuring their use, is important to standardize sampling efficiencies across programs. This synthesis shows that current practices make it difficult to compare biodiversity across the entire CCZ.

The many hundreds of macrofaunal species collected from the CCZ are mostly undescribed, there has been little intercalibration of morphological taxonomy, and DNA barcoding of macrofauna has been very limited. Most taxonomic effort to date has focused on polychaetes, tanaids, and isopods, yet much more work is needed for these groups as the vast majority of species remain undescribed. In addition, a full understanding of macrobenthos in the CCZ requires morphological descriptions and barcoding of species in additional taxonomic groups (e.g., mollusks, sipunculans, nemerteans, etc.). Morphological descriptions or intercalibrations of working species, combined with molecular barcoding, are desperately needed to elucidate species ranges and to compare species composition among sampling programs (Smith et al., 2020).

CONCLUSIONS

(1) Macrofaunal abundance and species diversity vary substantially across the CCZ, very likely in response to variations in POC flux and nodule abundance. POC flux and nodule abundance are thus important parameters to include in abyssal habitat mapping, and in designing and evaluating APEIs and other protected areas (e.g., Preservation Reference Zones) across the CCZ (as in Wedding et al., 2013).

(2) Nonetheless, macrofaunal biodiversity patterns remain poorly studied or unevaluated for much of the central and western CCZ, and in all APEIs.

(3) Sampling efficiencies likely vary across data sets and sampling programs in the CCZ. Varying sampling efficiencies, plus differences between programs in the identification of working species and limited barcoding, hinder quantitative comparisons of macrofaunal biodiversity patterns across the CCZ. Standardization of sampling equipment and protocols is urgently needed.

(4) Macrofaunal species accumulation curves are rising rapidly at all studied sites, indicating that species diversity remains under-sampled, even at the most intensely sampled sites (>50 box cores). Use of molecular techniques are likely to reveal even more undetected macrofaunal diversity in the form of morphologically cryptic species.

(5) Very limited data suggest lower abundance and diversity in APEI 3 compared to contractor areas 600 – 900 km away. No other direct comparisons can be made between APEIs and contractor areas.

(6) Some (but not all) common macrofaunal species range over 1000 – 3000 km. Some locally common species have been collected only over small distances (<200 km) and thus may have small ranges. However, the vast majority of identified macrofaunal species are rare and collected, thus far, only at single sites.

(7) Because rarity is often correlated with small species ranges in better known ecosystems (Pimm et al., 2014), we cannot assume that the numerous rare species in the CCZ are widely distributed, and simply under-sampled.

DATA AVAILABILITY STATEMENT

Publicly available datasets were analyzed in this study. This data can be found here: https://data.isa.org.jm/isa/map/.

AUTHOR CONTRIBUTIONS

CS conceived the project. TW and CS wrote the first draft of the manuscript. TW, LM, PB, EP, and CS performed the analyses. TW, LM, PB, EP, MB, GB-C, TD, TF, AG, SJ, SK,

OY, and CS provided the data, contributed the ideas for the synthesis, and reviewed and provided the comments for the manuscript. All the authors contributed to the article and approved the submitted version.

FUNDING

Funding to perform analyses for and to write this manuscript was provided by grants from the Pew Charitable Trusts (no. 32871) and the Gordon and Betty Moore Foundation (no. 5596) to CS.

ACKNOWLEDGMENTS

The authors thank individuals and institutions that collected and/or provided data for this synthesis. The *NUS* data set was provided by Koh Siang Tan and Cheah Hoay Chuar at the National University of Singapore. The *ABYSSLINE* data set was provided by CS, and funding for the Abyssline Project was provided by UKSRL. The *Smith* data set was provided by CS and was collected during the NSF US JGOFS Program, with funding from NSF Grant OCE-90-22116 to CS. The *Wilson* data set was obtained from the supplementary data of Wilson (2017). The JPIO data set received funding from the Ifremer program Ressources Minérales Marines (REMIMA), the National Science Centre grant: 2016/21/B/NZ8/02495, the JPI Oceans pilot action "Ecological aspects of deep-sea mining", the Narodowa Agencja Wymiany Akademickiej (NAWA, Poland) under the Ulam Program, and the European Union Seventh Framework Program (FP7/2007–2013) under the MIDAS project, grant agreement no. 603418. The Ghent data set, owned and provided by contractor Global Sea Mineral Resources N.V. (GSR), was collected in the frame of two environmental baseline surveys in the GSR license area and is supported by a service arrangement between GSR and Ghent University. The *KODOS* data set had been collected through environmental baseline studies for the polymetallic manganese nodules exploration contract of Republic of Korea (Ministry of Ocean and Fisheries R&D #: 20160099). The *Yuzhmor* data set was provided by Slava Melnik at JSC Yuzhmorgeologiya of the Russian Federation. See **Supplementary Data** for detailed acknowledgments. Much of the initial results for this manuscript have been released as a report through the ISA (https://ran-s3.s3.amazonaws.com/isa.org.jm/s3fs-public/files/documents/deep_ccz_biodiversity_synthesis_workshop_report_-_final.pdf) (Smith et al., 2019). This contribution is no. 11293, from SOEST, University of Hawai'i.

SUPPLEMENTARY MATERIAL

The Supplementary Material for this article can be found online at: https://www.frontiersin.org/articles/10.3389/fmars.2021.626571/full#supplementary-material

REFERENCES

Alvarez-Campos, P., Giribetfls, G., San Martin, G., Rouse, G. W., and Riesgo, A. (2017). Straightening the striped chaos: systematics and evolution of *Trypanosyllis* and the case of its pseudocryptic type species *Trypanosyllis krohnii* (Annelida, Syllidae). *Zool. J. Linnean Soc.* 179, 492–540. doi: 10.1111/zoj.12443

Barton, K. (2020). *Package 'MuMIn'*.

Bates, D., Maechler, M., Bolker, B., and Walker, S. (2015). *Package 'lme4'*.

Błażewicz, M., Jóźwiak, P., Jennings, R. M., Studzian, M., and Frutos, I. (2019a). Integrative systematics and ecology of a new deep-sea family of tanaidacean crustaceans. *Sci. Rep.* 9:18720. doi: 10.1038/s41598-019-53446-1

Błażewicz, M., Jóźwiak, P., Menot, L., and Pabis, K. (2019b). High species richness and unique composition of the tanaidacean communities associated with five areas in the Pacific polymetallic nodule fields. *Prog. Oceanogr.* 176:102141. doi: 10.1016/j.pocean.2019.102141

Boggemann, M. (2016). Glyceriformia (Annelida) of the abyssal SW Atlantic and additional material from the SE Atlantic. *Mar. Biodiver.* 46, 227–241. doi: 10.1007/s12526-015-0354-4

Bonifácio, P., Martinez-Arbizu, P., and Menot, L. (2020). Alpha and beta diversity patterns of polychaete assemblages across the nodule province of the Clarion-Clipperton Fracture Zone (Equatorial Pacific). *Biogeosciences* 14, 865–886. doi: 10.5194/bg-17-865-2020

Bonifácio, P., Neal, L., and Menot, L. (2021). Diversity of deep sea scale-worms (Polynoidae) in the Clarion-Clipperton Fracture Zone (equatorial Pacific). *Front. Mar. Sci.* doi: 10.3389/fmars.2021.626571

Borowski, C., and Thiel, H. (1998). Deep-sea macrofaunal impacts of a large-scale physical disturbance experiment in the Southeast Pacific. *Deep Sea Res. Part II Top. Stud. Oceanogr.* 45, 55–81. doi: 10.1016/s0967-0645(97)00073-8

Brix, S., Osborn, K. J., Kaiser, S., Truskey, S. B., Schnurr, S. M., Brenke, N., et al. (2020). Adult life strategy affects distribution patterns in abyssal isopods - implications for conservation in Pacific nodule areas. *Biogeosciences* 17, 6163–6184. doi: 10.5194/bg-17-6163-2020

Chuar, C. H., Tong, S. J. W., Chim, C. K., Wong, H. P. S., and Tan, K. S. (2020). Abyssal macrofaunal community structure in the polymetallic nodule exploration area at the easternmost region of the Clarion-Clipperton Fracture Zone, Pacific Ocean. *Deep Sea Res. Part I Oceanogr. Res. Pap.* 161, 103284. doi: 10.1016/j.dsr.2020.103284

Clarke, K. R., and Gorley, R. N. (2015). *PRIMER v7: User Manual/Tutorial*. Plymouth: PRIMER-E Ltd.

Colwell, R. K. (2013). *EstimateS 9.1.0 User's Guide*. Storr, CT: University of Connecticut.

Conway, J. R., Lex, A., and Gehlenborg, N. (2017). UpSetR: an R package for the visualization of intersecting sets and their properties. *Bioinformatics* 33, 2938–2940. doi: 10.1093/bioinformatics/btx364

De Smet, B., Pape, E., Riehl, T., Bonifácio, P., Colson, L., and Vanreusel, A. (2017). The community structure of deep-sea macrofauna associated with polymetallic nodules in the eastern part of the Clarion-Clipperton Fracture Zone. *Front. Mar. Sci.* 4:103. doi: 10.3389/fmars.2017.00103

Dinet, A., Desbruyeres, D., and Khripounolf, A. (1985). "Abondance des peuplements macro- et meiobenthiques dans la zone abyssale BIOGAS: repartition et strategie d'echantillonnage," in *Peup1ements Profonds du Golfe de Gascogne - Campagnes*, eds L. Biogas and L. C. Monniot (Brest: IFREMER), 121–142.

Drazen, J. C., Smith, C. R., Gjerde, K. M., Haddock, S. H. D., Carter, G. S., Choy, C. A., et al. (2020). Opinion: midwater ecosystems must be considered when evaluating environmental risks of deep-sea mining. *Proc. Natl. Acad. Sci. U.S.A.* 117, 17455–17460. doi: 10.1073/pnas.2011914117

Dymond, J., and Collier, R. (1998). *College of Oceanography*, Vol. 2. Corvallis: Oregon State University, 129–137.

Fox, J., Weisberg, S., and Price, B. (2020). *Package 'Car'*.

Glover, A. G., Dahlgren, T. G., Wiklund, H., Mohrbeck, I., and Smith, C. R. (2016). An end-to-end DNA taxonomy methodology for benthic biodiversity survey in the Clarion-Clipperton Zone, central Pacific abyss. *Journal of Marine Science and Engineering* 4:2. doi: 10.3390/jmse4010002

Glover, A. G., Smith, C. R., Paterson, G. L. J., Wilson, G. D. F., Hawkins, L., and Sheader, M. (2002). Polychaete species diversity in the central Pacific abyss: local and regional patterns, and relationships with productivity. *Mar. Ecol. Prog. Ser.* 240, 157–170.

Glover, A. G., Wiklund, H., Chen, C., and Dahlgren, T. G. (2018). Managing a sustainable deep-sea "blue economy" requires knowledge of what actually lives there. *eLife* 7:e41319.

Guggolz, T., Meißner, K., Schwentner, M., Dahlgren, T. G., Wiklund, H., Bonifácio, P., et al. (2020). High diversity and pan-oceanic distribution of deep-sea polychaetes: *Prionospio* and *Aurospio* (Annelida: Spionidae) in the Atlantic and Pacific Ocean. *Organ. Divers. Evol. Organ. Divers. Evol.* 20, 171–187. doi: 10.1007/s13127-020-00430-7

Hassack, E., and Holdich, D. M. (1987). The tubicolous habit amongst the Tanaidacea (Crustacea, Peracarida) with particular reference to deep-sea species. *Zool. Scripta* 16, 223–233. doi: 10.1111/j.1463-6409.1987.tb00069.x

Hauquier, F., Macheriotou, L., Bezerra, T. N., Egho, G., Martinez Arbizu, P., and Vanreusel, A. (2019). Distribution of free-living marine nematodes in the Clarion-Clipperton Zone: implications for future deep-sea mining scenarios. *Biogeosciences* 16, 3475–3489. doi: 10.5194/bg-16-3475-2019

Hein, J. R., Mizell, K., Koschinsky, A., and Conrad, T. A. (2013). Deep-ocean mineral deposits as a source of critical metals for high- and green-technology applications: comparison with land-based resources. *Ore Geol. Rev.* 51, 1–14. doi: 10.1016/j.oregeorev.2012.12.001

Hessler, R. R., and Jumars, P. A. (1974). Abyssal community analysis from replicate box cores in the central North Pacific. *Deep Sea Res. Oceanogr. Abstracts* 21:246.

Hutchings, P., and Kupriyanova, E. (2018). Cosmopolitan polychaetes - fact or fiction? Personal and historical perspectives. *Inverteb. Syst.* 32, 1–9. doi: 10.1071/is17035

ISA (2010). *A Geological Model of Polymetallic Nodule Deposits in the Clarion Clipperton Fracture Zone*. ISA Technical Study: NO. 6. Kingston: ISA.

ISA (2018). *Report of the Secretary-General on the Status of National Legislation Relating to Deep Seabed Mining and Related Matters, Including a Comparative Study of Existing National Legislation.* Agenda Item: NO. 8. Kingston: ISA.

Jakiel, A., Palero, F., and Błażewicz, M. (2019). Deep ocean seascape and Pseudotanaidae (Crustacea: Tanaidacea) diversity at the Clarion-Clipperton Fracture Zone. *Sci. Rep.* 9:17305. doi: 10.1038/s41598-019-51434-z

Jakiel, A., Palero, F., and Błażewicz, M. (2020). Secrets from the deep: Pseudotanaidae (Crustacea: Tanaidacea) diversity from the Kuril-Kamchatka Trench. *Prog. Oceanogr.* 183:102288. doi: 10.1016/j.pocean.2020.102288

Janssen, A., Kaiser, S., Meissner, K., Brenke, N., Menot, L., and Arbizu, P. M. (2015). A reverse taxonomic approach to assess macrofaunal distribution patterns in abyssal Pacific polymetallic nodule fields. *PLoS One* 10:e0117790. doi: 10.1371/journal.pone.0117790

Janssen, A., Stuckas, H., Vink, A., and Arbizu, P. M. (2019). Biogeography and population structure of predominant macrofaunal taxa (Annelida and Isopoda) in abyssal polymetallic nodule fields: implications for conservation and management. *Mar. Biodiver.* 49, 2641–2658. doi: 10.1007/s12526-019-00997-1

Jones, D. O. B., Kaiser, S., Sweetman, A. K., Smith, C. R., Menot, L., Vink, A., et al. (2017). Biological responses to disturbance from simulated deep-sea polymetallic nodule mining. *PLoS One* 12:e0171750. doi: 10.1371/journal.pone.0171750

Jóźwiak, P., Pabis, K., Brandt, A., and Błażewicz, M. (2020). Epibenthic sled versus giant box corer - Comparison of sampling gears for tanaidacean species richness assessment in the abyssal benthic ecosystem. *Prog. Oceanogr.* 181:102255. doi: 10.1016/j.pocean.2019.102255

Kakui, K., Nomaki, H., and Komatsu, H. (2020). Unexpected low genetic differentiation between Japan and Bering Sea populations of a deep-sea benthic crustacean lacking a planktonic larval stage (Peracarida: Tanaidacea). *Biol. J. Linnean Soc.* 2020:blaa106.

Kim, D., Choi, M. S., Oh, H. Y., Song, Y. H., Noh, J. H., and Kim, K. H. (2011). Seasonal export fluxes of particulate organic carbon from $^{234}Th/^{238}U$ disequilibrium measurements in the Ulleung Basin[1] (Tsushima Basin) of the East Sea[1] (Sea of Japan). *J. Oceanogr.* 67, 577–588. doi: 10.1007/s10872-011-0058-8

Kim, H. J., Kim, D., Yoo, C. M., Chi, S.-B., Khim, B. K., Shin, H.-R., et al. (2011). Influence of ENSO variability on sinking-particle fluxes in the northeastern equatorial Pacific. *Deep Sea Res. I* 58, 865–874. doi: 10.1016/j.dsr.2011.06.007

Lambshead, P. J. D., Brown, C. J., Ferrero, T. J., Hawkins, L. E., Smith, C. R., and Mitchel, N. J. (2003). Biodiversity of nematode assemblages from the region of the Clarion-Clipperton Fracture Zone, an area of commercial mining interest. *BMC Ecol.* 3:1. doi: 10.1186/1472-6785-3-1

Legendre, P. (2018). *Package 'lmodel2.' Montreal*.

Levin, L. A., Etter, R. J., Rex, M. A., Gooday, A. J., Smith, C. R., Pineda, J., et al. (2001). Environmental influences on regional deep-sea species diversity. *Ann. Rev. Ecol. Syst.* 32, 51–93. doi: 10.1146/annurev.ecolsys.32.081501.114002

Lutz, M., Dunbar, R., and Caldeira, K. (2002). Regional variability in the vertical flux of particulate organic carbon in the ocean interior. *Glob. Biogeochem. Cycles* 16, 11–18. doi: 10.1029/2000gb001383

Lutz, M. J., Caldeira, K., Dunbar, R. B., and Behrenfeld, M. J. (2007). Seasonal rhythms of net primary production and particulate organic carbon flux to depth describe the efficiency of biological pump in the global ocean. *J. Geophys. Res. Oceans* 112:JC003706.

Maciolek, N. J. (1981). A new genus and species of Spionidae (Annelida: Polychaeta) from the North and South Atlantic. *Proc. Biol. Soc. Washington* 94, 228–239.

Magurran, A. E. (2004). *Measuring Biological Diversity*. Oxford: Blackwell.

Martinez Arbizu, P., and Haeckel, M. (eds) (2015). *RV SONNE Fahrtbericht / Cruise Report SO239: EcoResponse Assessing the Ecology, Connectivity and Resilience of Polymetallic Nodule Field Systems, Balboa (Panama) - Manzanillo (Mexico) 11.03.-30.30.04.2015*. GEOMAR Report, N. Ser. 025. Kiel: GEOMAR Helmholtz-Zentrum für Ozeanforschung, 204.

McClain, C. R., Allen, A. P., Tittensor, D. P., and Rex, M. A. (2012). Energetics of life on the deep seafloor. *Proc. Natl. Acad. Sci. U.S.A.* 109, 15366–15371. doi: 10.1073/pnas.1208976109

McQuaid, D. A., Attrill, M. J., Clark, M. R., Cobley, A., Glover, A. G., Smith, C. R., et al. (2020). Using habitat classification to assess representativity of a protected area network in a large, data-poor area targeted for deep-sea mining. *Front. Mar. Sci.* 7:1066. doi: 10.3389/fmars.2020.558860

Mincks, S. L., Dyal, P. L., Paterson, G. L. J., Smith, C. R., and Glover, A. G. (2009). A new species of *Aurospio* (Polychaeta, Spionidae) from the Antarctic shelf, with analysis of its ecology, reproductive biology and evolutionary history. *Mar. Ecol.* 30, 181–197. doi: 10.1111/j.1439-0485.2008.00265.x

Montgomery, D. C., and Peck, E. A. (1992). *Introduction to Linear Regression Analysis*. New York, NY: Wiley.

Moore, J. C., and de Ruiter, P. C. (2000). "Invertebrates as webmasters in ecosystems," in *Invertebrates in Detrital Food Webs Along Gradients of Productivity*, eds D. C. Colman and P. F. Hendrix (Wallingford: CABI Publishing), 161–184.

Morgan, C. (2012). *A Geological Model of Polymetallic Nodule Deposits in the Clarion-Clipperton Fracture Zone - Briefing Paper 1/12*. ISA Briefing Paper. Honolulu: Planning Solutions Inc.

Nygren, A., Parapar, J., Pons, J., Meißner, K., Bakken, T., Kongsrud, J. A., et al. (2018). A mega-cryptic species complex hidden among one of the most common annelids in the north east Atlantic. *PLoS One* 13:e0198356. doi: 10.1371/journal.pone.0198356

Pape, E., Bezerra, T. N., Hauquier, F., and Vanreusel, A. (2017). Limited spatial and temporal variability in meiofauna and nematode communities at distance but environmentally similar sites in an area of interest for deep-sea mining. *Front. Mar. Sci.* 4:205. doi: 10.3389/fmars.2017.00205

Pasotti, F., Mevenkamp, L., Pape, E., Błażewicz, M., Bonifácio, P., Riehl, T., et al. (2021). A local scale analysis of manganese nodules influence on the Clarion-Clipperton Fracture Zone macrobenthos. *Deep Sea Res. Part I Oceanogr. Res. Pap.* 168:103449. doi: 10.1016/j.dsr.2020.103449

Paterson, G. L. J., Neal, L., Altamira, I., Soto, E. H., Smith, C. R., Menot, L., et al. (2016). New *Prionospio* and *Aurospio* species from the deep sea (Annelida: Polychaeta). *Zootaxa* 4092, 1–32. doi: 10.11646/zootaxa.4092.1.1

Paterson, G. L. J., Wilson, G. D. F., Cosson, N., and Lamont, P. A. (1998). Hessler and Jumars (1974) revisited: abyssal polychaete assemblages from the Atlantic and Pacific. *Deep Sea Res. Part II Top. Stud. Oceanogr.* 45, 225–251. doi: 10.1016/s0967-0645(97)00084-2

Pimm, S. L., Jenkins, C. N., Abell, R., Brooks, T. M., Gittleman, J. L., Joppa, L. N., et al. (2014). The biodiversity of species and their rates of extinction, distribution, and protection. *Science* 344:1246752. doi: 10.1126/science.1246752

Post, D. M. (2002). The long and short of food-chain length. *Trends Ecol. Evolut.* 17, 269–277. doi: 10.1016/s0169-5347(02)02455-2

Rex, M. A., McClain, C. R., Johnson, N. A., Etter, R. J., Allen, J. A., Bouchet, P., et al. (2005). A source-sink hypothesis for abyssal biodiversity. *Am. Naturalist* 165, 163–178. doi: 10.2307/3473143

Smith, C. R., De Leo, F. C., Bernardino, A. F., Sweetman, A. K., and Arbizu, P. M. (2008a). Abyssal food limitation, ecosystem structure and climate change. *Trends Ecol. Evol.* 23, 518–528. doi: 10.1016/j.tree.2008.05.002

Smith, C. R., Galeron, J., Gooday, A., Glover, A., Kitazato, H., Menot, L., et al. (2008b). Biodiversity, species ranges, and gene flow in the abyssal Pacific nodule province: predicting and managing the impacts of deep seabed mining. *Intern. Seabed Author. Techn.* 3:38.

Smith, C. R., Levin, L. A., Koslow, A., Tyler, P. A., and Glover, A. G. (2008c). "The near future of the deep seafloor ecosystems," in *Aquatic Ecosystems: Trends and Global Prospects*, ed. N. V. C. Polunin (Cambridge: Cambridge University Press), 334–351. doi: 10.1017/cbo9780511751790.030

Smith, C. R., and Demopoulos, A. W. J. (2003). The deep Pacific Ocean floor. *Ecosyst. World Ecosyst. Deep Oceans* 28, 179–218.

Smith, C. R., Tunnicliffe, V., Colaco, A., Drazen, J. C., Gollner, S., Levin, L. A., et al. (2020). Deep-sea misconceptions cause underestimation of seabed-mining impacts. *Trends Ecol. Evolut.* 35, 853–587.

Smith, C. R., Washburn, T., Menot, L., Bonifacio, P., Pape, E., Ju, S. J., et al. (2019). "Deep-sea biodiversity synthesis workshop - Macrofaunal report," in *Proceedings of the Deep CCZ Biodiversity Synthesis Workshop* (Friday Harbor, WA: University of Hawaii at Manoa & International Seabed Authority).

Smith, K. L., Ruhl, H. A., Kahru, M., Huffard, C. L., and Sherman, A. D. (2013). Deep ocean communities impacted by changing climate over 24 y in the abyssal northeast Pacific Ocean. *Proc. Natl. Acad. Sci. U.S.A.* 110, 19838–19841.

Snelgrove, P. V. R., Soetaert, K., Solan, M., Thrush, S., Wei, C.-L., Danovaro, R., et al. (2018). Global carbon cycling on a heterogeneous seafloor. *Trends Ecol. Evol.* 33, 96–105. doi: 10.1016/j.tree.2017.11.004

Stratmann, T., Lins, L., Purser, A., Marcon, Y., Rodrigues, C. F., Ravara, A., et al. (2018a). Abyssal plain faunal carbon flows remain depressed 26 years after a simulated deep-sea mining disturbance. *Biogeosciences* 15, 4131–4145. doi: 10.5194/bg-15-4131-2018

Stratmann, T., Mevenkamp, L., Sweetman, A. K., Vanreusel, A., and van Oevelen, D. (2018b). Has phytodetritus processing by an abyssal soft-sediment community recovered 26 years after an experimental disturbance. *Front. Mar. Sci.* 5:59. doi: 10.3389/fmars.2018.00059

Sun, Y., Wong, E., Tovar-Hernández, M. A., Williamson, J. E., and Kupriyanova, E. K. (2016). Is *Hydroides brachyacantha* (Serpulidae:Annelida) a widespread species? *Inverteb. Syst.* 30, 41–59. doi: 10.1071/is15015

Sweetman, A. K., Thurber, A. R., Smith, C. R., Levin, L. A., Mora, C., Wei, C.-L., et al. (2017). Major impacts of climate change on deep-sea benthic ecosystems. *Elem. Sci. Anth.* 5:4.

Thistle, D., Yingst, J. Y., and Fauchald, K. (1985). A deep-sea benthic community exposed to strong near-bottom currents on the Scotian Rise (western Atlantic). *Mar. Geol.* 66, 91–112. doi: 10.1016/0025-3227(85)90024-6

Ugland, K. I., Gray, J. S., and Ellingsen, K. E. (2003). The species-accumulation curve and estimation of species richness. *J. Anim. Ecol.* 72, 888–897. doi: 10.1046/j.1365-2656.2003.00748.x

Vanreusel, A., Hilario, A., Ribeiro, P. A., Menot, L., and Arbizu, P. M. (2016). Threatened by mining, polymetallic nodules are required to preserve abyssal epifauna. *Sci. Rep.* 6:26808.

Veillette, J., Sarrazin, J., Gooday, A. J., Galéron, J., Caprais, J. C., Vangriesheim, A., et al. (2007). Ferromanganese nodule fauna in the Tropical North Pacific Ocean: species richness, faunal cover and spatial distribution. *Deep Sea Res. Part I Oceanogr. Res. Pap.* 54, 1912–1935. doi: 10.1016/j.dsr.2007.06.011

Venables, W. N., Smith, D. M., and The R Core Team (2019). An Introduction to R Notes on R: A Programming Environment for Data Analysis and Graphics Version 2.15.2 (2012-10-26). N. Venables & D. M. Smith & R.G. Ihaka Adelaide. Available online at: https://cran.r-project.org/doc/manuals/r-release/R-intro.pdf (accessed June, 2019).

Volz, J. B., Mogollón, J. M., Geibert, W., Arbizu, P. M., Koschinsky, A., and Kasten, S. (2018). Natural spatial variability of depositional conditions, biogeochemical processes and element fluxes in sediments of the eastern Clarion-Clipperton Zone, Pacific Ocean. *Deep Sea Res. Part I Oceanogr. Res. Pap.* 140, 159–172. doi: 10.1016/j.dsr.2018.08.006

Vonnahme, T. R., Molari, M., Janssen, F., Wenzhofer, F., Haeckel, M., Titschack, J., et al. (2020). Effects of a deep-sea mining experiment on seafloor microbial communities and functions after 26 years. *Sci. Adv.* 6:eaaz5922. doi: 10.1126/sciadv.aaz5922

Washburn, T. W., Jones, D. O. B., Wei, C.-L., and Smith, C. R. (2021). Environmental heterogeneity throughout the Clarion-Clipperton Zone and the representativity of the APEI network. *Front. Mar. Sci.*

Washburn, T. W., Turner, P. J., Durden, J. M., Jones, D. O. B., Weaver, P., and Van Dover, C. L. (2019). Ecological risk assessment for deep-sea mining. *Ocean Coast. Manag.* 176, 24–39. doi: 10.1016/j.ocecoaman.2019.04.014

Watts, M. C., Etter, R. J., and Rex, M. A. (1992). "Effect of spatial and temporal scale on the relationship of surface pigment biomass to community structure in the deep-sea benthos," in *Deep-Sea Food Chains and the Global Cycle*, eds G. T. Rowe and V. Pariente (New York, NY: Kluwer Academic Publishing).

Wedding, L. M., Friedlander, A. M., Kittinger, J. N., Watling, L., Gaines, S. D., Bennett, M., et al. (2013). From principles to practice: a spatial approach to systematic conservation planning in the deep sea. *Proc. R. Soc. B Biol. Sci.* 280:20131684. doi: 10.1098/rspb.2013.1684

Wei, C.-L., Rowe, G. T., Escobar-Briones, E., Boetius, A., Soltwedel, T., Caley, M. J., et al. (2010). Global patterns and predictions of seafloor biomas using random forests. *PLoS One* 5:e15323. doi: 10.1371/journal.pone.0015323

Wilson, G. D. F. (2017). Macrofauna abundance, species diversity and turnover at three sites in the Clipperton-Clarion Fracture Zone. *Mar. Biodiver. Mar. Biodivers.* 47, 323–347. doi: 10.1007/s12526-016-0609-8

Wilson, G. D. F., and Hessler, R. R. (1987). "The effects of manganese nodule test mining on the benthic fauna in the North Equatorial Pacific," in *Environmental Effects of Deep-Sea Dredging. Scripps Institution of Oceanography Reference Series*, eds F. N. Speiss, R. R. Hessler, G. D. F. Wilson, and M. Weydert (California: University of California).

Woolley, S. N. C., Tittensor, D. P., Dunstan, P. K., Guillera-Arroita, G., Lahoz-Monfort, J. J., Wintle, B. A., et al. (2016). Deep-sea diversity patterns are shaped by energy availability. *Nature* 533, 393–396. doi: 10.1038/nature17937

Zuur, A., Ieno, E. N., Walker, N., Saveliev, A. A., and Smith, S. M. (2009). *Mixed Effects Models and Extensions in Ecology in R*. New York, NY: Springer.

Conflict of Interest: The authors declare that the research was conducted in the absence of any commercial or financial relationships that could be construed as a potential conflict of interest.

Copyright © 2021 Washburn, Menot, Bonifácio, Pape, Błażewicz, Bribiesca-Contreras, Dahlgren, Fukushima, Glover, Ju, Kaiser, Yu and Smith. This is an open-access article distributed under the terms of the Creative Commons Attribution License (CC BY). The use, distribution or reproduction in other forums is permitted, provided the original author(s) and the copyright owner(s) are credited and that the original publication in this journal is cited, in accordance with accepted academic practice. No use, distribution or reproduction is permitted which does not comply with these terms.

frontiers in Marine Science

ORIGINAL RESEARCH
published: 10 May 2021
doi: 10.3389/fmars.2021.632764

Mesopelagic Scattering Layer Behaviors Across the Clarion-Clipperton Zone: Implications for Deep-Sea Mining

Jessica N. Perelman[1], Eric Firing[1], Jesse M. A. van der Grient[1], Benjamin A. Jones[2] and Jeffrey C. Drazen[1]*

[1] Department of Oceanography, University of Hawai'i at Mānoa, Honolulu, HI, United States, [2] Applied Research Laboratory, University of Hawai'i, Honolulu, HI, United States

The Clarion-Clipperton Zone (CCZ) is a 4 million km^2 area in the eastern Central Pacific Ocean exhibiting large variability in environmental parameters, particularly oxygen and primary production, that is being targeted for deep-sea polymetallic nodule mining. This remote region's pelagic biology is very poorly sampled, including for micronekton and zooplankton that provide essential ecosystem services such as carbon flux and support for commercial fisheries. We built a baseline of deep scattering layer (DSL) depths and vertical migration behaviors, proxies for mesopelagic micronekton and zooplankton communities, using shipboard acoustic Doppler current profiler datasets. Acoustic data (38 kHz, 75 kHz) were compiled from research cruises passing near or through the CCZ (2004–2019), and environmental data (mean midwater oxygen partial pressure, surface chlorophyll-*a*, and sea surface height anomaly) were assembled from the World Ocean Atlas and satellite oceanographic datasets. Our results suggest that midwater oxygen, associated with the Eastern Tropical Pacific Oxygen Minimum Zone (OMZ), is the strongest predictor of daytime DSL depths and the proportions of midwater populations that undergo vertical migration in this region. We used these relationships to predict micronekton and zooplankton behaviors across the CCZ, including licensed mining exploration areas and no-mining reserves. While the OMZ encompasses most licensed exploration areas, the current network of reserves lies outside of the core OMZ and ultimately may not represent or protect the pelagic OMZ fauna at highest risk from mining impacts. This research will further assist in developing resource exploitation regulations by the International Seabed Authority, and will provide mesopelagic baseline information for monitoring changes that may occur in the CCZ once industrial-scale mining begins.

Keywords: Clarion-Clipperton Zone, deep-sea mining, mesopelagic, scattering layers, micronekton, oxygen minimum zone

OPEN ACCESS

Edited by:
Kerry Howell, University of Plymouth, United Kingdom

Reviewed by:
Michael Vecchione, National Oceanic and Atmospheric Administration (NOAA), United States
Thomas G. Dahlgren, Norwegian Research Institute (NORCE), Norway

****Correspondence:***
Jessica N. Perelman
jnperelm@hawaii.edu

Specialty section:
This article was submitted to Deep-Sea Environments and Ecology, a section of the journal Frontiers in Marine Science

Received: *24 November 2020*
Accepted: *12 April 2021*
Published: *10 May 2021*

Citation:
Perelman JN, Firing E, van der Grient JMA, Jones BA and Drazen JC (2021) Mesopelagic Scattering Layer Behaviors Across the Clarion-Clipperton Zone: Implications for Deep-Sea Mining. Front. Mar. Sci. 8:632764. doi: 10.3389/fmars.2021.632764

INTRODUCTION

The deep pelagic ocean likely contains a greater abundance and higher biomass of organisms than any other major ecosystem. Yet, this ecosystem is largely under-represented in global databases of marine biological records, and deep pelagic communities remain the least-known faunal group on Earth (Webb et al., 2010). Mesopelagic micronekton, small fishes and invertebrates (~2–20 cm in

size) that primarily inhabit depths between 200 and 1,000 m, form an essential trophic link between zooplankton and top predators such as tuna and billfishes (Choy et al., 2013; Young et al., 2015; Drazen and Sutton, 2017) and thus support pelagic fisheries. Diel vertical migration (DVM) by micronekton and zooplankton is the largest migration on Earth, and this contributes significantly to carbon and nutrient cycling in the ocean as organisms feed near the surface and respire at depth. Accordingly, the role of these communities in upper ocean carbon and nitrogen transport is substantial (Longhurst et al., 1990; Davison et al., 2013; Ariza et al., 2015).

When dense aggregations of micronekton and zooplankton form at midwater depths, these are frequently detected by shipboard sonars as acoustic backscatter and are thus termed "deep scattering layers" (DSLs). While swimbladdered fishes and gas-bearing siphonophores can dominate these acoustic signals, DSLs vary globally across pelagic ecosystems in their faunal composition, as well as daytime depths and vertical movements (Klevjer et al., 2016; Sutton et al., 2017). The fish families Myctophidae and Gonostomatidae (particularly *Cyclothone* spp.) are typically the dominant marine vertebrates caught in midwater trawls around the globe (e.g., Sutton et al., 2010) and likely comprise a large portion of mesopelagic scattering layers. Vertical migrations of DSLs are readily observable in echograms and this enables a visualization of largescale vertical community dynamics in the pelagic ocean (Dietz, 1948; Proud et al., 2018). The number of DSLs and their acoustic backscattering strength (a proxy for animal density) can vary widely at local and global scales (Urmy et al., 2012; Proud et al., 2017). Not all mesopelagic fauna migrate, which results in behavioral variation across the globe. Strong regional differences have been observed acoustically in the proportion of DSLs migrating out of the mesopelagic at night, from 20% migrating in the Indian Ocean and up to 90% migrating in the Eastern Pacific Ocean (Klevjer et al., 2016). However, information about the proportions of mesopelagic fauna actually carrying out DVM on local and regional scales is minimal, and this is a key attribute affecting active carbon flux and the coupling strength between the epi- and mesopelagic.

The ultimate driver of DVM by mid-trophic organisms is visual predator avoidance (Lampert, 1989, 1993). The behavior is thus thought to be driven primarily by downwelling light intensity in the water column where visual predation is common, as changes in the light environment at sunset and sunrise trigger these largescale animal migrations to and from the surface (Dickson, 1972; Kampa, 1975). The depth of daytime DSLs varies regionally (Bogorov, 1946; Dietz, 1948; Isaacs et al., 1974), and gradients in environmental conditions such as oxygen, chlorophyll, sea surface height, and water-column temperature have more recently been observed to drive largescale variability in scattering layer dynamics at regional and global scales (e.g., Bianchi et al., 2013; Netburn and Koslow, 2015; Urmy and Horne, 2016; Proud et al., 2017; Escobar-Flores et al., 2018). Oxygen-depleted zones act as strong bounding conditions for scattering layer depths globally, as hypoxia limits the depths to which animals can migrate and the duration they can spend at those depths. Phytoplankton chlorophyll affects light penetration in the ocean as light is scattered and absorbed by enhanced particle concentrations in surface waters (Yentsch and Phinney, 1989), and it can also be an indicator of surface food availability (Legendre and Michaud, 1999). Sea surface height anomalies can indicate the presence of oceanographic features (e.g., eddies) that may influence micronekton distribution via upwelling or downwelling (e.g., Drazen et al., 2011; Béhagle et al., 2016). Disturbances that alter these environmental drivers, such as climate change and human activities in the ocean, may stress midwater communities and alter their migration behavior. Knowledge of natural ecosystem dynamics and community sensitivities to environmental cues will thus enhance our ability to predict how the deep pelagic will respond to these stressors.

Growing interest in deep-sea polymetallic nodule mining may present a new human-induced stressor for midwater communities. This emerging industry could begin operations in the next several years in the Clarion-Clipperton Zone (CCZ)—a 4 million-km^2 area in the eastern Central Pacific Ocean (Wedding et al., 2015). This expansive region currently has mining exploration licenses by 15 countries regulated by the International Seabed Authority (ISA). Around the licensed exploration areas, a network of nine Areas of Particular Environmental Interest (APEIs) have been set up as no-mining zones by the ISA. They were developed on the basis of biophysical gradients, biologically unique seamounts, and socioeconomic impacts (Wedding et al., 2013). While nodule mining is expected to have major consequences for abyssal seafloor fauna (Amon et al., 2016; Jones et al., 2017), the industrial-scale operations are likewise expected to impact midwater ecosystems (Drazen et al., 2020). Namely, noise will be produced from vibrations in riser systems used to pump nodules to the surface, and heavy metal-laden sediment plumes generated from surface dewatering of the collected minerals will be released back into the water column. The resulting environmental influences could potentially hinder feeding, reproduction, DVM, and growth among organisms which may ultimately reduce pelagic biomass and diversity or alter their distributions (Christiansen et al., 2019; Drazen et al., 2020).

Only a handful of trawl and acoustic studies have documented midwater communities in the CCZ (e.g., Loeb and Nichols, 1984; Wishner et al., 2018), and this substantial knowledge gap hinders our ability to predict the influences of mining activities on the mesopelagic ecosystem. A recent global biogeographic classification suggests that the CCZ includes two mesopelagic "ecoregions" defined by geographically distinct faunal assemblages (Sutton et al., 2017): the Northern Central Pacific and Eastern Tropical Pacific ecoregions. In this framework, the Northern Central Pacific ecoregion is characterized as an oligotrophic gyre system with a fauna distinct from the central Equatorial Pacific, and the Eastern Tropical Pacific ecoregion is characterized as eutrophic with endemic taxa adapted to low oxygen. While this classification is broad, it is based on existing knowledge of faunal distributions and oceanographic patterns, and it may provide a good foundation from which to build hypotheses about mesopelagic ecosystems across the remote CCZ.

Light intensity and dissolved oxygen levels are known to be strong drivers of DVM and depth structure in deep scattering

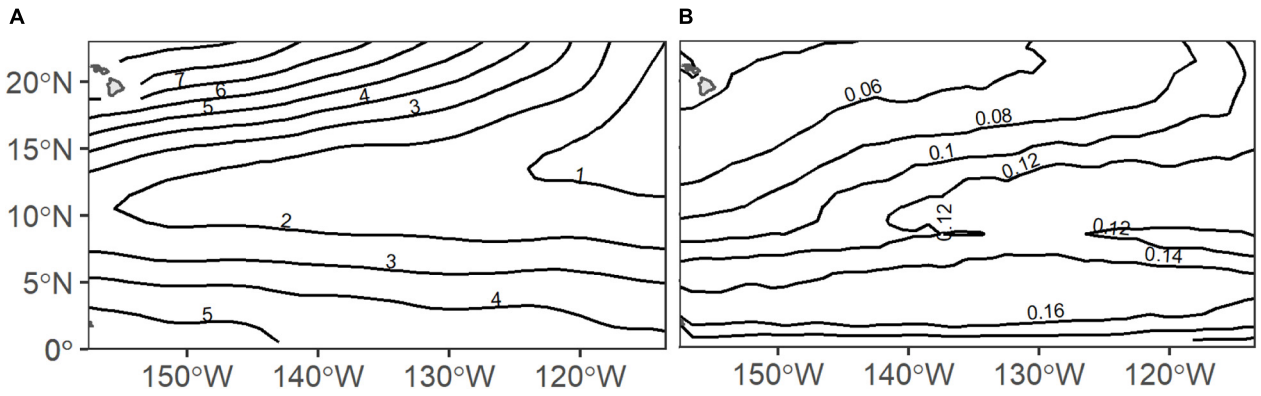

FIGURE 1 | Annual climatologies of **(A)** midwater oxygen partial pressure (pO_2; kPa) and **(B)** surface chlorophyll (chl-*a*; mg m^{-3}) across the eastern Central Pacific Ocean (source details in **Table 1**).

layers (Netburn and Koslow, 2015; Aksnes et al., 2017) and these parameters vary strongly within the CCZ mining region. Across the eastern Central Pacific Ocean, midwater oxygen partial pressures vary greatly with very low oxygen (∼0.5–2 kPa) extending from east to west and higher oxygen (∼4–7 kPa) in the north and south (**Figure 1A**). Further, surface chlorophyll and thus light penetration varies north to south and east to west with higher chlorophyll occurring to the east and to the south near equatorial upwelling (**Figure 1B**). Sea surface height anomalies, which may also influence DVM communities, are highly dynamic across the region due to the transient nature of the mesoscale features they indicate. Mesoscale eddies, for instance, may have a radius up to 100 km, a lifespan of several months, and typically propagate westward across the Pacific Ocean (Cheng et al., 2014; Aleynik et al., 2017). Such oceanographic gradients likely drive variability in the depths and behaviors of deep scattering layers across the CCZ.

The goal of this research is to build a baseline of deep scattering layer depths and DVM behaviors within and around the CCZ using opportunistic active acoustic data, and to reveal the dominant oceanographic factors driving variability in these dynamics. With the Eastern Tropical Pacific oxygen minimum zone (OMZ) extending throughout most of the region, we hypothesize that oxygen will play the largest role in structuring these communities by shallowing daytime DSL depths and increasing the proportions of migrating fauna in more hypoxic waters. The applied goal of this work is to inform developing resource exploitation regulations, which the ISA proposes to have in place by 2021, and to provide some mesopelagic baseline information for subsequently monitoring changes that may occur once largescale mining operations begin.

MATERIALS AND METHODS

Our analyses of scattering layers across the CCZ use publicly available shipboard acoustic Doppler current profiler (ADCP) measurements. At low frequencies (75 and 38 kHz), acoustic backscatter in pelagic ecosystems typically indicates the presence of large zooplankton and micronekton, and especially small mesopelagic fishes and siphonophores with gas-filled organs (Simmonds and MacLennan, 2008; Proud et al., 2019). Each frequency highlights the community of organisms whose size and morphology cause them to resonate most strongly at that frequency (Davison et al., 2015). We selected these two frequencies because the acoustic signals extend deep enough (roughly 650 m for 75 kHz and 1,000 m for 38 kHz) to encompass the daytime depths of dominant mesopelagic scattering layers, especially in the eastern Central Pacific where hypoxia limits migration depths (Bianchi et al., 2013; Klevjer et al., 2016; Aksnes et al., 2017; Proud et al., 2018). However, the shallowest measurements from ADCP systems are determined by the combination of transducer depth, blanking distance, and vertical resolution (cell size) which is a function of pulse length. Thus, the narrowband 75 kHz ADCPs in our dataset (with a cell size of 16 m, default blanking distance of 8 m, and transducer depth around 4 m) have the shallowest measurements at about 28 m, and the narrowband 38 kHz instruments (with a cell size of 24 m, default blanking distance of 16 m, and transducer depth around 7 m) have the shallowest measurements at about 47 m. Since these ADCP datasets include many instruments, all with uncalibrated backscatter, we analyzed relative structure within each dataset by evaluating the behaviors of dominant scattering layers, rather than assessing backscatter distributions as proxies for biomass (which is often done with calibrated echo sounder data).

ADCP Backscatter Processing

Shipboard ADCP datasets were compiled from the Joint Archive for Shipboard Acoustic Doppler Current Profilers (JASADCP)[1] and the NCEI Global Oceans Currents Database[2]. We analyzed a total of 44 cruise datasets from research vessels equipped with 75 and 38 kHz narrowband ADCPs (36 and 8 cruises, respectively) passing near or through the CCZ between 2004 and 2019 that showed at least one DVM event in the acoustic backscatter

[1]http://ilikai.soest.hawaii.edu/sadcp/

[2]https://www.ncei.noaa.gov/access/data/global-ocean-currents-database/saportal.html

(**Supplementary Table 1**). ADCP backscatter was converted from counts to decibel units using the common scaling factor (k_c) of 0.45 (Deines, 1999). We estimated the noise as the mean signal return from the bottom 6 depth cells, on the assumption that the signal-to-noise ratio (SNR) is small at those depths. After subtracting this estimated noise level from the received signal, we set a minimum SNR threshold of 3 dB. Acoustic intensity was thus calculated following the method of Gostiaux and Van Haren (2010):

$$I_{dB} = 10\log(10^{k_c E/10} - 10^{k_c E_{noise}/10}) \quad (1)$$

where E is the received signal strength indicator (RSSI; a logarithmic measure of acoustic intensity), E_{noise} is the noise level (counts), and I_{dB} is the acoustic intensity in decibels. Corrections were made for transmission loss due to spherical spreading and sound absorption. The attenuation coefficient was calculated as a function of depth using the formula of Ainslie and McColm (1998), with climatological temperature profiles from World Ocean Atlas. Due to highly variable noise and bubbles, particularly in the 75 kHz dataset, we flagged and removed cruise days with <10 intervals (5 min averaged profiles) that contained detectable backscatter during the daytime or nighttime timeframes of interest. Thus, while our original 75 kHz dataset included 50 cruises in the CCZ region, only 44 were included in these analyses. All acoustic data analyses were conducted in Python (version 3.7; Python Core Team, 2020).

Acoustic Metrics

Our examination of dominant scattering layers includes determination of dominant daytime DSL depths and DVM proportions (DVM_P). Daytime DSL depth was defined as the median depth of peak acoustic intensity from vertical backscatter profiles within 3 h around local solar noon. DVM_P, which was defined as the apparent proportion of midwater communities undergoing diel vertical migration, or vertical migration strength, was calculated as a ratio of integrated mesopelagic nighttime and daytime acoustic intensities similarly to Klevjer et al. (2016):

$$DVM_P = 1 - (10^{\tilde{I}_{dB-night}/10}/10^{\tilde{I}_{dB-day}/10}),\ DVMp > 0 \quad (2)$$

I_{dB} was calculated by integrating the acoustic intensity of each vertical profile (below 200 m) within 3 h around local solar midnight or noon. Then, we selected the median integrated value to represent I_{dB}. We did not correct for total water column changes between day and night acoustic intensities in our calculations of DVM_p due to lack of measurements in the shallowest 30–50 m as described previously. We further removed days or nights with > 5 noisy intervals within the noon or midnight time periods.

Environmental Variables

Due to the lack of high-resolution *in situ* oceanographic data to pair with opportunistic ADCP measurements for statistical models, environmental variables were extracted from global satellite and climatological datasets (**Table 1**). We explored the influences of oxygen, surface chlorophyll-*a*, sea surface height anomaly, sea surface temperature, and thermocline depth on DSL depth and DVM_p and ultimately focused on three of these variables: midwater oxygen partial pressure (pO_2), surface chlorophyll-*a* (chl-*a*), and sea surface height anomaly (SSHA). While we do expect temperature to affect swimming behaviors and habitat preferences, sea surface temperature is unlikely to influence migration deeper in the water column and it was excluded from these analyses. Thermocline depth was collinear with midwater oxygen (see collinearity method below), and because oxygen was ultimately a stronger predictor of DSL depth and DVM_p, we excluded thermocline depth from the models. After exploring several different monthly climatological oxygen metrics, including the depth of various oxygen isopleths and vertical oxygen averages over different depth ranges, mean pO_2 between 200 and 1,000 m (midwater pO_2) was selected as the best oxygen predictor of DSL behaviors, roughly encompassing the mesopelagic depth range. We further compared the pO_2 values at daytime DSL depths between the two frequency-defined communities. While pO_2 values were not concurrent in time with acoustic observations, the chl-*a* and SSHA values used for statistical models were extracted from satellite datasets and were thus matched as closely as possible to the empirical data (**Table 1**).

Statistical Analyses and Model Predictions

We evaluated the variance inflation factors (VIF) of each environmental variable in regression models to assess collinearity between predictors, with a cutoff of 2.5. After investigating for spatial and temporal autocorrelation in model residuals, the relationships between acoustic metrics (DSL depths and DVM_p) and environmental variables were evaluated using multiple linear regression (Eq. 3) and multiple beta regression (*betareg* R package; Cribari-Neto and Zeileis, 2009; Eq. 4), respectively.

$$\text{DSL depth} = \beta_0 + \beta_1 pO_2 + \beta_2 \text{chl}a + \beta_3 \text{SSHA} \quad (3)$$

$$\ln\left(\frac{DVM_p}{1-DVM_p}\right) = \beta_0 + \beta_1 pO_2 + \beta_2 \text{chl}a + \beta_3 \text{SSHA} \quad (4)$$

TABLE 1 | Environmental variables used to build statistical models for deep scattering layer (DSL) depth and vertical migration proportion (DVM_p).

Variable	Source	Spatial resolution	Temporal resolution	Units
Midwater pO_2	NODC World Ocean Atlas climatology (1955–2017)	1.0°	Monthly composite	kPa*
chl-*a*	ESA OC CCI (from NOAA OceanWatch)	0.04°	8-day mean	mg m^{-3}
SSHA	Global Ocean Gridded SSALTO/DUACS Sea Surface Height	0.25°	Daily mean	m

*Midwater pO_2 is the mean oxygen partial pressure between 200 and 1,000 m, chl-a is surface chlorophyll-a and SSHA is sea surface height anomaly. *Oxygen concentration (μmol kg^{-1}) was converted to pO_2 (kPa) following the methods of Hofmann et al. (2011).*

Since our ultimate goal was to best predict these acoustic metrics across the CCZ, models were averaged using a multi-model inference approach (Harrison et al., 2018) and parameter estimates were weighted based on Akaike information criteria (AICc; MuMIn package; Barton, 2018). Only models with ΔAICc < 4 (from the top ranked model) were included in these averages. AICc has become a favored approach for model selection over p-values when using multiple parameters to predict an outcome (Halsey, 2019). Full average models were used as opposed to conditional averages, as the full model mitigates biasing environmental parameters with weaker relationships. Explicitly, if a parameter is absent in a component model, its coefficient is set to zero and thus the full model average assumes a smaller response from that variable (Lukacs et al., 2010). To quantify the relative importance of environmental parameters in these model averages, we compared the sum of Akaike weights, or sum of model probabilities, for each parameter following the methods of Giam and Olden (2016). All statistical analyses were performed in R programming language (version 4.0.0; R Core Team, 2020).

To better understand the depths and migratory patterns of DSLs across the CCZ, we generated $1 \times 1°$ interpolated maps of DSL depths and DVM_p for each of the two frequencies (75 and 38 kHz). For these, we used predictions made with the empirical models described above in conjunction with annual $1 \times 1°$ climatological data for pO_2 and chl-*a* generated from the sources described in **Table 1**. Because SSHA is an anomaly and indicates dynamic and ephemeral mesoscale features, this parameter was set to zero for the climatological predictions. Using CCZ shapefiles provided by the ISA, we calculated the mean DSL depth and DVM_p in each licensed exploration area and APEI and averaged predictions across all mining exploration and no-mining zones. These were compared statistically using Wilcoxon rank sum tests. We further developed seasonal prediction maps for each acoustic frequency (**Supplementary Figures 4, 5**) to explore the temporal changes in DSLs between winter (Oct–Mar) and summer (Apr–Sep). All figures were produced in R or Python.

RESULTS

Acoustic Observations

Generally, ADCP backscatter indicated clear differences in scattering layer depth and migration patterns across the CCZ for both datasets. Observations from the northwest end of the region (e.g., 16.31°N, 146.45°W; **Figure 2A**) revealed relatively deep migratory scattering layers as well as strong non-migratory layers between ∼400 and 900 m. Observations from the eastern end of the region (e.g., 11.89°N, 116.61°W; **Figure 2B**) revealed shallower migrating layers in which most of the mesopelagic community appears to migrate, with several weak non-migratory layers residing in the deep mesopelagic below ∼650 m. These locations represent the upper and lower extremes of midwater oxygen levels in the CCZ (**Figure 1A**). While we mainly focused on strong mesopelagic DSLs, it is worth noting that weaker migratory and non-migratory DSLs extended below 1,000 m in our 38 kHz datasets (**Supplementary Figure 1**).

DSL Depth

The daytime DSL depth ranged from 270 to 510 m at 75 kHz and 290 to 890 m at 38 kHz, with median depths of 373 and 431 m, respectively. Observed daytime DSL depths at 75 kHz were shallowest in the eastern and central CCZ (**Figure 3A**), largely following the low-oxygen tongue extending out from the eastern tropical Pacific (**Figure 1A**). At 38 kHz, DSL depths were shallowest in the eastern and central CCZ as well as in the southwest (**Figure 3B**), generally following the low-oxygen and increased chl-a tongues extending out from the eastern tropical Pacific, and increased chl-*a* in the southern CCZ (**Figure 1B**). Since we lack 38 kHz data from the southcentral and southeastern CCZ, it is unclear whether the pattern of shallower DSL depths continues across the southern CCZ following enhanced chl-*a*.

DVM_p

DVM_p ranged from 0.03 to 0.99 at 75 kHz and 0.11 to 0.99 at 38 kHz, with median proportions of 0.86 and 0.63, respectively. DVM_p was highest in the eastern and central CCZ for both datasets (**Figure 4**), largely overlying the most hypoxic waters of the eastern tropical Pacific.

Environmental Influences on DSL Behavior

DSL Depth

At 75 kHz, daytime DSL depth was best described by a single model including pO_2, chl-*a*, and SSHA ($n = 77$, adjusted $R^2 = 0.56$; **Table 2**). DSL depth increased with increasing pO_2 and SSHA and decreased with increasing chl-*a* (**Supplementary Figure 2**). DSL depth at 38 kHz was more difficult to ascribe to the environmental predictors. Since DSL depths in this dataset were right-skewed (Shapiro-Wilk normality test; $p < 0.001$), we used a loglinear multiple regression model average that similarly included pO_2, chl-*a*, and SSHA as important predictors ($n = 76$, adjusted $R^2 = 0.31$; **Table 2**). Three component models comprised this model average: all included pO_2, two included chl-*a*, and one included SSHA. As in the 75 kHz model, DSL depth increased with increasing pO_2 and increasing SSHA and decreased with increasing chl-*a* in the 38 kHz model average (**Supplementary Figure 2**). For both frequency datasets, the order of relative variable importance based on sum of Akaike weight values was (1) pO_2, (2) chl-*a*, and (3) SSHA. Oxygen partial pressure at the depth of daytime DSLs ranged from 0.14 to 6.65 kPa at 75 kHz (median = 1.55 kPa, mode = 0.77 kPa) and from 0.12 to 4.80 kPa at 38 kHz (median = 1.65 kPa, mode = 0.73 kPa).

DVM_p

DVM_p was influenced by pO_2, chl-*a*, and SSHA at both 75 kHz ($n = 46$, adjusted pseudo-$R^2 = 0.60$; **Table 3**) and 38 kHz ($n = 56$, adjusted pseudo-$R^2 = 0.56$; **Table 3**). The model averages were comprised of two component models for both frequencies, one without and one with SSHA. According to these multiple beta regressions, DVM_p increased with decreasing pO_2 and with

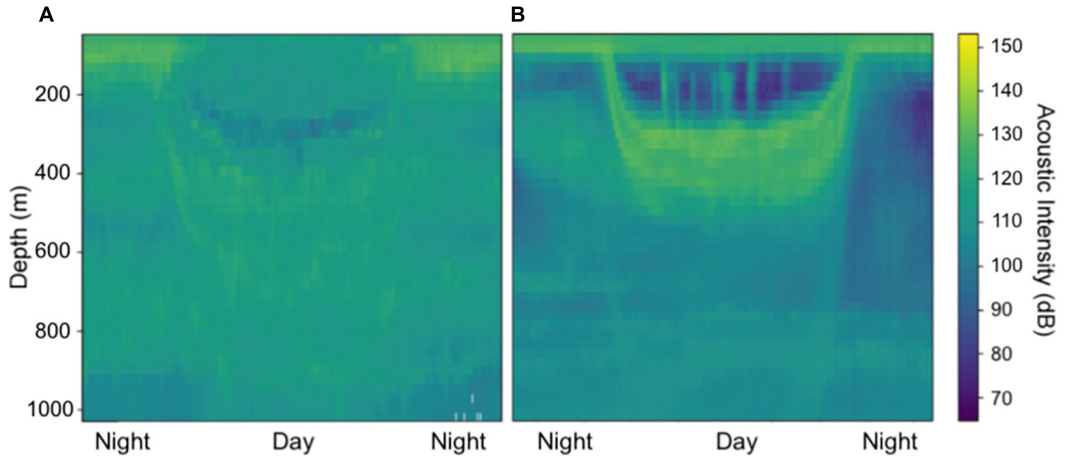

FIGURE 2 | Shipboard ADCP acoustic intensities at 38 kHz in **(A)** the northwest CCZ (16.31°N, 146.45°W) and **(B)** the eastern CCZ (11.89°N, 116.61°W) from November 2009. Acoustic intensity units are in decibels (RSSI counts*0.45).

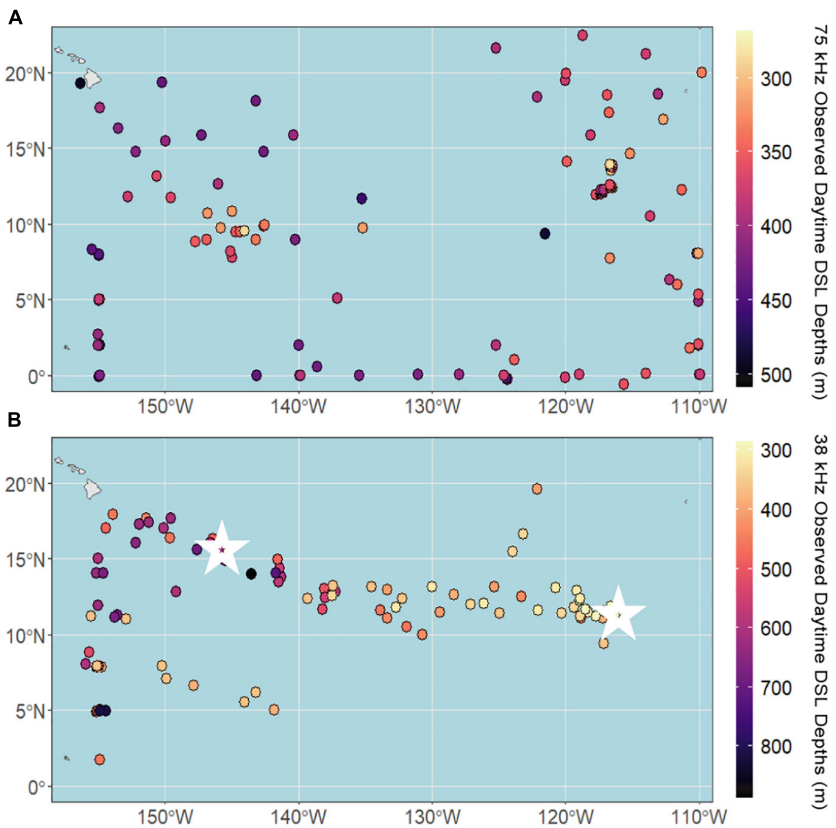

FIGURE 3 | Observed daytime deep scattering layer (DSL) depths across the CCZ region calculated from shipboard ADCP data between 2004 and 2019 at **(A)** 75 kHz and **(B)** 38 kHz. White stars indicate the locations of echogram examples (**Figure 2**).

increasing chl-*a* and SSHA (**Supplementary Figure 3**) at both frequencies. Similar to DSL depth, the order of relative variable importance for DVM_p in both datasets was (1) pO_2 (2) chl-*a*, and (3) SSHA. DVM_p always exceeded 0.9 when midwater oxygen partial pressure fell below 1.0 kPa (75 kHz) and 1.1 kPa (38 kHz).

CCZ Model Predictions

DSL Depth

Model predictions for both frequencies extended our observations of shallow DSL depths in the eastern and central CCZ, largely overlapping the most hypoxic waters of the OMZ

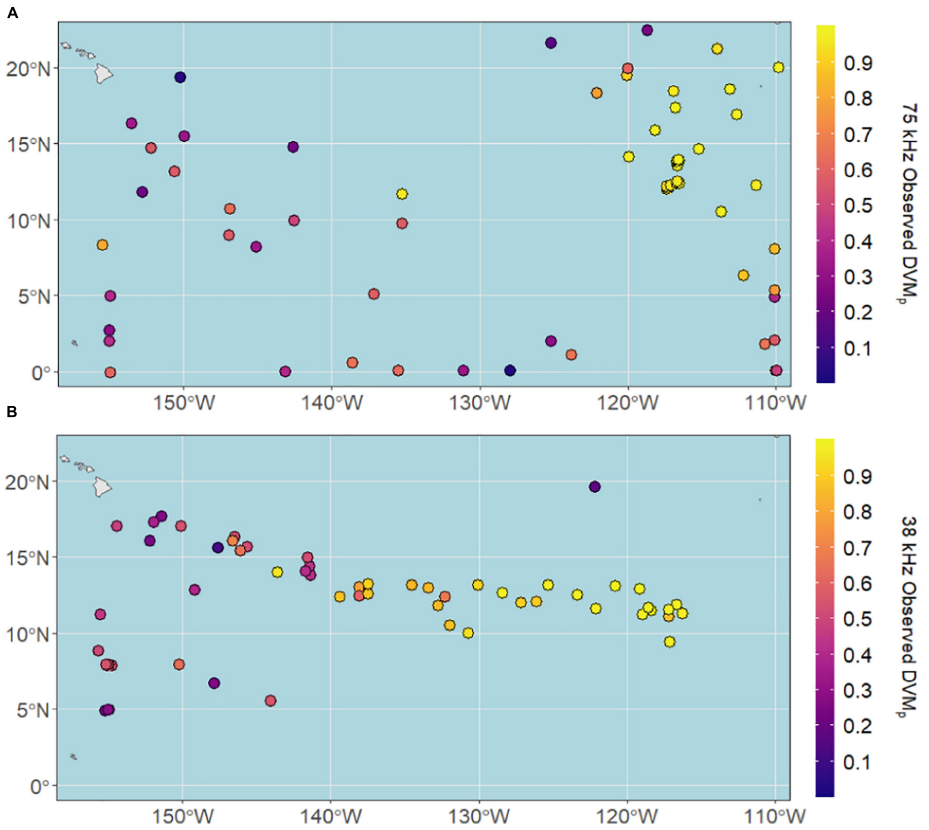

FIGURE 4 | Observed vertical migration proportions (DVM_p) across the CCZ region calculated from shipboard ADCP data between 2004 and 2019 at **(A)** 75 kHz and **(B)** 38 kHz.

TABLE 2 | Model parameters (component models and averages) from fitted regressions of observed deep scattering layer (DSL) depths for the two ADCP frequencies.

Frequency	Regression	N	Model	Model coefficients *(sum of Akaike weights)*			ΔAICc (weight)	Adjusted R^2
				pO_2	chl-*a*	SSHA		
75 kHz	Linear	77	*Component 1*	*20.89 (1.00)*	*−227.80 (0.99)*	*159.26 (0.99)*	*0.00 (0.99)*	*0.56*
38 kHz	Loglinear	76	Component 1	0.07	−1.78	0	0.00 (0.61)	0.33
			Component 2	0.06	−1.73	0.23	1.75 (0.26)	0.33
			Component 3	0.10	0	0	3.04 (0.13)	0.29
			Average	*0.07 (0.98)*	*−1.53 (0.82)*	*0.06 (0.31)*		*0.31*

Sample size (N) includes only data points with corresponding environmental variables for statistical analyses. The sum of Akaike weights is presented next to model coefficients for the models used to generate prediction maps (in italics). Model weights are presented next to ΔAICc values.

(**Figures 5A,B**). However, due to the low explanatory power of the 38 kHz model, the predictions for this frequency were less reliable. The predicted DSL depth ranges for 75 kHz (345–553 m) were shallower than those for 38 kHz (358–753 m), but similar DSL depths were predicted in the most hypoxic waters of the eastern CCZ for both datasets (∼355–370 m). Most licensed exploration areas had relatively shallow DSL depths, while most APEIs occurred where DSL depths changed most rapidly. The mean (±1 SD) predicted daytime DSL depths across current licensed exploration areas and APEIs were 365 ± 12 and 389 ± 14 m at 75 kHz ($p < 0.001$) and 388 ± 19 and 424 ± 24 m at 38 kHz ($p < 0.001$), respectively, with the eastern-most license areas having the shallowest DSLs. APEI-9 had the shallowest predicted DSL depths of the APEIs (370 and 393 m for 75 and 38 kHz, respectively), and APEI-3 had the deepest (410 and 468 m for 75 and 38 kHz, respectively). Our predictions showed minor seasonal trends in DSL depths for both frequencies (**Supplementary Figure 4**), with patterns suggesting a slight summertime deepening of DSL depths.

DVM_p

DVM_p predictions for the CCZ were similar in pattern to those for DSL depths. DVM_p was highest in the eastern and central CCZ for both frequencies (**Figures 5C,D**), overlapping with the OMZ and most licensed exploration areas (particularly the

TABLE 3 | Model parameters (component models and averages) from fitted regressions of observed vertical migration proportion (DVM_p) for the two ADCP frequencies.

Frequency	Regression	N	Model	Model coefficients *(sum of Akaike weights)*			ΔAICc (weight)	Adjusted Pseudo-R^2
				pO_2	chl-*a*	SSHA		
75 kHz	Beta (logit link)	46	Component 1	−0.77	7.27	0	0.00 (0.56)	0.58
			Component 2	−0.78	8.77	2.13	0.64 (0.40)	0.63
			Average	*−0.78 (1.00)*	*7.91 (0.96)*	*0.90 (0.41)*		*0.60*
38 kHz	Beta (logit link)	56	Component 1	−0.49	12.88	0	0.00 (0.74)	0.56
			Component 2	−0.49	12.87	0.06	2.41 (0.22)	0.56
			Average	*−0.49 (1.00)*	*12.87 (0.96)*	*0.01 (0.23)*		*0.56*

Sample size (N) includes only data points with corresponding environmental variables for statistical analyses. The sum of Akaike weights is presented next to model coefficients for the models used to generate prediction maps (in italics). Model weights are presented next to ΔAICc values.

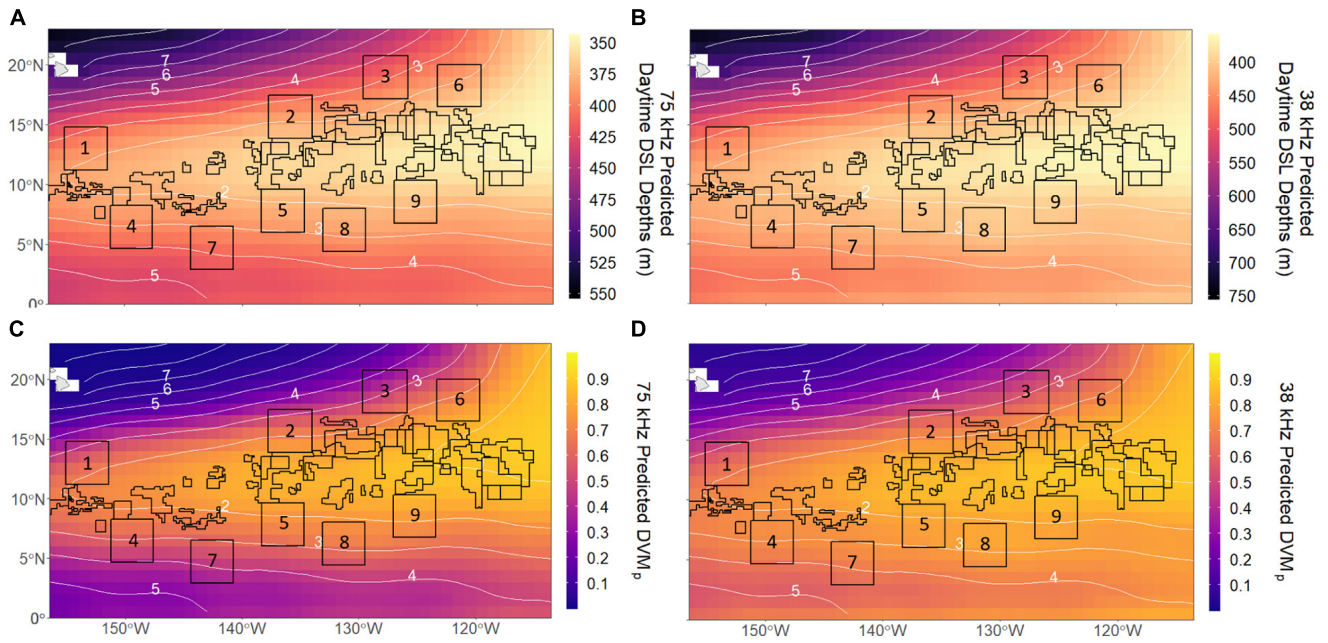

FIGURE 5 | Annual mean 1 × 1° predictions for daytime deep scattering layer (DSL) depths at **(A)** 75 kHz and **(B)** 38 kHz and vertical migration proportions (DVM_p) at **(C)** 75 kHz and **(D)** 38 kHz across the CCZ. Numbered boxes indicate Areas of Particular Environmental Interest (APEIs) and all other polygons represent mining exploration claim areas designated by the International Seabed Authority (ISA). White numbered contours represent mean midwater oxygen partial pressure (pO_2; kPa).

eastern-most license areas). DVM_p predictions ranged from 0.004 to 0.90 at 75 kHz and from 0.04 to 0.90 at 38 kHz, with values exceeding 0.85 in the most hypoxic waters for both frequencies. Overall, DVM_p was higher in the southern CCZ (∼0–5°N) at 38 kHz than at 75 kHz. Most APEIs had weaker migrations than license areas as they lie near the OMZ boundaries. The mean (±1 SD) predicted DVM_p among all license areas and APEIs were 0.80 ± 0.07 and 0.62 ± 0.11 at 75 kHz ($p < 0.001$) and 0.82 ± 0.06 and 0.71 ± 0.09 at 38 kHz ($p < 0.001$). APEI-9 was predicted to have the highest DVM_p (0.76 and 0.81 for 75 and 38 kHz, respectively) and APEI-3 was predicted to have the lowest (0.44 and 0.53 at 75 and 38 kHz, respectively). Similar to DSL depths, there were minor seasonal patterns in the predictions of DVM_p (slight summertime weakening of migration) for the CCZ region (**Supplementary Figure 5**).

DISCUSSION

Our analyses of acoustically measured micronekton and large zooplankton migratory behaviors highlight the significance of the Eastern Tropical Pacific OMZ in structuring mesopelagic communities across the CCZ. Amongst the environmental variables explored, midwater oxygen appears to be the strongest driver of daytime habitat depth and vertical migration strength in the CCZ. Midwater oxygen was present in all component models with the highest relative importance (sum of Akaike weights; **Tables 2**, **3**), and it largely structured the predicted behavioral patterns of these communities. As expected, DSL depths shoal and vertical migration strength increases along decreasing midwater oxygen gradients, leading to patterns in these behaviors that primarily follow the "tongue" shape of the

OMZ (**Figures 1A**, 5). Under low oxygen conditions, Klevjer et al. (2016) similarly observed midwater oxygen as a primary driver of global daytime scattering layer depths and migrating proportions. At more regional scales, other studies have also observed scattering layer organisms to closely follow oxyclines (Netburn and Koslow, 2015; Wishner et al., 2018). Although our 38 kHz dataset does not cover the southern and northern CCZ, we suspect that DVM_p in this community is lower across the southern and northwestern CCZ where oxygen is higher, and DVM_p is higher to the northeast following the trend with low oxygen.

By putting a physiological constraint on organisms, oxygen can impact the vertical distribution and duration spent at depth when oxygen levels are low. Above an OMZ, many organisms may only inhabit waters as deep as their hypoxia tolerance allows, and greater proportions of the mesopelagic community vertically migrate to higher oxygen surface waters at night in areas where midwaters are most hypoxic to offset oxygen limitation (Seibel, 2011; Klevjer et al., 2016). Metabolic suppression at depth in OMZs is a common strategy for vertical migrators (Seibel, 2011). Many mesozooplankton and micronekton can only adjust their capacity to acquire oxygen down to a critical oxygen partial pressure threshold of ∼0.8–1.0 kPa (though this varies regionally and between taxa), but some can migrate well into hypoxic waters of OMZs using a variety of adaptations to cope with low oxygen (Sameoto, 1986; Childress and Seibel, 1998; Hofmann et al., 2011; Seibel, 2011; Wishner et al., 2013; Seibel et al., 2016). Climatological oxygen partial pressures at DSL depths in this study had median values of 1.55 and 1.65 kPa for the 75 and 38 kHz communities, respectively, and were similar to critical oxygen thresholds reported for mesozooplankton and micronekton in OMZ regions (Seibel, 2011; Cade and Benoit-Bird, 2015; Seibel et al., 2016).

We identified mean oxygen partial pressure between 200 and 1,000 m as the most parsimonious oxygen metric to include in our models. This range likely encompasses the species-specific depths at which hypoxia tolerance thresholds are encountered, which follows the notion that there is no common oxygen preference across the global ocean (Aksnes et al., 2017). It is important to emphasize that the scattering layer is not singular; rather, multiple layers migrate at variable times and to different depths. Since responses to hypoxia are species-specific, community-wide metrics like single frequency acoustic backscatter might miss variability that is significant to food web dynamics and ecosystem services such as carbon cycling. Future work should thus employ additional techniques like broadband surveys and trawl sampling to assess the taxon-specific details underlying the community patterns we observed in this study.

DSL depths and migration strength were also influenced by other environmental factors according to our models. DSL depths shoaled and migration strength increased with increasing surface chlorophyll for both frequency-defined communities. Enhanced chlorophyll concentration in surface waters can absorb and scatter downwelling light (Yentsch and Phinney, 1989), leading to lower visual predation pressure that could allow zooplankton and micronekton to reside at shallower depths. Chlorophyll-*a* may also fuel enhanced secondary production that can be channeled up to higher trophic level organisms (Legendre and Michaud, 1999; Hirst and Bunker, 2003), and this food availability in surface waters could lead to enhanced migration strength. While our results evaluate DVM behaviors, recent work using global satellite-based light-detection-and-ranging (lidar) data calculated total DVM biomass (not DVM strength) to be higher in more productive regions with higher food availability, including the tropical Pacific (Behrenfeld et al., 2019).

Our models further suggest that DSL depths deepen and migration strength increases with increasing SSHA. SSHA can act as a surface proxy for meso- and macroscale oceanographic features such as eddies and fronts, both of which have been observed to influence micronekton vertical structure and aggregation in the pelagic ocean (e.g., Drazen et al., 2011; Béhagle et al., 2016). In the northern hemisphere, downwelling (+ SSHA) by anticyclonic eddies can bring micronekton and zooplankton to deeper waters, while upwelling (− SSHA) from cyclonic eddies may do the opposite by shoaling the thermocline and enhancing secondary production (food availability) in shallower waters (Bakun, 2007; Drazen et al., 2011; Béhagle et al., 2014). Enhanced surface chlorophyll associated with both cyclonic eddy interiors and anticyclonic eddy peripheries (e.g., Mizobata et al., 2002) could also decrease light penetration and further influence the shoaling of scattering layers. It is worth noting that SSHA was not important in every component model (**Tables 2**, **3**), and it is likely a weaker indicator of scattering layer dynamics across the CCZ than pO_2 and chl-*a*. SSHA indirectly influences the region-wide predictions of DSL depths and DVM_p because its inclusion in the empirical models changes the parameter estimates for chl-*a* and pO_2 during model fitting. However, the direct effect of SSHA is excluded from the region-wide predictions as mesoscale eddies and fronts only have short-term influences on scattering layer behaviors (i.e., weeks to months) in a fixed area (D'Ovidio et al., 2013). Although we lack a complete mechanistic understanding of how each environmental factor influences DVM behavior in micronekton and zooplankton, such satellite-based and climatological variables provide useful proxies that account for a portion of the variability in DSL behaviors in remote regions like the CCZ.

While we observed similar behaviors in relation to environmental factors in both frequency-defined communities, there were significant disparities between DSL depths and migration strengths worth noting. The ranges of observed daytime DSL depths were deeper for the 38 kHz community (290–890 m) than for the 75 kHz community (270–510 m). While there are variable hypoxia thresholds among marine fauna (Hofmann et al., 2011), oxygen partial pressure at daytime DSL depths was similar for 75 kHz (median 1.55 kPa, mode = 0.77 kPa) and 38 kHz (median = 1.65 kPa; mode = 0.73 kPa) communities in our observations. Thus, it is unlikely that differences in oxygen tolerance are driving the disparities in daytime depths between these communities. Clearly, the increased depths observed by the 38 kHz frequency itself may skew DSL locations toward greater possible depths. However, there was no evidence of strong DSLs approaching the maximum depth range in our 75 kHz dataset (i.e., the peak acoustic intensity

was well above 650 m). Additionally, there may be biological explanations for these differences. For instance, it is likely that larger organisms dominate lower frequency (longer wavelength) signals where near-resonance effects would amplify scattering by larger organisms with gaseous inclusions. It is possible that these organisms, such as swim-bladdered myctophids, are simply more mobile and thus can reach greater daytime depths. Following size-dependent predator-avoidance hypotheses (Lampert, 1993; De Robertis, 2002), larger micronekton are also more conspicuous to visual predators, and thus may need to reside at deeper daytime depths than smaller organisms to stay hidden, as has been observed with zooplankton (Bollens et al., 2010). Our observations of DVM_p likewise differed by frequency, with a higher median proportion for 75 kHz (0.86) than for 38 kHz (0.63), though total ranges were similar. One possible explanation for this difference is that non- or weakly migratory, lower mesopelagic and bathypelagic fishes (e.g., stomiids) contribute to 38 kHz nighttime backscatter at depths below 650 m (Andersen et al., 1992; Kenaley, 2008; Sutton et al., 2010), which is the limit of our 75 kHz observations. This would lower the day-to-night backscatter ratios and thus lead to lower values of DVM_p.

Although oxygen was an important factor controlling daytime DSL depths for both communities, it was not as influential for the 38 kHz community, and we were ultimately unable to account for as much variability in this group with the environmental variables in this study ($R^2 = 0.31$; **Table 2**). Although DSL depth predictions for this community still largely follow the shape of the Eastern Tropical Pacific OMZ similarly to the 75 kHz community, they deviate slightly from this pattern and appear to reflect a stronger influence of surface chlorophyll, with shallower DSL depths appearing across the southern CCZ (**Figure 5B**). DVM_p predictions for the 38 kHz community similarly reflect a stronger influence of chl-*a*, with higher migrating proportions extending south of the OMZ (**Figure 5D**). This model had higher explanatory power ($R^2 = 0.56$; **Table 3**) than that for DSL depth, but it underestimated DVM_p east of ∼130°W, highlighting the variance unaccounted for by this model (**Supplementary Figure 7D**). More 38 kHz observations across the southern and northern CCZ (**Figures 3B**, 4B) are required to fully evaluate predictions there. The relative influences of environmental factors on micronekton and zooplankton behavior may be different between these two mesopelagic communities in the CCZ, and it is possible that there are additional factors affecting the 38 kHz community that are not accounted for in this study.

The acoustic properties of organisms themselves can be a source of variability affecting the signals obtained. Evidence from recent depth-stratified broadband acoustic surveys in the Atlantic Ocean (Bassett et al., 2020) suggests that ship-based echo sounders at frequencies near 38 kHz under sample scattering layers at deeper depths. This is because the contribution to backscatter from marine organisms can be strongly frequency and depth dependent. For example, gaseous swimbladder-bearing fish that resonate near 38 kHz in the upper water column have a higher resonance frequency at greater depths. The combination of this shift in the resonance frequency of those fish, and increased attenuation of higher frequency signals (e.g., 75 kHz), may mean that neither the 38 kHz nor 75 kHz frequency is detecting many organisms in the lower mesopelagic that resonate near 38 kHz in shallower waters. Thus, the ship-based systems we employ here likely have a "blind-spot" at greater depths. In this regard, our observations of DSL depths across the CCZ assume that peak acoustic intensity represents the strongest or densest biomass layers, but we recognize that this may not necessarily be the case. Depths of peak acoustic intensity may also represent the depths of specific communities of organisms that happen to resonate most strongly at that particular frequency and depth (Davison et al., 2015). It is important to consider such complexities in acoustic data for addressing vertical community structure in the pelagic ocean when concurrent trawl or specimen data is lacking.

The community compositions of DSLs we observed from ADCP backscatter in the CCZ are unknown. However, the aforementioned mesopelagic biogeographical ecoregions defined for the CCZ (Sutton et al., 2017) are consistent with our observations of disparate scattering layer behaviors; shallower daytime DSLs and stronger vertical migration in the eastern and central CCZ (Eastern Tropical Pacific ecoregion), and deeper daytime DSLs and weaker vertical migration in the northwestern CCZ (the Northern Central Pacific ecoregion). Thus, it is possible that differences in scattering layer behaviors across the region are indicative of changes in mesopelagic faunal composition. The Northern Central Pacific ecoregion appears to hold high mesopelagic fish diversity and a dominant abundance of fish in the genus *Cyclothone* (Clarke, 1973, 1974, 1976; Maynard et al., 1975; Barnett, 1983). Despite high abundances of *Cyclothone* collected in trawls, several species within this genus have regressed or fat-invested swim bladders (Phleger, 1998; Davison, 2011; Dornan et al., 2019), rendering them weak acoustic scatterers. Thus, *Cyclothone* may not contribute significantly to the acoustic backscatter we observed and could be considered "acoustically cryptic" (Dornan et al., 2019). However, those species containing a gas-filled swim bladder (e.g., *C. pseudopallida*) are likely non-migrators (Davison, 2011) and may contribute to observed non-migratory scattering layers. Similarly to our observed DSL depths and DVM_P in the NW corner of the CCZ (**Figures 3**, **4**), nearly half of daytime micronekton biomass below 400 m has been found to migrate into the upper 400 m at night around Hawai'i (Maynard et al., 1975). Also consistent with our acoustic observations, micronekton and macrozooplankton vertical distributions in parts of the Eastern Tropical Pacific Ecoregion suggest that the upper water column down to 550 m is strongly influenced by DVM in and out of the upper oxycline and OMZ core (Maas et al., 2014). Fishes and crustaceans (particularly euphausiids) appear to dominate this community. Secondary biomass peaks in zooplankton and micronekton have also been observed at OMZ lower oxycline depths from trawls

and acoustics (**Supplementary Figure 6**; Bianchi et al., 2013; Wishner et al., 2013; Maas et al., 2014; Klevjer et al., 2016). This is consistent with our observations of additional, weaker scattering layers extending well below ∼500 m in the OMZ (**Figure 2** and **Supplementary Figure 1**), following the hypothesis that these low-oxygen waters provide some organisms with a refuge from large visual predators with greater oxygen demands (Seibel, 2011).

Despite our minimal understanding of mesopelagic community composition across the CCZ, these results provide basic information about deep pelagic communities that is relevant and significant to deep-sea mining in the region. After nodules are pumped from the abyssal seafloor to the surface, sediment plumes will be released into the water column after dewatering of polymetallic ore. As these sediment plumes will likely impact midwater communities, Drazen et al. (2020) recently recommended that they be discharged below depths of 1,500–2,000 m (i.e., well below the lower bounds of the mesopelagic), or be released all the way back to the abyssal seafloor. However, the ISA has yet to set that discharge depth, and if released too shallow (i.e., into the mesopelagic), these plumes could interact with and influence DVM behaviors and their associated ecosystem functions. An understanding of how DVM behaviors vary among licensed exploration areas and APEIs is crucial. For example, our overall findings suggest that dominant daytime DSLs are shallowest and vertical migration strength is highest in the eastern-most license areas (**Figure 5**). Mesopelagic mining impacts in this region could therefore have a greater influence on vertical coupling and DVM-mediated carbon transport (Longhurst et al., 1990; Ducklow et al., 2001) depending on the depth zones affected by mining.

Importantly, the majority of licensed mining exploration areas in the CCZ lie within the OMZ, and consequently these areas contain the shallowest scattering layer depths and strongest vertical migrations. However, the system of APEIs surrounding these mining zones lie on the boundaries or just outside of the OMZ, exhibiting relatively deeper scattering layers and weaker migrations. Many pelagic OMZ fauna are highly adapted (behaviorally and biologically) or endemic to low-oxygen habitats (Antezana, 2009; Seibel et al., 2016; Sutton et al., 2017). Our observations of disparate behavioral dynamics, combined with this knowledge of OMZ-specialist fauna, indicates that these protected, no-mining reserves likely do not adequately represent or protect the OMZ organisms in oceanic midwaters that could be impacted by deep-sea mining (Drazen et al., 2020). The APEI network of nine 400-km^2 reserve areas was spatially designed to protect the diversity of benthic habitats and fauna within the CCZ mining region (Wedding et al., 2013), so it is not surprising that these areas may not protect midwater habitats as they are currently placed. However, in order to prevent excessive harm to midwater ecosystems, whose services are closely linked to humans, the deep pelagic must be included in precautionary management plans and future environmental research in the CCZ (Christiansen et al., 2019; Drazen et al., 2020). Future work combining broadband acoustics and depth-stratified trawl sampling would provide a more thorough understanding of the organisms comprising DSLs in the CCZ (Kloser et al., 2002; Escobar-Flores et al., 2019), and to what extent different taxa contribute to the patterns of habitat depth and vertical migration that we observed here in opportunistic shipboard ADCP data. Nonetheless, this study provides the first major examination of midwater community dynamics across the remote CCZ, highlights the complexities of mesopelagic micronekton and zooplankton behavior in the open ocean, and raises concerns about the effectiveness of current no-mining areas for pelagic habitats.

DATA AVAILABILITY STATEMENT

The original contributions presented in the study are included in the article/**Supplementary Material**, further inquiries can be directed to the corresponding author/s.

AUTHOR CONTRIBUTIONS

JP and JD were responsible for the project design and funding was secured by JD. JP led ADCP and statistical analyses as well as manuscript writing. EF led the development of ACDP backscatter processing tools and interpretation. JD and EF aided in the refinement and selection of environmental variables. JG contributed to statistical analyses and statistical model development. BJ contributed to interpretation of the acoustic results. All authors contributed to manuscript writing and have approved the submitted document.

FUNDING

Funding support for this project came from the Benioff Ocean Initiative.

ACKNOWLEDGMENTS

We would like to thank Julia Hummon for formatting and providing access to shipboard ADCP data files, Phoebe Woodworth-Jefcoats for her assistance with environmental data extraction and climatology configuration, and Seth Bushinsky for his input on oxygen conversions. We also thank Justin Suca for his contributions to data interpretation, statistical modeling input, and R support. ADCP data was provided by JASADCP and KIOST. Finally, we would like to acknowledge our funding support for this project, the Benioff Ocean Initiative.

SUPPLEMENTARY MATERIAL

The Supplementary Material for this article can be found online at: https://www.frontiersin.org/articles/10.3389/fmars.2021.632764/full#supplementary-material

REFERENCES

Ainslie, M. A., and McColm, J. G. (1998). A simplified formula for viscous and chemical absorption in sea water. *J. Acoust. Soc. Am.* 103, 1671–1672. doi: 10.1121/1.421258

Aksnes, D. L., Røstad, A., Kaartvedt, S., Martinez, U., Duarte, C. M., and Irigoien, X. (2017). Light penetration structures the deep acoustic scattering layers in the global ocean. *Sci. Adv.* 3:e1602468. doi: 10.1126/sciadv.1602468

Aleynik, D., Inall, M. E., Dale, A., and Vink, A. (2017). Impact of remotely generated eddies on plume dispersion at abyssal mining sites in the Pacific. *Sci. Rep.* 7:16959.

Amon, D. J., Ziegler, A. F., Dahlgren, T. G., Glover, A. G., Goineau, A., Gooday, A. J., et al. (2016). Insights into the abundance and diversity of abyssal megafauna in a polymetallic-nodule region in the eastern Clarion-Clipperton Zone. *Sci. Rep.* 6:30492.

Andersen, V., Sardou, J., and Nival, P. (1992). The diel migrations and vertical distributions of zooplankton and micronekton in the Northwestern Mediterranean Sea. 2. Siphonophores, hydromedusae and pyrosomids. *J. Plankton Res.* 14, 1155–1169. doi: 10.1093/plankt/14.8.1155

Antezana, T. (2009). Species-specific patterns of diel migration into the Oxygen Minimum Zone by euphausiids in the Humboldt Current Ecosystem. *Prog. Oceanogr.* 83, 228–236. doi: 10.1016/j.pocean.2009.07.039

Ariza, A., Garijo, J. C., Landeira, J. M., Bordes, F., and Hernández-León, S. (2015). Migrant biomass and respiratory carbon flux by zooplankton and micronekton in the subtropical northeast Atlantic Ocean (Canary Islands). *Prog. Oceanogr.* 134, 330–342. doi: 10.1016/j.pocean.2015.03.003

Bakun, A. (2007). Fronts and eddies as key structures in the habitat of marine fish larvae: opportunity, adaptive response and competitive advantage. *Sci. Mar.* 70, 105–122. doi: 10.3989/scimar.2006.70s2105

Barnett, M. A. (1983). Species structure and temporal stability of mesopelagic fish assemblages in the Central Gyres of the North and South Pacific Ocean. *Mar. Biol.* 74, 245–256. doi: 10.1007/BF00403448

Barton, K. (2018). *MuMIn: Multi-Model Inference. R Package Version 1.15. 6. 2016*.

Bassett, C., Lavery, A. C., Stanton, T. K., and Cotter, E. D. (2020). Frequency- and depth-dependent target strength measurements of individual mesopelagic scatterers. *J. Acoust. Soc. Am.* 148:EL153. doi: 10.1121/10.0001745

Béhagle, N., Cotté, C., Ryan, T. E., Gauthier, O., Roudaut, G., Brehmer, P., et al. (2016). Acoustic micronektonic distribution is structured by macroscale oceanographic processes across 20-50°S latitudes in the South-Western Indian Ocean. *Deep. Res. Part I Oceanogr. Res. Pap.* 110, 20–32. doi: 10.1016/j.dsr.2015.12.007

Béhagle, N., Du Buisson, L., Josse, E., Lebourges-Dhaussy, A., Roudaut, G., and Ménard, F. (2014). Mesoscale features and micronekton in the Mozambique Channel: an acoustic approach. *Deep. Res. Part II Top. Stud. Oceanogr.* 100, 164–173. doi: 10.1016/j.dsr2.2013.10.024

Behrenfeld, M. J., Gaube, P., Della Penna, A., O'Malley, R. T., Burt, W. J., Hu, Y., et al. (2019). Global satellite-observed daily vertical migrations of ocean animals. *Nature* 576, 1–5.

Bianchi, D., Galbraith, E. D., Carozza, D. A., Mislan, K. A. S., and Stock, C. A. (2013). Intensification of open-ocean oxygen depletion by vertically migrating animals. *Nat. Geosci.* 6:545. doi: 10.1038/ngeo1837

Bogorov, B. G. (1946). Peculiarities of diurnal vertical migrations of zooplankton in polar seas. *J. Mar. Res* 6, 25–32.

Bollens, S. M., Rollwagen-Bollens, G., Quenette, J. A., and Bochdansky, A. B. (2010). Cascading migrations and implications for vertical fluxes in pelagic ecosystems. *J. Plankton Res.* 33, 349–355. doi: 10.1093/plankt/fbq152

Cade, D. E., and Benoit-Bird, K. J. (2015). Depths, migration rates and environmental associations of acoustic scattering layers in the Gulf of California. *Deep. Res. Part I Oceanogr. Res. Pap.* 102, 78–89. doi: 10.1016/j.dsr.2015.05.001

Cheng, Y.-H., Ho, C.-R., Zheng, Q., and Kuo, N.-J. (2014). Statistical characteristics of mesoscale eddies in the North Pacific derived from satellite altimetry. *Remote Sens.* 6, 5164–5183. doi: 10.3390/rs6065164

Childress, J. J., and Seibel, B. A. (1998). Life at stable low oxygen levels: adaptations of animals to oceanic oxygen minimum layers. *J. Exp. Biol.* 201, 1223–1232.

Choy, C. A., Portner, E., Iwane, M., and Drazen, J. C. (2013). Diets of five important predatory mesopelagic fishes of the central North Pacific. *Mar. Ecol. Prog. Ser.* 492, 169–184. doi: 10.3354/meps10518

Christiansen, B., Denda, A., and Christiansen, S. (2019). Potential effects of deep seabed mining on pelagic and benthopelagic biota. *Mar. Policy*. 114:103442. doi: 10.1016/j.marpol.2019.02.014

Clarke, T. A. (1973). Some aspects of the ecology of lanternfishes (myctophidae) in the Pacific Ocean near Hawaii. *Fish. Bull.* 71, 401–434.

Clarke, T. A. (1974). Some aspects of the ecology of stomiatoid fishes in the Pacific Ocean near Hawaii. *Fish. Bull.* 72, 337–351.

Clarke, T. A. (1976). Vertical distribution and other aspects of the ecology of certain mesopelagic fishes taken near Hawaii. *Fish. Bull.* 74, 635–645.

Cribari-Neto, F., and Zeileis, A. (2009). *Beta Regression in R**.

Davison, P. (2011). The specific gravity of mesopelagic fish from the northeastern Pacific Ocean and its implications for acoustic backscatter. *ICES J. Mar. Sci.* 68, 2064–2074. doi: 10.1093/icesjms/fsr140

Davison, P. C., Checkley, D. M., Koslow, J. A., and Barlow, J. (2013). Carbon export mediated by mesopelagic fishes in the northeast Pacific Ocean. *Prog. Oceanogr.* 116, 14–30. doi: 10.1016/j.pocean.2013.05.013

Davison, P. C., Koslow, J. A., and Kloser, R. J. (2015). Acoustic biomass estimation of mesopelagic fish: backscattering from individuals, populations, and communities. *ICES J. Mar. Sci.* 72, 1413–1424. doi: 10.1093/icesjms/fsv023

De Robertis, A. (2002). Size-dependent visual predation risk and the timing of vertical migration: an optimization model. *Limnol. Oceanogr.* 47, 925–933. doi: 10.4319/lo.2002.47.4.0925

Deines, K. L. (1999). "Backscatter estimation using broadband acoustic Doppler current profilers," in *Proceedings of the IEEE Sixth Working Conference on Current Measurement (Cat. No. 99CH36331)*, (Piscataway,NJ: IEEE), 249–253.

Dickson, R. R. (1972). On the relationship between ocean transparency and the depth of sonic scattering layers in the North Atlantic. *ICES J. Mar. Sci.* 34, 416–422. doi: 10.1093/icesjms/34.3.416

Dietz, R. S. (1948). Deep scattering layer in the Pacific and Antarctic Oceans. *J. Mar. Res.* 7, 430–442.

Dornan, T., Fielding, S., Saunders, R. A., and Genner, M. J. (2019). Swimbladder morphology masks Southern Ocean mesopelagic fish biomass. *Proc. R. Soc. B* 286:20190353. doi: 10.1098/rspb.2019.0353

D'Ovidio, F., De Monte, S., Penna, A. D., Cotté, C., and Guinet, C. (2013). Ecological implications of eddy retention in the open ocean: a Lagrangian approach. *J. Phys. A Math. Theor.* 46, 1–22. doi: 10.1088/1751-8113/46/25/254023

Drazen, J. C., De Forest, L. G., and Domokos, R. (2011). Micronekton abundance and biomass in Hawaiian waters as influenced by seamounts, eddies, and the moon. *Deep Sea Res. Part I Oceanogr. Res. Pap.* 58, 557–566. doi: 10.1016/j.dsr.2011.03.002

Drazen, J. C., Smith, C. R., Gjerde, K. M., Haddock, S. H. D., Carter, G. S., Choy, C. A., et al. (2020). Midwater ecosystems must be considered when evaluating environmental risks of deep-sea mining. *Proc. Natl. Acad. Sci. U.S.A.* 117, 17455–17460. doi: 10.1073/pnas.2011914117

Drazen, J. C., and Sutton, T. T. (2017). Dining in the deep: the feeding ecology of deep-sea fishes. *Ann. Rev. Mar. Sci.* 9, 337–366. doi: 10.1146/annurev-marine-010816-060543

Ducklow, H. W., Steinberg, D. K., and Buesseler, K. O. (2001). Upper ocean carbon export and the biological pump. *Oceanogr. DC-Oceanogr. Soc.* 14, 50–58. doi: 10.5670/oceanog.2001.06

Escobar-Flores, P. C., Ladroit, Y., and O'Driscoll, R. L. (2019). Acoustic assessment of the micronekton community on the Chatham Rise, New Zealand, using

a semi-automated approach. *Front. Mar. Sci.* 6:507. doi: 10.3389/fmars.2019.00507

Escobar-Flores, P. C., O'Driscoll, R. L., and Montgomery, J. C. (2018). Predicting distribution and relative abundance of mid-trophic level organisms using oceanographic parameters and acoustic backscatter. *Mar. Ecol. Prog. Ser.* 592, 37–56. doi: 10.3354/meps12519

Giam, X., and Olden, J. D. (2016). Quantifying variable importance in a multimodel inference framework. *Methods Ecol. Evol.* 7, 388–397. doi: 10.1111/2041-210X.12492

Gostiaux, L., and Van Haren, H. (2010). Extracting meaningful information from uncalibrated backscattered echo intensity data. *J. Atmos. Ocean. Technol.* 27, 943–949. doi: 10.1175/2009jtecho704.1

Halsey, L. G. (2019). The reign of the p-value is over: what alternative analyses could we employ to fill the power vacuum? *Biol. Lett.* 15:20190174. doi: 10.1098/rsbl.2019.0174

Harrison, X. A., Donaldson, L., Correa-Cano, M. E., Evans, J., Fisher, D. N., Goodwin, C. E. D., et al. (2018). A brief introduction to mixed effects modelling and multi-model inference in ecology. *PeerJ* 6:e4794.

Hirst, A. G., and Bunker, A. J. (2003). Growth of marine planktonic copepods: global rates and patterns in relation to chlorophyll a, temperature, and body weight. *Limnol. Oceanogr.* 48, 1988–2010. doi: 10.4319/lo.2003.48.5.1988

Hofmann, A. F., Peltzer, E. T., Walz, P. M., and Brewer, P. G. (2011). Hypoxia by degrees: establishing definitions for a changing ocean. *Deep. Res. Part I Oceanogr. Res. Pap.* 58, 1212–1226. doi: 10.1016/j.dsr.2011.09.004

Isaacs, J. D., Tont, S. A., and Wick, G. L. (1974). Deep scattering layers: vertical migration as a tactic for finding food. *Deep Sea Res. Oceanogr. Abstracts* 21, 651–656. doi: 10.1016/0011-7471(74)90049-7

Jones, D. O. B., Kaiser, S., Sweetman, A. K., Smith, C. R., Menot, L., Vink, A., et al. (2017). Biological responses to disturbance from simulated deep-sea polymetallic nodule mining. *PLoS One* 12:e0171750. doi: 10.1371/journal.pone.0171750

Kampa, E. M. (1975). Observations of a sonic-scattering layer during the total solar eclipse 30 June, 1973. *Deep Sea Res. Oceanogr. Abstracts* 22, 417–423. doi: 10.1016/0011-7471(75)90063-7

Kenaley, C. P. (2008). Diel vertical migration of the loosejaw dragonfishes (Stomiiformes: stomiidae: malacosteinae): a new analysis for rare pelagic taxa. *J. Fish Biol.* 73, 888–901. doi: 10.1111/j.1095-8649.2008.01983.x

Klevjer, T. A., Irigoien, X., Røstad, A., Fraile-Nuez, E., Benítez-Barrios, V. M., and Kaartvedt, S. (2016). Large scale patterns in vertical distribution and behaviour of mesopelagic scattering layers. *Sci. Rep.* 6:19873.

Kloser, R. J., Ryan, T., Sakov, P., Williams, A., and Koslow, J. A. (2002). Species identification in deep water using multiple acoustic frequencies. *Can. J. Fish. Aquat. Sci.* 59, 1065–1077. doi: 10.1139/f02-076

Lampert, W. (1989). The adaptive significance of diel vertical migration of zooplankton. *Funct. Ecol.* 3, 21–27. doi: 10.2307/2389671

Lampert, W. (1993). Ultimate causes of diel vertical migration of zooplankton: new evidence for the predator-avoidance hypothesis. *Diel Vertical Migration of Zooplankton* 79–88.

Legendre, L., and Michaud, J. (1999). Chlorophyll a to estimate the particulate organic carbon available as food to large zooplankton in the euphotic zone of oceans. *J. Plankton Res.* 21, 2067–2083. doi: 10.1093/plankt/21.11.2067

Loeb, V. J., and Nichols, J. A. (1984). Vertical distribution and composition of ichthyoplankton and invertebrate zooplankton assemblages in the eastern tropical Pacific. *Biol. Pesq.* 13, 39–66.

Longhurst, A. R., Bedo, A. W., Harrison, W. G., Head, E. J. H., and Sameoto, D. D. (1990). Vertical flux of respiratory carbon by oceanic diel migrant biota. *Deep Sea Res. Part A. Oceanogr. Res. Pap.* 37, 685–694. doi: 10.1016/0198-0149(90)90098-g

Lukacs, P. M., Burnham, K. P., and Anderson, D. R. (2010). Model selection bias and Freedman's paradox. *Ann. Inst. Stat. Math.* 62:117. doi: 10.1007/s10463-009-0234-4

Maas, A. E., Frazar, S. L., Outram, D. M., Seibel, B. A., and Wishner, K. F. (2014). Fine-scale vertical distribution of macroplankton and micronekton in the Eastern Tropical North Pacific in association with an oxygen minimum zone. *J. Plankton Res.* 36, 1557–1575. doi: 10.1093/plankt/fbu077

Maynard, S. D., Riggs, F. V., and Walters, J. F. (1975). Mesopelagic micronekton in Hawaiian waters: faunal composition, standing stock, and diel vertical migration. *Fish. Bull.* 73, 726–736.

Mizobata, K., Saitoh, S. I., Shiomoto, A., Miyamura, T., Shiga, N., Imai, K., et al. (2002). Bering Sea cyclonic and anticyclonic eddies observed during summer 2000 and 2001. *Prog. Oceanogr.* 55, 65–75. doi: 10.1016/s0079-6611(02)00070-8

Netburn, A. N., and Koslow, J. A. (2015). Dissolved oxygen as a constraint on daytime deep scattering layer depth in the southern California current ecosystem. *Deep Sea Res. Part I Oceanogr. Res. Pap.* 104, 149–158. doi: 10.1016/j.dsr.2015.06.006

Phleger, C. F. (1998). Buoyancy in marine fishes: direct and indirect role of lipids. *Am. Zool.* 38, 321–330. doi: 10.1093/icb/38.2.321

Proud, R., Cox, M. J., and Brierley, A. S. (2017). Biogeography of the global ocean's mesopelagic zone. *Curr. Biol.* 27, 113–119. doi: 10.1016/j.cub.2016.11.003

Proud, R., Cox, M. J., Le Guen, C., and Brierley, A. S. (2018). Fine-scale depth structure of pelagic communities throughout the global ocean based on acoustic sound scattering layers. *Mar. Ecol. Prog. Ser.* 598, 35–48. doi: 10.3354/meps12612

Proud, R., Handegard, N. O., Kloser, R. J., Cox, M. J., Brierley, A. S., and Demer, D. (2019). From siphonophores to deep scattering layers: uncertainty ranges for the estimation of global mesopelagic fish biomass. *ICES J. Mar. Sci.* 76, 718–733.

Python Core Team (2020). *Python: A dynamic, Open Source Programming Language*. Available online at*: https://www.python.org/

R Core Team. (2020). *R: A Language and Environment for Statistical Computing*. Available online at*: https://www.r-project.org/

Sameoto, D. D. (1986). Influence of the biological and physical environment on the vertical distribution of mesozooplankton and micronekton in the eastern tropical Pacific. *Mar. Biol.* 93, 263–279. doi: 10.1007/bf00508264

Seibel, B. A. (2011). Critical oxygen levels and metabolic suppression in oceanic oxygen minimum zones. *J. Exp. Biol.* 214, 326–336. doi: 10.1242/jeb.049171

Seibel, B. A., Schneider, J. L., Kaartvedt, S., Wishner, K. F., and Daly, K. L. (2016). Hypoxia tolerance and metabolic suppression in oxygen minimum zone euphausiids: implications for ocean deoxygenation and biogeochemical cycles. *Integr. Comp. Biol.* 56, 510–523. doi: 10.1093/icb/icw091

Simmonds, J., and MacLennan, D. N. (2008). *Fisheries Acoustics: Theory and Practice*. Hoboken, NJ: John Wiley & Sons.

Sutton, T. T., Clark, M. R., Dunn, D. C., Halpin, P. N., Rogers, A. D., Guinotte, J., et al. (2017). A global biogeographic classification of the mesopelagic zone. *Deep. Res. Part I Oceanogr. Res. Pap.* 126, 85–102. doi: 10.1016/j.dsr.2017.05.006

Sutton, T. T., Wiebe, P. H., Madin, L., and Bucklin, A. (2010). Diversity and community structure of pelagic fishes to 5000 m depth in the Sargasso Sea. *Deep Sea Res. Part II Top. Stud. Oceanogr.* 57, 2220–2233. doi: 10.1016/j.dsr2.2010.09.024

Urmy, S. S., and Horne, J. K. (2016). Multi-scale responses of scattering layers to environmental variability in Monterey Bay, California. *Deep Sea Res. Part I Oceanogr. Res. Pap.* 113, 22–32. doi: 10.1016/j.dsr.2016.04.004

Urmy, S. S., Horne, J. K., and Barbee, D. H. (2012). Measuring the vertical distributional variability of pelagic fauna in Monterey Bay. *ICES J. Mar. Sci.* 69, 184–196. doi: 10.1093/icesjms/fsr205

Webb, T. J., Berghe, E. V., and O'Dor, R. (2010). Biodiversity's big wet secret: the global distribution of marine biological records reveals chronic under-exploration of the deep pelagic ocean. *PLoS One* 5:e10223. doi: 10.1371/journal.pone.0010223

Wedding, L. M., Friedlander, A. M., Kittinger, J. N., Watling, L., Gaines, S. D., Bennett, M., et al. (2013). From principles to practice: a spatial approach to systematic conservation planning in the deep sea. *Proc. R. Soc. London B Biol. Sci.* 280:20131684. doi: 10.1098/rspb.2013.1684

Wedding, L. M., Reiter, S. M., Smith, C. R., Gjerde, K. M., Kittinger, J. N., Friedlander, A. M., et al. (2015). Managing mining of the deep seabed. *Science (80-.).* 349, 144–145.

Wishner, K. F., Outram, D. M., Seibel, B. A., Daly, K. L., and Williams, R. L. (2013). Zooplankton in the eastern tropical north Pacific: boundary effects of oxygen minimum zone expansion. *Deep Sea Res. Part I Oceanogr. Res. Pap.* 79, 122–140. doi: 10.1016/j.dsr.2013.05.012

Wishner, K. F., Seibel, B. A., Roman, C., Deutsch, C., Outram, D., Shaw, C. T., et al. (2018). Ocean deoxygenation and zooplankton: very small oxygen differences matter. *Sci. Adv.* 4:eaau5180. doi: 10.1126/sciadv.aau5180

Yentsch, C. S., and Phinney, D. A. (1989). A bridge between ocean optics and microbial ecology. *Limnol. Oceanogr.* 34, 1694–1705. doi: 10.4319/lo.1989.34.8.1694

Young, J. W., Hunt, B. P. V., Cook, T. R., Llopiz, J. K., Hazen, E. L., Pethybridge, H. R., et al. (2015). The trophodynamics of marine top predators: current knowledge, recent advances and challenges. *Deep. Res. Part II Top. Stud. Oceanogr.* 113, 170–187. doi: 10.1016/j.dsr2.2014.05.015

Conflict of Interest: The authors declare that the research was conducted in the absence of any commercial or financial relationships that could be construed as a potential conflict of interest.

Copyright © 2021 Perelman, Firing, van der Grient, Jones and Drazen. This is an open-access article distributed under the terms of the Creative Commons Attribution License (CC BY). The use, distribution or reproduction in other forums is permitted, provided the original author(s) and the copyright owner(s) are credited and that the original publication in this journal is cited, in accordance with accepted academic practice. No use, distribution or reproduction is permitted which does not comply with these terms.

frontiers in Marine Science

ORIGINAL RESEARCH
published: 13 May 2021
doi: 10.3389/fmars.2021.634803

Bacterial and Archaeal Communities in Polymetallic Nodules, Sediments, and Bottom Waters of the Abyssal Clarion-Clipperton Zone: Emerging Patterns and Future Monitoring Considerations

Emma K. Wear[1], Matthew J. Church[1,2], Beth N. Orcutt[3], Christine N. Shulse[4], Markus V. Lindh[5] and Craig R. Smith[6]*

[1] Flathead Lake Biological Station, University of Montana, Polson, MT, United States, [2] Department of Biological Sciences, University of Montana, Missoula, MT, United States, [3] Bigelow Laboratory for Ocean Sciences, East Boothbay, ME, United States, [4] Department of Biology, Los Medanos College, Pittsburg, CA, United States, [5] Swedish Meteorological and Hydrological Institute, Gothenburg, Sweden, [6] Department of Oceanography, University of Hawai'i at Mānoa, Honolulu, HI, United States

OPEN ACCESS

Edited by:
Cinzia Corinaldesi, Marche Polytechnic University, Italy

Reviewed by:
Eugenio Rastelli, University of Naples Federico II, Italy
Julia M. Otte, Aarhus University, Denmark

***Correspondence:**
Emma K. Wear
ekwear.oceans@gmail.com

Specialty section:
This article was submitted to Deep-Sea Environments and Ecology, a section of the journal Frontiers in Marine Science

Received: *28 November 2020*
Accepted: *12 April 2021*
Published: *13 May 2021*

Citation:
Wear EK, Church MJ, Orcutt BN, Shulse CN, Lindh MV and Smith CR (2021) Bacterial and Archaeal Communities in Polymetallic Nodules, Sediments, and Bottom Waters of the Abyssal Clarion-Clipperton Zone: Emerging Patterns and Future Monitoring Considerations. Front. Mar. Sci. 8:634803. doi: 10.3389/fmars.2021.634803

Bacteria and archaea are key contributors to deep-sea biogeochemical cycles and food webs. The disruptions these microbial communities may experience during and following polymetallic nodule mining in the Clarion-Clipperton Zone (CCZ) of the North Pacific Ocean could therefore have broad ecological effects. Our goals in this synthesis are to characterize the current understanding of biodiversity and biogeography of bacteria and archaea in the CCZ and to identify gaps in the baseline data and sampling approaches, prior to the onset of mining in the region. This is part of a large effort to compile biogeographic patterns in the CCZ, and to assess the representivity of no-mining Areas of Particular Environmental Interest, across a range of taxa. Here, we review published studies and an additional new dataset focused on 16S ribosomal RNA (rRNA) gene amplicon characterization of abyssal bacterial and archaeal communities, particularly focused on spatial patterns. Deep-sea habitats (nodules, sediments, and bottom seawater) each hosted significantly different microbial communities. An east-vs.-west CCZ regional distinction was present in nodule communities, although the magnitude was small and likely not detectable without a high-resolution analysis. Within habitats, spatial variability was driven by differences in relative abundances of taxa, rather than by abundant taxon turnover. Our results further support observations that nodules in the CCZ have distinct archaeal communities from those in more productive surrounding regions, with higher relative abundances of presumed chemolithoautotrophic *Nitrosopumilaceae* suggesting possible trophic effects of nodule removal. Collectively, these results indicate that bacteria and archaea in the CCZ display previously undetected, subtle, regional-scale biogeography. However, the currently available microbial community surveys are spatially limited and suffer from sampling and analytical differences that frequently confound inter-comparison; making

definitive management decisions from such a limited dataset could be problematic. We suggest a number of future research priorities and sampling recommendations that may help to alleviate dataset incompatibilities and to address challenges posed by rapidly advancing DNA sequencing technology for monitoring bacterial and archaeal biodiversity in the CCZ. Most critically, we advocate for selection of a standardized 16S rRNA gene amplification approach for use in the anticipated large-scale, contractor-driven biodiversity monitoring in the region.

Keywords: bacteria, archaea, 16S rRNA gene amplicons, Clarion-Clipperton Zone, polymetallic nodule, sediment, abyssal plain, biodiversity

INTRODUCTION

Deep-sea bacteria and archaea (hereafter referred to as microbes) are some of the most abundant lifeforms below the sunlit ocean (Whitman et al., 1998; Kallmeyer et al., 2012) and constitute the greatest standing stocks of biomass inhabiting the seafloor at depths of abyssal plains and below (Wei et al., 2010; Danovaro et al., 2015), in part because of the variety of habitats in which they can survive. In the abyssal plains of the Clarion-Clipperton Zone (CCZ), microbial habitats include polymetallic nodules as well as the more cosmopolitan habitats of sediments and the overlying water column. The CCZ, an approximately 6,000,000 km^2 region in international jurisdiction in the equatorial North Pacific (Wedding et al., 2013), contains the greatest observed concentrations of seabed nodule deposits (International Seabed Authority, 2010). Proposed polymetallic nodule mining operations, currently in the exploratory phase but expected to reach commercial feasibility within the coming decade (Hein et al., 2020) will therefore impact CCZ microbial habitats in a variety of ways, the most obvious being the physical removal of nodules from large swathes of the seafloor. Current mining technology will also necessitate removal of surface sediments and benthic boundary layer water along with nodules. This will result in a pronounced increase in sediment plumes from both direct seafloor disturbance and waste sediment disposal (Christiansen et al., 2020; Drazen et al., 2020), to which local biota – including microbes – are unlikely to be accustomed (Smith et al., 2020).

Microbes play critical and diverse roles in energy acquisition pathways and nutrient cycles in the abyss, including both chemoheterotrophic and chemoautotrophic metabolisms and substantial elemental transformations associated with nitrogen, phosphorus, sulfur, iron, and manganese cycling (Orcutt et al., 2011). There are therefore motivations beyond conservation of biodiversity to improve our understanding of the extant microbial communities in the abyssal CCZ prior to human-induced disturbance: in addition to critical ecological functions, mining activity may also detrimentally impact societally relevant ecosystem services provided by microbes in these regions (Thurber et al., 2014; Orcutt et al., 2020). Further, similar to the situation with other deep-sea organisms, abyssal microbes are poorly known to science – the putative metabolic functions and phylogeny of major groups of deep-sea bacteria and archaea are still actively being described in the literature (Baker et al., 2021): e.g., the little-known candidate order *Woeseiales* (Hoffmann et al., 2020) and putative heterotrophic deep-sea *Thaumarchaeota*, in contrast with the canonical autotrophic ammonia oxidizers (Aylward and Santoro, 2020).

This combination of factors suggests that, despite the likely importance of microbial communities to the overall biogeochemical and ecological function of the abyssal plains of the CCZ, we are unable to fully describe their roles in this ecosystem. And while bacteria and archaea in general have much shorter generation times than macro-organisms, current evidence indicates that deep-sea microbes impacted by mining will not recover quickly. A recent return visit to the site of the DISCOL simulated small-scale mining experiment in the Peru Basin found that portions of the disturbed areas retained persistently lower CO_2 fixation rates, reduced hydrolytic extracellular enzyme activity, and reduced microbial cell abundances relative to nearby reference sites, 26 years after the sediments were initially disturbed (Vonnahme et al., 2020). Deep-sea nodules themselves have been estimated to accrete at rates on the order of millimeters per 10^6 years (Ku and Broecker, 1969; Hein et al., 2020); thus, their removal will functionally lead to the extirpation of any microbes that rely on them for habitat. It is therefore particularly important that the reserve areas set aside from mining impacts, such as the nine current Areas of Particular Environmental Interest (APEIs), which cover 24% of the CCZ planning region (Wedding et al., 2013; see **Figure 1**), are representative of the taxonomic structure and metabolic function of microbial communities of the surrounding habitats.

Because the energy used by abyssal microbes at sites such as the CCZ that are distant from hydrothermal features ultimately derives from inputs from the surface ocean, the biogeochemical gradients in the upper water column of the south-eastern Pacific raise the possibility of similar, related habitat gradients at the seafloor. These biogeochemical gradients include particulate organic carbon flux to the sediments, which decreases northward from the equatorial upwelling region into the stratified gyre proper, as well as from east to west (Christian et al., 2002; McQuaid et al., 2020; Washburn et al., 2021). East-west variability in particulate organic carbon flux has been posited to explain spatial patterns in species richness of nodule-associated xenophyophores and metazoans (Veillette et al., 2007). The southeastern corner of the CCZ encompasses the pronounced oxygen minimum zone of the eastern tropical

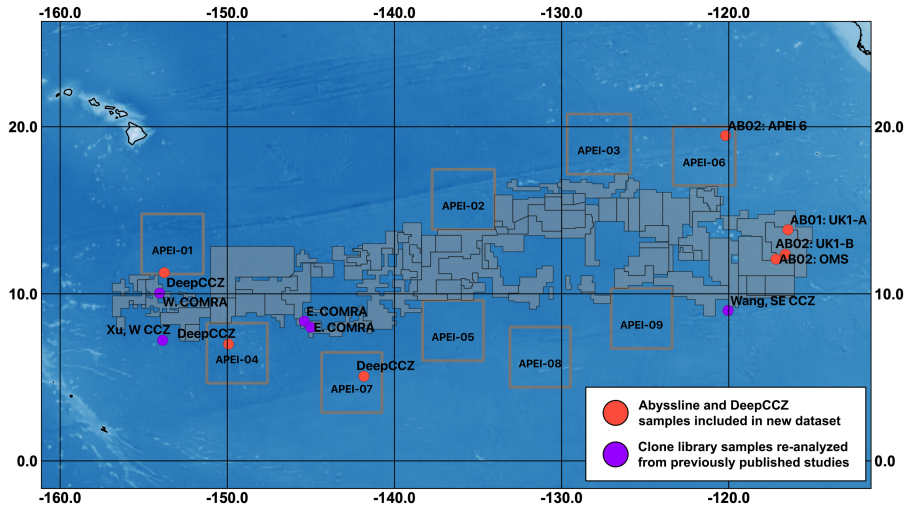

FIGURE 1 | Map of sampling sites for datasets included in this synthesis and designated exploration license and APEI areas within the CCZ. Sampling regions are labeled with unique cruise and/or location identifiers (see **Table 1**). Solid gray polygons represent both reserved and exploration areas, as designated by the International Seabed Authority; squares outlined in gray are APEIs. COMRA, China Ocean Mineral Resources R&D Association contract area (which is divided into east and west regions); UK1, UK Seabed Resources Ltd contract area, with two sampling sites (A and B); OMS, Ocean Mineral Singapore contract area. The three west COMRA sampling sites in the western CCZ share one location dot. For fine-scale sample locations for Abyssline (sampled from 30 × 30 km areas in UK1 and OMS; Lindh et al., 2017) and DeepCCZ (samples collected within 15 km of one another at each site) cruises, see **Supplementary Table 1**.

North Pacific (Talley, 2007), which may further impact the quantity and composition of organic matter reaching the benthos. More directly, nodule abundance and sediment composition also vary within the CCZ, inherently affecting habitat quality and availability for benthic microbes (International Seabed Authority, 2010; McQuaid et al., 2020).

To better understand the current state of knowledge of bacterial and archaeal microbes in the CCZ, here we synthesize a new dataset from polymetallic nodules, sediment, and bottom waters of the CCZ with published datasets from the CCZ and other regions. Our goals in this synthesis are to characterize the current understanding of biodiversity and biogeography of bacteria and archaea in the CCZ and to identify gaps in the baseline data and sampling approaches, prior to the onset of mining in the region. We describe observed biogeographic patterns as they relate both to habitat type (that is, nodules vs. sediments vs. bottom waters) and to spatial distribution. In addition, we highlight how gaps in available data hinder prediction in how these habitats might respond to mining disturbances. We focus here (1) on bacteria and archaea and not on eukaryotic microbes such as the protists or the fungi, as the former two groups have historically been sampled independently from the latter, and (2) on the abyssal water column and benthic habitats, as this is where the majority of published microbial datasets from the CCZ have concentrated their efforts. This is not to suggest that the shallower pelagic environments are expected to be spared the impact of nodule mining; on the contrary, the release of waste sediments into the water column will likely have substantial and still poorly understood impacts on the structure and activity of midwater pelagic communities of all taxa, including the microbes (Drazen et al., 2020). However, there are not at present sufficient, validly inter-comparable samples from the overlying water column of the CCZ to make a meaningful assessment of spatial heterogeneity.

Caveats in Assessing Microbial Biodiversity From DNA Sequencing Data

A substantial caveat limiting our ability to directly compare results across existing studies results from the rapid shifts in techniques used to characterize bacterial and archaeal communities over the past approximately 15 years. Marine bacteria and archaea are primarily identified through molecular techniques, in particular taxonomic profiling targeting various hypervariable regions of the 16S small subunit ribosomal RNA (rRNA) marker gene. The move from gene cloning and Sanger sequencing to next-generation sequencing (NGS) techniques such as Illumina sequencing (see review in Klindworth et al., 2013) has increased the number of sequences attainable per sample by several orders of magnitude, in turn increasing the detected richness and diversity of the microbial communities (e.g., Sogin et al., 2006), and this discrepancy only grows as technological advances continue to increase the sequencing depth per run and decrease the cost per read. Much of the early work on CCZ microbes was conducted with Sanger sequencing of cloned 16S rRNA gene amplicons, while many recent samples have been sequenced with NGS, complicating inter-cruise comparisons and detection of any potential temporal patterns in biodiversity.

Further, polymerase chain reaction (PCR) primers used to amplify 16S rRNA genes have changed substantially in recent years. Improvements in primer design have increased detection of abundant and cosmopolitan marine microbes such as the SAR11 clade in the water column (Apprill et al., 2015; Parada et al., 2016)

and the *Thaumarchaeota* (Parada et al., 2016). Studies within the CCZ have also used PCR primers that target different combinations of 16S rRNA gene hypervariable regions, which can affect measures of richness and diversity in addition to the taxonomic composition of the resulting libraries (Klindworth et al., 2013; Wear et al., 2018; see also **Supplementary Figures 1–3** for a direct example). These effects limit our ability to validly, directly compare results between studies conducted with different 16S rRNA gene primer sets at the level of taxonomic composition. Thus, where necessary, we qualify results with relevant caveats and in some cases omit comparisons between datasets that would otherwise be of interest. We conclude with recommendations that could help to minimize these issues in the future.

MATERIALS AND METHODS

Generation of New Dataset

To address the inter-comparability issues introduced by variability in primer choice, we re-sequenced selected benthic boundary layer water, sediment, and nodule genomic DNA samples from the Abyssline cruise program (see **Table 1**; Lindh et al., 2017; Shulse et al., 2017). We compared these samples with a new dataset collected as part of the DeepCCZ cruise to the western CCZ in spring 2018. DeepCCZ aimed to characterize biodiversity within the three westernmost APEIs. We report here a subset of samples focused on bottom water [nominally 5 m above bottom (MAB)], upper sediments (surface to 5 cm depth), and nodules; additional samples will be described elsewhere.

On the DeepCCZ cruise, water column samples were collected via Niskin bottles affixed to a sampling rosette, with an altimeter allowing sampling of water ∼5 MAB. Seawater (ca. 7.5–8 L) was prefiltered via gentle peristaltic pressure through 3 μm pore size, 25 mm diameter polycarbonate prefilters (Millipore Isopore) to remove macro-organisms and large particles followed by 0.2 μm pore size, 25 mm diameter polyethersulfone filters (Supor) in series to concentrate microbes. Only results from 0.2 μm pore size filters are reported here. Filters were stored dry at −80°C. Sampling bottles, tubing, and filter holders were rinsed in Milli-Q water between casts.

Sediments were collected via the ROV *Lu'ukai* using a push corer. Sediment was extruded and sliced into horizons; we report here the upper horizons, from surface−0.5 cm depth; 0.5–1 cm; and 1–5 cm. The upper two sections were transferred to sterile Whirl-Pak bags and frozen at −80°C. For the larger 1–5 cm section, sterile plastic syringes with the tips cut off were used to subsample sediment from the center of the slices (∼20–30 mLs) for freezing in Whirl-Pak bags. Core tubes were washed with dish soap and soaked in 10% bleach, followed by a Milli-Q water rinse, between ROV deployments. Sampling gear such as slicing plates was rinsed with Milli-Q water between cores and soaked in 10% bleach between dives.

Nodules were collected either from push cores or by targeted sampling with the manipulator arm of the ROV. Nodules were gently rinsed with 0.2-μm filtered seawater to remove attached sediments, measured and photographed, and frozen whole at −80°C.

DNA from water column filters was extracted using the DNeasy Plant Mini Kit as described in Shulse et al. (2017). Nodule and sediment DNA was extracted using the FastDNA Spin Kit for Soil (MP Biomedical) with modifications as described in Shulse et al. (2017). Sediment samples were homogenized in the Whirl-Pak bag before DNA was extracted from ∼0.5 g subsamples. Whole nodules were broken apart within a Whirl-Pak bag using a ceramic pestle and resulting particles were mixed; when nodules were large enough, DNA was extracted from replicate ∼0.5 g subsamples and then pooled (For detailed methods for DNA extraction through bioinformatics, see **Supplementary Information**). All extracted samples were concentrated with the Zymo Clean & Concentrator-5 kit.

On the Abyssline cruises, benthic sediment and nodule samples were retrieved using box corers and Megacorers. Sediments were collected from the surface to 5 cm depth horizon. Deep water samples (8 L) were collected whole on a 0.2 μm pore size filter without prefiltering. DNA was extracted using similar methods.

16S rRNA gene amplicons were generated using primers targeting the V4-V5 hypervariable regions: 515F-Y (5′-GTGYC AGCMGCCGCGGTAA-3′) and 926R (5′-CCGYCAATTYM TTTRAGTTT-3′) as recommended by Parada et al. (2016) with a multiplexing index on the forward primer following the design of the Earth Microbiome Project (Caporaso et al., 2012). Triplicate amplifications were combined and cleaned using an ENZA Cycle Pure Kit (Omega Bio-tek) then pooled into two libraries. Libraries were sequenced on an Illumina MiSeq using paired-end 250 v2 chemistry. Amplicon sequence variants (ASVs) were generated using DADA2 v1.14.1 (Callahan et al., 2016). ASVs are error-corrected, discrete DNA sequences which can differ from one another by as little as a single base pair, in contrast with operational taxonomic units (OTUs), which cluster closely related sequences based on a pre-defined percent nucleotide dissimilarity (Callahan et al., 2016). ASVs were classified to the Silva v138 database (Quast et al., 2013). All code is available at https://github.com/ekwear/DeepCCZreview.

Individual samples were randomly subsampled to 6,900 sequences using the "rrarefy" function in the R package vegan (Oksanen et al., 2019). Singlet ASVs were removed (for final totals of 6,805–6,876 sequences per sample) and relative abundances were calculated. Weighted UniFrac distance was generated using the R package phyloseq (McMurdie and Holmes, 2013).

Non-metric multidimensional scaling ordinations and multivariate statistics were conducted, and diversity metrics were calculated, in Primer-E v6 (Clarke and Gorley, 2006). Analysis of Similarity (ANOSIM) tests were conducted using weighted UniFrac distances between communities that had been calculated based on ASV-level composition. Two outlier samples from AB02 were discarded based on ordination patterns. Differentially abundant ASVs were identified using the R package DESeq2 (Love et al., 2014). We considered as significantly differentially abundant those ASVs with a greater than three-fold difference between categories (that is, a log2-fold change between categories > 1.585) and a false discovery rate-adjusted $p < 0.05$. Throughout the text, the phrase

"differential abundance" specifically refers to DESeq2 results that have met this significance threshold.

Literature Survey and Dataset Reanalysis

We aggregated datasets where community level, amplicon-based 16S rRNA gene sequences from the CCZ were publicly available, through a combination of literature surveys, public database reviews, and expert knowledge of cruises within the CCZ. **Figure 1** and **Table 1** highlight the locations of the datasets included in the analysis. We opted not to include microbial sequences from isolates or metagenomes in our spatial comparison of microbial community composition, as these approaches provide different types of information than 16S rRNA gene amplicon surveys; such studies from the CCZ are also numerically sparse and geographically clustered, limiting their utility for spatial analysis. A small number of published studies where raw sequence results were not available in a public database, or where the public database was missing metadata necessary for sample identification, were included in the discussion where relevant but not in the reanalysis. We also omitted those studies that sampled exclusively the upper water column.

To standardize taxonomic classifications to the greatest extent possible, we reanalyzed previously published sequences meeting the above qualifications (**Table 1**). Clone library sequences from Xu et al. (2005), Wang et al. (2010), and Wu et al. (2013) were

TABLE 1 | 16S rRNA gene amplicon datasets included in synthesis.

References	Cruise, year	General location in CCZ	Latitude(s) °N	Longitude(s) °W	Habitats (# of samples)	Bottom depth (m)	Taxa targeted	Hypervariable regions sequenced	Primer set(s) used
Amplicons sequenced from clone libraries									
Xu et al., 2005	DY105-11, 2001	Western CCZ	7.23	153.87	Sediment (1) [71 clones][2]	5,027	Bacteria Archaea	B: V1-V9 A: V1-V5	B: 27F, 1492R A: 21F, 958R
Wang et al., 2010	2005	East COMRA[1]	8.00–8.38	145.00–145.40	Sediment (2) [45–58 clones]	5,197–5,307	Bacteria	V1–V9	27F, 1492R
		West COMRA	10.04	154.02	Sediment (1) [49 clones]	5,120			
		Southeastern CCZ	9.00	120.42	Sediment (1) [71 clones]	4,299			
Wu et al., 2013	DY115-21	West COMRA	10.03–10.05	154.03–154.07	Sediment (2) Nodule (2) [179–351 clones]	5,178–5,189	Bacteria Archaea	B: V1–V9 A: V1–V7	B: 8F, 1492R A: 571F, 1204R
Next-gen (Illumina) amplicon sequencing									
Resequenced from Shulse et al. (2017)	Abyssline 1 (AB01), 2013	UK1-A[1]	13.75–13.96	116.46–116.71	Water (3) Sediment (18) Nodule (9)	4,025–4,166	Bacteria Archaea	V4–V5	515F-Y, 926R
Resequenced from Lindh et al. (2017)	Abyssline 2 (AB02), 2015	UK1-B	12.22–12.58	116.51–117.34	Water (4) Sediment (6) Nodule (8)	4,126–4,237	Bacteria Archaea	V4–V5	515F-Y, 926R
		OMS[1]	12.01–12.52	116.70–117.38	Water (3) Sediment (9) Nodule (10)	4,072–4,185			
		APEI 6	19.47	120.19	Water (1)[3] Sediment (2) Nodule (2)	4,115			
New, this manuscript	DeepCCZ, 2018	APEI 1	11.25–11.28	153.61–153.75	Water (2) Sediment (12)[3] Nodule (8)[4]	5,204–5,238[5]	Bacteria Archaea	V4–V5	515F-Y, 926R
		APEI 4	6.98–7.04	149.91–149.94	Water (2) Sediment (18)[2] Nodule (11)[4]	5,004–5,040[5]			
		APEI 7	5.05–5.12	141.83–141.93	Water (2) Sediment (14)[3]	4,860–4,877[5]			

[1] *COMRA, China Ocean Mineral Resources R&D Association contract area (which is divided into east and west regions); UK1, UK Seabed Resources Ltd contract area, with two sampling sites (A and B); OMS, Ocean Mineral Singapore contract area.*
[2] *The number of clones passing quality control in our bioinformatics pipeline.*
[3] *Because sediment cores were sliced at different depth horizons on the DeepCCZ cruise than on the Abyssline cruises, these sediment samples include multiple three-sample depth profiles encompassing the upper 5 cm (see section "Materials and Methods").*
[4] *Nodules were collected from APEIs 1 and 4 but were not present in the sampled region of APEI 7.*
[5] *As recorded for CTD casts.*

aligned and classified to the Silva v138 database using mothur v1.42.3 (Schloss et al., 2009). Published datasets sequenced with the Illumina platform included Lindh et al. (2017) and Shulse et al. (2017). We have focused on resequenced samples rather than using original sequences from these two publications to avoid potential confounding effects of different primer sets (e.g., see **Supplementary Figures 1–3**).

Taxonomic Nomenclature

The phylogenetic relationships between, and taxonomic classifications of, marine microbes remain in flux. We have chosen herein to follow the nomenclature used in Silva v138, with the sole exception of the *Thaumarchaeota*, which are referred to as the *Crenarchaeota* in Silva v138.

Data Availability

Sequence files from DeepCCZ samples, and re-sequenced samples from the Abyssline cruises, are available from the Sequence Read Archive[1] under project code PRJNA660809. Sample metadata are available in **Supplementary Tables 1, 2**, as well as archived on Zenodo[2]; analyzed sequence results are archived on Zenodo.

RESULTS AND DISCUSSION

Our survey of the community-level microbial literature focused in the CCZ yielded three clone library studies that met our criteria for inclusion, encompassing two nodule samples and seven sediment samples, and two published NGS studies from the Abyssline cruise program, from which we resequenced 75 samples (**Table 1**) – 29 from nodules, 35 from sediment, and 11 from bottom waters. The DeepCCZ dataset added an additional 69 new samples – 19 from nodules, 44 from sediment, and 6 from bottom waters. Altogether, these studies include samples from three exploration license areas and four APEIs, as well as some samples from outside currently allocated areas (**Table 1** and **Figure 1**).

Habitat Specificity Is the Primary Driver of Microbial Community Composition

Previous studies from the CCZ (Wu et al., 2013; Shulse et al., 2017; Lindh et al., 2017) have noted the selective effect of habitat – that is, water column vs. sediment vs. nodule – in determining overall microbial community composition as well as measures of diversity and richness, regardless of methodologies used (PCR primers, sequencing technique, etc.). Our literature survey and new dataset add further support to the assessment that habitat is the primary control of microbial community composition in the CCZ (**Figures 2A**, **3** and **Supplementary Figure 4**). Overall community composition across studies was similar (**Figure 3**): where archaeal 16S rRNA genes were measured, ASVs in the family *Nitrosopumilaceae* were dominant members of all habitat types. An assortment of members of the classes *Alphaproteobacteria* and *Gammaproteobacteria* were consistently abundant, with the composition varying by habitat: the SAR11 order was very abundant in the near-seabed water samples, while the sediment and nodule samples had high relative abundances of the alphaproteobacterial order *Kiloniellales* and the gammaproteobacterial genus *Woeseia*. Most samples also contained common deep-sea phyla including the *Acidobacteria*, members of the *Bacteroidota*, and the *Planctomycetota*. Where there were clear differences between studies at a broad taxonomic level (**Figure 3**), they were between habitat types rather than between geographic locations.

Within our new dataset of DeepCCZ and re-sequenced Abyssline samples, ANOSIM tests indicated that all habitat types were significantly different from one another, even the sediment and nodule communities that were in some cases collected in physical contact with one another (**Supplementary Table 3**). While sediment and nodule communities shared a high proportion (>85%) of abundant ASVs (with abundant ASVs defined here as those with a cumulative relative abundance within two orders of magnitude of the maximum cumulative relative abundance within a habitat; see **Supplementary Figure 5**), only about 16% of abundant ASVs were present in both water samples and at least one benthic habitat (**Supplementary Figure 5D**). In addition to the differences in ASV presence, there were strong patterns in differential abundance as identified by DESeq2 analysis between habitats, with 2,490 ASVs differentially abundant between nodules and water samples; 2,947 between sediment and water samples; and 1,607 between nodules and sediment (**Supplementary Figure 6** and **Supplementary Table 4**). Some of these differences at the ASV level reflect the clear ecological trends seen at broader phylogenetic levels (**Figure 3** and **Supplementary Figure 4**), such as significantly higher abundances of SAR11 and phylum *Thermoplasmatota* ASVs in water samples than in sediments and nodules.

Notably, many clades, even at taxonomic levels as low as genera, contained distinct ASVs that were enriched in each habitat (**Supplementary Figure 6**). This pattern included very common groups across CCZ habitats, such as the family *Nitrosopumilaceae*, the phylum *Planctomycetota*, and the gammaproteobacterial genus *Woeseia*. This ASV-level habitat selection adds an important nuance to the bulk views of microbial community composition, such as in **Figure 3** and **Supplementary Figure 4**: while a clade may be present and even dominant within multiple habitats in the CCZ, that does not necessarily mean the same members of that clade are present across all habitats. Tully and Heidelberg (2013) observed similar fine-scale habitat preferences within *Thaumarchaea* MG-1 OTUs collected from nodules and sediment from the South Pacific Gyre, with some OTUs shared across habitats and others limited to one habitat. Ultimately, this suggests that, to most correctly assess microbial diversity in the CCZ, we need to work at an ASV-level resolution – that is, at the highest possible resolution for amplicon data, able to identify taxa with marker genes differing by as little as a single base pair after application of an error-correction model (Callahan et al., 2017). While broad

[1] https://www.ncbi.nlm.nih.gov/sra

[2] http://doi.org/10.5281/zenodo.4214934

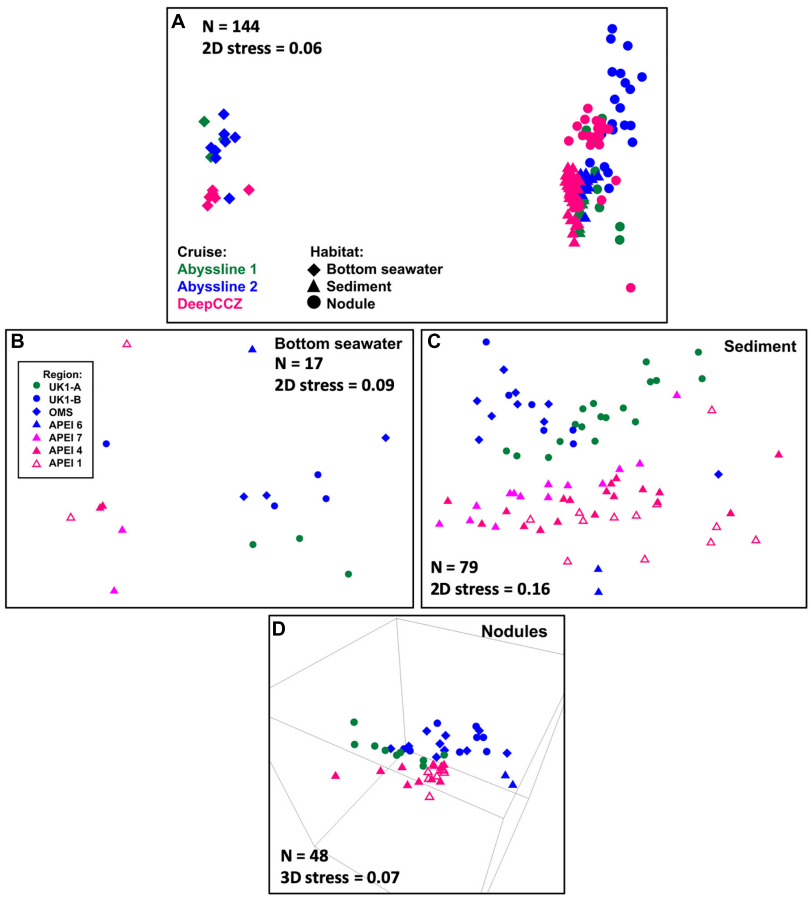

FIGURE 2 | NMS ordinations of samples from the Abyssline and DeepCCZ cruises. **(A)** Has a different legend than **(B–D)**. **(A)** All samples in the new dataset, with shape indicating benthic habitat and color indicating source cruise. For a further breakdown of sample numbers, see **Table 1**. **(B)** Bottom seawater samples. In this and subsequent panels, point color and shape indicate sample source region. **(C)** Sediment samples. This ordination is more correctly viewed as a 3D plot; see **Supplementary Video 1** for a 3D animation. The most notable difference in the 3D plot is that the two extremes of the *Y*-axis in the 2D ordination wrap around to approach each other, such that the samples from APEI 6 are not in reality as distinct from the other AB02 samples as they appear to be in this plot. **(D)** Nodules.

summaries such as **Figure 3** may be the best possible approach for combining currently available datasets that were sampled with different techniques, the fine-scale differential abundances within clades seen in this ASV-level analysis indicates that such an approach may overlook ecologically important levels of biodiversity.

Case Study: Eastern vs. Western CCZ Sites

The DeepCCZ and re-sequenced Abyssline samples allow for a direct comparison of microbial communities from the three westernmost APEIs with those from mining license exploration areas and an APEI in the northeastern CCZ. Based on non-metric multidimensional scaling (NMS) ordinations, spatial differences were present, though less pronounced than differences between spatially co-occurring habitats (e.g., sediments vs. seawater). The magnitude of spatial effects depended on habitat type. Spatial differences were most clear in the sediments (**Figure 2C** and **Supplementary Video 1**), where the samples from the western APEIs fell into a south-to-north gradient. The sediments from APEI 6 in the eastern CCZ most closely resembled those of the northernmost western APEI 1, while the sediments from the Abyssline license sites formed a distinct cluster. The bottom waters showed less spatial separation, with weak partitioning along the east-west divide (**Figure 2B**), while nodules appeared to vary more by cruise than by geographic location as such (**Figure 2D**). These biogeographic patterns are consistent with the broad patterns seen in physicochemical variables across the CCZ: bottom waters are similar across the region, while multiple parameters expected to affect benthic organisms (e.g., modeled particulate organic carbon flux to the seafloor, water depth, and sediment composition) vary both from the eastern to western CCZ and latitudinally within the western CCZ (Washburn et al., 2021).

ANOSIM comparisons indicated small but significant differences at the community level between nodules collected from the eastern CCZ versus the western CCZ (if APEI 6 is included: $R = 0.123$, $p = 0.008$; if APEI 6 is excluded: $R = 0.158$, $p = 0.003$). The majority of pairwise comparisons between

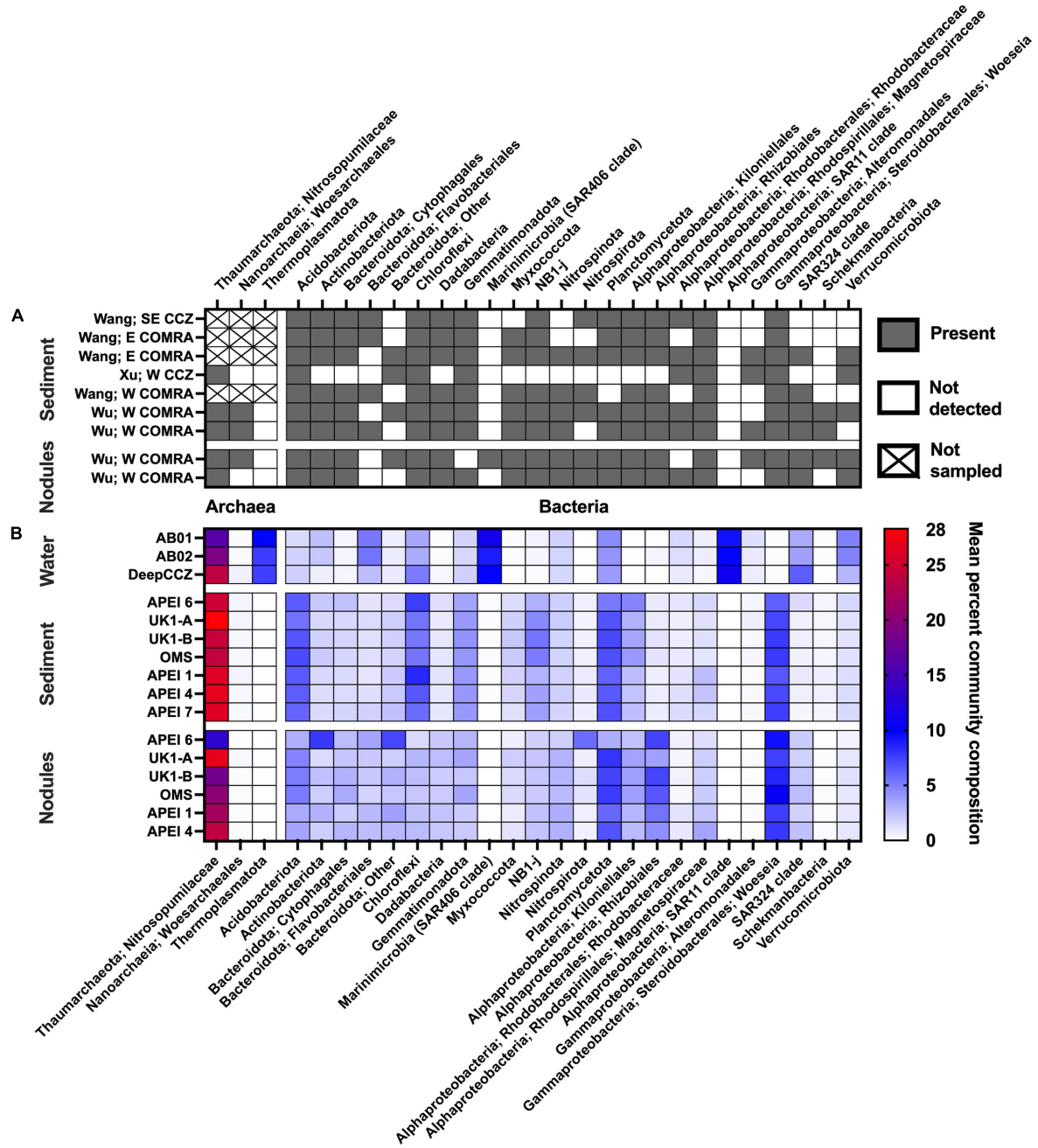

FIGURE 3 | Overview of prevalence of select clades across habitats within the CCZ. **(A)** Community composition from studies that sequenced amplicons from clone libraries, shown as presence/absence due to variable sequencing depths. "Not sampled" indicates archaeal primers were not used in the relevant study. Wang = sequences reanalyzed from Wang et al. (2010); Xu = Xu et al. (2005); and Wu = Wu et al. (2013). No clone library studies included in this synthesis reported results from water samples. **(B)** Community composition from the new dataset, shown as mean relative abundances within habitats and sites. Sites are arranged from roughly northeast to southwest, reading downward within a habitat; water samples are grouped within cruises due to limited sample numbers.

nodule communities from specific eastern and western sampling sites were likewise significantly different, while nodules from sites sampled on the same cruises did not differ at the community level (that is, APEI 4 vs. APEI 1 in the west and the UK1-B vs. OMS sites in the east; **Supplementary Table 5**). ANOSIM comparisons also suggested significant east-west differences in both bottom water and sediment samples (**Supplementary Table 5**). However, geographic distance in these comparisons is confounded with sampling differences between the DeepCCZ and Abyssline cruises, including in pre-filtering of water samples and sampling of different sediment depth horizons, and thus these observed differences may not be solely ecological in origin.

Consistent with these relatively subtle spatial patterns, the majority of abundant ASVs (defined based on cumulative relative abundances, as described above) within each habitat type (84–94%) were shared between all three cruises (**Supplementary Figure 5**), and spatial differences originated in large part from shifts in relative abundances rather than from presence/absence dynamics. DESeq2 analysis of differential abundances of ASVs within nodules (the habitat type sampled comparably across all cruises in this dataset) from the eastern and western CCZ indicated there were 375 ASVs enriched in the nodules from the eastern sites and 204 in the nodules from the western sites, out of 17,510 total ASVs present across the nodule samples (**Supplementary Figure 7** and **Supplementary Table 4**). However, these patterns were not driven by ASVs with high relative abundances, as only six differentially abundant ASVs were present at mean relative abundances of 0.5% or greater within a region (**Supplementary Table 6**). As was the case in the differential abundance analysis between habitats, several common taxonomic groups had ASVs that were enriched in each region, including the order *Nitrosopumilales*, the phylum *Gemmatimonadota*, the genus *Woeseia* in the *Gammaproteobacteria*, and the genus *Nitrospina*, suggesting some members of these groups may have preferred habitat niches across the CCZ when examined at a fine taxonomic resolution.

Diversity metrics varied between habitat types but not between geographic locations (**Figure 4**), with the exception of the benthic samples from APEI 6 (discussed below). Across cruises and stations, sediment samples had the highest observed ASV richness (mean of all samples: 1,774 ASVs), Pielou's evenness (0.91), and Shannon diversity (6.77) values; bottom water samples had the lowest values of all metrics (634; 0.82; and 5.30, respectively); and nodules were in between (1,166; 0.87; and 6.15, respectively). Although sampled volumes differed between habitats, these diversity metrics were calculated on a standardized number of sequences per sample (see section "Materials and Methods"). The bottom water samples from DeepCCZ had lower mean ASV richness and Shannon diversity than the bottom water samples from the Abyssline cruises, but as the DeepCCZ samples were subjected to a 3 μm pore-size pre-filtration step and the Abyssline samples were not, we do not have confidence that this difference is ecological rather than methodological in origin.

An unexpected result of this analysis was the relatively pronounced intra-habitat difference in sediments and nodules between spatially adjacent but temporally separated (∼17 months) Abyssline license area sites. The differences between samples collected on AB01 and AB02 were, by several measures, roughly as large as the differences between samples collected across the approximately 1,500 km latitudinal gradient of the DeepCCZ cruise or the differences between the eastern and western CCZ sites (**Figures 2**, **5** and **Supplementary Figure 8**). Nodule communities from the UK1-A site sampled on AB01 were significantly different from those from both AB02 license area sites according to an ANOSIM analysis, and sediment communities differed between the UK1-A site and the AB02 OMS license site (**Supplementary Table 5**). The Abyssline cruises had overlapping personnel and protocols, making it unlikely that this difference is solely a sampling artifact. This raises the possibility that there could be temporal as well as spatial variability in benthic microbial communities in the CCZ, which would need to be considered in assessing the extent of mining-induced community shifts, particularly in light of the relatively subtle spatial differences we find in microbial communities across the CCZ. Despite the stereotypical view of the abyssal sea as a largely stable habitat, there is evidence this is not the case for some trophic groups – for example, abyssal sediment macrofaunal community composition and function were observed to correlate with seasonal to interannual variability in particulate organic carbon flux in a decade-long study (Ruhl et al., 2008). Alternatively, our findings may indicate that spatial variability within the CCZ can be non-linear over fairly short geographic distances. Distinguishing between these effects will require more extensive datasets than are currently available, but such a distinction will be critical to designing sampling strategies that fully characterize the extant microbial biodiversity in the CCZ.

Case Study: APEI and Mining License Areas in the Eastern CCZ

Most studies of CCZ microbes have focused on either mining exploration license areas or on APEIs. An exception to this is Lindh et al. (2017), in which the authors sampled one box core and one rosette cast in an APEI (APEI 6) relatively close to the license areas that were the main focus of their work. However, given the large spatial extent of the CCZ, this still constituted an almost 900 km distance between the APEI sampling site and the closest license-area samples. Their sequencing of bacterial 16S rRNA gene amplicons indicated that community composition across all habitats – water column, sediment, and nodules – was significantly different between the APEI and corresponding samples from two nearby license areas.

Based on our spatially expanded analysis, it appears that the region of APEI 6 that Lindh et al. (2017) sampled may be an outlier relative to the CCZ in general, at least in sediments and nodules where we have enough samples for a confident assessment (see re-sequenced data in **Figures 2B–D** and **Supplementary Video 1**). Consistent with the observations of Lindh et al. (2017), the two nodules resequenced from APEI 6 had higher relative abundances of *Actinobacteria* (7.3 and 8.1%, vs. 0.4–6.1% in all other nodules) and *Nitrospira* (3.7 and 7.8%, vs. 0.1–2.8%) and lower relative abundances of *Planctomycetota* (3.1 and 3.2%, vs. 4.2–11.4%) than any other nodules included in the new dataset (**Supplementary Figure 4C**). The APEI 6 nodule samples also had low richness, evenness, and diversity metrics compared with those of the nearby license areas (**Figure 4**). These distinct benthic communities are perhaps not surprising given the location of APEI 6 on the far northeastern edge of the CCZ, and correspondingly we interpret this specific example as an illustration of the need for further comparisons between APEI and license area microbial communities. While our synthesis and new dataset both indicate that geographic variability within specific habitat types in the sampled portions of the CCZ is relatively low (that is, the absolute weighted UniFrac distances

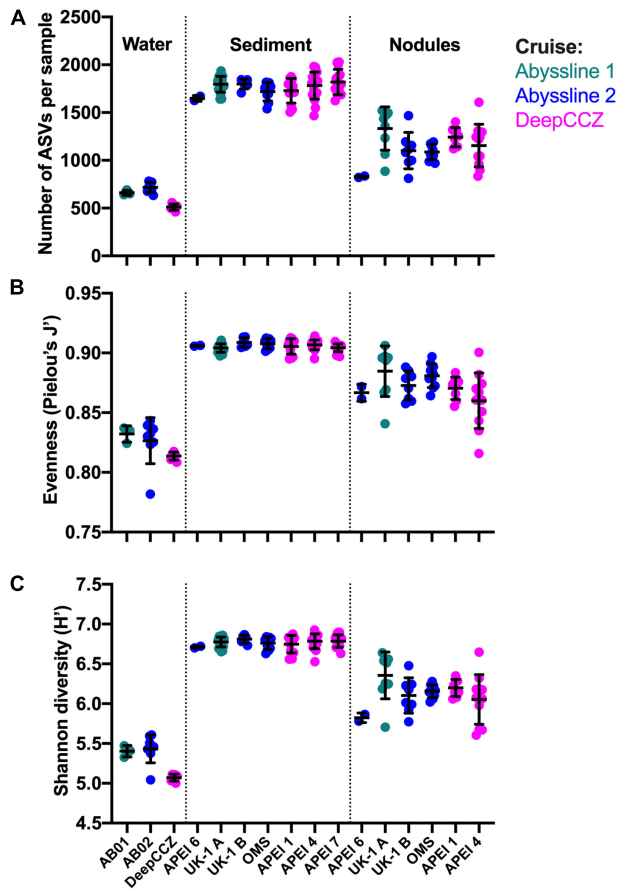

FIGURE 4 | Richness, evenness, and diversity across habitat types and sampling locations from the new dataset. **(A)** Observed richness: number of observed ASVs (amplicon sequence variants) per sample, after each sample was randomly subsampled to 6,900 reads and singlet ASVs were removed. Within each habitat type, sampling locations are arranged from roughly northeast to southwest. Because of the much smaller number of water column samples, these were grouped by cruise; no nodules were collected in APEI 7. Lines indicate mean ± one standard deviation. **(B)** Evenness calculated as Pielou's J′. **(C)** Shannon diversity, log base *e*.

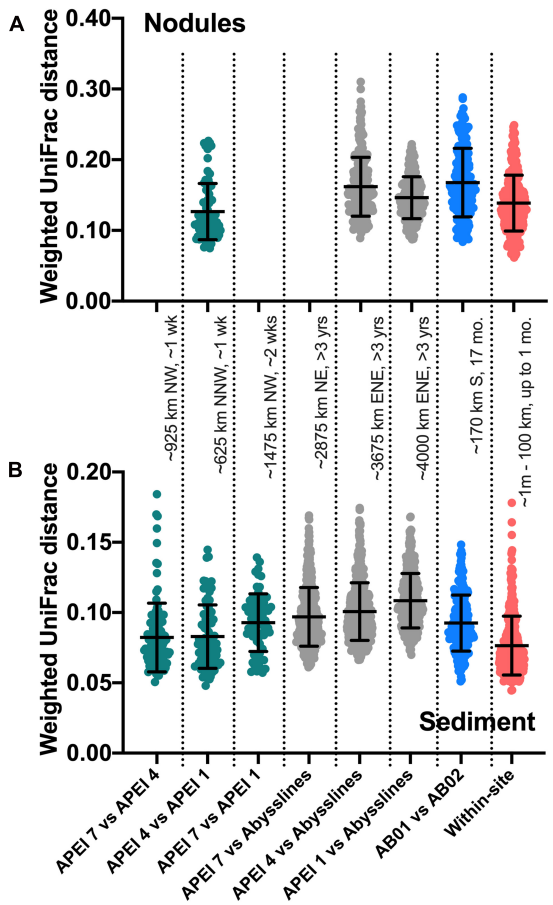

FIGURE 5 | Weighted UniFrac distances between comparable samples across spatial and temporal distances. AB01 and AB02 are Abyssline cruises 1 and 2, respectively; APEI 6 was omitted from AB02 for this analysis as it is spatially distant from the other sampled regions. Approximate distances and times between sample collections are listed between panels; cardinal directions are reported as traveling from the first to the second location. Colors are visual guides to distinguish categories of comparisons only. **(A)** Nodule samples; category labels as in **(B)**. **(B)** Sediment samples. For sediments, DeepCCZ samples were only compared within depth horizons between APEIs and within sites, as depth profiles are a distinct aspect of spatial ecology, but all depths were compared with Abyssline samples due to different depths sampled.

between samples are low (<0.3 between nodule samples and <0.2 between sediment samples; **Figure 5**) and the majority of ASVs are present within habitat types across the CCZ (**Supplementary Figure 5**), the current APEIs are generally located on the periphery of the CCZ, in some cases spanning the fracture zones (**Figure 1**), and thus could be prone to conditions promoting outlier microbial communities.

Nodule Communities Within the CCZ vs. Bordering Regions

While the CCZ is a particular target for potential mining activity due to the abundance and elemental composition of polymetallic nodules found there, microbial communities have also been studied from nodules collected from: the central South Pacific Gyre (Tully and Heidelberg, 2013); the Peru Basin, which is approximately 4,000 km to the southeast of the southeastern corner of the CCZ (Molari et al., 2020); the South China Sea (Zhang et al., 2015); and the western North Pacific Gyre (Jiang et al., 2020). The same issues with different sampling techniques that hinder direct comparisons between studies within the CCZ also arise in comparisons with bordering regions, yet several trends are clear despite these complications. Where both sediments and nodules have been examined, there are always pronounced overlaps in OTU or ASV presence between the two habitats, with habitat differences largely driven by differential relative abundances rather than unique organisms, consistent with the patterns we observed in the CCZ. Bacterial communities in nodules across sites have broadly similar composition when examined

at the class to phylum levels, dominated by diverse assemblages of both *Alphaproteobacteria* and *Gammaproteobacteria*, in particular members of the *Alteromonadales*. A further suite of phyla was frequently present in nodules across sites in the general range of circa 1 to 10% relative abundances, including the *Bacteroidota*, *Actinobacteria*, *Planctomycetota*, and *Verrucomicrobiota*.

However, differences in archaeal abundance are substantial enough to suggest that nodules in the CCZ, or perhaps more broadly within the meso- to oligotrophic central gyres of the North and South Pacific (Smith and Demopoulos, 2003), may constitute a distinct microbial habitat than nodules from more productive oceanic regions. In our CCZ dataset, we observed that members of the family *Nitrosopumilaceae* made up between 12 and 35% of nodule communities (mean 22%). Molari et al. (2020) reported lower relative abundances of *Nitrosopumilaceae* in nodules sampled from the Peru Basin compared with the CCZ results reported by Shulse et al. (2017); they observed total archaeal sequences constituting at most 7% of nodule communities, a difference the authors attribute to the higher particulate matter fluxes in the Peru Basin and subsequent differential selective pressure on the *Nitrosopumilaceae* from increased ammonium availability [although bacteria and archaea were amplified with distinct primers in Molari et al. (2020), which may additionally confound this comparison]. Zhang et al. (2015) also observed very low (0.01%) relative abundances of an OTU related to *Nitrosopumilus* in nodules collected from a dormant hydrothermal vent on a seamount in the South China Sea. While Zhang et al. (2015) used a primer set (515F and 806R) that is known to underrepresent the relative abundance of the *Thaumarchaeota*, the reported primer effects in direct comparisons have not been severe enough to solely explain that discrepancy from the much higher relative abundances of *Nitrosopumilaceae* seen in nodules across the CCZ (Parada et al., 2016; see also **Supplementary Figures 2, 3**). In contrast, Tully and Heidelberg (2013) found a high relative abundance (in some cases, >50% of the community) and OTU-level diversity of *Thaumarchaeota* in nodules from the South Pacific Gyre, and Jiang et al. (2020) reported a high proportion of cloned archaeal 16S rRNA genes from the *Thaumarchaeota*, and particularly those closely related to *Nitrosopumilus*, in the western North Pacific Gyre. This variable relative abundance of *Thaumarchaeota* raises the possibility that polymetallic nodules underlying meso- to oligotrophic regions such as the CCZ may play more of a role in supplying their local community with chemoautotrophic production of organic matter, and thus nodule removal could have different trophic implications between regions.

CONCLUSION

Our results strongly support a number of previously posited and novel conclusions about microbial communities across the CCZ. First, habitat type is the strongest determinant of microbial community composition; bottom waters share relatively few high resolution, ASV-level taxa with the benthic habitats, while sediments and nodules share many ASV-level taxa that differ in relative abundances. Second, we observe an east-vs.-west distinction in microbial community composition in the CCZ, although the magnitude of this effect, at least with current sample sizes, is relatively subtle and driven by changes in relative abundances rather than ASV-level taxon turnover. However, we also observed community-level differences between sites within the same claim area but sampled ∼17 months apart that were comparable in magnitude to differences between the eastern and western CCZ, suggesting either temporal variability or non-linear spatial shifts in community structure may be important. Either of these patterns would necessitate a specialized monitoring plan, accounting for seasonality or empirically determined spatial factors, to better characterize microbial biodiversity in the region. Finally, the observation that nodules in the CCZ harbor different microbial communities than nodules from more productive regions to the east and west of the CCZ, specifically higher relative abundances of putative chemoautotrophic organisms in CCZ nodules, suggests a possible effect of mining on trophic ecology in this meso- to oligotrophic region, although functional studies are required to confirm this. We can also unambiguously conclude that the currently available datasets do not represent a thorough spatial sampling of the microbial communities of the CCZ. In particular, the central and southeastern regions of the CCZ are poorly represented, and comparisons between proximate license areas and APEIs are extremely limited. We are aware of a small number of research cruises that have occurred but have not yet published microbial biodiversity data, which will improve but not fully alleviate these deficits.

Knowledge Gaps Concerning Microbial Biodiversity and Ecology in Nodule Regions

There remain several major gaps in our knowledge of CCZ microbes, in particular of those inhabiting polymetallic nodules, that we cannot address with current datasets. This includes the basic issue of whether reserve areas provide similar habitats to nearby exploration license areas. As noted above, available studies have largely sampled either APEIs or exploration areas, with scant paired comparisons between neighboring sites. Given the anticipated lengthy recovery time of sediment microbial communities after mining exposure (Vonnahme et al., 2020), and the presumably much longer time before nodules could re-form to be colonized (Ku and Broecker, 1969; Hein et al., 2020), it is particularly important that these reserves of intact habitat be representative of the broader CCZ.

This synthesis has focused on habitat selection and basin-scale spatial distribution patterns, but we lack knowledge of the basic ecology of deep-sea nodule-associated bacteria and archaea at much finer scales as well. This lack of basic ecological understanding has monitoring implications, in that it may inhibit our ability to design sampling programs that are robust to local variability when the goal is detecting spatial effects (see for example, some samples presenting high within-site variability in weighted UniFrac distances in **Figure 5**). At this point, we cannot confidently answer basic questions, including: how do

properties such as nodule size and metal composition affect microbial community composition? Is nodule density a factor in structuring small-scale microbial communities, as has been observed for megabenthic faunal composition (Simon-Lledó et al., 2019)? Does the frequent colonization of nodules by larger organisms including xenophyophores and sponges (e.g., Gooday et al., 2020) select for particular microbial communities, as has been observed with co-occurring epizoans in other marine habitats (e.g., on kelp blades: James et al., 2020)? Sediment-dwelling xenophyophores have been shown to contain enhanced and compositionally distinct bacterial fatty acids relative to surrounding sediments, suggesting some combination of bacterivory and/or bacterial growth on xenophyophore fecal pellets (Laureillard et al., 2004); both processes potentially could affect microbial community composition in a nodule to which a xenophyophore was attached. And like their shallow-water counterparts, deep-sea sponges host communities of bacteria and archaea that are distinct from those of the surrounding seawater, with deep-sea sponges particularly favorable habitats for members of the *Nitrosopumilaceae* (e.g., Steinert et al., 2020). Over the very long temporal duration of nodules (Ku and Broecker, 1969; Hein et al., 2020), attached macro-organisms would presumably episodically die; live vs. detrital epizoans would likely have different effects on microbes, and we speculate that changes in epizoan presence and health could potentially explain some nodule samples that have been observed to have outlier microbial communities, such as the three nodules from studies in the central Pacific that were each highly enriched in the chemoheterotrophic genus *Colwellia* (Tully and Heidelberg, 2013; Blöthe et al., 2015), which includes piezophilic members with chitin-degradation pathways (Peoples et al., 2020).

We also have an incomplete picture of how microbes use nodules as habitat. What are the proportions of microbes in surficial biofilms vs. shallow indentations vs. interior pore waters, and how do they differ? One study that compared the interior vs. exterior of a nodule found that microbial cell abundance was elevated at the nodule surface and decreased inward (Shiraishi et al., 2016). Studies that have compared interior and exterior bacterial and archaeal communities have seen differences in relative abundance and to a lesser extent in presence/absence of OTUs or higher clades between layers (Tully and Heidelberg, 2013; Shiraishi et al., 2016), while another observed higher OTU richness in layers closer to the exterior than in those closer to the nodule nucleus (Jiang et al., 2020). Other studies have found evidence for intra-nodule spatial heterogeneity, with differences in the microbial communities within the hydrogenetic (facing and formed by precipitation from the seawater) vs. diagenetic (facing the sediment and formed by precipitation from the pore waters) portions of individual nodules (Blöthe et al., 2015; Cho et al., 2018). The available nodule-associated microbial samples are insufficient to tease apart these potential factors, with the additional complication that different datasets have variable metadata that further reduce our ability to draw ecological conclusions.

Finally, what are the ecological and biogeochemical roles of bacteria and archaea inhabiting the benthos and near-seabed waters of the CCZ? While this information may be less important for designing sampling schemes, it could help us to better anticipate possible effects of mining on benthic community function. Rate measurements of key metabolic processes and molecular analyses of functional genes via metagenomics and metatranscriptomics would enable an accurate assessment of whether removing nodules and disturbing surface sediments will alter a key part of the abyssal elemental cycles in the CCZ. While rate measurements on deep-sea microbes are complicated by slow speeds and the need to maintain relevant hydrostatic pressures, with careful methodology such rates in the abyssal CCZ do appear to be quantifiable. For example, *in situ* tracer experiments in the eastern CCZ demonstrated that bacteria in nodule-containing sediments were active both in remineralization of added phytodetritus and in chemoautotrophic fixation of inorganic carbon, although the metabolic pathways underlying the latter process remain unknown (Sweetman et al., 2019).

Recommendations for Future Sampling

Beyond the limited number of extant microbial datasets from the CCZ, our ability to assess biodiversity and microbial ecosystem services is further hampered by the difficulties in directly comparing the samples that do exist. We make several recommendations for future microbial biodiversity work in the CCZ, contributing to the assessment guidelines recommended by the International Seabed Authority (2019), to facilitate future spatial and temporal inter-comparison efforts:

(1) Standardized sampling to the greatest extent practical, from field collection through DNA sequencing, will be key to enabling long-term monitoring of microbial diversity in response to mining activity – particularly in light of the very subtle spatial patterns within habitat types that we report in this analysis. International Seabed Authority guidelines already recommend next-generation (i.e., Illumina) amplicon-based sequencing. As the most pressing aspect of this standardization, we suggest adopting a single set of primers for consistent use, ideally one endorsed by a consortium, such as those validated by the Earth Microbiome Project[3] (Walters et al., 2015). The re-analysis included in this manuscript demonstrates how extant sequence information can be reprocessed as necessary to be compatible with future changes in bioinformatics processing routines (e.g., the shift in identifying working amplicon sequences from OTUs to ASVs) and updated reference databases. However, if the physical regions of the 16S rRNA gene, and original generation biases from factors such as PCR primers, constituting those sequences are not inter-comparable, that cannot be corrected for *in silico*. Yet we recognize that a static option may not be possible if improved primers are introduced over time; thus recommendation 2:

(2) As full DNA sequencing standardization over timescales of decades will be impossible in the face of expected

[3]https://earthmicrobiome.org

future technological improvements, we strongly encourage archiving of biological samples or extracted environmental DNA. This would enable the design of valid Before-After-Control-Impact studies (e.g., as are used to assess responses to the establishment of Marine Protected Areas or the effects of human-caused or natural perturbations; Osenberg and Schmitt, 1996) of the effects of mining processes on microbial communities, using the anticipated future sequencing approaches and instrumentation. Ideally there would be a central repository for such samples, but failing that, we encourage a strong commitment to long-term maintenance from individual research laboratories and contractors, as well as a willingness to share samples within the community when possible. Planned and coordinated archiving will likely be particularly important in the CCZ in light of the anticipated slow pace of post-disturbance community recovery and corresponding need for long-term monitoring (discussed in Jones et al., 2020).

(3) Collection of a standardized set of metadata for polymetallic nodules sampled for DNA will enable ecologically relevant comparisons and potentially help to identify those factors influencing microbial community composition. Beyond the basics of location and depth (both of the overlying water column and within the sediment), we encourage measures of nodule size and notes or photographs documenting attached organisms and unusual colors or features (e.g., see **Supplementary Table 2**). Additional information realistically may not always be feasible for all samples; for example, metal composition and nodule density could influence microbial communities associated with nodules and in nearby sediments. This list would likely expand or change as we better understand the ecology of nodule-inhabiting microbes.

(4) While a shift to non-targeted sequencing (i.e., shotgun metagenomics) could help to alleviate some of the primer-related inter-comparability issues and would have the additional benefit of providing functional information to address ecological questions, it is unlikely to be a panacea for biodiversity monitoring. This approach carries both technical and practical limitations. It too is affected by improvements in sequence yields and therefore changes in sequencing depth over timescales of decades. Functional gene analyses can be less precise for taxonomic identification than 16S rRNA genes, particularly in sparsely studied environments such as the deep sea. Finally, metagenomic analysis remains relatively expensive compared with 16S rRNA gene profiling and requires an arguably greater degree of specialist knowledge to interpret – it is highly unlikely to be accepted by commercial contractors as a component of routine monitoring activity in the near future. Metagenomics certainly has a place in furthering our understanding of the ecology of the CCZ in a research context, but for routine impact monitoring, we believe that the community should focus on optimizing amplicon-based approaches at this time.

We strongly encourage future sampling to better characterize the spatial and temporal biodiversity and activity of the microbial communities of the CCZ, to enable both more accurate management decisions and future detection of potential mining effects – particularly as our analysis here suggests that there are spatial differences in microbial communities within the CCZ. Careful planning of sampling techniques and target locations, to ensure inter-comparable datasets and alleviation of large areal gaps, will be key to obtaining an accurate understanding of microbial biodiversity in the CCZ prior to the onset of mining-related disturbances.

DATA AVAILABILITY STATEMENT

The datasets presented in this study can be found in online repositories. The names of the repository/repositories and accession number(s) can be found below: https://www.ncbi.nlm.nih.gov/genbank/, PRJNA660809; https://zenodo.org/record/4214934, 4214934; https://github.com/ekwear/DeepCCZreview.

AUTHOR CONTRIBUTIONS

EW drafted the manuscript, based in part on a conference report authored by MC, EW, and BO with input from CRS. EW, MC, CNS, ML, and CRS collected and/or conducted the initial analysis of samples included in the analysis. CRS led the DeepCCZ and Abyssline cruises that collected the samples. EW conducted the bioinformatics analyses. All the authors revised and approved the manuscript.

FUNDING

The review portion of this work originated in, and expands upon, a section of the workshop report from the DeepCCZ Biodiversity Synthesis Workshop in October 2019 (Church et al., 2019), funded by the Gordon and Betty Moore Foundation, the Pew Charitable Trusts, and the International Seabed Authority. New data included here were funded by the Gordon and Betty Moore Foundation (Grant 5596 to MC and CRS). Funding for collection of Abyssline samples derived from contracts from the UK Seabed Resources, LTD. (UKSRL) to CRS and MC. UKSRL had no influence in the study design, data collection, data analyses, and data interpretation. BO acknowledges funding support from the Center for Dark Energy Biosphere Investigations (C-DEBI) funded by the US National Science Foundation (award OIA-0939564). This is C-DEBI contribution number 566. This is contribution 11328 from SOEST, University of Hawai'i at Mānoa.

ACKNOWLEDGMENTS

We thank Jason Smith, Travis Washburn, C. Rob Young, other members of the DeepCCZ working groups, two reviewers, and

members of the Church lab for conversations and input that contributed to and improved this manuscript. We also thank the officers and crew of the R/V *Kilo Moana*, the members of the Hawaii Undersea Research Lab, and the DeepCCZ science party, in particular Jen Durden, Erica Goetze, Oliver Kersten, Kirsty McQuaid, Regan Drennan, Astrid Leitner, and Jeff Drazen.

SUPPLEMENTARY MATERIAL

The Supplementary Material for this article can be found online at: https://www.frontiersin.org/articles/10.3389/fmars.2021.634803/full#supplementary-material

Supplementary Figure 1 | Diversity parameters of microbial communities from Abyssline 1 samples sequenced by both this study and Shulse et al. (2017), using two different 16S rRNA gene primer sets.

Supplementary Figure 2 | Relative abundance of microbial communities from Abyssline 1 samples sequenced by both this study and Shulse et al. (2017), using two different 16S rRNA gene primer sets.

Supplementary Figure 3 | Log2-fold difference in relative abundances of selected taxa between Abyssline 1 samples sequenced in this study and in Shulse et al. (2017).

Supplementary Figure 4 | Microbial community composition, highlighting taxa of interest from genera to phylum level, in the new dataset.

Supplementary Figure 5 | Venn diagrams illustrating shared abundant ASVs between cruises and habitats.

Supplementary Figure 6 | Taxonomic distribution of differentially abundant ASVs between habitats, based on all samples from the new dataset.

Supplementary Figure 7 | Taxonomic distribution of differentially abundant ASVs in nodules between the eastern and western regions within the new dataset.

Supplementary Figure 8 | Cluster diagram of sediment samples from the new dataset, based on weighted UniFrac distance between samples.

Supplementary Table 1 | Metadata on samples included in new and re-sequenced dataset.

Supplementary Table 2 | Metadata on DeepCCZ nodule size and appearance.

Supplementary Table 3 | ANOSIM comparisons between habitats, based on weighted UniFrac distances.

Supplementary Table 4 | DESeq2 differential abundance analysis results of ASVs in nodules from the eastern vs. western CCZ sites and between different benthic habitat types.

Supplementary Table 5 | ANOSIM comparisons between eastern and western CCZ sites, based on weighted UniFrac distances.

Supplementary Table 6 | Highest relative abundance ASVs that are significantly different between eastern and western CCZ nodules.

Supplementary Video 1 | Animation showing the three-dimensional version of the sediment ordination in **Figure 2C**. 3D stress: 0.06.

REFERENCES

Apprill, A., McNally, S., Parsons, R., and Weber, L. (2015). Minor revision to V4 region SSU rRNA 806R gene primer greatly increases detection of SAR11 bacterioplankton. *Aquat. Microb. Ecol.* 75, 129–137. doi: 10.3354/ame01753

Aylward, F. O., and Santoro, A. E. (2020). Heterotrophic Thaumarchaea with small genomes are widespread in the dark ocean. *mSystems* 5:e0415-20. doi: 10.1128/mSystems.00415-20

Baker, B. J., Appler, K. E., and Gong, X. (2021). New microbial biodiversity in marine sediments. *Annu. Rev. Mar. Sci.* 13, 161–175. doi: 10.1146/annrev-marine-032020-014552

Blöthe, M., Wegorzewski, A., Müller, C., Simon, F., Kuhn, T., and Schippers, A. (2015). Manganese-cycling microbial communities inside deep-sea manganese nodules. *Environ. Sci. Technol.* 49, 7692–7700. doi: 10.1021/es504930v

Callahan, B. J., McMurdie, P. J., and Holmes, S. P. (2017). Exact sequence variants should replace operational taxonomic units in marker-gene data analysis. *ISME J.* 11, 2639–2643. doi: 10.1038/ismej.2017.119

Callahan, B. J., McMurdie, P. J., Rosen, M. J., Han, A. W., Johnson, A. J. A., and Holmes, S. P. (2016). DADA2: high-resolution sample inference from Illumina amplicon data. *Nat. Methods* 13, 581–583. doi: 10.1038/nmeth.3869

Caporaso, J. G., Lauber, C. L., Walters, W. A., Berg-Lyons, D., Huntley, J., Fierer, N., et al. (2012). Ultra-high-throughput microbial community analysis on the Illumina HiSeq and MiSeq platforms. *ISME J.* 6, 1621–1624. doi: 10.1038/ismej.2012.8

Cho, H., Kim, K. H., Son, S. K., and Hyun, J. H. (2018). Fine-scale microbial communities associated with manganese nodules in deep-sea sediment of the Korea Deep Ocean Study Area in the northeast equatorial Pacific. *Ocean Sci. J.* 53, 337–353. doi: 10.1007/s12601-018-0032-0

Christian, J. R., Verschell, M. A., Murtugudde, R., Busalacchi, A. J., and McClain, C. R. (2002). Biogeochemical modelling of the tropical Pacific Ocean. I: seasonal and interannual variability. *Deep Sea Res. II* 49, 509–543. doi: 10.1016/S0967-0645(01)00110-2

Christiansen, B., Denda, A., and Christiansen, S. (2020). Potential effects of deep seabed mining on pelagic and benthopelagic biota. *Mar. Policy* 114:103442. doi: 10.1016/j.marpol.2019.02.014

Church, M. J., Wear, E. K., Orcutt, B. N., Young, C. R., and Smith, J. M. (2019). *Taxonomic Diversity of Bacteria and Archaea in the Clarion-Clipperton Zone of the North Pacific Ocean*. Kingston, JM: International Seabed Authority. DeepCCZ Biodiversity Synthesis Workshop Report.

Clarke, K. R., and Gorley, R. N. (2006). *PRIMER v6: User Manual/Tutorial*. New Brunswick: PRIMER-E.

Danovaro, R., Corinaldesi, C., Rastelli, E., and Dell'Anno, A. (2015). Towards a better quantitative assessment of the relevance of deep-sea viruses, *Bacteria* and *Archaea* in the functioning of the ocean seafloor. *Aquat. Microb. Ecol.* 75, 81–90. doi: 10.3354/ame01747

Drazen, J. C., Smith, C. R., Gjerde, K. M., Haddock, S. H. D., Carter, G. S., Choy, C. A., et al. (2020). Midwater ecosystems must be considered when evaluating environmental risks of deep-sea mining. *Proc. Natl. Acad. Sci. U.S.A.* 117, 17455–17460. doi: 10.1073/pnas.2011914117

Gooday, A. J., Durden, J. M., Holzmann, M., Pawlowski, J., and Smith, C. R. (2020). Xenophyophores (Rhizaria, Foraminifera), including four new species and two new genera, from the western Clarion-Clipperton Zone (abyssal equatorial Pacific). *Eur. J. Protistol.* 75:125715. doi: 10.1016/j.ejop.2020.125715

Hein, J. R., Koschinsky, A., and Kuhn, T. (2020). Deep-ocean polymetallic nodules as a resource for critical materials. *Nat. Rev. Earth Environ.* 1, 158–169. doi: 10.1038/s43017-020-0027-0

Hoffmann, K., Bienhold, C., Buttigieg, P. L., Knittel, K., Laso-Pérez, R., Rapp, J. Z., et al. (2020). Diversity and metabolism of *Woeseiales* bacteria, global members of marine sediment communities. *ISME J.* 14, 1042–1056. doi: 10.1038/s41396-020-0588-4

International Seabed Authority (2010). *Technical Study No. 6: A Geological Model of Polymetallic Nodule Deposits in the Clarion-Clipperton Fracture Zone*. Kingston, JM: ISA.

International Seabed Authority (2019). *Recommendations for the Guidance of Contractors for the Assessment of the Possibl Environmental Impacts Arising from Exploration for Marine Minerals in the Area*. Kingston, JM: ISA. Report ISBA/25/LTC/6/Rev.1.

James, A. K., English, C. J., Nidzieko, N. J., Carlson, C. A., and Wilbanks, E. G. (2020). Giant kelp microbiome altered in the presence of epiphytes. *Limnol. Oceanogr. Lett.* 5, 354–362. doi: 10.1002/lol2.10157

Jiang, X.-D., Gong, J.-L., Ren, J.-B., Liu, Q.-S., Zhang, J., and Chou, Y. M. (2020). An interdependent relationship between microbial ecosystems and ferromanganese nodules from the Western Pacific Ocean. *Sediment. Geol.* 398:105588. doi: 10.1016/j.sedgeo.2019.105588

Jones, D. O. B., Ardron, J. A., Colaço, A., and Durden, J. M. (2020). Environmental considerations for impact and preservation reference zones for deep-sea polymetallic nodule mining. *Mar. Policy* 118:103312. doi: 10.1016/j.marpol.2018.10.025

Kallmeyer, J., Pockalny, R., Adhikari, R. R., Smith, D. C., and D'Hondt, S. (2012). Global distribution of microbial abundance and biomass in subseafloor sediment. *Proc. Natl. Acad. Sci. U.S.A.* 109, 16213–16216. doi: 10.1073/pnas.1203849109

Klindworth, A., Pruesse, E., Schweer, T., Peplies, J., Quast, C., Horn, M., et al. (2013). Evaluation of general 16S ribosomal RNA gene PCR primers for classical and next-generation sequencing-based diversity studies. *Nucleic Acids Res.* 41:e1. doi: 10.1039/nar/gks808

Ku, T. L., and Broecker, W. S. (1969). Radiochemical studies on manganese nodules of deep-sea origin. *Deep Sea Res.* 16, 625–637. doi: 10.1016/0011-7471(69)90063-1

Laureillard, J., Méjanelle, L., and Sibuet, M. (2004). Use of lipids to study the trophic ecology of deep-sea xenophyophores. *Mar. Ecol. Prog. Ser.* 270, 129–140. doi: 10.3354/meps270129

Lindh, M. V., Maillot, B. M., Shulse, C. N., Gooday, A. J., Amon, D. J., Smith, C. R., et al. (2017). From the surface to the deep-sea: bacterial distributions across polymetallic nodule fields in the Clarion-Clipperton Zone of the Pacific Ocean. *Front. Microbiol.* 8:1696. doi: 10.3389/fmicb.2017.01696

Love, M. I., Huber, W., and Anders, S. (2014). Moderated estimation of fold change and dispersion for RNA-seq data with DESeq2. *Genome Biol.* 15:550. doi: 10.1186/s13059-014-0550-8

McMurdie, P. J., and Holmes, S. (2013). phyloseq: an R package for reproducible interactive analysis and graphics of microbiome census data. *PLoS One* 8:e61217. doi: 10.1371/journal.pone.0061217

McQuaid, K. A., Attrill, M. J., Clark, M. R., Cobley, A., Glover, A. G., Smith, C. R., et al. (2020). Using habitat classification to assess representativity of a protected area network in a large, data-poor area targeted for deep-sea mining. *Front. Mar. Sci.* 7:558860. doi: 10.3389/fmars.2020.558860

Molari, M., Janssen, F., Vonnahme, T. R., Wenzhöfer, F., and Boetius, A. (2020). The contribution of microbial communities in polymetallic nodules to the diversity of the deep-sea microbiome of the Peru Basin (4130-4198 m depth). *Biogeosciences* 17, 3203–3222. doi: 10.5194/bg-17-3203-2020

Oksanen, J., Blanchet, F. G., Friendly, M., Kindt, R., Legendre, P., McGlinn, D., et al. (2019). *Vegan: Community Ecology Package. R Package Version 2.5-6*. Available online at: https://CRAN.R-project.org/package=vegan

Orcutt, B. N., Bradley, J. A., Brazelton, W. J., Estes, E. R., Goordial, J. M., Huber, J. A., et al. (2020). Impacts of deep-sea mining on microbial ecosystem services. *Limnol. Oceanogr.* 65, 1489–1510. doi: 10.1002/lno.11403

Orcutt, B. N., Sylvan, J. B., Knab, N. J., and Edwards, K. J. (2011). Microbial ecology of the dark ocean above, at, and below the seafloor. *Microbiol. Mol. Biol. R.* 75, 361–422. doi: 10.1128/MMBR.00039-10

Osenberg, C. W., and Schmitt, R. J. (1996). "Detecting ecological impacts caused by human activities," in *Detecting Ecological Impacts: Concepts and Applications in Coastal Habitats*, eds R. J. Schmitt and C. W. Osenberg (Cambridge, MA: Academic Press), 3–16.

Parada, A. E., Needham, D. M., and Fuhrman, J. A. (2016). Every base matters: assessing small subunit rRNA primers for marine microbiomes with mock communities, time series and global field samples. *Environ. Microbiol.* 18, 1403–1414. doi: 10.1111/1462-2920.13023

Peoples, L. M., Kyaw, T. S., Ugalde, J. A., Mullane, K. K., Chastain, R. A., Yayanos, A. A., et al. (2020). Distinctive gene and protein characteristics of extremely piezophilic *Colwellia*. *BMC Genom.* 21:692. doi: 10.1186/s12864-020-07102-y

Quast, C., Pruesse, E., Yilmaz, P., Gerken, J., Schweer, T., Yarza, P., et al. (2013). The SILVA ribosomal RNA gene database project: improved data processing and web-based tools. *Nucleic Acids Res.* 41, D590–D596. doi: 10.1093/nar/gks1219

Ruhl, H. A., Ellena, J. A., and Smith, K. L. Jr. (2008). Connections between climate, food limitation, and carbon cycling in abyssal sediment communities. *Proc. Natl. Acad. Sci. U.S.A.* 105, 17006–17011. doi: 10.1073/pnas.0803898105

Schloss, P. D., Westcott, S. L., Ryabin, T., Hall, J. R., Hartmann, M., Hollister, E. B., et al. (2009). Introducing mothur: open-source, platform-independent, community-supported software for describing and comparing microbial communities. *Appl. Environ. Microbiol.* 75, 7537–7541. doi: 10.1128/AEM.01541-09

Shiraishi, F., Mitsunobu, S., Suzuki, K., Hoshino, T., Morono, Y., and Inagaki, F. (2016). Dense microbial community on a ferromanganese nodule from the ultra-oligotrophic South Pacific Gyre: implications for biogeochemical cycling. *Earth Planet. Sci. Lett.* 447, 10–20. doi: 10.1016/j.epsl.2016.04.021

Shulse, C. N., Maillot, B., Smith, C. R., and Church, M. J. (2017). Polymetallic nodules, sediments, and deep waters in the equatorial North Pacific exhibit highly diverse and distinct bacterial, archaeal, and microeukaryotic communities. *Microbiol. Open* 6:e428. doi: 10.1002/mbo3.428

Simon-Lledó, E., Bett, B. J., Huvenne, V. A., Schoening, T., Benoist, N. M. A., and Jones, D. O. B. (2019). Ecology of a polymetallic nodule occurrence gradient: implications for deep-sea mining. *Limnol. Oceanogr.* 64, 1883–1894. doi: 10.1002/lno.11157

Smith, C. R., and Demopoulos, A. W. J. (2003). "The deep Pacific Ocean floor," in *Ecosystems of the World: Ecosystems of the Deep Ocean*, Vol. 28, ed. P. A. Tyler (Amsterdam: Elsevier), 179–218.

Smith, C. R., Tunnicliffe, V., Colaço, A., Drazen, J. C., Gollner, S., Levin, L. A., et al. (2020). Deep-sea misconceptions cause underestimation of seabed-mining impacts. *Trends Ecol. Evol.* 35, 853–857. doi: 10.1016/j.tree.2020.07.002

Sogin, M. L., Morrison, H. G., Huber, J. A., Welch, D. M., Huse, S. M., Neal, P. R., et al. (2006). Microbial diversity in the deep sea and the underexplored "rare biosphere". *Proc. Natl. Acad. Sci. U.S.A.* 103, 12115–12120. doi: 10.1073/pnas.0605127103

Steinert, G., Busch, K., Bayer, K., Kodami, S., Martinez Arbizu, P., Kelly, M., et al. (2020). Compositional and quantitative insights into bacterial and archaeal communities of South Pacific deep-sea sponges (*Demospongiae* and *Hexactinellida*). *Front. Microbiol.* 11:716. doi: 10.3389/fmicb.2020.00716

Sweetman, A. K., Smith, C. R., Shulse, C. N., Maillot, B., Lindh, M., Church, M. J., et al. (2019). Key role of bacteria in the short-term cycling of carbon at the abyssal seafloor in a low particulate organic carbon flux region of the eastern Pacific Ocean. *Limnol Oceanogr.* 64, 694–713. doi: 10.1002/lno.11069

Talley, L. D. (2007). "Hydrographic atlas of the World Ocean Circulation Experiment (WOCE)," in *Pacific Ocean*, Vol. 2, eds M. Sparrow, R. Chapman, and J. Gould (Southampton: International WOCE Project Office).

Thurber, A. R., Sweetman, A. K., Narayanaswamy, B. E., Jones, D. O. B., Ingels, J., and Hansman, R. L. (2014). Ecosystem function and services provided by the deep sea. *Biogeosciences* 11, 3941–3963. doi: 10.5194/bg-11-3941-2014

Tully, B. J., and Heidelberg, J. F. (2013). Microbial communities associated with ferromanganese nodules and the surrounding sediments. *Front. Microbiol.* 4:161. doi: 10.3389/fmicb.2013.00161

Veillette, J., Sarrazin, J., Gooday, A. J., Galéron, J., Caprais, J.-C., Vangriesheim, A., et al. (2007). Ferromanganese nodule fauna in the Tropical North Pacific Ocean: species richness, faunal cover, and spatial distribution. *Deep Sea Res. I* 54, 1912–1935. doi: 10.1016/j.dsr.2007.06.011

Vonnahme, T. R., Molari, M., Janssen, F., Wenzhöfer, F., Haeckel, M., Titschack, J., et al. (2020). Effects of a deep-sea mining experiment on seafloor microbial communities and functions after 26 years. *Sci. Adv.* 6:eaaz5922. doi: 10.1126/sciadv.aaz5922

Walters, W., Hyde, E. R., Berg-Lyons, D., Ackermann, G., Humphrey, G., Parada, A., et al. (2015). Improved bacterial 16S rRNA gene (V4 and V4-5) and fungal Internal Transcribed Spacer marker gene primers for microbial community surveys. *mSystems* 1:e00009-15. doi: 10.1128/mSystems.00009-15

Wang, C.-S., Liao, L., Xu, H. X., Xu, X. W., Wu, M., and Zhu, L. Z. (2010). Bacterial diversity in the sediment from polymetallic nodule fields of the Clarion-Clipperton Fracture Zone. *J. Microbiol.* 48, 573–585. doi: 10.1007/s12275-010-0151-5

Washburn, T. W., Jones, D. O. B., Wei, C.-L., and Smith, C. R. (2021). Environmental heterogeneity throughout the Clarion-Clipperton Zone and the representivity of the APEI network. *Front. Mar. Sci.* 8:661685. doi: 10.3389/fmars.2021.661685

Wear, E. K., Wilbanks, E. G., Nelson, C. E., and Carlson, C. A. (2018). Primer selection impacts specific population abundances but not community dynamics in a monthly time-series 16S rRNA gene amplicon analysis of coastal marine bacterioplankton. *Environ. Microbiol.* 20, 2709–2726. doi: 10.1111/1462-2920.14091

Wedding, L. M., Friedlander, A. M., Kittinger, J. N., Watling, L., Gaines, S. D., Bennett, M., et al. (2013). From principles to practice: a spatial approach to systematic conservation planning in the deep sea. *Proc. R. Soc. B.* 280:20131684. doi: 10.1098/rspb.2013.1684

Wei, C.-L., Rowe, G. T., Escobar-Briones, E., Boetius, A., Soltwedel, T., Caley, M. J., et al. (2010). Global patterns and predictions of seafloor biomass using random forests. *PLoS One* 5:e15323. doi: 10.1371/journal.pone.0015323

Whitman, W. B., Coleman, D. C., and Wiebe, W. J. (1998). Prokaryotes: the unseen majority. *Proc. Natl. Acad. Sci. U.S.A.* 95, 6578–6583. doi: 10.1073/pnas.95.12.6578

Wu, Y. H., Liao, L., Wang, C. S., Ma, W. L., Meng, F. X., Wu, M., et al. (2013). A comparison of microbial communities in deep-sea polymetallic nodules and the surrounding sediments in the Pacific Ocean. *Deep Sea Res. Pt. I* 79, 40–49. doi: 10.1016/j.dsr.2013.05.004

Xu, M., Wang, P., Wang, F., and Xiao, X. (2005). Microbial diversity at a deep-sea station of the Pacific nodule province. *Biodivers. Conserv.* 14, 3363–3380. doi: 10.1007/s10531-004-0544-z

Zhang, D.-C., Liu, Y.-X., and Li, X.-Z. (2015). Characterization of bacterial diversity associated with deep sea ferromanganese nodules from the South China Sea. *J. Microbiol.* 53, 598–605. doi: 10.1007/s12275-015-5217-y

Conflict of Interest: The authors declare that the research was conducted in the absence of any commercial or financial relationships that could be construed as a potential conflict of interest.

Copyright © 2021 Wear, Church, Orcutt, Shulse, Lindh and Smith. This is an open-access article distributed under the terms of the Creative Commons Attribution License (CC BY). The use, distribution or reproduction in other forums is permitted, provided the original author(s) and the copyright owner(s) are credited and that the original publication in this journal is cited, in accordance with accepted academic practice. No use, distribution or reproduction is permitted which does not comply with these terms.

frontiers in Marine Science

ORIGINAL RESEARCH
published: 17 May 2021
doi: 10.3389/fmars.2021.663798

Comparative Reproductive Biology of Deep-Sea Ophiuroids Inhabiting Polymetallic-Nodule Fields in the Clarion-Clipperton Fracture Zone

Sven R. Laming[1], Magdalini Christodoulou[2], Pedro Martinez Arbizu[2] and Ana Hilário[1]*

[1]*Department of Biology, Centre for Environmental and Marine Studies (CESAM), University of Aveiro, Aveiro, Portugal,*
[2]*German Centre for Marine Biodiversity Research (DZMB), Senckenberg am Meer, Wilhelmshaven, Germany*

Deep-sea mining in the Pacific Clarion-Clipperton Fracture Zone (CCZ), a low-energy sedimentary habitat with polymetallic nodules, is expected to have considerable and long-lasting environmental impact. The CCZ hosts extraordinarily high species diversity across representatives from all Domains of Life. Data on species biology and ecology remain scarce, however. The current study describes the reproductive biology of *Ophiosphalma glabrum* (Ophiosphalmidae) and *Ophiacantha cosmica* (Ophiacanthidae), two ophiuroids frequently found in the CCZ. Specimens collected in Spring 2015 and 2019 in four contract areas were examined morphologically and histologically. Size-class frequencies (disc diameter and oocytes feret diameters), sex ratios, gametogenic status, putative reproductive mode, and a simple proxy for fecundity are presented. Habitat use differs in each. While *O. glabrum* is epibenthic, occurring as single individuals, *O. cosmica* often forms size-stratified groups living on stalked sponges, suggesting gregarious settlement or retention of offspring (though no brooding individuals were found). Further molecular analyses are needed to establish whether *O. cosmica* groups are familial. In *O. glabrum*, for which sample sizes were larger, sex ratios approximated a 1:1 ratio with no size-structuring. In both species, individuals were at various stages of gametogenic maturity, but no ripe females were identified. Based on this, *O. glabrum* is most probably gonochoric. Reproductive mode remains inconclusive for *O. cosmica*. Both species are presumptively lecithotrophic, with vitellogenic-oocyte feret diameters exceeding 250 μm. Oocyte feret diameters at times exceeded 400 μm in *O. glabrum*, indicating substantial yolk reserves. Estimates of instantaneous fecundity (vitellogenic specimens of *O. glabrum* only) were confounded by interindividual variability in gonad characteristics. The well-furnished lecithotrophic larvae of *O. glabrum* would be capable of dispersing even under food-impoverished conditions. The current study examines ophiuroid reproductive biology over multiple localities in the CCZ concurrently for the first time, at sites characterised by differing productivity regimes. The reproductive biology of each species is thus discussed with reference to past evolutionary (habitat stability), contemporary (food supply), and future environmental drivers (potential impacts of deep-sea mining).

Keywords: maturation, lecithotrophy, deep-sea mining, ecology, brittle stars, ophiuroidea, echinodermata, gonochoric

OPEN ACCESS

Edited by:
Craig Randall Smith, University of Hawaii at Manoa, United States

Reviewed by:
Paul Alan Tyler, University of Southampton, United Kingdom
Mary A. Sewell, The University of Auckland, New Zealand

****Correspondence:***
Sven R. Laming
svenlaming@ua.pt

Specialty section:
This article was submitted to Interdisciplinary Physics, a section of the journal Frontiers in Marine Science

Received: *03 February 2021*
Accepted: *16 April 2021*
Published: *17 May 2021*

Citation:
Laming SR, Christodoulou M, Martinez Arbizu P and Hilário A (2021) Comparative Reproductive Biology of Deep-Sea Ophiuroids Inhabiting Polymetallic-Nodule Fields in the Clarion-Clipperton Fracture Zone. Front. Mar. Sci. 8:663798. doi: 10.3389/fmars.2021.663798

INTRODUCTION

The challenges of exploring remote deep-sea abyssal environments have, thus far, insulated the deep-sea benthos from the impacts of mineral resource extraction. However, the advent of the technological means to access and exploit the considerable mineral resources found in these environments (Ghosh and Mukhopadhyay, 2000), heralds imminent, unprecedented levels of disturbance in the deep-sea (Weaver et al., 2018). Fauna that have evolved under highly stable, food-limited environmental regimes are likely to be poorly adapted to large-scale disturbances that rapidly and/or irreversibly alter their environment (Stearns, 2000). The CCZ in the tropical Northeast (NE) Pacific exemplifies this scenario, where the largest known global reserve of polymetallic nodules is located, formed over geological timescales in abyssal soft sediments characterised by very low sedimentation rates (Hein et al., 2013). Recent studies that have sought to describe the benthic fauna that typify the CCZ have also revealed extraordinarily high taxonomic diversity across representatives from all Domains of Life (e.g., Amon et al., 2016; De Smet et al., 2017; Shulse et al., 2017; Wilson, 2017; Goineau and Gooday, 2019; Hauquier et al., 2019; Brix et al., 2020; Christodoulou et al., 2020), making the CCZ of critical importance for biodiversity conservation. In many of these studies, data (e.g., species-abundance curves) strongly suggest that many – arguably most – species remain unaccounted for, with high species turnover over relatively short spatial scales even in groups that are brooders like Isopoda (e.g., Wilson, 2017; Brix et al., 2020). Remoteness of habitat and spatial variability in species composition of this sort present challenges for performing robust ecological studies, as evidenced by the scarcity of ecologically meaningful data available for even the most conspicuous "common" epifaunal species in the CCZ (Danovaro et al., 2017), including many echinoderm species (Amon et al., 2016).

Members of the phylum Echinodermata represent some of the most biomass-dominant taxa found in deep-sea abyssal plains (Gage and Tyler, 1991). Echinoderms play a significant role in global marine carbon budget (Lebrato et al., 2010) and are abundant in many soft- and hard-substrate habitats globally (Gage and Tyler, 1991). The class Ophiuroidea are known to be particularly prevalent and diverse on bathyal slopes (e.g., O'Hara et al., 2008) but data concerning species diversity and abundances at abyssal depths are scarce by comparison (Stöhr et al., 2012). In the equatorial NE Pacific, such data is limited to select historic (e.g., HMS Challenger and Albatross expeditions, Lyman, 1878, 1879, 1882; Clark, 1911, 1949) and contemporary surveys (Amon et al., 2016; Vanreusel et al., 2016; Christodoulou et al., 2020). Drivers for large-scale regional variability in abyssal ophiuroid population densities are still poorly understood; however, in the CCZ it seems that local-scale patchiness in nodule substrate availability plays a key role in determining the distribution of many species. Under certain habitat conditions, ophiuroids and the echinoderms more generally, comprise one of the largest components of mobile epifauna at nodule-rich sites (Amon et al., 2016; Vanreusel et al., 2016: up to 15 individuals per 100 m^2, with major contributions from ophiuroids). The presence of nodules appears particularly relevant to certain ophiuroid and echinoid species; when nodules are absent, mobile epifaunal densities fall sharply to one or two encounters in an equivalent 100 m^2 area, largely due to much-reduced encounters with ophiuroid species (Vanreusel et al., 2016). Two recent studies published in 2020, one based on video-transect surveys and the other on specimens collected by remotely operated vehicle (ROV) and epibenthic sledge (EBS), have also identified ophiuroids in abundance and notably, at unexpectedly high levels of diversity in the easternmost regions of CCZ (Christodoulou et al., 2020; Simon-Lledó et al., 2020) with the discovery of previously unknown ancient lineages (Christodoulou et al., 2019, 2020).

Current knowledge of reproductive biology in abyssal ophiuroid species is limited to a few papers examining gametogenic and/or size-class patterns (e.g., *Ophiomusa lymani* in N Atlantic & NE Pacific, Gage, 1982; Gage and Tyler, 1982; *Ophiocten hastatum* in NE Atlantic, Gage et al., 2004; *Ophiura bathybia*, *Amphilepis patens*, *Amphiura carchara*, and *Ophiacantha cosmica* in NE Pacific, Booth et al., 2008; *Ophiuroglypha irrorata loveni*, *Ophiura lienosa*, *Salix daleus*, *O. cosmica*, *Ophiernus quadrispinus*, and *Ophioplexa condita* in S Indian Ocean, Billett et al., 2013), with no data available for specimens collected from polymetallic-nodule habitats. Two of the more frequently encountered ophiuroids within the eastern CCZ (Christodoulou et al., 2020) are the brittle stars *Ophiosphalma glabrum* (Lütken and Mortensen, 1899; Ophiosphalmidae) and *Ophiacantha cosmica* (Lyman, 1878; Ophiacanthidae). These two species make for an interesting comparative reproductive study due to their contrasting biology. *Ophiosphalma glabrum* is relatively large (35–40 mm maximum disc diameters, Clark, 1911, 1913), epifaunal on soft sediments (0–2 mm burial, Amon et al., 2016; Glover et al., 2016; Christodoulou et al., 2020) and likely a generalist deposit feeder, as is the case in the closely related genus *Ophiomusa* (Pearson and Gage, 1984, formerly *Ophiomusium*). *Ophiacantha cosmica*, by contrast, is considerably smaller (11–12 mm maximum disc diameters, Booth et al., 2008; Billett et al., 2013) and epizoic or epifaunal on hard substrata (Billett et al., 2013), where it filters feeds with its spinous arms (Pearson and Gage, 1984). Although reproductive data are currently not available for *Ophiosphalma glabrum*, a few data already exist for *Ophiacantha cosmica* in nodule-free habitats. These indicate that *O. cosmica* is probably both gonochoric and lecithotrophic (oocyte 30–560 μm in diameter in specimens from the Southern Indian Ocean, Billet et al., 2013), with seasonal fluctuations in body-size structure, suggesting that specimens spawn in response to peaks in particulate organic-carbon (POC) flux (Booth et al., 2008).

As part of a wider concerted effort to address significant knowledge gaps in our ecological understanding of nodule-rich seabeds while this habitat remains relatively pristine, the current study describes the reproductive biology of the brittle stars *Ophiosphalma glabrum* (Lütken and Mortensen, 1899; Ophiosphalmidae) and *Ophiacantha cosmica* (Lyman, 1878; Ophiacanthidae) in a nodule-rich environment, based on the histological analyses of specimens collected from several mining-contract areas within the eastern CCZ.

METHODOLOGY

Sample Collection, Fixation, Preservation, and Species Identification

Specimens were collected during ROV transects (ROV Kiel 6,000, GEOMAR, manipulator arm) undertaken over the course of two cruises in Spring 2015 and 2019 on the R/V Sonne in the eastern CCZ. Cruise SO239 (11 March–30 April 2015) visited four contract areas and one Area of Particular Environmental Interest (APEI, 400 × 400 square-km protected areas assigned to each of nine presumptive ecological subregions of the CCZ). The 2015 samples in the current study originate from three of these contract areas, where one or both of the species in the current study were found: BGR area (Federal Institute for Geosciences and Natural Resources, Germany), the southern IOM area (Interoceanmetal Joint Organization), and the easternmost GSR area (G-TEC Sea Mineral Resources NV, Belgium), where each area was located along a decreasing SE-to-NW POC gradient, concomitant with a decrease in surface primary productivity driven by basin-scale thermocline shoaling toward the N. Pacific subtropical gyre (Pennington et al., 2006). The 2019 samples from the follow-up cruise SO268 (18 February–21 May), originated from BGR (again) and the central GSR contract area (2015–2019 site separation: BGR ~ 50 km; GSR ~ 350 km). A site map is provided in **Figure 1**.

Following collection, the arms of each specimen were removed for molecular species identification, while the central disc was fixed for reproductive histology. Arm fixation was in pre-cooled 96% EtOH, with replacement after 24 h (stored at −20°C thereafter); disc fixation was in 4% phosphate-buffered formaldehyde (48 h) following by serial transfer to 70% ethanol, stored at room temperature. Specimens were later identified to species level based on morphological characteristics (*O. glabrum*: Lütken and Mortensen, 1899; Baker, 2016; *O. cosmica*: Lyman, 1878; Paterson, 1985), supported by mtDNA COI analyses of genomic DNA extracted from arm tissues, described in detail in Christodoulou et al. (2020).

Size Measurements, Dissection, and Tissue Preparation for Microscopy

Micrographs of the oral and aboral faces of central discs were created from focus-stacks taken under a stereomicroscope (Leica M125 and DMC5400 camera, LAS-Leica Application Suite 3.7; focus-stacking in Combine ZP 1.0). Disc diameter – the length from the radial shield's distal edge to the opposing interradial margin (Gage and Tyler, 1982) – was measured in LAS, to estimate size at first maturity and assess size-class frequencies as a function of sex. The aboral face, stomach, and bursa lining were then removed by dissection to reveal the bursal slits that border each arm base, along which the sac-like gonads are located, arranged in rows on each side. Intact gonad rows were dissected and then embedded either in paraffin wax or plastic resin, depending on tissue size. An additional decalcification step in 3% nitric acid in 70% ethanol (Wilkie, 2016) followed by a 70% ethanol rinse was required for smaller gonads, which were retained on a fragment of calcified tissue to facilitate tissue processing.

Larger gonad samples (all *Ophiosphalma glabrum* specimens and one *Ophiacantha cosmica* specimen with larger gonads) were infiltrated in molten paraffin at 60°C, following six-step serial transfer to 100% ethanol, four-step transfer to 100% MileGREEN™ (an iso-paraffin based solvent, Milestone) and final two-step transfer to paraffin in a mould to set. Blocks were trimmed and 5-µm sections cut, relaxed in a water bath, placed on Superfrost™+ slides, and dry-fixed by incubation at 50°C. Slides were stained in (Harris) Haematoxylin and Eosin(-Y) following standard protocols with dehydration by replacement using ethanol. Note that the *O. cosmica* specimen processed using paraffin wax was also processed with LR white resin (protocol below) using neighbouring gonads to identify any procedural biases in oocyte feret diameter.

Smaller tissue samples (all *O. cosmica* specimens) were blotted dry and then infiltrated directly in a hydrophilic methacrylate resin (LR white, London Resin Co.) at room temperature (three resin replacements by micropipette, 30-min. Each, fourth overnight) then transferred to a fresh resin-filled gelatine capsule (size 00, Electron Microscopy Sciences, United Kingdom), which was capped and polymerised at 50°C (20+ h). Having removed gelatine, LR-white resin pellets were trimmed and wet-sectioned on a Leica Ultracut UC6 Ultramicrotome (Germany), using a 45° glass knife. Sections 1-µm thick was transferred to individual aliquots arranged on Superfrost™+ slides. Periodic toluidine staining tracked progress through tissue. Standard H & E staining was modified by extending staining times and excluding ethanol, which distorts LR white. Slides were dried at 50°C with a desiccant (see Laming et al., 2020 for details). Regardless of protocol, sections were then cleared in MileGREEN™ and mounted with a cover slip (Omnimount™, Electron Microscopy Sciences).

Gametogenic Analyses

Stained serial sections were photographed under a compound microscope (Leica DM2500 with camera module ICC50W, LAS 3.7). Spermatogenesis was documented qualitatively only. Oogenesis was examined in more detail. Oocyte size frequencies were determined by image analysis of serial sections from ovaries, imported as image-stacks into Image-J (Schindelin et al., 2012) to track individual oocytes through the sample and prevent repeat counting. Up to 100 oocytes (with visible nuclei only) were counted per specimen, each measured along its longest axis (feret diameter) and classified into oogenic developmental stages, based on the presumption that germinal vesicle breakdown (GVBD) precedes oocyte release (Adams et al., 2019). Stages were: (1) *Previtellogenic* oocytes (Pv), smallest oocytes with no clear evidence of a germinal vesicle or vitellogenesis (i.e., eosinophilic granulated cytoplasm, rich in yolk proteins, has not yet developed); (2) *Vitellogenic I* (VI), "early" vitellogenic oocytes that are less than twice the diameter of previtellogenic oocytes, with the beginnings of an eosinophilic cytoplasm and a distinct germinal vesicle; (3) *Vitellogenic II* (VII), "mid-stage" vitellogenic oocytes that clearly

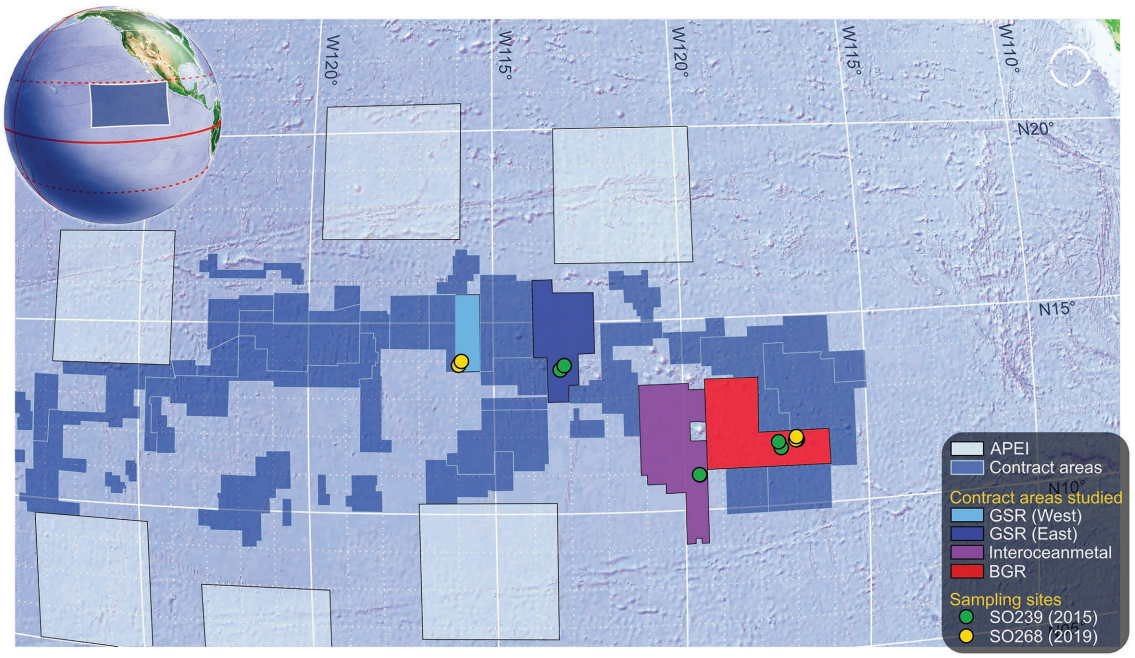

FIGURE 1 | Map of eastern CCZ with sampling details. Map depicts the eastern half of the Area within the CCZ. Large 400 km × 400 km square regions are Areas of Particular Environmental Interest (APEI) that border numerous exploration contract areas in the centre (N.B. so-called "reserved" areas are not shown). The areas in which specimens were collected are identified along with site locations for each cruise. These were from the BGR area (Federal Institute for Geosciences and Natural Resources, Germany); the southern IOM area (Interoceanmetal Joint Organization); and both the central and the easternmost GSR areas (G-TEC Sea Mineral Resources NV, Belgium). Map and globe adapted from Google Earth projections.

possess an eosinophilic granulated cytoplasm, but whose diameter is less than double that of the germinal vesicle; (4) *Vitellogenic III* (VIII), "late" vitellogenic oocytes with large eosinophilic cytoplasmic reserves, whose diameter exceeds double that of the germinal vesicle; (5) *Asymmetric* (As), late vitellogenic oocytes with germinal vesicles located asymmetrically and in contact with the cell membrane, the precursor to germinal vesicle breakdown (GVBD) and onset of meiosis I; (6) *Polar bodies* (PB), oocytes that have undergone GVBD, with evidence of peripheral polar bodies, germinal vesicle lacking; and (7) *Mature* (M), fully mature oocytes, possessing only a small pronucleus (after Wessel et al., 2004).

Overall state of gonad maturity was assessed visually in terms of gonad aspect within the bursa and histological appearance. Gonad state was either defined as "immature" (no gonad), "no gametes" (gonad but no gametogenesis), and "developing" (gametogenesis at all the stages of development but with interstitial spaces remaining, equivalent to stages I and II in Tyler, 1977), "nearly ripe" (late-stage gametes dominate – spermatozoa in males or *VIII*-to-*Mature*, denoted here as "$VIII_{plus}$" in females – but gonad is not yet replete, equivalent to stage III in Tyler, 1977), "ripe" (fully mature gametes and no interstitial space, equivalent to stage IV in Tyler, 1977), and "post-spawning/recovery" (some residual near-mature gametes remain alongside degraded material, epithelial and myoepithelial layers are thickened, and nutritive phagocytes are typically present, equivalent to stages V in Tyler, 1977). For *Ophiosphalma glabrum*, the percentage area occupied by oocytes relative to gonad area and a maturity stage index (MSI) were also calculated, the latter using the fourth formula proposed from Doyle et al. (2012): *Oocyte density* × *Size of individual*$^{-1}$ × *Oocyte surface area* × 0.01, where oocyte density in the current study refers to oocytes mm^{-2} of all gonads in cross section, size of individual is disc diameter in mm (whose reciprocal value compensates for any size bias) and oocyte surface area is derived from the mean feret diameter ($¼\pi d^2$).

Statistical Analyses

Sex ratios for each species were assessed by χ^2 test. The statistical significance of rank-based differences was tested by Kruskal-Wallis H test for: (1) disc diameter as a function of sex (including a juvenile category); (2) oocyte feret diameter as a function of year, and of disc diameter (for a given visual gonad state); and (3) percentage gonad occupied by oocytes, MSI and mean oocyte feret diameter each as a function of visual gonad state. *Post-hoc* pairwise comparisons were by Dunn test. To assess whether a trade-off exists between oocyte diameter and oocyte density (and thus, fecundity), a Spearman rank-order correlation was used to assess the strength of any proportional relationship between oocyte density and mean oocyte feret diameter. Expressions of variation around average values are standard deviation (sd., for means) and median absolute deviation (mad., for medians). All statistical and graphical analyses were performed in R 4.0.3

(R Core Team, 2020),[1] using packages *svglite*, *tidyverse*, *cowplot*, *ggExtra*, and *ggpubr* (Attali and Baker, 2019; Wickham et al., 2019, 2020; Kassambara, 2020; Wilke, 2020), with figures prepared in Inkscape 1.0.2 (Inkscape Project).[2]

RESULTS

Sex Ratios, Size-Class Frequencies, and Size at First Maturation

A total of 76 *Ophiosphalma glabrum* individuals (22 in 2015, 54 in 2019) and 23 *Ophiacantha cosmica* individuals (8 in 2015, and 15 in 2019) were processed. Molecular analyses of the arms of specimens in the current study used for species' confirmation in a subset of individuals have been compiled into dedicated DOI-indexed dataset containing accession codes (Genbank), BOLD IDs and photos, trace files and collection data, and specimen metadata.[3] Accession codes, BOLD IDs, and sample metadata are also provided in **Supplementary Table 1**. Of the two species, *Ophiosphalma glabrum* was larger (across entire sampling area, mean disc diameter 16.0 ± sd. 4.02 vs. *Ophiacantha cosmica* mean disc diameter 4.9 ± sd. 2.03, example specimens in **Figure 2**). Diameters ranged from 5.7–25.2 mm in *Ophiosphalma glabrum* and 2.2–10.0 mm in *Ophiacantha cosmica*. Although male *Ophiosphalma glabrum* specimens were numerically dominant (39 vs. 25 individuals), overall sex ratios did not differ significantly from a 1:1 ratio ($\chi^2_1 = 3.06$, $p > 0.05$). The three intermediate size classes for *O. glabrum* (together ranging from 12.5 to 20 mm) were characterised by equal numbers of males and females; however, smaller and larger mature *O. glabrum* individuals outside these size classes were exclusively male (**Figure 3**). Ranked-disc diameters did not significantly differ between sexes in *O. glabrum*, only between mature (male/female) and immature specimens, resulting in significant global differences across the three categories, when immature specimens were included in analyses (Kruskal-Wallis $\chi^2_2 = 31.39$, $p < 0.01$, **Figure 3**). Sample sizes were particularly small for specimens of *Ophiacantha cosmica*. Despite this, due to an over-whelming dominance of females (7:1), sex ratios were found to be significantly different ($\chi^2_1 = 4.50$, $p < 0.05$). The only male *Ophiacantha cosmica* collected was the largest individual of this species, making statistical comparisons of disc diameter between sexes impossible.

For both species, several immature specimens were retrieved (**Figures 2, 3**), allowing rough estimates of size at first maturity to be made. In *Ophiosphalma glabrum*, the largest immature specimen (lacking discernible gonads) had an 11.93-mm wide disc; a further 11 smaller specimens also lacked gonads. The smallest *O. glabrum* individual that possessed a gonad was a male at 12.07 mm disc diameter, while the smallest female was 14.14 mm (gametogenesis observed in both), placing approximate sizes at first maturity in males at <12 mm disc diameter and at <14.2 mm disc diameter in females. In *Ophiacantha cosmica*, size at first the maturity is less concrete. The largest specimen with no discernible gonad had a disc diameter of 5.12 mm, with two smaller (4.28, 4.34 mm) and two larger (6.00, 7.04 mm) specimens each in possession of 1–2 very small gonad buds (ca. 100 μm diameter) not yet furnished with gametes. The smallest individual in which gametogenesis was identified was a female of 4.96 mm with six larger females with disc diameters of 5.37–7.88 mm (**Figure 3**; select specimens in **Figure 2**). The largest individual – the only *O. cosmica* male – had a 9.98-mm wide disc.

Gonad State and Gametogenesis

Gonad state and gametogenesis were assessed qualitatively in males (**Figures 4, 5**) and both qualitatively and semi-quantitatively in females (**Figures 4–6**). No evidence of simultaneous or sequential hermaphroditism (i.e., ovotestes/sex-specific size stratification) was identified in either species. Most *Ophiosphalma glabrum* males' testes were *developing* (49%) with easily identifiable spermatogenic columns, composed of progressively more-advanced stages of spermatogenesis, extending from the inner-sac membrane into the central lumen (**Figure 4A**). Testes were somewhat angular (**Figure 4G**), lacking the creamy engorged appearance typical of ripe individuals (example in **Figure 4H**). A further 35% were considered *nearly ripe*, where testes aspect appears unchanged, but spermatogenic columns are no longer clearly visible, with roughly equal proportions of central mature spermatozoa, and surrounding tightly packed cells at earlier stages of spermatogenesis. Three specimens were *ripe* (8%), where gonads appear engorged, extensively spread throughout bursae and replete with spermatozoa (**Figures 4B,H**). Putative evidence of nutritive phagocytes was used as the basis for discriminating a minority of male specimens as being in a *post-spawn/recovery* state (8%, **Figure 4C**, with gonad aspect in **Figure 4I**). The single *Ophiacantha cosmica* male collected was at the *developing* stage, with evident spermatogenic columns (**Figure 5A**).

No *ripe* females were identified in either species. However, most *Ophiosphalma glabrum* females had ovaries in a *nearly ripe* state (56% overall, 100% in 2015, and 39% in 2019), where $VIII_{plus}$ oocytes dominate, but the ovary is not replete and has not yet spread far into the bursa (e.g., **Figures 4E,K**). A further 33% of individuals in *post-spawn/recovery* and 27% with *developing* ovaries (see **Figures 4D,F**) were also identified, all in 2019. All-but-one of the *Ophiacantha cosmica* females were *developing* (e.g., **Figure 5B**). The smallest female was in a *post-spawn/recovery* state (or possibly *developing* for the first time).

Oocytes at every stage of oogenesis were identified in *Ophiosphalma glabrum* (**Figures 6A–C**). Maximum oocyte feret diameters for *O. glabrum* and *Ophiacantha cosmica* were a mature oocyte of 453 μm and VIII oocyte of 273 μm, respectively. However, unlike *Ophiosphalma glabrum*, oocytes at stages more advanced than VIII were not observed in *Ophiacantha cosmica* generally (**Figures 6D,E**), so it is likely that maximum oocyte diameters in this species are underestimated. The higher proportion of *nearly ripe Ophiosphalma glabrum* females in 2015 vs. 2019, is reflected in significant differences in ranked

[1]https://www.R-project.org/
[2]https://inkscape.org
[3]http://dx.doi.org/10.5883/DS-CCZ4

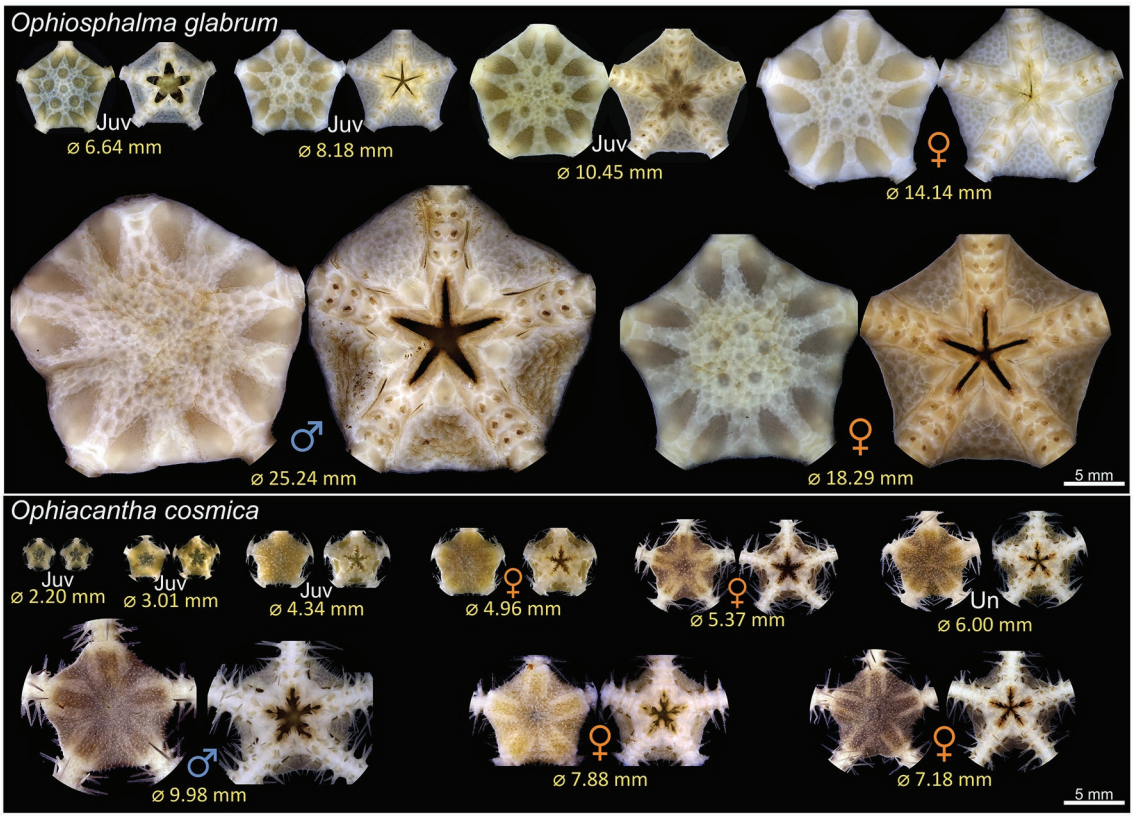

FIGURE 2 | Example discs of *O. glabrum* and *O. cosmica* from the current study. The aboral and oral faces of a subset of specimens encountered during the SO268 cruise in 2019 are pictured, representative of the size ranges encountered. Abbreviations: **Juv** *juvenile*; **Un** *undetermined sex* (see main text).

oocyte feret diameters between 2015 and 2019 (Kruskal-Wallis $\chi^2_1 = 63.5$, $p < 0.0001$). These differences, echoed by mean and median oocyte feret diameters for each year (2015-mean 159.1 ± sd. 91.7, median 149.5 ± mad. 109.0 and 2019-mean 112.0 ± sd. 78.3, median 88.0 ± mad. 57.8), relate to higher frequencies of $VIII_{plus}$ oocytes in the ovaries of specimens from 2015, clearly visible in the size-frequency data for both years (**Figure 6B**). Unfortunately, low sample sizes prohibit the quantitative comparison of oocyte frequency distributions as a function of contract area. That said, the proportion of large, late-stage oocytes found in specimens at the eastern-most sites appears higher (particularly for 2019, **Figure 5C**). No significant differences in ranked oocyte feret diameters between the two sampling years were found for *Ophiacantha cosmica* (Kruskal-Wallis $\chi^2_1 = 2.34$, $p > 0.05$), with similar oocyte size-class means, medians and distribution profiles identified for this species in both years (2015-mean 82.3 ± sd. 40.7, median 79.1 ± mad. 43.7; and 2019-mean 94.4 ± sd. 40.0, median 90.8 ± mad. 39.3; profiles in **Figure 6E**), though very low sampling sizes are likely undermining the statistical power of the test.

In addition to classifying oogenic stage and measuring oocyte feret diameters, the cross-sectional area occupied by oocytes relative to gonad area (inner-sac membrane) was calculated for *Ophiosphalma glabrum* – where tissue section quality allowed – as a proxy for the degree to which female gonads were full. A MSI previously demonstrated to be more sensitive to subtle changes in gonad maturation (Doyle et al., 2012) was also calculated for *O. glabrum*. Percentage of gonad occupied by oocytes (Kruskal-Wallis $\chi^2_2 = 11.37$, $p < 0.01$), mean oocyte feret diameter (Kruskal-Wallis $\chi^2_2 = 10.55$, $p < 0.01$) and MSI (Kruskal-Wallis $\chi^2_2 = 9.13$, $p < 0.05$) differed significantly as a function of *O. glabrum* gonad state (**Figure 7**). Evident differences existed in MSI and in the relative gonad area occupied by oocytes in *nearly ripe* females; however, these metrics both failed to resolve differences between *developing* and *post-spawn* females, with *post-hoc* pairwise comparisons revealing significant group differences only between *nearly ripe* females and the two other gonad states (**Figure 7**). Group differences in mean oocyte feret diameter were restricted to *nearly ripe* females and those classified as *post-spawn/recovery* (**Figure 6**), reflecting similar (non-significant) mean feret diameters between *developing* and *nearly ripe O. glabrum* females. Spearman-rank correlative analysis revealed oocyte density mm^{-2} of gonad cross-sectional area to be significantly, inversely related to mean oocyte feret diameter (coefficient $R = -0.74$, $p < 0.0001$, **Figure 7**), indicating a trade-off between investment per oocyte (i.e., size of yolk reserves) and the space available to house oocytes in each gonad.

Finally, intraindividual variation in the number and size of ovaries and oocyte densities per ovary in *O. glabrum* was considerable. Several *developing* females possessed

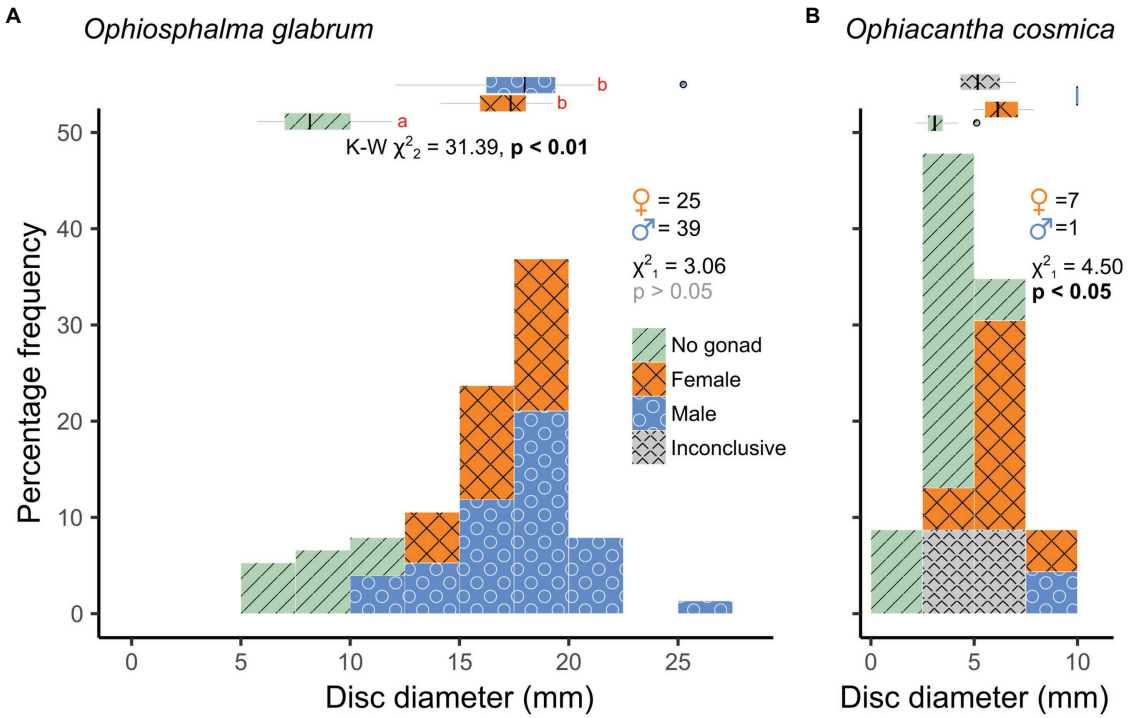

FIGURE 3 | Size-class frequency distributions of *O. glabrum* and *O. cosmica* disc diameters. Frequency histograms displayed for **(A)** O. glabrum and **(B)** O. cosmica are colour-coded by sex (including a "No gonad" category for immature specimens and an "Inconclusive" category for specimens with gonads devoid of gametes). Main χ^2 statistics relate to test for deviation from a 1:1 sex ratio (M vs. F only). Marginal box and whisker plots depict medians (vertical line), inter-quartile (box width), and 90% (whisker) ranges in disc diameter for each sex category. Proximate K-W χ^2 statistic and a value of *p* in a) relate to Kruskal-Wallis test for ranked differences in disc diameter as a function of all sex categories in *O. glabrum*. Significant *post-hoc* pairwise comparisons (Dunn's tests) are those with no letter annotations in common. Size-classes for each species are the same for comparative purposes.

neighbouring gonads at different stages of maturity based on visual aspect (e.g., **Figure 4J**). The presence of oocytes at various stages of oogenesis resulted in large variability in oocyte diameters (**Figure 8**), with large variances around median values (**Supplementary Figure 1**). Not unexpectedly – since one directly informed the other – the proportion of oocytes at each stage of oogenesis was relatively consistent in a given gonad state, irrespective of specimen size (**Figure 8**). However, overall ranked oocyte feret diameters were significantly higher in the largest *nearly ripe* disc-diameter size class, 17.5–20 mm, when compared with smaller size classes 12.5–15 mm and 15–17.5 mm (based on *post-hoc* comparisons, following a highly significant Kruskal-Wallis test for gonad state: Kruskal-Wallis χ^2_2 = 18.94, $p < 0.0001$, **Supplementary Figure 1**). Significant *post-hoc* differences in ranked oocyte feret diameters were also identified across size classes in individuals in a state of *post-spawn/recovery* (Kruskal-Wallis χ^2_2 = 12.63, $p < 0.01$), due to the relative dominance of previtellogenic oocytes in one individual from the intermediate 15–17.5 mm size category for this gonad state (**Figure 8**). No significant size-related differences were identified in the oocyte feret diameters of *developing* individuals of either species.

As a result of intra- and inter-individual variability in gonad maturity overall, a reliable measure of fecundity proved impossible. However, extrapolating from 25 µm of tissue sectioned per individual, late-stage ($VIII_{plus}$) oocyte counts mm-sectioned^{-1} ovary $^{-1}$ ranged from 1.3 to 12.0 oocytes in *developing* females (n = 4), 5.0–30.0 oocytes mm-sectioned^{-1} ovary $^{-1}$ in *nearly ripe* females (n = 14), and 1.5–5.0 oocytes mm-sectioned^{-1} ovary $^{-1}$ in *post-spawn/recovery* females (n = 2).

DISCUSSION

The current study provides new ecologically relevant reproductive data for two species of ophiuroid living in an oligotrophic, highly stable low-energy environment in the NE equatorial abyss which, due to the presence of polymetallic nodules, is under future threat from deep-sea mining activities (Weaver et al., 2018). The current study documents the reproductive biology of *O. glabrum* for the first time. Equal sex ratios for intermediate modal disc-diameter size classes and the absence of any simultaneous hermaphrodites both point to gonochorism in *O. glabrum*. Unfortunately, the manner (and possibly timing) of sampling may have created biases in the size classes of each sex. Large (and ripe) females (i.e., >20-mm disc diameters) were conspicuously absent, suggesting either an unlikely upper limit on female disc diameter, or most probably, that large females were overlooked.

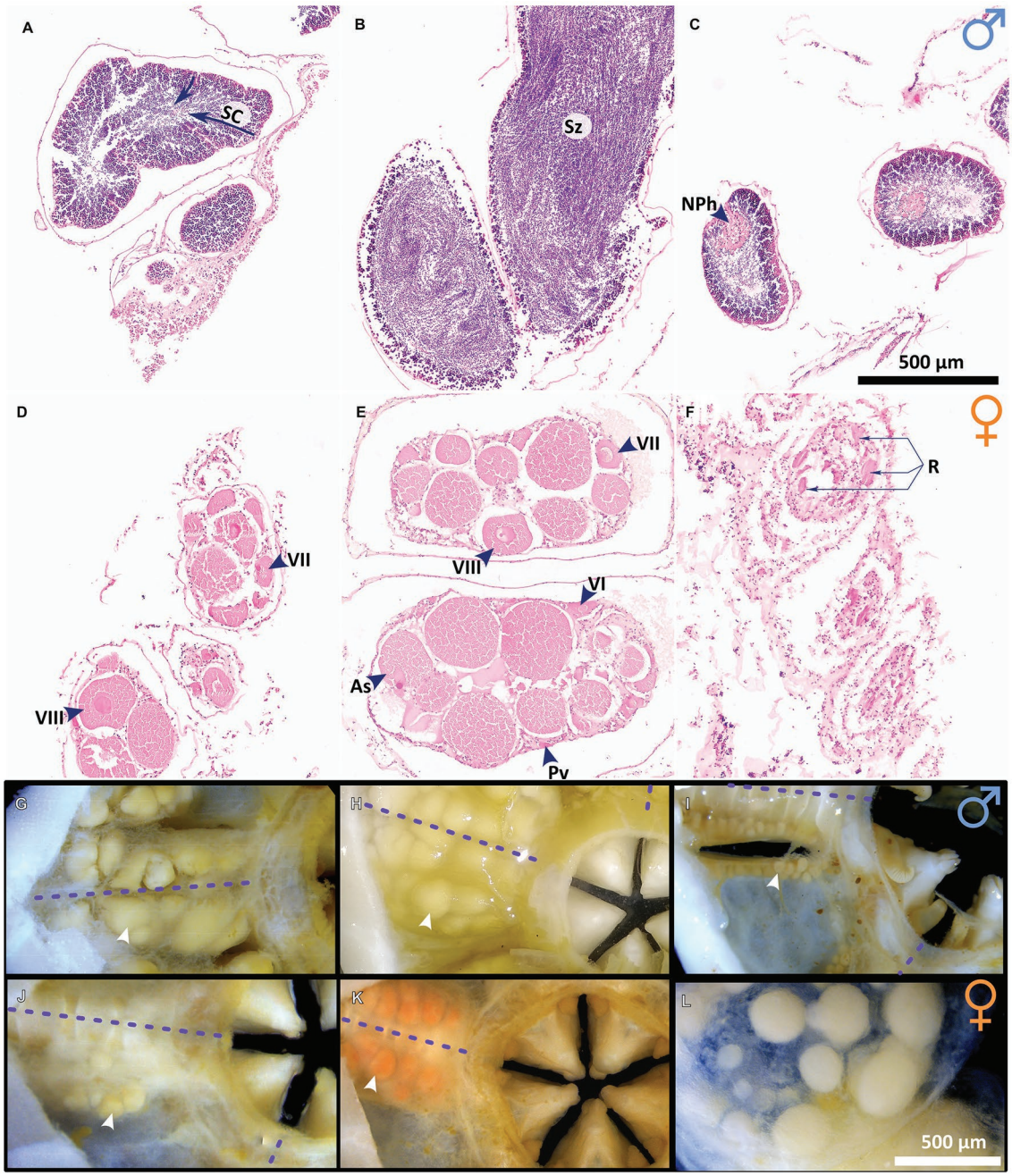

FIGURE 4 | Gametogenesis and gonad development in *O. glabrum*. Gonads at various stages of development in *O. glabrum*, as follows: **(A)** *developing* testes in which spermatogenic columns (**SC**) are evident (indicated with arrows), **(B)** *ripe* testes and **(C)** *post-spawn / recovery* testes; **(D)** *developing* ovaries, **(E)** *nearly ripe* ovaries, and **(F)** *post-spawn / recovery* ovaries; visual aspect of **G**) *developing* testes (corresponding to **A**), **(H)** *ripe* testes (corresponding to **B**) and **(I)** *post-spawn/recovery* testes (corresponding to **C**) and finally, visual aspect of **(J)** *developing* ovaries (corresponding to **D**), **(K)** *nearly ripe* ovaries (corresponding to **E**) and **(L)** a single ovary viewed down the distal-proximal axis, where late-stage oocytes are located distally (foreground), having previously developed from the basal region, where early-stage oocytes are visible beneath. White arrowheads in **(G-I)** indicate single gonads, and purple dotted lines are midlines of arm bases. Other abbreviations: **As** *Asymmetric oocytes*, **NPh** *Nutritive phagocytes*, **Pv** *Previtellogenic oocytes*, **R** *Residual oocytes*, **VI** *Vitellogenic I oocytes*, **VII** *Vitellogenic II oocytes*, **Sz** *Spermatazoa*, **VIII** *Vitellogenic III oocytes*.

This may simply be symptomatic of a patchy (or sex-specific) species distributions, where large communal echinoderm aggregations in the soft-sediment abyss only really occur during the episodic arrival of labile organic matter to the seafloor (Kuhnz et al., 2014; Smith et al., 2018) or during aggregative spawning events (Mercier and Hamel, 2009).

Oocyte feret diameters frequently exceeding 300 µm in the current study (max 453 µm in a mature oocyte) are indicative of

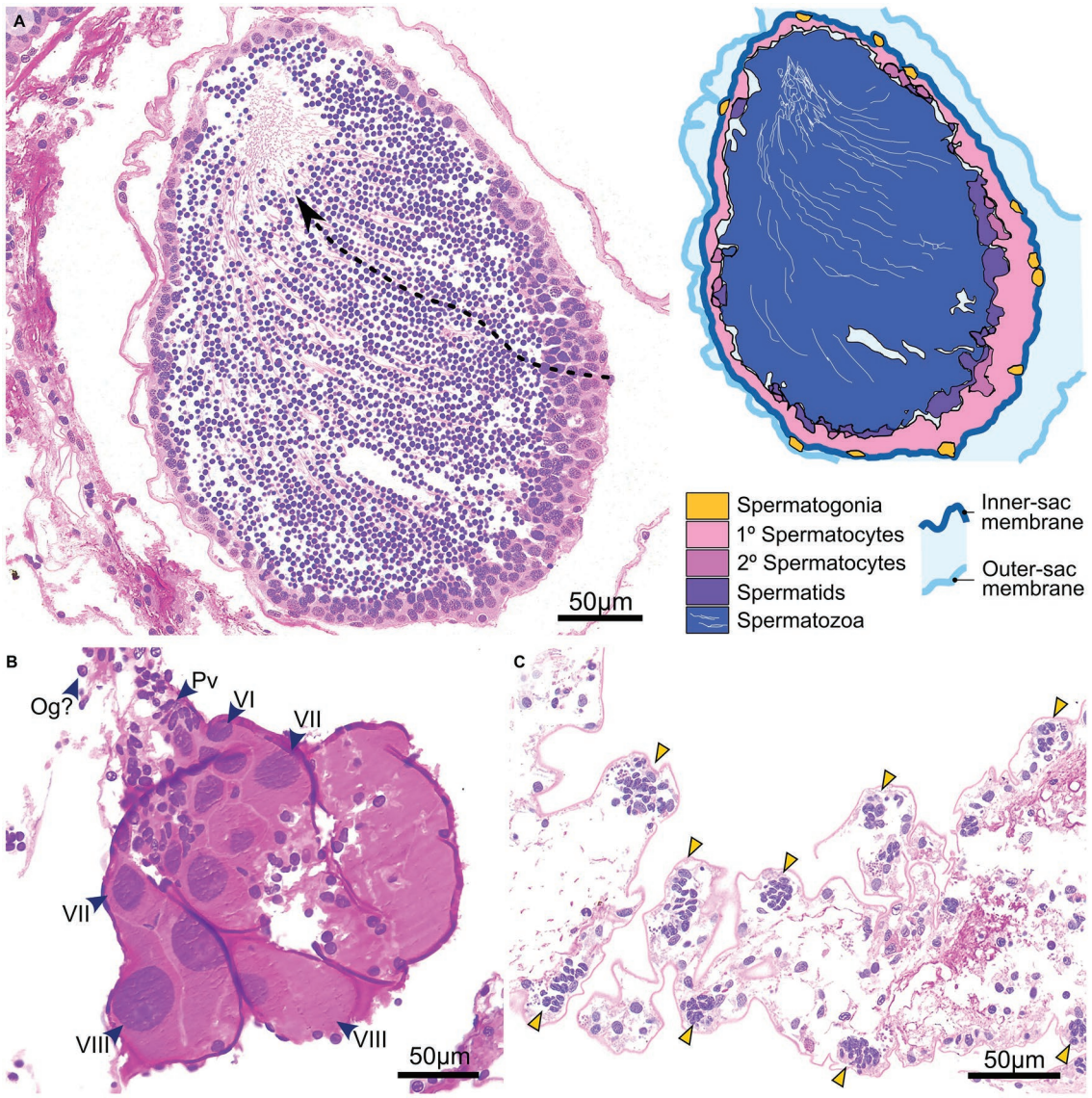

FIGURE 5 | Gametogenesis and gonad development in *O. cosmica*. Gonads at different stages of development in *O. cosmica*: **(A)** *developing* testes, in which spermatogenic columns are evident (dotted arrow), where cells at progressive developmental stages form chains that extend from the inner-sac membrane into the central lumen; **(B)** *developing* ovaries, in which various oogenic stages co-occur (the largest oocytes are distal-most to region of gonad attachment); and **(C)** pre-gametogenic gonadal tissue, with densely arranged pockets of putative primordial germ cells with basophilic nuclei that appear to form node-like gonadal precursors. Abbreviations: **Og** *Oogonia (putative)*, **Pv** *Previtellogenic oocytes*, **VI** *Vitellogenic I oocytes*, **VII** *Vitellogenic II oocytes*, **VIII** *Vitellogenic III oocytes*.

a lecithotrophic (non-feeding) larval mode with substantial yolk-protein and lipid reserves (Sewell and Young, 1997; Young, 2003). Although this places an upper limit on transport time relative to planktotrophy, lecithotrophy releases larvae of nutritional constraints that likely exist in food-impoverished transport environments. In addition, if lecithotrophic dispersal occurs in deep waters, where temperatures remain relatively low, this can act to extend transport times through metabolic suppression, with capacities for dispersal equivalent to planktotrophy (Mercier et al., 2013). Planktotrophic (feeding) larvae, by contrast, would be confined to water masses with higher detrital input (Young et al., 1997). Lecithotrophy necessitates greater energy investment per oocyte than in planktotrophy. This likely places constraints on fecundity in a food-limiting environment (Ramirez Llodra, 2002), as evidenced by the inverse relationship between oocyte densities and feret diameter in the current study. Ovaries in the current study when *nearly ripe*, were classified as such based mainly on oogenic characteristics, since striking external indications of maturity were lacking in female specimens. Coloration was inconsistent and ovaries were not engorged, nor had they spread extensively into the bursae, as was witnessed in at least one ripe male. This indicates considerable scope remained for further reproductive investment in the females collected, under suitable environmental conditions.

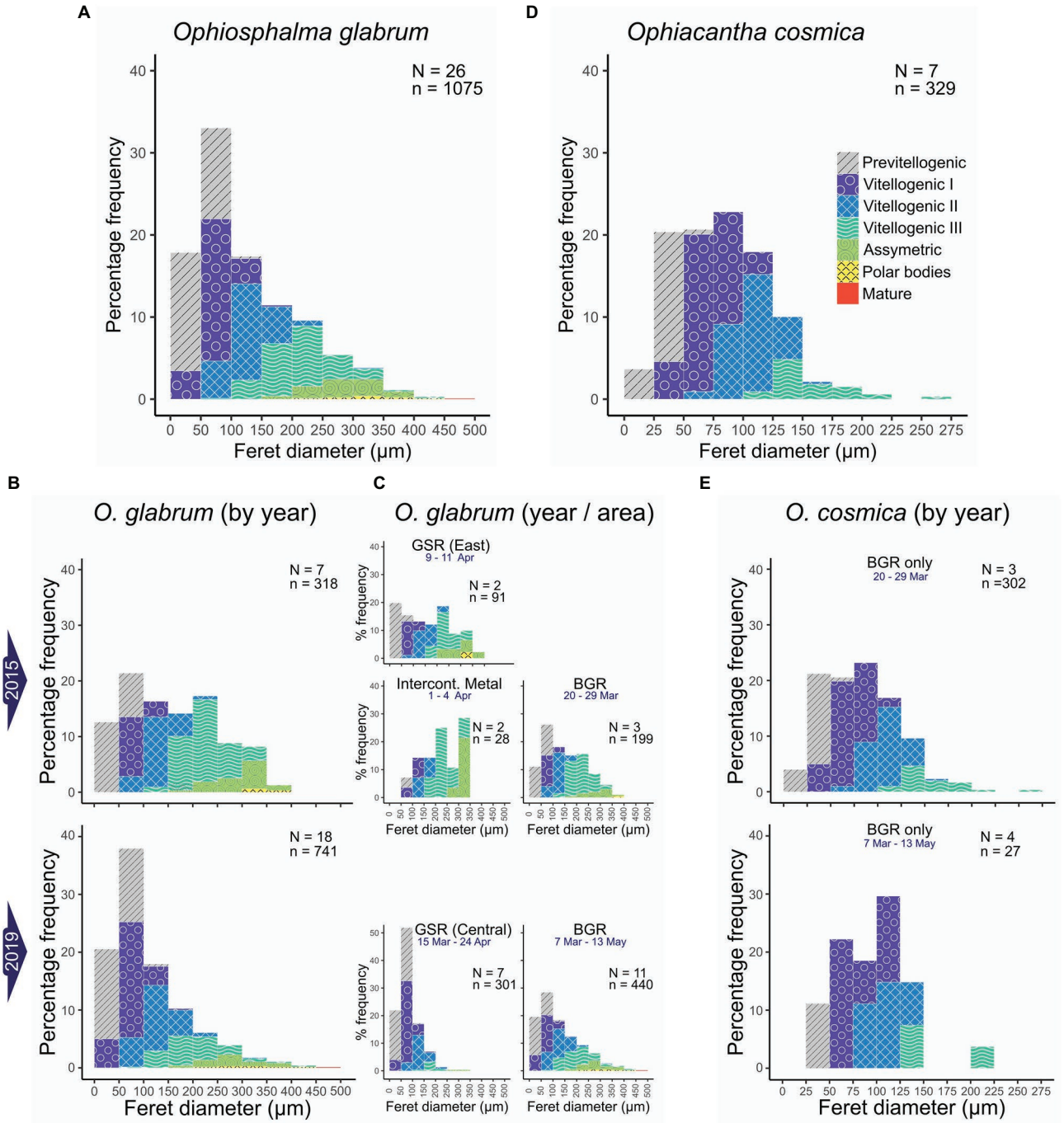

FIGURE 6 | Oocyte size-class frequency distributions. Frequency histograms display the relative proportions of oocytes in each size-class for feret diameters measured in females of each species. Only oocytes with nuclei were considered. Colour coding relates to associated oogenic developmental stages, assessed on a case-by-case basis for each oocyte counted and measured. Data for *O. glabrum* are on the left **(A–C)** displaying; **(A)** whole *O. glabrum* dataset; **(B)** data by sampling year and; **(C)** data by site for each year. Data for *O. cosmica* are on the right **(D,E)**, displaying; **(D)** whole *O. cosmica* dataset and **(E)** data by sampling year (this species was only recovered from the BGR contract area). *N* = total number of females, *n* = total number of oocytes pooled from N females.

Without ripe females and intra- and inter-annual time-series sampling it is not possible to ascertain whether gametogenesis is seasonal (Tyler and Gage, 1980; Gage and Tyler, 1982) or aperiodic ("continuous"), though the presence of all oogenic stages in most specimens suggests aperiodic or semi-continuous spawning behaviour (Brogger et al., 2013). Oocyte size-class data also appear to suggest that slight differences exist between 2015 and 2019, with a higher proportion of females approaching maturity in 2015. This could reflect the slightly different timing of cruises, as no *post-spawn recovery* females were found in

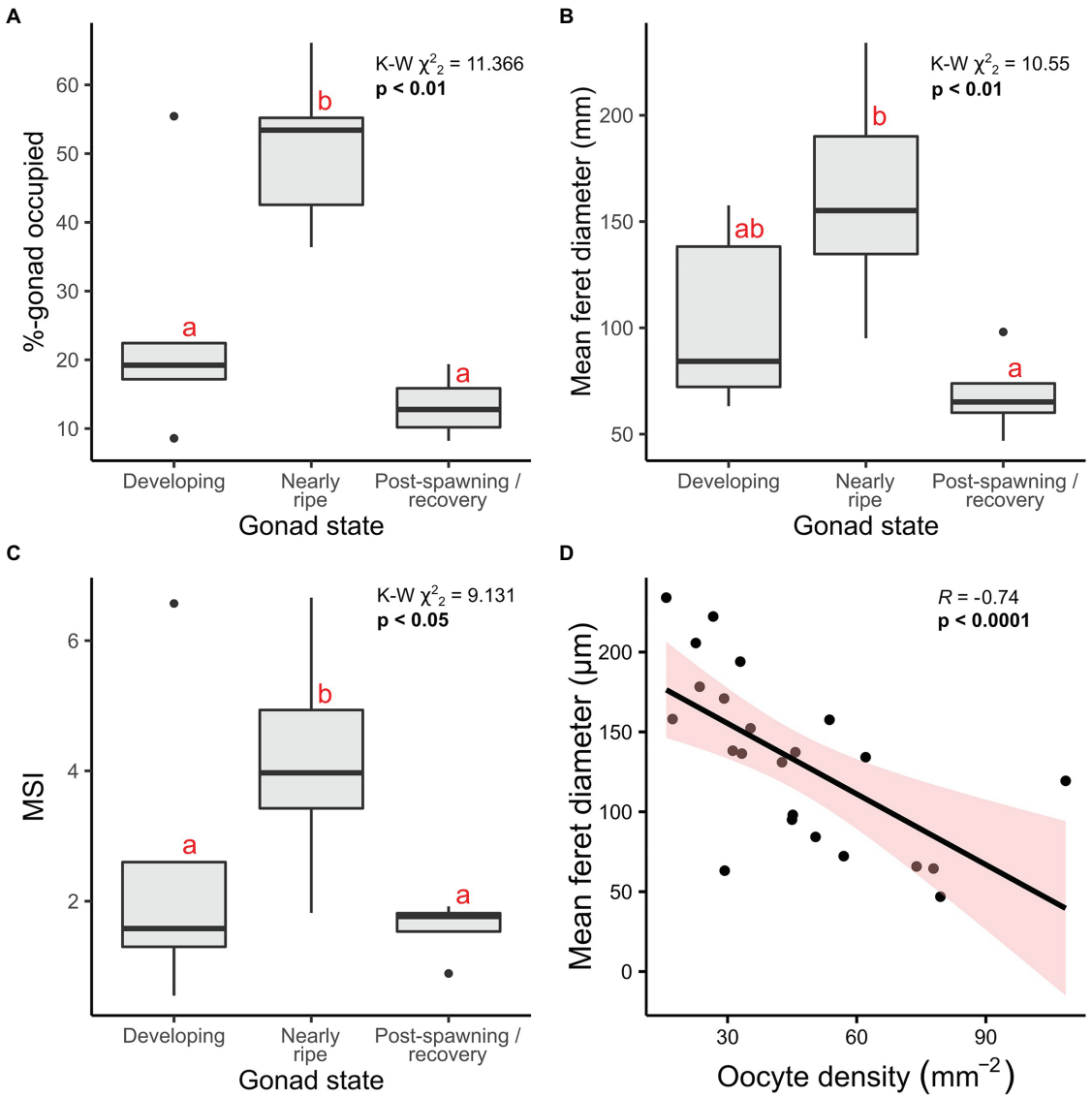

FIGURE 7 | Reproductive metrics plotted as a function of gonad state and oocyte density. Analyses are based on 23 female specimens, of which 14 were *nearly ripe*, five were *developing* and four were in *post-spawning/recovery*. **(A)** Percentage-gonad occupied by oocytes, **(B)** overall mean feret diameter per individual, and **(C)** a MSI developed by Doyle et al. (2012) were each calculated and evaluated as a function of gonad state, using Kruskall-Wallis Chi-squared tests on ranked data, the results of which are included in the top right corners for each. Significant *post-hoc* pairwise comparisons (Dunn's tests) are those with no letter annotations in common. Depicted in **(D)** is the Spearman rank-correlation analysis performed to identify any relationship between mean oocyte diameters and corresponding densities, with the resulting Rho statistic (R), a value of *p* and 95-% confidence intervals displayed.

2015 or site-related differences for each year since site locations were not the same. Further data are necessary to confirm this.

In an oligotrophic environment lacking strong seasonal fluctuations in POC flux, apparent aperiodic (or "continuous") gametogenesis may arise in species that spawn (1) periodically, but histological studies fail to identify their cyclical nature (Mercier et al., 2007; Mercier and Hamel, 2008) or (2) opportunistically, occurring in rapid response to increased food supply related to episodic massive changes in surface productivity and as such, remain undetected (Mercier and Hamel, 2009). Coupled with lecithotrophy, aperiodic opportunistic spawning would be resource-driven, allowing a species to respond to fluctuating food availability by investing in gametogenesis only when suitable conditions arise (e.g., Booth et al., 2008). Responsive reproductive modes of this sort appear to be a feature of bathyal and abyssal ecosystems in the tropical NE Pacific (Kuhnz et al., 2014; Smith et al., 2018), where the influences of episodic disturbance events are of greater influence than seasonal changes in surface productivity. However, additional sampling from highly oligotrophic NW regions of the CCZ (e.g., APEI 3, Vanreusel et al., 2016; Christodoulou et al., 2020)

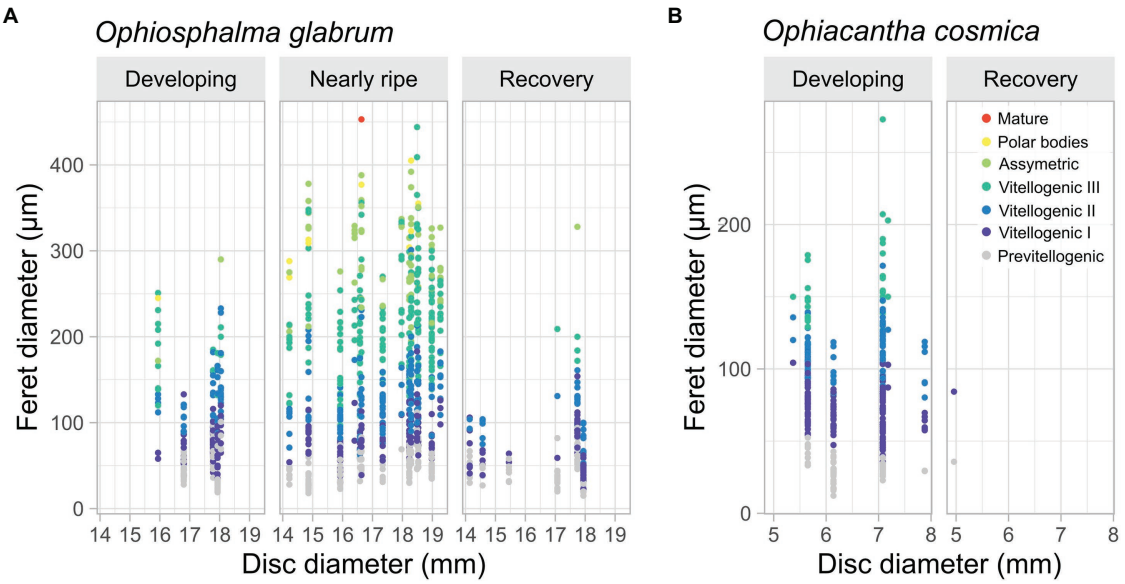

FIGURE 8 | Variation in oocyte feret diameter in *O. glabrum* and *O. cosmica* with specimen size. Scatterplots display variation in oocyte feret diameter with specimen size (disc diameter mm) for female gonad states identified in **(A)** *O. glabrum* and **(B)** *O. cosmica*. Colour-coding depicts oogenic developmental stage of each oocyte. Analyses are based on 25 *O. glabrum* specimens, of which 14 were nearly ripe, five were developing, and six were in post-spawning/recovery and seven *O. cosmica* specimens, of which all but one was developing. Significant differences in oocyte feret diameter across specimen size classes were assessed for each gonad state (where possible), using Kruskall-Wallis Chi-squared tests on ranked data (see main text and **Supplementary Figure 1** for Box and whisker plots of binned disc-diameter data).

would be needed to establish whether lower POC flux translates into reduced energetic investment in reproduction.

Maximum sizes recorded for *O. glabrum* vary considerably in the literature, but the largest attributed to this species is a 35 mm disc diameter (Clark, 1913), though there exists an *Ophiomusium multispinum* specimen – now synonymised with *Ophiosphalma glabrum* – with a 40-mm wide disc (Clark, 1911). In either case, the largest individual in the current study falls considerably short of these sizes, at 25.2 mm. Aside from some concerns around species assignation in historical samples and difficulties in collecting representative samples of species that occur at low densities in expansive and remote environments, these larger specimens also originate from shallower habitats (e.g., Cocos, Malpelo and Carnegie Ridge, Panama Basin, depths 800–3,200 m, Clark, 1911, 1913), where greater food availability arriving from productive coastal systems (Pennington et al., 2006) could enable larger maximum sizes. Although smaller specimens were undoubtedly underrepresented, enough immature *O. glabrum* were collected to establish a rough size at first maturity of <12 mm, around 30–35% maximum size. Without knowledge of growth rates, the time taken to reach these sizes remains unknown; however, if measures of growth (e.g., Gage et al., 2004) or temporal size-class frequency analyses can be compiled in future studies, this value could be easily converted to an estimate of age at first maturity, a highly relevant conservation metric for response to disturbance.

Sample sizes for the smaller species *Ophiacantha cosmica* limit any detailed interpretation of their reproductive biology. However, some data on size-class distributions and oocyte feret diameters already exist for this species from nodule-free habitats at Station M in the NE Pacific and around Crozet Island in the Southern Indian Ocean (Booth et al., 2008; Billett et al., 2013). Although sex ratios were significantly different in the current study, little stock can be placed in this result as the total number of mature specimens numbered less than 10 and maximum disc diameters for both sexes are markedly lower than in the literature. Evidence from other studies indicate that sex ratios follow a 1:1 ratio when sampled in larger numbers (Billett et al., 2013), with maximum disc diameters of 11–12 mm (Booth et al., 2008; Billett et al., 2013; M. Christodoulou, personal observations), although the disc diameter for this species' holotype is unaccountably large, at 18 mm (Lyman, 1878). Maximum oocyte feret diameter in the current study (VIII oocyte at 273 µm) also appears to be underestimated when compared with those of specimens from the Crozet Plateau (Billett et al., 2013), which reached maximum feret diameters exceeding 500 µm, indicating lecithotrophy (or direct development, though no evidence of brooding has ever been recorded, Billett et al., 2013; this study). This is to be expected as females in the current study were relatively small by comparison and only in *developing* states, with no oocytes in the final stages of meiosis (i.e., *asymmetric* or later). The only individual classified as *post-spawn/recovery* was probably developing for the first time, particularly in light of its small disc diameter. Unlike the protandric hermaphrodite *Ophiacantha fraterna* (Tyler and Gage, 1982; species identification updated from *Ophiacantha bidentata* by Martynov and Litvinova, 2008), data from the current study – corroborated by that of Billett et al. (2013) – indicate that *O. cosmica* is gonochoric. However, the current

study lacks sufficient data to confirm whether *O. cosmica* is also iteroparous, as is the case for *O. fraterna* (Tyler and Gage, 1982). Size at first maturity for *O. cosmica* was assessed in the current study but remains approximate at <4.96-mm disc diameter (in females), due to ambiguity around two relatively large specimens (6–7 µm disc diameters) that possessed tiny bud-like gonads in which no evidence for gametogenesis could be found. These gonads did possess nodes in which cell clumps with highly basophilic nuclei were located, which are believed to be gonadal precursors housing primordial germ cells (**Figure 5C**).

Ophiacantha spp. have been recorded from various hard substrata and vertically elevated fauna such as deep-sea corals (Tyler and Gage, 1980) and tube worms (Lauerman et al., 1996; Billett et al., 2013). In the current study, this species is recorded on stalked-sponge species *Caulophacus* sp. and *Hyalonema* spp. for the first time (**Figure 9**). Although alternative hard substrates are available in the CCZ (most obviously, polymetallic nodules), *O. cosmica* specimens here were exclusively epizoic; this species was not encountered elsewhere. Stalked sponges are some of the most elevated of fauna on the seafloor in the CCZ; colonising them at positions above the benthic boundary layer would mitigate the influences of shear on current speeds, which likely aids in a suspension-feeding lifestyle (Booth et al., 2008). The specimens in the current study either occurred as single individuals or, in certain instances, as size-stratified groups (**Figure 9**), suggestive of gregarious behaviour, offspring retention or fissiparity (though pentameral *Ophiacantha* spp. are not known to be fissiparous, Lee et al., 2019). A more detailed molecular work, beyond the scope of this study, would help to reveal common or distinct genetic origins for the members of these groups.

In contrast, *Ophiosphalma glabrum* examined in the current study was epibenthic as found in previous studies both within the CCZ (Amon et al., 2016; Glover et al., 2016; Christodoulou et al., 2020) and more generally in the NE Pacific (Booth et al., 2008). Stomach contents of dissected specimens also indicate that *O. glabrum* is a deposit feeder, like members of the closely related genus *Ophiomusa* (Pearson and Gage, 1984). Single individuals generally occurred in the sediment around nodules, or under habitat-forming fauna, such as non-stalked sponges and xenophyophores – giant, deep-sea foraminifera with delicate agglutinated tests (Goineau and Gooday, 2019).

The limited availability of food in the deep-sea soft-sediment benthos is a principal driver in structuring deep-sea benthic communities characterised by low population densities but high levels of diversity (Hardy et al., 2015). The CCZ is a vast, food-limited ecosystem, reliant on the arrival of particulate organic matter (POM) to the seafloor, dictated largely by productivity at the surface (Pennington et al., 2006). While nodule substrate availability plays a role in determining species distributions (Vanreusel et al., 2016), food availability – largely dependent on POM flux – will ultimately determine population densities. Having evolved under these relatively stable conditions, communities in the abyssal deep-sea may be poorly adapted, and thus highly susceptible to future mining impacts. If, for example, elevated substrata provide a nursery-type habitat for *Ophiacantha cosmica*, then the ramifications for reproductive success following future mining disturbance events are cause for concern. In addition, filter-feeding organisms are expected

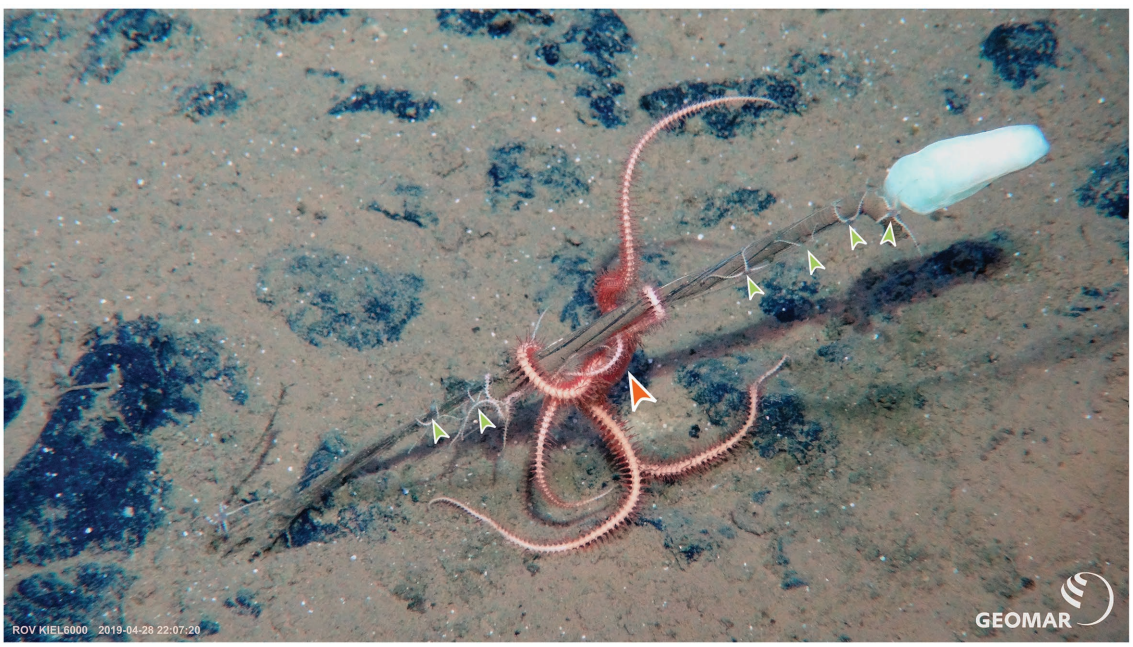

FIGURE 9 | *In-situ* photograph of a group of *O. cosmica* on a stalked sponge. Pictured is a female (large orange arrowhead) and several juvenile specimens (small green arrowheads) of *O. cosmica* that were sampled in the BGR contract area in 2019 during the SO268 R/V Sonne cruise. NB. Dark rock-like deposits in sediment are polymetallic nodules. Photo credit: ROV Kiel 6000, GEOMAR.

to be severely impacted by plumes and settling aggregates generated by the resuspension of sea-floor sediments during nodule collections, resulting in the long-term loss of suspension feeding organisms (Simon-Lledó et al., 2019). As with all deposit feeders, changes in surface-sediment chemical and physical characteristics following mining activity (e.g., remobilisation of formerly sequestered heavy metals and sediment compaction) could increase the toxicity of ingested sediments and impact *Ophiosphalma glabrum*'s ability to forage for food.

Food availability (i.e., POC flux) in soft-sediment abyssal habitats is subject to spatial variability both regionally, due to an undulating seafloor topography and at ocean-basin scales, as its dependency on surface productivity (Smith et al., 2008). Such heterogeneity in POC flux could create habitat networks of richer or poorer food supply over spatial scales at which reproductive kinetics and larval dispersal become ecologically relevant (Hardy et al., 2015). The CCZ lies along a POC flux gradient: lowest in regions that underlie central oligotrophic ocean gyres and highest beneath or adjacent to coastal and equatorial regions characterised by productive upwelling zones (Smith et al., 2008). Since population densities decrease concomitantly with POC flux (Tittensor et al., 2011), species in food impoverished areas often occur at densities below the minimum needed for reproductive success (e.g., critically low encounter rates for mating), rendering them wholly dependent on larval supply from populations in higher POC-flux habitats (the oligotrophic sink hypothesis, Hardy et al., 2015). The two species examined in the current study are relatively common in the CCZ and beyond (Booth et al., 2008; Amon et al., 2016; Christodoulou et al., 2019, 2020; Simon-Lledó et al., 2019). In fact, it is for this reason that the current reproductive study was even possible. However, the relative densities at which they occur at regional scales (such as between contract areas/APEIs) varies considerably (e.g., Christodoulou et al., 2020). Should mining activities proceed in regions of higher-POC flux that play a formative role as larval sources, this may have wide-reaching detrimental effects on the most food-limited populations of these and other species that employ planktonic larval dispersal.

Reproductive kinetics plays a fundamental role in mediating biogeographic patterns, population dynamics, metapopulation connectivity, and ultimately, species survival (Ramirez Llodra, 2002). While molecular approaches can be used to examine both historical and contemporary connectivity, the temporal resolution of these data remains too poor to discriminate between sporadic regional genetic exchange that then spreads locally over successive generations, and regular regional genetic exchange that acts to supplement local populations to a biologically meaningful degree. Reproductive ecology remains vital in bridging gaps in our understanding. The current study sought to add to the paucity of reproductive data for deep-sea species in nodule environments. It also highlights an uncomfortable truth in deep-sea ecology: these classical reproductive studies of this sort, which necessitate large numbers of individuals, may not be practicable in habitats such as the CCZ, where the most susceptible species are typically the rarest. Support for more ambitious approaches that compensate for sampling constraints, such as temporal studies or permanent monitoring networks are urgently needed in order for conservation measures to be effective and informed.

DATA AVAILABILITY STATEMENT

The original contributions presented in the study are included in the article/**Supplementary Material**, further inquiries can be directed to the corresponding author.

AUTHOR CONTRIBUTIONS

AH conceived the reproductive study. AH, MC, and PM coordinated the sample collection, fixation, and preservation. MC and PM performed all aspects of molecular ID. SL performed the specimen imagery, dissections, sectioning, histological, graphical and statistical analyses, prepared figures, and wrote manuscript with scientific input from remaining authors. All authors contributed to the article and approved the submitted version.

FUNDING

Cruises SO239 and SO268 were financed by the German Ministry of Education and Science (BMBF) as a contribution to the European project JPI Oceans "Ecological Aspects of Deep-Sea Mining." PM acknowledges funding from BMBF under contract 03F0707E and 03F0812E. SL and AH are supported by FCT/MCTES through CESAM (UIDP/50017/2020 + UIDB/50017/2020) funded by national funds, through the project REDEEM (PTDC/BIA-BMA/2986102/SAICT/2017) funded by FEDER within the framework of COMPETE2020 – Programa Operacional Competitividade e Internacionalização (POCI) and by Portuguese funds through FCT in special support of the JPIO pilot action "Ecological aspects of deep-sea mining" and the project MiningImpact2 (JPI Mining 2017, ref. Mining2/0002/2017), program 3599-PPCDT, Ciências do Mar – Sistemas Oceânicos e do Mar Profundo.

ACKNOWLEDGMENTS

The authors would like to acknowledge the captain and crew of the R/V Sonne and ROV Pilots for the Kiel 6000 (GEOMAR) and to the deep-sea scientists involved in cruise organisation as well as collection and processing of samples on board. The authors would also like to thank António and Sandra Calado for the use of an ultramicrotome. A pre-print of this manuscript is available on bioRxiv, Laming et al. (2020) at https://doi.org/10.1101/2021.02.06.428832.

SUPPLEMENTARY MATERIAL

The Supplementary Material for this article can be found online at: https://www.frontiersin.org/articles/10.3389/fmars.2021.663798/full#supplementary-material

REFERENCES

Adams, N. L., Heyland, A., Rice, L. L., and Foltz, K. R. (2019). Procuring animals and culturing of eggs and embryos. *Methods Cell Biol.* 150, 3–46. doi: 10.1016/bs.mcb.2018.11.006

Amon, D. J., Ziegler, A. F., Dahlgren, T. G., Glover, A. G., Goineau, A., Gooday, A. J., et al. (2016). Insights into the abundance and diversity of abyssal megafauna in a polymetallic-nodule region in the eastern Clarion-Clipperton Zone. *Sci. Rep.* 6:30492. doi: 10.1038/srep30492

Attali, D., and Baker, C. (2019). ggExtra: Add Marginal Histograms to "ggplot2", and More "ggplot2" Enhancements. Available at: https://CRAN.R-project.org/package=ggExtra

Baker, A. N. (2016). An illustrated catalogue of type specimens of the bathyal brittlestar genera *Ophiomusium* Lyman and *Ophiosphalma* HL Clark (Echinodermata: Ophiuroidea). *Zootaxa* 4097, 1–40. doi: 10.11646/zootaxa.4097.1.1

Billett, D. S. M., Bett, B. J., Evans, R., Cross, I., Tyler, P. A., and Wolff, G. A. (2013). The reproductive ecology of deep-sea ophiuroids around the Crozet plateau, Southern Indian ocean, under contrasting productivity regimes. *Deep-Sea Res. II Top. Stud. Oceanogr.* 92, 18–26. doi: 10.1016/j.dsr2.2013.03.002

Booth, J. A. T., Ruhl, H. A., Lovell, L. L., Bailey, D. M., and Smith, K. L. (2008). Size–frequency dynamics of NE Pacific abyssal ophiuroids (Echinodermata: Ophiuroidea). *Mar. Biol.* 154, 933–941. doi: 10.1007/s00227-008-0982-3

Brogger, M. I., Martinez, M. I., Zabala, S., and Penchaszadeh, P. E. (2013). Reproduction of Ophioplocus januarii (Echinodermata: Ophiuroidea): a continuous breeder in northern Patagonia, Argentina. *Aquat. Biol.* 19, 275–285. doi: 10.3354/ab00537

Brix, S., Osborn, K. J., Kaiser, S., Truskey, S. B., Schnurr, S. M., Brenke, N., et al. (2020). Adult life strategy affects distribution patterns in abyssal isopods–implications for conservation in Pacific nodule areas. *Biogeosciences* 17, 6163–6184. doi: 10.5194/bg-17-6163-2020

Christodoulou, M., O'Hara, T. D., Hugall, A. F., and Arbizu, P. M. (2020). Dark Ophiuroid biodiversity in a prospective abyssal mine field. *Curr. Biol.* 29, 3909–3912.e3. doi: 10.1016/j.cub.2019.09.012

Christodoulou, M., O'Hara, T., Hugall, A. F., Khodami, S., Rodrigues, C. F., Hilario, A., et al. (2020). Unexpected high abyssal ophiuroid diversity in polymetallic nodule fields of the Northeast Pacific Ocean and implications for conservation. *Biogeosciences* 17, 1845–1876. doi: 10.5194/bg-17-1845-2020

Clark, A. H. (1949). Ophiuroidea of the Hawaiian Islands. *Bull. Bernice P. Bishop Mus.* 195, 3–133.

Clark, H. L. (1911). *North Pacific Ophiurans in the Collection of the United States National Museum*. Washington, DC: US Government Printing Office.

Clark, H. L. (1913). *Echinoderms from Lower California, with descriptions of new species*. ed. J. A. Allen (Joel Asaph) (New York: American Museum of Natural History).

Danovaro, R., Aguzzi, J., Fanelli, E., Billett, D., Gjerde, K., Jamieson, A., et al. (2017). An ecosystem-based deep-ocean strategy. *Science* 355, 452–454. doi: 10.1126/science.aah7178

De Smet, B., Pape, E., Riehl, T., Bonifácio, P., Colson, L., and Vanreusel, A. (2017). The community structure of deep-sea macrofauna associated with polymetallic nodules in the eastern part of the Clarion-Clipperton Fracture Zone. *Front. Mar. Sci.* 4:103. doi: 10.3389/fmars.2017.00103

Doyle, G. M., Hamel, J.-F., and Mercier, A. (2012). A new quantitative analysis of ovarian development in echinoderms: the maturity stage index. *Mar. Biol.* 159, 455–465. doi: 10.1007/s00227-011-1823-3

Gage, J. D. (1982). Age structure in populations of the deep-sea brittle star *Ophiomusium lymani*: a regional comparison. *Deep Sea Res. A Oceano. Res. Papers* 29, 1565–1586. doi: 10.1016/0198-0149(82)90044-9

Gage, J. D., Anderson, R. M., Tyler, P. A., Chapman, R., and Dolan, E. (2004). Growth, reproduction and possible recruitment variability in the abyssal brittle star *Ophiocten hastatum* (Ophiuroidea: Echinodermata) in the NE Atlantic. *Deep-Sea Res. I Oceanogr. Res. Pap.* 51, 849–864. doi: 10.1016/j.dsr.2004.01.007

Gage, J. D., and Tyler, P. A. (1982). Growth and reproduction of the deep-sea brittlestar *Ophiomusium lymani* Wyville Thomson. *Oceanol. Acta* 5, 73–83.

Gage, J. D., and Tyler, P. A. (1991). *Deep-Sea Biology: A Natural History of Organisms at the Deep-Sea Floor*. Cambridge, UK: Cambridge University Press.

Ghosh, A. K., and Mukhopadhyay, R. (2000). *Mineral wealth of the ocean*. Rotterdam, The Netherlands: AA Balkema, Rotterdam, 260.

Glover, A. G., Wiklund, H., Rabone, M., Amon, D. J., Smith, C. R., O'Hara, T., et al. (2016). Abyssal fauna of the UK-1 polymetallic nodule exploration claim, Clarion-Clipperton Zone, Central Pacific Ocean: Echinodermata. *BDJ* 4:e7251. doi: 10.3897/BDJ.4.e7251

Goineau, A., and Gooday, A. J. (2019). Diversity and spatial patterns of foraminiferal assemblages in the eastern Clarion–Clipperton Zone (abyssal eastern equatorial Pacific). *Deep-Sea Res. I Oceanogr. Res. Pap.* 149:103036. doi: 10.1016/j.dsr.2019.04.014

Hardy, S. M., Smith, C. R., and Thurnherr, A. M. (2015). Can the source–sink hypothesis explain macrofaunal abundance patterns in the abyss? A modelling test. *Proc. R. Soc. B Biol. Sci.* 282:20150193. doi: 10.1098/rspb.2015.0193

Hauquier, F., Macheriotou, L., Bezerra, T. N., Egho, G., Martínez Arbizu, P., and Vanreusel, A. (2019). Distribution of free-living marine nematodes in the Clarion–Clipperton Zone: implications for future deep-sea mining scenarios. *Biogeo*. 16, 3475–3489. doi: 10.5194/bg-16-3475-2019

Hein, J. R., Mizell, K., Koschinsky, A., and Conrad, T. A. (2013). Deep-ocean mineral deposits as a source of critical metals for high-and green-technology applications: comparison with land-based resources. *Ore Geol. Rev.* 51, 1–14. doi: 10.1016/j.oregeorev.2012.12.001

Kassambara, A. (2020). ggpubr: "ggplot2" Based Publication Ready Plots. Available at: https://CRAN.R-project.org/package=ggpubr

Kuhnz, L. A., Ruhl, H. A., Huffard, C. L., and Smith, K. L. (2014). Rapid changes and long-term cycles in the benthic megafaunal community observed over 24 years in the abyssal Northeast Pacific. *Prog. Oceanogr.* 124, 1–11. doi: 10.1016/j.pocean.2014.04.007

Laming, S. R., Hourdez, S., Cambon-Bonavita, M.-A., and Pradillon, F. (2020). Classical and computed tomographic anatomical analyses in a not-so-cryptic *Alviniconcha* species complex from hydrothermal vents in the SW Pacific. *Front. Zool.* 17:12. doi: 10.1186/s12983-020-00357-x

Lauerman, L. M. L., Kaufmann, R. S., and Smith, K. L. (1996). Distribution and abundance of epibenthic megafauna at a long time-series station in the abyssal Northeast Pacific. *Deep-Sea Res. I Oceanogr. Res. Pap.* 43, 1075–1103. doi: 10.1016/0967-0637(96)00045-3

Lebrato, M., Iglesias-Rodríguez, D., Feely, R. A., Greeley, D., Jones, D. O. B., Suarez-Bosche, N., et al. (2010). Global contribution of echinoderms to the marine carbon cycle: $CaCO_3$ budget and benthic compartments. *Ecol. Monogr.* 80, 441–467. doi: 10.1890/09-0553.1

Lee, T., Stöhr, S., Bae, Y. J., and Shin, S. (2019). A new fissiparous brittle star, *Ophiacantha scissionis* sp. nov. (Echinodermata, Ophiuroidea, Ophiacanthida), from Jeju Island, Korea. *Zool. Stud.* 58, e8–e8. doi: 10.6620/ZS.2019.58-08

Lütken, C. F., and Mortensen, T. (1899). The Ophiuridae. *Mem. Museum Comp. Zoö.* 23, 93–208.

Lyman, T. (1878). Ophiuridae and Astrophytidae of the exploring voyage og HMS "Challenger" under Prof. Sir Wyville Thomson FRS. Part I. *Bull. Mus. Comp. Zool.* 5, 65–158.

Lyman, T. (1879). Ophiuridae and Astrophytidae of the exploring voyage og HMS "Challenger" under Prof. Sir Wyville Thomson FRS. Part II. *Bull. Mus. Comp. Zool.* 6, 17–83.

Lyman, T. (1882). Report on the Ophiuroidea dredged by HMS Challenger during the years 1873–1876. Report of the Scientific Results of the Voyage of HMS Challenger during 1873–1876, Zoology 5, 1–386.

Martynov, A. V., and Litvinova, N. M. (2008). Deep-water Ophiuroidea of the northern Atlantic with descriptions of three species and taxonomic remarks on certain genera and species. *Mar. Biol. Res.* 4, 76–111. doi: 10.1080/17451000701840066

Mercier, A., and Hamel, J.-F. (2008). Depth-related shift in life history strategies of a brooding and broadcasting deep-sea asteroid. *Mar. Biol.* 156, 205–223.

Mercier, A., and Hamel, J.-F. (2009). *Advances in Marine Biology: Endogenous and Exogenous Control of Gametogenesis and Spawning in Echinoderms*. Oxford, UK: Elsevier Science.

Mercier, A., Sewell, M. A., and Hamel, J.-F. (2013). Pelagic propagule duration and developmental mode: reassessment of a fading link. *Glob. Ecol. Biogeogr.* 22, 517–530. doi: 10.1111/geb.12018

Mercier, A., Ycaza, R. H., and Hamel, J.-F. (2007). Long-term study of gamete release in a broadcast-spawning holothurian: predictable lunar and diel periodicities. *Mar. Ecol.: Prog. Ser.* 329, 179–189. doi: 10.3354/meps329179

O'Hara, T. D., Rowden, A. A., and Williams, A. (2008). Cold-water coral habitats on seamounts: do they have a specialist fauna? *Divers. Distrib.* 14, 925–934. doi: 10.1111/j.1472-4642.2008.00495.x

Paterson, G. L. (1985). The deep-sea Ophiuroidea of the North Atlantic Ocean. *Bull. Br. Mus. Nat. Hist. Zool.* 49, 1–162.

Pearson, M., and Gage, J. D. (1984). Diets of some deep-sea brittle stars in the Rockall Trough. *Mar. Biol.* 82, 247–258. doi: 10.1007/BF00392406

Pennington, J. T., Mahoney, K. L., Kuwahara, V. S., Kolber, D. D., Calienes, R., and Chavez, F. P. (2006). Primary production in the eastern tropical Pacific: a review. *Prog. Oceanogr.* 69, 285–317. doi: 10.1016/j.pocean.2006.03.012

R Core Team (2020). R: A Language and Environment for Statistical Computing. Vienna, Austria: R Foundation for Statistical Computing. Available at: https://www.R-project.org/ (Accessed March 20, 2021).

Ramirez Llodra, E. (2002). Fecundity and life-history strategies in marine invertebrates. *Adv. Mar. Biol.* 43, 87–170. doi: 10.1016/S0065-2881(02)43004-0

Schindelin, J., Arganda-Carreras, I., Frise, E., Kaynig, V., Longair, M., Pietzsch, T., et al. (2012). Fiji: an open-source platform for biological-image analysis. *Nat. Methods* 9, 676–682. doi: 10.1038/nmeth.2019

Sewell, M. A., and Young, C. M. (1997). Are echinoderm egg size distributions bimodal? *Biol. Bull.* 193, 297–305. doi: 10.2307/1542932

Shulse, C. N., Maillot, B., Smith, C. R., and Church, M. J. (2017). Polymetallic nodules, sediments, and deep waters in the equatorial North Pacific exhibit highly diverse and distinct bacterial, archaeal, and microeukaryotic communities. *MicrobiologyOpen* 6:e00428. doi: 10.1002/mbo3.428

Simon-Lledó, E., Bett, B. J., Huvenne, V. A. I., Köser, K., Schoening, T., Greinert, J., et al. (2019). Biological effects 26 years after simulated deep-sea mining. *Sci. Rep.* 9:8040. doi: 10.1038/s41598-019-44492-w

Simon-Lledó, E., Pomee, C., Ahokava, A., Drazen, J. C., Leitner, A. B., Flynn, A., et al. (2020). Multi-scale variations in invertebrate and fish megafauna in the mid-eastern Clarion Clipperton Zone. *Prog. Oceanogr.* 187:102405. doi: 10.1016/j.pocean.2020.102405

Smith, C. R., De Leo, F. C., Bernardino, A. F., Sweetman, A. K., and Arbizu, P. M. (2008). Abyssal food limitation, ecosystem structure and climate change. *Trends Ecol. Evol.* 23, 518–528. doi: 10.1016/j.tree.2008.05.002

Smith, K. L., Ruhl, H. A., Huffard, C. L., Messié, M., and Kahru, M. (2018). Episodic organic carbon fluxes from surface ocean to abyssal depths during long-term monitoring in NE Pacific. *Proc. Natl. Acad. Sci. U. S. A.* 115, 12235–12240. doi: 10.1073/pnas.1814559115

Stearns, S. C. (2000). Life history evolution: successes, limitations, and prospects. *Naturwissenschaften* 87, 476–486. doi: 10.1007/s001140050763

Stöhr, S., O'Hara, T. D., and Thuy, B. (2012). Global diversity of brittle stars (Echinodermata: Ophiuroidea). *PLoS One* 7:e31940. doi: 10.1371/journal.pone.0031940

Tittensor, D. P., Rex, M. A., Stuart, C. T., McClain, C. R., and Smith, C. R. (2011). Species–energy relationships in deep-sea molluscs. *Biol. Lett.* 7, 718–722. doi: 10.1098/rsbl.2010.1174

Tyler, P. A. (1977). Seasonal variation and ecology of gametogenesis in the genus Ophiura (Ophiuroidea: Echinodermata) from the Bristol channel. *J. Exp. Mar. Biol. Ecol.* 30, 185–197. doi: 10.1016/0022-0981(77)90011-9

Tyler, P. A., and Gage, J. D. (1980). Reproduction and growth of the deep-sea brittlestar *Ophiura ljungmani* (Lyman). *Oceanol. Acta* 3, 177–185.

Tyler, P. A., and Gage, J. D. (1982). The reproductive biology of *Ophiacantha bidentata* (Echinodermata: Ophiuroidea) from the Rockall trough. *J. Mar. Biol. Assoc. U. K.* 62, 45–55. doi: 10.1017/S0025315400020099

Vanreusel, A., Hilario, A., Ribeiro, P. A., Menot, L., and Arbizu, P. M. (2016). Threatened by mining, polymetallic nodules are required to preserve abyssal epifauna. *Sci. Rep.* 6:26808. doi: 10.1038/srep26808

Weaver, P. P. E., Billett, D. S. M., and Van Dover, C. L. (2018). "Environmental risks of deep-sea mining," in *Handbook on Marine Environment Protection: Science, Impacts and Sustainable Management*. eds. M. Salomon and T. Markus (Cham: Springer International Publishing), 215–245.

Wessel, G. M., Voronina, E., and Brooks, J. M. (2004). Obtaining and handling echinoderm oocytes. *Methods Cell Biol.* 74, 87–114. doi: 10.1016/S0091-679X(04)74005-4

Wickham, H., Averick, M., Bryan, J., Chang, W., McGowan, L. D., François, R., et al. (2019). Welcome to the Tidyverse. *J. Open Source Softw.* 4:1686. doi: 10.21105/joss.01686

Wickham, H., Henry, L., Pedersen, T. L., Luciani, T. J., Decorde, M., and Lise, V. (2020). svglite: An "SVG" Graphics Device. Available at: https://CRAN.R-project.org/package=svglite

Wilke, C. O. (2020). cowplot: Streamlined Plot Theme and Plot Annotations for "ggplot2." Available at: https://CRAN.R-project.org/package=cowplot

Wilkie, I. C. (2016). Functional morphology of the arm spine joint and adjacent structures of the Brittlestar *Ophiocomina nigra* (Echinodermata: Ophiuroidea). *PLoS One* 11:e0167533. doi: 10.1371/journal.pone.0167533

Wilson, G. D. F. (2017). Macrofauna abundance, species diversity and turnover at three sites in the Clipperton-Clarion Fracture Zone. *Mar. Biodivers.* 47, 323–347. doi: 10.1007/s12526-016-0609-8

Young, C. M. (2003). "Reproduction, development and life-history traits," in *Ecosystems of the Deep Oceans*. ed. P. A. Tyler (Amsterdam: Elsevier), 381–426.

Young, C. M., Sewell, M. A., Tyler, P. A., and Metaxas, A. (1997). Biogeographic and bathymetric ranges of Atlantic deep-sea echinoderms and ascidians: the role of larval dispersal. *Biodivers. Conserv.* 6, 1507–1522.

Conflict of Interest: The authors declare that the research was conducted in the absence of any commercial or financial relationships that could be construed as a potential conflict of interest.

The handling editor declared a past co-authorship with one of the authors PM.

Copyright © 2021 Laming, Christodoulou, Martinez Arbizu and Hilário. This is an open-access article distributed under the terms of the Creative Commons Attribution License (CC BY). The use, distribution or reproduction in other forums is permitted, provided the original author(s) and the copyright owner(s) are credited and that the original publication in this journal is cited, in accordance with accepted academic practice. No use, distribution or reproduction is permitted which does not comply with these terms.

frontiers in Marine Science

ORIGINAL RESEARCH
published: 25 May 2021
doi: 10.3389/fmars.2021.671033

Eukaryotic Biodiversity and Spatial Patterns in the Clarion-Clipperton Zone and Other Abyssal Regions: Insights From Sediment DNA and RNA Metabarcoding

Franck Lejzerowicz[1,2], Andrew John Gooday[3,4], Inés Barrenechea Angeles[5,6], Tristan Cordier[5,7], Raphaël Morard[8], Laure Apothéloz-Perret-Gentil[9], Lidia Lins[10], Lenaick Menot[11], Angelika Brandt[12,13], Lisa Ann Levin[14], Pedro Martinez Arbizu[15], Craig Randall Smith[16] and Jan Pawlowski[5,9,17]*

[1] Center for Microbiome Innovation, University of California, San Diego, San Diego, CA, United States, [2] Department of Pediatrics, University of California, San Diego, San Diego, CA, United States, [3] National Oceanography Centre, Southampton, United Kingdom, [4] Life Sciences Department, Natural History Museum, London, United Kingdom, [5] Department of Genetics and Evolution, University of Geneva, Geneva, Switzerland, [6] Department of Earth Sciences, University of Geneva, Geneva, Switzerland, [7] NORCE Climate, NORCE Norwegian Research Centre AS, Bjerknes Centre for Climate Research, Bergen, Norway, [8] MARUM – Center for Marine Environmental Sciences, University of Bremen, Bremen, Germany, [9] ID-Gene Ecodiagnostics, Campus Biotech Innovation Park, Geneva, Switzerland, [10] Marine Biology Research Group, Ghent University, Ghent, Belgium, [11] IFREMER, REM/EEP/LEP, Centre de Bretagne, Plouzané, France, [12] Senckenberg Research Institute and Natural History Museum, Frankfurt, Germany, [13] Institute for Ecology, Evolution and Diversity, Goethe University Frankfurt, Frankfurt, Germany, [14] Integrative Oceanography Division, Center for Marine Biodiversity and Conservation, Scripps Institution of Oceanography, University of California, San Diego, San Diego, CA, United States, [15] German Centre for Marine Biodiversity Research, Senckenberg am Meer, Wilhelmshaven, Germany, [16] Department of Oceanography, University of Hawai'i at Mānoa, Honolulu, HI, United States, [17] Institute of Oceanology, Polish Academy of Sciences, Sopot, Poland

OPEN ACCESS

Edited by:
Chiara Romano,
Center for Advanced Studies of Blanes (CSIC), Spain

Reviewed by:
Owen S. Wangensteen,
UiT The Arctic University of Norway, Norway
Vera G. Fonseca,
Centre for Environment, Fisheries and Aquaculture Science (CEFAS), United Kingdom

***Correspondence:**
Franck Lejzerowicz
flejzerowicz@ucsd.edu

Specialty section:
This article was submitted to Deep-Sea Environments and Ecology, a section of the journal Frontiers in Marine Science

Received: 22 February 2021
Accepted: 19 April 2021
Published: 25 May 2021

Citation:
Lejzerowicz F, Gooday AJ, Barrenechea Angeles I, Cordier T, Morard R, Apothéloz-Perret-Gentil L, Lins L, Menot L, Brandt A, Levin LA, Martinez Arbizu P, Smith CR and Pawlowski J (2021) Eukaryotic Biodiversity and Spatial Patterns in the Clarion-Clipperton Zone and Other Abyssal Regions: Insights From Sediment DNA and RNA Metabarcoding. Front. Mar. Sci. 8:671033. doi: 10.3389/fmars.2021.671033

The abyssal seafloor is a mosaic of highly diverse habitats that represent the least known marine ecosystems on Earth. Some regions enriched in natural resources, such as polymetallic nodules in the Clarion-Clipperton Zone (CCZ), attract much interest because of their huge commercial potential. Since nodule mining will be destructive, baseline data are necessary to measure its impact on benthic communities. Hence, we conducted an environmental DNA and RNA metabarcoding survey of CCZ biodiversity targeting microbial and meiofaunal eukaryotes that are the least known component of the deep-sea benthos. We analyzed two 18S rRNA gene regions targeting eukaryotes with a focus on Foraminifera (37F) and metazoans (V1V2), sequenced from 310 surface-sediment samples from the CCZ and other abyssal regions. Our results confirm huge unknown deep-sea biodiversity. Over 60% of benthic foraminiferal and almost a third of eukaryotic operational taxonomic units (OTUs) could not be assigned to a known taxon. Benthic Foraminifera are more common in CCZ samples than metazoans and dominated by clades that are only known from environmental surveys. The most striking results are the uniqueness of CCZ areas, both datasets being characterized by a high number of OTUs exclusive to the CCZ, as well as greater beta diversity compared to other abyssal regions. The alpha diversity in the CCZ is high and correlated with

water depth and terrain complexity. Topography was important at a local scale, with communities at CCZ stations located in depressions more diverse and heterogeneous than those located on slopes. This could result from eDNA accumulation, justifying the interim use of eRNA for more accurate biomonitoring surveys. Our descriptions not only support previous findings and consolidate our general understanding of deep-sea ecosystems, but also provide a data resource inviting further taxon-specific and large-scale modeling studies. We foresee that metabarcoding will be useful for deep-sea biomonitoring efforts to consider the diversity of small taxa, but it must be validated based on ground truthing data or experimental studies.

Keywords: deep-sea sediment, eukaryotic biodiversity, Foraminifera, metazoans, 18S rRNA gene, bioinformatics, seafloor bathymetry

INTRODUCTION

The deep seabed encompasses a vast mosaic of poorly sampled habitats, many of them characterized by fine-grained sediments that, for more than 50 years, have been known to host surprisingly high levels of biodiversity (Hessler and Sanders, 1967; Ramirez-Llodra et al., 2010; Rex and Etter, 2010). It conceals a variety of material resources, services and history that are of cultural value to human societies (Wenhai et al., 2019; Turner et al., 2020) as well as ecosystems of considerable and growing economic importance (Armstrong et al., 2012; Thurber et al., 2014). However, estimating and conserving deep-sea biodiversity remain major challenges (Costello and Chaudhary, 2017), with many of the species found in deep-sea samples being undescribed (Glover et al., 2018). In some groups, this novelty is often at high taxonomic levels (Goineau and Gooday, 2019). Alongside biodiversity, understanding biogeographic patterns of benthic species on the ocean floor has been a long-standing and fundamental concern in deep-sea biology (Ekman, 1953; Vinogradova, 1997). In some cases, species horizontal ranges appear to be wider in the deep sea, particularly at abyssal depths, than in shelf and coastal waters (McClain and Hardy, 2010; Costello and Chaudhary, 2017), as landscapes of overlooked habitats such as bedrock offer corridors for dispersal (Riehl et al., 2020). However, the sheer scale of undescribed deep-sea biodiversity, combined with the rarity of many species and the vast spatial extent and chronic under-sampling of the deep seabed, make it very difficult to establish geographical ranges and the prevalence of endemicity, particularly for species that are small in size.

Previous attempts to tackle deep-sea biodiversity and biogeography have been based mainly on morphological analyses, with a bias toward larger, more conspicuous animals (Higgs and Attrill, 2015). These issues have been explored using metabarcoding (Taberlet et al., 2012), which is mainly based on environmental DNA (eDNA) and thus rather biased toward small, more inconspicuous taxa. Metabarcoding studies targeting the DNA of bacteria (Zinger et al., 2011), Foraminifera (Lecroq et al., 2011) as well as protists and meiofaunal animals (Bik et al., 2012; Guardiola et al., 2015; Sinniger et al., 2016) were conducted at global scale in the deep sea, but with relatively few samples. Evidence for DNA preservation, notably in the deep-sea sediment (Lejzerowicz et al., 2013a; Corinaldesi et al., 2018), justifies the use of environmental RNA (eRNA). Indeed, eRNA has been proposed as a proxy for active species in various environments (Logares et al., 2012; Adamo et al., 2020; Giner et al., 2020). It yields compositions that differ from eDNA in deep-sea sediments (Guardiola et al., 2016) and may therefore be more useful for interpreting biodiversity and biogeographic patterns. Yet further understanding of deep-sea processes can be obtained using metabarcoding, since this environment offers ideal conditions for the preservation of biomolecules, including eRNA which may persist in complex forms (Cristescu, 2019; Wood et al., 2020).

Besides fundamental methodological issues, the use of metabarcoding has practical benefits in the context of current and likely future human impacts on ocean-floor communities (Glover and Smith, 2003; Thiel, 2003; Levin et al., 2020a; Le et al. in revision), combined with the growing and far-reaching effects of global climatic changes (Levin and Le Bris, 2015; Danovaro et al., 2017; Sweetman et al., 2017; Morato et al., 2020), which will alter areas targeted for deep seabed mining (Levin et al., 2020b). The largest proportion of our samples was obtained in the eastern equatorial Pacific Clarion-Clipperton Zone (CCZ). This area lies beyond national jurisdictions (Rabone et al., 2019) and hosts vast deposits of polymetallic nodules (Hein et al., 2013; Petersen et al., 2016) that are the focus of an emerging seabed mining industry regulated by the International Seabed Authority (ISA). These activities will impact benthic ecosystems in a variety of ways (Levin et al., 2016) and likely lead to the irreversible loss of biodiversity (Niner et al., 2018), at least locally (Vonnahme et al., 2020). The ISA requires contractors licensed for mineral exploration and prospecting within the CCZ to conduct baseline surveys of benthic biodiversity, and subsequent exploitation contracts will require monitoring of mined areas to evaluate environmental impacts. Metabarcoding in the CCZ has been restricted to eDNA. It has been used to document prokaryotes in nodules (Blöthe et al., 2015) and in comparison with surrounding sediments and overlying water (Lindh et al., 2017, 2018), whereas eukaryotic studies pointing to the importance of habitat diversity and eDNA transport (Laroche et al., 2020a,b) were limited to the Western CCZ. No comparison with other abyssal regions was yet attempted.

Here, we perform eDNA and eRNA metabarcoding on 310 deep-sea sediment samples from the Eastern CCZ and other abyssal regions, including Northwest Pacific, Southern Ocean and several Atlantic regions in order to identify biogeographic patterns at larger scales and their relation to key environmental parameters at local scales, notably topographic heterogeneity. We rely on two 18S rRNA gene markers to reconstruct the taxonomic composition, diversity and distribution of benthic Foraminifera (37F marker) and Metazoa (V1V2 marker) that live or have lived in the Eastern CCZ region and explore some basic questions concerning: (1) the composition of sediment-dwelling eukaryotic assemblages at abyssal depths in the oceans; (2) levels of alpha diversity at particular abyssal sites and how they compare over different spatial scales; and (3) global (between oceans) to local (between stations) biogeographic patterns based on beta diversity turnover and dispersion. We rely on compositionally aware techniques that are necessary for omics data analysis, and on phylogenetic metrics to reflect on the evolutionary relatedness of communities sampled from eDNA or eRNA, that we systematically compare for more insightful interpretation. We discuss our conclusions in the context of recent metabarcoding and eco-evolutionary studies in the CCZ, in order to understand how environmental molecular data can be applied in future baseline surveys and the importance of small-sized organisms for deep-sea management and conservation in the face of rising pressures to mine minerals from the abyssal seafloor.

MATERIALS AND METHODS

Description of the Deep-Sea Sediment Sampling and Environmental Variable

Deep-sea sediments were collected at abyssal depths during eight expeditions to the Atlantic, Southern and Pacific Oceans (**Figure 1**). The largest number of samples originated from the Clarion-Clipperton Zone (CCZ) in the eastern Equatorial Pacific. They were taken mainly at the eastern end of this region, during the MANGAN'16 cruise in the BGR exploration license area and during the second ABYSSLINE cruise (AB02) in Stratum B (one of two 30 × 30 km study areas in which most samples were collected) of the UK-1 license area (hereafter called UK-1B) and a similar stratum within the OMS area. These two AB02 strata have very different topographies: UK-1B has approximately ten volcanic seamounts and hills on the abyssal plain, whereas the OMS stratum is much flatter with low, gently undulating abyssal ridges and troughs. Some samples were taken in the French (IFREMER) license area, located further to the west although still in the eastern half of the CCZ, during the BIONOD cruise. Sterile or disposable spoons were used to subsample the top surface sediment centimeter (ca. 2 g) according to a nested sampling design: up to three replicates per core; up to two cores per coring device deployment, and up to three deployments per station that were grouped into 16 areas and six larger regions (**Table 1**). Approximately 2 ml of fresh surficial sediments were collected with a multiple corer and placed in sterile tubes at −80°C with (VEMA, SYSTCO II, KuramBio I, MANGAN'16, and AB02) or without (MSM39, DIVA-3, and BIONOD) LifeGuard (Qiagen) Preservation Solution (6 ml) before shipment to the University of Geneva (Switzerland). For each station, the latitude and longitude were used to obtain environmental data layers presented in Howell et al. (2016), including seafloor slope (in degrees) and Bathymetric Position Indices (BPI, Broad, and Fine). A positive BPI value indicates a location higher than its surroundings (e.g., ridges) whereas a negative value indicates features such as valleys and troughs (Weiss, 2001).

Nucleic Acids Extraction, PCR Amplification and High-Throughput Sequencing

For each of 310 sediment samples, the total RNA and DNA contents of ca. 2 g of material were extracted as in Lejzerowicz et al. (2015) and cDNA was generated from DNase-treated RNA as in Pawlowski et al. (2014). It was ensured that no DNA molecules carried over into the RNA extracts based on the absence of PCR amplification with each primer set and after 60 cycles. From each sample, approximately 21 ng of DNA and cDNA extract were incorporated in 30-µl volume PCR amplifications performed in duplicate for each of the two 18S rRNA gene amplification primers pairs targeting Foraminifera and Eukaryota (**Supplementary Table 1** and **Supplementary Material**): the 37F hypervariable region using primers s14F1 and s15 (Lejzerowicz et al., 2014), and the V1V2 region using R22mod and F04 (Sinniger et al., 2016). Forward and reverse primers tagged at their 5′-ends with 8-nt tags were used in order to pool different amplicons to the same libraries and demultiplex the resulting reads to samples. The tagged primer combinations and their dispatching to libraries were designed to avoid and detect sequence-to-sample misidentifications due to mistagging (Esling et al., 2015) and to balance the base composition of the first sequenced positions (Illumina template cycles, see Mitra et al., 2015). The PCR duplicates of a given sample were amplified using the same tagged primer combinations, but pooled in different sequencing libraries in order to be able to analyze them separately. In total, 1,998 PCR products were mixed into 51 pools (on average: 44 ng per PCR; 39.2 PCRs per pool). The pools were transformed into sequencing libraries using the TruSeq Nano PCR-free Library Preparation Kit, which were Illumina-sequenced on two HiSeq 2500 runs (2 lanes; 36 libraries) and 5 MiSeq runs (5 lanes; 15 libraries). Strict procedures were respected to limit extraneous and cross contamination: (i) maximum 12 samples per session (one PCR session included the four markers and duplicates), (ii) separate laboratory spaces for no-DNA (PCR preparation), low-DNA (extraction and DNA/RNA/cDNA handling) and high-DNA (post-PCR) concentrations, (iii) lab coat and gloves worn at all time, (iv) cleaning with DNA AWAY^{TM} Surface Decontaminant (Thermo Fisher Scientific), and (v) wiping of each pipet tip on absorbent paper to avoid releasing the aerosols of primer, DNA or PCR products before gentle tip disposal. Technical information for each sample along with environmental variables and metadata information required by the MIMARKs standards (Yilmaz et al., 2011), including sequence frequencies after each filtering step (see next section), are available in **Supplementary Table 2**. Data and

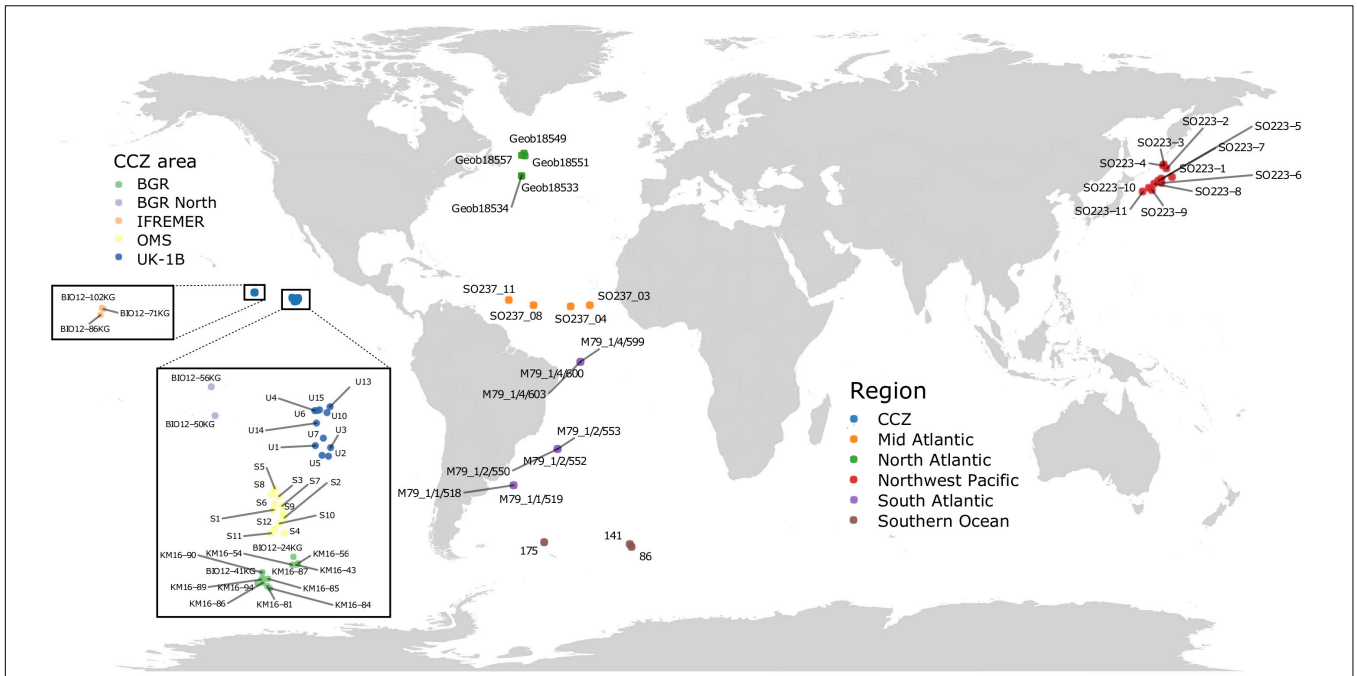

FIGURE 1 | Location of the sequenced sediment samples. Samples in the Pacific Ocean include two regions: the CCZ (five different areas, see inset) and the Northwest Pacific (Kuril-Kamchatka area). Samples in the Atlantic Ocean include three regions (North, Mid, and South Atlantic), as well as three areas (and stations) in the Southern Ocean region.

metadata are publicly available in FigShare[1] and at the European Bioinformatics Institute under accession number PRJEB44134.

Bioinformatic Sequence Data Processing

HiSeq sequencing generated ambiguous bases at a few positions corresponding to the amplification primer sequences (i.e., after the tags; **Supplementary Figure 1**). A python script was used to correct these ambiguities if their number corresponded to the hamming distance with the closest primer sequence. The corrected paired-end fastq files of each library were processed to (i) demultiplex sequences to samples using DTD (Dufresne et al., 2019)[2], which allows the counting of sequences associated with unexpected primer combinations (or *mistags*, see Esling et al., 2015), (ii) quality-filter and merge paired reads using pandaseq 2.11 (options -t 0.6 -A pear -T 24 -o 30) (Masella et al., 2012), (iii) filter mistags out of each sample (see Esling et al., 2015, **Supplementary Material**), (iv) dereplicate sequences using mothur (Schloss et al., 2009) and remove the resulting unique sequences that are singletons or that occur in only one of the two PCR replicates, (v) cluster sequences into operational taxonomic units (OTUs) to reduce diversity inflation due to PCR and sequencing errors using *swarm* v3 (option -f) (Mahé et al., 2015), (vi) filter potentially chimeric sequences using UCHIME (Edgar et al., 2011) in *de novo* mode as implemented in QIIME2 (Bolyen et al., 2019), and (vii) remove samples with less than 3,000 reads or less than 10 OTUs.

Reference Databases and Taxonomic Assignments

For the taxonomic assignment of foraminiferal OTUs, an alignment of 3,145 18S rRNA gene sequences belonging to classes Monothalamea, Globothalamea, and Tubothalamea as well as planktonic isolates was curated (PRF^2, Morard et al., 2015). Each sequence entails the hypervariable 37F region that has proved powerful for foraminiferal species identification (Pawlowski and Lecroq, 2010; Lecroq et al., 2011; Lejzerowicz et al., 2014), is flanked by at least 50 and 150 nucleotides at its 5′ and 3′ ends, and contains no ambiguous nucleotide (N) or species-level duplicate. A phylogeny built using RAxML v8.2.12 (1,000 bootstraps, GTRGAMMAI model; Stamatakis, 2014) was manually inspected using EMPress (Cantrell et al., 2020) to identify and remove rotaliid sequences branching with monothalamids, in contradiction with the current foraminiferal phylogeny (Holzmann and Pawlowski, 2017; **Supplementary Figure 2**). The resulting 3,002 18S fragments were harmonized to six taxonomic levels (class; order; family; genus; species; and isolate) in order to serve as a reference database.

For the taxonomic assignment of Eukaryota OTUs, both the Protist Ribosomal Reference database (PR^2, Guillou et al., 2013) and SILVA 138.1 (SSU Ref NR 99, Quast et al., 2013) were used, without Insecta and harmonized to the eight taxonomic levels of the PR^2 taxonomic framework (kingdom; domain; phylum; class; order; family; genus; species). Although the taxonomic ranks from PR^2 were employed, SILVA was kept because PR^2 is biased toward protists whereas SILVA remains a generalist database useful for Metazoa assignments. It is important to note

[1]https://figshare.com/account/home#/projects/98972

[2]github.com/yoann-dufresne/DoubleTagDemultiplexer

TABLE 1 | Origins and numbers of deep-sea sediment material, and successfully PCR-amplified and sequenced samples.

						PCRs				Reads			
						V1V2		37F		37F		V1V2	
Region	Expedition	Cruise report	Area/ Stratum	Stations	Sediment samples (DNA and RNA)	DNA	RNA	DNA	RNA	DNA	RNA	DNA	RNA
CCFZ	ABYSSLINE 02	Smith et al., 2013	OMS	12	67 (49)	118	122	130	85	5825513	1762646	9163968	4196374
			UK-1B	11	66 (60)	124	124	130	83	4068014	2060791	9060095	6002215
	BIONOD	Menot, 2012	BGR North	2	2 (1)	2	1	0	3	67503	5857	0	18236
			BGR	2	2 (1)	4	2	0	4	513177	11141	0	568777
			IFREMER	3	3 (2)	6	4	0	4	606679	62151	0	258482
	MANGAN'16	Not available	BGR	11	38 (20)	50	15	0	58	3135323	187228	0	2110184
Mid Atlantic	VEMA	Devey, 2015	East Basin	2	17 (7)	27	33	33	34	1243418	687412	1875064	1543698
			West Basin	2	10 (4)	12	8	18	12	547636	61634	387766	169837
North Atlantic	MSM39	Mulitza et al., 2015	Central Orphan Basin	3	11 (3)	16	10	0	20	1298106	315858	0	1156835
			SE Grand Banks	2	7 (0)	14	1	0	12	1680373	4623	0	462307
Northwest Pacific	KuramBio I	Brandt and Malyutina, 2015	Kuril-Kamchatka	11	33 (33)	62	66	64	66	7327166	2715442	3085158	2940135
South Atlantic	DIVA-3	Martínez Arbizu et al., 2015	Argentinean Basin	2	2 (0)	4	2	1	2	248527	77578	32564	250088
			Brazilian Basin	6	6 (0)	12	8	0	8	1123375	102496	0	307278
Southern Ocean	SYSTCO II	Wolf-Gladrow, 2013	HC_AEP	1	12 (12)	20	24	20	24	1035445	701209	1258836	825238
			HC_BEP	1	16 (10)	32	17	32	21	2571136	428049	3238188	1097734
			South Georgia	1	18 (14)	32	31	2	30	4332986	892373	60307	1811967
			Totals	**71**	**310**	**535**	**468**	**430**	**466**	**35624377**	**10076488**	**28161946**	**23719385**

that the PR2 taxonomy does not include Xenacoelomorpha, which in this database is not distinguished from Platyhelminthes (Ruiz-Trillo et al., 1999).

Each OTU representative sequence was assigned using four different methods, including (i) vsearch 2.7.0 (Rognes et al., 2016) and (ii) BLAST+ (Camacho et al., 2009) both as implemented in QIIME2, as well as (iii) IDTAXA (Murali et al., 2018) and (iv) SINTAX (Edgar, 2016). For every individual method, the deepest assignment associated with a probability of at least 0.9 was retained. Finally, OTUs were classified to the last common ancestor found by at least two out of the four assignment methods, and also across the two databases for Eukaryota OTUs.

Metazoa Novelty

A V1V2 subset composed of OTUs assigned to Metazoa was created for comparison with the OTUs reported in Sinniger et al. (2016). From the corresponding author, the Metazoa OTU read counts table (17 samples) was obtained, as well as their aligned representative sequences (8,517) and associated phylogeny, which was used as a guide tree for RAxML (GTRCAT model) to build a phylogeny suitable for phylogenetic sequence placement with SEPP (Mirarab et al., 2012). Then, our homologous V1V2 OTU sequences were placed onto this tree and their prevalence in CCZ samples was visualised in EMPress (for either or both types of molecule). In order to evaluate the quality of the placements, five SEPP repetitions were performed, using five different placement sizes (parameter "-P").

In parallel, our OTU sequences were co-clustered with the OTU sequences from Sinniger et al. (2016) in order to evaluate the amount of metazoan novelty in a deep-sea benthic sequencing survey. Two to 17 samples were randomly sub-sampled from Sinniger et al. (2016) and OTUs re-replicated into reads (following table counts) that were concatenated with a similar number of unique sequences per OTU randomly sampled from our study, using the same number of samples and the same reads proportions. Clustering was then performed using *swarm* v3 (as above) on the concatenated sequences of each sampling size and the proportion of resulting clusters containing sequences from both studies was measured (or "co-clusters"). Each random sub-sampling of sequences from 2 to 17 samples was repeated

one hundred times. The whole procedure was also repeated for each of three stations of Sinniger et al. (2016) from which were generated 2–6 samples in this study.

Alpha Diversity

Phylogenetic placement of the 37F OTUs sequences onto the foraminiferal phylogeny (without planktonic sequences) and of the V1V2 OTUs onto the SILVA v128 phylogeny pre-computed for use with SEPP was performed in QIIME2 (Janssen et al., 2018). QIIME2 was used to calculate the Faith's Phylogenetic Diversity (PD) index (Faith, 1992) based on these trees, in addition to the Shannon's entropy index for alpha diversity analyses. The Faith's PD metric computes the amount of root-to-tip branch length on the phylogeny represented by each community's OTUs, but it does not account for the number of reads associated with these OTUs. Hence, the Shannon's entropy index was also calculated as it incorporates relative read abundances. Both indices were computed after rarefaction to 3,000 reads per sample. For each marker, the difference between regions, areas, stations and coring device deployments was tested based on the Kruskal–Wallis *H* test for independent samples (Kruskal and Wallis, 1952) using the python library *scipy* (Virtanen et al., 2020). To satisfy sample independence, tests were performed for each set of replicates and for DNA and RNA separately, and *p*-values were adjusted using the python library *statsmodels* for false discovery rate control on multiple testing (Benjamini and Hochberg, 1995). Post-hoc pairwise comparisons between individual regions and areas were performed using the Faith's PD index (after Kruskal–Wallis *H* tests results showed significant differences at these scales; see section "Results") implemented in the R package *conover.test* (Conover and Iman, 1979). For these geographic scales, the difference in alpha diversity between DNA and RNA samples was also assessed using paired Kruskal–Wallis tests (Bonferroni adjusted per scale). Finally, the correlation between the Faith's PD index and each environmental variable was measured using Spearman's rho with *scipy*.

The OTU richness found exclusively at intersections of areas was measured across the 37F benthic Foraminifera and V1V2 Eukaryota datasets, as well as at intersections of stations within the CCZ UK-1B and OMS strata. The R package *upSetR* (Conway et al., 2017) was used to also report the number of sequence reads associated with each of the 30 most-important intersections in terms of OTU richness.

Beta Diversity

Based on placement trees, the Weighted and Unweighted UniFrac distances were computed for beta diversity analyses. These distances measure phylogenetic relatedness by quantifying the amount of unique branch length between communities (Lozupone and Knight, 2005; McDonald et al., 2018b). Metabarcoding and other environmental-sequencing data are compositional, as the true total of each sample is not known (Quinn et al., 2018). Hence, the compositionally robust Aitchison distance was employed to build sample dissimilarity matrices and identify clusters in Robust Principal Component Analysis (RPCA) (Aitchison, 1982, 1986) using the EMPeror visualization tool in QIIME2 (Vázquez-Baeza et al., 2013). This Aitchison metric includes a centered log-ratio transformation step, as performed in DEICODE, which also includes a matrix completion step for sparse data (Martino et al., 2019). Dissimilarity matrices were also built using the more traditional Jaccard and Bray-Curtis dissimilarity metrics (e.g., Legendre and Legendre, 2012).

These dissimilarity matrices were subject to one-way group comparisons of beta diversity between regions, areas or stations using PERMANOVA, as well as for differences in dispersion within each of these groups using PERMDISP (no group with fewer than 10 samples included, 999 permutations, performed using QIIME2). Additionally, the added beta diversity was evaluated by randomly sampling the matrices 10 times for each of an increasing number of samples and measuring the minimum distance among these samples, thus building dissimilarity-decay curves. These curves are similar to rarefaction curves but performed on samples dissimilarity, providing a way to explore the novelty space of communities, as proposed in Huttenhower et al. (2012, see Figures 3D,E) and McDonald et al. (2018a). The dissimilarity matrices and ordinations obtained before and after the removal of non-metazoan OTUs were also compared using Mantel tests (Mantel, 1967) with QIIME2 and PROTESTs (Jackson, 1995) with the R package *vegan* (Oksanen, 2011), respectively.

Local-Scale Heterogeneity and Relation to Bathymetry in the CCZ

Local-scale heterogeneity was assessed in terms of community turn-over by measuring the beta-diversity dispersion of each station within the UK-1B and OMS strata of the CCZ. First, RPCA ordination was performed (as above) but only for the CCZ samples and separately for the DNA and RNA versions of these samples. Then, the position of the centroid formed in these RPCA spaces (in three dimensions) by the maximum of six samples (three replicates from each of two sediment cores of the same deployment) was calculated at each station and the distances separating these samples from their centroid were collected. For an illustration, see **Supplementary Figure 20** where the samples are colored per station on the RPCAs used to calculate distance-to-centroids. This approach is similar to that proposed using the distance-to-plane in the human gut microbial ecosystem (Halfvarson et al., 2017). We describe the average and standard deviation of these distances-to-centroids at each station on the UK-1B and OMS maps and in relation to bathymetry. Maps and their isodepth contour lines were fetched using the function *getNOAA.bathy()* (R package *marmap*, Pante and Simon-Bouhet, 2013) and the Bathymetric Position Index environmental variable was smoothed over space using the function *Smooth()* (sigma = 0.05, R package *spatstat*, Baddeley et al., 2015). Finally, the DNA and RNA distributions of these distances to stations' centroids were compared using paired *t*-tests with the R package *ggpubr*. All code to perform and reproduce the analyses is available upon request.

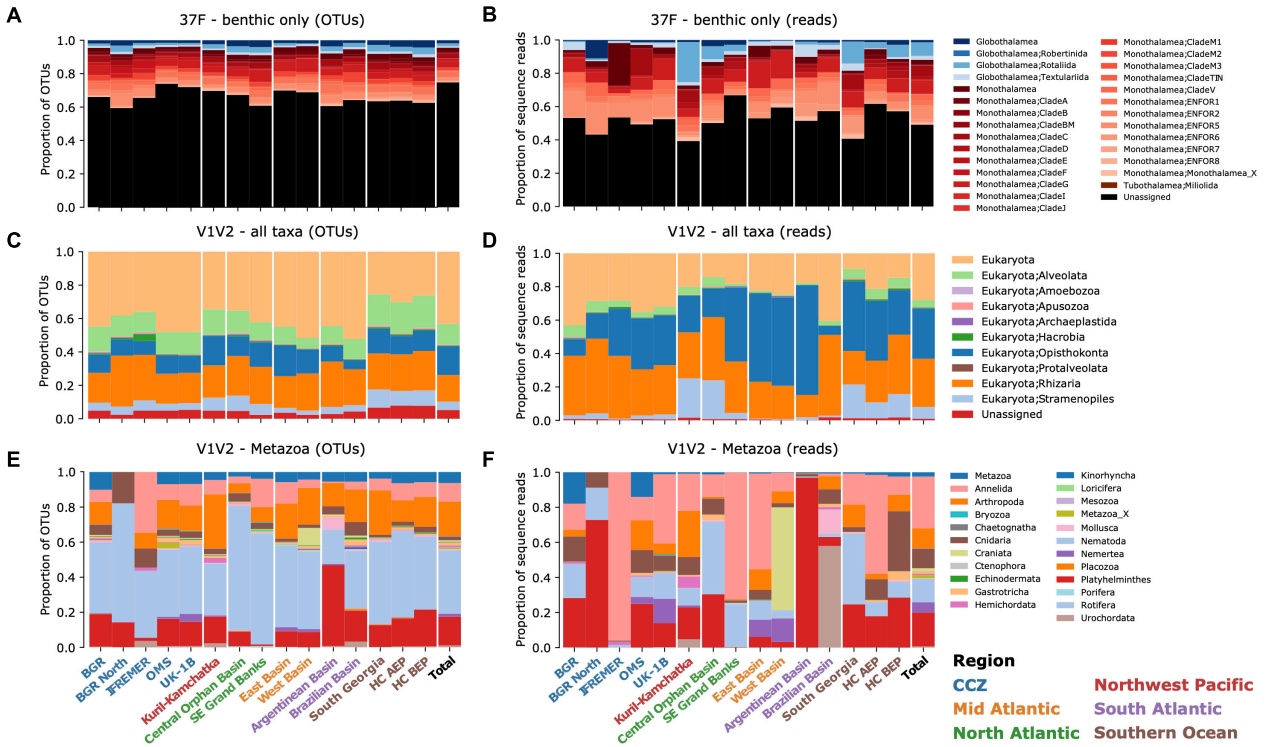

FIGURE 2 | Taxonomic composition and relative abundance. Proportions of OTUs found for each taxon across samples from each area **(A,C,E)** and relative abundances of reads per taxon **(B,D,F)**. **(A,B)** the 37F dataset (benthic Foraminifera only), **(C,D)** the full V1V2 dataset, and **(E,F)** the V1V2 dataset reduced to Metazoa. Bars are grouped per region and the total proportions are shown on the right of each panel.

RESULTS

Sequence Data and Taxonomic Assignment

Quality, replicates and frequency filtering discarded 13.4 and 26.9% of the 1,158 and 1,226 samples successfully PCR-amplified and sequenced for the 37F and V1V2 marker, respectively, with the more numerous CCZ samples being most affected (**Supplementary Figure 3A**). We performed analyses of an average of 474.7 ± 44 (standard deviation) samples and 24.4 ± 10.7 million reads per marker and molecule type (**Table 1**). The rarefaction depth of 3,000 reads per sample was chosen as a tradeoff between a high number of reads and a high number of samples for analysis, with the final number of samples being 1,003 for 37F and 896 for V1V2 (**Supplementary Figure 3B**). The sequencing depths obtained across PCR replicates are consistent for each marker and for DNA and RNA with an average Pearson's r correlation of 0.71 (**Supplementary Figure 3C**, all p-values < 0.001). Sequence clustering across markers and replicates resulted in a total of 12,742 and 43,091 OTUs for the 37F and V1V2 markers, respectively.

For taxonomic assignment of V1V2 OTUs, using PR^2 or SILVA resulted in very similar assignment profiles across taxonomic levels and methods intersections (**Supplementary Figure 4**). When the four methods agree, it is mainly for non-assignments, which is the case for the majority of OTUs, representing 74.5 and 43.6% of the total number of OTUs for 37F and V1V2, respectively. Yet, up to 619 V1V2 OTUs and almost a hundred 37F OTUs are consistently assigned to the same genus by the four methods. A few OTUs (max. 214) are assigned differently by two pairs of methods ("conflicts"), but are resolved at family (37F) and domain (V1V2) levels (**Supplementary Figure 5**). Assignments found consistent at the genus level by two or three methods represent 20.5 ± 0.01% of all V1V2 OTUs but only 5.6 ± 0.02% of all 37F OTUs.

High-Level Taxonomic Composition

We summarized the taxonomic composition of benthic foraminifera and eukaryotes in terms of OTU proportions and sequence read relative abundances in each area (**Figure 2**). The foraminiferal dataset is composed mainly of benthic species (**Figures 2A,B**). The proportion of planktonic sequences (order Globigerinida) is negligible (0.37% of OTUs, **Supplementary Figures 7, 8A,B**). The foraminiferal dataset is dominated by unassigned sequences, both in number of OTUs and abundance of reads (**Supplementary Tables 3, 4**). The assigned sequences belong mainly to the single-chambered class Monothalamea. Among them, the groups only known from previous environmental foraminiferal metabarcoding surveys ("ENFOR") can represent more than half of the reads assigned in a particular area. On average, the single group ENFOR5 accounts for 13.3 ± 3.1% of the reads in the six CCZ areas. The

proportion of multi-chambered Globothalamea is minor in the CCZ, although it is well represented in the Kuril-Kamchatka (Northwest Pacific) and South Georgia (Southern Ocean) areas, where it contributes 24.2 and 13.3% of the reads, respectively. Interestingly, the high-level taxonomic composition of OTUs is very similar in all sampled areas, in contrast to the relative abundance of reads, which are much lower for globothalamiids in the CCZ compared to other regions (Wilcoxon-Mann-Whitney tests on log-ratios, for DNA: $U = 2.82 \times 10^6$, p-value $= 3.27 \times 10^{-7}$; and for RNA: $U = 3.55 \times 10^6$, p-value $= 2.75 \times 10^{-14}$, **Supplementary Figure 9**).

The eukaryotic dataset (V1V2 all taxa) is composed mainly of OTUs assigned to Alveolata, Opisthokonta, Rhizaria, and Stramenopiles (**Figure 2C**), while Opisthokonta and Rhizaria dominate in terms of read abundances (**Figure 2D**). The average proportion of unassigned OTUs per area is 46.7 ± 0.05%, without the Southern Ocean areas, where it is 34.7 ± 0.02% (**Supplementary Tables 5–8**). The taxonomic profiles are very similar for the whole CCZ region. Overall, about a fourth of the reads (22.6 ± 0.09%) from CCZ belong to Opisthokonta, and these are distributed in 17.2% of the 43,091 OTUs, a proportion similar to that of the supergroup of Rhizaria (15.9% of OTUs). CCZ Opisthokonta includes Metazoa (6.2 ± 0.02% of OTUs), but also Fungi that represent 14.7 and 15.8% of reads in UK-1B and OMS, respectively (**Supplementary Figure 6**). In the other regions, the proportion of reads is also similar, except for the supergroup of Stramenopiles (dominated by diatoms), which represents a large fraction of the reads in the Kuril-Kamchatka (Northwest Pacific) and South Georgia (Southern Ocean) areas.

For analyses of the metazoan component, a large part of the V1V2 dataset was removed, including Alveolata, Amoebozoa, Apusozoa, Archaeplastida, Hacrobia, Stramenopiles, Rhizaria, non-metazoan Opisthokonta, as well as unassigned "Eukaryota" (**Supplementary Figure 7**). In the CCZ samples, these removed taxa are highly prevalent and altogether represent 85.8% of the reads (**Supplementary Figures 8C,D**). Among the most abundant metazoans prevalent in the CCZ are Nematoda (present in 97.9% of the samples), followed by Platyhelminthes/Xenacoelomorpha (77.9%), and Annelida (63.3%). The Echinodermata, Gastrotricha, Mollusca, Nemertea, and Porifera are present in, at most, only 23.3% of the CCZ samples.

Phylogenetic Novelty

To establish biodiversity novelty in the CCZ region we placed the metazoan and foraminiferal datasets in molecular phylogenies (**Figures 3**, **4**). In the case of metazoans, we performed OTU comparisons with the global-ocean study of Sinniger et al. (2016). An evaluation of the quality of this step reveals that for a given OTU, alternative placements associated with a low probability would place this OTU very close to the retained placement node on the tree (**Supplementary Figure 10C**). Hence, we are confident that our Metazoa placements can be interpreted in the framework of the Sinniger tree. To further measure metazoan novelty, we co-clustered at similar sampling effort the Metazoa OTUs of this study with the OTUs from Sinniger et al. (2016). With all Sinniger's samples included, only 1–2% of the clusters contained sequences from both studies (**Supplementary Figure 11A**) and the proportions remain low when comparing samples from exactly the same stations (**Supplementary Figure 11B**).

All metazoan clades recovered in Sinniger et al. (2016) are also found in the present study (**Figure 3**). The taxon that dominates in all deep-sea samples is the phylum Nematoda, the OTUs of which (in light blue) cover almost half of the tree (**Figure 3**). Some of them are assigned to species or genus level but many remain at order level. Another frequently occurring group is the Arthropoda (in dark blue), generally assigned to family level. Most of them belong to the class Maxillopoda, which includes the benthic harpacticoid and planktonic calanoid copepods. Next to the arthropods in the tree are annelids (in red) that also represent a highly diversified group, but with few OTUs assigned to genus or species level. The platyhelminthes/xenacoelomorphes (in dark green) branch separately and are assigned principally to the class level. The platyhelminthes/xenacoelomorphes branch closely to several unassigned sequences (in pink), which possibly also belong to this group.

An important proportion of metazoan OTUs are unique to the CCZ (**Figure 3**, yellow in inner ring). Many of them can be found among annelids and platyhelminthes/xenacoelomorphs. They are represented either in DNA or in RNA, but rarely in both datasets. Only a few OTUs have been found to be highly prevalent in CCZ samples (bars). Most of them belong to nematodes, but there are also a few hydrozoans, annelids, and platyhelminthes/xenacoelomorphes that are highly prevalent in the CCZ.

The phylogenetic placement of Foraminifera OTUs results in quite a different image (**Figure 4** and **Supplementary Figure 10A**), mainly because the reference tree comprises several taxonomic groups represented by shallow-water species. This applies particularly to the class Globothalamea and monothalamid Clade E, as well as the freshwater and soil clades. Compared to Metazoa, many foraminiferal sequences are highly prevalent in CCZ samples (both with DNA and RNA) and notably the environmental clades ENFOR5 and the highly diverse ENFOR1. High prevalence in the CCZ is also observed in Clades V and F. All these clades are dominated by undescribed monothalamous species, often represented by environmental sequences only. On the other hand, the CCZ foraminiferal dataset contains very few OTUs assigned to Clade C, despite the fact that this clade comprises the megafaunal xenophyophores, which are common in the CCZ.

Uniqueness of CCZ Areas

Areas within the CCZ region are distinct from the other regions studied in terms of exclusively shared OTUs, with 1,124 37F OTUs and 2,230 V1V2 OTUs (**Figure 5**) representing 19.8 and 14% of the CCZ OTUs, respectively. The numerous OTUs shared between UK-1B and OMS, the most-heavily sampled areas, are also rare in terms of sequence read abundances and half of them were detected both using eDNA and eRNA (**Figure 5** and **Supplementary Figure 12**). Among other regions, only the three Southern Ocean areas share relatively high numbers of OTUs that are unique to this region. This is especially true for the two

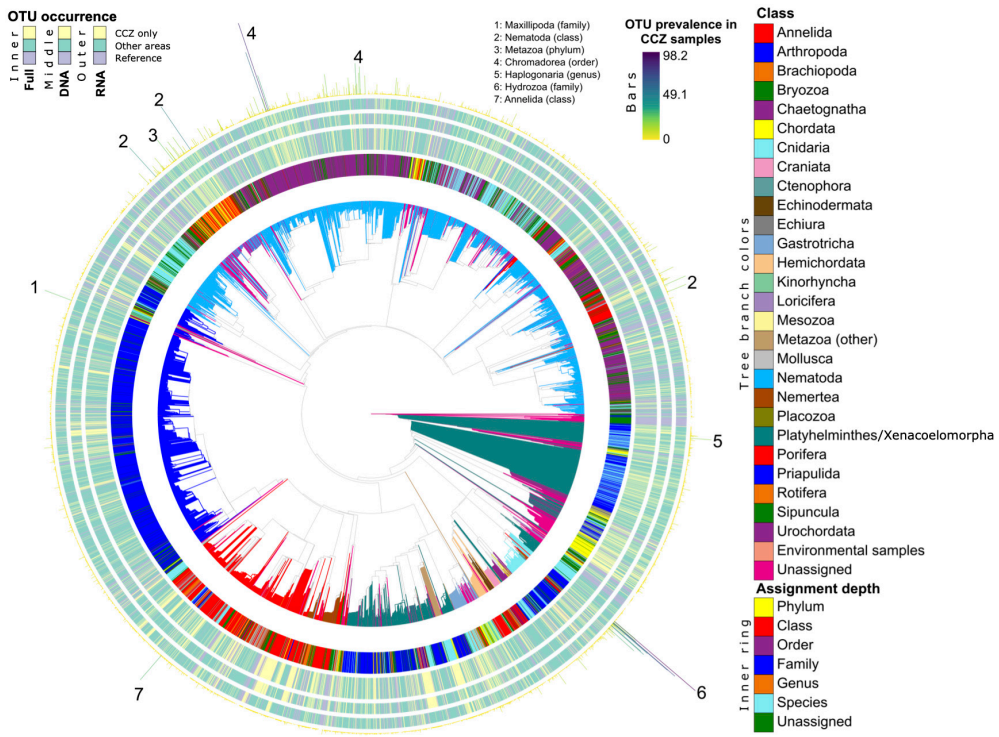

FIGURE 3 | Phylogenetic diversity and novelty of Metazoa OTUs. The phylogeny from Sinniger et al. (2016) is shown, expanded with V1V2 OTUs placements from this study. Tree branches are colored at the Class and Order levels. Concentric bar plots indicate, for each OTU its assignment depth (innermost ring), whether it is exclusive to the CCZ using both DNA and RNA (large inner ring), using DNA only (middle ring) or using RNA only (outer ring). These OTU-occurrence measures indicate whether a tip corresponds to an OTU found only in the CCZ ("CCZ only", in yellow), to an OTU also found in any other area ("Other areas", in turquoise), or whether a tip corresponds to a sequence from the reference phylogenies used for placement ("Reference", in purple). The prevalence of each OTU in the CCZ samples is indicated in terms of percent of samples where it is detected in this area (outermost bars). The finest taxonomy of OTUs highly prevalent in the CCZ are indicated.

stations exposed to high chlorophyll exports in the 37F dataset (HC_AEP and South Georgia), but less so in the V1V2 dataset where there are half the numbers of shared OTUs than in closely located areas (HC_AEP and HC_BEP). Interestingly, the CCZ areas also share exclusive OTUs at several intersections with the Kuril-Kamchatka area (Northwest Pacific region), although the number of shared OTUs is much lower than between CCZ areas.

There is a relationship between the number of reads in an OTU and the number of areas in which it occurs (**Figure 5**, box plots). Moreover, highly prevalent OTUs are detected by both DNA and RNA, which is also the case for the many OTUs present at all stations within each CCZ area (**Supplementary Figure 12**, box plots). Besides these cosmopolitan, high-frequency OTUs, the most important OTU intersections within CCZ areas are between pairs of stations, including OTUs only detected using DNA or RNA molecules (**Supplementary Figure 12**). Notably, any two stations within UK-1B and OMS strata tend to share between 10 and 15 exclusive 37F OTUs that can be represented by hundreds of reads (**Supplementary Figures 12A,B**). This number of OTUs exclusive to pairwise CCZ station intersections is higher for V1V2 (c.a. 40–100) than for 37F, and for OTUs associated with fewer reads (**Supplementary Figures 12D,E**).

Alpha Diversity

Different levels of alpha diversity characterize the benthic foraminiferal and eukaryotic communities at each spatial scale. Overall across datasets, this is seen more clearly when using Faith's PD (PD) compared to Shannon's entropy (H') and in most cases when using DNA (**Supplementary Figure 13**). For 37F, only the difference between regions using H' and RNA was not supported statistically, while other significant tests showed the largest difference effect using DNA at the region (Kruskal–Wallis H = 29.1 for PD; 17.8 for H') and area (H = 105.3 for PD; 77.3 for H') scales compared to RNA (for PD: H = 16.8 and 36.7 at region and area scales, respectively). Interestingly, this effect size was slightly larger using RNA for 37F PD at local scales, such as between stations (H = 76.7 for DNA; 82.1 for RNA) and deployments (H = 63.4 for DNA; 67 for RNA). For V1V2, the trend remains that RNA does not show alpha diversity difference between regions (for both indices), whereas it yields a greater difference between areas (H = 23.5 for PD; 16.5 for H') compared to DNA (H = 36.9 for PD; 22.6 for H'). However, alpha diversity differences are much more pronounced using DNA at local scales (between stations) both for PD (H = 92.6 for DNA; 37.3 for RNA) and H' (H = 89.9 for DNA; 35 for RNA) (all Kruskal–Wallis tests have adjusted p-values < 0.05). Also,

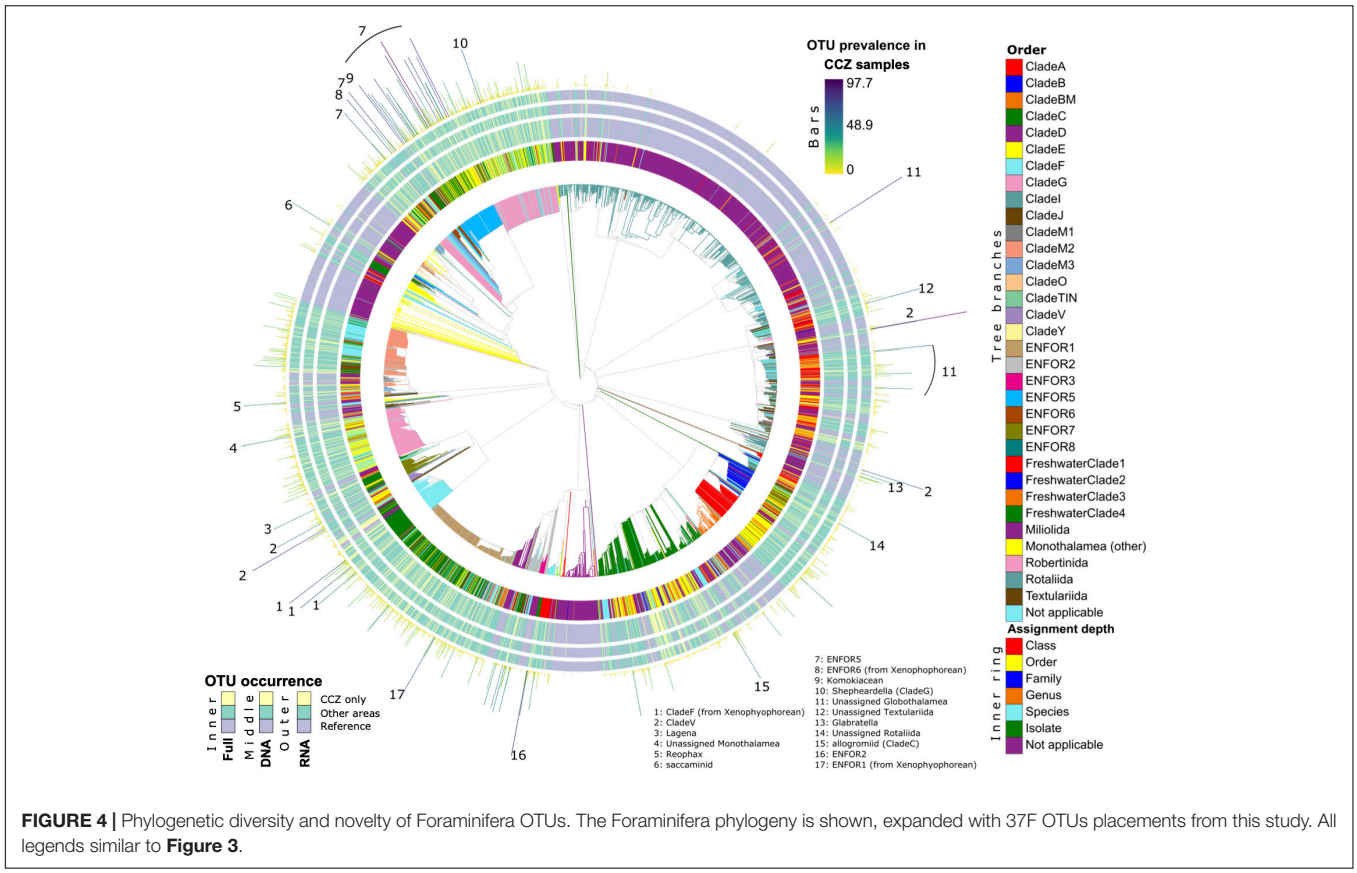

FIGURE 4 | Phylogenetic diversity and novelty of Foraminifera OTUs. The Foraminifera phylogeny is shown, expanded with 37F OTUs placements from this study. All legends similar to **Figure 3**.

it should be noted that for V1V2 not all areas (and stations) are compared since many DNA co-extractions failed (**Table 1** and **Supplementary Table 2**). For the CCZ, DNA and RNA yield similar levels of alpha diversity for V1V2, whereas for 37F, the diversity of DNA is higher than that of RNA, but only using Shannon's entropy (**Figure 6A** and **Supplementary Figures 14, 15A**). Hence, we restricted the following analyses to Faith's PD index.

Alpha diversity in the CCZ differs from that of every other region as assessed by post-hoc pairwise comparisons following Kruskal–Wallis *H* tests (37F: **Figure 6B**; V1V2: **Supplementary Figure 15B**). For the foraminiferal DNA dataset, the CCZ appears as the second most diverse region after Kuril-Kamchatka. Alpha diversity of the CCZ as a whole does not differ from the North Atlantic region because the diversity within its individual areas and stations (all confined to the eastern CCZ) varies significantly (**Figure 6C** and **Supplementary Figure 16A**). Indeed, the UK-1B and OMS strata have a similar, high Faith's PD whereas the BGR and IFREMER areas have very low values for this index (there were too few samples for testing against BGR North). In fact, the BGR stations exhibit consistently lower DNA diversity values than all other CCZ stations, with the notable exceptions of the two IFREMER stations where nodule abundance was particularly high (BIO12-102KG and BIO12-86), and station SO237-3 in the West Basin in the central Atlantic (**Supplementary Figure 16A**). This Atlantic station is also characterized by the presence of large polymetallic nodules (see cruise report; Devey, 2015). For the eukaryotic DNA dataset, the CCZ stands out as the most diverse region (no data for BGR and IFREMER) (**Supplementary Figures 15B,C**). Interestingly, within-station DNA and RNA diversity vary more for Eukaryota than for Foraminifera, as is clear from the wider dynamic range of values for the former dataset (**Supplementary Figures 16A** vs. **16B**, box plots). It also appears that between-station RNA diversity differences are more frequent for Foraminifera than for Eukaryota, as illustrated by the higher number of significant *post hoc* tests for the latter dataset (see dark yellow cells in heatmaps in **Supplementary Figures 16A** vs. **16B**).

Foraminifera 37F alpha diversity in the CCZ is associated with topography, but only for DNA (**Figure 6D**). Faith's PD was positively correlated with Broad BPI (Spearman's $rho = 0.36$, p-value < 0.05) and negatively with seafloor slope ($rho = -0.19$, $p < 0.05$). Eukaryota V1V2 alpha diversity is also associated with topography for DNA, but only with Fine BPI (Spearman's $rho = 0.23$, p-value < 0.05) (**Supplementary Figure 15D**). In relation to water depth, the Foraminifera RNA diversity exhibits a positive but weak correlation with increasing depth ($rho = 0.119$, p-value < 0.05). Conversely, only DNA associates with depth for the Eukaryota, in a stronger negative correlation (rho $= -0.222$, p-value < 0.05) (**Supplementary Figure 15D**).

Beta Diversity

For both Foraminifera and Eukaryota, the CCZ samples form clusters on the Robust PCAs that are well separated from the

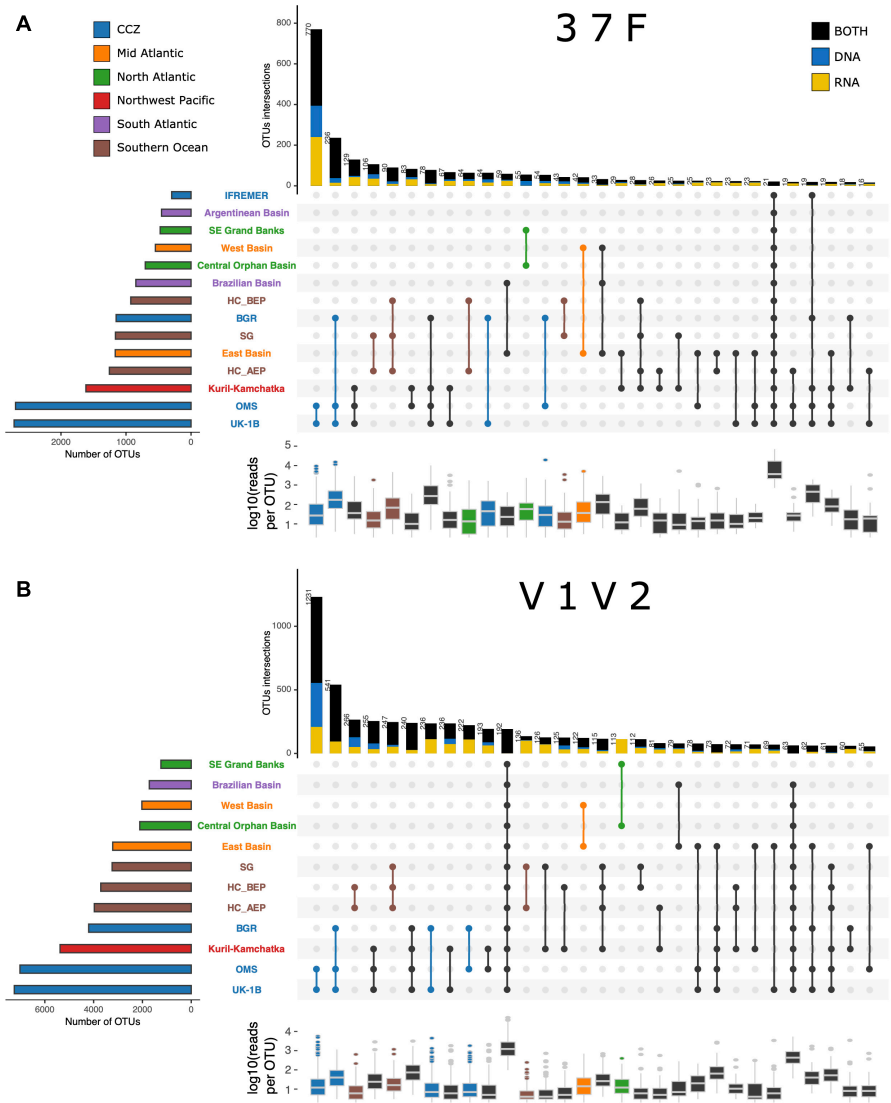

FIGURE 5 | Diversity specific to region intersections. Number and read frequencies for **(A)** the 37F (benthic) and **(B)** the V1V2 (all taxa) OTUs shared at different intersections of regions (matrix rows). Only the 30 intersections that are the largest in terms of numbers of OTUs are shown, and ordered by decreasing OTU numbers. The bars on the top panel indicate the number of OTUs in the intersection denoted by the connected dots on the middle panel. Bars are colored according to molecule (blue: DNA; yellow: RNA; black: both). The bars on the left panel indicate the total number of OTUs in each area (or station), while the box plots on the bottom panel indicate the distribution of reads in each OTU per intersection.

samples of other deep-sea regions (**Figures 7A,B**), except for the Mid Atlantic samples that intermingle to some extent with the CCZ samples in the case of V1V2 (**Figure 7B**). Strikingly, the DNA and RNA samples also formed two larger clusters, each of which shows separate groupings of CCZ samples. We therefore performed RPCA on DNA and RNA separately (as for alpha diversity analyses). For both 37F and V1V2, this also resulted in grouping samples according to region, and even areas, with the notable exception of CCZ areas, which formed a large and highly variable cluster (**Supplementary Figure 17**). Indeed, the beta diversity that we demonstrate within the CCZ is far from being representative of all that can be sampled there, as indicated by the dissimilarity-decay curves that do not saturate to an asymptotic minimum for both 37F and V1V2 and both for DNA and RNA (**Supplementary Figure 18**). Unsurprisingly, this pattern holds when sampling globally, with an increased baseline value of added beta diversity (**Supplementary Figure 18**, see "All samples").

For 37F, the separation between CCZ and Atlantic areas is driven by several ENFOR5 OTUs and several Unassigned OTUs pointing for DNA in these different, respective area directions whereas for RNA, it is two Unassigned and one poorly assigned Globothalamea OTUs that characterize CCZ samples, as opposed to two Rotaliida OTUs that are strongly associated with OTU-rich Atlantic samples. In the case of V1V2, it appears that for the DNA RPCA ordination, two

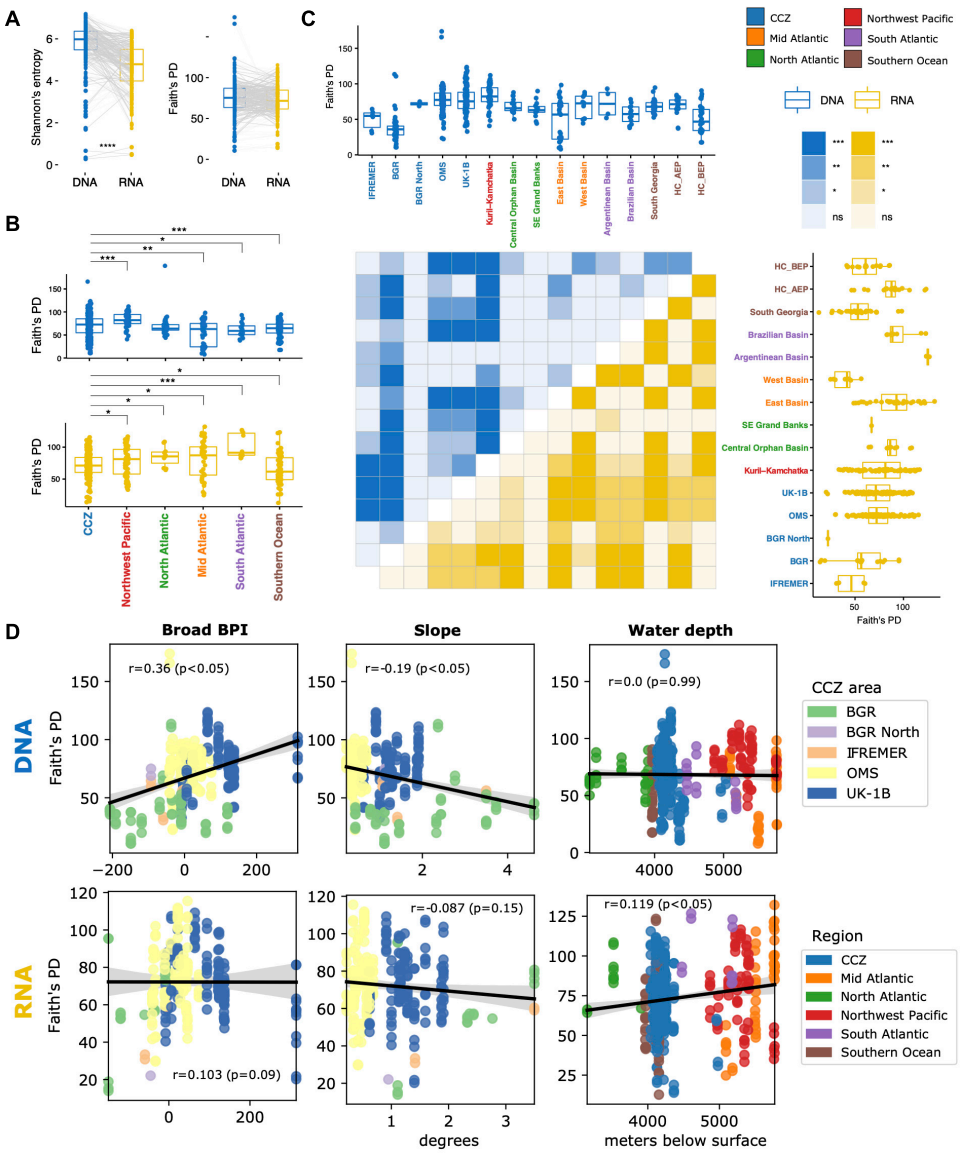

FIGURE 6 | Alpha diversity comparisons between molecules, regions and areas, and correlations with environmental variables for the Foraminifera dataset. **(A)** Paired Kruskal–Wallis test between DNA and RNA alpha diversity indices within the CCZ. Gray lines indicate same-sample paired comparisons. Pairwise *post hoc* tests separately for the DNA and RNA samples to compare the Faith's PD alpha diversity between individual regions **(B)** and areas **(C)**. Significant differences between regions are shown using box-to-box connectors **(B)** whereas for areas, these are indicated in the heatmaps (blue triangle: within-DNA comparisons; yellow triangle: within-RNA comparisons). **(D)** Spearman correlations between the Faith's PD alpha diversity of DNA or RNA samples and environmental variables in the CCZ. Slope and Broad BPI are only available for the CCZ region whereas water depth is shown across regions. Spearman's *rho* statistics and *p*-values are indicated on insets. ***p-value ≤ 0.01; **p-value ≤ 0.03; *p-value ≤ 0.05; no label/ns: p-values > 0.05; no color (heat map): no testing. Results for the V1V2 dataset are shown in **Supplementary Figure 15**.

OTUs assigned to the diatom *Chaetoceros* (pelagic) acting in one direction, and an OTU assigned the fungal taxon Sordariomycetes acting in the opposite direction, drive the separation along the first axis (PC1), i.e., the separation of Kuril-Kamchatka, Southern Ocean and CCZ samples (these taxa were already most influential with both DNA and RNA on the RPCA, **Figure 7B**). For the RNA ordination, the CCZ and Southern Ocean separate under the influence of an unassigned eukaryotic OTU and a Fungi OTU (along PC1) whereas a diversity of Cercozoa OTUs (including some assigned to Endomyxa-Ascetosporea parasites), and two OTUs assigned to Radiolaria (pelagic), strongly influence sample separation along the second axis (PC2).

No clear clustering of the areas results from the RPCAs based on the Metazoa subset, except for DNA where one Annelida OTU drives the separation between UK-1B and OMS samples and most of the Southern Ocean samples (**Supplementary Figure 17**). Beta diversity comparisons, performed before and after removal of

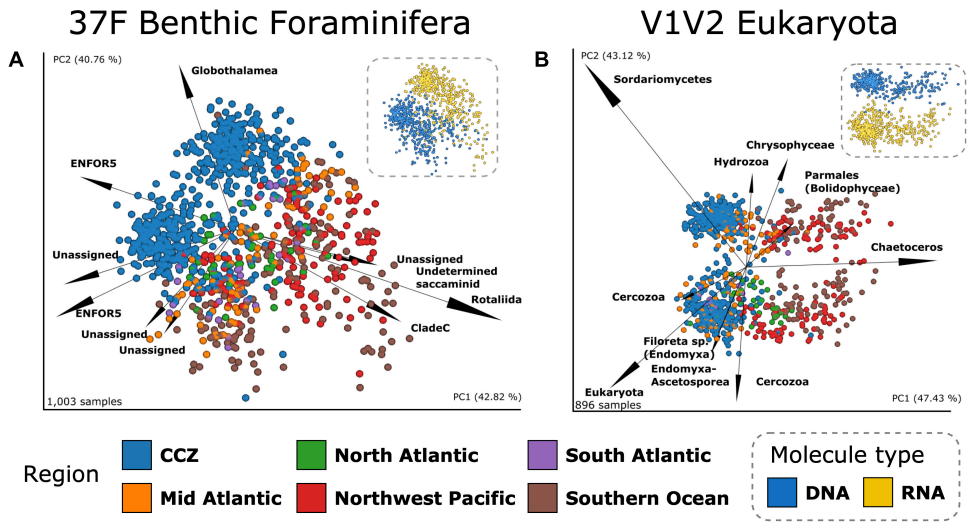

FIGURE 7 | Deep-sea benthic communities beta diversity. Robust PCAs based on the Aitchison metric for **(A)** the 1,003 37F samples **(B)** the 896 V1V2 samples. PCR-amplified samples (scatter), are colored according to region and the top 10 most influential OTUs biplots (arrows) are labeled with their deepest taxonomic assignment. Insets represent the same RPCAs but colored according to molecule type. The percentages indicated for PC1 and PC2 are large because they represent the variance explained in the three first dimensions.

non-Metazoa OTUs using Mantel tests on dissimilarity matrices or PROTEST on three-dimensional ordinations, revealed that the beta diversity changed considerably as a result of this filter. Mantel's r correlations were 0.65 and 0.59 for the Aitchison metric on DNA and RNA matrices, respectively, with an even lower procrustes PROTEST fit of ca. 0.4 for both DNA and RNA (**Supplementary Table 9**). Nevertheless, a relatively good conservation of the beta diversity pattern was achieved using the Jaccard binary metric (Mantel's r = 0.75 and PROTEST's 1-M^2 = 0.78, all p-values < 0.001, **Supplementary Table 9**).

Differences between regions, areas and stations were statistically supported for each dataset in PERMANOVA performed on the Aitchison metric (DNA Pseudo-$F_{37F/V1V2}$ = 20.44/20.43; RNA Pseudo-$F_{37F/V1V2}$ = 16.03/16.43; all p-values < 0.001) and for all other beta diversity metrics (**Supplementary Figures 19A–C**). However, the dispersion of the samples within each group was also significantly different between groups, except for the phylogenetic beta diversity metric Weighted UniFrac, which yielded the greatest difference between regions using DNA (Pseudo-F = 35.54, p-value < 0.01). We also tested for differences between areas and stations within the CCZ only and found statistical support unaffected by PERMDISP dispersion for comparisons based on DNA among 37F stations and V1V2 areas (PERMANOVA Pseudo-F = 4.027 and 3.194, respectively, both p-values < 0.001, **Supplementary Figures 19B–D**).

Spatial Heterogeneity

Since PERMDISP testing revealed differences in group dispersions and notably for stations, we calculated as a measure of local heterogeneity the distances to centroids for samples from each station on 37F CCZ RPCAs (for DNA and RNA separately, see section "Materials and Methods"). Since stations associated with steeper slopes seem more dissimilar on these RPCAs (**Supplementary Figure 20**), we plotted these distances to station centroids on bathymetric maps of the CCZ strata UK-1B and OMS (**Figure 8A**). Communities at stations located in depressions (i.e., associated with low Broad BPI values, blue background) were systematically more variable, as indicated by higher values for the distances to centroids in terms of average and standard deviation values (green circles). This relation was highly pronounced for the DNA samples and in the OMS stratum where distances to stations centroids increased with BPI, yielding more variable communities locally. Overall, the distances to station centroids computed based on the compositionally robust Aitchison metric are not different between DNA and RNA, while using the phylogenetic, Unweighted UniFrac metric, we found RNA heterogeneity to be significantly greater than DNA (**Figure 8B**).

DISCUSSION

Metabarcoding Data and the Abyss

Omics techniques allowing rapid and standardized profiling of environmental molecules may represent a powerful approach to filling deep-sea knowledge gaps (Levin et al., 2019) and addressing key goals for this decade (Howell et al., 2020). Metabarcoding, in particular, is being increasingly developed for biomonitoring purposes in marine environments (Chariton et al., 2010; Aylagas et al., 2018, 2020; Brandt et al., 2020; Le et al. in review). It has successfully documented the local impacts of marine industries, including aquaculture (Pawlowski et al., 2014; Lejzerowicz et al., 2015; Pochon et al., 2015; Cordier et al., 2018) and oil and gas extraction in coastal ecosystems (Lanzén et al., 2016; Laroche et al., 2016; Cordier et al., 2019;

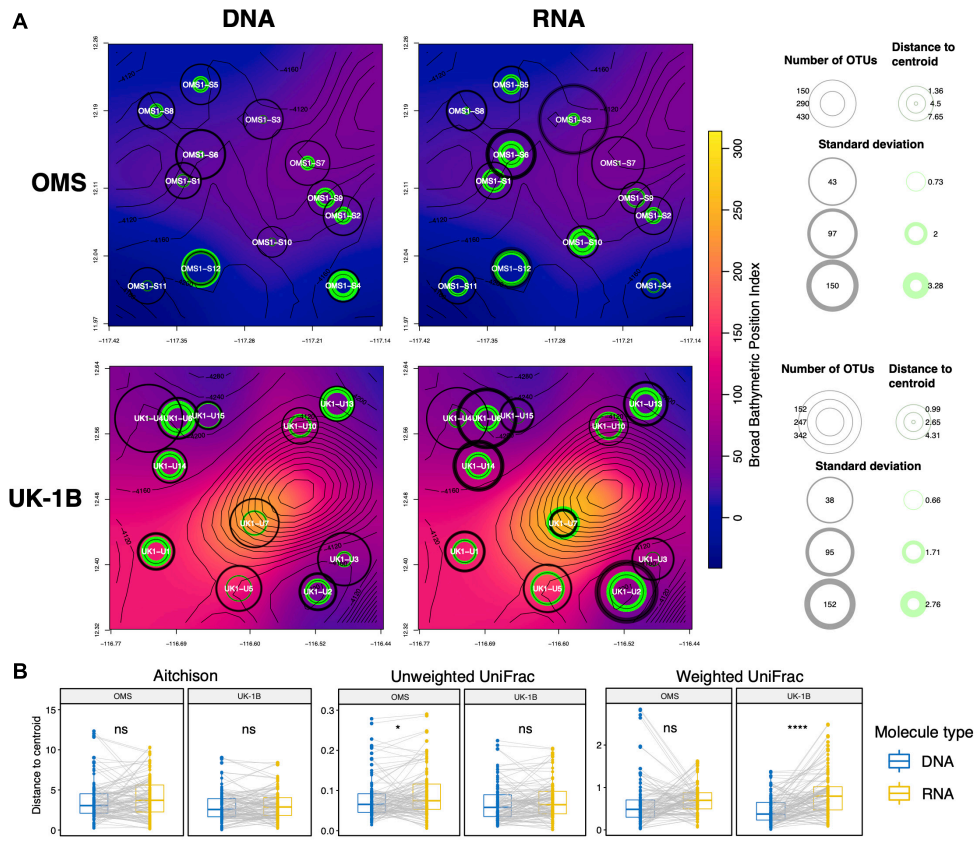

FIGURE 8 | Spatial heterogeneity expressed in terms of station beta diversity dispersion in relation to bathymetry for the 37F dataset. **(A)** At each station of the UK-1B and OMS strata (CCZ), we computed the distance separating the samples to the station centroid they form in the RPCA spaces obtained separately for DNA and RNA. Average and standard deviations for these distances-to-centroids are shown at each station (max. six samples per station) of each map panel (green rings), as well as for the number of OTUs (gray rings). The background color represents the Broad Scale BPI (Bathymetric Position Index) values smoothed over the plotted area. **(B)** Paired *t*-tests comparing the distributions of distance-to-centroid values between DNA and RNA are shown for the Aitchison dissimilarity metric (also used for the Robust PCA and maps) as well as for the phylogenetic, Weighted UniFrac dissimilarity metric.

Mauffrey et al., 2020) where extensive ecological knowledge has allowed ground truthing. Metabarcoding has also been used for surveys of CCZ areas focusing on prokaryotic microbial communities (Shulse et al., 2017), metazoans (Laroche et al., 2020a) and allochthonous pelagic eDNA deposited in sediments (Laroche et al., 2020b).

General methodological considerations regarding eukaryotic metabarcoding have been reviewed recently (Santoferrara et al., 2020). Besides the robust multiplexing design and PCR replicates that we used to filter cross-contaminations and spurious data (Esling et al., 2015), and extraction replicates to improve diversity estimates (Lanzén et al., 2017), another commonly overlooked issue is the compositional nature of sequencing data, which includes metabarcoding (Gloor et al., 2016, 2017; Martino et al., 2019). Indeed, a simple transformation (e.g., with the Aitchison metric) allows circumventing the fact that, following sediment sampling, extraction, PCR and sequence subsampling, it is impossible to know the true total abundance of taxa in samples and thus to compare compositions on the basis of abundance (or relative abundance) (Morton et al., 2017; Knight et al., 2018). Our analyses of beta diversity turnover and dispersion were performed in PCA spaces that are robust to this effect, allowing comparison and testing. These outstanding technical aspects are particularly relevant for the deep seafloor, which is characterized by substantial small-scale faunal patchiness (Snelgrove and Smith, 2002) that is difficult to sample, particularly using metabarcoding (Lejzerowicz et al., 2014).

Although metabarcoding is an important tool that can overcome some of the limitations inherent in morphology-based studies of deep-sea biota (Le et al., in review), there are some caveats to be born in mind when considering metabarcoding data obtained in deep-sea settings. First, because the amounts of sediment analyzed are small (2–10 g), the data will be weighted toward small-sized organisms (meiofauna and smaller). Macro- to megafauna would necessarily occur only as sloughed cells, eggs, larvae, or tissue fragments, which would yield high amounts of fresh, readily amplified molecules and explain the occasional dominance of large animals when taxonomic composition is expressed in terms of the relative abundances of reads (e.g., see Craniata in **Figure 2F**). This caveat may also apply to some protists, notably megafaunal xenophyophores. Although these giant agglutinated Foraminifera are abundant and diverse

across the CCZ (Gooday et al., 2017, 2020), no OTU was assigned to them, confirming the lack of representativeness of the metabarcoding samples for macro- to mega-fauna sized organisms.

Second, the V1V2 data also includes planktonic organisms, such as diatoms, radiolarians or calanoid copepods and hydrozoans among the Metazoa. It is well established that export fluxes deposit pelagic DNA traces, as well as entire cells, to the seafloor and that this DNA also conveys a strong biogeographic signal, as demonstrated for planktonic Foraminifera (Morard et al., 2017; Barrenechea et al., 2020). As a testament to this phenomenon, we were able recover the same clustering patterns for the CCZ and other regions using the benthic Foraminifera only, as well as the full V1V2 dataset that included a majority of planktonic sequences, as observed previously (Pawlowski et al., 2011). One compelling example is that of the Southern Ocean and Northwest Pacific regions (both highly productive), which clustered opposite to the CCZ (least productive), a separation associated with one OTU belonging to the large diatom genus *Chaetoceros*. Frustules from this diatom genus constituted the bulk of Southern Ocean sediment (Würzberg et al., 2014) and it was also found to be dominant in the Kuril-Kamchatka area (Golovan et al., 2019). One *Chaetoceros* OTU drove separation for the DNA samples, further highlighting the importance of pelagic DNA deposits in our data set.

A third point is that enormous quantities of extracellular DNA accumulate across the seafloor (Dell'Anno and Danovaro, 2005) and this material remains accessible for metabarcoding for extended periods of time ranging from centuries for settling, pelagic fish DNA (Kuwae et al., 2020) to millenia for benthic Foraminifera and even planktonic organisms (Coolen et al., 2013; Lejzerowicz et al., 2013a). The deep-sea environment favors the preservation of biomolecules and it has been found that up to half of 16S rDNA copies at abyssal depth originate from extracellular DNA pools (Corinaldesi et al., 2018). We found that the local heterogeneity for foraminiferal DNA is higher at stations characterized by low BPI values, compared to RNA and to stations located on slopes. This suggests that eDNA but not eRNA accumulates in depressions. In addition, we found that for eDNA – but again not for eRNA - there were significant correlations between alpha diversity and both BPI and slope. Faith's PD decreased with slope, suggesting winnowing (i.e., reduced permanent deposition) of eDNA in elevated areas, but increased with BPI. We stress that BPI interpretation is tightly linked to scale, and since this correlation is made across areas, it indicates that eDNA has a higher diversity in localities where there are more topographic depressions in which eDNA deposition may be focused. This suggests that eDNA winnowed off a slope would tend to become concentrated in these pools. Similar mechanisms of sediment winnowing and focusing related to abyssal seafloor topography have been postulated for labile particulate organic matter (Turnewitsch et al., 2015) and may determine its degradation (Volz et al., 2018). Nucleic acid is organic matter as well, and since RNA degrades more rapidly than DNA, it should be possible to model how these complex processes influence the distribution patterns inferred from environmental sequencing data. Interestingly, abyssal hills and more subtle topographic changes also appear to influence the distribution of live Foraminifera (Stefanoudis et al., 2016) and metazoan megafauna (Durden et al., 2020). Hence, if it can be assumed that DNA spreads with organic matter on the abyssal seafloor, we envision metabarcoding as a quantitative tool for trophic ecology and recommend RNA, which is likely to reflect contemporary faunas more accurately, for biodiversity assessments.

Corroborating this observation, we found that only beta-diversity comparisons measured from DNA (between regions, areas or stations) were not subject to differences in dispersion. The slow degradation time scales for DNA mentioned above may cause environmental DNA to integrate biodiversity over much longer time scales, combining past and present communities (Brandt et al., 2020), and thereby lowering variability amongst overlapping communities in RPCA ordinations. This can also explain the higher Shannon's entropy (compared to Faith's PD), because entropy increases with evenness, which will increase in turn with each set of DNA OTUs added to the pool. In contrast, RNA is more labile and therefore may exhibit more compositional variation that likely reflects spatial patchiness over shorter time scales. This potential advantage that RNA may confer by more accurately delineating deep-sea community patchiness in space and time is further indicated by the fact that we observe a higher distance to centroid for RNA compared to DNA across the entire CCZ (although reflecting local-scale, within-CCZ station heterogeneity). Higher RNA heterogeneity is a general trend for all beta-diversity metrics (higher median values, see **Figure 8B**) but was only statistically supported when accounting for evolutionary histories (i.e., using phylogenetic, UniFrac metrics). Interestingly, Macheriotou et al. (2020) relied on similar metrics to show a strong phylogenetic clustering for Nematoda in the CCZ, indicating highly heterogeneous, patchy communities, although their metabarcoding data derived from density-separated nematodes and not from bulk sediment. This makes their results more comparable to what eRNA conveys best, i.e., active, live species as shown for Foraminifera (Langlet et al., 2013; Lejzerowicz et al., 2013b), further strengthening our advocacy for use of eRNA for biomonitoring.

Wide Spectrum of Novel Benthic Taxa Revealed

This study is based on the largest collection ever assembled of deep-sea sediment samples covering a wide range of geographic areas. Using eDNA as well as eRNA sequence data, it represents a first attempt at understanding global to local biodiversity and distribution patterns for deep-sea benthic eukaryotes. Some metazoan clades could be assigned at the genus or species level, notably those belonging to the Nematoda, which are the best represented metazoan group in our data and consistently the dominant meiofaunal taxon in the deep sea (Thiel, 1983), including the CCZ (Pape et al., 2017). However, for many metazoan taxa, assignment was only possible to a Class, Order or Family (**Figure 3**). Among the Foraminifera, a large proportion of reads and OTUs could not be assigned to any known taxon (**Figures 2A,B**), a result that is also consistent with previous studies (Lecroq et al., 2009a; Lejzerowicz et al., 2014). Most of

those that were assigned could only be placed in a Class, Order, or Family, or in a particular isolate (i.e., an unidentified specimen).

These results undoubtedly indicate the existence of many new taxa, but it should be noted that the incompleteness of reference database coverage remains a major impediment to taxon assignment in biodiversity surveys. In a recent study based on samples from a well-studied and heavily sampled area of the North Sea, Hestetun et al. (2020) estimated that for the 18S rRNA gene, species coverage was 36% for GenBank and 27% for SILVA, which we used in this study (along with the curated, protist-focused PR^2). The species coverage in these databases is certain to be substantially lower for the sparsely sampled, species-rich deep sea. Molecular reference databases are undergoing major developments for animal groups that are important constituents of CCZ assemblage. However, these mainly concern macro- and mega-faunal taxa (e.g., Cnidaria, Mollusca and Polychaeta: Dahlgren et al., 2016; Glover et al., 2016; Wiklund et al., 2017, 2019) rather than meiofaunal organisms, which are potentially important ecologically (Smith et al., 2008; Ingels et al., 2020) and dominate metabarcoding data. We also recognize that querying very large, lightly curated databases may help improve high-level assignment, but relying on consistency across assignment methods applied to less complex databases could offer an equally interesting avenue to high-level assignment and with high confidence at the scale of such high-throughput data. In fact, one highly valuable approach is to improve such assignments using taxon-specific databases, as demonstrated for Nematoda (Macheriotou et al., 2020). Curated phylum-specific databases would best resolve assignments associated with long, detailed taxonomic paths that are not aligned with that of other phyla, as in the case of Platyhelminthes and Xenacoelomorpha. Indeed, these two distinct phyla are lumped together in the generalist, protist-oriented PR^2 database, whereas their taxonomic paths include more than the eight taxonomic ranks used here for taxonomic assignment.

Despite these caveats, the large proportion of reads that can only be assigned at higher taxonomic levels is quite consistent with the low level of basic taxonomic knowledge of deep-sea faunas (Glover et al., 2018). Many deep-sea species remain scientifically undescribed, particularly at abyssal depths, despite belonging to higher taxa that are commonly seen in deep-sea samples. Among the metazoan meiofauna, almost all (99.3%) of the 632 morphospecies of harpacticoid copepods recognized at two stations in the SE Atlantic (>5,000 m water depth) were considered to be new to science (George et al., 2014). In the eastern CCZ, 94.1% of 170 macrofaunal isopod species were undescribed (Brix et al., 2020). In the same area, undescribed monothalamid morphospecies, many of them previously unseen, are an important constituent of both meiofaunal (Goineau and Gooday, 2017, 2019; Gooday and Goineau, 2019) and macrofaunal (Gooday et al., 2021) foraminiferal assemblages.

Foraminifera and metazoan meiofaunal animals such as nematodes and harpacticoid copepods are common and familiar constituents of the abyssal sediment biota, as are, for example, polychaetes, isopods, and tanaids among the macrofauna and holothurians and sponges among the megafauna (Gage and Tyler, 1991; Washburn et al., 2021). However, as earlier shown by Sinniger et al. (2016), our V1V2 data reveal the presence in the eastern CCZ of animals that are rarely seen in deep-sea samples; for example, xenacoelomorphs (Rouse et al., 2016) platyhelminthes (Christensen, 1981), and priapulids (van der Land, 1972). As far as we know, the Placozoa and Mesozoa, for which we recovered some sequences from the Pacific and Southern Oceans, have never been reported from deep sea samples. Some of these taxa, notably some platyhelminthes (trematodes) and mesozoans, probably occur mainly as parasites (Bray, 2020), but others (turbellarian platyhelminthes, placozoans) may be free-living but too fragile to survive in a recognizable form in fixed samples. Thus, our metabarcoding data appears to reveal a fuller spectrum of animal diversity at our abyssal sites than could be recovered by traditional morphology-based methods. The same applies to the foraminifera, with OTUs that are known only from the environmental sequences constituting an important proportion of the assemblages, with an average of 8.4 ± 1.98% of OTUs of an area.

Interestingly, the metazoan diversity that Sinniger et al. (2016) revealed using eDNA metabarcoding is more readily detected at a similar sampling effort in our study using eRNA than eDNA. This suggests that this molecule is more reliable for analyzing diversity across studies and possibly, for future biomonitoring surveys. Yet, the amount of novel sequences that re-sampling yields is huge, as only c.a. 2% of the OTUs formed across studies contained sequences from both Sinniger et al. (2016) and the present study, even in the case of sediment sample extracts originating from the same station in the South Atlantic (DIVA-3 expedition, Martínez Arbizu et al., 2015).

Biogeographic Patterns From Global to Local Scales

The breadth and heterogeneity of the seafloor habitats (Howell et al., 2016) makes it challenging to establish patterns of deep-sea benthic biodiversity and biogeography at the spatial scales relevant to conservation efforts related to seabed mining (McQuaid et al., 2020) and climate change (Levin et al., 2020b). There is a general trend for morphological and genetic divergence to decrease with increasing water depth, and for species ranges to increase, reaching a maximal extent on abyssal plains where there should be fewer barriers for dispersal, in contrast to the topographically, hydrographically and environmentally more complex continental margins (Grassle and Morse-Porteous, 1987; Etter et al., 2005; McClain and Hardy, 2010). For example, in the geologically orientated literature, a number of well-documented, abyssal hard-shelled species of foraminifera, are considered to have 'cosmopolitan' distributions (Murray, 2006; Holbourn et al., 2013). This is confirmed by genetic data in the case of *Epistominella exigua* (Pawlowski et al., 2007; Lecroq et al., 2009b) and *Cibicidoides wuellerstorfi* (Burkett et al., 2020). Wide ranges are reported for certain species of harpacticoid copepods (Menzel et al., 2011) and polychaetes (Schüller and Hutchings, 2012; Guggolz et al., 2020), in the latter case with genetic support. At the same time, it is also common for abyssal assemblages of a particular taxon to combine a few dominant,

widely distributed species with many more rare species that are found only in one or two samples (e.g., Glover et al., 2002; Wilson, 2017; Washburn et al., 2021). Notably, Foraminifera OTUs that only occur in a single CCZ stratum also tend to occur in only one station of this stratum, even when highly sequenced (Gooday et al., 2021). Because rarity is often correlated with small species ranges in better known ecosystems (e.g., Pimm et al., 2014), these rare abyssal species may have limited distributions as well. Our metabarcoding data, as well as earlier genetic results (Janssen et al., 2015; Macheriotou et al., 2019), reveal a similar assemblage structure, with relatively few, highly sequenced OTUs but many rare OTUs that were confined to single or pairs of areas or stations (**Figure 5**). In addition to rare OTUs, the likely contribution of extracellular DNA (Corinaldesi et al., 2018) is another factor to consider in trying to generalize about biogeographic patterns and species ranges in the abyss based on metabarcoding.

Since establishing cosmopolitan and endemic patterns depends on sampling and sequencing efforts, we used rarefaction and propose to focus on the well-sampled UK-1B and OMS strata of the eastern CCZ. Here, the presence of cosmopolitan foraminiferal OTUs, and notably their high prevalence, are not surprising. Indeed, since the Pacific is the oldest ocean and nodule-rich environments are particularly stable, it is possible that the 'stability-time' hypothesis (Sanders, 1968), suggested as a key driver of niche diversification for Nematoda in the CCZ (Macheriotou et al., 2020), might also explain the diversity of Foraminifera, although other explanations are equally plausible (Snelgrove and Smith, 2002). Interestingly, the early evolution of Foraminifera is characterized by a large radiation of monothalamous species (Pawlowski et al., 2003) which remain highly diverse today in the abyss. Given the genomic potential of Foraminifera to adapt to changing environmental conditions (e.g., anoxia, Orsi et al., 2020), and the dramatic ecosystem transformation that could result from mining, it is important to also explore the distribution of functional-adaptation determinants and consider these for spatial planning in order to preserve adequate sources of biodiversity for recolonization.

At a global scale, we observed distinct faunal patterns in the foraminiferal and eukaryotic datasets. In particular, the CCZ is clearly different from the other regions from which we have data. The Southern Ocean and Kuril-Kamchatka, regions that were also well sampled and sequenced, also appear to be faunally distinct. The large-scale patterns observed in our data are broadly consistent with the abyssal seafloor provinces proposed by Watling (2013) and the marine realms of Costello et al. (2017), which integrate pelagic and benthic data. The CCZ sites fall within abyssal province A11 of Watling (2013), the Southern Ocean sites within AB5 and the SW Atlantic sites within AB3. Interestingly, we found the highest Faith's PD alpha diversity in the DNA data from the Kuril-Kamchatka region. This could reflect the location of this region at the intersection of three realms in Costello et al. (2017) and near the boundary of two benthic provinces in Watling (2013), although again other factors, including habitat heterogeneity, may also drive higher diversity.

Strong differences at the larger scale between regions do not necessarily indicate that sample compositions are homogeneous within these regions (especially when looking at tight clusters on global RPCAs). In fact, there exists a high degree of heterogeneity at smaller scales within regions and within areas. The dissimilarity-decay curves indicate that an enormous amount of faunal variability remains to be explored in deep-sea ecosystems, including within the CCZ. If seafloor areas such as the CCZ were sampled enough for random sampling to yield populations of truly comparable communities (e.g., for more specific statistical assessments), these curves would plateau out, as is the case in extensively sampled ecosystems (e.g., McDonald et al., 2018a). In addition, we hypothesize that exploring other habitats of the CCZ, such as nodules and other hard substrates hosting attached faunas (Amon et al., 2016; Smith, 2020), would shift the baseline we observe for this curve. Therefore, we propose this dissimilarity-decay analysis as a useful approach to evaluate sufficiency of biodiversity sampling for a given spatial scale. This beta diversity analysis can be made robust to the compositional nature of the data and is thus preferable to comparisons based on alpha diversity extrapolations, which remain promising to evaluate the importance of nodule habitats in the CCZ (Laroche et al., 2020b).

Implications for CCZ Conservation in the Face of Deep Seabed Mining

Although most of our samples originate from the CCZ, they cover only a tiny fraction of the CCZ's habitat heterogeneity, effectively 3 out of 24 habitat classes defined for the CCZ (McQuaid et al., 2020). This very uneven coverage limits the relevance of our results to conservation across the entire CCZ, as all samples come from the eastern half and, with the exception of the IFREMER area, from the eastern end of the CCZ. We did not obtain samples from the western half or from any of the no-mining protected areas, termed Areas of Particular Environmental Interest (APEIs). There is a general bias in our current knowledge toward the eastern half across all biological studies in the CCZ (e.g., Washburn et al., 2021), which limits our understanding of trends in relation to depth and productivity gradients. However, new knowledge for the CCZ and its comparison with the five other soft-bottom areas we included in our survey contributes to understanding of fine-sediment habitats in the deep sea. More widely, we suggest that the rapidly evolving field of environmental genomics has the potential to deliver new tools that could provide consistency across the kind of large international research efforts that are likely to dominate deep-ocean research in coming decades (e.g., Howell et al., 2020).

An important advance that will follow naturally from the present, descriptive study is the testing of predictive models that account for scale, topography and habitat heterogeneity. A plethora of statistical learning techniques are mature enough to make such predictions and inform the design of sampling protocols for baseline and monitoring studies in the CCZ and other industrially impacted areas, provided that high accuracy can be achieved. Machine learning predictions based

on metabarcoding data are useful for classification into biotic indices that are used for biomonitoring purposes in polluted, well-studied shallow-water benthic communities (e.g., Cordier et al., 2018, 2019), as well as for regressions accounting for the rare species of taxa susceptible to climate change at global scales (Busseni et al., 2020). By applying a similar approach, it also may be possible to test whether the cosmopolitan patterns we observed are real. Although we employed rigorous laboratory procedures comparable to those used in research on ancient DNA in order to avoid cross-contamination, OTUs that appear in every sample could, if rare, still be artifactual. Thus, studies based on the same genetic marker should be reanalyzed jointly to confirm patterns of cosmopolitanism and prove that harmonized, open-source metabarcoding data is a powerful tool for testing reproducibility and promoting capacity building.

To conclude, our study confirms the potential of metabarcoding for describing the deep-sea microbial and meiofaunal diversity of abyssal seafloor ecosystems. However, its use for the assessment of anthropogenic impacts, such as polymetallic nodule mining, would require better ecological understanding of the response of seafloor ecosystem to mining relating stressors (e.g., removal of nodules and surface sediments, enhanced turbidity, burial/smothering in disturbed-sediment plumes, Smith et al., 2020). Such ecological knowledge is necessary for ground truthing the metabarcoding analyses. As the ecological interpretation of metrics derived from metabarcoding improves, we anticipate that future surveys, combined with other omics analyses, will prove to be a powerful method for assessing the impact of deep-seabed mining on fragile benthic ecosystems.

DATA AVAILABILITY STATEMENT

The datasets presented in this study can be found in online repositories. The names of the repository/repositories and accession number(s) can be found below: European Nucleotide Archive accession PRJEB44134 and https://figshare.com/projects/Eukaryotic_eDNA_eRNA_From_CCZ_Benthos/98972.

AUTHOR CONTRIBUTIONS

AB, PMA, LM, LA-P-G, RM, and CRS organized deep-sea expedition or provided sediment material. FL, JP, and AJG conceived the study and wrote the manuscript. FL, IBA, and TC prepared the samples. FL performed the analyses. All authors provided comments and edits to the manuscript.

FUNDING

FL was supported by an Early Postdoc.Mobility Grant from the Swiss National Science Foundation (P2GEP3_171829). JP, LA-P-G, and IBA were supported by the Swiss National Science Foundation grants 31003A_179125 and 316030_150817. FL, TC, LAL, and JP were also supported by the Swiss Network for International Studies award (20170024). Samples from the UK-1 and OMS license areas in the Clarion-Clipperton Zone were collected as part of the ABYSSLINE project, funded by UK Seabed Resources Ltd. This funder was not involved in the study design, collection, analysis, interpretation of data, the writing of this article or the decision to submit it for publication. The material was collected and sorted within the framework of several large international projects. The expeditions with RV Polarstern were supported by the German Research Foundation, both expeditions with RV Sonne by the German Ministry for Science and Education. Pew Charitable Trusts payed for publications charges and for the Deep CCZ Biodiversity Synthesis Workshop which helped develop this manuscript.

ACKNOWLEDGMENTS

We thank the crews of the research vessels FS Polarstern, RV Sonne, FS Maria S. Merian, FS Meteor, R/V Kilo Moana, R/V Thompson, and RV L'Atalante for their help on board and all student helpers and technicians for support and help with sorting of the extensive expedition material. EU JPIO-Oceans project MinigImpact-2 (German BMBF contract 03F0812E). Samples from the German Contractor Area were kindly made available by Carsten Rühlemann and Annemiek Vink (Bundesanstalt für Geowissenschaften und Rohstoffe). We also thank Stefan Mulitza and MARUM for the North Atlantic samples collected during MSM39, Maria Holzmann for the alignments of the reference foraminifera tree, Frédéric Sinniger for the data and reference Metazoa tree, Stefan Janssen for early advice on placement in the eukaryotic SILVA reference tree, Kerry Howell for the collection of environmental data layers, Aurélie Goineau, Alexandra Anh-Thu Weber, Gan Bin Qi, Laura Würzberg, Tomas Cedhagen, and Ivan Voltsky for assistance during sampling at sea. Pew Charitable Trusts for supporting the participation of CRS, AJG and FL in the Deep CCZ Biodiversity Synthesis Workshop and for paying the publications charges.

SUPPLEMENTARY MATERIAL

The Supplementary Material for this article can be found online at: https://www.frontiersin.org/articles/10.3389/fmars.2021.671033/full#supplementary-material

REFERENCES

Adamo, M., Voyron, S., Chialva, M., Marmeisse, R., and Girlanda, M. (2020). Metabarcoding on both environmental DNA and RNA highlights differences between fungal communities sampled in different habitats. *PLoS One* 15:e0244682. doi: 10.1371/journal.pone.0244682

Aitchison, J. (1982). The statistical analysis of compositional data. *J. R. Stat. Soc. Ser. B Stat. Methodol.* 44, 139–160.

Aitchison, J. (1986). *The Statistical Analysis of Compositional Data. Monographs on Statistics and Applied Probability*. (Reprinted in 2003 with additional material by Blackburn Press), London: Chapman & Hall, 416.

Amon, D. J., Ziegler, A. F., Dahlgren, T. G., Glover, A. G., Goineau, A., Gooday, A. J., et al. (2016). Insights into the abundance and diversity of abyssal megafauna in a polymetallic-nodule region in the eastern Clarion-Clipperton Zone. *Sci. Rep.* 6:30492.

Armstrong, C. W., Foley, N. S., Tinch, R., and van den Hove, S. (2012). Services from the deep: steps towards valuation of deep sea goods and services. *Ecosyst. Serv.* 2, 2–13. doi: 10.1016/j.ecoser.2012.07.001

Aylagas, E., Borja, A., Pochon, X., Zaiko, A., Keeley, N., Bruce, K., et al. (2020). Translational molecular ecology in practice: linking DNA-based methods to actionable marine environmental management. *Sci. Total Environ.* 744:140780. doi: 10.1016/j.scitotenv.2020.140780

Aylagas, E., Borja, Á, Muxika, I., and Rodríguez-Ezpeleta, N. (2018). Adapting metabarcoding-based benthic biomonitoring into routine marine ecological status assessment networks. *Ecol. Indic.* 95, 194–202. doi: 10.1016/j.ecolind.2018.07.044

Baddeley, A., Rubak, E., and Turner, R. (2015). *Spatial Point Patterns: Methodology and Applications with R*. Boca Raton, FL: CRC press, 828.

Barrenechea, I. A., Lejzerowicz, F., Cordier, T., Scheplitz, J., Kucera, M., Ariztegui, D., et al. (2020). Planktonic Foraminifera eDNA signature deposited on the seafloor remains preserved after burial in marine sediments. *Sci. Rep.* 10:20351.

Benjamini, Y., and Hochberg, Y. (1995). Controlling the false discovery rate: a practical and powerful approach to multiple testing. *J. R. Stat. Soc. B* 57, 289–300. doi: 10.1111/j.2517-6161.1995.tb02031.x

Bik, H. M., Sung, W. A., De Ley, P., Baldwin, J. G., Sharma, J., Rocha-Olivares, A. X., et al. (2012). Metagenetic community analysis of microbial eukaryotes illuminates biogeographic patterns in deep-sea and shallow water sediments. *Mol. Ecol.* 21, 1048–1059. doi: 10.1111/j.1365-294x.2011.05297.x

Blöthe, M., Wegorzewski, A., Müller, C., Simon, F., Kuhn, T., and Schippers, A. (2015). Manganese-cycling microbial communities inside deep-sea manganese nodules. *Environ. Sci. Technol.* 49, 7692–7700. doi: 10.1021/es504930v

Bolyen, E., Rideout, J. R., Dillon, M. R., Bokulich, N. A., Abnet, C. C., Al-Ghalith, G. A., et al. (2019). Reproducible, interactive, scalable and extensible microbiome data science using QIIME 2. *Nat. Biotechnol.* 37, 852–857.

Brandt, A., and Malyutina, M. V. (2015). The German-Russian deep-sea expedition KuramBio (Kurile Kamchatka biodiversity studies) on board of the RV Sonne in 2012 following the footsteps of the legendary expeditions with RV Vityaz. *Deep Sea Res. II Top. Stud. Oceanogr.* 111, 1–9. doi: 10.1016/j.dsr2.2014.11.001

Brandt, M. I., Trouche, B., Henry, N., Liautard-Haag, C., Maignien, L., De Vargas, C., et al. (2020). An assessment of environmental metabarcoding protocols aiming at favoring contemporary biodiversity in inventories of deep-sea communities. *Front. Mar. Sci.* 7:234. doi: 10.3389/fmars.2020.00234

Bray, R. A. (2020). Digenean parasites of deep-sea teleosts: a progress report. *Int. J. Parasitol. Parasites Wildl.* 12, 251–264. doi: 10.1016/j.ijppaw.2020.01.007

Brix, S., Osborn, K. J., Kaiser, S., Truskey, S. B., Schnurr, S. M., Brenke, N., et al. (2020). Adult life strategy affects distribution patterns in abyssal isopods–implications for conservation in Pacific nodule areas. *Biogeosciences* 17, 6163–6184. doi: 10.5194/bg-17-6163-2020

Burkett, A., Rathburn, A., Pratt, R. B., and Holzmann, M. (2020). Insights into the ecology of epibenthic calcareous Foraminifera from a colonization study at 4000 m (Station M) in the NE Pacific Ocean. *Deep Sea Res. II Top. Stud. Oceanogr.* 173:104709. doi: 10.1016/j.dsr2.2019.104709

Busseni, G., Caputi, L., Piredda, R., Fremont, P., Hay Mele, B., Campese, L., et al. (2020). Large scale patterns of marine diatom richness: drivers and trends in a changing ocean. *Glob. Ecol. Biogeogr.* 29, 1915–1928. doi: 10.1111/geb.13161

Camacho, C., Coulouris, G., Avagyan, V., Ma, N., Papadopoulos, J., Bealer, K., et al. (2009). BLAST+: architecture and applications. *BMC Bioinformatics* 10:421. doi: 10.1186/1471-2105-10-421

Cantrell, K., Fedarko, M. W., Rahman, G., McDonald, D., Yang, Y., Zaw, T., et al. (2020). EMPress enables tree-guided, interactive, and exploratory analyses of multi-omic datasets. *bioRxiv [Preprint]* doi: 10.1101/2020.10.06.327080

Chariton, A. A., Court, L. N., Hartley, D. M., Colloff, M. J., and Hardy, C. M. (2010). Ecological assessment of estuarine sediments by pyrosequencing eukaryotic ribosomal DNA. *Front. Ecol. Environ.* 8:233–238. doi: 10.1890/090115

Christensen, A. M. (1981). The geographical and bathymetrical distribution of the Fecampiidae (Turbellaria, Rhabdocoela). *Hydrobiologia* 84, 13–16. doi: 10.1007/978-94-009-8668-8_3

Conover, W. J., and Iman, R. L. (1979). *On Multiple-Comparisons Procedures*. Technical report. New Mexico, NM: Los Alamos Scientific Laboratory.

Conway, J. R., Lex, A., and Gehlenborg, N. (2017). UpSetR: an R package for the visualization of intersecting sets and their properties. *Bioinformatics* 33, 2938–2940. doi: 10.1093/bioinformatics/btx364

Coolen, M. J., Orsi, W. D., Balkema, C., Quince, C., Harris, K., Sylva, S. P., et al. (2013). Evolution of the plankton paleome in the Black Sea from the deglacial to anthropocene. *Proc. Natl. Acad. Sci. U.S.A.* 110, 8609–8614. doi: 10.1073/pnas.1219283110

Cordier, T., Forster, D., Dufresne, Y., Martins, C. I., Stoeck, T., and Pawlowski, J. (2018). Supervised machine learning outperforms taxonomy-based environmental DNA metabarcoding applied to biomonitoring. *Mol. Ecol. Resour.* 18, 1381–1391. doi: 10.1111/1755-0998.12926

Cordier, T., Lanzén, A., Apothéloz-Perret-Gentil, L., Stoeck, T., and Pawlowski, J. (2019). Embracing environmental genomics and machine learning for routine biomonitoring. *Trends Microbiol.* 27, 387–397. doi: 10.1016/j.tim.2018.10.012

Corinaldesi, C., Tangherlini, M., Manea, E., and Dell'Anno, A. (2018). Extracellular DNA as a genetic recorder of microbial diversity in benthic deep-sea ecosystems. *Sci. Rep.* 8:1839.

Costello, M. J., and Chaudhary, C. (2017). Marine biodiversity, biogeography, deep-sea gradients, and conservation. *Curr. Biol.* 27, R511–R527.

Costello, M. J., Tsai, P., Wong, P. S., Cheung, A. K., Basher, Z., and Chaudhary, C. (2017). Marine biogeographic realms and species endemicity. *Nat. Commun.* 8:1057.

Cristescu, M. E. (2019). Can environmental RNA revolutionize biodiversity science? *Trends Ecol. Evol.* 34, 694–697. doi: 10.1016/j.tree.2019.05.003

Dahlgren, T. G., Wiklund, H., Rabone, M., Amon, D. J., Ikebe, C., Watling, L., et al. (2016). Abyssal fauna of the UK-1 polymetallic nodule exploration area, Clarion-Clipperton Zone, central Pacific Ocean: Cnidaria. *Biodivers. Data J.* 4:e9277. doi: 10.3897/bdj.4.e9277

Danovaro, R., Corinaldesi, C., Dell'Anno, A., and Rastelli, E. (2017). Potential impact of global climate change on benthic deep-sea microbes. *FEMS Microbiol. Lett.* 364:fnx214.

Dell'Anno, A., and Danovaro, R. (2005). Extracellular DNA plays a key role in deep-sea ecosystem functioning. *Science* 309:2179. doi: 10.1126/science.1117475

Devey, C. (2015). *Short Cruise Report R.V. "Sonne" Cruise SO-237 [SO237], Las Palmas - Santo Domingo, 14.12.2014 - 26.01.2015*, Vol. 11. Kiel: GEOMAR Helmholtz Centre for Ocean Science, doi: 10.3289/SCR_SO_237

Dufresne, Y., Lejzerowicz, F., Perret-Gentil, L. A., Pawlowski, J., and Cordier, T. (2019). SLIM: a flexible web application for the reproducible processing of environmental DNA metabarcoding data. *BMC Bioinformatics* 20:88. doi: 10.1186/s12859-019-2663-2

Durden, J. M., Bett, B. J., and Ruhl, H. A. (2020). Subtle variation in abyssal terrain induces significant change in benthic megafaunal abundance, diversity, and community structure. *Prog. Oceanogr.* 186:102395. doi: 10.1016/j.pocean.2020.102395

Edgar, R. C. (2016). SINTAX: a simple non-bayesian taxonomy classifier for 16S and ITS sequences. *bioRxiv [Preprint]*

Edgar, R. C., Haas, B. J., Clemente, J. C., Quince, C., and Knight, R. (2011). UCHIME improves sensitivity and speed of chimera detection. *Bioinformatics* 27, 2194–2200. doi: 10.1093/bioinformatics/btr381

Ekman, S. (1953). *Zoogeography of the Sea*. London: Sidgwick and Jackson, Ltd, 417.

Esling, P., Lejzerowicz, F., and Pawlowski, J. (2015). Accurate multiplexing and filtering for high-throughput amplicon-sequencing. *Nucleic Acids Res.* 43, 2513–2524. doi: 10.1093/nar/gkv107

Etter, R., Rex, M. A., Chase, M. R., and Quattro, J. M. (2005). Population differentiation decreases with depth in deep-sea bivalves. *Evolution* 59, 1479–1491. doi: 10.1554/04-538

Faith, D. P. (1992). Conservation evaluation and phylogenetic diversity. *Biol. Conserv.* 61, 1–10. doi: 10.1016/0006-3207(92)91201-3

Gage, J. D., and Tyler, P. A. (1991). *Deep-Sea Biology: A Natural History of Organisms at the Deep-Sea Floor*. Cambridge: Cambridge University Press.

George, K. H., Veit-Köhler, G., Martinez Arbizu, P., Seifried, S., Rose, A., Willen, E., et al. (2014). Community structure and species diversity of Harpacticoida (Crustacea: Copepoda) at two sites in the deep sea of the Angola Basin (Southeast Atlantic). *Org. Divers. Evol.* 14, 57–73. doi: 10.1007/s13127-013-0154-2

Giner, C. R., Pernice, M. C., Balagué, V., Duarte, C. M., Gasol, J. M., Logares, R., et al. (2020). Marked changes in diversity and relative activity of picoeukaryotes

with depth in the world ocean. *ISME J.* 14, 437–449. doi: 10.1038/s41396-019-0506-9

Gloor, G. B., Macklaim, J. M., Pawlowsky-Glahn, V., and Egozcue, J. J. (2017). Microbiome datasets are compositional: and this is not optional. *Front. Microbiol.* 8:2224. doi: 10.3389/fmicb.2017.02224

Gloor, G. B., Wu, J. R., Pawlowsky-Glahn, V., and Egozcue, J. J. (2016). It's all relative: analyzing microbiome data as compositions. *Ann. Epidemiol.* 26, 322–329. doi: 10.1016/j.annepidem.2016.03.003

Glover, A. G., Dahlgren, T. G., Wiklund, H., Mohrbeck, I., and Smith, C. R. (2016). An end-to-end DNA taxonomy methodology for benthic biodiversity survey in the Clarion-Clipperton Zone, central Pacific abyss. *J. Mar. Sci. Eng.* 4:2. doi: 10.3390/jmse4010002

Glover, A. G., and Smith, C. R. (2003). The deep-sea floor ecosystem: current status and prospects of anthropogenic change by the year 2025. *Environ. Conserv.* 1, 219–241. doi: 10.1017/s0376892903000225

Glover, A. G., Smith, C. R., Paterson, G. L., Wilson, G. D., Hawkins, L., and Sheader, M. (2002). Polychaete species diversity in the central Pacific abyss: local and regional patterns, and relationships with productivity. *Mar. Ecol. Prog. Ser.* 240, 157–170. doi: 10.3354/meps240157

Glover, A. G., Wiklund, H., Chen, C., and Dahlgren, T. G. (2018). Point of view: managing a sustainable deep-sea 'blue economy'requires knowledge of what actually lives there. *Elife* 7:e41319.

Goineau, A., and Gooday, A. J. (2017). Novel benthic Foraminifera are abundant and diverse in an area of the abyssal equatorial Pacific licensed for polymetallic nodule exploration. *Sci. Rep.* 7:45288.

Goineau, A., and Gooday, A. J. (2019). Diversity and spatial patterns of foraminiferal assemblages in the eastern Clarion–Clipperton zone (abyssal eastern equatorial Pacific). *Deep Sea Res. I Oceanogr. Res. Pap.* 149:103036. doi: 10.1016/j.dsr.2019.04.014

Golovan, O. A., Błażewicz, M., Brandt, A., Jażdżewska, A. Ì, Jóźwiak, P., Lavrenteva, A. V., et al. (2019). Diversity and distribution of peracarid crustaceans (Malacostraca) from the abyss adjacent to the Kuril-Kamchatka Trench. *Mar. Biodivers.* 49, 1343–1360. doi: 10.1007/s12526-018-0908-3

Gooday, A. J., and Goineau, A. (2019). The contribution of fine sieve fractions (63–150 μm) to foraminiferal abundance and diversity in an area of the eastern Pacific Ocean licensed for polymetallic nodule exploration. *Front. Mar. Sci.* 6:114. doi: 10.3389/fmars.2019.00114

Gooday, A. J., Holzmann, M., Caulle, C., Goineau, A., Kamenskaya, O., Weber, A. A., et al. (2017). Giant protists (Xenophyophores, Foraminifera) are exceptionally diverse in parts of the abyssal eastern Pacific licensed for polymetallic nodule exploration. *Biol. Conserv.* 207, 106–116. doi: 10.1016/j.biocon.2017.01.006

Gooday, A. J., Schoenle, A., Dolan, J. R., and Arndt, H. (2020). Protist diversity and function in the dark ocean–challenging the paradigms of deep-sea ecology with special emphasis on foraminiferans and naked protists. *Eur. J. Protistol.* 75:125721. doi: 10.1016/j.ejop.2020.125721

Gooday, A. J., Lejzerowicz, F., Goineau, A., Holzmann, M., Kamenskaya, O., Kitazato, H., et al. (2021). The biodiversity and distribution of abyssal benthic Foraminifera and their possible ecological roles: a synthesis across the Clarion-Clipperton Zone. *Front. Mar. Sci.* doi: 10.3389/fmars.2021.634726

Grassle, J. F., and Morse-Porteous, L. S. (1987). Macrofaunal colonization of disturbed deep-sea environments and the structure of deep-sea benthic communities. *Deep Sea Res. A Oceanogr. Res. Pap.* 34, 1911–1950.

Guardiola, M., Uriz, M. J., Taberlet, P., Coissac, E., Wangensteen, O. S., and Turon, X. (2015). Deep-sea, deep-sequencing: metabarcoding extracellular DNA from sediments of marine canyons. *PLoS One* 10:e0139633. doi: 10.1371/journal.pone.0139633

Guardiola, M., Wangensteen, O. S., Taberlet, P., Coissac, E., Uriz, M. J., and Turon, X. (2016). Spatio-temporal monitoring of deep-sea communities using metabarcoding of sediment DNA and RNA. *PeerJ* 4:e2807. doi: 10.7717/peerj.2807

Guggolz, T., Meißner, K., Schwentner, M., Dahlgren, T. G., Wiklund, H., Bonifácio, P., et al. (2020). High diversity and pan-oceanic distribution of deep-sea polychaetes: *Prionospio* and *Aurospio* (Annelida: Spionidae) in the Atlantic and Pacific Ocean. *Org. Divers. Evol.* 18, 171–187. doi: 10.1007/s13127-020-00430-7

Guillou, L., Bachar, D., Audic, S., Bass, D., Berney, C., Bittner, L., et al. (2013). The protist ribosomal reference database (PR2): a catalog of unicellular eukaryote small sub-unit rRNA sequences with curated taxonomy. *Nucleic Acids Res.* 41, D597–D604.

Halfvarson, J., Brislawn, C. J., Lamendella, R., Vázquez-Baeza, Y., Walters, W. A., Bramer, L. M., et al. (2017). Dynamics of the human gut microbiome in inflammatory bowel disease. *Nat. Microbiol.* 2:17004.

Hein, J. R., Mizell, K., Koschinsky, A., and Conrad, T. A. (2013). Deep-ocean mineral deposits as a source of critical metals for high-and green-technology applications: comparison with land-based resources. *Ore Geol. Rev.* 51, 1–4. doi: 10.1016/j.oregeorev.2012.12.001

Hessler, R. R., and Sanders, H. L. (1967). Faunal diversity in the deep-sea. *Deep Sea Res.* 14, 65–78. doi: 10.1016/0011-7471(67)90029-0

Hestetun, J. T., Bye-Ingebrigtsen, E., Nilsson, R. H., Glover, A. G., Johansen, P. O., and Dahlgren, T. G. (2020). Significant taxon sampling gaps in DNA databases limit the operational use of marine macrofauna metabarcoding. *Mar. Biodivers.* 50, 1–9.

Higgs, N. D., and Attrill, M. (2015). Biases in biodiversity: wide-ranging species are discovered first in the deep sea. *Front. Mar. Sci.* 2:61. doi: 10.3389/fmars.2015.00061

Holbourn, A., Henderson, A. S., and MacLeod, N. (2013). *Atlas of Benthic Foraminifera*. Hoboken, NJ: John Wiley & Sons, 642.

Holzmann, M., and Pawlowski, J. (2017). An updated classification of rotaliid Foraminifera based on ribosomal DNA phylogeny. *Mar. Micropaleontol.* 132, 18–34. doi: 10.1016/j.marmicro.2017.04.002

Howell, K. L., Hilário, A., Allcock, A. L., Bailey, D., Baker, M., Clark, M. R., et al. (2020). A decade to study deep-sea life. *Nat. Ecol. Evol.* 25, 265–267.

Howell, K. L., Piechaud, N., Downie, A. L., and Kenny, A. (2016). The distribution of deep-sea sponge aggregations in the North Atlantic and implications for their effective spatial management. *Deep Sea Res. I Oceanogr. Res. Pap.* 115, 309–320. doi: 10.1016/j.dsr.2016.07.005

Huttenhower, C., Gevers, D., Knight, R., Abubucker, S., Badger, J. H., Chinwalla, A. T., et al. (2012). Structure, function and diversity of the healthy human microbiome. *Nature* 486:207. doi: 10.1038/nature11234

Ingels, J., Valdes, Y., Pontes, L. P., Silva, A. C., Neres, P. F., Corrêa, G. V., et al. (2020). Meiofauna life on loggerhead sea turtles-diversely structured abundance and biodiversity hotspots that challenge the meiofauna paradox. *Diversity* 12:203. doi: 10.3390/d12050203

Jackson, D. A. (1995). PROTEST: a PROcrustean randomization TEST of community environment concordance. *Ecoscience* 2, 297–303. doi: 10.1080/11956860.1995.11682297

Janssen, A., Kaiser, S., Meissner, K., Brenke, N., Menot, L., and Martinez Arbizu, P. (2015). A reverse taxonomic approach to assess macrofaunal distribution patterns in abyssal Pacific polymetallic nodule fields. *PLoS One* 10:e0117790. doi: 10.1371/journal.pone.0117790

Janssen, S., McDonald, D., Gonzalez, A., Navas-Molina, J. A., Jiang, L., Xu, Z. Z., et al. (2018). Phylogenetic placement of exact amplicon sequences improves associations with clinical information. *mSystems* 3:e21-18.

Knight, R., Vrbanac, A., Taylor, B. C., Aksenov, A., Callewaert, C., Debelius, J., et al. (2018). Best practices for analysing microbiomes. *Nat. Rev. Microbiol.* 16, 410–422.

Kruskal, W. H., and Wallis, W. A. (1952). Use of ranks in one-criterion variance analysis. *J. Am. Stat. Assoc.* 47, 583–621. doi: 10.1080/01621459.1952.10483441

Kuwae, M., Tamai, H., Doi, H., Sakata, M. K., Minamoto, T., and Suzuki, Y. (2020). Sedimentary DNA tracks decadal-centennial changes in fish abundance. *Commun. Biol.* 3:558.

Langlet, D., Geslin, E., Baal, C., Metzger, E., Lejzerowicz, F., Riedel, B., et al. (2013). Foraminiferal survival after long-term in situ experimentally induced anoxia. *Biogeosciences* 10, 7463–7480. doi: 10.5194/bg-10-7463-2013

Lanzén, A., Lekang, K., Jonassen, I., Thompson, E. M., and Troedsson, C. (2016). High-throughput metabarcoding of eukaryotic diversity for environmental monitoring of offshore oil-drilling activities. *Mol. Ecol.* 25, 4392–4406. doi: 10.1111/mec.13761

Lanzén, A., Lekang, K., Jonassen, I., Thompson, E. M., and Troedsson, C. (2017). DNA extraction replicates improve diversity and compositional dissimilarity in metabarcoding of eukaryotes in marine sediments. *PLoS One* 12:e0179443. doi: 10.1371/journal.pone.0179443

Laroche, O., Kersten, O., Smith, C. R., and Goetze, E. (2020a). Environmental DNA surveys detect distinct metazoan communities across abyssal plains and

seamounts in the western Clarion Clipperton Zone. *Mol. Ecol.* 29, 4588–4604. doi: 10.1111/mec.15484

Laroche, O., Kersten, O., Smith, C. R., and Goetze, E. (2020b). From sea surface to seafloor: a benthic allochthonous eDNA survey for the abyssal ocean. *bioRxiv [Preprint]* doi: 10.1101/2020.05.07.082602

Laroche, O., Wood, S. A., Tremblay, L. A., Ellis, J. I., Lejzerowicz, F., Pawlowski, J., et al. (2016). First evaluation of foraminiferal metabarcoding for monitoring environmental impact from an offshore oil drilling site. *Mar. Environ. Res.* 120, 225–235. doi: 10.1016/j.marenvres.2016.08.009

Lecroq, B., Gooday, A. J., Cedhagen, T., Sabbatini, A., and Pawlowski, J. (2009a). Molecular analyses reveal high levels of eukaryotic richness associated with enigmatic deep-sea protists (Komokiacea). *Mar. Biodivers.* 39, 45–55.

Lecroq, B., Gooday, A. J., and Pawlowski, J. (2009b). Global genetic homogeneity in the deep-sea foraminiferan *Epistominella exigua* (Rotaliida: Pseudoparrellidae). *Zootaxa* 2096, 23–32. doi: 10.11646/zootaxa.2096.1.4

Lecroq, B., Lejzerowicz, F., Bachar, D., Christen, R., Esling, P., Baerlocher, L., et al. (2011). Ultra-deep sequencing of foraminiferal microbarcodes unveils hidden richness of early monothalamous lineages in deep-sea sediments. *Proc. Natl. Acad. Sci. U.S.A.* 108, 13177–13182. doi: 10.1073/pnas.1018426108

Legendre, P., and Legendre, L. (2012). *Numerical Ecology*. Amsterdam: Elsevier, 1006.

Lejzerowicz, F., Esling, P., Majewski, W., Szczuciński, W., Decelle, J., Obadia, C., et al. (2013a). Ancient DNA complements microfossil record in deep-sea subsurface sediments. *Biol. Lett.* 9:20130283. doi: 10.1098/rsbl.2013.0283

Lejzerowicz, F., Voltsky, I., and Pawlowski, J. (2013b). Identifying active Foraminifera in the Sea of Japan using metatranscriptomic approach. *Deep Sea Res. II Top. Stud. Oceanogr.* 86, 214–220. doi: 10.1016/j.dsr2.2012.08.008

Lejzerowicz, F., Esling, P., and Pawlowski, J. (2014). Patchiness of deep-sea benthic Foraminifera across the Southern Ocean: insights from high-throughput DNA sequencing. *Deep Sea Res. II Top. Stud. Oceanogr.* 108, 17–26. doi: 10.1016/j.dsr2.2014.07.018

Lejzerowicz, F., Esling, P., Pillet, L., Wilding, T. A., Black, K. D., and Pawlowski, J. (2015). High-throughput sequencing and morphology perform equally well for benthic monitoring of marine ecosystems. *Sci. Rep.* 5: 13932.

Levin, L. A., Amon, D. J., and Lily, H. (2020a). Challenges to the sustainability of deep-seabed mining. *Nat. Sustain.* 3, 784–794. doi: 10.1038/s41893-020-0558-x

Levin, L. A., Wei, C. L., Dunn, D. C., Amon, D. J., Ashford, O. S., Cheung, W. W., et al. (2020b). Climate change considerations are fundamental to management of deep-sea resource extraction. *Glob. Change Biol.* 26, 4664–4678. doi: 10.1111/gcb.15223

Levin, L. A., Bett, B. J., Gates, A. R., Heimbach, P., Howe, B. M., Janssen, F., et al. (2019). Global observing needs in the deep ocean. *Front. Mar. Sci.* 6:241. doi: 10.3389/fmars.2019.00241

Levin, L. A., and Le Bris, N. (2015). The deep ocean under climate change. *Science* 350, 766–768. doi: 10.1126/science.aad0126

Levin, L. A., Mengerink, K., Gjerde, K. M., Rowden, A. A., Van Dover, C. L., Clark, M. R., et al. (2016). Defining "serious harm" to the marine environment in the context of deep-seabed mining. *Mar. Policy* 74, 245–259. doi: 10.1016/j.marpol.2016.09.032

Lindh, M. V., Maillot, B. M., Shulse, C. N., Gooday, A. J., Amon, D. J., Smith, C. R., et al. (2017). From the surface to the deep-sea: bacterial distributions across polymetallic nodule fields in the clarion-clipperton zone of the Pacific Ocean. *Front. Microbiol.* 8:1696.

Lindh, M. V., Maillot, B. M., Smith, C. R., and Church, M. J. (2018). Habitat filtering of bacterioplankton communities above polymetallic nodule fields and sediments in the Clarion-Clipperton zone of the Pacific Ocean. *Environ. Microbiol. Rep.* 10, 113–122. doi: 10.1111/1758-2229.12627

Logares, R., Audic, S., Santini, S., Pernice, M. C., De Vargas, C., and Massana, R. (2012). Diversity patterns and activity of uncultured marine heterotrophic flagellates unveiled with pyrosequencing. *ISME J.* 6, 1823–1833. doi: 10.1038/ismej.2012.36

Lozupone, C., and Knight, R. (2005). UniFrac: a new phylogenetic method for comparing microbial communities. *Appl. Environ. Microbiol.* 71, 8228–8235. doi: 10.1128/aem.71.12.8228-8235.2005

Macheriotou, L., Guilini, K., Bezerra, T. N., Tytgat, B., Nguyen, D. T., Phuong Nguyen, T. X., et al. (2019). Metabarcoding free-living marine nematodes using curated 18S and CO1 reference sequence databases for species-level taxonomic assignments. *Ecol. Evol.* 9, 1211–1226. doi: 10.1002/ece3.4814

Macheriotou, L., Rigaux, A., Derycke, S., and Vanreusel, A. (2020). Phylogenetic clustering and rarity imply risk of local species extinction in prospective deep-sea mining areas of the Clarion–Clipperton Fracture Zone. *Proc. R. Soc. B* 287:20192666. doi: 10.1098/rspb.2019.2666

Mahé, F., Rognes, T., Quince, C., de Vargas, C., and Dunthorn, M. (2015). Swarm v2: highly-scalable and high-resolution amplicon clustering. *PeerJ* 3:e1420. doi: 10.7717/peerj.1420

Mantel, N. (1967). The detection of disease clustering and a generalized regression approach. *Cancer Res.* 27, 209–220.

Martínez Arbizu, P., Brix, S., Kaiser, S., Brandt, A., George, K., Arndt, H., et al. (2015). *Deep-Sea Biodiversity, Current Activity, and Seamounts in the Atlantic–Cruise no. M79/1–June 10–August 26, 2009–Montevideo (Uruguay)–Ponta Delgada (Portugal). METEOR-Berichte M79/1: 5–92, DFG-Senatskommission für Ozeanographie*. Berlin: Leibniz Assication.

Martino, C., Morton, J. T., Marotz, C. A., Thompson, L. R., Tripathi, A., Knight, R., et al. (2019). A novel sparse compositional technique reveals microbial perturbations. *mSystems* 4:e00016-19. doi: 10.1128/mSystems.00016-19

Masella, A. P., Bartram, A. K., Truszkowski, J. M., Brown, D. G., and Neufeld, J. D. (2012). PANDAseq: paired-end assembler for illumina sequences. *BMC Bioinformatics* 13:31. doi: 10.1186/1471-2105-13-31

Mauffrey, F., Cordier, T., Apothéloz-Perret-Gentil, L., Cermakova, K., Merzi, T., Delefosse, M., et al. (2020). Benthic monitoring of oil and gas offshore platforms in the North Sea using environmental DNA metabarcoding. *Mol. Ecol.* doi: 10.1111/mec.15698 Online Print ahead

McClain, C. R., and Hardy, S. M. (2010). The dynamics of biogeographic ranges in the deep sea. *Proc. R. Soc. B Biol. Sci.* 277, 3533–3546. doi: 10.1098/rspb.2010.1057

McDonald, D., Hyde, E., Debelius, J. W., Morton, J. T., Gonzalez, A., Ackermann, G., et al. (2018a). American gut: an open platform for citizen science microbiome research. *mSystems* 3:e31-18. doi: 10.1128/mSystems.00031-18

McDonald, D., Vázquez-Baeza, Y., Koslicki, D., McClelland, J., Reeve, N., Xu, Z., et al. (2018b). Striped UniFrac: enabling microbiome analysis at unprecedented scale. *Nat. Methods* 15, 847–848. doi: 10.1038/s41592-018-0187-8

McQuaid, K. A., Attrill, M. J., Clark, M. R., Cobley, A., Glover, A. G., Smith, C. R., et al. (2020). Using habitat classification to assess representativity of a protected area network in a large, data-poor area targeted for deep-sea mining. *Front. Mar. Sci.* 7:1066. doi: 10.3389/fmars.2020.558860

Menot, L. (2012). *BIONOD Cruise, RV L'Atalante*. Available online at: https://doi.org/10.17600/12010030 (accessed April 29, 2021).

Menzel, L., George, K. H., and Martinez Arbizu, P. (2011). Submarine ridges do not prevent large-scale dispersal of abyssal fauna: a case study of *Mesocletodes* (Crustacea, Copepoda, Harpacticoida). *Deep Sea Res. I Oceanogr. Res. Pap.* 58, 839–864. doi: 10.1016/j.dsr.2011.05.008

Mirarab, S., Nguyen, N., and Warnow, T. (2012). SEPP: SATé-enabled phylogenetic placement. *InBiocomputing* 2012, 247–258. doi: 10.1142/9789814366496_0024

Mitra, A., Skrzypczak, M., Ginalski, K., and Rowicka, M. (2015). Strategies for achieving high sequencing accuracy for low diversity samples and avoiding sample bleeding using illumina platform. *PLoS One* 10:e0120520. doi: 10.1371/journal.pone.0227431

Morard, R., Darling, K. F., Mahé, F., Audic, S., Ujiié, Y., Weiner, A. K., et al. (2015). PFR2: a curated database of planktonic Foraminifera 18S ribosomal DNA as a resource for studies of plankton ecology, biogeography and evolution. *Mol. Ecol. Resour.* 15, 1472–1485. doi: 10.1111/1755-0998.12410

Morard, R., Lejzerowicz, F., Darling, K. F., Lecroq-Bennet, B., Winther Pedersen, M., Orlando, L., et al. (2017). Planktonic Foraminifera-derived environmental DNA extracted from abyssal sediments preserves patterns of plankton macroecology. *Biogeosciences* 14, 2741–2754. doi: 10.5194/bg-14-2741-2017

Morato, T., González-Irusta, J. M., Dominguez-Carrió, C., Wei, C. L., Davies, A., Sweetman, A. K., et al. (2020). Climate-induced changes in the suitable habitat of cold-water corals and commercially important deep-sea fishes in the North Atlantic. *Glob. Change Biol.* 26, 2181–2202.

Morton, J. T., Sanders, J., Quinn, R. A., McDonald, D., Gonzalez, A., Vázquez-Baeza, Y., et al. (2017). Balance trees reveal microbial niche differentiation. *mSystems* 2:e162-16. doi: 10.1128/mSystems.00162-16

Mulitza, S., Bergmann, F., Brück, L., Chiessi, C. M., Govin, A., Klann, M., et al. (2015). *Cruise No. MSM39 –June 07 –June 25, 2014—St. John's (Canada)–St. John's (Canada). MARIA S. MERIAN-Berichte, MSM39. DFG-Senatskommission für Ozeanographie*. Berlin: Leibniz Assication, 89. doi: 10.2312/cr_msm39

Murali, A., Bhargava, A., and Wright, E. S. (2018). IDTAXA: a novel approach for accurate taxonomic classification of microbiome sequences. *Microbiome* 6, 1–4. doi: 10.1016/b978-0-12-512517-8.50014-x

Murray, J. W. (2006). *Ecology and Applications of Benthic Foraminifera*. Cambridge: Cambridge university press, 426.

Niner, H. J., Ardron, J. A., Escobar, E. G., Gianni, M., Jaeckel, A., Jones, D. O., et al. (2018). Deep-sea mining with no net loss of biodiversity—an impossible aim. *Front. Mar. Sci.* 5:53. doi: 10.3389/fmars.2018.00053

Oksanen, J. (2011). *Multivariate Analysis of Ecological Communities in R: Vegan Tutorial. R Package Version*. 1, 1–43.

Orsi, W. D., Morard, R., Vuillemin, A., Eitel, M., Wörheide, G., Milucka, J., et al. (2020). Anaerobic metabolism of Foraminifera thriving below the seafloor. *ISME J.* 8, 1–5.

Pante, E., and Simon-Bouhet, B. (2013). marmap: a package for importing, plotting and analyzing bathymetric and topographic data in R. *PLoS One* 8:e73051. doi: 10.1371/journal.pone.0073051

Pape, E., Bezerra, T. N., Hauquier, F., and Vanreusel, A. (2017). Limited spatial and temporal variability in meiofauna and nematode communities at distant but environmentally similar sites in an area of interest for deep-sea mining. *Front. Mar. Sci.* 4:205. doi: 10.3389/fmars.2017.00205

Pawlowski, J., Christen, R., Lecroq, B., Bachar, D., Shahbazkia, H. R., Amaral-Zettler, L., et al. (2011). Eukaryotic richness in the abyss: insights from pyrotag sequencing. *PLoS One* 6:e18169. doi: 10.1371/journal.pone.0018169

Pawlowski, J., Esling, P., Lejzerowicz, F., Cedhagen, T., and Wilding, T. A. (2014). Environmental monitoring through protist next-generation sequencing metabarcoding: assessing the impact of fish farming on benthic Foraminifera communities. *Mol. Ecol. Resour.* 14, 1129–1140. doi: 10.1111/1755-0998.12261

Pawlowski, J., Fahrni, J., Lecroq, B., Longet, D., Cornelius, N., Excoffier, L., et al. (2007). Bipolar gene flow in deep-sea benthic Foraminifera. *Mol. Ecol.* 16, 4089–4096. doi: 10.1111/j.1365-294x.2007.03465.x

Pawlowski, J., Holzmann, M., Berney, C., Fahrni, J., Gooday, A. J., Cedhagen, T., et al. (2003). The evolution of early Foraminifera. *Proc. Natl. Acad. Sci. U.S.A.* 100, 11494–11498.

Pawlowski, J., and Lecroq, B. (2010). Short rDNA barcodes for species identification in Foraminifera. *J. Eukaryot. Microbiol.* 57, 197–205. doi: 10.1111/j.1550-7408.2009.00468.x

Petersen, S., Krätschell, A., Augustin, N., Jamieson, J., Hein, J. R., and Hannington, M. D. (2016). News from the seabed–geological characteristics and resource potential of deep-sea mineral resources. *Mar. Policy* 70, 175–187. doi: 10.1016/j.marpol.2016.03.012

Pimm, S. L., Jenkins, C. N., Abell, R., Brooks, T. M., Gittleman, J. L., Joppa, L. N., et al. (2014). The biodiversity of species and their rates of extinction, distribution, and protection. *Science* 344:1246752. doi: 10.1126/science.1246752

Pochon, X., Wood, S. A., Keeley, N. B., Lejzerowicz, F., Esling, P., Drew, J., et al. (2015). Accurate assessment of the impact of salmon farming on benthic sediment enrichment using foraminiferal metabarcoding. *Marine Pollution Bulletin* 100, 370–382. doi: 10.1016/j.marpolbul.2015.08.022

Quast, C., Pruesse, E., Yilmaz, P., Gerken, J., Schweer, T., Yarza, P., et al. (2013). The SILVA ribosomal RNA gene database project: improved data processing and web-based tools. *Nucleic Acids Res.* 41, D590–D596.

Quinn, T. P., Erb, I., Richardson, M. F., and Crowley, T. M. (2018). Understanding sequencing data as compositions: an outlook and review. *Bioinformatics* 34, 2870–2878. doi: 10.1093/bioinformatics/bty175

Rabone, M., Harden-Davies, H., Collins, J. E., Zajderman, S., Appeltans, W., Droege, G., et al. (2019). Access to marine genetic resources (MGR): raising awareness of best-practice through a new agreement for biodiversity beyond national jurisdiction (BBNJ). *Front. Mar. Sci.* 6:520. doi: 10.3389/fmars.2019.00520

Ramirez-Llodra, E., Brandt, A., Danovaro, R., Mol, B. D., Escobar, E., German, C. R., et al. (2010). Deep, diverse and definitely different: unique attributes of the world's largest ecosystem. *Biogeosciences* 7, 2851–2899. doi: 10.5194/bg-7-2851-2010

Rex, M. A., and Etter, R. J. (2010). *Deep-Sea Biodiversity: Pattern and Scale*. Harvard: Harvard University Press, 388.

Riehl, T., Wölfl, A. C., Augustin, N., Devey, C. W., and Brandt, A. (2020). Discovery of widely available abyssal rock patches reveals overlooked habitat type and prompts rethinking deep-sea biodiversity. *Proc. Natl. Acad. Sci. U.S.A.* 117, 15450–15459. doi: 10.1073/pnas.1920706117

Rognes, T., Flouri, T., Nichols, B., Quince, C., and Mahé, F. (2016). VSEARCH: a versatile open source tool for metagenomics. *PeerJ* 4:e2584.

Rouse, G. W., Wilson, N. G., Carvajal, J. I., and Vrijenhoek, R. C. (2016). New deep-sea species of Xenoturbella and the position of Xenacoelomorpha. *Nature* 530, 94–97. doi: 10.1038/nature16545

Ruiz-Trillo, I., Riutort, M., Littlewood, D. T. J., Herniou, E. A., and Baguña, J. (1999). Acoel flatworms: earliest extant bilaterian metazoans, not members of platyhelminthes. *Science* 283, 1919–1923. doi: 10.1126/science.283.5409.1919

Sanders, H. L. (1968). Marine benthic diversity: a comparative study. *Am. Nat.* 102, 243–282. doi: 10.1086/282541

Santoferrara, L., Burki, F., Filker, S., Logares, R., Dunthorn, M., and McManus, G. B. (2020). Perspectives from ten years of protist studies by high-throughput metabarcoding. *J. Eukaryot. Microbiol.* 67, 612–622. doi: 10.1111/jeu.12813

Schloss, P. D., Westcott, S. L., Ryabin, T., Hall, J. R., Hartmann, M., Hollister, E. B., et al. (2009). Introducing mothur: open-source, platform-independent, community-supported software for describing and comparing microbial communities. *Appl. Environ. Microbiol.* 75, 7537–7541. doi: 10.1128/aem.01541-09

Schüller, M., and Hutchings, P. A. (2012). New species of *Terebellides* (Polychaeta: Trichobranchidae) indicate long-distance dispersal between western South Atlantic deep-sea basins. *Zootaxa* 3254, 1–31. doi: 10.11646/zootaxa.3254.1.1

Shulse, C. N., Maillot, B., Smith, C. R., and Church, M. J. (2017). Polymetallic nodules, sediments, and deep waters in the equatorial North Pacific exhibit highly diverse and distinct bacterial, archaeal, and microeukaryotic communities. *MicrobiologyOpen* 6:e00428. doi: 10.1002/mbo3.428

Sinniger, F., Pawlowski, J., Harii, S., Gooday, A. J., Yamamoto, H., Chevaldonné, P., et al. (2016). Worldwide analysis of sedimentary DNA reveals major gaps in taxonomic knowledge of deep-sea benthos. *Front. Mar. Sci.* 3:92. doi: 10.3389/fmars.2016.00092

Smith, C. R. (2020). The heterogeneous abyss. *Proc. Natl. Acad. Sci. U.S.A.* 117, 16729–16731. doi: 10.1073/pnas.2010215117

Smith, C. R., Dahlgren, T. G., Drazen, J., Gooday, A., Glover, A. G., Kurras, G., et al. (2013). *Abyssal Baseline Study (ABYSSLINE) Cruise Report*. Seafloor Investigations Report 2013-1304-051J-SRDL-AB01. Washington, DC: Seafloor Investigations. 1–160.

Smith, C. R., De Leo, F. C., Bernardino, A. F., Sweetman, A. K., and Martinez Arbizu, P. (2008). Abyssal food limitation, ecosystem structure and climate change. *Trends Ecol. Evol.* 23, 518–528. doi: 10.1016/j.tree.2008.05.002

Smith, C. R., Tunnicliffe, V., Colaço, A., Drazen, J. C., Gollner, S., Levin, L. A., et al. (2020). Deep-sea misconceptions cause underestimation of seabed-mining impacts. *Trends Ecol. Evol.* 35, 853–857. doi: 10.1016/j.tree.2020.07.002

Snelgrove, P., and Smith, C. R. (2002). A riot of species in an environmental calm. *Oceanogr. Mar. Biol.* 40, 311–342. doi: 10.1201/9780203180594.ch6

Stamatakis, A. (2014). RAxML version 8: a tool for phylogenetic analysis and post-analysis of large phylogenies. *Bioinformatics* 30, 1312–1313. doi: 10.1093/bioinformatics/btu033

Stefanoudis, P. V., Bett, B. J., and Gooday, A. J. (2016). Abyssal hills: influence of topography on benthic foraminiferal assemblages. *Prog. Oceanogr.* 148, 44–55. doi: 10.1016/j.pocean.2016.09.005

Sweetman, A. K., Thurber, A. R., Smith, C. R., Levin, L. A., Mora, C., Wei, C. L., et al. (2017). Major impacts of climate change on deep-sea benthic ecosystems. *Elementa* 5:4.

Taberlet, P., Coissac, E., Pompanon, F., Brochmann, C., and Willerslev, E. (2012). Towards next-generation biodiversity assessment using DNA metabarcoding. *Mol. Ecol.* 21, 2045–2050. doi: 10.1111/j.1365-294x.2012.05470.x

Thiel, H. (1983). "Meiobenthos and nanobenthos of the deep sea," in *Deep Sea Biology. The Sea*, ed. G. T. Rowe (New York, NY: John Wiley and Sons), 167–230.

Thiel, H. (2003). Anthropogenic impacts on the deep sea. *Ecosyst. World* 27, 427–472.

Thurber, A. R., Sweetman, A. K., Narayanaswamy, B. E., Jones, D. O., Ingels, J., and Hansman, R. L. (2014). Ecosystem function and services provided by the deep sea. *Biogeosciences* 11, 3941–3963. doi: 10.5194/bg-11-3941-2014

Turner, P. J., Cannon, S., DeLand, S., Delgado, J. P., Eltis, D., Halpin, P. N., et al. (2020). Memorializing the middle passage on the atlantic seabed in areas beyond national jurisdiction. *Mar. Policy* 122:104254. doi: 10.1016/j.marpol.2020.104254

Turnewitsch, R., Lahajnar, N., Haeckel, M., and Christiansen, B. (2015). An abyssal hill fractionates organic and inorganic matter in deep-sea surface sediments. *Geophys. Res. Lett.* 42, 7663–7672. doi: 10.1002/2015gl065658

van der Land, J. (1972). *Priapulus* from the deep sea (Vermes, Priapulida). *Zool. Meded.* 47, 358–368.

Vázquez-Baeza, Y., Pirrung, M., Gonzalez, A., and Knight, R. (2013). EMPeror: a tool for visualizing high-throughput microbial community data. *Gigascience* 2:16.

Vinogradova, N. G. (1997). Zoogeography of the abyssal and hadal zones. *Adv. Mar. Biol.* 32, 325–387. doi: 10.1016/s0065-2881(08)60019-x

Virtanen, P., Gommers, R., Oliphant, T. E., Haberland, M., Reddy, T., Cournapeau, D., et al. (2020). SciPy 1.0: fundamental algorithms for scientific computing in Python. *Nat. Methods* 17, 261–272.

Volz, J. B., Mogollón, J. M., Geibert, W., Martinez Arbizu, P., Koschinsky, A., and Kasten, S. (2018). Natural spatial variability of depositional conditions, biogeochemical processes and element fluxes in sediments of the eastern Clarion-Clipperton Zone, Pacific Ocean. *Deep Sea Res. I Oceanogr. Res. Pap.* 140, 159–172. doi: 10.1016/j.dsr.2018.08.006

Vonnahme, T. R., Molari, M., Janssen, F., Wenzhöfer, F., Haeckel, M., Titschack, J., et al. (2020). Effects of a deep-sea mining experiment on seafloor microbial communities and functions after 26 years. *Sci. Adv.* 6:eaaz5922. doi: 10.1126/sciadv.aaz5922

Washburn, T. W., Menot, L., Bonifácio, P., Pape, E., Błażewicz, M., Bribiesca-Contreras, G., et al. (2021). Patterns of macrofaunal biodiversity across the Clarion-Clipperton Zone: an area targeted for seabed mining. *Front. Mar. Sci.* 8:250. doi: 10.3389/fmars.2021.626571

Watling, L., Guinotte, J., Clark, M. R., and Smith, C. R. (2013). A proposed biogeography of the deep ocean floor. *Progr. Oceanogr.* 111, 91–112.

Weiss, A. (2001). "Topographic position and landforms analysis," in *Proceedings of the Poster Presentation, ESRI user Conference*, San Diego, CA.

Wenhai, L., Cusack, C., Baker, M., Tao, W., Mingbao, C., Paige, K., et al. (2019). Successful blue economy examples with an emphasis on international perspectives. *Front. Mar. Sci.* 6:261. doi: 10.3389/fmars.2019.00261

Wiklund, H., Neal, L., Glover, A. G., Drennan, R., Rabone, M., and Dahlgren, T. G. (2019). Abyssal fauna of polymetallic nodule exploration areas, eastern clarion-clipperton zone, central Pacific Ocean: annelida: capitellidae, opheliidae, scalibregmatidae, and travisiidae. *ZooKeys* 883, 1–82.

Wiklund, H., Taylor, J. D., Dahlgren, T. G., Todt, C., Ikebe, C., Rabone, M., et al. (2017). Abyssal fauna of the UK-1 polymetallic nodule exploration area, Clarion-Clipperton Zone, central Pacific Ocean: Mollusca. *ZooKeys* 707, 1–46. doi: 10.3897/zookeys.707.13042

Wilson, G. D. (2017). Macrofauna abundance, species diversity and turnover at three sites in the Clipperton-Clarion Fracture Zone. *Marine Biodiversity* 47, 323–347. doi: 10.1007/s12526-016-0609-8

Wolf-Gladrow, D. (2013). The expedition of the research vessel" Polarstern" to the Antarctic in 2012 (ANT-XXVIII/3). *Ber. Pol. Meeresforschung* 661:191. doi: 10.2312/BzPM_0661_2013

Wood, S. A., Biessy, L., Latchford, J. L., Zaiko, A., von Ammon, U., Audrezet, F., et al. (2020). Release and degradation of environmental DNA and RNA in a marine system. *Sci. Total Environ.* 704:135314. doi: 10.1016/j.scitotenv.2019.135314

Würzberg, L., Zinkann, A. C., Brandt, A., Janussen, D., Bohn, J. M., and Schwabe, E. (2014). Intensity of pelagic–benthic coupling in different regions along the Antarctic Polar Front–Clues from abyssal megafauna. *Deep Sea Res. II Top. Stud. Oceanogr.* 108, 85–92. doi: 10.1016/j.dsr2.2014.09.003

Yilmaz, P., Kottmann, R., Field, D., Knight, R., Cole, J. R., Amaral-Zettler, L., et al. (2011). Minimum information about a marker gene sequence (MIMARKS) and minimum information about any (x) sequence (MIxS) specifications. *Nat. Biotechnol.* 29, 415–420.

Zinger, L., Amaral-Zettler, L. A., Fuhrman, J. A., Horner-Devine, M. C., Huse, S. M., Welch, D. B., et al. (2011). Global patterns of bacterial beta-diversity in seafloor and seawater ecosystems. *PLoS One* 6:e24570. doi: 10.1371/journal.pone.0024570

Conflict of Interest: JP and LA-P-G were employed by ID-Gene Ecodiagnostics.

The remaining authors declare that the research was conducted in the absence of any commercial or financial relationships that could be construed as a potential conflict of interest.

Copyright © 2021 Lejzerowicz, Gooday, Barrenechea Angeles, Cordier, Morard, Apothéloz-Perret-Gentil, Lins, Menot, Brandt, Levin, Martinez Arbizu, Smith and Pawlowski. This is an open-access article distributed under the terms of the Creative Commons Attribution License (CC BY). The use, distribution or reproduction in other forums is permitted, provided the original author(s) and the copyright owner(s) are credited and that the original publication in this journal is cited, in accordance with accepted academic practice. No use, distribution or reproduction is permitted which does not comply with these terms.

frontiers in Marine Science

REVIEW
published: 28 June 2021
doi: 10.3389/fmars.2021.634726

The Biodiversity and Distribution of Abyssal Benthic Foraminifera and Their Possible Ecological Roles: A Synthesis Across the Clarion-Clipperton Zone

Andrew J. Gooday[1,2], Franck Lejzerowicz[3,4], Aurélie Goineau[1], Maria Holzmann[5], Olga Kamenskaya[6], Hiroshi Kitazato[7], Swee-Cheng Lim[8], Jan Pawlowski[5,9,10], Teresa Radziejewska[11], Zofia Stachowska[11] and Brygida Wawrzyniak-Wydrowska[11]*

[1] National Oceanography Centre, Southampton, United Kingdom, [2] Life Sciences Department, Natural History Museum, London, United Kingdom, [3] Center for Microbiome Innovation, University of California, San Diego, San Diego, CA, United States, [4] Department of Pediatrics, University of California, San Diego, San Diego, CA, United States, [5] Department of Genetics and Evolution, University of Geneva, Geneva, Switzerland, [6] Shirshov Institute of Oceanology Russian Academy of Sciences, Moscow, Russia, [7] Tokyo University of Science and Technology, Tokyo, Japan, [8] Keppel-NUS Corporate Laboratory, Tropical Marine Science Institute, National University of Singapore, Singapore, Singapore, [9] Institute of Oceanology, Polish Academy of Sciences, Sopot, Poland, [10] ID-Gene Ecodiagnostics, Campus Biotech Innovation Park, Geneva, Switzerland, [11] Institute of Marine and Environmental Sciences, University of Szczecin, Szczecin, Poland

OPEN ACCESS

Edited by:
Malcolm Ross Clark, National Institute of Water and Atmospheric Research (NIWA), New Zealand

Reviewed by:
Akkur Vasudevan Raman, Andhra University, India
Alessandra Asioli, Institute of Marine Science (CNR), Italy

***Correspondence:**
Andrew J. Gooday
ang@noc.ac.uk

Specialty section:
This article was submitted to Deep-Sea Environments and Ecology, a section of the journal Frontiers in Marine Science

Received: *28 November 2020*
Accepted: *19 April 2021*
Published: *28 June 2021*

Citation:
Gooday AJ, Lejzerowicz F, Goineau A, Holzmann M, Kamenskaya O, Kitazato H, Lim S-C, Pawlowski J, Radziejewska T, Stachowska Z and Wawrzyniak-Wydrowska B (2021) The Biodiversity and Distribution of Abyssal Benthic Foraminifera and Their Possible Ecological Roles: A Synthesis Across the Clarion-Clipperton Zone. Front. Mar. Sci. 8:634726. doi: 10.3389/fmars.2021.634726

Benthic foraminiferal research in the North Pacific has a long history, with works published over a century ago providing important information about the taxonomy and distribution of morphospecies. These studies focused mainly on areas outside the Clarion-Clipperton Zone (CCZ). Our knowledge of foraminiferal faunas within the CCZ originates largely from recent baseline investigations related to likely future seabed mining of the polymetallic nodule deposits. These have revealed highly diverse assemblages of sediment-dwelling morphospecies among the meiofauna and macrofauna, as well as megafaunal xenophyophores and nodule-attached fauna. Morphological analyses have been complemented by metabarcoding studies that yielded even higher numbers of molecular species (Operational Taxonomic Units - OTUs). Monothalamids, the vast majority undescribed, constitute a substantial proportion of both morphological and molecular datasets, with multichambered agglutinated and calcareous foraminifera being less common. Their importance in this abyssal (>4,000 m depth) habitat likely reflects food limitation combined with carbonate dissolution close to and below the carbonate compensation depth. Literature records, supported in a few cases by genetic data, suggest that many morphospecies found in the CCZ have wide geographical distributions across the Pacific abyss and in other oceans. At smaller spatial scales (several 100s of kilometers) there is a general uniformity in assemblage composition. Nevertheless, many morphospecies are too rare to conclude anything about their geographical distributions. Similarly, the part played by benthic foraminifera in CCZ ecosystems is largely a matter of speculation,

although their abundance across different size classes suggests that it is significant. Meiofauna-sized taxa that consume freshly-deposited organic detritus may be important in carbon cycling, particularly at the shallower, more eutrophic eastern end of the CCZ. Megafaunal xenophyophores can provide habitat structure for other organisms, potentially enhancing benthic biodiversity. Foraminifera of all sizes could be among the earliest recolonisers of disturbed or redeposited sediments. Their potential contributions in terms of both ecology and biodiversity make these protists significant members of benthic communities in the CCZ.

Keywords: polymetallic nodules, equatorial North Pacific Ocean, monothalamids, xenophyophores, metabarcoding analyses, biogeography, food webs, recolonization

INTRODUCTION

Foraminifera, shell-bearing protists in the supergroup Rhizaria, are common in all marine environments from the intertidal zone to the deepest ocean trenches and have also adapted to fresh water and damp terrestrial settings. They inhabit hard and soft substrates and flourish in the virtual absence of oxygen as well as in well-oxygenated environments. The extraordinary success of foraminifera may be attributable to unique physiological and ultrastructural adaptations, including their highly mobile system of reticulated pseudopodia that is involved in many life processes, including feeding, respiration and movement (Travis and Bowser, 1991). These protists become an increasingly important component of benthic communities with increasing water depth (Thiel, 1975, 1983), and on abyssal plains they may account for more than 50% of the meiofaunal and macrofaunal abundance and biomass (Gooday et al., 1992; Gooday, 2019). Interest in foraminifera is not confined to biologists. They have an outstanding fossil record and are widely used as indicators of seafloor conditions in ancient oceans (Jorissen et al., 2007). As a result, much of the more recent research on the ecology of modern deep-sea benthic foraminifera has been driven by efforts to refine their utility in palaeoceanography.

Foraminifera research in the Pacific Ocean has a long history, extending back well into the 19th century. This has generated a large body of information on species distributions, making foraminifera one of the better documented deep-sea benthic taxa. Much of this earlier research concerned species with relatively robust multichambered shells, composed either of secreted calcium carbonate or agglutinated particles. However, the true nature of foraminifera assemblages on Pacific abyssal plains, and the scale of their diversity, only started to become apparent as a result of research in the central North Pacific during the 1970s (Hessler, 1974). This revealed that the macrofauna is dominated by agglutinated foraminifera (Bernstein et al., 1978), many of them single-chambered monothalamids (class Monothalamea) including tubular forms and those with highly unusual test morphologies, for which Tendal and Hessler (1977) established the superfamily Komokiacea. A group of even larger monothalamids, the xenophyophores (Tendal, 1972), make a major contribution to the North Pacific megafauna (Gooday et al., 2017b; Simon-Lledó et al., 2019a), while largely undescribed sessile foraminifera are very abundant on polymetallic nodules (Veillette et al., 2007; Gooday et al., 2015).

Here, we focus on the Clarion-Clipperton Zone (CCZ). Spanning some 4.5 million km^2 of seafloor from about 115° to 155° W and 03° to 19° N, the region hosts some of the ocean's richest and most extensive seabed deposits of polymetallic nodules, a likely target for commercial mining in the near future (Hein et al., 2013; Washburn et al., 2019; Smith et al., 2020). The regulating body, the International Seabed Authority (ISA), has concluded contracts with 18 entities (states, enterprises and consortia) for polymetallic nodule deposit exploration in areas up to ∼75,000 km^2, and designated nine Areas of Particular Environmental Interest (APEIs) that will be protected from mining. These developments have prompted a sharp rise in ecological and taxonomic research across the CCZ during the last decade, aimed at assessing the present status of biodiversity in areas designated for future nodule extraction, and at finding potential repositories (gene banks) of taxa capable of recolonizing mined areas. Much of this effort has focused on the eastern CCZ (Washburn et al., 2021) and foraminifera have featured prominently in it. Our synthesis combines information from classical taxonomic and distributional studies of benthic foraminifera with morphological and genetic data, both published and unpublished, obtained during this recent phase of mining-related research. We first consider the important earlier literature on abyssal North Pacific foraminifera, before summarizing data on the biodiversity, biogeography, and species ranges of foraminifera within the CCZ. Finally, we speculate about possible ecological roles for foraminifera and suggest some plausible scenarios for their recovery from seabed mining impacts.

PREVIOUS RESEARCH ON MODERN BENTHIC FORAMINIFERA IN THE CCZ AND ADJACENT AREAS

Foraminifera have been collected at a large number of sites across the Pacific Ocean at depths of > 3000 m. The locations of sites sampled during some of the more important recent studies, as well as some early reports, are shown in **Figure 1**. The map is not intended to be comprehensive. In particular, it omits the numerous *Albatross* and *Nero*

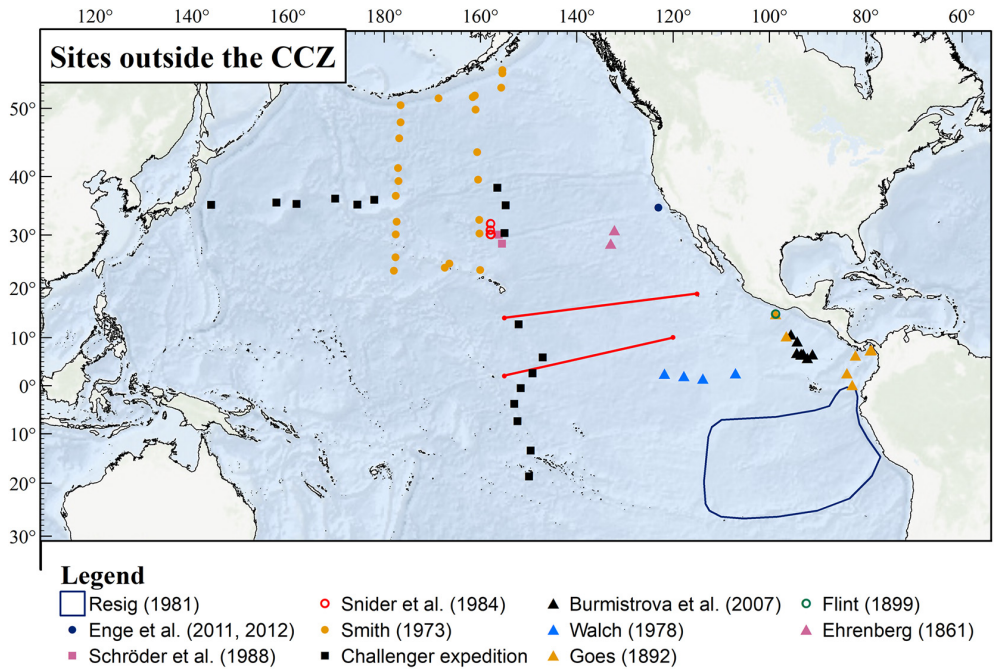

FIGURE 1 | The location of selected studies and sampling sites in the Pacific Ocean. Apart from two *Challenger* stations at the western end of the CCZ, all are located outside of the CCZ. The Clarion and Clipperton Fractures that delimit the CCZ are marked with red lines; the dark blue line outlines the Resig (1981) study area.

sites, which yielded many of the records summarized by Cushman (1910–1917).

The Megafaunal Xenophyophores

Earlier records of xenophyophores from within the CCZ and adjacent parts of the equatorial Pacific are summarized in Supplementary Table 3 in Gooday et al. (2017b). Gooday et al. (2020b) list the 24 described and 39 undescribed species reported from this region. Sampling sites are shown in **Figure 2a**. Xenophyophores from H.M.S. *Challenger* Station 270, located just to the south of APEI 4, and Stations 271, 272 and 274 to the south of the CCZ, were studied by Haeckel (1889), Schulze (1907a,b), and Tendal (1972). Fragments of *Aschemonella ramuliformis,* later shown to be a xenophyophore, were present in the sample from Station 272 (Brady, 1884), and two other *Challenger* stations (241, 244) in the NW Pacific to the east of Japan yielded species of *Stannophyllum.* Extensive Pacific collections were made during cruises in 1891, 1899, 1904, and 1905 of the American fisheries vessel *Albatross.* These included xenophyophores from sites located to the north, south and east of the CCZ (Goës, 1892; Schulze, 1907a,b; Tendal, 1972; Gooday et al., 2017b). More recently, Tendal (1980) described *Stannophyllum setosum* from a sample collected well within the CCZ (**Figure 2a**), Levin et al. (1986) and Levin and Thomas (1988) illustrated xenophyophores from seamounts located to the east and north of the CCZ (mostly from depths < 3000 m), Mullineaux (1987) and Veillette et al. (2007) reported undescribed species on polymetallic nodules from, respectively, the eastern and western CCZ, and Kamenskaya (2005) based the description of a new genus (*Spiculammina*) on material from the central CCZ. In the NW Pacific, a new species and genus, *Shinkaiya lindsayi,* was described by Lecroq et al. (2009c) from 5,435 m depth near the Japan Trench, and a new species, *Syringammina limosa,* was described by Voltski et al. (2018) from 3,351 to 3,366 m depth in the Sea of Okhotsk.

The latest and most intensive phase of xenophyophore research in the CCZ has been linked to mining-related baseline studies. This has resulted in the description of four new genera and 24 new species from the eastern (Gooday et al., 2017a,c, 2018a), central (Kamenskaya et al., 2015, 2017), and western (Gooday et al., 2020a) parts of the CCZ. Efforts to amplify DNA from xenophyophores collected in the eastern and western areas have had a high success rate (∼85% of extractions), a reflection of the multinucleate organization of these large foraminifera. As a result, sequence data have been obtained from 15 described and 10 undescribed species (Table 1 in Gooday et al., 2020b), more than for any other group of monothalamous foraminifera. At the same time, analyses of seafloor images have revealed xenophyophores to be a dominant component of the megafaunal assemblages across the CCZ nodule fields (Kamenskaya et al., 2013; Amon et al., 2016; Simon-Lledó et al., 2019a).

Other Foraminifera

The earliest record of benthic foraminifera in the deep Pacific Ocean is that of Ehrenberg (1861), who recorded a few species of "Polythalamien," together with a long list of radiolarians and diatoms, in two small sounding samples, one from 3,658 m and the other from 4,755 m to the north of the CCZ

(**Figure 1**). However, the first important study was based on material collected by H.M.S *Challenger*. She sailed south from Hawaii and sampled in a north to south direction along a line (approximately 150° W), crossing the western CCZ. The dredge sample from Challenger Station 265, one of eight (263-270) situated within the CCZ, was included in Brady's (1884) Challenger Report on the Foraminifera, together with samples from the more southerly stations 271, 272, 274. Picaglia (1892) listed planktonic and benthic species present in five samples from the equatorial Pacific (3647–4670 m depth), mainly to the west and east of the CCZ. *Albatross* samples were an important source of Pacific foraminifera and formed the basis for a number of papers and monographs. Goës (1896) worked on material collected in 1891 on the Californian, Mexican and Central American margins and the Galapagos region, to the south and east of the CCZ; the three deepest samples were from between 3,279 and 4,081 m. Flint (1899) included foraminifera from one North Pacific *Albatross* station deeper than 3,000 m in his "descriptive catalog" of foraminifera, the first work to illustrate foraminifera photographically. Bagg (1908) described species in *Albatross* samples collected down to 2,557 m around the Hawaiian Islands. Cushman's major monograph of North Pacific foraminifera, published in six parts between 1910 and 1917, was based on samples from the 1906 *Albatross* campaign obtained mainly from the NW Pacific, and those collected by the U.S.S. *Nero* during a 1899-1900 cable-laying survey west of Hawaii (Flint, 1905), together with a few other sources and literature records (Cushman, 1910–1917). Cushman's later monograph of foraminifera from the tropical Pacific (Cushman, 1932, 1933, 1942; completed by Todd, 1965) utilized samples from depths down to 4512 m in the South Pacific, as well as a few samples from deep-water sites (maximum depth 4,804 m) to the north and west of the CCZ. More recently, an unpublished thesis by Walch (1978) described "live" (stained) and dead foraminifera (>63-μm fraction) in box core subsamples from 5 sites located to the east and south of the CCZ (3189–4583 m). Other important papers on modern deep-sea foraminifera in areas more distant from the CCZ include those of CCZ include those of Smith (1973; transects running between the Aleutian Islands and the latitude of Hawaii), Resig (1981; SE Pacific), Schröder et al. (1988; CLIMAX II site north of Hawaii, material of Bernstein et al., 1978), Szarek et al. (2007; Sulu Sea), Enge et al. (2012; Station M on the Californian margin), and Shi et al. (2020; seamounts and abyssal plans in the tropical western Pacific).

It is remarkable that, apart from Challenger Stations 265 and 269, none of the early studies mentioned above includes sites within the CCZ. Saidova's (1975) monograph on Pacific foraminifera seems to be the first to include significant numbers of samples from this region. The bulk of her material came from the northeastern and particularly the northwestern margins, but some originated from more central parts of the North Pacific. Two transects crossed the western and central CCZ, although foraminiferal species were apparently not recorded by Saidova (1975) from all of the sites located between the two fracture zones. As in earlier Pacific studies, Saidova (1975) dealt mainly with "hard-shelled" multichambered taxa, both calcareous and agglutinated (mainly class Globothalamea). Appendix A (**Supplementary Material**) list 44 species and subspecies present at 12 of these stations within and immediately adjacent to the CCZ. Some have not been reported in the non-Russian foraminiferal literature. In other papers, Saidova (1965, 1976, 1981) compiled important syntheses of the geographical and bathymetric distribution of benthic foraminifera based on comprehensive species-level datasets from across the Pacific. These show large areas of the abyssal Pacific occupied entirely by agglutinated assemblages. Saidova (1974, 2000) also described different associations of foraminifera, related to seafloor topography within a 23 × 23 km area at the western end of the CCZ (Appendix B; **Supplementary Material**). A later Russian contribution (Burmistrova et al., 2007) summarizes the distribution of agglutinated species in samples from three areas, two in the central part of the CCZ (4918–4970 m depth) and the third to the east of the CCZ in the Guatemala Basin (3350–4040 m). Fifty of the 68 species listed are recorded from the two CCZ areas.

Renewed interest in seabed mining during the last two decades has generated an upsurge of research on benthic foraminifera within the CCZ (**Figures 2b,c**). The 1970s had seen the establishment of the Komokiacea and their recognition as an important component of the abyssal Pacific macrofauna (Tendal and Hessler, 1977), although this unusual group of what are presumed to be soft-bodied monothalamous foraminifera had been known to Russian scientists since the 1950s and a few were included in Saidova's (1975) monograph (summarized in Gooday et al., 2007). Most recent foraminiferal studies in the CCZ have included these and other delicate monothalamids. Kamenskaya et al. (2012) presented a survey of macrofauna-sized foraminifera (> 300 μm) from the IOM contract area. These included many komokiaceans, as well as chain-like forms, tube fragments, and other kinds of monothalamids. Meiofaunal assemblages (> 32 μm), again mainly monothalamids, were analyzed by Nozawa et al. (2006) from the Kaplan East site in the eastern CCZ, and Radziejewska et al. (2006) from the nearby IOM contract area. Ohkawara et al. (2009) described a particularly abundant new species of tiny agglutinated sphere that is very common at the Kaplan Central site. More recently, Goineau and Gooday (2017, 2019) and Gooday and Goineau (2019) have described highly diverse monothalamid-dominated assemblages (> 150 μm, > 63 μm fraction respectively) from the UK-1 and OMS areas, also in the eastern CCZ.

Nodule-Encrusting Foraminifera

Although the presence of foraminifera on nodules was noted briefly during the *Challenger* Expedition (Murray and Renard, 1891), they only attracted serious attention during the 1970s (e.g., Greenslate et al., 1974). The main initial studies of these novel faunas were those of Dugolinsky et al. (1977), based on samples from different parts of the Pacific including the CCZ, and Mullineaux (1987, 1988) who studied nodules from within (15°N, 125°W) and to the north (30°N, 125°W) of the CCZ (**Figure 2d**). Later, Veillette et al. (2007) conducted detailed studies of nodule assemblages in the two French contract areas located in the western and central CCZ, and Gooday et al. (2015) added a preliminary survey from the UK-1 contract area.

TABLE 1 | Distribution of samples from the CCZ used for published and unpublished foraminiferal studies.

Sampling site	MuC			EBS	Xenophyophores	Nodule fauna	eDNA/RNA
Sieve mesh (μm)	> 32	>150	> 250				
Eastern CCZ							
UK-1		Qt			Taxonomy[1]	Ql[4]	65/65[7]
OMS		Qt			Taxonomy[1]	Ql[4]	66/66[7]
BGR				Ql			43/28[7]
GSR				Ql			
IOM			Qt	Ql			
'ENP'						Ql[5]	
IFREMER (east)				Ql		Ql[6]	3/3[7]
Russian					Taxonomy[2]		
APEI-3				Ql			
APEI-6					Taxonomy[1]		
Kaplan East	Qt						
Kaplan Central	Qt						
Western CCZ							
IFREMER (west)						Ql[6]	
JET	Qt						
APEI-1					Taxonomy[3]		
APEI-4					Taxonomy[3]		
APEI-7					Taxonomy[3]		

[1]*Gooday et al. (2017a,b,c, 2018a).*
[2]*Kamenskaya et al. (2015, 2017).*
[3]*Gooday et al. (2020a,b).*
[4]*Gooday et al. (2015).*
[5]*Mullineaux (1987, 1988).*
[6]*Veillette et al. (2007).*
[7]*Lejzerowicz et al. (2021).*

Apart from the ENP (Equatorial North Pacific) site (Mullineaux, 1987, 1988), the two Kaplan sites (Smith et al., 2008) and the JET (Japan Deep-sea Impact Experiment) site, the sampling sites are either ISA contract areas or Areas of Particular Environmental Interest (APEIs). MuC = megacorer; EBS = epibenthic sledge; Qt = quantitative data; Ql = qualitative data. The right-hand column shows the numbers of sediment samples analyzed for eDNA and eRNA from different areas.

Other Data

In addition to published data, we have consulted a number of theses and unpublished datasets, mainly from the eastern CCZ (**Table 1**). Quantitative data (abundance, species richness etc.) for meiofaunal foraminifera are available from the Kaplan East (KE; Fusae Nozawa, 2005, M.Sc thesis) and Kaplan Central (KC; Nina Ohkawara, 2011, PhD thesis) sites, and for macrofaunal foraminifera (> 250 μm) from the IOM contract area (Zofia Stachowska, 2020, M.Sc thesis) (**Figure 2b**). Two undergraduate theses based on samples from the Japan Deep-Sea Impact Experiment (JET) site provide the only quantitative data from the western CCZ (Okamoto, 1998; Nozawa, 2003). Unpublished qualitative information (species occurrences) for macrofaunal foraminifera (>300 μm) come from epibenthic sledge samples obtained in the UK-1, OMS, IOM, German, Belgium, French and Russian contract areas and APEI-3 (Kamenskaya, unpublished; Wawrzyniak-Wydrowska, unpublished) (**Figure 2c**). Numerous qualitative observations on sessile foraminifera encrusting nodules from the OMS and UK-1 areas were made during cruises AB01 and AB02 of the ABYSSal baseLINE (ABYSSLINE) project (Gooday unpublished). Genetic data (SSU rRNA gene sequences) for some meiofaunal foraminiferal species were obtained from OMS and UK-1 samples (Voltski, Holzmann and Pawlowski, unpublished). Finally, samples for environmental DNA and RNA (eDNA/eRNA) metabarcoding were collected during the AB02 cruise, with additional samples being obtained from three parts of the BGR area (MANGAN cruise) and French area (BIONOD cruise, Apothéloz-Perret-Gentil, unpublished) (Lejzerowicz et al., 2021).

GENERAL OBSERVATIONS ON ABYSSAL PACIFIC ASSEMBLAGES

Smith et al. (1983) reported much lower Rose-Bengal-stained foraminiferal densities on central (5,755 to 5,904 m depth) and NE Pacific (4,392 to ∼4,800 m) abyssal plains than at shallower sites (1,300 and 3,815 m) on the Californian margin. Early studies also noted that foraminifera are very sparse in the deep North Pacific. Cushman (1910, p. 15 therein) found very few foraminifera ("practically nil") in "very deep water in red clay areas" sampled by the U.S.S. *Nero* during 1899 and 1900. More than half (51.5%) of the 466 Nero soundings between Midway atoll and Guam were deeper than 5,000 m (Flint, 1905). Cushman (1910) also concluded (p. 16) that, with a very few exceptions, "almost no" calcareous foraminifera were present at depths below 2,500 fathoms' (4,572 m) in the

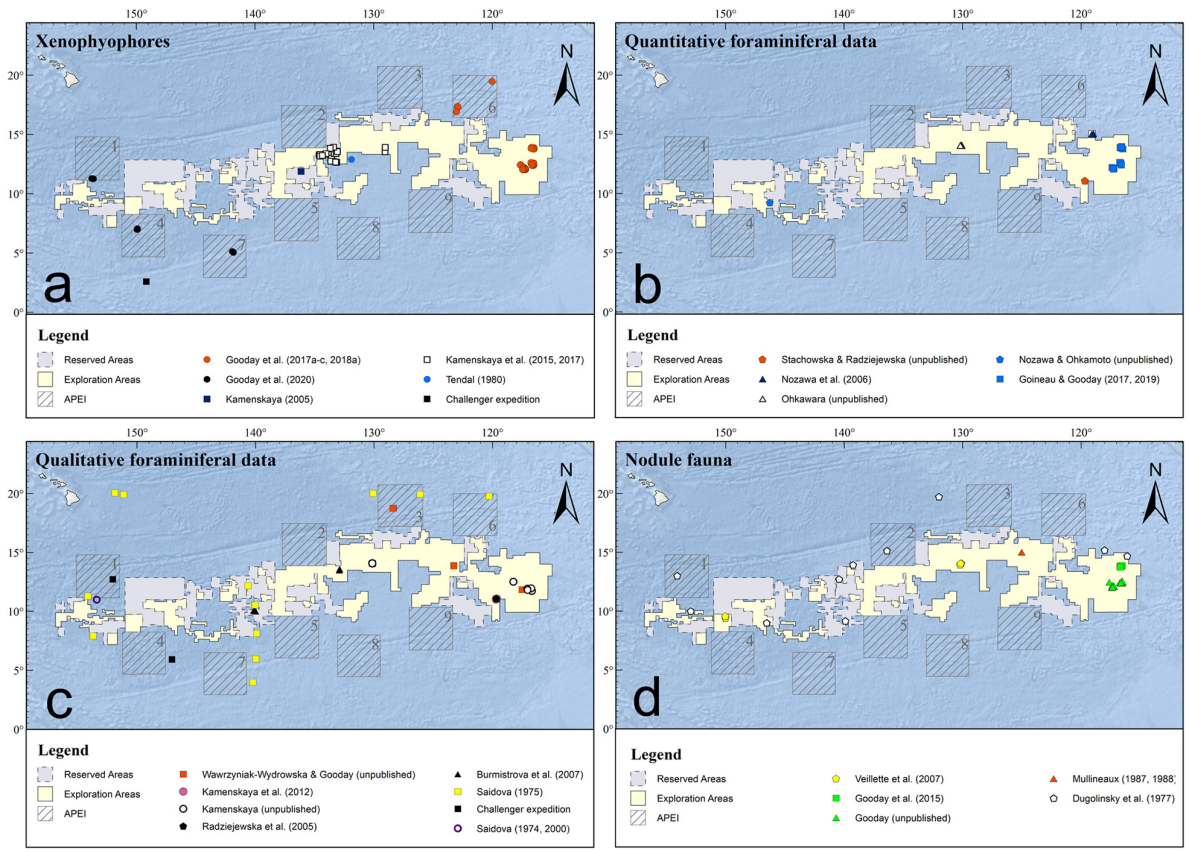

FIGURE 2 | Location of study sites within and in the vicinity of the Clarion-Clipperton Zone. **(a)** Xenophyophores. **(b)** Quantitative studies. **(c)** Qualitative studies. **(d)** Nodule-attached faunas.

North Pacific generally, although some agglutinated taxa were present. Similarly, Saidova (1966) found Pacific foraminiferal assemblages to be almost entirely agglutinated below 3,500–4,500 m depth. Maps based on her comprehensive dataset showed large areas of the central North and South Pacific, including much of the western CCZ, devoid of calcareous foraminifera (Saidova, 1976, 1981). Within the area (0°–20°N, 115°–155° W) that encompasses the CCZ, Figure 1 in Saidova (1965) shows calcareous benthic foraminifera confined to the southeastern part. This reflects the influence of the carbonate compensation depth (CCD), below which calcareous foraminifera cannot easily maintain their tests in a corrosive environment. The CCD is situated around 4,500 m depth in the southern North Pacific, deepening to ∼5,000 m near the equator (Lisitzin, 1996). The shallower eastern end of the CCZ, where calcareous foraminifera are a minor but consistent faunal component (Goineau and Gooday, 2017, 2019), is located somewhat above the CCD. At the western end, Brady (1884) found no calcareous foraminifera, apart from 2–3 miliolids and a few globigerinids, in reddish-brown siliceous mud at *Challenger* Station 265, located at 5,304 m depth, well below the CCD just to the east of the area now covered by APEI-1. He reports miliolids from stations deeper than 5000 m elsewhere in the North Pacific, but their calcareous shells were either completely dissolved (*Challenger* Station 238; 7,224 m) or very thin (*Challenger* Stations 245 and 253; 5,073 m and 5,715 m, respectively). Other calcareous taxa (rotaliids and lageniids) were present at shallower Challenger stations (241, 242, 271, 272, 276; 4,206–4,758 m) in the Pacific (Brady, 1884). Saidova (1974) reports that 80–90% of benthic foraminiferal tests in sediments containing 10–23% carbonate on the crests of hills at 4,780–4,790 m depth at the western end of the CCZ (**Figure 2b**) were calcareous. Elsewhere in the North Pacific, "live" (stained) calcareous foraminifera are found occasionally at depths as great as 6,560 m and 7,230 m (Smith, 1973).

BIODIVERSITY AND ASSEMBLAGE COMPOSITION

Morphological Data

Recent studies have shown foraminifera to be much more abundant and diverse in the CCZ than earlier data suggested. Eleven megacorer samples (0–1 cm layer, >150-μm size fraction) from three 30 × 30 km "strata" in the eastern CCZ, two in the UK-1 contract area and one in the OMS area, yielded a grand total of 580 meiofauna-sized morphospecies,

including live and dead tests and fragments (Goineau and Gooday, 2019). Between 310 and 411 species were found in particular strata and 132–228 in individual cores or core splits (**Table 2**). The combined dataset included a few relatively common (>100 specimens) morphospecies but the majority were uncommon and 29% were represented by singletons (**Supplementary Figure 1**), a pattern that is typical for the deep sea (Rex and Etter, 2010; McClain, 2021), including for benthic foraminifera (Douglas and Woodruff, 1981). Species were still being added after 11 samples (**Figure 3**), and rarefaction curves for individual cores did not reach an asymptote (**Supplementary Figure 2**), suggesting that the total number of species (>150 μm) was higher. Estimates ranged from 690 (abundance-based estimator ACE) to 877 (incidence-based estimator Jacknife 2) (Goineau and Gooday, 2019). A subset of 5 samples sieved on a 63-μm mesh yielded 462 morphospecies, of which 170 were absent in the >150-μm fractions (Gooday and Goineau, 2019). The number in individual cores ranged from 133 to 209 (**Table 2**). Finally, 158–252 morphospecies were recognized in the fine fractions (all foraminifera larger than 32 μm) of small subsamples from megacores taken at the Kaplan East (KE), Kaplan Central (KC) and JET sites. Between 18 and 100 were picked from single subcores (**Table 2**).

TABLE 2 | Species richness in core samples from the CCZ.

	Sieve mesh size	Cores (subcores)	Layer (cm)	Sample split	Species							References
					Live	Dead	Live frags	Dead frags	Total	Total per core/subcore	% Mono	
UK-1A	150 μm	5	0–1	8/8, 3/8	340	149	87	58	411	140–228	75.9	Goineau and Gooday, 2019
UK-1B	150 μm	3	0–1	4/8	224	138	55	51	324	132–197	75.6	Goineau and Gooday, 2019
OMS	150 μm	3	0–1	7/8,3/8	218	148	59	67	310	150–195	69.4	Goineau and Gooday, 2019
UK-1/OMS	63 μm	5	0–1	1/8	271	215	82	84	462	133–209	75.3	Gooday and Goineau, 2019
Kaplan E	32 μm	3(7)	0–1	–	168	–	84	–	252	66–100	75.6	Nozawa et al., 2006
Kaplan C	32 μm	1(2)	0–0.5	–	109	–	49	–	158	44, 84	88.6	Ohkawara, 2006
Kaplan C	32 μm	2(6)	0–1	–	202	–	–	–	208	51–70	83.7	Ohkawara, 2011
JET	32 μm	9(9)	0–3	–	179	–	33	–	196	18–87	80.6	Nozawa, 2003

The UK-1 and OMS data are from the 0–1 cm layer of complete megacores (10-cm internal diameter tubes; surface area 78.5 cm^2) or megacore splits. The Kaplan and JET data are from subcores taken with a cut-off 50-ml syringe (surface area 6.6 cm^2). The majority of species (particularly monothalamids) were either obviously undescribed, or could not be easily assigned to a described species.

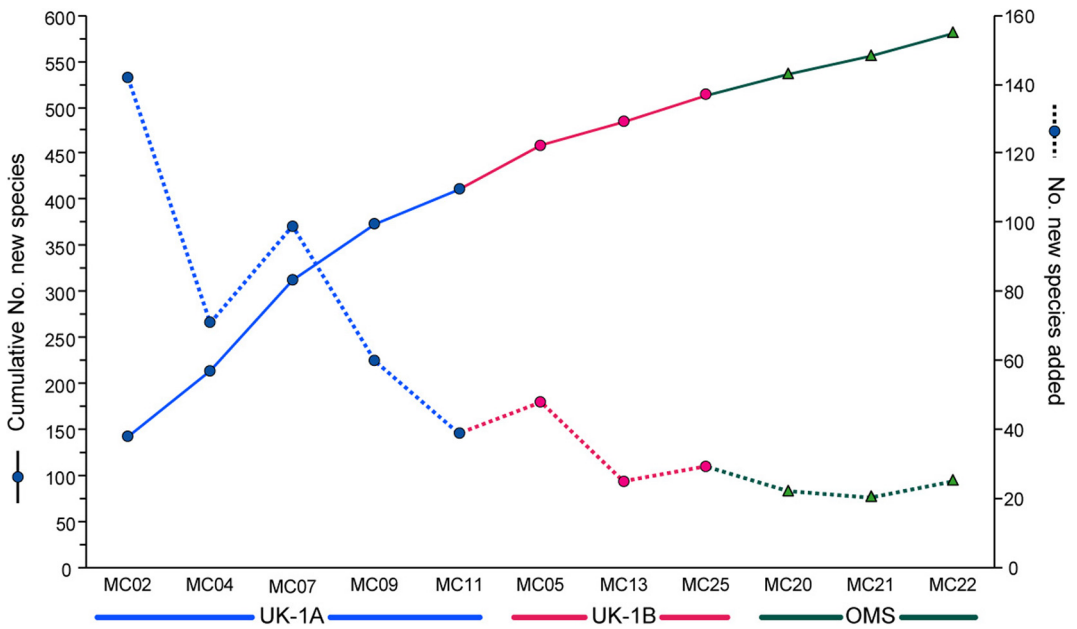

FIGURE 3 | Species accumulation curve (solid line; left-hand axis) showing the increase in the number of species with the addition of new samples from Strata A and B in the UK-1 contract area and the single Stratum in the OMS area (the 'strata' are 30 × 30 km study areas). The dotted line shows the number of new species added with each new sample (right-hand axis). Redrawn from Deep-Sea Research I, vol. 149, A. Goineau and A.J. Gooday, Diversity and spatial patterns of foraminiferal assemblages in the eastern Clarion–Clipperton zone (abyssal eastern equatorial Pacific), Article 103036, 2019, with permission from Elsevier.

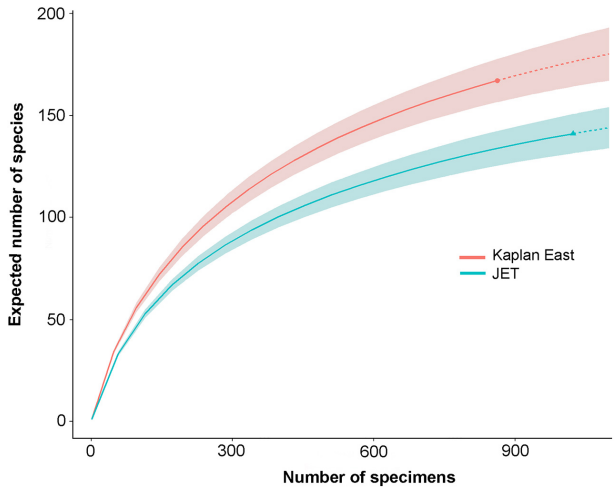

FIGURE 4 | Rarefaction curves with 95% confidence limits for foraminifera from the Kaplan East (~15°N, 119°W; ~4100 m depth) and JET (09° 14′ N, 146° 15′ W; 5300 m depth) sites. The curves are based on data from the 0-1 cm layer of subsamples (6.6 cm^2 surface area) of megacores, sieved on a 32-μm screen (Nozawa, 2003, 2005).

Monothalamids are always a dominant element of these meiofauna-sized assemblages, accounting for ~75% of species in the two UK-1 strata and the nearby KE site, and almost 70% in the OMS stratum, irrespective of the size fraction analyzed (**Table 2**). They contribute an even higher proportion of species (>80%) in the fine fractions (larger than 32 μm) at the KC and JET sites. Most other complete foraminiferal tests in these samples belong to multichambered agglutinated taxa. The inclusion of this important monothalamid component is the main difference between these recent and earlier foraminiferal studies in the Pacific.

The comparison of data across wider areas of the CCZ is hampered by inconsistencies in the sizes and methods used to analyze the samples (notably sieve mesh sizes) (**Table 2**), as well as the research bias toward the eastern CCZ (Washburn et al., 2021). The only quantitative samples that can be compared directly are those obtained at the KE (4000 m, eastern CCZ) and JET (5300 m, western CCZ) sites, which were analyzed by the same person using the same methods (Nozawa, 2003, 2005; **Table 2**). At the JET site, a total of 179 species (mean 46.1 ± 20.5 per subcore) was recognized among 1,702 specimens (excluding fragments) compared to 168 species among 983 specimens (mean 53.4 ± 9.36 per sample) at the KE site. The rarefied species richness is slightly higher at KE than at JET (**Figure 4**).

Macrofauna-sized (> 300 μm) monothalamids are very common in qualitative epibenthic sledge residues from the CCZ. Samples from five sites in the eastern CCZ (German, IOM, Belgium, French contract areas and APEI-3), sorted by the same people using consistent methods, yielded 224 monothalamid morphospecies (Wawrzyniak-Wydrowska and Gooday, unpublished). At least 30 additional forms have been recognized in samples analyzed by Kamenskaya (unpublished) from the French, German and Russian areas. Nine megacorer samples (> 250-μm fraction) from the IOM area have also yielded diverse foraminiferal assemblages, comprising more than 220 morphospecies, of which 78% are monothalamids (Stachowska, unpublished).

The eastern equatorial Pacific is notable for hosting diverse assemblages of megafaunal xenophyophores (Schulze, 1907a; Tendal, 1996; Gooday et al., 2017b). In total, 35 described species (>40% of the global total) have been reported from this region, of which 24 occur in the CCZ, where an additional 39 species have been recognized but not formally described (Gooday et al., 2020b). Most (52) of these 63 described and undescribed species have been found only in the eastern CCZ (i.e., east of 140° W), 8 only in the western CCZ, while three (*Aschemonella monilis, Moanammina semicircularis,* and *Stannophyllum zonarium*) span both sectors. Many xenophyophores species live attached to polymetallic nodules, suggesting that nodule occurrence may be a key driver of their diversity. However, since xenophyophores can colonize soft as well as hard substrates, the potential role of nodules in this respect has yet to be tested.

Other kinds of sessile foraminifera are also common on nodules (**Table 3**). Two early studies reported 28 (Dugolinsky et al., 1977) and 46 (Mullineaux, 1987, 1988) morphospecies from the CCZ and nearby areas (**Figure 2d**). In the eastern and western French contract areas, Veillette et al. (2007) distinguished 68 species attached to nodules, with a further 5 loosely associated species. In the UK-1 area seven nodules yielded a total of 75 attached species, with another eleven recognized during shipboard observations (Gooday et al., 2015). Further studies of nodule-attached foraminifera from the OMS area, as well as UK-1 area, would certainly increase this number further.

Based on these limited morphological analyses from a relatively small number of study sites, we estimate that the total number of foraminiferal morphospecies across all size fractions and substrates could easily exceed 1,000. Samples from sites in other parts of the CCZ will probably yield additional species. In the western CCZ, Saidova (1974, 2000) reported species-level variations in foraminiferal assemblages at a 10-km scale, particularly in relation to topographic features (abyssal hills). Heterogeneity of this kind would undoubtedly inflate species numbers further.

Environmental DNA and RNA Metabarcoding Data

Metabarcoding studies based on samples from the UK-1, OMS, BGR and eastern French (IFREMER) contract areas (Lejzerowicz et al., 2021), as well as previous studies in other regions (Lecroq et al., 2011; Lejzerowicz et al., 2014; Shi et al., 2020), provide further evidence that deep-sea foraminifera are highly diverse and include a substantial proportion of monothalamids. The Operational Taxonomic Units (OTUs) recognized in the CCZ encompass most of the existing monothalamid clades, some known only from environmental samples (Lejzerowicz et al., 2021). Environmental DNA (eDNA) and RNA (eRNA) was extracted from 166 sediment samples collected according to a nested design in four areas. Only 3 samples were processed for the French site, which is situated in the more central

TABLE 3 | Number of foraminiferal morphospecies associated with nodules within, and to the north of the CCZ.

Study area	Position	Depth (m)	Nodules	Morphospecies	References
UK-1 contract area	13° 50'N, 116° 37'W	4053–4160	7	75	Gooday et al., 2015
French area: East site A	14°N, 130°W	4955	15	47	Veillette et al., 2007
French area: East site B	14°N, 130°W	4974–5036	50	63	Veillette et al., 2007
French area: East site C	14°N, 130°W	4904–4954	39	66	Veillette et al., 2007
French area: West site	14°N, 130°W	5043–5059	131	63	Veillette et al., 2007
CCZ	15°N, 125°W	4500	65	46	Mullineaux, 1987
Central N. Pacific	30°N, 157°W	5800	64	25	Mullineaux, 1987
NE. eq. Pacific	02° 50'–19° 42'N, 116° 05'–154° 05'W	4500–5200	?	28	Dugolinsky et al., 1977

At the French East site, A, B, and C refer to nodule facies, differentiated by the shape, size and surface morphology of the nodules and their degree of burial in the sediment (Veillette et al., 2007).

part of the CCZ. Hence, the scope of the eDNA analyses is currently limited to faunal patterns in the UK-1 and OMS regions, which are relatively homogeneous in terms of nodule abundance and POC flux.

The processing of foraminiferal metabarcoding data was tailored for quality by using PCR replicates, cross-contamination filtering, four sequence assignment methods and compositional data analyses (Lejzerowicz et al., 2021). The eDNA and eRNA sequences clustered into 6,425 OTUs, including 21.7% assigned to the Monothalamea and 3.7% assigned to the multichambered Globothalamea (**Figure 5**). On average, the number of monothalamid OTUs obtained from samples at each site was 7.2 (± 3 standard deviation) times the number assigned to the Globothalamea. For both groups, the UK-1 and OMS areas yielded significantly higher richness than the well-sampled BGR South area (MANGAN16 cruise) (72 samples, **Figure 5**), and this is also true after normalizing sequencing read depths with rarefaction [Figure 6 in Lejzerowicz et al. (2021)]. Nevertheless, the majority of OTUs remained unassigned at lower taxonomic levels, suggesting that the foraminiferal genetic diversity in the CCZ is largely unknown and more effort is needed to complete the reference database necessary to assign the foraminiferal metabarcodes.

We first identified localized OTUs that occurred in only one of the CCZ areas, and then investigated those area-specific OTUs that a) also occurred at only one station per area and/or b) in only one sediment core per station (**Table 4**). More than half (3457 = 53.8%) of the 6,425 OTUs met the first criterion. In the OMS and UK-1 areas, a large majority (82.0% and 84.9%, respectively) of these area-specific OTUs do tend to occur at only one station; this proportion approaches 100% for BGR- and IFREMER-specific OTUs. Since OTUs associated with very few sequence reads are necessarily rare and strongly contribute to localized occurrences, we also determined these single-station and single-core occurrences for the 685 OTUs (19.8% of the localized OTUs and 10.7% of all OTUs) that include at least 1% of the total read count for each sample (**Table 5**). This reveals that even these more highly-sequenced OTUs tend to be found locally. This is notably the case for 2 and 4 OTUs assigned to Textulariida and 2 and 5 assigned to the Rotaliida in the OMS and UK1 areas, respectively. Some of these were genus- or species-level assignments (*Pullenia subcarinata, Cibicidoides wuellerstorfi, Eggerella* sp., and *Reophax* sp.). Even more striking is the fact that a large majority of these highly-sequenced OTUs are also found in one of the two sediment cores taken at each station (100% in column D of **Table 5**), suggesting a higher degree of local patchiness.

FAUNAL TRENDS AND SPECIES DISTRIBUTIONS ACROSS THE CCZ

Overall Trends

Across the CCZ, latitudinal and longitudinal gradients in surface productivity and food flux to the seafloor (Smith et al., 2019), together with the east to west increase in water depth and carbonate dissolution, are likely to influence faunal composition and therefore species ranges. The scarcity of data from the western CCZ means that longitudinal trends in foraminiferal assemblage composition are not well known. Saidova (1981) recognized a number of assemblages on Pacific abyssal plains that were linked partly to productivity. In the southern part of the CCZ, a *Cribrostomoides profundum* assemblage in the east gives way to a *Recurvoidatus spiculotestus* assemblage in the west, while the northern part is occupied by a *Rhabdammina inordita* assemblage. Our only across-CCZ data based on consistent sieve fractions (> 32 μm) come from three Japanese studies at the Kaplan East (KE), Kaplan Central (KC) and Japan Deep-Sea Impact Experiment (JET) sites, a total east to west distance of more than 3,000 km (**Table 6**). These reveal similar proportions of major groups. Monothalamids (which we interpret to include *Lagenammina* species and *Nodellum*-like forms) are dominant, particularly at the KE and KC sites (>80%). If monothalamids are excluded, then the main groups are hormosinids, and at the JET site, other textulariids. Calcareous rotaliids, which might be expected to be less common in the deeper and less productive western CCZ, represent the highest proportion (22%) of the monothalamid-free assemblages at the KC site, and the lowest proportion (8.2%) at the JET site. However, they are relatively more important at the JET (8.53%) compared to the KC and KE (4.54 and 4.29%, respectively) sites when all foraminiferal groups are included. Rotaliids persist at depths below the CCD, despite the fact that their tests are often dissolved, presumably as a result of carbonate dissolution on the seafloor.

At smaller spatial scales, all samples from UK-1 and OMS fall within 95% confidence limits in MDS plots (data not shown), indicating a high degree of assemblage uniformity at the contract-area scale (Goineau and Gooday, 2019). A decay-distance analysis based on Bray-Curtis similarity vs distance showed only minor differences in the species composition of UK-1 and OMS samples separated by increasing distances of up to ∼220 km (**Figure 6**). However, there was a general tendency for differences in species composition to increase with distance, and this overall trend was significant (p = 0.006). Thus, although particular morphospecies may have wide ranges, there seem to be gradual shifts in the species composition of foraminiferal assemblages in relation to environmental gradients within the CCZ.

Species Distributions

Relatively little is known about species ranges across the CCZ. Saidova (1974, 2000) provides some information on species found at R/V *Vityaz* Station 5996, located at the western extremity of the CCZ (153–154° W; **Figure 2c**, Appendices A and B in **Supplementary Material**). Although different names are sometimes used in Russian and non-Russian literature, a number of species reported by Saidova from this western site are probably the same as those found in the eastern CCZ (Goineau and Gooday, 2017, 2019). They include *Adercotryma glomeratum, Cyclammina trullissata* [= *Cyclammina. subtrullissata* (Parr, 1950) of Saidova, 1975], *Globocassidulina subglobosa* [= *Bradynella subglobosa*] and *Nuttallides umbonatus* [likely = *Osangulariella bradyi*]. Some meiofauna-sized monothalamid morphospecies that span similar distances within the CCZ (146°–150° W to ∼116°–117° W) are illustrated in **Figure 7**.

Five of the macrofaunal komokiacean morphospecies from epibenthic sledge samples taken in the German, IOM, Belgium, French, and APEI-3 areas (Wawrzyniak-Wydrowska and Gooday, unpublished) were originally described, either from the central North Pacific (30°N,

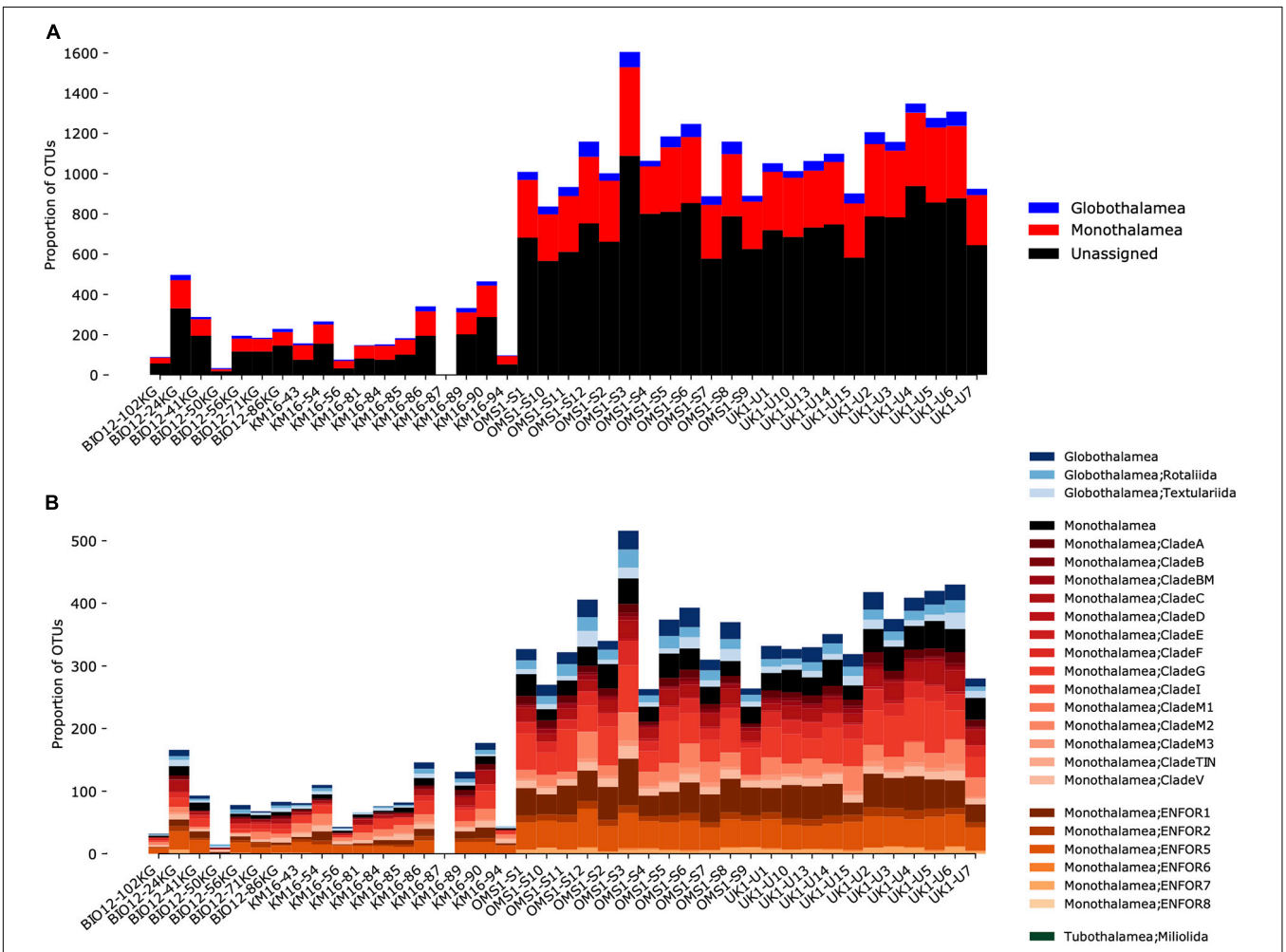

FIGURE 5 | Taxonomic composition of the OTUs found in samples from CCZ sites. The top panel includes the unassigned OTUs **(A)**, which are absent in the bottom panel where only OTUs that were assigned to Globothalamea, Tubulothalamea, and Monothalamea are shown, at a finer taxonomic level **(B)**; note the high diversity of monothalamid clades.

TABLE 4 | Number of OTUs that are confined to one CCZ area, station or single core. Data are arranged according to foraminiferal orders or clades and include only OTUs that are confined to the CCZ. **A** = number of OTUs found only in this area; **B** = total number of OTUs in the full dataset; **C** = percent of 'A' found at only one station; **D** = percent of 'A' found in only one core from this station. Note that a dash in column D indicates that only one core was sampled for metabarcoding. Two cores per station were always sampled in the OMS and UK-1 areas, but only one core was sampled per station in the IFREMER area and at some of the BGR stations.

Class	Order/Clade	BGR				IFREMER				OMS				UK-1			
		A	B	C%	D%	A	B	C%	D%	A	B	C%	D%	A	B	C%	D%
Unassigned		198	988	93.4	60.6	89	274	94.4	–	1331	3272	83.7	95.0	1096	3058	81.5	97.4
Globothalamea	Unassigned	7	30	100	85.7	1	7	100	–	18	67	72	94.4	24	70	91.7	100
	Rotaliida	3	21	100	66.7	0	0	0	0	17	60	76.5	82.4	12	50	91.7	100
	Textulariida	1	16	100	–	1	7	100	–	20	51	90.0	100	9	41	77.8	100
Tubulothalamea	Miliolida	0	0	0	0	0	0	0	0	0	0	0	0	2	2	100	100
Monothalamea	Unassigned	4	38	100	50.0	2	11	100	–	18	75	72.2	94.4	32	88	75.0	96.9
	Clade A	6	22	83.3	100	2	4	100	–	9	39	88.9	100	10	42	70.0	100
	Clade B	2	9	100	–	0	0	0	0	3	16	100	66.7	7	18	100	100
	Clade BM	0	0	0	0	0	0	0	0	0	0	0	0	3	15	100	100
	Clade C	22	58	77.3	86.4	0	0	0	0	41	95	80.5	78	48	103	81.2	100
	Clade D	1	4	100	100	0	0	0	0	0	0	0	0	2	10	100	50.0
	Clade E	0	0	0	0	0	0	0	0	0	0	0	0	1	1	100	100
	Clade F	1	24	100	100	9	20	100	–	15	70	66.7	80.0	15	72	93.3	93.3
	Clade G	10	87	100	70.0	2	12	100	–	63	193	81.0	90.5	69	205	71.0	100
	Clade I	0	0	0	0	0	0	0	0	0	0	0	0	2	2	50.0	100
	Clade M1	0	0	0	0	0	0	0	0	0	0	0	0	0	0	0	0
	Clade M2	8	50	100	87.5	1	17	100	0	15	86	73.3	93.3	19	92	68.4	100
	Clade M3	0	0	0	0	0	0	0	0	2	15	50.0	50.0	4	17	100	100
	Clade TIN	1	2	100	–	0	0	0	0	1	4	100	100	0	0	0	0
	Clade V	1	19	100	100	0	0	0	0	5	29	80.0	80.0	6	31	100	100
	ENFOR 1	5	52	100	80.0	1	4	100	–	45	161	80.0	84.4	38	157	78.9	97.4
	ENFOR 2	2	14	100	100	1	8	100	–	4	24	75.0	100	6	26	50.0	83.3
	ENFOR 5	1	38	100	–	3	19	100	–	21	101	71.4	100	19	98	89.5	94.7
	ENFOR 6	0	0	0	0	0	0	0	0	1	3	100	100	0	0	0	0
	ENFOR 7	0	0	0	0	0	0	0	0	3	24	100	100	6	27	100	100
	ENFOR 8	0	0	0	0	0	0	0	0	0	0	0	0	0	0	0	0
	Mono._X	0	0	0	0	1	2	100	–	3	17	100	66.7	6	20	83.3	100

156°W; 6070 m depth) (Tendal and Hessler, 1977) or the North Atlantic (Shires et al., 1994), indicating wide distributions. Similarly, some of the nodule-encrusting macrofaunal morphospecies in the UK-1 and OMS areas (Gooday et al., 2015; unpublished data) are also reported from the eastern and western CCZ sites of Veillette et al. (2007). These include two species of the komokiacean genus *Chrondrodapsis,* originally described from within the CCZ (15°N, 125°W) (Mullineaux, 1988). Delicate net-like formations assigned to the genus *Telammina* have been found growing on firm substrates in the CCZ and North Atlantic (Gooday et al., 2015), as well as the Indian Ocean (Figure 6D in Aranda da Silva and Gooday, 2009). However, there are no reliable genetic data for any komokiaceans or indeed for any nodule-encrusting species.

Previous studies have provided a wealth of information on the distribution of foraminiferal morphospecies, mainly hard-shelled, at abyssal depths in the wider Pacific Ocean. **Table 7** summarizes Pacific records for meiofauna-sized species, most of them with easily recognizable multichambered tests, recorded by Goineau and Gooday (2017, 2019) from the eastern CCZ. They all have wide geographical ranges at abyssal depths in the Pacific. There are also records of many of these species in other oceans, and some are considered to have "cosmopolitan" distributions (e.g., Holbourn et al., 2013).

Genetic studies (SSU rRNA sequences) provide some support for wide ranges. Those of two rotaliids, *Cibicidoides wuellerstorfi* and *Epistominella exigua,* span 17,000 km from the Arctic to the Southern Ocean (Pawlowski et al., 2007), extending into the NW Pacific in the case of *E. exigua* (Lecroq et al., 2009b) and the NE Pacific in the case of *C. wuellerstorfi* (Burkett et al., 2020). Sequences derived from *E. exigua* specimens collected in the UK-1 and OMS contract areas during the ABYSSLINE project were identical to those of Pawlowski et al. (2007) and Lecroq et al. (2009b) from the NW Pacific and other oceans. A SW Atlantic specimen of *Nuttallides umbonatus* was genetically identical to several from the UK-1 and OMS areas, where this is the most common rotaliid species. The greater degree of genetic differentiation reported in Arctic and Antarctic populations of other rotaliid species, *Oridorsalis umbonatus* (Pawlowski et al., 2007), however, suggests that some "cosmopolitan" morphospecies, particularly those found

across a wide depth range, may encompass a number of cryptic species.

Many xenophyophores species (described and undescribed) are represented in the CCZ by 1-2 specimens and are known from a single site, so nothing can be said about their wider distributions (Gooday et al., 2020b). *Psammina limbata,* described morphologically from the Russian area in the central CCZ (Kamenskaya et al., 2015), may also be present in the UK-1 and OMS areas, although without genetic data from Russian specimens this cannot be confirmed (Gooday et al., 2018a). However, wide ranges across a distance of 3,800 km (from APEI-4 to UK-1/OMS sites) have been confirmed genetically for two xenophyophore species (Gooday et al., 2020a). One of these (*Moanammina semicircularis*) is illustrated in **Figure 7I,J**. The other, *Aschemonella monilis,* is known from the Russian area (Gooday et al., 2017a) and APEI-6 (Simon-Lledó et al., 2019a), in addition to UK-1, OMS and APEI-4.

Undersampling, Patchiness and Rarity

Biogeographic patterns, including endemism, can be discerned with some confidence among benthic foraminiferal species living in coastal and shelf environments (Culver and Buzas, 1999; Murray, 2013; Hayward et al., 2021). However, limited sampling, combined with small-scale faunal patchiness, makes establishing geographical ranges and recognizing species with restricted distributions a much more difficult task in the deep ocean. The problem is compounded, particularly in the abyss, by the vast extent of the environment and the apparent rarity of many species. Around 60% of the 547 unfragmented species (> 150-μm fraction) in UK-1 and OMS samples are found at only 1 or 2 out of 11 sites but are represented by a relatively small proportion (16.7%) of specimens (**Figure 8**). Many species confined to one site are singletons. On the other hand, the few species (4.2%) that are recorded across 10 or 11 sites account for a relatively large proportion (35.9%) of specimens. Similarly, > 80% of macrofaunal foraminiferal species in epibenthic sledge samples from the Belgian, German, IOM, and French areas and APEI-3 are confined to one area, and 74% are confined to one of the 2 replicate samples analyzed from each area (Wawrzyniak-Wydrowska and Gooday, unpublished). The metabarcoding data summarized above (**Table 4**) also indicate that many OTUs are confined to one station and in some cases to

TABLE 5 | Number of OTUs that are confined to one CCZ area, station or single core. Data are arranged according to foraminiferal orders or clades and include only OTUs that are specific to CCZ areas and present in samples with >1% of sequence reads. **A** = number of OTUs found only in this area. **B** = total number of OTUs in the full dataset. **C** = percent of 'A' found at only one station. **D** = percent of 'A' found in only one core from this station. Note that a dash in column D indicates that only one core was sampled for metabarcoding. Two cores per station were always sampled in the OMS and UK-1 areas, but only one core was sampled per station in the IFREMER area and at some of the BGR stations.

Class	Order/Clade	BGR				IFREMER				OMS				UK-1			
		A	B	C%	D%	A	B	C%	D%	A	B	C%	D%	A	B	C%	D%
Unassigned		66	988	89.4	83.3	23	274	100	–	196	3272	85.7	97.4	218	3058	87.2	98.6
Globothalamea	Unassigned	2	30	50	100					3	67	100	100	4	70	75.0	100
	Rotaliida									2	60	50.0	100	5	50	80.0	100
	Textulariida									2	51	100	100	4	41	100	100
Tubulothalamea	Miliolida																
Monothalamea	Unassigned	2	38	100	50.0					8	75	87.5	100	4	88	25.0	100
	Clade A	1	22	0	100					3	39	100	100	2	42	100	100
	Clade B													1	18	100	100
	Clade BM													1	15	100	100
	Clade C	4	58	100	75.0					10	95	70.0	80.0	8	103	75.0	100
	Clade D																
	Clade E																
	Clade F									2	70	50.0	100	1	72	100	100
	Clade G	10	87	100	60.0					22	193	90.0	90.9	29	205	79.3	100
	Clade I																
	Clade M1																
	Clade M2	1	50	100	–												
	Clade V	2	19	50.0	100					2	29	100	100	1	31	0	100
	ENFOR 1	2	52	100	100					9	161	88.9	88.9	19	157	94.7	100
	ENFOR 2	1	14	100	100	1	8	100	–					1	26	0	100
	ENFOR 5	1	38	100	100					7	101	100	100	3	98	66.7	100
	ENFOR 6																
	ENFOR 7																
	ENFOR 8																
	Monoth._X													2	20	50.0	100

TABLE 6 | Proportions of major foraminiferal groupings in > 32-μm fraction of subsamples (0-1 cm layer) from Kaplan East (KE), Kaplan Central (KC) and JET sites.

	KE		KC		JET	
	N	%	N	%	N	%
Including monothalamids						
Hormosinids	98	*2.24*	334	*5.16*	95	*10.39*
Other textulariids	47	*1.07*	93	*1.44*	93	*10.18*
Rotaliids	27	*0.62*	125	*1.93*	17	*1.86*
Miliolids	2	*0.05*	12	*0.19*	0	*0*
Ammodiscus	1	*0.02*	2	*0.03*	2	*0.219*
Nodellum-like	150	*3.42*	271	*4.19*	49	*5.361*
Lagenammina	188	*4.29*	294	*4.54*	78	*8.534*
Monothalamids	3871	*88.3*	5345	*82.6*	580	*63.46*
Total numbers	4384		6470		914	
Excluding monothalamids						
Hormosinids	98	*56.0*	334	*59.0*	95	*45.9*
Other textulariids	47	*26.9*	93	*16.3*	93	*44.9*
Rotaliids	27	*15.4*	125	*22.1*	17	*8.21*
Miliolids	2	*1.14*	12	*2.12*	0	*0*
Ammodiscus	1	*0.57*	2	*0.35*	2	*0.97*
Total numbers	127		566		207	

Data are from Nozawa et al. (2006; KE), Nozawa (2003; JET), Ohkawara (2011; KC). The monothalamids from the KE and KC sites include a large proportion of tiny spheres. The most common form at the KC site was described as Saccammina minimus by Ohkawara et al. (2009), but others from both Kaplan sites could not be easily differentiated into species (Nozawa et al., 2006; Ohkawara et al., 2009).

one core. These OTUs are often rare (represented by few reads) and this, together with patchiness and under-sampling, most likely accounts for their localized occurrence. A minority of OTUs found only at one station or in one core are represented by > 1% of reads (**Table 5**) and therefore are not particularly rare. In these cases, under-sampling and a patchy distribution could still explain why they are only found in one place. The unique sequences that are combined to create OTUs may exhibit even more localized spatial distributions. These morphological andmetabarcoding studies highlight the likely prevalence of 'pseudo-endemism' and the need for more sampling.

Broad biogeographic patterns undoubtedly exist across the Pacific abyss. Several abyssal benthic provinces have been proposed for this ocean, most recently by Watling et al. (2013), while Saidova (1981) recognized a series of foraminiferal communities on Pacific abyssal plains related to surface productivity, combined with carbonate dissolution and bottom-water currents. Recent, metagenomic studies have revealed high number of OTUs that are confined to the CCZ (Lejzerowicz et al., 2021). However, whether some foraminiferal species are confined to smaller areas of the Pacific, including parts of the CCZ, and occur nowhere else in the global ocean, is difficult to establish. At present, it is not possible to distinguish strictly endemic distributions of this kind from artifacts resulting from rarity combined with under-sampling (i.e., 'pseudo-endemism'). It is worth noting that the ability of foraminiferal species to reproduce asexually may allow them to persist at very low population densities (Murray, 2013) over large, oligotrophic areas of the deep sea, without the need for propagules to be introduced from more productive areas, as postulated for some metazoan

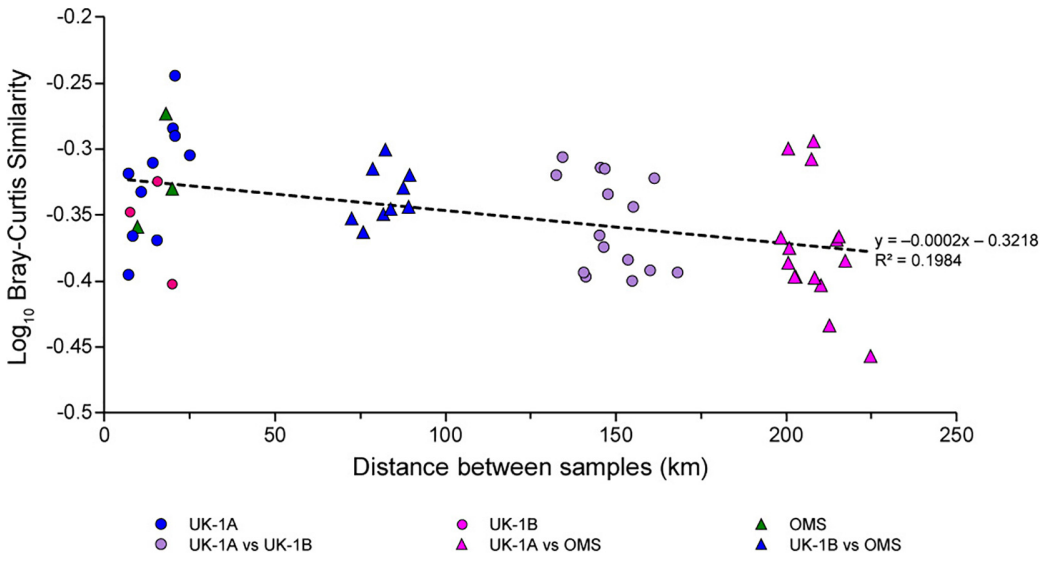

FIGURE 6 | Similarity between samples compared across increasing distances in the UK-1 and OMS contract areas. Based on Bray-Curtis similarity indices computed with species presence-absence data. The cluster of symbols at the left-hand side refers to comparisons of samples within each of the 30 × 30 km 'strata' (UK-1A, UK-1B, and OMS; 5, 3, and 3 samples, respectively); the other clusters refer to comparisons between these three strata. Similarity values within and between strata are significantly different (*t*-test, $p = 0.012$) only when the two most widely spaced strata, UK-1A and OMS, are compared (cluster of purple triangles on right-hand side). However, the overall trend indicated by the dotted line is significant (Spearman's rank correlation, rs = 0.373, $p = 0.006$). Redrawn from Deep-Sea Research I, vol. 149, A. Goineau and A.J. Gooday, Diversity and spatial patterns of foraminiferal assemblages in the eastern Clarion–Clipperton zone (abyssal eastern equatorial Pacific), Article 103036, 2019, with permission from Elsevier.

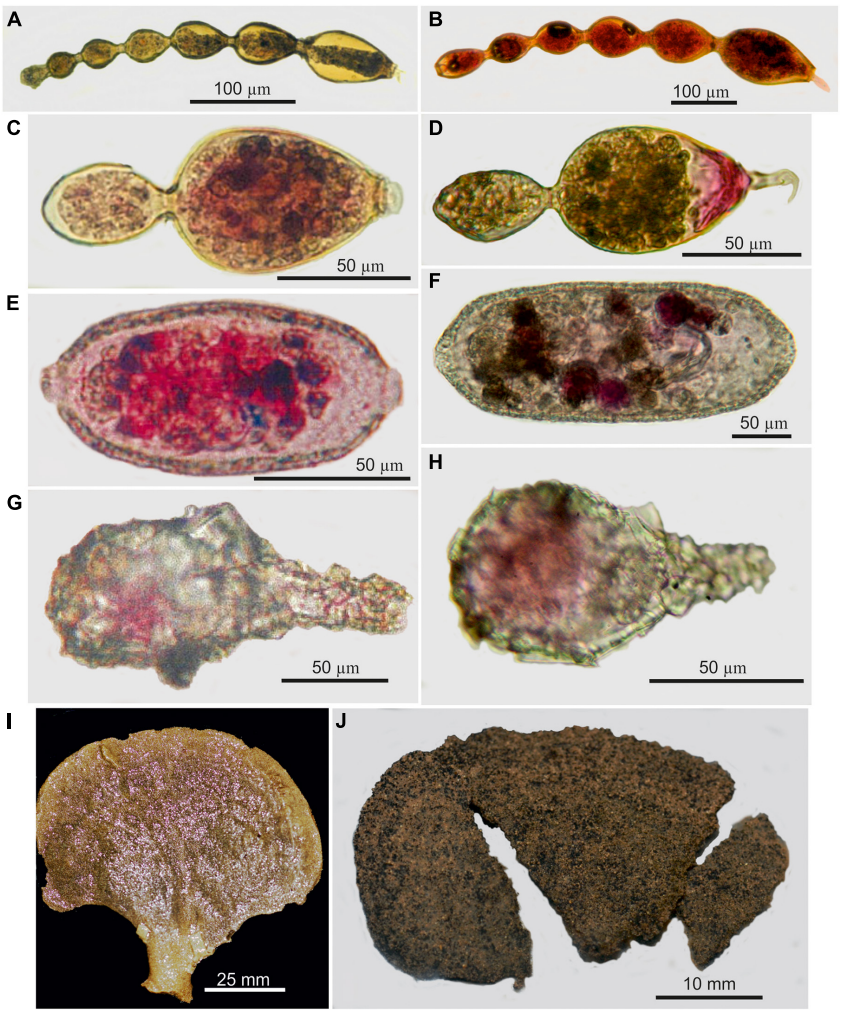

FIGURE 7 | Morphospecies occurring at the western **(A,C,E,G,I)** and eastern **(B,D,F,H,J)** ends of the CCZ. **(A,B)** *Resigella moniliforme* (Resig, 1982) from the JET site **(A)** and UK-1 contract area **(B)**. **(C,D)** Bilocular *Resigella* sp. from the JET **(C)** and KE **(D)** sites. **(E,F)** Saccamminid with terminal apertures from the JET site **(E)** and UK-1 contract area **(F)**. **(G,H)** *Lagenammina* sp. from the JET site **(G)** and OMS contract area. **(H)** *Moanammina semicircularis* Gooday and Holzmann, 2020 in Gooday et al. (2020a) from APEI4 **(I)** and the OMS contract area **(J)**; in this case, genetic data confirm that these two specimens are conspecific (Gooday et al., 2020a).

macrofaunal taxa ("source-sink hypothesis"; Rex et al., 2005; Hardy et al., 2015). This may enable even rare species to maintain wide geographical ranges.

GENETIC CONNECTIVITY

As indicated above, there is genetic evidence that some foraminiferal species have wide ranges across the CCZ and beyond. Lecroq et al. (2009b) analyzed the population genetics of *Epistominella exigua* (a calcareous species found in the UK-1 and OMS areas) from sites in the Arctic, North Atlantic, Southern Ocean, and the western Pacific off Japan, based on the complete ITS rDNA sequences. They found very little divergence between ITS haplotypes from different oceans. Whether or not these results for *E. exigua,* which is an unusually opportunistic species that exploits phytodetritus deposits (Gooday, 1988), are typical for other foraminifera living in the CCZ is an important question for the future.

POSSIBLE ECOLOGICAL ROLES FOR BENTHIC FORAMINIFERA IN THE CCZ

The abundance and diversity of foraminifera across different size classes and microhabitats in the CCZ suggest that they play an important ecological role in benthic communities (reviewed by Gooday, 2019; Gooday et al., 2020b). As a group, deep-sea foraminifera have a wide range of diets (Gooday et al., 1992, 2008; Nomaki et al., 2006). Species of Globothalamea and Tubothalamea, notably the calcareous rotaliids and miliolids, respectively, probably depend more on

TABLE 7 | Literature records from the Pacific Ocean of selected foraminiferal species that occur in the UK-1 and OMS contract areas.

Area or site	Sulu Sea[1]	North Pacific[2]	South Pacific[3]	Gulf of Panama[4]	North Pacific[5]	SE Pacific Abyssal assemblage[6]	35° 09' N, 123° 00'W[7]	~29°N, 155°W[8]	Guatemala Basin[9]
Depth (m)	**534–4635**	**3749–7224**	**3338–5353**	**1412–3436**	**2410–4810**	**>4,100**	**3953**	**5597–6036**	**3350–4040**
Resigella moniliformis	1053–4074					x			
Lag. difflugiformis	534–4635	4206–7224	1957–4435	2070–3436	4170–7230		x		3350–4040
Thurammina papillata		4435			x		x	x	3350–3785
T. albicans		3749							
Sorosphaera confusa		3749, 5304							
Hyperammina cylindrica	2055–4635				4650–5400				
Hyperammina laevigata	3059								3565–3785
Saccorhiza ramosa	534–4635			1564–2196				x	3350–4040
Rhizammina algaeformis	534–4635	3429–5304		2196–3436					
Hormosina ovicula		4206–7224	1957–3383	1443–3436			x		3350–4040
Hormosinella guttifera	534–4635					x	x	x	
Hormosinella distans	3059–4635	4206	1957–2515	1412–3182	4650–5230		x	x	3350–3735
Pseudo. nodulosa		3383–5715	1957–4252	2196	5500–7000		x		3600–4040
Reophax scorpiurus	534–4635	5394–7224	4343–4435		4650–7000	x			
Adercotryma glomeratum	2055–4635	4343	4435		443–7230	x	x		3350–4040
Ammobac. agglutinans	1053				4650–5160	x	x	x	3350–4040
Cribro. subglobosa	534–4635	3383–7224	1957–4435	1207–3436	4170–7230	x	x	x	3350–4040
Veleroninoides scitulus		5404			7000–7230				
Cyclammina trullissata		4206–7224	3458–4435	1789–2227	4170–5610			x	3350–4040
Cystammina galeatea		3383	3338		4170–5500	x		x	
C. pauciloculata	1053–2055	3383–7224	1957–4435	1845–2196		x			3350–4040
Glomospira gordialis	1053–4635	4206–5715	1957–4435		4210–5610	x	x		3350–4040
Epistominella exigua	534–1053			2227	4650–5160		x		
Nuttallides umbonatus					4650				
Globocassid. subglobosa	534–1053				4810	x	x		
Cibicidoides mundulus					4650				
Hoeglundina elegans	534				2410–4810				
Pyrgoella irregularis							x		
Pyrgo murrhyna	1053						x		

Depth ranges (m) are given for species where information from particular areas is available. Crosses (x) indicate occurrences within the depth range of the study. Note the wide bathymetric ranges for some species in the Sulu Sea. The 7 sites sampled in this semi-enclosed western Pacific basin were characterized by uniformly warm temperatures (10-11°C) and oxygen-depleted bottom water (2.06 ml/L from 534 to 2055 m; ~1 ml/L at 3059 m and deeper) (Szarek et al., 2007). Lag. = Lagenammina; Pseudo = Pseudonodosinella; Ammo = Ammobaculites; Cribro = Cribrostomoides; Globocassid. = Globocassidulina.
[1]Szarek et al. (2007); [2,3]Brady (1884); [4]Goës (1896); [5]Smith (1973); [6]Resig (1981); [7]Enge et al. (2012); [8]Schröder et al. (1988); [9]Burmistrova et al. (2007).

inputs of labile organic matter derived from surface production than most abyssal monothalamids, particularly those that accumulate stercomata, the likely waste products of feeding on sedimentary particles and detritus. Many rotaliids have smooth test morphologies consistent with movement through the sediment and are probably relatively active metabolically, whereas deep-sea monothalamids often have test morphologies that must make movement difficult or impossible, suggesting relatively low metabolic rates. Foraminiferal ecology is complex and this distinction is certainly too simplistic. Not all deep-sea monothalamids accumulate stercomata (Turley et al., 1993; Gooday et al., 2004) and some rotaliids ingest sediment and associated bacteria (Goldstein and Corliss, 1994); some small monothalamids are quite mobile (Groos, 2000) while some rotaliids are sessile (Mullineaux, 1987). However, it may be useful to bear this distinction in mind, particularly in abyssal settings where food limitation, combined with carbonate dissolution, favours stercomata-bearing monothalamids.

Role in Food-Webs and Carbon Cycling

Research conducted since the 1970s has documented the potentially important contribution of foraminifera to deep-sea food webs and carbon cycling. By typically feeding at a low trophic level and being consumed by specialist and incidental predators, foraminifera represent an important trophic link at the base of deep-sea foodwebs (Lipps and Valentine, 1970; Gooday et al., 1992; Nomaki et al., 2008; Würzberg et al., 2011). Feeding and reproductive responses to phytodetritus are reported in the bathyal and abyssal NE Atlantic (Gooday, 1988; Gooday and Lambshead, 1989; Gooday and Hughes, 2002), the bathyal western Pacific (Kitazato et al., 2003), and at Station M (4000

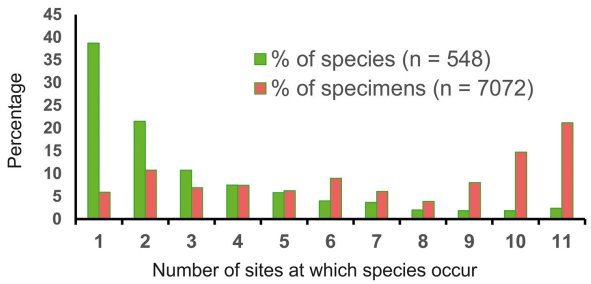

FIGURE 8 | The percentage abundance of species (total = 548) represented by complete tests and specimens (total = 7072) occurring at different numbers of sites (from a single site on the left of the x axis to all 11 sites on the right) within the UK-1 and OMS areas in the eastern CCZ. On the left-hand side, 60.2% of species are confined to 1 or 2 sites but these represent only 16.6% of specimens (i.e., species confined to 1 or 2 sites tend to be rare). In contrast, only 4.2% of species occur at 10 or 11 sites, but these represent 35.9% of specimens (i.e., widely-distributed species tend to be abundant). The relatively high percentage (10.7%) of specimens occurring at 2 sites (second point on x axis) reflects the high abundance (n = 296) of a single species. If this is removed, then the contribution of species confined to 1 or 2 sites decreases from 16.6% to 13.0% of specimens and that of species occurring at 10 or 11 sites increases 35.9 to 37.5%. Based on data from Goineau and Gooday (2019).

m depth) on the Californian margin to the north of the CCZ (Drazen et al., 1998). *In situ* "pulse-chase" experiments using ^{13}C-labelled diatoms as tracers of food uptake have likewise suggested a significant role for foraminifera in the short-term processing of fresh organic matter in the bathyal NW and NE Atlantic (Levin et al., 1999; Moodley et al., 2002), the bathyal NW Pacific (Nomaki et al., 2005), and at Station M (Enge et al., 2011). At the level of individual foraminifera, shipboard experiments and transmission electron microscopy have demonstrated the ingestion of fresh phytoplankton and zooplankton detritus, along with increases in the cellular carbon content and metabolic and enzymatic activity within days of artificial and natural food pulses (Heeger, 1990; Altenbach, 1992; Linke, 1992; Graf and Linke, 1992; Linke et al., 1995). Köster et al. (1991) found high levels of enzymatic activity associated with agglutinated foraminifera (*Hyperammina* and *Reophax*) in the Norwegian-Greenland Sea. They concluded that foraminifera can dominate the enzymatic hydrolysis of organic matter in areas where they are abundant.

How far are these observations, made mainly on eutrophic continental margins, applicable in the oligotrophic CCZ, where there is much less evidence for seasonality in food supply? Sweetman et al. (2018) carried out pulse-chase experiments to determine the uptake of ^{13}C-labeled diatoms by bacteria and macrofauna (>300 μm) in the UK-1 and OMS areas. Uptake was dominated by bacteria, with macrofaunal foraminifera contributing very little. This is not surprising since this size fraction in the abyssal Pacific comprises mainly low-biomass, stercomata-bearing monothalamids (Tendal and Hessler, 1977; Bernstein et al., 1978). Nevertheless, phytodetritus deposition events have been observed occasionally in the CCZ (Radziejewska, 2002) and are likely to evoke a response from small species such as *Epistominella exigua,* which occurs in the eastern CCZ (Gooday and Goineau, 2019). This and other rotaliids, including the most common calcareous species *Nuttallides umbonatus,* contain green cytoplasm, an indication of feeding on fresh phytoplankton-derived material. Moreover, the macrofaunal fraction in this area includes some large species (miliolids, the textulariid *Cribrostomoides subglobosa,* and the monothalamous *Crithionina hispida*), which were among those to respond strongly to food pulses on the Norwegian margin (Heeger, 1990; Thies, 1991; Altenbach, 1992; Linke, 1992; Linke et al., 1995). According to Enge et al. (2011), *Saccorhiza ramosa,* a common nodule-attached species across the CCZ (Gooday et al., 2015), was responsible for 61 and 99% of tracer uptake in the 1-2 and 2-3 cm layers, respectively, at Station M. These observations suggest that foraminifera play some role in the processing of organic carbon in the CCZ, although the contribution of calcareous taxa will probably be greater at the shallower eastern end where carbonate dissolution is less of an issue.

Limited knowledge about the ecology of abyssal foraminifera, and monothalamids in particular, hampers understanding of the overall contribution that these benthic protists make to carbon cycling in the CCZ. Although saccamminids (flask-shaped, soft-walled monothalamids) were a major component of foraminiferal assemblages at Station M, their contribution to carbon uptake in ^{13}C-tracer experiments was almost zero (Enge et al., 2011). Some small, organic-walled monothalamids have relatively featureless cytoplasm (Supplementary Figure 9A–C in Gooday and Goineau, 2019) and may consume bacteria (Turley et al., 1993), while gromiids are packed with waste pellets (stercomata) and often ingest cysts, fragments of other organisms, or mineral grains (Figures 3A,B in Renaud-Mornant and Gourbault, 1990). The storage of stercomata, which comprise mainly clay minerals, is typical of many abyssal monothalamids and probably reflects the ingestion of sediment and degraded organic matter. Lipid analyses suggest that bacteria may also be consumed by xenophyophores (Laureillard et al., 2004). Stercomata-retaining groups such as komokiaceans and xenophyophores, often have large tests but sparse cytoplasm. As a result, their biomass is much less than their macro- or mega-faunal sizes would suggest (Tendal, 1979; Levin and Gooday, 1992; Shires et al., 1994; Gooday et al., 2018b), a likely adaptation to severely energy-limited abyssal environments. This kind of organization also makes distinguishing "live" from dead specimens in fixed samples using Rose Bengal staining problematic, possibly leading to the over-estimation of "live" abundances. All of these factors suggest that the contribution of monothalamids to carbon cycling in the CCZ does not match their abundance and diversity although, given their large contribution to benthic communities, it may still be considerable. However, there are very few reliable data about their biomass or rates of metabolic activity, which are crucial parameters if foraminifera are to be included in carbon-based, food-web modeling studies (van Oevelen et al., 2011; de Jonge et al., 2020).

Provision of Heterogeneity

Gooday et al. (2020b) review the role of xenophyophores as a potentially important source of seafloor heterogeneity in parts of the deep sea where they are an abundant component of the

megafauna. Briefly, their tests, whether alive or dead, may (1) enhance the deposition of fine sediment and labile material in their immediate vicinity, creating food-rich hotspots (a likely reason why ophiuroids are often seen coiled around test bases; Levin and Thomas, 1988); (2) provide habitat structure that is utilized for multiple purposes by a wide range of meiofaunal and macrofaunal metazoans (e.g., Levin et al., 1986; Levin, 1991; Levin and Gooday, 1992), foraminifera (Hughes and Gooday, 2004), and even fish (Levin and Rouse, 2019), and (3) host an enhanced and distinctive microflora (Hori et al., 2013). These heterogeneity-enhancing attributes are either known or likely to apply in the CCZ.

Although the large test sizes of many xenophyophores makes them especially important in this regard, smaller meio- and macro-faunal foraminifera can also create habitat structure that is relevant to smaller organisms (Thistle, 1979, 1982). A genetic analysis of komokiacean tests (*Normanina conferta* and *Septuma ocotillo*) from the Weddell Sea revealed an extraordinary diversity of fungal and protistan sequences (Lecroq et al., 2009a), suggesting that these structures are hotspots of microbial diversity. An X-ray radiograph of a core from the eastern equatorial Pacific Panama Basin (3912 m depth) shows the sediment permeated by a network of fine burrows attributed to *Reophax* (Kaminski et al., 1988), the most common multichambered agglutinated genus in the eastern CCZ (Goineau and Gooday, 2017, 2019). Based on an analysis of "vegematic" box cores (i.e., partitioned into subcores) at the CLIMAX II site north of Hawaii, Bernstein et al. (1978) found that certain groups of foraminifera exhibited possible correlations with biological variables, such as prevalence of surface or subsurface deposit feeders and carnivores. These examples suggest that the diverse agglutinated foraminifera, including morphologically complex komokiaceans, mudballs, branching tubes, and chain-like formations that are common in CCZ samples, may help to structure sedimentary habitats and serve as microhabitats for other organisms.

Possible Recolonization Scenarios

Some clues to possible foraminiferal responses to the blanketing of the seafloor by sediment redeposited from the plume created by mining may be gleaned from studies in the South China Sea, where a large area was covered by a layer of volcanic ash (1 to 90 mm thick at sampled sites) following an eruption in the Philippines in 1991. Different parts of the impacted area (2338–3322 m depth) were sampled on 5 occasions: April 1994, June 1996, November/December 1996 and June/July 1998, and April 1999 (Hess and Kuhnt, 1996; Hess et al., 2001; Kuhnt et al., 2005). Among the observations that may be relevant to seabed mining impacts were the following. (1) Impact of the ash layer depended on its thickness. All foraminifera were killed where it was 60–80 mm thick; mobile infaunal species were significantly reduced where it was 20 mm thick, and epifaunal suspension feeders were eliminated by ash deposits <10 mm thick. (2) Twenty agglutinated species survived the ash fall at a site where the thickness was 15 mm, as shown by their use of quartz grains and biogenic particles in early chambers (pre-dating ash fall) and ash particles in later chambers. Most were considered to be mobile infaunal species. Some (*Ammobaculites agglutinans, Cribrostomoides subglobosum, Hormosinella distans, Hyperammina elongata, Reophax scorpiurus, Rhizammina algaeformis, Saccorhiza ramosa*) have been identified in the eastern CCZ. 3) A first wave of pioneer recolonizing species was recognized in 1994 samples. These were followed by a second wave that dominated in 1996. Suspension feeders, including large xenophyophores, appeared in the 1998 samples. Xenophyophores not reliant on nodules as an attachment substrate could therefore be among the first large immobile organisms to reappear in areas where seabed mining has destroyed the fauna (Gooday et al., 2020b), although there is no evidence of this having happened yet at experimental disturbance sites such as DISCOL (Figure 1 in de Jonge et al., 2020). 4) The earliest recolonizers were small, mobile, agglutinated forms, mainly *R. dentaliniformis* and *Textularia* sp., that were not present in the original pre-eruption assemblage or in control samples from unaffected areas. They were succeeded by two other *Reophax* species (*R. bilocularis, R. scorpiurus*) and the miliolid *Quinqueloculina seminula.*

The ash-fall observations are suggestive, but the South China Sea is a very different environment from the CCZ and they should be extrapolated only with considerable caution. Apart from being shallower, the South China Sea experiences monsoonal winds, leading to seasonal changes in productivity, as well as much stronger current activity than the CCZ. The ash substrate is very different geochemically and mineralogically from CCZ sediments, and is much coarser-grained (Kuhnt et al., 2005). Nevertheless, in the absence of any real evidence for how foraminiferal recolonization will proceed following mining impacts, these observations could provide pointers for what might happen. They are also consistent with other observations. Two species of *Reophax* (*R. dentaliniformis, R. excentricus*), a genus that included some of the pioneer ash-fall recolonizers, were the most common foraminifera after 9 months in 30 × 30 cm trays of defaunated sediments deployed at a 3,912-m-deep site in the Panama Basin (> 297-μm fraction; Kaminski et al., 1988). *Reophax dentaliniformis* also recolonized disturbed sediments at 1,478 m in the axis of the Cap Breton Canyon in the NE Atlantic (Duros et al., 2017). We suggest that members of this important uniserial genus, which is the most abundant multichambered foraminiferal taxon in the eastern CCZ (Goineau and Gooday, 2017, 2019), may be among the earliest to reappear following direct or indirect mining impacts. They might be accompanied by small biserial agglutinated taxa, notably *Textularia* spp. and *Spiroplectammina* spp., that also occur in the CCZ. Dispersal of such species could be mediated by the transport of propagules (tiny 1-2 chambered juveniles) (Alve and Goldstein, 2003, 2010), although very low current speeds in the CCZ suggest that recolonization would proceed at a slower rate than in the South China Sea.

CONCLUDING REMARKS

Foraminifera are unique among marine eukaryotes, and protists generally, in spanning a size range from meiofauna to megafauna.

They are also by far the most abundant benthic organisms to be preserved in the oceanic fossil record and important palaeoceanographic indicators of ancient seafloor environments. As a result, many deep-sea species have been described based on test morphology, and numerous publications record their distribution in modern oceans, making them one of the best documented of deep-sea benthic taxa and potential models for understanding biogeographic patterns in the abyss. The well-known, mainly multichambered foraminifera occur alongside delicate, monothalamous forms that have very little fossilization potential and include many undescribed species. In the CCZ and other parts of the abyssal Pacific, oligotrophic conditions, combined with increasing carbonate dissolution close to and below the carbonate compensation depth, favour the development of monothalamid-dominated assemblages. Some belong to known genera and species, or can be assigned to higher taxa like the Komokioidea and Xenophyophoroidea. However, other abyssal monothalamids are difficult to accommodate within current morphology-based taxonomic systems for agglutinated foraminifera (e.g., Kaminski, 2014).

The monothalamid component of CCZ assemblages poses further challenges. 1) Some tests, notably komokiaceans and tubular morphotypes, have a strong tendency to fragment, and are therefore difficult to quantify. The best solution is to count fragments separately from intact specimens (Bernstein et al., 1978; Nozawa et al., 2006) and include fragmented species in species numbers but not in calculations of species diversity. 2) Ecological studies of modern foraminifera need to distinguish between specimens that were living when collected and those that were dead. The simplest and most common method is Rose Bengal staining, but stercomata-bearing monothalamids have sparse cytoplasm and do not stain well, often making it difficult to discriminate between "live" and dead tests. 3) Although DNA sequences can be obtained easily from the megafaunal xenophyophores and smaller, more typical deep-sea monothalamids, including saccamminids (e.g., *Conqueria*) and allogromiids (e.g., *Bathyallogromia, Micrometula*), attempts to sequence the stercomata-bearing forms, such as komokiaceans, have often proved unsuccessful (e.g., Lecroq et al., 2009a). These difficulties limit understanding of the phylogenetic position and diversity of these problematic organisms, as well as hampering the description of new species. 4) Finally, although we can speculate that morphologically-complex, stercomata-bearing monothalamids probably consume sediment, degraded organic matter, and perhaps bacteria, and have lower energetic demands (metabolism) than multichambered foraminifera, we have very little direct information regarding their ecology. Experimental studies could help to address this important limitation. Because of difficulties such as these, there is a temptation to disregard monothalamids in surveys of the CCZ fauna. Given their importance, we would argue that they should be included, at least in assessments of seafloor biodiversity. As shown by several studies (Lecroq et al., 2011; Lejzerowicz et al., 2014; Cordier et al., 2019), metabarcoding of sediment DNA appears to be the best way to incorporate the smaller monothalamids in monitoring surveys. However, the biodiversity of komokiaceans and other enigmatic forms, which often dominate the abyssal Pacific macrofauna (Tendal and Hessler, 1977; Bernstein et al., 1978) and to a lesser extent the meiofauna (Goineau and Gooday, 2017, 2019), may still have to be evaluated morphologically.

In terms of data gaps, the most obvious is the scarcity of foraminiferal studies in the western CCZ. Apart from some species records, mainly in the works of Kh. Saidova (**Supplementary Material**), we have only some quantitative data from the JET site, some information on nodule-encrusting foraminifera from the western French site, and small collections of xenophyophores from APEIs 1, 4, 6 and 7. A transect of foraminiferal samples along east to west gradients of increasing depth and carbonate dissolution and decreasing surface productivity could prove very informative. Although xenophyophores have been collected (Gooday et al., 2017b, 2020a), and analyzed in seafloor images (Simon-Lledó et al., 2019a,b) in several APEIs, there are currently no quantitative morphological or metabarcoding data for foraminifera in samples from any of the nine present protected areas. This is an important gap to address given the importance of APEIs in protecting biodiversity and ecosystem functioning in the CCZ from future mining impacts. Finally, we agree with de Jonge et al. (2020) on the pressing need for more information about the biomass, metabolic activity, and ecology of abyssal foraminifera, particularly xenophyophores and other monothalamids, in order to include them in efforts to construct comprehensive carbon-flow models for the CCZ. Understanding the role of these remarkable protists in the functioning of deep-sea benthic ecosystems in the CCZ and across the globe remains a major challenge for the future.

DATA AVAILABILITY STATEMENT

Data from the UK-1 and OMS sites are available in published supplementary materials (Goineau and Gooday, 2017, 2019; Gooday and Goineau, 2019). Data from the Kaplan East, Kaplan Central, and Japan Deep-Sea Impact Experiment (JET) sites are available on reasonable request from AJG and HK. Data from the IOM BIE site are available on reasonable request from ZS and TR.

AUTHOR CONTRIBUTIONS

The original idea for a review was conceived by AJG and AG. AJG developed the idea, wrote much of the manuscript, and prepared **Figures 7**, **8**. FL did the metabarcoding analyses, wrote the section "Environmental DNA and RNA Metabarcoding Data" contributed to the section on 'Undersampling, Patchiness and Rarity' and prepared **Figure 5** and **Tables 4**, **5**. AG prepared the original versions of **Figures 3**, **6** and was jointly responsible with AJG for the collection and analysis of some of the data summarized in the review. MH and JP were responsible for the barcoding sequence data. JP supervised the metabarcoding analyses. OK contributed faunal data and prepared Appendix A (**Supplementary Material**). S-CL, HK, TR, ZS, and BW-W contributed faunal data. JP, TR, and BW-W edited the

manuscript. BW-W prepared **Figures 1**, **2**, **4**. All authors approved the final manuscript.

FUNDING

MH and JP were supported by Swiss National Science Foundation grants 31003A_179125 and 316030_150817 (JP). ZS, TR, and BW-W acknowledge support provided by the Polish National Science Center Grant No. 2014/13/B/ST10/02996 and by the JPI Oceans Pilot Action "Ecological Effects of Deep-Sea Mining". Additional support was provided by the Institute of Marine and Environmental Sciences of the University of Szczecin, Poland. Research by OK was funded by the Ministry of Education and Science of the Russian Federation, State Assignment No. 0149-2019-0009 and Grant No. 13.1902.21.0012). FL was supported by an Early Postdoc Mobility Grant from the Swiss National Science Foundation (P2GEP3_171829). Research conducted in the UK-1 and OMS contract areas in the Clarion-Clipperton Zone were collected as part of the ABYSSLINE project, funded by UK Seabed Resources Development Ltd.

ACKNOWLEDGMENTS

We thank Laure Apothéloz-Perret-Gentil, Ivan Voltski, and Alexandra Anh-Thu Weber who collected foraminiferal and eDNA samples from the CCZ during ABYSSLINE cruises. We thank the two reviewers for their comments that helped to improve the initial submission.

SUPPLEMENTARY MATERIAL

The Supplementary Material for this article can be found online at: https://www.frontiersin.org/articles/10.3389/fmars.2021.634726/full#supplementary-material

REFERENCES

Altenbach, A. V. (1992). Short term processes and patterns in the foraminiferal response to organic flux rates. *Mar. Micropaleontol.* 19, 119–129. doi: 10.1016/0377-8398(92)90024-e

Alve, E., and Goldstein, S. T. (2003). Propagule transport as a key method of dispersal in benthic foraminifera. *Limnol. Oceanogr.* 48, 2163–2170. doi: 10.4319/lo.2003.48.6.2163

Alve, E., and Goldstein, S. T. (2010). Dispersal, survival and delayed growth of benthic foraminiferal propagules. *J. Sea Res.* 63, 36–51. doi: 10.1016/j.seares.2009.09.003

Amon, D. J., Ziegler, A. F., Dahlgren, T. G., Glover, A. G., Goineau, A., Gooday, A. J., et al. (2016). Insights into the abundance and diversity of abyssal megafauna in a polymetallic-nodule region in the eastern Clarion-Clipperton Zone. *Sci. Rep.* 6:30492. doi: 10.1038/srep30492

Aranda da Silva, A. A. S., and Gooday, A. J. (2009). Large organic-walled Protista (*Gromia*) in the Arabian Sea: density, diversity, distribution and ecology. *Deep Sea Res. II* 56, 422–433. doi: 10.1016/j.dsr2.2008.12.027

Bagg, R. M. (1908). Foraminifera collected near the Hawaiian Islands by the steamer Albatross in 1902. *Proc. U.S. Nat. Mus.* 34, 113–172. doi: 10.5479/si.00963801.34-1603.113

Bernstein, B. B., Hessler, R. R., Smith, R., and Jumars, P. A. (1978). Spatial dispersion of benthic Foraminifera in the abyssal central North Pacific. *Limnol. Oceanogr.* 23, 401–416. doi: 10.4319/lo.1978.23.3.0401

Brady, H. B. (1884). Report on the foraminifera dredged by H.M.S. Challenger during the Years 1873-1876. Report of the Scientific Results of the Voyage of H.M.S. Challenger during the years 1873–76. *Zoology* 9 (Pt 22), 1–814, pls 1–115.

Burkett, A., Rathburn, A., Pratt, R. B., and Holzmann, M. (2020). Insight into the ecology of epibenthic calcareous foraminifera from a colonization study at 4000 m (Station M) in the NE Pacific Ocean. *Deep Sea Res. II* 173:104709. doi: 10.1016/j.dsr2.2019.104709

Burmistrova, I. I., Khusid, T. A., Belyaeva, N. V., and Chekhovskaya, M. P. (2007). Agglutinated abyssal foraminifers of the equatorial Pacific. *Oceanology* 47, 824–832. doi: 10.1134/s0001437007060070

Cordier, T., Barrenechea, I., Lejzerowicz, F., Reo, E., and Pawlowski, J. (2019). Benthic foraminiferal DNA metabarcodes significantly vary along a gradient from abyssal to hadal depths and between each side of the Kuril-Kamchatka trench. *Prog. Oceanogr.* 178:102175. doi: 10.1016/j.pocean.2019.102175

Culver, S. J., and Buzas, M. A. (1999). "Biogeography of neritic benthic Foraminifera," in *Modern Foraminifera*, ed. B. K. Sen Gupta (Dordrecht: Kluwer Academic Publisher), 93–102. doi: 10.1007/0-306-48104-9_6

Cushman, J. A. (1910). A monograph of the foraminifera of the North Pacific Ocean. Part 1. Astrorhizidae and Lituolidae. *Bull. U.S. Natl. Mus.* 71, 1–134. doi: 10.5479/si.03629236.104.1

Cushman, J. A. (1911). A monograph of foraminifera of the North Pacific Ocean. Pt. 2, Textulariidae. *Bull. U.S. Natl. Mus.* 71, 1–134.

Cushman, J. A. (1913). A monograph of foraminifera of the North Pacific Ocean. Pt. 3, Lagenidae. *Bull. U.S. Natl. Mus.* 71, 1–125, pls 1–47.

Cushman, J. A. (1914). A monograph of foraminifera of the North Pacific Ocean. Pt. 4, Chilostomellidae. *Bull. U.S. Natl. Mus.* 71, 1–46, pls 1–19.

Cushman, J. A. (1915). A monograph of foraminifera of the North Pacific Ocean. Pt. 5, Rotaliidae. *Bull. U.S. Natl. Mus.* 71, 1–81, pls 1–31.

Cushman, J. A. (1917). A monograph of foraminifera of the North Pacific Ocean. Pt. 6, Miliolidae. *Bull. U.S. Natl. Mus.* 71, 1–108, pls 1–39.

Cushman, J. A. (1932). The foraminifera of the tropical Pacific collections of the 'Albatross', 1899–1900. Pt. 1. Astrorhizidae to Trochamminidae. *Bull. U.S. Nat. Mus.* 161, 1–84, pls 1–17.

Cushman, J. A. (1933).). The foraminifera of the tropical Pacific collections of the 'Albatross', 1899–1900. Pt. 2. Lagenidae to Alveolinellidae. *Bull. U.S. Nat. Mus.* 161, 1–74, pls 1–19.

Cushman, J. A. (1942). The foraminifera of the tropical Pacific collections of the 'Albatross', 1899–1900. Pt. 3. Heterohelicidae and Buliminidae. *Bull. U.S. Nat. Mus.* 161, 1–67, pls 1–15.

de Jonge, D. S. W., Stratmann, T., Lins, L., Vanreusel, A., Purser, A., Marcon, Y., et al. (2020). Abyssal food-web model indicates faunal carbon flow recovery and impaired microbial loop 26 years after a sediment disturbance experiment. *Prog. Oceanogr.* 189:102446. doi: 10.1016/j.pocean.2020.102446

Douglas, R. G., and Woodruff, F. (1981). "Deep-sea benthic foraminifera," in *The Sea: The Oceanic Lithosphere*, Vol. 7, ed. E. Emiliani (New York, NY: John Wiley & Sons), 1233–1327.

Drazen, J. E., Baldwin, R. H., and Smith, K. L. (1998). Sediment community response to a temporally varying food supply at an abyssal station in the NE Pacific. *Deep Sea Res. II* 45, 893–913. doi: 10.1016/s0967-0645(98)00007-1

Dugolinsky, B. K., Margolis, S. V., and Dudley, W. C. (1977). Biogenic influence on growth of manganese nodules. *J. Sediment. Petrol.* 47, 428–445.

Duros, P., Silva Jacinto, R., Dennielous, B., Schmidt, S., Martinez Lamas, R., Gautier, E., et al. (2017). Benthic foraminiferal response to sedimentary disturbance in the Capbreton canyon (Bay of Biscay, NE Atlantic). *Deep Sea Res. I* 120, 61–75. doi: 10.1016/j.dsr.2016.11.012

Ehrenberg, C. G. (1861). Über den Tiefgrund des Stillen Oceans Zwischen Californien und den Sandwich-Inseln aus bis 15600' Tiefe nach Lieutenant Brooke. *Monatsberichte, Year 1860. Berlin: Königliche Preussische Akademie der Wissenschaften*, 819–833.

Enge, A. J., Kucera, M., and Heinz, P. (2012). Diversity and microhabitats of living benthic foraminifera in the abyssal Northeast Pacific. *Mar. Micropal.* 96–97, 84–104. doi: 10.1016/j.marmicro.2012.08.004

Enge, A. J., Nomaki, H., Ogawa, N. O., Witte, U., Moeseneder, M. M., Lavik, G., et al. (2011). Response of the benthic foraminiferal community to a simulated short-term phytodetritus pulse in the abyssal North Pacific. *Mar. Ecol. Prog. Ser.* 438, 129–142. doi: 10.3354/meps09298

Flint, J. M. (1899). Recent Foraminifera. A descriptive catalogue of specimens dredged by the U.S. Fish Commission steamer Albatross. *Rep. U.S. Natl. Mus.* 1897, 251–349, pls 1–80.

Flint, J. M. (1905). A contribution to the oceanography of the Pacific. *Bull U.S. Nat. Mus.* 55, 1–62. doi: 10.1594/PANGAEA.847719

Goës, A. (1892). On a peculiar type of arenaceous foraminifer from the American tropical Pacific. *Bull. Mus. Comp. Zool. Harv.* 23, 195–198.

Goës, A. (1896). Report on the dredging operations off the west coast of Central America to the Galapagos, to the west coast of Mexico, and the Gulf of California, in charge of Alexander Agassiz, carried on by the U.S. Fish Commission steamer 'Albatross', during 1891, Lieu. Z.L. Tanner U.S.N., commanding. XX. The Foraminifera. *Bull. Mus. Comp. Zool. Harv.* 29, 1–105, pls 1–9.

Goineau, A., and Gooday, A. J. (2017). Novel benthic foraminifera are abundant and diverse in an area of the abyssal equatorial Pacific licensed for polymetallic nodule exploration. *Sci. Rep.* 7:45288. doi: 10.1038/srep45288

Goineau, A., and Gooday, A. J. (2019). Diversity and spatial patterns of foraminiferal assemblages in the eastern Clarion-Clipperton zone (abyssal eastern equatorial Pacific). *Deep Sea Res. I* 149:103036. doi: 10.1016/j.dsr.2019.04.014

Goldstein, S. T., and Corliss, B. H. (1994). Deposit feeding in selected deep-sea and shallow-water benthic foraminifera. *Deep Sea Res.* 41, 229–241. doi: 10.1016/0967-0637(94)90001-9

Gooday, A. J. (1988). A response by benthic foraminifera to phytodetritus deposition in the deep sea. *Nature* 332, 70–73. doi: 10.1038/332070a0

Gooday, A. J. (2019). "Deep-sea benthic foraminifera," in *Encyclopedia of Ocean Science*, 3rd Edn, eds J. Cochran, J. Kirk, J. H. Bokuniewicz, and L. P. Yager (London: Elsevier), 684–705. doi: 10.1016/b978-0-12-409548-9.09071-0

Gooday, A. J., Cedhagen, T., Kamenskaya, O. E., and Cornelius, N. (2007). The biodiversity and biogeography of komokiaceans and other enigmatic foraminiferan-like protists in the deep Southern Ocean. *Deep Sea Res. II* 54, 1691–1719.

Gooday, A. J., Durden, J. M., Holzmann, M., Pawlowski, J., and Smith, C. R. (2020a). Xenophyophores (Rhizaria, Foraminifera), including four new species and two new genera, from the western Clarion-Clipperton Zone (abyssal equatorial Pacific). *Eur. J. Protist.* 75:125715. doi: 10.1016/j.ejop.2020.125715

Gooday, A. J., Durden, J. M., and Smith, C. R. (2020b). Giant, highly diverse protists in the abyssal Pacific: vulnerability to impacts from seabed mining and potential for recovery. *Commun. Integr. Biol.* 13, 189–197. doi: 10.1080/19420889.2020.1843818

Gooday, A. J., and Goineau, A. (2019). The contribution of fine sieve fractions (63–150 μm) to foraminiferal abundance and diversity in an area of the eastern Pacific Ocean licensed for polymetallic nodule exploration. *Front. Mar. Sci.* 6:114. doi: 10.3389/fmars.2019.00114

Gooday, A. J., Goineau, A., and Voltski, I. (2015). Abyssal foraminifera attached to polymetallic nodules from the eastern Clarion-Clipperton Fracture Zone: a preliminary description and comparison with North Atlantic dropstone assemblages. *Mar. Biodiv.* 45, 391–412. doi: 10.1007/s12526-014-0301-9

Gooday, A. J., Holzmann, M., Caulle, C., Goineau, A., Jones, D. O. B., Kamenskaya, O. E., et al. (2017a). New species of the xenophyophore genus *Aschemonella* (Rhizaria, Foraminifera) from areas of the abyssal eastern Pacific licensed for polymetallic nodule exploration. *Zool. J. Linn. Soc.* 182, 479–499. doi: 10.1093/zoolinnean/zlx052

Gooday, A. J., Holzmann, M., Caulle, C., Goineau, A., Kamenskaya, O. E., Weber, A. A.-T., et al. (2017b). Giant foraminifera (xenophyophores) are exceptionally diverse in parts of the abyssal eastern Pacific where seabed mining is likely to occur. *Biol. Conserv.* 207, 106–116. doi: 10.1016/j.biocon.2017.01.006

Gooday, A. J., Holzmann, M., Caulle, C., Goineau, A., Pearce, R. B., Voltski, I., et al. (2017c). Five new species and two new genera of xenophyophores (Foraminifera: Rhizaria) from part of the abyssal equatorial Pacific licensed for polymetallic nodule exploration. *Zool. J. Linn. Soc.* 183, 723–748. doi: 10.1093/zoolinnean/zlx093

Gooday, A. J., Holzmann, M., Goineau, A., Kamenskaya, O., Melnik, V. F., Pearce, R. B., et al. (2018a). Xenophyophores (Rhizaria, Foraminifera) from the Eastern Clarion-Clipperton Zone (equatorial Pacific): the genus *Psammina*. *Protist* 169, 926–957. doi: 10.1016/j.protis.2018.09.003

Gooday, A. J., Holzmann, M., Guiard, J., Cornelius, N., and Pawlowski, J. (2004). A new monothalamous foraminiferan from 100-6300 m water depth in the Weddell Sea: morphological and molecular characterisation. *Deep Sea Res. II* 51, 1603–1616. doi: 10.1016/j.dsr2.2004.06.025

Gooday, A. J., and Hughes, J. A. (2002). Foraminifera associated with phytodetritus deposits at a bathyal site in the northern Rockall Trough (NE Atlantic): seasonal contrasts and a comparison of stained and dead assemblages. *Mar. Micropaleontol.* 46, 83–110. doi: 10.1016/s0377-8398(02)00050-6

Gooday, A. J., and Lambshead, P. J. D. (1989). Influence of seasonally deposited phytodetritus on benthic foraminiferal populations in the bathyal northeast Atlantic: the species response. *Mar. Ecol. Prog. Ser.* 58, 53–67. doi: 10.3354/meps058053

Gooday, A. J., Levin, L. A., Linke, P., and Heeger, T. (1992). "The role of benthic foraminifera in deep-sea food webs and carbon cycling," in *Deep-Sea Food Chains and the Global Carbon Cycle*, eds G. T. Rowe and V. Pariente (Dordrecht: Springer), 63–91. doi: 10.1007/978-94-011-2452-2_5

Gooday, A. J., Nomaki, H., and Kitazato, H. (2008). "Modern deep-sea benthic foraminifera: a brief review of their biodiversity and trophic diversity," in *Biogeochemical Controls on Palaeoceanographic Environmental Proxies*, Vol. 303, eds W. E. N. Austin and R. H. James (London: Geological Society, Special Publications), 97–119. doi: 10.1144/SP303.8

Gooday, A. J., Sykes, D., Goral, T., Zubkov, M. V., and Glover, A. G. (2018b). Micro-CT 3D imaging reveals the internal structure of three abyssal xenophyophore species (Protista, Foraminifera) from the eastern equatorial Pacific Ocean. *Sci. Rep.* 8:12103. doi: 10.1038/s41598-018-30186-2

Graf, G., and Linke, P. (1992). "Adenosine nucleotides as indicators of deep-sea benthic metabolism," in *Deep-Sea Food Chains and the Global Carbon Cycle*, eds G. T. Rowe and V. Pariente (Dordrecht: Kluwer Academic), 237–243. doi: 10.1007/978-94-011-2452-2_14

Greenslate, J., Hessler, R. R., and Thiel, H. (1974). "Manganese nodules are alive and well on the sea floor," in *Proceedings of the Marine Technology Society 10th Annual Conference*, Washington, DC, 171–181.

Groos, O. (2000). The influence of temperature, oxygen and food availability on the migration activity of bathyal benthic foraminifera: evidence from microcosm experiments. *Hydrobiologia* 416, 123–137. doi: 10.1007/978-94-011-4148-2_12

Haeckel, E. (1889). Report on the Deep-Sea Keratosa collected by H.M.S. Challenger during the Years 1873-1876. Report of the Scientific Results of the Voyage of H.M.S. Challenger during the years 1873-76, Vol. 82, 1–92, pls 1–8.

Hardy, S. M., Smith, C. R., and Thurnherr, A. M. (2015). Can the source–sink hypothesis explain macrofaunal abundance patterns in the abyss? A modelling test. *Proc. Roy. Soc. Lond. B* 282:20150193. doi: 10.1098/rspb.2015.0193

Hayward, B. W., Holzmann, M., Pawlowski, J., Parker, J. H., Kaushik, T., Toyofuku, M. S., et al. (2021). Molecular and morphological taxonomy of living. *Ammonia* and related taxa (Foraminifera) and their biogeography. *Micropaleontology* 67, 109–313. doi: 10.47894/mpal.67.2-3.01

Heeger, T. (1990). Elektronmikrokopische untersuchungen zur ernährungsbiologie benthischer foraminiferen. *Berichte Sondersforschungsbereich* 313, 1–139.

Hein, J. R., Mizell, K., Koschinsky, A., and Conrad, T. A. (2013). Deep-ocean mineral deposits as a source of critical metals for high- and green-technology applications: comparison with land-based resources. *Ore Geol. Rev.* 51, 1–14. doi: 10.1016/j.oregeorev.2012.12.001

Hess, S., and Kuhnt, W. (1996). Deep-sea benthic foraminiferal recolonization of the 1991 Mt. Pinatubo ash layer in the South China Sea. *Mar. Micropaleontol.* 28, 171–197. doi: 10.1016/0377-8398(95)00080-1

Hess, S., Kuhnt, W., Hill, S., Kaminski, M. A., Holbourn, A., and de Leon, M. (2001). Monitoring the recolonization of the Mt. Pinatubo 1991 ash layer by benthic foraminifera. *Mar. Micropaleontol.* 43, 119–142. doi: 10.1016/s0377-8398(01)00025-1

Hessler, R. R. (1974). "The structure of deep-sea communities from central oceanic waters," in *The Biology of the Oceanic Pacific*, ed. C. B. Miller (Corvallis, OR: Oregon State University Press), 79–93.

Holbourn, A., Henderson, A., and McLeod, N. (2013). *Atlas of Benthic Foraminifera*. Chichester: Wiley-Blackwell, doi: 10.1002/9781118452493

Hori, S., Tsuchiya, M., Nishi, S., Arai, W., Yoshidam, T., and Takami, H. (2013). Active bacterial flora surrounding foraminifera (Xenophyophorea) living on the deep-seafloor. *Biosci. Biotechnol. Biochem.* 77, 381–384. doi: 10.1271/bbb.120663

Hughes, J. A., and Gooday, A. J. (2004). The influence of dead *Syringammina fragilissima* (Xenophyophorea) tests on the distribution of benthic foraminifera in the Darwin Mounds region (NE Atlantic). *Deep Sea Res. I* 51, 1741–1758. doi: 10.1016/j.dsr.2004.06.004

Jorissen, F., Fontanier, C., and Thomas, E. (2007). "Paleoceanographical proxies based on deep-sea benthic foraminiferal assemblage characteristics," in *Proxies in Late Cenozoic Paleoceanography*, eds C. Hillaire-Marcel and A. de Vernal (Amsterdam: Elsevier), 263–325. doi: 10.1016/s1572-5480(07)01012-3

Kamenskaya, O. E. (2005). *Spiculammina delicata* gen. et sp. n., a new xenophyophore from the eastern Pacific (Psamminidae). *Invert. Zool.* 2, 23–27. doi: 10.15298/invertzool.02.1.03

Kamenskaya, O. E., Gooday, A. J., Radziejewska, T., and Wawrzyniak-Wydrowska, B. (2012). Large, enigmatic foraminiferan-like protists in the eastern part of the Clarion-Clipperton Fracture Zone (abyssal eastern equatorial Pacific): biodiversity and vertical distribution in the sediment. *Mar. Biodiv.* 42, 311–327. doi: 10.1007/s12526-012-0114-7

Kamenskaya, O. E., Gooday, A. J., Tendal, O. S., and Melnik, V. F. (2015). Xenophyophores (Protista, Foraminifera) from the Clarion-Clipperton Fracture Zone with description of three new species. *Mar. Biodiv.* 45, 581–593. doi: 10.1007/s12526-015-0330-z

Kamenskaya, O. E., Gooday, A. J., Tendal, O. S., and Melnik, V. F. (2017). Xenophyophores (Rhizaria, Foraminifera) from the Russian license area of the Clarion-Clipperton Zone (eastern equatorial Pacific), with the description of three new species. *Mar. Biodiv.* 47, 299–306. doi: 10.1007/s12526-016-0595-x

Kamenskaya, O. E., Melnik, V. F., and Gooday, A. J. (2013). Giant protists (xenophyophores and komokiaceans) from the Clarion-Clipperton ferromanganese nodule field (Eastern Pacific). *Biol. Bull. Rev.* 3, 388–398. doi: 10.1134/s2079086413050046

Kaminski, M. (2014). The year 2010 classification of the agglutinated foraminifera. *Micropaleontology* 60, 89–108.

Kaminski, M. A., Grassle, J. F., and Whitlach, R. B. (1988). "Life history and recolonisation among agglutinated foraminifera in the Panama Basin," in *Proceedings of the 2nd Workshop on Agglutinated Foraminifera*, Vol. 41, eds M. F. Gradstein and F. Rögl (Wien: Abh. Geol. Bundesanst.), 229–243.

Kitazato, H., Nakatsuka, T., Shimanaga, M., Kanda, J., Soh, W., Kato, Y., et al. (2003). Long-term monitoring of the sedimentary processes in the central part of Sagami Bay, Japan: rationale, logistics and overview of results. *Prog. Oceanogr.* 57, 3–16. doi: 10.1016/s0079-6611(03)00047-8

Köster, M., Jensen, P., and Meyer-Reil, L.-A. (1991). "Hydrolytic activities of organisms and biogenic structures in deep-sea sediments," in *Microbial Enzymes in Aquatic Environments*, ed. R. J. Chrost (New York, NY: Springer-Verlag), 298–310. doi: 10.1007/978-1-4612-3090-8_19

Kuhnt, W., Hess, S., Holbourn, A., Paulsen, H., and Salomon, B. (2005). The impact of the 1991 Mt. Pinatubo eruption on deep-sea foraminiferal communities: A model for the Cretaceous–Tertiary (K/T) boundary? *Palaeogeogr. Palaeocl. Palaeoecol.* 224, 83–107. doi: 10.1016/j.palaeo.2005.03.042

Laureillard, J., Méjanelle, L., and Sibuet, M. (2004). Use of lipids to study the trophic ecology of deep-sea xenophyophores. *Mar. Ecol. Prog. Ser.* 270, 129–140. doi: 10.3354/meps270129

Lecroq, B., Gooday, A. J., Cedhagen, T., Sabbatini, A., and Pawlowski, J. (2009a). Molecular analyses reveal high levels of eukaryotic richness associated with enigmatic deep-sea protists (Komokiacea). *Mar. Biodiv.* 39, 45–55. doi: 10.1007/s12526-009-0006-7

Lecroq, B., Gooday, A. J., and Pawlowski, J. (2009b). Global genetic homogeneity in the deep-sea foraminiferan *Epistominella exigua* (Rotaliida: Pseudoparrellidae). *Zootaxa* 2096, 23–32. doi: 10.11646/zootaxa.2096.1.4

Lecroq, B., Gooday, A. J., Tsuchiya, M., and Pawlowski, J. (2009c). A new genus of xenophyophores (Foraminifera) from Japan Trench: morphological description, molecular phylogeny and elemental analysis. *Zool. J. Linn. Soc.* 156, 455–464. doi: 10.1111/j.1096-3642.2008.00493.x

Lecroq, B., Lejzerowicz, F., Bachar, D., Christen, R., Esling, P., Baerlocher, L., et al. (2011). Ultra-deep sequencing of foraminiferal microbarcodes unveils hidden richness of early monothalamous lineages in deep-sea sediments. *Proc. Nat. Acad. Sci. U.S.A.* 108, 13177–13182. doi: 10.1073/pnas.1018426108

Lejzerowicz, F., Esling, P., and Pawlowski, J. (2014). Patchiness of deep-sea benthic foraminifera across the Southern Ocean: insights from high-throughput DNA sequencing. *Deep Sea Res. II* 108, 17–26. doi: 10.1016/j.dsr2.2014.07.018

Lejzerowicz, F., Gooday, A. J., Barrenechea Angeles, I., Cordier, T., Morard, R., Apothéloz-Perret-Gentil, L., et al. (2021). Eukaryotic biodiversity and spatial patterns in the Clarion-Clipperton Zone and other abyssal areas: insights from sediment DNA and RNA metabarcoding. *Front. Mar. Sci.* doi: 10.3389/fmars.2021.671033

Levin, L. A. (1991). Interactions between metazoans and large, agglutinating protozoans: implications for the community structure of deep-sea benthos. *Am. Sci.* 31, 886–900. doi: 10.1093/icb/31.6.886

Levin, L. A., Blair, N. E., Martin, C. M., DeMaster, D. J., Plaia, G., and Thomas, C. J. (1999). Macrofaunal processing of phytodetritus at two sites on the Carolina margin: *in situ* experiments using 13C-labled diatoms. *Mar. Ecol. Prog. Ser.* 182, 37–54. doi: 10.3354/meps182037

Levin, L. A., DeMaster, D. J., McCann, L. D., and Thomas, C. L. (1986). Effects of giant protozoans (class: Xenophyophorea) on deep-seamount benthos. *Mar. Ecol. Prog. Ser.* 29, 99–104. doi: 10.3354/meps029099

Levin, L. A., and Gooday, A. J. (1992). "Possible roles for xenophyophores in deep-sea carbon cycling," in *Deep-Sea Food Chains and the Global Carbon Cycle*, eds G. T. Rowe and V. Pariente (Dordrecht: Kluwer Academic Publishers), 93–104. doi: 10.1007/978-94-011-2452-2_6

Levin, L. A., and Rouse, G. W. (2019). Giant protists (xenophyophores) function as fish nurseries. *Ecology* 101:e02933. doi: 10.1002/ecy.2933

Levin, L. A., and Thomas, C. L. (1988). The ecology of the xenophyophores (Protista) on eastern Pacific seamounts. *Deep Sea Res.* 35, 2003–2027. doi: 10.1016/0198-0149(88)90122-7

Linke, P. (1992). Metabolic adaptations of deep-sea benthic foraminifera to seasonally varying food input. *Mar. Ecol. Prog. Ser.* 81, 51–63. doi: 10.3354/meps081051

Linke, P., Altenbach, A. V., Graf, G., and Heeger, T. (1995). Response of deep-sea benthic foraminifera to a simulated sedimentation event. *J. Foram. Res.* 25, 75–82. doi: 10.2113/gsjfr.25.1.75

Lipps, J. H., and Valentine, J. W. (1970). The role of foraminifera in the trophic structure of marine communities. *Lethaia* 3, 279–286. doi: 10.1111/j.1502-3931.1970.tb01271.x

Lisitzin, A. P. (1996). *Oceanic Sedimentation: Lithology and Geochemistry*. Washington, DC: American Geophysical Union.

McClain, C. R. (2021). The commonness of rarity in a deep-sea taxon. *Oikos* doi: 10.1111/oik.07602

Moodley, L., Middelburg, J. J., Boschker, H. T. S., Duineveld, G. C. A., Pel, R., Herman, P. M. J., et al. (2002). Bacteria and foraminifera: key players in a short-term deep-sea benthic response to phytodetritus. *Mar. Ecol. Prog. Ser.* 236, 23–29. doi: 10.3354/meps236023

Mullineaux, L. S. (1987). Organisms encrusting manganese nodules and crusts: distribution and abundance at three North Pacific sites. *Deep Sea Res.* 34, 165–184. doi: 10.1016/0198-0149(87)90080-x

Mullineaux, L. S. (1988). Taxonomic notes on large agglutinated foraminifers encrusting manganese nodules, including the description of a new genus, *Chondrodapis* (Komokiacea). *J. Foram. Res.* 18, 46–53. doi: 10.2113/gsjfr.18.1.46

Murray, J., and Renard, A. F. (1891). *Report on Deep-Sea Deposits. Report of the Scientific Results of the Voyage of H.M.S. Challenger during the years 1873–76*. 1–529, pls 1–29.

Murray, J. W. (2013). Living benthic foraminifera: biogeographical distributions and the significance of rare morphospecies. *J. Micropalaeontol.* 32, 1–58. doi: 10.1144/jmpaleo2012-010

Nomaki, H., Heinz, P., Nakatsuka, T., Shimanaga, M., and Kitazato, H. (2005). Species-specific ingestion of organic carbon by deep-sea benthic foraminifera and meiobenthos: In situ tracer experiments. *Limnol. Oceanogr.* 50, 134–146. doi: 10.4319/lo.2005.50.1.0134

Nomaki, H., Heinz, P., Nakatsuka, T., Shimanaga, M., Ohkouchi, N., Ogawa, N. O., et al. (2006). Different ingestion patterns of ^{13}C-labeled bacteria and algae by deep-sea benthic foraminifera. *Mar. Ecol. Prog. Ser.* 310, 95–108. doi: 10.3354/meps310095

Nomaki, H., Ogawa, N. O., Ohkouchi, N., Suga, H., Toyofuku, T., Shimanaga, M., et al. (2008). Benthic foraminifera as trophic links between phytodetritus and

benthic metazoans: carbon and nitrogen isotopic evidence. *Mar. Ecol. Prog. Ser.* 357, 153–164. doi: 10.3354/meps07309

Nozawa, F. (2003). *Benthic Foraminifera from the JET Site, Equatorial Pacific Ocean.* Bachelors thesis. *Graduate School of Science*. Chiba: University of Chiba. (In Japanese).

Nozawa, F. (2005). *A deep-sea benthic foraminiferal assemblage in the equatorial Pacific Ocean,* Masters thesis. *Graduate School of Science*. Chiba: University of Chiba. (In Japanese).

Nozawa, F., Kitazato, H., Tsuchiya, M., and Gooday, A. J. (2006). 'Live' benthic foraminifera at an abyssal site in the equatorial Pacific nodule province: abundance, diversity and taxonomic composition. *Deep Sea Res. I* 51, 1406–1422. doi: 10.1016/j.dsr.2006.06.001

Ohkawara, N. (2006). *Deep-Sea Benthic Foraminiferal Distribution in the Central Pacific*, Masters thesis, Hirosaki University, Japan.

Ohkawara, N. (2011). *Deep-Sea Foraminiferal Fauna in the Equatorial Pacific: Abundance, Distribution and Species Diversity.* Doctoral thesis. Yokohama: Yokohama National University.

Ohkawara, N., Kitazato, H., Uematsu, K., and Gooday, A. J. (2009). A minute new species of *Saccammina* (monothalamous Foraminifera; Protista) from the abyssal Pacific. *J. Micropalaeontol.* 28, 143–151. doi: 10.1144/jm.28.2.143

Okamoto, T. (1998). *Responses of Deep-Sea Benthic Foraminiferal Distribution to Artificial Disturbance during JET*. Bachelors thesis. Shizuoka: University of Shizuoka. (In Japanese).

Pawlowski, J., Fahrni, J., Lecroq, B., Longet, D., Cornelius, N., Excoffier, L., et al. (2007). Bipolar gene flow in deep-sea benthic foraminifera. *Mol. Ecol.* 16, 4089–4096. doi: 10.1111/j.1365-294x.2007.03465.x

Picaglia, L. (1892). Foraminiferi dei Saggi di Fondo dragati nel viaggio di circumnavazione della R. Nave 'Vettor Pisani' comandante G. Palumbo negli anni 1882–85. *Atti. Soc. Nat. Modena Ser. 3* 7, 152–155.

Radziejewska, T. (2002). Responses of deep-sea meiobenthic communities to sediment disturbance simulating effects of polymetallic nodule mining. *Internat. Rev. Hydrobiol.* 87, 457–477. doi: 10.1002/1522-2632(200207)87:4<457::aid-iroh457>3.0.co;2-3

Radziejewska, T., Gooday, A. J., Koltan, M., and Szyrwiel, E. (2006). Deep-sea non-calcareous foraminifera: some examples from the Pacific abyssal nodule field. *Meiofauna Marina* 15, 3–10.

Renaud-Mornant, J., and Gourbault, N. (1990). Evaluation of abyssal meiobenthos in the eastern central Pacific (Clarion-Clipperton fracture zone). *Prog. Oceanogr.* 24, 317–329. doi: 10.1016/0079-6611(90)90041-y

Resig, J. M. (1981). Biogeography of benthic foraminifera of the northern Nazca plate and adjacent continental margin. *Geol. Soc. Am. Mem.* 154, 619–666. doi: 10.1130/mem154-p619

Rex, M. A., and Etter, R. J. (2010). *Deep-Sea Biodiversity: Pattern and Scale*. Cambridge, MA: Harvard University Press.

Rex, M. A., McClain, C. R., Johnson, N. A., Etter, R. J., Allen, J. A., Bouchet, P., et al. (2005). A source-sink hypothesis for abyssal biodiversity. *Am. Nat.* 165, 163–178. doi: 10.2307/3473143

Saidova, Kh. M (1965). Distribution of benthic foraminiferal in the Pacific. *Oceanology* 5, 72–83.

Saidova, Kh. M (1966). Benthic foraminiferal faunas of the Pacific. *Oceanology* 6, 222–227.

Saidova, Kh. M (1974). On large-scale facies confinement of deep-sea benthic foraminifera. *Oceanologica* 14, 534–540.

Saidova, Kh. M (1975). *Benthonic Foraminifera of the Pacific Ocean*. Moskva: Academy of Sciences of the USSR, Akademia Nauk, SSSR, Instituta Okeanologii, 1–875, pls 1–115. (in Russian).

Saidova, Kh. M (1976). *Benthic Foraminifera of the World Ocean (Zonal and Quantitative Distribution)*. Moscow: Akademia Nauk, SSSR, Instituta Okeanologii, 1–159. (in Russian).

Saidova, Kh. M (1981). Recent foraminiferal communities of the Pacific abyssal plains. *Oceanology* 21, 259–262.

Saidova, Kh. M (2000). Facial variability of benthic foraminiferal commuities of the open regions of the ocean. *Oceanology* 40, 66–72.

Schröder, C. J., Scott, D. B., Medioli, F. S., Bernstein, B. B., and Hessler, R. R. (1988). Larger agglutinated foraminifera: comparison of assemblages from central Pacific and western North Atlantic (Nares Abyssal Plain). *J. Foram. Res.* 18, 25–41. doi: 10.2113/gsjfr.18.1.25

Schulze, F. E. (1907a). Die Xenophyophoren, eine besondere Gruppe der Rhizopoden. Wiss Ergebn. Dt. Tiefsee Expedit. *Valdivia* 11, 1–55. doi: 10.1515/9783486745320-005

Schulze, F. E. (1907b). Report on the dredging operations off the west coast of Central America to the Galapagos, to the west coast of Mexico, and the Gulf of California, in charge of Alexander Agassiz, carried on by the U.S. Fish Commission steamer 'Albatross', during 1891, Lieu. Z.L. Tanner U.S.N., commanding. XI. Die Xenophyophoren. *Bull. Mus. Comp. Zool. Harv.* 51, 143–162.

Shi, J., Lei, Y., Li, Q., Lyu, M., and Li, T. (2020). Molecular diversity and spatial distribution of benthic foraminifera of the seamounts and adjacent abyssal plains in the tropical Western Pacific Ocean. *Mar. Micropaleontol.* 156:101850. doi: 10.1016/j.marmicro.2020.101850

Shires, R., Gooday, A. J., and Jones, A. R. (1994). The morphology and ecology of an abundant new komokiacean mudball (Komokiacea, Foraminiferida) from the bathyal and abyssal NE Atlantic. *J. Foram. Res.* 24, 214–225. doi: 10.2113/gsjfr.24.4.214

Simon-Lledó, E., Bett, B. J., Huvenne, V. A. I., Schoening, T., Benoist, N. M., and Jones, D. O. B. (2019b). Ecology of a polymetallic nodule occurrence gradient: Implications for deep-sea mining. *Limonol. Oceanogr.* 64, 1883–1894. doi: 10.1002/lno.11157

Simon-Lledó, E., Bett, B. J., Huvenne, V. A. I., Schoening, T., Benoist, N. M. A., Jeffreys, R. M., et al. (2019a). Megafaunal variation in the abyssal landscape of the Clarion-Clipperton Zone. *Prog. Oceanogr.* 170, 119–133. doi: 10.1016/j.pocean.2018.11.003

Smith, C. R., Paterson, G. L. J., Lambshead, P. J. D., Glover, A. G., Rogers, A. D., Gooday, A. J., et al. (2008). *Biodiversity, Species Ranges, and Gene Flow in the Abyssal Pacific Nodule Province: Predicting and Managing the Impacts of Deep Seabed Mining. ISA Technical Study*. Kingston: International Seabed Authority, ISA Technical Study No. 3, 1–38.

Smith, C. R., Tunnicliffe, V., Colaço, A., Drazen, J. C., Gollner, S., Levin, L. A., et al. (2020). Deep-sea misconceptions cause underestimation of seabed-mining impacts. *Trends Ecol. Evol.* 35, 853–857. doi: 10.1016/j.tree.2020.07.002

Smith, C. R., Washburn, T., Menot, L., Boniface, P., Pape, E., Bribiesca-Contreras, L., et al. (2019). "Sediment macrofauna – A synthesis of sediment macrofaunal biodiversity in the Clarion-Clipperton Zone," in *Deep CCZ Biodiversity Synthesis Workshop Friday Harbor, Washington, USA, 1-4 October 2019, Workshop Report*, Washington DC, 85–107.

Smith, K. L., Laver, M. B., and Brown, N. O. (1983). Sediment community oxygen consumption and nutrient exchange in the central and eastern North Pacific. *Limnol. Oceanogr.* 28, 882–898. doi: 10.4319/lo.1983.28.5.0882

Smith, P. B. (1973). Foraminifera of the North Pacific Ocean. *Geol. Surv. Prof. Pap.* 766. Washington, DC: United States Government Printing Office, 1–27.

Stachowska, Z. (2020). *Deep-sea Foraminiferal Assemblages at a Former Experimental Sediment Disturbance Site in the Clarion-Clipperton Fracture Zone (Subequatorial NE Pacific): Diversity and Distribution of Larger Size Fractions.* Masters thesis. Poland: University of Szczecin.

Sweetman, A. K., Smith, C. R., Shulse, C. N., Maillot, B., Lindt, M., Church, M. J., et al. (2018). Key role of bacteria in the short-term cycling of carbon at the abyssal seafloor in a low particulate organic carbon flux region of the eastern Pacific Ocean. *Limnol. Oceanogr.* 64, 694–713. doi: 10.1002/lno.11069

Szarek, R., Nomaki, H., and Kitazato, H. (2007). Living deep-sea benthic foraminifera from the warm and oxygen-depleted environment of the Sulu Sea. *Deep Sea Res. II* 54, 145–176. doi: 10.1016/j.dsr2.2006.02.017

Tendal, O. S. (1972). A monograph of the Xenophyophoria. *Galathea Rep.* 12, 7–103, pls 1–17.

Tendal, O. S. (1979). Aspects of the biology of Komokiacea and Xenophyophoria. *Sarsia* 64, 13–17. doi: 10.1080/00364827.1979.10411356

Tendal, O. S. (1980). *Stannophyllum setosum* sp. n., a remarkable xenophyophore (Rhizopodea, Protozoa) from the eastern Pacific. *Cah. Biol. Mar.* 21, 383–385.

Tendal, O. S. (1996). Synoptic checklist and bibliography of the Xenophyophorea (Protista), with a zoogeographical survey of the group. *Galathea Rep* 17, 79–101.

Tendal, O. S., and Hessler, R. R. (1977). An introduction to the biology and systematics of Komokiacea. *Galathea Rep.* 14, 165–194, pls 9–26.

Thiel, H. (1975). The size structure of the deep-sea benthos. *Int. Rev. Ges. Hydrobiol. Hydrogr.* 60, 575–606.

Thiel, H. (1983). "Meiobenthos and nanobenthos of the deep sea," in *The Sea*, Vol. 8, ed. G. T. Rowe (New York, NY: Wiley Interscience), 167–230.

Thies, A. (1991). *Die Benthos-Foraminiferen im Europäischen Nordmeer. Berichte aus dem Sondersforschungsbereich 313*, Vol. 31. Kiel: Christian-Albrechts-Universität, 1–97.

Thistle, D. (1979). "Harpacticoid copepods and biogenic structures: implications for deep-sea diversity maintenance," in *Ecological Processes in Coastal and Marine Systems*, ed. R. J. Livingston (New York, NY: Plenum Publishing Corporation), 217–231. doi: 10.1007/978-1-4615-9146-7_11

Thistle, D. (1982). Aspects of the natural history of the harpacticoid copepods of San Diego trough. *Biol. Oceanogr.* 1, 225–238. doi: 10.1080/00222935608655810

Todd, R. (1965). The foraminifera of the tropical Pacific collections of the 'Albatross', 1899–1900. Pt. 4. Rotaliform families and planktonic families. *Bull U.S. Nat. Mus.* 161, 1–127, pls 1–28.

Travis, J. L., and Bowser, S. S. (1991). "The motility of Foraminifera," in *Biology of Foraminifera*, eds J. J. Lee and O. R. Anderson (London: Academic Press), 92–115.

Turley, C. M., Gooday, A. J., and Green, J. C. (1993). Maintenance of abyssal benthic foraminifera under high pressure and low temperature: some preliminary results. *Deep Sea Res. I* 40, 643–652. doi: 10.1016/0967-0637(93)90063-9

van Oevelen, D., Soetaert, K., Garcia, R., de Stigter, H. C., Cunha, M. R., Pusceddu, A., et al. (2011). Canyon conditions impact carbon flows in food webs of three sections of the Nazare canyon. *Deep Sea Res. II* 58, 2461–2476. doi: 10.1016/j.dsr2.2011.04.009

Veillette, J., Sarrazin, J., Gooday, A. J., Galéron, J., Caprais, J. C., Vangriesheim, A., et al. (2007). Ferromanganese nodule fauna in the equatorial north Pacific Ocean: species richness, faunal cover and spatial distribution. *Deep Sea Res. I* 54, 1912–1935. doi: 10.1016/j.dsr.2007.06.011

Voltski, I., Weiner, A., Tsuchiya, M., and Kitazato, H. (2018). *Syringammina limosa* sp. nov., the first xenophyophore from the deep Sea of Okhotsk: morphological and genetic description. *Deep Sea Res. II.* 154, 32–46. doi: 10.1016/j.dsr2.2017.12.001

Walch, C. C. (1978). *Recent Abyssal Benthic Foraminifera from the Eastern Equatorial Pacific*. Masters thesis. University of Southern California. Available online at: http://digitallibrary.usc.edu/cdm/compoundobject/collection/p15799coll37/id/383807/rec/304 (accessed April 9, 2021).

Washburn, T. W., Menot, L., Bonifácio, P., Pape, E., Błażewicz, M., Bribiesca-Contreras, G., et al. (2021). Patterns of macrofaunal biodiversity across the Clarion-Clipperton Zone: an area targeted for seabed mining. *Front. Mar. Sci.* 8:626571. doi: 10.3389/fmars.2021.626571

Washburn, T. W., Turner, P. J., Durden, J. M., Jones, D. O. B., Weaver, P., and Van Dover, C. L. (2019). Ecological risk assessment for deep-sea mining. *Ocean Coast. Manag.* 176, 24–39. doi: 10.1016/j.ocecoaman.2019.04.014

Watling, L., Guinotte, J., Clark, M. R., and Smith, C. R. (2013). A proposed biogeography of the deep ocean floor. *Prog. Oceanogr.* 111, 91–112. doi: 10.1016/j.pocean.2012.11.003

Würzberg, L., Peters, J., and Brandt, A. (2011). Fatty acid patterns of Southern Ocean shelf and deep sea peracarid crustaceans and a possible food source, foraminiferans. *Deep Sea Res. II* 58, 2027–2035. doi: 10.1016/j.dsr2.2011.05.013

Conflict of Interest: JP was employed by ID-GENE Ecodiagnostics LTD.

The remaining authors declare that the research was conducted in the absence of any commercial or financial relationships that could be construed as a potential conflict of interest.

Copyright © 2021 Gooday, Lejzerowicz, Goineau, Holzmann, Kamenskaya, Kitazato, Lim, Pawlowski, Radziejewska, Stachowska and Wawrzyniak-Wydrowska. This is an open-access article distributed under the terms of the Creative Commons Attribution License (CC BY). The use, distribution or reproduction in other forums is permitted, provided the original author(s) and the copyright owner(s) are credited and that the original publication in this journal is cited, in accordance with accepted academic practice. No use, distribution or reproduction is permitted which does not comply with these terms.

frontiers in Marine Science

ORIGINAL RESEARCH
published: 01 July 2021
doi: 10.3389/fmars.2021.671062

Megafaunal Ecology of the Western Clarion Clipperton Zone

Jennifer M. Durden[1,2], Meagan Putts[2], Sarah Bingo[2], Astrid B. Leitner[2,3], Jeffrey C. Drazen[2], Andrew J. Gooday[1,4], Daniel O. B. Jones[1], Andrew K. Sweetman[5], Travis W. Washburn[2] and Craig R. Smith[2]*

[1] National Oceanography Centre, Southampton, United Kingdom, [2] Department of Oceanography, University of Hawai'i at Mānoa, Honolulu, HI, United States, [3] Monterey Bay Aquarium Research Institute, Moss Landing, CA, United States, [4] Life Science Department, Natural History Museum, London, United Kingdom, [5] The Lyell Centre for Earth and Marine Science, Heriot-Watt University, Edinburgh, United Kingdom

The Clarion Clipperton Zone (CCZ) is a vast area of the central Pacific Ocean where the abyssal seabed is a focus for future polymetallic nodule mining. Broad-scale environmental gradients occur east-to-west across the CCZ seabed, including organic matter supply and nodule abundance, factors that influence benthic faunal community structure and function. A network of protected areas across the CCZ, called Areas of Particular Environmental Interest (APEIs), has been designated to cover this variation. Most previous studies of the benthic environment and megafaunal communities have focussed on the eastern CCZ, leaving the impact of these large-scale gradients unexamined and the network design untested. Seamounts are a further source of heterogeneity in the region. We examined the benthic megafaunal ecology of three APEIs in the western CCZ, spanning a range of environmental conditions. We used a combination of seabed photography and direct sampling to assess the environment and megafauna on the soft sediment habitats on the abyssal plain in three APEIs, and seamounts in two of those APEIs. We found that environmental conditions on abyssal plains differed between the three APEIs in terms of water depth, nodule abundance and coverage, sediment particle size distribution, and estimated organic matter flux. Megafauna were low density and high diversity, with few common morphotypes between sites and many morphotypes being observed only once. Xenophyophores dominated the assemblages. The density and diversity of invertebrates were greater at the sites with lower organic matter inputs and greater nodule abundance. Seamounts in the same APEIs were nodule-free and had coarser sediments than on the plain. Invertebrate megafaunal diversity was lower on the seamounts than on the plains, and most morphotypes recorded on the seamounts were only found on seamounts. Low morphotype overlap also suggests little connectivity between APEIs, and between seamounts and adjacent abyssal plains. Our results provide the first evaluation of the seabed habitats and megafaunal ecology in the western CCZ, highlighting environmental gradients that influence benthic communities, and are important for evaluating the design of the network of protected areas.

Keywords: seamount, beta-diversity, polymetallic nodule, seabed mining, abyssal plain, Area of Particular Environmental Interest, Marine Protected Area, regional environmental management

OPEN ACCESS

Edited by:
Pedro A. Ribeiro, University of Bergen, Norway

Reviewed by:
Lenaick Menot, Institut Français de Recherche pour l'Exploitation de la Mer (IFREMER), France
Akkur Vasudevan Raman, Andhra University, India

****Correspondence:***
Jennifer M. Durden
jennifer.durden@noc.soton.ac.uk

Specialty section:
This article was submitted to Deep-Sea Environments and Ecology, a section of the journal Frontiers in Marine Science

Received: *22 February 2021*
Accepted: *24 May 2021*
Published: *01 July 2021*

Citation:
Durden JM, Putts M, Bingo S, Leitner AB, Drazen JC, Gooday AJ, Jones DOB, Sweetman AK, Washburn TW and Smith CR (2021) Megafaunal Ecology of the Western Clarion Clipperton Zone. Front. Mar. Sci. 8:671062. doi: 10.3389/fmars.2021.671062

INTRODUCTION

The abyssal seabed of the Clarion Clipperton Zone (CCZ) covers 6 million km^2 of the central Pacific Ocean and has become a focus for future deep-sea polymetallic nodule mining (Lodge et al., 2014). Large-scale gradients of environmental conditions occur across the CCZ, in east-to-west and north-to-south directions (Smith and Demopoulos, 2003; Wedding et al., 2013; Washburn et al., 2021a). These environmental conditions include the seabed substrate and the organic matter supply to the benthos, factors that influence the abundance, diversity, community composition and ecosystem function of deep-sea benthic faunal communities (Smith et al., 1997, 2008, 2009; Ruhl and Smith, 2004; Ruhl et al., 2008; Lacharité and Metaxas, 2017; Simon-Lledó et al., 2020). Across the CCZ, polymetallic nodule abundance and organic matter flux are generally higher in the east than in the west, and the abyssal seabed is deeper to the west (Wedding et al., 2013; Washburn et al., 2021a). The majority of studies of the CCZ, particularly in the last decade, have focused on the eastern portion. Several of these studies highlight the high diversity of benthic megafauna, a faunal group important to ecosystem function (Smith et al., 2008), of the eastern CCZ (e.g., Amon et al., 2016, 2017; Vanreusel et al., 2016; Gooday et al., 2017a,b,c, 2018a; Leitner et al., 2017; Simon-Lledó et al., 2019a; Cuvelier et al., 2020; Harbour et al., 2020; Jones et al., in review). The influence of substrate locally on the benthos in areas of the eastern CCZ was evident in these studies, particularly that of soft sediment texture, and nodule presence and size (Vanreusel et al., 2016; Simon-Lledó et al., 2019b). However, peer-reviewed studies on the benthic megafauna to the west remain few, even when those conducted outside the CCZ are included (e.g., Smith et al., 1997; Simon-Lledó et al., 2019c), or are focused on a single taxonomic or functional group (e.g., Leitner et al., 2017, 2020a; Gooday et al., 2020a,b). Thus, our understanding of the roles of environmental conditions in influencing megafaunal community structure and function, and their variation across the CCZ, is incomplete.

Bathymetric features are a source of heterogeneity in the seabed environment. Features providing positive elevation above the seabed, such as seamounts, are common on abyssal plains and specifically in the far western and eastern areas of the CCZ (Yesson et al., 2011; Wedding et al., 2013; Harris et al., 2014; Washburn et al., 2021a). Large variations in seabed environmental conditions found on seamounts, particularly those related to substrate and organic matter availability, influence the benthic communities present (Fock et al., 2002; Piepenburg and Muller, 2004; Samadi et al., 2007; Clark et al., 2009; McClain et al., 2009; Bo et al., 2011; Williams et al., 2011, 2015; Boschen et al., 2015; Rogers, 2018; Morgan et al., 2019; Cuvelier et al., 2020; Jones et al., in review). Current speeds are enhanced and directions altered around seamounts (Genin et al., 1986), resulting in enhancements to suspended particle flux and locally deposited organic matter (Kiriakoulakis et al., 2009; Vilas et al., 2009). Because seamount summits are shallower than the surrounding abyssal plain, the POC flux to the seabed may also be higher (Lutz et al., 2007). The enhanced currents can also alter the substrate texture, winnowing fine material and exposing hard substrate. Most studies on the megafauna of seamounts in relation to substrate focus on the availability of hard substrate, with little examination of soft sediment habitats. However, studies of smaller elevated features, such as knolls and abyssal hills, show that even subtle differences in elevation produce changes in soft sediments that have a large influence on megafaunal community diversity, standing stocks and assemblage composition (Durden et al., 2015, 2020b; Turnewitsch et al., 2015; Milligan et al., 2016; Leitner et al., 2017).

The governance of future polymetallic nodule mining by the International Seabed Authority (ISA) has included the development of a spatial environmental management plan (the "Regional Environmental Management Plain") for the CCZ, which designated areas to be protected from seabed mining. A network of these "Areas of Particular Environmental Interest" (APEIs) was designed to represent the environmental gradients across the CCZ (Wedding et al., 2013; Lodge et al., 2014). In addition, the APEIs were originally intended (Wedding et al., 2013) to represent similar habitats to those found in areas designated for mining. However, there has been very limited study of seafloor communities within APEIs; only small portions of some APEIs have been studied, leaving in question the extent to which this objective has been met. The APEIs in the western CCZ were located to span areas of high to low predicted nodule abundance, and moderate to low seabed organic matter supply. Recent studies have investigated APEIs in the eastern CCZ (Vanreusel et al., 2016; Simon-Lledó et al., 2019a; Jones et al., in review), but none have yet been conducted in the APEIs in the western CCZ.

Here, we report on the benthic megafaunal ecology of the abyssal plains in three APEIs in the western CCZ and examine the results in a regional context. We hypothesise that environmental conditions differ in the three abyssal plain areas, in terms of physical habitat (bathymetry, sediment conditions and nodule characteristics), in addition to known differences in resource (organic matter) inputs. We aim to determine whether standing stocks, diversity and assemblage structure of the invertebrate megafauna and highly mobile scavengers/predators differ across the region in response to these environmental gradients. We compare soft sedimented habitats on seamounts adjacent to these abyssal sites, and examine differences from the abyssal plain in both the sedimentary environment and faunal assemblages. We test these hypotheses using seabed photography and direct sampling of the sedimentary environment. We then use these data to comment on potential relationships between habitat heterogeneity and megafaunal assemblages in terms of regional variation (beta-diversity) across the western CCZ, and the potential for connectivity within and between habitats. Finally, we set these data in the contexts of regional variation across the whole CCZ, and conditions in nearby mining exploration areas, and comment on the suitability of these APEIs as part of regional environmental management of polymetallic nodule mining and conservation in the CCZ.

MATERIALS AND METHODS

Field Site Selection

Field operations in the western CCZ were conducted from the RV *Kilo Moana* between May 14 and June 16, 2018, as part of the DeepCCZ project, which included assessment of the benthic and benthopelagic environments and communities across an range of size classes from microbes to megafauna as well as ecosystem function (Drazen et al., 2019). Operations for this study were conducted using the remotely operated vehicle (ROV) *Lu'ukai*.

Field sites were selected in each of the three APEIs in the western CCZ (APEIs 1, 4, and 7), and included a location on the abyssal plain in each, and a location on a proximate seamount in APEIs 4 and 7 (**Figure 1**). Practical constraints precluded the examination of a seamount in APEI-1 for this study. Similar site locations were selected across the APEIs based on several criteria: (1) Site locations were selected to be within the CCZ. (2) Central location within the APEI was preferred, with locations in the APEI perimeter "buffer zone" (as described by Wedding et al., 2013) avoided, if possible. In order to meet the other criteria in APEI 1, the study site was located in the southern buffer zone. (3) Predicted high nodule abundance on the abyssal plain based on geological modelling (International Seabed Authority, 2010; Wedding et al., 2013) was preferred, so that abyssal plain sites would be comparable to those in areas to be mined. (4) The presence of a suitable seamount with an area of abyssal plain outside the presumed zone of seamount influence was required. The zone of influence was estimated to extend outwards from the seamount base for 15 km, based on a maximum influence of 30 km from the summit for very large seamounts with shallow summit depths (Gove et al., 2016). (5) Suitable seamounts each had a summit rising a minimum of 1,000 m above the abyssal plain estimated from satellite bathymetry (SRMT30+), with a "flat" area likely containing soft sediment near the top. Similar summit water depths and geomorphologies between seamounts were preferred, confirmed with shipboard multibeam.

Photo Capture and Processing

Seabed images were captured for the assessment of both the seabed environment and the megafaunal community (**Table 1**). ROV transects were undertaken at a randomly selected heading within the range of headings allowed by environmental conditions (surface winds and currents, bottom currents) and topography, with the aim of minimising suspended sediment from obscuring collected imagery and facilitating reasonable ship movement. Seabed transects at each location were planned to be 2 km in length on abyssal plains and 1 km on seamounts, at a target speed over ground of 0.5 knots, with a target camera altitude of 2.62 m above bottom. Still images were captured at 10-s intervals with a downward-facing Ocean Imaging Systems DSC 24000 digital camera system mounted to the front of the *Lu'ukai* ROV (Nikon 7100 camera set to aperture F8, shutter speed 1/60, focal distance 8.5 feet, images 4,000 × 6,000 pixels). Dedicated lighting was provided by two Ocean Imaging Systems 300 W-S remote head strobes synchronised to the camera shutter. Parallel lasers at a separation of 350 mm were used for scaling in the imagery.

Seafloor photos were examined if they met the following criteria: captured at camera altitudes up to 3 m above the seabed; ROV pitch and roll between −5 and 5 degrees; no overlap between photos; no obscuration (e.g., by large shadows or suspended sediment). The selected photos were cropped to 3,000 × 6,000 pixels to remove obscuration from ROV equipment in the image, and colour-corrected to approximate true-to-life colour in a well-lit environment. Annotations of photos was completed using the Monterey Bay Aquarium Research Institute's Video and Annotation Referencing System (Schlining and Stout, 2006).

Assessment of Environmental Characteristics

Four aspects of the benthic environment were examined: seabed bathymetry, estimated organic matter flux at the seabed, nodule abundance and sediment particle size. Seabed bathymetry was measured using a ship-borne multibeam echosounder (12 kHz Simrad EM120, Kongsberg Maritime), with a swath width of 12–14 km. Measured bathymetry was processed onboard using Qimera software (Quality Positioning Services), gridded at 100 m, with a correction for the sound velocity profile applied. Organic matter flux to the abyssal seabed was estimated as particulate organic matter (POC) flux for the study sites by Leitner et al. (2020a) based on a model by Lutz et al. (2007). POC flux to the seamount summits was not estimated because the coarse bathymetric model used by Lutz et al. (2007) to estimate of seafloor POC flux does not reliably capture seamount summit depth.

The density, seabed cover, and individual sizes of nodules were assessed in a randomly selected subset of 1090 seabed photographs (**Table 1**). A single annotator enumerated and measured all nodules in the central portion of each image in the subset (2,000 × 1,500 pixels; representing ∼0.92 m^2 seabed), a size selected for the practicality of annotating images with high densities of nodules.

Sediment was collected in pushcores (70 mm internal diameter) deployed by the ROV at locations near the seabed photograph transects (**Table 1**). Particle size distributions were determined by laser diffraction using a Malvern Mastersizer on the refrigerated collected sediment (0–50 mm horizon) suspended in reverse osmosis water (i.e., without digestion), following the removal of any nodules. Particle size distributions were divided into three size ranges for analysis, to divide the major modes in the distributions: fine particles (<17.5 μm), intermediate-sized particles (17.5–174 μm) and coarse particles (>174 μ m).

Megafaunal Community Assessment

Megafauna (generally > 10 mm in dimension, *sensu* Grassle et al., 1975) were enumerated in the photos and classified to the most detailed taxonomic level possible based on previously published studies of megafauna in the CCZ (**Figures 2**, **3**; Simon-Lledó et al., 2019a,b,c; Cuvelier et al., 2020;

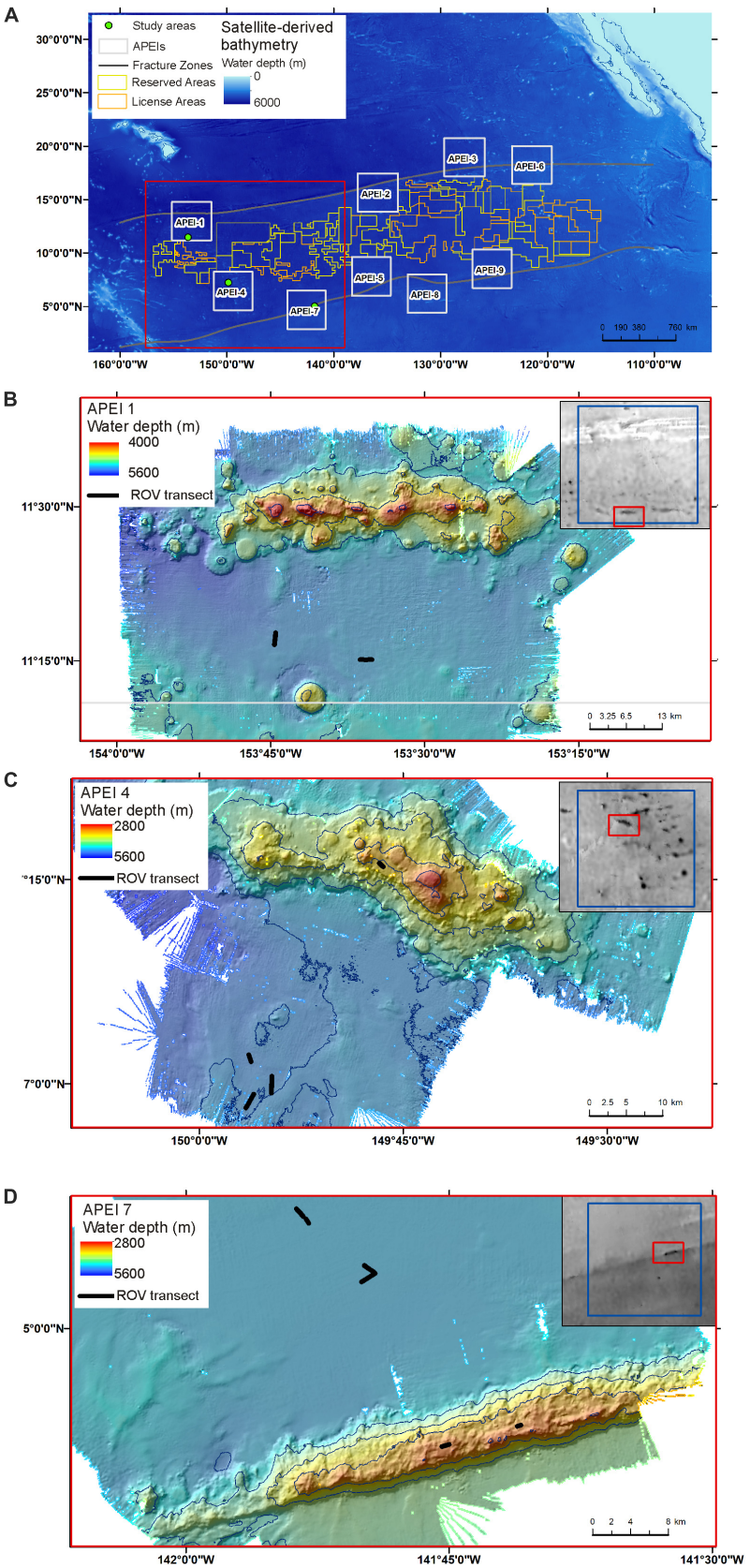

FIGURE 1 | Maps of the region **(A)**, and of the study areas in **(B)** APEI-1, **(C)** APEI-4, and **(D)** APEI-7.

TABLE 1 | Sediment coring and photographic transect information for the study sites in the western CCZ. Four sample units were created of 73 photos for nodule coverage and 312 photos for megafauna on the abyssal plain; on the seamounts, those sample unit sizes could not be achieved (indicated by *).

	Abyssal plain			Seamount	
Location	**APEI-1**	**APEI-4**	**APEI-7**	**APEI-4**	**APEI-7**
Centre latitude (°)	11.252	6.994	5.058	7.267	4.889
Centre longitude (°)	−153.604	−149.935	−141.827	−149.777	−141.753
Water depth (m)	5,198–5,251	4,999–5,039	4,855–4,873	3,538–3,570	3,095–3,247
Seabed photos for megafaunal assessment	1,250	1,706	1,347	233	325
Seabed area photographed for megafaunal assessment (m^2)	6,767	9,529	7,277	1,341	1,739
Seabed photos for nodule assessment	310	368	295	51	66
No. photo sample units	4	5	4	1*	1*
No. nodules measured	10,117	2,862	0	0	0
Sediment cores	3	4	3	1	1

Kahn et al., 2020). A six-digit alphanumeric code was assigned to each morphotype. Highly mobile scavengers and predators, and monothalamous Foraminifera (Xenophyophoroidea) were treated separately from the remaining "invertebrate megafauna" (see below), and additional investigations were made of key taxonomic groups (i.e., echinoderms, porifera and cnidarians).

Prepared seabed photos (3,000 × 6,000 pixels) were randomly assigned to two experts for megafaunal annotation. In addition to randomising the collections and order of images annotated by each expert, the following steps were taken to reduce annotator bias: (1) Prior to annotation of the main photo set, a subset of images was annotated by both experts, and their detections and classifications of megafauna in this "training" image set were discussed. These annotation data were removed and the images returned to the image pool. (2) Subsets of photos were randomly selected for repeated annotation for assessment and reduction of both inter- and intra-annotator bias in detection and classification of specimens. (3) Following annotation, all identified specimens were reviewed by a single expert on a morphotype basis, and reclassified where necessary to ensure consistency. Annotated counts are provided in **Supplementary Material 1**.

Individual body size (mm) was measured in each specimen in the images. Taxon-specific measurements (Durden et al., 2016a) were made for morphotypes with at least four individuals at each of a minimum of two sites. Fresh wet weight biomass was estimated for echinoderms (Holothuroidea, Crinoidea, Ophiuroidea, Asteroidea, and Echinoidea) from these measured dimensions in the seabed photographs and established length-to-wet weight relationships (Durden et al., 2016a). In the case of echinoids, fresh wet weight was estimated based on a spherical test volume of measured diameter, with an estimated tissue volume of 25% of test volume (Ebert, 2013) converted to fresh mass, assuming a density of 1 g cm^{-3}, a method similar to that employed by Durden et al. (2019).

Megafaunal xenophyophores were enumerated in the seabed photographs (as described above), with identification based on published literature on xenophyophores from the CCZ (Gooday et al., 2017a,b,c, 2018a,b). New morphotypes have been observed in seabed images (Gooday et al., 2020a), and new genera and species have been identified from specimens collected at these sites (Gooday et al., 2020b). The maximum diameter of a subset of 8750 specimens were measured in randomly selected images.

Highly mobile scavengers and predators of interest consisted of highly mobile benthopelagic morphotypes, including all fishes, shrimp-like arthropods and octopus. Individuals of these morphotypes were enumerated in seabed photographs (as described above), and classified based on (Drazen et al., in review). These morphotypes were treated separately to facilitate comparisons with other studies, since many megafaunal assessments omit these taxa, while studies using bait, including those from the wider DeepCCZ project, focus on them (Leitner et al., 2020a; Drazen et al., in review).

Statistical Comparisons Between APEIs

Statistical comparisons of conditions on the abyssal plain were made between APEIs by creating sample units from the set of pooled photos across all transects in an APEI. For statistical comparisons of nodule parameters, annotation data from the abyssal plain locations were aggregated into a minimum of four sample units of 73 randomly selected photographs each, the maximum sample unit size for the smallest nodule image set per APEI (**Table 1**; 295 photographs for nodule assessment at APEI-7). Mean fine, medium and coarse sediment content was computed across cores collected from a site. For statistical comparisons of density, diversity, echinoderm biomass, and community composition, annotation data from the abyssal plain locations were aggregated into a minimum of four sample units of 312 randomly selected photographs, the maximum sample unit size for the smallest image set per APEI (**Table 1**; 1250 seabed photos for megafaunal assessment at APEI-1). Comparisons of individual body size were conducted on a specimen basis. Although the limited photography and sampling on seamounts precluded statistical comparisons, all photographs captured at each seamount were aggregated into a single unit to facilitate computation of ecological metrics.

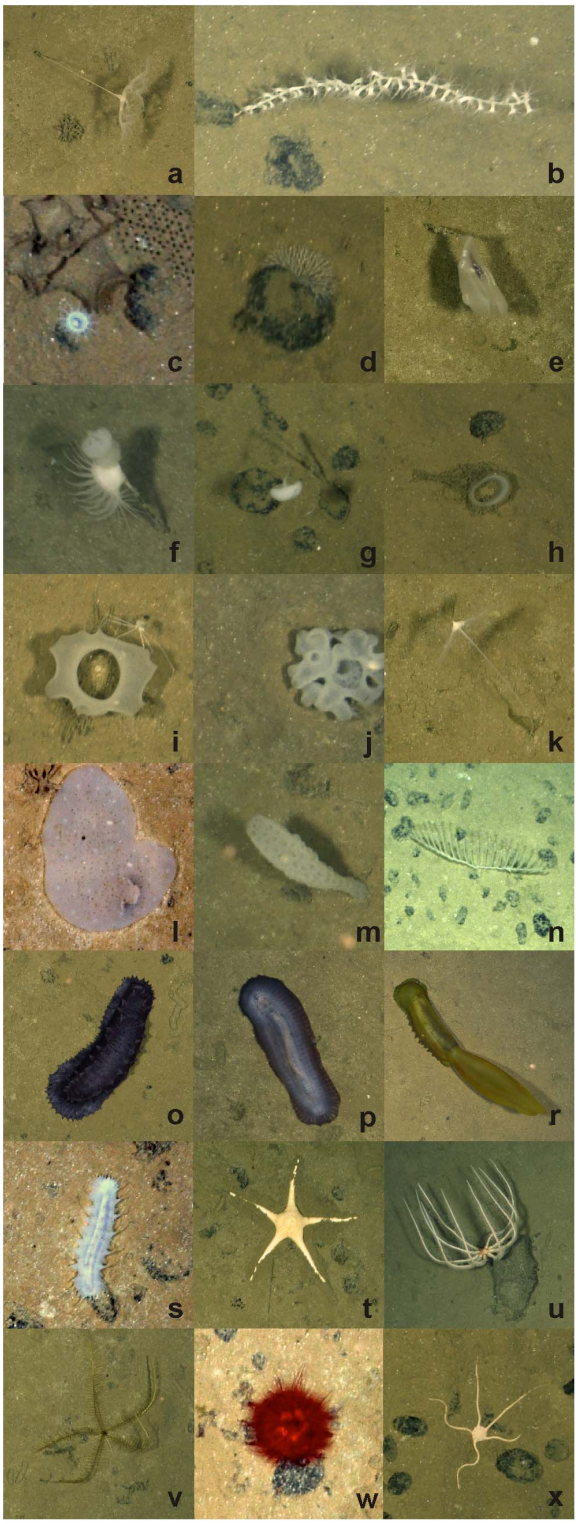

FIGURE 2 | Select invertebrate megafaunal specimens photographed on the abyssal plain in study areas of the western CCZ, with identifications and morphotype codes: **(a)** *Umbellula* sp. PEN003, **(b)** Isididae ALC005, **(c)** actiniarian ACT022 with large xenophyophore and *Paleodictyon* trace to top right; **(d)** Bryozoa BRY002; Ctenophora **(e)** *Lyrocteis* sp. CTE010; Porifera *(Continued)*

FIGURE 2 | Continued
(f) *Hyalonema* sp. POR030 with Actiniaria ACT042, **(g)** *Caulophacus* sp. HEX027 and nodules, **(h)** *Acanthascus* sp. HEX029, **(i)** *Euplectella* sp. HEX019 with Isopoda, **(j)** *Placopegma* sp. HEX005, **(k)** Cladorhizidae DES012, **(l)** *Docosaccus* sp. HEX015, **(m)** *Euplectellinae* sp. HEX011, **(n)** *Chondrocladia (Symmetrocladia)* cf. *lyra* DES014; Holothuroidea **(o)** *Galatheathuria* sp. HOL038, **(p)** *Benthodytes* sp. HOL042, **(r)** *Psychropotes* cf *dyscrita* HOL047, **(s)** Synallactidae HOL007; Asteroidea **(t)** *Dytaster* sp. AST005, **(u)** Brisingida AST001; **(v)** Pentametrocrinidae CRI002; Echinoidea **(w)** *Kamptosoma* sp. URC013; **(x)** Ophiuroidea OPH010. Image attribution: JM Durden & CR Smith, University of Hawai'i.

Nodule and faunal abundance, and echinoderm biomass were standardised to unit seabed area. Univariate Hill's diversity indices (Nq), morphotype richness (q = 0), exponential of the Shannon index (q = 1), and the inverse of the Simpson's index (q = 2; Magurran, 2013) were computed along with the rarefied number of morphotypes (Hurlbert, 1971) at the minimum number of individuals in any sampling unit (65). Environmental and univariate ecological metrics on the abyssal plains were compared between APEIs using ANOVA, with significance reported at α = 0.05 and *post hoc* testing using Tukey's honest significant difference. Normality was tested by visual inspection of normal quantile plots, and the Shapiro-Wilk normality test. Percentage data were arcsine transformed before assessment. Accumulation curves were computed for median values of density and diversity indices over aggregated images, repeated 500 times.

Differences in apparent assemblage composition were assessed using multivariate statistics (Bray-Curtis dissimilarity measure and 2-dimensional non-metric multidimensional scaling ordination), with the sample unit-like groupings of photographic data on the seamounts included in multidimensional analyses for illustration. Statistical comparisons between the community data on the abyssal plains were tested using ANOSIM and SIMPER routines (Clarke, 1993). All ecological metrics were calculated using the vegan package in R (Oksanen et al., 2012).

RESULTS

Environmental Characteristics

Abyssal Plains

The study sites were located in the three westernmost APEIs in the CCZ (**Figure 1**), with APEI-1 being the most northerly and westerly, and APEI-7 being the most easterly and southerly of the three. In APEI-1, the study site was located in the centre-south portion of the APEI, in a position between an elongated ("ridge-like") seamount to the north and a conical seamount to the south. In APEI-4, the study site was in centre-north portion of the APEI, and in APEI-7, the study site was in the northeast portion of the APEI. Seabed water depth across the region increased from east to west (**Table 2**), though the bathymetry between the APEI study sites is largely unknown, as these were the first seabed mapping exercises in these APEIs and large deviations from satellite-derived bathymetry were observed (e.g., presence or absence of large seamounts in contrast to anticipated bathymetry). The

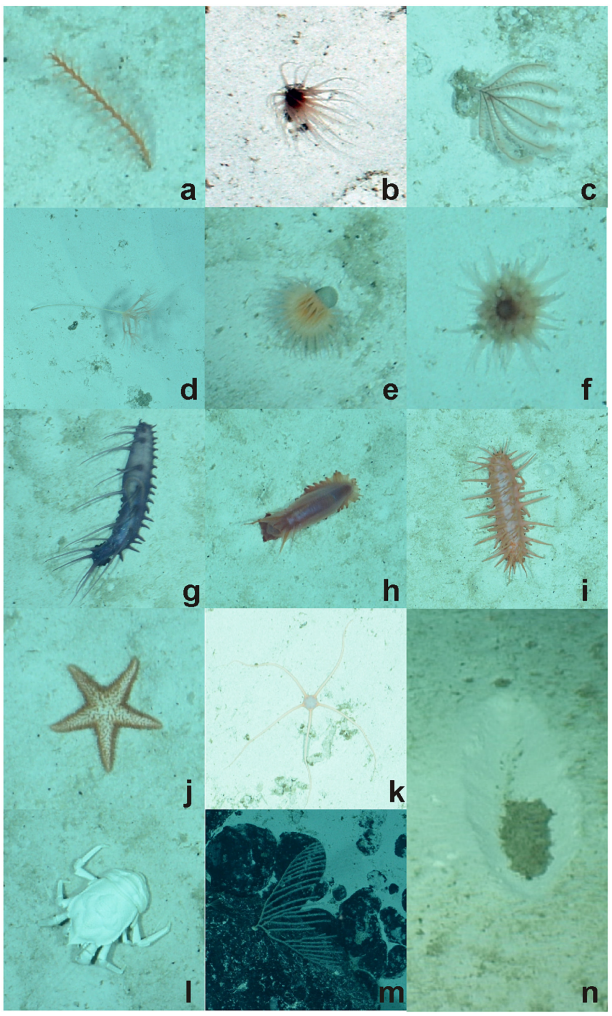

FIGURE 3 | Select invertebrate megafaunal specimens photographed on the seamount study areas in the western CCZ: Cnidaria **(a)** *Protoptilum* sp. PEN017, **(b)** Cerianthidae CER001, **(c)** *Heteropathes* cf. *americana* ALC021, **(d)** *Umbellula* sp. PEN012 with ripples in sediment, **(e)** Actiniaria ACT043, **(f)** Actiniaria ACT012; Holothuroidea: **(g)** *Laetmogone* sp. HOL030, **(h)** *Peniagone* sp. HOL064, **(i)** Deimatidae HOL060; **(j)** Asteroidea AST024; **(k)** Ophiuroidea OPH012; **(l)** Galatheoidea DEC007, **(m)** Actiniaria ACT011 on basalt-type hard substrate, **(n)** large depression in soft sediment (~0.5 × 1.5 m). Image attribution: JM Durden and CR Smith, University of Hawai'i.

seabed on the abyssal plain observed during seabed transects was "flattest" at APEI-7 (elevation difference of 18 m), while elevation differences at least double that (40 and 53 m) were found at APEIs 4 and 1, respectively (**Table 1**). Estimated POC flux at the abyssal seabed decreased from southeast to northwest across the western CCZ (**Table 2**).

Sedimentary conditions differed between the areas studied in the APEIs (**Table 2** and **Figure 4**). Nodule density (number m^{-2}) was significantly different between the APEI study sites [ANOVA $F(2, 10) = 141.9$, $p < 0.001$]. The nodule density observed in APEI-1 was four times that in APEI-4, while no nodules were observed in APEI-7. Seabed cover by nodules was significantly different in the areas studied in each APEI [$F(2, 10) = 187.3$, $p < 0.001$], and significantly higher in APEI-1 than in APEI-4 study sites. Mean nodule size (plan area; mm^2) measured in seabed photographs was significantly larger in the study sites in APEI-1 than in APEI-4 [$F(1, 12977) = 734.4$, $p < 0.0001$]. The observed nodule occurrence was patchy, with areas without nodules observed at APEIs 1 and 4, and nodule densities ranging over two orders of magnitude at APEI-1 (**Figure 4**).

Sediments (excluding nodules) were dark brown in colour (**Figure 2** and **Supplementary Material 2**) from the sediment surface to the full depth collected (~150–200 mm), except in some cores collected at APEI-4, where a colour change to lighter-brown sediment was observed at approximately 100 mm core depth (**Supplementary Material 2**). Particle size distributions had two main peaks (**Figure 4**), the greatest at 80 μm (in the intermediate size range) and a lesser peak at 8 μm (in the fine size range). The fraction of fine sediments on the plain differed between the APEIs [**Table 2**; $F(2, 7) = 16.8$, $p < 0.01$], as was the fraction of intermediate-sized particles [$F(2, 7) = 12.4$, $p < 0.01$], and the coarse sediments [$F(2, 7) = 14.1$, $p < 0.01$]. Sediments at APEI-1 had the highest fine particle content and the smallest fraction of intermediate-sized particles, those at APEI-4 had the greatest proportion of intermediate-sized particles, and those at APEI-7 had the least fine particle content (**Figure 4**).

In summary, a gradient of environmental conditions was observed across the three locations. At the most northwesterly location (APEI-1), the water depth of the abyssal plain was deepest, estimated POC flux was lowest, nodule density and cover were highest, nodules were largest, and sediment grains were finest. APEI-4 exhibited intermediate conditions, including lower nodule density and cover, and smaller nodules. In APEI-7, the seabed water depth was shallowest, estimated POC flux was greatest, nodules were absent, and sediment grains were coarsest.

Seamounts

Both seamounts were ridge features with similar geomorphologies (**Figure 1**), in contrast to conical features also found in the APEIs. The seamount summit in APEI-4 was at 2,800 m water depth, and was deeper at the seamount in APEI-7, at 2,936 m (1,452 and 1,744 m above the abyssal plain, respectively).

The benthic environments at the seamount sites differed substantially from those of the plain. Both were in areas of soft sediment near the ridge of the seamount, with areas of basalt-like hard substrate nearby. No nodules were present. Seamount sediments were a globigerina ooze of white calcareous planktonic foraminifera (**Supplementary Material 3**), with ripples evident. Particle size distributions on the seamounts were different from those on the plain. They were dominated by very coarse particles, with a peak at 480 μm in both APEIs (**Table 2** and **Figure 4**). Lesser peaks in particle size distributions occurred at approximately 120 and 11 μ m.

The environments at the two seamount sites also differed from one another. The site on the seamount at APEI-4 was 439 m deeper than the site on the seamount at APEI-7 (**Table 2**). The former was relatively flat (32 m elevation difference; **Table 1**), while the latter was sloping (152 m elevation difference), with

TABLE 2 | Environmental characteristics of the study areas by APEI and habitat type.

	Abyssal plain			Seamount	
Location	**APEI-1**	**APEI-4**	**APEI-7**	**APEI-4**	**APEI-7**
Mean seabed water depth (m)	5,222	5,013	4,866	3,561	3,122
Estimated seafloor POC flux* (gC_{org} m^{-2} y^{-1})	1.1	1.4	1.8	Not estimated	Not estimated
Mean [95% confidence interval] fine (<17.5 μm) sediment content (%)	46.3 [42.0, 50.6]	40.5 [38.9, 42.0]	39.0 [37.8, 40.1]	15.2	15.8
Mean [95% confidence interval] coarse (>174 μm) sediment content (%)	0.7 [0.4, 1.1]	1.3 [1.0, 1.6]	2.5 [1.8, 3.2]	45.8	44.6
Median nodule size (plan area; mm^2)	744	226	NA	NA	NA
Mean [95% confidence interval] nodule density (counts m^{-2})	34.6 [30.0, 39.1]	8.2 [5.8, 10.5]	0	0	0
Mean [95% confidence interval] seabed nodule cover (%)	3.3 [2.9, 3.8]	0.4 [0.3, 0.5]	0	0	0

Estimated particulate organic matter flux from Leitner et al. (2020a) and Washburn et al. (2021a) based on Lutz et al. (2007). The numbers and sizes of photo sample units or cores are given in **Table 1.*

clumps of phytodetritus visible, and large depressions in the sediment (**Figure 3**). Sediments on the seamount in APEI-4 were somewhat coarser than those on the seamount in APEI-7 (**Table 2**).

Abyssal Plain

Metazoan Invertebrates

Density

Total invertebrate megafaunal density was significantly different between the areas studied in the APEIs [ANOVA $F(2, 10) = 13.7$, $p < 0.01$; **Table 3**]. These differences were driven by significantly lower density at APEI-7 than at APEIs-1 and 4 (both $p < 0.01$; Tukey's HSD).

Diversity

A total of 126 morphotypes were detected at the abyssal plain sites. Similar numbers of morphotypes were found at APEIs 1 and 4 (81 and 80, respectively), while only 49 were found at APEI-7. Only about one sixth of all morphotypes (22) were found in all study areas (**Figure 5**). Many taxa were rare, with 34 morphotypes were only detected once. These morphotypes were spread across many taxonomic groups (e.g., Porifera, Holothuroidea, Asteroidea). APEIs 1 and 4 shared more than 3 times as many morphotypes as APEIs 4 and 7. Morphotypes from across all taxonomic groups were identified that were only found at each APEI study area.

Diversity as represented by the Hill numbers was significantly different between APEIs [N_0: ANOVA $F(2, 10) = 12.1$, $p < 0.01$; N_1: $F(2, 10) = 22.1$, $p < 0.001$; N_2: $F(2, 10) = 27.5$, $p < 0.0001$; **Table 3**]. For all Hill numbers, APEI-7 was significantly lower than APEIs-1 and 4 (all $p < 0.05$; Tukey's HSD). Rarefied morphotype richness (EM_{65}) was also significantly different between APEIs [$F(2, 10) = 9.6$, $p < 0.01$], driven by significantly higher richness in the areas studied at APEI-1 than at APEI-7 ($p < 0.01$; Tukey's HSD).

Assemblage Composition

The metazoan invertebrate assemblage was dominated by cnidarians (42% of individuals) and echinoderms (22%) in the study area at APEI-1 (**Figure 6** and **Table 4**), and by poriferans (35% and 50% of individuals) at APEIs 4 and 7, with the next phylum being cnidarians (32%) and annelids (13%), respectively.

The metazoan invertebrate composition by density was significantly different between the APEI study areas (**Figure 7**; ANOSIM $R = 1$, $p < 0.001$). Morphotypes contributing most to the dissimilarity between APEIs 1 and 4 were *Umbellula* sp. (PEN003) (8%) and unclassifiable Porifera (POR000) (6%), between APEIs 4 and 7 were *Umbellula* sp. (PEN003) (11%) and Echiura (ANN020) (8%) and, and between APEIs 1 and 7 were Echiura (ANN020) (6%) and an actiniarian (ACT022) (5%).

Individual Body Size

Individual body size of a sponge, *Docosaccus* sp. (HEX015), was significantly different between APEIs [ANOVA $F(2, 18) = 5.9$, $p < 0.05$; **Supplementary Material 4**]. TukeyHSD *post hoc* test indicated that body size was significantly greater at APEI-1 than 7. Individual body size of an antipatharian, *Abyssopathes lyra* (ANT002), was significantly greater at APEI-1 than at APEI-4 [$F(1, 16) = 6.8$, $p < 0.05$]. The individual body sizes of other morphotypes were not significantly different between sites.

Echinoderms

The density of echinoderms was significantly different between the APEI study areas [ANOVA $F(2, 10) = 21.9$, $p < 0.001$; **Table 3**], with the density at APEI-7 study site significantly lower than at APEIs 1 and 4 (both $p < 0.01$; TukeyHSD). Echinoderm biomass was not significantly different between APEIs, but mean echinoderm biomass at APEI-4 was approximately twice that of the other APEIs.

A total of 47 echinoderm morphotypes were observed on the abyssal plain. The number of morphotypes observed was significantly different between APEIs [ANOVA $F(2, 10) = 11.48$, $p < 0.01$], with the number at APEI-7 being significantly lower from the other APEIs (both $p < 0.01$; TukeyHSD). Two echinoderm morphotypes were shared between all APEIs (*Galatheathuria* sp. HOL038 and Unclassified holothurians HOL000), while 8 were unique to APEI-1, 13 were unique to APEI-4, and 5 were unique to APEI-7. Holothurians dominated the echinoderms observed at the abyssal plain sites (**Figure 6** and **Table 4**), contributing 39% to echinoderm density, across 21 morphotypes, approximately double the density of the next most common group (echinoids).

The echinoderm assemblage composition by density was significantly different between the APEIs (ANOSIM $R = 0.84$,

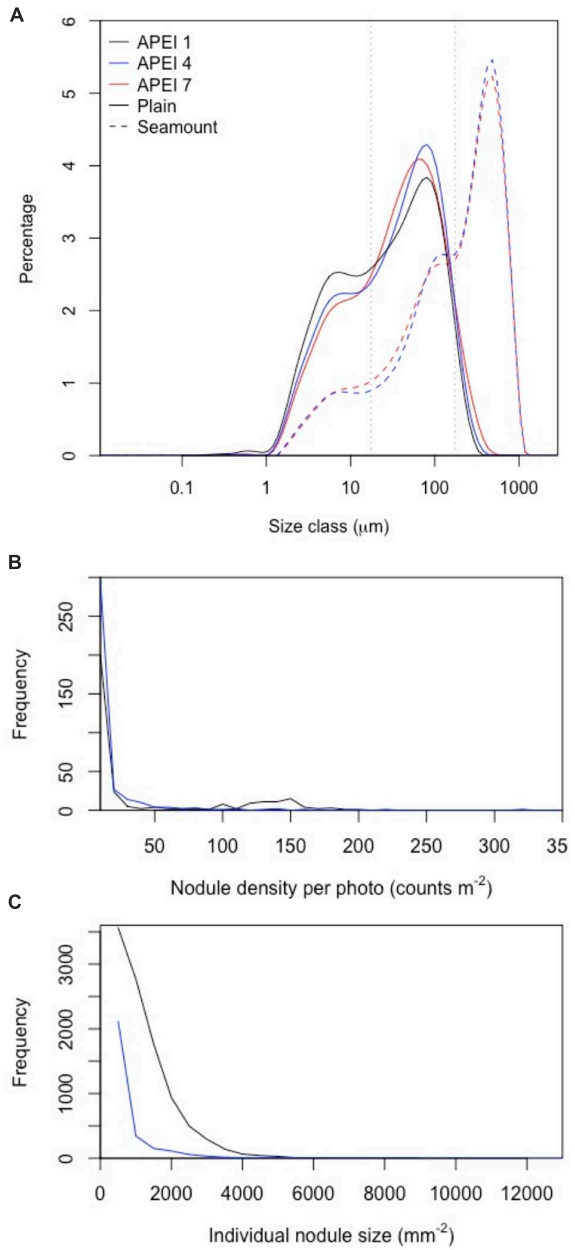

FIGURE 4 | Distributions of particle and nodule parameters at the study sites in the three APEIs in the western CCZ. **(A)** Particle size distributions in sediments collected in cores (0–5 cm horizon) on the plain and seamounts. Grey dotted lines indicate size divisions between fine, intermediate and coarse particles (17.5 and 174 μm). **(B,C)** Distribution of nodule density (per image) and nodule size in APEIs 1 and 4.

$p < 0.001$; **Figure 7**). Morphotypes contributing most to the dissimilarity between APEIs 1 and 4 were *Kamptosoma* sp. URC013 (14%) and Unclassified holothurians HOL000 (8%), between APEIs 4 and 7 were *Kamptosoma* sp. URC013 (17%) and Synallactidae HOL007 (9%), and between APEIs 1 and 7 were Asteroid AST004 (10%) and Synallactidae HOL007 (8%). The echinoderm assemblage composition by biomass was also significantly different between the APEIs (ANOSIM $R = 0.43$, $p < 0.01$). Morphotypes contributing most to this dissimilarity between the APEIs were all large holothurians, with *Galatheathuria* sp. HOL 038 contributing significantly in all comparisons. Differences in assemblage by biomass between APEIs 1 and 4 were principally driven by *Psychropotes* cf *dyscrita* HOL 047 (SIMPER 37%) and *Galatheathuria* sp. HOL 038 (15%), differences between APEIs 4 and 7 driven by *P. dyscrita* HOL 047 (34%) and *Galatheathuria* sp. HOL 038 (26%), and differences between APEIs 1 and 7 driven by *Galatheathuria* sp. HOL 038 (26%) and *Benthodytes* sp. HOL 042 (21%).

Porifera

The density of sponges was significantly different between APEIs [ANOVA $F(2, 10) = 26.9$, $p < 0.0001$]. The lowest density of sponges was observed at APEI-1, where it was less than half the densities observed at APEIs 4 and 7.

The number of sponge morphotypes observed was significantly different between APEIs [$F(2, 10) = 4.2$, $p < 0.05$], with the highest number observed at APEI-7. A total of 29 sponge morphotypes were observed at the abyssal plain sites, with 9 morphotypes being common to all three APEIs (*Cladorhiza* sp. DES010, *Hyalonema* sp. HEX002, *Hyalonema* sp. HEX003, *Placopegma* sp. HEX005, Euplectellinae HEX014, *Docosaccus* sp. HEX015, *Euplectella* sp. HEX019, *Acanthascus* sp. HEX029, Unclassified poriferans POR000). Six unique morphotypes were observed at APEI-1, one at APEI-4 and 7 at APEI-7.

The sponge assemblage composition by density differed significantly between APEIs (ANOSIM $R = 0.65$, $p < 0.001$; **Figure 7**). Morphotypes contribution most to dissimilarity between APEIS 1 and 4 were Unclassified poriferans POR000 (SIMPER 24%) and *Hyalonema* sp. POR002 (SIMPER 18%), between APEIs 4 and 7 were Unclassified poriferans POR000 (13%) and *Docosaccus* sp. HEX015 (13%), and between APEIs 1 and 7 were Unclassified poriferans POR000 (20%) and *Hyalonema* sp. POR002 (16%).

Cnidaria

The density of cnidarians was significantly different between APEIs [ANOVA $F(2, 10) = 42.3$, $p < 0.0001$], and was highest in APEI-1 and lowest in APEI-7.

A total of 37 cnidarian morphotypes were observed on the abyssal plain, with only 6 morphotypes observed at all three sites (Actiniaria ACT009; Actiniaria ACT022; Ceriantharia CER002; Ceriantharia CER005; *Umbellula* sp. PEN003; and Unclassified actiniarians ACT000). Ten morphotypes were unique to APEI-1, five to APEI-4 and one to APEI-7. The number of cnidarian morphotypes observed was significantly different between APEIs [ANOVA $F(2, 10) = 65.8$, $p < 0.0001$], with the number of morphotypes at APEI-7 significantly lower than at the other two APEIs (both $p < 0.0001$) by about threefold, and a significant increase in the number of morphotypes at APEI-1 from APEI-4 ($p < 0.05$). Actiniairians comprised 45% of cnidarian abundance at the sites on the abyssal plain, across 13 morphotypes, more than double the abundance of the other groups.

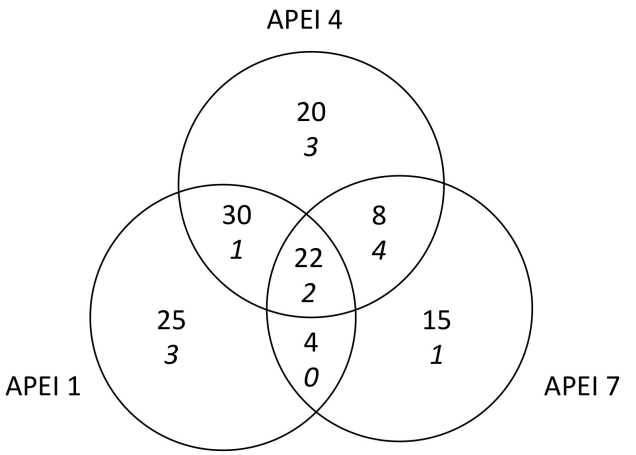

FIGURE 5 | Shared megafaunal morphotypes between APEIs on the abyssal plain for both invertebrates (plain font) and highly mobile scavengers and predators (italics).

The cnidarian assemblage composition by density differed significantly between APEIs (ANOSIM $R = 0.93$, $p < 0.001$; **Figure 7**). Morphotypes contributing most to the dissimilarity between APEIs 1 and 4 were *Umbellula* sp. PEN003 (SIMPER 19%) and Actiniarian ACT022 (13%), between APEIs 4 and 7 were *Umbellula* sp. PEN003 (31%) and *Abyssopathes lyra* ANT002 (8%), and between APEIs 1 and 7 were Actiniarian ACT022 (13%) and Unclassified Alcyonaria ALC000 (10%).

Xenophyophores

Xenophyophores dominated the benthic megafaunal assemblage; densities of xenophyophores on the abyssal plains were two orders of magnitude greater than the densities of invertebrate megafauna (**Table 3** and **Figure 6**). Densities of xenophyophores were significantly different between APEIs [$F(2, 10) = 1876.3$, $p < 0.001$]. The magnitude of difference between APEIs was much greater than in the densities of invertebrate megafauna; densities of xenophyophores at APEI-4 were 1.8 times those at APEI-1 and 5.5 times those at APEI-7. The size of xenophyophore tests ("specimens") on the abyssal plain was significantly different between the APEIs [$F(2, 2889) = 10.1$, $p < 0.001$), driven by specimens at APEI-4 being larger than specimens at the other two APEIs ($p < 0.05$).

Highly Mobile Scavengers and Predators

The total density of highly mobile scavengers/predators differed significantly between the APEIs [$F(2, 10) = 6.0$, $p < 0.05$; **Table 3**], driven by 50% lower densities at APEI-1 than at APEI-7 (TukeyHSD $p < 0.05$). The density at APEI-4 was an intermediate value, and not significantly different from those at APEIs 1 or 7. Diversity was not significantly different between APEIs (ANOVA for all Hill numbers $p > 0.05$). A total of 14 morphotypes were found across the abyssal plain sites, with only two morphotypes (*Aristeidae* sp. DEC003 and unclassified fish OST000) common to all APEIs (**Figure 5**).

Seamounts

Metazoan Invertebrates

Density

Invertebrate megafaunal densities were substantially different between the two seamounts (**Table 3**). At APEI-4, the density on the seamount was within the range of densities found on the abyssal plain sites generally but less than on the plain in APEI-4. The density on the seamount at APEI-7 was approximately 4 times that observed on the seamount at APEI-4.

Diversity

The diversity of invertebrate megafauna in the study areas on the seamounts was generally lower than in those on the abyssal plain (**Table 3**). The number of morphotypes on the seamount at APEI-7 was double that found on the seamount at APEI-4, and more similar to the lowest value found on the plain (also at APEI-7). The Hill numbers and rarefied number of morphotypes were both substantially smaller on the seamounts than on the plain, and were slightly higher at the APEI-4 seamount than at the APEI-7 seamount.

A total of 28 morphotypes of invertebrate megafauna were observed on the seamounts (**Figure 3**). Of these, 61% were only found on the seamounts, while 11 were also found on the plain. A total of 6 were common to both seamounts. Each seamount shared four morphotypes with the adjacent abyssal plain. Only two morphotypes were common to both seamounts and all abyssal plain sites. The metazoan invertebrate assemblage on the seamounts were dominated by cnidarians (83% of individuals at APEI-4 and 78% at APEI-7; **Figure 6**), with echinoderms being the second largest major taxonomic group (15% of individuals at APEI-4 and 20% at APEI-7).

Individual Body Size

Individual body size of a cerianthid CER001, was significantly larger at the seamount at APEI-7 than at APEI-4 [ANOVA $F(1, 28) = 6.8$, $p < 0.05$; **Supplementary Material 4**]. The individual body sizes of other morphotypes were not significantly different between seamounts.

Echinoderms

The density of echinoderms on the seamount at APEI-4 was within the range found at the abyssal plain sites, though half that found on the abyssal plain at APEI-4 (**Table 3**). However, the density of echinoderms on the seamount at APEI-7 was very high, about six times that found at the seamount at APEI-4 and an order of magnitude higher than on the adjacent plain. Echinoderm biomass at APEI-4 was within the range found at the abyssal plain sites, but lower than the biomass found on the abyssal plain at APEI-4. By contrast, echinoderm biomass at APEI-7 was approximately 5 times that found on the adjacent abyssal plain, and more than double the maximum echinoderm biomass found at the plain sites.

The number of echinoderm morphotypes found on the seamounts was within the range of numbers of morphotypes found on the abyssal plain. At APEI-4, the number of echinoderm morphotypes found on the seamount was less than one third

TABLE 3 | Megafaunal community metrics by APEI and habitat type expressed as means [95% confidence interval of the mean] determined in photographic sample units: density, univariate diversity metrics (Hill numbers N_0 [number of morphotypes], N_1 [Shannon index] and N_2 [Simpson's index]; expected number of morphotypes rarefied to 65 specimens, EM_{65}), fresh wet weight biomass of echinoderms.

	Abyssal plain			Seamount	
Location	**APEI-1**	**APEI-4**	**APEI-7**	**APEI-4**	**APEI-7**
Seabed area (m^2)	1,689 [1,682, 1,696]	1,743 [1,733, 1,754]	1,686 [1,677, 1,695]	1,341	1,739
Metazoan invertebrates					
Density (ind m^{-2})	0.058 [0.053, 0.063]	0.059 [0.053, 0.065]	0.042 [0.038, 0.046]	0.049	0.216
N_0	43.0 [40.9, 45.1]	38.6 [33.0, 44.3]	26.3 [21.4, 31.1]	11	23
N_1	30.6 [29.3, 31.9]	24.4 [21.5, 27.3]	16.8 [13.3, 20.3]	4.8	3.9
N_2	22.3 [20.5, 24.0]	15.3 [13.6, 17.1]	11.4 [8.9, 13.8]	3.4	2.2
EM_{65}	33.8 [32.8, 34.7]	29.9 [27.1, 32.7]	24.9 [21.3, 28.5]	10.9	9.7
Echinoderms					
Density (ind m^{-2})	0.013 [0.011, 0.014]	0.015 [0.013, 0.017]	0.004 [0.001, 0.007]	0.007	0.043
N_0	12.8 [11.3, 14.2]	13.2 [10.1, 16.3]	4.8 [1.9, 7.6]	4	9
Biomass (g_{wet} m^{-2})	0.87 [0.41, 1.34]	2.04 [0.55, 3.53]	0.99 [0.23, 1.75]	1.79	4.90
Porifera					
Density (ind m^{-2})	0.012 [0.011, 0.013]	0.021 [0.017, 0.024]	0.021 [0.017, 0.025]	0	0
N_0	7.3 [5.1, 9.4]	8.0 [6.9, 9.1]	11.5 [8.5, 14.5]	0	0
Cnidaria					
Density (ind m^{-2})	0.025 [0.023, 0.027]	0.019 [0.017, 0.022]	0.006 [0.002, 0.009]	0.041	0.170
N_0	17.0 [17.0, 17.0]	14.0 [12.4, 15.6]	5.0 [3.2, 6.8]	6	12
Xenophyophores					
Density (ind m^{-2})	2.065 [1.967, 2.163]	3.734 [3.644, 3.824]	0.680 [0.655, 0.706]	0.128	0.034
Highly mobile scavengers and predators					
Density (ind m^{-2})	0.0013 [0.0010, 0.0016]	0.0020 [0.0015, 0.0024]	0.0028 [0.0019, 0.0037]	0.0037	0.0040
N_0	2.3 [1.8, 2.7]	3.0 [2.1, 3.9]	3.0 [1.6, 4.4]	3.0	2.0

*The numbers and sizes of photographic sample units are given in **Table 1**.*

of the number found on the abyssal plain, while at APEI-7, the number of morphotypes observed on the seamount was almost double that found on the adjacent abyssal plain. In contrast to the abyssal plain sites, holothurians contributed only 25% to echinoderm density at the seamount sites, in 4 morphotypes, while ophiuroids contributed 67% to density, almost entirely in a single morphotype (OPH 012).

Ophiuroidea OPH012 and *Laetmogone* sp. HOL030 were the two morphotypes found in the highest densities at both seamount sites (**Figure 6**). The density of Ophiuroid 012 at the seamount at APEI-7 was particularly high (0.030 ind m^{-2}), 4.4 times the density of the second-ranked *Laetmogone* sp. (0.007 ind m^{-2}); the most common morphotype at the APEI-4 seamount occurred at lower densities than these (0.004 ind m^{-2}). *Laetmogone* sp. was the highest-ranked morphotype in terms of biomass at both seamounts, contributing 99% of biomass at APEI-4 and 53% at APEI-7.

The echinoderm assemblage structures (by density and biomass) on the seamounts appear to be more similar to each other than to the corresponding adjacent abyssal plain (**Figure 7**).

Porifera

No porifera were observed in the soft sedimented environment on the seamounts.

Cnidaria

The density of cnidarians on the seamounts was greater than on the respective adjacent abyssal plain; at APEI-4 the density on the seamount was double that on the plain, while at APEI-7 it was 28 times that observed on the plain. The density of cnidarians was much greater than that of echinoderms on the seamounts, while only slightly greater on the plains.

The number of cnidarian morphotypes found at each of the two seamount sites was within the range found at the sites on the abyssal plain (**Table 3**). The observed morphotype richness at the APEI-7 seamount site was double the number found at the APEI-4 seamount site. A total of 15 cnidarian morphotypes were found on the seamounts, with seven also found on the abyssal plain. Only three cnidarian morphotypes were common to both seamounts. At APEI-4, three morphotypes were found on both the seamount and abyssal plain, while 8 were common to both habitats in APEI-7. In contrast to the abyssal plain, where the dominant actinians were accompanied by much smaller densities of alcyonacea and antipatharia, one seamount assemblage was dominated by alcyonaceans and at the other cerianthids contributed highly to cnidarian and invertebrate density.

As found for echinoderms, the cnidarian assemblage structures by density on the seamounts appear to be more similar

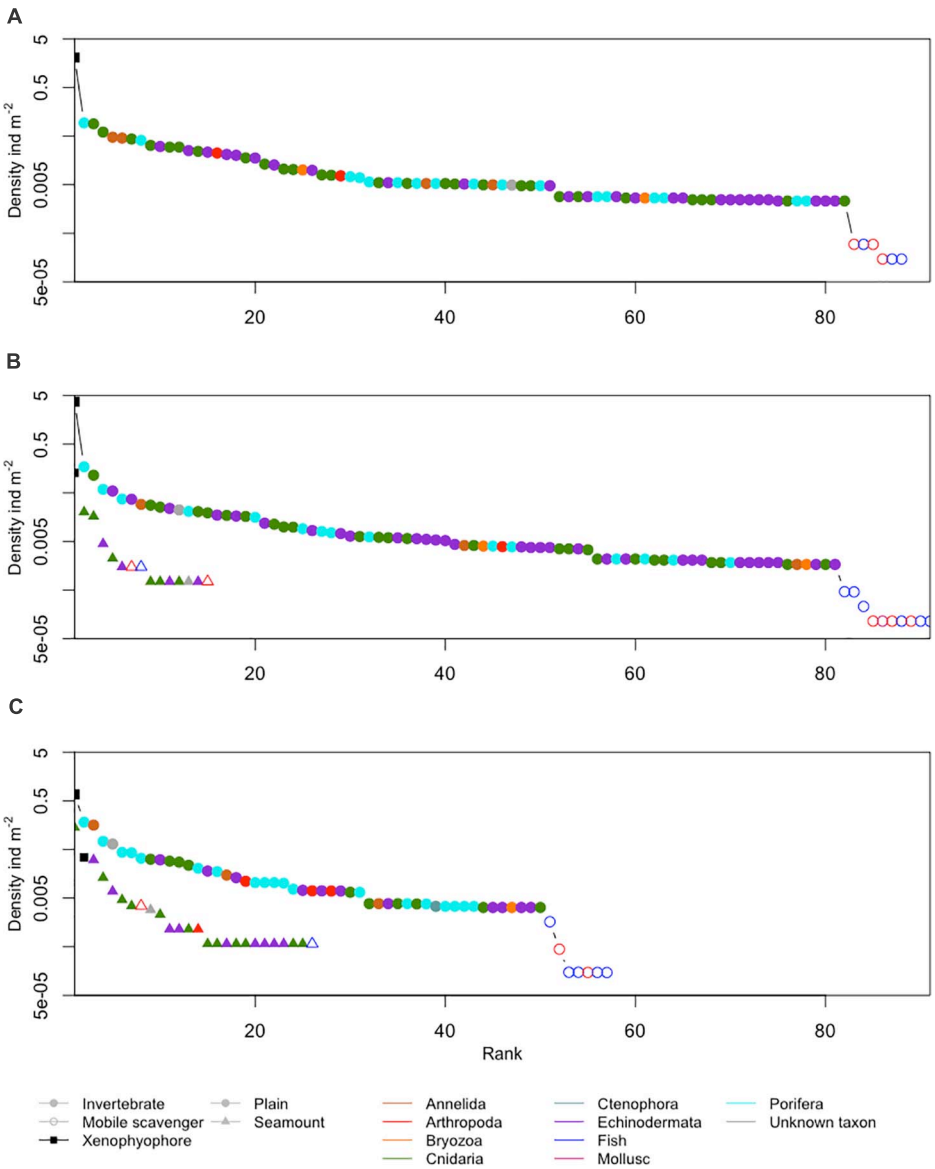

FIGURE 6 | Ranked densities of all seabed megafaunal morphotypes (metazoan invertebrates, highly mobile scavengers/predators, and xenophyophores) observed at **(A)** APEI-1, **(B)** APEI-4, and **(C)** APEI-7. Note the log scale in the y-axis.

to each other than to the corresponding adjacent abyssal plain (**Figure 7**).

Summary

Megafaunal communities in the soft sedimented environments on the seamounts were different from those on the abyssal plain. Invertebrate megafaunal densities were comparable or higher, and diversity was lower on the seamounts than on the plains, and most morphotypes found on the seamounts were unique to that environment. The density of cnidarians was higher on the seamounts than on the plains; in contrast, no porifera were found on the seamounts.

The megafaunal communities on the two seamounts differed from one another. Invertebrate megafaunal density and diversity were lower at APEI-4 than APEI-7. Echinoderm density, diversity and biomass, and cnidarian density and diversity were greater on the seamount at APEI-7.

Xenophyophores

The density of xenophyophores was substantially lower on the seamounts than on the abyssal plain, 29 times smaller at APEI-4 and 22 times smaller at APEI-7 (**Table 3**). There was also substantial difference between the seamounts, with the density of xenophyophores on the seamount at APEI-4 being 3.7 times that at APEI-7. However, xenophyophores were still important to the megabenthic assemblages on the seamounts (**Figure 6**). At APEI-4, the density of xenophyophores was greater than

TABLE 4 | Contributions of major taxonomic groups to the metazoan invertebrate assemblage at the study sites: mean percentage of metazoan invertebrate density (%) and morphotype richness (N_0) over all sample units.

Phylum	Class or order	Abyssal plain						Seamount			
		APEI-1		APEI-4		APEI-7		APEI-4		APEI-7	
		%	N_0	%	N_0	%	N_0	%	N_0	%	N_0
Echinodermata	Asteroidea	1	*4*	1	*2*	5	*4*	0	*0*	1	*3*
	Crinoidea	3	*4*	6	*9*	0	*0*	0	*0*	0.2	*1*
	Echinoidea	5	*4*	6	*4*	0	*0*	2	*1*	0	*0*
	Holothuroidea	8	*10*	9	*15*	5	*6*	9	*1*	4	*4*
	Ophiuroidea	5	*5*	3	*4*	0.3	*1*	5	*2*	14	*1*
Total		22	*27*	25	*34*	10	*11*	16	*4*	19	*9*
Cnidaria	Actiniaria	26	*11*	7	*7*	9	*5*	45	*2*	8	*3*
	Alcyonacea	12	*8*	4	*7*	0	*0*	2	*1*	66	*2*
	Antipatharia	2	*3*	6	*6*	0.3	*1*	0	*0*	0	*0*
	Ceriantharia	1	*3*	1	*2*	3	*3*	35	*2*	4	*5*
	Corallimorpharia	0.2	*1*	2	*1*	0	*0*	0	*0*	0	*0*
	Pennatulacea	0.8	*1*	12	*3*	0.3	*1*	2	*1*	0.5	*2*
Total		42	*27*	32	*26*	13	*10*	82	*6*	79	*12*
Porifera	Desmospongiae	2	*4*	1	*2*	0.3	*1*	0	*0*	0	*0*
	Hexactinellida	8	*11*	10	*9*	20	*12*	0	*0*	0	*0*
	Unclassified porifera	9	*2*	24	*5*	30	*7*	0	*0*	0	*0*
Total		19	*17*	35	*16*	50	*20*	0	*0*	0	*0*

that of invertebrate megafauna (2.6 times), while at APEI-7, xenophyophores were the second ranked morphotype in terms of density (**Figure 6**). Test sizes were significantly smaller on the seamounts than on the plain [$F(1, 78) = 6.3$, $p < 0.05$], but were not different between seamounts.

Highly Mobile Scavengers and Predators

Highly mobile scavengers and predators were observed in greater densities on the seamounts than on the plain. Only the morphotype unclassified Arthropoda (ART000) was common to both seamounts and the abyssal plain.

DISCUSSION

Environmental Drivers of Megafaunal Assemblages on the Abyssal Plains of the Western CCZ

We found low density, high diversity benthic megafaunal communities on the abyssal plains of the western CCZ, with significant differences between the study areas in the three APEIs in both the megafaunal communities and habitat. These community differences were observed in terms of density, diversity and assemblage composition, with few common morphotypes between sites and many rare morphotypes observed only once. Metazoan invertebrate density and diversity were lower to the southeast, at APEI-7, where estimated POC flux was highest, sediments were finest and no nodules were observed. Conversely, metazoan invertebrate density and diversity were higher at APEIs-1 and 4 to the northwest, where nodules were observed on the coarser sediment, and POC flux was estimated to be lower. These environmental factors (nodule abundance, sediment texture, POC flux) are likely to have impacted the observed megafaunal density, diversity and assemblage composition, both directly and in combination.

Nodule Occurrence and Sediment Characteristics as Drivers of Metazoan Megafaunal Assemblages

Nodules are an important source of habitat heterogeneity on abyssal plains, and exert a major influence on megafaunal assemblages across the CCZ. At the western CCZ study sites, there was a 40% increase in density and an increase of 30 morphotypes at the study sites with nodules compared to the site without (**Table 3**). At a local scale, nodule presence has been observed to increase densities twofold, with nodules harbouring specific megafauna, such as antipatharians and alcyonaceans, while some fauna have been observed only in nodule-free areas (Amon et al., 2016; Vanreusel et al., 2016; Simon-Lledó et al., 2019b). Metazoan and foraminiferal densities have been observed to increase substantially, and metazoan assemblage composition to vary, with nodule cover at low nodule coverage (∼1–3%; Simon-Lledó et al., 2019b). Similarly, metazoan diversity was higher at lower nodule densities (<15% seabed cover; Amon et al., 2016) than at higher nodule densities. These community-level variations were a result of changes in the densities of both mobile and non-mobile taxa. The low nodule coverages are comparable to those found at the study sites in APEIs 1 and 4, suggesting that the presence or absence of nodules may have influenced the assemblages observed there. Since nodule cover was

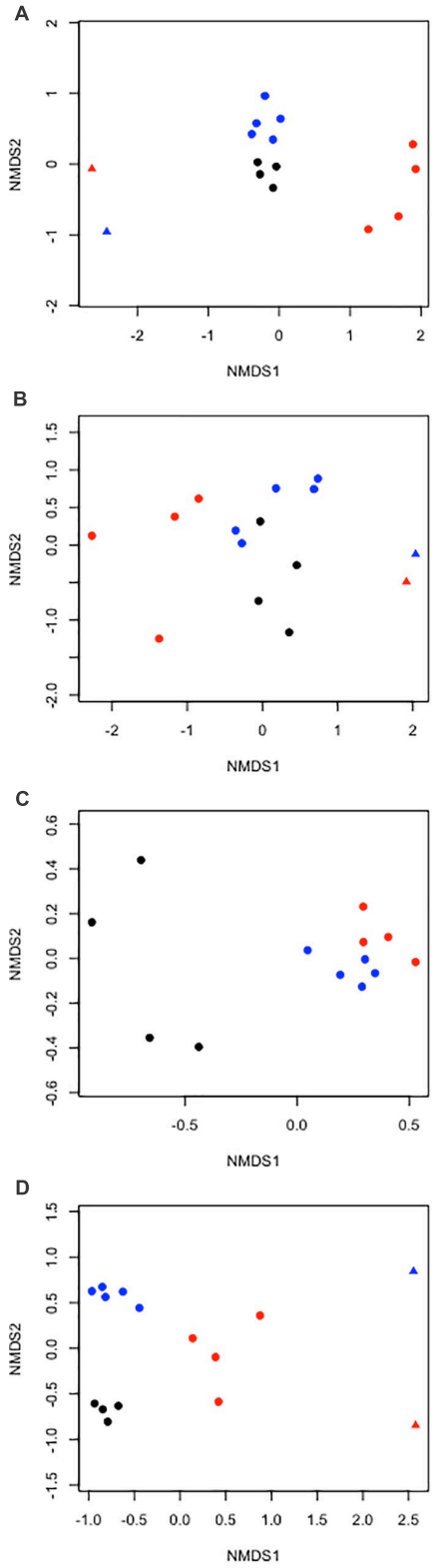

FIGURE 7 | Two-dimensional non-metric multidimensional scaling ordination plots of community composition similarity for echinoderm **(A)** density and **(B)** biomass (fresh wet weight), **(C)** poriferan density, and **(D)** cnidarian density on the abyssal plain (circles) and seamounts (triangles) in the APEIs (1 = black, 4 = blue, 7 = red symbols).

patchy at these two study sites (**Figure 3**), the megafauna observed likely include a combination of morphotypes suited to both nodules and nodule-free areas. These habitat niches are favoured by different taxa, leading to switches in major groups dominant in areas with contrasting nodule presence. For example, while densities of holothurians and (largely nodule-attaching) actiniarians at the high nodule density APEI-1 site were double and triple those observed at the nodule-free APEI-7 study site, densities of (largely non-nodule attaching) hexactinellids and sponges of indeterminate class were halved (**Table 4**). *Docossacus* sp., a plate-shaped glass sponge that is supported on soft sediments by spicules (Kahn et al., 2020), contributed significantly to the high density of hexactinellids at APEI-7. The preference of some taxa for the presence or absence of nodules (latter for hexactinellids) at these sites were confirmed through the analysis of environmental DNA (Laroche et al., 2020). Thus, the habitat heterogeneity provided by the patchy abundance of nodules at APEIs 1 and 4 is likely a substantial driver of variation in the megafaunal communities in the western CCZ.

Nodule-related seabed heterogeneity is accompanied by differences in the soft sediment particle size, which likely also influences the megabenthic assemblage. Taxa that interact with the sediment, such as deposit feeding and burrowing fauna, are sensitive to its granulometric characteristics (Hudson et al., 2005). Nodule-free areas were observed at all three APEIs (**Figure 3**), and few soft-sediment interacting taxa were common to all sites (though the lack of overlapping morphotypes may be related to the small sample size). However, these contributed only a small proportion of all morphotypes observed at the nodule-free APEI-7 study site. Morphotypes that interact with soft sediments (e.g., holothurians, annelids, some asteroids) were observed at all abyssal plain study sites, but the morphotypes present and their densities both varied. Densities of echiurans (ANN020), deposit feeding burrowing annelids that leave large feeding traces on the sediment surface (Bett and Rice, 1993), were highest at APEI-7, with 3.5- and 5.4-fold higher densities than in APEIs 1 and 4, respectively. Differences in densities and observed morphotypes may be related to differences in sediment particle size distributions between the sites (**Figure 3**), with the APEI-7 having the coarsest sediment. Similar relationships between soft-sediment adapted megafaunal morphotypes and sediment texture have been observed with small changes to sediment texture at the nodule-free abyssal Porcupine Abyssal Plain in the Atlantic Ocean (Durden et al., 2020b). Other sediment conditions not measured at these sites, such as porosity and biogeochemical parameters (e.g., Volz et al., 2018), may also influence the assemblage in areas of soft sediments. Finally, the observed sediment particle size distribution is related to other environmental factors important to the faunal assemblage, including the near surface current regime, and deposition and bioturbation of organic material (Turnewitsch et al., 2015), which are influenced by seabed bathymetry. Even small changes in seabed water depth (12.5 m), smaller than those in the study areas (18–50 m), can result in changes in sediment particle size, with corresponding alterations to megafaunal assemblage related to deposit feeders

and burrowing organisms (Durden et al., 2020b). While the effects of sediment texture on megafaunal density and diversity may not be comparable to those of nodules (Simon-Lledó et al., 2019a), our results suggest that particle size may influence the presence and densities of morphotypes in the western CCZ.

Organic Matter Flux as a Driver of Metazoan Megafaunal Assemblages

The differences in the density and diversity of metazoan megafaunal assemblages between APEI study sites were also likely related to the differences in POC flux, a relationship previously observed in the equatorial Pacific and other abyssal areas (Smith et al., 1997). The largest difference in estimated annual POC flux was between the most distant APEIs, with estimated annual POC flux 73% higher at APEI-7 than at APEI-1. The densities of highly mobile scavengers and predators, a group that can be equally surveyed regardless of nodule occurrence, paralleled estimated annual POC flux. This finding contrasts with a regional assessment that found no relationship between POC flux and fish density (though the conclusions of regional synthesis may be confounded by methodological differences of the studies involved) (Drazen et al., in review). In contrast to the pattern for mobile scavengers and predators, observed densities of metazoan invertebrates in this study were lower where POC flux was highest. The relationship between POC flux and megafaunal assemblages is likely complicated by the presence of nodules, as a link between low organic matter deposition and nodule abundance has been observed (Mewes et al., 2014). However, observations of this relationship from a nodule-free abyssal site provide an interesting comparison. Temporal variation in POC flux at the eastern Pacific abyssal time-series site Station M was linked to major alterations to the megafaunal community observed. The densities of suspension and filter feeders decreased while holothurian density increased in relation to an increase in POC flux of two orders of magnitude (0.07–7 gC m^{-2} y^{-1})(Kuhnz et al., 2014). This contrasts with our observations from the western CCZ, where higher densities of porifera (largely filter feeders) were found along with increased POC flux, though the range of POC flux was smaller in magnitude to that of Station M. These high densities of porifera in the western CCZ may be related to nodule presence for attachment, as suggested for the eastern CCZ (Vanreusel et al., 2016). However, the soft sediment-dwelling *Docosaccus* sp. contributed substantially to the relatively high hexactinellid density at APEI-7, where POC flux was highest. The high density of *Docosaccus* sp. was accompanied by smaller individual body sizes, in similarity to observations from Station M, where this sponge recruited quickly after increased POC flux, resulting in increased densities and small body sizes (Kahn et al., 2012; Kuhnz et al., 2014). The high sponge density observed at APEI-7 included only relatively low densities of carnivorous Desmospongiae (0.00015 ind m^{-2}), which were ten times more abundant and diverse at APEI-1 (0.0012 ind m^{-2}), where POC flux was lowest. The densities and diversity of these carnivorous sponges have been observed to increase as filter feeding sponges decline, both at Station M (Kuhnz et al., 2014) and at other nodule fields in the Pacific with similar desmosponge densities (Maldonado et al., 2015). The increase in holothurian densities along with POC flux at Station M were driven by large changes to densities of small holothurians selecting fresh organic matter (e.g., *Peniagone* spp., *Elpidia*); similar morphotypes (e.g., *Peniagone* sp. HOL028, *Deima* sp. HOL018, Elpidiidae HOL020) were observed at APEI-7 but not at APEI-1. The high densities of echiurans at APEI-7 may also be related to their affinity for fresh organic matter (Durden et al., 2020a), in addition to soft sediment texture (above).

The Abyssal Plains of the Western CCZ as Part of the Region

Invertebrate megabenthic densities in the three APEIs in the western CCZ were low compared to other study locations in the central Pacific, without a straightforward relationship to POC flux. Two other studies provide east/west end members to our study locations, with an east-to-west increase in POC flux and megafaunal density between them: the Kiribati Area C to the west, where estimated POC flux (1.5 gC m^{-2} y^{-1}) was 125% and total density (0.12 ind m^{-2}) was 200% of those observed at APEI-1 (Simon-Lledó et al., 2019c); and a central equatorial Pacific site (5°N, 140°W) to the east, where POC flux (1.9 gC m^{-2} y^{-1}; Washburn et al., 2021a) was similar and density (0.18 ind m^{-2}; Smith et al., 1997) was more than four times those at APEI-7. The lower POC flux and difference in megafaunal densities observed at APEIs-1 and 4 may be related to latitude, as more labile organic matter has observed closer to the equator in the Pacific, where upwelling leads to much greater primary production (Smith et al., 1997). Both the Kiribati Area C and the central equatorial Pacific that bookend our study sites east-to-west are at 5°N, similar to APEI-7, and also used photographic methods for estimating megafaunal densities. Thus, it appears that the relationship between estimated POC flux and metazoan densities across the area is not simple.

The observed megafaunal densities in the western APEIs were similar to or lower than those previously observed in the eastern CCZ. Metazoan megafaunal density in APEI-3 (∼0.05 ind m^{-2}) (Vanreusel et al., 2016) was similar to those observed in APEIs 1, 4 and 7. However, the APEI-3 densities are likely an underestimate, as organisms less than 30 mm in size were excluded based on image resolution. In contrast, observed megafaunal densities from the easternmost APEI-6 and eastern CCZ contract areas (BGR, GSR, IFREMER, IOM, TOML, UK-1 contract areas) were substantially higher than those found in the APEIs of the western CCZ: reported metazoan densities ranged from 0.11 to 1.5 ind m^{-2} (Amon et al., 2016; Vanreusel et al., 2016; Simon-Lledó et al., 2019a, 2020; Jones et al., in review), values that may also be underestimates because of similar exclusion of small organisms. Where values were reported, the locations with higher megafaunal densities than the western APEIs also had higher nodule abundance (134 m^{-2} in APEI-6) (Simon-Lledó et al., 2019a) or greater seabed nodule cover (13–37% in TOML contract areas)

(Simon-Lledó et al., 2020), and POC flux similar to or lower (0.5–1.6 gC m^{-2} y^{-1}) than those observed in the western APEIs. These comparisons suggest that environmental and the megafaunal density variations are substantial across the CCZ, and that the relationships between environmental factors and the megafaunal assemblage are complex.

These spatial variations in megafaunal densities across the CCZ may be substantially confounded by temporal variation. The temporal mismatch between studies, often with seasons and years separating observations (e.g., observations from 2013 in Amon et al., 2016; observations from 2018 in this study), makes differentiating spatial from temporal variations difficult. Metazoan megafaunal assemblages have been observed to vary with seasonal and interannual changes to organic matter inputs at other abyssal sites, with densities of some taxa changing by orders of magnitude over periods of 1–2 years (Billett et al., 2001, 2010; Kuhnz et al., 2014). Shorter-term factors altering behaviour of some abyssal organisms, such as movements in sponges that may impact their consistent identification in images, have only just been discovered (Kahn et al., 2020), and longer-term changes to megabenthic biomass and biodiversity are anticipated as a result of climate change (Smith et al., 2008; Jones et al., 2014; Levin et al., 2020).

Diversity of metazoan megafauna on the abyssal plain is high across the CCZ and central Pacific, as evidenced by the high numbers of morphotypes observed (e.g., 136 morphotypes at APEI-6, Simon-Lledó et al., 2019a; 145–189 invertebrate taxa at three TOML sites, Simon-Lledó et al., 2020; 126 morphotypes, this study). The combination of high diversity with low density results in substantial proportions of rare morphotypes. At APEI-6 in the eastern CCZ, 40% of morphotypes were observed fewer than 3 times (Simon-Lledó et al., 2019a), while in the APEIs of the western CCZ, 27% of morphotypes were observed only once. Although direct comparisons of beta-diversity across the region using images is currently precluded by a lack of standardisation of taxonomic identifications and methodological differences including sampling effort, some studies using consistent methodologies have found few overlapping morphotypes between the multiple areas they examined. At the three sites near Kiribati, nearly half (49%) of all morphotypes were detected only at a single location, with only 33% of morphotypes found across all study sites (Simon-Lledó et al., 2019c). Similarly, in the APEIs of the western CCZ, 48% of morphotypes were found only at one of the APEIs, and only 18% of morphotypes were found at all locations. In reviewing taxonomic identifications used in previous studies (see "Megafaunal Community Assessment"), approximately 100 of those observed in this study were not observed in those previous studies. However, the small seabed areas surveyed precludes robust assessments of endemicity from morphotype presence in photographs. Genetic techniques have been used to examine the connectivity of individual species, with connectivity between APEI-6 and adjacent contract areas in the eastern CCZ found for a common demosponge (Taboada et al., 2018).

Xenophyophores on the Abyssal Plains of the Western CCZ

Despite the low densities of megafauna generally in the western CCZ, there was one highly abundant group: agglutinated monothalamous benthic foraminifera (xenophyophores). These giant protists dominated the megafauna at the abyssal plain sites, and were found in the highest densities and largest test sizes at APEI-4. Why this group was particularly successful at this site, characterised by intermediate depth, nodule cover and estimated POC flux, is difficult to assess. Although it was impractical to discriminate between morphotypes among all the specimens (>58,000 were observed), the assemblages are clearly quite diverse. At least 22 morphotypes, some attached to nodules, were recognised in a subset of specimens from the abyssal plain sites (Gooday et al., 2020a). The lack of nodules observed at APEI-7 may result in a lower foraminiferal diversity at the site, similar to the nodule effect on metazoan invertebrates (Amon et al., 2016; Simon-Lledó et al., 2019b). Many of the morphotypes project well above the sediment surface and have morphologies that suggest suspension-feeding or particle trapping trophic strategies (Levin and Gooday, 1992; Gooday et al., 2020b). However, those that are flat-lying are more likely to feed directly on the sediment surface. The combination of species represented may also explain the differing sizes of specimens observed between sites, the large test sizes at APEI-4 possibly being related to a prevalent morphotype.

Although found in high densities and with large test size, the relatively small proportion of test volume occupied by cytoplasm means that megafaunal foraminifera are unlikely to contribute substantially to megafaunal biomass (Levin and Gooday, 1992; Gooday et al., 2018b, 2020a). Estimates were made using a hemisphere to represent the test volume (reasonable for those with reticulated and folded plate-like morphologies) and the method described by Gooday et al. (1993). Mean foraminiferal biomass was estimated at 2.2×10^{-5} g m^{-2} on the abyssal plain in APEI-1 and 4.6×10^{-8} g m^{-2} at APEI-4, a tiny fraction of the observed echinoderm biomass at these sites (**Table 3**). Thus, this group may contribute substantially to biodiversity in the western CCZ, but their contributions to megafaunal biomass appears to be small in these areas.

Xenophyophores dominate the megafauna across much of the CCZ. High densities of these protists were observed from the west, in the Kiribati Area C (0.5 ind m^{-2}) (Simon-Lledó et al., 2019c), to the extreme east of the CCZ, in APEI-6 (2 ind m^{-2}), with lower absolute densities reported in the Russian contract area (0.16 ind m^{-2}) (Kamenskaya et al., 2013) and UK-1 contract area (0.08–0.16 ind m^{-2}) (Amon et al., 2016). The diversity of xenophyophores is often difficult to estimate from seafloor imagery, partly due to the morphological variability of some morphotypes and genetic evidence that morphologically similar specimens may encompass several distinct species (Gooday et al., 2018a). Nevertheless, observations in APEIs 1, 4 and 7 have contributed substantially to the number of observed morphotypes across the CCZ (Gooday et al., 2020a,b). At least one species, *Aschemonella monilis,* has been observed at multiple locations including APEI-4 east to UK-1 contract

area. Morphotype diversity is discussed in more detail in Gooday et al. (2020a).

Seamount Communities in the Western CCZ

The seabed environment at the soft sedimented study areas on the seamounts in APEIs 4 and 7 differ substantially from those found on the adjacent abyssal plain. The white sediments, rich in planktonic foraminiferan shells, are characteristic of many Pacific seamount summits above the carbonate compensation depth (Smith and Demopoulos, 2003). This depth is approximately 4,500 m across the CCZ, but is likely deeper to the west (Mewes et al., 2014). Sediments at these two seamount sites appeared similar in terms of composition and particle size (**Table 2** and **Supplementary Material 3**), but differed from the thin coccolithophore-rich sediment observed at seamount in APEI-6 (Jones et al., in review). Although the seamount study sites in APEIs 4 and 7 are located at low latitudes, the depth of their summits suggest that they likely do not benefit from surface chlorophyll enhancements (Leitner et al., 2020b), but organic matter may be enhanced by resuspension and increased horizontal flux. These alterations to the seabed environment likely influence the megafaunal communities observed.

Differences in the seabed environments between the two seamounts likely influence the differences in the observed megafaunal densities. The relatively high density (approximately fourfold) and diversity (double the morphotype richness) of metazoan invertebrates observed at the seamount in APEI-7 in comparison to the seamount in APEI-4 is echoed in the density (approximately four times greater) and diversity (double richness) of Cnidaria, and Echinoderm density (approximately six times greater). These differences are likely related to the differences in the mean seabed depths of the surveyed areas, where the APEI-7 seamount is substantially shallower, but also the range of seabed depths surveyed, which was 5 times greater at APEI-7. Such depth differences likely influence megafaunal communities, as observed for relatively small topographic features on the plains (Durden et al., 2015, 2020b; Simon-Lledó et al., 2019a, 2020), with significant differences in megafaunal communities related to species replacement at elevation differences of only 12.5 m (Durden et al., 2020b). The differences in the depth ranges of seabed observations at each seamount has been highlighted as a limitation to comparability between seamounts in the eastern CCZ (Cuvelier et al., 2020).

The significant community differences and lack of morphotype overlap between the metazoan megafaunal communities on seamounts and the abyssal plain are unsurprising, given the > 1,400 m elevation of the study areas above the abyssal plain and significantly different sediment environments. Analysis of environmental DNA in sediments at the same sites also found that communities on the seamounts differed from the plain (Laroche et al., 2020). Dissimilarity between megafaunal communities on seamounts and nearby abyssal plains related to density and diversity was also observed in APEIs-3 and 6 (Cuvelier et al., 2020; Jones et al., in review), with some morphotypes found exclusively on the seamounts. Abyssal hills, similar but comparatively small topographic features, result in significant changes to the seabed environment (Turnewitsch et al., 2015; Morris et al., 2016), megafaunal community structure and ecosystem function (Durden et al., 2015; Mitchell et al., 2020). Depth and substrate are important to the composition and distribution of organisms on seamounts (Tittensor et al., 2009), with species replacement observed to dominate beta diversity processes in seamount communities with depth, rather than changes to species richness (Victorero et al., 2018). The Cuvelier et al. (2020) study of multiple seamounts in the eastern CCZ similarly found reduced similarity in megafaunal communities between seamounts with larger depth differences than between those of similar depth, though the comparison was non-statistical and included both hard and soft substrates. The study areas on the seamounts in the western CCZ focused on soft sediments, thus controlling for differences between hard and soft substrate, and found a high proportion of morphotypes only on the seamounts (61%, representing 89% of individuals on the seamounts), which was likely related to both sediment texture (as described above) and depth differences. Some fauna observed exclusively on the seamounts in APEIs 4 and 7 are likely depth-limited; for example, *Laetmogone* sp. have been observed elsewhere at bathyal rather than abyssal depths (Tyler et al., 1985). Of the morphotypes found on both the seamounts and the abyssal plain, 45% were groups only identifiable to class or order, precluding our ability to assess their ranges specifically. Thus, it may be reasonable to exclude these morphotypes, leaving only 29% of morphotypes (representing 8% of individuals on the seamounts) found in both habitats. This low species overlap between seamounts and abyssal plain, a finding shared by Cuvelier et al. (2020), suggests low connectivity between the habitats.

Low morphotype overlap (21%) between the seamounts in APEIs 4 and 7 is a source of community dissimilarity, and suggests that connectivity between seamounts may also be low. However, the assessment of morphotype overlap must be tempered by the fact that morphotypes were still accumulating at the two seamounts (**Supplementary Material 5**). The limited connectivity between seamounts sites in APEIs 4 and 7 was also reflected in environmental DNA analysis from the same sites (Laroche et al., 2020). These community differences in the seamounts in APEIs 4 and 7 may be related to the ∼440 m difference in water depths of the study areas contributing to range restriction of particular taxa. High variation in connectivity has been observed between seamounts, related to some taxa having wide distributions while others are more localised (Clark et al., 2009). Order and class-level differences between the seamounts in APEIs 4 and 7 are evident, with Asteroidea, Crinoidea, Echinoidea, and Decapoda only observed at the seamount at APEI-7, and Actiniaria, Ceriantharia, Alcyonacea, Pennatulacea, Holothuroidea, and Ophiuroidea at both seamounts, with large differences in abundances of each between seamounts. Similar higher taxonomic-level differences were observed between seamounts in APEI-3 and contract areas in the eastern CCZ (Cuvelier et al., 2020), with Alcyonacea found at all seamounts, but large differences in densities of Antipatharia, Pennatulacea, Porifera, and Echinodermata contributing to the significant

differences in megafaunal communities observed. This apparent lack of connectivity between the seamounts observed in the western CCZ, and variation in connectivity between those studied in the east, may require additional consideration in terms of regional management and conservation planning, as seamount habitats could be impacted by plumes from mining activities on nearby abyssal plains. The high percentage of species represented by singletons, and the continuing accumulation of species at each site (**Supplementary Material 5**), indicate that substantially more sampling of seamounts is required to fully document biodiversity and connectivity of the CCZ seamount fauna. Undersampling is a concern at other seamounts (Cuvelier et al., 2020), which limits the evaluation of biodiversity and connectivity among seamounts and between habitats across the CCZ.

Implications for Regional Management of Polymetallic Nodule Mining

Observations of environmental and faunal conditions across the APEIs are needed to provide evidence to evaluate the design and efficacy of the regional environmental management plan for polymetallic nodule mining. The design of the APEI network aimed to conserve biodiversity and ecosystem function, and was originally planned to span the range of habitat and biological variation across the CCZ, based on modelled biophysical parameters (Wedding et al., 2013). The high diversity of megafauna observed and apparently low connectivity at the western APEIs reinforces the need for the distributed nature of the APEI network. The observations from APEIs 1, 4, and 7 provide important western end members to combine with observations from the eastern CCZ, in creating a regional picture that could be used to evaluate whether the APEI network design is suitable for its aims. Some examples of potential network evaluation perspectives using these data include:

(1) One evaluation could include adjusting the modelled variation in parameters across the CCZ to reflect ground-truthing from gathered baseline environmental information. The low values of observed polymetallic nodule and invertebrate abundance at the western APEIs, and the bathymetry collected during the DeepCCZ project expedition (**Figure 1**), directly address three of the biophysical parameters used in the APEI network design. The bathymetric data revealed previously unknown seamounts, suggesting that the number of seamounts used in the original design may be an underestimate.

(2) A second evaluation of the APEI network design could include assessing the suitability of these biophysical parameters as suitable proxies of the habitats, biodiversity and ecosystem function. The results of this study suggest that many of the original biophysical parameters continue to be important to the benthic assemblage at the regional scale, as the observed variations in megafaunal assemblages between the study sites in the western CCZ likely result from combined effects of environmental factors, including nodule presence and occurrence, organic matter inputs, depth, and topographic undulation on the abyssal plains. The evaluation would benefit from considering the results of habitat mapping of the region (McQuaid et al., 2020), to assist in evaluating the weighting of these parameters.

(3) Continued evaluation of whether the APEIs represent the habitats and fauna of the mined areas, could incorporate baseline environmental information from the APEIs as it becomes available. Observations from the APEIs could be used in aggregate to compare with those aggregated from contract areas, or more locally to compare with adjacent contract areas directly to determine whether they contain the same habitats and biodiversity, and any overlaps in species. Such comparisons could include syntheses of environmental or habitat parameters (Washburn et al., 2021a), biological data across multiple size classes (e.g., Washburn et al., 2021b, for macrofauna), and habitat mapping (McQuaid et al., 2020). At the contract area scale, the results of this study and those at other APEIs will be vital for spatial planning of work in the contract area in preparation of the environmental impact assessment (Durden et al., 2018; Clark et al., 2020), designation of reference zones (Jones et al., 2018), and wider environmental management (Durden et al., 2017).

Despite the need for baseline information on the APEIs, studies of these areas remain few, and limited in spatial and temporal scope. For example, the seabed areas photographed in each of our study areas encompass only $\sim 5 \times 10^{-7}$% of an APEI that is 1.44×10^{6} km^2 in area (**Table 1**), and whether the photographed areas represent the habitats and megafauna of the remaining portions of the APEIs is unknown. Despite the lack of areal coverage, the observed low density and high diversity of the megafaunal assemblages of the western CCZ provides important information for designing future studies across the APEIs (**Supplementary Material 5**), and points to the potential areal coverage required to ensure the observed area is representative of an APEI (e.g., survey design calculations in Durden et al., 2016b). The observed prevalence of rare morphotypes is particularly important to future survey design, as the detection of rare morphotypes is sensitive to the area surveyed, resulting in the need for a larger study area to document the biodiversity and assess species overlaps than in habitats with few rare morphotypes. A further factor precluding robust comparisons between APEIs and evaluation of the APEI network is the lack of consideration of temporal variation. Studies of the APEIs to date have been conducted in different seasons and years (as noted above), though some studies of APEIs have been conducted at similar times to those of adjacent exploration contract areas, facilitating comparisons (e.g., Amon et al., 2016; Vanreusel et al., 2016). Finally, the practicalities of studying the APEIs must be considered. The paucity of studies conducted at the APEIs in the western CCZ may be in part related to their inaccessibility, as they are distant from shore. Thus, a comprehensive plan to study the APEIs is needed to ensure that observations and data are captured with sufficient consideration for these spatial, temporal and practical factors to produce the necessary data for understanding patterns in the environment and fauna regionally, and for evaluating, maintaining and updating the regional management plan.

CONCLUSION

We provide the first assessment of the megafaunal communities along with aspects of the benthic environment on the abyssal plains and on two seamounts in the APEIs of the western CCZ. Our findings suggest that megafaunal communities are low in density with high biodiversity, including many rare morphotypes. Megafaunal communities differed between abyssal plain sites, and from and between seamount communities, with minimal apparent overlap in morphotypes between these communities (but note the potential influence of small sample sizes). Densities were lower than elsewhere in the CCZ, expanding the variation in observed abundance across the region.

This study provides preliminary, but critical baseline data on these APEIs. In addition to beginning the collection of baseline information on the habitats and megafaunal assemblages of these APEIs, our results provide a western end member for any regional CCZ assessment and ground-truthed evaluation of the APEI network design. Detection of rare morphotypes is sensitive to study size, which was small relative to the area of each APEI. Their prevalence highlights the need for further sampling to cover sufficient seabed areas of these habitats, both in the APEIs and the contract areas, to understand the breadth of biodiversity, and the role of rare species in the ecosystem.

DATA AVAILABILITY STATEMENT

Photographic data used in this study are available from the Deep Sea Animal Research Center at the University of Hawai'i and via the NOAA Deep-Sea Coral & Sponge Map Portal (https://www.ncei.noaa.gov/maps/deep-sea-corals/mapSites.htm). The original contributions presented in the study are included in the article/**Supplementary Material**.

ETHICS STATEMENT

Ethical review and approval was not required for the animal study because this study observed these organisms in their natural environment without interaction.

AUTHOR CONTRIBUTIONS

JMD, JCD, and CS designed the study. JMD, MP, SB, AL, AS, TW, and CS conducted the field work and collected the data. MP, SB, AL, JCD, and AG provided taxonomic expertise. JMD, DJ, and CS planned the statistical analysis. JMD wrote the first draft of the manuscript. All authors contributed to manuscript revision.

FUNDING

This work was supported by the Gordon and Betty Moore Foundation (grant no. 5596), NOAA OAR Office for Ocean Exploration and Research (award no. NA17OAR0110209) and Pew Charitable Trusts (contract no. 30788). Support was also received from the UK Natural Environment Research Council through National Capability funding to NOC as part of the Climate Linked Atlantic Section Science (CLASS) programme (grant no. NE/R015953/1).

ACKNOWLEDGMENTS

We thank the captain and crew of the R/V *Kilo Moana,* the ROV *Lu'ukai* team, and the DeepCCZ Biodiversity Project members for their support at sea. Thanks to James Hunt (NOC) for his assistance with the laser diffraction meter, to Brian Schlining (MBARI) for his assistance in configuring VARS, to Erik Simon-Lledó for the invitation to participate in a megafaunal taxonomic workshop, and the taxonomists who assisted in identifying specimens in images: Rich Mooi (California Academy of Sciences), David Billett (Deep Seas Environmental Solutions Ltd.), Chris Kelley and Les Watling (University of Hawai'i), Antonina Kremenetskaya and Andrey Gebruk (P.P. Shirshov Institute of Oceanology). Photographic data used in this study are available from the Deep Sea Animal Research Center at the University of Hawai'i and via the NOAA Deep-Sea Coral and Sponge Map Portal (https://www.ncei.noaa.gov/maps/deep-sea-corals/mapSites.htm), our thanks to Virginia Moriwake for facilitating the data availability. This is contribution number 11355 from SOEST, University of Hawai'i.

SUPPLEMENTARY MATERIAL

The Supplementary Material for this article can be found online at: https://www.frontiersin.org/articles/10.3389/fmars.2021.671062/full#supplementary-material

REFERENCES

Amon, D., Ziegler, A., Dahlgren, T., Glover, A., Goineau, A., Gooday, A., et al. (2016). First insights into the abundance and diversity of abyssal megafauna in a polymetallic-nodule region in the eastern Clarion-Clipperton Zone. *Sci. Rep.* 6:30492. doi: 10.1038/srep30492

Amon, D. J., Ziegler, A. F., Drazen, J. C., Grischenko, A. V., Leitner, A. B., Lindsay, D. J., et al. (2017). Megafauna of the UKSRL exploration contract area and eastern Clarion-Clipperton Zone in the Pacific Ocean: Annelida, Arthropoda, Bryozoa, Chordata, Ctenophora, Mollusca. *Biodivers. Data J.* 14:e14598. doi: 10.3897/BDJ.5.e14598

Bett, B. J., and Rice, A. L. (1993). The feeding-behavior of an abyssal echiuran revealed by in-situ time-lapse photography. *Deep Sea Res. I Oceanogr. Res. Papers* 40, 1767–1779.

Billett, D. S. M., Bett, B. J., Reid, W. D. K., Boorman, B., and Priede, I. G. (2010). Long-term change in the abyssal NE Atlantic: the 'Amperima Event' revisited. *Deep Sea Res. II. Top. Stud. Oceanogr.* 57, 1406–1417. doi: 10.1016/j.dsr2.2009.02.001

Billett, D. S. M., Bett, B. J., Rice, A. L., Thurston, M. H., Galeron, J., Sibuet, M., et al. (2001). Long-term change in the megabenthos of the Porcupine Abyssal Plain (NE Atlantic). *Progr. Oceanogr.* 50, 325–348.

Bo, M., Bertolino, M., Borghini, M., Castellano, M., Covazzi Harriague, A., Di Camillo, C. G., et al. (2011). Characteristics of the mesophotic megabenthic assemblages of the vercelli seamount (north tyrrhenian sea). *PLoS One* 6:e16357. doi: 10.1371/journal.pone.0016357

Boschen, R. E., Rowden, A. A., Clark, M. R., Barton, S. J., Pallentin, A., and Gardner, J. P. A. (2015). Megabenthic assemblage structure on three New Zealand seamounts: implications for seafloor massive sulfide mining. *Mar. Ecol. Progr. Ser.* 523, 1–14. doi: 10.3354/meps11239

Clark, M. R., Durden, J. M., and Christiansen, S. (2020). Environmental impact assessments for deep-sea mining: can we improve their future effectiveness? *Mar. Pol.* 114. doi: 10.1016/j.marpol.2018.11.026

Clark, M. R., Rowden, A. A., Schlacher, T., Williams, A., Consalvey, M., Stocks, K. I., et al. (2009). The ecology of seamounts: structure, function, and human impacts. *Annu. Rev. Mar. Sci.* 2, 253–278. doi: 10.1146/annurev-marine-120308-081109

Clarke, K. R. (1993). Non-parametric multivariate analyses of changes in community structure. *Aust. J. Ecol.* 18, 117–143.

Cuvelier, D., Ribeiro, P. A., Ramalho, S. P., Kersken, D., Martinez Arbizu, P., and Colaço, A. (2020). Are seamounts refuge areas for fauna from polymetallic nodule fields? *Biogeosciences* 17, 2657–2680. doi: 10.5194/bg-17-2657-2020

Drazen, J., Church, M., Dahlgren, T., Durden, J., Glover, A., Goetze, E., et al. (2019). Exploration of biodiversity and ecosystem structure on seamounts in the Western CCZ. *Oceanogr*.

Drazen, J. C., Leitner, A. B., Jones, D. O. B., and Simon-Lledó, E. (in review). Regional variation in communities of demersal fishes and scavengers across the CCZ. *Front. Mar. Sci.*

Durden, J. M., Bett, B. J., Billett, D. S. M., Horton, T., Morris, K. J., Serpell-Stevens, A., et al. (2016a). Improving the estimation of deep-sea megabenthos biomass: dimension-to-wet weight conversions for abyssal invertebrates. *Mar. Ecol. Progr. Ser.* 552, 71–79. doi: 10.3354/meps11769

Durden, J. M., Bett, B. J., Huffard, C., Ruhl, H. A., and Smith, K. L. Jr. (2019). Abyssal deposit-feeding rates consistent with the metabolic theory of ecology. *Ecology* 100:e02564. doi: 10.1002/ecy.2564

Durden, J. M., Bett, B. J., Huffard, C. L., Pebody, C., Ruhl, H. A., and Smith, K. L. (2020a). Response of deep-sea deposit-feeders to detrital inputs: a comparison of two abyssal time-series sites. *Deep Sea Res. II Top. Stud. Oceanogr.* 173:104677. doi: 10.1016/j.dsr2.2019.104677

Durden, J. M., Bett, B. J., Jones, D. O. B., Huvenne, V. A. I., and Ruhl, H. A. (2015). Abyssal hills–hidden source of increased habitat heterogeneity, benthic megafaunal biomass and diversity in the deep sea. . *Progr. Oceanogr.* 137 (Pt A), 209–218. doi: 10.1016/j.pocean.2015.06.006

Durden, J. M., Bett, B. J., and Ruhl, H. A. (2020b). Subtle variation in abyssal terrain induces significant change in benthic megafaunal abundance, diversity and community structure. *Progr. Oceanogr.* 186:102395. doi: 10.1016/j.pocean.2020.102395

Durden, J. M., Lallier, L. E., Murphy, K., Jaeckel, A., Gjerde, K., and Jones, D. O. B. (2018). Environmental impact assessment process for deep-sea mining in 'the Area'. *Mar. Pol.* 87, 194–202. doi: 10.1016/j.marpol.2017.10.013

Durden, J. M., Murphy, K., Jaeckel, A., Van Dover, C. L., Christiansen, S., Ortega, A., et al. (2017). A procedural framework for robust environmental management of deep-sea mining projects using a conceptual model. *Mar. Pol.* 84, 193–201. doi: 10.1016/j.marpol.2017.07.002

Durden, J. M., Schoening, T., Althaus, F., Friedman, A., Garcia, R., Glover, A., et al. (2016b). "Perspectives in visual imaging for marine biology and ecology: from acquisition to understanding," in *Oceanography and Marine Biology: an Annual Review*, eds R. N. Hughes, D. J. Hughes I, P. Smith, and A. C. Dale (Boca Raton, FL: CRC Press), 1–72.

Ebert, T. (2013). "Potential use of production and biomass for life-history comparisons of sea urchins," in *Echinoderms in a Changing World*, ed. C. Johnson (London: Taylor & Francis Group), 141–150.

Fock, H., Uiblein, F., Koster, F., and von Westernhagen, H. (2002). Biodiversity and species-environment relationships of the demersal fish assemblage at the Great Meteor Seamount (subtropical NE Atlantic), sampled by different trawls. *Mar. Biol.* 141, 185–199. doi: 10.1007/S00227-002-0804-Y

Genin, A., Dayton, P. K., Lonsdale, P. F., and Spiess, F. N. (1986). Corals on seamount peaks provide evidence of current acceleration over deep-sea topography. *Nature* 322, 59–61.

Gooday, A., Durden, J., and Smith, C. (2020a). Giant, highly diverse protists in the abyssal Pacific: vulnerability to impacts from seabed mining and potential for recovery. *Commun. Integr. Biol.* 13, 189–197. doi: 10.1080/19420889.2020.1843818

Gooday, A. J., Bett, B. J., and Pratt, D. N. (1993). Direct observation of episodic growth in an abyssal xenophyophore (Protista). *Deep Sea Res. I* 40, 2131–2143.

Gooday, A. J., Durden, J. M., Holzmann, M., Pawlowski, J., and Smith, C. R. (2020b). Xenophyophores (Rhizaria, Foraminifera), including four new species and two new genera, from the western Clarion-Clipperton Zone (abyssal equatorial Pacific). *Eur. J. Protistol.* 75:125715. doi: 10.1016/j.ejop.2020.125715

Gooday, A. J., Holzmann, M., Caulle, C., Goineau, A. L., Jones, D. O. B., Kamenskaya, O., et al. (2017a). New species of the xenophyophore genus *Aschemonella* (Rhizaria: Foraminifera) from areas of the abyssal eastern Pacific licensed for polymetallic nodule exploration. *Zool. J. Linn. Soc.* 182, 479–499. doi: 10.1093/zoolinnean/zlx052/4554273/New-species-of-the-xenophyophore-genus

Gooday, A. J., Holzmann, M., Caulle, C., Goineau, A. L, Kamenskaya, O., Weber, A. A. T., et al. (2017b). Giant protists (xenophyophores, Foraminifera) are exceptionally diverse in parts of the abyssal eastern Pacific licensed for polymetallic nodule exploration. *Biol. Conserv.* 207, 106–116. doi: 10.1016/j.biocon.2017.01.006

Gooday, A. J., Holzmann, M., Goineau, A. L., Pearce, R. B., Voltski, I., Weber, A. A.-T., et al. (2017c). Five new species and two new genera of xenophyophores (Foraminifera: Rhizaria) from part of the abyssal equatorial Pacific licensed for polymetallic nodule exploration. *Zool. J. Linn. Soc.* 183, 723–748. doi: 10.1093/zoolinnean/zlx093/4757204

Gooday, A. J., Holzmann, M., Goineau, A.l, Kamenskaya, O., Melnik, V. F., Pearce, R. B., et al. (2018a). Xenophyophores (Rhizaria, Foraminifera) from the Eastern Clarion-Clipperton Zone (equatorial Pacific): the genus *Psammina*. *Protist* 169, 926–957. doi: 10.1016/j.protis.2018.09.003

Gooday, A. J., Sykes, D., Goral, T., Zubkov, M. V., and Glover, A. G. (2018b).). Micro-CT 3D imaging reveals the internal structure of three abyssal xenophyophore species (Protista, Foraminifera) from the eastern equatorial Pacific Ocean. *Sci. Rep.* 8:12103. doi: 10.1038/s41598-018-30186-2

Gove, J. M., McManus, M. A., Neuheimer, A. B., Polovina, J. J., Drazen, J. C., Smith, C. R., et al. (2016). Near-island biological hotspots in barren ocean basins. *Nat. Commun.* 7:10581. doi: 10.1038/ncomms10581

Grassle, J. F., Sanders, H. L., Hessler, R. R., Rowe, G. T., and Mclellan, T. (1975). Pattern and zonation–study of Bathyal Megafauna using research submersible alvin. *Deep Sea Res.* 22, 457–481.

Harbour, R. P., Leitner, A. B., Ruehlemann, C., Vink, A., and Sweetman, A. K. (2020). Benthic and demersal scavenger biodiversity in the eastern end of the Clarion-Clipperton Zone–an area marked for polymetallic nodule mining. *Front. Mar. Sci.* 7:458. doi: 10.3389/fmars.2020.00458

Harris, P. T., Macmillan-Lawler, M., Rupp, J., and Baker, E. K. (2014). Geomorphology of the oceans. *Mar. Geol.* 352, 4–24. doi: 10.1016/j.margeo.2014.01.011

Hudson, I. R., Wigham, B. D., Solan, M., and Rosenberg, R. (2005). Feeding behaviour of deep-sea dwelling holothurians: inferences from a laboratory investigation of shallow fjordic species. *J. Mar. Syst.* 57, 201–218. doi: 10.1016/j.jmarsys.2005.02.004

Hurlbert, S. H. (1971). Nonconcept of species diversity–critique and alternative parameters. *Ecology* 52, 577–586.

International Seabed Authority (2010). *A Geological Model of Polymetallic Nodule Deposits in the Clarion Clipperton Fracture Zone*. Kingston: International Seabed Authority.

Jones, D. O. B., Ardron, J. A., Colaco, A., and Durden, J. M. (2018). Environmental considerations for impact and preservation reference zones for deep-sea mining. *Mar. Pol.* 118. doi: 10.1016/j.marpol.2018.10.025

Jones, D. O. B., Yool, A., Wei, C.-L., Henson, S. A., Ruhl, H. A., Watson, R. A., et al. (2014). Global reductions in seafloor biomass in response to climate change. *Glob. Change Biol.* 20, 1861–1872. doi: 10.1111/gcb.12480

Jones, D. O. B., Simon-Lledo, E., Amon, D. J., Bett, B. J., Caulle, C., Clément, L., et al. (in review). *Environment, Ecology, and Potential Effectiveness of an Area Protected From Deep-Sea Mining (Clarion Clipperton Zone, Abyssal Pacific)*.

Kahn, A. S., Pennelly, C. W., McGill, P. R., and Leys, S. P. (2020). Behaviors of sessile benthic animals in the abyssal northeast Pacific Ocean. *Deep Sea Res. II Top. Stud. Oceanogr.* 173:104729. doi: 10.1016/j.dsr2.2019.104729

Kahn, A. S., Ruhl, H. A., and Smith, K. L. (2012). Temporal changes in deep-sea sponge populations are correlated to changes in surface climate and food supply. *Deep Sea Res. I Oceanogr. Res. Papers* 70, 36–41. doi: 10.1016/j.dsr.2012.08.001

Kamenskaya, O. E., Melnik, V. F., and Gooday, A. J. (2013). Giant protists (xenophyophores and komokiaceans) from the Clarion-Clipperton ferromanganese nodule field (eastern Pacific). *Biol. Bull. Rev.* 3, 388–398. doi: 10.1134/s2079086413050046

Kiriakoulakis, K., Vilas, J. C., Blackbird, S. J., Aristegui, J., and Wolff, G. A. (2009). Seamounts and organic matter-Is there an effect? The case of sedlo and seine seamounts, part 2. Composition of suspended particulate organic matter. *Deep Sea Res. II Top. Stud. Oceanogr.* 56, 2631–2645. doi: 10.1016/j.dsr2.2008.12.024

Kuhnz, L. A., Ruhl, H. A., Huffard, C. L., and Smith, K. L. Jr. (2014). Rapid changes and long-term cycles in the benthic megafaunal community observed over 24 years in the abyssal northeast Pacific. *Progr. Oceanogr.* 124, 1–11. doi: 10.1016/j.pocean.2014.04.007

Lacharité, M., and Metaxas, A. (2017). Hard substrate in the deep ocean: How sediment features influence epibenthic megafauna on the eastern Canadian margin. *Deep Sea Res. I Oceanogr. Res. Papers* 126, 50–61. doi: 10.1016/j.dsr.2017.05.013

Laroche, O., Kersten, O., Smith, C. R., and Goetze, E. (2020). Environmental DNA surveys detect distinct metazoan communities across abyssal plains and seamounts in the western Clarion Clipperton Zone. *Mol. Ecol.* 29, 4588–4604. doi: 10.1111/mec.15484

Leitner, A. B., Durden, J. M., Smith, C. R., Klingberg, E., and Drazen, J. C. (2020a). Synaphobranchid eel swarms on abyssal seamounts: largest aggregation of fishes ever observed at abyssal depths. *Deep Sea Res. I Oceanogr. Res. Papers* 167:103423. doi: 10.1016/j.dsr.2020/103423

Leitner, A. B., Neuheimer, A. B., Donlon, E., Smith, C. R., and Drazen, J. C. (2017). Environmental and bathymetric influences on abyssal bait-attending communities of the Clarion Clipperton Zone. *Deep Sea Res. I Oceanogr. Res. Papers* 125, 65–80. doi: 10.1016/j.dsr.2017.04.017

Leitner, A. B., Neuheimer, A. B., and Drazen, J. C. (2020b). Evidence for long-term seamount-induced chlorophyll enhancements. *Sci. Rep.* 10:12729. doi: 10.1038/s41598-020-69564-0

Levin, L. A., and Gooday, A. J. (1992). "Possible roles for xenophyophores in deep-sea carbon cycling," in *Deep-Sea Food Chains and the Global Carbon Cycle*, eds G. T. Rowe and V. Pariente (Dordrecht: Kluwer Academic Publishers), 93–104.

Levin, L. A., Wei, C. L., Dunn, D. C., Amon, D. J., Ashford, O. S., Cheung, W. W. L., et al. (2020). Climate change considerations are fundamental to management of deep-sea resource extraction. *Glob. Chang. Biol.* 26, 4664–4678. doi: 10.1111/gcb.15223

Lodge, M., Johnson, D., Le Gurun, G., Wengler, M., Weaver, P., and Gunn, V. (2014). Seabed mining: international seabed authority environmental management plan for the Clarion–Clipperton Zone. A partnership approach. *Mar. Pol.* 49, 66–72. doi: 10.1016/j.marpol.2014.04.006

Lutz, M. J., Caldeira, K., Dunbar, R. B., and Behrenfeld, M. J. (2007). Seasonal rhythms of net primary production and particulate organic carbon flux to depth describe the efficiency of biological pump in the global ocean. *J. Geophys. Res.* 112. doi: 10.1029/2006jc003706

Magurran, A. E. (2013). *Measuring Biological Diversity*. Oxford: Blackwell Publishing.

Maldonado, M., Aguilar, R., Bannister, R. J., Bell, J. J., Conway, K. W., Dayton, P. K., et al. (2015). "Sponge grounds as key marine habitats: a synthetic review of types, structure, functional roles, and conservation concerns," in *Marine Animal Forests.*), eds S. Rossi, L. Bramanti, A. Gori, and C. Orejas Saco del Valle (Cham: Springer International Publishing), 1–39.

McClain, C. R., Lundsten, L., Ream, M., Barry, J. P., and DeVogelaere, A. P. (2009). Endemicity, biogeography, composition and community structure on a northeast Pacific seamount. *PloS One* 4:e4141. doi: 10.1371/journal.pone.0004141

McQuaid, K. A., Attrill, M. J., Clark, M. R., Cobley, A., Glover, A. G., Smith, C. R., et al. (2020). Using habitat classification to assess representativity of a protected area network in a large, data-poor area targeted for deep-sea mining. *Front. Mar. Sci.* 7:1066. doi: 10.3389/fmars.2020.558860

Mewes, K., Mogollón, J. M., Picard, A., Rühlemann, C., Kuhn, T., Nöthen, K., et al. (2014). Impact of depositional and biogeochemical processes on small scale variations in nodule abundance in the Clarion-Clipperton Fracture Zone. *Deep Sea Res. I Oceanogr. Res. Papers* 91, 125–141. doi: 10.1016/j.dsr.2014.06.001

Milligan, R. J., Morris, K. J., Bett, B. J., Durden, J. M., Jones, D. O. B., Robert, K., et al. (2016). High resolution study of the spatial distributions of abyssal fishes by autonomous underwater vehicle. *Sci. Rep.* 6:26095. doi: 10.1038/srep26095

Mitchell, E. G., Durden, J. M., and Ruhl, H. A. (2020). First network analysis of interspecific associations of abyssal benthic megafauna reveals potential vulnerability of abyssal hill community. *Progr. Oceanogr.* 187:102401. doi: 10.1016/j.pocean.2020.102401

Morgan, N. B., Goode, S., Roark, E. B., and Baco, A. R. (2019). Fine scale assemblage structure of benthic invertebrate megafauna on the North Pacific Seamount Mokumanamana. *Front. Mar. Sci.* 6:715. doi: 10.3389/fmars.2019.00715

Morris, K. J., Bett, B. J., Durden, J. M., Benoist, N. M. A., Huvenne, V. A. I., Jones, D. O. B., et al. (2016). Landscape-scale spatial heterogeneity in phytodetrital cover and megafauna biomass in the abyss links to modest topographic variation. *Sci. Rep.* 6:34080. doi: 10.1038/srep34080

Oksanen, J., Blanchet, F. G., Kindt, R., Legendre, P., Minchin, P. R., O'Hara, R. B., et al. (2012). *"vegan: Community Ecology Package". R Package Version 2.0-5 ed.*

Piepenburg, D., and Muller, B. (2004). Distribution of epibenthic communities on the Great Meteor seamount (North-East Atlantic) mirrors pelagic processes. *Arch. Fish. Mar. Res.* 51, 55–70.

Rogers, A. (2018). The biology of seamounts: 25 years on. *Adv. Mar. Biol.* 79, 137–224. doi: 10.1016/bs.amb.2018.06.001

Ruhl, H. A., Ellena, J. A., and Smith, K. L. (2008). Connections between climate, food limitation, and carbon cycling in abyssal sediment communities. *Proc. Natl. Acad. Sci. U.S.A.* 105, 17006–17011. doi: 10.1073/pnas.0803898105

Ruhl, H. A., and Smith, K. L. (2004). Shifts in deep-sea community structure linked to climate and food supply. *Science* 305, 513–515. doi: 10.1126/science.1099759

Samadi, S., Schlacher, T. A., and Richer de Forges, B. (2007). "Seamount benthos," in *Seamounts: Ecology, Fisheries, and Conservation*, eds T. J. Pitcher, T. Morato, P. J. B. Hart, M. R. Clark, N. Haggan, and R. S. Santos (Oxford: Blackwell), 119–140.

Schlining, B. M., and Stout, N. J. (2006). "MBARI's video Annotation and Reference System," in *Proceedings of the OCEANS 2006*, (Piscataway, NJ: IEEE), 1–5.

Simon-Lledó, E., Bett, B. J., Huvenne, V. A. I., Schoening, T., Benoist, N. M. A., Jeffreys, R. M., et al. (2019a). Megafaunal variation in the abyssal landscape of the Clarion Clipperton Zone. *Progr. Oceanogr.* 170, 119–133. doi: 10.1016/j.pocean.2018.11.003

Simon-Lledó, E., Bett, B. J., Huvenne, V. A. I., Schoening, T., Benoist, N. M. A., and Jones, D. O. B. (2019b). Ecology of a polymetallic nodule occurrence gradient: implications for deep-sea mining. *Limnol. Oceanogr.* 64, 1883–1894. doi: 10.1002/lno.11157

Simon-Lledó, E., Pomee, C., Ahokava, A., Drazen, J. C., Leitner, A. B., Flynn, A., et al. (2020). Multi-scale variations in invertebrate and fish megafauna in the mid-eastern Clarion Clipperton Zone. *Progr. Oceanogr.* 187:102405.

Simon-Lledó, E., Thompson, S., Yool, A., Flynn, A., Pomee, C., Parianos, J., et al. (2019c). Preliminary observations of the abyssal megafauna of Kiribati. *Front. Mar. Sci.* 6:605. doi: 10.3389/fmars.2019.00605

Smith, C., and Demopoulos, W. R. (2003). "The deep Pacific ocean floor," in *Ecosystems of the World*, ed. P. A. Tyler (Amsterdam: Elsevier), 179–218.

Smith, C. R., Berelson, W., Demaster, D. J., Dobbs, F. C., Hammond, D., Hoover, D. J., et al. (1997). Latitudinal variations in benthic processes in the abyssal equatorial Pacific: control by biogenic particle flux. *Deep Sea Res. II Top. Stud. Oceanogr.* 44, 2295–2317. doi: 10.1016/S0967-0645(97)00022-2

Smith, C. R., De Leo, F. C., Bernardino, A. F., Sweetman, A. K., and Arbizu, P. M. (2008). Abyssal food limitation, ecosystem structure and climate change. *Trends Ecol. Evol.* 23, 518–528. doi: 10.1016/j.tree.2008.05.002

Smith, K. L. Jr., Ruhl, H. A., Bett, B. J., Billett, D. S. M., Lampitt, R. S., and Kaufmann, R. S. (2009). Climate, carbon cycling, and deep-ocean ecosystems. *Proc. Natl. Acad. Sci. U.S.A.* 106, 19211–19218. doi: 10.1073/pnas.0908322106

Taboada, S., Riesgo, A., Wiklund, H., Paterson, G. L. J., Koutsouveli, V., Santodomingo, N., et al. (2018). Implications of population connectivity studies for the design of marine protected areas in the deep sea: an example of a demosponge from the Clarion-Clipperton Zone. *Mol. Ecol.* 27, 4657–4679. doi: 10.1111/mec.14888

Tittensor, D. P., Baco, A. R., Brewin, P. E., Clark, M. R., Consalvey, M., Hall-Spencer, J., et al. (2009). Predicting global habitat suitability for stony corals on seamounts. *J. Biogeogr.* 36, 1111–1128. doi: 10.1111/j.1365-2699.2008.02062.x

Turnewitsch, R., Lahajnar, N., Haeckel, M., and Christiansen, B. (2015). An abyssal hill fractionates organic and inorganic matter in deep-sea surface sediments. *Geophys. Res. Lett.* 42, 7663–7672. doi: 10.1002/2015GL065658

Tyler, P. A., Muirhead, A., Billett, D. S. M., and Gage, J. D. (1985). Reproductive biology of the deep-sea holothurians *Laetmogone violacea* and *Benthogone rosea* (Elasipoda: Holothurioidea). *Mar. Ecol. Progr. Ser.* 23, 269–277.

Vanreusel, A., Hilario, A., Ribeiro, P. A., Menot, L., and Arbizu, P. M. (2016). Threatened by mining, polymetallic nodules are required to preserve abyssal epifauna. *Sci. Rep.* 6:26808. doi: 10.1038/srep26808

Victorero, L., Robert, K., Robinson, L. F., Taylor, M. L., and Huvenne, V. A. I. (2018). Species replacement dominates megabenthos beta diversity in a remote seamount setting. *Sci. Rep.* 8:4152. doi: 10.1038/s41598-018-22296-8

Vilas, J. C., Aristegui, J., Kiriakoulakis, K., Wolff, G. A., Espino, M., Polo, I., et al. (2009). Seamounts and organic matter–is there an effect? The case of sedlo and seine seamounts: part 1. Distributions of dissolved and particulate organic matter. *Deep Sea Res. II: Top. Stud. Oceanogr.* 56, 2618–2630. doi: 10.1016/j.dsr2.2008.12.023

Volz, J. B., Mogollón, J. M., Geibert, W., Arbizu, P. M., Koschinsky, A., and Kasten, S. (2018). Natural spatial variability of depositional conditions, biogeochemical processes and element fluxes in sediments of the eastern Clarion-Clipperton Zone, Pacific Ocean. *Deep Sea Res. I Oceanogr. Res. Papers* 140, 159–172. doi: 10.1016/j.dsr.2018.08.006

Washburn, T. W., Jones, D. O. B., Wei, C.-L., and Smith, C. R. (2021a). Environmental Heterogeneity throughout the Clarion-Clipperton Zone. *Front. Mar. Sci.* 8:661685. doi: 10.3389/fmars.2021.661685

Washburn, T. W., Menot, L., Bonifaìcio, P., Pape, E., Błaz?ewicz, M., Bribiesca-Contreras, G., et al. (2021b). Patterns of macrofaunal biodiversity across the Clarion-Clipperton Zone: an area targeted for seabed mining. *Front. Mar. Sci.* 8:250. doi: 10.3389/fmars.2021.626571

Wedding, L. M., Friedlander, A. M., Kittinger, J. N., Watling, L., Gaines, S. D., Bennett, M., et al. (2013). From principles to practice: a spatial approach to systematic conservation planning in the deep sea. *Proc. R. Soc. Lond. B Biol. Sci.* 280:20131684. doi: 10.1098/rspb.2013.1684

Williams, A., Althaus, F., Clark, M. R., and Gowlett-Holmes, K. (2011). Composition and distribution of deep-sea benthic invertebrate megafauna on the Lord Howe Rise and Norfolk Ridge, southwest Pacific Ocean. *Deep Sea Res. II Top. Stud. Oceanogr.* 58, 948–958. doi: 10.1016/j.dsr2.2010.10.050

Williams, A., Althaus, F., and Schlacher, T. A. (2015). Towed camera imagery and benthic sled catches provide different views of seamount benthic diversity. *Limnol. Oceanogr. Methods* 13, 62–73.

Yesson, C., Clark, M. R., Taylor, M. L., and Rogers, A. D. (2011). The global distribution of seamounts based on 30 arc seconds bathymetry data. *Deep Sea Res. I Oceanogr. Res. Papers* 58, 442–453. doi: 10.1016/j.dsr.2011.02.004

Conflict of Interest: The authors declare that the research was conducted in the absence of any commercial or financial relationships that could be construed as a potential conflict of interest.

Copyright © 2021 Durden, Putts, Bingo, Leitner, Drazen, Gooday, Jones, Sweetman, Washburn and Smith. This is an open-access article distributed under the terms of the Creative Commons Attribution License (CC BY). The use, distribution or reproduction in other forums is permitted, provided the original author(s) and the copyright owner(s) are credited and that the original publication in this journal is cited, in accordance with accepted academic practice. No use, distribution or reproduction is permitted which does not comply with these terms.

frontiers in Marine Science

ORIGINAL RESEARCH
published: 26 July 2021
doi: 10.3389/fmars.2021.663420

Spatial Variability of Abyssal Nitrifying Microbes in the North-Eastern Clarion-Clipperton Zone

Anita L. Hollingsworth[1,2], Daniel O. B. Jones[2] and C. Robert Young[2]*

[1] Ocean and Earth Science, National Oceanography Centre Southampton, University of Southampton, Southampton, United Kingdom, [2] National Oceanography Centre, Southampton, United Kingdom

Abyssal microbes drive biogeochemical cycles, regulate fluxes of energy and contribute to organic carbon production and remineralization. Therefore, characterizing the spatial variability of benthic microbes is important for understanding their roles in benthic environments and for conducting baseline assessments of areas of the seabed that might be targeted by commercial mining activities. Yet, detailed assessments of the spatial distributions of benthic microbial communities in these regions are still incomplete, and these efforts have not yet considered the influence of seafloor topography and heterogeneity on microbial distributions across a range of scales. In this study, we investigated the composition and spatial variability of benthic microbial assemblages found in sediments and polymetallic nodules collected from the Clarion Clipperton Zone (CCZ) in the equatorial Pacific (4000–4300 m water depth). We used 16S rRNA gene sequences to characterize these communities. The upper 20 cm of abyssal sediments harbored diverse and distinctive microbial communities in both sediments and their associated polymetallic nodules, with high similarity across topographical areas of the seabed. Assemblage composition differed vertically through the sediment, by habitat and across small to mesoscales. Potential carbon-fixing microbes formed more than 25% relative abundance of sediment assemblages, which were dominated by ammonia-oxidizing Archaea *Nitrosopumilus*. Non-photosynthetic Cyanobacteria were more frequent in the deeper sediment layers and nodules. Sediment communities had a higher abundance of taxa involved in nitrogen cycling, such as *Nitrosopumilus*, *Nitrospina*, *Nitrospira*, *AqS1* (Nitrosococcaceae), and methanogens *wb1-A12* (NC10 phylum). In contrast, nodules were more enriched in Alphaproteobacteria, Gammaproteobacteria, Planctomycetes, Acidobacteria, Bacteroidetes, Nanoarchaeaeota, and *Calditrichaeota*. Microbes related to potential metal-cycling (Magnetospiraceae and *Kiloniellaceae*), organic carbon remineralization (*Woeseia*), and sulfur-oxidizing Thiohalorhabdaceae were also more enriched in nodules. Our results indicate that benthic microbial community composition

OPEN ACCESS

Edited by:
Adrian Glover, Natural History Museum (United Kingdom), United Kingdom

Reviewed by:
Massimiliano Molari, Max Planck Institute for Marine Microbiology (MPG), Germany
Gustavo Fonseca, Federal University of São Paulo, Brazil

***Correspondence:**
Anita L. Hollingsworth
a.l.hollingsworth@southampton.ac.uk

Specialty section:
This article was submitted to Deep-Sea Environments and Ecology, a section of the journal Frontiers in Marine Science

Received: *02 February 2021*
Accepted: *06 July 2021*
Published: *26 July 2021*

Citation:
Hollingsworth AL, Jones DOB and Young CR (2021) Spatial Variability of Abyssal Nitrifying Microbes in the North-Eastern Clarion-Clipperton Zone. Front. Mar. Sci. 8:663420. doi: 10.3389/fmars.2021.663420

is driven by sediment profile depth and seafloor heterogeneity at small and mesoscales. The most abundant microbial taxa within the sediments were nitrifying and putative carbon-fixing microbes, and may have key ecological roles in mediating biogeochemical cycles in this habitat.

Keywords: 16S rRNA, microbial diversity, nitrifiers, deep-sea mining, polymetallic nodules, sediment, Clarion-Clipperton Zone

INTRODUCTION

The high abundances of polymetallic nodules and the possibility of deep-sea mining has heightened scientific and commercial interest in the environment of the Clarion Clipperton Zone (CCZ) in the eastern Pacific (Wedding et al., 2015). In an area of seafloor covering ∼ 6 million km^2 (Wedding et al., 2013), seventeen exploration licenses for nodule mining have been granted since 2001 by the International Seabed Authority (ISA) (Jones et al., 2020). In addition, the ISA have also designated nine Areas of Particular Environmental Interest (APEIs), protected from mining activities and these conservation areas surround the belt of mining contract areas (Lodge et al., 2014). The aim of these conservation areas is to form a network of sites that represent the range of habitats and communities of the CCZ. Ideally, these sites will help to preserve biodiversity in the region, should any mining exploration and activities take place (Wedding et al., 2013). The potential impacts of mining on the benthic assemblages are poorly understood (Jones et al., 2017). Recovery is likely to be very slow, from decades to millions of years (Jones et al., 2017), particularly as nodule formation and growth can range from thousands to millions of years (Kerr, 1984). The process of nodule removal would remove the top layers of sediment and generate plumes near the seabed from the action of the mining collector vehicle as well as in the water column from discharge of sediment-laden water from shipboard dewatering of nodules (Jones et al., 2018). This activity could lead to widespread ecological disturbance on the seafloor. These effects could result from direct physical disturbance of communities, the removal of nodule habitat by the collector, and/or to the resettling of plume sediments to the surrounding seabed over 100's to 1000's km (Rolinski et al., 2001; Smith et al., 2008a). Recovery of benthic assemblages is likely to be very slow in an area with naturally low sedimentation rates (approximately 0.35 cm/kyr; Mewes et al., 2014) and stable physical conditions (Levin et al., 2016). Additionally, the CCZ is a food limited environment, and the benthic ecosystems are structured by a very low flux of particulate organic carbon (POC; fluxes 1 mg C_{org} m^{-2} d^{-1}; Volz et al., 2018) from oligotrophic overlying waters (Smith et al., 2008a; Levin et al., 2016). As a result of a low POC flux, the soft sediments of the CCZ are oxygenated down to 300 cm below seafloor (cmbsf: Mewes et al., 2014; Volz et al., 2018; Menendez et al., 2019).

Despite a low input of carbon, there are highly diverse benthic microbial communities in this region that inhabit the sediment and nodules (Durbin and Teske, 2011; Tully and Heidelberg, 2013; Wu et al., 2013; Blöthe et al., 2015; Shulse et al., 2016; Lindh et al., 2017; Molari et al., 2020). Benthic microbes form a key part of benthic ecosystems by mediating biogeochemical cycles, regulating fluxes of energy and contributing to organic carbon production and remineralization. As well as the input of energy into abyssal ecosystems from photosynthetically derived particulate organic carbon (Ruhl et al., 2008; Smith et al., 2008b, 2009), microbially mediated inorganic C-fixation by chemolithoautotrophic microbes, (Middelberg, 2011; Molari et al., 2013) appear to provide an important carbon subsidy to benthic ecosystems in the CCZ (Sweetman et al., 2019), and more generally (Brunnegård et al., 2004; Tully and Heidelberg, 2016).

Owing to our limited knowledge of microbial communities and their functions in these environments, our ability to predict the impact of commercial mining activities on benthic microbial communities inhabiting the sediment and nodules is also limited. Benthic impact experiments designed to mimic the consequences of mining have indicated that along with metazoans, microbial assemblage recovery is poor (Gjerde et al., 2016; Jones et al., 2017). Microbial abundance in sediments has been reduced by up to 50% following sediment disturbance from plowing at the abyssal DISCOL site (Peru Basin) and recovery times for organic matter (OM) remineralization rates and microbial activity to return to baseline are more than 50 years (De Jonge et al., 2020; Vonnahme et al., 2020).

The CCZ is heterogenous, with bathymetry varying over 2000 m (Washburn et al., 2021), and clear variability in visible seafloor habitats (Simon-Lledó et al., 2019a). The CCZ is characterized by landscape-scale topographical features, such as ridges, valleys and flat plains (Macdonald et al., 1996). This topography influences the diversity and distribution of metazoans (Cosson et al., 1997; Durden et al., 2015, 2020; Stefanoudis et al., 2016; Leitner et al., 2017; Simon-Lledó et al., 2019a), possibly owing to the influence of topography on bottom currents, sediment grain size and food supply (Durden et al., 2015; Morris et al., 2016). These factors would also be likely to influence benthic microbial communities, but have not been assessed at a landscape scale. Such information is an important component of baseline environmental assessment for commercial mining activities and subsequent monitoring (Ingels et al., 2020), particularly as benthic microbes represent an important energy and nutrient source for abyssal ecosystems. Previous work examining the regional-scale structure of CCZ benthic microbial communities using 16S rRNA gene sequencing has indicated that microbial communities may have a spatial variability over distances of less than 1000 km (Tully and Heidelberg, 2013; Lindh et al., 2017), but finer-scale patterns or their controls are unknown.

Here we characterize bacterial and archaeal assemblages via amplicon sequencing of the 16S rRNA genes, from sediment and nodule samples collected from one of the CCZ conservation areas, APEI-6, in order to determine environmental controls on microbial community structure and compare these with one of the proximal exploration areas (UK-1). Specifically, we tested the following hypotheses: (1) Benthic microbes vary in their spatial distribution from small scales (cm) to larger scales (100's m) within sediments at APEI-6 analogous to that previously observed in metazoans and (2) the broad landscape-scale features of APEI-6 (ridges, valleys, and plains) will influence the diversity and distribution of benthic microbial assemblages.

MATERIALS AND METHODS

Sample Collection

Sediment samples and polymetallic nodules were collected during the RRS *James Cook* cruise JC120, April-May 2015 to the eastern CCZ in the northern equatorial Pacific. Samples were obtained from 20 megacores (Bowers and Connelly type; Barnett et al., 1984) that were deployed in the south western part of APEI-6 (Sampling area centered: 17° 10 N, 122° 75 W) and 2 megacores deployed in the UK-1 Exploration Contract Area, ∼750 km away from APEI-6 (13° 28 N, 116° 35 W) (**Table 1**). Megacores were deployed in four distinct topographical landscape areas in APEI-6 that were each defined by bathymetric data: Deep-Plain, Flat, Ridge and Trough [**Figure 1**; definition details in Simon-Lledó et al. (2019a)]. Megacores of sediment were sliced at 1 cm intervals down to 10 cm, below which slices were taken every 2 cm. The following sediment depth layers were used for analysis of eDNA studies: 0–1 cm below seafloor (cmbsf), 1–2, 5–6, 10–12, and 20–22 cmbsf. Only sediment from the center of the core that had not been in contact with the sides of the megacore tube was sampled. Sediment was placed into sterile Whirl-pak bags and frozen at −80°C immediately on board. Surface nodules in the top 1 cm of the megacore were removed with forceps, rinsed with filtered seawater and frozen immediately at −80°C in sterile Whirl-pak bags for microbial analysis.

Environmental data was collected during the JC120 cruise and included sediment grain size, nodule density (no. m^{-2}), total carbon (TC,% sediment dry weight), total organic carbon (TOC, wt%), total nitrogen (TN, wt%), the ratio of total organic carbon to total nitrogen (TOC:TN), the ratio of total carbon to total nitrogen (TC:TN) and carbonate content ($CaCO_3$, wt%). Manganese (Mn, wt%) values are from Menendez et al. (2019). Collection and calculation of these values is detailed in Simon-Lledó et al. (2019a) and Menendez et al. (2019).

DNA Extraction and Sequencing

Genomic DNA was extracted from 500 mg of wet sediment and 500 mg of crushed nodule samples using the FastDNA Spin Kit for Soil (MP Biomedicals, United States) following the manufacturer's protocol. Nodules were first crushed with an autoclaved pestle and mortar. Additional extraction blanks containing only the FastDNA Spin Kit reagents were processed with the sediment samples. The concentrations of DNA from all samples was below 0.1 ng/μl and required further concentration. DNA was concentrated using the Zymo Clean & Concentrator-5 kits with a 2:1 DNA Binding Buffer ratio and eluted into 50 μl sterile, DNase-free water. The V4 region of the 16S bacterial and archaeal rRNA gene was amplified by the polymerase chain reaction (PCR), following the Earth Microbiome Project (EMP) protocol (Thompson et al., 2017), using the oligonucleotide primers Pro515f/Pro806r. The amplified 16S rRNA gene products and extraction blanks were prepared with the Nextera XT v2 Kit (Illumina, San Diego, CA, United States) and sequenced on an Illumina MiSeq platform at the Environmental Genomics Sequencing Facility (University of Southampton, National Oceanography Centre, Southampton).

Data Analysis

The demultiplexed sequences were analyzed with the microbiome analysis software package QIIME 2 (Quantitative Insights Into Microbial Ecology), version 2019.1 (Bolyen et al., 2019). The DADA2 pipeline (Callahan et al., 2016) within QIIME 2 was implemented for sequence quality control and chimera removal. Amplicon Sequence Variants (ASVs) or features were resolved using the DADA2 denoise-single method. Features that were observed in the PCR blanks were considered to be contaminants and were filtered from the samples. A Naïve Bayes classifier that was pre-trained on the V4 region of reference sequences from the Silva database (version 132; Quast et al., 2013) was used to classify representative sequences of ASVs in our dataset and clustered at 99% identity. A rooted phylogenetic tree was generated within QIIME2, using MAFFT and FastTree, which was used for calculating diversity metrics.

The generated feature table contained 48,198 ASVs and 4,383,878 reads, with an average of 36,839 reads per sample. The feature table was normalized to 4600 sequences per sample in QIIME 2 prior to abundance and diversity analysis, to account for uneven sampling depth and library sizes. Samples were categorized by substrate (sediment and nodules), topographical landscape and sediment horizon. Relative abundances were calculated on ASV feature tables with raw counts that had been normalized by library size to get the proportions of species within each library and then square-root transformed. Alpha diversity (observed features (q = 0), Shannon-Wiener index, evenness (Pielou's evenness values, Chao-1 index) and beta diversity (Bray-Curtis distance) were calculated in QIIME 2 on the normalized samples and formatted along with the generated feature-table for further analysis in R. Community composition and statistical analyses were performed using the "vegan" package in R v 3.3.2 (Oksanen, 2007, 2017). To determine if there were significant differences between alpha diversity in sediments and nodules at APEI-6 (Flat and Deep Plain sites), a one-way ANOVA test was performed in "vegan." Given the low numbers of replicates, the data from different topographies were combined for the testing. Tables of ASV counts were double square-root transformed and Bray-Curtis dissimilarity measures applied to determine variations in community composition between the four topographic areas and sediment layers in APEI-6. Non-metric multidimensional scaling (NMDS) ordination was used to visualize community variation

TABLE 1 | Sampling site locations of megacore deployments in APEI-6 SW and UK-1 (UK Seabed Resources Limited eastern contract area) that were collected during cruise JC120 with location and depths shown for each sample taken.

Station	Location	Seafloor topography	Latitude	Longitude	Water depth (m)	Sediment (cm)	Nodule	No. of samples
JC120-010	Deep Plain 1	Deep Plain	16° 54.77	122° 59.82	4297	0–22		5
JC120-012	Deep Plain 1	Deep Plain	16° 54.77	122° 59.82	4297	0–22		5
JC120-019	Flat 2	Flat	17° 14.94	123° 1.28	4162	0–22		5
JC120-020	Flat 3	Flat	17° 15.03	123° 1.75	4155	0–1*		1
JC120-023	Flat 1	Flat	17° 14.45	123° 3.98	4156	0–22		5
JC120-024	Flat 4	Flat	17° 13.19	123° 2.67	4180	0–22		5
JC120-028	Trough 1	Trough	17° 13.07	123° 49.39	4236	0–22		5
JC120-034	Trough 2	Trough	17° 9.45	122° 48.78	4291	0–1		1
JC120-048	Ridge 1	Ridge	17° 21.56	122° 54.17	4015	0–22		5
JC120-049	Ridge 1	Ridge	17° 21.56	122° 54.17	4015	0–1		1
JC120-058	Ridge 2	Ridge	17° 18.84	122° 54.05	4038	0–22		5
JC120-059	Ridge 3	Ridge	17° 22.02	122° 53.93	4029	0–1*		1
JC120-062	Trough 3	Trough	17° 8.73	122° 48.52	4282	0–22		5
JC120-063	Trough 1	Trough	17° 13.07	122° 49.39	4245	0–22		5
JC120-065	Ridge 4	Ridge	17° 17.30	122° 53.07	4012	0–22		5
JC120-066	Ridge 5	Ridge	17° 19.69	122° 53.27	4012	0–22		5
JC120-067	Trough 5	Trough	17° 17.77	122° 50.12	4234	0–22		5
JC120-075	Flat 5	Flat	17° 14.38	123° 1.59	4158	0–22	2	7
JC120-076	Flat 3	Flat	17° 15.04	123° 1.76	4153	0–1	6	7
JC120-084	Deep Plain 3	Deep Plain	16° 54.44	123° 1.50	4300	0–22		5
JC120-092	Deep Plain 2	Deep Plain	16° 54.14	123° 0.97	4290	0–22	3	8
JC120-105	UK-1	UK-1	13° 27.79	116° 36.49	4108	0–22		5
JC120-106	UK-1	UK-1	13° 27.81	116° 34.50	4108	0–1*		1

*All nodules were taken from the top 0–1 cm of the megacore. *These were short cores (less than 30 cm) when megacores were collected. A total of 102 samples were analyzed (91 sediment samples and 11 nodules). One sample from each horizon (0–1, 1–2, 5–6, 10–12, and 20–22 cm, n = 5) within each megacore was taken. Nodules were analyzed individually with one replicate per nodule.*

between geographic location (APEI-6 vs. UK1), topographical landscape and sediment horizon, along with environmental parameters, with the "envfit" method in the "vegan" package (Oksanen, 2007).

Permutational multivariate analysis of variance (PERMANOVA; Anderson et al., 2001) and *post hoc* pair-wise tests were performed on Bray-Curtis dissimilarity matrices using PRIMER v.7 (Clarke and Gorley, 2015). A mixed effect model was used to partition variance among factors and to test whether microbial assemblage composition varied significantly between factors at APEI-6 (20 megacore samples, **Table 1**). In this model, topography and sediment horizon were treated as fixed factors. To account for potential covariance between depth strata sampled from individual megacores and to reflect the stratified random sampling within topographical regions, megacore was treated as a random factor nested within topographical region. This model is analogous to a classical repeated measures ANOVA design. Topography contained four levels: Deep Plain, Flat, Ridge, and Trough. Sediment Horizon contained five levels: 0–1, 1–2, 5–6, 10–12, and 20–22 cm. The main effects, topography and depth, the nested factor, core, and the interaction term, topography × depth, were included in the model. Methods of permutation used was "method (ii) *permutation of residuals under a reduced model*." Nodules and the UK-1 samples were excluded from the PERMANOVA mixed-effect model due to lack of sufficient replication.

We were not able to carry out comparative statistics on UK-1 samples as there was only one full megacore taken from this region. The second megacore from UK-1 was a short core owing to a large nodule that was retrieved in the eDNA core, so only the top 1 cm of undisturbed sediment could be recovered. Nevertheless, samples from UK-1 and nodule samples were qualitatively evaluated using taxon abundance plots and NMDS. To aid in visualization, ASVs were grouped by taxonomy at phylum, class and genus levels, and the higher classification taxonomic groups that represented more than 1% of the total abundance in at least one substrate type, one depth horizon or one topographical landscape type were further analyzed and discussed. Graphical outputs from abundance and statistical analysis were displayed using the "ggplot2" package in R (Wickham, 2016). Raw sequences were deposited in the National Center for Biotechnology Information (NCBI) Sequence Read Archive under BioProject ID PRJNA694451.

RESULTS

Microbial Diversity at APEI-6 and UK-1

After the data were normalized, 547,400 reads comprising of 36,815 ASVs were identified in 91 sediment and 11 nodule samples (**Table 1**). Of these ASVs from APEI-6, 19% were classified as Archaea and 81% as Bacteria. In UK-1, the

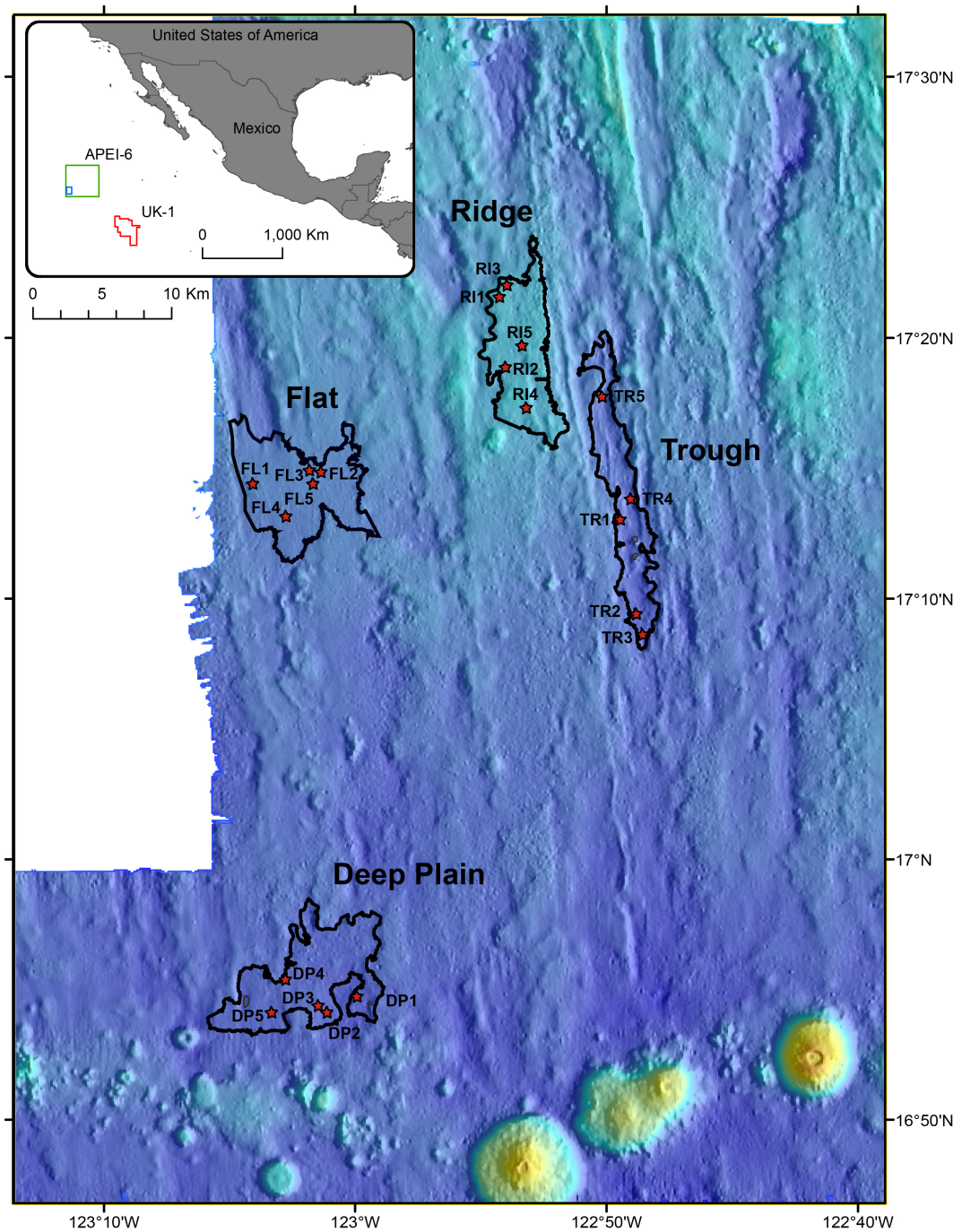

FIGURE 1 | Location of the Area of Particular Environmental Interest (APEI-6) and UK-1 exploration contract area in the Clarion-Clipperton Zone (CCZ) of the Pacific Ocean, where sampling occurred (insert map). Coring locations within the four landscape regions of the APEI-6 are shown with a red star. Red polygon shows location of UK-1, the green box indicates the location of APEI-6, and the blue box delineates the location of the sampling sites within APEI-6.

proportion of Archaea was slightly higher, with 21% of ASVs classified as Archaea and 79% as Bacteria.

Sediment assemblages in the upper 2 cm of sediment were more diverse than polymetallic nodule-associated assemblages in APEI-6 (One-way ANOVA, $P = 0.005$, $F_{1,46} = 8.99$, $R^2 = 0.17$). Alpha diversity (**Figures 2A–C**) in UK-1 sediments (Observed ASVs: mean = 755, SE ± 82; Shannon diversity 8.75 ± 0.15) is higher compared to alpha diversity in APEI-6 sediments (ASVs: 675 ± 14; Shannon: 8.72 ± 0.01) and nodules (ASVs: 288 ± 8; Shannon: 7.34 ± 0.18). Despite non-significant alpha diversity between sediment horizons or between topographical regions within APEI-6, mid to deeper layers (5–22 cm) of sediment at

APEI-6 were more diverse than those at the sediment surface, except at Ridge, where the reverse was true. Sediments at Flat sites were the most diverse, with the 5–6 cm layer being the most diverse overall (Observed ASVs 2000 ± 447, Shannon; 9.35 ± 0.52) and least diverse in the 20–22 cm horizon at Ridge (Observed ASVs 534 ± 114, Shannon; 8.36 ± 0.38). At UK-1, greater alpha diversity was also observed in the surface layers, particularly in the 1–2 cm horizon (Observed ASVs 1089 ± 412; Shannon 9.15 ± 0.68). Estimated richness, (Chao1, **Figure 2D**) was also higher overall at UK-1 (978 ± 159), compared to APEI-6 sediments (805 ± 46).

General Patterns in Microbial Community Composition

Non-metric multidimensional scaling plots were used to visualize differences in microbial community composition between the sediment layers at APEI-6, UK-1, and nodule samples (**Figure 3**). Microbial assemblages associated with nodules clustered separately from sediment samples within APEI-6 (**Figure 3A**). Benthic topography only explained 2.7% of the variance in beta diversity and was not statistically significant. We observed a significant influence of sediment horizon depth on assemblage composition within APEI-6, (PERMANOVA, p = 0.001, $F_{4,83}$ = 6.977, Table 2) accounting for 23% of variance in community composition and structure of sediment assemblages overall. The interaction between topography and depth was not statistically significant, but accounted for 9.6% of the variance (**Table 2**). We observed a relatively large between core variance (20%), suggesting a degree of heterogeneity in microbial assemblage composition between megacores within topographical regions (PERMANOVA, p = 0.001, $F_{18,83}$ = 1.3212, **Table 2**). We also noted that UK-1 sediment samples formed a distinct cluster from APEI-6 sediment and nodules (**Figure 3B**). It was not possible, however, to perform statistical analysis on UK-1 samples, owing to lack of replication.

Environmental variables were largely homogenous within APEI-6. Relative proportions of TC, TOC, TN, TOC:TN, TC:TN, $CaCO_3$, Mn, and mean grain size were very similar across the four sampled regions of APEI-6 with no significant differences detected. Nodule coverage was significantly different between the study areas (Simon-Lledó et al., 2019b), with greatest nodule density observed at Deep Plain (**Table 3**).

Microbial Assemblage Composition of Sediments at APEI-6 and UK-1

Overall, 32% of the community in the whole dataset consisted of Proteobacteria, including Gammaproteobacteria (13%), Alphaproteobacteria (12%), Deltaproteobacteria (5%), and Betaproteobacteria (1.5%) (**Figure 4**). Sequences assigned to the Thaumarchaeota phylum comprised a significant proportion of the sediment microbial assemblages overall (UK-1 = 20%, APEI-6 = 19%). This proportion was lower in the nodules at APEI-6 (11%). The dominant class within Thaumarchaeota was Nitrososphaeria, which composed 12–23% of sediment communities and 11% of the nodule-associated communities. Within both sediment and nodule communities, the most

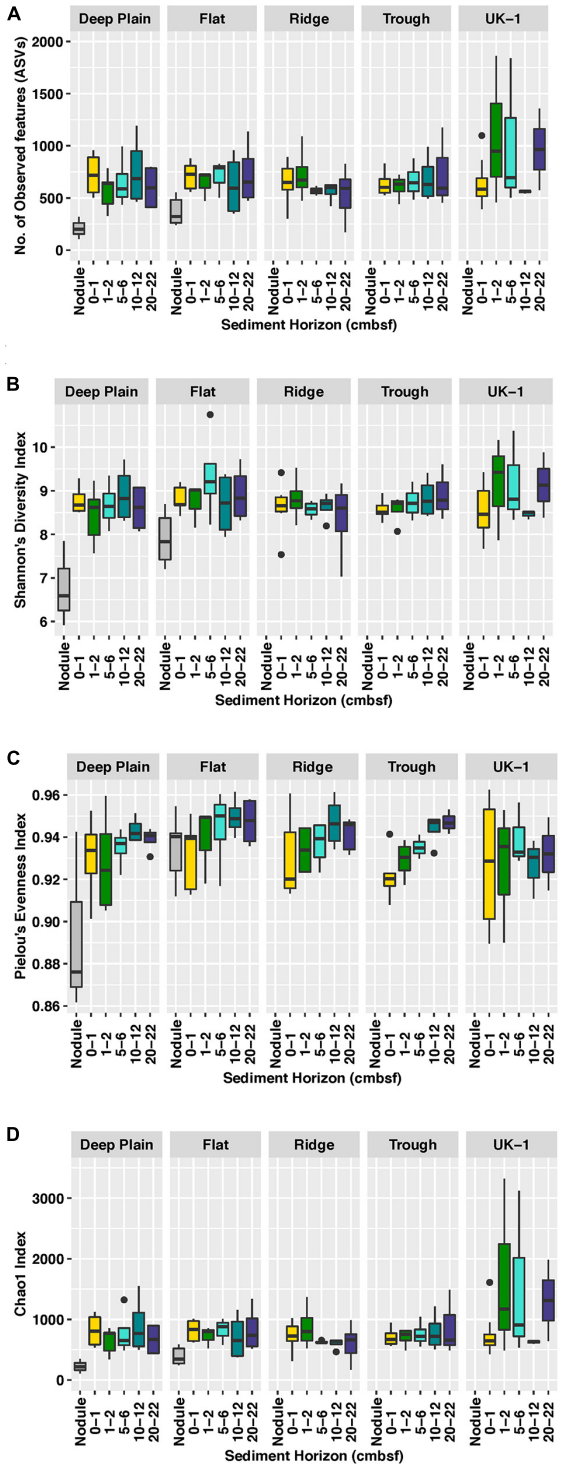

FIGURE 2 | Comparisons of diversity indices between sediment and nodule-associated microbial communities, at APEI-6 and UK-1, based on **(A)** Number of observed features or amplicon sequence variants (ASVs), **(B)** Shannon's Diversity Index, **(C)** Pielou's Evenness Index, and **(D)** Chao1 richness Index. Boxplots show the median (horizontal line), interquartile ranges (box limits), range (whiskers), and outliers (black dots). Diversity indices were calculated on samples that had been rarefied to account for uneven sampling depth.

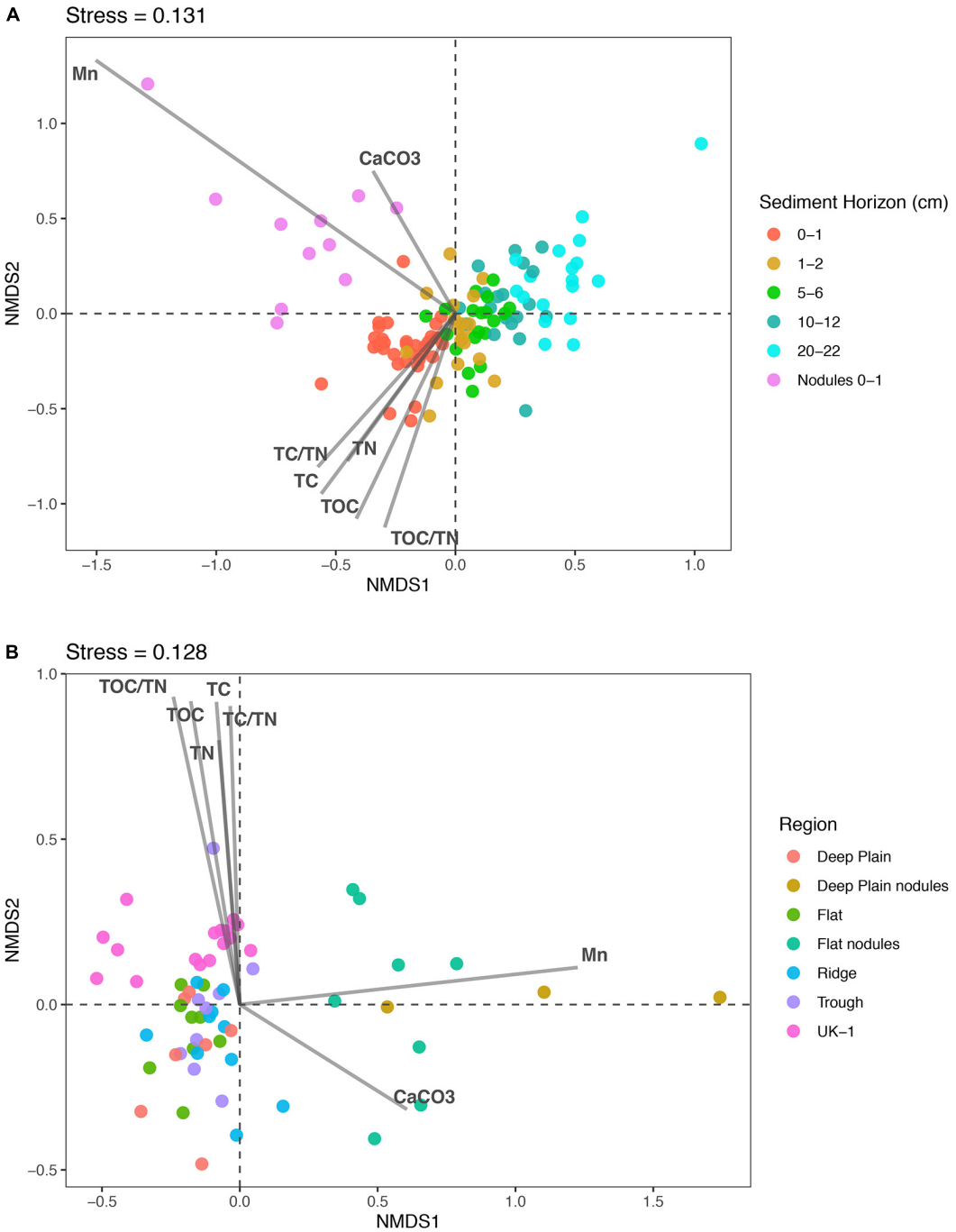

FIGURE 3 | Non-metric multidimensional scaling (nMDS) plots of microbial community dissimilarity based on Bray-Curtis distances. The points represent individual samples and their proximity to one another indicates their similarity. The closer the points are to each other, the more similar the samples are to each other based on community structure and composition. **(A)** Nodule-associated and sediment communities through the sediment profile (0–22 cm) from APEI-6 and UK-1 in the CCZ. Nodules are from the surface sediments (0–1 cm) of the Deep Plain and Flat regions of APEI-6. **(B)** Sediment communities in the top 2 cm of sediment across the four regions in APEI-6 and sediment at UK-1. Nodules are from the surface sediments (0–1 cm) of the Deep Plain and Flat regions of APEI-6. The relationship of environmental variables to the samples are shown with arrows, where the greater the arrow length, the stronger the correlation. Environmental variables are from Jones et al., 2021, in prep.) and Menendez et al. (2019).

dominant genera within Nitrososphaeria was *Candidatus* Nitrosopumilus, which comprised on average 12% of the sediment communities and 7% of the nodule-associated assemblages (**Figure 5**). Within sediments, the highest abundance of *Nitrosopumilus* was in the surface sediments, ranging from 10–14.5% (±2.10) across all topographical landscapes in

TABLE 2 | Output permutational multivariate analysis of variance (PERMANOVA) on relative abundance counts that have been square-root transformed prior to creation of Bray-Curtis dissimilarity matrices for sediment microbial assemblages at APEI-6, showing the following: all 16S microbial assemblages; putative carbon-fixing and nitrifying taxa within sediment microbial assemblages; and taxa within the Nitrososphaeria class in the Thaumarchaeota phylum.

Source	d.f.	SS	MS	*F*	*P*	*% var.*
All 16S microbial sediment assemblages						
Topography	3	2098.7	699.56	0.9025	0.694	2.7
Sediment Horizon	4	17661	4415.2	6.9772	0.001	23.0
Core (Topography)	18	15049	836.06	1.3212	0.001	20.0
Topography x Horizon	12	7245.7	603.81	0.95418	0.801	9.6
Residuals	46	29109	632.81			38.6
Total	83	75400				
Putative carbon-fixing and nitrifying taxa						
Topography	3	62.12	20.707	0.40553	0.864	1.0
Sediment Horizon	4	2491.9	622.97	15.566	0.001	41.1
Core (Topography)	18	1004.2	55.79	1.3941	0.125	16.6
Topography x Horizon	12	223.81	18.651	0.46605	0.981	3.7
Residuals	46	1840.9	40.02			30.4
Total	83	6061				
Nitrososphaeria taxa (Thaumarchaeota)						
Topography	3	713.94	237.98	0.85126	0.648	1.8
Sediment Horizon	4	15002	3750.6	14.499	0.001	37.4
Core (Topography)	18	5193.1	288.5	1.1153	0.222	13.0
Topography x Horizon	12	3059.2	254.94	0.98551	0.555	7.6
Residuals	46	11899	258.68			30.0

The interaction effect "Core" refers to Megacore and is nested within Topography. The interaction effects Topography and Sediment horizon are crossed. Percent variation based on Sum of Squares (SS) is shown as column "% var."

TABLE 3 | Sediment biogeochemistry and environmental data for each APEI-6 SW landscape type and UK-1 (UK Seabed Resources Limited eastern contract area) which were collected during cruise JC120 (Jones et al., 2021, in prep.).

Parameter	APEI-6 Deep Plain	APEI-6 Flat	APEI-6 Ridge	APEI-6 Trough	UK-1
n	3	6	5	5	1
TC (%) ± SD	0.46 ± 0.07	0.49 ± 0.08	0.47 ± 0.06	0.49 ± 0.06	0.72
TOC (%) ± SD	0.42 ± 0.04	0.44 ± 0.05	0.41 ± 0.04	0.44 ± 0.05	0.71
TN (%) ± SD	0.11 ± 0.01	0.11 ± 0.01	0.11 ± 0.01	0.11 ± 0.01	0.14
TOC:TN ± SD	4.5 ± 0.2	4.7 ± 0.3	4.5 ± 0.2	4.7 ± 0.5	5.7
TC:TN ± SD	4.89 ± 0.43	5.23 ± 0.44	5.11 ± 0.31	5.17 ± 0.50	5.8
$CaCO_3$ (%) ± SD	0.3 ± 0.36	0.4 ± 0.05	0.5 ± 0.16	0.4 ± 0.09	0.1
Mn wt% (range across 5 cm interval)	0–5 cm: 0.48–0.51 5–10 cm: 0.44–0.46 10–15 cm: 0.44	0–5 cm: 0.47–0.52 5–10 cm: 0.51–0.53 10–15 cm: 0.56	0–5 cm: 0.54–0.58 5–10 cm: 0.55–0.61 10–15 cm: 0.58	0–5 cm: 0.42–0.48 5–10 cm: 0.44–0.46 10–15 cm: 0.44	0–5 cm: 0.77–0.95 5–10 cm: 0.72–0.79 10–15 cm: 0.56
Nodule density, no m^{-2}	632 (484–776)	307 (200–388)	246 (137–370)	200 (14–455)	16
Grain size, μm (min–max range across 5 cm interval)	0–5 cm: 6.53–8.86 5–10 cm: 6.19- 7.89 10–15 cm: 5.72–8.76 15–20 cm: 5.68–8.89	0–5 cm: 7.15–7.61 5–10 cm: 6.50–8.52 10–15 cm: 6.06–7.24 15–20 cm: 5.77–8.55	0–5 cm: 6.71–9.21 5–10 cm: 6.56–8.72 10–15 cm: 6.33–11.67 15–20 cm: 6.07–10.61	0–5 cm: 7.60–8.50 5–10 cm: 7.49–11.16 10–15 cm: 6.47–20.08 15–20 cm: 6.35–20.15	0–5 cm: 18.06 5–10 cm: 17.6 10–15 cm: 17.58 15–20 cm: 18.74

Parameters are shown as averages (mean) with standard deviation (SD) and ranges (minimum-maximum) shown in brackets. Grain size for each 5 cmbsf sediment profile interval are listed as sample means, showing minimum and maximum. No ranges are given for UK-1 owing to lack of replication. Manganese (Mn) values are from Menendez et al. (2019), collected during cruise JC120, and show ranges within the uppermost 14 cmbsf of sediment at APEI-6 and UK-1.

APEI-6 and within UK-1. Overall, *Nitrosopumilus* was more enriched in UK-1 sediments (10%) than those of APEI-6 (5%). The highest abundances of *Nitrosopumilus* were found at Trough in APEI-6 (14.5% ± 1.29) and UK-1 (14%) in the top cm of sediment.

Other prevalent groups that were also well-represented in sediment assemblages at phylum level were Planctomycetes (11.5%), Chloroflexi (9%), Acidobacteria (5%), Bacteroidetes (4%), Gemmatimonadetes (4%), Nitrospinae (3%), Nitrospirae (2%), and Actinobacteria (1%). Abundant taxa at class level in sediment assemblages in APEI-6 and UK-1 included Dehalococcoidia (Chloroflexi, 7%), Phycisphaerae (Planctomycetes, 7%), Bacteroidia (Bacteroidetes, 3%), Nitrospinia (Nitrospinae, 2.5%), Gemmatimonadetes

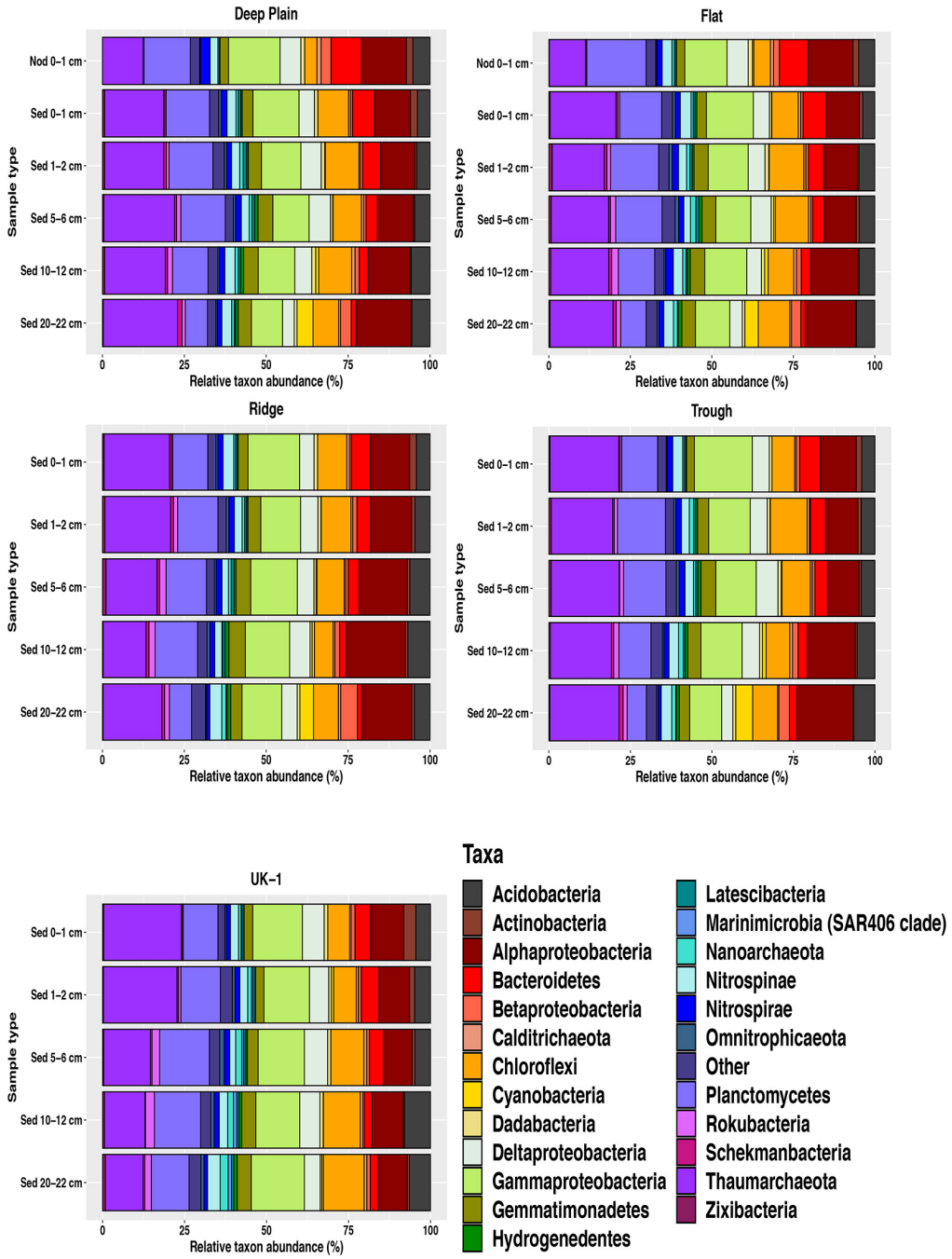

FIGURE 4 | Relative abundances of amplicon sequence variants (ASVS) at phylum level nodule-associated and sediment (0–22 cm) from APEI-6 and UK-1 in the CCZ. Nodules are from the surface sediments (0–1 cm) of the Deep Plain and Flat regions of APEI-6. Only taxa ≥1% relative abundance are shown. Category "Other" represents taxa <1% relative abundance. Relative abundances were calculated on samples that had first been normalized to account for uneven sampling depth, by scaling sequence counts by library sizes.

(Gemmatimonadetes, 2%), Nitrospira (Nitrospirae, 1.5%), Planctomycetacia (Planctomycetes, 1.5%), and OM190 (Planctomycetes, 1.5%). The most dominant genera in sediment assemblages were *Ca. Nitrosopumilus* (6.5–10%), the *Urania-1B-19 marine sediment group* (Planctomycetes, Phycisphaerae, 3%), uncultured bacterium in the Kiloniellaceae family (Alphaproteobacteria, 2.5–3%), *Woeseia* (Gammaproteobacteria (2.5–3%), uncultured Nitrosopumilales archaeon in the Nitrososphaeria class (Thaumarchaeota, 2–2.5%), uncultured bacterium in the Magnetospiraceae family (Alphaproteobacteria, 1.5–2%), *Nitrospina* (Nitrospinae, 1.5%), and *Nitrospira* (Nitrospirae, 1.5%).

Microbial community composition differed among the vertical layers of the sediment, and these differences were influenced by topography (**Table 2**). For example, the abundance of taxa within the Nitrososphaeria class (Thaumarchaeota) varied through the sediment profile within each topographical region, explaining 37.4% of the variance in beta diversity (PERMANOVA, p = 0.001, $F_{3,83}$ = 14.50, **Table 2**; **Figure 5**). However, at Deep Plain, Thaumarchaeota increased with depth through the sediment, whereas at Ridge, the opposite was observed. In contrast, at Flat and Trough, the top one cm of sediment contained a high abundance of Thaumarchaeota (>20% of sequences), which declined with depth to the mid-layers, then increased in abundance again in the 20–22 cm layer. At UK-1, the top 2 cm had the highest observed abundances of Thaumarchaeota (24%). However, the abundance of this group rapidly declined through the sediment profile, to 11.5% in the deepest layer. Certain groups of microbial taxa increased in abundance with increasing depth through the sediment profile. The abundance of Acidobacteria and Rokubacteria followed this pattern at both APEI-6 and UK-1. Rokubacteria were most abundant at UK-1 and peaked at 10–12 cm before declining in abundance in deeper layers. Alphaproteobacteria only increased in deeper layers at the APEI, whereas the reverse was true in UK-1 sediments. Cyanobacteria were largely absent in sediments, except for the 20–22 cm layer in APEI-6. Other groups such as Actinobacteria and Bacteroidetes decreased in abundance with depth through APEI-6 and UK-1 sediments. Gammaproteobacteria and *Nitrospina* declined in abundance in mid-layers (5–6 cm) of sediment at both locations, before increasing in deeper layers again (10–22 cm). Other taxa followed the opposite pattern, such as Chloroflexi, Gemmatimonadetes, *Nitrospira,* and Planctomycetes, which reached a peak in relative abundance in the 5–6 cm layers before declining deeper into the sediment profile.

Microbial Assemblage Composition of Nodules at APEI-6

Nodule-associated communities were dominated by a higher abundance of Proteobacteria than sediments, forming 37% of total sequences, compared to 32% in sediments, driven by the classes Gammaproteobacteria (14%), Alphaproteobacteria (14%), Deltaproteobacteria (6.5%), and Betaproteobacteria (2%). The dominance of Gammaproteobacteria was driven by the families Thiohalorhabdaceae, Woeseiaceae (*Woeseia* genera), Arenicellaceae and the KI89A clade. Within Alphaproteobacteria, the most abundant families were Kiloniellaceae and Magnetospiraceae and the most represented groups within Deltaproteobacteria were the Orders Myxococcales and the SAR324 clade. Betaproteobacteria were largely dominated by ASVs affiliated with *Nitrosomonas* genera. Nodule communities also had a higher abundance of the Planctomycetes phylum, which formed 17% of assemblages associated with nodules, compared to 11.5% of sequences in sediments. This difference was driven by the enrichment of classes Phycisphaerae, OM190, Planctomycetacia and Pla4 lineage. The Bacteroidetes phylum was also more abundant in nodule communities, forming 9% of nodule communities compared to 4% in sediment communities and enriched by uncultured genera in the Rhodothermaceae family and the Cyclobacteriaceae family. Nodule-associated assemblages were also depleted in certain phyla compared to sediments, namely Thaumarchaeota (11% nodules, 19% sediments), Chloroflexi (5% nodules, 9% sediments), Gemmatimonadetes (2.5% nodules, 4% sediments), and Rokubacteria (0.2% nodules, 1% sediments).

We also observed differences in community composition and abundance of the main taxa found within the microbiomes of nodules retrieved from Deep Plain and Flat (**Supplementary Tables 1, 2**). The most dominant genera in nodule-associated communities, *Ca. Nitrosopumilus*, on average formed 10% relative abundance from Deep Plain nodules, and 6% from nodules from Flat (**Figure 5**). The family Thiohalorhabdaceae within the Gammaproteobacteria, formed 5% relative abundance in Deep Plain nodules, compared with 2% in Flat nodules. There was also a greater number of taxa that exceeded 1% relative abundance in nodule assemblages from Deep Plain than Flat. Groups such as *Cohaesibacter* (Alphaproteobacteria), *AqS1* (Gammaproteobacteria), *Pelagibius* (Alphaproteobacteria), *JdFR-76* (Calditrichaeota) and *LS-NOB* (Nitrospinae) exceeded 1% relative abundance in Deep Plain nodule assemblages but were below the 1% cut-off in nodules from Flat. *Aquibacter* (Bacteroidetes) and the Pir4 lineage (Planctomycetes) were present only in the most abundant taxa in nodule-associated assemblages from Flat but not Deep plain nodules.

DISCUSSION

Spatial Differences in Benthic Assemblages Between Substrates

Microbial assemblages in sediments were more diverse than those associated with polymetallic nodules at both APEI-6 and UK-1, a finding that agrees with studies conducted in other areas of the Pacific (Tully and Heidelberg, 2013; Wu et al., 2013; Zhang et al., 2014; Shulse et al., 2016; Lindh et al., 2017; Molari et al., 2020). Microbes related to potential metal-cycling (Magnetospiraceae and Kiloniellaceae), organic carbon remineralization (*Woeseia*), and sulfur-oxidizing Thiohalorhabdaceae were also more enriched in nodules than sediments. Other ASVs that were more prevalent in nodules included *AqS1*, *Cohaesibacter*, *JdFR-76*, *Pelagibius*, *Nitrospina,* and *Nitrospira*. These ASVs have been previously reported in other nodule-associated communities (Wu et al., 2013; Blöthe et al., 2015; Molari et al., 2020).

Spatial Differences in Sediment Benthic Assemblages

Previously, abyssal plain habitats were considered to be homogenous landscapes, and the microbial constituents inhabiting the sediments were assumed to be cosmopolitan in their distribution. Yet, the distributions of metazoans, such as megafauna (Durden et al., 2015, 2020; Leitner et al., 2017; Simon-Lledó et al., 2019a), macrofauna (Cosson et al., 1997),

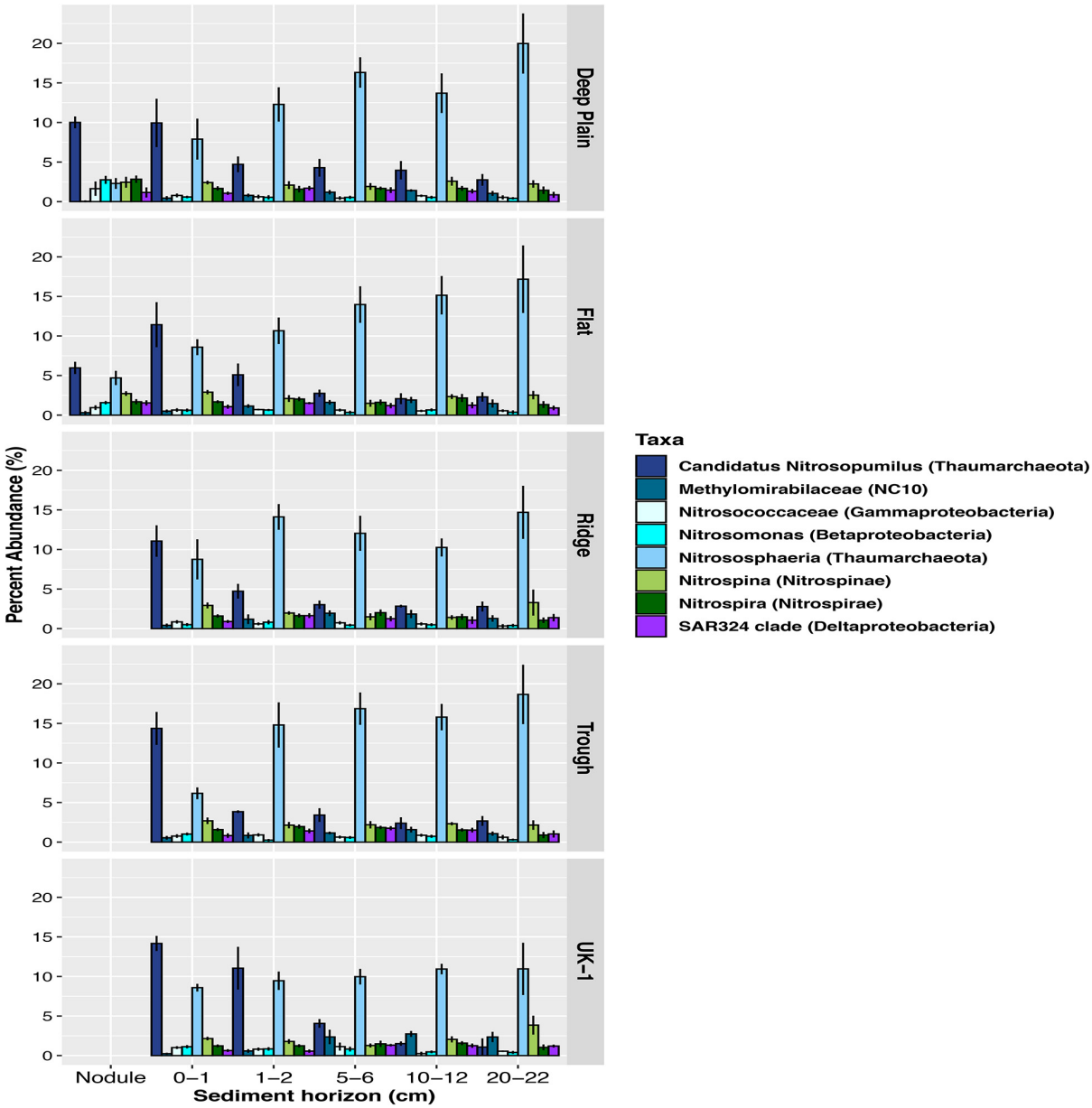

FIGURE 5 | Relative abundances of amplicon sequence variants (ASVs) of the most abundant putative carbon-fixing and nitrifying microbes in sediments and nodules within each region at APEI-6 and at UK-1, defined at genera or family level. The class Nitrososphaeria includes all taxa within that class excluding the genera *Candidatus Nitrosopumilus*, which is shown in a separate category. Only taxa ≥1% relative abundance are shown. Relative abundances were calculated on samples that had first been normalized to account for uneven sampling depth, by scaling sequence counts by library sizes.

and meiofauna (Stefanoudis et al., 2016), are influenced by seafloor heterogeneity.

Bathymetric variation of the seafloor can modify bottom current velocities, which in turn effect local sedimentation rates (Mewes et al., 2014) and POM deposition (Durden et al., 2015; Morris et al., 2016). In the CCZ, however, environmental features were generally homogenous between the landscape regions. Grain size distribution, relative proportions of TC, TOC, TN, TOC:TN, TC:TN, $CaCO_3$, and Mn did not vary significantly between the landscape regions of this area (**Table 3**; Menendez et al., 2019; Simon-Lledó et al., 2019a), which has also been reported in nearby areas of the CCZ (Khripounoff et al., 2006; Volz et al., 2018). Sediments at the CCZ have been reported to be oxygenated (50 μmol L^{-1}) down to 2–3 m depth (Haeckel et al., 2001; Mewes et al., 2014; Volz et al., 2018; Menendez et al., 2019), and across the four landscape types at APEI-6, the oxygen penetration depth (OPD) was similar, at >2.0 m depth (Menendez et al., 2019; Jones et al., 2021, in prep.). One factor that did vary between the landscape regions, however, was nodule density across the seafloor, which was twice as high

at Deep Plain, compared to Flat, Ridge and Trough (**Table 3**; Simon-Lledó et al., 2019a).

At APEI-6, we observed spatial differences in the structure and composition of sediment assemblages, across small scales (cm), through the sediment depth profiles, to mesoscales (m to km) between cores within topographical regions. Across a range of 100's meters to kilometers, the structure of assemblages varied between coring locations within each topographical region, a phenomenon previously observed in meiofauna (Stefanoudis et al., 2016).

Benthic assemblages also varied at larger scales of hundreds of km, between APEI-6 and UK-1. However, the lack of replicates at UK-1 prevented robust statistical analysis. We noted higher alpha diversity at UK-1 compared to APEI-6, a pattern also reported by Lindh et al. (2017). Putative chemolithoautotrophic microbes, such as *Nitrosopumilus*, were more prevalent in UK-1 sediments, particularly in surface layers. Another group, non-photosynthetic Cyanobacteria, Melainabacteria group bacterium S15B-MN24 CBMW_12, was found in the deeper sediment layers of APEI-6 but were largely absent from UK-1 sediments. Differences in assemblages between the two locations may be driven by varying biogeochemistry. The chemical composition of sediments at UK-1 differs from that at APEI-6, with higher proportions of total carbon (TC), total organic carbon (TOC), total nitrogen (TN), TOC:TN and TC:TN ratios, and $CaCO_3$ (**Table 3**), as well as minerals Mn, Ni, and Cu in the sediments of UK-1 (Menendez et al., 2019). Differences in the biogeochemistry of sediments of the neighboring APEI-3 compared to contract areas, as well as lower faunal abundances have also been reported (Volz et al., 2018). The UK-1 area is also closer to the equatorial region of higher primary production in the overlying waters than APEI-6, giving rise to a higher flux of POC to the sediments (Menendez et al., 2019). As a result, the oxygen penetration depth (OPD) in UK-1 sediments is shallower (∼150 cmbsf) than it is at APEI-6 (>300 cmbsf) (Menendez et al., 2019), which is likely to influence benthic assemblage structure and composition.

High Abundance of Chemoautotrophic and Nitrogen Cycling Taxa

In the dark ocean, it is now recognized that chemolithoautotrophic microbes form a significant source of organic carbon through inorganic carbon fixation (Middelberg, 2011; Swan et al., 2011; Molari et al., 2013; Tully and Heidelberg, 2016; Sweetman et al., 2019), which could be equal to or slightly greater than phytoplankton export production in some regions (Reinthaler et al., 2010). Nitrification is an important process in benthic nitrogen cycling and accounts for a large proportion of the chemoautotrophic carbon fixation in the deep ocean (Herndl et al., 2005; Wuchter et al., 2006; Middelberg, 2011). Although not well constrained, using reduced compounds to drive energy for carbon fixation, alongside anabolic processes of inorganic carbon incorporation, may be potentially important strategies for supplementing recalcitrant carbon in oligotrophic deep-sea sediments (Brunnegård et al., 2004; Molari et al., 2013; Sweetman et al., 2019; Trembath-Reichert et al., 2021). Ammonia (NH_3) released from organic matter decay is converted to nitrite (NO_2) mediated by ammonia-oxidizing archaea (AOA) or ammonia-oxidizing bacteria (AOB), in the first step (Bock and Wagner, 2013). The second reaction, the oxidation of nitrite to nitrate (NO_3) is catalyzed by nitrite-oxidizing bacteria (NOB), providing an important source of organic material to the benthic community (Middelberg, 2011). Indeed, benthic impact experiments have indicated that microbial nitrification was reduced following sediment disturbance and plowing (Vonnahme et al., 2020), hence likely impacting nutrient cycling and the availability of labile organic matter (Haeckel et al., 2001).

Across all four of the topographical landscape types of APEI-6 and within UK-1, both sediment and nodule-associated communities were dominated by putatively chemoautotrophic and nitrogen-cycling microbes, up to 29% in sediments and 21% from nodules (**Figure 6**). We observed a community of nitrifying microbes at CCZ, that was numerically dominated by AOA *Nitrosopumilus* (Nitrososphaeria class), which oxidize ammonia to nitrite (Könneke et al., 2005) and have previously been observed in deep-sea sediments in this region, despite the low input of phytodetritus (Nitahara et al., 2011, 2017; Shulse et al., 2016). There were also other nitrifiers present, including the AOA: *Candidatus* Nitrosopelagicus, *Candidatus Nitrosopumilus*, *Candidatus* Nitrosotenuis, taxa within the Nitrososphaeria class; ammonia-oxidizing bacteria (AOB) *Nitrosomonas* (Betaproteobacteria), and *AqS1* (Gammaproteobacteria); and nitrite-oxidizing bacteria (NOB) *Nitrospina* (Nitrospinae) and *Nitrospira* (Nitrospirae).

The relatively high abundances of sequences corresponding to AOA *Ca. Nitrosopumilus* and NOB genera *Nitrospina and Nitrospira* have also been reported in other oligotrophic sediments with Fe-Mn deposits in the South Pacific Gyre (Tully and Heidelberg, 2016; Kato et al., 2019), in the CCZ (Nitahara et al., 2011, 2017: Shulse et al., 2016) and in the Peru Basin (Molari et al., 2020). The high proportions of these AOA and NOB groups at CCZ suggest a coupling between ammonia and nitrite oxidation. This co-occurrence has also been noted in marine environments, from water column (Mincer et al., 2007; Santoro et al., 2010), to shallow sediments (Herbert, 1999; Mills et al., 2008) and deep sediments (Shulse et al., 2016; Tully and Heidelberg, 2016; Molari et al., 2020) to freshwater environments such as oligotrophic lakes (Parro et al., 2019). For the AOA at least, greater numbers have been reported in oligotrophic sediments with low ammonium concentrations, and as AOA have a higher affinity for ammonia, they outcompete AOB in these environments (Martens-Habbena et al., 2009). The nitrate produced by the NOB may be used in other microbial metabolisms, such as oxidation of organic molecules and reduced sulfur compounds (Parro et al., 2019).

In addition to nitrification, carbon fixation in abyssal ecosystems might take place through other metabolic pathways and microbial lineages. Sediment assemblages at APEI-6 and UK-1 contained the methanotrophic taxon *wb1-A12* (family Methylomirabilaceae, phylum NC10). This group are nitrite-dependent anaerobic methane oxidizing (N-damo) bacteria that utilize nitrate or nitrite as an electron acceptor to oxidize methane into CO_2 (Ettwig et al., 2010). In addition, we observed the SAR324 clade (Deltaproteobacteria) in sediment assemblages,

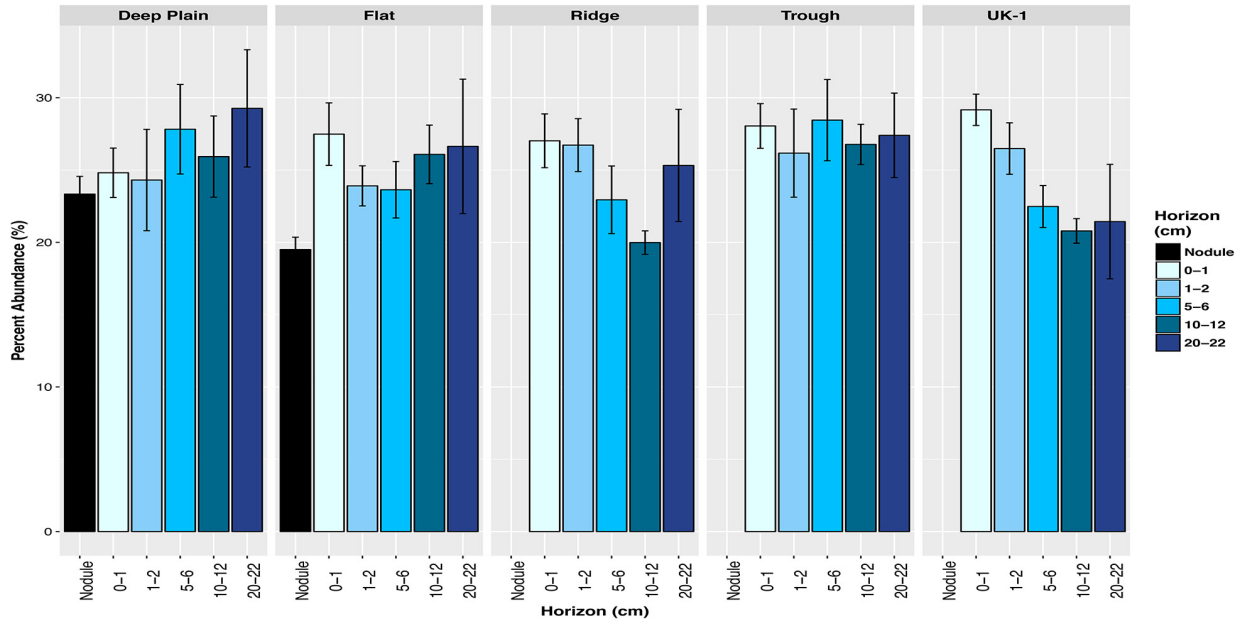

FIGURE 6 | Total relative abundances of amplicon sequence variants (ASVs) of putative carbon-fixing and nitrifying microbes in sediments and nodule-associated communities at APEI-6 and UK-1. Error bars represent standard deviation of the 3 or more replicates for each category. Relative abundances were calculated on samples that had first been normalized to account for uneven sampling depth, by scaling sequence counts by library sizes.

a metabolically flexible taxon capable of heterotrophy as well as autotrophy, that is capable of oxidizing reduced sulfur compounds to fix inorganic carbon (Swan et al., 2011; Sheik et al., 2014). Hence, the ubiquity of these microbial groups, in particular the nitrifiers, in the sediment might provide a source of organic carbon and nitrate for the benthic communities at CCZ. Indeed, microbial carbon incorporation mechanisms in deep-sea environments that lack high quantities of reduced compounds are variable (Trembath-Reichert et al., 2021) and warrant further study in these environments.

As many of the microbial taxa in the CCZ have neither been cultured or genomically sequenced, and with few *in situ* microbial activity or cultivation experiments available for this region (Gillard et al., 2019; Sweetman et al., 2019; Vonnahme et al., 2020), it is difficult to definitely infer metabolic capability from 16S sequences alone. For this reason, metagenomics should be conducted to confirm the metabolic functions that we hypothesize, here, and to link those back to taxonomic markers. Developing a comprehensive microbial ecology of the CCZ will contribute to our knowledge of microbially mediated biogeochemical cycling and will help to develop a mechanistic understanding of the contribution that benthic microbial communities provide to the overall resilience of nodule-associated communities.

CONCLUSION

Differences in microbial community composition at APEI-6 were predominantly driven by depth through the sediment profile and seafloor heterogeneity at small and mesoscales. We observed a diverse and varied microbial assemblage through the sediment, both within APEI-6 and at UK-1. Communities differed between nodules and sediments. The predominance of nitrifying and putative carbon-fixing microbes within sediment assemblages suggests a key ecological role of these groups of taxa in the CCZ, and our results emphasize the importance of microbial communities in mediating carbon, nitrogen and sulfur cycling in this habitat.

Understanding the diversity and functional roles of benthic microbes is vital for the sustainable use and preservation of ecosystems targeted for commercial-scale deep-sea mining. Therefore, ascertaining the composition and diversity of benthic microbial assemblages in both APEI-6 and mining exploration contract regions of the CCZ will be essential ahead of mining activities and will be a useful tool for monitoring in the future.

DATA AVAILABILITY STATEMENT

The datasets presented in this study can be found in online repositories. The names of the repository/repositories and accession number(s) can be found below: https://www.ncbi.nlm.nih.gov/, BioProject ID PRJNA694451.

AUTHOR CONTRIBUTIONS

CY and DJ performed sampling. AH processed the samples, analyzed the data, and wrote the manuscript with the contribution from all authors. All authors conceived the study.

FUNDING

This work was part of the Managing Impacts of Deep-seaA reSource exploitation (MIDAS) European Union Seventh Framework Programme (FP7/2007-2013; grant agreement no. 603418) and UK National Environmental Research Council (NERC) Seabed Mining And Resilience To EXperimental impact (SMARTEX) project (Grant Reference NE/T003537/1). Funding was jointly supported by a studentship from the NERC (Grant NE/L002531/1).

ACKNOWLEDGMENTS

We thank the captain, crew and scientists of the RRS *James Cook* for their assistance during the JC120 research cruise. We are grateful to P. Lam for helpful advice and suggestions with data analysis and interpretation. We are grateful to R. Jeffreys, University of Liverpool, for carrying out the sediment biogeochemical analysis. We would like to thank N. Pratt and A. Baylay for their technical support and assistance with Illumina sequencing (Environmental Sequencing Facility, National Oceanography Centre, Southampton). We also thank two reviewers for their constructive and helpful comments and suggestions, which significantly improved the quality of the manuscript.

SUPPLEMENTARY MATERIAL

The Supplementary Material for this article can be found online at: https://www.frontiersin.org/articles/10.3389/fmars.2021.663420/full#supplementary-material

Supplementary Table 1 | Most abundant taxa associated with polymetallic nodules sampled from the top cm of sediment in the "Deep plain" region of APEI-6. Taxa forming ≥1% average relative abundances (% of total sequences) are given along with standard deviation (SD).

Supplementary Table 2 | Most abundant taxa associated with polymetallic nodules sampled from the top cm of sediment in the "Flat" region of APEI-6. Taxa forming ≥1% average relative abundances (% of total sequences) are given along with standard deviation (SD).

Supplementary Table 3 | Pair-wise *post hoc* tests for fixed term "Sediment Horizon" for sediment microbial assemblages at APEI-6, showing the following: all 16S microbial assemblages; putative carbon-fixing and nitrifying taxa within sediment microbial assemblages; and taxa within the Nitrososphaeria class in the Thaumarchaeota phylum.

REFERENCES

Anderson, M. J. (2001). A new method for non-parametric multivariate analysis of variance. *Austral. Ecol.* 26, 32–46. doi: 10.1111/j.1442-9993.2001.01070

Barnett, P. R. O., Watson, J., and Connelly, D. (1984). The multiple corer for taking virtually 712 undisturbed samples from shelf, bathyal and abyssal sediments. *Oceanologica Acta* 7, 399–408.

Blöthe, M., Wegorzewski, A., Müller, C., Simon, F., Kuhn, T., and Schippers, A. (2015). Manganese-cycling microbial communities inside deep-sea manganese nodules. *Environ. Sci. Technol.* 49, 7692–7700. doi: 10.1021/es504930v

Bock, E., and Wagner, M. (2013). "Oxidation of Inorganic Nitrogen Compounds as an Energy Source," in *The Prokaryotes*, eds E. Rosenberg, E. F. DeLong, S. Lory, E. Stackebrandt, and F. Thompson (Berlin: Springer), doi: 10.1007/978-3-642-30141-4_64

Bolyen, E., Rideout, J. R., Dillon, M. R., Bokulich, N. A., Abnet, C. C., Al-Ghalith, G. A., et al. (2019). Reproducible, interactive, scalable and extensible microbiome data science using QIIME 2. *Nat. Biotechnol.* 37, 852–857. doi: 10.1038/s41587-019-0209-9

Brunnegård, J., Grandel, S., Ståhl, H., Tengberg, A., and Hall, P. O. J. (2004). Nitrogen cycling in deep-sea sediments of the Porcupine Abyssal Plain, NE Atlantic. *Prog. Oceanogr.* 63, 159–181. doi: 10.1016/j.pocean.2004.09.004

Callahan, B. J., McMurdie, P. J., Rosen, M. J., Han, A. W., Johnson, A. J. A., and Holmes, S. P. (2016). DADA2: High-resolution sample inference from Illumina amplicon data. *Nat. Methods* 13, 581–583. doi: 10.1038/nmeth.3869

Clarke, K. R., and Gorley, R. N. (2015). *PRIMER v7: User Manual/Tutorial. PRIMER-E, Plymouth.*

Cosson, N., Sibuet, M., and Galeron, J. (1997). Community structure and spatial heterogeneity of the deep-sea macrofauna at three contrasting stations in the northeast Atlantic. *Deep Sea Res. Part I.* 44, 247–269. doi: 10.1016/S0967-0637(96)00110-0

De Jonge, D. S. W., Stratmann, T., Lins, L., Vanreusel, A., Purser, A., Marcon, Y., et al. (2020). Abyssal food-web model indicates faunal carbon flow recovery and impaired microbial loop 26 years after a sediment disturbance experiment. *Prog. Oceanogr.* 2020:102446. doi: 10.1016/j.pocean.2020.102446

Durbin, A. M., and Teske, A. (2011). Microbial diversity and stratification of South Pacific abyssal marine sediments. *Environ. Microbiol.* 13, 3219–3234. doi: 10.1111/j.1462-2920.2011.02544.x

Durden, J. M., Bett, B. J., and Ruhl, H. A. (2020). Subtle variation in abyssal terrain induces significant change in benthic megafaunal abundance, diversity, and community structure. *Prog. Oceanogr.* 186, 1–11. doi: 10.1016/j.pocean.2020.102395

Durden, J. M., Bett, B. J., Jones, D. O. B., Huvenne, V. A. I., and Ruhl, H. A. (2015). Abyssal hills – hidden source of increased habitat heterogeneity, benthic megafaunal biomass and diversity in the deep sea. *Prog. Oceanogr.* 137, 209–218. doi: 10.1016/j.pocean.2015.06.006

Ettwig, K. F., Butler, M. K., Le Paslier, D., Pelletier, E., Mangenot, S., Kuypers, M. M. M., et al. (2010). Nitrite-driven anaerobic methane oxidation by oxygenic bacteria. *Nature* 464, 543–550. doi: 10.1038/nature08883

Gillard, B., Chatzievangelou, D., Thomsen, L., and Ullrich, M. S. (2019). Heavy-metal-resistant microorganisms in deep-sea sediments disturbed by mining activity: an application toward the development of experimental *in vitro* systems. *Front. Mar. Sci.* 6, 1–12. doi: 10.3389/fmars.2019.00462

Gjerde, K. M., Weaver, P., Billett, D., Paterson, G., Colaco, A., Dale, A., et al. (2016). *Implications of MIDAS Results for Policy Makers: Recommendations for Future Regulations. Managing Impacts of Deep Sea Resource Exploitation Consortium*. 16. Available online at: https://www.eu-midas.net/sites/default/files/downloads/MIDAS_recommendations_for_policy_lowres.pdf (accessed date 20th October 2020)

Haeckel, M., König, I., Reich, V., Weber, M. E., and Suess, E. (2001). Pore water profiles and numerical modelling of biogeochemical processes in Peru Basin deep-sea sediments. *Deep-Sea Res. Pt. II.* 48, 3713–3736. doi: 10.1016/S0967-0645(01)00064-9

Herbert, R. A. (1999). Nitrogen cycling in coastal marine ecosystems. *FEMS* 23, 563–590. doi: 10.1111/j.1574-6976.1999.tb00414.x

Herndl, G. J., Reithaler, T., Teira, E., van Aken, H., Veth, C., Pernthaler, A., et al. (2005). Contribution of *Archaea* to total prokaryotic production in the deep Atlantic Ocean. *Appl. Environ. Microbiol.* 71, 2303–2309. doi: 10.1128/aem.71.5.2303-2309.2005

Ingels, J., Vanreusel, A., Pape, E., Pasotti, F., Macheriotou, L., Arbizu, P. M., et al. (2020). Ecological variables for deep-ocean monitoring must include microbiota and meiofauna for effective conservation. *Nat. Ecol. Evol.* 2020:1335. doi: 10.1038/s41559-020-01335-6

Jones, D. O. B., Amon, D. J., and Chapman, A. S. A. (2018). Mining Deep-Ocean Mineral Deposits: What are the Ecological Risks? *Elements* 14, 325–330. doi: 10.2138/gselements.14.5.325

Jones, D. O. B., Amon, D. J., and Chapman, A. S. A. (2020). "Chapter 5: Deep-sea mining: processes and impacts," in *Natural Capital and Exploitation of the*

Deep Ocean, eds M. Baker, E. Ramirez-Llodra, and P. Tyler (Oxford: Oxford University Press).

Jones, D. O. B., Kaiser, S., Sweetman, A. K., Smith, C. R., Menot, L., Vink, A., et al. (2017). Biological responses to disturbance from simulated deep-sea polymetallic nodule mining. *PLoS One* 12:e0171750. doi: 10.1371/journal.pone.0171750

Jones, D. O. B., Simon-Lledó, E., Amon, D. J., Bett, B. J., Caulle, C., Clement, L., et al. (2021). Environment, ecology, and potential effectiveness of an area protected from deep-sea mining (Clarion Clipperton Zone, abyssal Pacific).

Kato, S., Hirai, M., Ohkuma, M., and Suzuki, K. (2019). Microbial metabolisms in an abyssal ferromanganese crust from the Takuyo-Daigo Seamount as revealed by metagenomics. *PLoS One* 2019:224988. doi: 10.1371/journal.pone.0224888

Kerr, R. A. (1984). Manganese nodules grow by rain from above. *Science* 223, 576–577. doi: 10.1126/science.223.4636.576

Khripounoff, A., Caprais, J. C., Crassous, P., and Etoubleau, J. (2006). Geochemical and biological recovery of the disturbed seafloor in polymetallic nodule fields of the Clarion-Clipperton Fracture Zone (CCFZ) at 5,000 m depth. *Limnol. Oceanogr.* 51, 2033–2041. doi: 10.4319/lo.2006.51.5.2033

Könneke, M., Bernhard, A. E., de la Torre, J. R., Walker, C. B., Waterbury, J. B., and Stahl, D. A. (2005). Isolation of an autotrophic ammonia-oxidising marine archaeon. *Nature* 437, 543–546. doi: 10.1038/nature03911

Leitner, A. B., Neuheimer, A. B., Donlon, E., Smith, C. R., and Drazen, J. C. (2017). Environmental and bathymetric influences on abyssal bait-attending communities of the Clarion Clipperton Zone. *Deep Sea Res. Part I.* 125, 65–80. doi: 10.1016/j.dsr.2017.04.017

Levin, L. A., Mengerink, K., Gjerde, K. M., Rowden, A. A., Van Dover, C. L., Clark, M. R., et al. (2016). Defining "serious harm" to the marine environment in the context of deep-seabed mining. *Mar. Policy* 74, 245–259. doi: 10.1016/j.marpol.2016.09.032

Lindh, M. V., Maillot, B. M., Shulse, C. N., Gooday, A. J., Amon, D. J., Smith, C. R., et al. (2017). From the surface to the deep-sea: bacterial distributions across polymetallic nodule fields in the Clarion-Clipperton Zone of the Pacific Ocean. *Front. Microbiol.* 8, 1–12. doi: 10.3389/fmicb.2017.01696

Lodge, M., Johnson, D., Le Gurun, G., Wengler, M., Weaver, P., and Gunn, V. (2014). Seabed mining: International Seabed Authority environmental management plan for the Clarion-Clipperton Zone. A partnership approach. *Mar. Policy* 49, 66–72. doi: 10.1016/j.marpol.2014.04.006

Macdonald, K. C., Fox, P. J., Alexander, R. T., Pockalny, R., and Gente, P. (1996). Volcanic growth faults and the origin of Pacific abyssal hills. *Nature* 380:125. doi: 10.1038/380125a0

Martens-Habbena, W., Berube, P. M., Urakawa, H., de la Torre, J., and Stahl, D. A. (2009). Ammonia oxidation kinetics determine niche separation of nitrifying Archaea and Bacteria. *Nature* 461, 976–979. doi: 10.1038/nature08465

Menendez, A., James, R. H., Lichtschlag, A., Connelly, D., and Peel, K. (2019). Controls on the chemical composition of ferromanganese nodules in the Clarion-Clipperton Fracture Zone, eastern equatorial Pacific. *Mar. Geo*. 409, 1–14. doi: 10.1016/j.margeo.2018.12.004

Mewes, K., Mogollón, J. M., Picard, A., Rühlemann, C., Kuhn, T., Nöthen, K., et al. (2014). Impact of depositional and biogeochemical processes on small scale variations in nodule abundance in the Clarion-Clipperton Fracture Zone. *Deep Sea Res. Part I.* 91, 125–141. doi: 10.1016/j.dsr.2014.06.001

Middelberg, J. J. (2011). Chemoautotrophy in the ocean. *Geophys. Res. Lett.* 38, 1–4. doi: 10.1029/2011GL049725

Mills, H. J., Hunter, E., Humphrys, M., Kerkhof, L., McGuiness, L., Huettel, M., et al. (2008). Characterization of nitrifying, denitrifying and overall bacterial communities in permeable marine sediments of the Northeastern Gulf of Mexico. *Appl. Environ. Microbiol.* 74, 4440–4453. doi: 10.1128/aem.02692-07

Mincer, T. J., Church, M. J., Trent Taylor, L., Preston, C., Karl, D. M., and DeLong, E. F. (2007). Quantitative distribution of presumptive archaeal and bacterial nitrifiers in Monterey Bay and the North Pacific Subtropical Gyre. *Environ. Microbiol.* 9, 1162–1175. doi: 10.1111/j.1462-2920.2007.01239.x

Molari, M., Janssen, F., Vonnahme, T., Wenzhöfer, F., and Boetius, A. (2020). Microbial communities associated with sediment and polymetallic nodules of the Peru Basin. *Biogeosciences* 2020:11. doi: 10.5194/bg-2020-11

Molari, M., Manini, E., and Dell'Anno, A. (2013). Dark inorganic carbon fixation sustains the functioning of benthic deep-sea ecosystems. *Global Biogeochem. Cycles*. 27, 212–221. doi: 10.1002/gbc.20030

Morris, K. J., Bett, B. J., Durden, J. M., Benoist, N. M. A., Huvenne, V. A. I., Jones, D. O. B., et al. (2016). Landscape-scale spatial heterogeneity in phytodetrital cover and megafauna biomass in the abyss links to modest topographical variation. *Sci. Rep*. 6, 1–10. doi: 10.1038/srep34080

Nitahara, S., Kato, S., Urabe, T., Usui, A., and Yamagishi, A. (2011). Molecular characterization of the microbial community in hydrogenetic ferromanganese crusts of the Takuyo-Daigo Seamount, northwest Pacific. *FEMS* 321, 121–129. doi: 10.1111/j.1574-6968.2011.02323.x

Nitahara, S., Kato, S., Usui, A. S., Urabe, T., Suzuki, K., and Yamagishi, A. (2017). Archaeal and bacterial communities in deep-sea hydrogenetic ferromanganese crusts on old seamounts of the northwestern Pacific. *PLoS One* 12:e0173071. doi: 10.1371/journal.pone.0173071

Oksanen, J. (2007). *Multivariate analyses of ecological communities in R: vegan tutorial*. 39. Available online at: http://cc.oulu.fi/jarioksa/opetus/metodi/vegantutor.pdf (accessed on August 15th, 2020).

Oksanen, J., Blanchet, F. G., Friendly, M., Kindt, R., Legendre, P., McGlinn, D., et al. (2017). *Vegan: Community ecology package. R Package version 2.4-2*.

Parro, V., Puente-Sánchez, F., Cabrol, N. A., Gallardo-Carreño, I., Moreno-Paz, M., Blanco, Y., et al. (2019). Microbiology and nitrogen cycle in the benthic sediments of a glacial oligotrophic deep Andean lake as analog of ancient Martian lake-beds. *Front. Microbiol.* 10, 1–14. doi: 10.3389/fmicb.2019.00929

Quast, C., Pruesse, E., Yilmaz, P., Gerken, J., Schweer, T., Yarza, P., et al. (2013). The SILVA ribosomal RNA gene database project: improved data processing and web-based tools. *Nucleic Acids Res.* 41, 590–596. doi: 10.1093/nar/gks1219

Reinthaler, T., van Aken, H. M., and Herndl, G. J. (2010). Major contribution of autotrophy to microbial carbon cycling in the deep North Atlantic's interior. *Deep Sea Res. II.* 57, 1572–1580. doi: 10.1016/j.dsr2.2010.02.023

Rolinski, S., Segschneider, J., and Sündermann, J. (2001). Long-term propagation of tailing from deep-sea mining under variable conditions by means of numerical simulations. *Deep Sea Res. Part I.* 48, 3469–3485. doi: 10.1016/S0967-0645(01)00053-4

Ruhl, H. A., Ellena, J. A., and Smith, K. L. Jr. (2008). Connections between climate, food limitation, and carbon cycling in abyssal sediment communities. *PNAS* 105, 17006–17011. doi: 10.1073/pnas.0803898105

Santoro, A. E., Casciotti, K. L., and Francis, C. A. (2010). Activity, abundance and diversity of nitrifying archaea and bacteria in the central California Current. *Environ. Microbiol.* 12, 1989–2006. doi: 10.1111/j.1462-2920.2010.02205.x

Sheik, C. S., Jain, S., and Dick, G. J. (2014). Metabolic flexibility of enigmatic SAR324 revealed through metagenomics and metatranscriptomics. *Environ. Microbiol.* 16, 304–317. doi: 10.1111/1462-2920.12165

Shulse, C. N., Maillot, B., Smith, C. R., and Church, M. J. (2016). Polymetallic nodules, sediments and deep waters in the North Pacific exhibit highly diverse and distinct bacterial, archaeal and microeukaryotic communities. *MicrobiologyOpen* 6, 1–16. doi: 10.1002/mbo3.428

Simon-Lledó, E., Bett, B. J., Huvenne, V. A. I., Schoening, T., Benoist, N. M. A., Jeffreys, R. M., et al. (2019a). Megafaunal variation in the abyssal landscape of the Clarion Clipperton Zone. *Progr. Oceanogr*. 170, 119–133. doi: 10.1016/j.pocean.2018.11.003

Simon-Lledó, E., Bett, B. J., Huvenne, V. A. I., Schoening, T., Benoist, N. M. A., and Jones, D. O. B. (2019b). Ecology of a polymetallic nodule occurrence gradient: Implications for deep-sea mining. *Limnol. Oceanogr.* 64, 1883–1894. doi: 10.1002/lno.11157

Smith, C. R., De Leo, F. C., Bernardino, A. F., Sweetman, A. K., and Martinez Arbizu, P. (2008b). Abyssal food limitation, ecosystem structure and climate change. *Trends Ecol. Evol.* 23, 518–528. doi: 10.1016/j.tree.2008.05.002

Smith, C. R., Gaines, S., Friedlander, A., Morgan, C., Thurnherr, A., Mincks, S., et al. (2008a). Preservation reference areas for nodule mining in the Clarion-Clipperton Zone: rationale and recommendations to the International Seabed Authority. *Manoa.* 2008:2008.

Smith, K. L., Ruhl, H. A., Bett, B. J., Billett, D. S. M., Lampitt, R. S., and Kaufmann, R. S. (2009). Climate, carbon cycling and deep-ocean ecosystems. *PNAS* 106, 19211–19218. doi: 10.1073/pnas.0908322106

Stefanoudis, P. V., Schiebel, R., Mallet, R., Durden, J. M., Bett, B. J., and Gooday, A. J. (2016). Agglutination of benthic foraminifera in relation to mesoscale bathymetric features in the abyssal NE Atlantic (Porcupine Abyssal Plain). *Mar. Micropaleontol.* 123, 15–28. doi: 10.1016/j.marmicro.2015.12.005

Swan, B. K., Martinez-Garcia, M., Preston, C. M., Sczyrba, A., Woyke, T., Lamy, D., et al. (2011). Potential for chemolithoautotrophy among ubiquitous bacterial

lineages in the dark ocean. *Science* 333, 1296–1300. doi: 10.1126/science.1203690

Sweetman, A. K., Smith, C. R., Shulse, C. N., Maillot, B., Lindh, M., Church, M. J., et al. (2019). Key role of bacteria in the short-term cycling of carbon at the abyssal seafloor in a low particulate organic carbon flux region of the eastern Pacific Ocean. *Limnol. Oceanogr.* 64, 694–713. doi: 10.1002/lno.11069

Thompson, L. R., Sanders, J. G., McDonald, D., Amir, A., Ladau, J., Locey, K. J., et al. (2017). A communal catalogue reveals Earth's multiscale microbial diversity. *Nature* 551, 457–463.

Trembath-Reichert, E., Shah Walter, S. R., Fontánez Ortis, M. A., Carter, P. D., Girguis, P. R., and Huber, J. A. (2021). Multiple carbon incorporation strategies support microbial survival in cold subseafloor crustal fluids. *Sci. Adv*. 7:18.

Tully, B. J., and Heidelberg, J. F. (2013). Microbial communities associated with ferromanganese nodules and the surrounding sediments. *Front. Microbiol.* 4, 1–10. doi: 10.3389/fmicb.2013.00161

Tully, B. J., and Heidelberg, J. F. (2016). Potential Mechanisms for Microbial Energy Acquisition in Oxic Deep-Sea Sediments. *Appl. Environ. Microbiol.* 82, 4232–4243. doi: 10.1128/aem.01023-16

Volz, J. B., Mogollón, J. M., Geibert, W., Martínez Arbizu, P., Koschinsky, A., and Kasten, S. (2018). Natural spatial variability of depositional conditions, biogeochemical processes and element fluxes in sediment of the eastern Clarion-Clipperton Zone, Pacific Ocean. *Deep Sea Res. Part I.* 140, 159–172. doi: 10.1016/j.dsr.2018.08.006

Vonnahme, T. R., Molari, M., Janssen, F., Wenzhöfer, F., Haeckel, M., Tischack, J., et al. (2020). Effects of a deep-sea mining experiment on seafloor microbial communities and functions after 26 years. *Sci. Adv*. 6, 1–14.

Washburn, T. W., Jones, D. O. B., Wei, C.-L., and Smith, C. R. (2021). Environmental Heterogeneity Throughout the Clarion-Clipperton Zone and the Potential Representativity of the APEI Network. *Front. Mar. Sci.* 8:661685. doi: 10.3389/fmars.2021.661685

Wedding, L. M., Friedlander, A. M., Kittinger, J. N., Watling, L., Gaines, S. D., Bennett, M., et al. (2013). From principles to practice: a spatial approach to systematic conservation planning in the deep sea. *Proc. R. Soc. B.* 280, 1–10. doi: 10.1098/rspb.2013.1684

Wedding, L. M., Reiter, S. M., Smith, C. R., Gjerde, K. M., Kittinger, J. N., Friedlander, A. M., et al. (2015). Managing mining of the deep seabed. *Science* 349, 144–145.

Wickham, H. (2016). *ggplot2: Elegant Graphics for Data Analysis*, 2nd Edn. New York, NY: Springer Publishing Company, Incorporated.

Wu, Y. H., Liao, L., Wang, C. S., Ma, W. L., Meng, F. X., Wu, M., et al. (2013). A comparison of microbial communities in deep-sea polymetallic nodules and the surrounding sediments in the Pacific Ocean. *Deep Sea Res. Part I.* 79, 40–49. doi: 10.1016/j.dsr.2013.05.004

Wuchter, C., Abbas, B., Coolen, M. J. L., Herfort, L., van Bleijswijk, J., Timmers, P., et al. (2006). Archaeal nitrification in the ocean. *PNAS* 104, 12317–12322. doi: 10.1073/pnas.0600756103

Zhang, D. C., Liu, Y. X., and Li, X. Z. (2014). Characterization of bacterial diversity associated with deep-sea ferromanganese nodules from the South China Sea. *J. Microbiol.* 53, 598–605. doi: 10.1007/s12275-015-5217-y

Conflict of Interest: The authors declare that the research was conducted in the absence of any commercial or financial relationships that could be construed as a potential conflict of interest.

Publisher's Note: All claims expressed in this article are solely those of the authors and do not necessarily represent those of their affiliated organizations, or those of the publisher, the editors and the reviewers. Any product that may be evaluated in this article, or claim that may be made by its manufacturer, is not guaranteed or endorsed by the publisher.

Copyright © 2021 Hollingsworth, Jones and Young. This is an open-access article distributed under the terms of the Creative Commons Attribution License (CC BY). The use, distribution or reproduction in other forums is permitted, provided the original author(s) and the copyright owner(s) are credited and that the original publication in this journal is cited, in accordance with accepted academic practice. No use, distribution or reproduction is permitted which does not comply with these terms.

frontiers in Marine Science

ORIGINAL RESEARCH
published: 27 July 2021
doi: 10.3389/fmars.2021.705237

Biogeography and Connectivity Across Habitat Types and Geographical Scales in Pacific Abyssal Scavenging Amphipods

Guadalupe Bribiesca-Contreras[1], Thomas G. Dahlgren[2,3], Tammy Horton[4], Jeffrey C. Drazen[5], Regan Drennan[1], Daniel O.B. Jones[4], Astrid B. Leitner[5,6], Kirsty A. McQuaid[7], Craig R. Smith[5], Sergio Taboada[1,8,9], Helena Wiklund[1,2] and Adrian G. Glover[1]*

[1] Life Sciences Department, Natural History Museum, London, United Kingdom, [2] Department of Marine Sciences, University of Gothenburg, Gothenburg, Sweden, [3] NORCE Norwegian Research Centre, Bergen, Norway, [4] National Oceanography Centre, Southampton, United Kingdom, [5] Department of Oceanography, University of Hawai'i at Mānoa, Honolulu, HI, United States, [6] Monterey Bay Aquarium Research Institute, Moss Landing, CA, United States, [7] School of Biological and Marine Sciences, University of Plymouth, Plymouth, United Kingdom, [8] Departamento de Biodiversidad, Ecología y Evolución, Universidad Complutense de Madrid, Madrid, Spain, [9] Departamento de Ciencias de la Vida, EU-US Marine Biodiversity Group, Universidad de Alcalá, Alcalá de Henares, Spain

OPEN ACCESS

Edited by:
Sylvie Marylène Gaudron, Sorbonne Université, France

Reviewed by:
Sven Richard Laming, University of Aveiro, Portugal
Jorge Paramo, University of Magdalena, Colombia

***Correspondence:**
Guadalupe Bribiesca-Contreras
l.bribiesca-contreras@nhm.ac.uk

Specialty section:
This article was submitted to Deep-Sea Environments and Ecology, a section of the journal Frontiers in Marine Science

Received: *04 May 2021*
Accepted: *07 July 2021*
Published: *27 July 2021*

Citation:
Bribiesca-Contreras G, Dahlgren TG, Horton T, Drazen JC, Drennan R, Jones DOB, Leitner AB, McQuaid KA, Smith CR, Taboada S, Wiklund H and Glover AG (2021) Biogeography and Connectivity Across Habitat Types and Geographical Scales in Pacific Abyssal Scavenging Amphipods. Front. Mar. Sci. 8:705237. doi: 10.3389/fmars.2021.705237

Recently, there has been a resurgent interest in the exploration of deep-sea mineral deposits, particularly polymetallic nodules in the Clarion-Clipperton Zone (CCZ), central Pacific. Accurate environmental impact assessment is critical to the effective management of a new industry and depends on a sound understanding of species taxonomy, biogeography, and connectivity across a range of scales. Connectivity is a particularly important parameter in determining ecosystem resilience, as it helps to define the ability of a system to recover post-impact. Scavenging amphipods in the superfamilies Alicelloidea Lowry and De Broyer, 2008 and Lysianassoidea Dana, 1849 contribute to a unique and abundant scavenging community in abyssal ecosystems. They are relatively easy to sample and in recent years have become the target of several molecular and taxonomic studies, but are poorly studied in the CCZ. Here, a molecular approach is used to identify and delimit species, and to investigate evolutionary relationships of scavenging amphipods from both abyssal plain and deep (>3000 m) seamount habitats in three APEIs (Areas of Particular Environmental Interest, i.e., designated conservation areas) in the western CCZ. A total of 17 different morphospecies of scavenging amphipods were identified, which include at least 30 genetic species delimited by a fragment of the cytochrome *c* oxidase subunit I (COI) barcode gene. The scavenging communities sampled in the western CCZ included the most common species (*Abyssorchomene gerulicorbis* (Shulenberger and Barnard, 1976), *A. chevreuxi* (Stebbing, 1906), *Paralicella caperesca* Shulenberger and Barnard, 1976, and *P. tenuipes* Chevreux, 1908) reported for other ocean basins. Only four morphospecies, representing five genetic species, were shared between APEIs 1, 4, and 7. The two abyssal plain sites at APEIs 4 and 7 were dominated by two and three of the most common scavenging species, respectively, while the APEI 1 seamount site was

dominated by two species potentially new to science that appeared to be endemic to the site. The presence of common species in all sites and high genetic diversity, yet little geographic structuring, indicate connectivity over evolutionary time scales between the areas, which span about 1500 km. Similar to recent studies, the differences in amphipod assemblages found between the seamount and abyssal sites suggest that ecological conditions on seamounts generate distinct community compositions.

Keywords: scavenging amphipods, connectivity, biodiversity, Clarion-Clipperton Zone, deep-sea mining, seamount

INTRODUCTION

For decades, it has been known that large deposits of metals such as nickel, iron, copper, cobalt, and manganese, in the form of polymetallic nodules exist in the abyssal deep sea (Mewes et al., 2014). However, with an increasing demand for these metals to fuel high-technology industry, deep-sea mining is now being more actively considered (Hein et al., 2020). The Clarion-Clipperton Zone (CCZ), located in the central Pacific, has one of the largest known deposits of polymetallic nodules and deep-sea mining exploration in the area has greatly increased in the last decade. The seafloor minerals in the CCZ lie in areas beyond national jurisdiction and are managed by the International Seabed Authority (ISA), which has granted 18 exploration contracts to date (ISA, 2021). In addition, the ISA has implemented a regional environmental management plan, provisionally designating nine representative areas where mining activities will be prohibited (Areas of Particular Environmental Interest, APEI) to preserve the biodiversity and ecosystem functions across the region (Wedding et al., 2013). Yet, their effectiveness depends on several key ecological criteria, particularly the degree to which APEI community compositions are representative of mining contract areas and whether they could maintain regional connectivity in the event of mining-related habitat loss.

Connectivity is a particularly important parameter in determining ecosystem resilience, as it helps to define the ability of a system to recover post-impact (Gollner et al., 2017). Thus, connectivity studies are critical for the effective management of nodule fields targeted for deep-sea mining. Many biodiversity baseline surveys have been conducted in the CCZ (Glover et al., 2015). However, most of these have focused on surveying contract areas, which is an ISA regulatory requirement, with the APEIs remaining largely unexplored. Moreover, while most surveys have aimed to describe general patterns of biodiversity and community structure, our understanding of species ranges and genetic connectivity is still very limited. To date, only two studies have investigated genetic connectivity patterns in the CCZ (Taboada et al., 2018; Janssen et al., 2019), with data restricted to the eastern CCZ. However, larger scale studies spanning the entire CCZ and adjacent areas are obviously required to fully understand species ranges and connectivity.

Necrophagous amphipods in the superfamiles Alicelloidea Lowry and De Broyer, 2008 and Lysianassoidea Dana, 1849, could provide insight into connectivity patterns for highly mobile, demersal species in the CCZ given their ubiquity in bathyal and abyssal ecosystems (Lacey et al., 2016). Scavenging amphipods can be easily collected in large numbers using baited traps, which have been in use since 1888 (Horton and Thurston, 2014). They are highly motile, with some deep-sea species within the genus *Paralicella* Chevreux, 1908 showing remarkably high and reciprocal pan-Pacific migration between hadal trench populations (Ritchie et al., 2017). Many deep-sea scavenging amphipod species were previously considered to be cosmopolitan (Christiansen et al., 1990), with large distributional and bathymetric ranges, occurring in bathyal, abyssal, and hadal zones. More recently, genetic diversity studies have uncovered complexes of cryptic species within these "cosmopolitan" taxa (Havermans, 2016), revealing biogeographic patterns and bathymetric structuring within the deep sea (Havermans et al., 2013; Lacey et al., 2016).

Although scavenging amphipods are generally well studied at shallower depths (Sainte-Marie, 1992), they remain little studied in the abyssal CCZ. Two recent studies have looked into the diversity of this group, using morphological and molecular data, in contractor areas and APEIs in the eastern CCZ (Patel et al., 2020; Mohrbeck et al., 2021). In our study, the DeepCCZ expedition targeted APEIs in the western CCZ, which remains largely unexplored. During the expedition in May–June 2018, on board the *R/V Kilo Moana*, baited traps were deployed in APEIs 1, 4, and 7, collecting more than 5,000 specimens of scavenging amphipods. Here, the biodiversity and connectivity patterns of necrophagous amphipods within these areas, spanning approximately 1500 km, are explored. Species delimitation is performed using both morphological and genetic data, and phylogenetic relationships are inferred. Additionally, the biodiversity of assemblages from the three sites is described, and connectivity between these sites, across the CCZ, and amongst other abyssal regions is inferred.

MATERIALS AND METHODS

Study Sites, Specimen Sampling and Processing

APEIs 1, 4, and 7 are the westernmost APEIs (**Figure 1**), and were surveyed during the DeepCCZ expedition on board the *R/V Kilo Moana* in May–June 2018. Scavenging amphipods were collected using a large baited trap (∼1.2 m wide, 1 m high, 2 m long), with two PVC tube traps (10" diameter with funneled entrances; Leitner et al., 2017) inside, specifically designed to

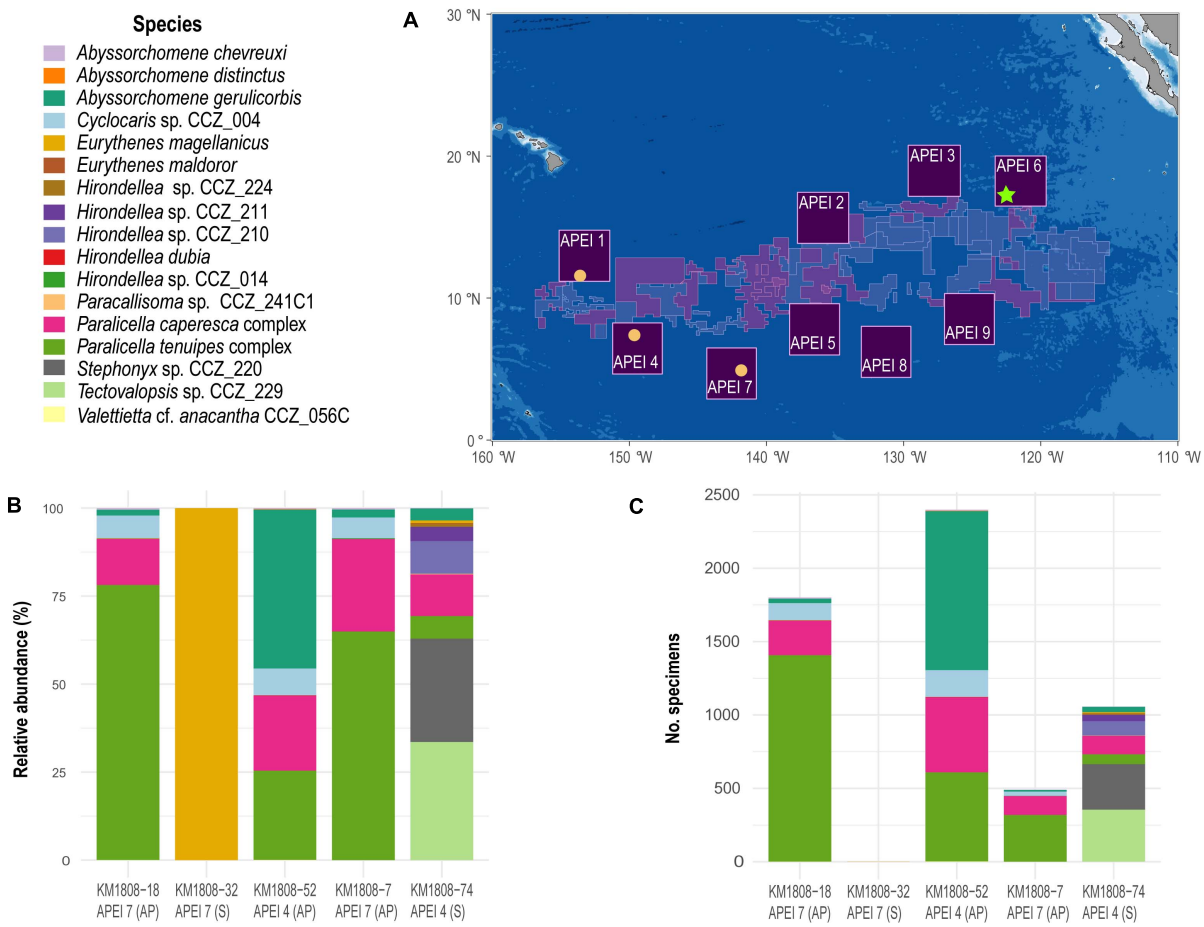

FIGURE 1 | Map of the Clarion-Clipperton Zone indicating the Areas of Particular Environmental Interest [APEIs; **(A)**]. Yellow circles indicate the sites where baited-traps were deployed during the DeepCCZ expedition, with bar plots indicating the relative abundance **(B)** and total number of specimens collected **(C)** of each of the different morphospecies of scavenging amphipod recovered at each site. During deployment KM1808-32 on APEI 7, only a single specimen was recovered. The green star indicates the site where the baited trap was deployed during the JC120 expedition, and from which only a few specimens were included in this study. S, seamount, AP, abyssal plain.

trap necrophagous amphipods. The PVC tube traps were baited with ∼1 kg of chopped Pacific mackerel (*Scomber japonicus*). Baited traps were deployed five times for a minimum of 22 h (22.7–47.1 h) on benthic landers at less than 50 cm above the seafloor at four different sites: APEI 1 seamount (deployment KM1808-074: 4175 m depth, 22.7 h), APEI 4 abyssal plain (deployment KM1808-052: 4872 m depth, 43.4 h), twice on APEI 7 abyssal plain (deployment KM1808-007: 4871 m depth, 30.7 h; and deployment KM1808-018: 4871 m depth, 47.1 h), and APEI 7 seamount (deployment KM1808-032: 3203 m, 25.1 h) (Leitner et al., 2017). More than 5700 specimens were collected during the four deployments (see **Figure 1**), but unfortunately only a single specimen was recovered from the deployment on the seamount on APEI 7. This was likely due to the large numbers of synaphobranchid eels observed at this site, with 12 individuals recovered from this trap (Leitner et al., 2021). Amphipods from each deployment were processed separately, and a total of about 850 specimens from all traps were sorted and grouped into morphospecies at sea. These sorted specimens were photographed and preserved in 80%, non-denatured ethanol. The remaining unsorted amphipods were also preserved in 80%, non-denatured ethanol. Preserved specimens were shipped to the Natural History Museum, London for further analyses.

An additional 36 amphipods from the APEI 6 (**Figure 1**), collected during the JC120 cruise on the Royal Research Ship *James Cook* in 2015 (Jones, 2015), were included in our genetic analyses.

Alpha-Diversity

All specimens were morphologically examined and sorted into different morphotypes using external morphological characters. Specimens were identified to the lowest taxonomic level possible, considering both morphological characters and genetic sequences. Additionally, representatives of the different morphotypes identified were morphologically examined in more detail by a taxonomic expert (TH). Taxonomic classification and authorities follow WoRMS (Horton et al., 2020b) and can be checked by following the hyperlinks in **Table 1**.

TABLE 1 | Morphospecies and genetic species of scavenging amphipods found in the Areas of Particular Environmental Interest (APEIs) 1, 4, and 7.

Morphospecies	Genetic species	APEI 1 (S)	APEI 4 (P)	APEI 7 (P)	APEI 7 (S)	Mean genetic divergence (%)
Alicelloidea Lowry and De Broyer, 2008						
Alicelloidea Lowry and De Broyer, 2008e						
Paralicella Chevreux, 1908						
Paralicella caperesca Shulenberger and Barnard, 1976 complex		125	510	365	–	**2.33–15.33**
	Paralicella cf. *caperesca* 1	(7)	–	–	–	1.14 ± 0.27
	Paralicella cf. *caperesca* 10	–	–	(1)	–	NA
	Paralicella cf. *caperesca* 12	-	–	(1)	–	0.35 ± 0.16
	Paralicella cf. *caperesca* 14	–	–	(3)	–	0.08 ± 0.03
	Paralicella cf. *caperesca* 4	–	–	(1)	–	0.00
	Paralicella cf. *caperesca* 5	–	(1)	(1)	–	0.00
	Paralicella cf. *caperesca* 6	–	–	(1)	–	NA
	Paralicella cf. *caperesca* 7	(1)	(18)	(16)	–	0.55 ± 0.11
	Paralicella cf. *caperesca* 9	–	(1)	(3)	–	0.08 ± 0.07
Paralicella tenuipes Chevreux, 1908 complex		68	608	1726	–	**3.32**
	Paralicella cf. *tenuipes* 1	(2)	(6)	(7)	–	0.19 ± 0.09
	Paralicella cf. *tenuipes* 2	(4)	(11)	(11)	–	0.81 ± 0.19
Tectovalopsis Barnard and Ingram, 1990						
Tectovalopsis sp. CCZ_229		355	–	–	–	**3.1**
	Tectovalopsis sp. CCZ_229	(26)	–	–	–	0.65 ± 0.26
	Tectovalopsis sp. CCZ_229 2	(1)	–	–	–	2.49 ± 0.87
Valettiopsidae Lowry and De Broyer, 2008						
Valettietta Lincoln and Thurston, 1983						
Valettietta cf. *anacantha* CCZ_056C	*Valettietta* cf. *anacantha* CCZ_056C	–	2 (2)	1 (1)	–	0.19 ± 0.09
Lysianassoidea Dana, 1849						
Cyclocaridae Lowry and Stoddart, 2011						
Cyclocaris Stebbing, 1888						
Cyclocaris sp. CCZ_004	*Cyclocaris* sp. CCZ_004	–	183 (19)	145 (23)	–	4 ± 0.48
Eurytheneidae Stoddart and Lowry, 2004						
Eurythenes S. I. Smith in Scudder, 1882						
Eurythenes magellanicus (H. Milne Edwards, 1848)		8	–	2	1	**2.19**
	Eurythenes cf. *magellanicus*	(8)	–	–	–	0.12 ± 0.06
	Eurythenes cf. *magellanicus* 2	–	–	(2)	(1)	0.3 ± 0.13
Eurythenes maldoror d'Udekem d'Acoz and Havermans, 2015		3	–	–	–	**4.98**
	Eurythenes cf. *maldoror* CCZ_232	(1)	–	–	–	0.16 ± 0.15
	Eurythenes maldoror	(2)	–	–	–	0.73 ± 0.23
Hirondelleidae Lowry and Stoddart, 2010						
Hirondellea Chevreux, 1889						
Hirondellea sp. CCZ_224	*Hirondellea* sp. CCZ_224	8 (3)	–	–	–	NA
Hirondellea sp. CCZ_211	*Hirondellea* sp. CCZ_211	43 (5)	–	–	–	0.00
Hirondellea sp. CCZ_210	*Hirondellea* sp. CCZ_210	98 (7)	–	–	–	0.00
Hirondellea dubia Dahl, 1959	*Hirondellea dubia*	–	3 (3)	–	–	0.41 ± 0.13
Hirondellea sp. CCZ_014	*Hirondellea* sp. CCZ_014	–	–	2 (2)	–	0.49 ± 0.3
Scopelocheiridae Lowry and Stoddart, 1997						
Paracallisoma Chevreux, 1903						
Paracallisoma sp. CCZ_241C1	*Paracallisoma* sp. CCZ_241C1	2 (2)	–	–	–	0.42 ± 0.19
Uristidae Hurley, 1963						
Abyssorchomene De Broyer, 1984						
Abyssorchomene chevreuxi (Stebbing, 1906)		1	7	10	–	**3.94**
	Abyssorchomene cf. *chevreuxi*	–	(2)	(1)	–	0.05 ± 0.05
	Abyssorchomene chevreuxi	(1)	(5)	(6)	–	0.87 ± 0.19
Abyssorchomene distinctus (Birstein and Vinogradov, 1960)	*Abyssorchomene distinctus*	–	3 (3)	–	–	0.22 ± 0.06
Abyssorchomene gerulicorbis (Shulenberger and Barnard, 1976)	*Abyssorchomene gerulicorbis*	36 (16)	1083 (27)	41 (19)	–	0.23 ± 0.12
Stephonyx Lowry and Stoddart, 1989						
Stephonyx sp. CCZ_220	*Stephonyx* sp. CCZ_220	310 (17)	–	–		0.00
Total no. of specimens collected		**1057**	**2399**	**2292**	**1**	

Number of specimens per morphotype is given in the same line as morphotype name, with number of specimens sequenced per genetic species indicated in parentheses. These sequenced specimens are also included in the total number of specimens per morphotype. Mean intraspecific genetic divergence values are given for each genetic species, while mean or ranges of mean interspecific genetic divergence between all species within each morphospecies are indicated in bold. "S" indicates seamount, "P" indicates abyssal plain.

Analyses were performed in R version 4.0.2 (R Development Core Team, 2017), using several packages, and all plots generated using *ggplot2* (Wickham, 2009). Individual-based abundance data were used to describe alpha-diversity of morphospecies in the three APEIs. The seamount site on APEI 7 was excluded from these analyses, as only a single specimen was recovered here. Rarefaction curves were used to visualize sampling effort, and were generated using the R package *vegan* (Oksanen et al., 2018). Diversity was estimated as effective number of species (i.e., Hill numbers; Jost, 2006) for different orders of diversity (q), that indicate sensitivity to common and rare species, using the R package *iNEXT* (Hsieh et al., 2020). Diversity profiles were generated using a continuum of q values (from 0 to 5 every 0.10) to visualize the contribution of rare and abundant species in the community (See **Supplementary S1**). Order zero diversity ($q = 0$) only takes into account presence, thus representing species richness. Order one diversity ($q = 1$) weighs all species frequencies equally without favoring rare or common species and is equivalent to the inverse of the Shannon-Wiener entropy index. The order two diversity ($q = 2$) places more weight on the frequencies of abundant species and discounts rare species, equivalent to the inverse of Simpson's concentration index.

DNA Extraction, Amplification, and Sequencing

A reverse taxonomic approach was used to improve and speed up taxonomic assignments, as well as to allow comparisons between studies for which sequences of indeterminate species have been provided. Several representatives of each morphotype were thus photographed and one or several pleopods were used for DNA extraction. DNA extraction was performed using the DNeasy Blood and Tissue Kit (Qiagen). A fragment of the barcoding gene cytochrome *c* oxidase subunit I (COI) was amplified for all selected specimens in order to perform single-locus species delimitation. A fragment of the genes 16S rRNA (16S) and 18S rRNA (18S) were additionally amplified for at least a single representative of each morphotype for phylogenetic inference. The PCR mix for each reaction contained 10.5 μl of Red Taq DNA Polymerase 1.1X MasterMix (VWR), 0.5 μl of each primer (10 μM) and 1 μl of DNA template. The mitochondrial COI was amplified using the LCO1490 (GGTCAACAAATCATAAAGATATTGG) and HCO2198 (TAAACTTCAGGGTGACCAAAAAATCA) primers (Folmer et al., 1994) with an initial denaturation at 95°C for 5 min, followed by 35 cycles of denaturation at 95°C for 45 s, annealing at 51°C for 45 s, and extension at 72°C for 1 min, with a final extension of 72°C for 10 min. The mitochondrial 16S was successfully amplified with the universal primers 16sar-L (CGCCTGTTTATCAAAAACAT) and 16sbr-H (CCGGTCTGAACTCAGATCACGT) (Palumbi, 1996) using an initial denaturation at 94°C for 2 min, followed by 30 cycles of denaturation at 94°C for 15 s, annealing at 55°C for 30 s, extension at 68°C for 30 s, and a final extension at 68°C for 4 min. The nuclear 18S was amplified using the primers 18SA (AYCTGGTTGATCCTGCCAGT; Medlin et al., 1988) and 18SB (ACCTTGTTACGACTTTTACTTCCTC; Nygren and Sundberg, 2003) with an initial denaturation at 95°C for 5 min, followed by 30 cycles of denaturation at 95°C for 30 s, annealing at 59°C for 30 sec, and extension at 72°C for 1 min, with a final extension at 72°C for 2 min. The primers used for sequencing were the same as those for amplifications, with an additional set of internal primers for 18S, 620F (TAAAGYTGYTGCAGTTAAA; Nygren and Sundberg, 2003) and 1324R (CGGCCATGCACCACC; Cohen et al., 1998). PCR products were purified using a Millipore Multiscreen 96-well PCR Purification System and sequenced using the forward and reverse primers mentioned above using an ABI 3730XL DNA Analyzer (Applied Biosystems) at The Natural History Museum Sequencing Facilities. For each gene fragment, contigs were assembled by aligning both forward and reverse sequences using Geneious 7.0.6[1]; chromatograms were visually inspected and ambiguous base calls were corrected manually. Sequences were deposited on GenBank with accession numbers MZ443996–MZ444014 (16S), MZ444015–MZ444046 (18S), and MZ474200–MZ474475 (COI).

Phylogenetic Analyses

In addition to the sequences generated for this study, sequences from Genbank were included in downstream analyses (see **Supplementary Table 1**). Sequences for COI (276 sequences generated for this study and 482 sequences from public databases; **Supplementary Table 1**) were aligned using MUSCLE in MEGA X (Kumar et al., 2018); with nucleotides translated into amino acids to identify pseudogenes based on the presence of stop codons. Sequences of 16S (19 generated for this study and 55 from public databases) and 18S (32 generated for this study and 32 from public databases) were aligned using MAFFT version 7 (Katoh et al., 2019) with the iterative refinement method FFT-NS-i, and unalignable regions were filtered in Gblocks server http://molevol.cmima.csic.es/castresana/Gblocks_server.html (Castresana, 2000), allowing gap positions within final blocks and less strict flanking positions. These alignments were used in three different datasets: (1) concatenated COI, 16S, and 18S alignment of a few representatives per morphotype, (2) a reduced dataset: COI alignment from a single representative per unique haplotype, and (3) complete dataset: all COI sequences. For the concatenated dataset, individual gene-alignments were concatenated in Geneious. Also, best substitution models for each partition (each marker, and each codon position for COI) were determined using PartitionFinder (Lanfear et al., 2017).

Phylogenetic trees were estimated using partitioned maximum-likelihood (RAxML v8.2.10; Stamatakis, 2006) and Bayesian inference (BEAST v2.4.7; Bouckaert et al., 2014), with the best inferred substitution model for each partition. In RAxML, the most common substitution model for each taxon was selected, with the best maximum-likelihood (ML) tree and support values estimated from 1000 rapid Bootstrap and 20 ML searches. BEAST analyses were performed with trees and clock models linked, a Yule tree model, and relaxed clock log normal. Two independent runs of a maximum 100M steps were combined after discarding 20% as burn-in. Runs were checked

[1]https://www.geneious.com

for convergence and a median consensus tree was estimated from the combined post-burn-in samples.

Species Delimitation

In order to estimate the number of species of scavenging amphipods collected during the DeepCCZ expedition, single-locus species delimitation was carried out (**Supplementary S3**). Three different methods were considered, including both distance- and tree-based approaches, because different methods are known to yield different results on the same dataset (Dellicour and Flot, 2018). Two different datasets for species delimitation were also used, the complete COI-only dataset and the reduced COI-only dataset that included a single representative per haplotype.

The barcode gap method ABGD (Automatic Barcode Gap Discovery; Puillandre et al., 2012) is a distance-based approach that separates Molecular Operational Taxonomic Units (MOTUs), hereby referred to as species, by identifying a threshold pairwise distance known as the barcode gap. ABGD was run on both full and reduced datasets, with K80 distances, default parameters for P (P = 0.001000, 0.001668, 0.002783, 0.004642, 0.007743, 0.012915, 0.021544, 0.035938, 0.059948, and 0.100000), and different values of X (X = 0.5, 0.8, 1.0, and 1.5).

Also, two different tree-based delimitation approaches were used: single-threshold GMYC (General Mixed Yule Coalescent; Pons et al., 2006) and PTP (Poisson tree processes; Zhang et al., 2013). Both tree-based approaches require a phylogenetic tree, with GMYC requiring an ultrametric (i.e., BEAST) tree to fit models of inter- and intraspecific processes and defining the limits of these. PTP does not require an ultrametric tree, as the speciation rate is modeled directly from the number of substitutions which is reflected in the branch lengths. Herein, the most conservative approach was considered, hence basing species delimitation on results from ABGD on the full dataset. However, some clusters/singletons identified by ABGD as separate putative species were nested in well-supported clades, from both ML and BI trees. These were combined to ensure all species were monophyletic. The full dataset of 758 barcodes, including GenBank sequences, was reduced to a CCZ dataset with 585 barcodes, excluding putative species delimited that were not found in the CCZ, to facilitate visualization of results.

Genetic Diversity, Population Differentiation and Connectivity

In order to investigate genetic diversity, as well as genetic differentiation, and qualitatively assess connectivity between localities, only the six species for which there were at least 30 COI sequences available were considered. mtDNA diversity metrics including haplotype number (h), haplotype diversity (Hd), nucleotide diversity (pi), and number of segregating sites (S), were estimated for each species using the R packages *pegas* (Paradis, 2010) and *ape* (Paradis and Schliep, 2019) (See **Supplementary S4**). Basic statistics of genetic diversity, including the analysis of molecular variance (AMOVA; Excoffier et al., 1992) and pairwise Fixation index (Fst; Weir and Cockerham, 1984), were estimated between different localities (e.g., APEIs 1, 4, 6, and 7, UK-1, OMS) using the R packages *poppr* (Kamvar et al., 2014) and *hierfstat* (Goudet and Jombart, 2020). Fst values were not estimated for *Paralicella* cf. *caperesca* 14, as two of the haplotypes differed in a single base and the other two haplotypes defined had a missing base. Genetic connectivity was visualized using minimum-spanning tree haplotype networks built using *pegas* (Paradis, 2010).

RESULTS

A total of 5749 specimens were captured during five 22 + hour deployments of baited traps, of which 1057 individual amphipods were captured on the APEI 1 seamount, 2399 on the APEI 4 abyssal plain site, 2292 (1801 plus 491 individuals from two different deployments) on the APEI 7 abyssal plain site, and a single specimen on the APEI 7 seamount site (**Table 1**). Thus, samples were collected from three different APEIs (APEI 1, APEI 4, and APEI 7) and from two different habitats (seamount and abyssal plain).

Alpha-Diversity and Compositional Assemblages

The 5749 amphipods recovered were morphologically identified as 17 morphospecies, belonging to seven families and nine genera (**Table 1**). Seven of these species are likely new to science. Four morphospecies were found in all three investigated western APEIs (*Abyssorchomene gerulicorbis* (Shulenberger and Barnard, 1976), *A. chevreuxi* (Stebbing, 1906), *Paralicella caperesca* Shulenberger and Barnard, 1976, and *P. tenuipes* Chevreux, 1908); three were found only in two APEIs, and 10 were found in a single APEI (**Table 1**; **Figure 2**). APEI 1 was the most species-rich area with 12 morphotypes recorded, and both APEIs 4 and 7 had eight. The assemblage composition of the three areas was highly dominated by a few species (**Figure 1**), with common deep-sea amphipod scavenger species dominating the communities in APEI 4 (*Abyssorchomene gerulicorbis*: 45%, *Paralicella tenuipes* complex: 25%, and *P. caperesca* complex: 21%) and APEI 7 (*P. tenuipes* complex: 75%, and *P. caperesca* complex: 16%). However, the seamount in APEI 1, the only seamount site with a large sample, was dominated by two new species that were also restricted to this site (*Tectovalopsis* sp. CCZ_229: 34%, *Stephonyx* sp. CCZ_220: 29%). The APEI 1 seamount site was the most species-rich, as well as the most diverse when accounting for the contribution of common and rare species using the inverse of Simpsons concentration (4.7 spp.), followed by APEI 4 (3.6 spp.), and APEI 7 (1.7 spp.). Diversity profiles for the three sites showed highly uneven communities (**Figure 3**).

There were two deployments on the abyssal plain in APEI 7, KM1808-007, and KM1808-018, with different bottom times of 30.7 and 47.1 h, respectively. The number of morphospecies recovered was higher (8) in the deployment with the longest bottom time than in deployment KM1808-007 with shorter bottom time (6 morphospecies; **Figure 1**, **Supplementary S1**). The number of specimens was also higher in the trap with longest bottom time (1801 vs. 491), and this general trend was

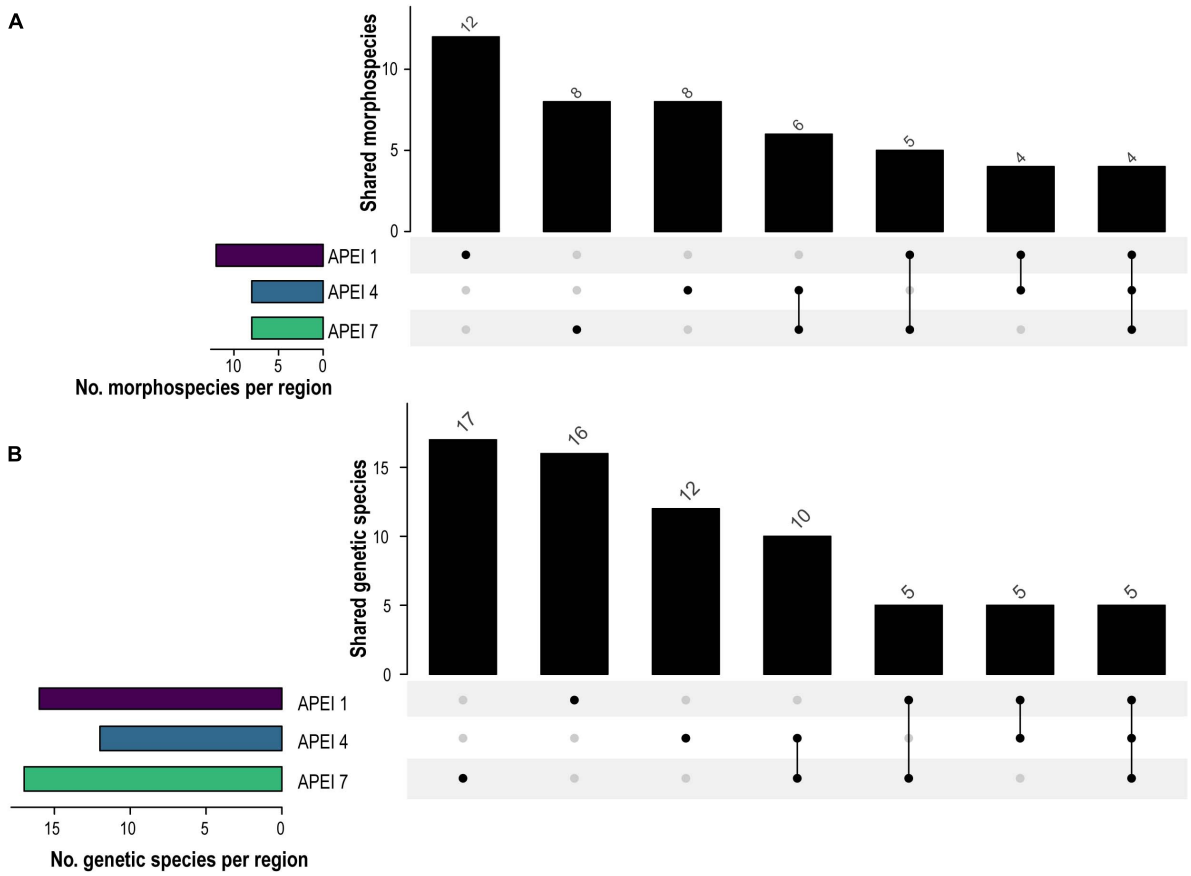

FIGURE 2 | UpSet plots showing shared number of morphospecies **(A)** and genetic species **(B)** species between western CCZ APEIs (APEI 1, 4, and 7) in vertical bars and total number of species per site indicated by horizontal bars.

also observed for the other deployments, except KM1808-032 (**Supplementary S1**) which recovered a single specimen. Relative abundance of species was very similar for both deployments on the abyssal plain in APEI 7, but *P. caperesca* relative abundance declined (from 26.27 to 13.1%) with increased bottom time while *P. tenuipes* relative abundance increased (from 64.9 to 78.1%) with increased bottom time.

Phylogenetic Analyses

In this study, a total of 239 sequences of the barcoding gene COI, with average length of 612 bp, were generated from samples from the western CCZ and 36 from samples from the eastern CCZ. Nucleotide composition was T: 36.6%, C: 18.2%, A: 26.7%, and G: 18.5. In addition, 22 and 32 sequences for the 16S and 18S markers, respectively, were generated from specimens belonging to different morphotypes to infer phylogenetic relationships (**Figure 4**).

The Bayesian phylogenetic tree showed a distinct clade belonging to the superfamily Alicelloidea, represented in the phylogeny by the families Alicellidae and Valettiopsidae (**Figure 4**). However, the family Cyphocarididae Lowry and Stoddart, 1997, belonging to the Lysianassoidea, was recovered within the Alicelloidea. Members of the superfamily Lysianassoidea were not recovered in the same clade. The family Alicellidae was not recovered as monophyletic, with *Paralicella* forming a separate clade from *Tectovalopsis*, *Civifractura* Weston, Peart and Jamieson, 2020 and *Alicella* Chevreux, 1899. The family Uristidae appeared also as paraphyletic, with *Stephonyx* and *Abyssorchomene* forming two separate clades. The phylogeny showed that *Stephonyx* is more closely related to *Eurythenes* (Eurytheneidae) than to *Abyssorchomene*. The latter appeared as a sister taxon to Orchomene Boeck, 1871 in the Tryphosidae Lowry and Stoddart, 1997 family.

Species Delimitation

Different species delimitation methods identified a different number of putative species within the 758 barcodes, being assigned to 35–131 putative species (ABGD: 35–41, PTP: 44–131, GMYC: 43–45; **Figure 5**, **Table 2**). The 239 COI sequences from the western CCZ were assigned to 29–80 putative species (ABGD: 29–33, PTP: 34–85, GMYC: 34–36). PTP performed poorly on the complete dataset, greatly over-splitting taxa. Although there was no clear barcode gap identified when plotting pairwise divergence distances (**Supplementary S3**), both ABGD and GMYC species hypotheses on the full dataset were similar. Hence, species delimitation was based on the output from ABGD as it was more

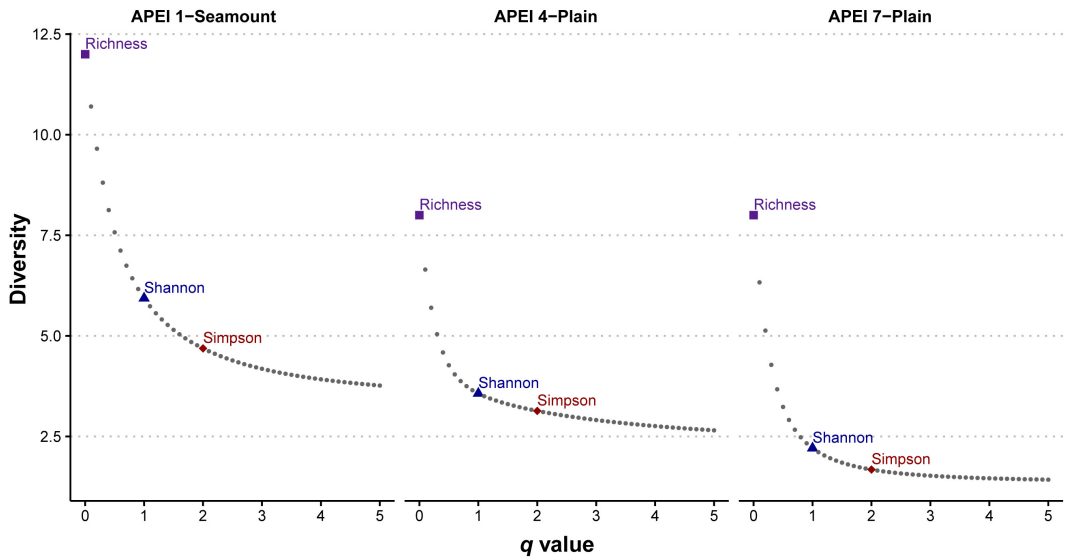

FIGURE 3 | Diversity profile plots for scavenging amphipods in western APEIs (Area of Particular Environmental Interest) 1, 4, and 7 showing higher diversity in APEI 1 and a strong dominance of species in each community. X-axis indicates different values of *q* (i.e., diversity order), with y-axis indicating diversity as effective number of species (i.e., Hill numbers). Values of q = 0, q = 1, and q = 2 are indicated as this correspond to values of species richness, the inverse of Shannon-Wiener entropy index, and the inverse of Simpson's concentration index, respectively.

conservative, and because a few species delimited by GMYC were recovered with low posterior values. Some clusters/singletons recovered as separate putative species were considered the same to ensure monophyly of all species.

Mean intraspecific divergence (K2P distance) varied between putative species, ranging from 0% (e.g., *Hirondellea* sp. CCZ_210) to 4% (*Cyclocaris* sp. CCZ_004) (**Table 1**). Mean interspecific divergence between species within the same morphotypes ranged from 2.19% (*Eurythenes magellanicus*) to 15.33% (*Paralicella caperesca* complex) (**Table 1** and **Supplementary Table 2**).

In total, 30 putative species of scavenging amphipods were found in the western CCZ. Considering previously published sequences from the eastern CCZ (Mohrbeck et al., 2021), and sequences generated for this study from some specimens collected during the MIDAS expedition, 11 of the species delimited were found only in the western CCZ. A total of 36 species were found to occur in the CCZ, with 20 distributed in the eastern CCZ, 14 of those spanning the entire CCZ and 3 being restricted to the eastern CCZ (the remaining two are shared with areas adjacent to the CCZ). APEI 7 had the highest species richness (17), followed by APEI 1 (16), and APEI 4 (12) (**Figures 2**, **5**). APEI 1, the seamount site, had the highest number of unique species (6), as well as fewest species shared with other sites. The most shared species (10) occurred between both abyssal plain sites, APEIs 4 and 7.

Several morphospecies were separated into multiple genetic species (**Table 1**, **Supplementary S5**), for which further morphological analyses are needed in order to determine diagnostic characters for each group. A few of these genetic species are consistent with previous studies. *Valettietta* cf. *anacantha* was recovered as two separate clades (**Figure 6**), Va2 and Va1 in Mohrbeck et al. (2021). Both lineages were also recovered in our samples from the eastern CCZ, but only Va2 (*V. cf. anacantha* CCZ_056C) was found in the western CCZ.

Eurythenes magellanicus was also recovered as two separate genetic species, both found in the western CCZ (**Figure 7**, **Supplementary S5**). Havermans (2016) identified two clades, Eg4 and Eg5, within the species, plus an additional sequence (TAI-1; Havermans et al., 2013) recovered outside of both clades. In the western CCZ, representatives of Eg4 were found, along with a clade including the sequence TAI-1, but did not recover representatives of Eg5. The clade including the sequence TAI-1 includes specimens collected in the Pacific Ocean (Sea of Okhotsk: OKI-3 (Narahara-Nakano et al., 2018), and off Taiwan: TAI-1, and the western CCZ), but also a specimen collected in the Porcupine Abyssal Plain (DY077_83_B2; Horton et al., 2020a). In a recent revision of the genus *Eurythenes* (d'Udekem d'Acoz and Havermans, 2015), specimens from both clades Eg4 and Eg5 were included as voucher sequences for *E. magellanicus*, and a detailed morphological description was provided based on a specimen from Eg5. *Eurythenes maldoror* was also recovered as two separate clades, both collected in the western CCZ. Specimens from the clade including the holotype sequence (ArgB-7, GenBank JX887151) were thus listed as *E. maldoror*, and the remaining ones as *E.* cf. *maldoror* CCZ_232.

Genetic Structuring of Scavenging Amphipods

Six species, for which there were at least 30 COI sequences available, were chosen for connectivity analyses –two species within the *Paralicella caperesca* complex, two species within the *P. tenuipes* complex, *Abyssorchomene gerulicorbis*, and *Cyclocaris* sp. CCZ_004. A total of 363 individuals were included in

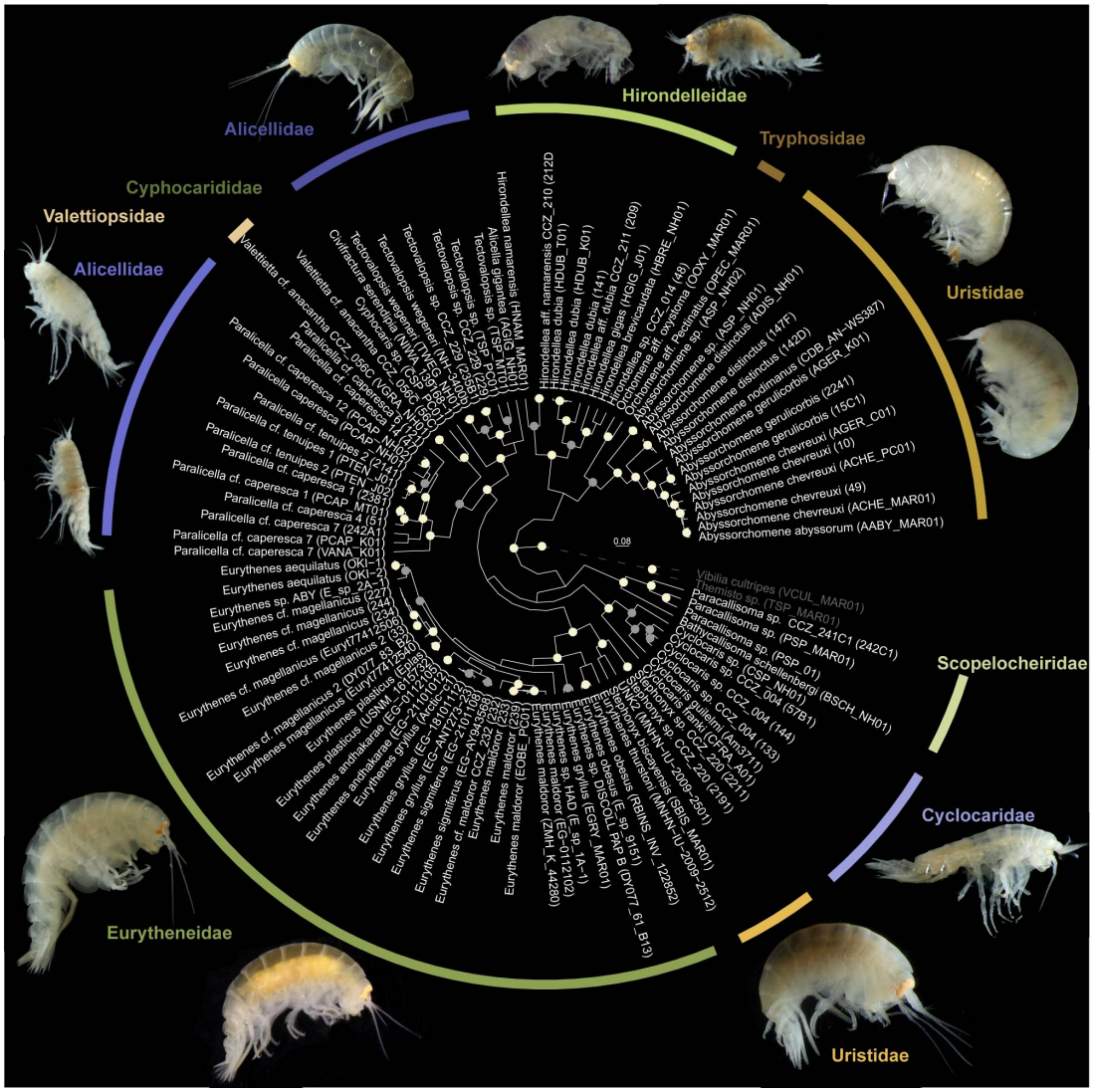

FIGURE 4 | Bayesian phylogenetic tree from a concatenated alignment of the COI, 16S, and 18S genes of the superfamilies Alicelloidea and Lysianassoidea. Only highly supported nodes are highlighted, with posterior support values of 1.0 colored in white and ≥0.95 in gray.

the analyses (154 from the western CCZ), with 77 unique haplotypes found (**Table 3**). These species are also distributed in the eastern CCZ, and in other regions except for a single species for which the only samples were from the CCZ (*Paralicella* cf. *caperesca* 14). Several haplotypes were found in all species, with haplotype diversity (Hd) being high for all except *P.* cf. *caperesca* 14. *Cyclocaris* sp. CCZ_004 had the highest Hd (0.92), with 20 different haplotypes (h) found across 31 samples.

Minimum-spanning tree haplotype networks were constructed to visualize genetic differentiation between regions (**Figure 8**). No genetic differentiation was observed, with haplotypes being shared across different localities. This is also consistent with the results obtained from the AMOVA, with most of the variation being found within localities (>89.06%; **Table 3** and **Supplementary S4**). Pairwise fixation index (Fst) also suggested there is no divergence between areas in the CCZ (**Table 4**, **Supplementary S4**), with very low values estimated for all species but *P.* cf. *tenuipes* 1. Fst values considered as significant for differentiating population (>0.15) were found between APEI 1-APEI 7, APEI 1-OMS, APEI 4-APEI 6, APEI 4-OMS, APEI 6-APEI 7, APEI 6-OMS, and APEI 6-UK-1.

DISCUSSION

With increasing interest in deep-sea mining, there is an urgent need for accurate estimates of species diversity, as well as understanding the processes generating and maintaining it, in order to inform environmental management plans. Despite the large number of scientific expeditions that have been carried out in the CCZ, only two studies have focused on necrophagous

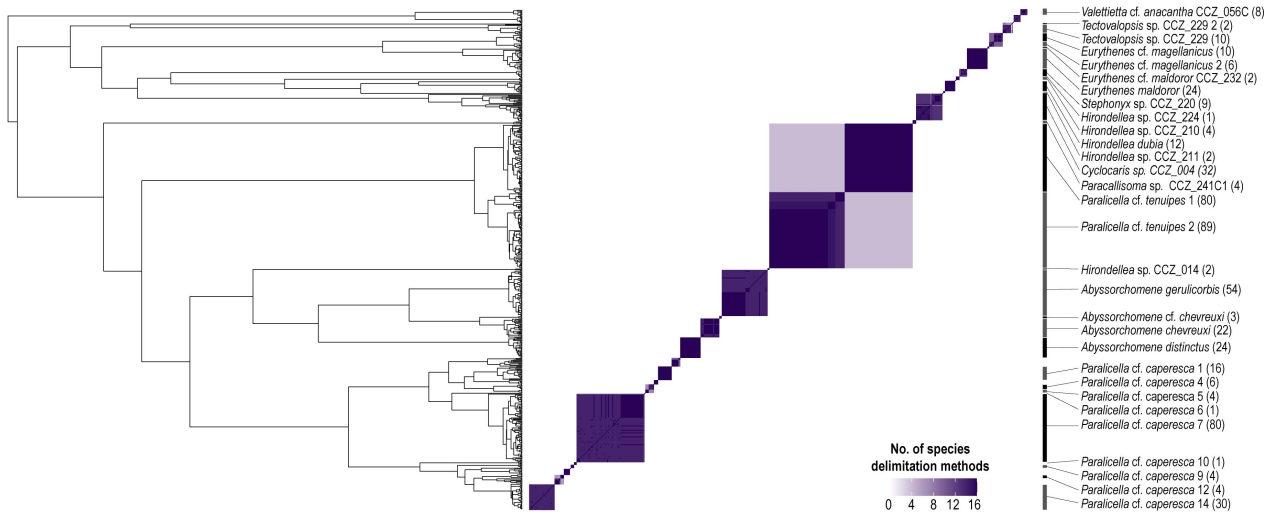

FIGURE 5 | Bayesian phylogenetic tree from COI-only data (CCZ dataset; i.e., 585 sequences) indicating species delimitation for the 30 genetic species found to occur in the western CCZ. Tip labels representing specimens distributed in the western CCZ are highlighted. The heatmap indicates the number of species delimitation methods that recovered each different cluster, with species boundaries considered for downstream analyses indicated on the right. Number in brackets indicates number of specimens.

amphipods (Patel et al., 2020; Mohrbeck et al., 2021), which are important components of abyssal ecosystems. This study contributes to our understanding of the diversity, biogeography, and connectivity of bait-attending necrophagous amphipods in the CCZ and is the first carried out in the western CCZ.

TABLE 2 | Table indicating the 16 different approaches for species delimitation considered in this study.

Method	Dataset	Notes	# Clusters	# singletons	Total species
ABGD	complete	X = 0.5; K80	33(22)	7(11)	40(33)
		X = 0.8; K80	33(22)	7(11)	40(33)
		X = 1.0; K80	33(22)	7(11)	40(33)
		X = 1.2; K80	33(22)	7(11)	40(33)
		X = 0.1.5; K80	29(21)	5(8)	34(29)
	reduced	X = 0.5; K80	29(21)	5(8)	34(29)
		X = 0.8; K80	29(21)	5(8)	34(29)
		X = 1.0; K80	29(21)	5(8)	34(29)
		X = 1.2; K80	29(21)	5(8)	34(29)
		X = 1.5; K80	29(21)	5(8)	34(29)
PTP	complete	Bayesian	50(27)	80(58)	130(85)
		ML	52(30)	63(40)	115(70)
	reduced	B	34(21)	9(13)	43(34)
		ML	34(21)	12(14)	46(35)
GMYC	complete	single-threshold	38(27)	6(9)	44(36)
	reduced	single-threshold	36(26)	6(8)	42(34)
Mean			34.4(22.9)	14.6(14.6)	49(37.5)

Number of species defined from the 758 barcodes are shown, with the number of species defined from the 239 barcodes from the western CCZ indicated in parentheses. Some singletons from the western CCZ were found in other areas, hence the number of singletons in only the western CCZ can be higher than when considering all barcodes. ABGD, Automated Barcode Gap Discovery; GMYC, General Mixed Yule Coalescent; PTP, Poisson Tree Process.

Morphological Diversity of Scavenging Amphipods

The western CCZ, with 17 different morphospecies, appears to be much more species rich than the eastern CCZ. However, this apparent higher diversity could be an artifact of sampling. Although the western CCZ has sustained considerably less sampling effort, with only five baited trap deployments, sampling has encompassed a wider range of habitats (abyssal plains and seamounts), as well as larger depth ranges (3203–4872 m). Nonetheless, sampling adequacy has been evaluated using rarefaction plots for a previous study in the eastern CCZ (Patel et al., 2020), as well as herein (see **Supplementary S1**), with all species accumulation curves plateauing except for one CCZ station included in Patel et al. (2020). The recent study by Mohrbeck et al. (2021) included a subsample of 645 specimens and found the same species richness (10 morphospecies) for the eastern CCZ (Patel et al., 2020). Because one study was strictly morphology-based, it is not possible to determine if some of the species identified to genus level only are shared between the eastern CCZ studies. Nonetheless, both reported the same genera (*Eurythenes, Paralicella, Abyssorchomene, Paracallisoma*, and *Valettietta*), with the addition of a single species of *Hirondellea* only reported by Patel et al. (2020). Based on the species overlap found in the present study, it is very likely that most of the species reported in Patel et al. (2020) represent the same species reported in Mohrbeck et al. (2021).

In the western CCZ, species richness was highest in APEI 1, the seamount site, with 12 morphospecies. The abyssal APEI 4 and 7 sites had eight morphospecies each, although composition differed between the assemblages. APEI 7 was highly dominated (91%) by species of the *Paralicella tenuipes* and *P. caperesca* complexes, as reported for the eastern areas in 2015 (UK-1 Stratum B, OMS and APEI 6; Mohrbeck et al., 2021) and previous

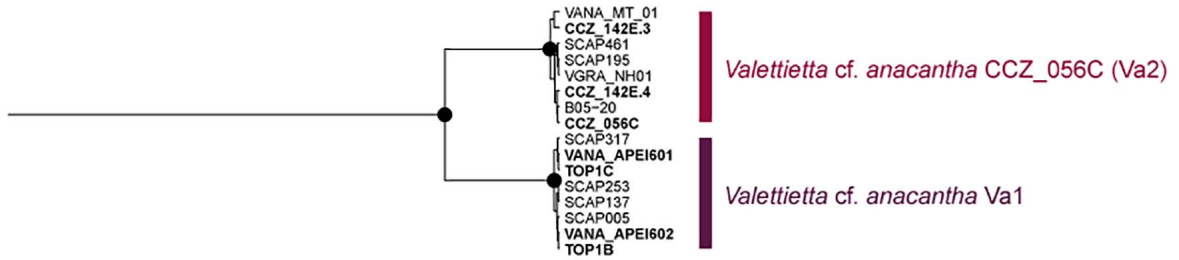

FIGURE 6 | Bayesian COI-only phylogenetic tree for the morphospecies *Valettietta* cf. *anacantha*. The two genetic clades are indicated on the right. Node posterior support values of 1.0 are indicated as black circles. Sequences generated in this study are highlighted in bold, with western CCZ labels starting with "CCZ_".

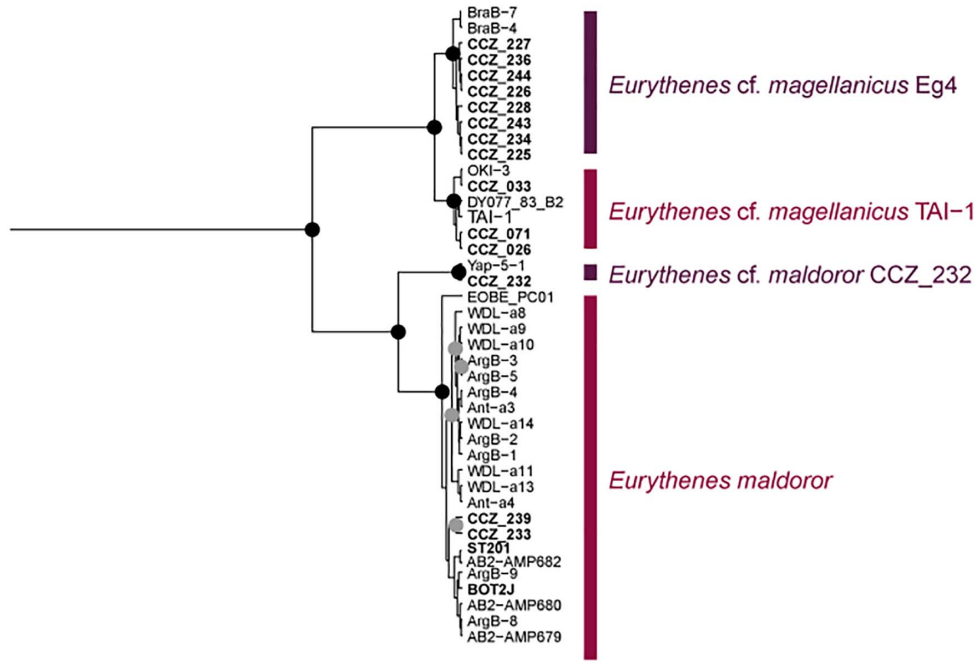

FIGURE 7 | Bayesian COI-only phylogenetic tree for species of *Eurythenes* distributed in the western CCZ. Genetic species are indicated on the right. Node posterior support values of 1.0 are indicated as black circles, and values ≥ 0.95 in gray circles. Sequences generated in this study are highlighted in bold, with western CCZ labels starting with "CCZ_".

TABLE 3 | Population genetic statistics for six genetic species of scavenging amphipods occurring in the western CCZ.

Species	No. samples	S	h	Hd	π	AMOVA		
						Variation between regions%	Variation between samples within regions%	Variation within samples%
Abyssorchomene gerulicorbis	54	7	10	0.78	0.0024	0.19	4.25	95.56
Cyclocaris sp. CCZ_004	31	61	20	0.92	0.0051	−59.77	−3.11	162.88
Paralicella cf. *caperesca* 14	30	2	4	0.25	0.0001	−20.84	1.50	119.34
Paralicella cf. *caperesca* 7	80	31	25	0.81	0.0047	0.97	−1.89	101.92
Paralicella cf. *tenuipes* 1	80	7	6	0.63	0.0019	−1.51	12.46	89.06*
Paralicella cf. *tenuipes* 2	88	22	12	0.76	0.0072	−0.58	−0.11	100.69

Number of samples per species, number of segregating sites (S), number of haplotypes (h), haplotype diversity (Hd), and nucleotide diversity (π) are given for each species, as well as the percentage of variation explained between regions, between samples within regions, and within samples as estimated from the analysis of molecular variance (AMOVA).
**Monte-Carlo tests $p < 0.05$.*

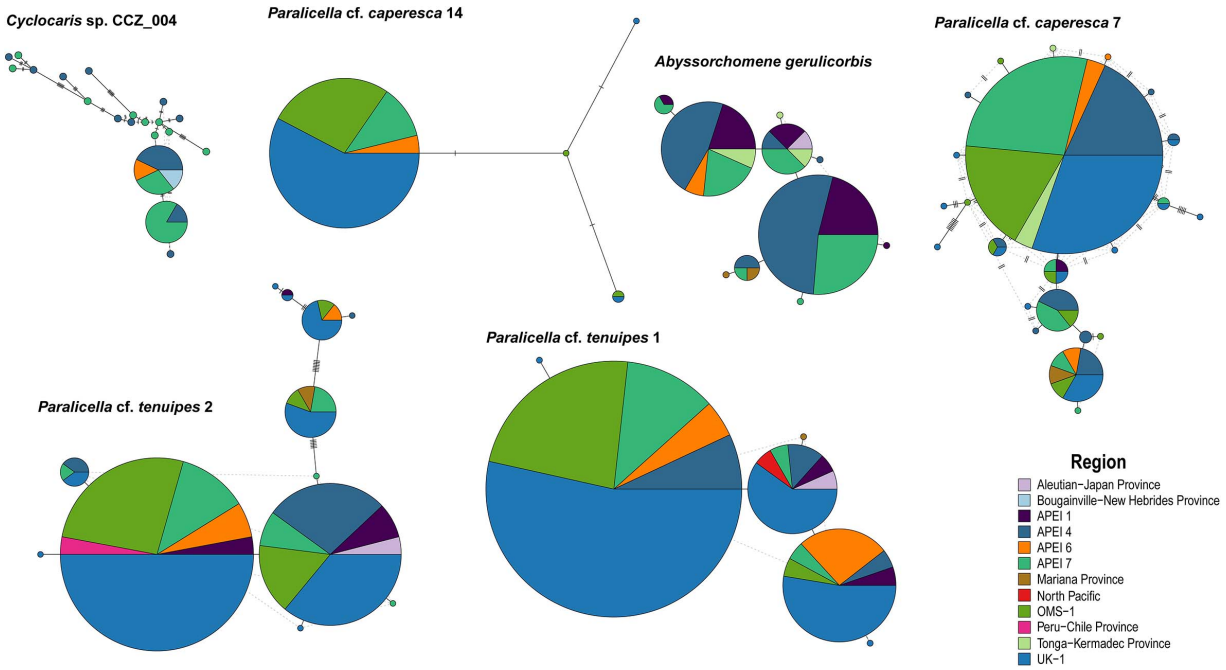

FIGURE 8 | Minimum-spanning tree haplotype networks for COI for six species of scavenging amphipods. Circles are proportional to the number of samples and all regions are color-coded.

studies north of Hawaii (Ingram and Hessler, 1983). APEI 4 was dominated by *Abyssorchomene gerulicorbis, P. tenuipes* complex, and *P. caperesca* complex, differing from APEI 7 and previous findings for the eastern CCZ. Both Mohrbeck et al. (2021) and Patel et al. (2020) reported another species of *Abyssorchomene*, *A. distinctus*, to be dominant in several sites, with a westward decrease in abundance. In our study, *A. distinctus* only occurred in APEI 4, with 3 specimens identified. Interestingly, the most common abyssal species (*Abyssorchomene gerulicorbis, A. chevreuxi*, *Paralicella caperesca*, and *P. tenuipes*) were not found in large numbers in APEI 1, the seamount site, with the community dominated (∼63%) instead by two new species restricted to this site (*Tectovalopsis* sp. CCZ_229 and *Stephonyx* sp. CCZ_220).

While scavenging amphipods are easily collected using baited-traps, and trapping is the only method to collect them in large numbers, this sampling strategy is always biased (Kaïm-Malka, 2005). Different species have different chemosensory abilities, as well as different swimming speeds, which affect distance of attraction to the bait (Horton et al., 2020c). Stronger odor plumes can also be more attractive, and while these depend on currents, no correlation has been found between current speeds and relative abundance of trapped amphipods (Leitner et al., 2017). Relative abundances of different species attracted to baited traps can also be biased because some developmental stages might be fasting (e.g., brooding females) or have different diets (e.g., juveniles), therefore not attend bait (Kaïm-Malka, 2005). Very few replicated bait-trap studies have been carried out, but differences in species composition between these traps, with different deployment times and at different heights above the seabed, have suggested a possible succession of scavenging species (Horton et al., 2020c). Two baited traps were deployed in the abyssal plains at APEI 7. Morphospecies diversity was higher in the deployment with the longest bottom time, where the "rare" species *Eurythenes magellanicus* and *Valettietta* sp. were recovered in low numbers (two and one individuals, respectively). This possibly indicates a later arrival to the trap, as previously suggested (Horton et al., 2020a), indicating that collection of "rare" species necessitates increased time on the seabed. Despite the limited data with few deployments, our results suggest that abundance increases with deployment times (**Supplementary S1**). However, the overall relative abundance of the common species seem to be similar between the only replicated deployments on the abyssal plain on APEI 7, but relative abundances of *P. caperesca* decreased while *P. tenuipes* increased with longer bottom times. While longer deployment times seem to better recover "rare" species (Horton et al., 2020a), the dominance of new or "rare" species (*Stephonyx* sp. and *Tectovalopsis* sp.) in the seamount site is unlikely to be explained by sampling bias.

Temporal and spatial variability in scavenging communities have been linked to environmental conditions. A recent study found that compositional changes in amphipod scavenging communities in the Atlantic were related to changes in Particulate Organic Carbon (POC) flux to the seafloor, shifting between communities dominated by specialist scavengers of food-falls (*Paralicella*) (Duffy et al., 2016; Havermans and Smetacek, 2018) to opportunistic scavengers (*Eurythenes* and *Abyssorchomene*) that include organic matter in their diets (Horton et al., 2020c). While the differences in community composition observed

TABLE 4 | Pairwise Fixation index (FST) for genetic species of scavenging amphipods collected in different areas within the Clarion-Clipperton Zone (CCZ).

Abyssorchomene gerulicorbis

	APEI 1	APEI 4	APEI 7
APEI 1	–		
APEI 4	0.00000	–	
APEI 7	0.00000	0.00000	–

***Cyclocaris* sp. CCZ_004**

	APEI 4	APEI 7
APEI 4	–	
APEI 7	0.00849	–

***Paralicella* cf. *caperesca* 7**

	APEI 4	APEI 6	APEI 7	OMS-1	UK-1
APEI 4	–				
APEI 6	0.00000	–			
APEI 7	0.00000	0.00000	–		
OMS-1	0.00000	0.00000	0.00000	–	
UK-1	0.03660	0.00000	0.00000	0.00000	–

***Paralicella* cf. *tenuipes* 1**

	APEI 1	APEI 4	APEI 6	APEI 7	OMS-1	UK-1
APEI 1	–					
APEI 4	0.04673	–				
APEI 6	0.00000	0.17469	–			
APEI 7	0.32426	0.00000	0.31148	–		
OMS-1	0.67346	0.15535	0.54812	0.00000	–	
UK-1	0.07118	0.00000	0.15727	0.00000	0.10164	–

***Paralicella* cf. *tenuipes* 2**

	APEI 1	APEI 4	APEI 6	APEI 7	OMS-1	UK-1
APEI 1	–					
APEI 4	0.00000	–				
APEI 6	0.00000	0.07942	–			
APEI 7	0.00000	0.03616	0.02197	–		
OMS-1	0.00000	0.01638	0.00568	0.00000	–	
UK-1	0.00000	0.04897	0.00000	0.00000	0.00000	–

APEI, Areas of Particular Environmental Interest.

in the three western CCZ sites may be driven by different environmental conditions across the three sites, the difference in species composition between the seamount and abyssal plain sites is striking, with the seamount site dominated by genera not commonly reported in the literature such as *Paralicella, Eurythenes* and *Abyssorchomene* (e.g., Fujii et al., 2013; Lacey et al., 2016).

Net primary production and POC data suggest there is a southeast to northwest gradient of declining food availability and productivity in the western CCZ (Washburn et al., 2021b); for example, APEI 1 site is considered oligotrophic (0.06 mg m-3; McQuaid et al., 2020; Washburn et al., 2021b). Despite the low food availability, the seamount site in APEI 1 had the highest diversity of scavenging amphipods. For this site, very low abundances of predators, with an overall maximum of 3 individuals of a single predator species observed in either of the two baited camera deployments, were reported (Leitner et al., 2021). The high diversity could be driven by the low abundance of predators, but could also be driven by the seamount higher habitat heterogeneity (Washburn et al., 2021a) or by its oligotrophic condition (McQuaid et al., 2020). Oligotrophy has been associated with lower abundances but higher species diversity of scavenging amphipods compared to eutrophic sites (Horton et al., 2020c), and higher habitat heterogeneity has been also linked to higher diversity. Seamounts have been suggested to be biodiversity hotspots (Rowden et al., 2010). Additionally, seamounts have been posited to have endemic faunas, while also acting as faunal reservoirs for surrounding areas (Clark et al., 2010). However, very little overlap has been reported for megafauna between seamount and abyssal plain sites in the CCZ (Cuvelier et al., 2020), with large differences in the composition of scavenging fish communities. This may indicate seamount faunas in the CCZ are distinct from those of abyssal plains. The species composition of necrophagous amphipods between the seamount and abyssal plain sites in this study differed drastically, with the seamount appearing to have a distinct scavenging fauna. Five out of the seven potentially new species identified in this study were only found in APEI 1 on the seamount. The seamount site was also the shallowest (4084 m; abyssal plain sites > 4800 m depth). While depth has been identified to structure scavenging communities (Lacey et al., 2016), it is very unlikely this explains the difference in composition since these bathymetric changes in species assemblages occur at the abyssal-hadal transition zone around 6000 m depth (Jamieson et al., 2011; Lacey et al., 2016), and the eastern CCZ sites are also shallower (∼4200 m depth). Owing to the lack of sampling in abyssal plains in APEI 1, and in seamounts in APEIs 4 and 7, it is not possible to determine if the difference in species composition and diversity is attributed to the geoform, or to different environmental conditions in APEI 1 leading to general differences in species composition from other CCZ sites (Patel et al., 2020; Mohrbeck et al., 2021).

Commonly reported species (i.e., *Abyssorchomene gerulicorbis*, *A. chevreuxi*, *Eurythenes maldoror,* and *E. magellanicus*) were found in very low numbers in our samples, in at least one of the three sites. This is in accordance with previous findings in amphipods (Mohrbeck et al., 2021) and gastropods (McClain and Hardy, 2010; McClain, 2021), suggesting that local rarity is not necessarily linked to small geographic ranges. There was also overlap of species with narrow ranges in adjacent areas. *Hirondellea dubia* had only been reported for southwest Pacific trenches, where it is a dominant component of the hadal scavenging amphipod community (Lacey et al., 2016). This species was found in very low numbers in APEI 4, the southwestern most APEI, closer to the likely core area of distribution of the species. Moreover, four putative new species of *Hirondellea* were also found. These also appear to be restricted to a single area, with three of them only occurring at the seamount site in APEI 1.

Genetic Diversity, Population Differentiation and Connectivity

Single-locus species delimitation is being more commonly used for uncovering biodiversity in remote and poorly studied systems,

as it can provide a fast and accurate assessment (Glover et al., 2015, 2016; Dahlgren et al., 2016; Wiklund et al., 2017). Species delimitation was performed using a fragment of the barcoding cytochrome *c* oxidase subunit I (COI), which has been used in scavenging amphipods previously (e.g., Havermans, 2016; Horton et al., 2020a). In our study, it revealed a diversity greater than that estimated from morphological characters, with at least 30 species identified from barcode sequences compared to 17 morphospecies identified from external morphological characters, similar to a previous study for the CCZ (Mohrbeck et al., 2021). However, there was disagreement between the different methods for species delimitation with regard to the inferred species numbers. This has been previously reported (Rubinoff et al., 2006), and it has been suggested that estimates of species boundaries should be treated with caution and different approaches should be compared (Dellicour and Flot, 2018).

The distance-based approach ABGD is known to lump species (Dellicour and Flot, 2018) and, as expected, it inferred the lowest number of species in our datasets (35–41 putative species for the complete dataset; **Table 2**). In contrast, the GMYC approach (Pons et al., 2006) tends to oversplit lineages (Correa et al., 2017; da Silva et al., 2017), yet it yielded only a slightly larger number of species than ABGD (43–45 putative species for the complete dataset; **Table 2**). bPTP (bayesian Poisson tree processes; Zhang et al., 2013) has been found to be sensitive to different mutation rates and has been reported to produce the least accurate results in empirical datasets (Hofmann et al., 2019). In this study, the results produced using the reduced dataset, excluding redundant haplotypes, were very similar to those from GMYC (44–47 species for the complete dataset; **Table 2**). However, when all haplotypes were considered, bPTP greatly oversplit lineages (116–131 species for the complete dataset; **Table 2**), even for those in which genetic divergences were low (e.g., *Abyssorchomene gerulicorbis*; mean intraspecific divergence: 0.23%).

Several widespread lineages of scavenging amphipods have been identified as complexes of species using COI. While several differ morphologically and have subsequently been described as new species (e.g., Havermans et al., 2011; d'Udekem d'Acoz and Havermans, 2015; Havermans, 2016; Weston et al., 2020), cryptic lineages have yet to be subjected to more detailed morphological analyses, despite having been identified within common species such as *Paralicella caperesca* (Ritchie et al., 2017). The morphological characters commonly used to separate *P. caperesca* from *P. tenuipes* have been reported as not being robust enough to accurately discriminate the species (Ritchie et al., 2015; 2017), but these two species were easily separated by the conspicuous red eyes in *P. tenuipes*, as reported by Mohrbeck et al. (2021). However, both species were found to represent complexes of cryptic species. Mohrbeck et al. (2021) identified at least four genetically distinct clusters within *P. caperesca*, whereas nine (mean interspecific divergence ranging from 2.33–15.33%) were identified in this study, five of which were found in both the western and eastern CCZ and belong to three of the clades identified by Mohrbeck et al. (2021) (Pc1, Pc3, and Pc4), with Pc2 being absent from the western CCZ. It is important to highlight that some of the *P. caperesca* MOTUs hypothesized by Mohrbeck et al. (2021) differ from the ones in this study, with some considered in here as multiple MOTUs. This reflects differences between methods for species delimitation and highlights the need to carry out further studies targeting a larger number of genes, as well as detailed morphological studies that will provide evidence to support one of the different species hypotheses available. For instance, several thresholds for species discrimination in amphipods have been proposed, ranging from the widely used 3% (Hebert et al., 2003) to 16% (e.g., Fiser et al., 2015). Although a more recent study proposed a threshold of 7% to discriminate amphipod species (Tempestini et al., 2018), and was also used for scavenging amphipods in the CCZ (Mohrbeck et al., 2021), no clear barcode gap was found in this study (**Supplementary S3**), and interspecific distances were estimated >2%. There was also support for this as the different approaches considered inferred a similar number of species.

There was no evidence of geographic genetic differentiation, with haplotypes being shared across different sites in the CCZ and with other adjacent areas (e.g., Kermadec, Peru-Chile, South Fiji, Mariana, and New Hebrides trenches; **Figure 8**). Additionally, none of the haplotype networks showed a strong star-like pattern, with only *P.* cf. *caperesca* 14 and *P.* cf. *caperesca* 7 having a somewhat predominant central haplotype. However, the starburst pattern of *P.* cf. *caperesca* 7 is indicative of low geographic structure and might suggest rapid population expansion (Neubaum et al., 2007). Although we acknowledge that the use of COI alone could prevent us from detecting genetic geographic structuring, COI has shown similar patterns to nuclear microsatellite markers in squat lobsters (Yan et al., 2020). Thus, the lack of geographic structuring observed in the widespread scavenging amphipods included in this study might not necessarily be an artifact of COI lacking resolution, but rather the result of them being highly motile, with high levels of gene flow across the Pacific Ocean, as has been shown for a study on *Paralicella* spp. using microsatellites (Ritchie et al., 2017).

Available data thus currently support the hypothesis that many mobile necrophagous amphipods are wide ranging and thus could be relatively resistant to localized mining impacts, although apparent endemism (e.g., the species found in APEI 1) and/or reduced motility in select species could place them under greater threat (Havermans et al., 2011). There are very few comparable studies of other CCZ taxa, but in the small nodule-dwelling sponge, *Plenaster craigi* Lim and Wiklund, 2017, evidence of geographic genetic structure was found using microsatellite DNA, suggesting recolonization of this sessile species into disturbed areas may be much slower (Taboada et al., 2018). These two groups of taxa, sessile nodule dwelling *P. craigi* and highly motile scavenging amphipods may make useful contrasts in future monitoring studies, being functionally very different, relatively easy to collect and with potentially differing patterns of resilience to mining impacts.

Phylogenetic Relationships of Scavenging Amphipods

Our phylogenetic analyses of scavenging amphipods recovered all genera included as monophyletic. However, higher taxa were recovered as polyphyletic, differing from the current

classification (Horton et al., 2020b). A finding consistent with other published phylogenies (Corrigan et al., 2014; Ritchie et al., 2015; Copilas-Ciocianu et al., 2020) was the recovery of the superfamilies Alicelloidea and Lysianassoidea as non-monophyletic. Those published phylogenies also recovered the families Alicellidae and Uristidae as polyphyletic, and while our results are concordant, they all differ in phylogenetic relationships at the family level. Most families were recovered with high support values, but there was no resolution for deeper nodes in the phylogeny, most likely due to targeting only three genetic markers (COI, 16S, and 18S), as these were the most abundant in the datasets considered for this study. In contrast, both phylogenies from Ritchie et al. (2015) and Copilas-Ciocianu et al. (2020) showed high support values in deeper nodes in the phylogeny, but showed contrasting hypotheses of phylogenetic relationships between families, possibly also as a result of choice of genetic markers and taxa representativeness. Further studies to elucidate phylogenetic relationships of scavenging amphipods should therefore consider a wider sample of scavenging genera and a much larger number of genetic markers.

CONCLUSION

This study has again demonstrated the advantages of molecular taxonomy over morphology-based taxonomy in taxa where cryptic speciation is pervasive, allowing for fast but reliable diversity estimates in poorly studied groups. However, different approaches for species delimitation yielded different results, making it necessary to contrast results from different approaches and datasets. The finding of potentially cryptic species within described, widely distributed morphospecies such as *Paralicella caperesca* highlights the need for detailed, integrative studies that aim to identify and describe cryptic diversity. The study also contributes to our understanding of the diversity and connectivity of necrophagous amphipods in the western Clarion-Clipperton Zone (CCZ), in particular within the poorly studied APEI regions. A higher diversity, of both morphospecies and genetic species was found from a single expedition to the western CCZ than from multiple expeditions in eastern CCZ spanning several years. Within the western CCZ, differences in composition and diversity of scavenging communities between sites on seamounts and those on abyssal plains were observed, possibly driven by habitat heterogeneity and different environmental conditions between the sites, but further studies are required to understand the drivers of the diversity patterns observed. It is critical to understand the drivers of diversity, and the potential for biodiversity reservoirs within different topographic features in the CCZ, and in the currently conserved APEI regions, to allow sustainable management of any future deep-sea mining industry.

DATA AVAILABILITY STATEMENT

The original contributions presented in the study are publicly available. This data can be found here: Sequences were deposited in GenBank with accession numbers MZ443996–MZ444014 (16S), MZ444015–MZ444046 (18S), and MZ474200–MZ474475 (COI). Code used for all analyses has been made available as **Supplementary Material**.

AUTHOR CONTRIBUTIONS

JD, RD, AL, KM, HW, ST, DJ, and CS collected and processed samples. GB-C and ST generated genetic sequences. TH carried out detailed morphological examination. AG, TD, and GB-C designed the study, with GB-C carrying out the analyses. All authors contributed to drafting and reviewing the manuscript.

ACKNOWLEDGMENTS

We thank the masters, crew and technical support staff on the *R/V Kilo Moana* and ROV Luukai for their expertise in collecting samples. We thank the primary funder, the Gordon and Betty Moore Foundation grant no. 5596 and NOAA Office of Ocean Exploration (grant #NA17OAR0110209). We also acknowledge funding from UK Seabed Resources, the UK Natural Environment Research Council grant numbers NE/T003537/1 and NE/T002913/1, and The Norwegian Research Council (JPIO Mining Impact 2). We also acknowledge Dr. Lauren Hughes and Muriel Rabone (NHM) for curatorial support, and Elena Luigli (NHM) and Claire Griffin (NHM) for lab support. This is a contribution from SOEST, University of Hawai'i at Mānoa.

SUPPLEMENTARY MATERIAL

The Supplementary Material for this article can be found online at: https://www.frontiersin.org/articles/10.3389/fmars.2021.705237/full#supplementary-material

REFERENCES

Bouckaert, R., Heled, J., Kuhnert, D., Vaughan, T., Wu, C. H., Xie, D., et al. (2014). BEAST 2: a software platform for Bayesian evolutionary analysis. *PLoS Comput. Biol.* 10:e1003537. doi: 10.1371/journal.pcbi.1003537

Castresana, J. (2000). Selection of conserved blocks from multiple alignments for their use in phylogenetic analysis. *Mol. Biol. Evol.* 17, 540–552. doi: 10.1093/oxfordjournals.molbev.a026334

Christiansen, B., Pfannkuche, O., and Thiel, H. (1990). Vertical distribution and population structure of the necrophagous amphipod *Eurythenes gryllus* in the west European basin. *Mar. Ecol. Prog. Ser.* 66, 35–45. doi: 10.3354/meps066035

Clark, M. R., Rowden, A. A., Schlacher, T., Williams, A., Consalvey, M., Stocks, K. I., et al. (2010). The ecology of seamounts: structure, function, and human impacts. *Ann. Rev. Mar. Sci.* 2, 253–278. doi: 10.1146/annurev-marine-120308-081109

Cohen, B. L., Gawthrop, A., and Cavalier-Smith, T. (1998). Molecular phylogeny of brachiopods and phoronids based on nuclear-encoded small subunit ribosomal RNA gene sequences. *Philos. Trans. R. Soc. Lond. B Biol. Sci.* 353, 2039-2061.

Copilas-Ciocianu, D., Borko, S., and Fiser, C. (2020). The late blooming amphipods: global change promoted post-Jurassic ecological radiation despite Palaeozoic origin. *Mol. Phylogenet. Evol.* 143:106664. doi: 10.1016/j.ympev.2019.106664

Correa, C., Vasquez, D., Castro-Carrasco, C., Zuniga-Reinoso, A., Ortiz, J. C., and Palma, R. E. (2017). Species delimitation in frogs from South American temperate forests: the case of *Eupsophus*, a taxonomically complex genus with high phenotypic variation. *PLoS One* 12:e0181026. doi: 10.1371/journal.pone.0181026

Corrigan, L. J., Horton, T., Fotherby, H., White, T. A., and Hoelzel, A. R. (2014). Adaptive evolution of deep-sea amphipods from the superfamily lysiassanoidea in the North Atlantic. *Evol. Biol.* 41, 154–165. doi: 10.1007/s11692-013-9255-2

Cuvelier, D., Ribeiro, P. A., Ramalho, S. P., Kersken, D., Martinez Arbizu, P., and Colaço, A. (2020). Are seamounts refuge areas for fauna from polymetallic nodule fields? *Biogeosciences* 17, 2657–2680. doi: 10.5194/bg-17-2657-2020

da Silva, R., Peloso, P. L. V., Sturaro, M. J., Veneza, I., Sampaio, I., Schneider, H., et al. (2017). Comparative analyses of species delimitation methods with molecular data in snappers (Perciformes: Lutjaninae). *Mitochondrial DNA A DNA Mapp. Seq. Anal.* 29, 1108–1114. doi: 10.1080/24701394.2017.1413364

Dahlgren, T. G., Wiklund, H., Rabone, M., Amon, D. J., Ikebe, C., Watling, L., et al. (2016). Abyssal fauna of the UK-1 polymetallic nodule exploration area, Clarion-Clipperton zone, central Pacific Ocean: Cnidaria. *Biodivers. Data J.* 4:e9277. doi: 10.3897/bdj.4.e9277

Dellicour, S., and Flot, J. F. (2018). The hitchhiker's guide to single-locus species delimitation. *Mol. Ecol. Resour.* 18, 1234–1246. doi: 10.1111/1755-0998.12908

d'Udekem d'Acoz, C., and Havermans, C. (2015). Contribution to the systematics of the genus *Eurythenes* S.I. Smith in Scudder, 1882 (Crustacea: Amphipoda: Lysianassoidea: Eurytheneidae). *Zootaxa* 3971, 1–80. doi: 10.11646/zootaxa.3971.1.1

Duffy, G. A., Lawler, S. F., and Horton, T. (2016). Scavenging amphipods of the Angolan deep-sea habitat, with a focus on *Abyssorchomene distinctus* (Birstein and Vinogradov, 1960) (Amphipoda: Lysianassoidea). *J. Crustac. Biol.* 36, 417–426. doi: 10.1163/1937240x-00002448

Excoffier, L., Smouse, P. E., and Quattro, J. M. (1992). Analysis of molecular variance inferred from metric distances among DNA haplotypes: application to human mitochondria DNA restriction sites. *Genetics* 131, 479–491. doi: 10.1093/genetics/131.2.479

Fiser, Z., Altermatt, F., Zaksek, V., Knapic, T., and Fiser, C. (2015). Morphologically cryptic amphipod species are "ecological clones" at regional but not at local scale: a case study of four *Niphargus* species. *PLoS One* 10:e0134384. doi: 10.1371/journal.pone.0134384

Folmer, O., Black, M., Hoeh, W., Lutz, R., and Vrijenhoek, R. C. (1994). DNA primers for amplification of mitochondrial cytochrome c oxidase subunit I from diverse metazoan invertebrates. *Mol. Mar. Biol. Biotechnol.* 3, 294–299.

Fujii, T., Kilgallen, N. M., Rowden, A. A., and Jamieson, A. J. (2013). Deep-sea amphipod community structure across abyssal to hadal depths in the Peru-Chile and Kermadec trenches. *Mar. Ecol. Prog. Ser.* 492, 125–138. doi: 10.3354/meps10489

Glover, A., Dahlgren, T., Wiklund, H., Mohrbeck, I., and Smith, C. (2015). An end-to-end DNA taxonomy methodology for benthic biodiversity survey in the Clarion-Clipperton zone, central Pacific Abyss. *J. Mar. Sci. Eng.* 4:2. doi: 10.3390/jmse4010002

Glover, A. G., Wiklund, H., Rabone, M., Amon, D. J., Smith, C. R., O'hara, T., et al. (2016). Abyssal fauna of the UK-1 polymetallic nodule exploration claim, Clarion-Clipperton Zone, central Pacific Ocean: echinodermata. *Biodivers. Data J.* 4:e7251.

Gollner, S., Kaiser, S., Menzel, L., Jones, D. O. B., Brown, A., Mestre, N. C., et al. (2017). Resilience of benthic deep-sea fauna to mining activities. *Mar. Environ. Res.* 129, 76–101.

Goudet, J., and Jombart, T. (2020). *hierfstat: Estimation and Tests of Hierarchical F-Statistics. R package version 0.5-7*. Available online at: https://CRAN.R-project.org/package=hierfstat. (accessed April 7, 2021)

Havermans, C. (2016). Have we so far only seen the tip of the iceberg? Exploring species diversity and distribution of the giant amphipod *Eurythenes*. *Biodiversity* 17, 12–25. doi: 10.1080/14888386.2016.1172257

Havermans, C., Nagy, Z. T., Sonet, G., De Broyer, C., and Martin, P. (2011). DNA barcoding reveals new insights into the diversity of Antarctic species of orchomene sensu lato (Crustacea: Amphipoda: Lysianassoidea). *Deep Sea Res. 2 Top Stud. Oceanogr.* 58, 230–241. doi: 10.1016/j.dsr2.2010.09.028

Havermans, C., and Smetacek, V. (2018). Bottom-up and top-down triggers of diversification: a new look at the evolutionary ecology of scavenging amphipods in the deep sea. *Prog. Oceanogr.* 164, 37–51. doi: 10.1016/j.pocean.2018.04.008

Havermans, C., Sonet, G., D'udekem D'acoz, C., Nagy, Z. T., Martin, P., Brix, S., et al. (2013). Genetic and morphological divergences in the cosmopolitan deep-sea amphipod *Eurythenes gryllus* reveal a diverse abyss and a bipolar species. *PLoS One* 8:e74218. doi: 10.1371/journal.pone.0074218

Hebert, P. D., Ratnasingham, S., and Dewaard, J. R. (2003). Barcoding animal life: cytochrome c oxidase subunit 1 divergences among closely related species. *Proc. R. Soc. B Biol. Sci.* 270(Suppl 1), S96–S99.

Hein, J. R., Koschinsky, A., and Kuhn, T. (2020). Deep-ocean polymetallic nodules as a resource for critical materials. *Nat. Rev. Earth Environ.* 1, 158–169. doi: 10.1038/s43017-020-0027-0

Hofmann, E. P., Nicholson, K. E., Luque-Montes, I. R., Kohler, G., Cerrato-Mendoza, C. A., Medina-Flores, M., et al. (2019). Cryptic diversity, but to what extent? discordance between single-locus species delimitation methods within mainland anoles (Squamata: Dactyloidae) of Northern Central America. *Front. Genet.* 10:11. doi: 10.3389/fgene.2019.00011

Horton, T., Cooper, H., Vlierboom, R., Thurston, M., Hauton, C., and Young, C. R. (2020a). Molecular phylogenetics of deep-sea amphipods (Eurythenes) reveal a new undescribed species at the Porcupine Abyssal plain, north east Atlantic ocean. *Prog. Oceanogr.* 183:102292. doi: 10.1016/j.pocean.2020.102292

Horton, T., Lowry, J., De Broyer, C., Bellan-Santini, D., Coleman, C. O., Corbari, L., et al. (2020b). *World Amphipoda Database. Lysianassidira [Online]*. Available online at: http://www.marinespecies.org/aphia.php?p=taxdetails&id=1055696 (accessed April 7, 2021)

Horton, T., and Thurston, M. H. (2014). A revision of the bathyal and abyssal necrophage genus Cyclocaris Stebbing, 1888 (Crustacea: Amphipoda: Cyclocaridae) with the addition of two new species from the Atlantic Ocean. *Zootaxa* 3796, 507–527. doi: 10.11646/zootaxa.3796.3.6

Horton, T., Thurston, M. H., Vlierboom, R., Gutteridge, Z., Pebody, C. A., Gates, A. R., et al. (2020c). Are abyssal scavenging amphipod assemblages linked to climate cycles? *Prog. Oceanogr.* 184:102318. doi: 10.1016/j.pocean.2020.102318

Hsieh, T. C., Ma, K. H., and Chao, A. (2020). *iNEXT: iNterpolation and EXTrapolation for Species Diversity*. Available online at: http://chao.stat.nthu.edu.tw/wordpress/software-download/. (accessed April 7, 2021)

ISA (2021). *Exploration Contracts [Online]*. Available online at: https://isa.org.jm/exploration-contracts (accessed April 29, 2021).

Jamieson, A. J., Kilgallen, N. M., Rowden, A. A., Fujii, T., Horton, T., Lörz, A. N., et al. (2011). Bait-attending fauna of the kermadec trench, SW Pacific Ocean: evidence for an ecotone across the abyssal–hadal transition zone. *Deep Sea Res. 1 Oceanogr. Res. Pap.* 58, 49–62. doi: 10.1016/j.dsr.2010.11.003

Janssen, A., Stuckas, H., Vink, A., and Arbizu, P. M. (2019). Biogeography and population structure of predominant macrofaunal taxa (Annelida and Isopoda) in abyssal polymetallic nodule fields: implications for conservation and management. *Mar. Biodivers.* 49, 2641–2658. doi: 10.1007/s12526-019-00997-1

Jones, D. O. B. (2015). RRS James Cook Cruise JC120 15 Apr–19 May 2015. Manzanillo to Manzanillo, Mexico. Managing Impacts of Deep-Sea Resource Exploitation (MIDAS): Clarion-Clipperton Zone North Eastern Area of Particular Environmental Interest. (Southampton, National Oceanography Centre, Southampton)

Jost, L. (2006). Entropy and diversity. *Oikos* 113, 363–375.

Kaïm-Malka, R. A. (2005). Biology and life cycle of *Tmetonyx similis* (G. O. Sars, 1891) (Amphipoda, Lysianassidae), a scavenging amphipod from the

continental slope of the Mediterranean. *J. Nat. Hist.* 39, 3163–3186. doi: 10.1080/00222930500240502

Kamvar, Z. N., Tabima, J. F., and Grunwald, N. J. (2014). Poppr: an R package for genetic analysis of populations with clonal, partially clonal, and/or sexual reproduction. *PeerJ* 2:e281. doi: 10.7717/peerj.281

Katoh, K., Rozewicki, J., and Yamada, K. D. (2019). MAFFT online service: multiple sequence alignment, interactive sequence choice and visualization. *Brief Bioinform.* 20, 1160–1166. doi: 10.1093/bib/bbx108

Kumar, S., Stecher, G., Li, M., Knyaz, C., and Tamura, K. (2018). MEGA X: molecular evolutionary genetics analysis across computing platforms. *Mol. Biol. Evol.* 35, 1547–1549. doi: 10.1093/molbev/msy096

Lacey, N. C., Rowden, A. A., Clark, M. R., Kilgallen, N. M., Linley, T., Mayor, D. J., et al. (2016). Community structure and diversity of scavenging amphipods from bathyal to hadal depths in three South Pacific Trenches. *Deep Sea Res. 1 Oceanogr. Res. Pap.* 111, 121–137. doi: 10.1016/j.dsr.2016.02.014

Lanfear, R., Frandsen, P. B., Wright, A. M., Senfeld, T., and Calcott, B. (2017). PartitionFinder 2: new methods for selecting partitioned models of evolution for molecular and morphological hylogenetic analyses. *Mol. Biol. Evol.* 34, 772–773.

Leitner, A. B., Durden, J. M., Smith, C. R., Klingberg, E. D., and Drazen, J. C. (2021). Synaphobranchid eel swarms on abyssal seamounts: largest aggregation of fishes ever observed at abyssal depths. *Deep Sea Res. 1 Oceanogr. Res. Pap.* 167:103423. doi: 10.1016/j.dsr.2020.103423

Leitner, A. B., Neuheimer, A. B., Donlon, E., Smith, C. R., and Drazen, J. C. (2017). Environmental and bathymetric influences on abyssal bait-attending communities of the Clarion Clipperton Zone. *Deep Sea Res. 1* 125, 65–80. doi: 10.1016/j.dsr.2017.04.017

McClain, C. R. (2021). The commonness of rarity in a deep-sea taxon. *Oikos* 130, 863–878. doi: 10.1111/oik.07602

McClain, C. R., and Hardy, S. M. (2010). The dynamics of biogeographic ranges in the deep sea. *Proc. Biol. Sci.* 277, 3533–3546. doi: 10.1098/rspb.2010.1057

McQuaid, K. A., Attrill, M. J., Clark, M. R., Cobley, A., Glover, A. G., Smith, C. R., et al. (2020). Using habitat classification to assess representativity of a protected area network in a large, data-poor area targeted for deep-sea mining. *Front. Mar. Sci.* 7:558860. doi: 10.3389/fmars.2020.558860

Medlin, L., Elwood, H., Stickel, S., and Sogin, M. (1988). The characterization of enzymatically amplified eukaryotic 16S-like rRNA-coding regions. *Gene* 71, 491–499. doi: 10.1016/0378-1119(88)90066-2

Mewes, K., Mogollón, J. M., Picard, A., Rühlemann, C., Kuhn, T., Nöthen, K., et al. (2014). Impact of depositional and biogeochemical processes on small scale variations in nodule abundance in the Clarion-Clipperton fracture zone. *Deep Sea Res. 1 Oceanogr. Res. Pap.* 91, 125–141. doi: 10.1016/j.dsr.2014.06.001

Mohrbeck, I., Horton, T., Jażdżewska, A. M., and Martínez Arbizu, P. (2021). DNA barcoding and cryptic diversity of deep-sea scavenging amphipods in the Clarion-Clipperton zone (Eastern Equatorial Pacific). *Mar. Biodivers.* 51:26.

Narahara-Nakano, Y., Nakano, T., and Tomikawa, K. (2018). Deep-sea amphipod genus *Eurythenes* from Japan, with a description of a new *Eurythenes* species from off Hokkaido (Crustacea: Amphipoda: Lysianassoidea). *Mar. Biodivers.* 48, 603–620. doi: 10.1007/s12526-017-0758-4

Neubaum, M. A., Douglas, M. R., Douglas, M. E., and O'shea, T. J. (2007). Molecular ecology of the big brown bat (Eptesicus fuscus): genetic and natural history variation in a hybrid zone. *J. Mammal.* 88, 1230–1238. doi: 10.1644/06-mamm-a-228r1.1

Nygren, A., and Sundberg, P. (2003). Phylogeny and evolution of reproductive modes in Autolytinae (Syllidae, Annelida). *Mol. Phylogenet. Evol.* 29, 235–249.

Oksanen, J., Blanchet, G., Friendly, M., Kindt, R., Legendre, P., Mcglinn, D., et al. (2018). *vegan: Community Ecology Package. R package Version 2.4-6.* Available online at: http://CRAN.Rproject.org/package=vegan. (accessed April 7, 2021).

Palumbi, S. R. (1996). "Nucleic acid II: the polymerase chain reaction," in *Molecular Systematics*, eds D. M. Hillis, G. Moritz, and B. K. Mable (Sunderland, MA: Sinauer Associates).

Paradis, E. (2010). pegas: an R package for population genetics with an integrated-modular approach. *Bioinformatics* 26, 419–420. doi: 10.1093/bioinformatics/btp696

Paradis, E., and Schliep, K. (2019). ape 5.0: an environment for modern phylogenetics and evolutionary analyses in R. *Bioinformatics* 35, 526–528. doi: 10.1093/bioinformatics/bty633

Patel, T., Robert, H., D'udekem D'acoz, C., Martens, K., De Mesel, I., Degraer, S., et al. (2020). Biogeography and community structure of abyssal scavenging Amphipoda (Crustacea) in the Pacific Ocean. *Biogeosciences* 17, 2731–2744. doi: 10.5194/bg-17-2731-2020

Pons, J., Barraclough, T., Gomez-Zurita, J., Cardoso, A., Duran, D., Hazell, S., et al. (2006). Sequence-based species delimitation for the DNA taxonomy of undescribed insects. *Syst. Biol.* 55, 595–609. doi: 10.1080/10635150600852011

Puillandre, N., Lambert, A., Brouillet, S., and Achaz, G. (2012). ABGD, automatic barcode gap discovery for primary species delimitation. *Mol. Ecol.* 21, 1864–1877. doi: 10.1111/j.1365-294x.2011.05239.x

R Development Core Team (2017). *R: A Language and Environment for Statistical Computing. R Foundation for Statistical Computing*. Vienna: R Foundation for Statistical Computing.

Ritchie, H., Jamieson, A. J., and Piertney, S. B. (2015). Phylogenetic relationships among hadal amphipods of the Superfamily lysianassoidea: implications for taxonomy and biogeography. *Deep Sea Res. 1 Oceanogr. Res. Pap.* 105, 119–131.

Ritchie, H., Jamieson, A. J., and Piertney, S. B. (2017). Population genetic structure of two congeneric deep-sea amphipod species from geographically isolated hadal trenches in the Pacific Ocean. *Deep Sea Res. 1 Oceanogr. Res. Pap.* 119, 50–57. doi: 10.1016/j.dsr.2016.11.006

Rowden, A. A., Dower, J. F., Schlacher, T. A., Consalvey, M., and Clark, M. R. (2010). Paradigms in seamount ecology: fact, fiction and future. *Mar. Ecol.* 31, 226–241. doi: 10.1111/j.1439-0485.2010.00400.x

Rubinoff, D., Cameron, S., and Will, K. (2006). A genomic perspective on the shortcomings of mitochondrial DNA for "barcoding" identification. *J. Hered.* 97, 581–594. doi: 10.1093/jhered/esl036

Sainte-Marie, B. (1992). "Foraging of scavenging deep-sea lysianassoid amphipods," in *Deep-Sea Food Chains and the Global Carbon Cycle*, eds G. T. Rowe and V. Pariente (Dordrecht: Springer).

Stamatakis, A. (2006). RAxML-VI-HPC: maximum likelihood-based phylogenetic analyses with thousands of taxa and mixed models. *Bioinformatics* 22, 2688–2690. doi: 10.1093/bioinformatics/btl446

Taboada, S., Riesgo, A., Wiklund, H., Paterson, G. L. J., Koutsouveli, V., Santodomingo, N., et al. (2018). Implications of population connectivity studies for the design of marine protected areas in the deep sea: an example of a demosponge from the Clarion-Clipperton Zone. *Mol. Ecol.* 27, 4657–4679. doi: 10.1111/mec.14888

Tempestini, A., Rysgaard, S., and Dufresne, F. (2018). Species identification and connectivity of marine amphipods in Canada's three oceans. *PLoS One* 13:e0197174. doi: 10.1371/journal.pone.0197174

Washburn, T. W., Jones, D. O. B., Wei, C.-L., and Smith, C. R. (2021a). Environmental heterogeneity throughout the Clarion-Clipperton zone and the potential representativity of the APEI Network. *Front. Mar. Sci.* 8:661685. doi: 10.3389/fmars.2021.661685

Washburn, T. W., Menot, L., Bonifácio, P., Pape, E., Błaz˙Ewicz, M., Bribiesca-Contreras, G., et al. (2021b). Patterns of macrofaunal biodiversity across the Clarion-Clipperton zone: an area targeted for deep-sea mining. *Front. Mar. Sci.* 8:626571. doi: 10.3389/fmars.2021.626571

Wedding, L. M., Friedlander, A. M., Kittinger, J. N., Watling, L., Gaines, S. D., Bennett, M., et al. (2013). From principles to practice: a spatial approach to systematic conservation planning in the deep sea. *Proc. R. Soc. Lond. B Biol. Sci.* 280:20131684. doi: 10.1098/rspb.2013.1684

Weir, B. S., and Cockerham, C. C. (1984). Estimating F-statistics for the analysis of population structure. *Evolution* 38, 1358–1370. doi: 10.2307/2408641

Weston, J. N. J., Carrillo-Barragan, P., Linley, T. D., Reid, W. D. K., and Jamieson, A. J. (2020). New species of *Eurythenes* from hadal depths of

the Mariana Trench, Pacific Ocean (Crustacea: Amphipoda). *Zootaxa* 4748, 4741–4749.

Wickham, H. (2009). *ggplot2: Elegant Graphics for Data Analysis*. New York, NY: Springer-Verlag.

Wiklund, H., Taylor, J. D., Dahlgren, T. G., Todt, C., Ikebe, C., Rabone, M., et al. (2017). Abyssal fauna of the UK-1 polymetallic nodule exploration area, Clarion-Clipperton Zone, central Pacific Ocean: Mollusca. *Zookeys* 707, 1–46. doi: 10.3897/zookeys.707.13042

Yan, R.-J., Schnabel, K. E., Rowden, A. A., Guo, X.-Z., and Gardner, J. P. A. (2020). Population structure and genetic connectivity of squat lobsters (Munida Leach, 1820) associated with vulnerable marine ecosystems in the Southwest Pacific Ocean. *Front. Mar. Sci.* 6:791. doi: 10.3389/fmars.2019.00791

Zhang, J., Kapli, P., Pavlidis, P., and Stamatakis, A. (2013). A general species delimitation method with applications to phylogenetic placements. *Bioinformatics* 29, 2869–2876. doi: 10.1093/bioinformatics/btt499

Conflict of Interest: The authors declare that the research was conducted in the absence of any commercial or financial relationships that could be construed as a potential conflict of interest.

Publisher's Note: All claims expressed in this article are solely those of the authors and do not necessarily represent those of their affiliated organizations, or those of the publisher, the editors and the reviewers. Any product that may be evaluated in this article, or claim that may be made by its manufacturer, is not guaranteed or endorsed by the publisher.

Copyright © 2021 Bribiesca-Contreras, Dahlgren, Horton, Drazen, Drennan, Jones, Leitner, McQuaid, Smith, Taboada, Wiklund and Glover. This is an open-access article distributed under the terms of the Creative Commons Attribution License (CC BY). The use, distribution or reproduction in other forums is permitted, provided the original author(s) and the copyright owner(s) are credited and that the original publication in this journal is cited, in accordance with accepted academic practice. No use, distribution or reproduction is permitted which does not comply with these terms.

frontiers in Marine Science

ORIGINAL RESEARCH
published: 19 August 2021
doi: 10.3389/fmars.2021.636305

Testing the Seamount Refuge Hypothesis for Predators and Scavengers in the Western Clarion-Clipperton Zone

Astrid B. Leitner[1,2], Jeffrey C. Drazen[2] and Craig R. Smith[2]*

[1] Monterey Bay Aquarium Research Institute, Moss Landing, CA, United States, [2] Department of Oceanography, University of Hawai'i at Mānoa, Honolulu, HI, United States

Seamounts are common in all ocean basins, and most have summit depths >3,000 m. Nonetheless, these abyssal seamounts are the least sampled and understood seamount habitats. We report bait-attending community results from the first baited camera deployments on abyssal seamounts. Observations were made in the Clarion Clipperton Zone (CCZ), a manganese nodule region stretching from south of Hawaii nearly to Mexico. This zone is one of the main target areas for (potential) large-scale deep-sea nodule mining in the very near future. The Seamount Refuge Hypothesis (SRH) posits that the seamounts found throughout the CCZ provide refugia for abyssal fauna likely to be disturbed by seabed mining, yielding potential source populations for recolonization of mined areas. Here we use baited cameras to test a prediction of this hypothesis, specifically that predator and scavenger communities are shared between abyssal seamounts and nearby abyssal plains. We deployed two camera systems on three abyssal seamounts and their surrounding abyssal plains in three different Areas of Particular Environmental Interests (APEIs), designated by the International Seabed Authority as no-mining areas. We found that seamounts have a distinct community, and differences in community compositions were driven largely by habitat type and productivity changes. In fact, community structures of abyssal-plain deployments hundreds of kilometers apart were more similar to each other than to deployments ∼15 km away on seamounts. Seamount communities were found to have higher morphospecies richness and lower evenness than abyssal plains due to high dominance by synaphobranchid eels or penaeid shrimps. Relative abundances were generally higher on seamounts than on the plains, but this effect varied significantly among the taxa. Seven morphotypes were exclusive to the seamounts, including the most abundant morphospecies, the cutthroat eel *Ilyophis arx.* No morphotype was exclusive to the abyssal plains; thus, we cannot reject the SRH for much of the mobile megafaunal predator/scavenging fauna from CCZ abyssal plains. However, the very small area of abyssal seamounts compared to abyssal plains suggest that seamounts are likely to provide limited source populations for recolonizing abyssal plains post-mining

OPEN ACCESS

Edited by:
Daphne Cuvelier, Center for Marine and Environmental Sciences (MARE), Portugal

Reviewed by:
Frine Cardone, Anton Dohrn Zoological Station, Italy
Rui Pedro Vieira, Centre for Environment, Fisheries and Aquaculture Science (CEFAS), United Kingdom

***Correspondence:**
Astrid B. Leitner
aleitner@mbari.org

Specialty section:
This article was submitted to Deep-Sea Environments and Ecology, a section of the journal Frontiers in Marine Science

Received: *01 December 2020*
Accepted: *26 July 2021*
Published: *19 August 2021*

Citation:
Leitner AB, Drazen JC and Smith CR (2021) Testing the Seamount Refuge Hypothesis for Predators and Scavengers in the Western Clarion-Clipperton Zone. Front. Mar. Sci. 8:636305. doi: 10.3389/fmars.2021.636305

disturbance. Because seamounts have unique community compositions, including a substantial number of predator and scavenger morphospecies not found on abyssal plains, they contribute to the beta biodiversity of the Clarion-Clipperton Zone, and thus indirect mining impacts on those distinct communities are of concern.

Keywords: seamount, baited camera, deep-sea, scavenger, CCZ, nodule

INTRODUCTION

Seamounts are submarine mountains that rise at least 1,000 m above the surrounding seafloor (Pitcher et al., 2007). Seamounts are common seafloor features, with tens to hundreds of thousands of seamounts estimated globally (Kim and Wessel, 2011; Yesson et al., 2011). Seamounts are still understudied habitats, but current data suggest that seamounts with summits shallower than 3000 m are often characterized by rich benthic and demersal megafaunal communities with high abundance, high biomass, and high diversity (Pitcher et al., 2007; Morato et al., 2010; Schlacher et al., 2010). The vast majority of these features are small, deep seamounts, but these are also the least studied and least understood class of seamounts (Wessel, 2001; Kim and Wessel, 2011).

The Clarion-Clipperton Zone (CCZ), a large region rich in polymetallic nodules in the eastern equatorial Pacific between Hawaii and Mexico, is currently being considered for deep seabed nodule mining. The International Seabed Authority (ISA) is responsible for environmental management in the CCZ and to that end has established nine, 400 km × 400 km no-mining zones called Areas of Particular Environmental Interest (APEIs; Wedding et al., 2013). The APEIs were designing as a representative system of protected areas to cover the biophysical gradients in productivity, nodule cover, and depth across the CCZ, as well as to protect the range of seafloor habitat types in the CCZ, including abyssal hills and seamounts (Wedding et al., 2013). The CCZ hosts approximately 221 seamounts, whose average summit depth is 2850 m below sea-level (data extracted from Yesson et al., 2011; **Figure 1**). It has recently been hypothesized that these seamounts, which will be spared from direct mining activities due to the rugosity and complexity of their terrain, may provide refugia for many species from the abyssal plain displaced or disturbed by mining and thus may provide source populations for recolonization of mined areas (Cuvelier et al., 2020). A prediction of this hypothesis is that seamounts and nearby abyssal plains share a substantial proportion of their fauna. Thus far, this hypothesis, referred to throughout this manuscript as the Seamount Refuge Hypothesis (SRH), has been evaluated and rejected for benthic megafauna (excluding highly mobile groups like fishes and crustaceans) in the eastern CCZ, where only 10% of fauna were observed on both seamounts and plains (Cuvelier et al., 2020). In addition, a recent study using a multi-gene environmental DNA metabarcoding approach, suggests substantial differences in metazoan communities with limited taxonomic overlap between seamounts and plains in the western CCZ (Laroche et al., 2020). However, an evaluation specific to fishes and other mobile top predators and scavengers is still lacking.

Knowledge of the distribution, ecology, and behavior of top predators is crucial to establish environmental baselines and conduct ecosystem-based management (Estes et al., 2011; Wedding et al., 2015, 2013). Even at low densities, predators can exert top-down control on prey populations, thereby controlling prey abundance, biomass, and diversity, and influencing habitat use/choice and behavior of prey (Myers et al., 2007; Polovina et al., 2009; Estes et al., 2011; Drazen and Sutton, 2017). In the CCZ, top seafloor predators are large fishes, crustaceans, and octopods, many of which are opportunistic scavengers readily attracted to baited cameras (Leitner et al., 2017; Drazen et al., 2019; Harbour et al., 2020). While these highly mobile predators are also detected in seafloor imaging transects, they are often observed in a very low (<1%) percentage of images (e.g., Milligan et al., 2016) due to their sparse distribution and avoidance of light, noise, and vibrations from survey vehicles, making baited imaging a key technique for studying the predator-scavenger component of abyssal seafloor ecosystems (Drazen et al., 2021, this vol.; Leitner et al., 2017).

Here we test the "shared-fauna" prediction of the SRH for bait-attending fauna in the western CCZ using data from two baited camera landers which were deployed a total of 17 times on three different seamounts and their proximate abyssal plains, one in each of the three western APEIs. Collectively, the DeepCCZ expedition has provided the first baited camera data from the western APEI regions. The data presented here also represent the first baited experiments on abyssal-depth seamounts. Thus, in addition to evaluating the SRH, we also report on the diversity and composition of the bait-attending megafauna and the potential importance of environmental characteristics such as seafloor habitat type and productivity in structuring this community.

MATERIALS AND METHODS

Study Site

Data were collected during the DeepCCZ cruise to the western CCZ aboard the R/V Kilo Moana in May-June of 2018 (**Figure 1**). All sampling took place within three APEIs: APEI 1, APEI 4, and APEI 7 (north to south, **Figures 2A–C**). These APEIs lie on a strong primary productivity gradient. APEI 7, the southernmost, is under the influence of equatorial upwelling with a decadal average chlorophyll-a concentrations of 0.15 mg m^{-3} Chl-a [National Oceanic & Atmospheric Administration (NOAA), and National Aeronautics and Space Administration (NASA), n.d.] and an estimated average particulate organic carbon (POC) flux to depth of 1.9 mg C_{org} m^{-2} d^{-1} (Lutz et al., 2007). The mid-latitude APEI, APEI 4, is characterized by lower surface

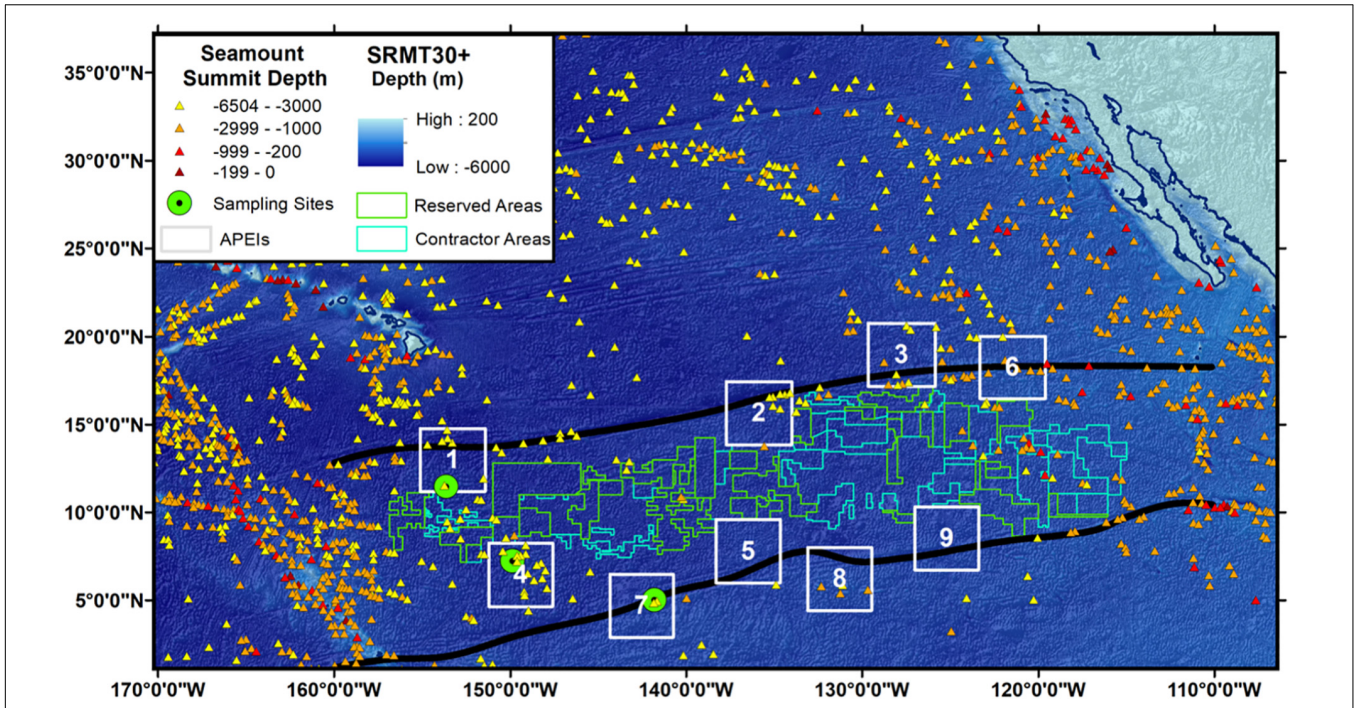

FIGURE 1 | Map of the CCZ (Clarion and Clipperton Fracture Zones are black lines) with sampling locations. Bathymetry data is drawn from the SRMT30 + satellite-derived bathymetry dataset (Becker et al., 2009). Satellite-estimated seamount locations and summit depths are plotted with abyssal seamounts in yellow, lower bathyal seamounts in orange, upper bathyal seamounts in red, and shallow seamounts in dark red (data from Yesson et al., 2011). Current regions licensed by the ISA for mining exploration are pictured as green polygons, areas currently reserved for future mining contracts are delineated by blue polygons, and Areas of Particular Environmental Interest (APEIs), i.e., areas currently protected from direct mining are shown, in white, with APEI number indicated. The Main Hawaiian Islands and the western coast of Mexico and California are shown.

chlorophyll concentrations and seafloor POC flux (0.12 mg m^{-3} Chl-a and 1.4 mg C_{org} m^{-2} d^{-1}). The northernmost APEI, APEI 1, is in the least productive waters with just 0.07 mg m^{-3} Chl-a and an estimated average seafloor POC flux of 1.1 mg C_{org} m^{-2} d^{-1}.

One abyssal seamount was selected in each APEI to test the SRH. Because these APEIs were all unmapped and unsampled prior to the expedition, seamount targets were selected from the best available satellite-estimated bathymetry: the Shuttle Radar Topography Mission (SRTM30+) 30 arc-second global bathymetry grid (Becker et al., 2009), which combines both high resolution (~1 km) ship-based bathymetry data and ~9 km satellite-gravity data.[1] Seamounts were chosen to have elevations between 1,000 and 1,500 m above the surrounding seafloor and summits at abyssal depths (>3,000 m) to meet the classic definition of "seamount" (Pitcher et al., 2007) while still minimizing differences in community composition stemming from depth distributions. During the cruise, each seamount was mapped at 50 m resolution using shipboard multibeam sonar (see details below).

After mapping of the initial seamount target in APEI 7, additional seamount targets were selected to be as similar to the first as possible, with roughly similar summit depths, elevations, and geomorphologies. All were elongated, ridge-like features. Lander deployment locations on the seamount summits were strategically chosen to be in large, flat areas to allow for successful lander deployments. Landers were deployed in soft sediment habitats on both seamounts and proximate abyssal plains. Seamount effects on benthic larval distributions have been documented to extend 7 km away from shallow seamount summits, and possibly as far as 40 km (Mullineaux and Mills, 1997), and island effects on productivity extend up to 30 km from shore declining exponentially with distance (Gove et al., 2016). While seamount effect radius is not known for abyssal seamounts, the radius is likely much smaller given the low average current speeds at abyssal depths; thus a 15 km seamount buffer (more than twice the documented shallow seamount effect and half the island mass effect) was instituted such that all abyssal plain deployments were >15 km from the seamount summit ridgeline and well out onto the abyssal plain (**Figure 2**).

Data Collection

Bathymetric data was collected at 50 m resolution using the R/V Kilo Moana's deep-water multibeam system (12 kHz Simrad EM120) at a constant ship speed of eight knots. Raw pings were manually edited in near real time with the software Qimera^{R}. Sound velocity profiles (SVP) were taken every 6 h during surveys. Processed multibeam bathymetry was then used to find suitable lander deployment sites (large, flat areas atop each seamount) and for subsequent spatial analysis in ArcGIS 10.4.

[1]https://topex.ucsd.edu/WWW_html/srtm30_plus.html

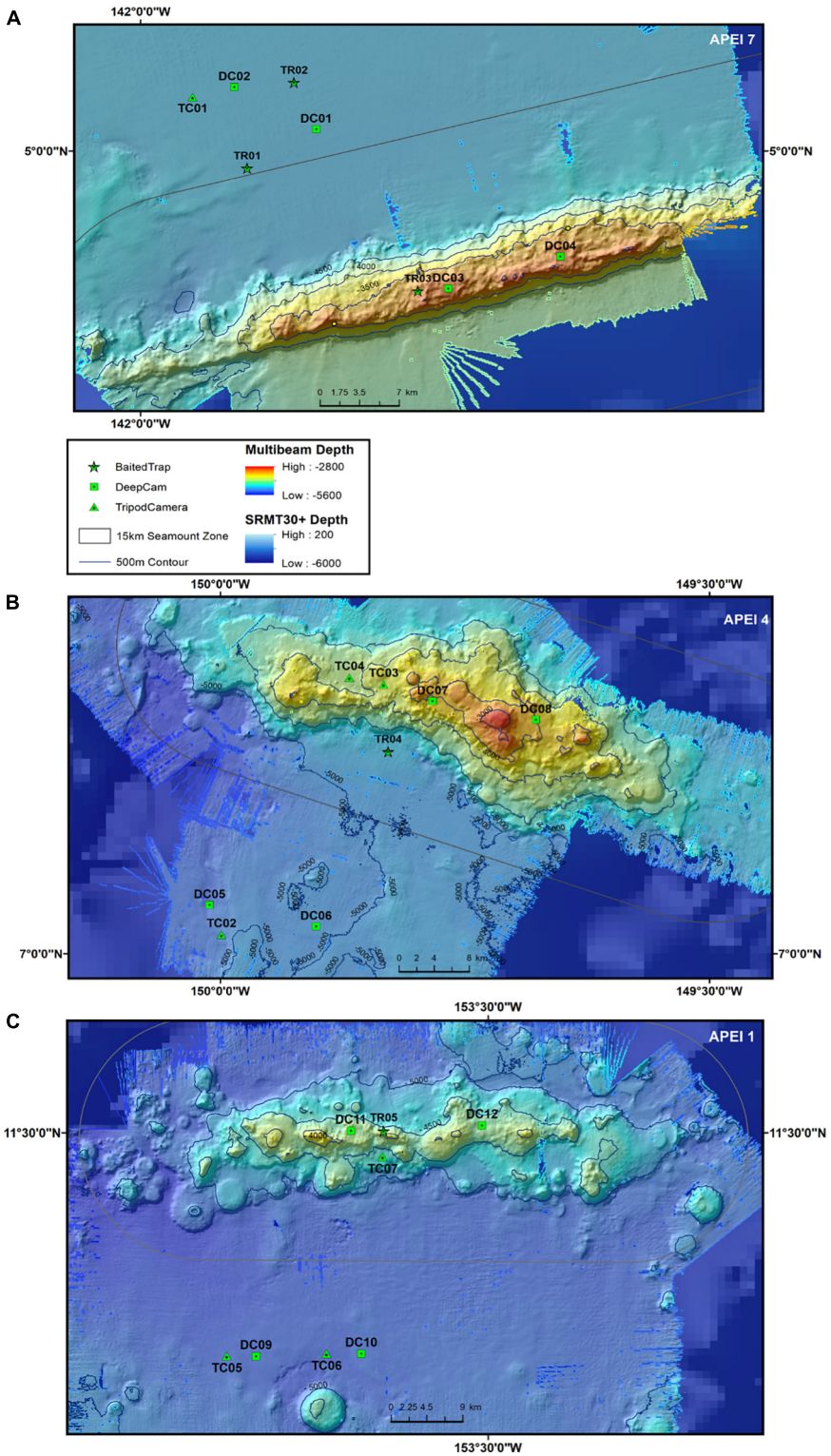

FIGURE 2 | Detailed multibeam bathymetry and sampling locations from three APEIs **(A)** APEI 7, **(B)** APEI 4, **(C)** APEI 1. Baited trap (TR) deployment locations (stars) and baited camera deployment locations [DeepCam lander deployments (DC) as squares, Tripod Camera Lander (TC) as triangles] are shown in each panel. Finer scale multibeam bathymetry (rainbow color scale) overlays coarser satellite-estimated bathymetry (blue, pixelated color scale). The "seamount zone" denoted by a 15 km buffer (as measured from the seamount ridge-line) is shown in gray. Depth contours (500 m) are shown in black. Note TC01 (the first tripod deployment) was not successful.

Two baited-camera landers were used to collect seafloor imagery. The first, DeepCam (DC), is a baited, geometrically calibrated stereo-video system. Details of this system are described elsewhere (Leitner et al., 2017) but in brief, two identical cameras were mounted with an overlapping horizontal field of view at a slightly downward angle at 0.56 m above the seafloor. Geometric calibration (done using the CAL software by SeaGIS)[2] provided a precise estimation of the seafloor area within the field of view that was illuminated by the system's lights (1.86 m^2). To minimize light disturbance on bait-attending fauna and maximize battery life, videos were recorded for 2-min intervals (clips) interrupted by 8-min lights-off intervals. This lander was also equipped with a Nortek Aquadopp 6000 current meter, though this instrument was lost during the ninth recovery. The current meter provided true bottom depth, bottom temperature, and current velocities. Videos from both synchronous cameras were annotated using the EventMeasure software by SeaGIS for all visible megafauna to the lowest taxonomic level possible, although only bait-attending (scavengers and necrophagivores) fauna are considered in the analysis. Identifications were made using the collaborative CCZ abyssal photographic fish guide, published as supplementary material to Drazen et al. (2021, this vol.). This guide provides an image-based identifications and ensures naming standardization across the greater CCZ region (Drazen et al., 2021, this vol.). As such, all taxa are considered morphospecies except in a few instances, where concurrent capture of specimens allowed for confirmation of image-based identification (e.g., *Ilyophis arx*). MaxN, a conservative relative abundance metric, was extracted for each clip and for each deployment for each bait-attending taxon (Cappo et al., 2006). MaxN represents the maximum number of individuals of each single taxon present in a single frame of a clip (clipwise MaxN) or deployment (dropwise MaxN). MaxN eliminates the possibility of double counting individuals over the course of a video, and is therefore a conservative relative abundance metric.

The second lander, Tripod Camera (TC), is a deep-sea time-lapse photography camera tripod described in Ziegler et al. (2020). Camera angle and elevation were modified to match the DC to make the two systems as comparable as possible. This lander took one still photograph every minute. Because of the horizontal camera angle and lack of stereo calibration, a precise estimate of the seafloor area in view is not possible. By comparing images between landers, the field of view of the Tripod lander was determined to be slightly smaller than that of the DC. Still images were annotated manually to the lowest taxonomic level possible for all visible megafauna, though only bait-attending fauna were used in analyses. It should be noted that species level identification is more challenging for still photos than for video, especially for the large, red decapod shrimps (known from the DC to be a mix of penaeid and aristeid shrimps), necessitating a taxa that combines the two as a single morphospecies for comparison across landers. MaxN was extracted for each deployment (dropwise MaxN) for subsequent analyses.

[2]www.seagis.com.au

Both landers were baited with ∼1 kg of Pacific mackerel (*Scomber japonicus*), positioned 1.5 m in front of the cameras. This resulted in a complete view of the entire area around the bait package in the DC video. For the Tripod, the field of view included only the bait package and the seafloor beyond it. Deployment times for landers ranged from 12.7 to 44.2 h (**Table 1**).

Finally, whenever possible given shiptime constraints, a baited trap (details provided in Leitner et al., 2017) was deployed to collect voucher specimens for morphological and genetic identification. To minimize interactions between the bait plumes of the three landers, simultaneous deployments were spaced at least 4 km apart.

Statistics

The "shared-fauna" prediction of the SRH was evaluated for bait-attending fauna (scavengers and predators) by comparing taxonomic overlap, diversity metrics, and community composition between seamounts and proximate abyssal plains at the three APEIs in the western CCZ.

Diversity and Taxonomic Overlap

In order to evaluate differences in diversity, rarified and extrapolated abundance-based Hill numbers (q = 0,1,2) were compared between habitat (seamount vs. abyssal plain) and APEI using the {iNEXT} R package (Chao et al., 2014; Hsieh et al., 2016). Hill numbers correspond to morphospecies richness (q = 0), Shannon diversity (q = 1), and Simpson diversity (q = 2). Significant differences in diversity metrics were evaluated using the bootstrapped 95% confidence intervals (CI) around the sampling curves, such that non-overlapping CI around each curve were interpreted as significant differences (Chao et al., 2014; Hsieh et al., 2016). To evaluate data coverage, morphospecies accumulation curves were also compared between seamounts and abyssal plains and between APEIs. To evaluate morphospecies overlaps across APEI and habitat type, morphospecies intersections were visualized and quantified for each station (APEI and habitat combination) using the {UpSetR} package (Gehlenborg, 2019). Taxonomic overlap uses taxon-presence data to compare how many taxa are shared between different sites. It is reported in percent overlap, in this case the percentage of the total number of observed morphospecies that are shared between sites.

Community Analysis

In order to visualize and quantify differences in community composition across all deployments and specifically across habitat types, a constrained ordination based on a Bray-Curtis dissimilarity matrix calculated from the square root transformed relative abundances (MaxN) of all bait-attending taxa (N = 20) was run using the capscale function in the R package {vegan} (Oksanen et al., 2015). Capscale performs a principal coordinates analysis (PCoA) and then uses given predictors to conduct an eigenanalysis to determine the axes along which the predictor explains as much of the dissimilarity between communities as possible (Oksanen et al., 2015). Permutations (N = 9,999) were stratified by APEI to account for the spatial

TABLE 1 | Metadata and deployment information for all lander deployments.

Drop	Stratum	Habitat Type	Lander	Image Type	Imaging Interval	Duration	Latitude	Longitude	Depth
					(min)	(hr)	(dd N)	(dd E)	(m)
DC1	**APEI7**	Abyssal Plain	DeepCam	video	2(10)	23.9	5.018	−141.860	4878.3
DC2		Abyssal Plain	DeepCam	video	2(10)	28.3	5.053	−141.926	4859.9
DC3		Seamount	DeepCam	video	2(10)	16.4	4.884	−141.755	3083.4
DC4		Seamount	DeepCam	video	2(10)	17.6	4.911	−141.666	3140.4
DC5	**APEI4**	Abyssal Plain	DeepCam	video	2(10)	20.5	7.052	−150.011	5216.5
DC6		Abyssal Plain	DeepCam	video	2(10)	21.2	7.029	−149.902	5003.7
DC7**		Seamount	DeepCam	video	2(10)	21.7**	7.270	−149.783	3541.8
DC8		Seamount	DeepCam	video	2(10)	44.2	7.250	−149.677	3496.8
TC02		Abyssal Plain	Tripod	stills	1	21.3	7.020	−149.999	5096
TC03		Seamount	Tripod	stills	1	17.6	7.287	−149.833	3885
TC04		Seamount	Tripod	stills	1	29.9	7.295	−149.868	4134
DC9	**APEI1**	Abyssal Plain	DeepCam	video	2(10)	43.1	11.249	−153.761	5236
DC10		Abyssal Plain	DeepCam	video	2(10)	23.4	11.252	−153.643	5213
DC11		Seamount	DeepCam	video	2(10)	18.4	11.502	−153.654	4218
DC12		Seamount	DeepCam	video	2(10)	12.7	11.508	−153.507	4346
TC05		Abyssal Plain	Tripod	stills	1	18.3	11.250	−153.794	5225
TC06		Abyssal Plain	Tripod	stills	1	18.4	11.252	−153.682	5249
TC07		Seamount	Tripod	stills	1	17.6	11.473	−153.619	4622
TR01	**APEI7**	Abyssal Plain	Baited Trap	–	–	30.7	4.985	−141.915	4872
TR02		Abyssal Plain	Baited Trap	–	–	47.1	5.057	−141.878	4871
TR03		Seamount	Baited Trap	–	–	25.1	4.883	−141.779	3203
TR04	**APEI4**	Abyssal Plain*	Baited Trap	–	–	43.3	7.216	−149.828	4872
TR05	**APEI1**	Seamount	Baited Trap	–	–	22.7	11.502	−153.617	4175

Imaging interval for the DeepCam lander is 2 min of video during every 10 min.
**Within 15 km seamount buffer zone.*
***Bait was consumed on initial descent, and so this deployment was almost entirely unbaited and therefore excluded from quantitative analyses.*

dependence in the data. Significant clusters of deployments ($p < 0.05$) were identified using similarity profile analysis (SIMPROF) using the simprof function in the {clustsig} R package (Whitaker and Christman, 2014).

The predictors used to constrain the ordination were broad-scale benthic position index (BBPI), Lutz et al. (2007) estimates of seafloor POC flux at the drop locations, nodule abundance in the camera view, latitude, and lander type. Benthic position index (BPI), whether broad BBPI or fine scale (FBPI), is a relative position index defined as the difference in elevation between the location of interest (given as radius of cells around the sampling location) and the surrounding area (outer radius) (Modeler, 2012). Positive BPI values correspond to local high points, negative values correspond to local depressions, and values close to zero either represent flat areas or areas of constant slope (Lundblad et al., 2006; Verfaillie et al., 2007). BPI provides a continuous variable for quantifying bathymetric habitat differences. BBPI was calculated using GEBCO bathymetry data interpolated to 1 km^2 with the (Mcquaid et al., 2020) PDC Mercator projection. The inner radius was 1 bathymetry cell and the outer radius was 100 cells (scale factor = 100 km). Using a coarse resolution bathymetry allowed for a single BBPI layer to be calculated across the dataset. This method successfully captured the habitat differences between abyssal plain deployments (BBPI $\leq$ 25) and seamounts (BBPI $\geq$ 500) in all three APEIs (**Table 2**). FBPI was calculated from fine-scale (50 m) multibeam bathymetry for each APEI and was standardized for comparison across all three strata. However, because of seamount deployment locations in large, flat areas surrounded by higher elevations, FBPI was similar between seamount and abyssal plain deployments and was not used as a predictor. Estimated POC flux was derived from the Lutz et al. (2007) model. POC flux was highly correlated with longitude (Pearson correlation = 0.99) and with all surface productivity metrics (monthly average Chl-a concentration: 0.84, yearly average Chl-a concentration: 0.95, decadal average Chl-a concentration: 0.94). Because POC flux to depth is a good proxy for deep seafloor food availability (Smith et al., 2008), it was included while other correlated predictors (including longitude) were excluded. Nodule abundance was roughly estimated for each deployment using pixel image color analysis for each deployment. For the most consistent and evenly illuminated portion of the field of view, the proportion of that area that was covered by nodules was calculated with an online color-extraction tool set to 5 colors and a delta of 24.[3] Latitude was also included as a predictor in the analysis because seafloor depth gets deeper with increasing latitude, and depth is too highly correlated to BBPI for both predictors to be included in the same model. Therefore, while habitat related differences in depth are captured by BBPI and habitat type, latitude is used to account for this depth

[3]http://www.coolphptools.com/color_extract#demo

TABLE 2 | Environmental characteristics for all camera deployments.

Drop	Station Name	Depth	BBPI	FBPI	POC	Decadal Avg Chl	Monthly Avg Chl	Nodule Cover	Avg Temp	Avg Speed	Max Speed	Avg Current Direction
		(m)	1:100 km	50:250 m								
DC1	APEI7 AP	4878	−235	−2	1.850	0.147	0.125	0.000	1.62	0.05	0.12	230.4
DC2	APEI7 AP	4860	−208	−2	1.850	0.147	0.125	0.000	1.62	0.05	0.12	333.3
DC3	APEI7 S	3083	903	44	1.973	0.147	0.124	0.000	1.8	0.06	0.14	328.2
DC4	APEI7 S	3140	1345	12	2.014	0.147	0.124	0.000	1.79	0.08	0.18	29.7
DC5	APEI4 AP	5216	−217	−16	1.380	0.117	0.119	0.526	1.67	0.09	0.13	176.1
DC6	APEI4 AP	5004	−138	−2	1.430	0.117	0.120	0.148	1.64	0.08	0.14	1.3
DC7	APEI4 S	3542	1098	−36	1.327	0.116	0.108	0.000	1.68	0.05	0.15	27.3
DC8	APEI4 S	3497	1310	−9	1.428	0.116	0.106	0.000	1.7	0.04	0.16	129.5
DC9	APEI1 AP	5236	−81	−10	1.105	0.073	0.062	0.142	NA	NA	NA	NA
DC10	APEI1 AP	5213	25	−18	1.156	0.073	0.063	0.099	NA	NA	NA	NA
DC11	APEI1 S	4218	932	−56	1.158	0.071	0.061	0.470	NA	NA	NA	NA
DC12	APEI1 S	4346	831	4	1.118	0.072	0.063	0.738	NA	NA	NA	NA
TC02	APEI4 AP	5096	−150	17	1.430	0.117	0.120	0.000	NA	NA	NA	NA
TC03	APEI4 S	3885	1201	−22	1.327	0.115	0.106	0.000	NA	NA	NA	NA
TC04	APEI4 S	4134	1218	−2	1.355	0.115	0.106	0.000	NA	NA	NA	NA
TC05	APEI1 AP	5225	−46	27	1.105	0.073	0.062	0.299	NA	NA	NA	NA
TC06	APEI1 AP	5249	14	−10	1.156	0.073	0.063	0.079	NA	NA	NA	NA
TC07	APEI1 S	4622	688	−3	1.149	0.072	0.062	0.383	NA	NA	NA	NA

AP, abyssal plain; S, seamount.

gradient and any additional variability introduced with a change in latitude not accounted for by productivity/POC changes.

In addition to the PCoA analysis, PERMANOVA was used to evaluate how much the community composition was influenced by each available predictor, with the adonis function in the R package {vegan}. The permutations (N = 9,999) were again stratified by APEI. Significance was evaluated using marginal tests: PERMANOVA analyses were repeated so that each predictor could be evaluated as the last predictor added to the model, since the results depend on the order of the terms. Finally, in order to understand which animals were most responsible for driving differences between habitat types, a similarity percentages (SIMPER) analysis was conducted on the dissimilarity matrix using habitat type as the grouping variable (simper function in {vegan}). The eight taxa that represent >70% of the variation in community composition were considered the most significant taxa.

RESULTS

Seamounts vs. Plains: Environmental Characteristics

A total of 17 baited camera deployments and 5 baited trap deployments were conducted (**Table 1**, Note, DC7 was excluded due to bait consumption on descent). All deployment locations were on soft sediment. Nodule cover varied across the three APEIs, with no manganese nodules in APEI 7 deployments. APEI 4 was highly heterogeneous in nodule abundance with nodules covering 0 to 53% at abyssal locations (mean 13%; **Table 2**), and with no nodules observed in any of the four APEI 4 seamount deployments. All deployments in APEI 1, both on plains and seamounts, observed nodules, with the average percent coverage at 32% (8–74%). Across all sites, there were no clear relationships between nodule cover and habitat type.

For the eight deployments for which current meter data was available (APEI 7 and 4), seamount and abyssal plain deployments had similar mean current speeds around 0.06 m s^{-1} (seamount mean ± sd 0.0575 ± 0.02 m s^{-1}; plain mean ± sd 0.0675 ± 0.02 m s^{-1}; **Table 2**). Although seamounts average speeds were slightly lower than plains, this difference was not significant (p = 0.65). However, maximum recorded speeds were significantly higher on seamounts (0.15 m s^{-1}) than on abyssal plains (0.13 m s^{-1}). Seamount sediments were rippled, bright white, and much coarser than plain sediments in all APEIs, indicating bouts of active sediment transport and winnowing. Large gouge marks (>1 m in length), which may be some sort of feeding traces, were also visible in several seamount deployments.

Seamounts vs. Plains: Diversity

A total of 22 bait-attending taxa were identified across all 17 baited camera deployments (**Figure 3** and **Table 3**). Twelve fish morphotaxa (family, genus, or species) were observed from six families, Synaphobranchidae, Macrouridae, Ophidiidae, Alepocephalidae, Halosauridae, Zoarcidae. Seven crustacean morphotaxa were also observed including a squat lobster (*Munidopsis* sp.) and several types of shrimps (Period, Aristeid, and Caridean shrimps). Additionally, one genus of octopus was observed, *Grimpoteuthis* sp. Finally, bait-attending echinoderms were represented by the brittle star *Ophiosphalma* cf. *glabrum*, and an unidentified echinoid. At the APEI 7 seamount (DC3). One deployment (DC7) was not considered in the statistical analysis because shallow-water sharks ate nearly all of the bait before the lander reached bottom, leaving the deployment with some bait scent, but essentially un-baited for the entire duration. Fifteen taxa were observed across the abyssal plain deployments, and 22 taxa were observed across the seamount deployments.

Rarified diversity showed that seamounts have significantly higher morphospecies richness (q = 0) than plains (**Figure 4B**), and morphospecies accumulation curves suggest that while abyssal plains seem to have been sufficiently sampled, seamount richness has not yet reached an asymptote (**Figure 4A**). Extrapolated morphospecies richness at 614 individuals was calculated to be 15.4, [standard error (se) = 2.7] for abyssal plains and 22.3 (se = 3.9) for seamounts, and CI were non-overlapping by 450 individuals. For both Shannon and Simpson diversity metrics (q = 1,2), seamounts were significantly less diverse than abyssal plains (**Figures 4C,D**). This is due to low evenness scores on seamounts, driven by the extremely high abundances of the predator and scavenger *I. arx*, identified to species from baited-trap specimens (Leitner et al., 2020; **Table 3**).

Comparisons between APEIs (with habitat types combined within each APEI) showed no significant differences in morphospecies richness (q = 0) among APEIs, but significantly lower Shannon and Simpson diversities (q = 1,2) in APEI 7 (**Figures 5B–D**). The diversity metrices were lower in APEI 7 due to the extreme dominance of *I. arx* on the APEI 7 seamount, with MaxN for *I. arx* an order of magnitude greater than for all other morphospecies. Morphospecies accumulation curves for each APEI indicate that only APEI 4 approached an asymptote, suggesting that more morphospecies are likely to be found upon further sampling in APEI 1 and 7 (**Figure 5A**).

Seamounts vs. Plains: Taxonomic Overlap

Seven morphospecies were only found on seamounts, including the most abundant bait-attending taxon observed, the synaphobranchid eel *I. arx* (MaxN = 115). *Ilyophis arx* dominated scavenger abundance and was responsible for the vast majority of the bait consumption on seamounts in APEI 7 and 4. Four morphotaxa (*Asquamiceps*, Halosaur, *Bassogigas walkeri*, and Zoarcidae sp. 2) were unique to the seamount in APEI 7. One morphotaxon (echinoid) was unique to the seamount in APEI 4. The seamount in APEI 1 had no exclusive morphotaxa but shared one morphotaxon (*Acanthephyra* sp.) exclusively with the seamount in APEI 7. No bait-attending morphotaxon was exclusively found on abyssal plains. The greatest amount of morphospecies overlap (N = 6) was found between all sites except APEI 7 seamount, which was clearly the most distinct site (**Figure 6** and **Table 4**). Only two taxa were common to all sites, the ophidiid *Bassozetus* sp. B, and the summed taxonomic category of large penaeid and aristeid shrimps (a category used when distinguishing characteristics like rostrum length and

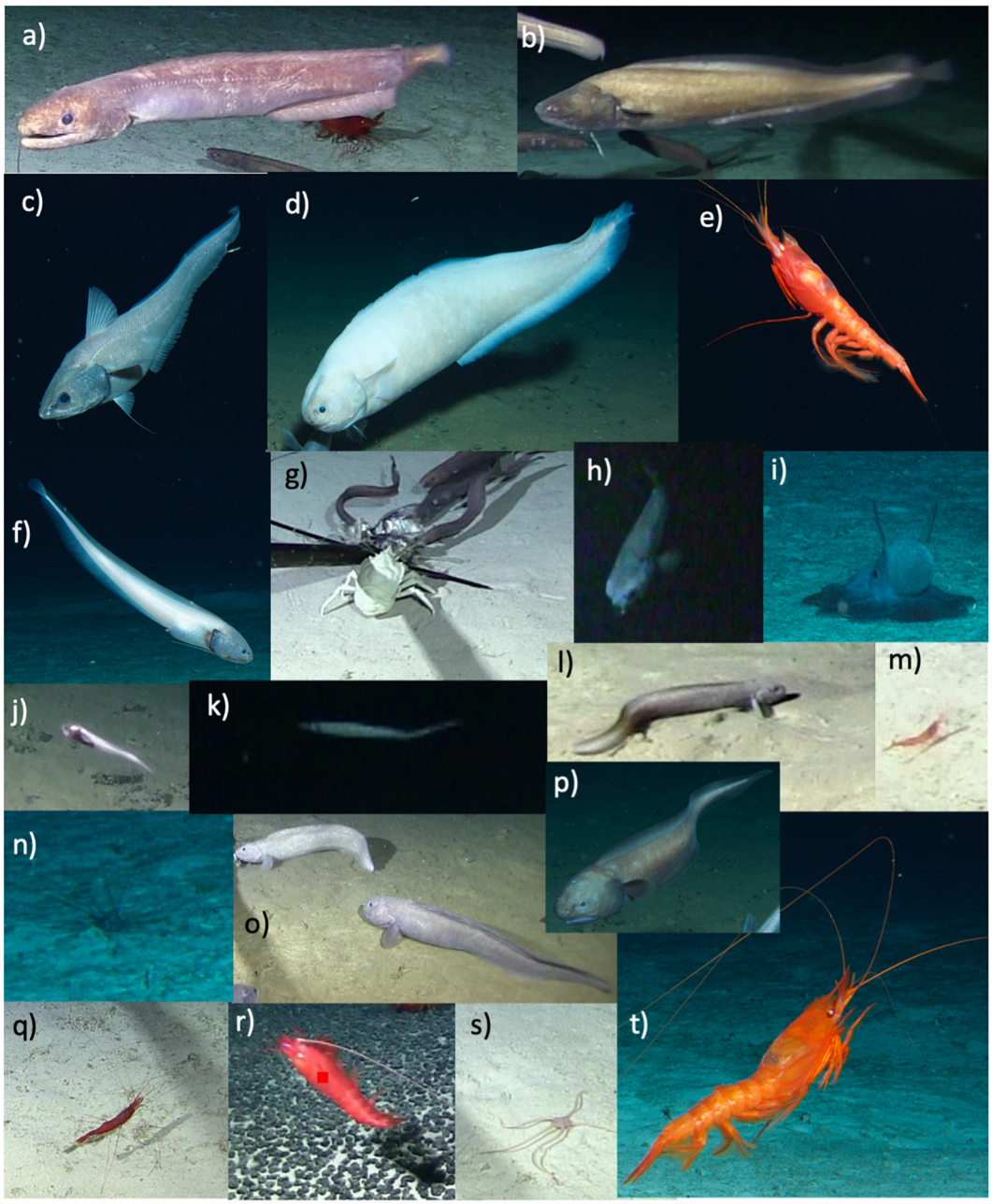

FIGURE 3 | Twentymorphospecies seen across the seventeen successful baited camera deployments. **(a)** *Ilyophis arx* **(b)** *Bassogigas walkeri* **(c)** *Coryphaenoides armatus/yaquinae* complex **(d)** *Barathrites iris* **(e)** *Benthiscymus* sp. **(f)** *Bassozetus* sp. B **(g)** *Munidopsis* sp. **(h)** *Asquamiceps* sp. **(i)** *Grimpoteuthis* sp. **(j)** *Bassozetus* juvenile sp. **(k)** Halosaur **(l)** Zoarcid sp. 2 **(m)** *Hymenopenaeus nereus* **(n)** Echinoid **(o)** *Pachycara nazca* **(p)** *Bassozetus nasus* **(q)** *Nematocarcinus* sp. **(r)** *Acanthephyra* sp. **(s)** *Ophiosphalma* c.f. *glabrum* **(t)** *Cerataspis monstrosus*.

shape were not visible to distinguish *Cerataspis monstrosus* from *Benthiscymus* sp.).

Seamounts vs. Plains: Community Composition

Seamounts have significantly different community compositions than plains (PERMANOVA $p < 0.001$). From the SIMPER analysis, the eight morphotaxa most influential in driving the differences between seamount and abyssal plain communities were the synaphobranchid eel *I. arx* (21% of the difference), the abyssal rattail *Coryphaenoides armatus/yaquinae* (12%), large decapod shrimp (as a general taxonomic category, 9%), the shrimp morphospecies *C. monstrosus* (7%), the ophidiid *Barathrites iris* (6%), the zoarcid *Pachycara nazca* (6%), and two ophidiids: juvenile *Bassozetus* sp. (5%) and *Bassozetus* sp. B (5%).

TABLE 3 | (A) Relative abundances (MaxN) of all bait-attending fishes in all successful deployments. (B) Relative abundances (MaxN) of all bait-attending invertebrate fauna in all successful deployments.

(A)

Station name	Drop	*Asquamiceps* sp.	Halosaur	*Coryphaenoides armatus/ yaquinae*	*Barathrites iris*	*Bassogigas walkeri*	*Bassozetus nasus*	*Bassozetus* spp	*Bassozetus* sp.B	*Bassozetus* sp. juv	*Ilyophis arx*	*Pachycara nazca*	*Zoarcidae* sp.2
APEI7 AP	**DC1**	0	0	20	2	0	1	0	0	0	0	3	0
APEI7 AP	**DC2**	0	0	21	2	0	0	0	1	0	0	2	0
APEI7 S	**DC3**	1	0	0	0	2	0	0	2	0	115	0	1
APEI7 S	**DC4**	0	1	0	0	2	0	1	2	0	110	0	2
APEI4 AP	**DC5**	0	0	10	2	0	4	0	1	3	0	0	0
APEI4 AP	**DC6**	0	0	20	1	0	1	0	1	1	0	8	0
APEI4 S	**DC7**	0	0	0	0	0	0	0	1	0	4	0	0
APEI4 S	**DC8**	0	0	3	0	0	1	0	2	0	56	8	0
APEI1 AP	**DC9**	0	0	15	2	0	2	0	0	2	0	0	0
APEI1 AP	**DC10**	0	0	8	2	0	2	3	1	5	0	0	0
APEI1 S	**DC11**	0	0	2	0	0	2	0	0	0	1	0	0
APEI1 S	**DC12**	0	0	3	0	0	2	0	1	0	0	0	0
APEI4 AP	**TC02**	0	0	11	4	0	2	0	1	0	0	9	0
APEI4 S	**TC03**	0	0	0	1	0	2	0	6	1	15	1	0
APEI4 S	**TC04**	0	0	1	1	0	7	0	5	5	3	1	0
APEI1 AP	**TC05**	0	0	5	5	0	3	0	0	4	0	1	0
APEI1 AP	**TC06**	0	0	4	1	0	3	0	1	4	0	0	0
APEI1 S	**TC07**	0	0	3	0	0	2	0	0	1	0	0	0

TABLE 3 | Continued

(B)

Station Name	Drop	*Munidopsis* sp.	*Acanthephyra* sp.	total shrimp Penaeid /*Aristeidae*	*Cerataspis monstrosus*	*Benthiscymus* sp	*Hymenop-enaeus nereus*	*Nemato-carcinus* sp	*Grimpoteuthis* sp	*Echinoidea*	*Ophiosphalma glabrum*
APEI7 AP	**DC1**	0	0	3	3	2	1	0	0	0	0
APEI7 AP	**DC2**	1	0	0	2	2	1	1	0	0	0
APEI7 S	**DC3**	0	1	1	0	0	0	0	0	0	0
APEI7 S	**DC4**	1	1	1	0	0	0	0	0	0	1
APEI4 AP	**DC5**	0	0	5	3	2	1	0	1	0	1
APEI4 AP	**DC6**	0	0	3	3	1	1	0	1	0	0
APEI4 S	**DC7**	0	0	2	1	1	0	0	0	0	0
APEI4 S	**DC8**	0	0	7	5	0	0	0	0	0	0
APEI1 AP	**DC9**	0	0	4	1	2	1	0	0	0	0
APEI1 AP	**DC10**	0	0	6	3	3	1	0	0	0	2
APEI1 S	**DC11**	0	0	23	23	1	1	0	0	0	0
APEI1 S	**DC12**	0	1	11	5	1	0	0	0	0	0
APEI4 AP	**TC02**	0	0	5	4	2	1	1	0	0	1
APEI4 S	**TC03**	0	0	14	9	1	0	1	0	1	0
APEI4 S	**TC04**	0	0	12	9	2	1	1	1	0	0
APEI1 AP	**TC05**	0	0	3	3	2	2	0	0	0	3
APEI1 AP	**TC06**	0	0	7	3	3	1	1	0	0	0
APEI1 S	**TC07**	0	0	18	10	2	7	1	1	0	0

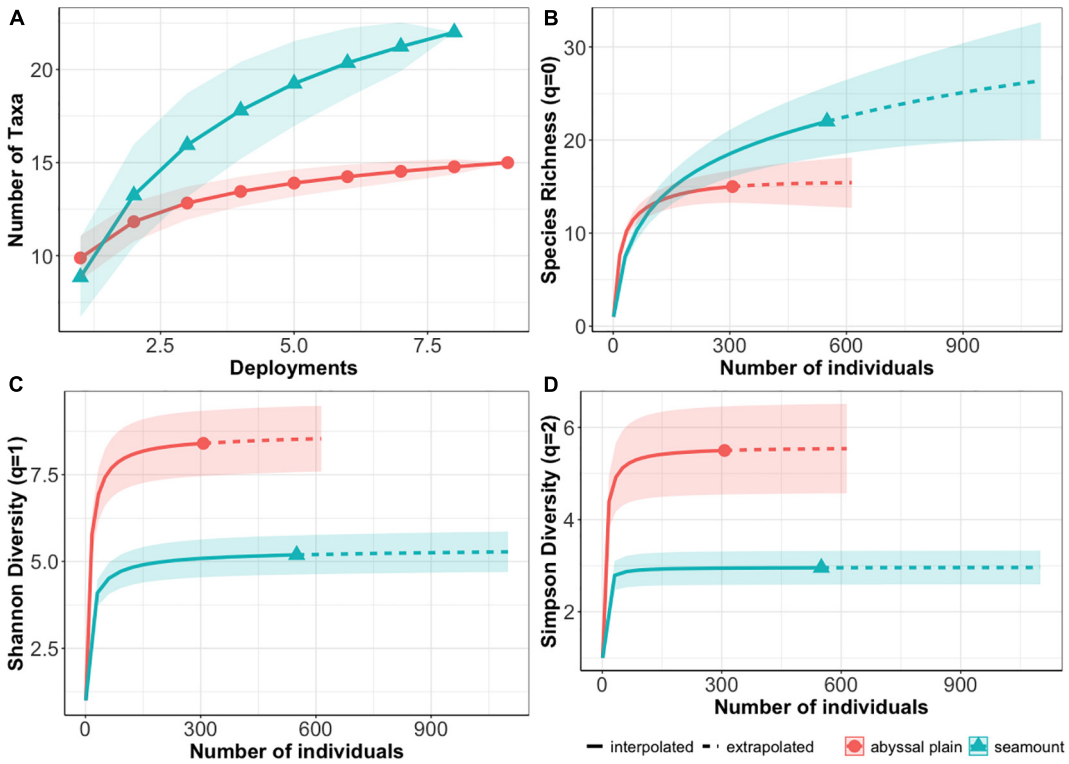

FIGURE 4 | Comparisons of sampling effort and diversity metrics between seamounts (blue triangle) and abyssal plains (red circle). **(A)** Morphospecies accumulation curves by habitat type. **(B)** Species richness (Hill number $q = 0$), **(C)** Shannon diversity (Hill number $q = 1$) and **(D)** Simpson Diversity (Hill number $q = 2$) with 95% confidence intervals (CI) (shaded areas) for each habitat type. For panel **(B–D)** interpolated values are shown with solid lines and extrapolated values with dashed lines.

The three APEIs also had significantly different community compositions (PERMANOVA $p < 0.05$), and *I. arx* was always the most influential taxa in driving the differences in community compositions in the areas. Over one quarter of the differences between each APEI pair is explained by the relative abundances of *I. arx* and *C. armatus/yaquinae*; though for the APEI 1 and 4 pair, *P. nazca* (12%) accounts for more variation than *C. armatus/yaquinae* (10%).

Of the environmental predictors analyzed, marginal significance tests consistently found that BBPI (habitat type), latitude, and POC flux had significant influences on relative abundances and community composition ($p < 0.05$). Lander type did not have a significant effect. The constrained ordination with these predictors as well as with nodule abundance and lander type (not significant) was able to explain 69% of the variability in the community compositions across the deployments (**Figure 7**). The first two ordination axes alone explained 61% of the variation.

Cluster analysis (simprof) found eight significant clusters of deployments, and no seamount deployments clustered with any abyssal plain deployments (**Figure 7** and **Supplementary Figure 1**). Deployments from the two different landers, DC and Tripod, were never included in the same significant clusters; however, marginal tests found that lander type did not significantly affect the community composition ($p > 0.05$). The APEI 7 seamount deployments formed their own significant, unique cluster. These two deployments were part of another cluster with the only successful DC deployment on the APEI 4 seamount. These three seamount deployments were all marked by high abundances of *I. arx* (Leitner et al., 2021). Both Tripod deployments on the APEI 4 seamount cluster together, though separately from one the DC deployment on that same seamount. Likewise, both DC deployments on the APEI 1 seamount cluster together, while the only tripod deployment on the APEI 1 seamount was in a separate cluster on its own. Abyssal plain communities were more similar to each other than to those at their proximate seamounts, as evidenced by the cluster analysis. Seamounts host distinct communities from plains, though the differences decrease with increasing latitude such that the seamounts in APEI 1 were the closest in composition to that of the plains. Abyssal plain deployments seem to be grouped by APEI; though APEI 4 plain deployments showed a transitional community, with one deployment grouping with the APEI 1 plain cluster and the others with the APEI 7 plain cluster (**Figure 7** and **Supplementary Figure 1**).

While the abyssal seamounts sampled here generally had higher overall relative abundances (MaxN) than the surrounding abyssal plains, this "seamount-effect" was highly taxon-specific, with some animals found at significantly higher abundances

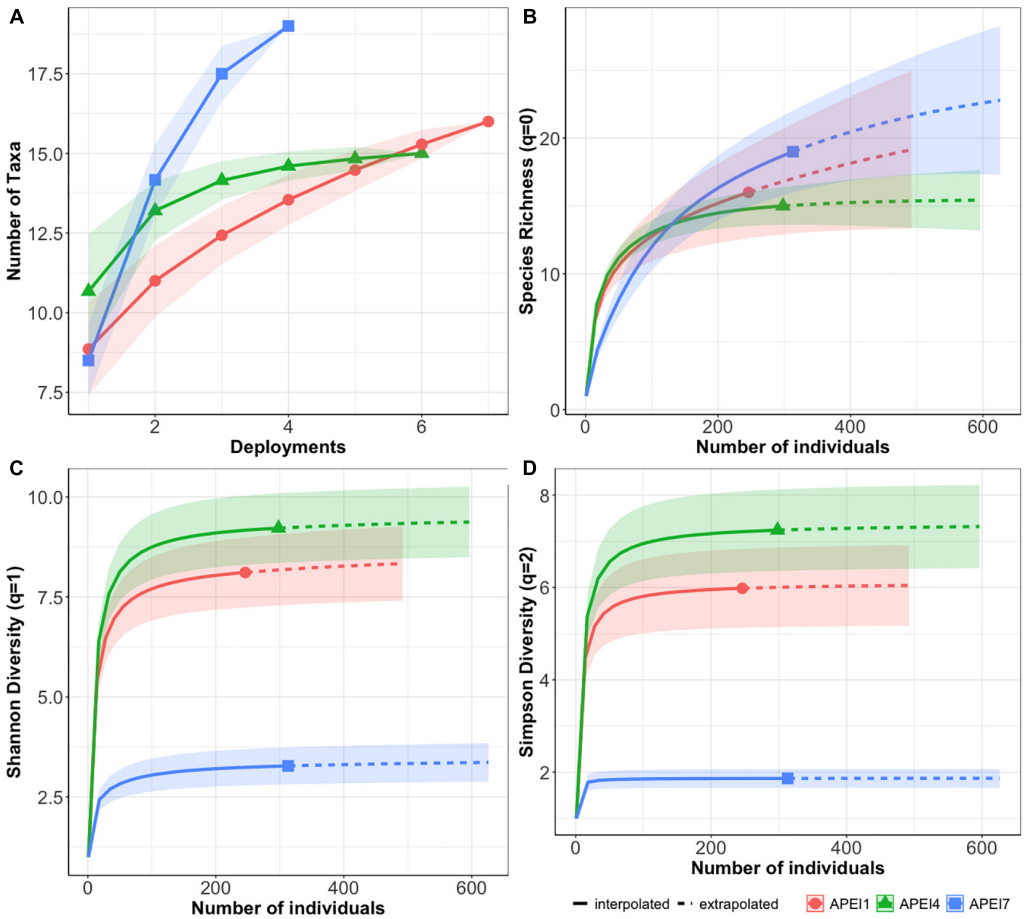

FIGURE 5 | Comparisons of sampling effort and diversity metrics between APEIs (red circle, APEI 1, green triangle APEI 4, blue square APEI 7). **(A)** Species accumulation curves for all APEIs. **(B)** Species richness (hill number $q = 0$), **(C)** Shannon diversity (Hill number $q = 1$) and **(D)** Simpson Diversity (Hill number $q = 2$) with 95% confidence intervals (shaded areas) for each APEI. For panel **(B–D)** interpolated values are shown with solid lines and extrapolated values with dashed lines.

on seamounts and others on abyssal plains. The abyssal plain communities were distinguished by higher abundances of *C. armatus/yaquinae*, *B. iris*, juvenile *Bassozetus* sp., *P. nazca*, *Benthiscymus* sp., and *O. glabrum*. The abyssal seamount communities were distinguished by higher abundances of *I.arx*, *Bassozetus* sp. B, *B. walkeri*, total shrimp, and *C. monstrosus* (**Figure 8**).

DISCUSSION

The main goals of this study were to describe the bait-attending assemblage from abyssal seamounts for the first time and to test the "shared-fauna" prediction of the SRH in the western CCZ in the context of deep-sea mining for bait-attending abyssal-demersal fauna. These are mid-level and top predators, necrophagivores, and scavengers in abyssal seafloor ecosystems. From our observations, we cannot reject the SRH for the bait-attending community. All abyssal plain morphospecies were also seen on at least one seamount deployment. However, the reverse was not true. In fact, seven morphospecies were exclusive to seamount deployments. Therefore, these abyssal seamounts were found to host diverse and different bait-attending assemblages in comparison to their neighboring abyssal plains. In fact, abyssal plain assemblages hundreds of kilometers apart were more similar to each other, than to those assemblages on seamounts just 15 km away. The seamounts sampled also had different dominant fauna, with synaphobranchid eels dominating in the southern two seamounts, and large decapod shrimps dominating the community in the northern seamount. The significant differences in community structure make it unlikely that displaced animals will venture up into the seamount habitat in sufficient numbers to create and sustain viable populations on the timescales required for recovery (>26 years), even to avoid negative mining impacts such as extensive sediment plumes and reduction or elimination of infaunal and benthic prey (Gollner et al., 2017; Jones et al., 2017; Simon-Lledó et al., 2019). While highly mobile animals are often found in a variety of habitats, their core habitat, where they are naturally the most abundant, is often needed to sustain reproductive populations (Drazen et al., 2019). Moreover, seamounts make up only 0.3% of the habitat area of the CCZ (Washburn et al., 2021) and ecological research shows that a 99%

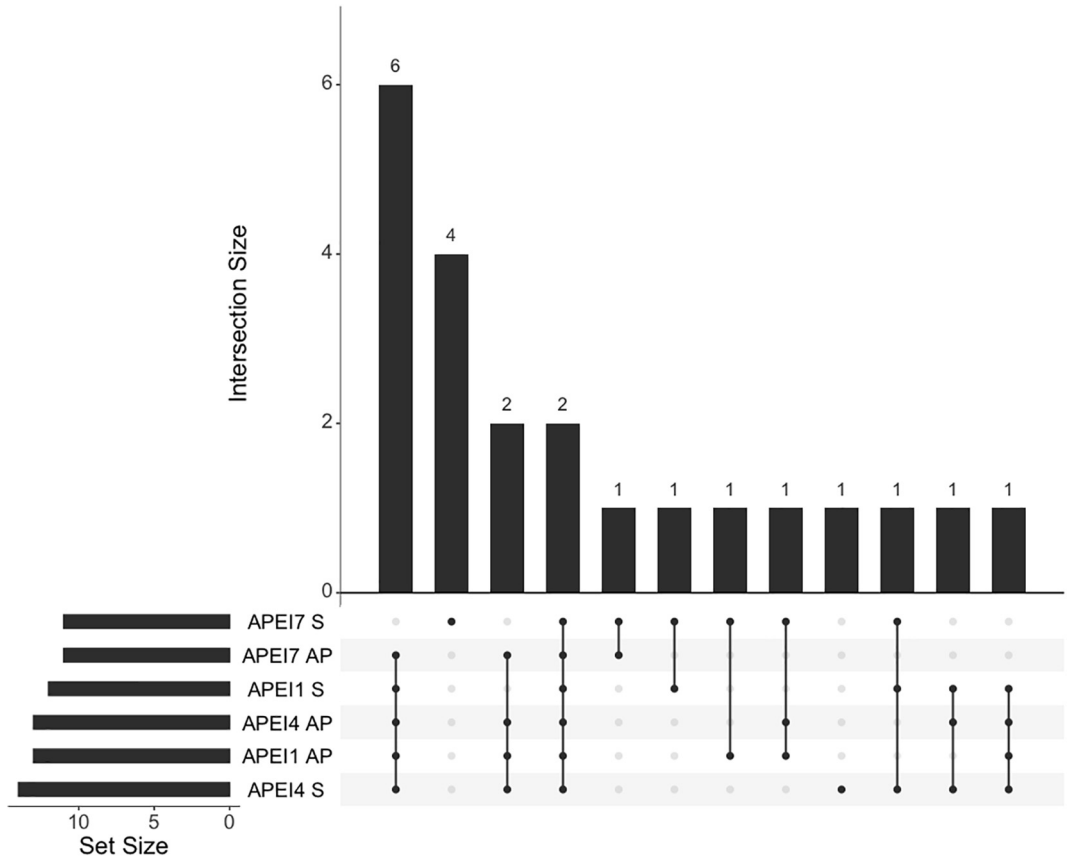

FIGURE 6 | Intersection sizes in community composition between sampling station. Numbers of samples at each station are displayed on the bottom left bar chart. Vertical bars show intersection sizes between stations marked with dots listed along the *x* axis. Chart produced with {UpSetR} (Gehlenborg, 2019).

habitat loss results in extinctions of essentially all species reliant on that habitat (Hanski et al., 2013; Rybicki and Hanski, 2013). Thus, protection of seamounts in the CCZ region alone does not appear to be sufficient to preserve abyssal biodiversity, even if all the mobile abyssal species can live on seamounts. Therefore, while we found no morphospecies exclusive to abyssal plains, we argue that distinct differences in densities indicate that only preserving seamounts is likely to be insufficient refuge for top predators and scavengers of the CCZ.

Often, seamounts are considered unusual habitats in the deep-sea because they provide hard substrate, which can be rare in much of the deep sea (but see Riehl et al., 2020; Smith et al., 2020). Previous works comparing seamounts to surrounding abyssal plains face two complications. Firstly, these studies mostly attempted to compare fauna at bathyal depths on seamounts to fauna at abyssal depths on plains (e.g., Christiansen et al., 2015; Vieira et al., 2018), so any difference between seamounts and abyssal plains may result from the strong vertical zonation of fauna across this depth gradient (Christiansen et al., 2015; Denda et al., 2017; Linley et al., 2017) instead of geomorphology. Secondly, most studies compared hard-substrate habitats, which predominate on seamounts, to soft-substrate plain habitats, making it difficult to distinguish a seamount effect from a substrate effect (e.g., Christiansen et al., 2015; Vieira et al., 2018). Here we specifically compared soft-sediment habitats on abyssal seamounts to surrounding soft-sediment abyssal plains, making the clear community differences between seamounts and abyssal plains reported particularly noteworthy, especially because bait-attending fauna are mobile and generally widespread. One study in the Atlantic abyssal plains for example, showed no difference in the fish communities between abyssal plains and abyssal highs with elevations less than 1,000 m (Milligan et al., 2016). However, for the same area, abyssal hills were found to have significantly higher biomass, higher diversity, and a different trophic composition for the invertebrate, benthic megafaunal community (Durden et al., 2015). Moreover, across a gradient of low relief bathymetric change within the CCZ, another study found significantly higher abundances, larger body sizes, higher diversity, and different community composition for bait-attending fauna at higher relative elevations (abyssal hills) vs. plains and depressions (Leitner et al., 2017). Finally, a recent study has found that even changes in depth as small as 10s of meters can significantly influence the benthic megafaunal community (Durden et al., 2020). Thus, a bathymetric change of 1,000 m, even without a substrate change, would be expected to affect the megafaunal community.

TABLE 4 | Presence table for each bait-attending taxon in order of most widely observed.

Taxon	Total N sites	APEI1 AP	APEI1 S	APEI4 AP	APEI4 S	APEI7 AP	APEI7 S	SM	AP
Bassozetus spB	6	**1**	**1**	**1**	**1**	**1**	**1**	3	3
Total Shrimp Penaeidae/Aristeidae	6	**1**	**1**	**1**	**1**	**1**	**1**	3	3
Coryphaenoides armatus/yaquinae	5	**1**	**1**	**1**	**1**	**1**	0	2	3
Bassozetus nasus	5	**1**	**1**	**1**	**1**	**1**	0	2	3
Cerataspis monstrosus	5	**1**	**1**	**1**	**1**	**1**	0	2	3
Benthiscymus sp.	5	**1**	**1**	**1**	**1**	**1**	0	2	3
Hymenopenaeus nereus	5	**1**	**1**	**1**	**1**	**1**	0	2	3
Nematocarcinus sp.	5	**1**	**1**	**1**	**1**	**1**	0	2	3
Barathrites iris	4	**1**	0	**1**	**1**	**1**	0	1	3
Bassozetus sp. juv	4	**1**	**1**	**1**	**1**	0	0	2	2
Pachycara nazca	4	**1**	0	**1**	**1**	**1**	0	1	3
Ilyophis arx	3	0	**1**	0	**1**	0	**1**	3	0
Grimpoteuthis sp.	3	0	**1**	**1**	**1**	0	0	2	1
Ophiosphalma glabrum	3	**1**	0	**1**	0	0	**1**	1	2
Bassozetus spp.	2	**1**	0	0	0	0	**1**	1	1
Munidopsis sp.	2	0	0	0	0	**1**	**1**	1	1
Acanthephyra sp.	2	0	**1**	0	0	0	**1**	2	0
Asquamiceps	1	0	0	0	0	0	**1**	1	0
Halosaur	1	0	0	0	0	0	**1**	1	0
Bassogigas walkeri	1	0	0	0	0	0	**1**	1	0
Zoarcidae sp.2	1	0	0	0	0	0	**1**	1	0
Echinoidea	1	0	0	0	**1**	0	0	1	0

The first column displays the number of sites (APEI and habitat type combinations, N = 6) where each taxon was observed at least once. The middle columns show presence (1) or absence (0) at each site. The last two columns show the number of sites where each taxon was observed at least once split by habitat type, SM, seamount; AP, abyssal plain. Gray fill color highlights seamount exclusive taxa. Bolded 1 values represent present, plain text 0s represent absences.

Cuvelier et al. (2020) and Laroche et al. (2020) conducted the only other tests of the SRH in the CCZ, and their results differ from ours in finding lower taxonomic overlap between seamounts and abyssal plains than reported here for bait-attending fauna. Cuvelier et al. (2020) used ROV video and compared the megafaunal communities, excluding fishes, of four seamounts and surrounding nodule fields and found, similar to the results here, that seamounts hosted distinct benthic megafaunal communities. However, they found only 10% taxonomic overlap between abyssal plains and seamounts. Laroche et al. (2020) also found that abyssal seamounts and neighboring abyssal-plain communities (the same locations studied here) were distinct based on eDNA sampling of sediment and bottom waters, finding only 16–19% seamount vs. plain overlap in amplicon sequence variants. Both studies concluded that the SRH was not valid for mining impacts in the CCZ due to low degrees of faunal overlap (Cuvelier et al., 2020). While we did find 7 of 22 morphospecies unique to the sampled seamounts, we found much higher (68%) taxonomic overlap between seamounts and plains. Moreover, all of the abyssal bait-attending morphospecies were also found on seamounts, though often in much lower numbers. Thus, seamounts may provide better refugia for the highly mobile scavengers/predators than for the much less mobile megafaunal deposit and suspension feeders. It should be noted that while Cuvelier et al. (2020) did have data from abyssal depths on three of the visited seamounts, all but one of their seamounts extended into bathyal depths, making these bathyal seamounts rather than the abyssal seamounts as discussed here. In addition, fishes were left out of their comparative statistical analysis due to their lack of representativity and possibly attraction to the ROV lights, although the authors did report greater fish diversity on seamounts than in abyssal nodule fields (Cuvelier et al., 2020). Laroche et al. (2020) found that fishes represented only a small fraction of the amplicon sequence variants identified, making seamount vs. abyssal-plain comparisons difficult.

Studies from bathyal seamounts in other regions, though shallower than the present work, show some similarities to our findings. Witte (1999) reported results from a large carcass experiment on a bathyal seamount summit (1,900 m depth) in the Arabian sea. High numbers of large aristeid shrimps were recorded at the bait, similar to our observations at the seamount in APEI 1. However, Witte also found a high number of macrourids at the bathyal seamount summit, which were absent at the nearby abyssal plain site, which was instead dominated by scavenging amphipods and large numbers of zoarcid fishes (Witte, 1999). Nevertheless, similar to our findings here, Witte found a distinct scavenging community at the seamount summit, though the dominant seamount taxa were different from those we found in the western CCZ. The only other baited camera data available from deep, oceanic seamounts come from Wilson et al. (1985), who studied the bait-attending community of one bathyal seamount (1,443 m) in the North Pacific. They observed halosaurs and shrimp from the genus *Acanthephyra*,

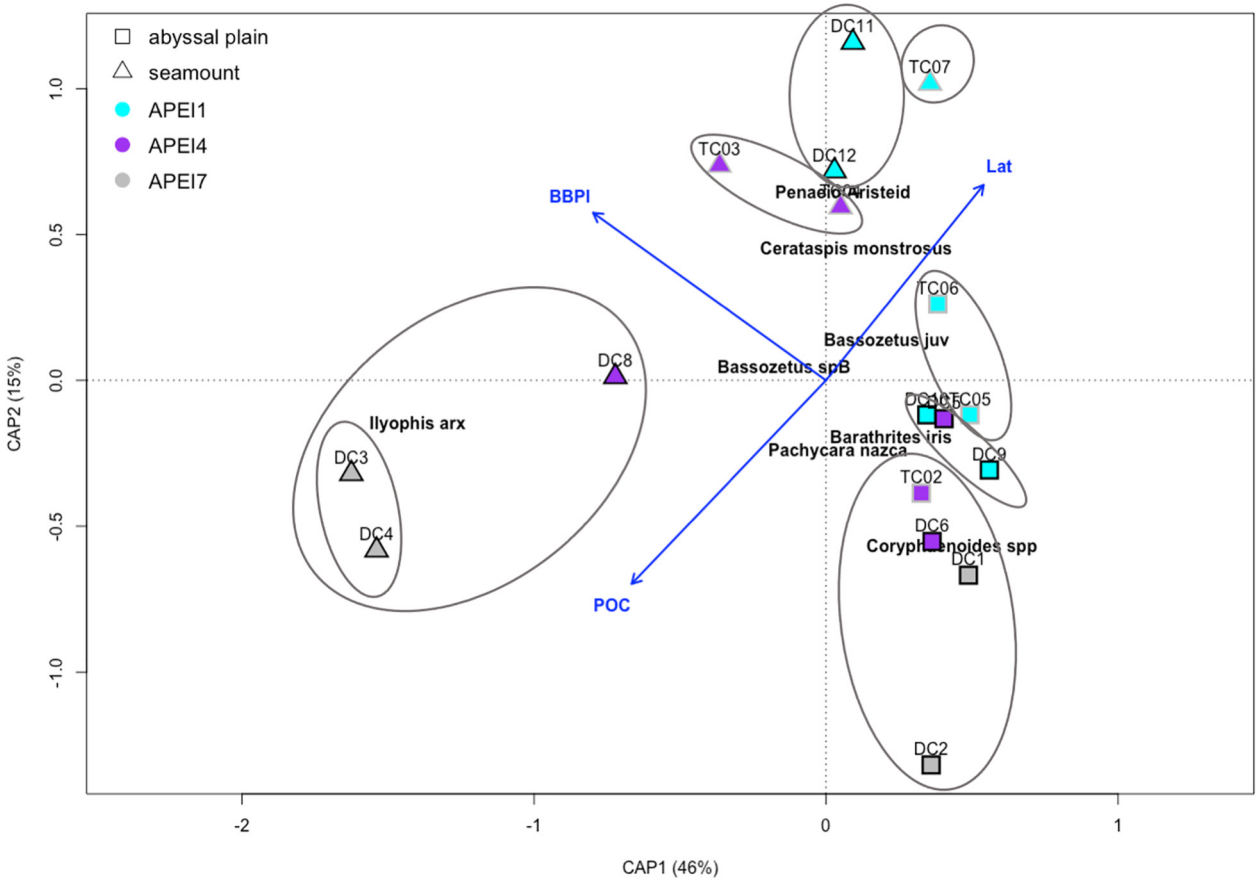

FIGURE 7 | Constrained ordination of square root transformed abundance data (MaxN). Blue arrows with labels represent the biplot scores for each constraining variable. Marker shape denotes habitat type (triangle = seamount; square = abyssal plain), fill color denotes APEI, outline color denotes lander (Deepcam, black outline; Tripod, gray outline). Proportion of variation explained by each axis is in parentheses. Species names show the most influential species as identified by SIMPER analysis with a cumulative contribution to the ordination of 0.72. Circles show significant (alpha = 0.05) clusters of deployments as determined by similarity profile analysis.

which we find to be seamount-associated and absent from the proximate abyssal plains. Wilson et al. (1985) also observed high numbers of penaeid shrimp around the bait, as well as several morphospecies of synaphobranchid eels, though none in high numbers (MaxN = 4). Our results are also consistent with a study on the shallow Ampere Seamount in the NE Atlantic by Christiansen et al. (2015), who found large numbers of synaphobranchid eels on the bathyal slopes of the seamount. In this study only a single species (an alepocephalid) was shared between the deep slopes of Ampere seamount and the abyssal reference site.

Despite the fact that small abyssal seamounts (seamounts whose summit depths are ≥3,000 m) are the most common class of seamounts (Wessel et al., 2010), they are some of the most understudied, least explored habitats in the deep sea. The deployments discussed here, to our knowledge, yielded the first baited camera data published from abyssal seamounts. To date, seamount research has generally focused on shallower seamounts, which can be productivity hotspots, with abundant, high biomass, and diverse pelagic and benthic communities (Holland and Grubbs, 2007; Pitcher et al., 2007; Morato et al., 2010; Rowden et al., 2010; Leitner et al., 2020). This "seamount effect" is still not fully understood, but is likely due to the added habitat heterogeneity provided by the seamount structure and increased food availability due to modified hydrodynamics and topographic blocking of mesopelagic migrators (Genin et al., 1988; Genin, 2004; Genin and Dower, 2007; Morato et al., 2009; Lavelle and Mohn, 2010). Whether this "seamount effect" extends to the deepest, and most ubiquitous seamounts in the global ocean, remains uncertain, mostly due to the lack of data from deep features (Wilson et al., 1985; Wessel, 2001; Rowden et al., 2010). Evidence from abyssal hills suggest that such seamount effects may extend to the abyss, since abyssal hills can have higher detrital food availability (Morris et al., 2016; Durden et al., 2017).

Our observations provide initial evidence that this "seamount effect" can apply to abyssal seamounts in some cases. Seamounts in the western CCZ hosted higher community relative abundances than the proximate abyssal plains and had higher morphospecies richness. Moreover, our analysis showed that there are likely more as of yet unrecorded taxa on seamounts.

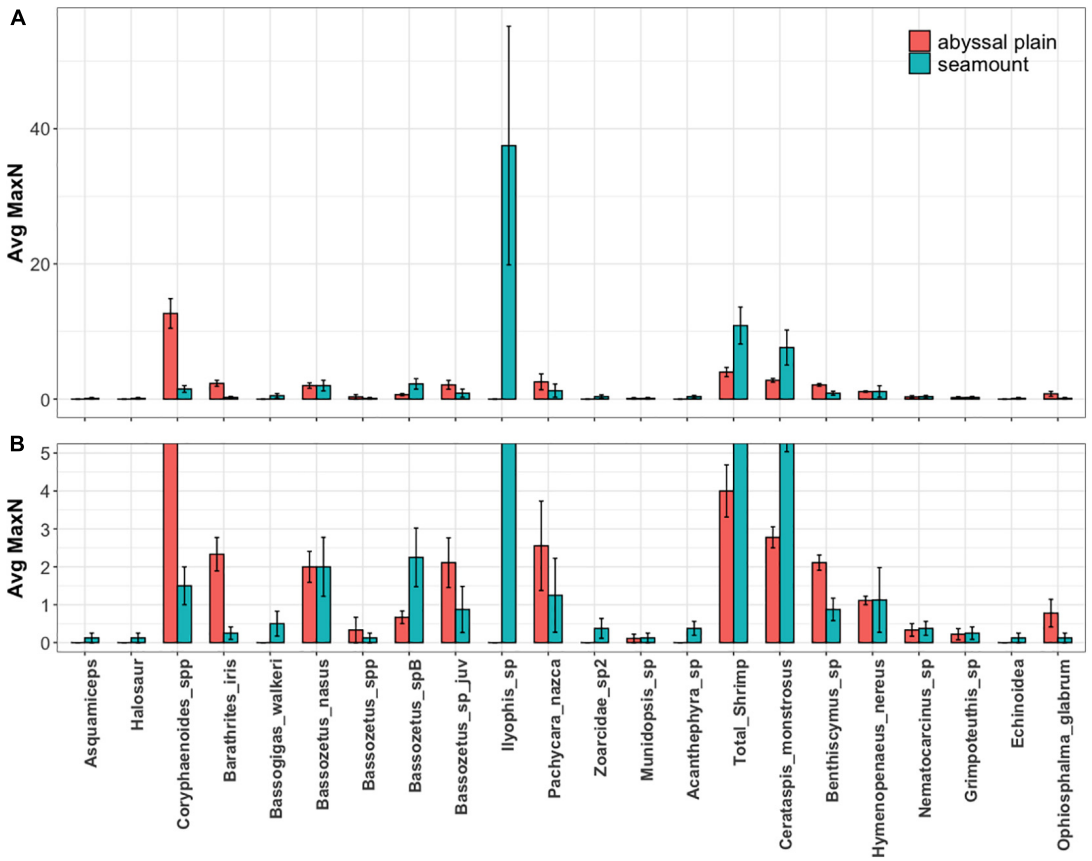

FIGURE 8 | (A) Average relative abundance (MaxN) of bait attending fauna on seamount (blue) and abyssal plain (red) habitats with error bars represent standard error. **(B)** Bottom panel shows a restricted range of abundance to more clearly display differences for all taxa beside *Ilyophis* sp (*I. arx*).

Higher order diversity metrics showed that seamount diversity was lower than abyssal plain diversity, though this was due to low evenness, not to low richness. The extraordinarily high relative abundances of eels (in APEI 4 and 7) and shrimps (APEI 1) on these seamounts resulted in lower Shannon and Simpson diversity estimates. It must also be noted that the individual seamounts themselves had distinct communities, with each feature in each of the APEIs clustering separately. Therefore, while the communities on the three sampled seamounts were more similar to each other than to those on the surrounding plains, each seamount also had a unique community. Therefore, these abyssal seamounts enhance regional biodiversity, though the mechanisms are not yet fully clear. POC flux, a proxy for food availability in the deep-sea, was found to be a significant driver of differences in community composition (in addition to BBPI/habitat type). More sampling should be conducted on abyssal seamounts, especially on those within high productivity regimes, to examine further the relationship found here between high relative abundances on seamounts as well as high single taxon dominance and productivity.

Currently, community and diversity analyses are hampered by limited taxonomic resolution. While baited cameras are an efficient and unobtrusive method for observing abyssal fishes, scavengers, and predators, physical sampling through trawls and additional traps are important complementary sampling methods that would enable additional species level identifications (Drazen and Sutton, 2017; Priede, 2017; Drazen et al., 2021, this vol). This information is currently lacking for many megafaunal species in the CCZ, because there has been no trawling in this area. Nevertheless, ISA-mandated environmental baselines require detailed taxonomic resolution in order to be effective (Wedding et al., 2015; Smith et al., 2020). Thus, there is a need for additional complementary physical sampling at this stage.

Our results show that abyssal seamounts host distinct, morphospecies-rich, communities that contribute to the regional biodiversity of the CCZ. These seamounts may not face direct mining impacts due to their challenging terrain but, it must not be assumed that because CCZ seamounts will not face manganese nodule mining, that they will not be impacted by mining activities. Nodule extraction on abyssal plains will likely generate large sediment plumes, both at the seafloor and in the midwater, that potentially could spread over 100s of kilometers (Drazen et al., 2020; Smith et al., 2020). Nearby seamount habitats therefore could also sustain impacts from these sediment plumes. Therefore, these distinct habitats merit consideration for environmental protection and further scientific study.

DATA AVAILABILITY STATEMENT

The original contributions presented in the study are included in the article/**Supplementary Material**, further inquiries can be directed to the corresponding author/s.

ETHICS STATEMENT

Ethical review and approval was not required for the animal study because this was a non-extractive video study.

AUTHOR CONTRIBUTIONS

AL, JD, and CS conceived of the project and conducted the field work, interpreted the results and drew final conclusions. AL annotated the video data, conducted statistical analyses, and wrote the body of the manuscript. JD and CS edited and made substantial contributions to the manuscript writing. All authors contributed to the article and approved the submitted version.

FUNDING

We thank the NOAA Office of Ocean Exploration (grant # NA17OAR0110209), the Gordon and Betty Moore Foundation (grant no. 5596), and the University of Hawaii School of Ocean and Earth Science and Technology (SOEST) for financial support. Open Access fees were funded by The Pew Charitable Trusts.

ACKNOWLEDGMENTS

We thank the captain and crew of the RV *Kilo Moana* and the science team of the DeepCCZ expedition for making this research possible. We thank taxonomic experts David G. Smith and Kenneth Tighe of the Smithsonian Institute for assistance with identification of all trapped specimens, and Ben Frable and Philip A. Hastings of the Scripps Institute of Oceanography fish collection for allowing us to examine the synaphobranchid specimens archived there. We also thank Kirsty McQuaid and Kerry Howell for extracting the seafloor POC flux for our deployment locations from the Lutz et al. (2007) model. This is SOEST contribution #11380.

SUPPLEMENTARY MATERIAL

The Supplementary Material for this article can be found online at: https://www.frontiersin.org/articles/10.3389/fmars.2021.636305/full#supplementary-material

REFERENCES

Becker, J. J., Sandwell, D. T., Smith, W. H. F., Braud, J., Binder, B., Depner, J., et al. (2009). Global bathymetry and elevation data at 30 Arc seconds resolution: SRTM30_PLUS. *Mar. Geod.* 32, 355–371. doi: 10.1080/01490410903297766

Cappo, M., Harvey, E., and Shortis, M. (2006). "Counting and measuring fish with baited video techniques – an overview," *Proceedings of the Cutting-Edge Technologies in Fish and Fisheries Science*, 101–114. doi: 10.1007/978-1-62703-724-2_1

Chao, A., Gotelli, N. J., Hsieh, T. C., Sander, E. L., Ma, K. H., Colwell, R. K., et al. (2014). Rarefaction and extrapolation with Hill numbers: a framework for sampling and estimation in species diversity studies. *Ecol. Monogr.* 84, 45–67. doi: 10.1890/13-0133.1

Christiansen, B., Vieira, R. P., Christiansen, S., Denda, A., Oliveira, F., and Goncalves, J. M. S. (2015). The fish fauna of ampere seamount (NE Atlantic) and the adjacent abyssal plain. *Helgol. Mar. Res.* 69, 13–23. doi: 10.1007/s10152-014-0413-4

Cuvelier, D., Ribeiro, P. A., Ramalho, S. P., Kersken, D., Martinez Arbizu, P., and Colaço, A. (2020). Are seamounts refuge areas for fauna from polymetallic nodule fields? *Biogeosciences* 17, 2657–2680. doi: 10.5194/bg-2019-304

Denda, A., Stefanowitsch, B., and Christiansen, B. (2017). From the epipelagic zone to the abyss: trophic structure at two seamounts in the subtropical and tropical Eastern Atlantic - Part I zooplankton and micronekton. *Deep. Res. Part I Oceanogr. Res. Pap.* 130, 63–77. doi: 10.1016/j.dsr.2017.10.010

Drazen, J. C., Leitner, A. B., Morningstar, S., Marcon, Y., Greinert, J., and Purser, A. (2019). Observations of deep-sea fishes and mobile scavengers from the abyssal DISCOL experimental mining area. *Biogeosciences* 16, 3133–3146. doi: 10.5194/bg-16-3133-2019

Drazen, J. C., Smith, C. R., Gjerde, K. M., Haddock, S. H. D., Carter, G. S., Choy, C. A., et al. (2020). Midwater ecosystems must be considered when evaluating environmental risks of deep-sea mining. *Proc. Natl. Acad. Sci. U.S.A.* 117, 17455–17460. doi: 10.1073/pnas.2011914117

Drazen, J. C., and Sutton, T. T. (2017). Dining in the deep: the feeding ecology of deep-sea fishes. *Ann. Rev. Mar. Sci.* 9, 1–26. doi: 10.1146/annurev-marine-010816-060543

Drazen, J. C., Leitner, A. B., Jones, D. O. B., and Simon-Lledó, E. (2021). Regional variation in communities of demersal fishes and scavengers across the Clarion Clipperton Zone and Pacific ocean. *Front. Mar. Sci.* (in press).

Durden, J. M., Bett, B. J., Jones, D. O. B., Huvenne, V. A. I., and Ruhl, H. A. (2015). Abyssal hills – hidden source of increased habitat heterogeneity, benthic megafaunal biomass and diversity in the deep sea. *Prog. Oceanogr.* 137, 209–218. doi: 10.1016/j.pocean.2015.06.006

Durden, J. M., Bett, B. J., and Ruhl, H. A. (2020). Subtle variation in abyssal terrain induces significant change in benthic megafaunal abundance, diversity, and community structure. *Prog. Oceanogr.* 186:102395. doi: 10.1016/j.pocean.2020.102395

Durden, J. M., Ruhl, H. A., Pebody, C., Blackbird, S. J., and van Oevelen, D. (2017). Differences in the carbon flows in the benthic food webs of abyssal hill and plain habitats. *Limnol. Oceanogr.* 62, 1771–1782. doi: 10.1002/lno.10532

Estes, J. A., Terborgh, J., Brashares, J. S., Power, M. E., Berger, J., Bond, W. J., et al. (2011). Trophic downgrading of planet Earth. *Science* 333, 301–306. doi: 10.1126/science.1205106

Gehlenborg, N. (2019). *UpSetR: A More Scalable Alternative to Venn and Euler Diagrams for Visualizing Intersecting Sets*.

Genin, A. (2004). Bio-physical coupling in the formation of zooplankton and fish aggregations over abrupt topographies. *J. Mar. Syst.* 50, 3–20.

Genin, A., and Dower, J. F. J. (2007). "Seamount plankton dynamics," in *Seamounts: Ecology, Fisheries & Conservation*, eds T. J. Pitcher, T. Morato, P. J. B. Hart, M. R. Clark, N. Haggan, and R. S. Santos (Oxford: Blackwell Publishing), 85–100.

Genin, A., Haury, L., and Greenblatt, P. (1988). Interactions of migrating zooplankton with shallow topography: predation by rockfishes and intensification of patchiness. *Deep Sea Res. Part A* 35, 151–175. doi: 10.1016/0198-0149(88)90034-9

Gollner, S., Kaiser, S., Menzel, L., Jones, D. O. B., Brown, A., Mestre, N. C., et al. (2017). Resilience of benthic deep-sea fauna to mining activities. *Mar. Environ. Res.* 129, 76–101. doi: 10.1016/j.marenvres.2017.04.010

Gove, J. M., McManus, M. A., Neuheimer, A. B., Polovina, J. J., Drazen, J. C., Smith, C. R., et al. (2016). Ocean Oases: near-island biological hotspots in barren ocean basins. *Nat. Commun.* 7, 1–34. doi: 10.1038/ncomms10581

Hanski, I., Zurita, G. A., Bellocq, M. I., and Rybicki, J. (2013). Species-fragmented area relationship. *Proc. Natl. Acad. Sci. U.S.A.* 110, 12715–12720. doi: 10.1073/pnas.1311491110

Harbour, R. P., Leitner, A. B., Ruehlemann, C., Vink, A., and Sweetman, A. K. (2020). Benthic and demersal scavenger biodiversity in the eastern end of the clarion-clipperton Zone – An area marked for polymetallic nodule mining. *Front. Mar. Sci.* 7:458. doi: 10.3389/fmars.2020.00458

Holland, K. N., and Grubbs, R. D. (2007). "Fish visitors to seamounts: tunas and billfish at seamounts," in *Seamounts: Ecology, Fisheries and Conservation*, eds T. J. Pitcher, T. Morato, P. J. B. Hart, M. R. Clark, N. Haggan, and R. S. Santos (Oxford: Blackwell Publishing), 189–206.

Hsieh, T. C., Ma, K. H., and Chao, A. (2016). iNEXT: an R package for rarefaction and extrapolation of species diversity (Hill numbers). *Methods Ecol. Evol.* 7, 1451–1456. doi: 10.1111/2041-210X.12613

Jones, D. O. B., Kaiser, S., Sweetman, A. K., Smith, C. R., Menot, L., Vink, A., et al. (2017). Biological responses to disturbance from simulated deep-sea polymetallic nodule mining. *PLoS One* 12:e0171750. doi: 10.1371/journal.pone.0171750

Kim, S.-S., and Wessel, P. (2011). New global seamount census from altimetry-derived gravity data. *Geophys. J. Int.* 186, 615–631. doi: 10.1111/j.1365-246X.2011.05076.x

Laroche, O., Kersten, O., Smith, C. R., and Goetze, E. (2020). Environmental DNA surveys detect distinct metazoan communities across abyssal plains and seamounts in the western Clarion Clipperton Zone. *Mol. Ecol* 29, 4588–4604. doi: 10.1111/mec.15484

Lavelle, W. J., and Mohn, C. (2010). Motion, commotion, and biophysical connections at deep ocean seamounts. *Oceanography* 23, 90–103. doi: 10.5670/oceanog.2010.64

Leitner, A. B., Durden, J. M., Smith, C. R., Klingberg, E. D., and Drazen, J. C. (2021). Synaphobranchid eel swarms on abyssal seamounts: largest aggregation of fishes ever observed at abyssal depths. *Deep Sea Res. Part I Oceanogr. Res. Pap.* 167:103423. doi: 10.1016/j.dsr.2020.103423

Leitner, A. B., Neuheimer, A. B., and Drazen, J. C. (2020). Evidence for long-term seamount-induced chlorophyll enhancements. *Sci. Rep.* 10, 1–10. doi: 10.1038/s41598-020-69564-0

Leitner, A. B., Neuheimer, A. B., Donlon, E., Smith, C. R., and Drazen, J. C. (2017). Environmental and bathymetric influences on abyssal bait-attending communities of the Clarion Clipperton Zone. *Deep. Res. Part I Oceanogr. Res. Pap.* 125, 65–80. doi: 10.1016/j.dsr.2017.04.017

Linley, T. D., Stewart, A. L., McMillan, P. J., Clark, M. R., Gerringer, M. E., Drazen, J. C., et al. (2017). Bait attending fishes of the abyssal zone and hadal boundary: community structure, functional groups and species distribution in the Kermadec, New Hebrides and Mariana trenches. *Deep Sea Res. Part I Oceanogr. Res. Pap.* 121, 38–53. doi: 10.1016/j.dsr.2016.12.009

Lundblad, E. R., Wright, D. J., Miller, J., Larkin, E. M., Rinehart, R., Naar, D. F., et al. (2006). A benthic terrain classification scheme for American Samoa. *Mar. Geod.* 29, 89–111. doi: 10.1080/01490410600738021

Lutz, M. J., Caldeira, K., Dunbar, R. B., and Behrenfeld, M. J. (2007). Seasonal rhythms of net primary production and particulate organic carbon flux to depth describe the efficiency of biological pump in the global ocean. *J. Geophys. Res.* 112:C10011. doi: 10.1029/2006JC003706

Mcquaid, K. A., Attrill, M. J., Clark, M. R., Cobley, A., Glover, A. G., Smith, C. R., et al. (2020). Using habitat classification to assess representativity of a protected area network in a large, data-poor area targeted for deep-sea mining. *Front. Mar. Sci.* 7, 1–21. doi: 10.3389/fmars.2020.558860

Milligan, R. J., Morris, K. J., Bett, B. J., Durden, J. M., Jones, D. O. B., Robert, K., et al. (2016). High resolution study of the spatial distributions of abyssal fishes by autonomous underwater vehicle. *Sci. Rep.* 6, 1–12. doi: 10.1038/srep26095

Modeler, B. T. (2012). Benthic terrain modeler v3 .0 for ArcGIS 10.x. *ESRI* 2012, 1–14.

Morato, T., Bulman, C., and Pitcher, T. J. (2009). Modelled effects of primary and secondary production enhancement by seamounts on local fish stocks. *Deep Sea Res. Pt. II* 56, 2713–2719.

Morato, T., Hoyle, S. D., Allain, V., and Nicol, S. J. (2010). Seamounts are hotspots of pelagic biodiversity in the open ocean. *Proc. Natl. Acad. Sci. U.S.A.* 107, 9707–9711. doi: 10.1073/pnas.0910290107

Morris, K. J., Bett, B. J., Durden, J. M., Benoist, N. M. A., Huvenne, V. A. I., Jones, D. O. B., et al. (2016). Landscape-scale spatial heterogeneity in phytodetrital cover and megafauna biomass in the abyss links to modest topographic variation. *Sci. Rep.* 6:34080. doi: 10.1038/srep34080

Mullineaux, L. S., and Mills, S. W. (1997). A test of the larval retention hypothesis in seamount-generated flows. *Deep. Res. Part I Oceanogr. Res. Pap.* 44, 745–770. doi: 10.1016/S0967-0637(96)00130-6

Myers, R. A., Baum, J. K., Shepherd, T. D., Powers, S. P., and Peterson, C. H. (2007). Cascading Effects of the Loss of Apex Predatory Sharks from a Coastal Ocean. *Science* 315, 1846–1850. doi: 10.1126/science.1138657

National Oceanic & Atmospheric Administration (NOAA), and National Aeronautics and Space Administration (NASA) (n.d.). *Chlorophyll-a, Aqua MODIS, NPP, 4km, Science Quality, 2003-present (Monthly Composite)*.

Oksanen, J., Blanchet, F. G., Kindt, R., Legendre, P., Minchin, P. R., O'Hara, R. B., et al. (2015). *vegan: Community Ecology Package*.

Pitcher, T. J., Morato, T., Hart, P. J. B., Clark, M. R., Haggan, N., and Santos, R. S. (Eds). (2007). *Seamounts: Ecology, Fisheries and Conservation. Blackwell Fisheries and Aquatic Resources* Vol. 12 (Oxford: Blackwell Publishing).

Polovina, J. J., Abecassis, M., Howell, E. A., and Woodworth, P. (2009). Increases in the relative abundance of mid-trophic level fishes concurrent with declines in apex predators in the subtropical North Pacific, 1996-2006. *Fish. Bull.* 107, 523–531.

Priede, I. (2017). *Deep-Sea Fishes: Biology, Diversity, Ecology and Fisheries*. Cambridge: Cambridge University Press.

Riehl, T., Wölfl, A.-C., Augustin, N., Devey, C. W., and Brandt, A. (2020). Discovery of widely available abyssal rock patches reveals overlooked habitat type and prompts rethinking deep-sea biodiversity. *Proc. Natl. Acad. Sci.* 117, 15450–15459. doi: 10.1073/pnas.1920706117

Rowden, A. A., Dower, J. F., Schlacher, T. A., Consalvey, M., and Clark, M. R. (2010). Paradigms in seamount ecology: fact, fiction and future. *Mar. Ecol.* 31, 226–241. doi: 10.1111/j.1439-0485.2010.00400.x

Rybicki, J., and Hanski, I. (2013). Species-area relationships and extinctions caused by habitat loss and fragmentation. *Ecol. Lett.* 16, 27–38. doi: 10.1111/ele.12065

Schlacher, T. A., Rowden, A. A., Dower, J. F., and Consalvey, M. (2010). Seamount science scales undersea mountains: new research and outlook. *Mar. Ecol.* 31, 1–13. doi: 10.1111/j.1439-0485.2010.00396.x

Simon-Lledó, E., Bett, B. J., Huvenne, V. A. I., Köser, K., Schoening, T., Greinert, J., et al. (2019). Biological effects 26 years after simulated deep-sea mining. *Sci. Rep.* 9, 1–13. doi: 10.1038/s41598-019-44492-w

Smith, C. R., De Leo, F. C., Bernardino, A. F., Sweetman, A. K., and Arbizu, P. M. (2008). Abyssal food limitation, ecosystem structure and climate change. *Trends Ecol. Evol.* 23, 518–528.

Smith, C. R., Tunnicliffe, V., Colaço, A., Drazen, J. C., Gollner, S., Levin, L. A., et al. (2020). Deep-sea misconceptions cause underestimation of seabed-mining impacts. *Trends Ecol. Evol.* 35, 853–857. doi: 10.1016/j.tree.2020.07.002

Verfaillie, E., Doornenbal, P., Mitchel, A. J., White, J., and Van Lancker, V. (2007). *The Bathymetric Position Index (BPI) as a Support Tool for Habitat Mapping, Mapping European Seabed Habitats*. Available online at: http://www.emodnet-seabedhabitats.eu/PDF/GMHM4_Bathymetric_position_index_(BPI).pdf (accessed February 06, 2017).

Vieira, R. P., Coelho, R., Denda, A., Martin, B., Gonçalves, J. M. S., and Christiansen, B. (2018). Deep-sea fishes from Senghor Seamount and the adjacent abyssal plain (Eastern Central Atlantic). *Mar. Biodivers.* 48, 963–975. doi: 10.1007/s12526-016-0548-4

Washburn, T. W., Jones, D. O. B., Wei, C. L., and Smith, C. R. (2021). Environmental heterogeneity throughout the clarion-clipperton zone and the potential representativity of the APEI network. *Front. Mar. Sci.* 8:661685. doi: 10.3389/fmars.2021.661685

Wedding, L. M., Friedlander, A. M., Kittinger, J. N., Watling, L., Gaines, S. D., Bennett, M., et al. (2013). From principles to practice: a spatial approach to systematic conservation planning in the deep sea. *Proc. Biol. Sci.* 280:20131684. doi: 10.1098/rspb.2013.1684

Wedding, L. M., Reiter, S. M., Smith, C. R., Gjerde, K. M., Kittinger, J. N., Friedlander, A. M., et al. (2015). Managing mining of the deep seabed. *Science* 349, 144–145. doi: 10.1126/science.aac6647

Wessel, P. (2001). Global distribution of seamounts inferred from gridded Geosat/ERS-1 altimetry. *J. Geophys. Res.* 106:19431.

Wessel, P., Sandwell, D. T., and Kim, S.-S. (2010). The global seamount census. *Oceanography* 23, 24–33.

Whitaker, D., and Christman, M. (2014). *clustsig: Significant Cluster Analysis*.

Wilson, R. R. Jr., Smith, K. L. Jr., and Rosenblatt, R. H. (1985). Megafauna associated with bathyal seamounts in the central North Pacific Ocean. *Deep Sea Res. Part A. Oceanogr. Res. Pap.* 32, 1243–1254. doi: 10.1016/0198-0149(85)90007-X

Witte, U. (1999). Consumption of large carcasses by scavenger assemblages in the deep Arabian Sea: observations by baited camera. *Mar. Ecol. Prog. Ser.* 183, 139–147. doi: 10.3354/meps183139

Yesson, C., Clark, M. R., Taylor, M. L., and Rogers, A. D. (2011). Deep-sea research I the global distribution of seamounts based on 30 arc seconds bathymetry data. *Deep. Res. Part I* 58, 442–453. doi: 10.1016/j.dsr.2011.02.004

Ziegler, A. F., Cape, M., Lundesgaard, Ø, and Smith, C. R. (2020). Intense deposition and rapid processing of seafloor phytodetritus in a glaciomarine fjord, Andvord Bay (Antarctica). *Prog. Oceanogr* 187:102413. doi: 10.1016/j.pocean.2020.102413

Conflict of Interest: The authors declare that the research was conducted in the absence of any commercial or financial relationships that could be construed as a potential conflict of interest.

Publisher's Note: All claims expressed in this article are solely those of the authors and do not necessarily represent those of their affiliated organizations, or those of the publisher, the editors and the reviewers. Any product that may be evaluated in this article, or claim that may be made by its manufacturer, is not guaranteed or endorsed by the publisher.

Copyright © 2021 Leitner, Drazen and Smith. This is an open-access article distributed under the terms of the Creative Commons Attribution License (CC BY). The use, distribution or reproduction in other forums is permitted, provided the original author(s) and the copyright owner(s) are credited and that the original publication in this journal is cited, in accordance with accepted academic practice. No use, distribution or reproduction is permitted which does not comply with these terms.

frontiers in Marine Science

ORIGINAL RESEARCH
published: 25 August 2021
doi: 10.3389/fmars.2021.656899

Diversity of Deep-Sea Scale-Worms (Annelida, Polynoidae) in the Clarion-Clipperton Fracture Zone

Paulo Bonifácio[1,2]*, *Lenka Neal*[3] *and Lénaïck Menot*[2]

[1] *Independent Researcher, Brest, France,* [2] *Ifremer, Centre Bretagne, REM EEP, Laboratoire Environnement Profond, Plouzané, France,* [3] *The Natural History Museum, London, United Kingdom*

The polymetallic nodules lying on the seafloor of the Clarion-Clipperton Fracture Zone (CCFZ) represent over 30 billion metric tons of manganese. A single mining operation has potential to directly impact approximately 200 km^2 of the seabed per year. Yet, the biodiversity and functioning of the bentho-demersal ecosystem in the CCFZ remain poorly understood. Recent studies indicate a high species diversity in a food-poor environment, although the area remains poorly sampled. Undersampling is aggravated by a combination of low densities of fauna and high habitat heterogeneity at multiple spatial scales. This study examines the Polynoidae, a diverse family of mobile polychaetes. Sampling with an epibenthic sledge and a remotely operated vehicle was performed during the cruise SO239 within the eastern CCFZ. Five areas under the influence of a sea surface productivity gradient were visited. Specimens were identified using morphology and DNA: (i) to provide a more comprehensive account of polynoid diversity within the CCFZ, (ii) to infer factors potentially driving alpha and beta diversity, and (iii) to test the hypothesis that epibenthic polychaetes have low species turnover and large species range. Patterns of species turnover across the eastern CCFZ were correlated with organic carbon fluxes to the seafloor but there was also a differentiation in the composition of assemblages north and south of the Clarion fracture. In contrast to the previous studies, patterns of alpha taxonomic and phylogenetic diversity both suggest that polynoid assemblages are the most diverse at Area of Particular Environmental Interest no. 3, the most oligotrophic study site, located north of the Clarion fracture. Without ruling out the possibility of sampling bias, the main hypothesis explaining such high diversity is the diversification of polynoid subfamily Macellicephalinae, in response to oligotrophy. We propose that macellicephalins evolved under extremely low food supply conditions through adoption of a semi-pelagic mode of life, which enabled them to colonise new niches at the benthic boundary layer and foster their radiation at great depths.

Keywords: diversity and distribution, Clarion-Clipperton Fracture Zone, nodule province, scale-worms, Polychaeta, diversification

OPEN ACCESS

Edited by:
Erica Goetze,
University of Hawai'i at Mânoa,
United States

Reviewed by:
Gustavo Fonseca,
Federal University of São Paulo, Brazil
Pat Hutchings,
Australian Museum, Australia

***Correspondence:**
Paulo Bonifácio
bonif@me.com

Specialty section:
This article was submitted to Deep-Sea Environments and Ecology, a section of the journal Frontiers in Marine Science

Received: *21 January 2021*
Accepted: *19 July 2021*
Published: *25 August 2021*

Citation:
Bonifácio P, Neal L and Menot L (2021) Diversity of Deep-Sea Scale-Worms (Annelida, Polynoidae) in the Clarion-Clipperton Fracture Zone. Front. Mar. Sci. 8:656899. doi: 10.3389/fmars.2021.656899

INTRODUCTION

Polymetallic nodules are potato-shaped structures varying in size and mineral concentration, and patchily distributed on the seafloor (Morgan, 2000). They are mainly composed of manganese and iron, but also copper, nickel, and cobalt (Hein and Petersen, 2013). The Clarion-Clipperton Fracture Zone (CCFZ), an area of ca. 6 million km^2 of seabed in the central Pacific, has attracted increasing commercial interest. This largest polymetallic nodule field in the world sits between 4000 and 6000 m depth. The CCFZ potentially holds 34 billion metric tons of manganese, representing at least 25 trillion USD (Morgan, 2000; Volkmann et al., 2018). This area is managed by the International Seabed Authority (ISA), which issues exploration mining contracts. To date, 18 such contracts have been signed with the latest one in 2021 (International Seabed Authority, 2021). When moving from exploration to exploitation, a single mining operation could directly impact 182 km^2 year^{-1} of seafloor to achieve a production of 2 Mt annually, while sediment plume re-deposition might indirectly increase the footprint of mining by a factor of two to five (Oebius et al., 2001; Glover and Smith, 2003; Volkmann and Lehnen, 2018). The ISA has approved a regional management plan that has designated nine zones each measuring 400 × 400 km, known as Areas of Particular Environmental Interest (APEIs). Such areas are protected from the mining activities and expected to be representative of the full range of biodiversity, ecosystem structure, and habitats within the management area (Lodge et al., 2014). These nine APEIs are located at the periphery of the CCFZ, however, their location is currently not completely supported by the scientific data. Unsupervised classification of benthic habitats based on derivatives of the GEBCO bathymetry, particulate organic carbon (POC) fluxes estimated from satellite data and nodule abundances derived from low-resolution kriging suggested that habitats in the network of APEIs are not fully representative of habitats within mineable areas (McQuaid et al., 2020). To provide quality knowledge for management and conservation strategies, we need to better constrain habitat distribution models, which in turn requires enhanced comprehension of the factors determining biodiversity patterns.

The CCFZ is a heterogeneous environment composed of abundant hills (approximately 200 m high), numerous seamounts, and nodule fields, which may explain why biodiversity appears to be richer than previously thought (Smith et al., 2008; Wedding et al., 2013; Glover et al., 2016). For example, a megafauna diversity assessment within APEI no. 6 found 129 morphospecies in a survey covering 15,840 m^2 of seabed. Changes in assemblage composition were associated with variations in geomorphology and nodule abundance (Simon-Lledó et al., 2019). Beyond species restricted to hard substrates, the presence of nodules may also increase the diversity of macro-infauna at a local scale (De Smet et al., 2017; Bonifácio et al., 2020; Chuar et al., 2020). On a regional scale, northward and westward gradients of decreasing primary productivity are important drivers of variations in meiofaunal and macrofaunal community structure (Hauquier et al., 2019; Bonifácio et al., 2020). The structure of megafaunal assemblages is also highly variable at a 100-km scale although the influence of productivity gradients is not as clear (Simon-Lledó et al., 2020).

Understanding the ecology of benthic communities in the CCFZ is however still impaired by the incomplete diversity assessment. For polychaetes, a species-rich group at abyssal depths representing 36–55% of total macrofaunal abundances (Hessler and Jumars, 1974; Hecker and Paul, 1979; De Smet et al., 2017; Chuar et al., 2020), the incomplete species inventories can be attributed to undersampling, species lumping and sampling inaccuracy. Undersampling is visible at all scales. At local scale, the species rarefaction curve did not level off after extensive sampling of 54 box-cores at Domes A in the western and most oligotrophic site of the CCFZ (Wilson, 2017; Washburn et al., 2021). In the eastern CCFZ, a total of 30 box-cores across four contract zones and one APEI yielded 275 species of which 49% were singletons (Bonifácio et al., 2020). Moreover, most polychaete species remain undescribed (only 5–10% of collected polychaete species were identified to named species; Glover et al., 2002) and the recent combination of morphological and molecular criteria to delineate species suggests that morphology significantly underestimates the magnitude of biodiversity (Janssen et al., 2015; Bonifácio and Menot, 2018). Sampling needs to be more comprehensive because polychaetes encompass a large range of sizes and life modes, from minute infaunal to large epibenthic and commensal species (Hutchings, 1998). In the CCFZ, polychaete assemblages are sampled with a box core, in accordance with the recommendations issued by the ISA (ISBA/25/LTC/6/Rev.1, International Seabed Authority, 2020). While macro-infaunal polychaetes are quantitatively and accurately sampled with a box core (Hessler and Jumars, 1974), large epifaunal and commensal species are not. Such groups are better targeted by trawls and epibenthic sledges (EBS). Among the poorly sampled polychaetes, EBS samples showed that the family Polynoidae is a highly diverse yet poorly studied group at abyssal depths (Schüller et al., 2009; Guggolz et al., 2018; Bonifácio and Menot, 2018).

Of all polychaetes, Polynoidae is one of the most diverse families, both in the number of genera and species (868 valid species; Read and Fauchald, 2021). Polynoids belong to a group of organisms called scale-worms (Aphroditiformia), distinguishable by their scale-like dorsal elytra. Of the eight subfamilies of Polynoidae recognised by Bonifácio and Menot (2018) and followed in this study, the subfamily Macellicephalinae appears to be restricted to the deep sea, the deep Antarctic shelf, and submarine caves (Pettibone, 1985b; Neal et al., 2018b; Bonifácio and Menot, 2018). In a census of deep-sea polychaete species, Paterson et al. (2009) counted 91 polynoid species (12% of total polychaete records) below 2000 m depth with 15 polynoid species below 4000 m depth (hadal depths), 13 of these belonging to Macellicephalinae, including the deepest known polynoid found at 10,190 m depth (Kirkegaard, 1956). According to Bonifácio and Menot (2018), the subfamily Macellicephalinae forms a monophyletic group characterized by the loss of the lateral antennae compared to other polynoid subfamilies, which bear two lateral and one median antennae. Within the Macellicephalinae, which currently contains 121 species (Read and Fauchald, 2021), a monophyletic clade of 15 species, the

so-called Anantennata clade, also lost the median antenna. Macellicephalins seem to have been particularly successful in colonizing and radiating in the deep sea (Uschakov, 1982; Levenstein, 1984; Bonifácio and Menot, 2018). Numerous genera are endemic to deep-sea chemosynthetic ecosystems such as hydrothermal vents and cold seeps (Pettibone, 1983; Chevaldonné et al., 1998; Hatch et al., 2020), whereas others were successful in colonizing pelagic deep-sea, nodule fields, abyssal depths, and even trenches (Pettibone, 1976, 1985a,b; Bonifácio and Menot, 2018). Predating the discovery of hydrothermal vents, Levenstein (1984) studied macellicephalin distribution around the world and pointed out that the Pacific Ocean hosts a high rate of diversity with 21 of the 40 species (known at that time) and 15 endemic species.

From EBS and remotely operated vehicle (ROV) samples collected during the SO239 cruise across the eastern half of the CCFZ (Martínez Arbizu and Haeckel, 2015), Bonifácio and Menot (2018) described 17 new polynoid species, of which 16 were macellicephalins, with many remaining undescribed. In the present study, we aim to provide a more comprehensive account of polynoid diversity within the CCFZ and improve our understanding of macellicephalin species radiation in the deep sea. Additionally, we aim to further test hypotheses regarding the drivers of species turnover in the CCFZ. Based on quantitative box-core sampling, Bonifácio et al. (2020) showed a high species turnover among infaunal polychaete assemblages across the eastern CCFZ, attributing it to variations in trophic inputs and barriers to dispersal. In particular, the Clarion fracture was hypothesized to limit dispersal between the APEI no. 3 to the north and the core of the CCFZ to the south. Dispersal ability has also been advocated as a driver of differential distribution patterns between polychaete and isopods as well as among isopod families in the CCFZ (Janssen et al., 2015, 2019; Brix et al., 2020). By focusing on polynoids, we aspired to test whether mobile epifaunal polychaetes would show lower species turnover and greater species ranges than the more sedentary infaunal polychaete assemblages.

MATERIALS AND METHODS

Clarion-Clipperton Fracture Zone

Within the Equatorial Pacific Ocean, the CCFZ is bordered by the Clarion fracture to the north, the Clipperton Fracture to the south, the Kiribati islands to the west, and Mexico to the east (**Figure 1**). As part of the JPI Oceans project "Ecological aspects of deep-sea mining," the EcoResponse cruise SO239 on board the *RV* Sonne covered the eastern part of the CCFZ from March 9 to April 30, 2015 (Martínez Arbizu and Haeckel, 2015). Sampling took place within four exploration contract areas and the APEI no. 3 at water depths ranging from 4000 to 5000 m (**Figure 1**). While the ISA administers the APEIs, the exploration contracts were issued by ISA to the Federal Institute for Geosciences and Natural Resources of Germany (BGR); the InterOceanMetal Joint Organization (IOM); the G-TEC Sea Mineral Resources NV (GSR); and the Institut Français de Recherche pour l'Exploitation de la Mer (Ifremer). Only 243 km of distance separates BGR and IOM areas whereas 1440 km separates BGR and Ifremer or APEI no. 3.

Sampling Strategy

The overarching aim of the sampling strategy was to cover the whole range of biodiversity of benthic communities, crossing all faunal size groups (from meio- to megafauna) and habitats (from soft-sediments with no nodules to basalt on seamounts). A variety of methods were used to collect biological samples from large and qualitative EBS samples to smaller and quantitative box-core samples and targeted samples with a ROV.

The EBS (Brenke, 2005) consists of a supra- and epibenthic net with cod ends of 300 μm each and an opening and closing mechanism. A total of 12 EBS were recovered but only eight were fully examined (**Table 1**). The ROV Kiel 6000 fitted with various sampling tools was also used to recover benthic macrofauna (**Figure 1**). One of the features employed was the bio-box, a large box in which megafaunal specimens collected with the manipulator arm were stored. The United States Naval Electronics Laboratory (USNEL) spade box corer of 0.25 m^2 (Hessler and Jumars, 1974) is proven to be an accurate and quantitative tool for benthic biological studies.

Polynoids were recovered from box corer and EBS deployments, as well as from the ROV bio-box. Polynoids were not intentionally sampled using the ROV but were most likely associated with the collected sponges or corals. Once on board, the megafauna specimens were sorted from the bio-box and the water was sieved through a 300 μm mesh in a cold room (full methods in Martínez Arbizu and Haeckel, 2015). Polynoids were sorted from the sieved residues.

Sieving and sorting were performed on board. The samples were maintained in cold seawater (4°C) and sieved through a 300 μ mesh in a cold room. All specimens from ROV sampling and some specimens from box corer and EBS sampling were sorted alive. The upper 10 cm of the box-core sample was sliced into three layers (0–3, 3–5, and 5–10 cm), the first was sieved on board in the cold room with cold seawater (4°C) whereas the deeper layers were fixed in formalin for 48–96 h, preserved in 96% ethanol and sorted back on land (for detailed processing of box corer sampling, see Bonifácio et al., 2020). Sieving residues from the EBS samples were preserved in 96% ethanol at −20°C. The ethanol was changed after 24–48 h and the sieved residues were then sorted on board under ice. The collected polychaetes were fixed/preserved in cold (−20°C) 80% ethanol and stored at −20°C. In the laboratory (on land), a few parapodia or small pieces of tissue were dissected, preserved in cold 96% ethanol, and stored at −20°C for molecular extraction.

Molecular Methods

Briefly, the DNA was extracted from sampled tissues using a NucleoSpin Tissue kit (Macherey-Nagel). Two mitochondrial genes (i.e., COI, cytochrome c oxidase subunit I; and 16S) and one nuclear gene (18S) were amplified using the following primers: polyLCO, polyHCO, LCO1490, and HCO2198 for COI (Folmer et al., 1994; Carr et al., 2011); Ann16SF and 16SbrH

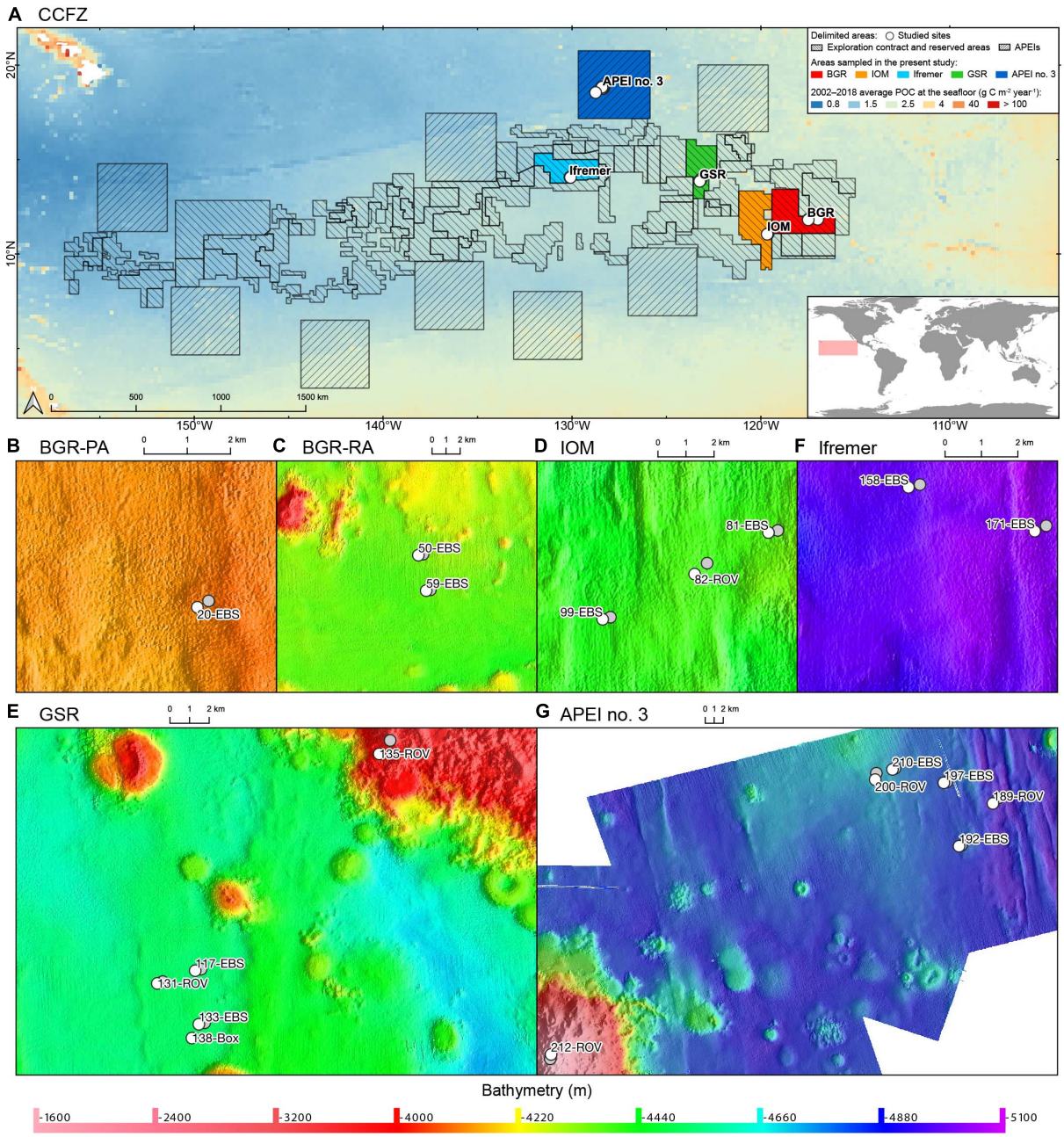

FIGURE 1 | (A) Map of the nodule exploration contract areas, reserved areas and Areas of Particular Environmental Interest (APEIs) in the Clarion-Clipperton Fracture Zone (CCFZ) showing the sampled areas (in color). The background map shows the average particulate organic carbon (POC) flux at the seafloor during the 2002–2018 period estimated by Bonifácio et al. (2020). The sampled areas are enlarged in the following panels: BGR **(B,C)**, IOM **(D)**, GSR **(E)**, Ifremer **(F)** and APEI no. 3 **(G)**, with start positions in white and end positions in grey. Each has a detailed local hydro-acoustic map based on the multibeam system EM122 (Martínez Arbizu and Haeckel, 2015; Greinert, 2016) in the background.

for 16S (Palumbi, 1996; Sjölin et al., 2005); and 18SA, 18SB, 620F, and 1324R for 18S (Medlin et al., 1988; Cohen et al., 1998; Nygren and Sundberg, 2003) for 18S. The polymerase chain reaction (PCR) mixtures were prepared as suggested for the Green GoTaq® by the manufacturers. The profile of temperature was as follows: 95°C/240 s – [94°C/30 s – 52°C/60 s – 72°C/75 s (for COI and 16S) or 180 s (for 18S) for 35 cycles (for 16S or 18S) or for 40 cycles (for COI)] – 72°C/480 s. PCR products which resulted in bands of expected size after electrophoresis on 1% agarose gel, were sent to the MacroGen Europe Laboratory in Amsterdam (Netherlands) to be sequenced with the same set of primers.

Overlapping sequence fragments (forward and reverse) were assembled into consensus sequences using Geneious Pro 8.1.7

TABLE 1 | Details of sampling sites, total number of polynoid specimens (ind., individuals), and number of polynoid species collected from epibenthic sledges (EBS), box corer, and ROV deployments across the eastern Clarion-Clipperton Fracture Zone during the SO239 cruise.

Area – locality	Station	Date (dd/mm/yyyy)	Depth (m)	Sampling start latitude	Sampling start longitude	Sampling end latitude	Sampling end longitude	Trawling distance (m)	Number of specimens (ind. gear^{-1})	Total species (taxa gear^{-1})
EBS									**Per EBS**	**Per EBS**
BGR-PA	20	21/03/2015	4144–4093	11.83717	−116.982	11.8385	−116.97967	2769	11	9
BGR-RA	50	26/03/2015	4360–4328	11.83117	−117.4915	11.83183	−117.4885	2469	1	1
BGR-RA	59	28/03/2015	4384–4307	11.8085	−117.4865	11.809	−117.48383	2469	2	2
IOM	81*	1/04/2015	4365–4346	11.07083	−119.60783	11.0715	−119.60483	2739	31	15
IOM	99*	4/04/2015	4398–4402	11.043	−119.661	11.04367	−119.6585	2529	23	16
GSR	117*	7/04/2015	4498–4521	13.879	−123.23317	13.87967	−123.2305	3129	54	15
GSR	133*	10/04/2015	4516–4427	13.8545	−123.2315	13.85517	−123.22883	2289	19	9
Ifremer	158*	15/04/2015	4946–4976	14.06283	−130.11083	14.0635	−130.108	3789	30	16
Ifremer	171*	17/04/2015	5024–5017	14.052	−130.07967	14.05333	−130.07683	2979	6	4
APEI no. 3	192*	21/04/2015	4821–4820	18.75417	−128.3425	18.755	−128.34017	2799	47	33
APEI no. 3	197*	22/04/2015	4805–4823	18.81717	−128.35767	18.818	−128.35467	2529	29	22
APEI no. 3	210	24/04/2015	4700–4740	18.8305	−128.40867	18.8315	−128.40617	3399	3	2
Total									256	89
ROV									**Per ROV dive**	**Per ROV dive**
IOM	82	1–2/04/2015	4347	11.0575	−119.6315	11.061	−119.6275	–	1	1
GSR	131	9–10/04/2015	4478	13.87317	−123.2505	13.874	−123.248	–	1	1
GSR	135	10–11/04/2015	3593	13.97817	−123.149	13.98433	−123.144	–	2	2
APEI no. 3	189	20–21/04/2015	4931	18.79667	−128.30883	18.80217	−128.30333	–	10	3
APEI no. 3	200	22–23/04/2015	4672	18.82033	−128.42583	18.82667	−128.42467	–	1	1
APEI no. 3	212	24–25/04/2015	1844	18.54717	−128.748	18.54283	−128.74883	–	8	2
Total									23	6
Box corer									**Per box core**	**Per box core**
GSR	138	11/04/2015	4503	13.84817	−123.23467	–	–	–	1	1

Asterisk indicates fully processed EBS samples.

2005–2015 (Biomatters Ltd.). For COI, the sequences were translated into amino-acid alignments and checked for stop codons to avoid pseudogenes.

Newly assembled sequences were blasted in GenBank to check for contamination. Each set of genes was aligned separately using: MAAFT (Katoh et al., 2002) for 16S and 18S; and MUSCLE (Edgar, 2004) for COI. All sequences obtained in this study have been deposited in BOLD[1] (Ratnasingham and Hebert, 2007) or GenBank[2].

Integrative Taxonomy

The specimens were examined under a Leica M125 stereomicroscope and a Nikon Eclipse E400 microscope. Only the specimens with heads were counted and morphologically identified using deep-sea polynoid fauna bibliography (Pettibone, 1976; Uschakov, 1982; Bonifácio and Menot, 2018), to the lowest taxonomic level possible (morphospecies). The naming of morphospecies is consistent with previous studies (Bonifácio and Menot, 2018; Bonifácio et al., 2020). Naming refers to the Ifremer code of the specimen, which served as a reference for morphological characters defined in the diagnosis of the morphospecies (similar to *type material*). For specimens that could not be morphologically discriminated, the principle of the phylogenetic species concept was applied. Through this approach, the genetic divergence among specimens belonging to the same species (intraspecific) is smaller than the divergence among specimens from different species (interspecific) (Hebert et al., 2003b). This creates a gap between intraspecific and interspecific variations when plotted in a distribution of pairwise divergences among all sequences. When data were insufficient to define a barcode gap, molecular operational taxonomic units (MOTUs) were recognised using a threshold of 97 or 99% similarity between COI and 16S sequences, respectively (Hebert et al., 2003a,b). Hereafter, for the sake of simplicity, we use the term species to refer to the lowest taxonomic resolution achieved by using this combination of morphospecies and MOTU concepts.

Environmental Data

The environmental data used are those compiled by Bonifácio et al. (2020) from previous studies (Volz et al., 2018a; Hauquier et al., 2019) which are publicly available (Hauquier et al., 2017; Volz et al., 2018b,c,d,e,f,g). Sediment samples were recovered from the same areas as biological samples during the same cruise, using a multi-corer or a gravity corer (see Martínez Arbizu and Haeckel, 2015 for details). Hauquier et al. (2019) reported

[1]http://www.boldsystems.org

[2]https://www.ncbi.nlm.nih.gov/genbank/

data for clay fraction (<4 μm), silt fraction (4–63 μm), total nitrogen (TN in weight per cent), total organic carbon (TOC in weight per cent), and chloroplastic pigment equivalents (CPE in μg ml^{-1}). Volz et al. (2018a) reported POC flux (POC, mg C m^{-2} d^{-1}) at the seafloor for all areas (eastern CCFZ). This POC flux at the seafloor was used as a proxy for food supply to benthic communities.

Data Analysis

Phylogenetic Analyses

Maximum likelihood and Bayesian phylogenetic analyses were run for two datasets. The first dataset included all 428 sequences (COI, 16S, and 18S) from 238 specimens collected by all types of gear from all study sites. Two sigalionids [*Neoleanira tetragona* (Örsted, 1845) and *Sthenelais boa* (Johnston, 1833)] were chosen as outgroups. The phylogenetic analyses aimed at providing a comprehensive account of known polynoid diversity in the eastern CCFZ. The second dataset was limited to specimens collected from the fully processed EBS samples and included 156 sequences (COI, 16S, and 18S) from 81 species. *N. tetragona* was used as an outgroup. The phylogenetic analyses were run to compute phylogenetic diversity indices (see below).

The three genes were combined in a partitioned dataset with SequenceMatrix (Vaidya et al., 2011). The maximum likelihood analyses were carried out using Randomized Axelerated Maximum Likelihood (RAxML v.8.2.10; Stamatakis, 2014) on XSEDE with rapid bootstrapping (1000 iterations). The Bayesian phylogenetic analyses were achieved using MrBayes v.3.2.6 on XSEDE (Ronquist et al., 2012) with 60,000,000 generations in which every 1000 generation chain was sampled and 25% discarded as burn-in. TRACER v.1.7.1 (Rambaut et al., 2018) was used to check the convergence chain runs. Both phylogenetic analyses were computed in CIPRES Science Gateway (Miller et al., 2010). Node support is given as a maximum likelihood bootstrap and Bayesian posterior probability values. The tree files were plotted using RStudio environment or FigTree v.1.4.2[3].

Alpha and Beta Phylogenetic Diversity (PD)

Phylogenetic diversity was assessed using Faith's PD (Faith, 1992). PD is the most widely used phylogenetic diversity measure and is defined as the sum of branch lengths of a phylogenetic tree connecting all species in a given assemblage. Similar to species richness, Faith's PD is also dependent on sample size and inventory completeness (Hsieh and Chao, 2017). We thus used sample-size-based rarefaction and extrapolation curves to compare PD between polynoid assemblages (Hsieh and Chao, 2017). Extrapolations were computed for a sample twice the size of the empirical sample. The 95% confidence intervals were computed using a bootstrap method with 200 replications. For PD, the phylogenetic ultrametric tree was pruned to only reflect species with at least one sequence present in the entire dataset (i.e., without outgroup species or specimens without a sequence).

Unweighted (presence/absence) UniFrac metric (Lozupone et al., 2006) was computed to assess beta phylogenetic diversity between assemblages. The metric measures the difference between assemblages based on the unique branch length (branch leading to another tip in the same sample) over the total branch length observed among assemblages. UniFrac metric ranges from 0 (i.e., no unique branch, all the terminals on the tree are shared among all assemblages) to 1 (i.e., only unique branches, the terminals leading to another tip are not shared between assemblages). Ordination of samples based on UniFrac distance metric was performed using Principal Coordinate Analysis (PCoA; Gower, 1966). PCoA, also known as metric multidimensional scaling, is an ordination method similar to PCA but that can handle semimetric and non-metric dissimilarity measures (Borcard et al., 2018). Furthermore, a correlation between UniFrac distance and geographical distance was sought to test for a distance decay of phylogenetic similarity between polynoid assemblages. The UpSet plots were used to illustrate the distribution of rare, widely distributed and common species across the CCFZ. Haplotype networks were constructed considering the infinite site model and a pairwise uncorrected distance between mitochondrial (COI or 16S genes) haplotypes, and the quantitative distribution of haplotypes within putative populations (sampling site).

Alpha and Beta Taxonomic Diversity

Diversity patterns were analysed using rarefaction curves based on the total number of individuals from fully examined EBS samples (Hurlbert, 1971; Gotelli and Colwell, 2001). Based on this rarefied dataset, the expected number of species was calculated for 12 (ES12) and 35 (ES35) individuals for comparison with previous studies. Non-parametric and abundance-based estimators included Chao1 and an abundance-based coverage estimator (ACE; O'Hara, 2005; Chiu et al., 2014).

A Hypergeometric Principal Component Analysis (H-PCA) was used to describe variations in assemblage composition between fully examined EBS samples. The H-PCA relies on Chord-Normalized Expected Species Shared (CNESS) distance (Trueblood et al., 1994; Gallagher, 1999), which is computed from probabilities of species occurrence in random draws of m individuals. The CNESS distance thus allows rarefying samples to a similar number of individuals, limiting the bias due to different sample sizes. Low values of m give high weight to dominant species whereas high values of m give high weight to rare species. To choose the value of m, distance matrices are computed for all possible values of m, then Kendall's τ correlations are calculated between each of these matrices and both matrices for $m = 1$ and $m = m$ max (minimum sample total). The value of m used for calculation is the one that gives correlation with CNESS $m = 1$ which is roughly equivalent to its correlation with CNESS $m = m$ max. The CNESS distance, which provides an objective trade-off between giving weight to either dominant or rare species was preferred over the Euclidean distance classically used in PCA, which gives high weight to abundant species, and a Chi-square distance classically used in Correspondence Analysis that gives high weight to rare species (Legendre and Gallagher, 2001). CNESS is also a metric distance, which contrary to semimetrics such as the Bray–Curtis dissimilarity, respects the relative distance between samples and can be plotted in the Euclidean space of a PCA. The influence of environmental

[3]http://tree.bio.ed.ac.uk/software/figtree/

variables on assemblage patterns was explored by fitting clay fraction, silt fraction, TN, TOC, CPE, and POC flux at the seafloor onto the PCA ordination (*envfit* function in R library Vegan). The accuracy of fit of each variable was tested with a permutation test (n = 999). This *post hoc* explanation of ordination axes was preferred over a constrained multivariate analysis such as a Redundancy Analysis (RDA). RDA involves multiple linear regressions of species abundance data, but our data are not truly quantitative. For comparison with previous studies and to evaluate the distance decay of taxonomic similarity between assemblages, the New Normalized Expected Species Shared (NNESS; Trueblood et al., 1994; Gallagher, 1999) was also computed. NNESS is a similarity measure, which as for CNESS is computed on rarefied samples (Trueblood et al., 1994; Gallagher, 1999).

All analyses were conducted with R language (R Core Team., 2020) using RStudio (R Studio Team., 2020) and the following specific packages or functions: adespatial (Dray et al., 2020), ade4 (Dray and Dufour, 2007), ape (Paradis and Schliep, 2019), BiodiversityR (Kindt and Coe, 2005), Biostrings (Pagès et al., 2017), dplyr (Wickham et al., 2020), fossil (Vavrek, 2011), geiger (Pennell et al., 2014), ggplot2 (Wickham, 2016), ggtree (Yu et al., 2017), iNextPD (Hsieh and Chao, 2017), ness (Menot, 2019), pegas (Paradis, 2010), picante (Kembel et al., 2010), reshape2 (Wickham, 2007), treeio (Wang et al., 2020), UpSetR (Conway et al., 2017), and vegan (Oksanen et al., 2016).

RESULTS

Diversity and Distribution

A total of 280 polynoid specimens were sampled along the five areas studied within the eastern CCFZ, of which 256 specimens were collected with the EBS, 23 with the ROV and one from a box-core sample (**Tables 1**, **2**). The combination of morphological examination and DNA sequencing enabled the identification of all but five poorly preserved specimens for which DNA sequencing was unsuccessful. The success rate of the DNA sequencing varied according to the targeted genes. COI sequences were obtained from 136 specimens, 16S sequences from 217 specimens, and 18S sequences from 68 specimens. Collectively, 238 specimens were successfully sequenced for at least one of the targeted genes (**Figure 2**) while 38 specimens were sequenced for all three genes and 107 specimens were sequenced for at least two of the studied genes.

The identified polynoids (275 specimens) accounted for 95 species belonging to the subfamilies Eulagiscinae, Polynoinae, and Macellicephalinae (**Figure 2** and **Table 2**). Eulagiscinae was represented by nine specimens belonging to the same species, *Bathymoorea lucasi*, which was found only at APEI no. 3. Polynoinae was represented by 12 specimens belonging to two species (*Harmothoe* sp. 207 and *Harmothoe* sp. 414) found at BGR, IOM, GSR and Ifremer areas (**Figure 2**). Macellicephalinae was the most abundant and diverse group with 259 specimens (92.5% of total number of specimens) belonging to 92 species (**Figure 2** and **Table 2**). Within Macellicephalinae, a clade called Anantennata was also abundant and surprisingly very diverse with 65 specimens belonging to 42 species (**Figure 2**). Anantennata corresponded to 25.1% of the total number of specimens and 45.6% of the total number of macellicephalin species. Of the 11 genera identified, the following were the most abundant (>10% of the total number macellicephalin specimens) and/or diverse: *Macellicephala* with 77 specimens (29.7%) and 11 species; *Polaruschakov* with 38 specimens (14.7%) and 24 species; *Macellicephaloides* with 37 specimens of *Macellicephaloides moustachu*; and *Bathyfauvelia* with 35 specimens (13.5%) and nine species. The most abundant species was *Macellicephala* sp. 180 with 45 specimens (16.1% of the total number of polynoid specimens). The identification of 38 specimens (29 species) remained incomplete due to poor conservation or no fit within currently recognised genera. Eight specimens probably belong to new genera and 21 were identified at least as Anantennata.

The UpSet plot (**Figure 3**) shows that 74 species were restricted to only one area with 59 species represented by a single specimen (**Table 2**). These singletons accounted for 62.1% of the total number of species and 21.1% of the total number of polynoid specimens. Seventeen species were sampled at two or three areas whereas only five species were recovered from four areas. No species was common to all five studied areas. APEI no. 3 was the most species-rich zone, with 55 species in total, of which 80% were unique to this site, a percentage that drops to a maximum of 52.7% for the other sites within the CCFZ. Interestingly, the two most abundant species *Macellicephala* sp. 180 and *Macellicephaloides moustachu* together representing 29% of the total number of specimens were widely distributed in all areas except APEI no. 3.

The relationships among DNA sequences within putative populations were explored for two relatively abundant and widely distributed species. The haplotype networks for *Bathyfauvelia* sp. 224 and *Macellicephala* sp. 180 based on sampled sites (putative populations) showed relatively high numbers of haplotypes separated mostly by one or a few mutational steps (**Figure 4**). The data did not show phylogeographic structure.

Polynoidae Assemblages

The structure of polynoid assemblages was analysed from eight fully processed EBS samples from IOM, GSR, Ifremer, and APEI no. 3 areas totalling 239 specimens (**Table 1**). The proportion among subfamilies varied among the sites (**Figure 5**). The subfamily Macellicephalinae was dominant while the subfamily Polynoinae was represented by a few specimens at IOM, GSR, and Ifremer areas. Within the subfamily Macellicephalinae, the proportion of the Anantennata group (Macellicephalinae without median antenna) showed a two to fivefold increase at APEI no. 3.

Taxonomic Diversity

Of the 239 specimens, 234 were identified to species (**Table 3**). In the case of five poorly preserved specimen, DNA sequencing was not successful, preventing any identification. Based on an integrative taxonomy, 84 species were recognised. The total number of species showed high variability between areas and

TABLE 2 | Species list and total number of specimens per study area of Polynoidae sampled during the SO239 cruise in the eastern Clarion-Clipperton Fracture Zone.

	BGR	IOM	GSR	Ifremer	APEI no. 3	Total		BGR	IOM	GSR	Ifremer	APEI no. 3	Total
Macellicephalinae Hartman-Schröder, 1971	**10**	**46**	**64**	**24**	**50**	**194**	**Anantennata macellicephalins**	**2**	**6**	**8**	**10**	**39**	**65**
Abyssarya acus Bonifácio and Menot, 2018					4	4	*Bathyedithia retierei* Bonifácio and Menot, 2018				1		1
Bathyeliasona mariaae Bonifácio and Menot, 2018	1		1	1	1	4	*Hodor anduril* Bonifácio and Menot, 2018					2	2
Bathyfauvelia glacigena Bonifácio and Menot, 2018		1	4	1		6	*Hodor hodor* Bonifácio and Menot, 2018					1	1
Bathyfauvelia ignigena Bonifácio and Menot, 2018		1	1		3	5	*Hodor* sp. 666-2		1			3	4
Bathyfauvelia sp. 224		3	2	2	3	10	*Nu aakhu* Bonifácio and Menot, 2018			1			1
Bathyfauvelia sp. 225	1	3	2			6	*Polaruschakov lamellae* Bonifácio and Menot, 2018	1				2	3
Bathyfauvelia sp. 626					1	1	*Polaruschakov limaae* Bonifácio and Menot, 2018				1		1
Bathyfauvelia sp. 636-5-2				1	2	3	*Polaruschakov omnesae* Bonifácio and Menot, 2018		1	1			2
Bathyfauvelia sp. 636-5-3				1	1	2	*Polaruschakov* sp. 211	1					1
Bathyfauvelia sp. 666-1-3					1	1	*Polaruschakov* sp. 219		1				1
Bathyfauvelia sp. 698					1	1	*Polaruschakov* sp. 315		1	1			2
Bathypolaria sp. 173	1	1	1			3	*Polaruschakov* sp. 343			2			2
Bathypolaria sp. 608					6	6	*Polaruschakov* sp. 514				1		1
Bruunilla nealae Bonifácio and Menot, 2018				1		1	*Polaruschakov* sp. 615					2	2
Bruunilla sp. 651					1	1	*Polaruschakov* sp. 636-4-2				1		1
Bruunilla sp. 659-8					3	3	*Polaruschakov* sp. 636-4-3				1		1
Bruunilla sp. 664					1	1	*Polaruschakov* sp. 639-2				1		1
Bruunilla sp. 668-1					1	1	*Polaruschakov* sp. 642				1		1
Bruunilla sp. 668-2					1	1	*Polaruschakov* sp. 655-3-1					2	2
Bruunilla sp. 692					1	1	*Polaruschakov* sp. 655-3-4					1	1
Macellicephala clarionensis Bonifácio and Menot, 2018					4	4	*Polaruschakov* sp. 655-3-5					1	1
Macellicephala parvafauces Bonifácio and Menot, 2018			1		1	2	*Polaruschakov* sp. 655-3-6					1	1
Macellicephala sp. 180	1	12	29	3		45	*Polaruschakov* sp. 655-3-7					1	1
Macellicephala sp. 308		5	1			6	*Polaruschakov* sp. 659-1-2					1	1
Macellicephala sp. 320		1				1	*Polaruschakov* sp. 666-3-1				1	4	5
Macellicephala sp. 35	2	4	3			9	*Polaruschakov* sp. 666-3-2					1	1
Macellicephala sp. 437		1				1	*Polaruschakov* sp. 685					1	1
Macellicephala sp. 442b		2				2	*Polaruschakov* sp. 686					1	1
Macellicephala sp. 444		1			1	2	*Polaruschakov* sp. 690					1	1
Macellicephala sp. 464		1	1		1	3	*Polaruschakov* spp.					3	3
Macellicephala sp. 687					2	2	Polynoidae sp. 303		1				1
Macellicephaloides moustachu Bonifácio and Menot, 2018	2	7	15	13		37	Polynoidae sp. 450			1			1
Polynoidae sp. 153	1					1	Polynoidae sp. 513				1		1
Polynoidae sp. 197	1					1	Polynoidae sp. 537-1-2			2			2
Polynoidae sp. 299		1				1	Polynoidae sp. 609					1	1
Polynoidae sp. 306		1				1	Polynoidae sp. 655-4					2	2
Polynoidae sp. 314		1				1	Polynoidae sp. 657-1-3					3	3
Polynoidae sp. 353			1			1	Polynoidae sp. 659-7					1	1
Polynoidae sp. 465a			1			1	Polynoidae sp. 670-2					1	1
Polynoidae sp. 521-4			1			1	Polynoidae sp. 679		1				1

(Continued)

TABLE 2 | Continued

	BGR	IOM	GSR	Ifremer	APEI no. 3	Total		BGR	IOM	GSR	Ifremer	APEI no. 3	Total
Polynoidae sp. 655-5					1	1	Polynoidae sp. 688					1	1
Polynoidae sp. 659-4					1	1	Polynoidae sp. 693					1	1
Polynoidae sp. 659-5					1	1	Polynoidae sp. 697					1	1
Polynoidae sp. 666-5					1	1	Polynoidae spp.				1		1
Polynoidae sp. 666-6					1	1	**Eulagiscinae Pettibone, 1997**					**9**	**9**
Polynoidae sp. 673					1	1	*Bathymoorea lucasi* Bonifácio and Menot, 2018					9	9
Polynoidae sp. 691					1	1	**Polynoinae Kinberg, 1856**	**2**	**3**	**5**	**2**		**12**
Polynoidae sp. 696					1	1	*Harmothoe* sp. 207	1	2	2	2		7
Polynoidae spp.					1	1	*Harmothoe* sp. 414	1	1	3			5
Yodanoe desbruyeresi Bonifácio and Menot, 2018				1		1							
Yodanoe sp. 659-3					1	1	**Total**	**14**	**55**	**77**	**36**	**98**	**280**

Subfamilies and species' grouping are marked in bold. Values represent a sum of specimens belonging to the given taxon or grouping of species.

no clear trend. A total of 24 species were identified at IOM area from 54 individuals, 19 species at GSR area from 73 individuals, 19 species at Ifremer from 35 individuals, and 49 species identified at APEI no. 3 from 72 individuals (**Table 3**). Species rarefaction curves (individual-based) did not reach an asymptote at any sampled area and suggested higher diversity at APEI no. 3 (**Figure 6A**). The results also suggest that the diversity at Ifremer and IOM areas is similar and possibly higher than at the GSR area. The non-parametric estimation of species richness followed the same patterns as rarefaction curves, showing the highest values at APEI no. 3 (123 species with Chao1; **Table 3**). The richness estimates computed by Chao1 and ACE for APEI no. 3 are four to five times higher than for the GSR area, which presented a similar sample size. When data from the four areas were pooled, the rarefaction curve did not level-off (**Figure 6C**). The non-parametric estimation of species richness at this regional scale yielded estimates ranging from 176 to 202 polynoid species for Chao1 and ACE estimators respectively.

The ordination of EBS samples in the two first axes of an H-PCA based on polynoid assemblage structure is illustrated in **Figure 7A**. The first two axes explained 61% of total variance in the composition of polynoid assemblage (**Figure 7A**). The first axis explained 40% of total variance and discriminated eastern areas (IOM and GSR) from APEI no. 3. The second axis, explaining 21% of total variance, discriminated the Ifremer area, and particularly one EBS sample. TOC was identified (*post hoc)* as the environmental variable most significantly related ($p < 0.01$) to the first axis (**Figure 7A**). POC, silt and clay were also significantly related to the first axis ($p < 0.05$). The ordination of species (**Figure 7A**) showed that *Macellicephala* sp. 180 and *Macellicephaloides moustachu* were the species most characteristic in eastern areas (particularly in IOM and GSR for the first, and in GSR and Ifremer for the second).

The relationship between distance and assemblage similarity showed no significant correlation ($R^2 = 0.12$, $p = 0.49$; **Supplementary Figure 1A**) but two groups of pairwise comparisons can be highlighted. The three pairwise comparisons between exploration contracts and APEI no. 3 consistently show the lowest values of similarity, irrespective of distance. For pairwise comparison among the three exploration contracts, similarity decreases with distance but the correlation is not statistically significant ($R^2 = 0.84$, $p = 0.26$; **Supplementary Figure 1C**).

Phylogenetic Diversity

Out of the 239 specimens recovered from fully examined EBS, 230 were sequenced and identified to one of the 80 species represented in the phylogenetic tree. Maximum likelihood and Bayesian inference resulted in very similar phylogenetic trees (**Supplementary Figure 2**). For phylogenetic diversity analyses, the distance between species in the Bayesian inference tree has been considered. The rarefaction curves of the Faith phylogenetic diversity showed significantly higher diversity in APEI no. 3 than Ifremer, GSR, and IOM areas (**Figure 6B**). The same pattern was observed for the estimated asymptotes where APEI no. 3 was expected to have two to three times higher diversity (**Table 4**). Pooling of samples from the four areas did not result in rarefaction curve levelling off either (**Figure 6D**).

The PCoA based on phylogenetic distance showed similar patterns to the H-PCA ordination (**Figure 7B**). APEI no. 3 was discriminated from southern areas, and Ifremer separated from GSR and IOM, which are closely related.

The phylogenetic distance showed no relationship with geographic distance ($R^2 = 0.10$, $p = 0.54$; **Supplementary Figure 1B**). Two groups of pairwise comparison were evident, as previously found with taxonomic similarity. Pairwise comparison with the APEI no. 3 had the highest phylogenetic distances irrespective of geographic distances while pairwise comparison among exploration contracts showed a pattern of increasing phylogenetic distance as a function of geographic distance. This pattern was however not statistically significant ($R^2 = 0.84$, $p = 0.26$; **Supplementary Figure 1D**).

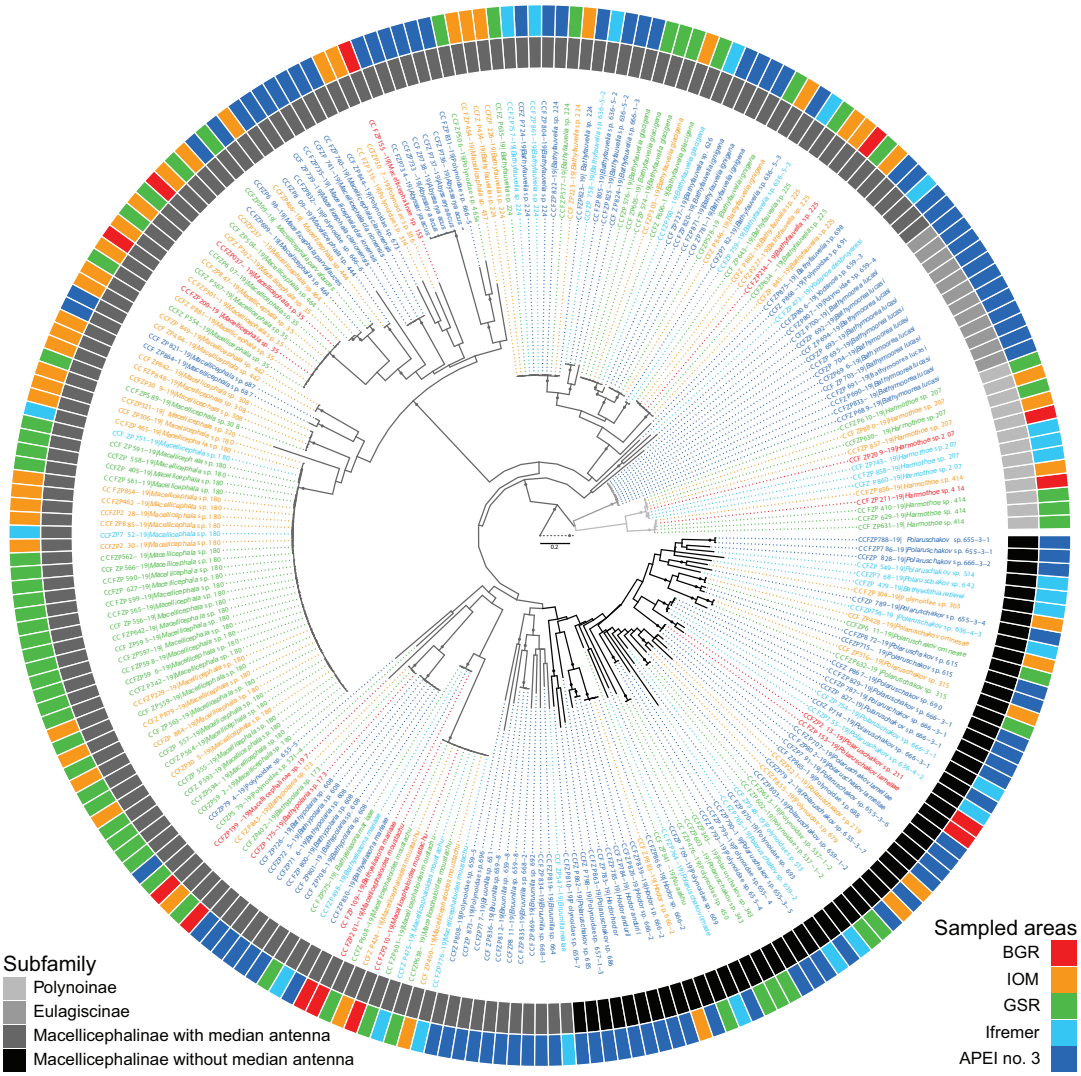

FIGURE 2 | Maximum likelihood inference of polynoid phylogeny based on concatenated gene data (COI, 16S, and 18S) showing distribution of each sequence within the eastern CCFZ. Some species and respective DNA data were already published by Bonifácio and Menot (2018). Dataset includes all sequences of specimens from ROV, EBS, and box corer. Colors indicate subfamilies or sampled area. Circles on branches represent bootstrap supports ≥90%. Bayesian inference has not converged to the stationary distribution (not presented).

DISCUSSION

Causes of Polynoid Species Turnover in the Clarion-Clipperton Fracture Zone

Taxonomic and phylogenetic beta diversity patterns were similar for polynoid assemblages across the eastern CCFZ. The composition of polynoid assemblages discriminated the eastern (i.e., IOM and GSR) from the western areas (i.e., Ifremer and APEI no. 3). It was also possible to notice clear differences between the Ifremer and APEI no. 3. These patterns in species turnover resemble those already reported among the same sampling sites for infaunal polychaetes (Bonifácio et al., 2020), tanaids (Błażewicz et al., 2019), and nematodes (Hauquier et al., 2019). So far, the three main processes evoked to explain these patterns were food inputs, sediment grain size, and a barrier to dispersal.

Conflicting Patterns of Community Structure Along a Gradient of Surface Primary Productivity

Sea surface primary productivity decreases from south-east to north-west across the eastern CCFZ with POC fluxes ranging from 1.54 mg C m^{-2} d^{-1} at IOM to 1.07 mg C m^{-2} d^{-1} at APEI no. 3 (Volz et al., 2018a). In previous studies, beyond species turnover, the influence of food inputs on community structure was supported by positive correlations between POC fluxes and the abundance or taxonomic richness of infauna (Błażewicz et al., 2019; Hauquier et al., 2019; Bonifácio et al., 2020). However, here, the highest species richness of polynoids was found at

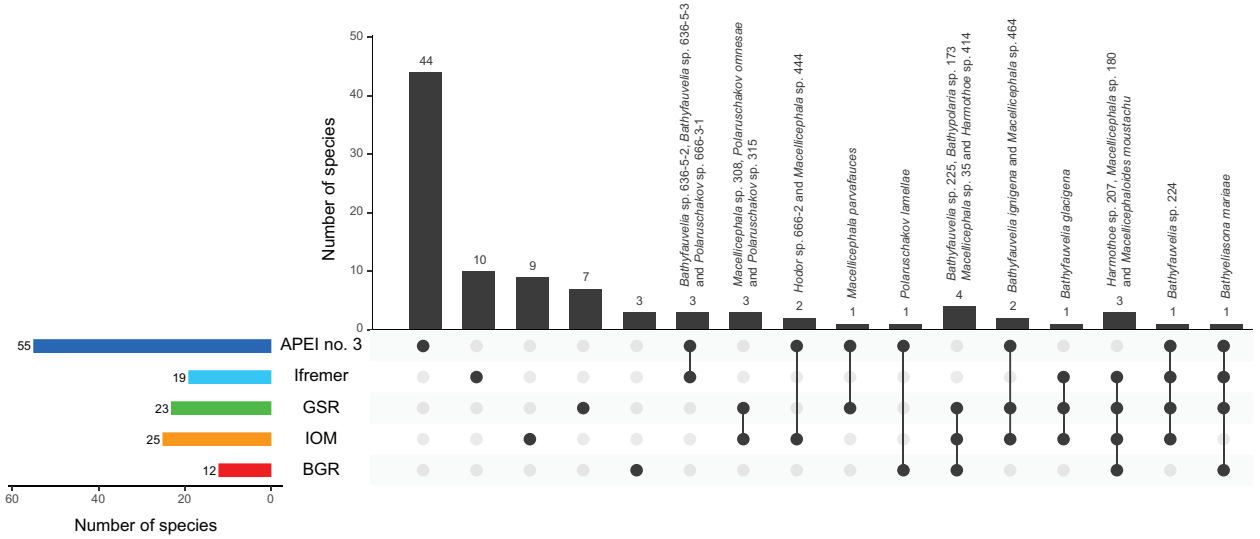

FIGURE 3 | UpSet plot showing the intersection of species distribution along sampled areas within the eastern CCFZ. Horizontal (colored) bars present total number of species for corresponding areas with vertical (black) bars presenting restricted (dots) or shared species (linked dots). Shared species are indicated.

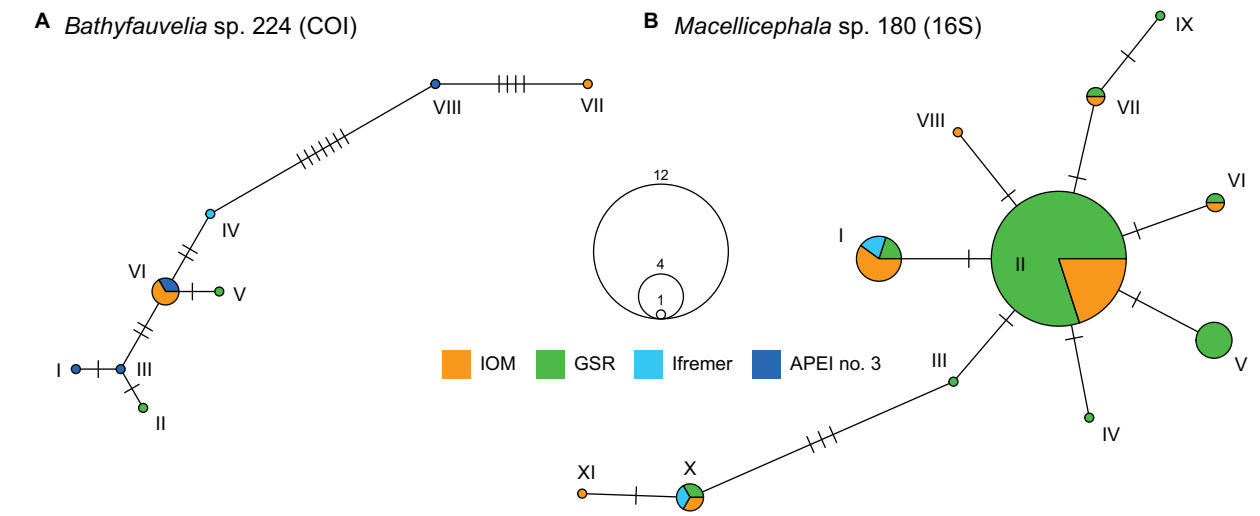

FIGURE 4 | Haplotype networks for *Bathyfauvelia* sp. 224 (10 sequences) based on COI gene **(A)** and for *Macellicephala* sp. 180 (36 sequences) based on 16S gene **(B)**. Each roman number indicates one haplotype with colors indicating sampling areas and dashes indicating mutational steps between haplotypes. Circle size is proportional to the number of samples observed for a specific haplotype.

APEI no. 3, the most oligotrophic site. The EBS used in this study, while very efficient in sampling the poorly known vagile epifauna (Brandt and Schnack, 1999), is a qualitative sampler contrary to the box corer used to sample infauna. Diversity data extrapolated from EBS trawls should thus be interpreted with caution. Yet, without ruling out the sample bias, a high number of specimens and species of polynoids at APEI no. 3, driven mainly by Macellicephalinae, might also be explained by adaptations to oligotrophy (see below).

The Influence of Sediment Grain Size – Fact or Artefact?

In addition to low POC flux, the sediments at APEI no. 3 were characterised by a lower average grain size, higher clay content and lower porosity (Volz et al., 2018a; Hauquier et al., 2019). Higher contents of finer sediments have been postulated to increase sediment shear strength making it more difficult for fauna to burrow (Trueman et al., 1966). Chuar et al. (2020) pointed out that sediment shear strength may impact negatively infaunal abundance in the OMS area located at the south-eastern end of the CCFZ. Together with low food input, inhospitable sediments may thus have contributed to the low abundance of infaunal polychaetes, tanaids, and nematodes at APEI no. 3 (Błażewicz et al., 2019; Hauquier et al., 2019; Bonifácio et al., 2020). In turn, the low infaunal standing stock may increase the relative availability of resources to epifaunal communities. Like polynoids, isopods from EBS samples also showed a number of specimens and species similar to or even higher at APEI no.

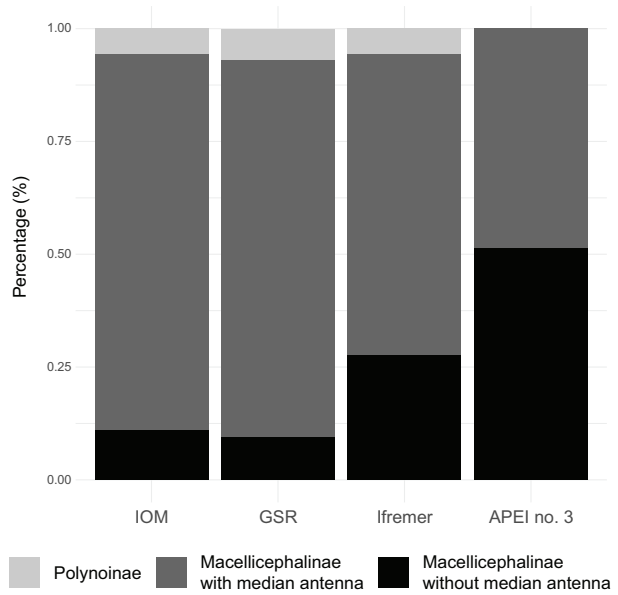

FIGURE 5 | Bar chart of the relative abundance of two polynoid subfamilies – Polynoinae and Macellicephalinae, and within Macellicephalinae with median antenna only or no antennae (i.e., the "Anantennata clade"). Comparisons of data from fully processed EBS samples from the IOM, GSR, Ifremer, and APEI no. 3 study areas.

TABLE 3 | Observed species richness (Sobs) and individual-based estimators of polynoid species richness for each sampled area and for the eastern CCFZ (pooled areas) from the fully processed EBS samples.

Assemblage	Sobs	Sample size *n*	Chao1	ACE	ES12	ES35
IOM	24	54	64 ± 29	62 ± 4	9 ± 1	18 ± 2
GSR	19	73	25 ± 5	27 ± 3	6 ± 1	13 ± 2
Ifremer	19	35	54 ± 26	68 ± 2	8 ± 1	19 ± 0
APEI no. 3	49	72	123 ± 36	114 ± 4	11 ± 1	28 ± 2
Eastern CCFZ	84	234	176 ± 36	202 ± 9	9 ± 1	22 ± 2

ES indicates the expected number of species for a given number of individuals "n." "±" indicates the standard error.

3 than at the southern areas (Ifremer, GSR, IOM, and BGR; Brix et al., 2020). Contrasting patterns in community structure between infaunal and epifaunal assemblages at APEI no. 3 are thus consistent for different taxonomic groups. However, sampling bias cannot be ruled out, as sediment heterogeneity may influence the sampling efficiency of an EBS (Guggolz et al., 2018). At APEI no. 3, the higher clay content might have facilitated sediment flushing through the nets, limiting sediment clogging and increasing the effective sampling time, contrary to southern sites where the EBS mesh would have filled up faster.

Clarion Fracture, a True Barrier to Dispersal?

The pairwise comparisons of taxonomic and phylogenetic composition show that the polynoid assemblage from APEI no. 3 is systematically the most different from all other assemblages, regardless of geographic distance between sites. This may suggest that the Clarion fracture is a biogeographic barrier between the northern APEI no. 3 and the southern exploration contract areas (Ifremer, GSR, IOM, and BGR). This fracture represents a long and narrow submarine mountain range displaying peak-and-trough patterns with up to 1800 m of difference in elevation (Hall and Gurnis, 2005).

Ridges and fractures can work as physiographic barriers affecting the dispersal of different taxa to a lesser or greater degree. For example, the Mid-Atlantic Ridge (MAR) allows the dispersal of nematodes of the genus *Acantholaimus* (Lins et al., 2018), copepods of the genus *Mesocletodes* (Menzel et al., 2011) and isopods of the family Munnopsidae (Bober et al., 2018), but is mostly impermeable to isopods of the families Macrostylidae, Desmosomatidae, and Nannoniscidae (Bober et al., 2018). Polychaetes did not show a clear pattern in the permeability of the MAR as a barrier (Guggolz et al., 2018). Guggolz et al. (2018) examined the distribution of polychaetes and species composition of spionids and polynoids along the Vema Fracture Zone across the MAR. They observed significant changes in species composition across the MAR and suggested them to be the result of limited dispersal potential and different habitat characteristics. Only six of 32 polynoid species crossed the MAR (Guggolz et al., 2018).

Based on our CCFZ samples, 11 of 96 polynoid species (10%) were found on both sides of the Clarion Fracture Zone, which is a much higher proportion of faunal sharing than for infaunal polychaetes (1%; Bonifácio et al., 2020) or infaunal tanaidaceans (0%; Błażewicz et al., 2019), in the same order of magnitude as isopods sampled with an EBS (5%; Brix et al., 2020), and still lower than scavenging amphipods (90%; Patel et al., 2020). For isopods, variations in species ranges across the CCFZ were attributed to variable swimming habits, and thus dispersal abilities (Brix et al., 2020; Janssen et al., 2015). Among the most abundant species of polynoids, *Bathyfauvelia* sp. 224 (10 specimens) remarkably occurs on both sides of the fracture while *Macellicephaloides moustachu* (37 specimens), and *Macellicephala* sp. 180 (45 specimens) were clearly restricted to south of the fracture. The subfamily Macellicephalinae, which is dominant among deep-sea polynoids, shows morphological characters that facilitate a benthopelagic lifestyle (see below). However, *M. moustachu* has been described as having very thin neurochaetae which would evidently affect its ability to swim, and may have contributed to limit its distribution south of the Clarion fracture. This species also has morphological structures attached to the body that may potentially be related to reproduction (Bonifácio and Menot, 2018).

The life cycle of polynoids is mostly known from shallow water species, which have generally a planktotrophic larval development (Giangrande, 1997). A few species in the deep sea are however assumed to undergo lecithotrophic development (Glover et al., 2005), a more suitable condition in oligotrophic waters (Tyler and Young, 1999). External brooding of eggs under the dorsal elytra has also been observed in polynoids of the Antarctic shelf (Gambi et al., 2001). Species from the CCFZ also showed swollen or sac-like structures on the dorsal side, which may be linked to reproduction (Bonifácio and Menot, 2018).

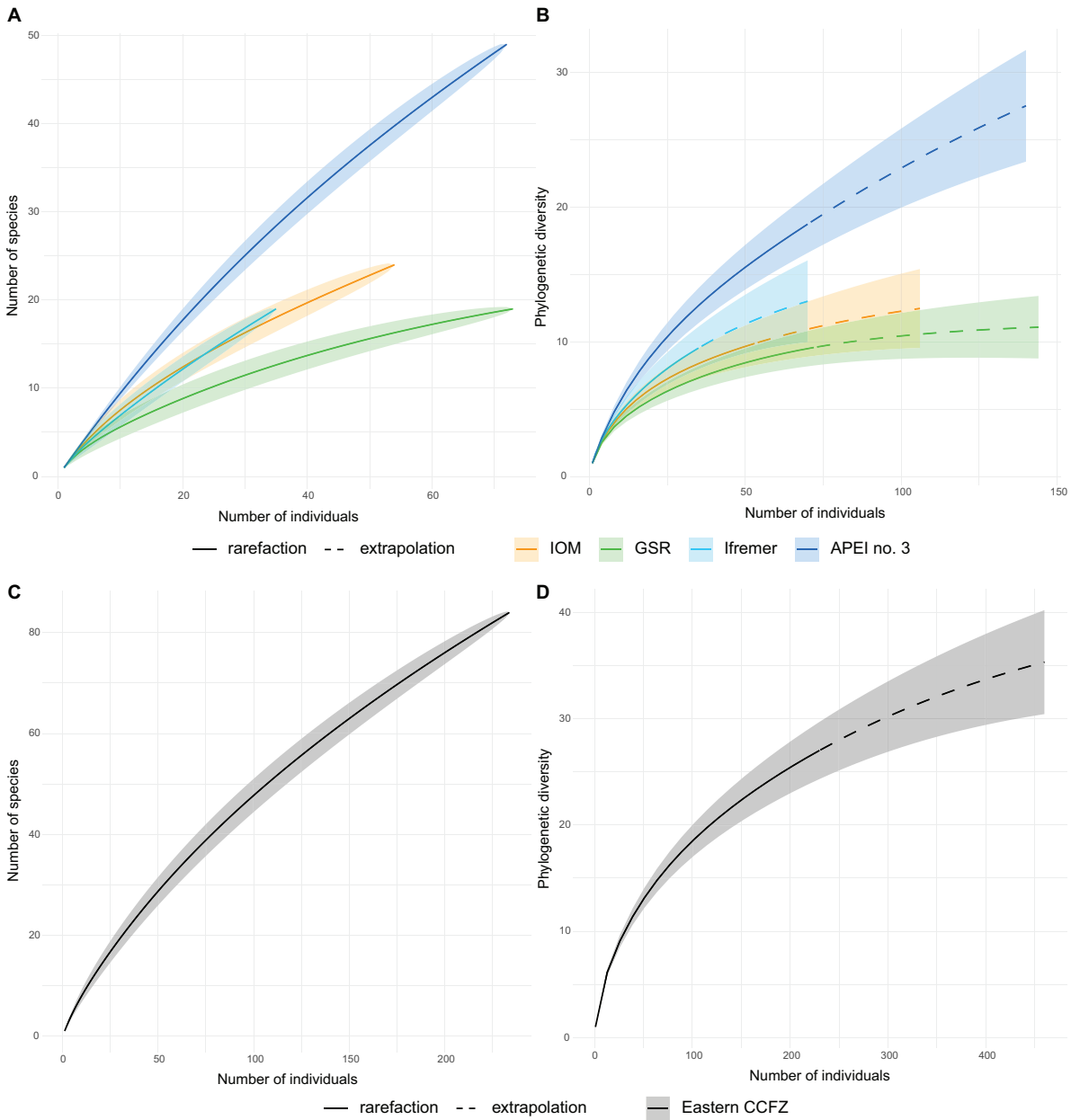

FIGURE 6 | Individual-based rarefaction curves of fully processed EBS samples based on species richness for each sampled area **(A)** and for the eastern CCFZ **(**pooled areas, **C)**; and based on phylogenetic diversity for each sampled area **(B)**, and for the eastern CCFZ **(**pooled areas, **D)**.

Overall, the benthopelagic lifestyle of some deep-sea polynoids combined with the planktotrophic larval development inherited from their shallow-water relatives might explain the relatively large geographic ranges of Polynoidae at community scale in the CCFZ, with 10% of species shared between north and south of the Clarion fracture. However, this is still a low sharing proportion, considering that the purpose of APEI no. 3 is to preserve representative biodiversity of benthic communities within the CCFZ (Wedding et al., 2013). Further, while some polynoids radiated in the deep sea, much remains to be learned about their reproduction and mode of life.

Enhanced Diversity at Great Depths Potentially Related to Low Food Input and Mode of Life

In a global census of abyssal polychaetes (Paterson et al., 2009), polynoids represented the most species-rich family with 91 species out of a total of 768 polychaete species occurring below 2000 m depth. In addition, 13 out of the 15 species occurring below 4000 m depth belonged to the subfamily Macellicephalinae. Interrogation of the Ocean Biodiversity Information System yielded 125 valid species of polynoids below 2000 m depth (OBIS,

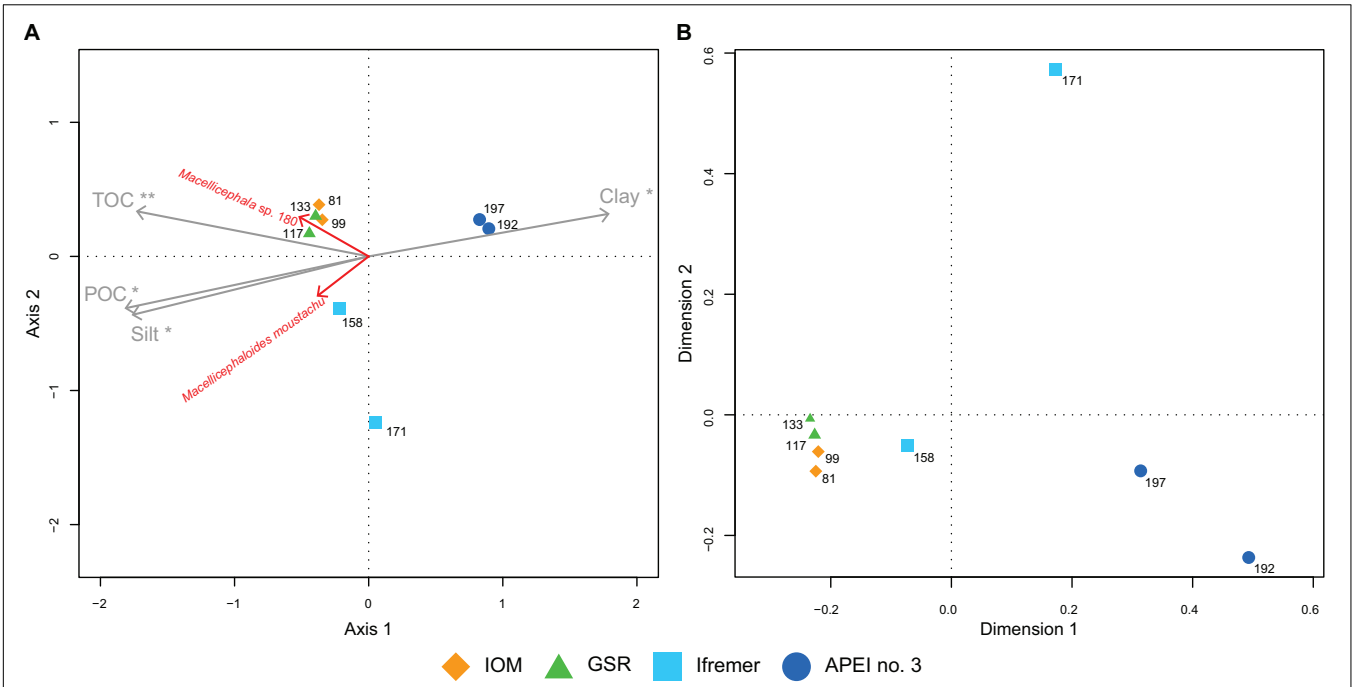

FIGURE 7 | Ordination plot of polynoid assemblages from fully processed EBS samples. **(A)** H-PCA biplot based on the Chord-Normalized Expected Species Shared (CNESS with $m = 3$) distance of species (scaling 2) with variables significantly correlated to the projected points (*post hoc envfit* permutation test) and showing species contributing most to two first axes (**A**, scaling 2). Significance codes: $^{**}p < 0.01$ and $^{*}p < 0.05$. **(B)** PCoA plot based on UniFrac phylogenetic distances.

TABLE 4 | Individual-based phylogenetic diversity (PD) of polynoid assemblages.

Assemblage	Sobs	Sample size *n*	Observed PD	Sample coverage (%)	Estimated asymptote PD	95% confidence interval
IOM	53	23	9.9	72	15 ± 4	9.9, 23.2
GSR	72	18	9.6	89	12 ± 1	9.6, 14.3
Ifremer	35	19	9.5	58	17 ± 5	9.5, 25.8
APEI no. 3	70	47	18.7	53	47 ± 10	26.8, 67.9
Eastern CCFZ	80	230	27	79	43 ± 6	31.7, 54.7

Dataset includes all sequenced specimens from fully examined EBS. Sobs indicates observed species richness. Eastern CCFZ comprises IOM, GSR, Ifremer, and APEI no. 3 data pooled. "±" indicates the standard error. The 95% confidence intervals were calculated by a bootstrap method based on 200 replications.

2020). The Macellicephalinae (*sensu* Bonifácio and Menot, 2018) is the most species-rich deep-sea subfamily with 70 species, followed by Polynoinae with 41 species. The depth ranges of OBIS records differ for these two subfamilies. For 311 valid species of Polynoinae, the depth range varies from 0 to 5400 m depth, with a median at 21 m; while for 89 valid species of Macellicephalinae the depth range varies from 298 to 10,180 m, with a median at 2451 m. In total, 121 species are currently described within Macellicephalinae (36 genera) including only 15 Anantennata (Read and Fauchald, 2021), with the recent additions of 37 new species and four new genera (Bonifácio and Menot, 2018; Jimi et al., 2018; Neal et al., 2018a; Zhang et al., 2018; Zhou et al., 2018; Lindgren et al., 2019; Wu et al., 2019; Hatch et al., 2020; Kolbasova et al., 2020).

Our results (including 16 named species from Bonifácio and Menot, 2018) indicate the presence of at least 92 Macellicephalinae species with 42 being Anantennata in the eastern CCFZ, in the north-east Pacific. In the Atlantic Ocean, Guggolz et al. (2018) were able to identify eight Anantennata species among the 31 Macellicephalinae species recognised. Macellicephalins are thus polychaetes thriving in cold and dark environments that have successfully colonised deep-sea habitats such as chemosynthetic ecosystems (hydrothermal vents and cold seeps; Pettibone, 1983; Chevaldonné et al., 1998; Hatch et al., 2020), trenches (Levenstein, 1971; Pettibone, 1976), manganese nodules (Bonifácio and Menot, 2018), and the deep Antarctic shelf (Neal et al., 2018a,b) but also analogous shallow water habitats such as submarine caves (Pettibone, 1985b).

Macellicephalins differ from other polynoid subfamilies in having lost their antennae. Polynoids from shallow waters typically possess two lateral and one median antennae, whereas macellicephalins have either only a median antenna or no antennae at all. Macellicephalins without antennae form a monophyletic group (i.e., the "Anantennata clade"; Bonifácio and Menot, 2018). Macellicephalinae probably originated from

short-body polynoids such as *Bathymoorea* (Eulagiscinae), a morphology that is reminiscent of macellicephalins from chemosynthetic habitats (a robust body, thick elytra and short body appendages; Desbruyères and Hourdez, 2000) and is likely associated with a basal position within Macellicephalinae (Bonifácio and Menot, 2018).

Deep-sea, polar and cave-endemic macellicephalins not living in chemosynthetic habitats share mostly distinct morphological characters such as a soft body, delicate elytra, loss of eyes, relatively thin, flattened and long chaetae, elongated parapodia, and sometimes extremely long dorsal cirri or reduction of jaws (Uschakov, 1977, 1982; Bonifácio and Menot, 2018; Gonzalez et al., 2018). Pettibone (1985a) also observed some of these morphological characters specific for pelagic life in *Natopolynoe kensmithi* Pettibone, 1985a which was described to be abundant not only on the seafloor but also swimming up to 10 m above it. Some Macellicephalinae seem to be benthopelagic, swimming in near-bottom water in search of food (Knox, 1959; Pettibone, 1976; Uschakov, 1977, 1982). Other studies, examining megafauna, have also recorded macellicephalins swimming in the water column (Smith and Hamilton, 1983; Rybakova et al., 2019). Some macellicephalins also have elongated papillae on their pharynx, assumed to be helpful in rapid capture of small suspended particles, a character also shared with the pelagic family Alciopidae (Pettibone, 1976; Uschakov, 1982). Evidence presented so far supports the hypothesis of Gonzalez et al. (2018) of a secondary pelagic mode of life as a deep-sea adaptation in polynoids. These authors also suggested that scale worms living in aphotic environments (i.e., submarine caves and the deep-sea) are subjected to the "darkness syndrome" promoting morphological and behavioral changes such as loss of eyes, elongation of appendages and shifting to swimming behavior.

Elongated appendages could provide an evolutionary advantage in two ways for deep-sea polynoids. Firstly, cirri elongation increases the surface area thus contributing to attainment of neutral buoyancy (Gonzalez et al., 2018). Secondly, cirri elongation could increase their sensitivity to prey detection. By removing the sensory appendages in *Harmothoe* species, Daly (1972) showed that the ability to locate a source of vibrations is an important factor in feeding behavior. His experiments further suggested that palps provide the worm with contact exploration of the object and chemical information (e.g., if suitable as prey or not) whereas dorsal cirri were responsible for relaying chemical information and vibration source location (Daly, 1972). Therefore, the elongation of appendages in deep-sea polynoids could represent an adaptation of the subfamily Macellicephalinae to food limitation by increasing the access to food (invasion of new niches) and prey detection.

The swimming behavior in Macellicephalinae was likely the key to exploitation of new trophic resources, unavailable to worms with a benthic lifestyle. This rare semi-pelagic mode of life within polynoids has been well-documented for a Polynoinae species, *Bylgides sarsi* (Kinberg in Malmgren, 1866), which rises above the bottom to mid-water during the night, escaping the poor oxygen conditions close to the bottom and feeding on small pelagic crustaceans or scavenging dead planktonic organisms on the bottom (Pettibone, 1993). Evolution of similar behavior may have enabled macellicephalins to explore benthic and pelagic niches in the deep sea, particularly within hadal depths where they are the most characteristic and diverse polychaetes (Paterson et al., 2009; Jamieson, 2015).

CONCLUSION

Variations in epibenthic polynoid assemblages across the CCFZ show similarities with other faunal groups in that species turnover covaries with POC flux and thus food supply. A major difference from the infaunal pattern (Bonifácio et al., 2020) is that species richness was similar to or even higher at APEI no. 3, the most oligotrophic site located north of the Clarion fracture, in comparison to other exploration mining areas to the south. This unexpected pattern may result from sampling bias, but could also be due to: (i) higher shear strength of APEI no. 3 sediments making them less hospitable to infauna to the benefit of epifauna and (ii) evolutionary adaptations of macellicephalins towards a benthopelagic life strategy under oligotrophic conditions in the deep sea. The difference in species composition and community structure at APEI no. 3 brings into question the key principles of the APEI network, as this area appears not representative of the biogeography and habitat of the broader region (Wedding et al., 2013). However, such a conclusion is tentative, given the limited sampling within this APEI.

The polynoids in the CCFZ are highly diverse, with most diversity confined to the subfamily Macellicephalinae, which has particularly radiated in the deep sea. Together with the results of Bonifácio and Menot (2018) from the same areas in the CCFZ, our results increase the number of known Macellicephalinae species worldwide. We have newly identified 42 Anantennata species whereas only eight species have been described worldwide prior to our visit in 2015. This number indicates, how underestimated macellicephalin diversity currently is. Other questions remain unanswered as well: Do they have a pattern of vertical movement? Is the elongation of appendages driven by swimming behavior or prey detection? How do they interact with other species? How do they reproduce and disperse?

DATA AVAILABILITY STATEMENT

DNA sequences are available in BOLD (https://dx.doi.org/10.5883/DS-POLYNOID; Bonifácio, 2021) and GenBank. The total number of specimens and species data examined in the present study with respective BOLD IDs and GenBank accession numbers are available in the PANGAEA database (https://doi.org/10.1594/PANGAEA.926674; Bonifácio et al., 2021).

AUTHOR CONTRIBUTIONS

LM was responsible for the project planning and sampling design. All authors carried out the sampling and the subsequent sample

processing on board. PB was responsible for the identification of Polynoidae and data analysis. All authors involved in data interpretation and preparation of the manuscript.

FUNDING

This study received funding from the Ifremer programme "Ressources Minérales Marines" (REMIMA), the JPI Oceans pilot action "Ecological Aspects of Deep-Sea Mining," and the European Union Seventh Framework Programme (FP7/2007–2013) under the MIDAS project, grant agreement no. 603418.

ACKNOWLEDGMENTS

We are grateful to Pedro Martínez, the crew of the *RV* Sonne, the team of the ROV Kiel 6000 and all people who participated in the field sampling and sample processing during the SO239 cruise. Many thanks for sample processing to Stefanie Kaiser, Sarah Schnurr and Ana Hilário; and to Emmanuelle Omnes for assistance with DNA extraction and amplification. Special thanks to Helena Wiklund and Thomas Dahlgren who initiated PB in phylogenetic and connectivity studies. We are thankful to Alison Chalm for the English editing. Finally, we extend our sincere thanks to Erica Goetze and the two referees for their critical reviews and helpful comments on the manuscript.

SUPPLEMENTARY MATERIAL

The Supplementary Material for this article can be found online at: https://www.frontiersin.org/articles/10.3389/fmars.2021.656899/full#supplementary-material

Supplementary Figure 1 | Distance decay of New Normalized Expected Species Shared (NNESS) between IOM, GSR, Ifremer, and APEI no. 3 **(A)** and the same areas excluding APEI no. 3 **(C)**. Distance decay of UniFrac phylogenetic distance between IOM, GSR, Ifremer, and APEI no. 3 **(B)** and the same areas excluding APEI no. 3 **(D)**.

Supplementary Figure 2 | Molecular phylogenetic relationship among sampled polynoid species based on concatenated genes (COI, 16S, and 18S) and performed with maximum-likelihood **(A)** and Bayesian inference **(B)** analyses. Outgroup (sigalionid species) colored in gray. Node values indicate the maximum-likelihood bootstrap **(A)** and Bayesian posterior probabilities **(B)**.

REFERENCES

Błażewicz, M., Jóźwiak, P., Menot, L., and Pabis, K. (2019). High species richness and unique composition of the tanaidacean communities associated with five areas in the Pacific polymetallic nodule fields. *Prog. Oceanogr.* 176:102141. doi: 10.1016/j.pocean.2019.102141

Bober, S., Brix, S., Riehl, T., Schwentner, M., and Brandt, A. (2018). Does the Mid-Atlantic Ridge affect the distribution of abyssal benthic crustaceans across the Atlantic Ocean? *Deep Sea Res. Part II Top. Stud. Oceanogr.* 148, 91–104. doi: 10.1016/j.dsr2.2018.02.007

Bonifácio, P. (2021). Polynoidae from Clarion-Clipperton Fracture Zone sampled during SONNE cruise SO239. *Bold* 2021:5883. doi: 10.5883/DS-POLYNOID

Bonifácio, P., and Menot, L. (2018). New genera and species from the Equatorial Pacific provide phylogenetic insights into deep-sea Polynoidae (Annelida). *Zool. J. Linn. Soc.* 185, 555–635. doi: 10.1093/zoolinnean/zly063

Bonifácio, P., Martínez Arbizu, P., and Menot, L. (2020). Alpha and beta diversity patterns of polychaete assemblages across the nodule province of the eastern Clarion-Clipperton Fracture Zone (equatorial Pacific). *Biogeosciences* 17, 865–886. doi: 10.5194/bg-17-865-2020

Bonifácio, P., Neal, L., Omnes, E., and Menot, L. (2021). Polychaete fauna belonging to family Polynoidae of the Clarion-Clipperton Fracture Zone sampled during SONNE cruise SO239. *Pangaea* 2021:926674. doi: 10.1594/PANGAEA.926674

Borcard, D., Gillet, F., and Legendre, P. (2018). *Numerical Ecology With R*. Cham: Springer International Publishing, doi: 10.1007/978-3-319-71404-2

Brandt, A., and Schnack, K. (1999). Macrofaunal abundance at 79°N off East Greenland: opposing data from epibenthic-sledge and box-corer samples. *Polar Biol.* 22, 75–81. doi: 10.1007/s003000050392

Brenke, N. (2005). An epibenthic sledge for operations on marine soft bottom and bedrock. *Mar. Technol. Soc. J.* 39, 10–21. doi: 10.4031/002533205787444015

Brix, S., Osborn, K. J., Kaiser, S., Truskey, S. B., Schnurr, S. M., Brenke, N., et al. (2020). Adult life strategy affects distribution patterns in abyssal isopods – implications for conservation in Pacific nodule areas. *Biogeosciences* 17, 6163–6184. doi: 10.5194/bg-17-6163-2020

Carr, C. M., Hardy, S. M., Brown, T. M., Macdonald, T. A., and Hebert, P. D. N. (2011). A tri-oceanic perspective: dna barcoding reveals geographic structure and cryptic diversity in canadian polychaetes. *PLoS ONE* 6:e22232. doi: 10.1371/journal.pone.0022232

Chevaldonné, P., Jollivet, D., Feldman, R. A., Desbruyères, D., Lutz, R. A., and Vrijenhoek, R. C. (1998). Commensal scale-worms of the genus Branchipolynoe (Polychaeta: Polynoidae) at deep-sea hydrothermal vents and cold seeps. *Cah. Biol. Mar.* 39, 347–350.

Chiu, C.-H., Wang, Y.-T., Walther, B. A., and Chao, A. (2014). An improved nonparametric lower bound of species richness via a modified good-turing frequency formula: An improved nonparametric lower bound of species richness. *Biom.* 70, 671–682. doi: 10.1111/biom.12200

Chuar, C. H., Tong, S. J. W., Chim, C. K., Wong, H. P. S., and Tan, K. S. (2020). Abyssal macrofaunal community structure in the polymetallic nodule exploration area at the easternmost region of the clarion-clipperton fracture zone, pacific ocean. *Deep Sea Res. Part 1 Oceanogr. Res. Pap.* 161:103284. doi: 10.1016/j.dsr.2020.103284

Cohen, B. L., Gawthrop, A., and Cavalier–Smith, T. (1998). Molecular phylogeny of brachiopods and phoronids based on nuclear–encoded small subunit ribosomal RNA gene sequences. *Phil. Trans. R. Soc. Lond. B* 353, 2039–2061. doi: 10.1098/rstb.1998.0351

Conway, J. R., Lex, A., and Gehlenborg, N. (2017). UpSetR: an R package for the visualization of intersecting sets and their properties. *Bioinformatics* 33, 2938–2940. doi: 10.1093/bioinformatics/btx364

Daly, J. M. (1972). The ability to locate a source of vibrations as a prey—capture mechanism in *Harmothoë imbricata* (Annelida Polychaeta). *Mar. Freshw. Behav. Physiol.* 1, 305–322. doi: 10.1080/10236247209386906

De Smet, B., Pape, E., Riehl, T., Bonifácio, P., Colson, L., and Vanreusel, A. (2017). The Community structure of deep-sea macrofauna associated with polymetallic nodules in the eastern part of the Clarion-Clipperton Fracture Zone. *Front. Mar. Sci.* 4:103. doi: 10.3389/fmars.2017.00103

Desbruyères, D., and Hourdez, S. (2000). A new species of scale-worm (Polychaeta: Polynoidae), *Lepidonotopodium atalantae* sp nov., from the East Pacific Rise at 13°N and 9°50'N. *Cah. Biol. Mar.* 41, 47–54.

Dray, S., Bauman, D., Blanchet, G., Borcard, D., Clappe, S., Guenard, G., et al. (2020). *adespatial: Multivariate Multiscale Spatial Analysis*. Available online at: https://CRAN.R-project.org/package=adespatial (accessed April 07, 2021).

Dray, S., and Dufour, A.-B. (2007). The ade4 Package: Implementing the Duality Diagram for Ecologists. *J. Stat. Soft.* 22:04. doi: 10.18637/jss.v022.i04

Edgar, R. C. (2004). MUSCLE: multiple sequence alignment with high accuracy and high throughput. *Nucleic Acids Res.* 32, 1792–1797. doi: 10.1093/nar/gkh340

Faith, D. P. (1992). Conservation evaluation and phylogenetic diversity. *Biol. Conserv.* 61, 1–10. doi: 10.1016/0006-3207(92)91201-3

Folmer, O., Black, M., Hoeh, W., Lutz, R., and Vrijenhoek, R. (1994). DNA primers for amplification of mitochondrial cytochrome c oxidase subunit I from diverse metazoan invertebrates. *Mol. Mar. Biol. Biotechnol.* 3, 294–299.

Gallagher, E. (1999). *Compah Documentation*. Available online at: http://citeseerx.ist.psu.edu/viewdoc/download?doi=10.1.1.9.1334&rep=rep1&type=pdf (accessed June 18, 2021).

Gambi, M., Patti, F., Micaletto, G., and Giangrande, A. (2001). Diversity of reproductive features in some Antarctic polynoid and sabellid polychaetes, with a description of *Demonax polarsterni* sp. n. (Polychaeta, Sabellidae). *Polar Biol.* 24, 883–891. doi: 10.1007/s003000100287

Giangrande, A. (1997). Polychaete reproductive patterns, life cycles and life histories: an overview. *Oceanogr. Mar. Biol.* 35, 323–386.

Glover, A., Dahlgren, T., Taboada, S., Paterson, G., Wiklund, H., Waeschenbach, A., et al. (2016). The london workshop on the biogeography and connectivity of the clarion-clipperton zone. *RIO* 2:e10528. doi: 10.3897/rio.2.e10528

Glover, A., Smith, C., Paterson, G., Wilson, G., Hawkins, L., and Sheader, M. (2002). Polychaete species diversity in the central Pacific abyss: local and regional patterns, and relationships with productivity. *Mar. Ecol. Prog. Ser.* 240, 157–170. doi: 10.3354/meps240157

Glover, A. G., Goetze, E., Dahlgren, T. G., and Smith, C. R. (2005). Morphology, reproductive biology and genetic structure of the whale-fall and hydrothermal vent specialist, *Bathykurila guaymasensis* Pettibone, 1989 (Annelida: Polynoidae). *Mar. Ecol.* 26, 223–234. doi: 10.1111/j.1439-0485.2005.00060.x

Glover, A. G., and Smith, C. R. (2003). The deep-sea floor ecosystem: current status and prospects of anthropogenic change by the year 2025. *Environ. Conserv.* 30, 219–241. doi: 10.1017/S0376892903000225

Gonzalez, B. C., Worsaae, K., Fontaneto, D., and Martínez, A. (2018). Anophthalmia and elongation of body appendages in cave scale worms (Annelida: Aphroditiformia). *Zool. Scr.* 47, 106–121. doi: 10.1111/zsc.12258

Gotelli, N. J., and Colwell, R. K. (2001). Quantifying biodiversity: procedures and pitfalls in the measurement and comparison of species richness. *Ecol. Lett.* 4, 379–391. doi: 10.1046/j.1461-0248.2001.00230.x

Gower, J. C. (1966). Some distance properties of latent root and vector methods used in multivariate analysis. *Biometrika* 53:325. doi: 10.2307/2333639

Greinert, J. (2016). Swath sonar multibeam EM122 bathymetry during SONNE cruise SO239 with links to raw data files. *Pangaea* 2016:859456. doi: 10.1594/PANGAEA.859456

Guggolz, T., Lins, L., Meißner, K., and Brandt, A. (2018). Biodiversity and distribution of polynoid and spionid polychaetes (Annelida) in the vema fracture zone, tropical north atlantic. *Deep Sea Res. Part II Top. Stud. Oceanogr.* 148, 54–63. doi: 10.1016/j.dsr2.2017.07.013

Hall, C. E., and Gurnis, M. (2005). Strength of fracture zones from their bathymetric and gravitational evolution. *J. Geophys. Res.* 110:B01402. doi: 10.1029/2004JB003312

Hartman-Schröder, G. (1971). "Teil 58. Annelida, Borstenwürmer, Polychaeta," in *Die Tierwelt Deutschlands und der angrenzenden Meeresteile nach ihren Merkmalen und nach ihrer Lebensweise*, eds M. Dahl and F. Peus (Stuttgart: Gustav Fischer Verlag Jena), 1–594.

Hatch, A. S., Liew, H., Hourdez, S., and Rouse, G. W. (2020). Hungry scale worms: Phylogenetics of *Peinaleopolynoe* (Polynoidae, Annelida), with four new species. *Zookeys* 932, 27–74. doi: 10.3897/zookeys.932.48532

Hauquier, F., Macheriotou, L., Bezerra, T. N., Egho, G., Martínez Arbizu, P., and Vanreusel, A. (2019). Distribution of free-living marine nematodes in the Clarion–Clipperton Zone: implications for future deep-sea mining scenarios. *Biogeosciences* 16, 3475–3489. doi: 10.5194/bg-16-3475-2019

Hauquier, F., Macheriotou, L., Vanreusel, A., Janssen, F., and Boetius, A. (2017). Sedimentary parameters from multicorer and ROV pushcore samples during SONNE cruise SO239. *Mariene Biologie, Universiteit Gent. Pangaea* 2017:873272. doi: 10.1594/PANGAEA.873274

Hebert, P. D. N., Cywinska, A., Ball, S. L., and deWaard, J. R. (2003a). Biological identifications through DNA barcodes. *Proc. R. Soc. Lond. B* 270, 313–321. doi: 10.1098/rspb.2002.2218

Hebert, P. D. N., Ratnasingham, S., and de Waard, J. R. (2003b). Barcoding animal life: cytochrome *c* oxidase subunit 1 divergences among closely related species. *Proc. R. Soc. Lond. B* 270:25. doi: 10.1098/rsbl.2003.0025

Hecker, B., and Paul, A. Z. (1979). "Abyssal Community Structure of the Benthic Infauna of the Eastern Equatorial Pacific: DOMES Sites A, B, and C," in *Marine Geology and Oceanography of the Pacific Manganese Nodule Province*, eds J. L. Bischoff and D. Z. Piper (Boston, MA: Springer), 287–308. doi: 10.1007/978-1-4684-3518-4_8

Hein, J. R., and Petersen, S. (2013). "The geology of Manganese nodules," in *Deep Sea Minerals: Manganese Nodules, a Physical, Biological, Environmental and Technical Review*, eds Y. Beaudoin and E. Baker (Nouméa: Secretariat of the Pacific Community).

Hessler, R. R., and Jumars, P. A. (1974). Abyssal community analysis from replicate box cores in the central North Pacific. *Deep- Sea Res. Oceanogr. Abstr.* 21, 185–209. doi: 10.1016/0011-7471(74)90058-8

Hsieh, T. C., and Chao, A. (2017). Rarefaction and extrapolation: making fair comparison of abundance-sensitive phylogenetic diversity among multiple assemblages. *Syst. Biol.* 66, 100–111. doi: 10.1093/sysbio/syw073

Hurlbert, S. H. (1971). The nonconcept of species diversity: a critique and alternative parameters. *Ecology* 52, 577–586. doi: 10.2307/1934145

Hutchings, P. (1998). Biodiversity and functioning of polychaetes in benthic sediments. *Biodivers. Conserv.* 7, 1133–1145. doi: 10.1023/A:1008871430178

International Seabed Authority. (2021). *Minerals: Polymetallic Nodules*. Available online at: https://www.isa.org.jm/exploration-contracts/polymetallic-nodules (accessed June 18, 2021).

International Seabed Authority (2020). *ISBA/25/LTC/6/Rev.1: Recommendations for the Guidance of Contractors for the Assessment of the Possible Environmental Impacts Arising From Exploration for Marine Minerals in the Area*. Kingston: International Seabed Authority.

Jamieson, A. (2015). *The Hadal Zone: Life in the Deepest Oceans*. Cambridge, MA: Cambridge University Press, doi: 10.1017/CBO9781139061384

Janssen, A., Kaiser, S., Meißner, K., Brenke, N., Menot, L., and Martínez Arbizu, P. (2015). A reverse taxonomic approach to assess macrofaunal distribution patterns in abyssal pacific polymetallic nodule fields. *PLoS ONE* 10:e0117790. doi: 10.1371/journal.pone.0117790

Janssen, A., Stuckas, H., Vink, A., and Arbizu, P. M. (2019). Biogeography and population structure of predominant macrofaunal taxa (Annelida and Isopoda) in abyssal polymetallic nodule fields: implications for conservation and management. *Mar. Biodivers.* 49, 2641–2658. doi: 10.1007/s12526-019-00997-1

Jimi, N., Fujiwara, Y., and Kajihara, H. (2018). New annelid species from the deepest known whale-fall environment: *Bathykermadeca thanatos* sp. nov. (Annelida: Polynoidae). *Zootaxa* 4450:575. doi: 10.11646/zootaxa.4450.5.4

Johnston, G. (1833). Illustration in British Zoology. *Mag. Nat. Hist. J. Zool. Bot. Mineral. Geol. Meteorol.* 34, 320–324.

Katoh, K., Misawa, K., Kuma, K., and Miyata, T. (2002). MAFFT: a novel method for rapid multiple sequence alignment based on fast Fourier transform. *Nucleic Acids Res.* 30, 3059–3066. doi: 10.1093/nar/gkf436

Kembel, S. W., Cowan, P. D., Helmus, M. R., Cornwell, W. K., Morlon, H., Ackerly, D. D., et al. (2010). Picante: R tools for integrating phylogenies and ecology. *Bioinformatics* 26, 1463–1464. 10.1093/bioinformatics/btq166

Kindt, R., and Coe, R. (2005). *Tree Diversity Analysis. A Manual and Software for Common Statistical Methods for Ecological and Biodiversity Studies*. Nairobi: World Agroforestry Centre (ICRAF).

Kinberg, J. G. H. (1856). Nya slägten och arter af Annelider. Öfversigt af kongl. *Vetensk. Akadem. Förhhand.* 12, 381–388.

Kirkegaard, J. B. (1956). Benthic Polychaeta from depths exceeding 6000 meters. *Galathea Rep.* 2, 63–78.

Knox, G. (1959). Pelagic and benthic polychaetes of the central Arctic Basin. *Geophys. Res. Pap.* 63, 105–114.

Kolbasova, G., Kosobokova, K., and Neretina, T. (2020). Bathy- and mesopelagic Annelida from the Arctic Ocean: description of new, redescription of known and notes on some "cosmopolitan" species. *Deep Sea Res. Part 1 Oceanogr. Res. Pap.* 165:103327. doi: 10.1016/j.dsr.2020.103327

Legendre, P., and Gallagher, E. D. (2001). Ecologically meaningful transformations for ordination of species data. *Oecologia* 129, 271–280. doi: 10.1007/s004420100716

Levenstein, R. Y. (1971). A new polychaete species of the genus *Macellicephaloides* from the Aleutian Trench. *J. Fish Res. Board Can.* 28, 1429–1431. doi: 10.1139/f71-220

Levenstein, R. Y. (1984). On the ways of the formation of the deep-sea polychaete fauna of the family Polynoidae. *Proc. First Int. Polychaete Conf.* 1984, 72–85.

Lindgren, J., Hatch, A. S., Hourdez, S., Seid, C. A., and Rouse, G. W. (2019). Phylogeny and biogeography of *Branchipolynoe* (Polynoidae, Phyllodocida, Aciculata, Annelida), with descriptions of five new species from methane seeps and hydrothermal vents. *Diversity* 11:153. doi: 10.3390/d11090153

Lins, L., da Silva, M. C., Neres, P., Esteves, A. M., and Vanreusel, A. (2018). Testing deep-sea biodiversity paradigms on abyssal nematode genera and *Acantholaimus* species. *Deep Sea Res. Part II Top. Stud. Oceanogr.* 148, 208–222. doi: 10.1016/j.dsr2.2016.12.005

Lodge, M., Johnson, D., Le Gurun, G., Wengler, M., Weaver, P., and Gunn, V. (2014). Seabed mining: international seabed authority environmental management plan for the clarion–clipperton zone. A partnership approach. *Mar. Policy* 49, 66–72. doi: 10.1016/j.marpol.2014.04.006

Lozupone, C., Hamady, M., and Knight, R. (2006). UniFrac – An online tool for comparing microbial community diversity in a phylogenetic context. *BMC Bioinforma.* 7:371. doi: 10.1186/1471-2105-7-371

Malmgren, A. J. (1866). Nordiska hafs-annulater. Öfversigt af kÃűniglich vetenskapsakademiens förhandlingar. *Stockholm* 22, 355–410.

Martínez Arbizu, P., and Haeckel, M. (2015). RV SONNE Fahrtbericht/cruise report SO239: EcoResponse assessing the ecology, connectivity and resilience of polymetallic nodule field systems, balboa (Panama) - Manzanillo (Mexico). *Geomar. Rep.* 25:204. doi: 10.3289/GEOMAR_REP_NS_25_2015

McQuaid, K. A., Attrill, M. J., Clark, M. R., Cobley, A., Glover, A. G., Smith, C. R., et al. (2020). Using habitat classification to assess representativity of a protected area network in a large, data-poor area targeted for deep-sea mining. *Front. Mar. Sci.* 7:558860. doi: 10.3389/fmars.2020.558860

Medlin, L., Elwood, H. J., Stickel, S., and Sogin, M. L. (1988). The characterization of enzymatically amplified eukaryotic 16S-like rRNA-coding regions. *Gene* 71, 491–499. doi: 10.1016/0378-1119(88)90066-2

Menot, L. (2019). ness: hypergeometric standardization and probabilistic measures of similarity for community ecology. *Zenodo* 2019:3254750. doi: 10.5281/ZENODO.3254750

Menzel, L., George, K. H., and Arbizu, P. M. (2011). Submarine ridges do not prevent large-scale dispersal of abyssal fauna: a case study of *Mesocletodes* (Crustacea, Copepoda, Harpacticoida). *Deep Sea Res. Part 1 Oceanogr. Res. Pap.* 58, 839–864. doi: 10.1016/j.dsr.2011.05.008

Miller, M. A., Pfeiffer, W., and Schwartz, T. (2010). *Creating the CIPRES Science Gateway for Inference of Large Phylogenetic Trees. in 2010 Gateway Computing Environments Workshop (GCE)*. New Orleans, LA: IEEE, 1–8. doi: 10.1109/GCE.2010.5676129

Morgan, C. L. (2000). "Resource Estimates of the Clarion-Clipperton Manganese Nodule Deposits," in *Handbook of Marine Mineral Deposits*, ed. D. S. Cronan (Milton Park: Routledge), 145–170. doi: 10.1201/9780203752760

Neal, L., Brasier, M. J., and Wiklund, H. (2018a). Six new species of *Macellicephala* (Annelida: Polynoidae) from the Southern Ocean and south Atlantic with re-description of type species. *Zootaxa* 4455:1. doi: 10.11646/zootaxa.4455.1.1

Neal, L., Linse, K., Brasier, M. J., Sherlock, E., and Glover, A. G. (2018b). Comparative marine biodiversity and depth zonation in the Southern Ocean: evidence from a new large polychaete dataset from Scotia and Amundsen seas. *Mar. Biodiv.* 48, 581–601. doi: 10.1007/s12526-017-0735-y

Nygren, A., and Sundberg, P. (2003). Phylogeny and evolution of reproductive modes in Autolytinae (Syllidae, Annelida). *Mol. Phylogenet. Evol.* 29, 235–249. doi: 10.1016/S1055-7903(03)00095-2

OBIS (2020). *Ocean Biodiversity Information System. Intergovernmental Oceanographic Commission of UNESCO*. Available online at https://www.obis.org (accessed June 18, 2021).

Oebius, H. U., Becker, H. J., Rolinski, S., and Jankowski, J. A. (2001). Parametrization and evaluation of marine environmental impacts produced by deep-sea manganese nodule mining. *Deep Sea Res. Part II Top. Stud. Oceanogr.* 48, 3453–3467. doi: 10.1016/S0967-0645(01)00052-2

O'Hara, R. B. (2005). Species richness estimators: how many species can dance on the head of a pin? *J. Anim. Ecol.* 74, 375–386. doi: 10.1111/j.1365-2656.2005.00940.x

Oksanen, J., Blanchet, F. G., Friendly, M., Kindt, R., Legendre, P., McGlinn, D., et al. (2016). *vegan: Community Ecology Package. R package version 2.4-3*. Vienna: R Foundation for Statistical Computing.

Örsted, A. S. (1845). Fortegnelse over Dyr, samlede i Christianiafjord ved Drobak fra 21–24 Juli, 1844. *Naturhistorisk Tidsskrift, Köbenhavn Ser.* 2, 400–427.

Pagès, H., Aboyoun, P., Gentleman, R., and DebRoy, S. (2017). Biostrings: Efficient manipulation of biological strings. *Bioconductor* 2017:18129. doi: 10.18129/B9.BIOC.BIOSTRINGS

Palumbi, S. R. (1996). "The polymerase chain reaction," in *Molecular Systematics*, eds D. M. Hillis, C. Moritz, and B. K. Mable (Sunderland, MA: Sinauer Associates), 205–247.

Paradis, E. (2010). Pegas: an R package for population genetics with an integrated-modular approach. *Bioinformatics* 26, 419–420. doi: 10.1093/bioinformatics/btp696

Paradis, E., and Schliep, K. (2019). Ape 5.0: an environment for modern phylogenetics and evolutionary analyses in R. *Bioinformatics* 35, 526–528. doi: 10.1093/bioinformatics/bty633

Patel, T., Robert, H., D'Udekem, D., Acoz, C., Martens, K., De Mesel, I., et al. (2020). Biogeography and community structure of abyssal scavenging Amphipoda (Crustacea) in the Pacific Ocean. *Biogeosciences* 17, 2731–2744. doi: 10.5194/bg-17-2731-2020

Paterson, G. L. J., Glover, A. G., Barrio Froján, C. R. S., Whitaker, A., Budaeva, N., Chimonides, J., et al. (2009). A census of abyssal polychaetes. *Deep Sea Res. Part II Top. Stud. Oceanogr.* 56, 1739–1746. doi: 10.1016/j.dsr2.2009.05.018

Pennell, M. W., Eastman, J. M., Slater, G. J., Brown, J. W., Uyeda, J. C., FitzJohn, R. G., et al. (2014). Geiger v2.0: an expanded suite of methods for fitting macroevolutionary models to phylogenetic trees. *Bioinformatics* 30, 2216–2218. doi: 10.1093/bioinformatics/btu181

Pettibone, M. H. (1976). Revision of the genus *macellicephala* mcintosh and the subfamily macellicephalinae hartmann-schröder (polychaeta: polynoidae). *Smithson. Contr. Zool.* 229, 1–71. doi: 10.5479/si.00810282.229

Pettibone, M. H. (1983). A new scale worm (Polychaeta: Polynoidae) from the hydrothermal rift-area off western Mexico at 21°N. *Proc. Biol. Soc. Wash.* 96, 392–399.

Pettibone, M. H. (1985a). New genera and species of deep sea macellicephalinae and harmothoinae galapagos and western mexico at 21°n and from the santa catalina channel. *Proc. Biol. Soc. Wash.* 98, 740–757.

Pettibone, M. H. (1985b). Polychaete worms from a cave in the Bahamas and from experimental wood panels in deep water of the North Atlantic (Polynoidae, Macellicephalinae, Harmothoinae). *Proc. Biol. Soc. Wash.* 98, 127–149.

Pettibone, M. H. (1993). Revision of some species referred to *Antinoe*, *Antinoella*, *Antinoana*, *Bylgides*, and *Harmothoe* (Polychaeta: Polynoidae: Harmothoinae). *Smithson. Contr. Zool.* 545, 1–41. doi: 10.5479/si.00810282.545

Pettibone, M. (1997). Revision of the scaleworm genus Eulagisca McIntosh (Polychaeta: Polynoidae) with the erection of the subfamily Eulagiscinae and the new genus Paraeulagisca. *Proc. Biol. Soc. Wash.* 110, 537–551.

R Core Team. (2020). *R: A Language and Environment for Statistical Computing*. Vienna: R Foundation for Statistical Computing.

R Studio Team. (2020). *RStudio: Integrated Development Environment for R*. Boston, MA: RStudio, PBC.

Rambaut, A., Drummond, A. J., Xie, D., Baele, G., and Suchard, M. A. (2018). Posterior summarization in bayesian phylogenetics using Tracer 1.7. *Syst. Biol.* 67, 901–904. doi: 10.1093/sysbio/syy032

Ratnasingham, S., and Hebert, P. D. N. (2007). BARCODING: bold: The Barcode of Life Data System: barcoding. *Mol. Ecol. Notes* 7, 355–364. doi: 10.1111/j.1471-8286.2007.01678.x

Read, G. B., and Fauchald, K. (2021). *World Polychaeta database. Polynoidae Kinberg, 1856*. Available online at: http://www.marinespecies.org/aphia.php?p=taxdetails&id=939 (accessed June 05, 2021).

Ronquist, F., Teslenko, M., van der Mark, P., Ayres, D. L., Darling, A., Höhna, S., et al. (2012). MrBayes 3.2: Efficient Bayesian phylogenetic inference and model choice across a large model space. *Syst. Biol.* 61, 539–542. doi: 10.1093/sysbio/sys029

Rybakova, E., Kremenetskaia, A., Vedenin, A., Boetius, A., and Gebruk, A. (2019). Deep-sea megabenthos communities of the Eurasian Central Arctic are influenced by ice-cover and sea-ice algal falls. *PLoS One* 14:e0211009. doi: 10.1371/journal.pone.0211009

Schüller, M., Ebbe, B., and Wägele, J.-W. (2009). Community structure and diversity of polychaetes (Annelida) in the deep Weddell Sea (Southern Ocean) and adjacent basins. *Mar. Biodiv.* 39, 95–108. doi: 10.1007/s12526-009-0009-4

Simon-Lledó, E., Bett, B. J., Huvenne, V. A. I., Schoening, T., Benoist, N. M. A., Jeffreys, R. M., et al. (2019). Megafaunal variation in the abyssal landscape of the

Clarion Clipperton Zone. *Prog. Oceanogr.* 170, 119–133. doi: 10.1016/j.pocean.2018.11.003

Simon-Lledó, E., Pomee, C., Ahokava, A., Drazen, J. C., Leitner, A. B., Flynn, A., et al. (2020). Multi-scale variations in invertebrate and fish megafauna in the mid-eastern Clarion Clipperton Zone. *Prog. Oceanogr.* 187:102405. doi: 10.1016/j.pocean.2020.102405

Sjölin, E., Erséus, C., and Källersjö, M. (2005). Phylogeny of Tubificidae (Annelida, Clitellata) based on mitochondrial and nuclear sequence data. *Mol. Phylogenet. Evol.* 35, 431–441. doi: 10.1016/j.ympev.2004.12.018

Smith, C., Deleo, F., Bernardino, A., Sweetman, A., and Arbizu, P. (2008). Abyssal food limitation, ecosystem structure and climate change. *Trends Ecol. Evol.* 23, 518–528. doi: 10.1016/j.tree.2008.05.002

Smith, C. R., and Hamilton, S. C. (1983). Epibenthic megafauna of a bathyal basin off southern California: patterns of abundance, biomass, and dispersion. *Deep Sea Res. Part A Oceanogr. Res. Pap.* 30, 907–928. doi: 10.1016/0198-0149(83)90048-1

Stamatakis, A. (2014). RAxML version 8: a tool for phylogenetic analysis and post-analysis of large phylogenies. *Bioinformatics* 30, 1312–1313. doi: 10.1093/bioinformatics/btu033

Trueblood, D. D., Gallagher, E. D., and Gould, D. M. (1994). Three stages of seasonal succession on the Savin Hill Cove mudflat, Boston Harbor. *Limnol. Oceanogr.* 39, 1440–1454. doi: 10.4319/lo.1994.39.6.1440

Trueman, E. R., Brand, A. R., and Davis, P. (1966). The effect of substrate and shell shape on the burrowing of some common bivalves. *J. Molluscan Stud.* 37, 97–109. doi: 10.1093/oxfordjournals.mollus.a064983

Tyler, P. A., and Young, C. M. (1999). Reproduction and dispersal at vents and cold seeps. *J. Mar. Biol. Ass.* 79, 193–208. doi: 10.1017/S0025315499000235

Uschakov, P. V. (1977). "Phylogenetic relationship in the family Polynoidae (Polychaeta)," in *Essays on the Polychaetous Annelids in Memory of Dr. Olga Hartman*, eds D. Reish and K. Fauchald (Los Angeles: Allan Hancock Foundation), 29–38.

Uschakov, P. V. (1982). *Fauna of the USSR. (2)1: Polychaetes. Polychaetes of the suborder Aphroditiformia of the Arctic Ocean and the Northwestern Part of the Pacific Ocean. Families Aphroditidae and Polynoidae*. Moscow: NAUKA, Academy of Sciences of the USSR, Zoological Institute.

Vaidya, G., Lohman, D. J., and Meier, R. (2011). SequenceMatrix: concatenation software for the fast assembly of multi-gene datasets with character set and codon information. *Cladistics* 27, 171–180. doi: 10.1111/j.1096-0031.2010.00329.x

Vavrek, M. (2011). fossil: palaeoecological and palaeogeographical analysis tools. *Palaeontol. Electron.* 14:2011.

Volkmann, S. E., Kuhn, T., and Lehnen, F. (2018). A comprehensive approach for a techno-economic assessment of nodule mining in the deep sea. *Miner. Econ.* 31, 319–336. doi: 10.1007/s13563-018-0143-1

Volkmann, S. E., and Lehnen, F. (2018). Production key figures for planning the mining of manganese nodules. *Mar. Georesour. Geotechnol.* 36, 360–375. doi: 10.1080/1064119X.2017.1319448

Volz, J. B., Mogollón, J. M., Geibert, W., Arbizu, P. M., Koschinsky, A., and Kasten, S. (2018a). Natural spatial variability of depositional conditions, biogeochemical processes and element fluxes in sediments of the eastern Clarion-Clipperton Zone, Pacific Ocean. *Deep Sea Res. Part A Oceanogr. Res. Pap.* 140, 159–172. doi: 10.1016/j.dsr.2018.08.006

Volz, J. B., Mogollón, J. M., Geibert, W., Martinez Arbizu, P., Koschinsky, A., and Kasten, S. (2018b). Total organic carbon contents of sediment cores retrieved during R/V SONNE cruise SO239 in the BGR area. *Pangaea* 2018:894854. doi: 10.1594/PANGAEA.894854

Volz, J. B., Mogollón, J. M., Geibert, W., Martinez Arbizu, P., Koschinsky, A., and Kasten, S. (2018c). Total organic carbon contents of sediment cores retrieved during R/V SONNE cruise SO239 in the IOM area. *Pangaea* 2018:894858. doi: 10.1594/PANGAEA.894858

Volz, J. B., Mogollón, J. M., Geibert, W., Martinez Arbizu, P., Koschinsky, A., and Kasten, S. (2018d). Total organic carbon contents of sediment cores retrieved during R/V SONNE cruise SO239 in the GSR area. *Pangaea* 2018:894855. doi: 10.1594/PANGAEA.894855

Volz, J. B., Mogollón, J. M., Geibert, W., Martinez Arbizu, P., Koschinsky, A., and Kasten, S. (2018e). Total organic carbon contents of sediment cores retrieved during R/V SONNE cruise SO239 in the IFREMER-1 area. *Pangaea* 2018:894856. doi: 10.1594/PANGAEA.894856

Volz, J. B., Mogollón, J. M., Geibert, W., Martinez Arbizu, P., Koschinsky, A., and Kasten, S. (2018f). Total organic carbon contents of sediment cores retrieved during R/V SONNE cruise SO239 in the IFREMER-2 area. *Pangaea* 2018:894857. doi: 10.1594/PANGAEA.894857

Volz, J. B., Mogollón, J. M., Geibert, W., Martinez Arbizu, P., Koschinsky, A., and Kasten, S. (2018g). Total organic carbon contents of sediment cores retrieved during R/V SONNE cruise SO239 in the APEI3 area. *Pangaea* 2018:894795. doi: 10.1594/PANGAEA.894795

Wang, L.-G., Lam, T. T.-Y., Xu, S., Dai, Z., Zhou, L., Feng, T., et al. (2020). Treeio: an r package for phylogenetic tree input and output with richly annotated and associated data. *Mol. Biol. Evol.* 37, 599–603. doi: 10.1093/molbev/msz240

Washburn, T. W., Menot, L., Bonifácio, P., Pape, E., Błażewicz, M., Bribiesca-Contreras, G., et al. (2021). Patterns of macrofaunal biodiversity across the clarion-clipperton zone: an area targeted for seabed mining. *Front. Mar. Sci.* 8:250. doi: 10.3389/fmars.2021.626571

Wedding, L. M., Friedlander, A. M., Kittinger, J. N., Watling, L., Gaines, S. D., Bennett, M., et al. (2013). From principles to practice: a spatial approach to systematic conservation planning in the deep sea. *Proc. R. Soc. B.* 280:20131684. doi: 10.1098/rspb.2013.1684

Wickham, H. (2007). Reshaping Data with the reshape Package. *J. Stat. Soft.* 21:12. doi: 10.18637/jss.v021.i12

Wickham, H. (2016). *ggplot2: Elegant Graphics for Data Analysis*. New York, NY: Springer.

Wickham, H., François, R., Henri, L., and Müller, K. (2020). *dplyr: A Grammar of Data Manipulation*. Available online at: https://CRAN.R-project.org/package=dplyr (accessed June 18, 2021).

Wilson, G. D. F. (2017). Macrofauna abundance, species diversity and turnover at three sites in the Clipperton-Clarion Fracture Zone. *Mar. Biodiv.* 47, 323–347. doi: 10.1007/s12526-016-0609-8

Wu, X., Zhan, Z., and Xu, K. (2019). Two new and two rarely known species of *Branchinotogluma* (Annelida: Polynoidae) from deep-sea hydrothermal vents of the Manus Back-Arc basin, with remarks on the diversity and biogeography of vent polynoids. *Deep Sea Res. Part 1 Oceanogr. Res. Pap.* 149:103051. doi: 10.1016/j.dsr.2019.05.011

Yu, G., Smith, D. K., Zhu, H., Guan, Y., and Lam, T. T. (2017). Ggtree: an r package for visualization and annotation of phylogenetic trees with their covariates and other associated data. *Methods Ecol. Evol.* 8, 28–36. doi: 10.1111/2041-210X.12628

Zhang, Y., Chen, C., and Qiu, J.-W. (2018). Sexually dimorphic scale worms (annelida: polynoidae) from hydrothermal vents in the okinawa trough: two new species and two new sex morphs. *Front. Mar. Sci.* 5:112. doi: 10.3389/fmars.2018.00112

Zhou, Y., Wang, Y., Zhang, D., and Wang, C. (2018). *Branchinotogluma bipapillata* n. sp., a new branchiate scale worm (Annelida: Polynoidae) from two hydrothermal fields on the Southwest Indian Ridge. *Zootaxa* 4482:527. doi: 10.11646/zootaxa.4482.3.5

Conflict of Interest: The authors declare that the research was conducted in the absence of any commercial or financial relationships that could be construed as a potential conflict of interest.

Publisher's Note: All claims expressed in this article are solely those of the authors and do not necessarily represent those of their affiliated organizations, or those of the publisher, the editors and the reviewers. Any product that may be evaluated in this article, or claim that may be made by its manufacturer, is not guaranteed or endorsed by the publisher.

Copyright © 2021 Bonifácio, Neal and Menot. This is an open-access article distributed under the terms of the Creative Commons Attribution License (CC BY). The use, distribution or reproduction in other forums is permitted, provided the original author(s) and the copyright owner(s) are credited and that the original publication in this journal is cited, in accordance with accepted academic practice. No use, distribution or reproduction is permitted which does not comply with these terms.

frontiers in Marine Science

ORIGINAL RESEARCH
published: 30 August 2021
doi: 10.3389/fmars.2021.630616

Regional Variation in Communities of Demersal Fishes and Scavengers Across the CCZ and Pacific Ocean

Jeffrey C. Drazen[1], Astrid B. Leitner[1,2], Daniel O. B. Jones[3] and Erik Simon-Lledó[3]*

[1] Department of Oceanography, University of Hawai'i at Mānoa, Honolulu, HI, United States, [2] Monterey Bay Aquarium Research Institute, Moss Landing, CA, United States, [3] Ocean BioGeosciences Group, National Oceanography Centre, Southampton, United Kingdom

We synthesize and analyze data from visual transecting approaches and baited camera studies to evaluate fish and invertebrate scavenger communities across the Clarion-Clipperton Zone (CCZ), an area of intense deep-sea mining interest, and neighboring areas of the abyssal Pacific. In abyssal regions including the CCZ most of the top predators are large mobile fishes and crustaceans, and the majority of these are also opportunistic scavengers. Top predators can exert important ecosystem influences and they can be susceptible to sustained anthropogenic disturbances, necessitating their study in the CCZ mining region. In total 157 baited camera deployments from 3 mining exploration license areas, 4 APEIs (Areas of Particular Environmental Interest – one type of no mining zone) and 4 other areas in the Pacific (Hawaii, California, New Zealand and Guam) and 122 visual transects from 7 exploration license areas, 4 no mining zones, and the Peru Basin (DISCOL area) were examined. Many taxa were observed in both sampling techniques but visual transects viewed few fishes overall. Fish and scavenger communities and diversity varied across the CCZ, significantly for baited camera data with a parallel but insignificant pattern for visual transects suggesting that even for these highly mobile species, not all regions of the CCZ are equivalent and the CCZ cannot be managed as one homogenous region. Further CCZ communities were different than communities elsewhere in the abyssal Pacific. The regional variations in community composition are largely the result of varying abundances of species rather than species presence/absence given that most, but not all, of the fishes and scavengers observed have very large ranges. On a more local scale, seamounts had a significantly different scavenger community than neighboring abyssal plains and thus contribute to regional diversity. Visual transect data revealed a similar but insignificant pattern due to low sample sizes. Given the coarse spatial resolution of sampling of fish and scavenger communities in the CCZ, it is not possible to evaluate if no mining zones (APEIs) adequately represent these communities nor where, or if, any biogeographic boundaries exist in the CCZ region. It is possible to conclude that a network of APEIs that covers the spectrum of available habitats at regional and more local scales will be key to conserving fish and scavenger biodiversity.

Keywords: baited camera, deep sea mining, marine protected areas, visual transects, abyssal

OPEN ACCESS

Edited by:
Malcolm Ross Clark, National Institute of Water and Atmospheric Research (NIWA), New Zealand

Reviewed by:
Francis Neat, World Maritime University, Sweden
Rosanna J. Milligan, Nova Southeastern University, United States

****Correspondence:***
Jeffrey C. Drazen
jdrazen@hawaii.edu

Specialty section:
This article was submitted to Deep-Sea Environments and Ecology, a section of the journal Frontiers in Marine Science

Received: *18 November 2020*
Accepted: *20 July 2021*
Published: *30 August 2021*

Citation:
Drazen JC, Leitner AB, Jones DOB and Simon-Lledó E (2021) Regional Variation in Communities of Demersal Fishes and Scavengers Across the CCZ and Pacific Ocean. Front. Mar. Sci. 8:630616. doi: 10.3389/fmars.2021.630616

INTRODUCTION

Interest in exploitation of manganese nodules on the deep seafloor has increased dramatically in the last two decades. Much of this interest continues to be focused on the Clarion Clipperton Zone (CCZ). The CCZ covers about 6 million km^2 of the subtropical eastern North Pacific, roughly between Hawaii and central America (Lodge et al., 2014). This abyssal region ranges in depth from about 4,000 to 5,500 m. It is bounded by the Clarion fracture zone to the north and the Clipperton fracture zone to the south. This area spans gradients in overlying primary production, nodule density and includes a large number of deep seamounts and abyssal hills (Wedding et al., 2013).

Research into the ecological effects of deep-sea polymetallic nodule mining began in the 1970's and it has informed the International Seabed Authority (ISA) in its task of the management of deep-sea mining including the need to ensure the effective protection of the marine environment. Early research in the CCZ focused on understanding the potential for recovery of benthic communities to simulated mining disturbances. Six experiments in the CCZ and another in the south Pacific at the DISCOL site have shown severe reductions in faunal densities and diversity post-disturbance with generally slow recovery (reviewed in Jones et al., 2017). As a means of protecting the marine environment in the Area, the ISA has formalized a process of regional environmental management plans that includes a spatial management component for the CCZ (Wedding et al., 2013). This largely consists of a system of nine no mining areas or Areas of Particular Environmental Interest (APEI) that were established based on ecological principals and what was known of the distribution of community drivers such as seafloor organic matter flux and nodule density. Furthermore, the ISA requires that mining contractors develop ecological baselines in their exploration license areas (hereafter simply called license areas) as part of their applications for mining and by which to assess future environmental impacts. To meet the goals of effective spatial management and monitoring of environmental effects, a flurry of new research has occurred. This research has focused on establishing ecological baselines prior to mining, generating faunal habitat associations (Amon et al., 2017; Simon-Lledó et al., 2019b,c, 2020), and evaluating biogeography and species or population connectivity (Kersten et al., 2017; Taboada et al., 2018; Bribiesca-Contreras et al., 2021). Given the accumulated, yet sparse, knowledge about abyssal CCZ ecosystems and faunal groups, broad scale syntheses of the distributions of communities and their spatial variability are timely and could help evaluate spatial management plans such as the appropriateness of the APEI network.

It is vital to include studies on the abundance, diversity, and community structure of top predators both in broad scale syntheses and when conducting the mandated baseline surveys, assessing possible environmental impacts of mining activities, and planning spatial management strategies. In abyssal regions, including the CCZ most of the top predators are large mobile fishes and crustaceans, and the majority of these are also opportunistic scavengers (Drazen and Sutton, 2017). Top trophic level animals have been shown to control prey biomass or abundance, exert selective pressures, influence prey diversity, and alter the behavior and habitat choices of potential prey (Myers et al., 2007; Polovina et al., 2009; Estes et al., 2011; Ripple et al., 2014; Drazen and Sutton, 2017). Top predators are also highly susceptible to both direct and indirect anthropogenic changes, particularly habitat alteration, because many have large habitat requirements (Fosså et al., 2002; Ryall and Fahrig, 2006; Ripple et al., 2014; Wenger et al., 2017). The importance of this faunal group is recognized by the ISA and demersal fishes and scavengers are a baseline taxonomic group recommended for study. Changes in the abundance, composition, and size distribution of deep-sea fishes and shrimps have been documented in response to direct activities such as fishing and to its indirect habitat alteration (Watling and Norse, 1998; Devine et al., 2006; Morato et al., 2006; Puig et al., 2012; Pusceddu et al., 2014; Mindel et al., 2017) and in at least one case for mine tailings disposal at upper bathyal depths (Brewer et al., 2007). Fishes and mobile scavengers have been sampled in the CCZ during various programs (Jones et al., 2017; Linley et al., 2017; Harbour et al., 2020) and ecologically, they are an important group for a regional synthesis.

Abyssal top predators are most frequently sampled using visual transecting approaches and baited cameras. Visual transecting with remotely operated vehicles (ROVs), towed cameras and autonomous underwater vehicles (AUVs) can provide valuable and quantitative measures of density and diversity (e.g., Milligan et al., 2016; Drazen et al., 2019). However, these animals are highly mobile, sensitive to light and noise, and generally occur at low densities. For example, in an extensive underwater survey of the Porcupine Abyssal Plain in the Atlantic, only 0.11 to 0.29% of images from AUV camera surveys contained fish (Milligan et al., 2016). This can lead to underestimations of top predator densities, unless large areas are surveyed. A complementary approach is the use of baited cameras (Bailey et al., 2007) that can attract these scavenging fishes and invertebrates to the camera system where they can be quantified (e.g., Linley et al., 2017; Harbour et al., 2020). Baited camera systems have been used to census fish populations from shallow to deep water and to evaluate the fish diversity, relative abundance and community composition and to assess the efficacy of spatial management plans (Priede and Bagley, 2000; Bailey et al., 2007; Linley et al., 2017; Sackett et al., 2017). However, baited cameras do present the challenge that only a subset of the fauna will be attracted and its often very difficult to quantify absolute densities because the area of attraction is unknown or roughly approximated (Priede and Bagley, 2000; Farnsworth et al., 2007). Given the pros and cons of both methods, it is most useful to combine visual transect and baited camera techniques (e.g., Drazen et al., 2019).

In this paper we synthesize and analyze data from both visual transecting approaches and baited camera studies to evaluate the diversity, abundance, distribution and community structure of fishes and scavengers across the CCZ region. Our goals were to describe these communities across the region for the first time, address whether these mobile animal communities differ across the region and to other abyssal regions in the Pacific, begin to understand some of the environmental drivers of any

differences found, evaluate if biogeographic boundaries exist, and finally address whether the current system of APEIs are likely to contain fish and scavenger communities that are representative of the region overall.

MATERIALS AND METHODS

Image Transect Data

Quantitative and qualitative assessments of fish distributions were made using seabed imaging transects at abyssal depths (3,000–6,000 m). Images were obtained using cameras mounted on ROVs, autonomous underwater vehicles (AUVs) and towed cameras (**Table 1**; and see caption for a list of acronyms for station abbreviations). We considered these methods broadly comparable. All the data compared quantitatively used downward-facing imagery at similar altitudes. Only the data from Vanreusel et al. (2016) and Cuvelier et al. (2020) were taken at a slightly oblique angle (to avoid the ROV frame in the image), and these data were only used in the presence-only analysis (see below). All three platform types create noise, light and water movement, which may influence fish behavior, leading to avoidance or attraction, usually on a species-specific basis. There are some differences between platforms, including in survey speed (all < 1.5 m s^{-1}), light (AUVs do not have continuous lighting, the other platforms do), size (ROVs are bigger and less hydrodynamic than other platforms) and propulsion method (ROV and AUVs are self-propelled), so comparisons between gear types should be treated with some caution. It appears that there is greater variation between species responses than between platform types (e.g., Trenkel et al., 2004).

A total of 24 areas were evaluated including six APEIs, contractor areas and areas to the periphery of the CCZ. Out of these, the 13 datasets with the highest image resolution, lowest above-seabed altitude (2–5 m) of collection, and with precise measurements of the seabed area encompassed by sampling (minimum 4,000 m^2) were used for quantitative evaluation. These included data from (east to west): two sites within the eastern Kiribati EEZ (data from Kiribati A was excluded as only 3 fish were observed, Simon-Lledó et al., 2019d); western CCZ APEIs 1, 4, and 7 (Durden et al., 2021); TOML areas B, C, and D (Simon-Lledó et al., 2020); eastern CCZ APEI6 (Simon-Lledó et al., 2019b,c), and the UK-1 area (Amon et al., 2016). Fish abundance, diversity, and community composition were extracted from each quantitative dataset (**Table 1**). In addition, we included fish community data collected in 2015 from the Peru Basin (DISCOL area; **Figure 1**), a well-studied abyssal nodule area, for some comparisons (Drazen et al., 2019; Simon-Lledó et al., 2019a).

We also evaluated several datasets for presence of taxa only. The area surveyed is very important. Few fish in a small area may be an artifact of low sampling effort but few fish in a large surveyed area suggests that there is truly a low density of fishes rather than a sampling artifact. We used a threshold of 1,000 m^2, based upon an analysis of sample area effects on all megafauna (Simon-Lledó et al., 2019b). Data from a towed camera used in the OMCO A-G sites (McQuaid, 2020), fell below this threshold and were used only for presence information. Measures of diversity and community composition are dependent upon adequate number of specimens sampled. Hence, even if a large area is sampled and density may be derived, the observation of few animals reduces confidence in community composition metrics. For this reason, Kiribati A was only used for presence data (3 fish observed, each representing a different taxa). Data were also made available from towed cameras from KODOS and APEI 9 areas and while counts of fishes were available only a subset of images were available to confirm identities (Ju et al., unpublished data). ROV data from BGR, GSR, and APEI 3 plains and seamounts (Cuvelier et al., 2020) included exploration and opportunistic sampling and Cuvelier et al. (2020) did not feel data for fishes were representative of the whole community, so only taxon presence was used.

Baited Camera Data

Baited cameras are deployed as free vehicle moorings for short (12–48 h) deployments to the seabed. Bait attracts mobile fishes and scavengers to the area in front of the camera for a census. Still photographs or video clips are recorded in time lapse over the duration of the deployment from either an overhead vertical position or a horizontal/oblique position.

Given the mobile nature of the abyssal fish and scavenger fauna, all available baited camera deployments across the Pacific Ocean, including those in the CCZ, were assembled. Data were gathered from the literature and by contribution of raw data by lead scientists of past studies. A total of 12 studies representing 158 deployments were compiled (**Table 2** and **Figure 1**). Three studies representing 43 deployments were directly from the CCZ region: OMS and UK1 (Linley et al., 2017), APEIs 1, 4, 6, and 7 (Linley et al., 2017; Leitner et al., 2021a) and BGR (Harbour et al., 2020). The remainder ranged from New Zealand to California and south to the Peru Basin DISCOL site (Priede and Smith, 1986; Priede et al., 1990, 1994; Jamieson et al., 2009, 2011; Yeh and Drazen, 2009, 2011; Linley et al., 2017; Drazen et al., 2019). Data included camera viewing angle and area, duration of deployment and sampling interval to facilitate sample intercomparison. Only studies that occurred at abyssal depths (3,000–6,000 m) and presented the maximum number of animals visible during deployment (MaxN) were included. Many studies also presented the time of first arrival for each taxon which has been used as an indicator of relative abundance if current speeds and fish swimming speeds are available (Priede and Bagley, 2000). Often these metrics were not available in the studies examined so we used MaxN for assessment of diversity and community composition.

Several methodological issues were evaluated. First, deployment durations varied considerably across the dataset from <5 to 67 h. Examination of this data showed that deployments <5 h had much lower MaxN compared to regionally co-occurring deployments, and so they were eliminated ($n = 4$; Linley et al., 2017). One deployment used non-standard bait (Yeh and Drazen, 2011) which is also known to affect survey results (Fleury and Drazen, 2013; Wraith et al., 2013) and was eliminated. Finally, while no differences between vertical and oblique camera views was detectable, six deployments used

TABLE 1 | Camera survey areas, sampling metrics and associated estimates for fish density (mean ± std dev), number of taxa observed (see also **Figure 3**), and asymptotic taxa richness (see section "Materials and Methods") with 95% confidence intervals (for quantitative transects).

Area	Method	# transects	Area surveyed (ha)	# of fish	Fish density (# ha^{-1})	# taxa	asymptotic richness
UK 1	ROV	4	0.42	7	16 ± 15.2	4	5.70 ± 2.81
BGR*	ROV	2/2		98		19	
APEI 6	AUV	12	1.86	74	39.6 ± 13.7	9	11.05 ± 4.04
GSR*	ROV	2/1		16		4	
TOML D	Towed	3	2.02	79	36.5 ± 8.9	10	12.90 ± 4.80
OMCO G*	Towed	1	0.08	0		0	
APEI 3*	ROV	2/1		13		7	
APEI 9*	Towed	3		48		5	
OMCO F*	Towed	2	0.16	0		0	
OMCO E*	Towed	1	0.08	2		0	
TOML C	Towed	4	2.93	83	27.3 ± 13.9	14	17.42 ± 5.94
OMCO D*	Towed	1	0.08	0		0	
KODOS*	Towed	7		78			
TOML B	Towed	4	2.50	46	16.3 ± 7.3	11	15.09 ± 5.56
OMCO C*	Towed	1	0.08	1		1	
OMCO A*	Towed	1	0.08	2		1	
OMCO B*	Towed	2	0.16	1		1	
APEI 7	ROV	3/1	1.24/0.30	59	42.5 ± 22.3	9	11.17 ± 4.24
APEI 4	ROV	5/1	2.07/0.30	46	19.5 ± 6.3	9	10.26 ± 4.22
APEI 1	ROV	4	1.82	12	6.6 ± 4.1	4	4.14 ± 2.78
Kiribati A*	Towed	4	0.60	3	3.8 ± 4.7	3	
Kiribati B	Towed	1	0.44	8	18.4	4	5.72 ± 2.71
Kiribati C	Towed	1	0.45	19	42.7	5	7.12 ± 4.28
DISCOL	Towed	46	8.83	281	30.0 ± 18.1	13	18.26 ± 3.72
DISCOL	AUV	2	11.11	376	33.5 ± 9.4	9	
Totals		124	37.59	1344	28.0 ± 17.7	32	

*Areas are organized from east to west in the CCZ (see **Figure 1** for locations) with DISCOL (South Pacific) given last. *indicates an area for which data were used for presence only analysis (see section "Materials and Methods"). # taxa does include those that are higher taxonomic level (e.g., Stephanoberycidae) but does not include unidentified teleost. Numbers of transects and areas surveyed are divided into abyssal plains/seamounts where applicable. Methods for image acquisition include towed camera (towed), autonomous underwater vehicle (AUV) and remotely operated vehicle (ROV). Abbreviations are as follows: Areas of Particular Environmental Interest (APEI), Federal Institute for Geosciences and Natural Resources Germany (BGR), Disturbance and Recolonization experiment (DISCOL), Global Sea Mineral Resources Netherlands (GSR), South Korea Deep Ocean Study (KODOS), Ocean Minerals Company (OMCO), Tonga Offshore Mining Limited (TOML), United Kingdom Seabed Resources Limited (UK).*

a very small viewing area (<0.5 m^2; Jamieson et al., 2009, 2011), MDS results (not shown) suggested different community structure for these deployments compared to other deployments in their area/depth, so they were excluded. The final data set for analysis included 106 deployments across the Pacific of which 43 deployments where from the CCZ (**Table 2**).

Taxonomic Standardization

To standardize fish identification across the datasets we compiled imagery of abyssal fish observations into a single CCZ abyssal photographic fish guide (**Supplementary Material**). It included inputs from taxonomists, from the University of Hawaii video annotation group (The Deep-sea Animal Research Center[1]) who had worked on observations elsewhere in the Pacific as part of the CAPSTONE project (Kennedy et al., 2019), and from the Hawaii Undersea Research Laboratory database (see above link). Voucher specimens from trapping studies were available for a small number of taxa. For instance, morphological taxonomy and/or barcoding approaches were used to confirm identities of the most common and widespread taxon *Coryphaenoides armatus/yaquinae* (Gaither et al., 2015; Linley et al., 2017) and for a few other species such as *Pachycara nazca*, *Illyophis arx*, *Cerataspis monstrosus*, and *Hymenopenaeus nereus*. All transects were annotated using this consistent photo guide, most in the annotation platform BIIGLE (Langenkämper et al., 2017). This ensured a high degree of taxonomic consistency which is required for a broad synthesis of the data.

Considerable effort was applied to ensure that all of the data used the same taxonomy and identified taxa consistently (**Supplementary Material**). A number of earlier studies from off California and in the central North Pacific (Priede and Smith, 1986; Priede et al., 1990, 1994) had been conducted for purposes other than biodiversity assessment and taxa were all identified as *Coryphaenoides armatus/yaquinae*. These studies had to be omitted from the analysis. For the remaining studies there was variability in a few key taxa (Macrouridae, *Bassozetus*, and Synaphobranchidae) as these groups have few obvious visual characteristics to confirm identifications. In a few cases higher

[1]http://www.soest.hawaii.edu/UMC/cms/DARC/index.php

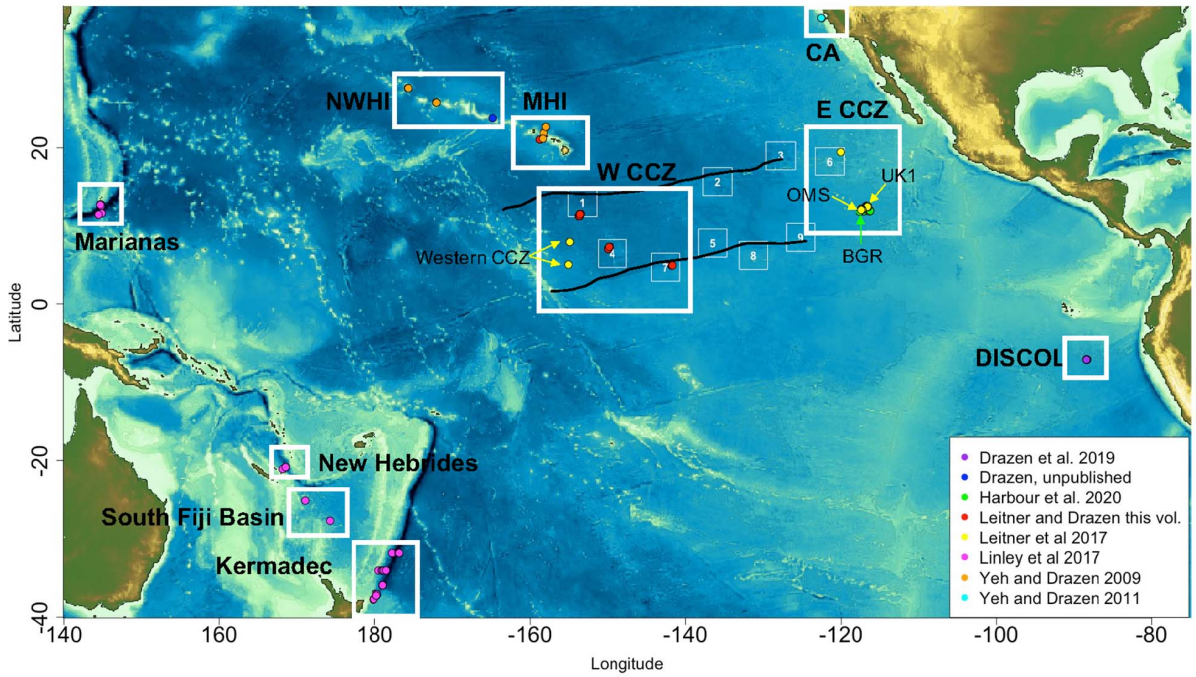

FIGURE 1 | Baited camera sample locations across the Pacific and CCZ region by study. White boxes represent general provinces of sampling.

taxa (genus, family) had to be used for consistency across studies (**Supplementary Table 2**).

Statistical Analysis

Environmental Data

Environmental data were obtained from literature sources. Depth was taken from measurements made during sampling. Particulate organic carbon (POC) flux to the seafloor was obtained from Lutz et al. (2007) and extracted for all sample positions from an equal-area grid of 9-km resolution. These data were calculated using an exponential flux algorithm applied to satellite-derived net primary production data obtained during the period from August 1997 to June 2004. Nodule abundance was taken from regional models with an interpolated resolution of 1 km^2 (McQuaid, 2020). Relative elevation, quantified using broadscale Bathymetric Position Index (BPI), was calculated using a 100 km scale factor from 1 km^2 (inner radius) resolution General Bathymetric Chart of the Oceans (GEBCO) bathymetry data and extracted from McQuaid (2020) for all sample locations[2]. Deployments were also identified by their habitat or stratum, including seamount, abyssal plain, island flank and trench edge.

Diversity

Diversity of fish assemblages sampled with both quantitative image transecting and baited cameras were assessed using Hill numbers which calculate rarified taxa richness (q = 0), exponential Shannon diversity (q = 1), and the inverse of Simpson diversity (q = 2) for each region as well as asymptotic diversity estimates for each site. This approach was used to help constrain the disparities between numbers of observations in each region. Hill numbers were calculated using the iNEXT function in the iNEXT R package (R version 4.0.2) including 95% confidence intervals around the resulting rarefaction and extrapolation sampling curves, which allows for robust comparison of the diversity metrics between sites (Chao et al., 2014; Hsieh et al., 2020).

To further explore differences in fish and scavenger diversity between the eastern and western CCZ, rarified and extrapolated diversity was compared between the two regions also using the iNEXT function in the iNEXT R package. To evaluate the additional diversity provided by samples from CCZ seamounts, the diversity metrics were compared between the eastern and western CCZ excluding seamount deployments. To investigate the drivers of the spatial variability in diversity across the CCZ and across the Pacific from the baited camera dataset, we also used generalized linear models with a gamma error distribution and a log link function to relate observed and asymptotic diversity estimates (for q = 0,1,2) to average station environmental predictors. For the CCZ analysis the predictors used were: POC flux, nodule abundance, and BPI as well as habitat stratum to account for clustering by sampling area. Longitude was excluded due to correlation with stratum and POC flux across the CCZ. For the Pacific analysis the predictors used were: POC flux, habitat type, and longitude.

Community Composition

Community composition was evaluated for both transect and baited camera approaches using multidimensional scaling

[2]https://www.gebco.net/

TABLE 2 | Summary of available published and unpublished baited camera datasets from across the Pacific Ocean between 3,000–6,000 m depth (abyssal) by region and data source.

Region	Data source	# camera deployments
Eastern CCZ		
BGR	Harbour et al., 2020	10
OMS	Linley et al., 2017	6
K1	Linley et al., 2017	6
APEI6	Linley et al., 2017	1
Western CCZ		
Western CCZ	Linley et al., 2017	2
APEI1	Leitner et al., 2021a	7
APEI4	Leitner et al., 2021a	7
APEI7	Leitner et al., 2021a	4
CCZ total		**43**
California, Sta. F	Priede et al., 1990	14/0
California, Sta. M	Priede et al., 1994	11/0
Central California	Yeh and Drazen, 2011	3/2
Central North Pacific Gyre	Priede and Smith, 1986	6/0
	Priede et al., 1990	9/0
DISCOL	Drazen et al., 2019	6
Hawaiian Islands – Main	Leitner et al., unpublished	2
	Yeh and Drazen, 2009	3
Hawaiian Islands – Northwestern	Yeh and Drazen, 2009	4
	Drazen, unpublished	1
Kermadec	Jamieson et al., 2009	1/0
	Jamieson et al., 2011	4/0
	Linley et al., 2017	28/26
Marianas	Jamieson et al., 2009	2/0
	Linley et al., 2017	10
New Hebrides	Linley et al., 2017	7/5
South Fiji Basin	Linley et al., 2017	4
Pacific wide total		158/**106**

# of camera deployments illustrates the samples evaluated/samples used in analysis after methodological standardization.

(MDS), cluster analysis (group average linkage) with associated significance testing using SIMPROF (1,000 permutations) in Primer v6.1 (Clarke and Gorley, 2006). Transect data used fish densities to standardize for variations in total sampling and observations between studies. Densities were square root transformed and a Bray-Curtis similarity matrix was used. For the baited camera data, we used a similar approach with square root transformed MaxN data and a Bray-Curtis similarity matrix. For all sampling approaches, the taxa most responsible for significant (SIMPROF) differences between groups of deployments were identified using a similarity percentages (SIMPER) approach. Where significant structuring in community composition was found, we evaluated the effects of the potential environmental drivers including estimated POC flux (Lutz et al., 2007), depth, habitat stratum (seamount, abyssal plain, trench edge, island flank), and longitude. Nodule abundance was not included because of a high correlation with the longitude predictor (Pearson correlation 0.81) since the dataset included areas outside the CCZ with no nodules. Habitat type was used in favor of the continuous variable BPI because the main goal of this analysis was to ask whether community compositions varies across these morphological habitat categories rather than whether it varies across a gradient of local elevation where island flanks, for example, would have similar values (close to 0) as abyssal plains. PERMANOVA tests with marginal significance tests were used to evaluate the significance of each predictor variable such that the test was repeated multiple times, each time with the full dataset, with the predictors reordered each time so that each predictor variable was the last one to be added to the analysis (reordered model, not reduced model). Significance for each predictor was then evaluated only from partial R-squared values (the proportion of the sum of squares from the total) generated by the corresponding marginal PERMANOVA test (Oksanen et al., 2016, adonis documentation). Data were visualized using a constrained ordination using the same taxa data and predictors using the function capscale() from the R package vegan (Oksanen et al., 2016), which performs a canonical analysis of principle coordinates analysis (CAP). Permutations (n = 9,999) were stratified by region to account for spatial autocorrelation and nestedness.

Biogeography

To evaluate species ranges and biogeographies of fishes and scavengers, we took two approaches. First, using baited camera data (both fishes and other scavengers) we examined overlap in taxa occurrence between individual deployment locations as a function of the geographic distance between the stations. Every pair of stations was assigned a geographic separate distance based on their locations and a number of shared taxa. Shared taxa were then plotted as a function of geographic separation. Second, using both baited camera and transect data (both quantitative and qualitative transects) converted to presence data we compared species overlap (fishes only in this case) by location to estimate how widespread these animals are both across the CCZ and across the Pacific. The overlap was as a frequency histogram of the number of taxa observed in numbers of sampled areas (e.g., how many taxa in one area, two areas etc.).

Diversity and community composition analyses were run in PRIMER v6. Other statistics were run in R version 4.0.2.

RESULTS

Camera Transect Data (CCZ Only)

The camera transect data frequently included very few fishes (**Table 1**). For instance, four transects in Kiribati A (0.60 ha) observed only 3 fish each its own taxon. Some of the OMCO stations only sampled ∼800 m^2 (0.08 ha) in a single transect and observed no fish at all. In contrast some of the TOML areas in the eastern/central CCZ and the APEIs had survey data covering 1.5 to over 2 hectares and observed up to 83 fishes. The DISCOL site in the south Pacific was the most intensively sampled location by far, with a survey that covered nearly 20 hectares and observed 649 individual fishes.

Fish density and diversity varied greatly across the CCZ. From the quantitative transects total fish density ranged from 6.6 fish

ha^{-1} in the northwestern APEI 1 to just over 42 fish ha^{-1} in the west equatorial APEI 7 and Kiribati C areas (**Table 1** and **Figure 2**). There was no significant correlation between mean fish density at each station and its corresponding seafloor POC flux ($r = 0.64$, $p = 0.17$). Rarefied diversity curves suggested that species richness was highest in two areas of Kiribati and lowest in APEI 6 and the DISCOL site (**Figure 3**). Generally, most of the rarefaction curves were not yet nearing an asymptote suggesting that additional sampling is required to characterize the full fish community. The exception was for the DISCOL area (649 fishes representing 17 taxa).

The fish community across the CCZ was dominated by a few common taxa. The most frequently encountered taxa and the one with the highest density was by far *Ipnops meadi*. Other abundant

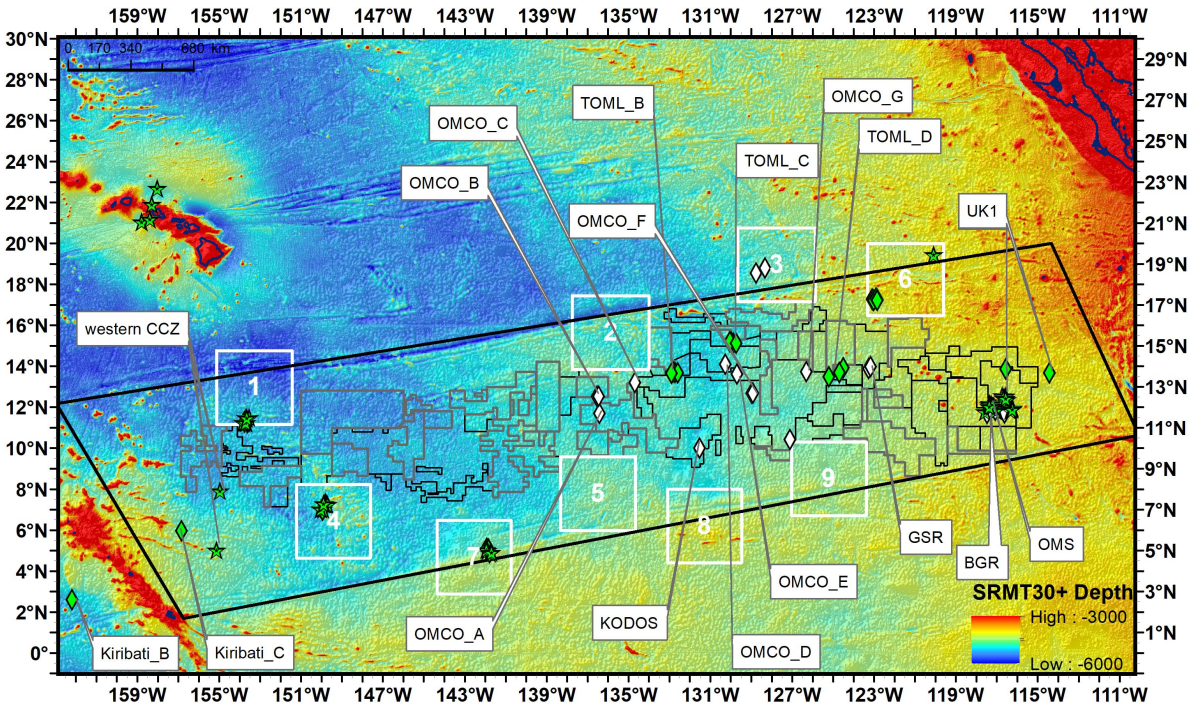

FIGURE 2 | Locations of visual transects (diamonds) and baited camera sample (stars) locations across the CCZ. Quantitative visual transects are in green and non-quantitative in white symbols. Study locations are given as abbreviations (see **Table 1**).

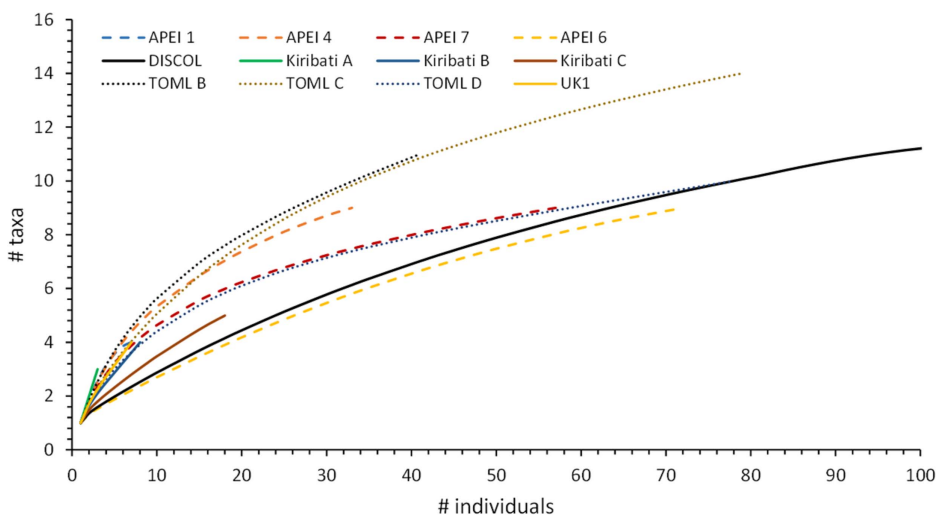

FIGURE 3 | Rarefied fish diversity from quantitative camera transect data by region. Note that for DISCOL considerably more fish were observed and the curve extends to 17 taxa.

taxa included *Abyssoberyx* sp., *Bassozetus* sp. B, *Coryphaenoides armatus/yaquinae*, Ophidiid sp. 5, *Ilyophis arx*, and *Typhlonus nasus* (**Figure 4**). These were also the most frequently observed across transects except for *Ilyophis arx* that was locally abundant at only a few locations (Leitner et al., 2021a, see below and **Supplementary Table 1**). Variability in community composition was high between the transects, so while there was some apparent structure across the CCZ, no statistically significant groupings were found (SIMPROF, $p > 0.05$; **Figure 5**). Generally, transects that were located farther to the west in the CCZ were located to the right of the MDS space progressing from APEIs 1 and 4 and the Kiribati transects to transects from the TOML and APEI6 locations to the left of the MDS space. Additionally, transects in APEI 4 and 7 (one each) that occurred on seamounts rather than the abyssal plain were located to the bottom of the MDS with high densities of the synaphobranchid eel, *I. arx* (**Figure 5**).

Baited Camera Data

Baited camera studies provide a complementary examination of fish and scavenger communities across the CCZ. From the 43 deployments the most commonly observed fish were *C. armatus/yaquinae*, *Bassozetus nasus*, *Barathrites iris*, and *Pachycara* spp. (**Figure 4**; **Supplementary Table 2**). A total of 16 fish taxa were observed in the CCZ region. This represents 44% (14 of 32) of the total fish fauna observed in the camera transects. Furthermore, the baited cameras observed two taxa (Ophididae sp1, *Histiobranchus bathybius*) that were not observed in the camera transects and the *Pachycara* spp., observed with both methods, could be resolved to two species in the baited camera observations. Sixteen invertebrate taxa were observed from the CCZ baited camera deployments including shrimps, ophiuroids, a Plesiodiatematid urchin, Munidopsis crabs, and a few octopuses (**Figure 4**; **Supplementary Table 2**). Shrimp dominated the invertebrate scavenger assemblage across the CCZ, including *Hymenopenaeus nereus* and Penaeoids represented by *Cerataspis monstrosus* and Benthesicymidae. This latter group was very difficult to distinguish from imagery. Across the Pacific abyss, a total of 48 scavenging taxa were observed. There were sixteen taxa not observed in the CCZ, 10 that were restricted to the CCZ observations and 22 taxa that were held in common.

Scavenger assemblages varied significantly across the Pacific (**Figure 6**; SIMPROF, $p < 0.05$). The CCZ communities generally grouped by sampling area and were distinct from those found off California, the Northwestern Hawaiian Islands, and the

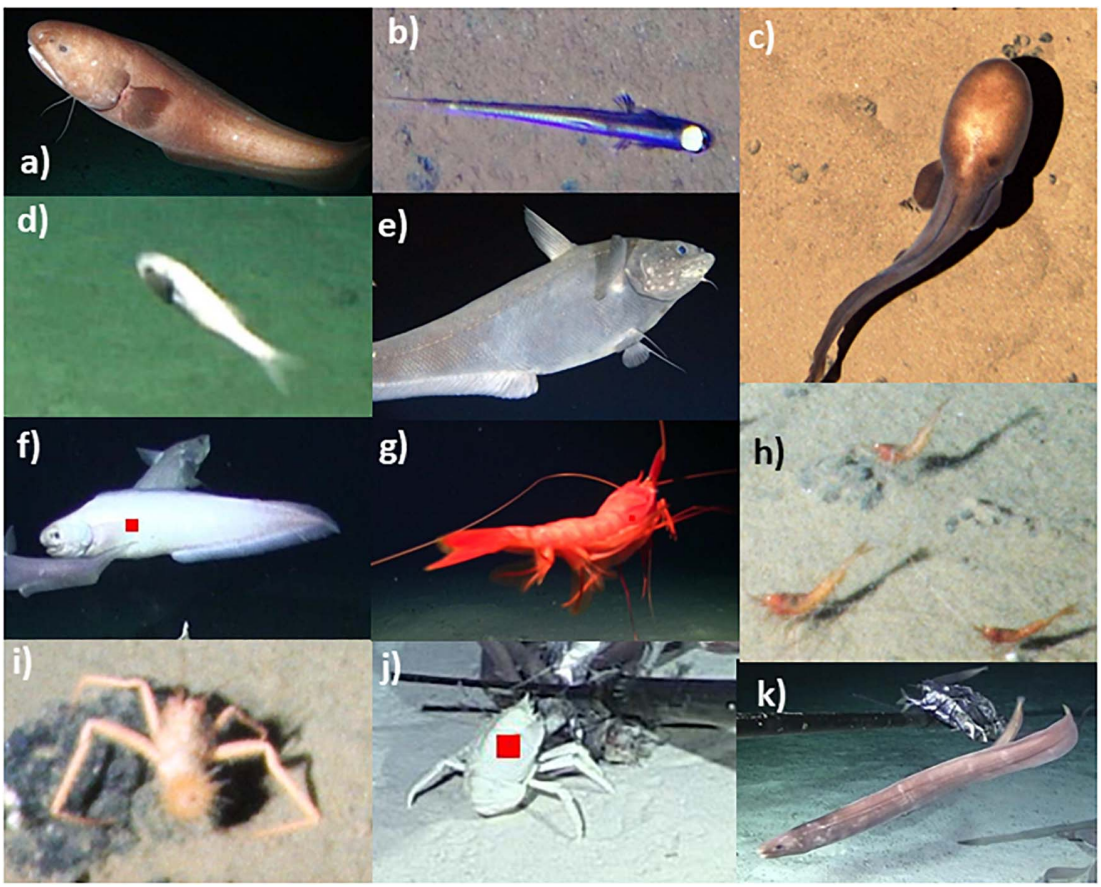

FIGURE 4 | Representative fishes and invertebrate scavengers observed in visual transects and baited cameras. **(a)** *Bassozetus* cf. *nasus*, **(b)** *Ipnops meadi*, **(c)** *Typhlonus nasus*, **(d)** *Abyssoberyx* sp., **(e)** *Coryphaenoides armatus/yaquinae*, **(f)** *Barathrites iris*, **(g)** *Cerataspis monstrosus*, **(h)** *Hymenopenaeus nereus*, **(i)** *Probeebei mirabilis*, **(j)** *Munidopsis* sp., **(k)** *Ilyophis arx*.

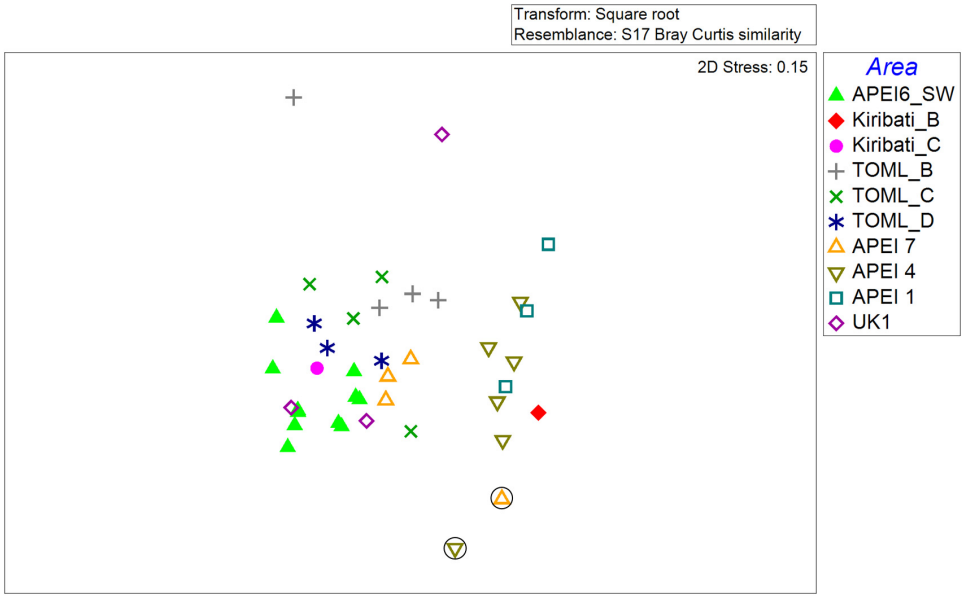

FIGURE 5 | MDS plot of fish community composition based on a square root transformed Bray-Curtis similarity matrix of fish densities for each quantitative transect in each area across the CCZ. Circled symbols represent transects on abyssal seamounts.

western Pacific (e.g., Kermadec and Marianas areas). The CCZ communities were similar to deeper abyssal samples off the main Hawaiian Islands which were occasionally included in significant groups of primarily CCZ samples ($p < 0.05$; SIMPROF). DISCOL samples were also more similar to CCZ samples but these still formed a statistically different outgroup ($p < 0.05$; SIMPROF) because of the frequent occurrence of the hermit crab *Probeebei mirabilis* (SIMPER dissimilarity to CCZ groups = 10–15%).

The scavenger assemblages also varied significantly within the CCZ (**Figure 6**). There was an east to west variability with the most eastern license areas (e.g., OMS, UK1, group e) clustering significantly from the western APEIs ($p < 0.05$; SIMPROF, groups g and h). The differences between these groups was largely driven by higher abundances of the shrimp *H. nereus* and lower abundances of the fishes *Barathrites iris* and *C. armatus/yaquinae* and in the eastern license areas (SIMPER group e vs. g, h). It was even more evident that the seamount samples from the western APEIs had a distinct community from their surrounding abyssal plains. These represented three distinct clusters of deployments (see a, i, and k in **Figure 6**) much less similar to the rest of the deployments. The two clusters representing seamounts in APEI 4 and 7 were largely driven by the occurrence of the eel, *Ilyophis arx*, for APEI 7 deployments (SIMPER, *I. arx* drove 33 to 39% of dissimilarity compared to neighboring plains) and fewer *C. armatus/yaquinae* and both more *I. arx* and *C. monstrosus* for APEI 4 seamounts. Interestingly, the main and northwestern Hawaiian island deployments that were on the island flanks (similar to seamounts) at depths of about 3,000 meters also clustered together (SIMPROF, $p < 0.05$, group b in **Figure 6**).

Diversity also varied across the Pacific and CCZ. Asymptotic taxa richness values were slightly higher on the abyssal plains in the western CCZ compared to the license areas in the eastern CCZ (**Table 3**). These diversities were comparable to those found in Hawaii and DISCOL and higher than those from California and the western Pacific. Looking only at the samples from within the CCZ, the eastern CCZ seems to have a significantly lower estimated species richness than the west (18 versus 29.5 with non-overlapping confidence intervals; **Figure 7A**); however, excluding the additional diversity that the western seamount deployments give to the west, the estimated number of species is no longer significantly different between the regions (22.2 in the east versus 22.5 in the western abyssal plains, overlapping confidence intervals; **Figure 7B**) and no differences were found for H' or Simpson diversity either. This finding again highlights the importance of macroscale habitat features such as seamounts.

We evaluated the drivers of the spatial variability in diversity across the CCZ from the baited camera dataset. In all cases models of the asymptotic diversity estimate agreed with models of observed values. None of these environmental variables significantly explained variation in species richness metrics across the CCZ (glm, $p > 0.05$). There was a significant positive relationship between nodule abundance and both Shannon ($q = 1$) and Simpson ($q = 2$) diversity across the CCZ (glm, $p < 0.05$). There was a significant negative relationship between Simpson diversity and POC flux within CCZ stations (glm, $p < 0.05$). In particular, the APEI7 seamount sites ($n = 2$) had very low diversity and high seafloor POC flux. When these data points were removed the relationship was no longer significant. Across the Pacific there was a significant negative relationship between observed morphospecies richness and POC flux (glm, $p < 0.05$), though this relationship was marginally significant for the asymptotic richness estimate ($p = 0.057$). Across the Pacific baited camera deployments there was also a significant

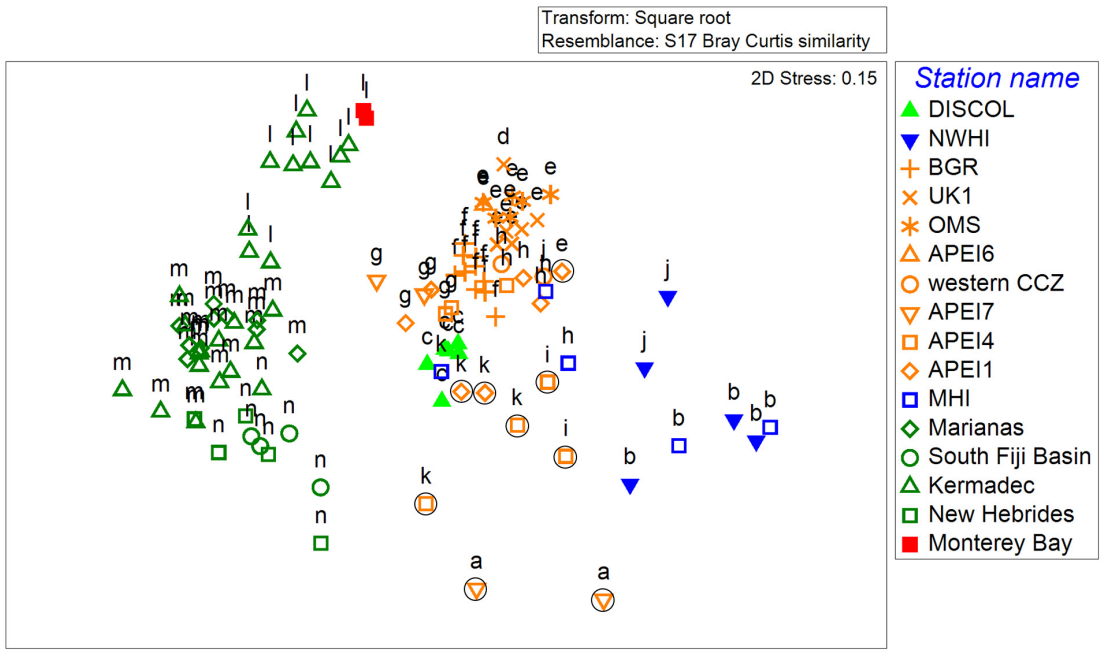

FIGURE 6 | MDS analysis of scavenger communities (MaxN data) across the Pacific. CCZ deployments are in orange, Hawaii locations in blue, DISCOL in light green, the western Pacific locations in dark green, and central California in red. Seamount deployments from the CCZ are circled. Letters above symbols represent significantly similar deployments ($p < 0.05$; SIMPROF).

TABLE 3 | Diversity measures (with standard errors) from baited camera deployments in the abyssal Pacific ordered from east to west in the CCZ followed by other areas of the Pacific.

Region	Area	S ($q = 0$)	*N*	H'($q = 1$)	S ($q = 2$)	Asymptotic richness
Eastern CCZ	UK1	16	152	8.06 ± 0.78	5.73 ± 0.40	24.94 ± 10.11
	OMS	12	140	7.44 ± 0.61	5.84 ± 0.45	16.47 ± 7.15
	APEI6	4	15	3.83 ± 0.53	3.75 ± 0.64	4.00 ± 0.52
	BGR	10	213	7.73 ± 0.36	6.70 ± 0.38	10.0 ± 0.36
Western CCZ	APEI7 AP	11	68	5.19 ± 1.00	2.66 ± 0.41	18.88 ± 11.50
	APEI7 S	12	248	1.74 ± 0.16	1.21 ± 0.05	18.23 ± 7.5
	APEI4 AP	15	110	8.84 ± 1.04	5.42 ± 0.76	22.93 ± 11.56
	APEI4 S	16	186	7.31 ± 0.65	4.42 ± 0.44	18.65 ± 3.47
	APEI1 AP	14	113	9.41 ± 0.67	6.92 ± 0.73	14.99 ± 1.86
	APEI1 S	13	102	6.19 ± 0.84	3.93 ± 0.44	21.91 ± 10.08
	Western CCZ	6	46	4.43 ± 0.54	3.64 ± 0.54	6.49 ± 1.30
Other areas	DISCOL	16	190	9.78 ± 0.67	6.78 ± 0.70	16.50 ± 1.32
	Monterey Bay	5	45	3.98 ± 0.40	3.25 ± 0.45	5.00 ± 0.27
	NWHI	16	128	7.44 ± 0.76	4.76 ± 0.53	18.97 ± 5.25
	MHI AP	19	98	9.86 ± 1.22	5.09 ± 0.81	21.97 ± 3.21
	MHI S	6	9	10.87 ± 6.67	9.00 ± 7.06	13.11 ± 10.40
	Kermadec	12	354	5.31 ± 0.28	3.90 ± 0.24	11.25 ± 0.73
	Marianas	8	78	4.66 ± 0.52	3.74 ± 0.32	12.44 ± 7.11
	New Hebrides	6	83	5.07 ± 0.28	4.56 ± 0.39	6.00 ± 0.16
	South Fiji Basin	8	58	5.52 ± 0.60	4.22 ± 0.61	8.98 ± 2.21

S, observed species richness (q = 0); N, number of fishes observed; H', Shannon diversity (q = 1); S, Simpson diversity (q = 2); and asymptotic taxa richness (this excludes APEI6 and MHI S). Under area, abyssal plains (AP) and seamount (S) are denoted.

effect of seamounts on Simpson diversity, where seamounts had significantly lower Simpson diversity than abyssal plains ($p < 0.05$).

We also evaluated the drivers of the large variation in community composition across the Pacific and CCZ (**Figure 6**) using CAP analysis (**Figure 8**). The first axis was largely related

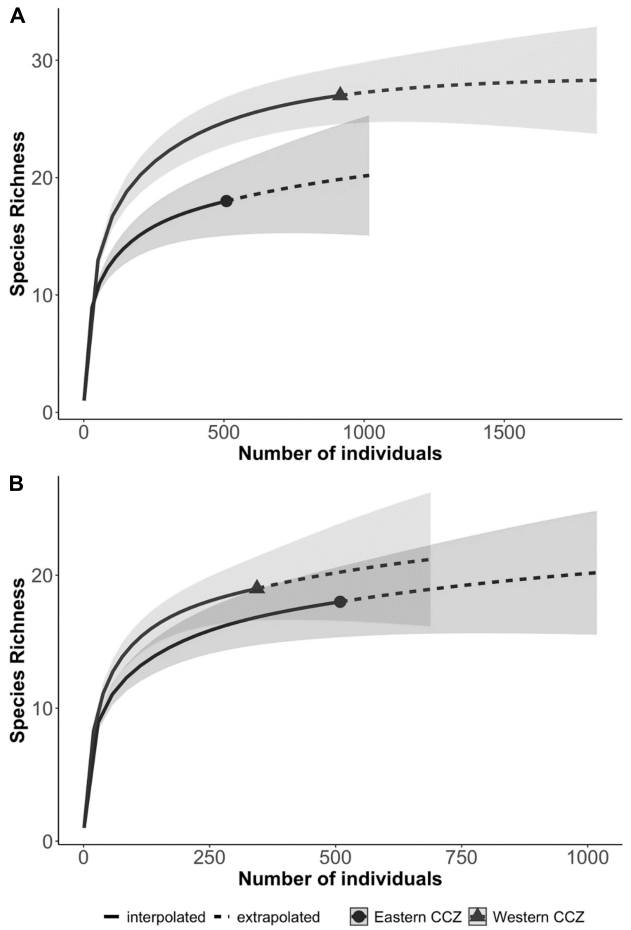

FIGURE 7 | Fish and scavenger diversity (estimated morphotype richness) compared between the eastern and western CCZ **(A)** including all CCZ baited camera deployments and **(B)** excluding all seamount deployments (bottom).

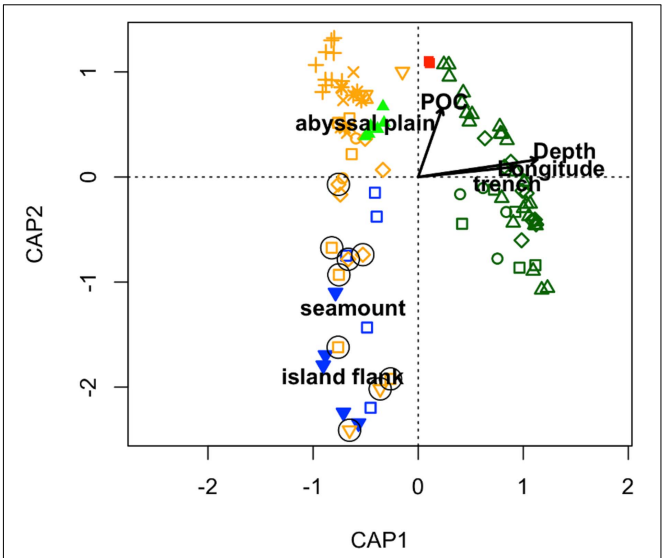

FIGURE 8 | Principal coordinate analysis of the baited camera community composition data (points) across the Pacific evaluated in relation to the environmental drivers particulate organic carbon flux as estimated by Lutz et al. (2007) (lutz_poc), longitude, and depth (arrows with lengths twice biplot scores) and habitat types (centroids). Seamount deployments are circled and symbols are as in **Figure 5**.

to longitude (east to west across the Pacific), suggesting regional variations, but without an indication of why this variation exists environmentally (PERMANOVA marginal significance test, $p = 0.057$). The first axis was also highly correlated with the trench edge habitat type; the communities from the western Pacific region (still at depths of 3,000–6,000 m). Depth was also correlated with this axis which explained some variation and generally the western sites were deeper than the eastern ones (**Supplementary Table 2**). The second axis is largely aligned with variations in POC flux and to a lesser extent, with depth. The cluster of points representing the CCZ, the top left quadrat (**Figure 8**), is largely distributed along this axis. Deployments on seamounts and island flanks are generally clustered together as well. The effect of POC flux was non-significant (PERMANOVA marginal significance test, $p > 0.05$), and both depth and habitat type (abyssal plain, seamount, island flank, trench, and basin) were highly statistically significant (PERMANOVA marginal significance test, $p < 0.01$) in structuring scavenger communities across the Pacific. When evaluating only the CCZ deployments, a second CAP showed dramatic clustering by BBPI (significant marginal test, $p < 0.05$; result not shown), which indicates that macroscale habitat is the most important driver in determining the structure of scavenger communities within the CCZ only. Other factors included in the CCZ-only analysis were non-significant (CAP; modeled POC flux, model predicted nodule abundance, depth).

Fish and Scavenger Ranges and Overlap

The biogeographic ranges of scavenging taxa were evaluated using the baited camera data. Many species of mobile fishes and scavengers had wide ranges as expected (**Figure 9** and **Table 4**) with several locations <2,000 km from one another having as many as 14 shared taxa. Numbers of shared species decline with increasing distance between station locations. At the scale of the CCZ (∼4000 km across) sites share from ∼1 to 6 species, which matches the result of changes in the fish community across the CCZ region.

The transect and baited camera data were combined to evaluate the ranges of fish species across the abyssal Pacific and in relation to the APEI network. Many fishes have very broad overlap between the sites (**Figure 10**), with *C. armatus/yaquinae* occurring at 20 of the 28 locations evaluated. In contrast to these widespread taxa, 9 taxa were found at a single site and a further 9 at only two sites across the Pacific.

DISCUSSION

We present the first synthesis of fish and scavenger communities across the CCZ. Data are still limited. We have taken care to standardize our use of data across different types of

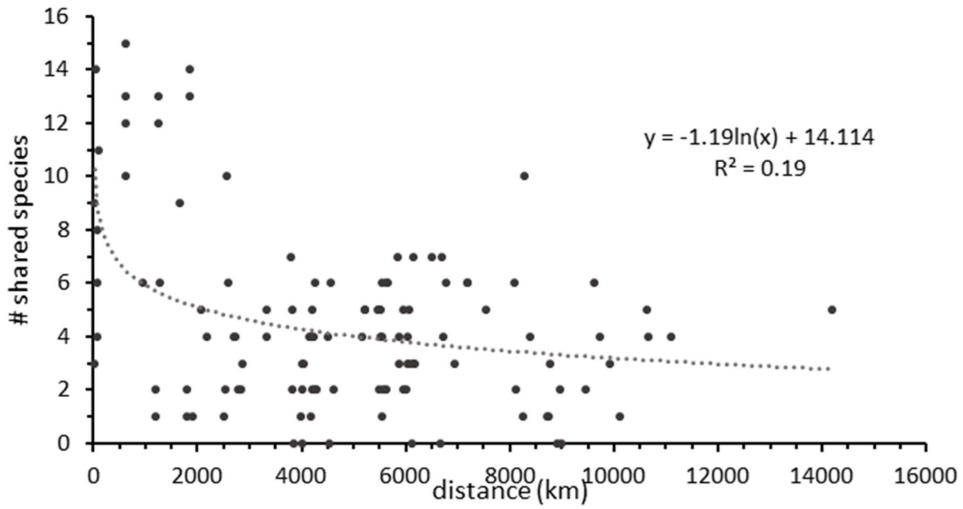

FIGURE 9 | The number of shared scavenger taxa between all possible combinations of baited camera station pairs as a function of distance (km) between the pair.

visual transecting and baited camera deployments (see section "Materials and Methods"). Future studies utilizing parallel ROV and AUV or towed camera methods within the CCZ may provide more robust comparisons than possible here for visual transecting approaches. It is possible that more subtle differences in community composition between areas within the CCZ exist but were not detectable with the current analysis due to low sample sizes or variance between studies. Given many ongoing studies in the region, additional synthesis will be warranted in the future.

Recognizing the limitations with the data available, it is clear that there is a relatively diverse fish and scavenger community across the CCZ that has a number of similarities and differences to the communities of other regions. 32 taxa were observed in the transects and an additional 2 were only seen in baited camera deployments. The most common taxa observed in transects was the fish *Ipnops meadi*. This fish is also commonly observed at the DISCOL site but neither it, nor its congeners, are common in the abyssal NE Pacific (Pearcy et al., 1982; Cailliet et al., 1999; Priede et al., 2020) or the NE Atlantic (Priede et al., 2010) except south of about 32° N where a lower productivity regime apparently alters the abyssal fish community and the confamilial, *Bathymicrops regis,* can be very abundant (Merrett and Fasham, 1998; Christiansen et al., 2015). Ophidiids are particularly abundant and speciose in the CCZ similar to findings in other abyssal subtropical regions such as the Caribbean (Anderson et al., 1985; Crabtree et al., 1991) and subtropical Atlantic (Merrett and Fasham, 1998) but in contrast to temperate latitudes (Merrett et al., 1991; Cailliet et al., 1999; Cousins and Priede, 2012; Milligan et al., 2016). Common to nearly all abyssal studies is the macrourid *C. armatus/yaquinae* (reviewed in King and Priede, 2008), and the CCZ is no exception. Indeed, while the baited camera studies show that the CCZ has a distinct fish and scavenger community compared to other areas of the Pacific, *C. armatus/yaquinae* is seen throughout (**Table 4**).

The CCZ is very large and while general comparisons can be made across the globe, it is clear that the abyssal fish and scavenger communities vary significantly across the CCZ. While the transect data was only suggestive in this regard, the communities differed significantly from east to west in the baited camera data. Using smaller amounts of data this regional variation in community composition has been observed before (Linley et al., 2017; Harbour et al., 2020; Simon-Lledó et al., 2020). This suggests that even for mobile fishes that not all regions of the CCZ are equivalent. Abyssal fish and/or scavenger community change has been attributed to variation in overlying surface water productivity (Crabtree et al., 1991; Merrett and Fasham, 1998; Linley et al., 2017) and, more recently, nodule cover (Linley et al., 2017), as has also been seen in other megafauna (Simon-Lledó et al., 2019c). We did find a positive correlation between Shannon and Simpson diversity and nodule cover but these drivers did not significantly covary with community composition in the CCZ. However, this may derive from sparse data (e.g., $n = 10$ regions/habitats for CCZ) and environmental data layers that were model predictions rather than empirically derived variables, suggesting low statistical power to detect environmental patterns. Depth was a significant driver ($p < 0.01$) of community composition in the baited camera dataset. Depth clearly creates zonation in deep-sea communities (Carney, 2005; Priede, 2017). Though most frequently evaluated at slope depths, even small changes in depth (∼10 m) have now been shown to alter abyssal benthic invertebrate megafaunal communities (Durden et al., 2020). Whether depth is related to the CCZ fish and scavenger community composition because of differences in species pressure adaptations or, more likely, if depth is a proxy for some other covarying environmental driver (e.g., local variation in food accumulation or current regime), cannot be ascertained.

One environmental driver that had a strong effect on fish and scavenger communities was macroscale habitat type, and BPI, a continuous variable that describes habitat types based on their bathymetric profile. Across the Pacific habitat types, seamounts,

TABLE 4 | Presence and absence of fishes and scavengers observed in visual transects (black cells), baited camera deployments (white cells with "bc"), or both (gray cells).

Family	Taxa	East CCZ	Middle CCZ	West CCZ	DISCOL	Monterey Bay	Main HI Islands	NW HI Islands	Kermadec	Marianas	New Hebrides	South Fiji Basin
Chaunacidae	*Chaunacops coloratus*											
Bathysauridae	*Bathysaurus mollis*											
Halosauridae	*Aldrovandia affinis*											bc
	Halosauridae/*Porogadus*											
	Halosauridae											
Ipnopidae	*Bathypterois* spp.											
	Bathytyphlops cf *sewelli*											
	Ipnops meadi		vt	vt								
Liparidae	liparid sp. 1											
	Liparidae							bc	bc			
Macrouridae	*Coryphaenoides armatus/yaquinae*					bc	bc		bc	bc		
	Coryphaenoides filifer					bc						
	Coryphaenoides longicirrhus						bc	bc				
	Coryphaenoides rudis							bc				
	Coryphaenoides leptolepis								bc			
	Coryphaenoides other								bc	bc		
	Macrouridae											
Moridae	*Antimora microlepis*					bc		bc				
Myxinidae	*Eptatretus carlhubbsi*						bc	bc				
Ophidiidae	*Barathrites iris*			bc	bc		bc	bc	bc	bc		bc
	Bassogigas walker			bc				bc			bc	bc
	Bassozetus spp.			bc			bc		bc	bc	bc	bc
	Bassozetus cf *nasus*						bc	bc				
	Bassozetus sp. B						bc			bc		
	Bassozetus sp. juvenile			bc			bc					
	Bathyonus caudalis								bc			
	cf *Holcomycteronus*	v										
	Leucicoris sp.											
	Spectrunculus grandis					bc			bc			
	Ophidiidae sp1	bc										
	Ophidiid sp2						bc	bc				
	Ophidiid sp. 3				v							
	Ophidiid sp. 5	v		v								
	Ophidiid sp. 6											
	Ophidiid sp. 7			v								
	Porogadus sp.											
	Typhlonus nasus											
	Ophidiidae	v										
Stephanoberycidae	*Abyssoberyx* sp.											
	Stephanoberycidae											
Synaphobranchidae	*Histiobranchus bathybius*	bc		bc				bc				
	Ilyophis aryx			bc			bc	bc				
	Ilyophis sp.											
	Synaphobranchus brevidorsalis						bc	bc				
	Synphobranchidae				bc				bc		bc	bc
Zoarcidae	*Pachycara* spp.	bc		bc		bc	bc	bc	bc	bc	bc	bc
	Zoarcidae sp1	bc										
	Zoarcidae sp2	bc		bc								
	Zoarcidae											

(Continued)

TABLE 4 | Continued

Family	Taxa	East CCZ	Middle CCZ	West CCZ	DISCOL	Monterey Bay	Main HI Islands	NW HI Islands	Kermadec	Marianas	New Hebrides	South Fiji Basin
Invertebrate scavengers												
Isopoda	Munnopsidae				bc		bc					
Mysidacea	Mysidae			bc	bc		bc					
Crabs	*Munidopsis*_sp.	bc		bc	bc							
	Probeebei mirabilis				bc							
	Sympagurus birkenroadii						bc	bc				
Shrimp	*Acanthephyra* sp			bc			bc	bc				
	Cerataspis monstrosus	bc		bc	bc		bc		bc	bc	bc	bc
	Benthiscymus spp.			bc	bc		bc		bc	bc	bc	bc
	Penaeid shrimp	bc		bc	bc		bc	bc				
	Hymenopenaeus nereus	bc		bc	bc		bc					
	Nematocarcinus sp			bc			bc					
Octopoda	Cirroteuthidae	bc										
	Grimpoteuthis sp			bc								
	Octopoda			bc	bc							
Echinodermata	Echinoidea	bc		bc								
	Plesiodiadema sp.	bc										
	Urechinidae	bc										
	Ophiosphalma glabrum	bc		bc								
	Ophiuroidea			bc	bc							

For simplicity the CCZ locations have been pooled into east (east of 130° W, UK1 to OMCO D), middle and west (west of 145° W, APEI 7 to Kiribati C) regions. Note that regions outside of the CCZ and DISCOL do not have visual transect data and invertebrates were only enumerated in baited cameras where their status as scavengers could be confirmed.

abyssal plains, island flanks, and trenches, significantly influenced the composition of the fish and scavenger community. In the CCZ, seamounts had a greater influence on scavenger assemblages than sampling region in many cases (**Figure 6**). Indeed some taxa appear to specialize on abyssal seamounts such as the eel *Ilyophis arx* (Leitner et al., 2021a). Synaphobranchid eels also were present in the two seamount visual transects but couldn't be identified to species (**Figure 5**). However, these transects were not statistically different from plains. It is clear that abyssal seamounts contribute to regional diversity in the CCZ (Cuvelier et al., 2020). These results corroborate our findings and suggest that seamount habitats must be considered in spatial management as distinct from the plains. Further differentiation of the fish community between finer-scale habitats (e.g., ridges and troughs) are not possible with the dataset, but cannot be excluded.

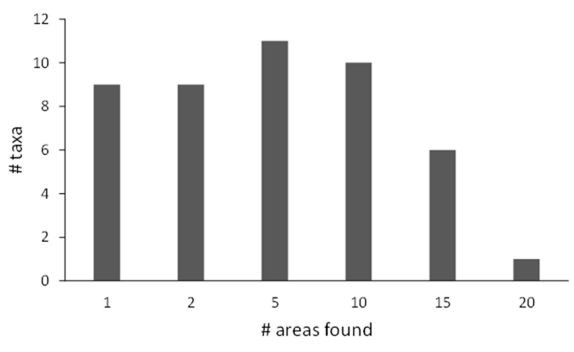

FIGURE 10 | Frequency distribution of the numbers of fish taxa with varying levels of species overlap (# of sites in which each was found out of 28 sites that had identified fish) across the Pacific from both camera transect and baited camera data.

Many fishes and scavengers have very large (as shown here), even worldwide, biogeographic ranges (King and Priede, 2008; Gaither et al., 2015). Indeed, the regional variations in community composition discussed above are largely the result of varying abundances of species rather than species presence/absence. It should be noted that there are a few species that have small ranges too (**Figure 10**). Though sampling in this analysis is sparse which can lead to erroneous conclusions about ranges (pseudoendemism) we observed some taxa only on seamounts (even with abyssal deployments from 15 to 20 km away; Leitner et al., 2021b) and 9 fish taxa were observed in only one region each and another 9 in two regions each (see also Simon-Lledó et al., 2020; Leitner et al., 2021a). Taxa such as the Liparidae and Zoarcidae frequently have regional endemics (Anderson and Fedorov, 2004; Chernova et al., 2004). Despite generally large ranges

it is not presently possible to determine if any biogeographic boundaries exist in the CCZ region owing to the coarse spatial resolution of the data. It is also important to note that the present analysis is largely based on morphological taxonomy, specifically photographic identification. Future physical sampling could yield greater diversity and split existing taxa, such that taxa with apparently widespread distributions are actually confined to smaller biogeographies. Additionally, we have not evaluated any population level ranges which can be quite important to evaluate connectivity and recolonization rates. Ideally datasets could be compared to those employing eDNA approaches. However, specimens for fishes and scavengers are limited which makes their coverage in barcoding databases very sparse. We need a concentrated fish and scavenger sampling effort using benthic trawls and traps across the CCZ where captured specimens are first morphologically identified and then barcoded with entry into global databases for future reference.

The changes in fish and scavenger community composition across the CCZ suggest that the distributed nature of the network of APEIs is likely very important for their conservation. It is clear already that the CCZ communities are different than those in much of the rest of the Pacific including some large protected areas such as Mariana Trench National Monument and Papahānaumokuākea Marine National Monument (the Northwestern Hawaiian Islands in our analysis) (Kennedy et al., 2019). Even for very mobile fishes and scavengers protected areas are needed in the immediate mining region to protect fish and scavenger communities. The regional environmental management plan for the CCZ is currently being reviewed by the ISA to ensure that the APEIs will preserve a fauna that is similar to the neighboring license areas (Wedding et al., 2015). While it seems clear that their distributed nature is beneficial for conservation of fish communities, at this stage fish and scavenger data is too limited to compare communities between license areas and neighboring APEIs to evaluate their representivity on more local scales. In those regions where we have data from APEIs, we are missing data from neighboring license areas (western CCZ), and in those regions where we have data from license areas, we are missing data from neighboring APEIs (eastern CCZ). Additionally, there is no currently available data from the central CCZ.

The ISA requires contractors to perform baseline assessment of license areas in the CCZ that include studies of top predators and scavengers (ISBA/25/LTC/6/Rev.1[3]). This initial synthesis (including the fish guide in **Supplementary Materials**) will hopefully provide a foundation for these future studies. We urge contractors to conduct megafaunal transect studies that cover enough area to provide robust fish data. Many transecting studies done to date were not quantitative or did not cover enough area to provide robust estimates of fish density, diversity and community composition. Exact areas will vary based on local densities and diversities but the areas with the most asymptotic rarefaction curves in this study included DISCOL, APEIs 6 and 7, and TOML D where the survey areas ranged from 1.3 to 11 hectares. Comparative methodological studies that more fully evaluate potential differences between ROV, AUV and towed camera systems are also needed. Baited camera studies will complement such transecting approaches. Though their effort is hard to quantify, they captured a large fraction (44%) of the fish taxa observed in visual transects and two that were not observed otherwise. At least one study has suggested that at one place and time, ∼10 deployments may adequately capture diversity and relative abundances of scavenging taxa within one habitat type (Harbour et al., 2020). Baited camera approaches already enable statistically meaningful comparisons between locations within the CCZ (**Figure 6**) but are currently unevenly distributed, existing for eastern CCZ license areas and western CCZ APEIs only. Baited camera deployments should be expanded into more CCZ regions using standard methods: a view area of 1–3 m^2, duration of 18–24 h at the seafloor, and using 1 kg of mackerel or similar bait tied tightly to the camera system in the field of view. We must urge taxonomic consistency during annotation (see **Supplementary Material**) by working with others to ensure consistency and especially with taxonomists by providing samples and funding (e.g., Glover et al., 2016). There are a number of taxa, particularly the diverse ophidiids, where we need significant additional specimens for vouchers and tissue to create DNA barcodes for eDNA work. Results from all analyses should be shared and will enable further evaluation of the APEIs, environmental drivers of community patterns, identify biogeographic boundaries, and perhaps lead to understanding seasonal and interannual variations that have been documented in other parts of the abyss (Priede et al., 2003; Drazen et al., 2012). As well as the scientific value, this will form an important part of the broad-scale understanding needed to inform regional management.

DATA AVAILABILITY STATEMENT

The original contributions presented in the study are included in the article/**Supplementary Material**, further inquiries can be directed to the corresponding author.

ETHICS STATEMENT

The animal study was reviewed and approved by the Animal Care and Use Committee, Office of Research Compliance, University of Hawai'i at Mānoa, protocol #14-1934.

AUTHOR CONTRIBUTIONS

JD and AL conceived of the study, compiled, and analyzed the baited camera data. DJ and ES-L compiled the visual transect data and assisted JD and AL in analysis. JD wrote the first draft of the manuscript. All authors contributed to manuscript revision, read, and approved the submitted version.

[3]www.isa.org.jm

FUNDING

This project was provided to JD and AL by the Gordon and Betty Moore Foundation (grant no. 5596), NOAA Office of Exploration and Research (grant # NA17OAR0110209), the Pew Charitable Trusts, and the Benioff Ocean Initiative. DJ received funding through the One Ocean Hub, a collaborative research for sustainable development programme funded by UK Research and Innovation (UKRI) through the UK Global Challenges Research Fund (GCRF) under NERC grant NE/S008950/1. This work was part of the NERC Seabed Mining And Resilience To EXperimental impact (SMARTEX) project (Grant Reference NE/T003537/1). This is SOEST contribution # 11379.

ACKNOWLEDGMENTS

Many thanks to the many scientists who assisted by contributing raw data from published and unpublished works: Monty Priede (U. Aberdeen), Tom Linley and Alan Jamieson (Newcastle U.), Se-Jong Ju (Korea Institute of Ocean Science and Technology), Andrew Sweetman and Rob Harbour (Heriot-Watt U.), Jennifer Durden (U. Southampton), Daphne Cuvelier (U. of Azores), Kirsty McQuaid and Kerry Howell (Plymouth U), John Parianos and Christina Pomee (Tonga Ocean Minerals Limited). Thanks to Victoria Gronwald for assistance in annotation of video transects from the DeepCCZ cruise, Sage Morningstar and Eric Klingberg for assistance in annotation of baited camera data from DISCOL and Station ALOHA. Numerous taxonomists assisted with animal identification: Mary Wicksten, Bruce Mundy, M. Eric Anderson, David G. Smith, Virginia Moriwake, Meagan Putts, Sarah Bingo, and Michelle Gaither. Thanks to Craig Smith and all the organizers of the CCZ data synthesis workshop held at Friday Harbor Marine Laboratory in October 2019. Malcolm Clark provided thoughtful insights and discussion during the workshop. This manuscript, in a more preliminary form, was released as part of a report published by the International Seabed Authority (ISA, 2020).

SUPPLEMENTARY MATERIAL

The Supplementary Material for this article can be found online at: https://www.frontiersin.org/articles/10.3389/fmars.2021.630616/full#supplementary-material

REFERENCES

Amon, D. J., Ziegler, A. F., Dahlgren, T. G., Glover, A. G., Goineau, A., Gooday, A. J., et al. (2016). Insights into the abundance and diversity of abyssal megafauna in a polymetallic-nodule region in the eastern Clarion-Clipperton Zone. *Sci. Rep.* 6:30492.

Amon, D., Ziegler, A. F., Drazen, J. C., Grisschenko, A. V., Leitner, A. B., Lindsay, D. J., et al. (2017). Megafauna of the UKSRL exploration contract area and eastern clarion-clipperton zone in the pacific ocean: Annelida, Arthropoda, Bryozoa, Chordata, Ctenophora, Mollusca. *Biodivers. Data J.* 5:e14598.

Anderson, M. E., Crabtree, R. E., Carter, H. J., Sulak, K. J., and Richardson, M. D. (1985). Distribution of demersal fishes of the Caribbean Sea found below 2,000 meters. *Bull. Mar. Sci.* 37, 794–807.

Anderson, M. E., and Fedorov, V. V. (2004). Family Zoarcidae Swainson 1839 eelpouts. *California Acad. Sci. Annotated Checklists Fishes* 34, 1–58.

Bailey, D. M., King, N. J., and Priede, I. G. (2007). Cameras and carcasses: historical and current methods for using artificial food falls to study deep-water animals. *Mar. Ecol. Prog. Ser.* 350, 179–191. doi: 10.3354/meps07187

Brewer, D. T., Milton, D. A., Fry, G. C., Dennis, D. M., Heales, D. S., and Venables, W. N. (2007). Impacts of gold mine waste disposal on deepwater fish in a pristine tropical marine system. *Mar. Pollut. Bull.* 54, 309–321. doi: 10.1016/j.marpolbul.2006.10.011

Bribiesca-Contreras, G., Dahlgren, T. G., Drazen, J. C., Drennan, R., Horton, T., Jones, D. O. B., et al. (2021). Biogeography and connectivity across habitat types and geographical scales in Pacific abyssal scavenging amphipods. *Front. Mar. Sci.* 8, 705237. doi: 10.3389/fmars.2021.705237

Cailliet, G. M., Andrews, A. H., Wakefield, W. W., Moreno, G., and Rhodes, K. L. (1999). Fish faunal and habitat analyses using trawls, camera sleds and submersibles in benthic deep-sea habitats off central California. *Oceanologica Acta* 22, 579–592. doi: 10.1016/s0399-1784(00)88949-5

Carney, R. S. (2005). Zonation of deep biota on continental margins. *Oceanogr. Mar. Biol. Annu. Rev.* 43, 211–278. doi: 10.1201/9781420037449.ch6

Chao, A., Gotelli, N. J., Hsieh, T., Sander, E. L., Ma, K., Colwell, R. K., et al. (2014). Rarefaction and extrapolation with Hill numbers: a framework for sampling and estimation in species diversity studies. *Ecol. Monogr.* 84, 45–67. doi: 10.1890/13-0133.1

Chernova, N. V., Stein, D. L., and Andriashev, A. P. (2004). Family Liparidae (Scopoli 1777) — snailfishes. *California Acad. Sci. Annotated Checklists Fishes* 31, 1–72.

Christiansen, B., Vieira, R. P., Christiansen, S., Denda, A., Oliveira, F., and Gonçalves, J. M. S. (2015). The fish fauna of Ampère Seamount (NE Atlantic) and the adjacent abyssal plain. *Helgol. Mar. Res.* 69, 13–23. doi: 10.1007/s10152-014-0413-4

Clarke, K. R., and Gorley, R. N. (2006). *PRIMER v6: User Manual and Tutorial*. Plymouth: PRIMER-E Ltd.

Cousins, N. J., and Priede, I. G. (2012). Abyssal demersal fish fauna composition in two contrasting productivity regions of the Crozet Plateau, Southern Indian Ocean. *Deep Sea Res. Part I Oceanogr. Res. Papers* 64, 71–77. doi: 10.1016/j.dsr.2012.02.003

Crabtree, R. E., Carter, J., and Musick, J. A. (1991). The comparative feeding ecology of temperate and tropical deep-sea fishes from the western North Atlantic. *Deep Sea Res.* 38, 1277–1298. doi: 10.1016/0198-0149(91)90027-d

Cuvelier, D., Ribeiro, P. A., Ramalho, S. P., Kersken, D., Martinez Arbizu, P., and Colaço, A. (2020). Are seamounts refuge areas for fauna from polymetallic nodule fields? *Biogeosciences* 17, 2657–2680. doi: 10.5194/bg-17-2657-2020

Devine, J. A., Baker, K. D., and Haedrich, R. L. (2006). Deep-sea fishes qualify as endangered. *Nature* 439:29. doi: 10.1038/439029a

Drazen, J. C., Bailey, D. M., Ruhl, H., and Smith, K. L. Jr. (2012). The role of carrion supply in the abundance of deep-water fish off California. *PLoS One* 7:e49332. doi: 10.1371/journal.pone.0049332

Drazen, J. C., Leitner, A. B., Morningstar, S., Marcon, Y., Greinert, J., and Purser, A. (2019). Observations of deep-sea fishes and mobile scavengers from the abyssal DISCOL experimental mining area. *Biogeosciences* 16, 3133–3146. doi: 10.5194/bg-16-3133-2019

Drazen, J. C., and Sutton, T. T. (2017). Dining in the deep: the feeding ecology of deep-sea fishes. *Annu. Rev. Mar. Sci.* 9, 337–366. doi: 10.1146/annurev-marine-010816-060543

Durden, J. M., Bett, B. J., and Ruhl, H. A. (2020). Subtle variation in abyssal terrain induces significant change in benthic megafaunal abundance, diversity, and community structure. *Progr. Oceanogr.* 186:102395. doi: 10.1016/j.pocean.2020.102395

Durden, J. M., Putts, M., Bingo, S., Leitner, A. B., Drazen, J. C., Gooday, A., et al. (2021). Megafaunal ecology of the western Clarion Clipperton Zone. *Front. Mar. Sci.* 8:671062. doi: 10.3389/fmars.2021.671062

Estes, J. A., Terborgh, J., Brashares, J. S., Power, M. E., Berger, J., Bond, W. J., et al. (2011). Trophic downgrading of planet Earth. *Science* 333, 301–306.

Farnsworth, K. D., Thygesen, U. H., Ditlevsen, S., and King, N. J. (2007). How to estimate scavenger fish abundance using baited camera data. *Mar. Ecol. Prog. Series* 350, 223–234. doi: 10.3354/meps07190

Fleury, A. G., and Drazen, J. C. (2013). Abyssal scavenging communities attracted to sargassum and fish in the Sargasso sea. *Deep Sea Res. I* 72, 141–147. doi: 10.1016/j.dsr.2012.11.004

Fosså, J. H., Mortensen, P. B., and Furevik, D. M. (2002). The deep-water coral Lophelia pertusa in Norwegian waters: distribution and fishery impacts. *Hydrobiologia* 471, 1–12.

Gaither, M. R., Bowen, B. W., Rocha, L. A., and Briggs, J. C. (2015). Fishes that rule the world: circumtropical distributions revisited. *Fish Fish.* 17, 664–679.

Glover, A., Dahlgren, T., Wiklund, H., Mohrbeck, I., and Smith, C. (2016). An end-to-end DNA taxonomy methodology for benthic biodiversity survey in the clarion-clipperton zone, central Pacific abyss. *J. Mar. Sci. Eng.* 4:2. doi: 10.3390/jmse4010002

Harbour, R. P., Leitner, A., Ruehlemann, C., Vink, A., and Sweetman, A. K. (2020). Benthic and demersal scavenger biodiversity in the eastern end of the Clarion-Clipperton Zone - an area marked for polymetallic nodule mining. *Front. Mar. Sci.* 7:458. doi: 10.3389/fmars.2020.00458

Hsieh, T. C., Ma, K. H., and Chao, A. (2020). *iNEXT: iNterpolation and EXTrapolation for Species Diversity. R Package Version 2.0.20*. Available online at: http://chao.stat.nthu.edu.tw/wordpress/software-download/ (Online) (accessed January 28, 2020).

ISA (2020). "Deep CCZ Biodiversity Synthesis Workshop Friday Harbor, Washington, USA, 1-4 October 2019: WORKSHOP REPORT," in *ISA Workshop Report*, eds C. R. Smith and M. R. Clark (Kingston: International Seabed Authority).

Jamieson, A., Fujii, T., Solan, M., Matsumoto, A. K., Bagley, P. M., and Priede, I. G. (2009). Liparid and macrourid fishes of the hadal zone: in situ observations of activity and feeding behaviour. *Proc. R. Soc. B: Biol. Sci.* 276, 1037–1045. doi: 10.1098/rspb.2008.1670

Jamieson, A. J., Kilgallen, N. M., Rowden, A. A., Fujii, T., Horton, T., Lörz, A. N., et al. (2011). Bait-attending fauna of the Kermadec Trench, SW Pacific Ocean: evidence for an ecotone across the abyssal-hadal transition zone. *Deep Sea Res. Part I: Oceanogr. Res.arch Papers* 58, 49–62. doi: 10.1016/j.dsr.2010.11.003

Jones, D. O. B., Kaiser, S., Sweetman, A. K., Smith, C. R., Menot, L., Vink, A., et al. (2017). Biological responses to disturbance from simulated deep-sea polymetallic nodule mining. *PLoS One* 12:e0171750. doi: 10.1371/journal.pone.0171750

Kennedy, B. R. C., Cantwell, K., Malik, M., Kelley, C., Potter, J., Elliott, K., et al. (2019). The unknown and the unexplored: Insights into the Pacific deep-sea following NOAA CAPSTONE expeditions. *Front. Mar. Sci.* 6:480. doi: 10.3389/fmars.2019.00480

Kersten, O., Smith, C. R., and Vetter, E. W. (2017). Abyssal near-bottom dispersal stages of benthic invertebrates in the Clarion-Clipperton polymetallic nodule province. *Deep Sea Res. I* 127, 31–40. doi: 10.1016/j.dsr.2017.07.001

King, N. J., and Priede, I. G. (2008). "Coryphaenoides armatus, the Abyssal Grenadier: Global distribution, abundance, and ecology as determined by baited landers," in *Grenadiers of the World Oceans: Biology, Stock Assessment, and Fisheries*, eds A. M. Orlov and T. Iwamoto (Bethesda, MD: American Fisheries Society), 139–161.

Langenkämper, D., Zurowietz, M., Schoening, T., and Nattkemper, T. W. (2017). BIIGLE 2.0 – Browsing and annotating large marine image collections. *Front. Mar. Sci.* 4:83. doi: 10.3389/fmars.2017.00083

Leitner, A. B., Durden, J. M., Smith, C. R., Klingberg, E., and Drazen, J. C. (2021a). Synaphobranchid swarms at an abyssal seamount summit: the largest aggregation of fishes ever observed at abyssal depths. *Deep Sea Res. I* 167, 103423. doi: 10.1016/j.dsr.2020.103423

Leitner, A. B., Neuheimer, A. B., Donlon, E., Smith, C. R., and Drazen, J. C. (2017). Environmental and bathymetric influences on abyssal bait-attending communities of the Clarion Clipperton Zone. *Deep Sea Res. I* 125, 65–80. doi: 10.1016/j.dsr.2017.04.017

Leitner, A. B., Smith, C. R., and Drazen, J. C. (2021b). Testing the seamount refuge hypothesis for predators and scavengers in the western Clarion-Clipperton Zone. *Front. Mar. Sci.* 8, 636305. doi: 10.3389/fmars.2021.636305

Linley, T. D., Stewart, A., Mcmillan, P., Clark, M., Gerringer, M., Drazen, J. C., et al. (2017). Bait attending fishes of the abyssal zone and hadal boundary: community structure, functional groups and species distribution in the Kermadec, New Hebrides and Mariana trenches. *Deep Sea Res. I* 121, 38–53.

Lodge, M., Johnson, D., Le Gurun, G., Wengler, M., Weaver, P., and Gunn, V. (2014). Seabed mining: international seabed authority environmental management plan for the Clarion–Clipperton Zone. A partnership approach. *Mar. Policy* 49, 66–72. doi: 10.1016/j.marpol.2014.04.006

Lutz, M. J., Caldeira, K., Dunbar, R. B., and Behrenfeld, M. J. (2007). Seasonal rhythms of net primary production and particulate organic carbon flux to depth describe the efficiency of biological pump in the global ocean. *J. Geophys. Res. C. Oceans* 112:C10011.

McQuaid, K. (2020). *Ecological Studies of an Abyssal Nodule Province to Inform the Management of deep-Sea Mining*. Ph.D. dissertation. Plymouth: University of Plymouth.

Merrett, N. R., and Fasham, M. J. R. (1998). Demersal ichthyofauna distribution in the abyssal North Atlantic revisited: the effect of sample size on ordination. *Mar. Ecol. Progr. Series* 173, 267–274. doi: 10.3354/meps173267

Merrett, N. R., Haedrich, R. L., Gordon, J. D. M., and Stehmann, M. (1991). Deep demersal fish assemblage structure in the Porcupine Seabight (eastern North Atlantic): Results of single warp trawling at lower slope to abyssal soundings. *J. Mar. Biol. Assoc. U.K. Plymouth* 71, 359–373. doi: 10.1017/s002531540005164x

Milligan, R. J., Morris, K. J., Bett, B. J., Durden, J. M., Jones, D. O. B., Robert, K., et al. (2016). High resolution study of the spatial distributions of abyssal fishes by autonomous underwater vehicle. *Sci. Rep.* 6:26095.

Mindel, B. L., Neat, F. C., Webb, T. J., and Blanchard, J. L. (2017). Size-based indicators show depth-dependent change over time in the deep sea. *ICES J. Mar. Sci.* 75, 113–121. doi: 10.1093/icesjms/fsx110

Morato, T., Watson, R., Pitcher, T. J., and Pauly, D. (2006). Fishing down the deep. *Fish Fish.* 7, 24–34. doi: 10.1111/j.1467-2979.2006.00205.x

Myers, R. A., Baum, J. K., Shepherd, T. D., Powers, S. P., and Peterson, C. H. (2007). Cascading effects of the loss of apex predatory sharks from a coastal ocean. *Science* 315, 1846–1850. doi: 10.1126/science.1138657

Oksanen, J., Blanchet, F., Kind, R., Legendre, P., Minchin, P., O'hara, R., et al. (2016). *Vegan: Community Ecology Package*.

Pearcy, W. G., Stein, D. L., and Carney, R. S. (1982). The deep-sea benthic fish fauna of the northeastern Pacific Ocean on Cascadia and Tufts abyssal plains and adjoining continental slopes. *Biol. Oceanogr.* 1, 375–428.

Polovina, J., Abecassis, M., Howell, E. A., and Woodworth, P. (2009). Changes among the upper trophic levels in the central North Pacific subtropical gyre ecosystem, 1996-2006. *Fish. Bull.* 107, 523–531.

Priede, I. G. (2017). *Deep-Sea Fishes: Biology, Diversity, Ecology and Fisheries*. Cambridge: Cambridge University Press.

Priede, I. G., and Bagley, P. M. (2000). In situ studies on deep-sea demersal fishes using autonomous unmanned ladder platforms. *Oceanogr. Mar. Biol. Annu. Rev.* 38, 357–392.

Priede, I. G., Bagley, P. M., and Smith, K. L. Jr. (1994). Seasonal change in activity of abyssal demersal scavenging grenadiers *Coryphaenoides* (Nematonurus) armatus in the eastern North Pacific Ocean. *Limnol. Oceanogr.* 39, 279–285. doi: 10.4319/lo.1994.39.2.0279

Priede, I. G., Deary, A. R., Bailey, D. M., and Smith, K. L. Jr. (2003). Low activity and seasonal change in population size structure of grenadiers in the oligotrophic abyssal Central North Pacific Ocean. *J. Fish Biol.* 63, 187–196. doi: 10.1046/j.1095-8649.2003.00142.x

Priede, I. G., Drazen, J. C., Bailey, D. M., Kuhnz, L. A., and Fabian, D. (2020). Abyssal demersal fishes recorded at station M (34°50′N, 123° 00′W, 4100 m depth) in the northeast Pacific Ocean: an annotated check list and synthesis. *Deep Sea Res. Part II Top. Stud. Oceanogr.* 173:104648. doi: 10.1016/j.dsr2.2019.104648

Priede, I. G., Godbold, J. A., King, N. J., Collins, M. A., Bailey, D. M., and Gordon, J. D. M. (2010). Deep-sea demersal fish species richness in the Porcupine Seabight. NE Atlantic Ocean: global and regional patterns. *Mar. Ecol.* 31, 247–260. doi: 10.1111/j.1439-0485.2009.00330.x

Priede, I. G., Smith, K. L. Jr., and Armstrong, J. D. (1990). Foraging behavior of abyssal grenadier fish: Inferences from acoustic tagging and tracking in the North Pacific Ocean. *Deep Sea Res.* 37, 81–101. doi: 10.1016/0198-0149(90)90030-y

Priede, I. G., and Smith, K. L. (1986). Behaviour of the abyssal grenadier, Coryphaenoides yaquinae, monitored using ingestible acoustic transmitters in the Pacific Ocean. *J. Fish Biol.* 29, 199–206. doi: 10.1111/j.1095-8649.1986.tb05011.x

Puig, P., Canals, M., Company, J. B., Martin, J., Amblas, D., Lastras, G., et al. (2012). Ploughing the deep sea floor. *Nature* 489, 286–289. doi: 10.1038/nature11410

Pusceddu, A., Bianchelli, S., Martín, J., Puig, P., Palanques, A., Masqué, P., et al. (2014). Chronic and intensive bottom trawling impairs deep-sea biodiversity and ecosystem functioning. *Proc. Natl. Acad. Sci.U.S.A.* 111, 8861–8866. doi: 10.1073/pnas.1405454111

Ripple, W. J., Estes, J. A., Beschta, R. L., Wilmers, C. C., Ritchie, E. G., Hebblewhite, M., et al. (2014). Status and ecological effects of the World's largest carnivores. *Science* 343:1241484. doi: 10.1126/science.1241484

Ryall, K. L., and Fahrig, L. (2006). Response of predators to loss and fragmentation of prey habitat: a review of theory. *Ecology* 87, 1086–1093. doi: 10.1890/0012-9658(2006)87[1086:roptla]2.0.co;2

Sackett, D., Kelley, C. D., and Drazen, J. C. (2017). Spilling over deepwater boundaries; evidence of spillover from two deepwater protected areas in Hawaii. *Mar. Ecol. Progr. Series* 568, 175–190. doi: 10.3354/meps12049

Simon-Lledó, E., Bett, B. J., Huvenne, V. A. I, Köser, K., Schoening, T., Greinert, J., et al. (2019a). Biological effects 26 years after simulated deep-sea mining. *Sci. Rep.* 9:8040.

Simon-Lledó, E., Bett, B. J., Huvenne, V. A. I, Schoening, T., Benoist, N. M. A., Jeffreys, R. M., et al. (2019b). Megafaunal variation in the abyssal landscape of the Clarion Clipperton Zone. *Progr. Oceanogr.* 170, 119–133. doi: 10.1016/j.pocean.2018.11.003

Simon-Lledó, E., Bett, B. J., Huvenne, V. A. I, Schoening, T., Benoist, N. M. A., and Jones, D. O. B. (2019c). Ecology of a polymetallic nodule occurrence gradient: Implications for deep-sea mining. *Limnol. Oceanogr.* 64, 1883–1894. doi: 10.1002/lno.11157

Simon-Lledó, E., Thompson, S., Yool, A., Flynn, A., Pomee, C., Parianos, J., et al. (2019d). Preliminary observations of the abyssal megafauna of kiribati. *Front. Mar. Sci.* 6:605.

Simon-Lledó, E., Pomee, C., Ahokava, A., Drazen, J. C., Leitner, A. B., Flynn, A., et al. (2020). Multi-scale variations in invertebrate and fish megafauna in the mid-eastern Clarion Clipperton Zone. *Progr. Oceanogr.* 187:102405. doi: 10.1016/j.pocean.2020.102405

Taboada, S., Riesgo, A., Wiklund, H., Paterson, G. L. J., Koutsouveli, V., Santodomingo, N., et al. (2018). Implications of population connectivity studies for the design of marine protected areas in the deep sea: an example of a demosponge from the Clarion-Clipperton Zone. *Mol. Ecol.* 27, 4657–4679. doi: 10.1111/mec.14888

Trenkel, V. M., Lorance, P., and Mahevas, S. (2004). Do visual transects provide true population density estimates for deepwater fish? *ICES J. Mar. Sci.* 61, 1050–1056.

Vanreusel, A., Hilario, A., Ribeiro, P. A., Menot, L., and Arbizu, P. M. (2016). Threatened by mining, polymetallic nodules are required to preserve abyssal epifauna. *Sci. Rep.* 6:26808.

Watling, L., and Norse, E. A. (1998). Disturbance of the sea bed by mobile fishing gear: a comparison to forest clearcutting. *Conservation. Biology* 12, 1180–1197. doi: 10.1046/j.1523-1739.1998.0120061180.x

Wedding, L. M., Friedlander, A. M., Kittinger, J. N., Watling, L., Gaines, S. D., Bennett, M., et al. (2013). From principles to practice: a spatial approach to systematic conservation planning in the deep sea. *Proc. R. Soc. B Biol. Sci.* 280:20131684. doi: 10.1098/rspb.2013.1684

Wedding, L. M., Reiter, S. M., Smith, C. R., Gjerde, K. M., Kittinger, J. N., Friedlander, A. M., et al. (2015). Managing mining of the deep seabed. *Science* 349, 144–145.

Wenger, A. S., Harvey, E., Wilson, S., Rawson, C., Newman, S. J., Clarke, D., et al. (2017). A critical analysis of the direct effects of dredging on fish. *Fish Fish.* 18, 967–985. doi: 10.1111/faf.12218

Wraith, J., Lynch, T., Minchinton, T. E., Broad, A., and Davis, A. R. (2013). Bait type affects fish assemblages and feeding guilds observed at baited remote underwater video stations. *Mar. Ecol. Progr. Series* 477, 189–199. doi: 10.3354/meps10137

Yeh, J., and Drazen, J. C. (2009). Depth zonation and bathymetric trends of deep-sea megafaunal scavengers of the Hawaiian Islands. *Deep Sea Res. I* 56, 251–266. doi: 10.1016/j.dsr.2008.08.005

Yeh, J., and Drazen, J. C. (2011). Baited-camera observations of deep-sea megafaunal scavenger ecology on the California slope. *Mar. Ecol. Progr. Series* 424, 145–156. doi: 10.3354/meps08972

Conflict of Interest: The authors declare that the research was conducted in the absence of any commercial or financial relationships that could be construed as a potential conflict of interest.

Publisher's Note: All claims expressed in this article are solely those of the authors and do not necessarily represent those of their affiliated organizations, or those of the publisher, the editors and the reviewers. Any product that may be evaluated in this article, or claim that may be made by its manufacturer, is not guaranteed or endorsed by the publisher.

Copyright © 2021 Drazen, Leitner, Jones and Simon-Lledó. This is an open-access article distributed under the terms of the Creative Commons Attribution License (CC BY). The use, distribution or reproduction in other forums is permitted, provided the original author(s) and the copyright owner(s) are credited and that the original publication in this journal is cited, in accordance with accepted academic practice. No use, distribution or reproduction is permitted which does not comply with these terms.

Advantages of publishing in Frontiers

OPEN ACCESS
Articles are free to read for greatest visibility and readership

FAST PUBLICATION
Around 90 days from submission to decision

HIGH QUALITY PEER-REVIEW
Rigorous, collaborative, and constructive peer-review

TRANSPARENT PEER-REVIEW
Editors and reviewers acknowledged by name on published articles

Frontiers
Avenue du Tribunal-Fédéral 34
1005 Lausanne | Switzerland

Visit us: www.frontiersin.org
Contact us: frontiersin.org/about/contact

REPRODUCIBILITY OF RESEARCH
Support open data and methods to enhance research reproducibility

DIGITAL PUBLISHING
Articles designed for optimal readership across devices

FOLLOW US
@frontiersin

IMPACT METRICS
Advanced article metrics track visibility across digital media

EXTENSIVE PROMOTION
Marketing and promotion of impactful research

LOOP RESEARCH NETWORK
Our network increases your article's readership